UGR-3129

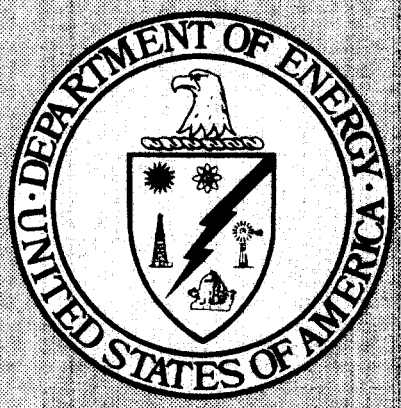

MERC/SP-77/5

PROCEEDINGS
FIRST EASTERN GAS SHALES SYMPOSIUM

October 17-19, 1977

MARCH 1978

United States Department of Energy
Morgantown Energy Research Center
Morgantown, West Virginia

TECHNICAL INFORMATION CENTER
UNITED STATES DEPARTMENT OF ENERGY

NOTICE

This report was prepared as an account of work sponsored by the United States Government. Neither the United States nor the United States Department of Energy, nor any of their employees, nor any of their contractors, subcontractors, or their employees, makes any warranty, express or implied, or assumes any legal liability or responsibility for the accuracy, completeness or usefulness of any information, apparatus, product or process disclosed, or represents that its use would not infringe privately owned rights.

This report has been reproduced directly from the best available copy.

Available from the National Technical Information Service, U. S. Department of Commerce, Springfield, Virginia 22161.

Price: Paper Copy $21.50
Microfiche $3.00

MERC/SP-77/5
Distribution Category UC-92

PROCEEDINGS

FIRST EASTERN GAS SHALES SYMPOSIUM

OCTOBER 17–19, 1977

LAKEVIEW INN AND COUNTRY CLUB
MORGANTOWN, WEST VIRGINIA

EDITORS: GARRY L. SCHOTT
WILLIAM K. OVERBEY, JR.
ARLEN E. HUNT
CHARLES A. KOMAR

COORDINATOR: HILMA D. BARLOW

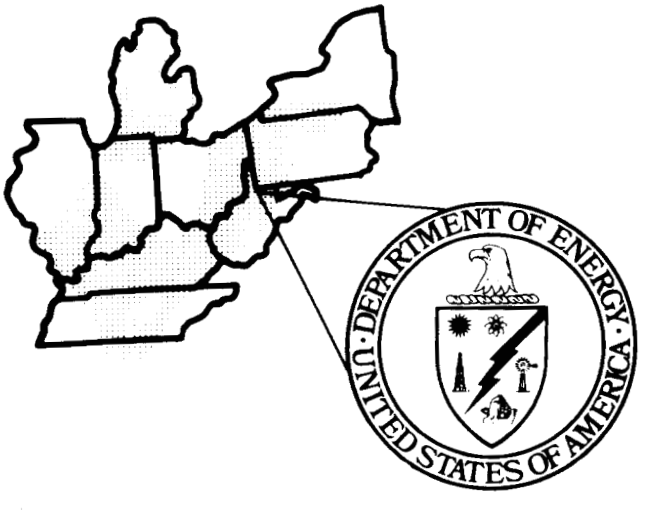

SPONSORED BY:

MORGANTOWN ENERGY RESEARCH CENTER
MORGANTOWN, WEST VIRGINIA

TABLE OF CONTENTS

ITEM	PAGE NO.
Opening Remarks by W. K. Overbey, Jr.	vii
"Unconventional Gas Resources: DOE Program in Enhanced Gas Recovery" Jeffrey B. Smith	1
GENERAL SESSION I	
EGS-1 "Some Preliminary Results of Regional Stratigraphic Studies of the Devonian Black Shales in the Appalachian Basin" John B. Roen, Wallace de Witt, Jr., Roy C. Kepferle, Laure G. Wallace, Mareta West	22
EGS-2 "Update Concerning the Three-Dimensional Seismic Investigations in the Cottageville Field" Edward R. Tegland	23
EGS-3 "In Situ Examination of Hydraulic Fractures" L. D. Tyler, W. C. Vollendorf, D. A. Northrop	37
EGS-4 "Abundance and Distribution of Some Chemical Elements in the Chattanooga, Ohio, and New Albany Shales in Kentucky" William H. Dennen, William H. Blackburn, Philip A. Davis	49
EGS-5 "Wireline Evaluation of the Devonian Shale: A Progress Report" Jon Hilton	68
EGS-6 "Update on the LLL Gas Stimulation Program" M. E. Hanson, R. J. Shaffer, J. R. Hearst, G. D. Anderson, D. N. Montan, H. C. Heard, D. Emerson	80
STRATIGRAPHY/GEOLOGY	
EGS-7 "Subsurface Stratigraphy and Extent of the Upper Devonian Dunkirk and Rhinestreet Black Shales in New York" Arthur M. Van Tyne, John C. Peterson, Lawrence V. Rickard, David G. Kamakaris	111
EGS-8 "Stratigraphy and Gas Occurrence in the Devonian Organic Rich Shales of Pennsylvania" R. G. Piotrowski, S. A. Krajewski, Louis Heyman	127
EGS-9 "Wireline Logs and Sample Studies in Stratigraphy and Gas Occurrence of the Devonian Shales Along the Southern Tie Section in Eastern Kentucky and Vicinity" Edward N. Wilson, Jaffery S. Zafar	145
EGS-10 "Tioga Bentonite Time-Marker Associated With Devonian Shales in Appalachian Basin" John M. Dennison, Daniel A. Textoris	166

TABLE OF CONTENTS (CONT'D)

ITEM		PAGE NO.
EGS-11	"New Albany Shale and Correlative Strata in Indiana" John L. Bassett, Nancy R. Hasenmueller	183
EGS-12	"Preliminary Model of Catskill Delta in West Virginia" Joseph F. Schwietering	195
CHARACTERIZATION/PHYSICAL - MINERALOGICAL		
EGS-13	"Physio-Chemical Characterization of Devonian Gas Shale R. E. Zielinski, A. Attalla, E. Stacy, B. D. Craft, and R. L. Wise	206
EGS-14	"Characterization and Analysis of Devonian Shales: 1. Physical Characterization" R. S. Kalyoncu, W. G. Coppins, D. T. Hooie, M. J. Snyder.	230
EGS-15	"New Data for Uranium, Thorium, Carbon, and Sulfur in Devonian Black Shale, from West Virginia, Kentucky, and New York" Joel S. Leventhal, Martin B. Goldhaber	259
EGS-16	"Geochemical Characterization of the Devonian Black Shale from Cottageville, West Virginia: A Preliminary Look at Multivariate Analysis" Stephanie J. Bialobok, Steven C. Lamey, Jojok Sumartojo	297
EGS-17	"A Petrologic Study of the Devonian Shales from Central Tennessee and West Virginia" Jojok Sumartojo, Peter Waldstein	311
EGS-18	"Petrology of New Albany Shale Group (Upper Devonian and Kinderhookian) in the Illinois Basin, A Preliminary Report" R. D. Harvey, W. A. White, R. M. Cluff, J. K. Frost, P. B. DuMontelle	328
EGS-19	"The Relationship Between Density and Gamma-Ray Intensity in the Devonian Shale Sequence, Lincoln County, West Virginia" James W. Schmoker	355
GENERAL SESSION II		
EGS-20	"AMEX/VESCORP Devonian Shale Project - Lawrence & Scioto Counties, Ohio" John N. Cochrane, F. Daniel Ryan, Steven H. Alkire	361
EGS-21	"Chemical Explosive Fracturing of Eight Tight Gas Gas Wells" S. J. LaRocca, Arthur M. Spencer	368
EGS-22	"Dynamic Properties of Devonian Shales" W. J. Carter, B. W. Olinger	381
EGS-23	"Novel Fracturing Treatments in the Devonian Shale" Stephen P. Cremean	389

TABLE OF CONTENTS (CONT'D)

	ITEM	PAGE NO.
EGS-24	"Rock Mechanics Aspects of MHF Design in Eastern Devonian Shale Gas Reservoirs" A. H. Jones, A. S. Abou-Sayed, L. A. Rogers	410
EGS-25	"Tilt Monitoring of Massive Hydraulic Fracture Experiments in Devonian Shale of West Virginia" M. D. Wood	425
EGS-26	"Results from a MHF Surface Electrical Potential Mapping Experiment" Carl L. Schuster, Leon J. Keck	426
GEOLOGY/STRUCTURE		
EGS-27	"Paleocurrent Systems in Shaly Basins: Preliminary Results for Appalachian Basin (Upper Devonian) R. C. Kepferle, Paul Lundegard, J. B. Maynard, Paul E. Potter, W. A. Pryor, Neil Samuels, Fred Schauf	434
EGS-28	"Stress Trajectory Simulations Accross the Appalachian Plateau Province in West Virginia" Sunder H. Advani, Hota V. S. GangaRao, H. Y. Chang. Claude S. Dean, William K. Overbey, Jr.	442
EGS-29	"Seismic Modelling of Complexly Deformed Fold-and-Thrust-Belt Rocks, Central Appalachians" William J. Perry, Jr., Gerald Smith, Myung W. Lee	449
EGS-30	"Regional Seismic Investigations in Eastern Tennessee" Edward R. Tegland, Lloyd Johnson	450
EGS-31	"Interrelationships of Photolineaments, Geological Structures, and Fracture Production of Natural Gas in the Appalachian Plateau of West Virginia" Eberhard Werner	474
EGS-32	"Correlation Between Outcrop Fractures, Geophysics and Rome Trough Structure in Kanawha County West Virginia" Byron R. Kulander, Stuart L. Dean, Richard E. Williams	484
EGS-33	"Analysis of Structural Geological Parameters that Influence Gas Production from the Devonian Shale of the Appalachian Basin" Robert C. Shumaker, Keith G. Kirk, E. B. Nuckols III, Brian R. Long	496
GEOCHEMISTRY - GAS AND ORGANIC		
EGS-34	"Characterization and Analysis of Devonian Shales: Gas Composition and Release Rates" M. Jack Snyder, M. P. Rausch, J. S. Ogden, R. W. Coutant	524
EGS-35	"Geochemical Characterization of Devonian Gas Shale" Ron E. Zielinski	546

TABLE OF CONTENTS (CONT'D)

ITEM		PAGE NO.
EGS-36	"Structural Characterization of Bitumen and Kerogen from Devonian Shale" T. F. Yen, C. S. Wen, J. I. S. Tang, J. T. Kwan, D. K. Young, Edith Chow	572
EGS-37	"Internal Surface Area and Porosity in Eastern Gas Shales from the Sorption of Nitrogen, Carbon Dioxide, and Methane - A Status Report Josephus Thomas, Jr., Robert R. Frost	589
EGS-38	"Chemical and Isotopic Composition of Gas from Devonian Black Shale Canned Core Samples, Martin County, Kentucky, and Wise County, Virginia" George F. Claypool, Charles N. Threlkeld	596
EGS-39	"The Relationship of Thermodynamic and Kinetic Parameters to Well Production in Devonian Shale" Paul D. Schettler, Jr., Dale L. Wampler, Philip J. Sipling, Donald J. Mitchell	608
OTHER PAPERS		
EGS-40	"Conodont Color Alteration, an Organo-Mineral Metamorphic Index, and its Application to Appalachian Basin Geology" Anita G. Harris	620
EGS-41	"Devonian Harrell and Millboro Shales in Parts of Pennsylvania, Maryland, West Virginia and Virginia" Kenneth O. Hasson, John M. Dennison	634
EGS-42	"Petrology of Lower Huron Devonian Shale, Columbia Gas Transmission Co. Well #20403, Lincoln County, West Virginia" Robert J. Vinopal	642
EGS-43	"Procedures for the Characterization of Devonian Shales" W. E. Brownell	659
EGS-44	"A Report on Variations of Stimulation Treatments on the ERDA Shale Projects" J. L. Norton	667
EGS-45	"Progress Report on Characterization of the Devonian Black Shales in Ohio" Frank L. Majchszak	668
EGS-46	"Use of the Scintillometer and Gamma-Ray Logs for Correlation from the Subsurface to the Surface in Black Shale" Frank R. Ettensohn, Linda Provo Fulton, Roy C. Kepferle	678
EGS-47	"Hybrid Computers for Simulation of Gas Diffusion in Fractured Shale" Thomas E. Springer	691

	ITEM	PAGE NO.
EGS-48	"Devonian Shale Evaluation in Stimulation Fluid Recommendations" D. E. Simon, A. R. Jennings, Jr.	701
EGS-49	"Carbonaceous Shales of Indiana as Sources of Energy, Petrochemicals, and Ceramic Materials: First Annual Progress Report" John B. Patton	702
EGS-50	"Characterization of Devonian Shales Using Laser Pyrolysis-Gas Chromatography" Nicholas E. Vanderborgh, J. M. Williams, E. M. Wewerka, J. P. Bertino	709
EGS-51	"SRI International's Computational Fracture Model and its Application to Devonian Shales" S. L. McHugh, L. Seaman, D. R. Curran, D. A. Shockley	717
EGS-52	"Gas Chromatographic Analysis of Fischer Retort Products of the New Albany Shale" Gianfranco Rinaldi, Paolo Ciccioli, W. Bradley Wimberg, W. G. Meinschein	734
EGS-53	"An Interactive Data Management and Analysis System for the Eastern Gas Shales Program" Pyrtle W. Seabaugh, Ronald E. Zielinski	748

APPENDICES

A-1	Submitted Biographical Sketches	756
A-2	List of Attendees	760
A-3	Photographs of Symposium Events	778

FIRST EASTERN GAS SHALES SYMPOSIUM

OPENING REMARKS

W. K. Overbey, Jr., Symposium Chairman

Welcome to the First Eastern Gas Shales Symposium. This symposium is designed to allow those of us associated with the Eastern Gas Shales Project (EGSP) to report the results of the many laboratory and field R & D studies conducted during the past year. It is encouraging to see this large attendance, which exemplifies the great interest in our project.

First of all I would like to introduce to you, and thank, the following people who have been instrumental in making preparations for the symposium and who will assist in its conduction:

Arlen E. Hunt.....Vice Chairman, Chairman Session I
Charles A. Komar.....Vice Chairman, Chairman Session III
Hilma Barlow.....Symposium Coordinator and Treasurer
Diane Manilla.....Registration
Brenda McDilda.....Registration
Charles Whieldon.....Special Arrangements

I would also like to thank and introduce the session chairmen who have spent considerable time arranging the sessions and reviewing papers:

Wallace de Witt, Jr.	Chairman Session IIA, Geology/Stratigraphy
Charles W. Byrer	Chairman Session IIB, Characterization/ Physical and Mineralogical
Claude S. Dean	Chairman Session IVA, Geology/Structure
Garry L. Schott	Chairman Session IVB, Geochemistry/Gas and Organic

The objective of this symposium is to promote "A Free Exchange of Results and Ideas". The purpose, of course, is to pass on to those who can apply it, the knowledge we have gained during the past year.

In March of 1976 at a seminar conducted by the West Virginia Geological Survey, West Virginia University and Morgantown Energy Research Center, we summarized the state of knowledge at that point with a number of papers, most of which are published in MERC/SP-76/2 "Devonian Shale Production and Potential".

Today we will hopefully be taking a giant step forward as we listen to the results of research conducted during the past year and add to our previous knowledge of the organic rich, gas-bearing shales of the eastern United States.

Goals and Objectives

The Eastern Gas Shales Project was formally initiated in 1976 by the Energy Research and Development Administration (now DOE) at its Morgantown Energy Research Center (MERC). The ultimate objective is to increase production of natural gas from the Eastern Shales through advanced exploration and extraction techniques.

The project is specifically directed toward:

1. Determining the Magnitude of potential gas reserves
2. Thoroughly characterizing the shale
3. Improving current stimulation technology and developing new stimulation techniques.

The Eastern Gas Shales Project expects to achieve the following goals:

In Appalachian basin

Add 3.5 to 7.0 trillion cubic feet of gas to reserves in the Appalachian basin

Increase average total gas reserve added per well drilled from 200 to 600 million cubic feet

Increase the average open-flow production rate of new shale wells from 100,000 to 300,000 cubic feet of gas per day, or more

In Illinois and Michigan basins

To stimulate interest in testing the New Albany and Antrim shales for gas production

Strategy

The overall project consists of a large number of separate, but closely related, activities involving State and Federal organizations, universities, and industry working within a planned project structure coordinated by DOE.

Accomplishments

I would like to highlight just a few of the accomplishments which I think are of significance to those of you who test our ideas and results by actually drilling and stimulating gas wells.

Geological Resource Evaluations

Stratigraphy - An intensive study and effort to map the thickest, most consistently productive shale unit - the Huron outcrop and Brown shale in the subsurface has been made by state surveys and the USGS who cooperated in a crash effort to complete a basin-wide series of stratigraphic sections which will be distributed shortly. An example is on display.

Sedimentation - The collection, review, and annotation of 381 references on argillaceous sediment by Messrs. Potter, Maynard, and Pryor of the University of Cincinnati represents a tremendous achievement and will prove to be an outstanding source of information. Definition of paleocurrent directions by this group is important to sedimentation Patterns.

The postulation of a structural and depositional model of the Catskill Delta, which provided much of the sediments for the upper Devonian shales in the Appalachian basin, by Dr. Joe Schwietering is an important step to provide insight in establishing exploration models.

The completion of detailed petrographic studies on core material has provided new insights into various types of depositional environments and associated sedimentary structures, which may be important in the generation of fractures during sediment maturation processes. This data can be used in establishing exploration models.

Fifty-three (53) stratigraphic cross sections in all three basins and thirty-seven maps of various types have been completed this past year. We are now preparing to publish many of these.

We obtained more than 5000 feet of core material and conducted thousands of geochemical and physical property determinations. We also developed new techniques for examining core fractures and determining their genetic origin.

We have made measurements of residual gas liberated from encapsulated shale core samples to estimate potential gas reserves. We have looked in depth at kerogen and the maturity of the organic matter in the shales. We have conducted material-balance fischer assays of the shale to determine the gas and oil content. Results to date indicate a residual gas saturation of .8 cu. ft. gas/cu. ft. of shale. Seismic techniques being investigated as exploration tools are showing considerable promise. Stress trajectory models over the Rome Trough area, when combined with seismic information, point to possibly a new technique for locating fractured reservoirs. Stimulation tests are inconclusive but appear promising. Foam Fracs permit well-clean-up much more quickly than conventional H_2O fracs. We have had one successful demonstration of a displaced liquid explosive stimulation in Lincoln County, WV. This well is currently being tested.

We need to examine statistically the effects of various completion techniques used historically, such as cleaning-out versus not-cleaning-out a shot well. We would like further discussions with those of you having experience in this area.

We feel we have had a good first year and that we will have an even better second year as we focus on the key issues of our various research efforts. The synthesis of this year's results with next year's should provide us with some very interesting evaluations about the potential for a major shale gas contribution to the energy economy.

The challenge to develop new sources of gas for the nation is being met by all of you who are participating in this project. To set the theme of this symposium I would like to show you a film we have prepared which we think illustrates well the depth and thoroughness of studies that we are conducting with the Eastern Gas Shales Project.

I would like to introduce now Mr. Leo Schrider, Assistant Director for Oil, Gas & In Situ Coal at MERC, who will introduce Mr. Hugh Guthrie our keynote speaker for the Symposium.

UNCONVENTIONAL GAS RESOURCES:
DOE PROGRAM IN ENHANCED GAS RECOVERY

Jeffrey B. Smith
Enhanced Gas Recovery Branch
Division of Oil, Gas, Shale and In Situ Technology

Rather than discuss the status of natural gas research - as indicated in your program - I hope that you will excuse me if I confine my remarks merely to a short synopsis of the overall DOE program in Enhanced Gas Recovery. A program, I might add, in which the Eastern Gas Shales Project is one of the key initiatives.

First, I would like to say something that most everyone in this room is well aware of - the gas shortage is real and it is going to be with us for some time to come. If we can set aside all of the ongoing political and industry rhetoric (along with our own subjective personal opinions) we are still confronted by two serious "facts of life":

(1) For almost a decade the United States has been consuming nautral gas at a greater rate than we have been finding new reserves to replace those consumed and

(2) There is a finite amount of natural gas present within the earth's crust - it is not a renewable resource.

Much of the known and easily exploitable sources of gas - the so-called "conventional" sources, such as the high permeability sand reservoirs of the Tertiary sequence along the Gulf Coast - have already been developed and production is declining rapidly. The total producible reserves from conventional gas reservoirs amount to only 216 Tcf - less than an 11 year supply.

However...several large potential resources of natural gas remain to be developed. These resources are collectively referred to as "unconventional sources" because of their inherent low permeability and/or peculiar producing characteristics. Furthermore, the oil and gas industry are not enthusiastically pursuing development of these potential gas resources because of poor or non-existent profit incentives.

The Federal Government - primarily ERDA, and now the DOE - stepped into the picture in order to support Research, Development and Demonstration work and provide the "extra incentive" to overcome the existing inertia associated with commercial development of these resources.

The total DOE program for development of these unconventional sources of gas is called the Enhanced Gas Recovery Program. The primary goal of this program is to provide a data base of resource characterization and production technology which will lead to commercial development of these gas resources. DOE will encourage and support industry participation in developing and demonstrating technologies needed to reach this goal.

We feel that there are four major unconventional resources of gas that have a high potential for commercial development. There are other unconventional sources - such as the gas hydrates - however, these sources are simply too poorly defined to warrant a major development thrust at this time.

The four unconventional sources of gas currently included in our EGR program are as follows:

(1) The carbonaceous shales of Devonian age located in the Appalachian, Illinois and Michigan Sedimentary Basins are the target resource for the project which you all are most familiar with - the Eastern Gas Shales Project.

(2) The low permeability, low porosity so-called "tight" gas sandstones of the Upper Cretaceous/Lower Tertiary in the Rocky Mountain areas constitute the resource target for our Western Gas Sands Project.

(3) The free methane trapped in coal beds of both the eastern and western United States constitute the Methane from Coal Beds Project.

(4) The abnormally high pressured, high temperature saltwater aquifers of the Texas-Louisiana Gulf Coast are targets of our Geopressured Aquifer Project.

Having discussed the DOE role and resource targets for Enhanced Gas Recovery, I would like to talk about implementation of the program. Our basic implementation strategy consists of:

(1) assessing and characterizing the resource potential of each unconventional gas resource.

(2) conducting cost-shared field test with industry to improve, develop and demonstrate various stimulation and production technologies. I have included the caveat "when advantageous" on the slide to convey to you that all field tests will be tailored to the constantly changing Program Plan and must have to have a large component of R&D - we will not fund stimulation tests merely because the operator needs to fracture a well in order to insure commercial production volumes.

(3) we will coordinate our activities with both DOE divisions and other Federal agencies (such as the Bureau of Mines) to minimize duplication of effort and overlapping costs to the government

(4) finally, all projects will be directored toward commercial development of the gas resources. We cannot continue to fund stimulation technology experiments once they have been statistically proven to be ineffective from the cost/benefit standpoint. Simply stated, if it won't be self-supporting at some time in the forseeable future (say 10 years from now), DOE support will be withdrawn.

Before I go over a brief synopsis of activities planned for each project, I would like to disgress for just a moment. Since many of you have, at one time or another, expressed some confusion as to how the managment of our program in EGR is handled let me show you a simplified organization chart which hopefully, will shed some light on this matter.

All oil and gas research and development activities involving drilling, stimulation and production technologies (that is, field development) is conducted by the DOE Division of Oil, Gas and Shale Technology. The division Director is Hugh D. Guthrie, who was yesterday's keynote speaker. Under Hugh are two Directorates - Oil and Gas and In Situ Technology. The In Situ Technology Directorate, conducts work in underground coal gasification and in situ retorting of oil shale. The Oil and Gas Directorate includes programs in EOR, EGR, and Drilling and Exploration Technology. Under Don Ward, the EGR Branch Chief, are the four projects I have mentioned previously. All funding for these projects is channeled through the Branch Chief. However, the actual day to day field management of three of the projects has been delegated to personnel at our Energy Research Centers.

At best, we in Headquarters can only be classified as "well-informed", technically, when it comes to evolving technologies relevant to developing these unconventional gas resources. The actual day-to-day field management of the EGSP is entrusted to more knowledgeable personnel like Bill Overbey and his technical support staff. Field management of our Western Gas Sands Project is provided by personnel from the Bartlesville (Oklahoma) Energy Research Center. The soon to be initiated Methane from Coal Project, will be managed at MERC. Bob Wise is the designated project manager. Both Bob and Bill Overbey report to Leo Schrider, the Assistant Director for the Oil, Gas, Shale, and In Situ Division at MERC. Our Geopressured Aquifer project will be managed out of Headquarters because none of our field ERC's has done any research in this area, and therefore, are just as "qualified" as we at Headquarters!

I see little benefit to be derived from my discussing the EGSP. You have been exposed to a thorough discussion of its potential as a resource, and its physical/chemical parameters at yesterday's sessions. This slide will serve as a quick reminder of the geography areas encompassed by the EGSP.

The next slide gives a quick look at what type of "geological animal" the EGSP is dealing with. While gas is undeniably related to the occurrence of natural fracture systems within the shale, the overall producing mechanism and precise location of fractured, gas-bearing locales within each basin is still poorly understood. By developing reliable resource characterization techniques and applying effective stimulation technologies we (and I mean the collective "we" represented by all of you present in this room) intend to elevate the Devonian shale from the status of a potential gas resource to that of a proven gas reserve. Once we have done this then the private sector can take over the large-scale commercial development of the Devonian shale gas resource.

The second largest project (both in terms of complexity and level of funding) is our WGSP. The primary targets for this project are the low permeability (<1md) gas sandstones of the Piceance, Uinta, Greater Green River Basins and the Northern Great Plains Province (shown by the diagonally cross-hatched pattern on the slide).

Success of our project in these four primary geologic locales will permit us to investigate additional low permeability sandstones in the 16 other sedimentary basins included on the slide.

This very generalized schematic cross-section of the Piceance Basin shows the geometry of these tight sandstones. They are a series of individual lenticular sand bodies deposited in a complexy interfingering fluvial/deltaic sequence. Individual sand lenses have thicknesses measured in 10's of feet and lateral extents of less than 3000'.

Some of the basic problems which we are attempting to solve in the WGSP are shown on this slide. Without ruling out CEF completely, I have to say that at this time, it appears that the only practical means of increasing permeability and resultant flow rates from these sandstones lies in the use of massive hydraulic fracturing techniques. Unfortunately, we still have some way to go before we can design MHF jobs with predictable results. To date our experiments have been very encouraging w/2x-10x increase in post-frac flow rates over the initial natural open flow rates over the initial natural open flow rates - (from 100 Mcf to as much as 1.1 MMcf/d).

Unlike the eastern United States where there are many very strong state geological surveys and universities (most of which are represented in this room today), the major source of geologic, geochemical and geophysical knowledge relating to these tight gas sandstones in the West resides in one institution -- the USGS. Under an interagency agreement with DOE the USGS is responsible for a wide variety of assignments in providing an inventory and thorough characterization of these tight gas sandstones. Regional universities and labs will be utilized for work which the USGS cannot handle or which would be more cost-effective to contract out.

In addition to conducting resource characterization and stimulation field experiments, several institutions are engaged in applied research aimed at developing new supporting technology for our field stimulation experiments. The activities shown on this slide support development of both the EGSP and WGSP. I won't dwell upon these activities as you've already heard, or shortly will hear, talks by some of these contractors such as Sandia, Los Alamos Laboratories, Lawrence Livermore Laboratory and Mound Lab.

Our Methane from Coal Project is relegated neither to the eastern or the western part of the United States. However, the size of our budget for FY-1978 will preclude any widespread and/or large-scale activities. There have even been rumors to the effect that Bob Wise, the project manager, has gone out and rented a Honda 350 to cut down on his travel expenses.

The next slide shows some of the programs involved in producing and utilizing methane derived from coal beds. The top statement alludes to the fact that the coal, like portions of the Devonian shale, is impermeable, highly fractured (termed "cleat" by mining personnel) and produces gas by desorption. However...the greatest similarity between shale gas production and methane drainage production is their generally unpredictable nature, especially with regard to predicting open flow production rates prior to actually production testing the wells.

The EGR project in Methane Drainage will be confined to unminable coal beds -- those which are too thin and/or too deep to be conventionally mined. The project goals are pretty straight forward.

This project is a new initiative in FY-78 and we (meaning MERC and Headquarters) have not finished drafting a complete, fully integrated project plan.

The fourth EGR project, and another new initiative in FY-78, is the Geopressured Aquifer (GPA) Project. Both the Division of Geothermal Energy and the Enhanced Gas Recovery Branch are cooperating in a joint venture to develop the energy resources (both geothermal and gas) of the abnormally high pressure, high temperature, saltwater aquifers of the TX-LA Gulf Coast.

Some of the requirements for a viable field project in the geopressured aquifers are given in this slide. The first 2 requirements are obvious. Flowing a well at a rate of 40,000 BWPD for 20 years with a minimum gas saturation of 30 SCF/bbl (1.2 MMcf of gas/day) is a pretty good trick. If this was Saudi Arabia and we were talking about 40,000 BPD of light Arabian crude the economic picture would be quite different. Finally, for such a high risk, low profit venture you have to be able to pin down the aquifer to reduce the risk to virtually nil.

Currently most of the money available for this program is in the Geothermal Program, which has been underway for over one year.

The final statement pretty much sums up the general assessment by informed experts. And I do wish to stress the work informed, especially with the current atmosphere wherein the press is quoting the resource as being thousands of trillion cubic feet or hundreds of years supply. I only wish I were as knowledgeable as the New York Times copy writers.

There is a large potential source of gas in these aquifers, but the risk and technical problems are formidable. I once read, somewhere, that there are tons and tons of gold in a cubic mile of seawater; the "trick" is to get it out and yield a profit for your labor. This analogy applies to all of the unconventional sources of gas, but it is especially pertinent with regard to the geopressured aquifers.

The proposed work in developing the GPA's is shown on this slide. The EGR project activities are directed primarily toward implementing studies defined by the bottom two bullets.

In summary, the primary objective to the EGR Program is to stimulate commercial development of large known gas resource. The figures shown here were derived from an independent study by the old ERDA organization entitled the Market Oriented Program Planning Study or MOPPS. Those of you who are subscribers to the New York Times have undoubtedly heard of the study. I won't dwell upon the methods employed in generating these numbers. I think the main point of this slide is to show that there are indeed very impressive reserves of potentially (and I emphasize the word "potentially") recoverable gas. However...the wide range of the estimates should provide a strong clue as to the reliability of an reserves figures at this time.

In order to turn these estimates into commercial reserves capable of being put into the pipeline the DOE, Enhanced Gas Recovery Branch is following the program strategy outlined here. We fully intend to meet our stated goals to:

(1) provide a reliable data base of technological information

(2) improve upon existing and/or develop new stimulation and production technologies and

(3) demonstrate the commercial feasibility of successful techniques

Of all Fossil Energy programs in DOE, the EGR Program has the greatest potential for near-term impact. Relative to the building of coal gasification plants and the like, our program activities have fast response time (weeks to D & C a well versus months or years to construct a plant), it costs less to do the work, and has minimal effect upon the environment.

With your support and technical expertise we can take a major step toward solving the current energy crisis. If this program is to become a success it will only happen because dedicated professionals such as yourselves make it happen. Thank you.

Overview

- Several Large Potential Resources of Gas.
- Industry Is Not Developing These Resources.
- DOE Sponsored R&D Will Provide Data Base for Commercialization .
  - — Resource Characterization
  - — Production Technology
- Transfer Technology and Support Industry Development

JEFFREY B. SMITH

5

UNCONVENTIONAL SOURCES OF GAS

GAS SOURCE	OGST ACTIVITY
TIGHT GAS SANDS	WESTERN GAS SANDS PROJECT (WGSP)
EASTERN DEVONIAN SHALES	EASTERN GAS SHALES PROJECT (EGSP)
METHANE FROM COAL BEDS	COORDINATING WITH DIVISION OF CONSERVATION RESEARCH AND TECHNOLOGY AND BUREAU OF MINES
GEOPRESSURED AQUIFERS	COORDINATING WITH DIVISION OF GEOTHERMAL ENERGY

Implementation Strategy

- Assess and Characterize the Resource Potential of These Unconventional Gas Sources.
- When Advantageous, Conduct Cost-Shared Field Tests With Industry.
- Coordinate Planning and Implementation Within DOE and Other Government Agencies.
- Structure Integrated Projects Directed Specifically at Development of These Gas Sources.

Eastern Gas Shales
Gas-Bearing Devonian and Mississippian
Shale Deposits

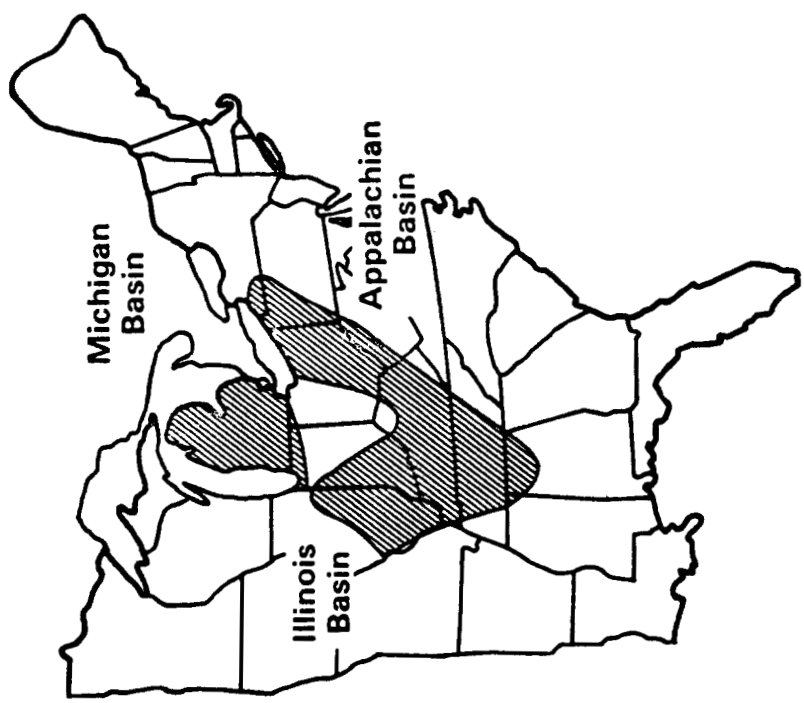

Eastern Gas Shales Project

(EGSP)

- Gas Production Appears To Be Related to the Occurrence of Natural Fracture Systems
- Resource Characterization Techniques:
  - Surface Mapping of Lineaments and Faults
  - Subsurface Detection by Logging and/or Coring
  - Correlation of Potentially Productive Intervals Through Stratigraphic and Geochemical Studies
- Stimulation Techniques Techniques:
  - Hydraulic Fracturing
  - Chemical Explosive Fracturing
  - Directional Drilling
- Field Management (MERC)

JEFFREY B. SMITH

9

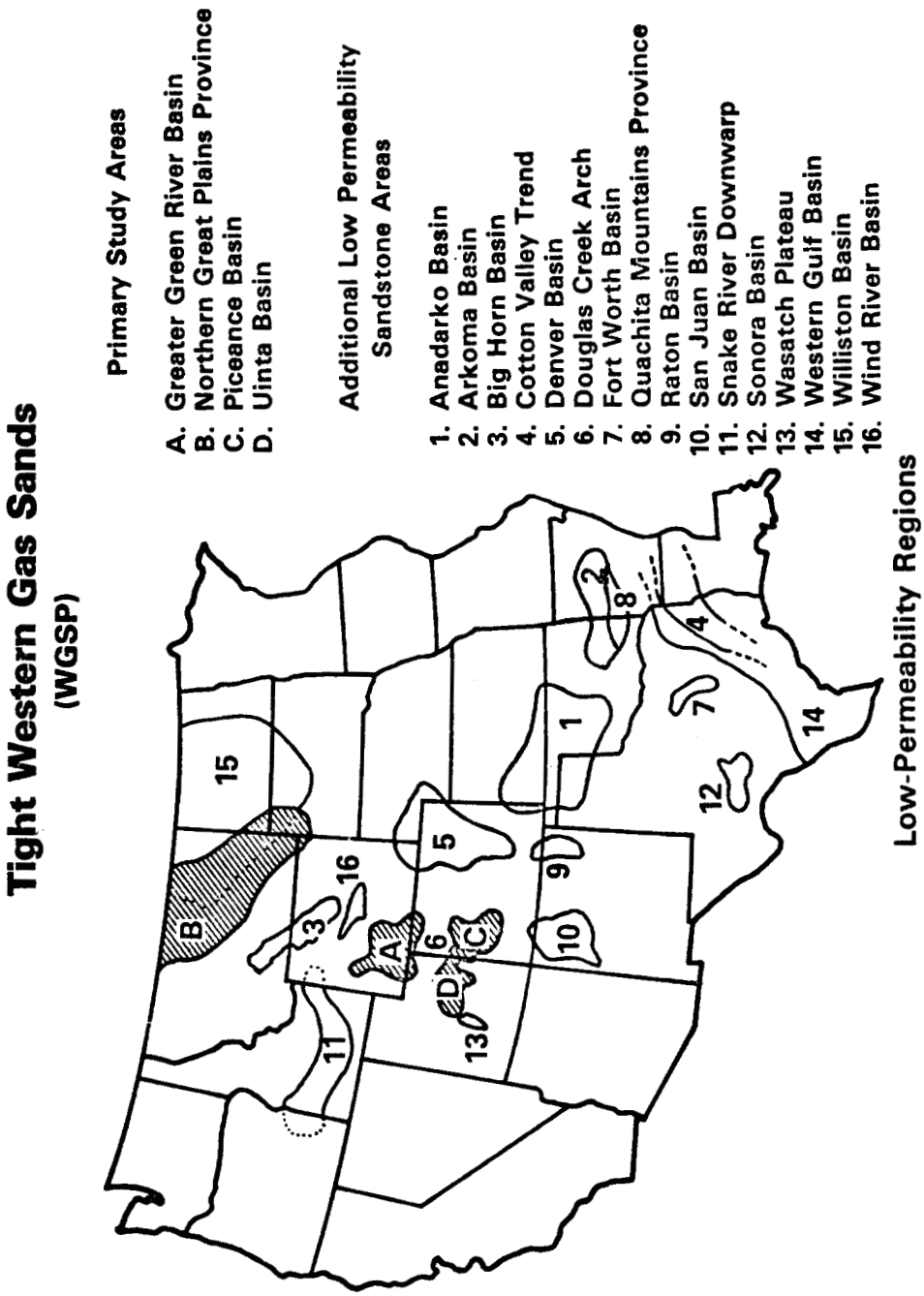
Tight Western Gas Sands
(WGSP)
Primary Study Areas
A. Greater Green River Basin
B. Northern Great Plains Province
C. Piceance Basin
D. Uinta Basin
Additional Low Permeability Sandstone Areas
1. Anadarko Basin
2. Arkoma Basin
3. Big Horn Basin
4. Cotton Valley Trend
5. Denver Basin
6. Douglas Creek Arch
7. Fort Worth Basin
8. Quachita Mountains Province
9. Raton Basin
10. San Juan Basin
11. Snake River Downwarp
12. Sonora Basin
13. Wasatch Plateau
14. Western Gulf Basin
15. Williston Basin
16. Wind River Basin
Low-Permeability Regions

PICEANCE BASIN SCHEMATIC GEOLOGIC CROSS SECTION

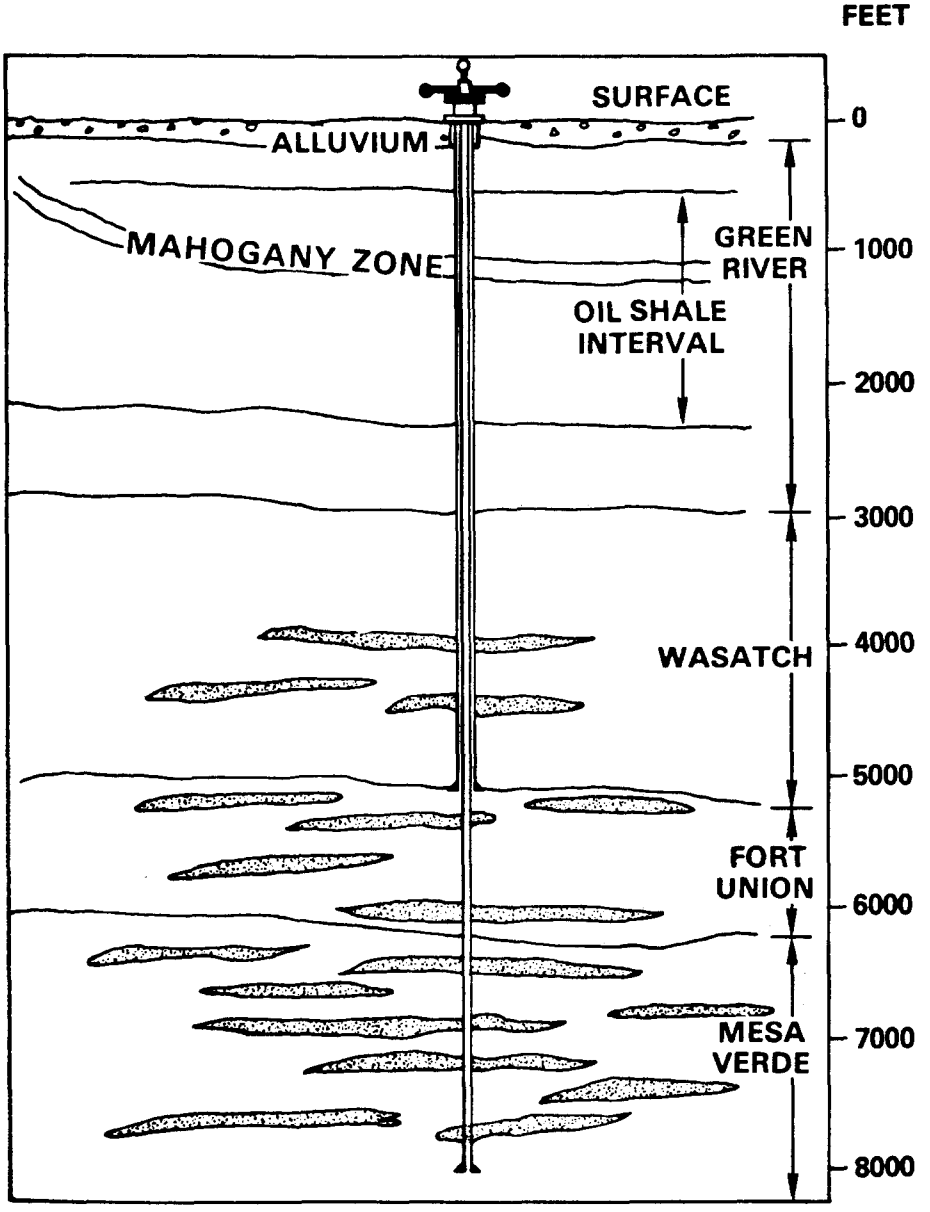

Western Gas Sands Project
(WGSP)

- Geometry and Fluid Saturations of Sand Lenses Are Unknown
- Extent, Direction, and Inclination of Hydraulically Induced Fractures Are Unknown
- Two Approaches to MHF
  - Single MHF Over Large Interval of Borehole
  - Optimum Designed MHF For Discrete Sand Intervals for With Emphasis on Control of:
    (1) Fracture Length
    (2) Fracture
- Field Management (BERC)

WGSP Resource Inventory and Characterization

- **USGS Research Activities (Interagency Agreement)**
  - Stratigraphy and Structural Geology
  - Geochemistry
  - Reservoir Engineering
  - Clay Mineralogy
  - Data Acquisition and Processing
  - Resource Appraisal
- **Special Studies To Be Contracted With Universities and Research Labs**

JEFFREY B. SMITH

13

Technology Support

Stimulation Research

- Determine Extent and Direction of Hydraulically Induced Fractures
  - Sandia Resistivity Mapping Technique
  - USGS Tiltmeter Experiments
- Sandia Mineback Program to Evaluate AHF Experiments

Resource Characterization

- Development of Downhole Logging Tools to Determine Basic Reservoir Properties
  - LLL ^{3}-D Dry-Hole Sonic Tool
  - USGS Small Diameter Borehold Gravimeter
- Subcontracts for Support (Rock Mechanics, Core Analyses, Etc...) Being Let to Private Labs and Institutions

Methane From Coal Beds

- Production Characteristics Are Similar to Shale Gas Production
- EGR Project to Assess Resource and Perfect Technologies for Methane Recovery From Unminable Coal Beds
- DOE Conservation Program to Address Utilization of Recovered Methane
- Bureau of Mines Engaged in Methane Drainage for Coal-Mine Safety
- Field Management (MERC)

JEFFREY B. SMITH

15

Methane From Unminable Coalbeds

Project Goals

1. Locate, Identify and Characterize the Unminable Coalbeds.

2. Develop Drilling and Fracturing Techniques for Economical Methane Recovery.

3. Determine the Mechanisms and Kinetics Which Control Gas Production.

4. Identify Environmental Effects Associated with Methane Recovery From Deep Deposits.

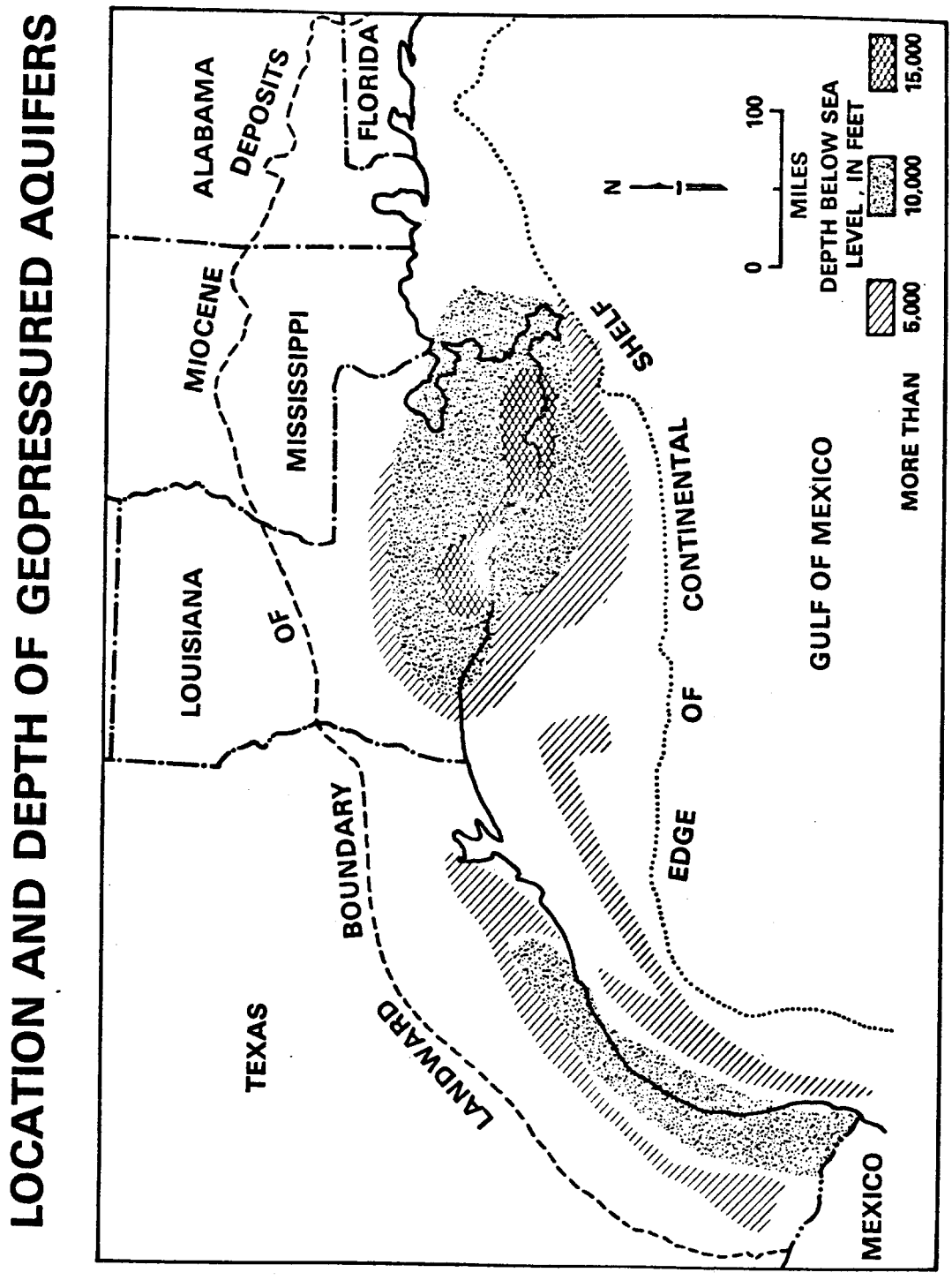
LOCATION AND DEPTH OF GEOPRESSURED AQUIFERS
ALABAMA
DEPOSITS
FLORIDA
MIOCENE
MISSISSIPPI
LOUISIANA
OF
TEXAS
BOUNDARY
LANDWARD
SHELF
CONTINENTAL
OF
EDGE
GULF OF MEXICO
MEXICO
N
0
100
MILES
DEPTH BELOW SEA LEVEL, IN FEET
5,000
10,000
15,000
MORE THAN

GEOPRESSURED AQUIFERS

- REQUIREMENTS FOR VIABLE PROJECT:
  - GEOPRESSURED RESERVOIR
  - LARGE VOLUME RESERVOIR
  - WELL FLOW RATES OF 40,000 BWPD OVER 20 YEAR PERIOD
  - METHANE CONTENT 30 SCF/BARREL OF WATER PRODUCED
  - WELL-DEFINED TARGET AQUIFER
- DOE GEOTHERMAL ENERGY PROGRAM CONDUCTING FIELD TESTS TO
  - ELECTRIC POWER GENERATION
  - GAS RECOVERY
- CURRENT ASSESSMENT OF GEOPRESSURED AQUIFERS:
  - GREATEST POTENTIAL SOURCE OF GAS
  - HIGHEST RISK GAS RESOURCE

Geopressured Aquifers
Proposed Work

- Coordinate All Work With Division of Geothermal Energy (DGE)
- Determine Magnitude and the Production Characteristics of Resource
- Determine Economic Factors Governing Gas Recovery

JEFFREY B. SMITH

19

Conclusions

Objectives

- Stimulate Commercial Development of Large Known Gas Resoures

Resources	* Potentially Recoverable Gas
Eastern Devonian Shales	10-520 Trillion SCF
Western Tight Gas Sands	50-320 Trillion SCF
Methane From Coal Beds	16-500 Trillion SCF
Geopressured Aquifers	150-2000 Trillion SCF

* MOPPS Estimates

CONCLUSIONS (CONT.)

PROGRAM STRATEGY

- PROVIDE RELIABLE DATA BASE FOR EACH RESOURCE
- IMPROVE STATE-OF-THE-ART STIMULATION AND PRODUCTION TECHNOLOGIES
- DEMONSTRATE COMMERCIAL FEASIBILITY

NEAR-TERM IMPACT

- FAST RESPONSE TIME
- LESS CAPITAL INTENSIVE
- GAS READILY AVAILABLE TO MARKET
- PROGRAM IS CONTINUING TO ACCELERATE

21

Some Preliminary Results of Regional Stratigraphic Studies of the Devonian Black Shales in the Appalachian Basin*

John B. Roen[1]
Wallace de Witt, Jr.[1]
Roy C. Kepferle[1]
Laure G. Wallace[1]
Mareta West[1]
[1]U.S. Geological Survey, Reston, Virginia

ABSTRACT

THE U.S. GEOLOGICAL SURVEY (USGS) UNDER A COOPERATIVE AGREEMENT WITH THE ENERGY RESEARCH AND DEVELOPMENT ADMINISTRATION (ERDA) IS INVESTIGATING THE REGIONAL STRATIGRAPHY OF THE DEVONIAN BLACK SHALES IN THE APPALACHIAN BASIN. IN ADDITION TO WORK BY USGS PERSONNEL, STRATIGRAPHIC DATA FOR THIS STUDY ARE BEING PROVIDED BY STATE AGENCIES AND UNIVERSITIES UNDER CONTRACT TO ERDA.

SEVERAL REGIONAL STRATIGRAPHIC CROSS SECTIONS BASED ON GAMMA RAY LOGS COMPILED BY THE USGS CONFIRM PREVIOUS SUGGESTIONS THAT THE DUNKIRK SHALE MEMBER OF THE PERRYSBURG FORMATION OF NEW YORK IS CORRELATIVE WITH THE LOWER PART OF THE HURON MEMBER OF THE OHIO SHALE OF OHIO AND KENTUCKY. THE CORRELATION IS SUBSTANTIATED BY THE REGIONAL DISTRIBUTION OF A MARKER BED JUST BELOW THE DUNKIRK-HURON BLACK SHALE. THIS BED, THE PIPE CREEK SHALE MEMBER OF THE JAVA FORMATION OF NEW YORK HAS BEEN TRACED FROM NEW YORK THROUGH WESTERN PENNSYLVANIA, EASTERN OHIO, AND EASTERN OHIO, AND EASTERN KENTUCKY INTO SOUTHWESTERN VIRGINIA. IN ADDITION, THE REGIONAL DISTRIBUTION OF THE CLEVELAND SHALE MEMBER OF THE OHIO SHALE IN OHIO, KENTUCKY AND WEST VIRGINIA HAS BEEN VERIFIED.

*Paper not available at time of publication

UPDATE CONCERNING THE THREE-DIMENSIONAL SEISMIC INVESTIGATIONS IN THE COTTAGEVILLE FIELD

by

Edward R. Tegland, Geophysical Services, Inc.

ABSTRACT

In June of 1977 Geophysical Service Inc. undertook an ERDA sponsored three-dimensional seismic program in the Cottageville field in conjunction with Consolidated Gas Supply Corporation.

The program was aimed at defining the seismic characteristics of the Devonian shale section and accurately mapping deep seated faults which might control fracturing and production in the shale.

The complete results available as of September 1, 1977, will be presented.

INTRODUCTION

During late June and early July 1977 a seismic program (figure 1) was undertaken in the Cottageville field area of Mason and Jackson counties, West Virginia. The program consisted of three elements: (1) an experimental program, (2) conventional 12-fold reflection program, and (3) a three-dimensional reflection survey. One objective of the program was to determine the relationship, if any, between the occurrence of significant fracture zones in the Devonian shale section and a deep normal fault system. In the developed portion of the field Martin and Nuckols (1976) indicate an interesting trend of wells which had high (1000 mcf+) open flow rates. Their paper also establishes a correlation between this trend and fracture trends measured in work by ERDA. To establish the fault pattern through the field, a three-dimensional approach was employed.

Other objectives of the program were to characterize the total geologic section in the area in terms of seismic response and to track any fault trends found in the area outward to the southwest. The conventional seismic program consisting of four lines tied into the 3D program was chosen for the latter task.

The seismic characterization of the geologic section was accomplished by means of an experimental expanded spread collected at well 11940 on the county line in the southern portion of the 3D area and two refraction studies, one near well 11940 and one along a straight segment of the PRIME conventional line.

EXPERIMENTAL FIELD METHODS

The expanded spread collection technique is diagramed in figure 2. In practice the seismometers were positioned along a road which ran past well 11940 (figure 1), and some slight bending of the seismometer line was required. The vibrators were required to stay on the road, and some horizontal offset did take place.

Several sweep ranges were collected using the same layout to provide a means of choosing the sweep range for this project and a benchmark for any future seismic work in the area. Since the crew was equipped with a CFS* I field computer system, playbacks of the field data following diversity vertical stack and correlation were made as the data was collected. Field analysis of this data indicated that the 60-20 sweep was providing the best overall result, although some events looked better at the higher frequencies.

The location of this experimental work was chosen because well 11940 had a considerable amount of geologic data available in the zone of interest. To interpret the data in this form one simply picks each seismic event and tabulates time (T) against source-to-detector distance (X). A straight line fit is then made to the relationship between X^2 and T^2. The slope of this line is $1/V^2$, and the intercept is T_o^2. This procedure follows from the normal moveout expression:

$$T_X^2 = \frac{X^2}{V^2} + T_o^2 \qquad \text{(Eq. 1)}$$

where

T_X = reflection arrival time and a trace at distance X from source

X = distance from source to receiver

V = velocity (RMS) through overburden medium from surface to reflector

T_o = travel time of a trace having zero source-to-detector distance.

The knowns, of course, are T_X and X. A simple hand calculator program was developed for the TI-59 calculator which allowed direct entry of the knowns and automatic calculation of the unknowns. Near-surface corrections were made to the expanded spread data to reduce it to a datum equivalent to the average elevation of the spread. A correctional velocity of 9000 fps (2743 mps) was used in equation 2.

$$TC = \frac{DE - DS}{VC} \qquad \text{(Eq. 2)}$$

where

TC = time correction

DE = datum elevation

DS = source or receiver elevation.

At the time of this writing, final interpretation of this data was not complete. However, it will be reviewed in the oral presentation.

*Trademark of Texas Instruments Incorporated.

Two refraction studies were collected using the layout shown in figure 3. These studies were also collected using various sweeps. Figures 4A, 4B and 5 are results of study No. 1 with two sweeps and study No. 2 with one sweep. Vibrator locations could not be obtained where originally planned, hence the variation in offset patterns. It is interesting to note that the event with an apparent velocity of 5250 fps (1600 mps) is attenuated at the higher sweep frequency. The lower velocity noise at 1250 fps (381 mps) appears to propagate at both frequencies. More detailed evaluation of these studies will be included in the oral presentation also.

REFLECTION FIELD METHODS

The reflection data was collected with a 60-20 Hz sweep of 10-second duration using a vertical redundancy of 15 sweeps from two vibrators or 10 sweeps when three units were working simultaneously. Diversity vertical stacking of individual sweeps and correlation were carried out in the field using a CFS I system. The geophone array consisted of 24 geophones separated by 5 feet (1.52 meters). The conventional common depth point reflection lines were collected using the surface layout shown in figure 6. This asymmetric split provided good near-offset coverage coupled with sufficiently long offsets to provide good velocity control out to approximately 8000 feet (2438 meters). Four lines of this type were collected which have been designated as "PRIME," I, II, and III (figure 1). The intent of these lines was to provide control for tracking structure from the field area outward to the south and west.

The field area itself was covered by the 3D Seisloop* approach. Nine closed loops identified as A through J were established using existing roads and trails within the field (shaded area of figure 1). The final survey locations of the loops are shown in figure 7. The field procedure consisted of laying seismometer groups on alternate stations around each loop and occupying each station with the source. The result causes an in-fill of subsurface coverage throughout the loop. Subsequently, data are gathered into a series of parallel equally spaced output lines using techniques discussed by Tegland (1974). The output line and trace spacing are designed so that no greater than one-fourth wavelength exists between data points.

The high density of control points allows very accurate tracing of faults and other features through the area. The density also allows implementation of three-dimensional migration to provide true vertical image sections (Schneider 1977).

SEISMIC PROCESSING

The seismic processing sequence involved use of the common depth point gathering scheme just mentioned for both the conventional and 3D data. The conventional lines yielded a single "stack track" for each line with 110-foot (33.5-meter) trace spacing.

All data were gain recovered and deconvolved prior to any other processing. Datum corrections were made as per equation 2 using a datum elevation of 800 feet (243.8 meters) and a correctional velocity of 9000 fps (2743 mps). The datum and correctional velocity were chosen to be consistent with older dynamite data in the area which will possibly be used to supplement the new work.

Automated residual near-surface corrections were employed with good success on all data. Velocity analysis followed residual near-surface correction. An example of velocity data extracted from conventional Line 2 is shown in figure 9. In this analytical approach trial functions V1 and V11 are chosen such that there is a 6-db change in stack response from one function to another. The events are monitored by power computations made on the stacked traces after a rotating dip search is employed. Besides calculating and plotting stacking velocity,

---

*Trademark of Geophysical Service Inc.

the process plots dip and amplitude estimates. This and similar techniques will be employed throughout the 3D area also, to produce a "velocity field" for stacking the data. This velocity field will be upgraded where possible and tied to the available subsurface in order to depth convert and perform 3D migration.

Final display of the conventional data will be simple conventional profiles. The 3D area will be displayed in two orientations as vertical sections and in horizontal sections called SEISCROPS* (Giles, Bone, Tegland, 1976). Figure 9 is an example of data from Line 1 of the conventional program. The data quality is very good as can be readily seen. Events within the Devonian shale section are expected to correlate to the "Brown Shale Zones" discussed by several authors in MERC/SP-76/2.

CONCLUSIONS AND COMMENTS

Since this is a progress report, no specific conclusions have yet been reached concerning the objectives of the program. However, one can conclude at this point that excellent data quality may be obtained in this area with the field collection and processing techniques used in this project. More information and conclusions should be available at the time of the oral presentation.

The author wishes to express appreciation to Mr. Jim Wilson and others with Consolidated Gas Supply Corporation for their extensive help in conducting this project.

BIBLIOGRAPHY

MARTIN and NUCKOLS, 1976, "Geology and Gas Occurrence in the Devonian Shales: Northern West Virginia," Devonian Shale Production and Potential, MERC/SP-76/2.

TEGLAND, 1974, "CDP Techniques and Crooked Traverses," 44th International Meeting of the SEG, Dallas, Texas, 1974.

TEGLAND, BONE, GILES, 1976, " SEISCROP Maps for Direct Mapping of 3D Seismic Data," Silver Anniversary Meeting EAEG, The Hague, The Netherlands, June 1976.

*Trademark of Geophysical Service Inc.

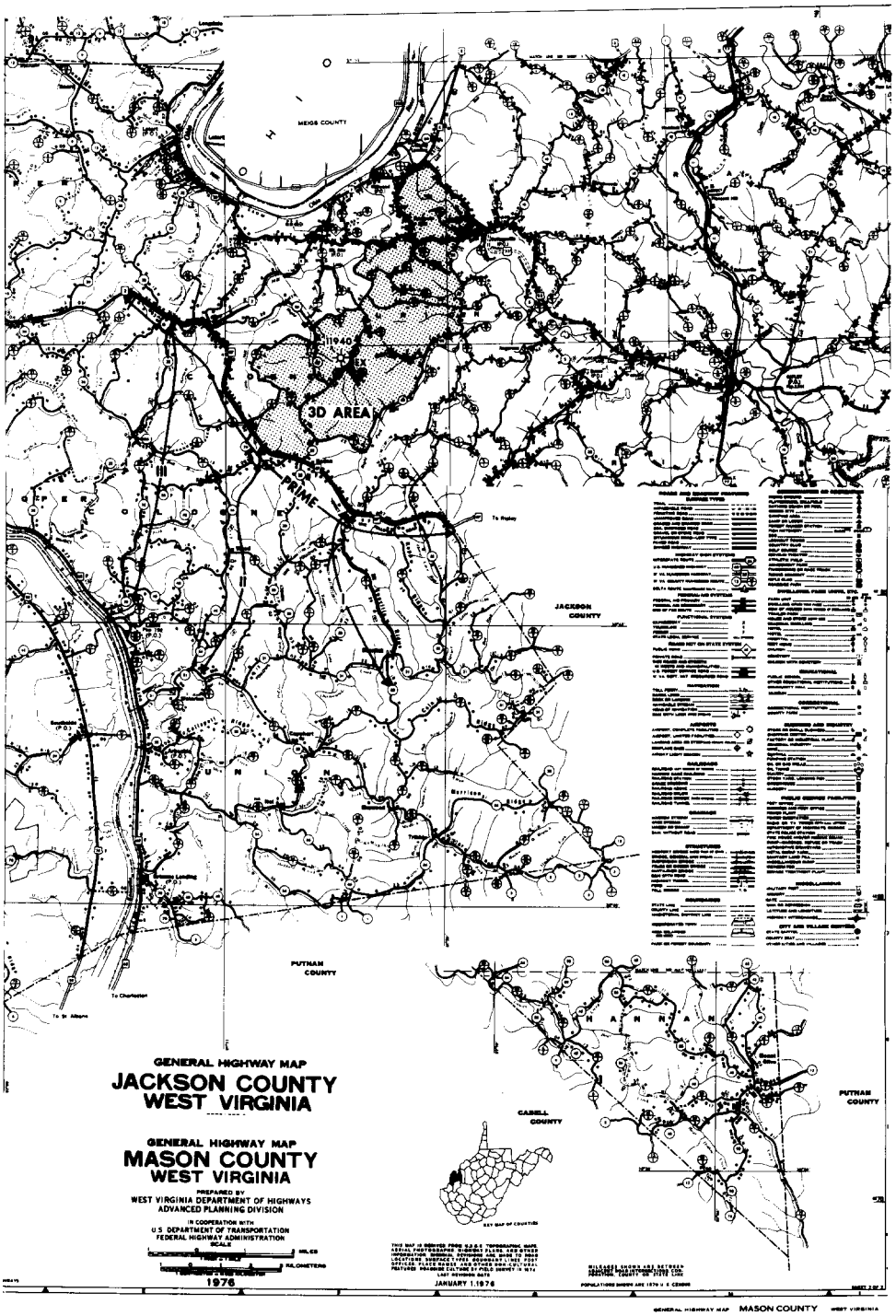
MEIGS COUNTY
3D AREA
PRIME
JACKSON COUNTY
PUTNAM COUNTY
CABELL COUNTY
GENERAL HIGHWAY MAP
JACKSON COUNTY
WEST VIRGINIA
GENERAL HIGHWAY MAP
MASON COUNTY
WEST VIRGINIA
PREPARED BY
WEST VIRGINIA DEPARTMENT OF HIGHWAYS
ADVANCED PLANNING DIVISION
IN COOPERATION WITH
U.S. DEPARTMENT OF TRANSPORTATION
FEDERAL HIGHWAY ADMINISTRATION
1976
JANUARY 1, 1976
GENERAL HIGHWAY MAP MASON COUNTY WEST VIRGINIA

FIGURE 1

SHOOTING PLAN
FOR EXPANDED SPREAD ANALYSIS

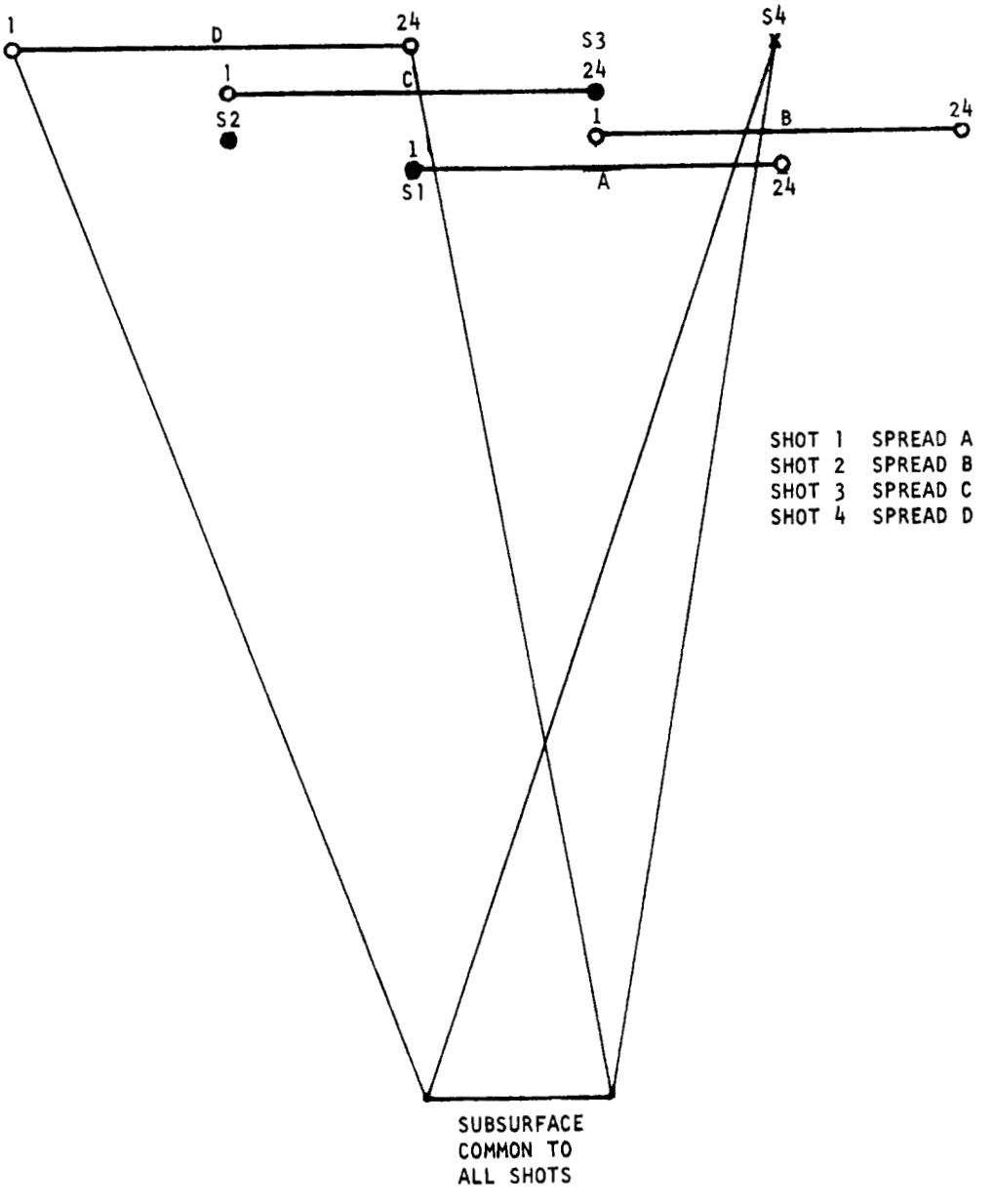

FIGURE 2

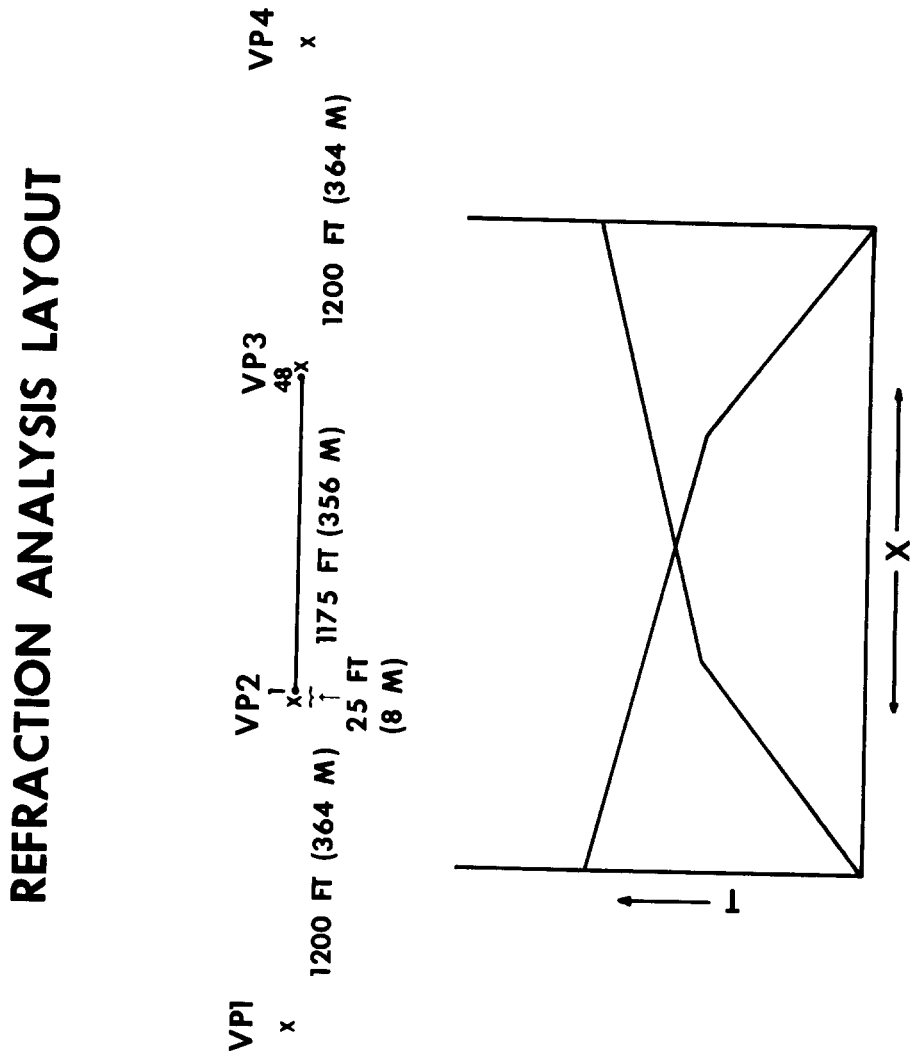
REFRACTION ANALYSIS LAYOUT
VP1
VP2
VP3
VP4
48
1200 FT (364 M)
1175 FT (356 M)
25 FT
(8 M)
1200 FT (364 M)
T
X

FIGURE 3

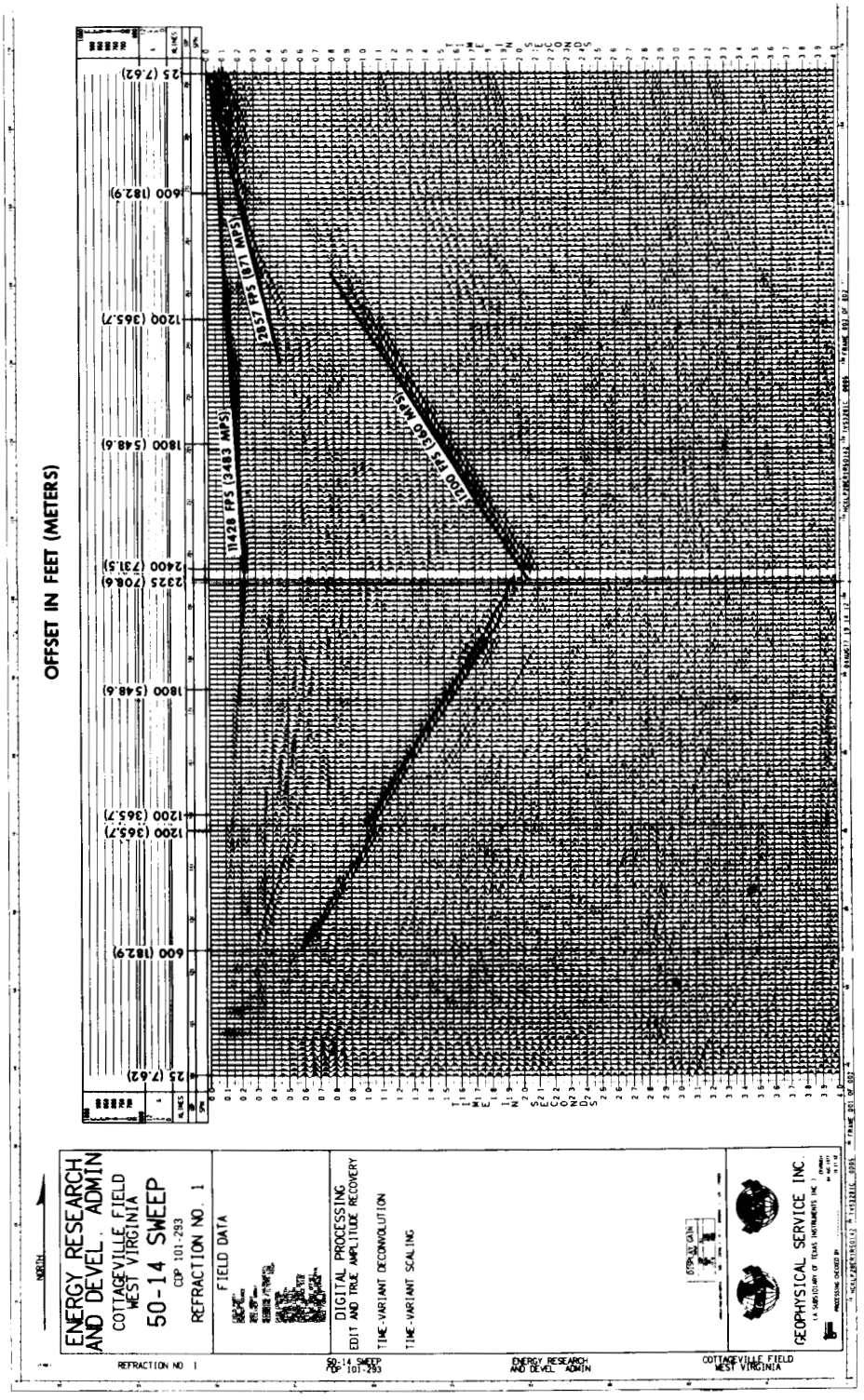
OFFSET IN FEET (METERS)
25 (7.62)
600 (182.9)
1200 (365.7)
1800 (548.6)
2400 (731.5)
2225 (708.6)
11428 FPS (3483 MPS)
12857 FPS (3871 MPS)
ENERGY RESEARCH AND DEVEL. ADMIN
COTTAGEVILLE FIELD
WEST VIRGINIA
50-14 SWEEP
CDP 101-293
REFRACTION NO. 1
FIELD DATA
DIGITAL PROCESSING
EDIT AND TRUE AMPLITUDE RECOVERY
TIME-VARIANT DECONVOLUTION
TIME-VARIANT SCALING
GEOPHYSICAL SERVICE INC.

FIGURE 4A

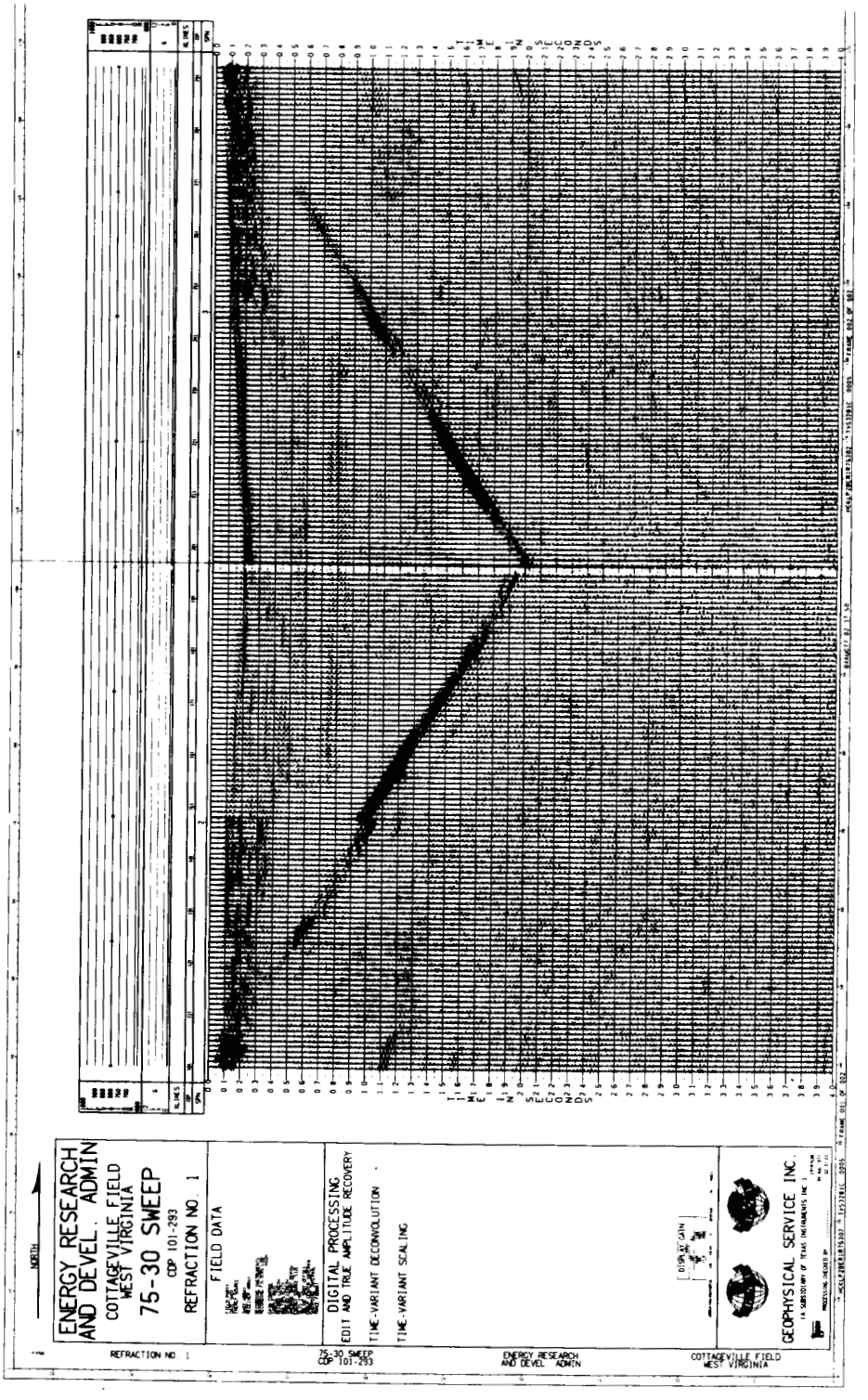
NORTH
ENERGY RESEARCH AND DEVEL. ADMIN
COTTAGEVILLE FIELD WEST VIRGINIA
75-30 SWEEP
CDP 101-293
REFRACTION NO. 1
FIELD DATA
DIGITAL PROCESSING
EDIT AND TRUE AMPLITUDE RECOVERY
TIME-VARIANT DECONVOLUTION
TIME-VARIANT SCALING
DISPLAY DATA
GEOPHYSICAL SERVICE INC.
TIME IN MILLISECONDS
REFRACTION NO. 1
75-30 SWEEP CDP 101-293
ENERGY RESEARCH AND DEVEL. ADMIN
COTTAGEVILLE FIELD WEST VIRGINIA

FIGURE 4B

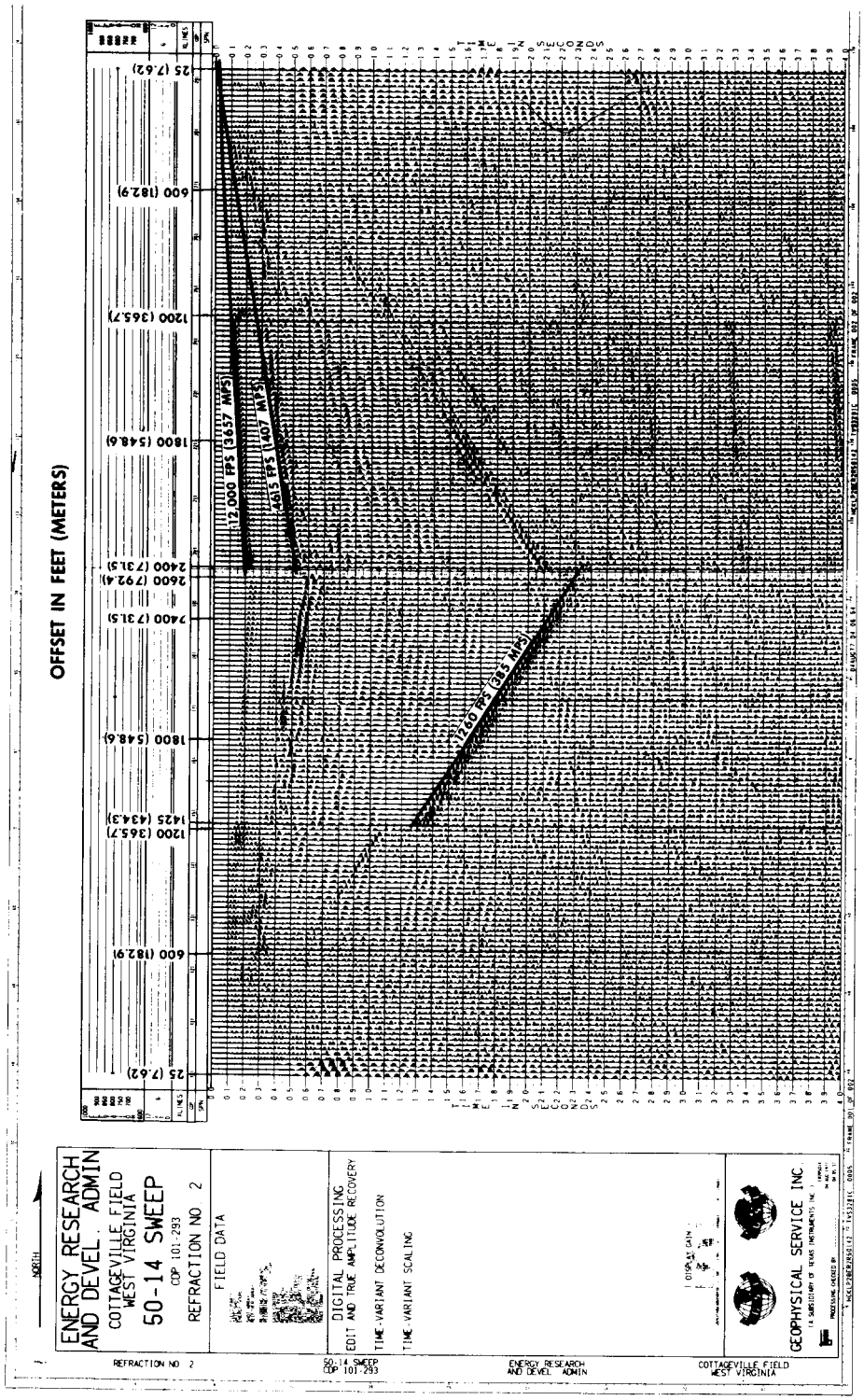
OFFSET IN FEET (METERS)
25 (7.62)
600 (182.9)
1200 (365.7)
1800 (548.6)
2400 (731.5)
2600 (792.4)
2400 (731.5)
1800 (548.6)
1425 (434.3)
1200 (365.7)
600 (182.9)
25 (7.62)
12,000 FPS (3657 MPS)
4615 FPS (1407 MPS)
1260 FPS (385 MPS)
NORTH
ENERGY RESEARCH AND DEVEL. ADMIN
COTTAGEVILLE FIELD WEST VIRGINIA
50-14 SWEEP
CDP 101-293
REFRACTION NO 2
FIELD DATA
DIGITAL PROCESSING
EDIT AND TRUE AMPLITUDE RECOVERY
TIME-VARIANT DECONVOLUTION
TIME-VARIANT SCALING
DISPLAY GAIN
GEOPHYSICAL SERVICE INC.
REFRACTION NO 2
50-14 SWEEP CDP 101-293
ENERGY RESEARCH AND DEVEL. ADMIN
COTTAGEVILLE FIELD WEST VIRGINIA

FIGURE 5

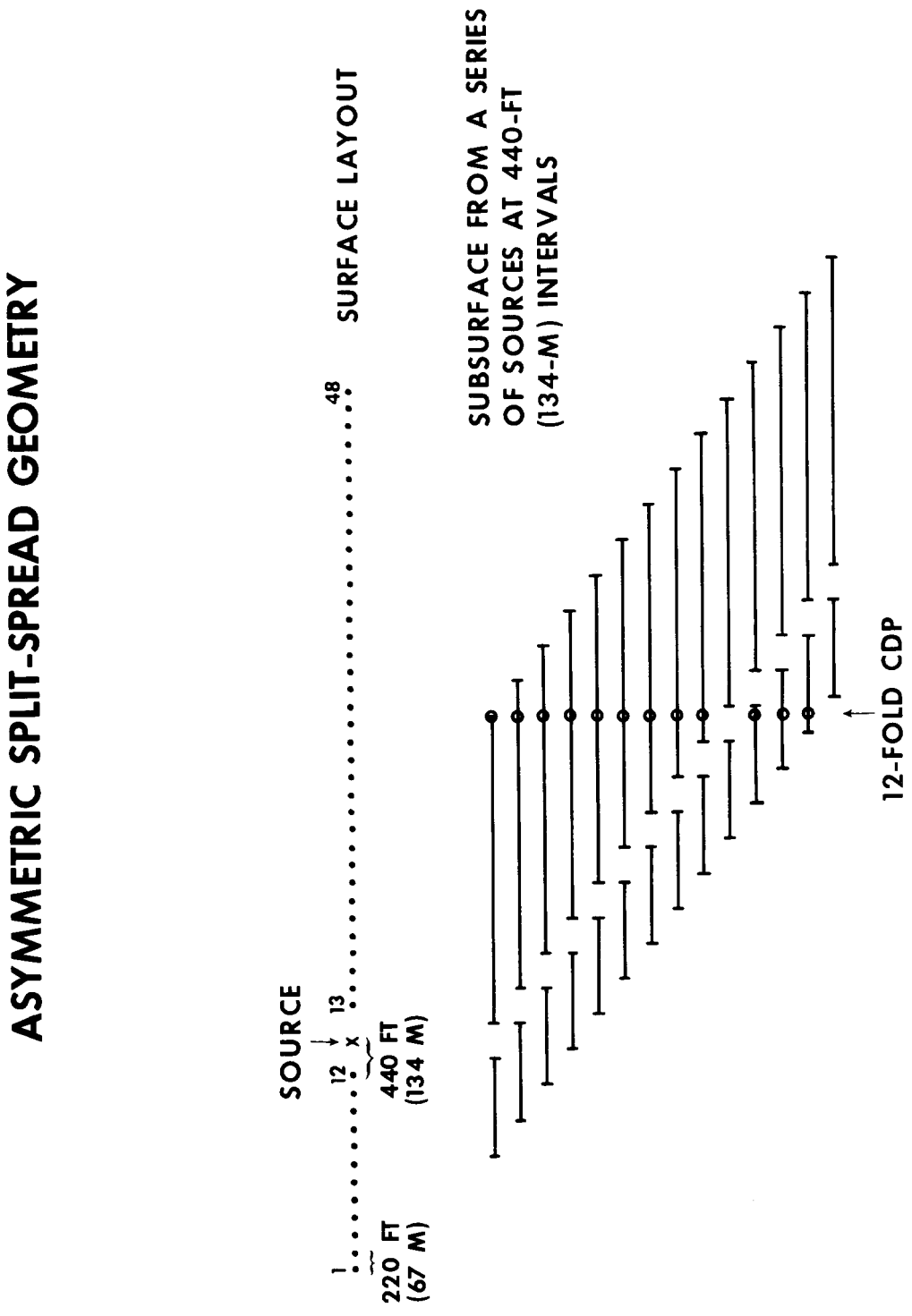
ASYMMETRIC SPLIT-SPREAD GEOMETRY
SURFACE LAYOUT
SOURCE
1
12
13
48
220 FT
(67 M)
440 FT
(134 M)
SUBSURFACE FROM A SERIES
OF SOURCES AT 440-FT
(134-M) INTERVALS
12-FOLD CDP

FIGURE 6

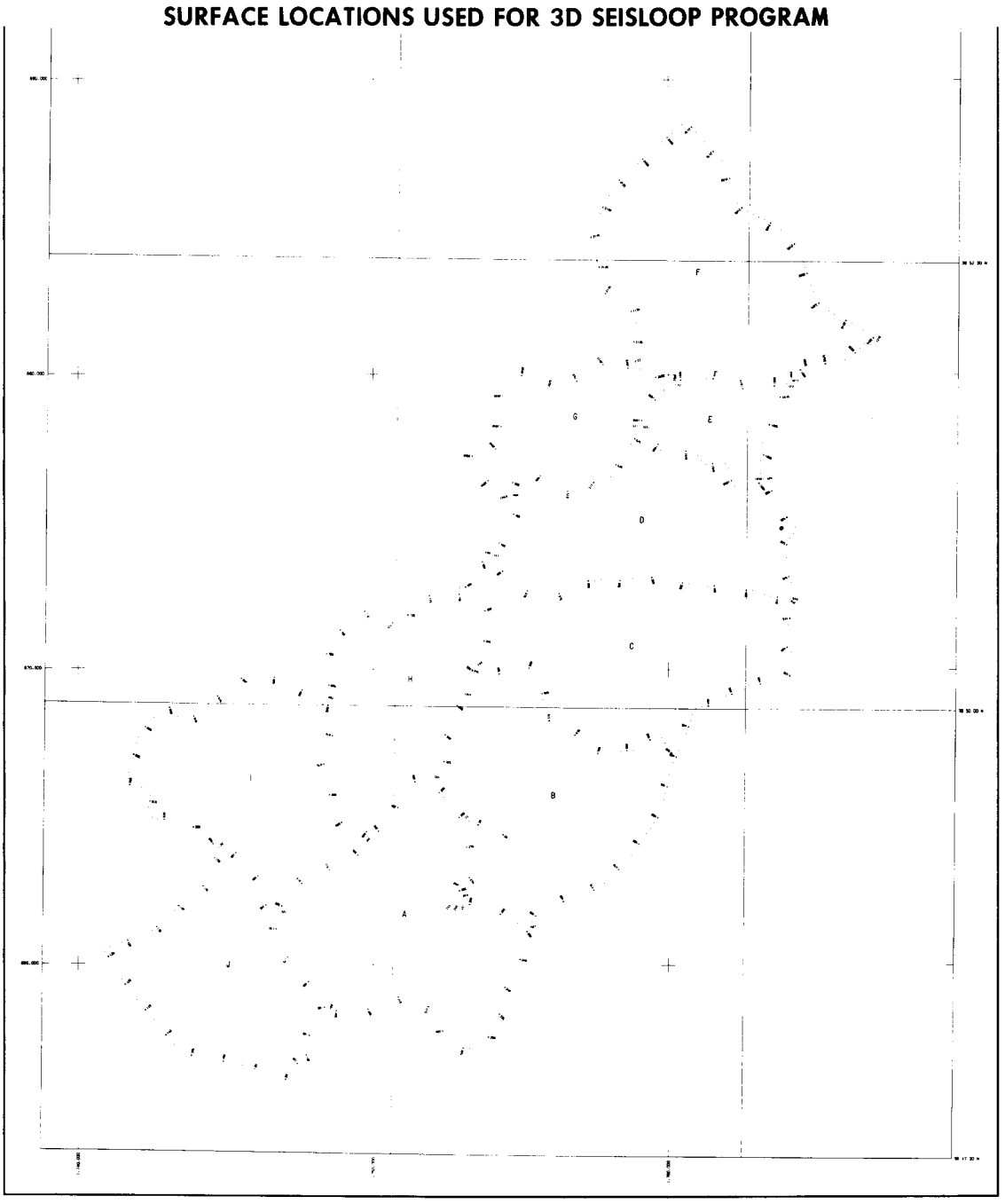
SURFACE LOCATIONS USED FOR 3D SEISLOOP PROGRAM
A
B
C
D
E
F
G
H
I
J

FIGURE 7

SAMPLE VELOCITY ANALYSIS

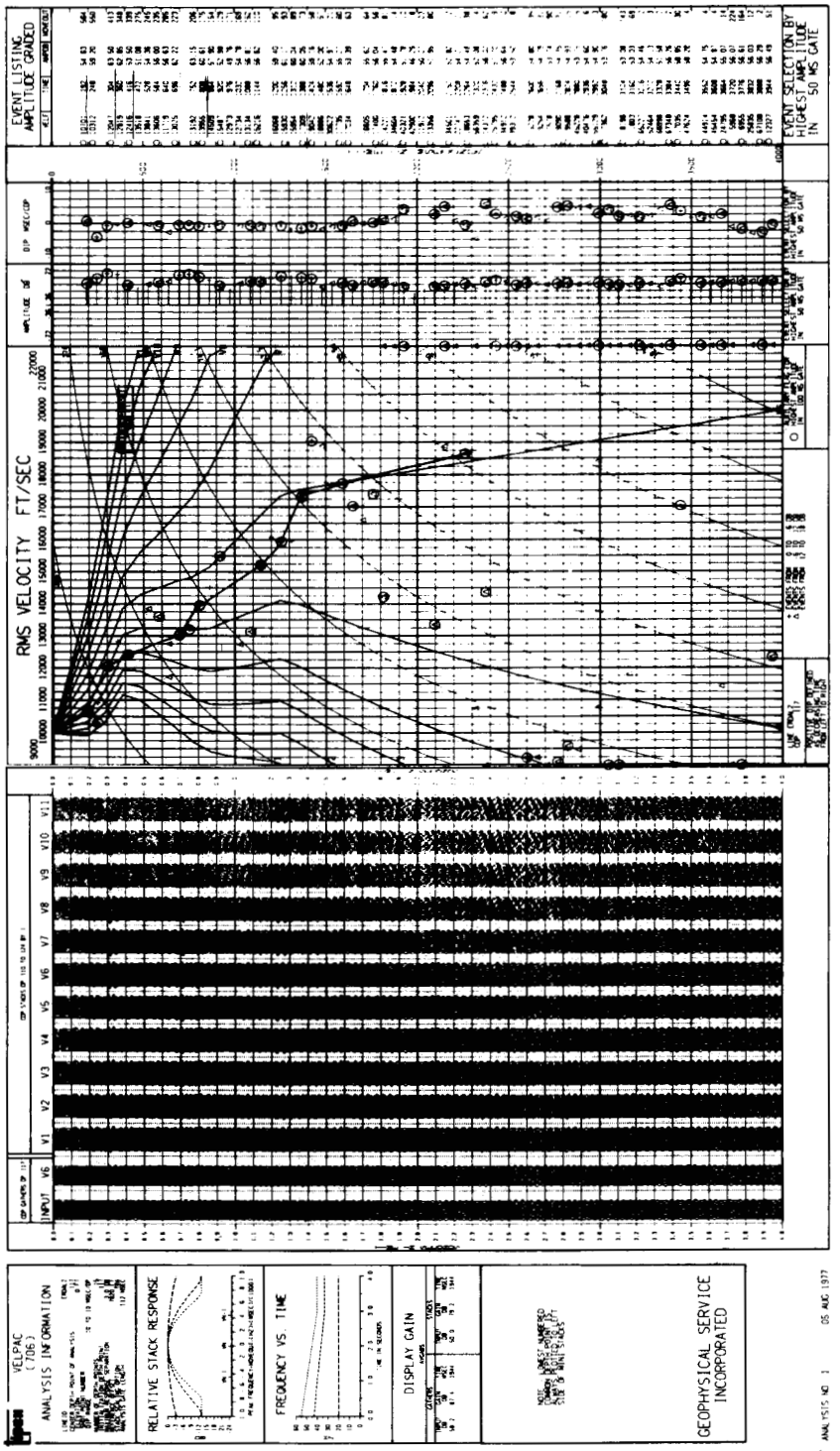

FIGURE 8

CONVENTIONAL VIBROSEIS* DATA
EXAMPLE 1

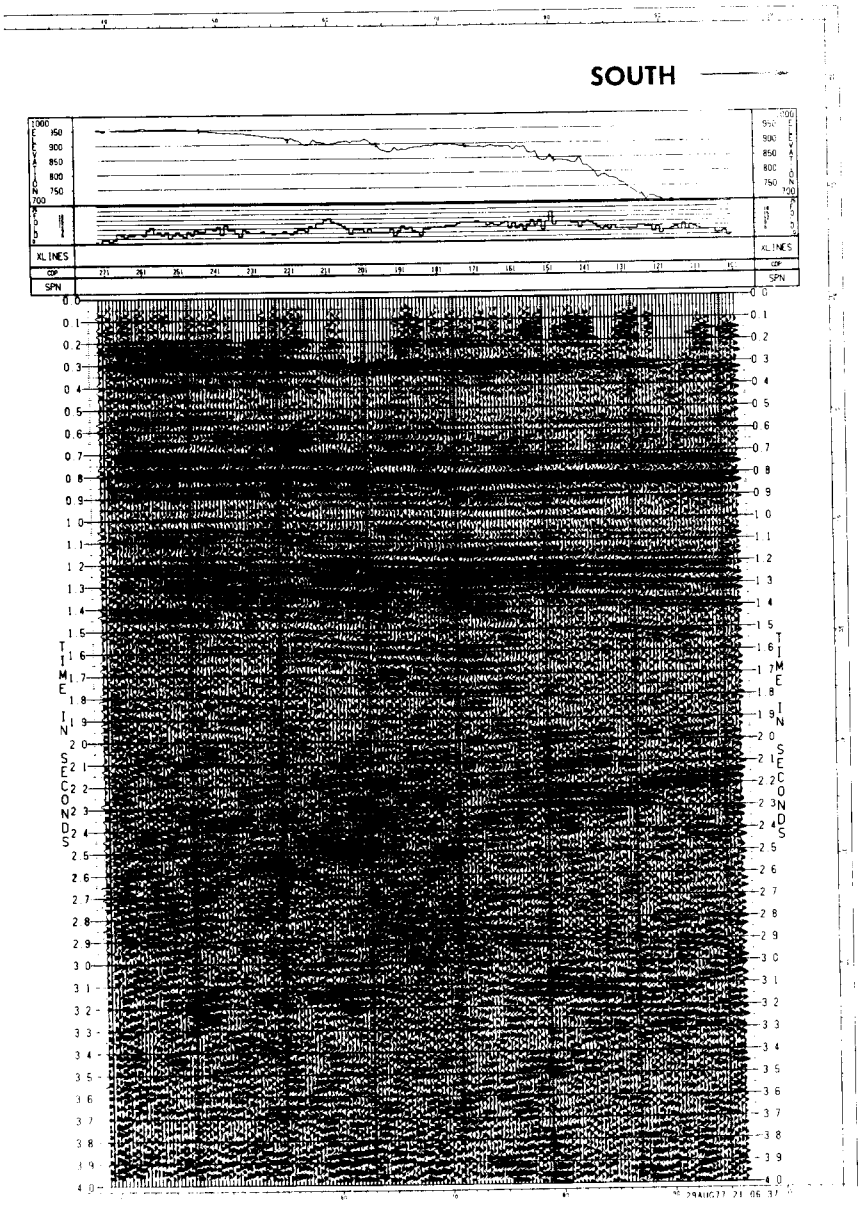

*TRADEMARK OF CONTINENTAL OIL COMPANY

FIGURE 9

IN SITU EXAMINATION OF HYDRAULIC FRACTURES*

by

L. D. Tyler, W. C. Vollendorf, and D. A. Northrop
Sandia Laboratories
Albuquerque, New Mexico 87115

ABSTRACT

Hydraulic fracture experiments have been performed in Rainier Mesa at ERDA's Nevada Test Site as part of a nuclear containment study. An expanded program to understand hydraulic fractures as part of ERDA's Enhanced Gas Recovery Program is underway. Three fracture experiments conducted to date and plans for this mineback test project will be discussed.

The fracture experiments were performed in a 4-in diameter uncased hole at a nominal depth of 1400 ft in a uniform ash-fall tuff formation. Two experiments were conducted in one hole with different colored grout. The results showed the strong influence of in situ stress on fracture direction and orientation. The third experiment used a water gel frac fluid which was designed to place 20-40 sand, injected in three stages with different concentration and color, uniformly in the fracture. The resulting fracture system was very complex. The effects of faults and bedding planes on blocking fracture growth and changing fracture orientation were pronounced. Data collection and analysis have not been completed, but valuable insight into in situ fracture behavior has been obtained.

Further experiments are planned as part of this project to understand hydraulic fracturing. Direct fracture observation by mineback and correlation with geologic and material properties, fluid behavior, and fracture parameters will form a bridge between modeling and laboratory studies and empirical field production results.

INTRODUCTION

Hydraulic, explosive, and nuclear fracturing stimulation techniques have been applied to low permeability natural gas reservoirs with varying, but generally noneconomic, results. Massive hydraulic fractureing (MHF) as being practiced is based on extensive, "conventional" fracturing experience, laboratory experimentation, and empirical design models; the extrapolation to the massive scale has not been generally successful. Industry has stated the need to perform experiments in an environment which allows for direct fracture examination and evaluation. ERDA's Nevada Test Site provides this opportunity. An existing tunnel complex and support facilities of the Site have been used for the direct examination of hydraulic fractures. These mineback experiments form the basis of a new project aimed at the understanding of complex fracturing processes

* This work was supported by the United States Energy Research and Development Administration, ERDA, Under Contract No. AT(29-1)789.

This paper is divided into two parts. The first part, In Situ Mineback Experimental Results, presents the results of the mineback hydraulic fracturing experiment performed at the Nevada Test Site. The second part, Mineback Test Project, outlines the role of Sandia's project in the gas stimulation work done by industry.

IN SITU MINEBACK EXPERIMENTAL RESULTS

Since 1974 Sandia Laboratories has had an active research program in hydraulic fracturing. Our initial motivation for the research came from the underground nuclear test program, where our concern was how a leak might occur due to hydrofracing by a condensible fluid. The objectives of the fracturing program were to establish small-scale hydraulic fracture experiments as an in situ stress tool and study the behavior of hydraulically formed cracks in an in situ environment. This work was done in the G Tunnel Complex of Rainer Mesa at ERDA's Nevada Test Site. All the experiments were conducted adjacent to the tunnel so that the fracture data could be collected during a mining operation. The first objective related to in situ stress measurements has been met and hydraulic fracturing is routinely used to measure in situ stresses in the tunnel with a low volume, high pressure pumping system. The aims of the second objective have been expanded to include requirements for hydraulic fracturing research to support ERDA's Enhanced Gas Recovery Program.

Three hydraulic fracture experiments are described below. All of the experiments were conducted in 4-in diameter uncased holes at a nominal depth of 1400 ft. Two experiments were conducted in Hole U12g10.3 using colored grouts as a fracture fluid. The third experiment was done in Hole U12g10.5 using a water based gel as a fracture fluid.

Hole U12g10.3. Two hydraulic fracture experiments were conducted in this hole at different depths. The bottom fracture used a red grout fracture fluid at a bottom hole depth of 1395 feet. After the first experiment was accomplished, a grout plug was poured and the second experiment was done with a yellow grout at a depth of 1365 feet. The fracture interval in the hole for both experiments was 10 feet with a bridge plug set at the top of the interval. Formation breakdown was done by initially injecting 200 gallons of water. This was followed by 272 gallons of grout with water to flush the system. The total volume injected was 700 gallons. The average treatment rate was 3.2 barrels per minute. Flow rate and surface injection pressure were only measured.

The formation rock for these experiments was a uniform ash-fall tuff which has the properties listed in Table I. The mineback investigation showed that both fractures were almost vertical with a dip that varied between 83° and 87° NW. The fractures were also planar in that the bearing for the yellow fracture was N 53° E for 20 feet of recovery and the red fracture bearing varied from N 47°E to N 53° E over a distance of 50 feet. No lateral and vertical extents of the fractures have been defined as yet, but a coring program is underway to complete the fracture geometry definition. The dip and bearing directions of the two fractures correspond to the minimum horizontal principal stress direction. The calculated down hole shut-in pressures compared well with those measured by small hydraulic

fracture in situ stress tests done in the tunnel complex.[1] The tunnel tests gave 894 psi for the minimum principal stress with a value of 1065 psi for the Hole 12g10.3 fractures. The dip and bearings found for the small test agreed well with the two grouted fractures.

Hole U12g10.5. A single fracture experiment was done in this hole. The purpose of this experiment was to try to gain some information on the fracture fluid motion during the fracture creation and to get some data on fracture width. The experiment was done in the ash-fall tuff rock described in Table I. The fracture design called for a water based gel (PWG/FR2GL) with colored 20-40 sand of different concentrations to be phased into the fracture schedule at an injection rate of 4 barrels/minute. The design schedule is given in Table II. Flow rate and surface pressures were measured. An annulus pressure was measured to help determine the down hole values.

The mineback evaluation of the experiment has not been completed, but some very interesting results have been obtained. The hole drilled for this experiment penetrated a region of the formation between two faults which strongly influenced the fracture growth and orientation. The faults had small displacements of the order of an inch and contained a rubble zone which was about an inch wide. The formation also had a number of thin bedding planes in the experimental area. The effect of these features on fracture geometry are presented below.

The plan view shown in Figure 1 shows the outline of the tunnel excavated for fracture examination. The enclosed area shown at the bottom of the figure is an excavated bench. The experiment hole is shown at the 55 foot station. The first view of the fracture system is a profile along the line A-A. The A-A view, Figure 2, shows the entire mined fracture system projected on the A-A line. Two fractures were formed. The primary fracture was nearly vertical with a dip varying between 85° NE to 85° NW and essentially lies in the A-A plane except for the tail from CS20 to CS40 which curved out of the plane. The faults and bedding planes are as observed in the A-A plane. The secondary fracture system shown was projected on the A-A plane from the tunnel bench noted in Figure 1. The experiment hole is shown as VDH #5 with the fracture initiation interval being the thin line below the wide line. Two important results about the primary fracture can be seen in this profile. First, the fault to the left of the hole blocked the lateral growth to the north and, secondly, a bedding plane a few feet above the initiation level served as a barrier to vertical growth. The effect of the fault to the right of the hole is shown in later views. Basically, the path of least resistance was downward.

A vertical cross-section, plane D-D, is shown in Figure 3. The primary fracture system is shown passing through the hole and stopping just below the upper bedding plane. The secondary fracture is shown to the left. This fracture has a dip which varies from 10° NE to 80° NE. The marked changes in fracture dip are due to very thin bedding planes. The dashed line at the intersection of the two fractures denotes the absence of sand. Referring to Figure 2, the next view of the fracture system is a plan view of plane E-E. The E-E plane is shown in Figure 4. The fault to the left has retarded the lateral growth, as mentioned earlier, to the north and a new weak fault is evident between the other two faults. The fracture is not connected

across the fault to the right in this plane. On the right side of this fault, the fracture begins to change bearing by approximately 40° to the east. Another observation is that the secondary fracture system does not extend to this depth.

From the observations of the placement of the sand and the shape of the fracture system, it appears that the fracture initiated and grew in the downward direction because of barriers due to the fault to the north and the parting plane above. The fault to the south did not stop growth but there is evidence that a marked change of in situ stress exists across the fault because of the direction change of the fracture. Continued exploration of this fracture is planned which includes in situ stress determinations across the faults and bedding planes in addition to further fracture examination.

The above results from the mineback investigation of the hydraulic fracture experiments have demonstrated how different geological features affect fracture growth. In a uniform media, the fractures are vertical with a consistent dip and bearing. When faults or bedding planes are present, the fracture growth may be retarded or reoriented. Additional in situ stress measurements and material property data are being obtained to further quantify the observed fracture behavior in these experiments.

MINEBACK TEST PROJECT

The mineback experiments just presented have been performed as part of a nuclear containment program; their commonality and application to enhanced gas recovery is obvious. An expanded scope of activities is planned for a recently initiated Sandia Laboratories project which is part of ERDA's Enhanced Gas Recovery Program and which is aimed at the understanding of complex fracturing processes. This mineback test project is intended to form a bridge between the design modeling and laboratory studies and the empirical field production results which are the basis for today's fracturing technology.

One view of the role of mineback testing is given in Figure 5. A fracture stimulation as undertaken today is indicated by the upper half of the figure. Industry and service company experience, plus inputs from well logs and other geological information, results in a frac design, the frac job in the field, and a final evaluation. This evaluation is based primarily upon gas production in combination with the operational parameters (fluid type, pumping rate, proppant, etc.) of the job. The evaluation is empirical in nature with the experience contributing to the design of further jobs. Mineback testing offers more information which can contribute directly to production design and practice. As seen in the figure, Sandia would serve as a catalyst in the planning,conduct, and evaluation of a mineback fracture experiment. Evaluation here is accomplished by direct observation of the produced fracture and correlations can be made with the material property, fluid behavior, physical description, and operational parameters as listed. Note that the evaluation feeds back into the same industry-service company experience and knowledge base used in production.

The Mineback Test Project's objective is to understand, and thus improve, fracturing processes for enhanced natural gas production from low

permeability reservoirs. Tasks contributing to this objective are: (1) mineback testing for direct fracture observation and evaluation; (2) rock mechanics, fluid dynamics, and geochemical studies required to interpret observed fracture behavior; (3) incorporation of the results into improved stimulation design models and calculations; (4) assessment and calibration of logging and instrumentation techniques for fracture mapping and characterization; and (5) testing of innovative stimulation techniques.

Industry and service company participation in all aspects of this program is essential. Such industrial interest has been high, and further participation is solicited in this paper. This program will provide a unique opportunity to quantify fracture behavior and is not being done elsewhere to our knowledge.

The trade-offs between number and scale of the experiments and the costs, time and "real estate" consumed by mineback for adequate characterization must be carefully assessed in the test planning. Important experimental areas include: (1) the effects of different fluids, proppants, and pumping schedules upon proppant distribution and fracture conductivity; (2) interaction of the created fracture with naturally-occurring fractures and formation interfaces; (3) the effects of different or novel completion, preforation, and frac techniques upon fracture initiation and propagation; and (4) chemical explosive fracturing. Initial tests would be small-scale, but subsequent larger tests would be conducted to establish scaling parameters apprepriate to MHF. Extension of these tests to deep uranium mines which underlie Cretaceous formation of the San Juan Basin is envisioned to provide similar information in a more representative environment.

A formation interface experiment is planned for late summer 1977. Hydraulic fractures will be created above and below an ash-fall tuff-welded tuff interface at a depth of $\sim$ 1350 ft. The two formations have contrasting densities and Young's modulii of 1.77 and 2.19 g/cm^3 and 0.24 and 2.41 x 10^6 psi for the ash-fall and welded tuffs, respectively.

Supportive rock mechanics, fluid dynamics, and geophysical and geochemical studies will be performed to aid in the interpretation of observed fracture behavior. The mineback experiments will allow for confirmation, in a field environment, of the laboratory and modeling efforts. Formation properties (fracture toughness, spallation, uniaxial and triaxial stress-strain relationships, anisotropy, etc.) will be measured under different conditions of stress, temperature, and water saturation. Fluid dynamics during fracturing involves investigation of frac fluid viscosity as a function of time and temperature, proppant mobility, and fluid loss to the formation. Finally, the resultant permeability for gas flow from the formation to the fracture and along a propped fracture to the well will be investigated and modeled. The geophysical and geochemical effects of the formations on these properties will receive particular attention to make the results applicable to other field environments.

The mineback tests will be used for the assessment and calibration of instrumentation techniques for fracture characterization. Borehole and adjacent-station seismic techniques which map the source of signals generated by the growing fracture appear promising but are known to be complex. Electrical, displacement via tiltmeters, trace, and improved pressure

measurements will be investigated. Logging technique--in situ property--observed fracture correlations will be made. Finally, in situ stress measurement technique comparisons will be made in "side-by-side" tests.

CONCLUSIONS

The feasibility of the in situ examination of hydraulic fractures by mineback has been demonstrated. Preliminary results have shown the effects of in situ stress distributions, material properties, and other geologic features upon fracture behavior. An expanded project has been initiated aimed at the understanding of complex fracturing processes by correlating direct fracture observations with laboratory and modeling studies and field production experience. Applications to enhanced gas recovery will be emphasized.

REFERENCES

1. L. D. Tyler and W. C. Vollendorf, "Physical Observations and Mapping of Cracks Resulting from Hydraulic Fracturing In Situ Stress Measurements," 50th Annual Technical Conference and Exhibition, Society of Petroleum Engineers of AIME, SPE-5542, Dallas, Texas, September 28 - October 1, 1975.

TABLE I

ASH-FALL TUFF ROCK PROPERTIES

Bulk Density (gm/cc)	1.77
Grain Density (gm/cc)	2.42
Porosity (%)*	44.6
Modulus of Elasticity (x 10^6 psi)	0.236
Poisson's Ratio	0.312
Bulk Modulus (x 10^6 psi)*	0.211
Shear Modulus (x 10^6 psi)*	0.111
Permeability (millidarcy)**	0.01

* Calculated

** Helium permeability test on 4.75-cm diameter by 5.18-cm long specimens. Test conducted on as-received specimen with zero confining pressure and 300 psi driving pressure. (Our experience shows with small confining pressures the permeability values may be one or two orders of magnitude smaller.)

TABLE II

DESIGN SCHEDULE FOR HOLE U12g10.5

Fracturing Fluid PWG/FR26L

μ = 79 cp

Schedule: Injection Rate = 4 barrels/minute

Volume		
350 gal	Pad	
450 gal	1 lb/gal	20-40 Sand-Black
400 gal	2 lb/gal	20-40 Sand-Red
400 gal	3 lb/gal	20-40 Sand-Blue
1600 gal	TOTAL	

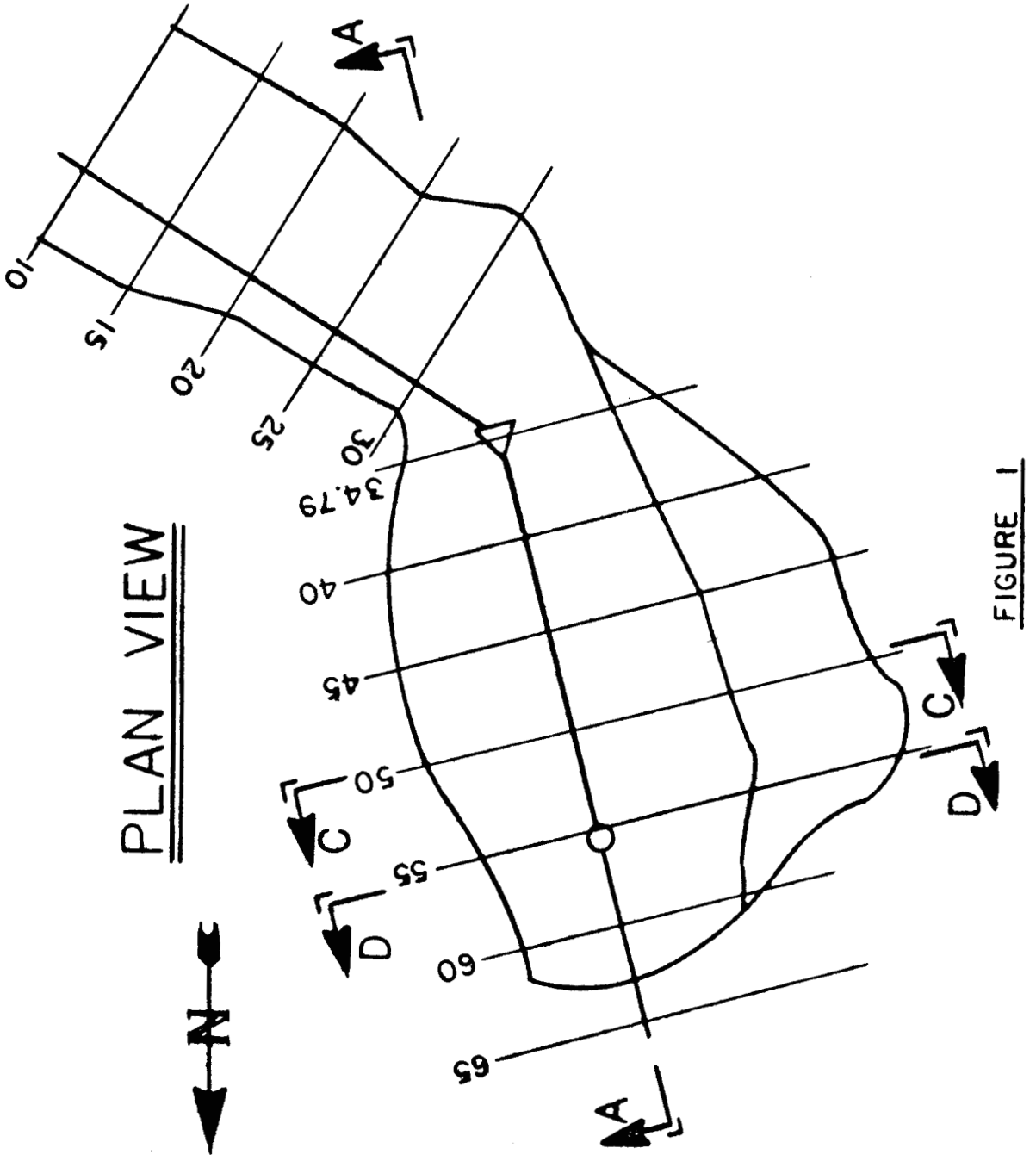

FIGURE 1

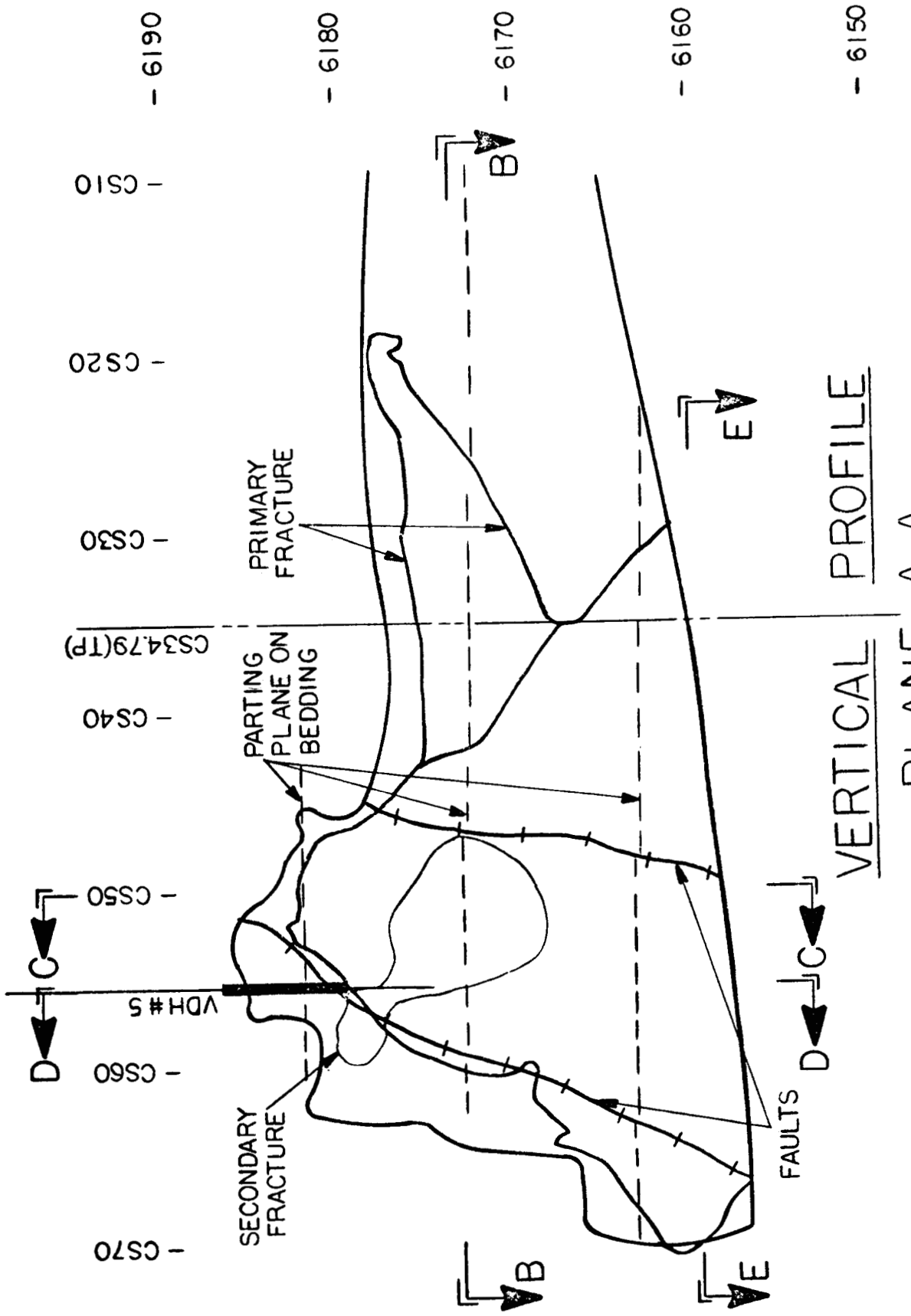
- 6190
- 6180
- 6170
- 6160
- 6150
- CS10
- CS20
- CS30
CS34.79(TP)
- CS40
- CS50
- CS60
- CS70
VDH # 5
PRIMARY FRACTURE
PARTING PLANE ON BEDDING
SECONDARY FRACTURE
FAULTS
A
B
C
D
E
VERTICAL PLANE A-A PROFILE

FIGURE 2

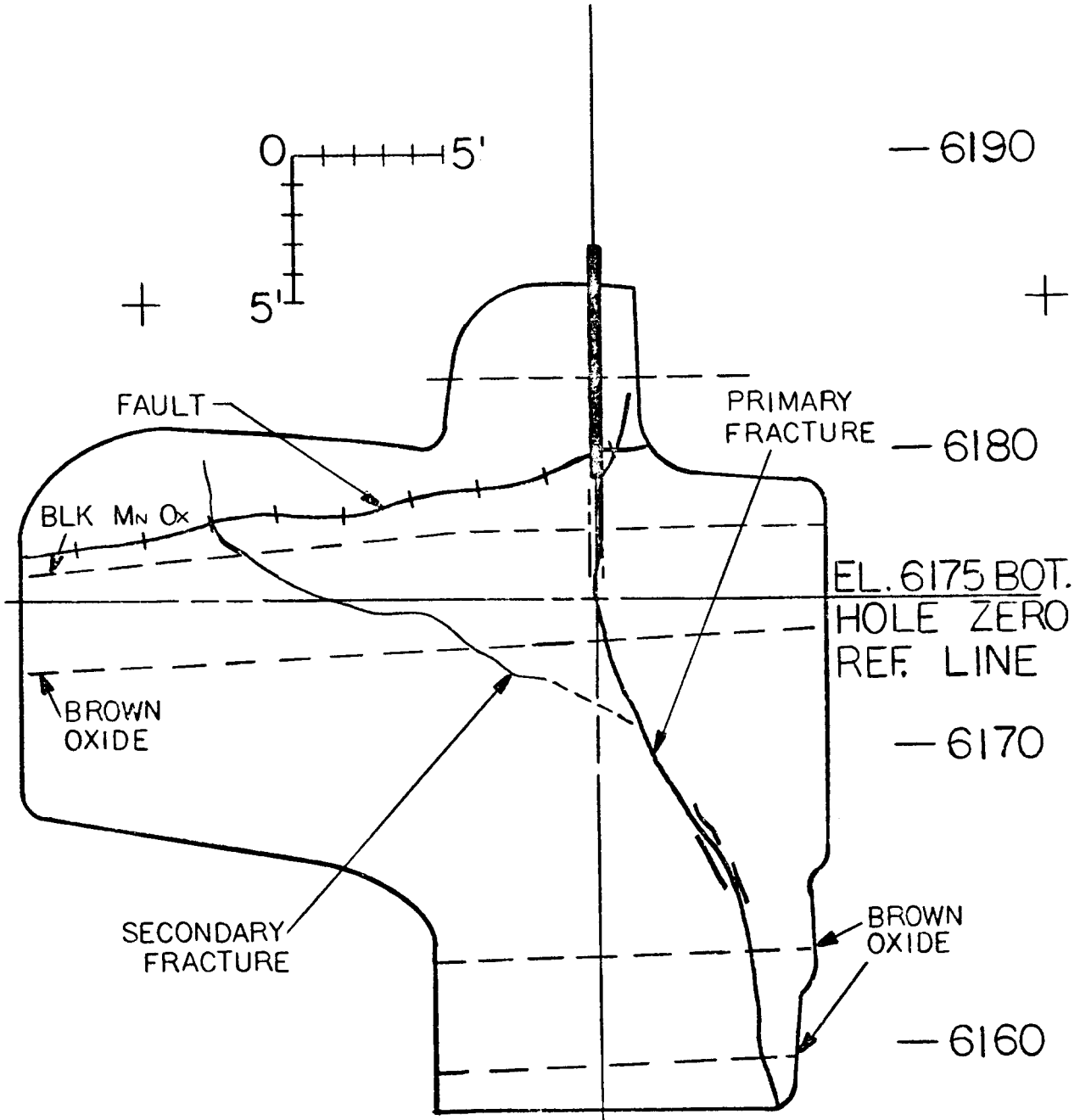

VERTICAL SECTION D-D
THROUGH VDH #5
(CSO+55.5' NOTES)
(LOOKING NORTH)

FIGURE 3

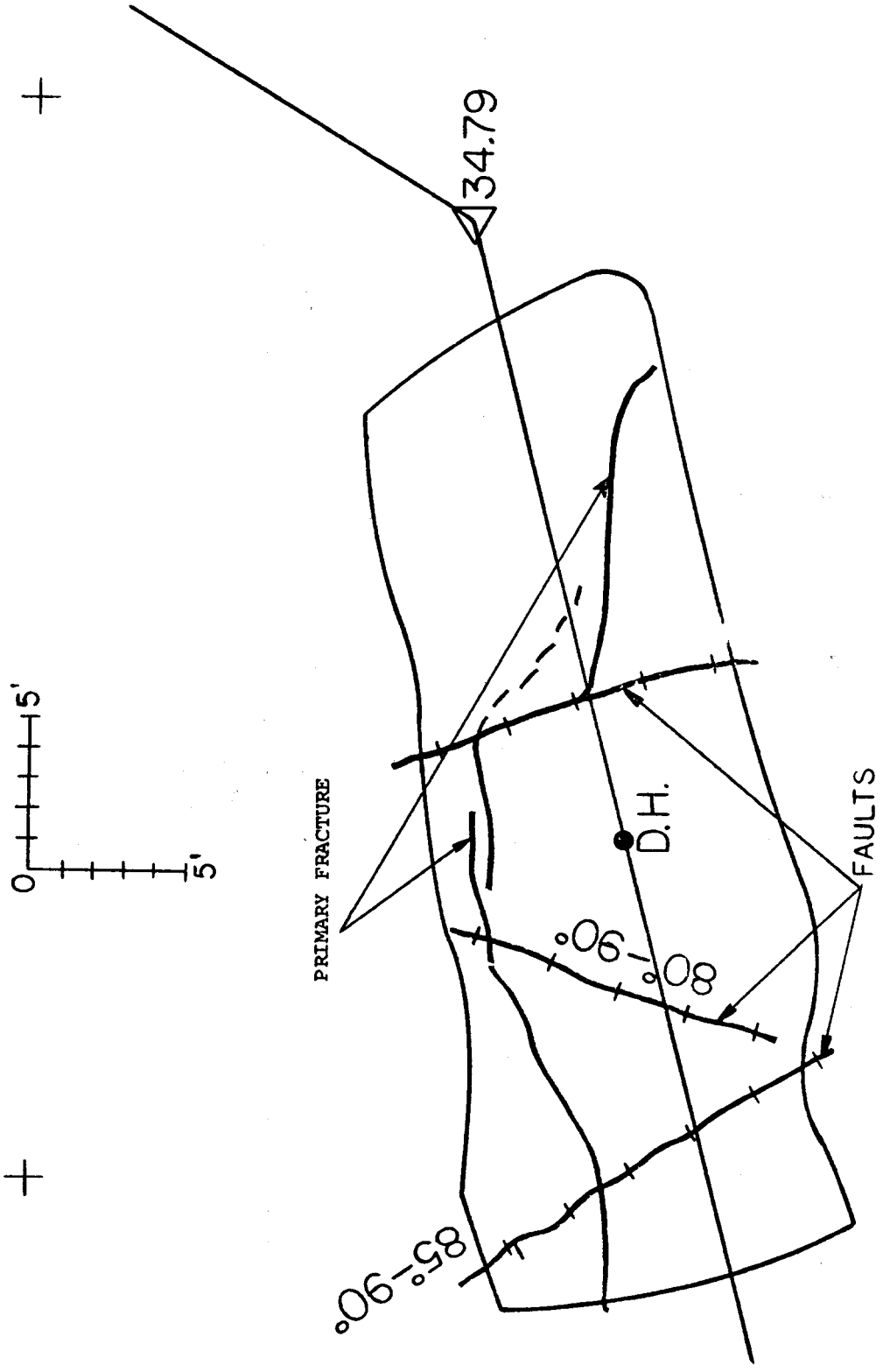

PLAN E-E (6160 ELEV.)
-15'

FIGURE 4

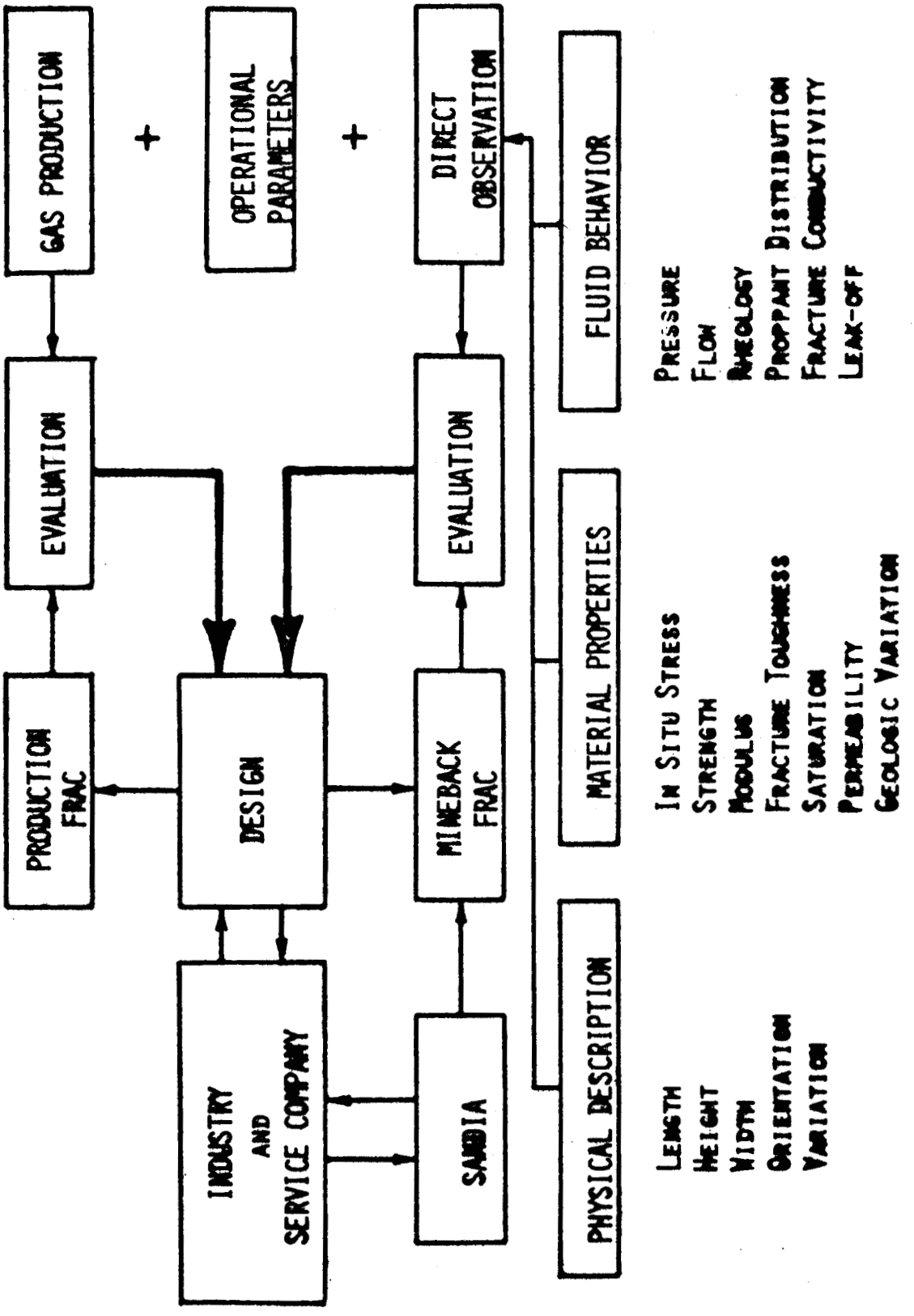
GAS PRODUCTION
+
OPERATIONAL PARAMETERS
+
DIRECT OBSERVATION
EVALUATION
EVALUATION
FLUID BEHAVIOR
PRESSURE
FLOW
RHEOLOGY
PROPPANT DISTRIBUTION
FRACTURE CONDUCTIVITY
LEAK-OFF
PRODUCTION FRAC
DESIGN
MINEBACK FRAC
MATERIAL PROPERTIES
IN SITU STRESS
STRENGTH
MODULUS
FRACTURE TOUGHNESS
SATURATION
PERMEABILITY
GEOLOGIC VARIATION
INDUSTRY AND SERVICE COMPANY
SANDIA
PHYSICAL DESCRIPTION
LENGTH
HEIGHT
WIDTH
ORIENTATION
VARIATION

FIGURE 5

ABUNDANCE AND DISTRIBUTION OF SOME CHEMICAL ELEMENTS IN THE CHATTANOOGA, OHIO, AND NEW ALBANY SHALES IN KENTUCKY

by

William H. Blackburn, Department of Geology, University of Kentucky
William H. Dennen, Department of Geology, University of Kentucky
Philip A. Davis[1], Department of Geology, University of Kentucky

ABSTRACT

The chemical characterization of the Devonian shales must involve examination of large amounts of data to ascertain which elements may be considered as independent variables and which, through their areal and stratigraphic variability, carry the greatest amount of geochemical information.

Chemical determinations of 25 major, minor and trace elements have been made on 60 outcrop samples of the Devonian shale collected around the Cincinnati Arch. No attempt was made to provide stratigraphic control and, since all the material was weathered to some extent, the data probably represent the maximum geochemical range to be anticipated in core samples. Elements showing bimodal or wide variability may be expected to be most useful in stratigraphic or areal analyses. These include V, Co, Ni, Zn, Mo, Ca, S, Y, Sr, and U. Other elements examined are unimodal with little variability and are probably least useful in this context. A relationship between concentrations of variable elements and modal components is also noted.

INTRODUCTION

Modern analytic instrumentation allows the determination of a large number of chemical elements in geologic materials with such speed and precision that data may often be accumulated at rates beyond the capacity for geochemical interpretation of the problem in hand. Indeed, too much data may obscure the more important and useful aspects of a study. In these circumstances, it is requisite that the intended use of the geochemical information be kept clearly in mind and that every effort be made to cull out such data as will contribute only noise.

Several procedures for selecting those elements which carry a high geochemical information content are available and this work is, in part, an example of their application. The procedure is outlined below:

I. Preselection of elements for study:
   include: elements of possible commercial value or environmental hazard and elements generally unaffected by diagenetic processes and post-consolidation solutional activity.
   exclude: elements of high mobility in the sedimentary environment and those whose natural abundance is so low as to require preconcentration.

II. Selection of elements from reconnaissance data:
   (acquisition of an adequate data base is essential at the outset of a study but continued determination of elements contributing no information should cease thereafter)
   include: elements acting as independent variables and having a recognizable statistical variation.

---

[1]Present address: Department of Chemistry, University of California-San Diego, San Diego, CA

exclude: one or the other of element pairs showing strong covariance and elements showing little inter-sample variability.

Application of these general procedures will usually lead to the selection of minor and trace elements (high variance, cohesive distribution patterns) of small size and high charge (geochemically stable) and eliminate such typically invariant major elements as silicon, aluminum, or iron as well as the highly mobile alkali metals.

ANALYTICAL TECHNIQUES

Sixty outcrop samples were collected from the exposed belt of Devonian Black Shale around the Cincinnati Arch in Kentucky. Collection sites were selected to afford maximum coverage with a minimum number of samples. To this end, an attempt was made to collect at least one sample from each Kentucky Carter Coordinate Quadrangle in the exposed belt. No attempt was made to provide stratigraphic control. Further, the samples were all weathered to some extent. The samples were crushed in a jaw crusher and subsequent splits of the resultant pea-size material taken for the various analytical methods described below.

Gamma-ray Spectrometry

Sample splits taken for the determination of U, Th, and K were further reduced to -100 mesh in a puck and ring grinder. The resulting powder was homogenized and approximately 150 g sealed in a 25 x 75 mm can. All samples were set aside for at least two weeks to allow attainment of radioactive equilibrium with radon which may have been lost in the grinding process. The pulverizing process was checked for contamination by preparing samples of quartz and dunite: no increase in activity was detected.

U, Th, and K were determined by gamma-ray spectrometry using a 75 x 75 mm thallium activated sodium iodide detector. All counting took place inside a lead brick castle with walls at least 50 mm thick. The detector was coupled to a Tracor/Northern TN1705 1024 channel pulse height analyzer with teletype output. Counts were made at three energy levels in order to solve for the three unknown count rates (U, Th, K). The 1.47 MeV peak (K^{40}) was used for potassium, the 1.76 MeV peak (Bi^{214} in the uranium series) for U, and the 2.62 MeV peak (Tl^{208} in the thorium series) for Th.

The γ-ray spectrometric system was calibrated using standard radioactive samples acquired from the Canadian Certified Reference Materials Project and U.S. Atomic energy standard consisting of uraninite diluted with dunite. KCl was used as the potassium standard. Precision of the analyses was checked by replicate sample determinations and by estimate of counting precision using the method of Loevinger and Berman (1951). Uranium determinations generally had a coefficient of variation of close to 2% as calculated by replicate determinations and thorium generally had a coefficient of variation of about 5%. These values were always less than the errors calculated using only counting statistics.

X-ray Fluorescence Spectrometry

Na, S, Ti, Ni, Cu, Rb, Sr, Y, and Zr were determined using x-ray fluorescence spectrometry. Sample splits were reduced to -250 mesh in an agate mortar and pestle and homogenized. Close to 3 g were then pressed into a boric acid backed pellet. Determinations were made on a Philips 1410/70 vaccum x-ray spectrometer. Mass absorption coefficients and backgrounds were calculated using the techniques of Reynolds (1967) and Feathers and Willis (1976). Analytical calibrations employed the use of international rock standards and secondary standards produced at the University of Kentucky.

Optical Emission Spectrography

Al, B, Ca, Co, Cr, Cu, Fe, Ga, Mg, Mn, Mo, P, Pb, Si, V, Zr were determined by optical emission spectrography employing a large quartz-glass, Littrow-mounted prism instrument manufactured by Adam Hilger, Ltd. Sample splits were -100 mesh powders mixed with equal parts by volume of specpure graphite powder and tamped into 1.5 x 3 mm craters in 3 mm diameter prearced specpure graphite electrodes. Samples were arced to completion as the anode at 8 amperes using a 6.4 mm diameter carbon counter-electrode and a 7 mm analytic gap. Incident light was focused on the collimating lens of the spectrograph after passing a rotating mechanical sector having a 4^n aperture ratio located at the entrance slit.

Spectra were recovered on Kodak Spectrum Analysis-1 plates, developed for 4 1/2 minutes at 19°C with constant stirring in a temperature controlled tank, fixed, washed, rinsed with distilled water,

and air dried.

Photometry was accomplished by use of Jarrell-Ash Co. nonrecording digital microphotometer-comparator. Line density and background were recorded and transformed to concentration values through the use of appropriate standards.

The precision of the spectrographic method is not high, usually being $\pm$ 5-15% of the reported value, but is generally more than adequate for trace element comparisons whose natural variations are often integral multiples.

RESULTS

For simplicity, the reduced data is presented as 1) histograms summarizing each element's distribution and 2) "blot plot" maps of relative concentration of elements showing regional variability. The logarithm of the concentration is used as the abscissae in the histograms to normalize the data and allow direct visual comparison of the chemical variability from plot to plot. On each diagram, an open triangle represents the concentration of the element in "APSC", an Appalachian Paleozoic Shale Composite collected by Julian Feiss, Kennecott Copper Corp., along the Pennsylvania Turnpike and composited by thickness. APSC is thought to be representative of the average Paleozoic shale and is routinely used in this laboratory as a reference material.

As discussed earlier, elements (or oxides) showing a bimodal distribution or wide variability as expressed by the histograms (Figs. 1, 2, 3) may be expected to be most useful in distinguishing stratigraphic units and in kerogen type discrimination. Taking phosphorus as 1.00 to be the least useful in this context (Fig. 1) the elements and their relative discriminatory values are given in Table 1.

U and Th distributions are given in Fig. 4 and show the latter to be relatively invariant with an average value of 9.8 ppm for Th. Potassium was also found to be relatively invariant with an average value of 2.96% as K_2O. Uranium, however, shows a wide concentration range from less than 5 to nearly 80 ppm with an average for the 60 samples of 36.4 ppm. The histogram of uranium content is either bimodal or has a strong positive skew; assuming bimodality, modes are at about 15 and 44 ppm. The U/Th ratio, shown in Fig. 4, has an average value of 3.71 close to that of APSC, 4.00. The possible presence of two populations of uranium is supported by the U/Th histogram.

In light of the variability shown by the determined elements, a consideration of the geochemical properties of the elements may be made leading to conclusions as to their usefulness for stratigraphic discrimination. Table 2 presents the elements listed in groups according to their discriminatory value. It should be remembered that the data is directly applicable to outcrop data and may change on examination of unweathered core material. The outcrop data, however, probably represents the maximum geochemical range to be anticipated in core samples.

Regional chemical variations of the elements showing most promise as discriminatory are shown in Figs. 5, 6, and 7. A bold interpretation of regional chemical trends, where recognized, is indicated by dashed iso-concentration lines on the plots (Fig. 6). These lines all have an east-northeasterly to east-west strike and suggest regional chemical changes in a generally north-south direction.

If the uranium and yttrium are associated with a heavy mineral suite as they commonly are in sedimentary rocks, a close correlation of these elements might be expected. The regional variance of the elements (Fig. 5) shows a tendency toward correlation in the eastern and southern exposed areas. The association breaks down in the area south of Louisville where yttrium is depleted in the same area of a uranium anomaly. The pattern for Mo, however, follows that for U quite closely. This feature is also shown by Fig. 8. This relationship between U and Mo is not well understood and is under study at this time. A covariance of uranium and organic carbon (100 - % Ash) is shown by Fig. 9. More scatter is observed than might be expected but this may be explained by the varying degrees of alteration of these outcrop samples.

Trace elements of the First Transition Series seem to correlate rather well. Cobalt (Fig. 7) and Nickel (Fig. 6) both increase to the south and vanadium, while exhibiting the same southerly increase (Fig. 7) does so at a slower rate.

Three distinct V/Ni ratios seem to be evident on Fig. 10 but these are not geographically discernable. On the other hand, Cr/Ni ratios (Fig. 11) have distinct geographic relationships. This feature may prove to be stratigraphically controlled and explained by detailed studies of core and

outcrop sections.

Iron and sulfur (Fig. 12) values are generally correlatable and corroborates mineralogic evidence of pyrite being the sole residence of sulfur in these rocks. It may also indicate that the great bulk of Fe is pyritiferous.

Kerogen Discrimination

An attempt is being made to distinguish terrestrially-derived from marine-derived kerogens on the basis of their inorganic chemical content. It is presumed that the elements of interest are originally adsorbed on the kerogen and that a different suite or proportion of critical elements will be present in the different kerogen types. It is recognized, however, that sample processing may remove or alter the concentrations of elements of interest and both concepts require testing.

To date, a routine has been developed for the separation of the kerogen fraction from the shale samples. The flow sheet for sample preparation is shown as Fig. 13 where boxed products are satisfactory for inorganic analysis. To identify those elements which may be useful in the characterization of kerogen, a sample of New Albany shale has been treated along with a portion of the Appalachian Paleozoic Shale Composite (APSC) described above. Comparison of element concentrations between APSC is quite argillaceous and kerogen-poor while the black shale sample is arenaceous and kerogen-rich. The element enrichments may thus be ascribable to adsorption on kerogen in the black shale.

The benzene extraction process removed approximately 7 percent by weight of soluble hydrocarbons from the New Albany Shale but had no appreciable effect on the concentration of the inorganic constituents except for boron. This element was reduced to one-half its original concentration and, therefore, must be markedly concentrated in the extracted substances.

The kerogen content of the New Albany sample amounts to approximately 13 percent by weight. The kerogen contains detectable quantities of Cr, Cu, Fe, Pb, Mn, Mo, Ni, P, Si, Ti, and Zr. Boron could not be determined because of the use of boric acid in the silicate dissolution process. It should be noted that Cu, Fe, Mo, Ni and Zr are particularly high.

On consideration of the geochemical properties of these elements coupled with the probable effects of sample processing, conclusions may be drawn regarding the relative usefulness of these elements for kerogen discrimination. This data is presented as Table 4.

SUMMARY

One of the tasks of the Eastern Gas Shales Project is to search for methods of stratigraphic interpretation and kerogen discrimination using inorganic chemistry. To this end, an attempt is made to evaluate the usefulness of various elements for discriminatory purposes. The selection process must include geochemical reasoning to select those elements which have potential commercial value, those which may have environmental impact, those which are generally unaffected by secondary processes. This suite, of preselected elements can be further reduced by consideration of results obtained in a reconnaissance study to evaluate the variability of the elements in the lithology under study. At this stage, elements which show little variability or act as dependent variables may be eliminated.

The results of this study show that the elements Cu, Cr, Pb, Ga, Fe, Mn, Y, U, V, Na, Co, Ni, S, Mo, and Ca may be best for stratigraphic interpretation. Similarly, Cr, Cu, Ni, Mo, and Pb may prove best for kerogen discrimination.

REFERENCES

Feathers, C. E. and Willis, J. P. (1976) A simple method for background and matrix correction of spectral peaks in trace element determination by x-ray fluorescence spectrometry. X-ray Spectrometry 5, 41-48.

Loevinger, R. and Berman, m. (1951) Efficiency criteria in radioactivity counting. Nucleonics 9, 26-39.

Reynolds, R. C. (1967) Estimation of mass absorption coefficient by Compton scattering: Improvement and extensions of the method. Amer. Mineralogist 52, 1493-1502.

TABLE 1

Relative discriminating values of elements and oxides based on a value of 1.00 for phosphorus.

UNIMODAL DISTRIBUTION			
P	1.00	Zr	2.70
SiO_2	1.15	Cu	2.78
B	1.20	S	2.87
Rb	1.40	Cr	3.22
Sr	1.40	Pb	3.57
TiO_2	1.54	Ga	4.00
Al_2O_3	2.30	Fe_2O_3*	4.35
MgO	2.70	MnO	5.55
BIMODAL DISTRIBUTION			
Y	1.17	Ni	5.55
U	3.49	Na_2O	6.25
V	4.45	Mo	8.00
Co	4.87	CaO	33.00

TABLE 2

Preliminary listing of usefulness of elements for stratigraphic discrimination.

Excellent - CaO, U, Mo, Co, Ni

Good - Na_2O, V, Y, S, MnO, Fe, Ga

Fair - Pb, Cr, Cu, K

Poor - P, SiO_2, B, TiO_2, Al_2O_3, MgO, Zr, Rb, Na, Sr

TABLE 3

Comparison of elemental concentrations between the Appalachian Paleozoic Shale Composite and the New Albany Shale.

Element	New Albany/APSC	Element	New Albany/APSC
Al	0.53	Mn	0.62
B	1.43	Mo	4.67
Ca	0.29	Na	0.32
Co	1.75	Ni	1.91
Cr	0.70	P	0.92
Cu	2.07	Pb	0.68
Fe	0.78	Si	1.05
Ga	0.69	Ti	0.74
Mg	0.51	V	0.83
		Zr	0.81

TABLE 4

Relative usefulness of some elements for kerogen discrimination.

Good - Cr, Cu, Ni, Mo, Pb

Possible - Fe, Mn, P, Ti

Unlikely - Si, Zr

Figure 1.- Histograms showing variability of Cu, Pb, Sr, Rb, Ga, Zr, P, B in Devonian shale outcrop samples. Class interval in each case is equal to $\log_{10}$ 1.2. The open triangle represents the value for the Appalachian Paleozoic Shale Composite APSC.

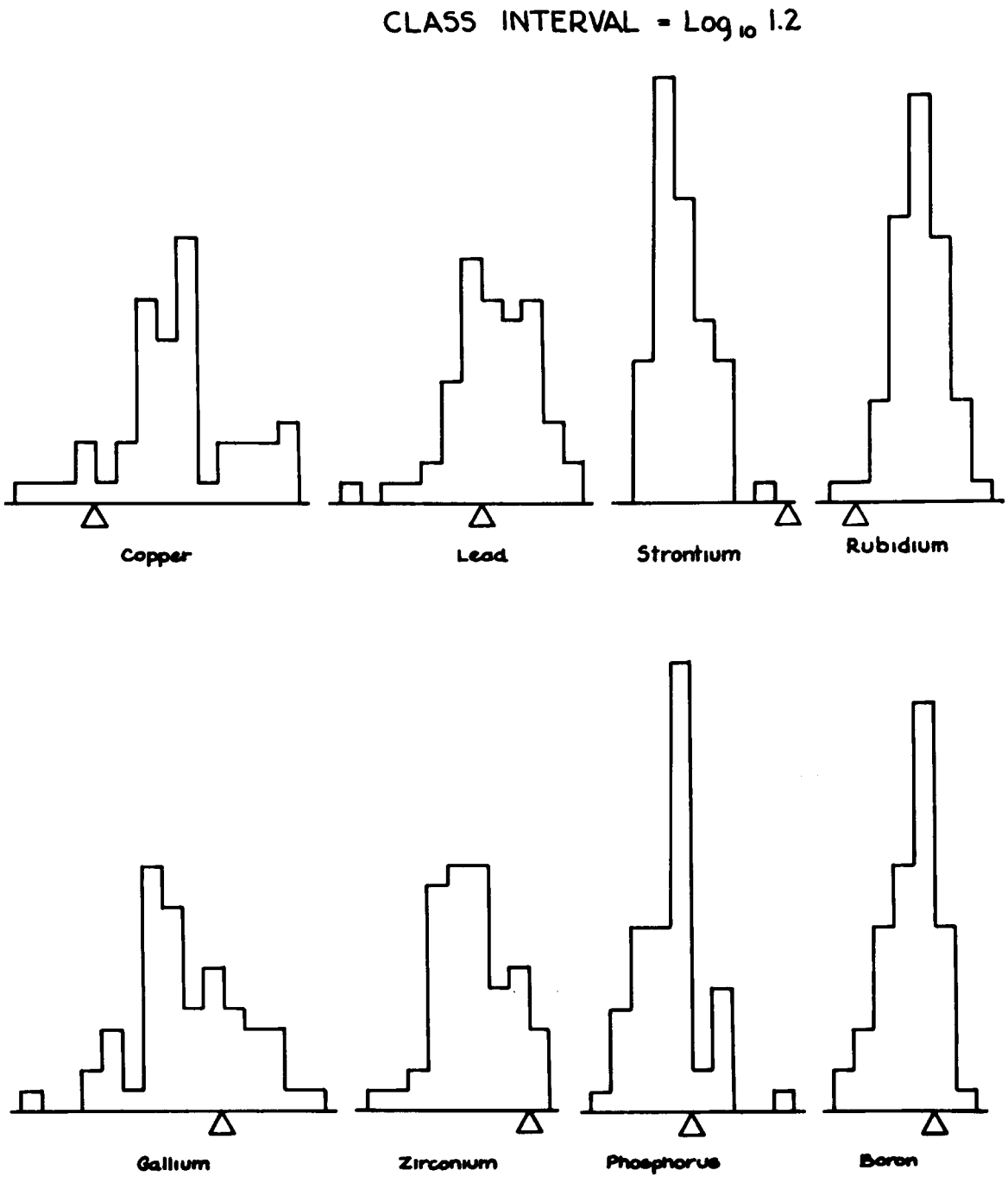

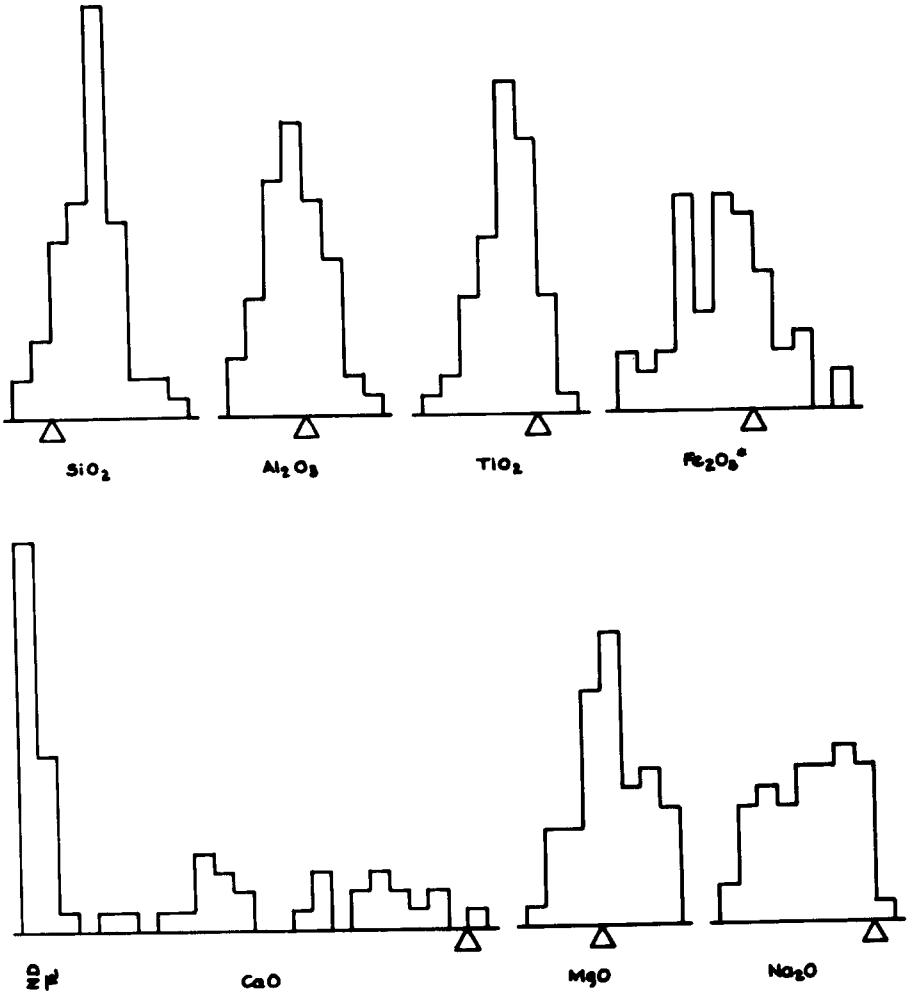

Fig. 2. Histograms showing variability of SiO_2, Al_2O_3, TiO_2, Fe_2O_3*, CaO, MgO, Na_2O, Co, Ni. Class interval is equal to $\log_{10}$ 1.2. The open triangle represents the value for APSC.

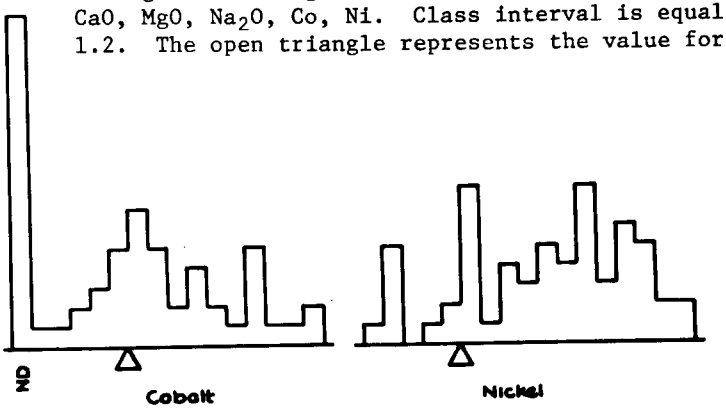

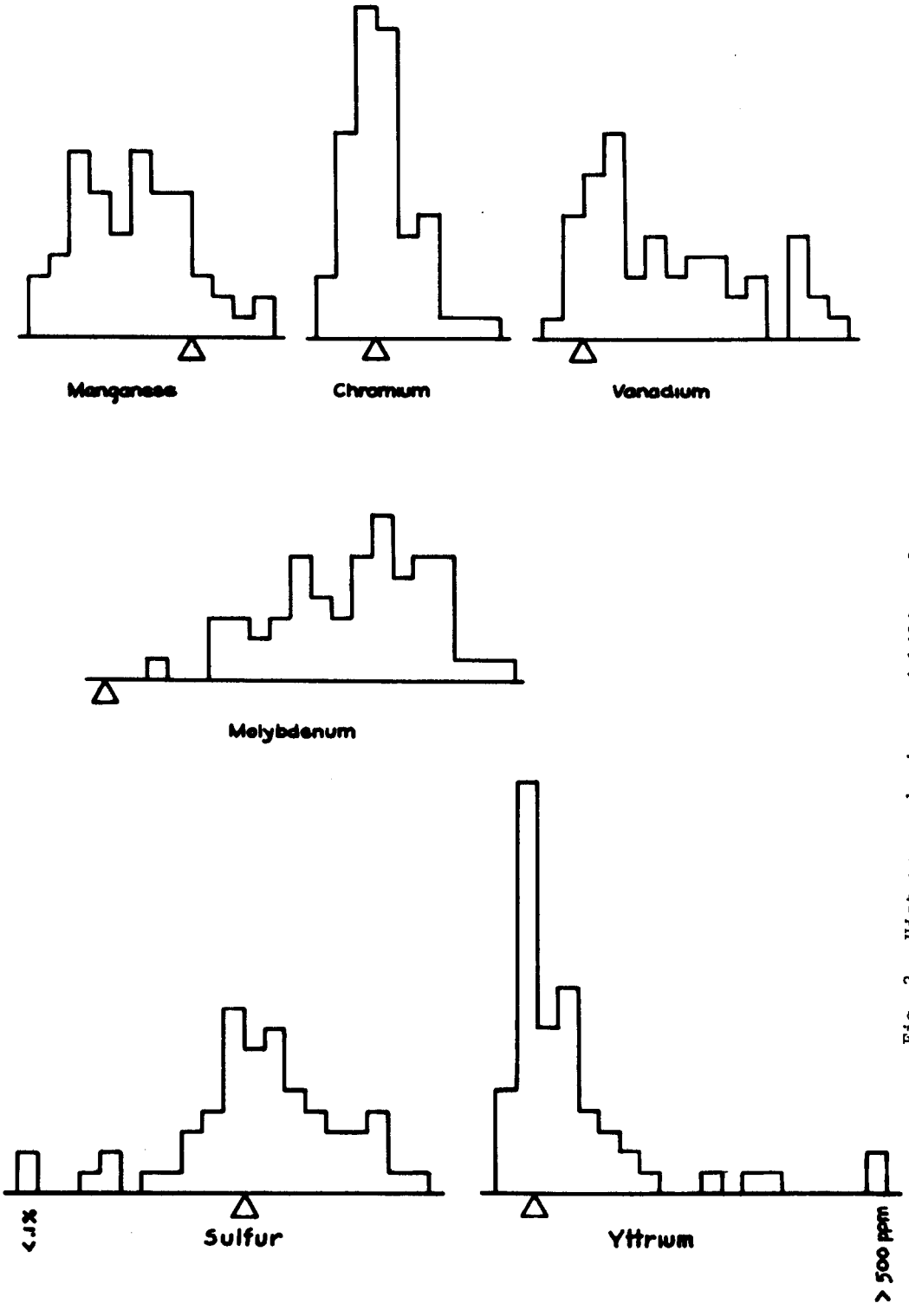

Fig. 3. Histograms showing variability of Mn, Cr, V, Mo, S, Y. Class interval is equal to $\log_{10}$ 1.2. The open triangle represents the value for APSC.

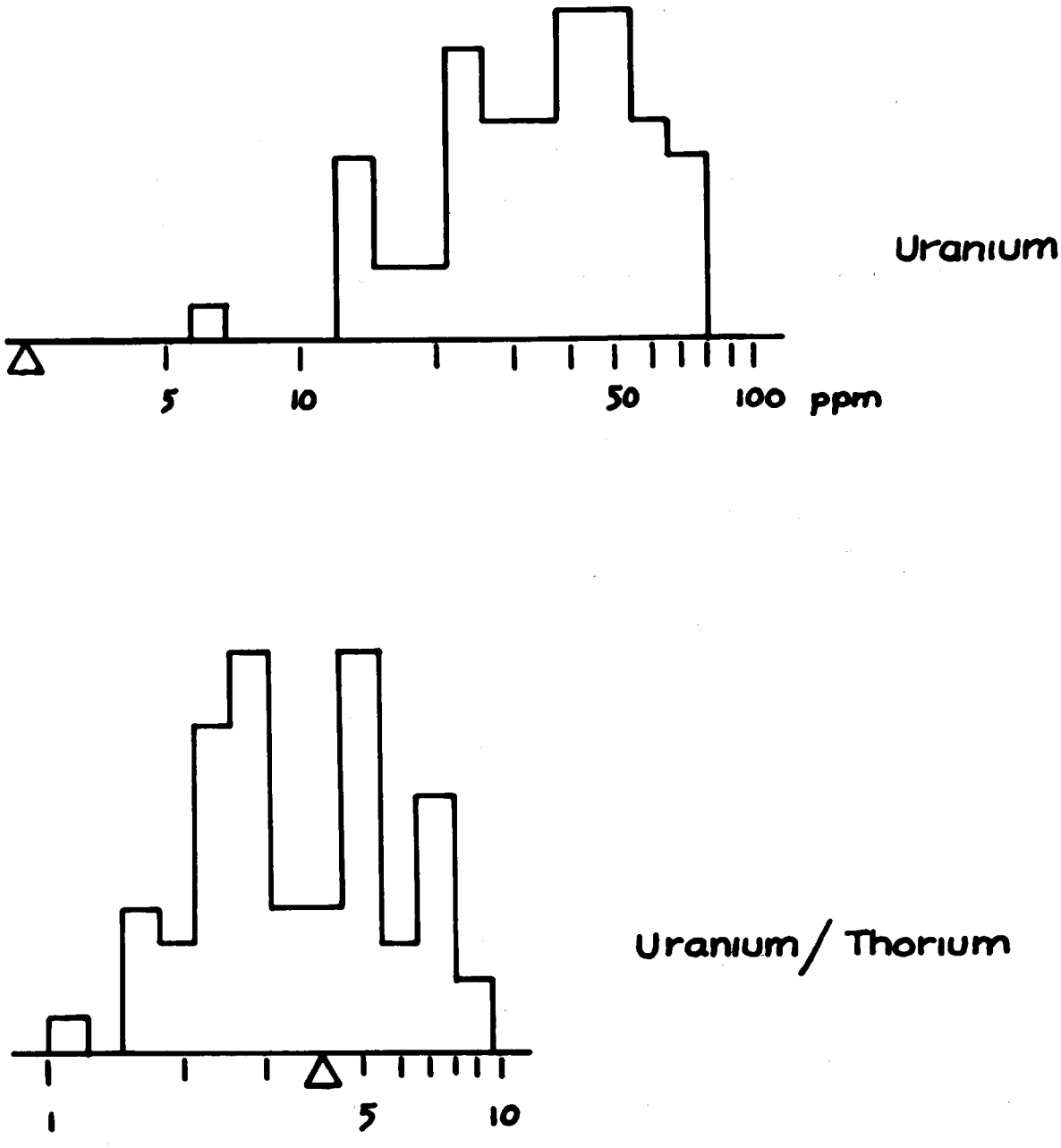

Fig. 4. Histograms showing the variability of U and U/Th. The class interval is equal to $\log_{10} 1.2$. The open triangle gives the value for APSC.

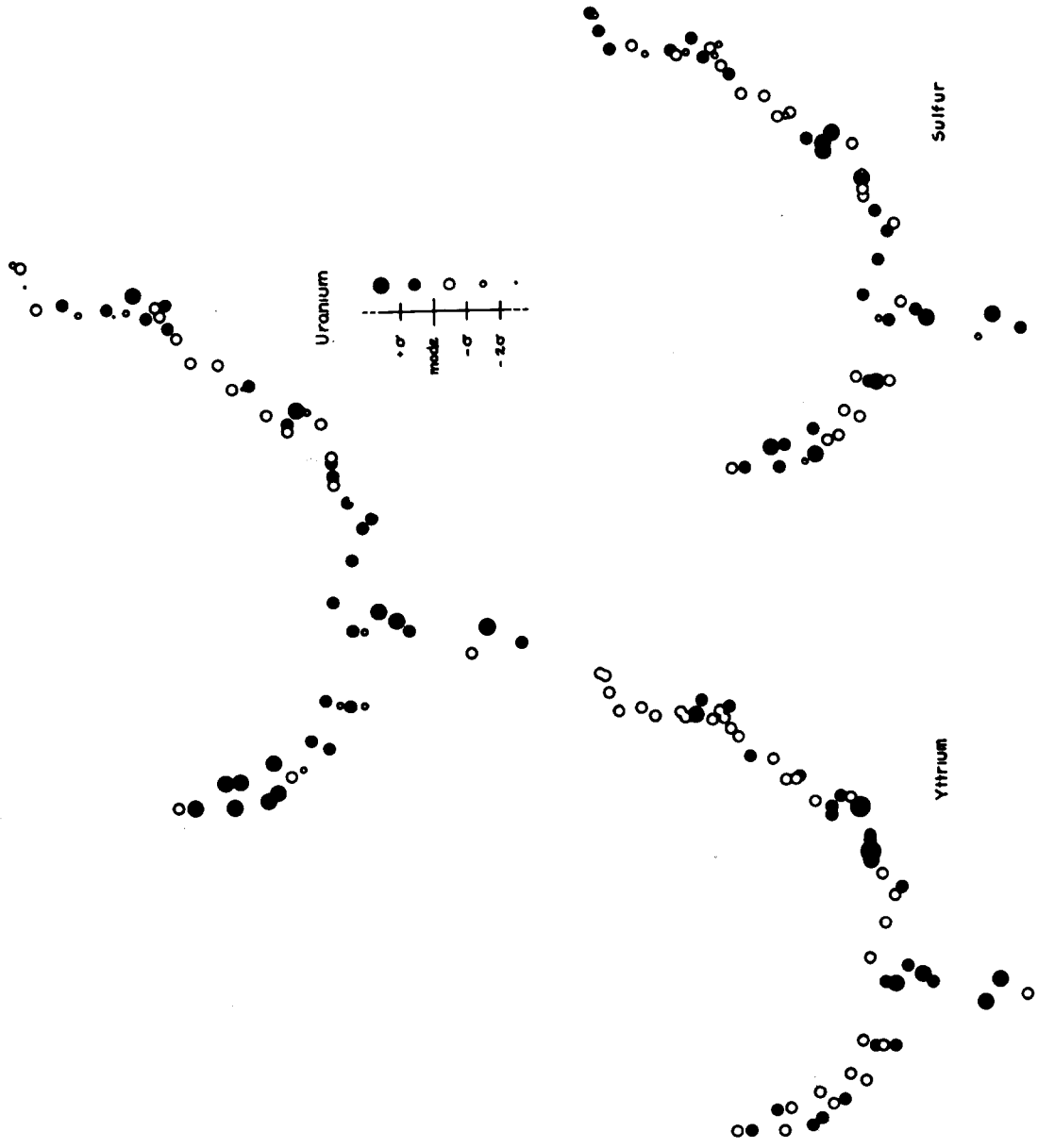

Fig. 5. Blot plot showing regional variability of U, Y, and S in outcrop samples taken around the Cincinnati Arch in Kentucky. Concentration ranges are taken from the histogram plots in + and - σ and 2σ increments.

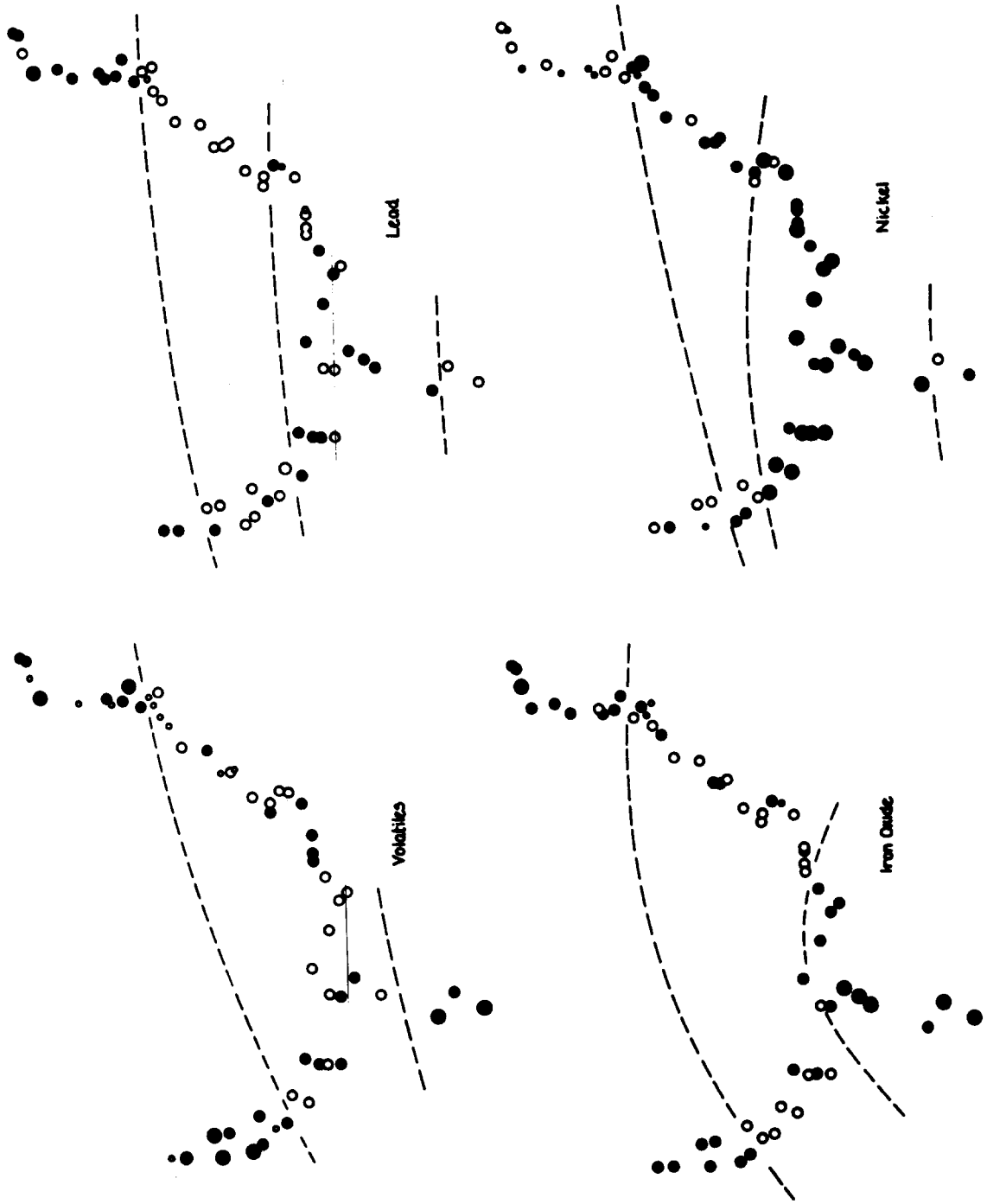

Fig. 6. Blot plot showing regional variability of Pb, Ni, Fe_2O_3* and total volatiles (H_2O + soluble hydrocarbon) in outcrop samples taken around the Cincinnati Arch in Kentucky. The scale for concentration ranges is as for Fig. 5.

Fig. 7. Blot plot showing regional variability of Co, Mo, V, and CaO in outcrop samples taken around the Cincinnati Arch in Kentucky. The scale for concentration ranges is as for Fig. 5.

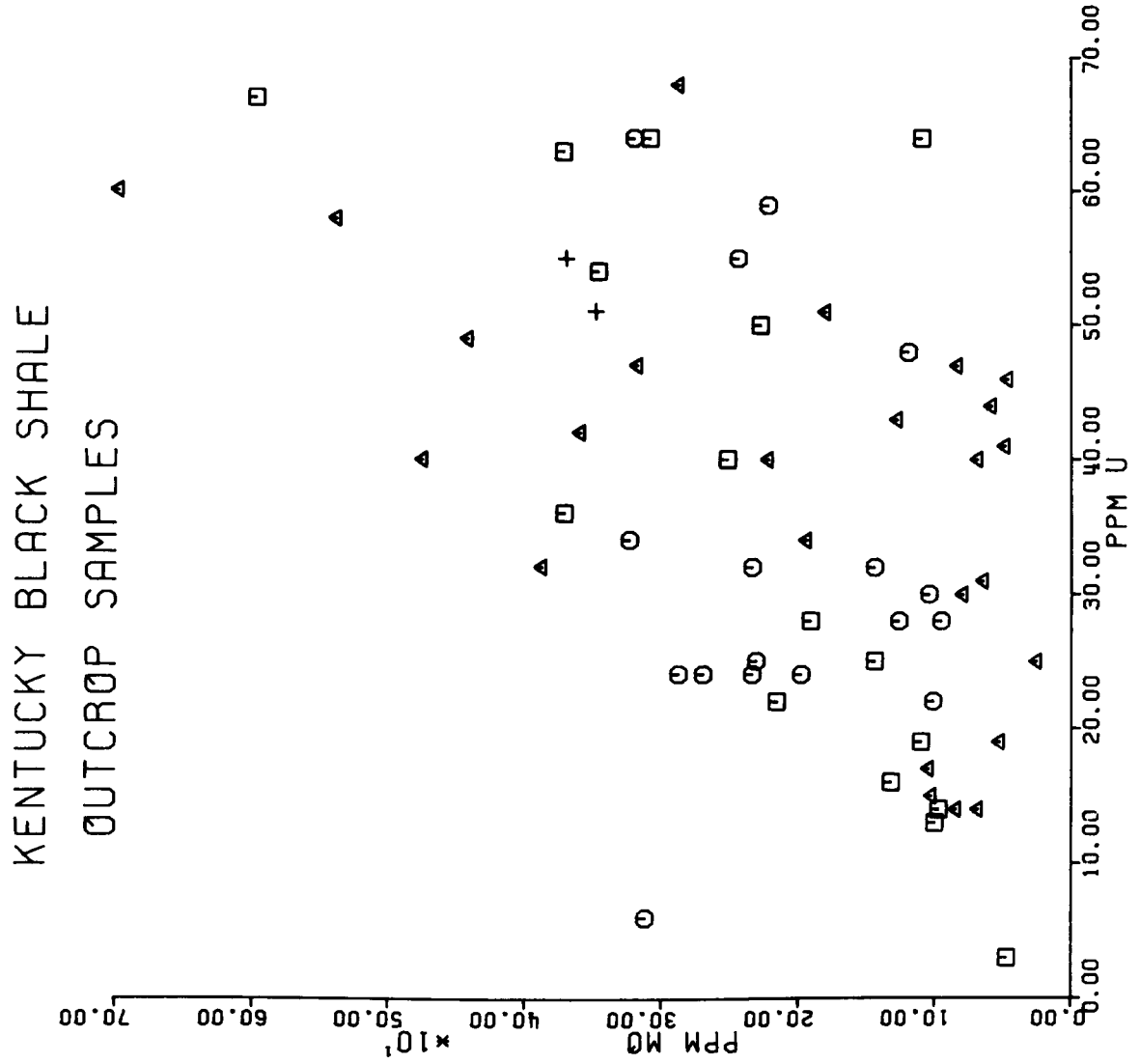

Figure 8.- The relationship between U and Mo in 60 outcrop samples of Devonian Black Shale in Kentucky.

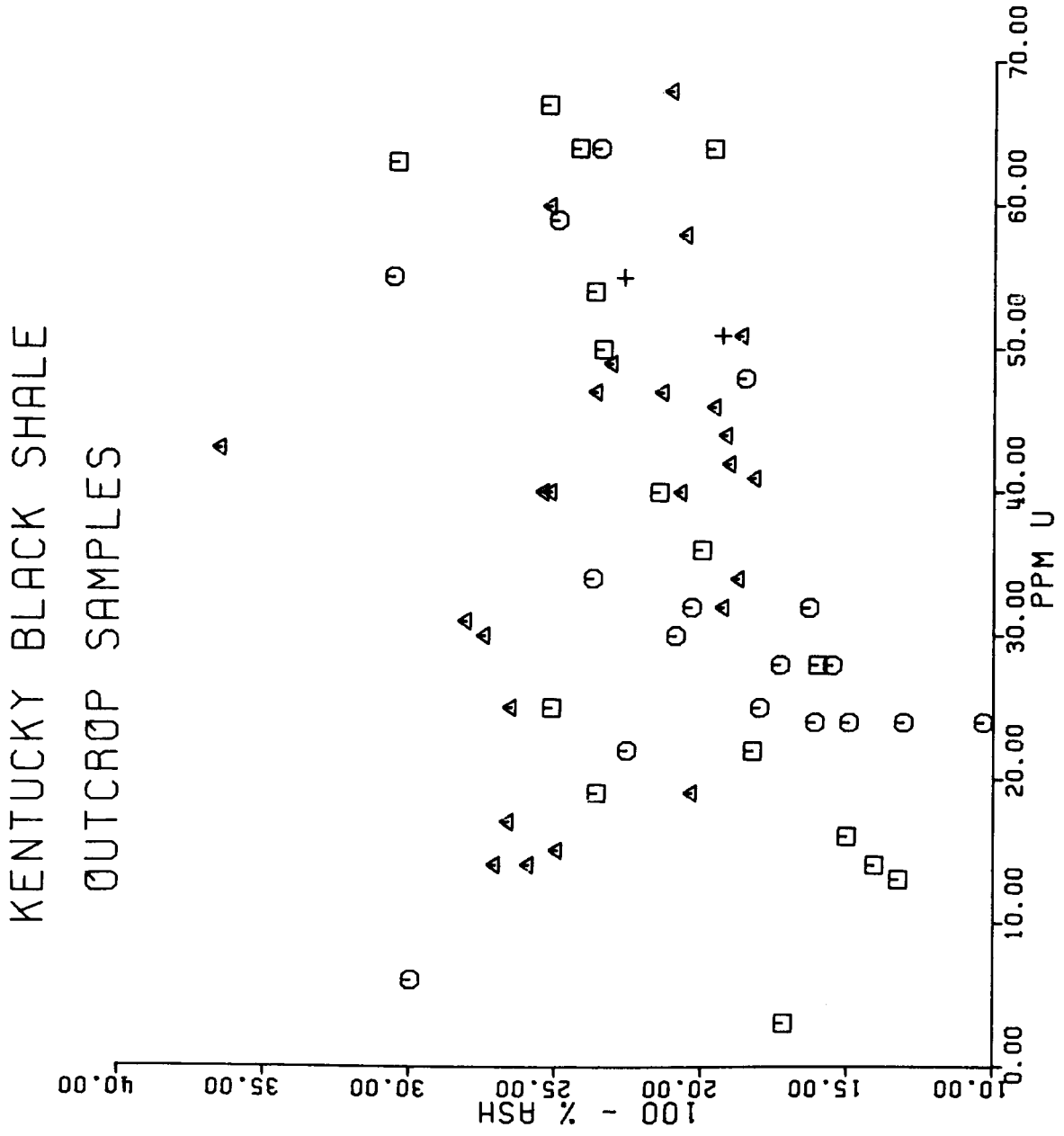

Figure 9.- Uranium vs a measure of total organic carbon, (100 - % Ash)

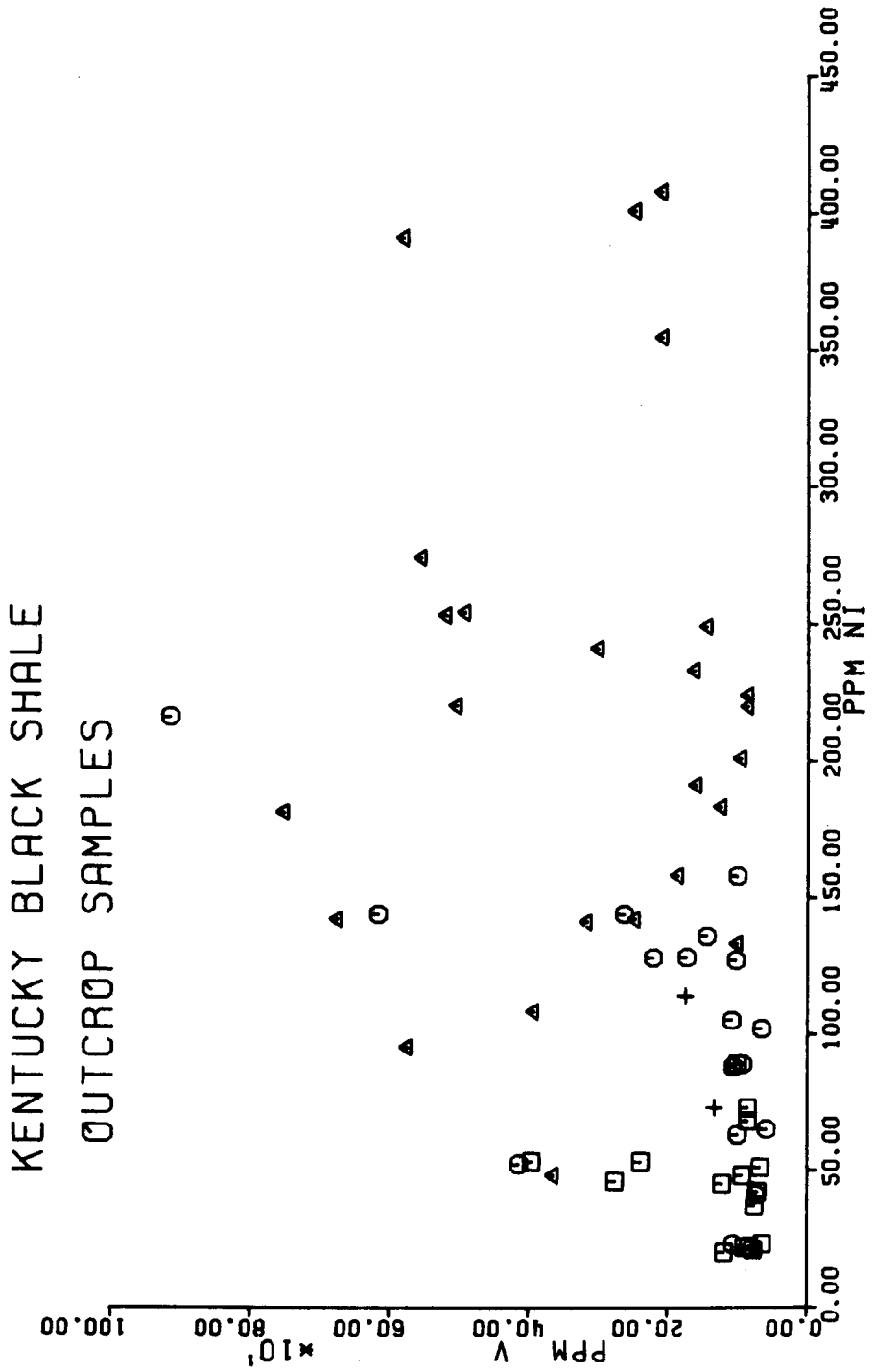

Figure 10.- Vanadium vs nickel in 60 outcrop samples. Geographic source of the samples is represented by the symbols going in a southerly direction; square, circle, triangle, cross.

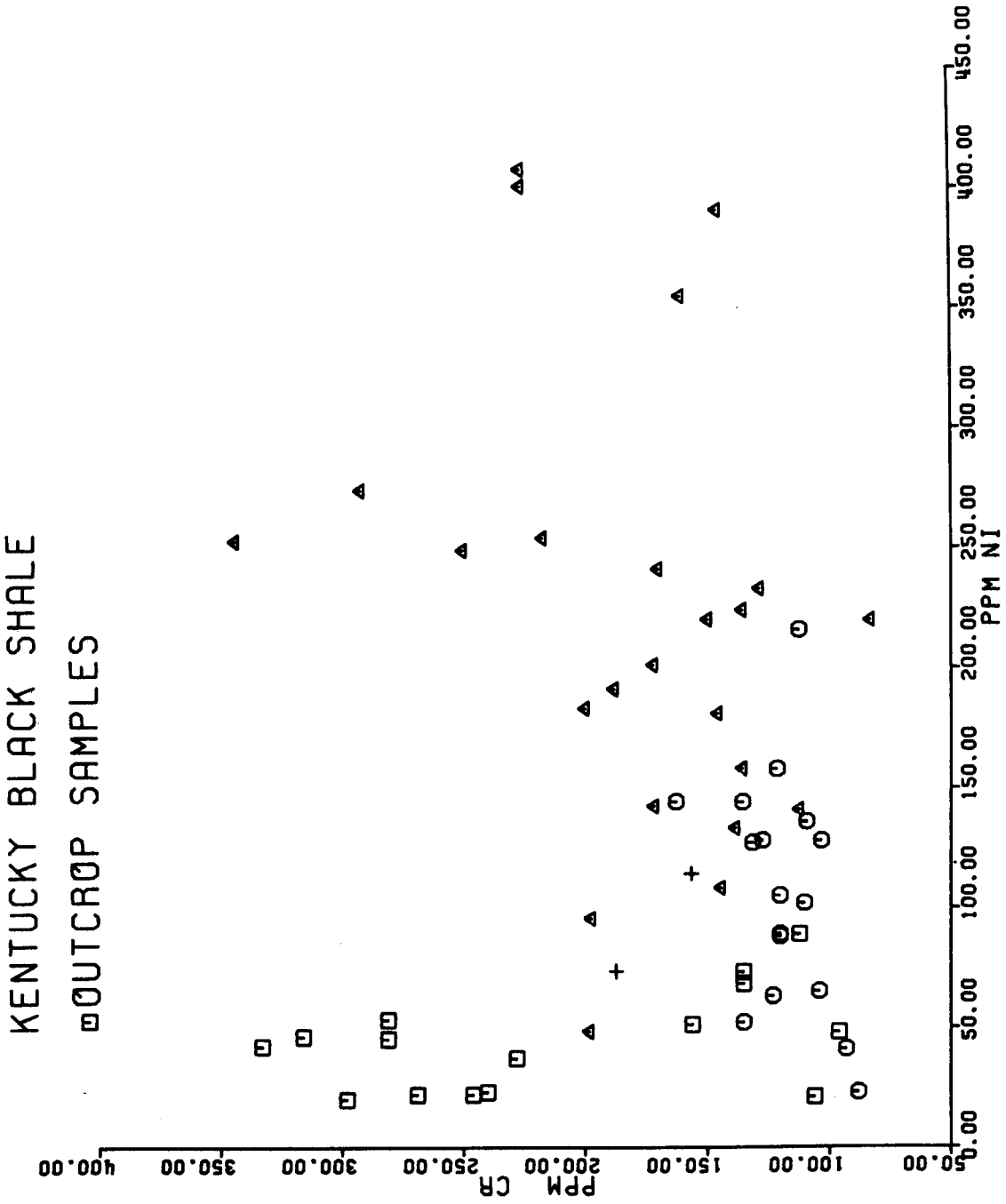

Figure 11.- Chromium vs nickel in 60 outcrop samples. Symbols as in Figure 10.

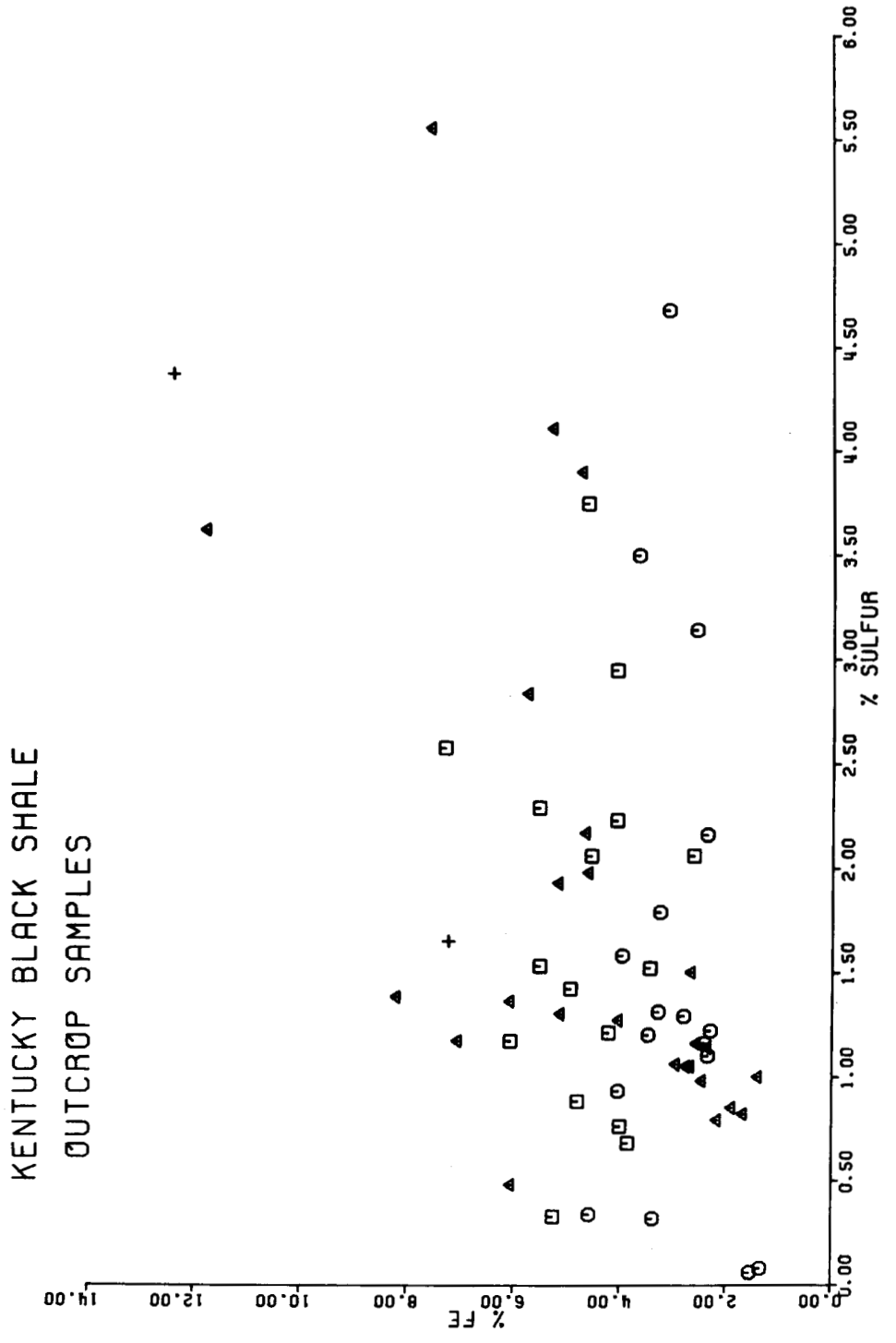

Figure 12.- Iron vs Sulfur in 60 outcrop samples. Symbols as in Figure 10.

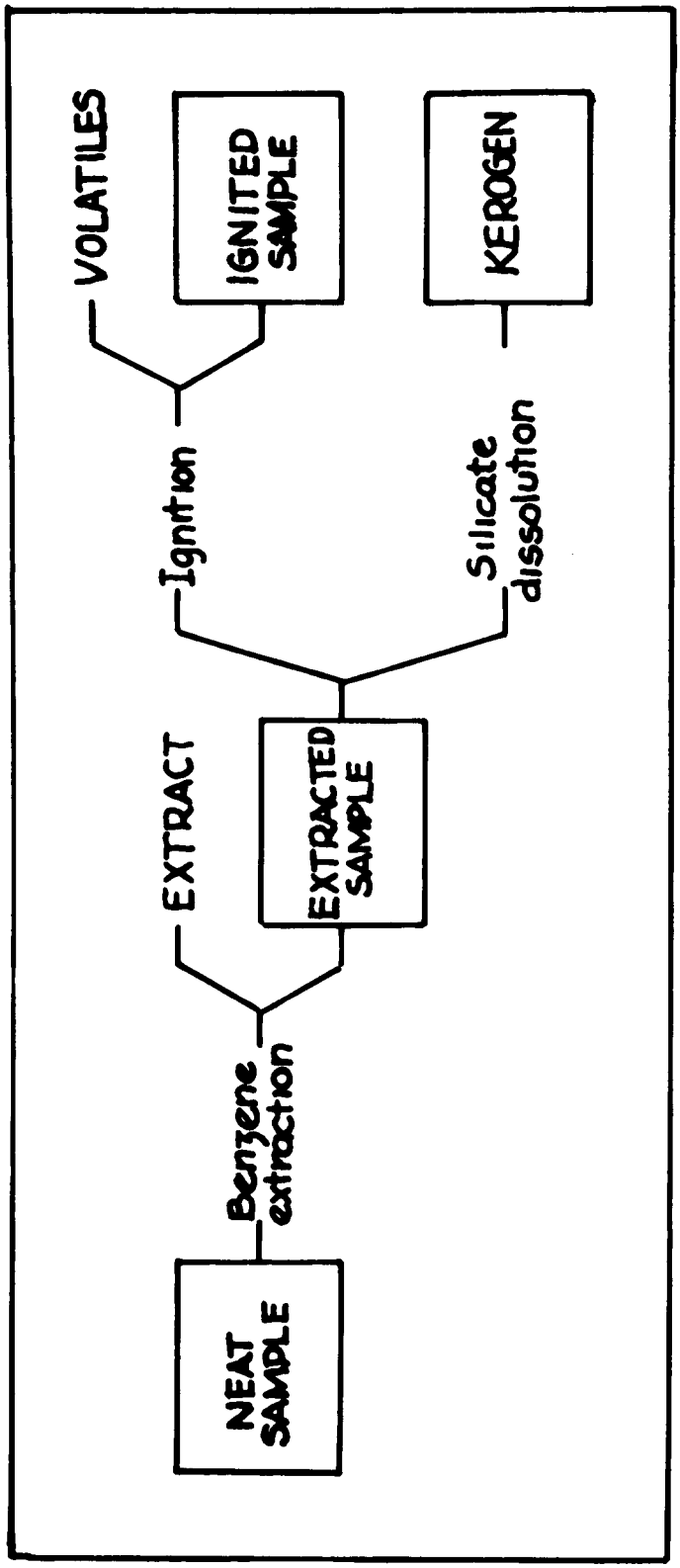

Figure 13.- Flow sheet for sample preparation to isolate kerogen in Devonian shale samples.

WIRELINE EVALUATION OF THE DEVONIAN SHALE: A PROGRESS REPORT

by

Jon Hilton, Schlumberger Well Services, Wooster, Ohio

ABSTRACT

Wireline evaluation of the Devonian shale has always been difficult because of the complex nature of the formation. However, research projects of recent years and the growing interest of independent operators have presented an opportunity for some much-needed study of the problems.

To understand the problems of log analysis, it was first necessary to understand the lithology and its affect on log response. Once this was known, the next step was to determine what information was required for evaluation and how this information could be found.

Since the lithology of the Devonian shale is complex, a comprehensive logging program was needed. To obtain the maximum value from the program, a computer-processes interpretation, "Kerogen Analysis", was developed by Schlumberger. The output of this program is a qualitative analysis of the reservoir. In addition, the need of a positive fracture-detection system was recognized. Resistivity-profile measurements and the Fracture Identification Log (FIL*) have been very useful for this purpose.

INTRODUCTION

Although the Devonian shale in the Appalachian Basin has been known to be productive for many years, the interest of the industry has been limited because of the technical and economic problems involved. However, the gas shortage of recent times and the accompanying increase in industrial drilling have focused some much-deserved attention on this formation.

With this attention came the realization that existing wireline techniques were inadequate for proper evaluation. Fortunately, on-going research projects have permitted the adaptation of existing logs and interpretation techniques (both computer-processed and wellsite) to the analysis problem in Devonian shales. The short-term objectives have been:

- to identify hydrocarbon-bearing zones within the section.
- to identify permeable intervals within the section.

The first objective has been accomplished, at least qualitatively, with the computer-processed interpretation called "Kerogen Analysis". This program uses data from several down-hole services, and the output is a rather complete formation analysis. Permeable zones, which at the present are believed to result from fractures, have been successfully located by means of shallow-reading resistivity tools and/or the Fracture Identification Log.

GEOLOGY

The Devonian shale, which is a widespread Chattanooga age marine shale, has been known by many names: Brown, Black, Antrim, New Albany, Cinnamon, and Ohio. Fig. 1 is a typical Gamma Ray-Neutron log from the State of Ohio. It shows that the Devonian shale section extends from just below the Berea sandstone and Bedford shale to the top of the Columbus lime. The section can range in thickness from a few hundred to a few thousand feet.

*Mark of Schlumberger.
Figures are placed at the end of the paper.

Production is known to occur in several zones within this section. In certain portions of the basin, sandstones and silts exist just below the Bedford shale, as shown by Zone A. Production has also come from the "Brown and Black" shales, which includes the Marcellus shale, shown as Zone B. Since the sandstones and siltstones lend themselves to more conventional log analysis, only the Brown and Black shales will be considered from this point forward.

Core analysis has shown that the mineral content of the Brown and Black shales commonly consists of quartz (approximately 40 percent), illite (approximately 40 percent), chlorite, and kaolinite. Various trace elements, such as pyrite, uranium, thorium, titanium, barium, and boron, have also been found. In addition, the shale can contain as much as 15 percent organic matter. This matter is identified as Kerogen, a light hydrocarbonic solid.

There is still some question about the maximum porosity that can be expected; however, it is generally believed that it seldom exceeds 5 percent. A portion of this porosity can be due to a system of natural fractures. Matrix permeability values, generally less than 0.1 millidarcy, suggest that production comes from fracture systems.

OBJECTIVES OF LOG ANALYSIS

As with most other formations, the ultimate log analysis would result in the calculation of the volume of producible hydrocarbons. Since this total evaluation is somewhere in the future, short-term goals have been set. The first of these goals was simply to locate hydrocarbons within the section. The second was to locate any natural fracture systems. When both hydrocarbons and fractures (permeability) are present, production may be expected.

This information permits us to restrict our interest to only those zones which contain both hydrocarbons and fractures, eliminating all others. Stimulation procedures should thus be simplified and made more efficient.

To meet these objectives, the present log-based evaluation consists of determining:

- Pore space
- Hydrocarbon saturation
- Clay volume
- Kerogen volume
- Fracture detection

LOG RESPONSE

As stated previously, conventional log analysis appears to be inadequate when dealing with the Brown and Black shale. This is due to the several minerals and Kerogen that can be present in varying quantities. Fig. 2 shows densities and CNL* Neutron responses for some of these minerals. To permit an appreciation of the problems encountered, several log types will be examined individually. Typical responses are summarized in Fig. 3, and examples of actual logs (Gamma Ray, FDC* Density, CNL, Dual Induction-Laterolog*-8, and BHC* Sonic) are shown in Figs. 4, 5, and 6.

1. Gamma-Ray--In Zone A, the curve response is approximately 120 API units. This is the normal response in a shale section. Zone B, on the other hand, exhibits a much higher level of radioactivity. This higher response is due to the presence of larger quantities of uranium and thorium. Conventional log analysis depends very heavily on the Gamma Ray for determination of clay content. However, this technique can be misleading when dealing with the Devonian shale.

2. FDC Density--The porosity in the example is computed from the Density log, assuming a limestone matrix. The normal shale response of 2 to 5 porosity units is seen in Zone A. The porosity in Zone B appears much higher due to the presence of Kerogen which, we will see later, has a very low density.

*Mark of Schlumberger.

3. CNL Neutron--This neutron porosity is also computed assuming a limestone matrix. The porosity indicated in Zone A is in the 22-25 percent range. The neutron porosity in Zone B is higher, due to the presence of Kerogen, a hydrocarbon, which contributes to the hydrogen index and thus, to the porosity indicated by neutron logging systems.

4. Resistivity (Dual Induction-Laterolog-8)--The resistivity in Zone A is in the 15-20 ohm-m range. Because of the Kerogen, Zone B exhibits a much higher resistivity.

5. BHC Sonic--70 to 80 microseconds per foot is the interval transit time expected in a normal, highly compacted shale. This is the response in Zone A. Zone B has a longer transit time because of the presence of Kerogen.

The Brown and Black shales, thus the zones of interest, can be readily identified from the raw log data. However, when these data are used directly in a routine log analysis, the result is an unrealistically high porosity and correspondingly low water saturation. The problem is the presence of Kerogen. It is a hydrocarbon and is seen as such by the logs. However, in the mechanics of normal fluid production, it is a matrix constituent.

To eliminate the problem, the volume of Kerogen must be determined and the log data corrected for its effects. This is the basis of Kerogen Analysis.

Kerogen Analysis

Due to the complex nature of the Devonian shale (i.e., varying mineral and Kerogen content and relatively low porosity and permeability) a rather extensive logging program is required for complete analysis. This program consists of the logs discussed previously, namely:

1. Gamma Ray
2. FDC Density
3. CNL (or SNP) Neutron
4. BHC Sonic
5. Dual Laterolog or Dual-Induction Laterolog-8

The CORIBAND*[1,2] computer program was introduced some years ago for analysis of complex lithologies. To evaluate the Devonian shale, this technique was modified, resulting in the Kerogen Analysis program. It is based on known and assumed matrix characteristics of Kerogen, silt, and clay, as shown in Fig. 7. From this information, various crossplots can be made and the volume of the organic material calculated. The most useful crossplots appear to be the Neutron-Density, Fig. 8, and Sonic-Density, Fig. 9.

Kerogen volume is determined from the above crossplots by comparing the distance from the data point (x) to the Silt-Clay line with the distance of the Kerogen point from this same line. The Kerogen volume is selected from the minimum value from the two crossplots. The data point is then shifted to the Silt-Clay line, along the line projected through the data point from the Kerogen point. The Kerogen-free data thus obtained is then analyzed by CORIBAND.

The results of the computations are coded and presented as shown in Fig. 10.

TRACK 1 -- Formation Characteristics

- Secondary porosity indicator (cross-hatched areas)
  This indicates porosity other than intergranular, such as fractures or vugs.
- Gamma Ray (dotted curve)
  A reduced-scale Gamma Ray used for correlation.
- Average grain density (solid curve)
  A computed apparent grain density, including clay.

*Mark of Schlumberger.

TRACK 2 -- Production Characteristics

- Water saturation
  The percentage of clay-free pore space filled with water.

TRACK 3 -- Porosity and Fluids Analysis by Volume

- Porosity
  The curve to the left represents total clay-free porosity.

- Water-filled porosity
  The curve to the right represents the pore space that is water-filled.

- Hydrocarbon-filled porosity
  The area between the total porosity and water-filled porosity curves.

- Caliper minus bit size
  This curve represents hole size minus bit size in inches.

TRACK 4 -- Formation Analysis by Volume

- Clay volume
  The leftmost curve represents the percentage of clay.

- Kerogen volume
  This is the area just to the right of the clay volume, also a percentage.

- Other matrix
  This area represents the percentage sum of all other solids present in the formation.

- Porosity
  Clay-free porosity, as presented in Tract 3.

In addition to the film display, a tabular listing is alos presented, as shown in Fig. 11. The information is identical with the following exceptions:

1. Column 6 -- Average grain density of matrix other than clay.

2. Column 8 -- Cumulative porosity feet.

3. Column 9 -- Cumulative hydrocarbon feet.

Field Example of Kerogen Analysis (Fig. 12)

This is an example of a well in Northern Ohio which was completed by reference to the Kerogen Analysis log. Casing was set through the interval and perforated, one perforation at each point indicated by an arrow in Track 3. The perforations were placed at points where both hydrocarbons (Track 3) and secondary porosity (Track 1) were indicated.

The well was hydro-fraced. After a period of cleanup, a Temperature survey was run to locate gas entry into the borehole; a reduced-scale temperature curve is shown in Track 3. Although the temperature survey is not completely diagnostic, it does indicate that gas was being produced from those zones shown by Kerogen Analysis to contain hydrocarbons. However, the volume of gas produced by this well was too low to constitute a commercial success.

Fracture Detection

As stated previously, the existence of a natural fracture system is of the utmost importance if the Devonian shale is to be productive. To date, three separate techniques have been used with varying degrees of success.

1. Secondary porosity calculation; Kerogen Analysis

2. Resistivity profile

3. Fracture Identification Log

The following examples of fracture location with Kerogen Analysis and resistivity profiles are all from the same zone of the same well.

Secondary Porosity: Kerogen Analysis

In the earlier discussion of Kerogen Analysis, it was stated that corrections were applied to the log values for the presence of Kerogen. Other corrections are made for the effects of clay and light hydrocarbons. After these corrections, lithology is determined, and secondary porosity is found from the following relationship:

$$\phi_2 = \frac{\phi_{N\text{-}D} - \phi_{SV}}{\phi_{N\text{-}D}}$$

where ϕ = secondary porosity

$\phi_{N\text{-}D}$ = Neutron-Density crossplot porosity

ϕ_{SV} = Sonic porosity

Fig. 13 is an example of a well in West Virginia in which the shale section was cored. In Track 1 there is a comparison of the secondary porosity indicated by Kerogen Analysis and the fractures found in the core. It can be seen that there is some correlation; however, a more positive fracture detection system is needed.

Resistivity Profile

The qualitative analysis of resistivity-profile variations is a long-established technique for locating permeable zones. Even though we are searching for fractures instead of intergranular permeability, this technique seems to work quite well in the Devonian shale.

When dealing with a permeable zone and a salt mud system, a resistivity profile similar to Fig. 14 would be expected. The portion of the formation near the borehole would exhibit a lower resistivity than the undisturbed formation, due to invasion by the conductive drilling fluid.

Fig. 15 is a Dual Induction-Laterolog*-8-Microlaterolog* combination. There are four resistivity measurements, each having a different depth of investigation. The Deep Induction is the deepest measurement, then in order of decreasing depth of investigation we have the Medium Induction, Laterolog-8, and Microlaterolog. Also shown are the fractures found in the core. The resistivity profile indicated by the character of the log curves suggests that invasion of a low-resistivity fluid has occurred. It can be seen that a very good correlation exists between the fractures seen in the core and the invaded (therefore permeable) zones.

Fracture Identification Log

The log presentation of Schlumberger's High Resolution Dipmeter has been modified so that it can be used for fracture detection.† The technique is similar to that used in resistivity-profile evaluation.

The HDT* is designed to detect changes in conductivity. This is accomplished by using four focused electrodes on sidewall pads. The pads are spaced 90° apart so that all four sides of the borehole are covered. A separate conductivity-sensitive curve is recorded for each electrode. Any conductive fluid in a fracture will be detected if one or more of the pads cut that fracture. Fig. 16 illustrates the expected curve response.

* Mark of Schlumberger

† The suggestion for this overlay presentation is credited to John Humston of Hughes and Hughes, Beeville, Texas.

For fracture detection the log presentation of the High Resolution Dipmeter has been modified. It was found that by stacking curves from adjacent pads (1 and 2, 3 and 4) and by recording the curves on a 1:48 scale (25 inches = 100 ft.), a fracture will usually be seen on only one of each pair, and will thus produce separations between the two. Fig. 17 is an example of an FIL* run across a section of Devonian shale. The curve separation is quite apparent.

CONCLUSION

The original objectives of locating hydrocarbons and natural fractures in the Devonian shale have been met. More data is required, from both production and cores, to permit a more definitive evaluation of the Kerogen Analysis, but in the meantime it can be used qualitatively. Positive fracture detection, on the other hand, appears to be a reality. Either the resistivity profile method or the Fracture Identification Log provides satisfactory fracture identification under the conditions described here.

The logging program required to obtain the reservoir evaluation, including fracture detection, is as follows:

1. Gamma Ray
2. FDC* Density
3. CNL* or SNP* Neutron
4. BHC* Sonic
5. Dual Laterolog* or Dual Induction-Laterolog-8
6. Microlaterolog* and/or Fracture Identification Log

*Mark of Schlumberger

REFERENCES

1. Poupon, A., Hoyle, W.R., and Schmidt, A.W.: "Log Analysis in Formations with Complex Lithologies", Society of Petroleum Engineers of AIME, October, 1970. SPE Paper 2925.

2. Schmidt, A.W., Land, A.G., Yunker, J.D., and Kilgore, E.C.: "Applications of the CORIBAND Technique to Complex Lithologies", SPWLA Logging Symposium, May, 1971.

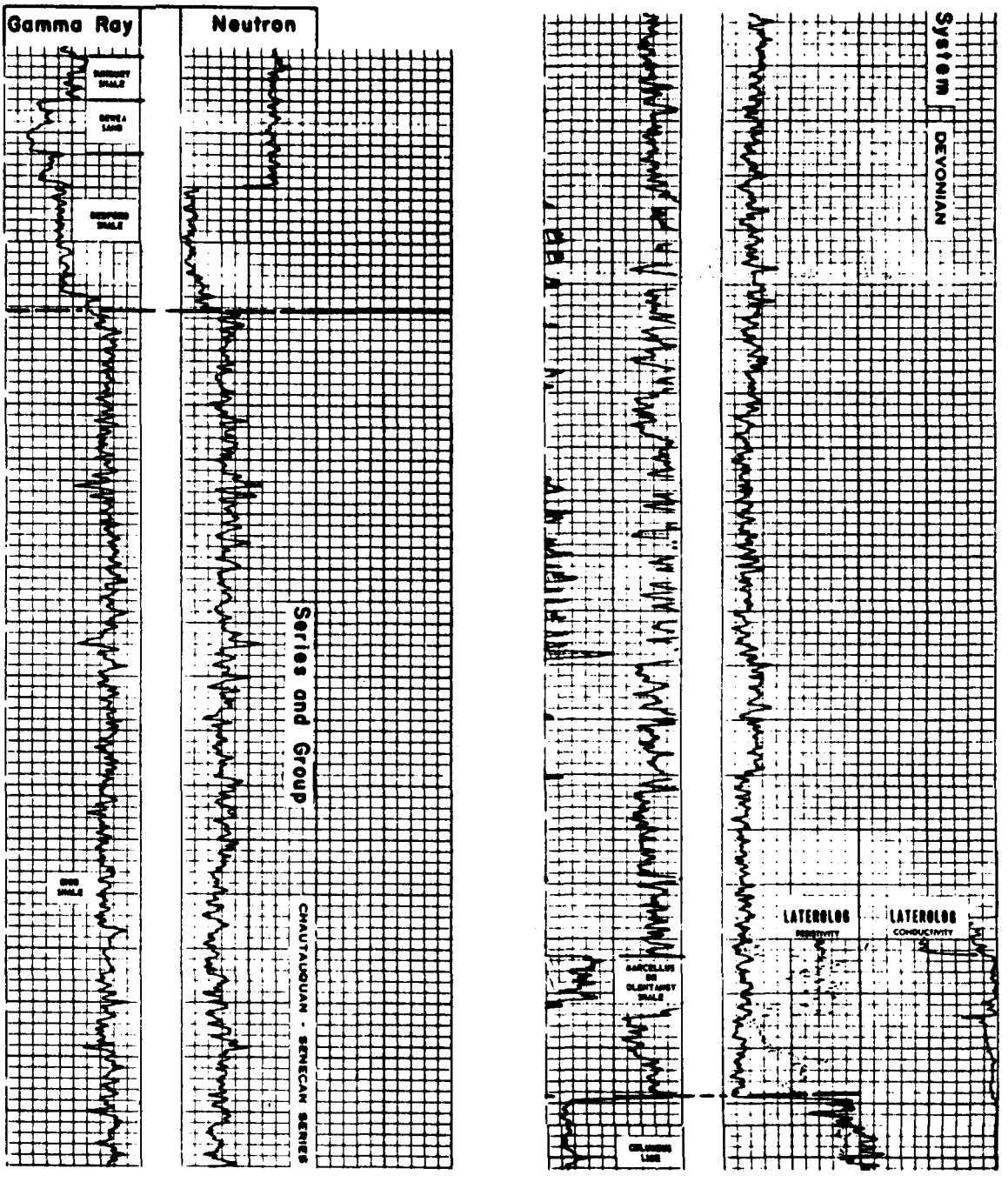

Fig. 1 - Typical Devonian shale sequence in Ohio.

MINERAL DENSITIES & CNL POROSITY

	ρ_g (gm/cc)	ϕ_{CNL} (Limestone)
KAOLINITE	2.65	51
CHLORITE	2.62-3.08	26-54
ILLITE	2.58-2.65	20-30
PYRITE	5.0	-6.7

Fig. 2

TYPICAL LOG RESPONSES IN DEVONIAN SHALE

DEVICE	SHALE (no Korogen)	SILT	SHALE (w/Korogen)
ILD ohm-m	10-20	30-50	Up to 2000
GAMMA RAY API Units	120	100	150-400
DENSITY gm/cc	2.6-2.7	2.5-2.6	2.3-2.6
SNP ϕ(Limestone)	14	15-18	18-20
CNL ϕ(Limestone)	26	20-30	20-36

Fig. 3

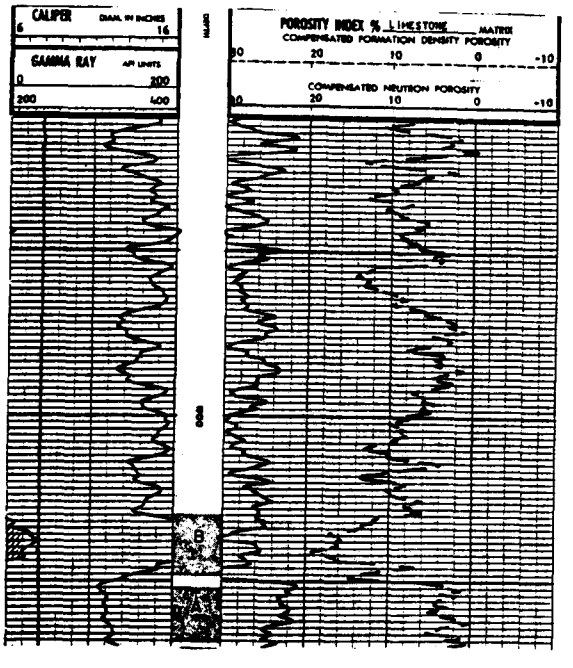

Fig. 4 - A typical CNL-FDC-GR log in Ohio.

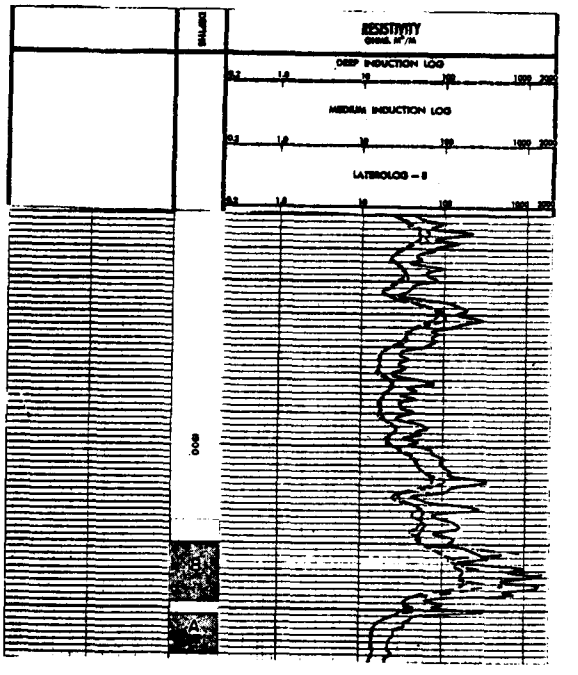

Fig. 5 - Dual Induction, same interval as Fig. 4.

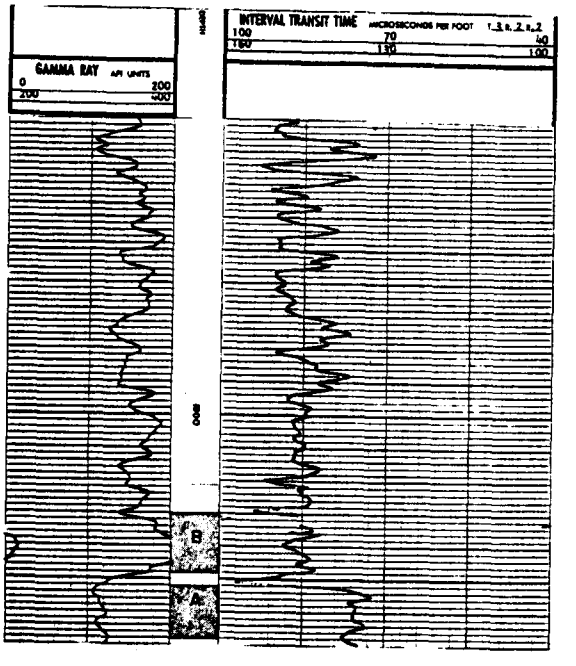

Fig. 6 - Sonic, same interval as Fig. 4.

PARAMETER SELECTION

DEVICE	SILT	CLAY	KEROGEN
SONIC (microsec/ft)	55.5	85	174
DENSITY (gm/cc)	2.68	2.82	1.10
SNP ϕ (Limestone)	-0.02	0.27	0.87
CNL ϕ (Limestone)	0.14	0.315	0.87

Fig. 7 - Parameters used in Kerogen Analysis processing.

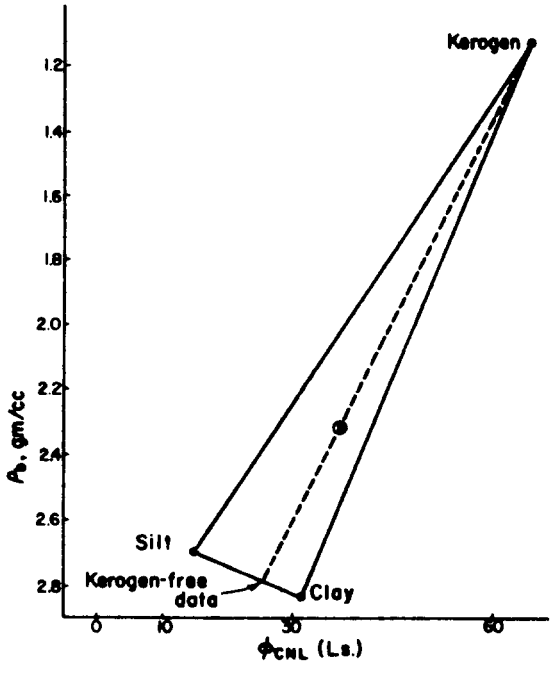

Fig. 8 - A typical N-D crossplot in Kerogen-bearing shale.

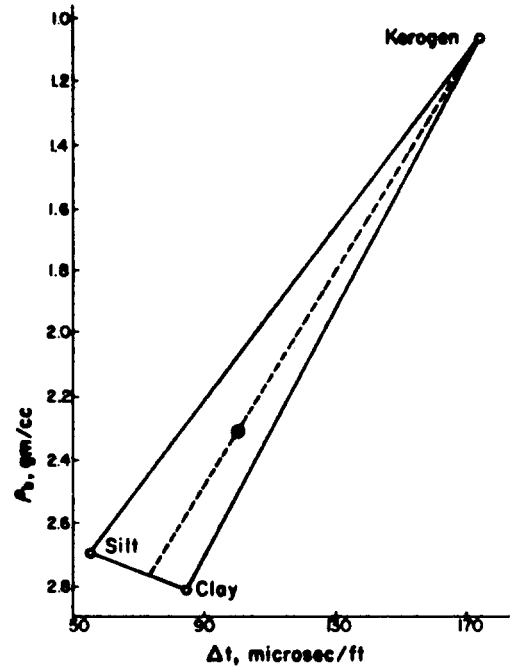

Fig. 9 - A Sonic-Density crossplot from the same zone as Fig. 8.

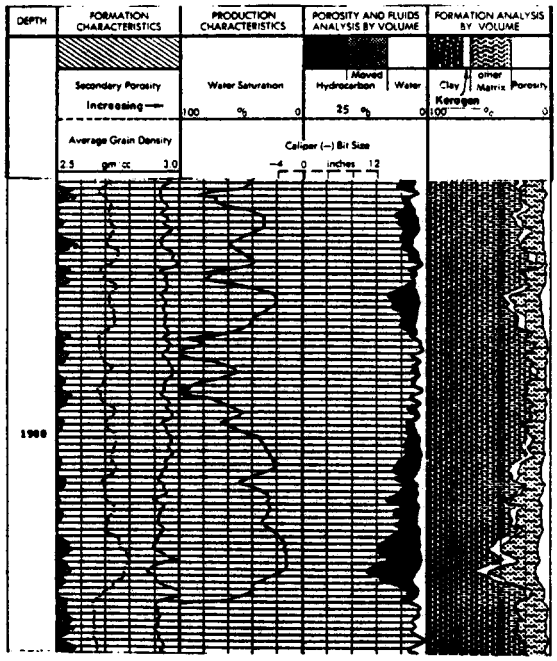

Fig. 10 - Representative output of the Kerogen Analysis.

DEPTH	KEROGEN VOLUME	WATER SAT.	POROSITY TOTAL	POROSITY SEC.	MATRIX DENSITY GM/CC	CLAY VOLUME	CUMULATIVE INTEGRATIONS PORE-FT	CUMULATIVE INTEGRATIONS HC-FT
1892.0	3.88	48	3.1	0.0	2.72	84	77.98	23.66
1893.0	3.38	51	2.7	0.0	2.71	86	77.95	23.65
1894.0	2.66	57	3.0	0.0	2.69	84	77.92	23.64
1895.0	1.34	66	3.9	1.2	2.68	76	77.89	23.62
1896.0	1.76	59	4.1	1.1	2.68	79	77.85	23.61
1897.0	1.73	53	3.7	0.9	2.69	81	77.81	23.59
1898.0	2.60	48	4.0	0.1	2.69	79	77.77	23.57
1899.0	4.47	39	3.7	0.0	2.74	81	77.73	23.55
1900.0	4.98	34	3.8	0.0	2.76	81	77.69	23.53
1901.0	5.91	32	4.1	0.0	2.78	79	77.66	23.50
1902.0	5.42	30	4.6	0.0	2.76	76	77.61	23.48
1903.0	4.74	28	4.3	0.0	2.75	78	77.57	23.44
1904.0	5.03	27	3.7	0.0	2.79	81	77.52	23.41
1905.0	4.02	25	3.9	0.0	2.78	80	77.49	23.39
1906.0	4.92	23	4.7	0.0	2.77	76	77.45	23.36
1907.0	5.26	22	5.0	0.0	2.76	76	77.40	23.32
1908.0	6.45	21	4.1	0.6	2.78	69	77.34	23.27
1909.0	7.46	22	6.5	0.5	2.79	67	77.28	23.22
1910.0	7.81	27	6.7	0.0	2.75	66	77.21	23.17
1911.0	5.99	37	6.0	0.0	2.73	69	77.15	23.13
1912.0	3.63	43	6.2	0.0	2.70	69	77.09	23.09
1913.0	1.68	51	4.7	1.8	2.68	73	77.02	23.06
1914.0	0.41	44	3.3	1.3	2.69	79	76.98	23.04
1915.0	2.75	38	4.8	0.8	2.71	75	76.95	23.02
1916.0	3.05	32	5.1	0.2	2.75	74	76.90	22.98
1917.0	3.33	27	6.2	0.0	2.70	68	76.84	22.95
1918.0	2.72	29	6.1	0.0	2.74	59	76.78	22.90
1919.0	3.22	27	7.7	0.7	2.71	61	76.69	22.84
1920.0	4.69	29	5.7	0.0	2.72	71	76.62	22.79
1921.0	5.64	25	5.8	0.1	2.74	70	76.57	22.75
1922.0	5.58	29	6.5	0.9	2.73	67	76.51	22.70
1923.0	4.92	27	6.5	1.0	2.72	67	76.44	22.65
1924.0	3.82	29	6.1	0.7	2.71	69	76.38	22.61
1925.0	3.48	31	5.6	0.6	2.70	70	76.32	22.56
1926.0	4.10	30	6.4	0.0	2.70	67	76.26	22.52
1927.0	3.66	27	5.2	0.0	2.72	73	76.20	22.48
1928.0	2.59	22	5.2	0.0	2.72	73	76.15	22.44
1929.0	3.51	20	6.6	0.0	2.73	67	76.09	22.40
1930.0	6.17	17	7.7	0.0	2.75	61	76.02	22.35
1931.0	7.59	15	8.3	0.0	2.76	58	75.95	22.28
1932.0	7.62	14	9.0	2.2	2.76	56	75.86	22.21
1933.0	8.54	13	9.6	0.9	2.76	51	75.77	22.13
1934.0	9.61	13	9.7	2.8	2.78	51	75.67	22.05
1935.0	11.23	12	8.8	1.8	2.83	55	75.58	21.98
1936.0	11.33	12	8.0	1.2	2.85	59	75.49	21.89
1937.0	11.72	12	7.4	0.8	3.00	62	75.41	21.82
1938.0	11.47	12	9.4	1.3	2.81	52	75.33	21.75
1939.0	11.38	12	10.8	1.9	2.79	48	75.24	21.66

Fig. 11 - Tabular listing of Fig. 10 data.

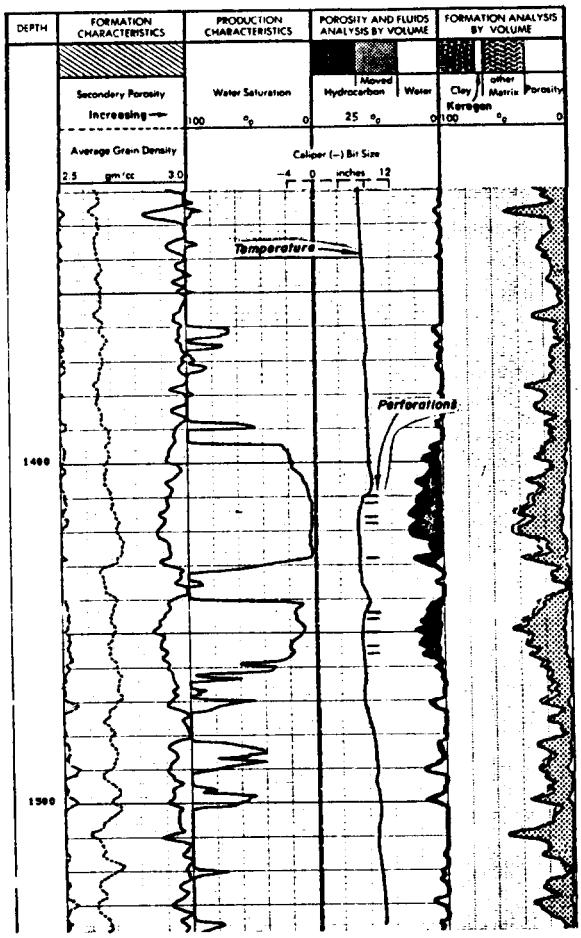

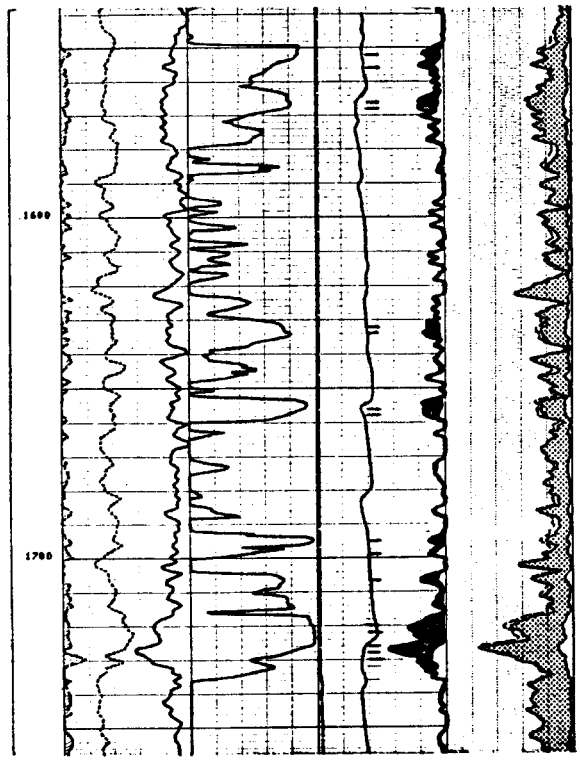

Fig. 12 - Computed log shows use of Kerogen Analysis in guiding completion.

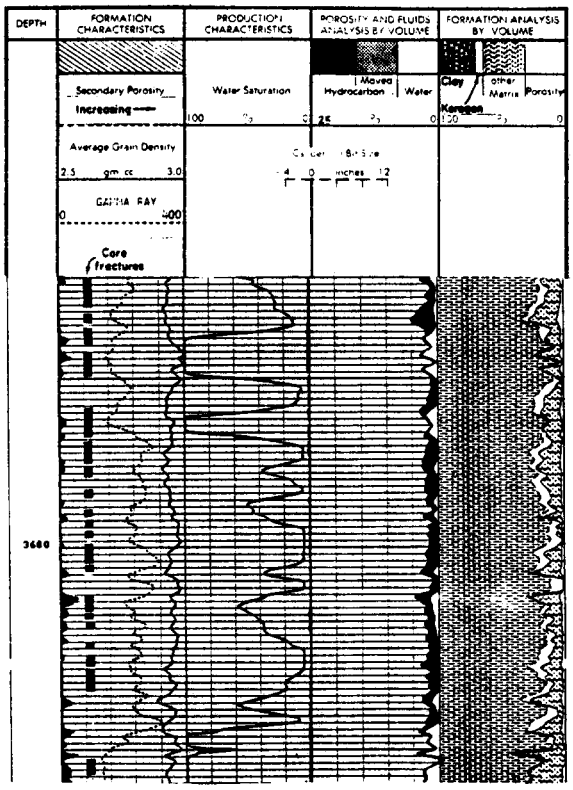

Fig. 13 - Kerogen Analysis shows some correlation with fractures.

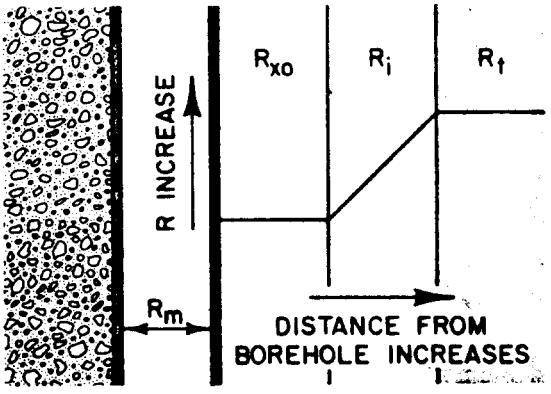

Fig. 14 - Schematic cross-section showing assumed resistivity profile.

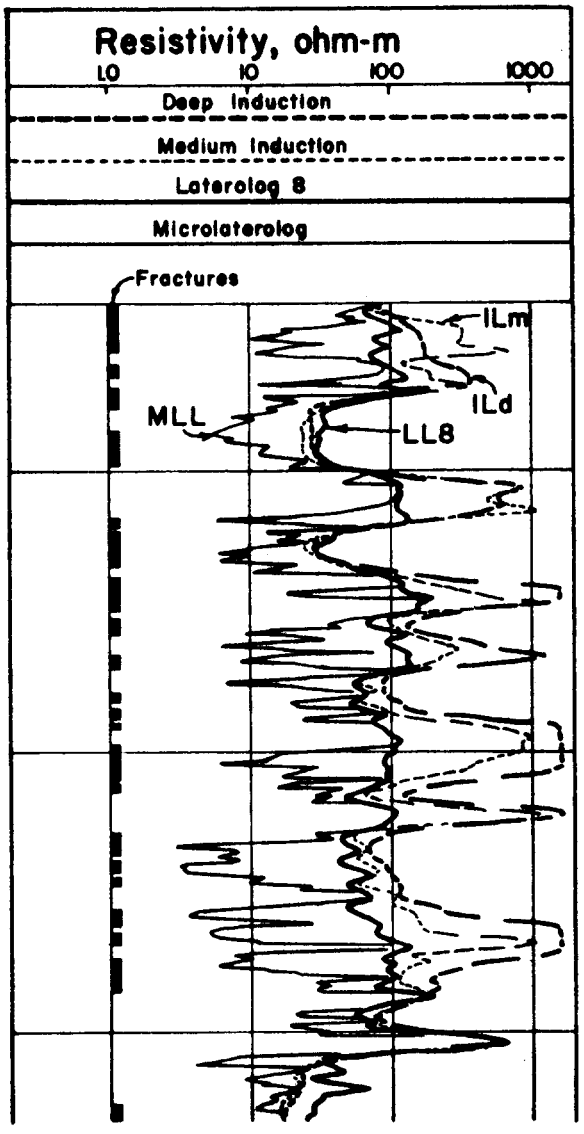

Fig. 15 - Resistivity log with four different depths of investigation shows influence of salt-mud invasion. Note correlation with fractures (shaded).

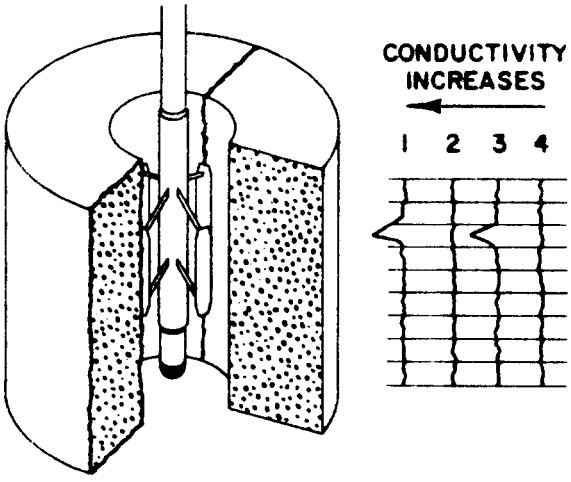

Fig. 16 - Schematic of Fracture Identification logging model; transverse fracture is seen by opposing pads.

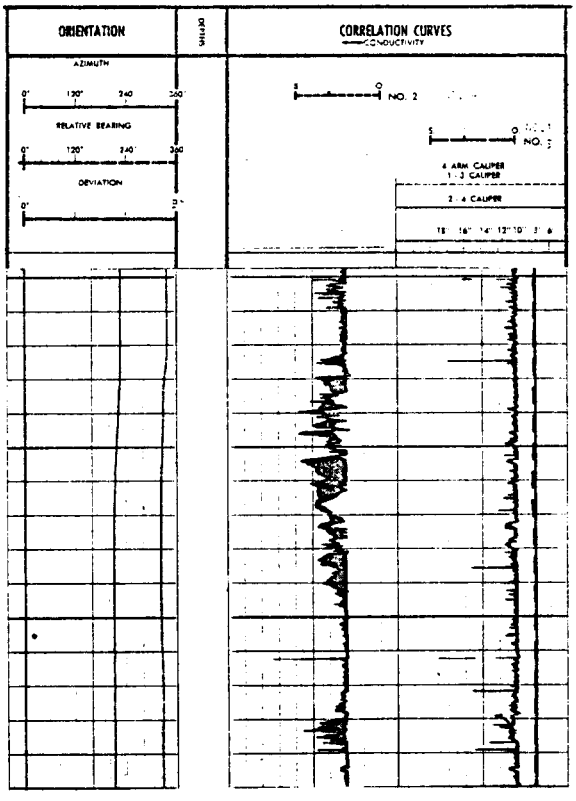

Fig. 17 - A typical FIL, showing separations between adjacent-pad recordings when fractures are present.

UPDATE ON THE LLL GAS STIMULATION PROGRAM*

M. E. Hanson, R. J. Shaffer, J. R. Hearst, G. D. Anderson,
D. N. Montan, H. C. Heard, and D. Emerson

Lawrence Livermore Laboratory, University of California
Livermore, California 94550

ABSTRACT

This report discusses the progress and current state of the Lawrence Livermore Laboratory research program on the stimulation of tight gas reservoirs. This is primarily a theoretical and laboratory program; however, the application and interpretation of geophysical logging is an essential part of it. The theoretical hydraulic fracturing models in their current state of development show that as the pore pressure is increased, the matrix stress around a fracture becomes more tensile. Laboratory experiments, which use unconfined specimens, show that both the characteristics of a layer and the mechanical properties of the adjacent materials control the fracturing in the region of the layer. We have acquired and interpreted some long-period seismic logging data. The preliminary analysis indicates gas-producing fractures intersecting the wellbore. Other fractures, which are either barren or do not intersect the wellbore, are also indicated by the data. Mechanical measurements of the Devonian shale indicate fairly uniform mechanical characteristics; however, a degree of mechanical anisotropy was noted for sections oriented horizontally or vertically with respect to the shale structure. Reservoir analyses of the Rio Blanco nuclear stimulation experiment and the nearby MHF experiment indicate that characteristic lens dimensions were 40 to 60 ft (12 to 18 m) vertically and 400 to 600 ft (120 to 180 m) horizontally.

INTRODUCTION

Although U.S. gas resources remain large, the proven U.S. reserves have declined to 230 trillion ft^3 (TCF). The current reserves/production ratio is 10 to 1. It is estimated that tight nuclear gas reservoirs and eastern Devonian gas shales contain large quantities of gas, but these resources have been difficult to recover. Some gas has been produced from these reservoirs already, but industry needs more economical recovery techniques.

Several techniques have been used to stimulate gas production. One of the most promising is massive hydraulic fracturing (MHF). MHF differs from hydraulic fracturing, which has been used in oil well completion and cleanup for many years, in that much larger amounts of fluid and proppant are pumped down the well and out into the formation to create and prop fractures at greater distances from the well. Other techniques include high explosive

*This work was performed under the auspices of the U.S. Energy Research and Development Administration under contract No. W-7405-Eng-48.

and nuclear explosive stimulation. They involve detonating explosives underground to fracture the rock and allow production. High explosive stimulation has been used extensively in the Devonian shales, and nuclear explosive stimulation has been tried in three western locations.

The application of MHF techniques to tight gas formations has given variable and sometimes disappointing results. The best efforts of a CER/Industry/Government consortium to stimulate the Piceance Basin near Rio Blanco, Colorado, have not been successful. On the other hand, Amoco has used MHF techniques in the Wattenburg field near Denver with a high degree of success. Significant differences in these reservoirs apparently contribute to the differences in the success ratio.

The Devonian shales present similar problems. It is believed that production from these gas shales results from the connection of the wells to the existing fracture patterns. Hence, the problems here include locating the producing zones, locating the natural fractures near the wellbore, and fracturing from the wellbore to the existing fractures.

The Lawrence Livermore Laboratory has embarked on a research program to help develop tight gas reservoirs in the United States. We are trying to obtain a more detailed understanding of the stimulation processes, including how the formation properties interact with and affect these processes. The problem is to determine how to connect the maximum amount of productive reservoir rock to the wellbore through a highly permeable fracture system. There are several questions that we would like to be able to answer in advance about Rocky Mountain areas. Can we identify particular sections where the fractures may be expected to be preferentially confined to the productive sands, resulting in a maximum volume of reservoir stimulated? What is the geometry (length, width, and number) of the fractures? What is the nature of the treatment (fluid composition, volumes, pumping rates, perforation intervals) which, when applied to a formation of certain properties, will result in optimum and economic recovery. What are some of the important geophysical measurements and experiments that can aid in this endeavor? What data and experiences exist that are relevant? Most of the western reservoirs contain a high degree of water saturation. High degrees of water saturation can significantly reduce the already low permeability of these reservoirs. Is it possible to use existing logging techniques supplemented by new geophysical measurements to ascertain the in-situ water saturation?

Devonian shales are also very low in permeability and therefore present many of the same challenges as the tight Rocky Mountain formations. There are, however, some special problems. Logging techniques for these shales are just being developed, and we have not been able to locate fractures that do not intersect the wellbore by means of standard logs. The effect of the hydraulic fracturing method on Devonian shales is not well understood. Water, one of the standard hydraulic fracturing fluids, can cause significant formation damage; organic and cryogenic fluids are expensive; high explosive fracturing makes well clean-out and completion costly and uncertain, and as we have shown previously,[1] the diameter of permeability enhancement is small. Gas fracturing is a developing art, and it shows promise for application in the shales.

Our program is primarily investigative in nature. No major field programs are currently proposed. We are constructing and applying theoretical models and performing laboratory experiments to develop an understanding of the stimulation processes. However, one facet of the program is directed toward geophysical measurement (logging) to provide insight into the environments where these stimulation processes are applied. Close association with the ERDA-supported field programs will provide the interaction and direction necessary to the program. The LLL program can be broken into seven task areas: (1) theoretical modeling of the hydraulic fracturing process; 2) hydraulic fracturing laboratory experiments; (3) log tool development and application and analysis of log data; (4) cataloging and evaluation of pertinent geological and geophysical reservoir data; (5) measurements of pertinent reservoir properties; (6) reservoir analysis; and (7) evaluation of other stimulation techniques.

THEORETICAL MODELING OF THE HYDRAULIC FRACTURING PROCESS

At the present time, two models are being used. One is designed to analyze the local effects of the hydraulic fracturing process (that is, the effects that control the orientation of the hydraulically created fracture) and the other to calculate some of the long range effects of fracturing processes such as surface deformations and stress fields across layering near the fracture. Results from the latter model are being compared with field measurements[2] to interpret fracture geometries.

The first model is much more complete in that pore fluid flow and pore pressure effects are included with the elastic model of the continuum. The model consists of the numerical solution of the two-dimensional time-dependent porous-flow equations, which overlays a static two-dimensional finite element description of the elastic continuum.[3] This allows the time solution to be controlled by the fluid flow into the fracture, while the static solution follows as a set of equilibrium states at each time step. We ignore the wave effects in the elastic solution. This approximation is valid since the wave speed is much larger than the propagation velocity of a fluid-driven fracture. For example, a fracture is driven on the order of 2000 ft in 5 to 8 h, while an elastic wave traverses this distance in 0.2 s. At present, the coupling between the elastic and flow parts of the code is in the pore pressure effects using the equation generally attributed to Terzaghi:[4]

$$\sigma^1 = \sigma^o - p, \tag{1}$$

where σ^1 is the total stress, σ^o is the solid matrix stress, and p is the pore pressure. The permeability of the fracture is calculated using

$$k = \delta^2/12, \tag{2}$$

where k is the permeability of the fracture and δ is the fracture aperature.

The hydraulic fracturing model, which includes the fluid flow and pore pressure effect is in an advanced development stage, and we will proceed with further development as application warrants. Calculations show that the model can allow a fracture to be pushed open by the fluid pressure

and then to close as the fluid is withdrawn. A failure criterion, which would permit fractures to nucleate and propagate has not yet been incorporated into the model.

The model has been applied in several check problems. The effects of the pore pressure on the elastic strain field can be readily seen by examination of Figs. 1 and 2. Figure 1 shows contours of the dilatation shortly after the fracture was pushed open by an injected fluid. Here we note two dilatational or tensional lobes near the crack tips and compressional lobes adjacent to the fracture faces. Figure 2 displays contours of dilatation after the pore fluid has propagated from the fracture into the medium. Here, we note that the compressional lobes have significantly decreased and the tensional lobes are more predominant.

The second model is essentially a static/elastic model. Pore pressure effects are not included. We used this model to study the effect of a layer on the general stress field and surface deflection properties above a vertical hydrofracture. As the problem geometry in Fig. 3 shows, we used half-plane symmetry to simplify the calculations. The layer, typified by Poisson's ratio ν_2, is embedded in a medium typified by Poisson's ratio ν_1. Young's modulus was held constant for both materials. We kept the hydrofracture location and width constant, but varied the layer depth a and the layer width w independently. We made ten calculations, then reversed the Poisson's ratios and redid the calculations. In some calculations, the layer was wholly below the hydrofracture. In most cases, the layer completely or partially contained the hydrofracture. For the problem shown in Fig. 3, we used $\nu_1 = 0.35$ and $\nu_2 = 0.20$.

At the top of Fig. 3 is a plot of the surface vertical displacements we obtained for the layer geometry shown. The general character of this curve was similar for the different cases, but a change in the hydrofracture location or width sometimes shifted the peak of the curve slightly and also caused the amplitude to change. The parallel strain along the surface, when plotted, also exhibited the same general characteristics as the surface displacement curve with the peak corresponding to the peak in surface deflection.

Figure 4 shows the general distortional field in the region of the hydrofracture. The most compressive stress is near the middle of the hydrofracture and the most tensile near the ends of the hydrofracture. Some of the lines have been omitted near the hydrofracture due to the large gradients in that region. The position of the layer is clearly visible on the contour map.

LOGGING

Acoustic velocity logs are often used in finding fractures near the wellbore.[5] We have used them for that purpose in the Devonian shales. A wet-hole tool often used is the variable-intensity-recording continuous-velocity log, marketed under such names as Microseismogram or 3-D log.[6] The data obtained with this log are normally recorded on film that moves past a slit at a rate proportional to the logging speed. An oscilloscope sweeps across the slit with each pulse of the sonde transmitter. The oscilloscope beam is intensity-modulated by the acoustic signal, producing a bright trace

for large positive amplitude, no trace for a large negative amplitude, and a medium trace for zero amplitude. This is recorded on the film as light and dark lines, with neutral gray for zero amplitude. Figure 5 shows such a record.

Such logs are satisfactory for locating fractures near the borehole, but since their sweep is generally quite short, the depth of observation is quite limited. The equipment can be operated with much longer sweeps if desired, although this is rarely done. At Columbia gas well No. 20403 near Huntington, West Virginia, two wet-hole logs were run with sweeps of about 30 ms (an order of magnitude longer than normal). Part of the record is shown in Fig. 6. The solid-looking straight vertical lines are water waves, boundary waves, etc.; the "hash" beyond them is presumably signal returned from reflectors far from the borehole. We hope to extract useful information from this late-time record, or "coda."

The coda is rather difficult to interpret as it stands. Therefore it was digitized on a microdensitometer. Unfortunately, the digitization had to be performed piecemeal, and the result was a record of film density vs position on the film, corresponding to signal amplitude vs depth and time. These records were input to a contour-plotting computer program, and two film-density contours were plotted for each section of record (Fig. 7). The contours were then redigitized with a hand-tracing type digitizer so that a new continuous record of a contour for the entire hole could be plotted. The result is shown in Fig. 8. Also shown in Fig. 8 are two logs (a sibilation log and a "fracture intensity log"), which are indicative of gas entering the borehole. Peaks in these logs seem to be associated with dips in the contour log. These dips indicate that a signal of a given intensity dies away sooner at that depth than at depths nearby; thus, the signal at that depth is weaker.

An explanation of why such a dip might be associated with a gas show has been suggested by R. C. Carlson of LLL. Assume that the signals seen in Fig. 6 have been scattered many times from fractures before arriving at the detector. If there are very few scatterers (fractures), no signal will be returned to the detector. This situation obtains in the top part of Fig. 6. If there are very many scatterers, the scattered signal will be greatly attenuated, and there will be very little signal at the detector. With an optimum number of scatterers, the signal will be largest. The dips in the contour, then, indicate a situation in which the signal has been greatly attenuated. This would suggest that there are many fractures and therefore recoverable gas.

Figure 9 compares the logs in Fig. 8 with a number of others in the same hole. Of them, only the acoustic-amplitude and the 3-D logs (run with a transmitter/receiver spacing of 30 cm) seem to show anomalies not associated with lithology. In both logs, the gas shows at 3100 ft and 3800 ft are associated with anomalies. The 3-D log suggests that a fractured region begins at 3100 ft and ends at 3800 ft. The amplitude log shows a low-amplitude region there, which indicates fracturing, but there is nothing on these logs to indicate the individual gas shown. Therefore, the log-sweep acoustic log seems to be the most promising one currently available.

Eric Smith of Columbia Gas Company has shown that peaks on a natural gamma-ray log are associated with the presence of kerogen in Devonian shale. A number of samples from Columbia Gas well No. 20403 near Huntington, West Virginia, were analyzed with gamma-ray spectroscopy. David Coles of LLL performed the analysis. Four of the samples were light in color, presumably low in kerogen, and four were dark, presumably because of high kerogen content. A high gamma count was found associated with the dark samples.

David Coles of LLL also analyzed for gamma-rays due to ^{40}K and the chains of ^{232}Th, ^{238}U, and ^{235}U. He used a Ge(Li) detector, which sees each gamma peak in detail, and came out with a table of disintegrations per minute for each of the four nuclides of interest. The table does not explain the gamma-ray log of well No. 20403 by itself, and so it is not reproduced here.

The gamma-ray log in that hole was evidently performed with a Geiger-Muller counter, which does not discriminate between the gamma rays. The ^{232}U chain produces eight. When Coles' results are multiplied by these factors, the result clearly explains the log. Figure 10 shows the gamma-ray log in well No. 20403, with Coles' data, multiplied as above, properly scaled, and with the two uranium chains added. It is obvious that the majority of the count-rate difference is caused by the uranium.

Table 1 shows a geologist's description of the cores at each depth point. The high-count points are also the darkest in color. Looking at the powdered samples, the color difference is very clear between the dark samples at 2740, 3055, 3220, and 3720 and the other four.

We may safely conclude that the difference in count rate between the dark and light samples is caused by isotopes of uranium. Cole has written a paper that shows that coal is similarly enriched in uranium.[7] This paper may explain why the uranium is present in the kerogen.

MECHANICAL MEASUREMENTS OF DEVONIAN SHALE

Prediction of fracture intensity, geometry, and extent resulting from high-explosive or hydraulic-fracturing stimulation of a low-permeability, gas-bearing formation requires certain equation of state (EOS) or mechanical measurements as input to the calculational codes. These measurements include: tensile strength, failure envelope (under pressure), loading moduli, loading path (up to the failure envelope), and pressure/volume behavior.

To characterize the mechanical behavior of the 10-cm core from Columbia gas well No. 20403, we elected to subdivide it into four distinct units. These were:

Upper gray member	807-1039 m
brown gaseous member	1039-1116 m
white slate member	1116-1203 m
Marcellos black shale member	1203-1233 m

Each of these units was then treated as an individual rock for the purposes of defining an EOS. For each unit, we have planned to determine:

1. The tensile strength parallel and perpendicular to bedding, 0.1 MPa.

2. The uniaxial stress failure envelope in compression to $\sim$ 300 MPa confining pressure, parallel and perpendicular to bedding.

3. The uniaxial stress failure envelope in extension to 400-600 MPa confining pressure, parallel and perpendicular to bedding.

4. The pressure/volume behavior to 1.5 GPa.

5. The loading path in uniaxial strain (compression) beginning at 0.1 and 50 MPa confining pressure. Loading direction both parallel and perpendicular to bedding.

6. The shear and compressional wave velocities to confining pressures of 1.0 GPa (measurements made both parallel and perpendicular to bedding for the determination of dynamic elastic constants).

During this past year, we have determined all eight sets of measurements under item 1 above (two directions in each of four rock units). These are summarized in Table 2. In general, there does not appear to be any discernible trend in strength with either depth or between rock units (for the same orientation). The tensile strength parallel to the bedding seems to be about two times that measured normal to bedding.

We have also completed all measurements outlined in item 2. Typical results are illustrated in Figs. 11-14. In each figure, the compression failure envelope for the virgin shale is defined by the points. At low-moderate pressures, the failure mode is termed brittle in all cases and is the result of combined tensile and shear fracture. The former dominates at low pressure and is oriented parallel to the maximum principal stress σ_1. However, the latter becomes dominant at moderate-high pressures and is oriented at $\sim$ 30° to σ_1. At the highest pressures tested, these shale units frequently become ductile, that is, all deformation is quasi-uniformally distributed within the test sample. The brittle-ductile (B.D.) transition point usually occurs at lower pressures for loading normal to bedding than for compression parallel to it (Figs. 11 and 12). Also shown in these figures is the post-failure strength envelope, designated by points Δ. This surface delineates the shear strength of the fractured shale vs confining pressure. At the brittle-ductile transition, there is no strength decrease upon failure, only distributed flow, and hence, the two curves become identical at higher pressures (Figs. 11-14). Comparison between Figs. 11 and 12 suggests that at similar pressures, this shale unit has only about a 10 to 20% strength anisotropy with loading direction. Loading parallel to bedding seems to be strongest (except at the lowest pressure), but more brittle than for perpendicular to bedding.

Determination of the failure envelope in uniaxial stress loading for extension (item 3) has been completed for 5 of the 8 possible combinations (two directions in each of four rock units). Examples of these failure envelopes are illustrated in Figs. 13 and 14 for comparison with the compression curve. At low pressures, this extension envelope always is much lower than that for compression; at high pressure, it may remain lower (Fig. 13) or it may exceed it (Fig. 14).

The pressure/volume behavior (item 4) of units 1 through 3 is summarized to 4.0 GPa in Fig. 15. This figure clearly indicates that the known gaseous shale member is the most compressible (except at low pressure), followed by the Marcellus black shale member, and the white slate member. Volume changes at 210 GPa, for example, are about 9.2%, 8.3% and 6.5%, respectively for the three members. Each curve shown in Fig. 15 is based on the average of 3 or more tests. These results are unaffected by sample orientation.

Also shown in Figs. 11 through 13 are the uniaxial strain loading paths as described in item 5 (above). In each case, regardless of the initial starting pressure, this loading path rapidly becomes sub-parallel to the virgin compression envelope curve at about one-half of that value. Large hysteresis occurs upon unloading (Fig. 11).

Acoustic velocities listed under item 6 have not been completed. These, as well as the remaining work noted above, will be completed in the next quarter.

LABORATORY EXPERIMENTS ON HYDRAULIC FRACTURE

A laboratory experimental program has been established to provide a better understanding of the initiation and growth of a fluid-driven crack. The parameters to be considered are: (1) the mechanical properties of the solid, i.e., elastic moduli, strength, etc., (2) the physical state of the solid, i.e., presence of pre-existing cracks, porosity, layering, etc., (3) the boundary conditions, such as free surfaces, applied overburden stresses, etc., and (4) the manner in which the crack-driving fluid is injected into the solid.

The overall goal of this research is to explain how these parameters determine the details of crack growth such as direction, orientation with respect to fluid injection hole, growth rate, and forking or dividing. We also seek an understanding of how a crack behaves in the region near an interface, both in a single material and between two materials having dif different properties. Clearly, laboratory-scale experiments cannot simulate all conditions encountered in an actual in-situ hydraulic fracture experiment. However, it is felt that the understanding gained will definitely be useful in the design of large-scale fracture operations.

We have begun by investigating experimental techniques of generating hydraulic fractures and controlling and observing their growth. A few experiments have been performed on rocks, but for the majority, we have used polymethylmethacrylate (PMMA) as the fracture medium. Its transparency permits easy observation of interior cracks.

The technique used to induce hydraulic fractures in all experiments so far has been to inject pressurized oil into the sample through a borehole cased with a steel injection tube. A short, uncased, smaller-diameter portion of the borehole is located at the bottom of the injection tube so that the injection tube rests on a shoulder as shown in Fig. 16. The steel injection tube (0.250 in. O.D.) is slightly smaller in diameter than the borehole

(0.280 in. I.D.) and is secured in the borehole by a mixture of Hysol epoxy. To give a definite direction to the work, we sometimes use a special tool to make a small pre-crack in the open portion of the borehole below the injection tube. The dashed line in Fig. 16 denotes such a pre-crack. This technique has been used so far only in PMMA fracture experiments. In each experiment, prior to connecting the injection tube to the hydraulic pressure line, we fill the injection tube and borehole section with hydraulic fluid so that all air is displaced. Pressure is applied with a hand-operated pump.

Early in the program, a series of experiments were performed to assess the relative fracturability of several rock types to be used in future experiments. The test samples were generally cylinders 2 to 5 in. in diameter and 6 to 12 in. in height. The rocks chosen were Indiana limestone (porosity about 15%), Nugget sandstone (porosity about 5%) and three types of shale. Fluid injection holes were fabricated along the cylinder axis as described above. The Indiana limestone and Nugget sandstone were found to be the strongest of the rocks tested. They fractured in the 5000 to 6000 psi injection-fluid pressure range. The planes of these fractures were parallel to the borehole as shown in Fig. 17. The shales were found to be much weaker, fracturing in the 1200 to 1600 psi injection-fluid pressure range. The shale fractures were in the bedding planes, which in these experiments were perpendicular to the boreholes.

These preliminary experiments in rocks yielded little quantitative data other than the relative fracture strengths of the different rock types. Future experiments are planned to assess the effects of externally applied stress fields and the rate of fluid injection on hydraulic fracture generation.

Experiments to study the effect of an external stress field were performed using PMMA. The test specimens were 4 in. cubes. In the first two experiments, the pre-crack was oriented parallel and perpendicular to the faces upon which a 2000 psi load was applied as shown in Figs. 18a and 18b. In the first case (Fig. 18a), the crack developed from the pre-crack at a borehole pressure of 2500 psi and grew parallel to the applied stress. In the second case (Fig. 18b), a new crack formed at a borehole pressure of 7000 psi and grew parallel to the applied stress. This new crack was independent of the pre-crack. In a second set of two experiments, the pre-crack was oriented at 45° to the cube faces along the diagonal as shown in Figs. 19a and 19b. In one case no external load was applied, and the crack grew as a continuation of the pre-crack at a fluid pressure of 2500 psi as shown by the dashed line in Fig. 19a. In the second experiment, a 2000 psi load was applied. At a 3000 psi borehole pressure a crack grew from the pre-crack but turned and grew parallel to the applied load as shown by the dashed line in Fig. 19b.

To study hydraulically driven crack motion near an interface, a block of PMMA (8 in. x 8 in. x 4 in.) was sectioned into three pieces as shown in Fig. 20. The interfaces I_1 and I_2 were machined flat. Interface I_1 was

bonded by a thin film of chloroform. Interface I_2 had no bond. The assembly was loaded with a stress of 2000 psi as shown in Fig. 20. The borehole was pressurized to 3000 psi, where fracture occurred. The fracture did not cross either of the interfaces, but was contained in the shaded area shown in Fig. 20. In a similar experiment in which Indiana limestone was bonded to PMMA with no external applied stress, the crack crossed the interface from PMMA into the limestone. However, when the injection hole was put in the limestone and an attempt was made to drive the crack from limestone into PMMA, the crack would not cross the PMMA-limestone interface.

RESERVOIR ANALYSIS

As part of our study of hydraulic fracturing as a stimulation method, we have performed further evaluations of the nuclear-explosive-stimulated well (RB-E-01) located about one mile from the massive hydraulic fracture experimental well (RB-MHF-3) near Rio Blanco, Colorado. In this experiment, three 30-kt nuclear explosives were emplaced at depths of 5480, 6230, and 6690 ft, respectively. The upper explosive was in the Fort Union formation, while the lower two were in the Mesa Verde formation. These are the same two formations studied in the MHF well.

The explosives were detonated as planned on 17 May 1973. The explosively fractured region was reentered thru the emplacement well and initial production testing commenced in November 1973. The initial drawdown (during which $\sim$ 35 mmscf of gas were produced) indicated that contrary to original expectations, the production originated only from the chimney volume created by the top explosive, not from the three chimneys combined. Additional production of about 65 mmscf during the first two weeks of February 1974 reduced the chimney pressure to about 450 psi, and there was still no indication of communication with the lower chimneys. (Rare gas tracers had been emplaced with each of the explosives to give a measure of the contribution from each chimney.)

In late 1974, the lowermost chimney was entered by slant drilling from a well (RB-AR-2) offset about a quarter of a mile. Approximately 25 mmscf of gas were produced in December 1974, and this lowered the chimney pressure from an initial 1900 psia to just over 1200 psia. The well was then shut-in to monitor the pressure buildup. An early indication that the well was connected to gas sands of limited extent was the initial pressure of 1900 psia, which was about 1000 psi lower than hydrostatic.

After several months of pressure buildup, an attempt was made (via modeling studies) to evaluate the characteristics of the formation feeding the chimney and the stimulation due to explosive fracturing. We used a computer model, which simulated the chimney, fractures, and formation. The gas-flow calculations were done using the TRUMP computer program.

The basic modeling procedure involved assigning values to the various model parameters (permeability, pay height, permeability enhancement due to fracturing, and chimney size), driving the model with the known production history, and then comparing the calculated chimney pressure history with the measured pressures. After changing the value of one or more of the parameters, the process was repeated over and over until a reasonable match was obtained between the calculated and measured pressure histories.

This early modeling led to a pair of models that appeared to bracket the somewhat scattered data. These models used permeabilities of 5 and 10 μd, respectively, and a pay height of 50 ft. The radial extent of the models was effectively infinite. With the passing of time, the effect of finite lens size became evident as the calculated pressures continued to rise while the observed buildup essentially stopped. Further modeling directed at a study of the lens size led to the conclusion that a 10-μd permeability and a 50-ft pay height, with an effective outer boundary radius of womewhat under 400 ft would fit the data reasonably well. However, the observation that the pressure history could be interpreted as showing a slight late-time decline (within the scatter of the data) prompted a reconsideration of the model.

It was recognized that the chimney, initially at a temperature of perhaps 600°F, would be very slowly cooling; however the low rate, on the order of 0.1°F/day, would be only a small perturbation as far as the change in gas density was concerned. It was then realized that the vapor pressure of water (which contributes to the total pressure in the chimney) changes many times more rapidly in this temperature range than does the absolute temperature. A thermal model of the chimney and surrounding rock was constructed to obtain an approximate thermal history of the chimney. This model indicated that during the 600 days following the start of buildup the chimney temperature declined only 40°F (from 500°F to 460°F), while the vapor pressure of water dropped 300 psi (from 700 to 400 psia).

Further work led to a model with a formation permeability of 10 μd, a pay height of 60 ft, and an effective lens radius of 450 ft. The calculated and measured pressure-vs-time histories are shown in Fig. 21. Figure 22 shows the fracture-induced permeability used in the model.

GEOLOGIC STUDIES FOR GAS STIMULATION MODELS

Realistic models for the stimulation of gas from the Devonian brown shale of the Appalachian Basin and the low-permeability western gas sandstone require a careful consideration of the geology of each reservoir. In contrast to the tight sandstone, the shale has a lower gas-filled porosity, (about 2% versus 5%) a lower reservoir pressure (they are shallower and have less-than-normal pressure gradients), and a very low gas permeability (less than 1 μd vs about 2 μd). However, the reservoirs are thick (about 400 ft) and extensive (55,000 to 110,000 square miles).

The Western sandstone formations are considerably more variable. Not only do they show a wider range of physical properties, they are geometrically variable. Figure 23 shows the geographical distribution of basins with low-permeability sandstone reservoirs. Areas like the Denver Basin have predominantly thin, but extensive marine margin sandstone deposits that are amenable to stimulation by long fractures. A few units of this type exist near the basin of the Mesa Verde formation in the Piceance and Uinta Basins. However, most of the reservoirs in these latter basins are flurial and lacustrine deposits, elongated lenses within shale. The stimulation technique and analysis must take the spatial variations of these continental deposits into consideration. A typical channel-fill deposit in the Piceance Basin Mesa Verde formation is 25 ft thick, 350 ft wide, and 3,500 ft long. Clearly, a fracture generated across the width need not exceed 350 ft in length. To be

effective, a single well should be completed by stimulating each sand zone according to its own characteristics. Detailed studies of typical basins are now underway to provide the necessary information for an understanding of local variations and their effect on stimulation methods.

REFERENCES

1. C. R. McKee, M. Hanson, and R. Terhune, Permeability from Single and Multiple Detonations of Explosive Charges, Lawrence Livermore Laboratory, Livermore, CA., Rept. UCRL 28207, Rev. 1 (1976).

2. M. McKann, R. Hay, and L. Bartel, Massive Hydraulic Fracture Mapping and Characterization Program, First Annual Report, August 1975 through July 1976, Sandia Laboratories, Rept. SAND-77-0286 (1977).

3. M. Hanson, C. McKee, D. Emerson, B. Qualheim, J. Hearst, and R. Terhune, Quarterly Report: The LLL Massive Hydraulic Fracturing Program for Gas Stimulation, April-June 1976, Lawrence Livermore Laboratory, Rept. UCRL 50036-76-2 (1976).

4. J. C. Jaeger and N. G. W. Cook, Fundamentals of Rock Mechanics, Chapman and Hall, 1969.

5. J. I. Myung and R. W. Baltosser, Fracture Evaluation by the Borehole Logging Method, Birdwell Division, Seismograph Service Corporation, Tulsa, Oklahoma.

6. R. L. Geyer and J. Myung, "The 3-D Velocity Log: A tool for in-situ determination of the elastic moduli of rocks," 12th Annual Symposium on Rock Mechanics, University of Missouri, Rolla, Missouri, Nov. 16, 1970.

7. D. G. Coles, R. C. Rogaini and J. M. Ondov, The Behavior of the Natural Radionuclides in Western Coal-Fired Power Plants, Lawrence Livermore Laboratory, Rept. UCRL 78940 (1976).

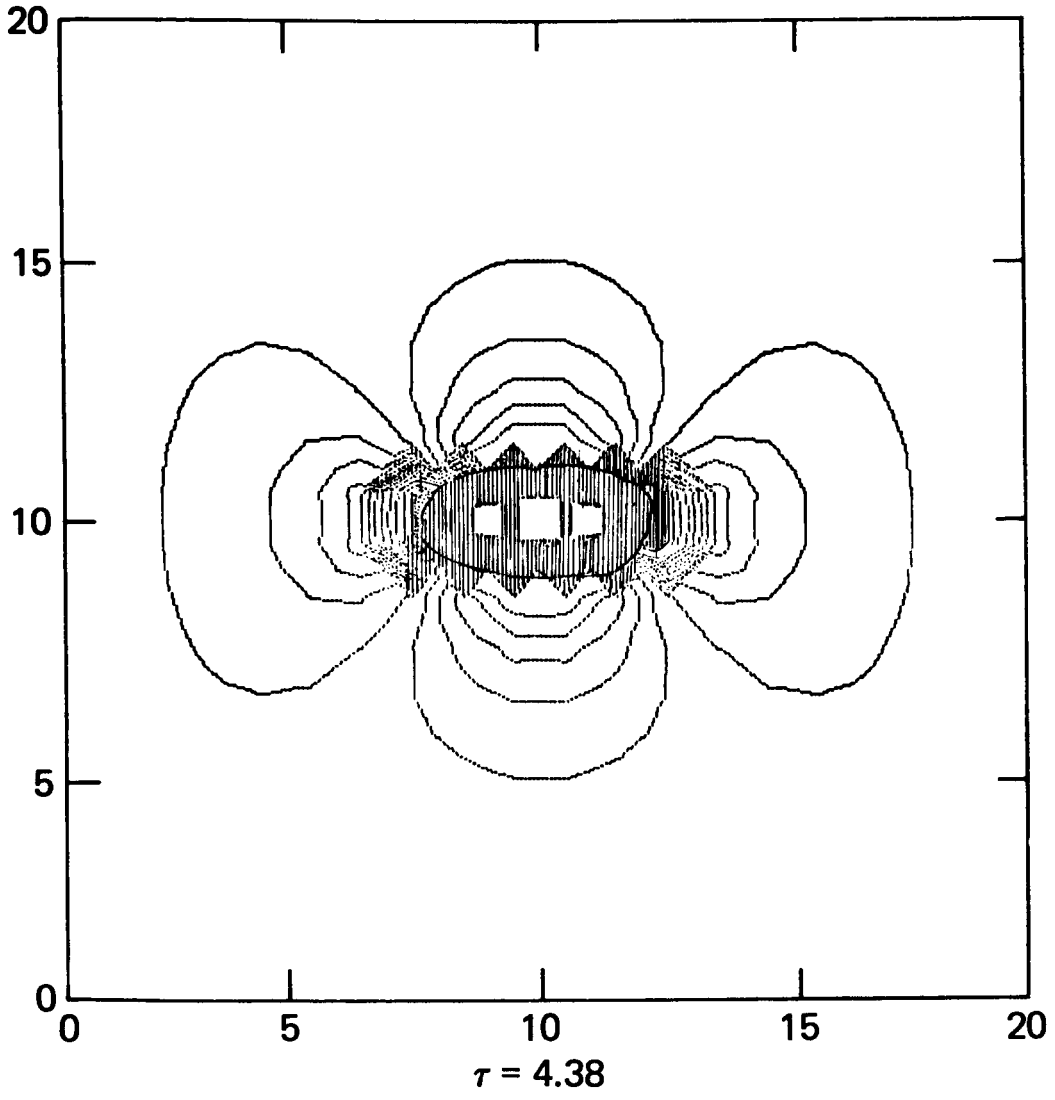

FIGURE 1. Dilatation contours around a pressure-opened fracture at $\tau = 0.44$, where $\tau = \frac{k}{\mu(\alpha+\eta\ \beta)}\frac{t}{L^2}$; k is the permeability of the medium, μ is the viscosity of the injected fluid, α is the compressibility of the elastic matrix, η is the porosity, β is the compressibility of the injected fluid, t is the problem time, and L is the length of the fracture.

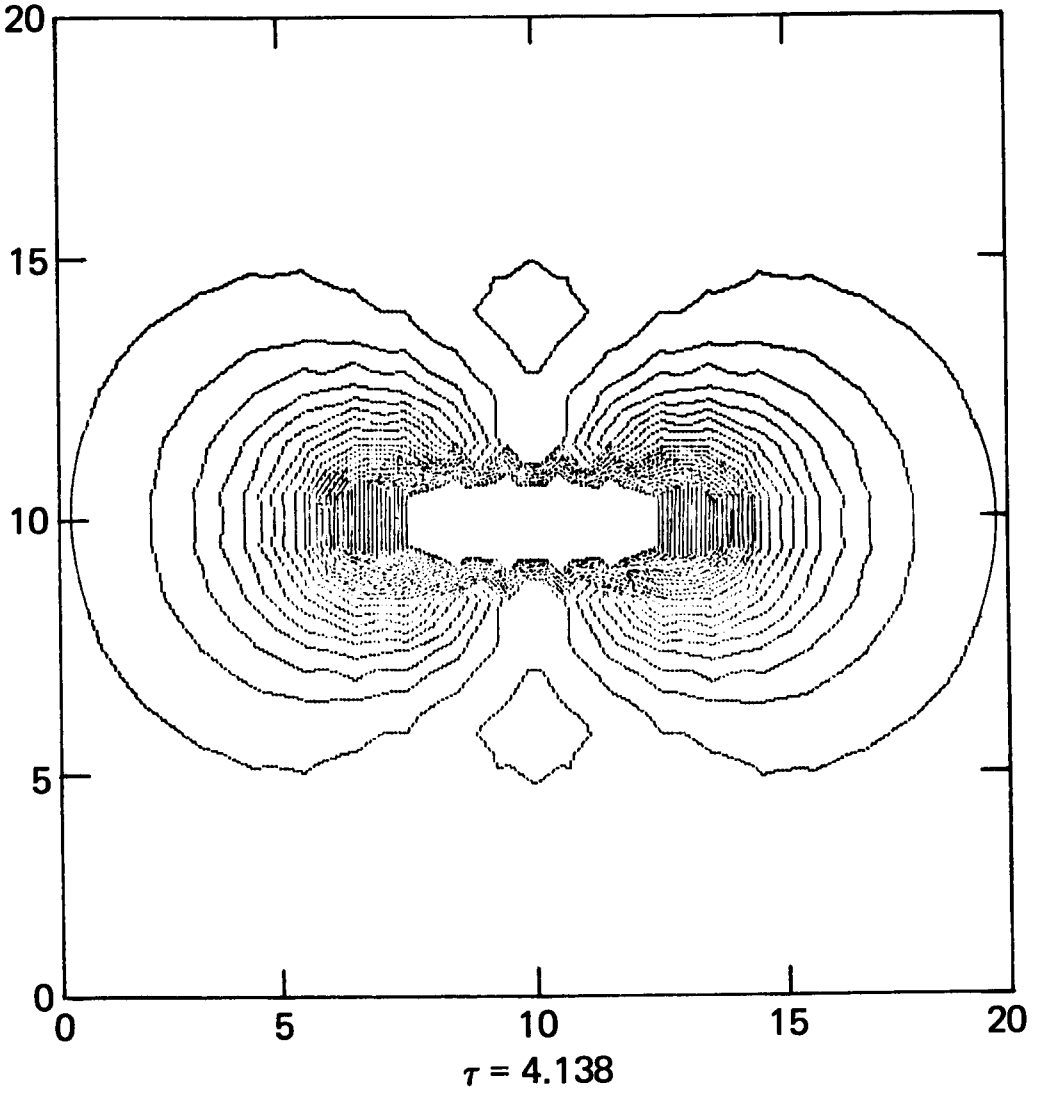

FIGURE 2. Dilatation contours around a pressurized fracture at $\tau = 4.138$. See Fig. 1 for a definition of the nondimensional time τ.

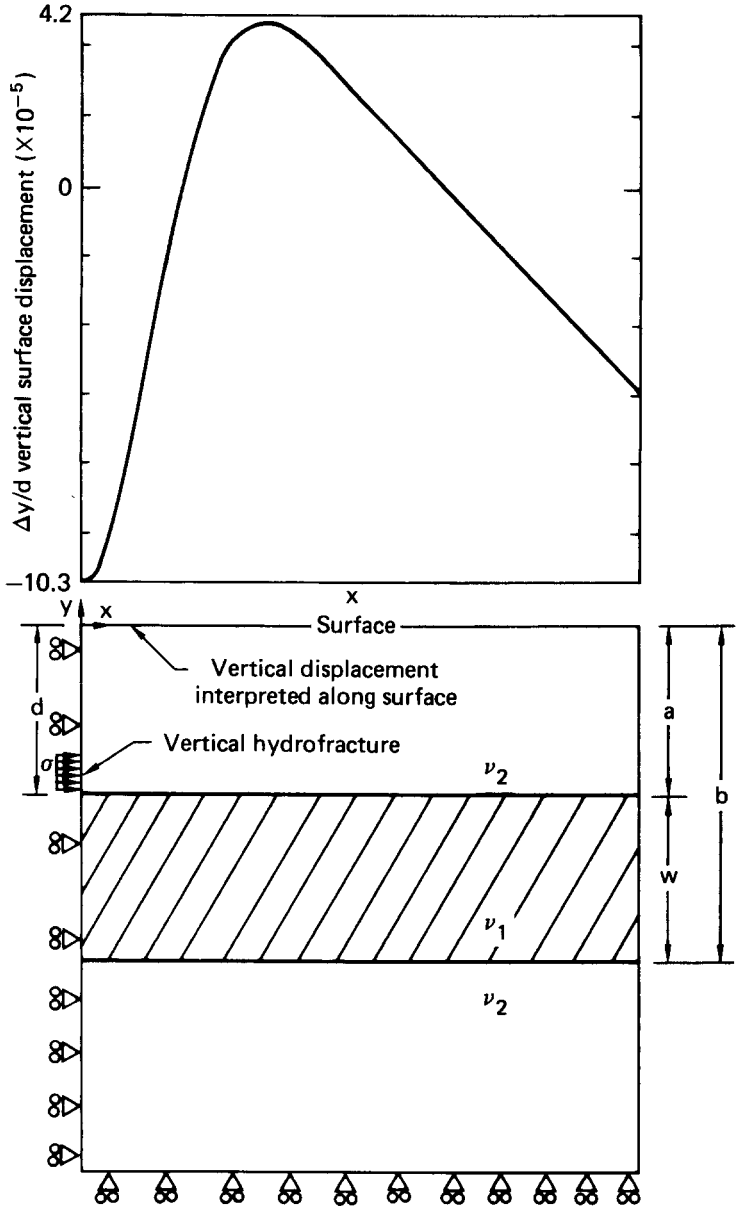

FIGURE 3. Representation of a vertical hydrofracture in a layered medium. Vertical displacements of the surface are shown at the top of the figure.

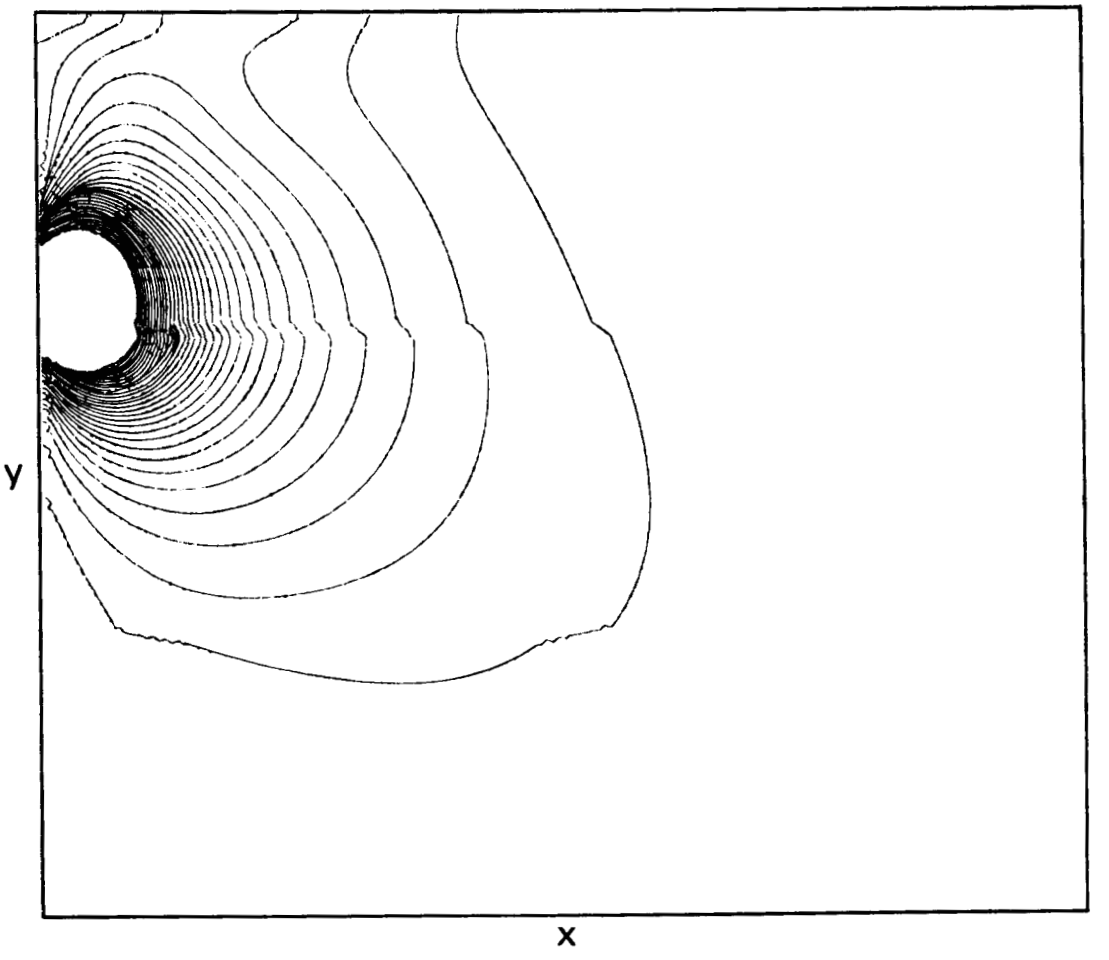

FIGURE 4. Distortional contours for the problem geometry shown in Fig. 3. Distortion is defined as $|\varepsilon_1-\varepsilon_2|$ where ε_1 and ε_2 are the principal strains.

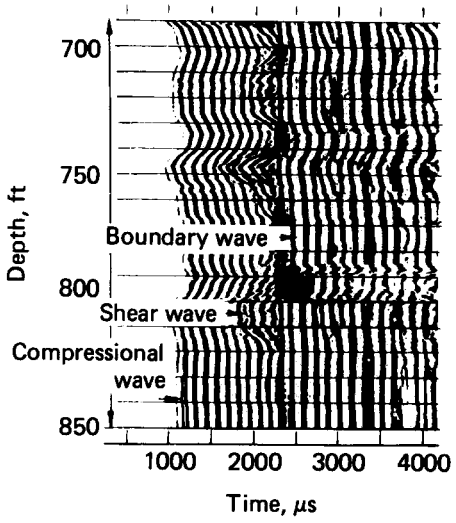

FIGURE 5. Illustration of typical intensity-modulated, continuous-velocity (3-D) log.

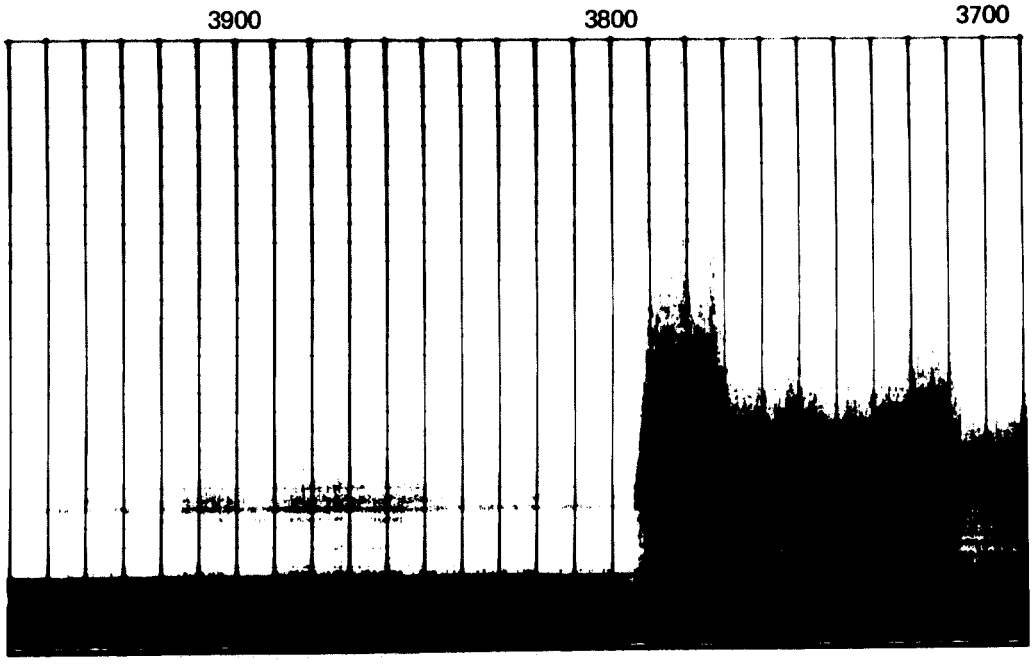

FIGURE 6. Part of long sweep logging record for Columbia gas well No. 20403 (signal is for 3690 ft to 3960 ft).

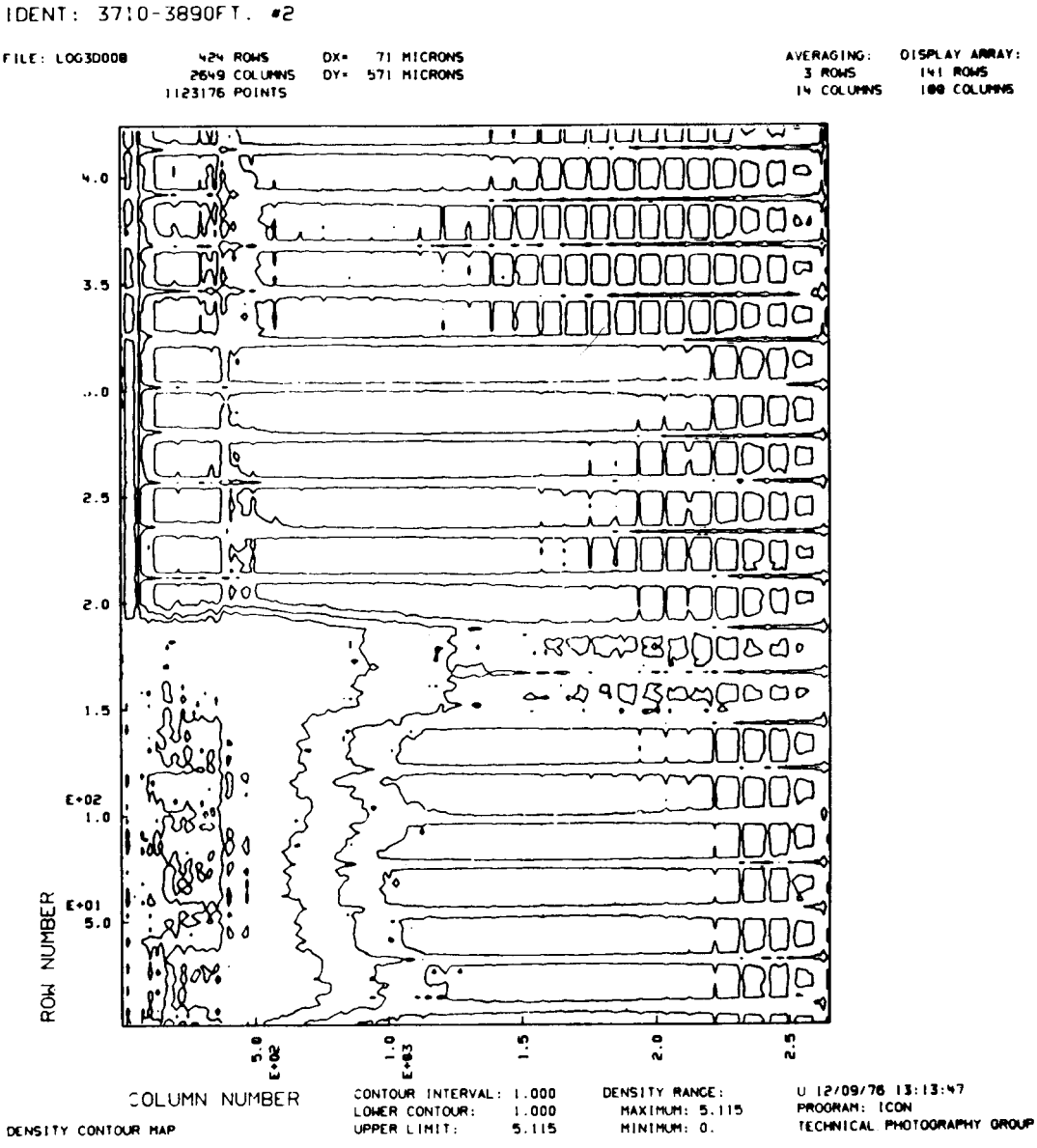

FIGURE 7. Initial contours for a segmented, digitized, sonic-logging record for Columbia gas well No. 20403.

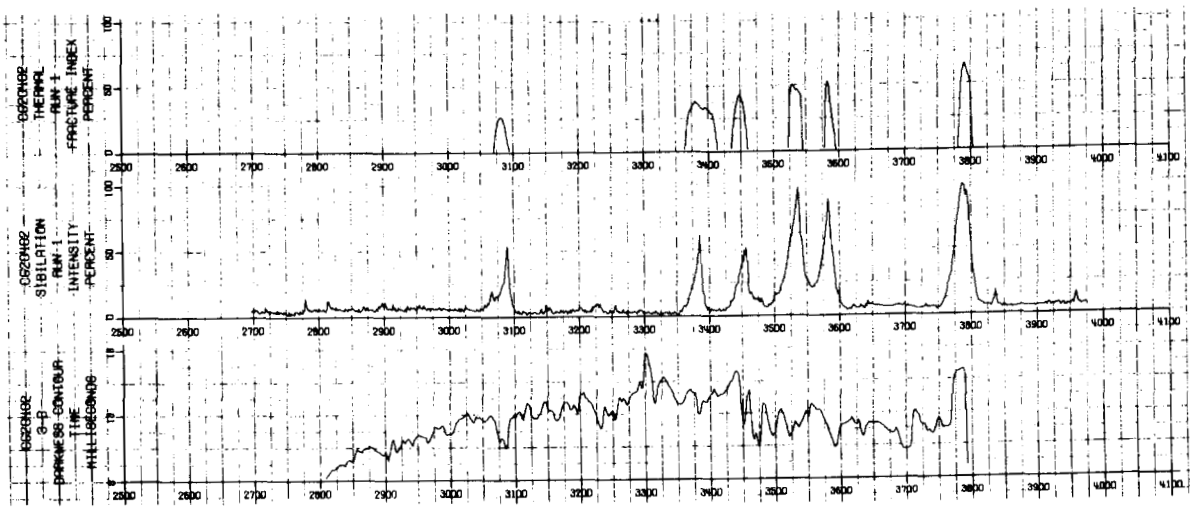

FIGURE 8. Composite of processed sonic logging record with two other logs (the sibilation log and a fracture intensity log), which indicate gas entering the borehole.

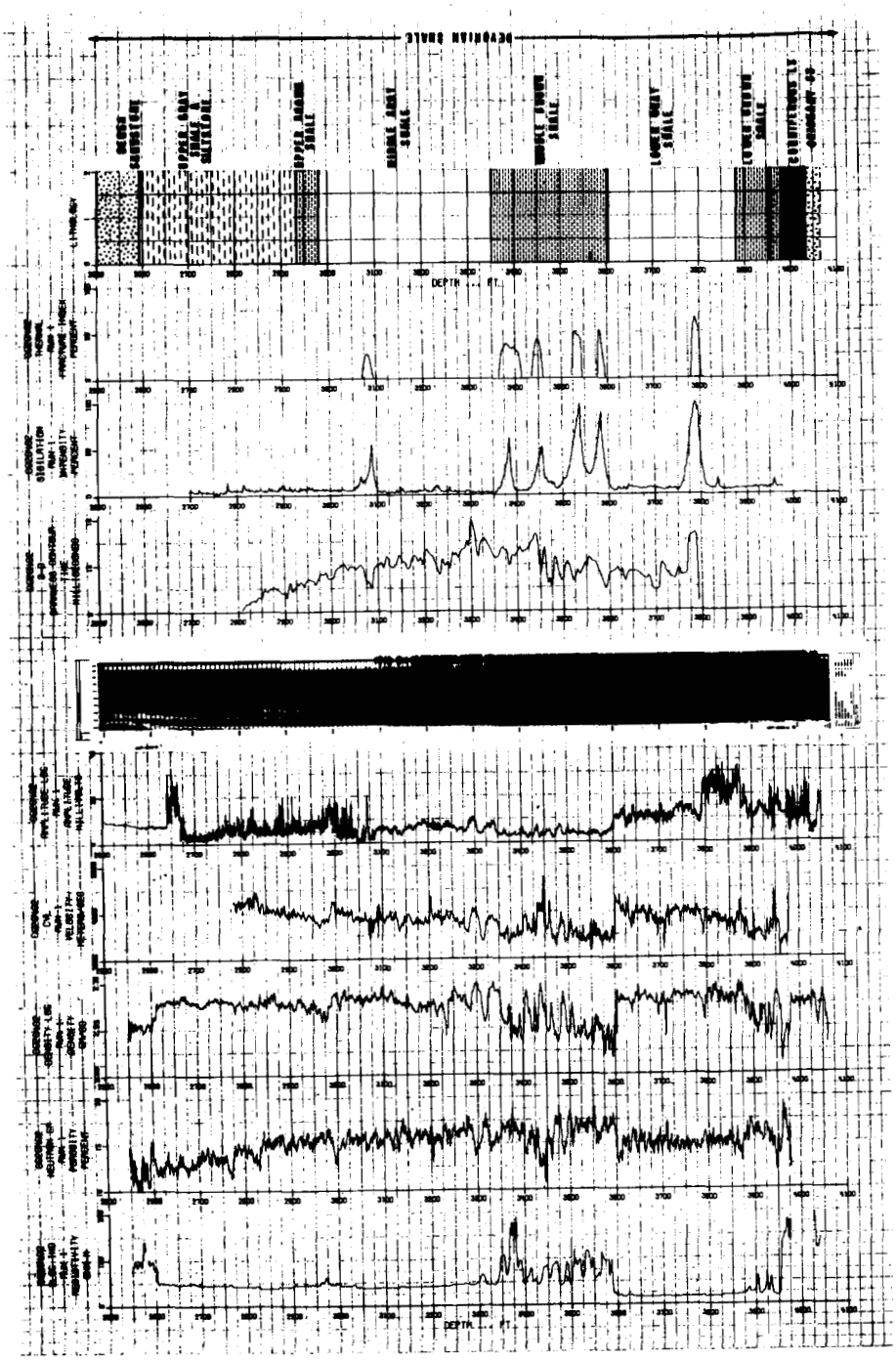

FIGURE 9. Composite borehole geophysical logs for Columbia gas well No. 20403.

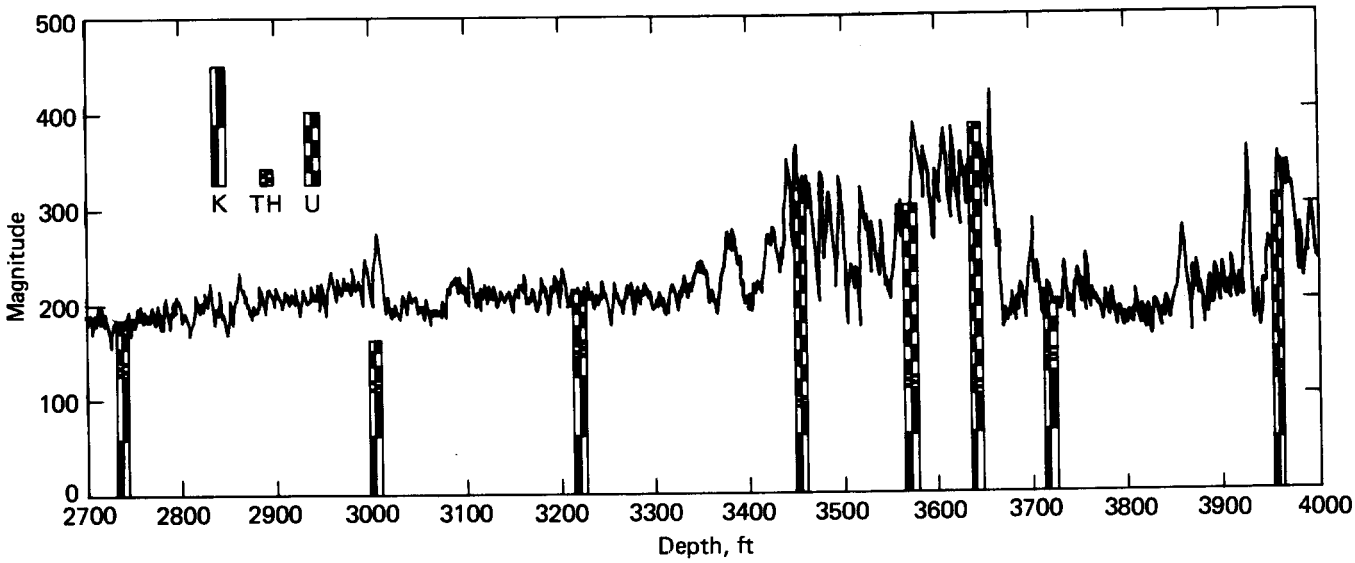

FIGURE 10. Gamma ray log for Columbia gas well No. 20403, properly scaled showing ^{40}k, ^{232}Th and ^{238}U.

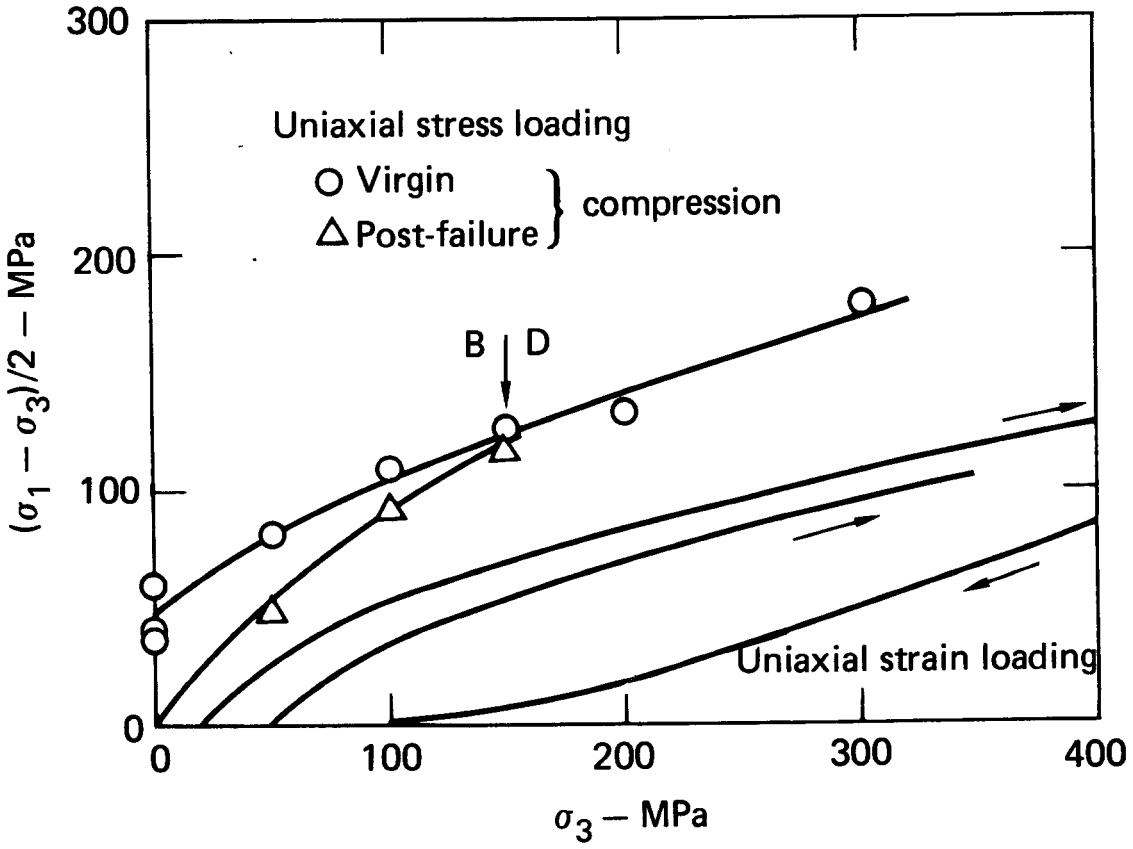

FIGURE 11. Failure envelopes for core from Marcellus black shale section for Columbia gas well No. 20403. Samples tested were perpendicular to bedding.

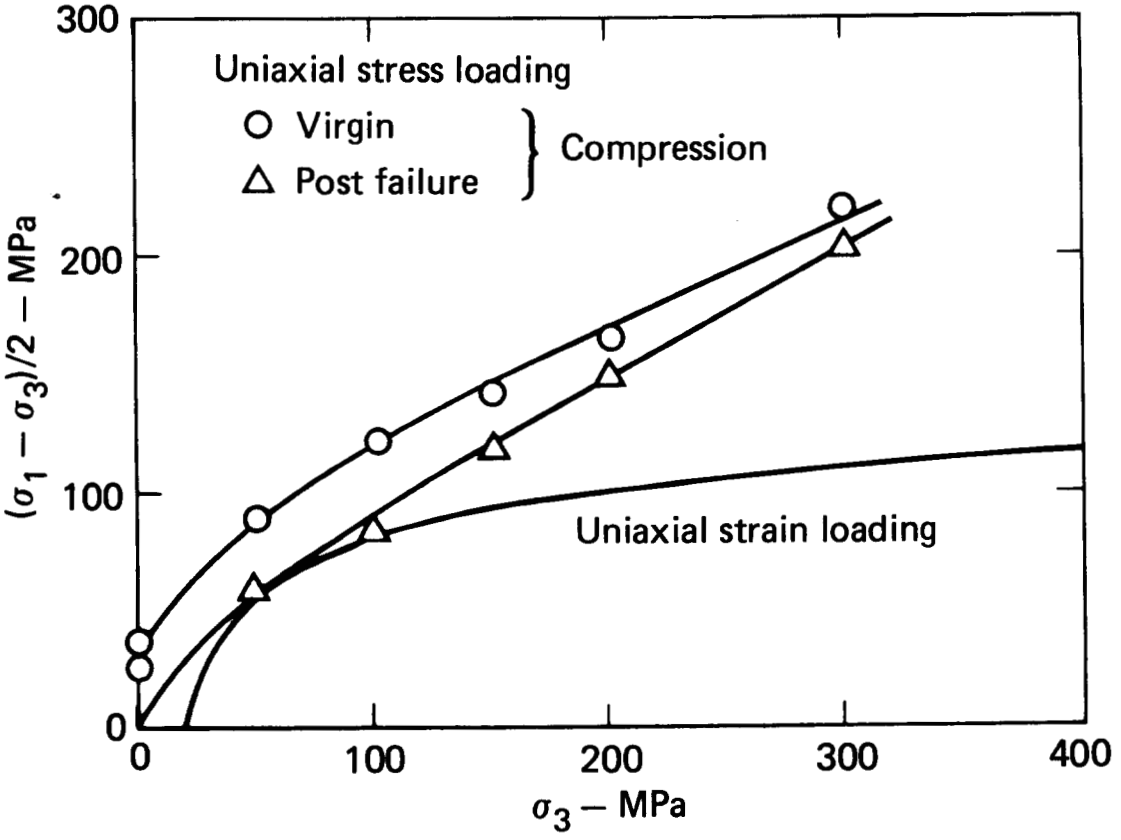

FIGURE 12. Failure envelopes for core from Marcellus black shale section for Columbia gas well No. 20403. Samples tested were parallel to bedding.

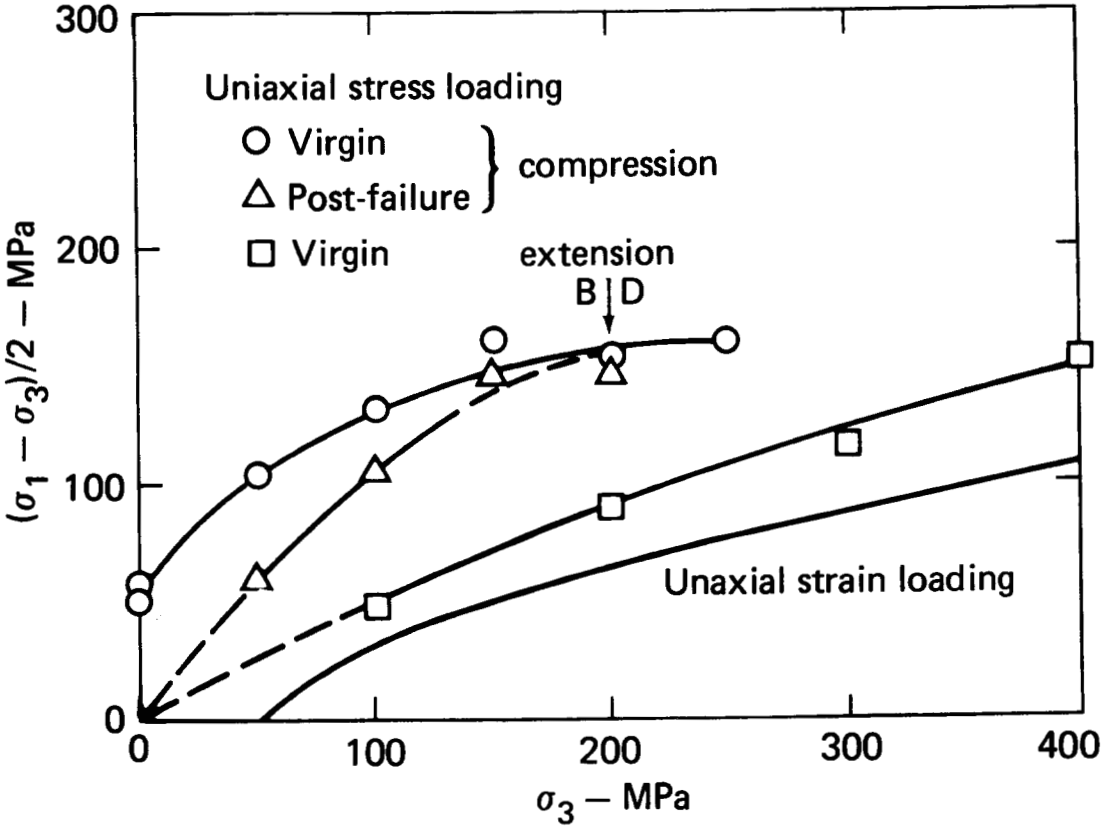

FIGURE 13. Failure envelopes for core from brown gaseous shale section for Columbia gas well No. 20403. Samples were perpendicular to bedding.

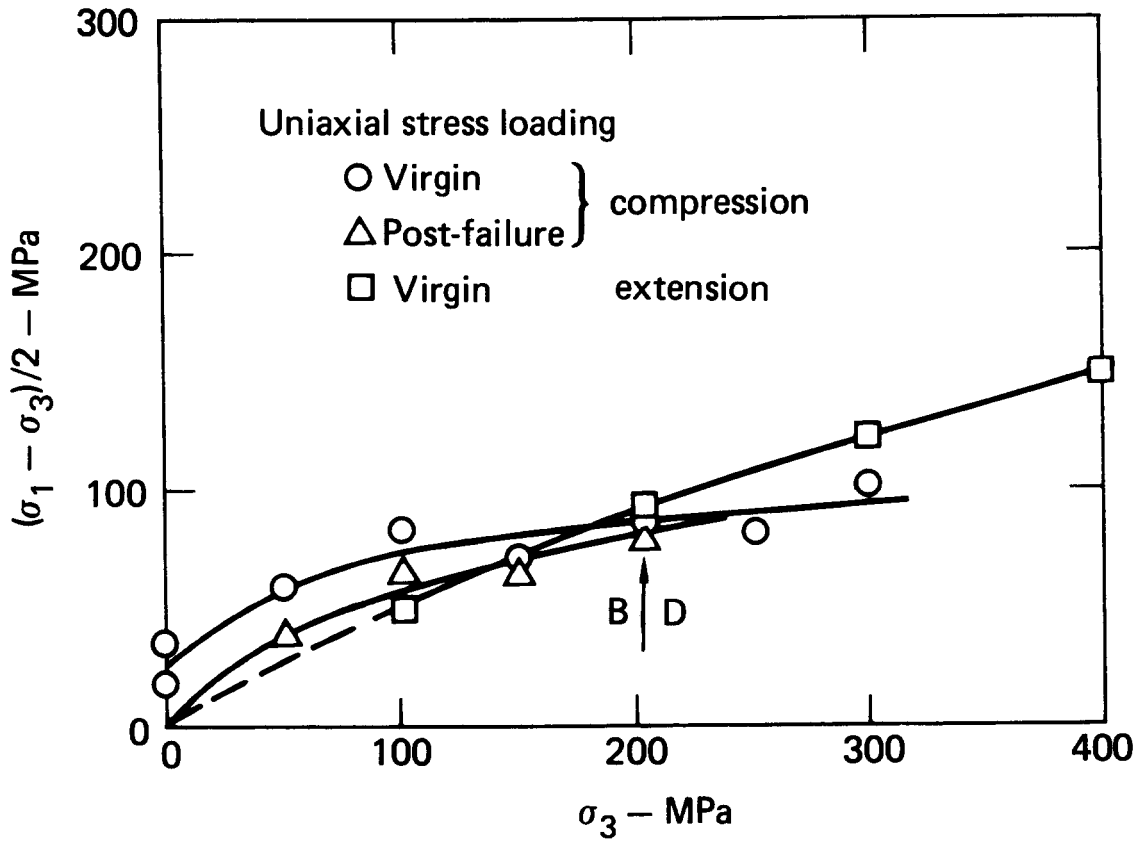

FIGURE 14. Failure envelopes for core from white shale section for Columbia gas well No. 20403. Samples were perpendicular to bedding.

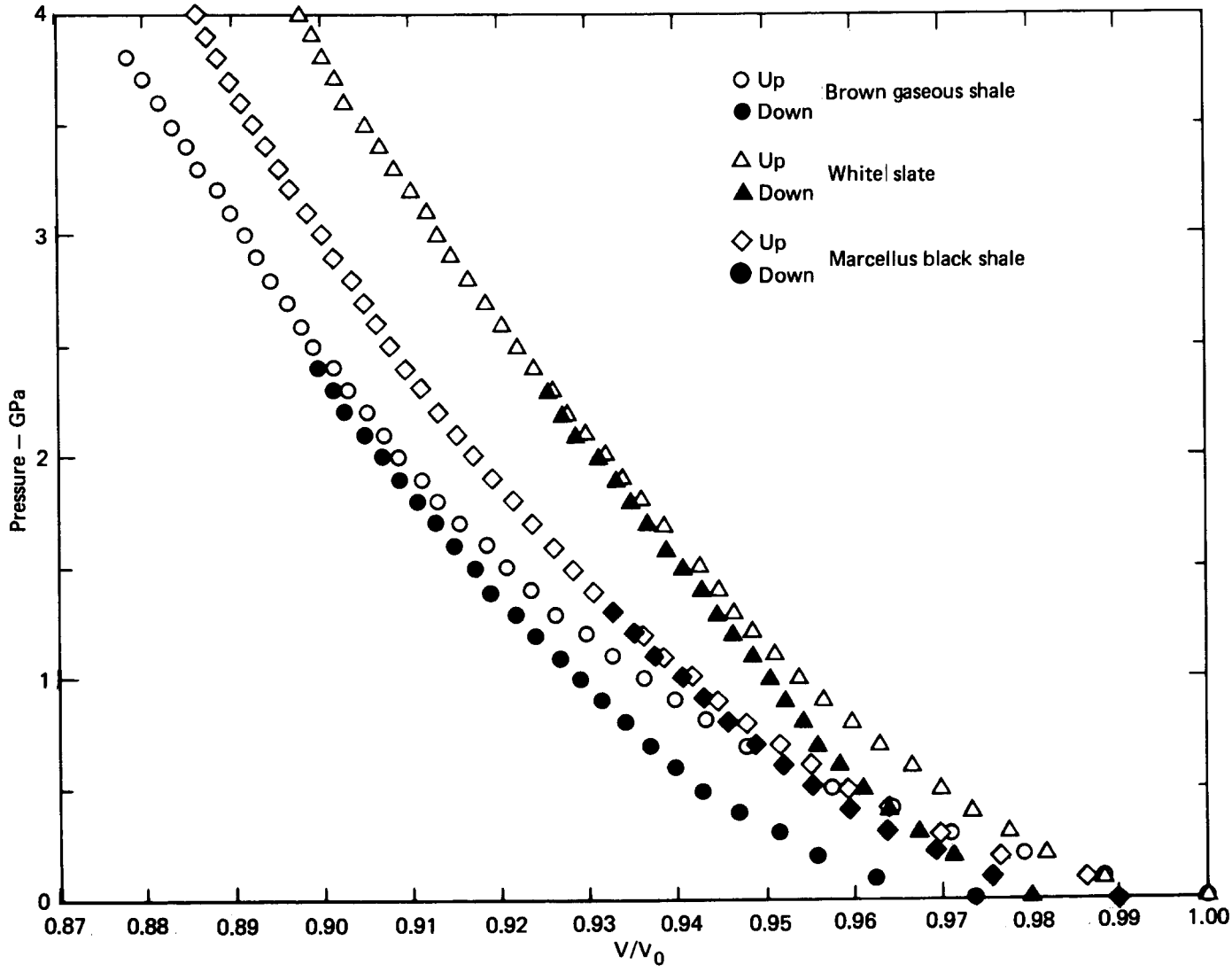

FIGURE 15. Compressibility curves for cores from Columbia gas well No. 20403.

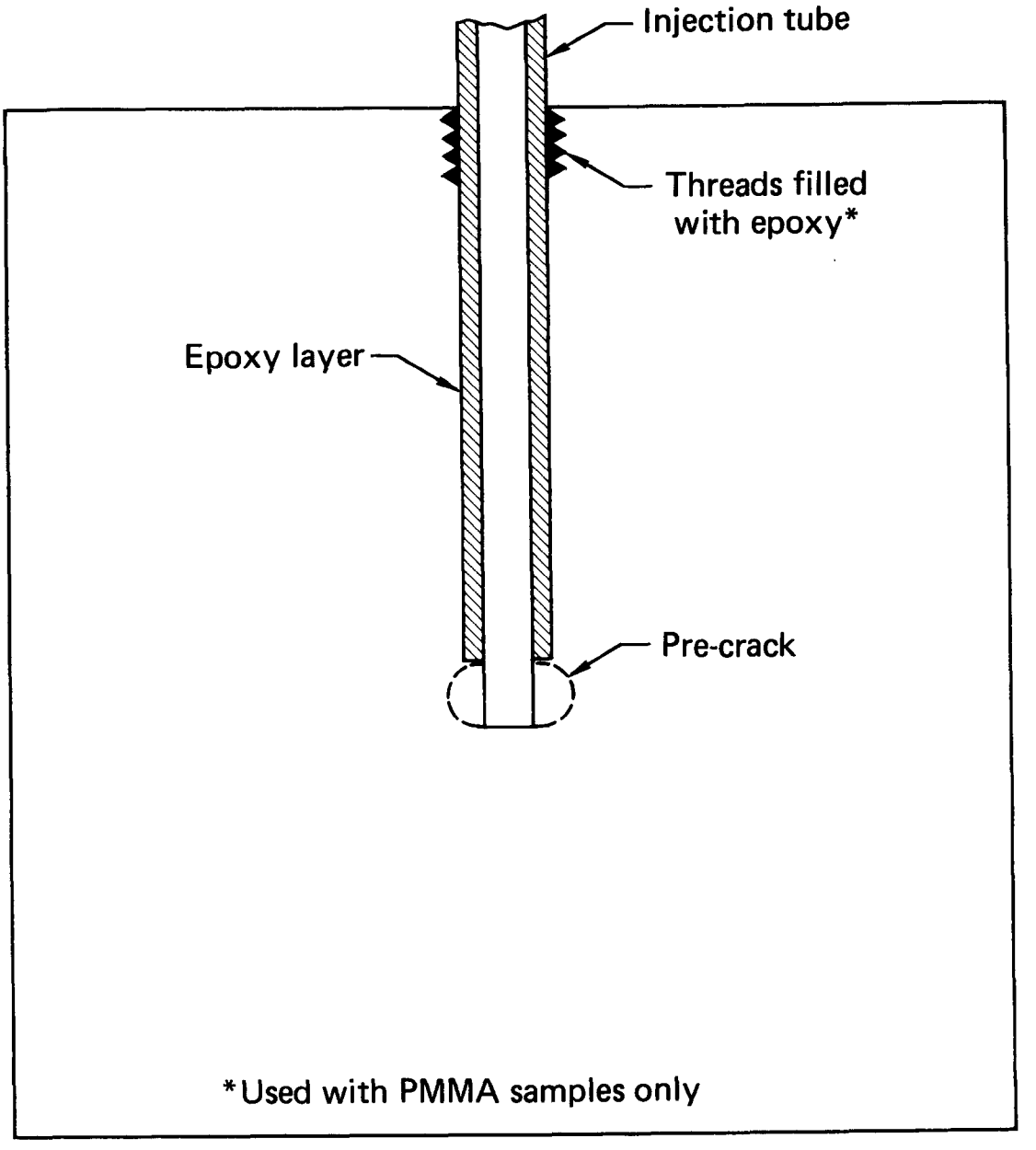

FIGURE 16. Technique of securing injection tube in borehole (used with PMMA samples only).

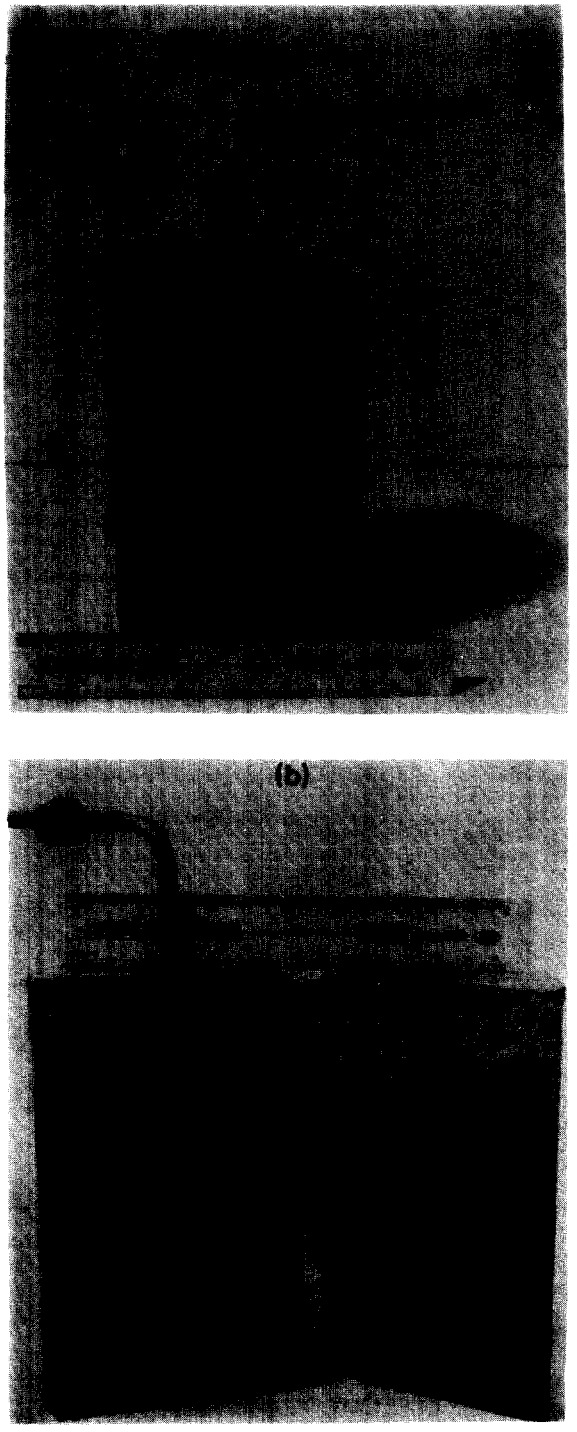

FIGURE 17. Hydraulic fracture in Indiana limestone.

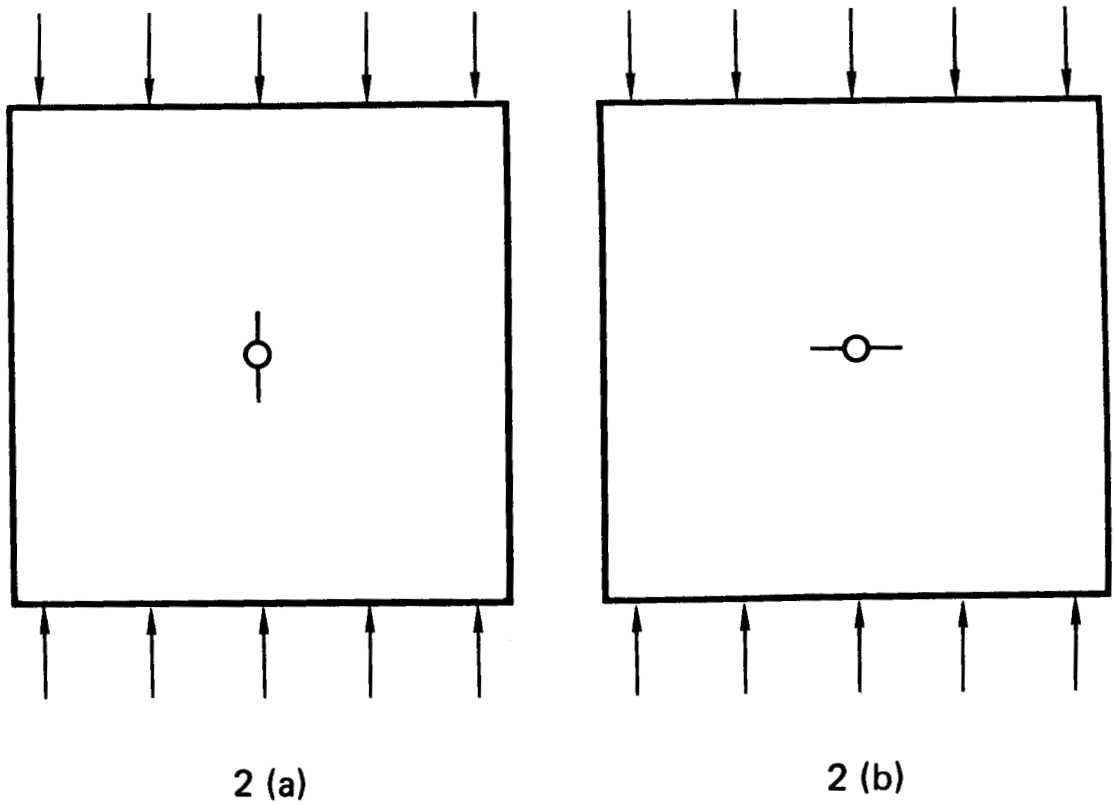

FIGURE 18. Orientation of pre-crack with respect to applied load.

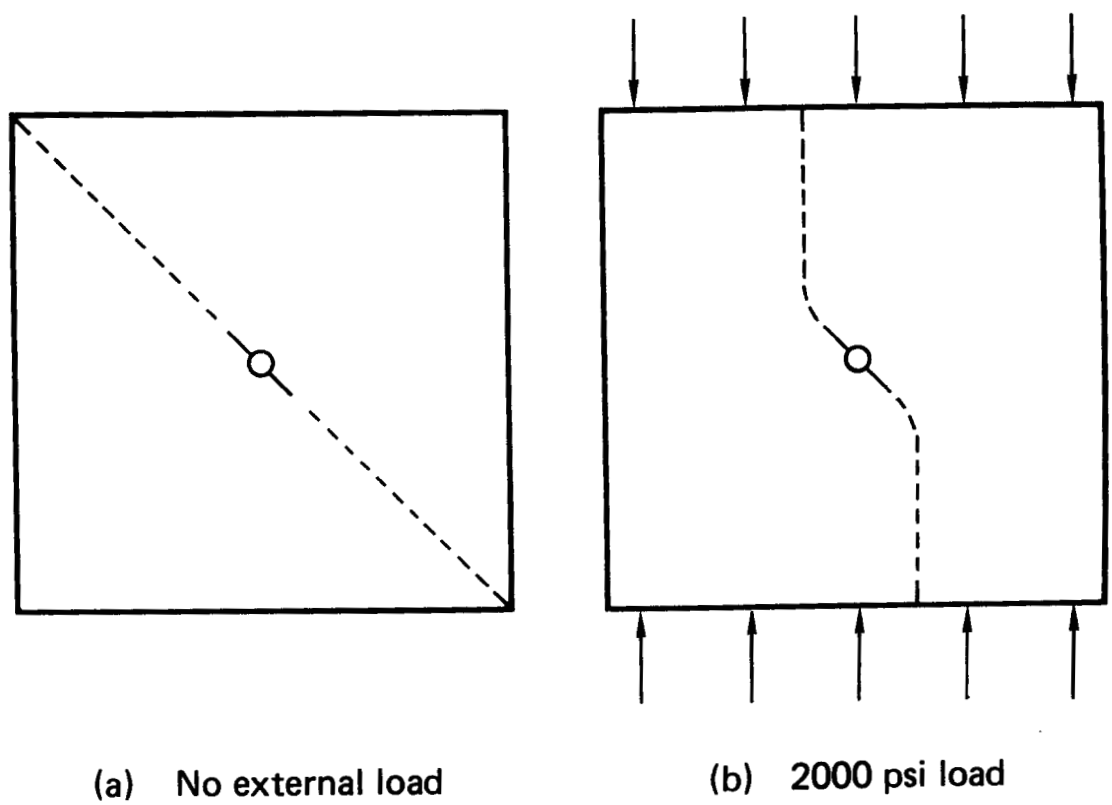

FIGURE 19. The effect of an external load on direction of crack growth.

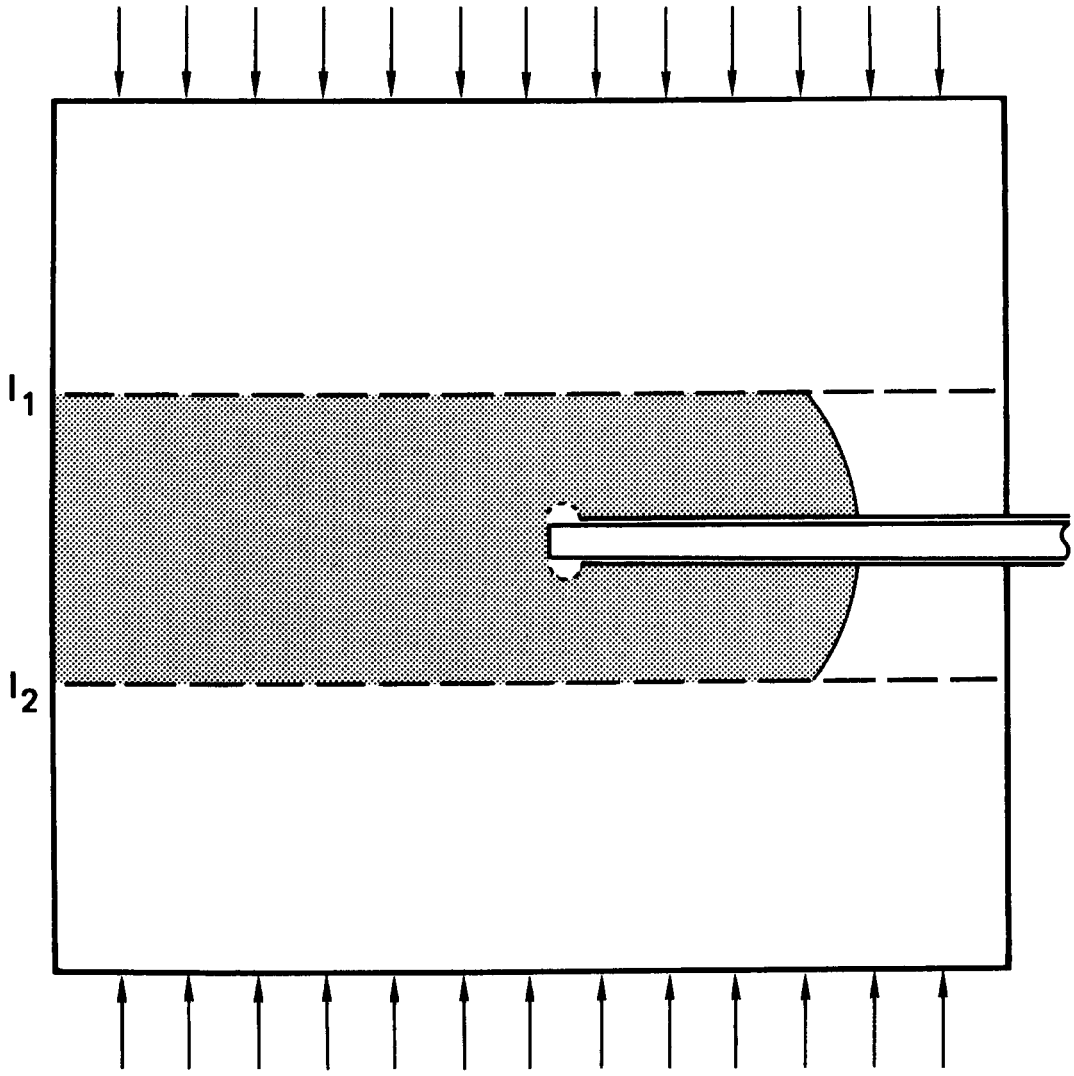

FIGURE 20. Crack growth pattern in layered PMMA.

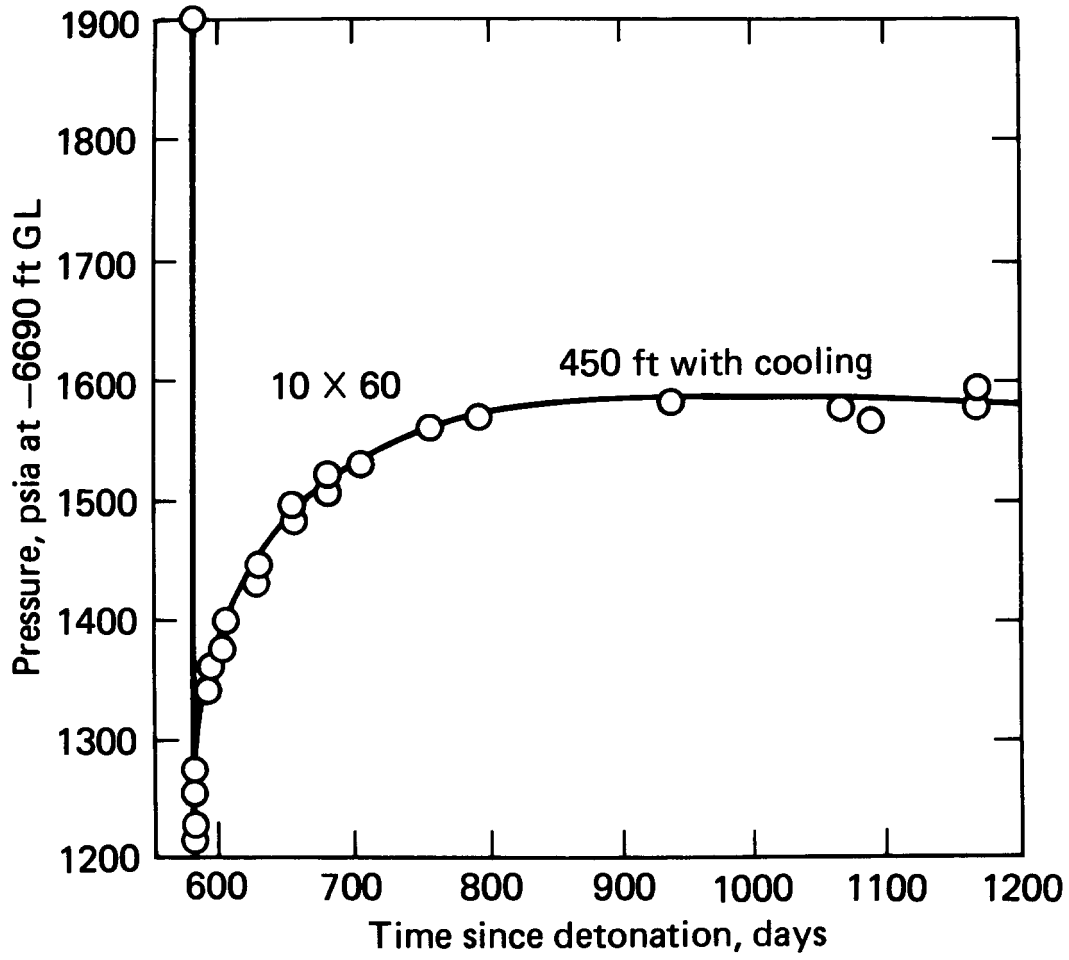

FIGURE 21. Pressure-buildup history of the lower Rio Blanco nuclear chimney compared to a theoretical match.

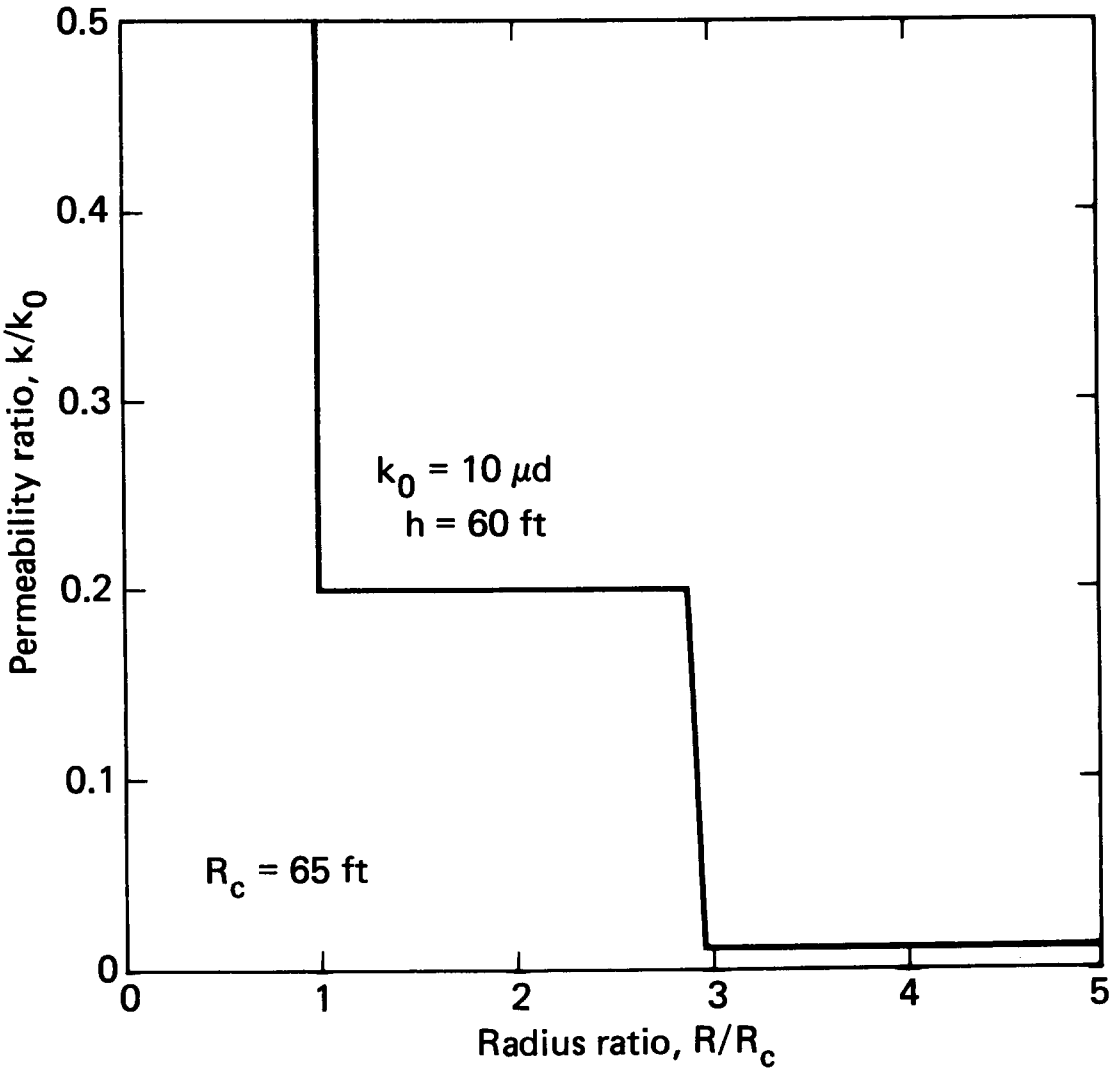

FIGURE 22. Permeability profile for theoretical model of lower Rio Blanco nuclear chimney.

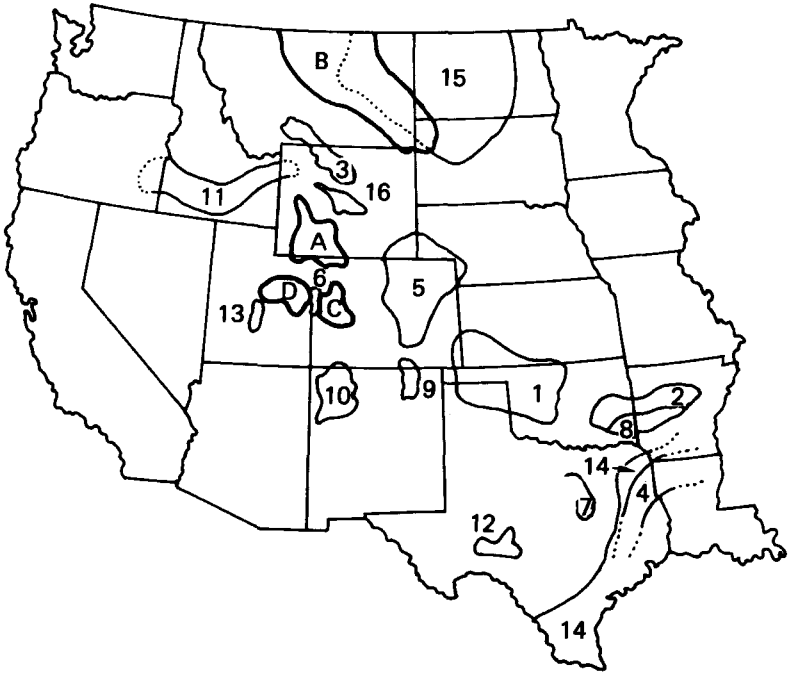

PRIMARY STUDY AREAS

A. GREATER GREEN RIVER BASIN
B. NORTHERN GREAT PLAINS PROVINCE
C. PICEANCE BASIN
D. UINTA BASIN

ADDITIONAL LOW PERMEABILITY SANDSTONE AREAS

1. ANADARKO BASIN
2. ARKOMA BASIN
3. BIG HORN BASIN
4. COTTON VALLEY TREND
5. DENVER BASIN
6. DOUGLAS CREEK ARCH
7. FORT WORTH BASIN
8. OUACHITA MOUNTAINS PROVINCE
9. RATON BASIN
10. SAN JUAN BASIN
11. SNAKE RIVER DOWNWARP
12. SONORA BASIN
13. WASATCH PLATEAU
14. WESTERN GULF BASIN
15. WILLISTON BASIN
16. WIND RIVER BASIN

FIGURE 23. Low-permeability regions.

SUBSURFACE STRATIGRAPHY AND EXTENT OF THE UPPER DEVONIAN DUNKIRK AND RHINESTREET BLACK SHALES IN NEW YORK

Arthur M. Van Tyne[1], John C. Peterson[1],

Lawrence V. Rickard[2], David G. Kamakaris[1]

ABSTRACT

Gamma Ray log correlations of the Dunkirk and Rhinestreet shales were made for 142 wells in western New York. The total Dunkirk section, from West to East, ranges in thickness from 40 feet at the Lake Erie shoreline outcrop to more than 80 feet in Allegany County. The massive black shale portion of the Dunkirk varies from 50 feet thick in Chautauqua County to less than 25 feet in Cattaraugus County. The structure on base Dunkirk indicates a southwestward dipping surface with southwestward trending anticlinal features in Chautauqua and Cattaraugus Counties.

The deeper total Rhinestreet, from West to East, ranges from 113 feet at Lake Erie to 1,450 feet in Steuben County. The massive black shale zone of the Rhinestreet varies from 113 feet in Chautauqua County to less than 5 feet in Allegany County. The structure on base Rhinestreet indicates a northeast-southwest trending basinal area with the same anticlinal features seen in the Dunkirk structure.

INTRODUCTION

There are four major black shale intervals in the Upper Devonian of New York. The two uppermost intervals, which lie at the base of the Canadaway and West Falls Groups, are the Dunkirk and Rhinestreet units. (Fig.1) Their subsurface expression as massive black shales is limited to the far western part of the state and this forms only a portion of their full stratigraphic thickness further to the east. Although they are mapped as lithostratigraphic units, their bases also represent time-lines or chronostratigraphic horizons which are present at the base of most of the Upper Devonian Groups in New York.

A detailed study of subsurface facies changes has been a necessary step in beginning to appraise the gas potential of these units. Correlation difficulties can be attributed to an eastward thickening of the total section and the replacement of organic-rich, radioactive black shale with gray shales, siltstones and sandstones. This is seen in increasing grain size, decreasing radioactivity, decreasing organic content and lighter color, indicative of changes in transportation processes and/or the depositional environment. An understanding of the nature of such lateral variations will aid in further evaluation of potential reservoirs adjacent to the eastward thinning black shales.

DUNKIRK SHALE

The type locality of the Dunkirk Shale is on the Lake Erie shoreline at Dunkirk, New York.(Fig.2)

[1] New York State Museum, Geological Survey, Oil and Gas Office, Alfred, New York.
[2] New York State Museum, Geological Survey, Albany, New York

At this outcrop it is about 40 feet thick and consists of massive medium gray to grayish-black shale. A bed of calcareous septaria occurs in the middle of the shale and pyritized algae, carbonized plant stems and conodonts have also been found in the section (Tesmer, 1963). The subsurface lithology of the Dunkirk in a well about 18 miles southwest of this outcrop is 25% black shale, 20% medium gray shale and 55% medium dark gray shale with a thickness of 42 feet.

In Erie County outcrops, further to the north, the Dunkirk is an olive-gray to black shale with little interbedded medium gray shale. Calcareous and argillaceous concretions occur in the gray shale (Buehler & Tesmer, 1963). The subsurface Dunkirk from a well in Erie County occurs as 69% dark gray shale and 31% medium gray shale.

In northern Cattaraugus County, the outcrop section consists of grayish-black to black shales with interbedded thin calcareous zones (Tesmer, 1975). In the subsurface in southern Cattaraugus County, it is a dark to light gray shale.

In the past, correlation of the type Dunkirk with units east of Cattaraugus County has been problematical due to a seeming lack of black shale continuity. The eastern Hume black shale was thought to be a higher unit and not correlative with the Dunkirk. However, recent study (Rickard, 1975) has shown that the Dunkirk and Hume are correlative.

The general lithology of the Hume Shale, which outcrops in northern Allegany County, is black, brown and dark gray shale (Pepper & deWitt, 1951). The subsurface lithology in central Allegany County (from a limited number of wells) is: 20% dark gray shale, 18% medium gray shale and 62% medium dark gray shale and minor gray siltstones.

In the southwesternmost part of New York state, the total Dunkirk consists of dark gray to black shale. Eastwards from there the total Dunkirk section expands to include more gray shales and siltstones with lessening amounts of black shale. In the vicinity of central Cattaraugus County, the black shale has lost its character and cannot be distinguished from the total dark gray shale and siltstone section. The loss of the massive black shale section is interpreted as a change in depositional environment from anoxic basin to a slope environment. The top of the Dunkirk becomes more poorly defined on the G-R log as the black shale becomes interbedded with gray shales and siltstones. (Fig.3) Near its pinchout close to the Allegany-Steuben County line, the Dunkirk Shale is 18 feet thick in the subsurface and contains 20% dark gray shale, 64% medium dark gray shale and 6% gray siltstone at its base. Here it occurs within a sandstone section which is an oil producer and is locally known as the Fulmer Valley sand.

The lower contact of the Dunkirk is sharp and easily recognized in both outcrop and subsurface. The upper contact is generally transitional through thinly interbedded black and gray shales and siltstones.

In the subsurface of central Chautauqua County, the Dunkirk shows a high G-R response with a correspondingly low density response. This appears to be typical of organic-rich shale. (Fig.4) This is the massive Dunkirk black shale which can be traced into outcrop at the type section. Both radioactivity and organic content decrease eastward.

The total Dunkirk isopach map varies from 40 feet in Chautauqua County to 80 feet in central Allegany County. (Fig.5) It is believed to pinch-out to the east where it abruptly thins from 70 feet to 15 feet, then to 0 in western Steuben County. The isopach of the massive black shale section of the Dunkirk varies from 50 feet in Chautauqua County, where it comprises the total Dunkirk section, to less than 25 feet in Cattaraugus County. (Fig.6)

The structure of the base of the Dunkirk indicates a southwestward dipping surface with a series of NE-SW trending anticlinal features in western New York not seen in previous structural studies. In central New York, structures reflect those already known from mapping on the Oriskany sandstone. (Fig.7)

RHINESTREET SHALE

The Rhinestreet type section is located just north of Naples, in Ontario County, New York. Here it is a fissile, massive black shale with minor gray shale rapidly thickening to the East into interbedded gray shales and siltstones (Sutton, 1960). In Erie County, interbedded medium gray to dark gray shales occur in the upper part of the Rhinestreet as do thin gray siltstones and argillaceous limestones (Buehler & Tesmer, 1963). One sample study in Chautauqua County showed the subsurface Rhinestreet to be composed of 52% dark gray shale, 41% black shale and 7% medium gray

shale.

The basal contact is sharp in outcrop and in the subsurface. The top is picked at the base of the so-called Scraggy Black Shale member of the Angola Shale and eastward equivalent Nunda shales and sandstones. The base is readily picked at a pronounced G-R decrease which marks the top of the gray, silty Cashaqua shale.

The Rhinestreet is similar to the Dunkirk in that the total section in the western Chautauqua County area consists of massive black shale. Within the 25 miles eastward to the central part of the County this massive black shale thins and becomes overlain and underlain by interbedded gray shales and siltstones so that the total Rhinestreet section becomes greatly expanded. (Fig.8) This eastward thickening of the total Rhinestreet section and thinning of the central massive black shale continues into eastern Allegany County where the central black shale is only a few feet thick. The total Rhinestreet section in this area consists of interbedded gray and brown shales and siltstones and numerous thin black shale beds.

From the Allegany-Steuben County line eastward the Rhinestreet continues to thicken but the section containing interbedded black shales decreases in vertical extent from 1,200 feet to less than 400 feet at the Steuben-Chemung County line, a distance of 40 miles. This eastward stepping-down of the black shales in the section is interpreted as offlap caused by a westwardly prograding shoreline. (Fig.9)

The Density log, where run, readily indicated the black Rhinestreet shales as lower density, organic-rich intervals. In Chautauqua County, an overall average lower density is indicated for the total Rhinestreet section due to the predominance of black shale. From Cattaraugus County east this overall density decline is not so apparent but individual black shale zones in the Rhinestreet are still clearly shown as zones of lower density.

The total Rhinestreet varies from 113 feet in Chautauqua County to 1,450 feet in Steuben County. (Fig.10) The Massive Black Shale zone of the Rhinestreet varies from a maximum of 148 feet in Chautauqua County to less than 25 feet in western Cattaraugus County. (Fig.11) This zone can be traced to southeastern Allegany County where it is less than 5 feet thick.

Structures are similar to those in the Dunkirk but reveal a NE-SW trending basin with a depocenter in Steuben County. (Fig.12)

SUMMARY

Gamma Ray logs for 142 wells were studied to ascertain the subsurface stratigraphy of the Dunkirk and Rhinestreet shales from far western to central New York State. Both units contain massive black shales (in western New York) which thin and pinch-out to the east. The maximum massive black shale thickness in the Dunkirk is 50 feet and in the Rhinestreet 148 feet, both occurring in Chautauqua County.

The total Dunkirk appears to pinch-out in western Steuben County while the total Rhinestreet still thickens eastwards of this area to 1,500 feet and contains many scattered, thin black shale beds.

Structure maps on the base of these units indicate a generally NE-SW trending basin flattening to E-W in the far western part of New York State. Some new anticlinal features are revealed in Chautauqua and Cattaraugus Counties as are previously known faulted anticlines in Allegany and Steuben Counties.

ACKNOWLEDGEMENT

Support for this study was provided by ERDA contract E(40-1)-5206 as part of the Eastern Gas Shales Project (EGSP) managed by the Morgantown Energy Research Center.

REFERENCES

Buehler, E. J., and I. H. Tesmer. Geology of Erie County New York. Buffalo Soc. of Nat. Sci. Bull., v. 21, no. 3, 1963, 118 pp.

Pepper, J. F., and W. deWitt, Jr. Stratigraphy of the Late Devonian Perrysburg Formation in Western and West-Central New York. U. S. Geol. Survey Oil and Gas Investigations Chart OC-45, 1951.

Rickard, L. V. Correlation of the Silurian and Devonian Rocks in New York State. N. Y. State Mus. and Sci. Service, Geol. Survey Map and Chart Series No. 24, 1975, 16 pp.

Sutton, R. G. Stratigraphy of the Naples Group (Late Devonian) in Western New York. N. Y. State Mus. Bull., no. 380, 1960, 56 pp.

Tesmer, I. H. Geology of Chautauqua County, New York: Part 1, Stratigraphy and Paleontology (Upper Devonian). N. Y. State Mus. Bull., no. 391, 1963, 65 pp.

_____. Geology of Cattaraugus County, New York. Buffalo Soc. of Nat. Sci. Bull., v. 27, 1975, 105 pp.

	NEW YORK	PENNSYLVANIA	OHIO
UPPER DEVONIAN	CONEWANGO GROUP		
	CONNEAUT GROUP		
	CANADAWAY GROUP		
	DUNKIRK SHALE *	DUNKIRK	OHIO SHALE LOWER HURON MEMBER
	WEST FALLS GROUP		
	RHINESTREET SHALE *	RHINESTREET	MIDDLE OLENTANGY
	SONYEA GROUP		
	MIDDLESEX SHALE *		
	GENESEE GROUP	BURKETT	
	GENESEO SHALE *		
MIDDLE DEVONIAN	TULLY FORMATION	TULLY	
	HAMILTON GROUP	MAHANTANGO	LOWER OLENTANGY
	MARCELLUS FM *	MARCELLUS	
	ONONDAGA FORMATION	ONONDAGA	DELAWARE COLUMBUS

Figure 1. GENERAL STRATIGRAPHY AND MAJOR BLACK SHALE UNITS (*) OF THE MIDDLE AND UPPER DEVONIAN OF NEW YORK

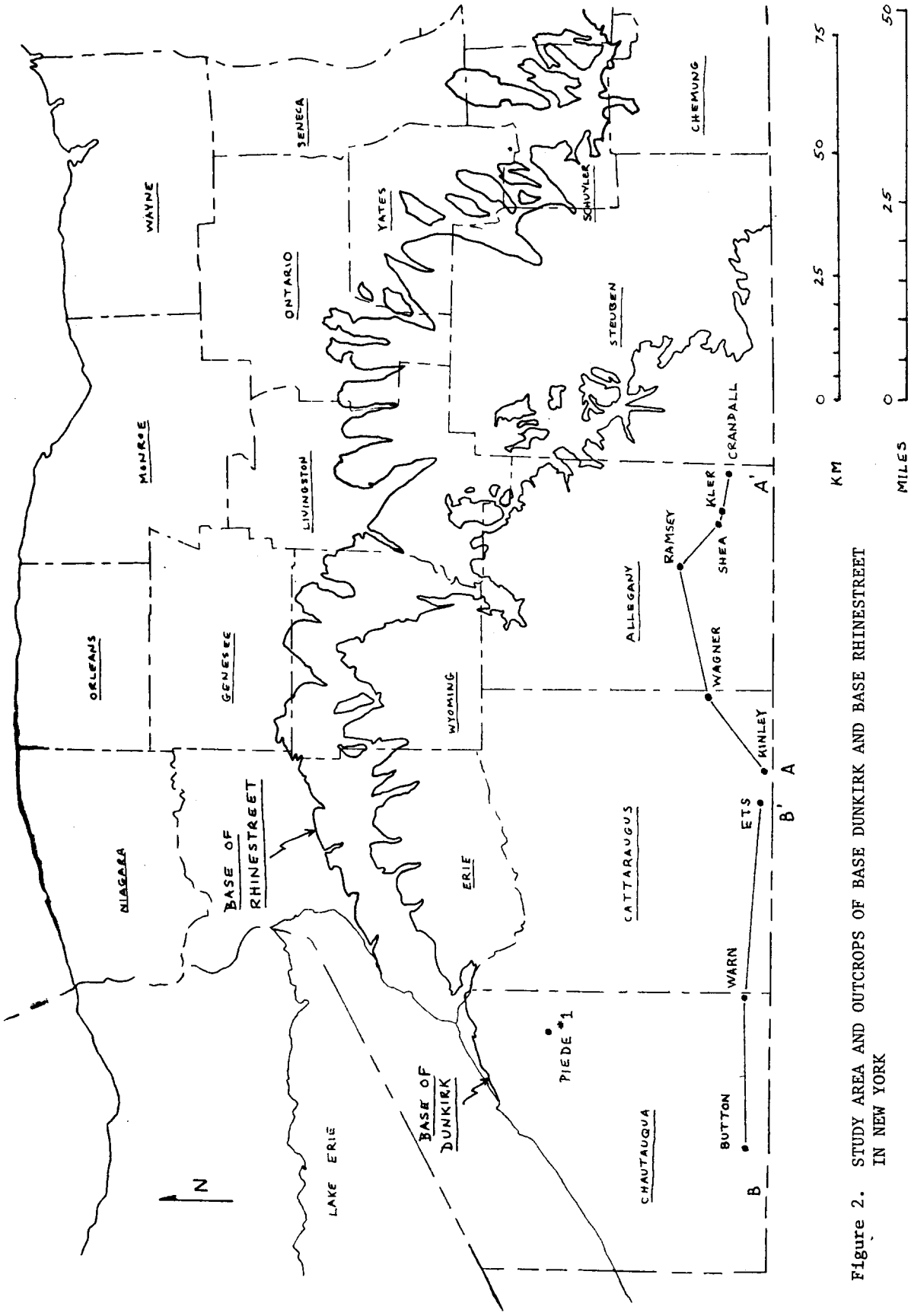

Figure 2. STUDY AREA AND OUTCROPS OF BASE DUNKIRK AND BASE RHINESTREET IN NEW YORK

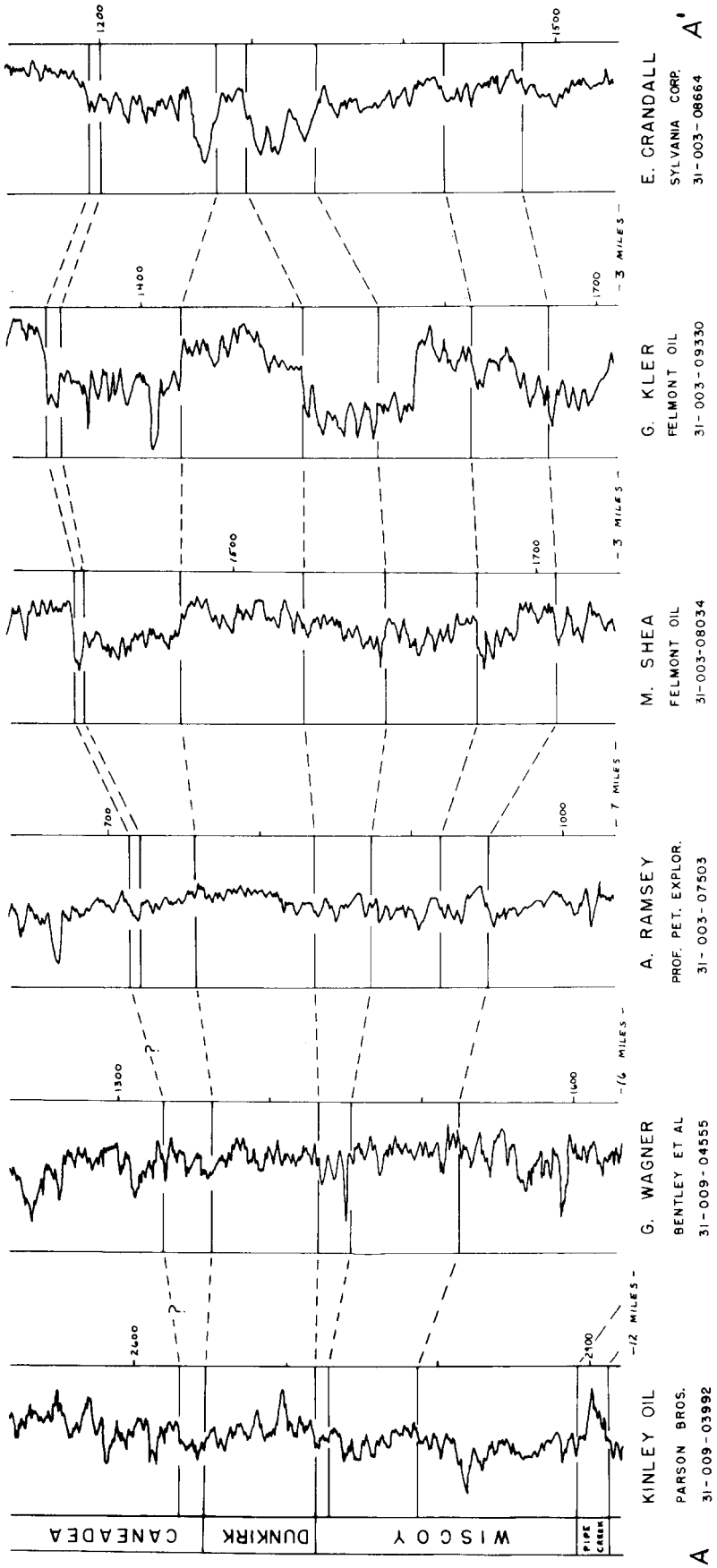

Figure 3. G-R STRATIGRAPHY OF THE DUNKIRK SHALE

Figure 4. TYPICAL G-R AND BULK DENSITY LOGS IN CHAUTAUQUA COUNTY, NEW YORK

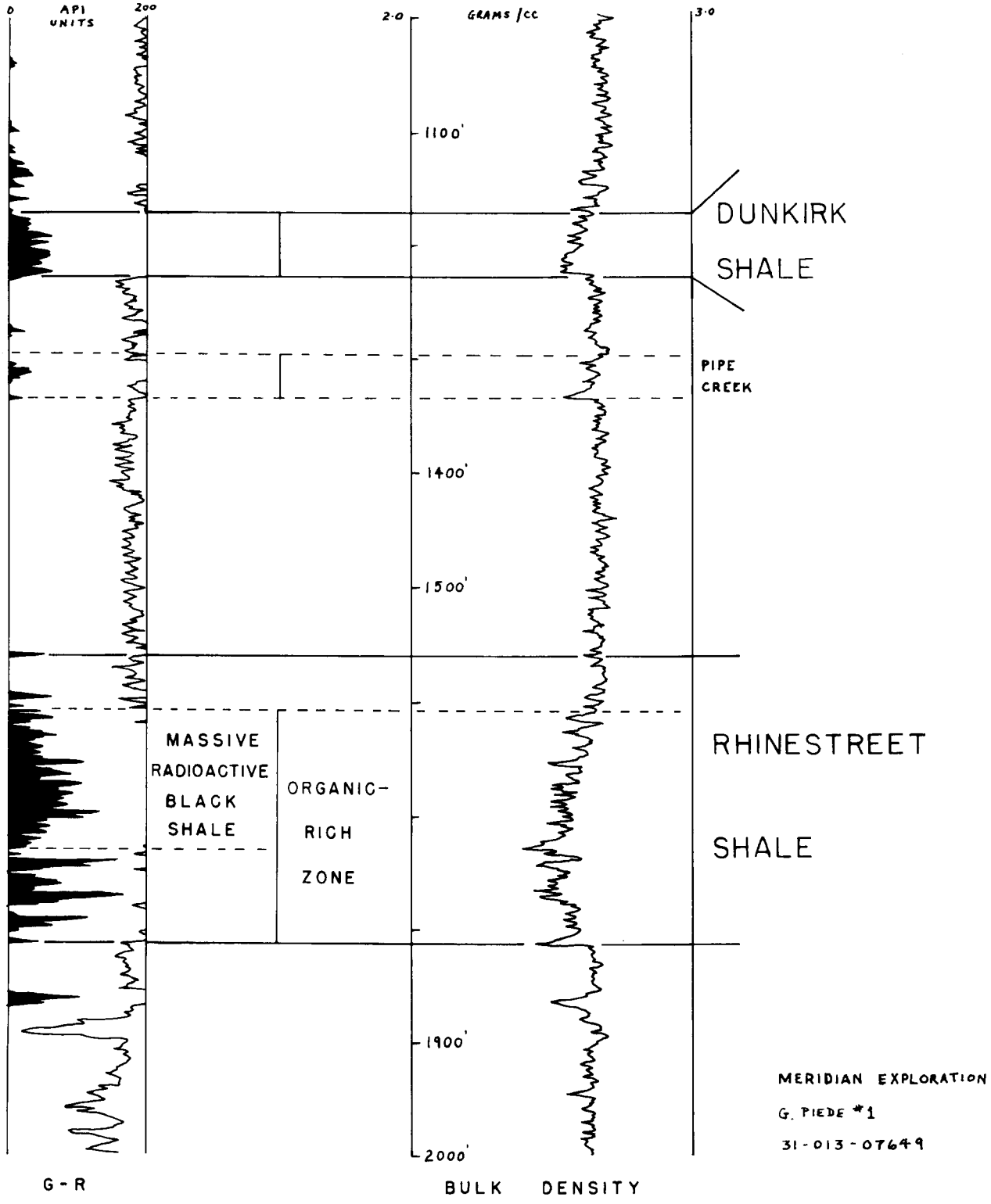

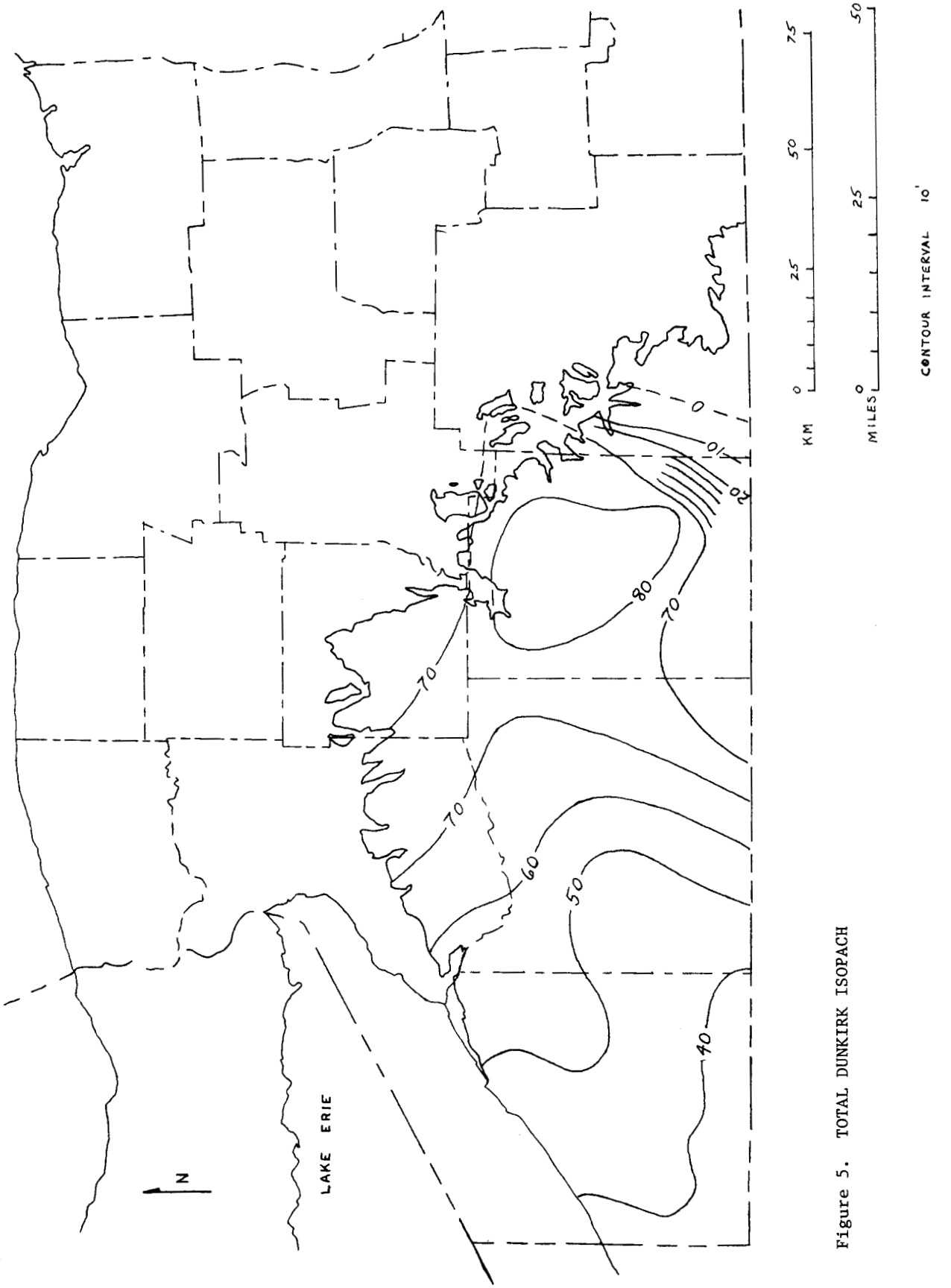

Figure 5. TOTAL DUNKIRK ISOPACH

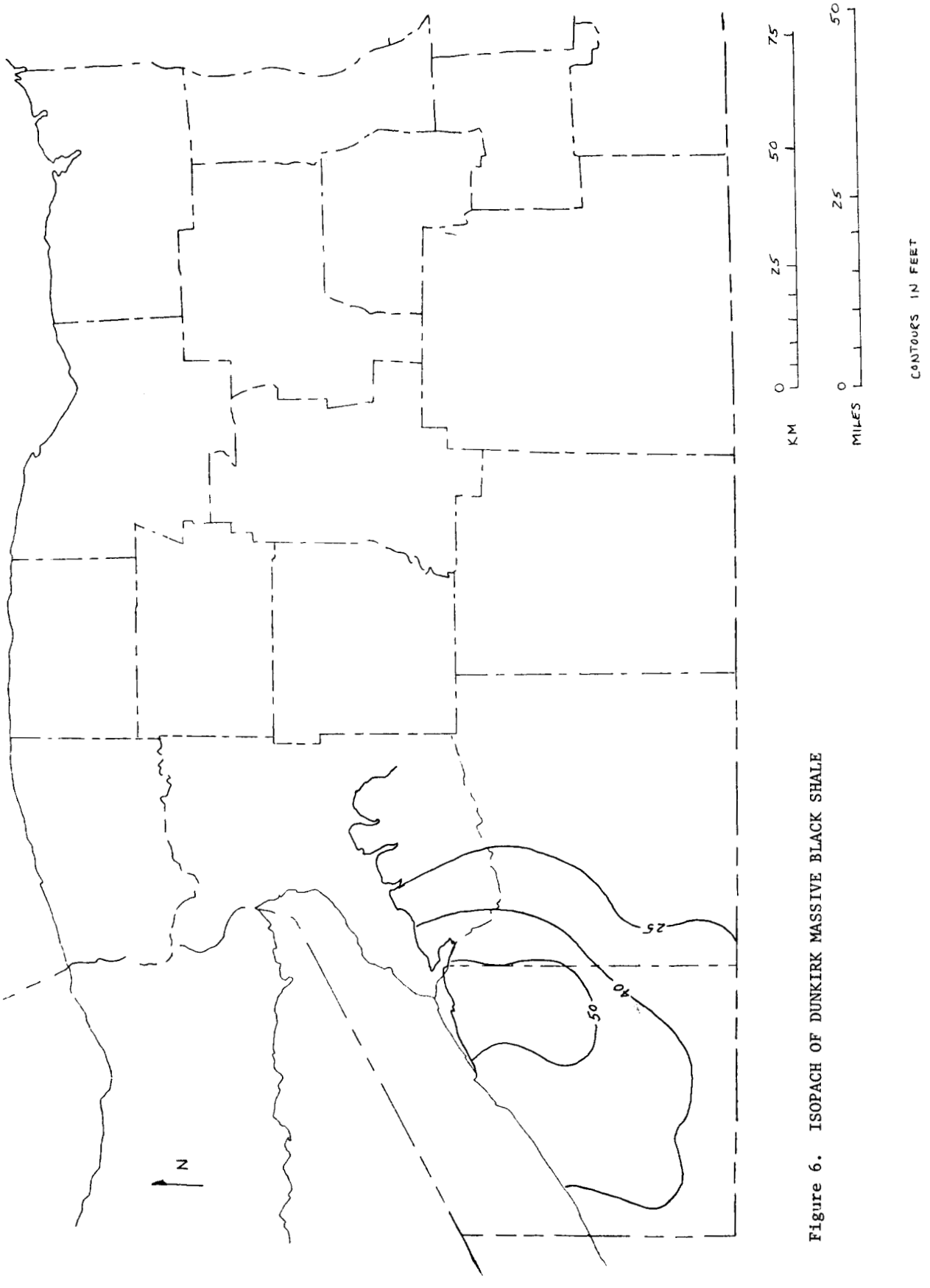

Figure 6. ISOPACH OF DUNKIRK MASSIVE BLACK SHALE

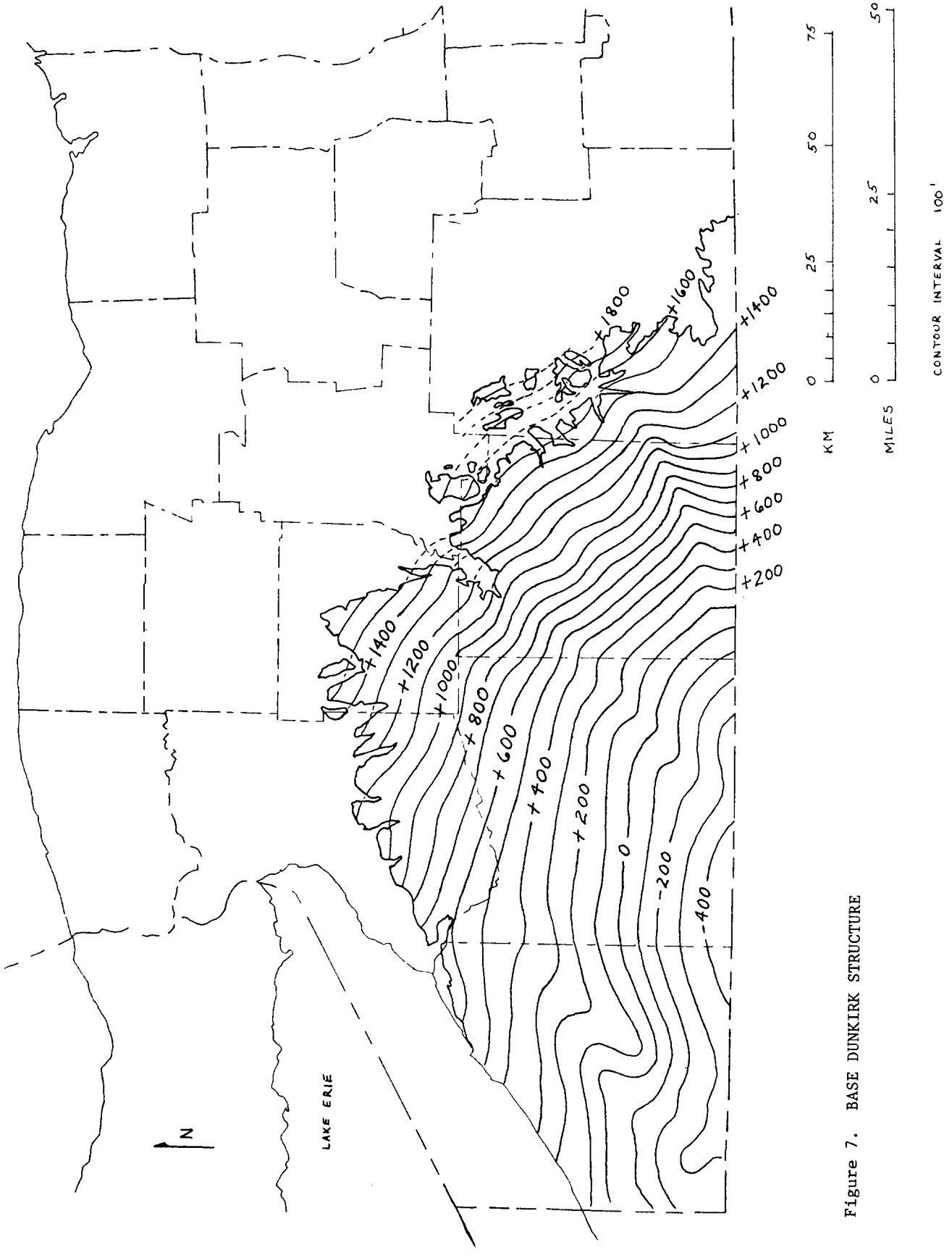

Figure 7. BASE DUNKIRK STRUCTURE

SUBSURFACE STRATIGRAPHY AND EXTENT OF THE UPPER DEVONIAN
DUNKIRK AND RHINESTREET BLACK SHALES IN NEW YORK

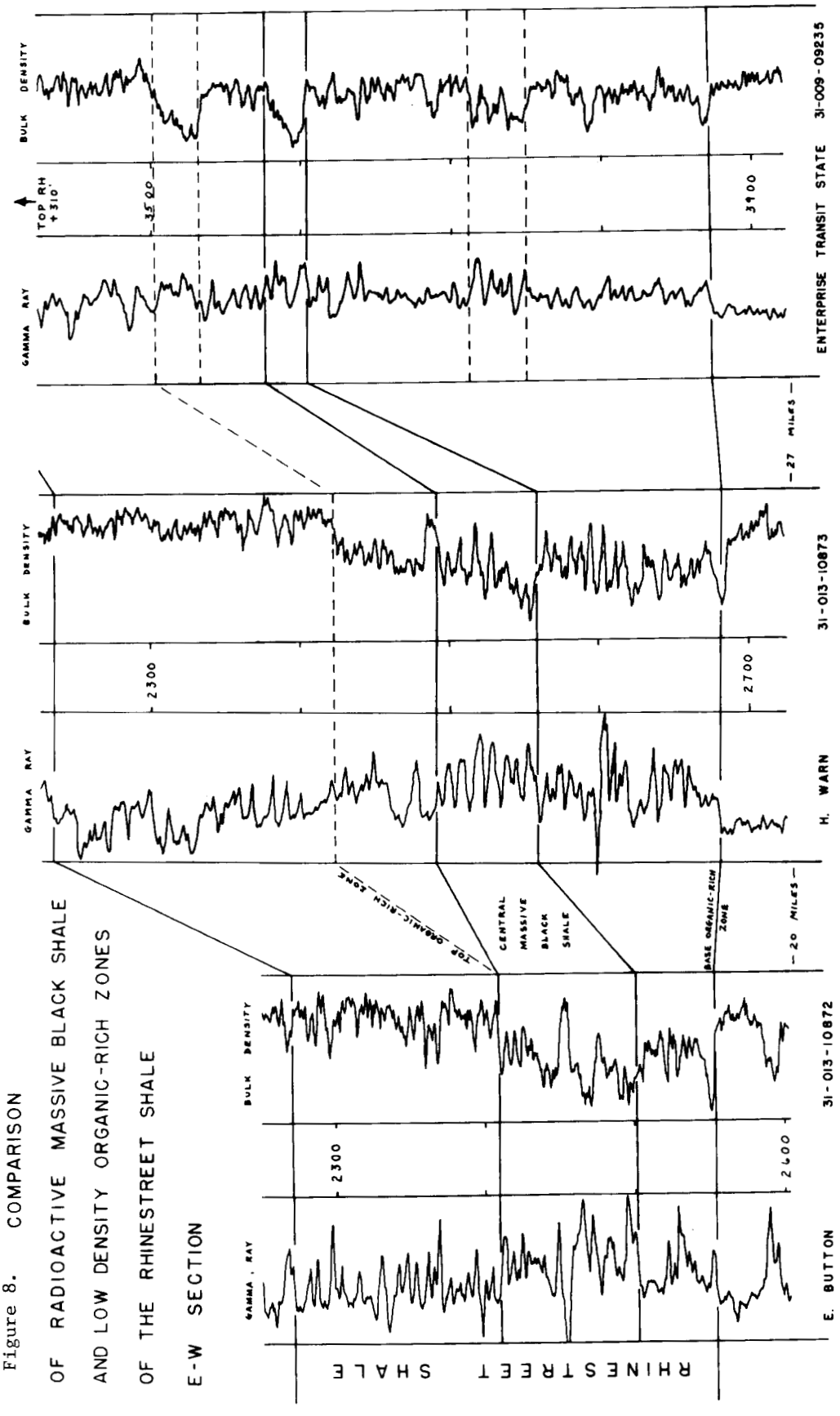

Figure 8. COMPARISON OF RADIOACTIVE MASSIVE BLACK SHALE AND LOW DENSITY ORGANIC-RICH ZONES OF THE RHINESTREET SHALE E-W SECTION

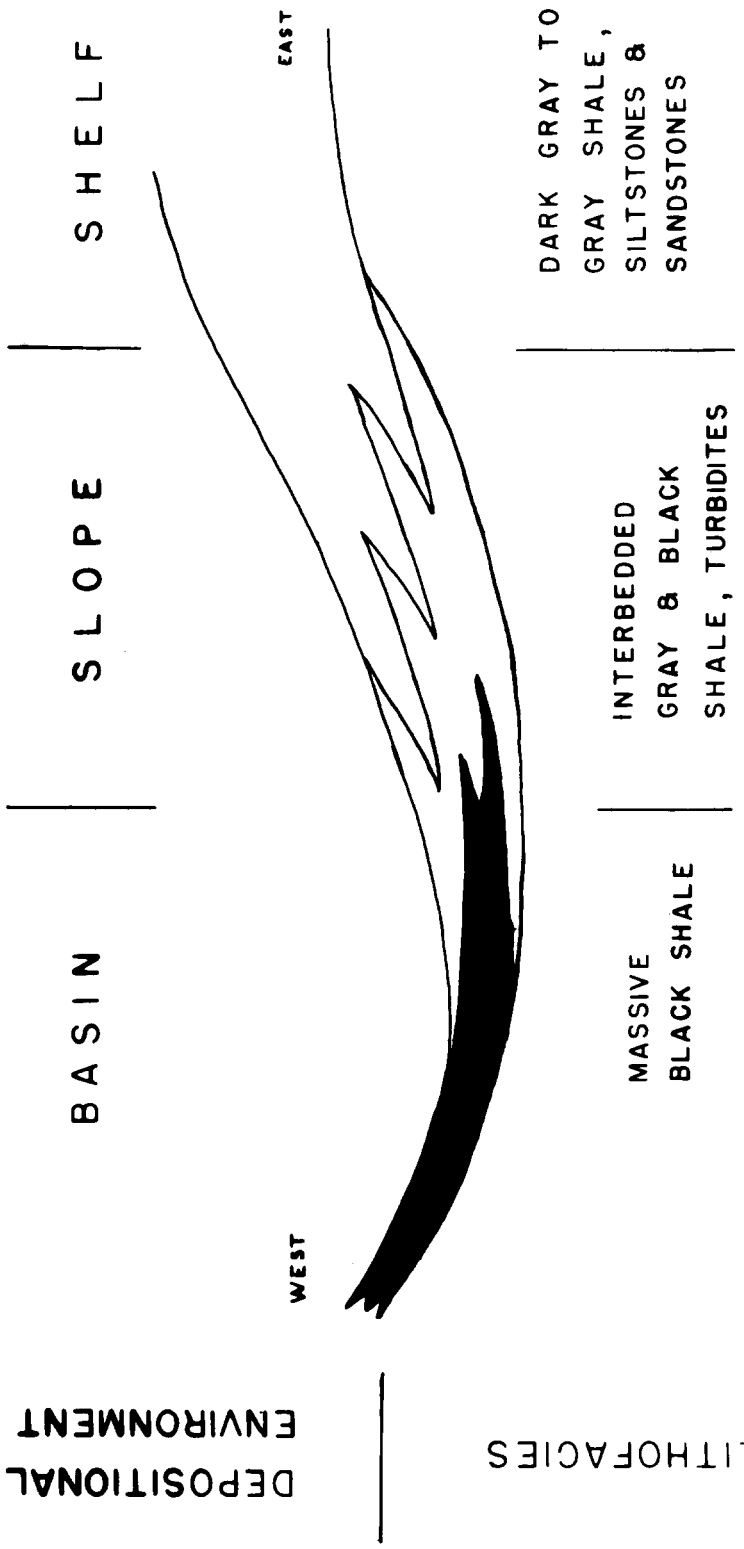

Figure 9. SCHEMATIC CROSS-SECTION SHOWING THE RELATIONSHIP OF MASSIVE BLACK SHALE TO THE TOTAL RHINESTREET SECTION

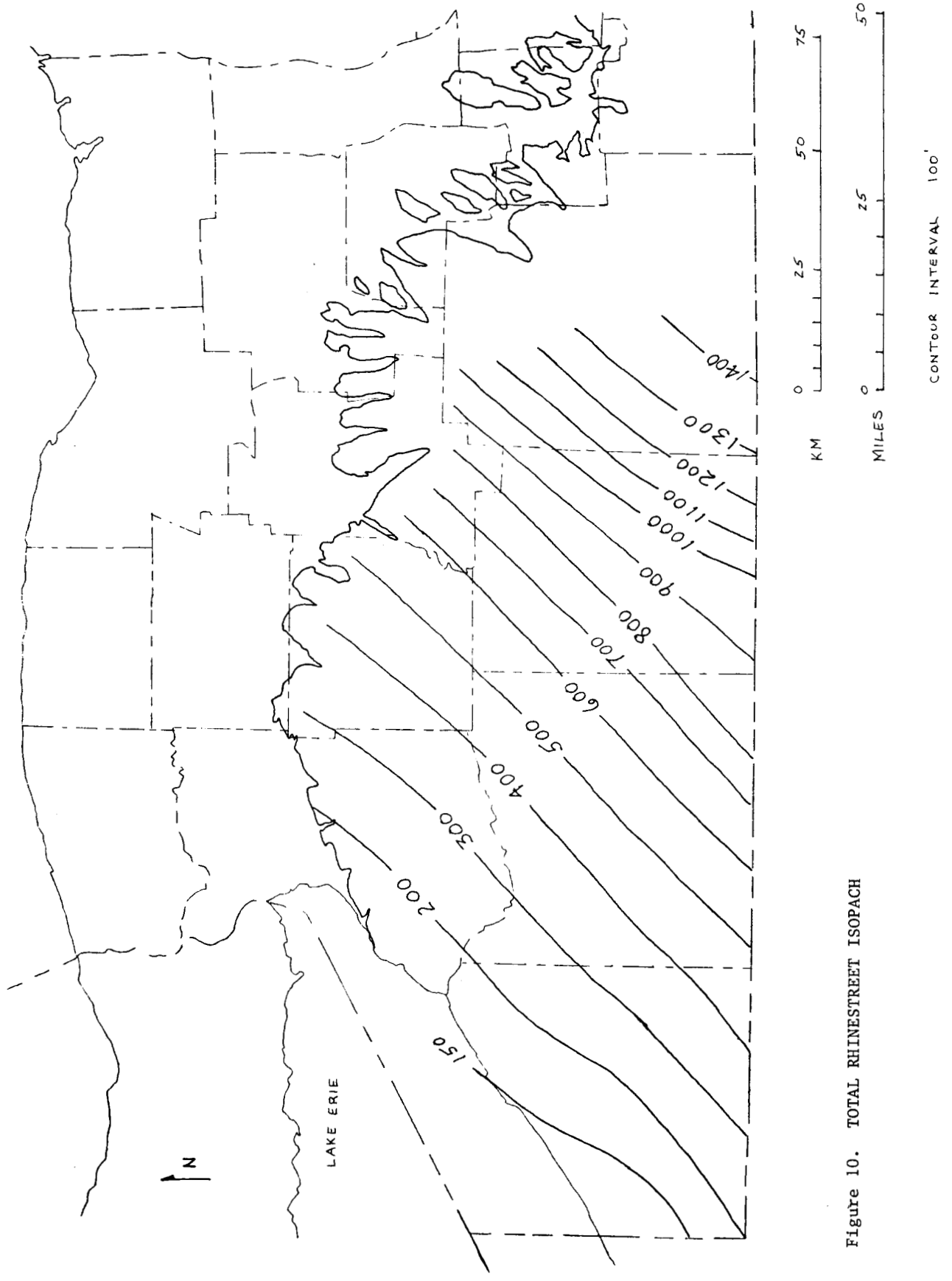

Figure 10. TOTAL RHINESTREET ISOPACH

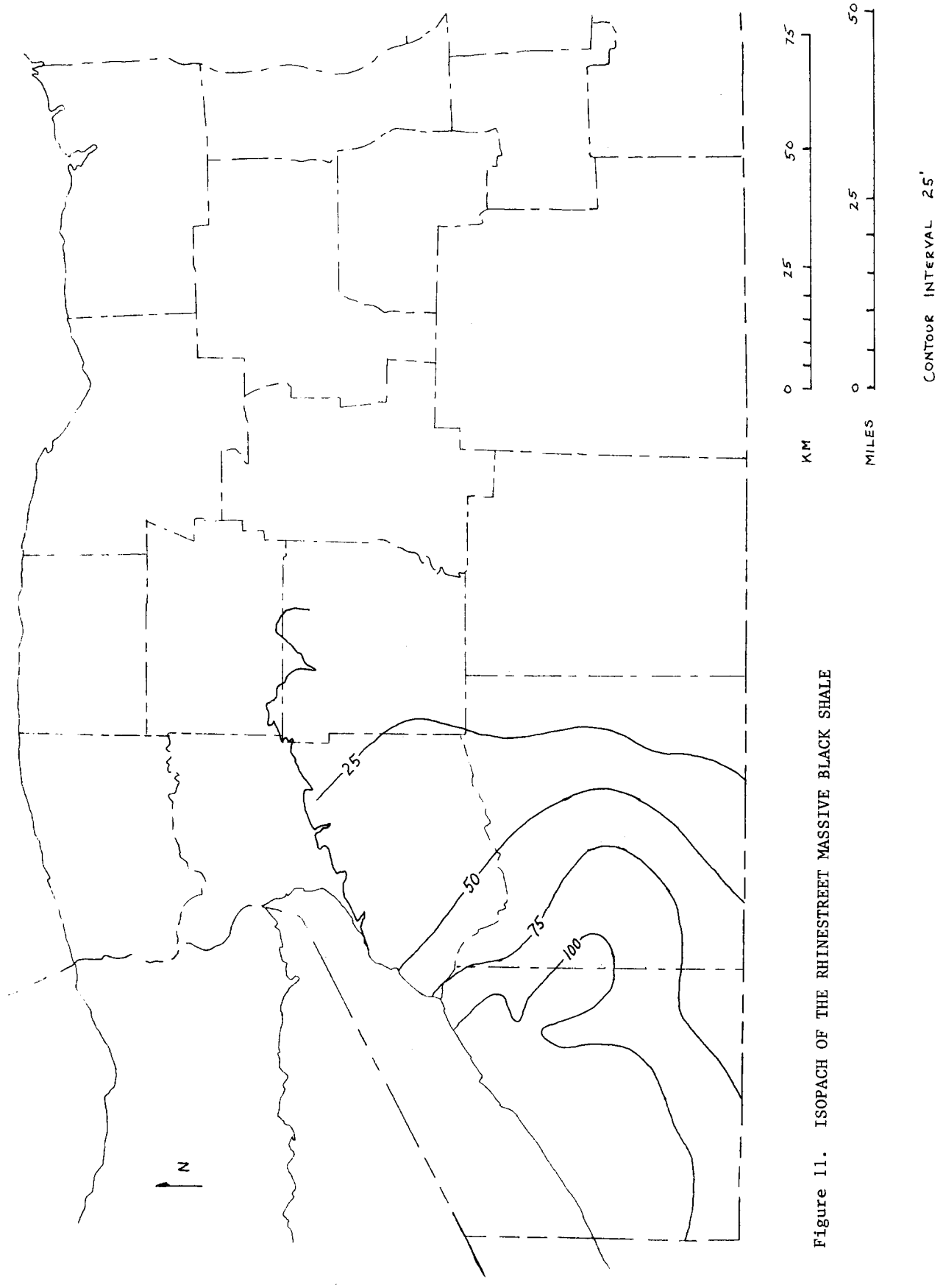

Figure 11. ISOPACH OF THE RHINESTREET MASSIVE BLACK SHALE

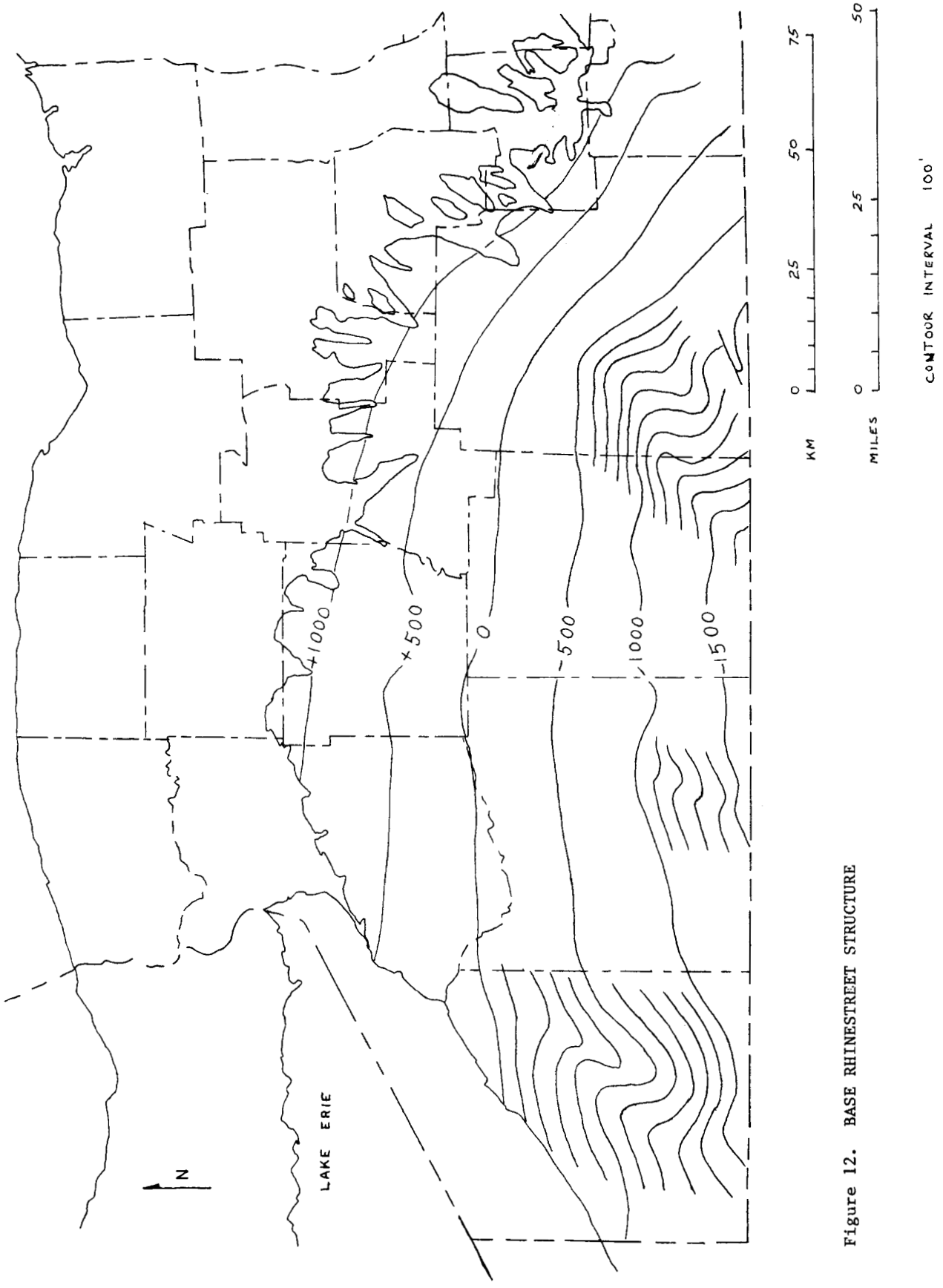

Figure 12. BASE RHINESTREET STRUCTURE

STRATIGRAPHY AND GAS OCCURRENCE IN THE DEVONIAN ORGANIC RICH SHALES OF PENNSYLVANIA

R. G. Piotrowski
S. A. Krajewski
Louis Heyman
- Pennsylvania Geological Survey -

ABSTRACT

Devonian shale gas was produced from shallow low pressure wells along Lake Erie in northwestern Pennsylvania between 1821 and 1880. Unfortunately, little information on these wells is available. Current production from the Devonian shales in Pennsylvania is limited to two wells, the Welch Foods, Inc. #3 well in Erie County and the Metropolitan Brick #1 well in Beaver County. Using these wells as a starting point, a network of nine stratigraphic cross-sections is in preparation. The sections provide a stratigraphic framework for the rocks between the Mississippian-Devonian boundary and the Onondaga limestone, Middle Devonian. Special emphasis is given to the highly radioactive organic rich shales in the lower part of this stratigraphic sequence. Three major radioactive shale units are defined: the Marcellus, the Rhinestreet, and the Dunkirk. Preliminary mapping of two of these major radioactive shales, Rhinestreet and Dunkirk, has been completed. These units were mapped since they are the primary producing intervals in the recent shale gas wells in Pennsylvania. The maps indicate excellent exploration potential in northwest Pennsylvania. The Rhinestreet is the more extensive and thicker of the two. It reaches a maximum thickness of approximately 200 feet and extends over most of northwest Pennsylvania. The area of maximum Rhinestreet thickness in eastern Erie and Crawford Counties looks very promising. The Dunkirk is prospective in the extreme northwest portion of the state, primarily in Erie County.

Black organic rich shales of Devonian age underlie a large portion of the eastern U. S. (Figure 1). In 1821, the first well drilled specifically for natural gas in the U. S. produced from these black shales. The well was located in Fredonia, Chautauqua County in western New York State. Between the discovery of this well in 1821 and at least to 1880, natural gas was produced from many shallow low pressure wells in a belt along Lake Erie from Dunkirk, New York, through Erie, Pennsylvania, to Sandusky, Ohio. However, other than some descriptive information, little data is available.

In Pennsylvania, three field areas are indicated on old maps of Erie County. These fields, which are the Girard, Erie, and North East fields (Figure 2), are part of the gas trend which extended along the Lake and are believed to be associated with the black shale facies. Locations and driller's logs are not available for the wells in these fields. Since the gas is known to have been used locally, the field outlines may simply define major population areas and actual production may have been more extensive.

At present black shale production is limited to two wells in Pennsylvania. These are the #1 Metropolitan Brick well drilled by Quaker State in Beaver County, and the #3 well drilled by Welch Foods, Inc. in Erie County (Figure 2).

Details of the Metropolitan Brick well are shown in Figure 3. The well was completed in February, 1975 with no natural gas production but with an initial potential of 150 Mcf gas per day at 1150 pounds rock pressure after fracturing. The various stratigraphic units are indicated on the log, and the gas productive shales which were perforated are indicated. The logs demonstrate that the productive shales have a high gamma ray response, low density response and a high porosity indicated on the neutron log; the resistivity log shows a reading of 100 ohms or greater; and the sonic log cycle skips through the productive shales. The cycle skipping may be caused by natural fractures or gas in the formation. The high resistivity presumably indicates hydrocarbon content. The low density and high gamma radiation responses may result from high organic content.

Details of the Welch Foods, Inc. #3 well in Erie County are shown in Figure 4. This well is located in the old shale producing area along Lake Erie, specifically in the old North East shale gas field, and may be a model for the type of production which occurred along the Lake. The well was completed in September of 1976 with gas production of 12 Mcf per day natural flow, and an initial potential of 150 Mcf per day with 80 lb. rock pressure after fracture. The various stratigraphic units are indicated on the log, and it is noted that the highly radioactive zones have low density log responses and high porosity readings on the neutron log. Resistivity in these zones is 100 ohms or greater. These are identical to the characteristics of the gas productive zones in the Metropolitan Brick well. A sibilation log was also run in the well, and the positive readings may indicate fracturing. The sibilation log was not run in the lower portion of the well, probably due to fluid in the hole. Treatment of the well appears to have been based primarily on the sibilation log.

The relationship between natural gas production and high gamma ray responses indicated in the Metropolitan Brick well and the Welch Foods well demonstrate that stratigraphy based primarily on gamma ray log correlations is a reasonable approach to establishing the stratigraphic framework of the gas bearing shales. Published work by Martin and Nuckols [1976] and Bagnal and Ryan [1976] in West Virginia support the concept that the highly radioactive zones are the gas bearing zones. Martin and Nuckols plotted the gas shows in thirty-seven wells in the Cottageville shale gas field located in Jackson and Mason Counties, West Virginia, on a typical gamma ray log from the field. This plot shows a direct correlation between the gas shows in the wells and the high radioactive zones on the gamma ray log. Bagnal and Ryan analyzed well cuttings for gas content from the Columbia Gas Transmission Corp. #9842 well in Kanawha County, West Virginia. Their results show a direct correlation between the total gas content of the cuttings and high radioactivity on the gamma ray log of this well.

In this study, shales which are called black or organic rich correspond to highly radioactive zones defined on the gamma ray log. This response appears to be due primarily to high organic content with some possible relationship to fractures. Highly radioactive zones on the gamma ray logs can also be correlated generally to black shale zones as defined on sample logs. Gamma ray logs were also employed for basic correlations since they are commonly run in most Pennsylvania wells, are readily available, and can be interpreted consistently.

The stratigraphic terminology used in the study for the black shales is based upon common usage in Pennsylvania. However, since most of the black shales have not been previously defined in

Pennsylvania, New York terminology is applied to the majority of the black shale units [Oliver, et al., 1969]. The radioactive portions of the formal stratigraphic units are also indicated on the logs and cross-sections and are divided into massive radioactive and interbedded radioactive zones. Radioactivity in shales is believed to be due primarily to the degree of K^{40} concentration. Radioactive shales in this paper are those having a response which is 20 API units above a base line for normal shales. These abnormally high responses are believed to be due to the presence of elements of the uranium-thorium series which themselves may be related to the presence of organic matter. Twenty API units was selected for the cutoff line because this amount was thought to be consistently above any recognizable instrument or operator induced deviations of the gamma ray logs. Massive radioactive units are defined as those greater than 25 feet thick with split beds included only if the thickness of the overlying radioactive bed is greater than that of the intervening split. Highly radioactive beds which are not massive are defined as interbedded. Most of the black shales tend to be massive radioactive near the base and gradational or interbedded toward the top.

Using the established criteria, three major black shale units have been defined. These are the Middle Devonian Marcellus shale and the Upper Devonian Rhinestreet and Dunkirk shales. The Rhinestreet is the primary producing interval in the previously mentioned Metropolitan Brick well in Beaver County (Figure 3). The thin Burket and Middlesex shales were also gas productive in this well, but the Rhinestreet is the primary producing interval. The Dunkirk shale is the primary producing interval in the previously mentioned Welch Foods, Inc. well in Erie County (Figure 4). The Dunkirk shale is believed to be equivalent to the Lower Huron shale of Ohio [Schwietering, 1970] and to the primary producing interval in the Cottageville and Big Sandy shale gas fields of West Virginia. The Rhinestreet shale in the Welch Foods well (Figure 4) also appears to have good potential. The reason the Rhinestreet was not tested in this well is unknown.

The distribution of reported gas shows in the Devonian organic rich shales is shown in Figure 2. Marcellus shale gas shows have been reported mainly from wells in the north central and southeastern portions of the study area, whereas gas shows in the brown shales above the Tully have been reported mainly from wells in the northwestern portion of the state. The reported gas shows in the Marcellus appear to be closely related to the Chestnut Ridge anticline in Fayette and Westmoreland Counties. This may indicate that the shows are related to structure; however, it may also be a result of drilling density since most wells are drilled on structure. The reported shows from brown shales above the Tully Limestone are primarily located in two areas: one along Lake Erie, which is closely related to the old shale gas fields that extended along the Lake and to the recent shale gas producing well, the Welch Foods, Inc. #3. The other area is in Beaver County which is in the vicinity of recent shale gas production from the #1 Metropolitan Brick well drilled by Quaker State.

A series of nine stratigraphic cross-sections have been constructed across Pennsylvania (Figure 5). The sections are based primarily on the gamma ray log correlations with some sample descriptions. The stratigraphic sections provide a framework for the rock units between the Mississippian-Devonian contact and the top of the Onondaga Limestone of Middle Devonian age. These rocks encompass the Catskill clastic wedge in Pennsylvania and special emphasis is placed on the black, organic rich shales in the lower portion of this rock sequence.

Figure 6 and Figure 7 are two schematic diagrams across western Pennsylvania, east-west section C1-C3, and north-south section A1-D1. The stratigraphic sections use the base of the Marcellus black shale as the datum with the top of the section at the Mississippian-Devonian boundary. This boundary is placed at the base of one of the following sands: the Berea - the Cussewago - the Corry-the Knapp - the Murrysville. Although these sands are not exactly correlative, their position marks what is called the "traditional" Mississippian-Devonian boundary [Kelley and Wagner, 1970]. This time line is difficult to pick in the subsurface since there is no time linked lithologic break at the boundary. The same depositional system was continuous from Upper Devonian into Mississippian time.

As mentioned previously, three major radioactive shales are defined in Pennsylvania. In sequence upward, these are the Marcellus, the Rhinestreet, and the Dunkirk shales (Figure 7). The cross-sections demonstrate that the Marcellus shale is a massive radioactive unit in southeastern Pennsylvania and becomes interbedded and thin toward the northwest. The Rhinestreet shale is an entirely massive radioactive unit in northwestern Pennsylvania and interfingers with less radioactive shales toward the southeast. In some wells only a portion of the rocks equivalent to the Rhinestreet shale appear to be radioactive. In the southeastern portion of the study area no radioactive shale occurs in the Rhinestreet interval and in some wells, markers defining the interval of Rhinestreet equivalents could not be picked. This probably reflects dilution of the organic black shales by clastics derived from the southeast. It should also be noted that the

radioactive portion of the Rhinestreet climbs slightly in the section defined as Rhinestreet equivalent. The Dunkirk shale, like the Rhinestreet, is massive radioactive in northwest Pennsylvania and becomes interbedded and increasingly undefinable toward the southeast. The black shale environment shifts toward the west from Marcellus to Rhinestreet to Dunkirk. This black shale environment shift probably reflects the progradation of the Catskill clastic wedge.

The rocks which both overlie the black shales and are equivalent to the black shale in the eastern portion of the study area are primarily grey shales and siltstones with some thin sands. This thick sequence is undivided since the gamma ray log displays very little character through these rocks. Above these grey shales and siltstones are the sandstones of the Upper Devonian which are the traditional shallow oil and gas reservoirs of western Pennsylvania (Figures 6, 7). The indicated sandstones are defined by a 50% sand cutoff limit on the gamma ray log. In the oil and gas belt of western Pennsylvania, two major sandstone bundles are defined which are informally designated sandstone zone B and sandstone zone D. These lithic zones are further subdivided into intervals based upon driller's terminology for known producing sands. This informal division of the Upper Devonian sandstones is based upon Pennsylvania Geological Survey Progress Report 178 [Wagner, 1969] and Pennsylvania Geological Survey Open File Report #1 [Kelley and Wagner, 1970]. In the eastern portion of the study area sandstones are also present stratigraphically below the traditional producing sands of the oil and gas belt of Pennsylvania. These sands have been informally labeled sandstone zone Bo. Also in the eastern portion of the study where sandstone zones B and D are not separated by the shaly and silty zone C, all the sandstone zones merge and are not subdivided. This is the combined sandstone zone D-B-Bo. Red beds, where reported in the rock sequence, are also defined on the section.

Preliminary mapping of two of the major radioactive zones defined on the cross-sections has been completed. The Rhinestreet and the Dunkirk shales were chosen since they are the primary productive zones in the two currently producing shale gas wells in Pennsylvania. The radioactive portion of the shales were mapped because as demonstrated previously they define the gas productive organic rich black shale facies.

Figures 8, 9, and 10 are maps of the Rhinestreet shale including structure on the base of the shale, isopach of the massive radioactive shale, and total net feet of radioactive shale. The structure map shows a uniform dip to the southeast. The base of the shale is 500 feet below sea level along Lake Erie and dips to 4000 feet below sea level near the 25 net feet limit of radioactive shale in Beaver, Butler, and Clarion Counties. The massive radioactive Rhinestreet is observed to be limited to northwest Pennsylvania where it has a maximum thickness of approximately 200 feet. The Metropolitan Brick well in Beaver County which was mentioned previously produces gas primarily from the Rhinestreet shale. This well has approximately 50 feet of massive radioactive shale within the Rhinestreet and if this is taken as a minimum to predict possible gas production, the area of possible production from the Rhinestreet is quite extensive. The area of thick massive radioactive shale within the Rhinestreet in eastern Crawford and Erie Counties looks especially promising (Figure 9). The total net feet of radioactive shale within the Rhinestreet is shown in Figure 10. The net feet value includes both massive and interbedded radioactive shales. The radioactive shale is restricted to the northwest portion of Pennsylvania and has a maximum thickness of about 225 feet. It is noted that in comparing the massive radioactive shale map to the map of total net feet of radioactive shale that the thick massive area in eastern Crawford and Erie Counties is very close to the total amount of radioactive shale, whereas toward the southwest in Venango and Butler Counties, even though the total amount of radioactive shale is relatively high, no single bed is greater than 25 feet in thickness. It is unknown at this time if potential gas production will be found only in the massive radioactive zones or if the interbedded zones are also prospective. The presence of a natural fracture system may also be critical for production.

Figures 11, 12, and 13 are maps of the Dunkirk shale, including structure on the base of the shale, isopach of the massive radioactive shale and total net feet of radioactive shale. Structural dip again is uniform to the southeast with some minor structural nosing. The base of the Dunkirk is just at or above sea level along Lake Erie and dips to approximately 2500 feet below sea level at the limit of 25 feet of total radioactive shale in the Beaver County area. The area of massive radioactive Dunkirk shale (Figure 12) is restricted almost exclusively to Erie County with a maximum thickness of 75 feet near the New York border. Present production is restricted to one well, the Welch Foods well in the North East quadrangle near the Lake and the 50 foot thickness contours. The old Lake Erie shale gas production of the late 1880's is believed to have been primarily from this zone also. If 25 feet is taken as minimum for possible production, the potential area is restricted to Erie County. The total amount of radioactive shale in the Dunkirk is shown in Figure 13. The radioactive shale is restricted to extreme northwest Pennsylvania,

primarily in Erie and Crawford Counties. A small area of radioactive shale is located in Beaver County, with the 25 foot contour line probably extending through Ohio parallel to the Pennsylvania border, as shown by the dashed contour line.

Commercial production in shale gas fields in West Virginia and Kentucky is known to be related to natural fracture systems [Martin and Nuckols, 1976] [Patchen and Larese, 1976]. The organic shales serve as the source beds and the fracture system the reservoir. Whether similar natural fracture systems occur in the shales in Pennsylvania, or whether the shales can be artificially stimulated to produce a reservoir is unknown at this time. What is known is that there are three major black shale bodies in the Upper and Middle Devonian of Pennsylvania. Mapping of two of these black shales, the Rhinestreet and Dunkirk, indicate excellent exploration potential in northwest Pennsylvania. The Rhinestreet is the more extensive and thicker of the two in Pennsylvania, but the Dunkirk is prospective in the extreme northwest portion of the state primarily in Erie County. Currently gas is produced from both shales but is limited to one well from each zone. A third well, the Peoples Natural Gas #1 Fleck in Mercer County (Figure 2), is being considered by ERDA and the operator, Peoples Natural Gas Co., for fracturing. Radioactive zones within the Rhinestreet appear to have potential, and a successful completion would make the well the third current shale gas producer in the state. Future exploration work, primarily drilling and testing of the shale with extensive coring and logging, will be needed to determine the feasibility of economic development of this resource.

ACKNOWLEDGEMENTS

The authors thank Ms. Karen Elmeier, Ms. Ann M. Tasillo and Messrs. Lee R. Golden and Phillip H. Golden who aided in the collection, processing, and illustration of well data. Mr. Lajos J. Balogh is responsible for all illustration preparation. The cooperation and advice of Mr. John Roen of the U. S. Geological Survey is greatly appreciated. Support for this study was provided by the U. S. Energy Research and Development Administration under contract E(40-1)-5198.

REFERENCES

Bagnal, W. D. and Ryan, W. M., 1976, *The geology, reserves, and production characteristics of the Devonian shale in southwestern West Virginia*, in *Devonian shale production and potential: Proceedings of the 7th Appalachian Petroleum Geology Symposium*, MERC/SP-76/2, ERDA, Morgantown, WV, p. 41-53.

Kelley, D. R. and Wagner, W. R., 1970, *Surface to Middle Devonian (Onondaga) subsurface stratigraphy, Part I*, PA Geol. Survey, 4th Survey, Open File Report No. 1.

Martin, P., and Nuckols, E. B., 1976, *Geology and oil and gas occurrence in the Devonian shales: northern West Virginia*, in *Devonian shale production and potential: Proceedings of the 7th Appalachian Petroleum Geology Symposium*, MERC/SP-76/2, ERDA, Morgantown, WV, p. 20-40.

Oliver, W. A., Jr., DeWitt, W., Jr., Dennison, J. M., Hoskins, D. M., and Huddle, J. W., 1969, *Correlation of Devonian rock units in the Appalachian Basin*, U. S. Geol. Survey, Oil and Gas Investigations Chart OC-64.

Patchen, D. G., and Larese, R. E., 1976, *Stratigraphy and petrology of the Devonian "brown" shale in West Virginia*, in *Devonian shale production and potential: Proceedings of the 7th Appalachain Petroleum Geology Symposium*, MERC/SP-76/2, ERDA, Morgantown, WV, p. 4-19.

Schwietering, J. B., 1970, *Devonian shales of Ohio and their eastern equivalents:* unpublished Ph.D dissertation, Ohio State University, Columbus, Ohio, 79 p.

Wagner, W. R., 1969, *Representative gamma ray logs from shallow and deep wells of western Pennsylvania*, PA Geol. Survey, 4th Survey, Progress Report No. 178.

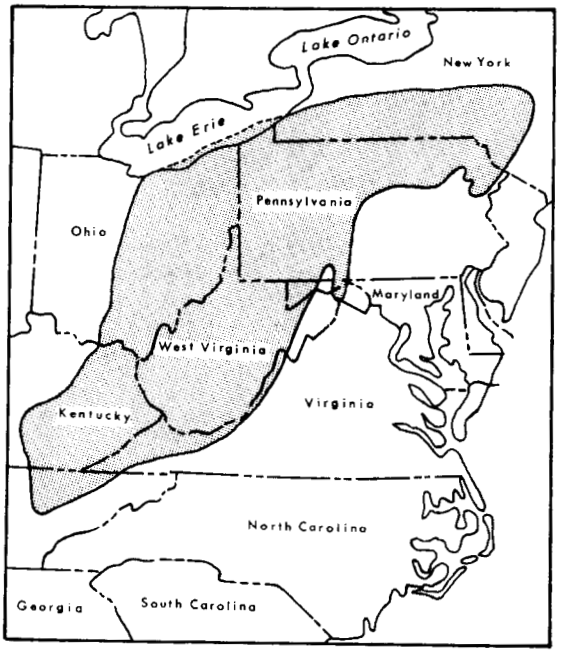
Lake Ontario
New York
Lake Erie
Pennsylvania
Ohio
Maryland
West Virginia
Virginia
Kentucky
North Carolina
Georgia
South Carolina
Area of Devonian black shales
From Dewitt, 1976

FIGURE 1

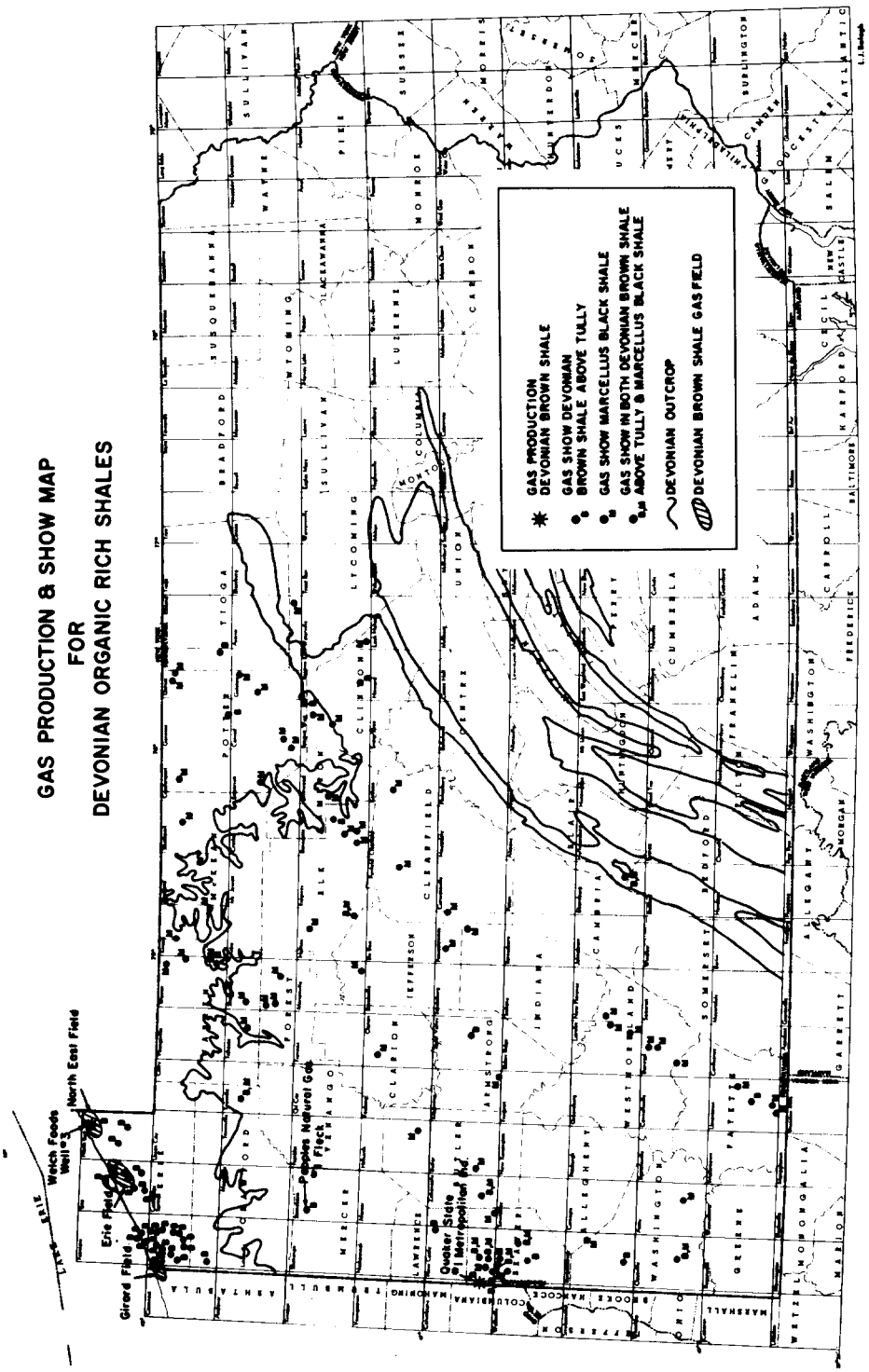
GAS PRODUCTION & SHOW MAP
FOR
DEVONIAN ORGANIC RICH SHALES
GAS PRODUCTION
DEVONIAN BROWN SHALE
GAS SHOW DEVONIAN
BROWN SHALE ABOVE TULLY
GAS SHOW MARCELLUS BLACK SHALE
GAS SHOW IN BOTH DEVONIAN BROWN SHALE
ABOVE TULLY & MARCELLUS BLACK SHALE
DEVONIAN OUTCROP
DEVONIAN BROWN SHALE GAS FIELD
North East Field
Welch Foods Well #3
Erie Field
Girard Field
Peoples Natural Gas Fleck
Quaker State #1 Metropolitan Ind.

FIGURE 2

Columbiana I 5

Beaver Co.
Metropolitan Brick I
Quaker State
El= 948 gl.

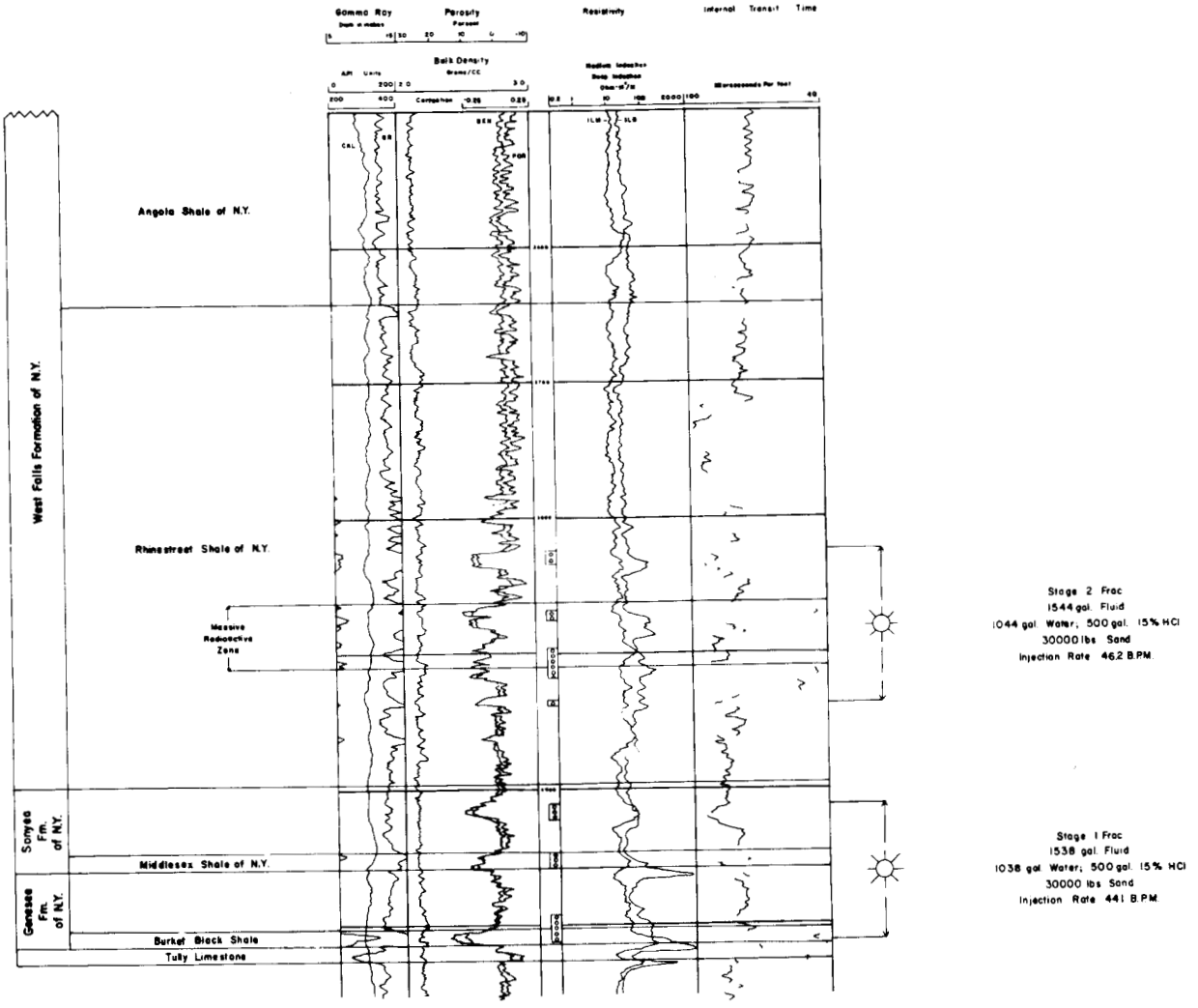

Shale Gas Discovery, Darlington Field
Completed 2/6/75
Gas Pay Natural-None; 150 MCF After Frac 1150 lb R.P

FIGURE 3

Northeast B38

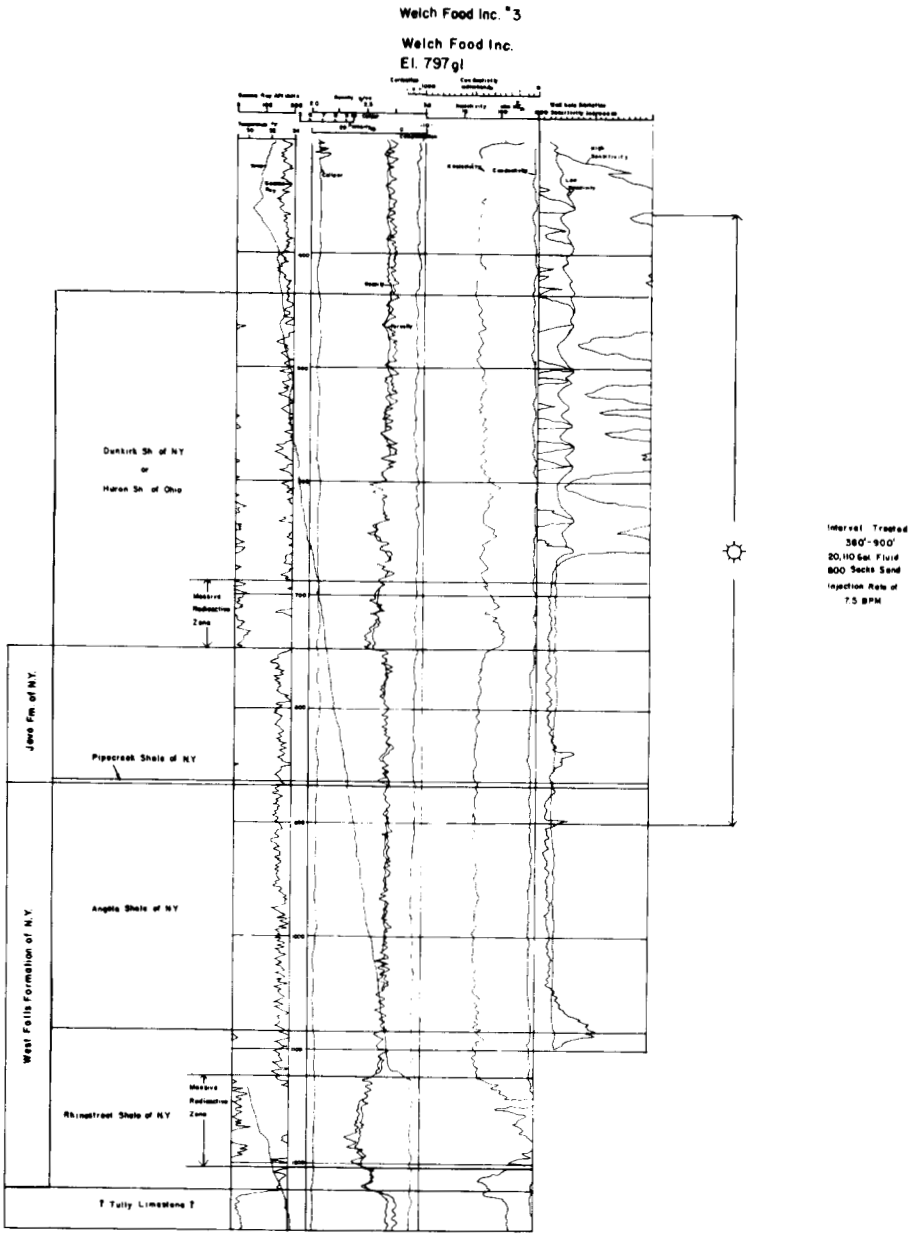

Shale Gas Discovery
Completed 9/30/76
Gas Pay 12 MCF Natural;
150 MCF After Frac,
80 Lbs. Rock Pressure

FIGURE 4

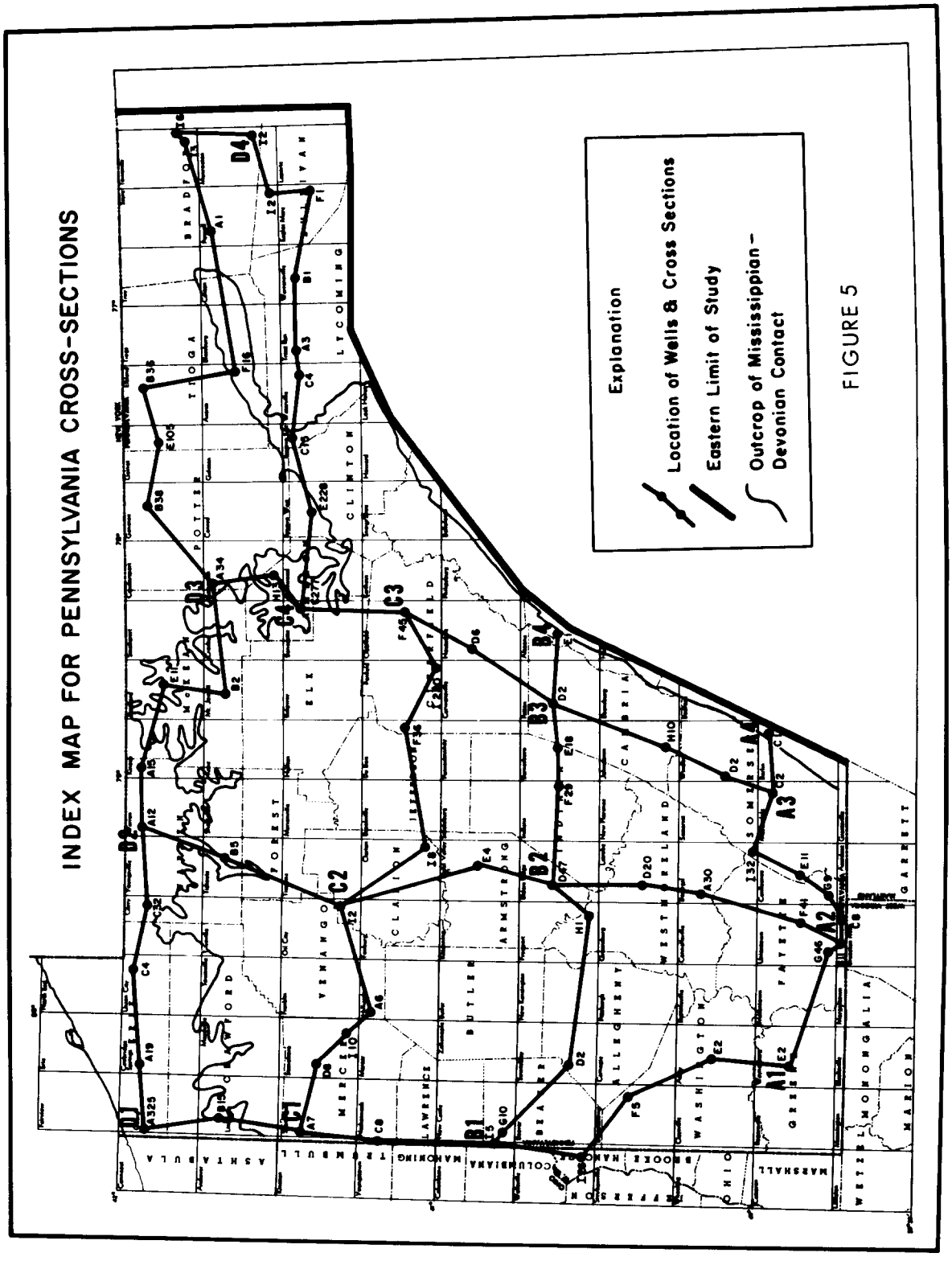
INDEX MAP FOR PENNSYLVANIA CROSS-SECTIONS
Explanation
Location of Wells & Cross Sections
Eastern Limit of Study
Outcrop of Mississippian – Devonian Contact
FIGURE 5

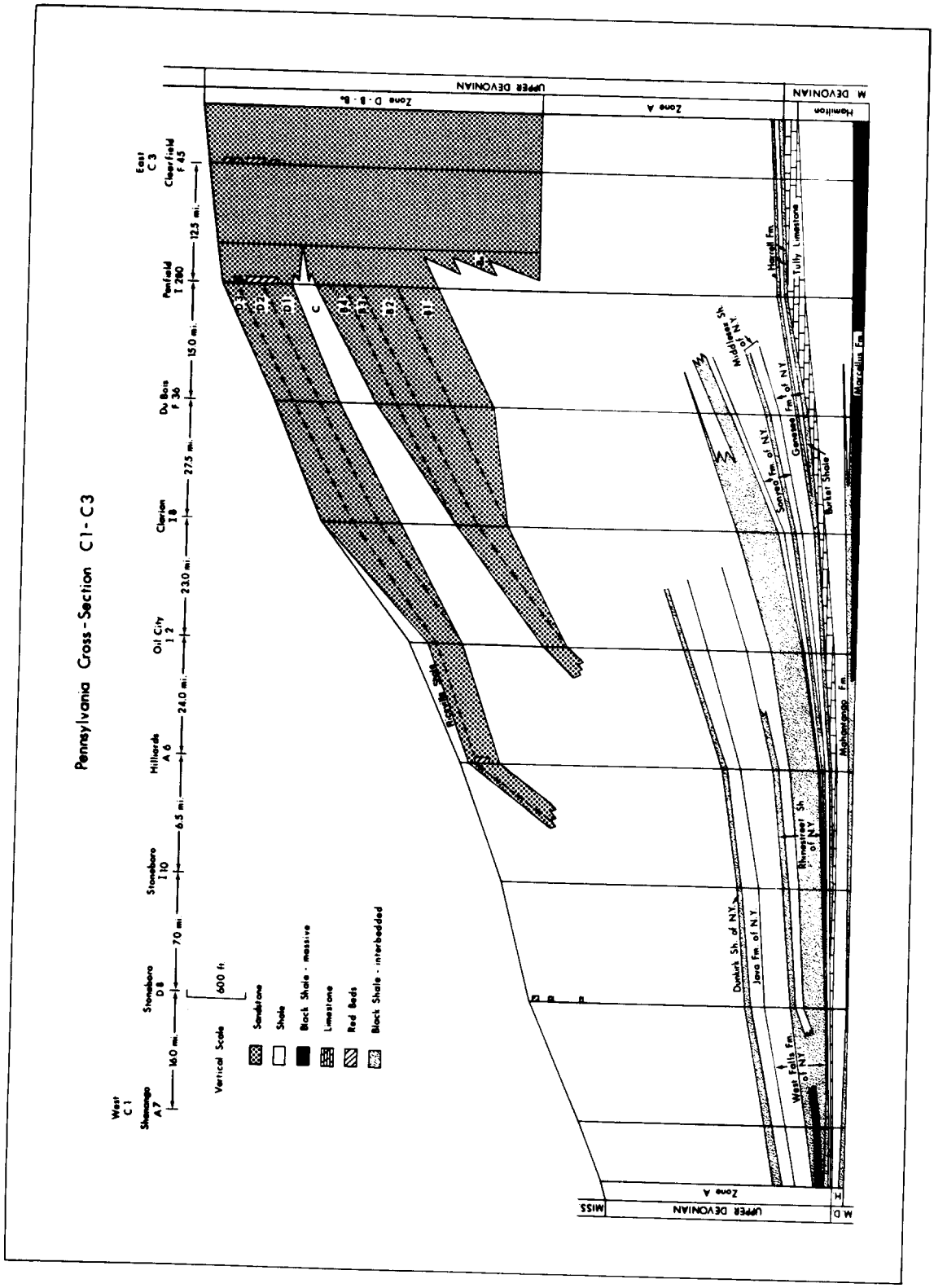
Pennsylvania Cross-Section C1-C3
West C1 Shenango A7
Stoneboro D8
Stoneboro I10
Hilliards A6
Oil City I2
Clarion I8
Du Bois F36
Penfield I280
East C3 Clearfield F45
16.0 mi.
7.0 mi.
6.5 mi.
24.0 mi.
23.0 mi.
27.5 mi.
15.0 mi.
12.5 mi.
Vertical Scale
600 ft
Sandstone
Shale
Black Shale - massive
Limestone
Red Beds
Black Shale - interbedded
UPPER DEVONIAN
Zone D-B-B
Zone A
M DEVONIAN
Hamilton
Harrell Fm.
Tully Limestone
Middlesex Sh. of N.Y.
Genesee Fm. of N.Y.
Sonyea Fm. of N.Y.
Burket Shale
Marcellus Fm.
Mahantango Fm.
Rhinestreet Sh. of N.Y.
Dunkirk Sh. of N.Y.
Java Fm. of N.Y.
West Falls Fm. of N.Y.
MISS
M.D.

FIGURE 6

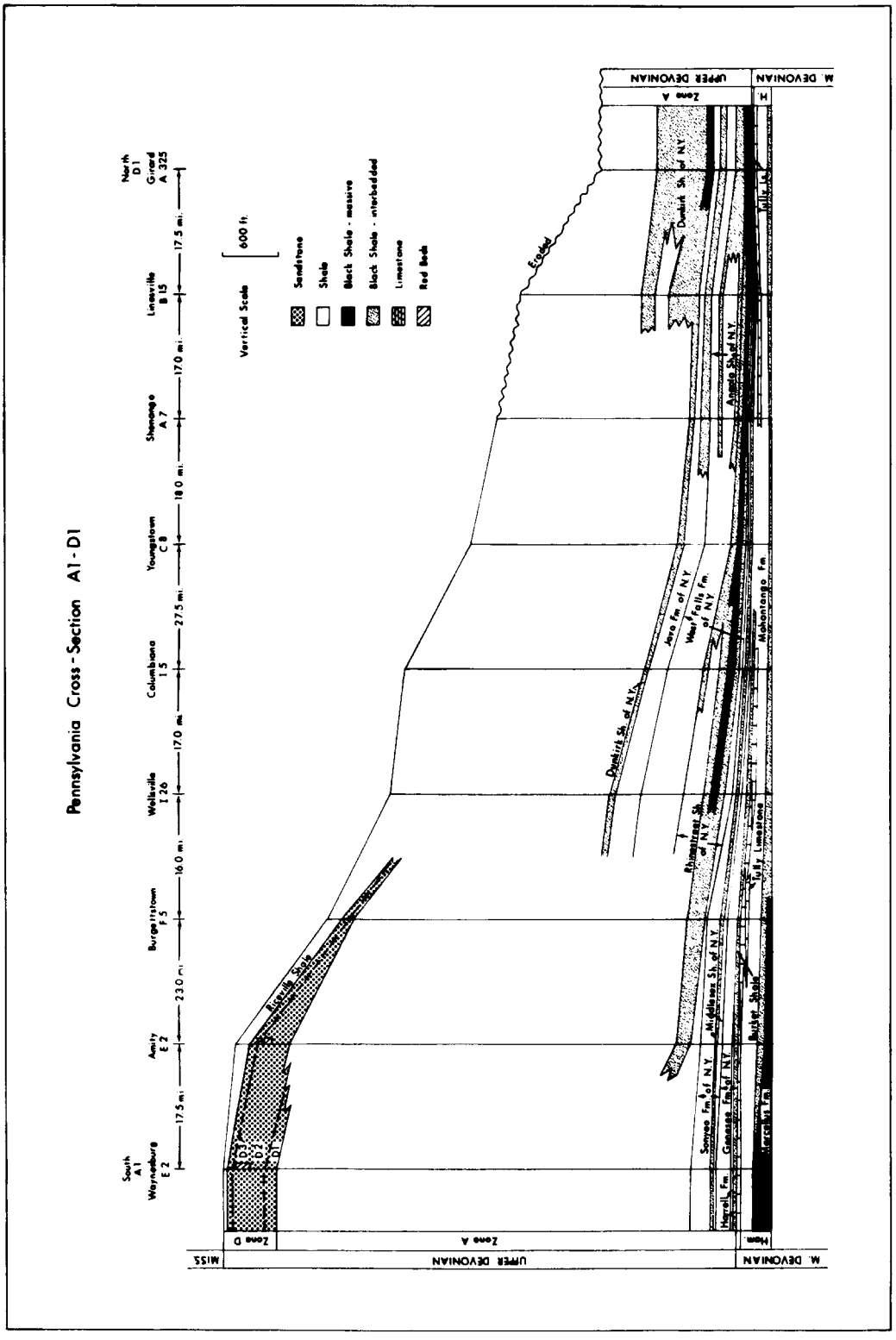
Pennsylvania Cross-Section A1-D1
South A1 Waynesburg E2
Amity E2
Burgettstown F5
Wellsville I26
Columbiana I5
Youngstown C8
Shenango A7
Linesville B15
North D1 Girard A325
17.5 mi.
23.0 mi.
16.0 mi.
17.0 mi.
27.5 mi.
18.0 mi.
17.0 mi.
17.5 mi.
Vertical Scale
600 ft.
Sandstone
Shale
Black Shale - massive
Black Shale - interbedded
Limestone
Red Beds
Eroded
Rickville Shale
Dunkirk Sh. of N.Y.
Java Fm. of N.Y.
West Falls Fm. of N.Y.
Angola Sh. of N.Y.
Mahantango Fm.
Tully Limestone
Rhinestreet Sh. of N.Y.
Middlesex Sh. of N.Y.
Sonyea Fm. of N.Y.
Genesee Fm. of N.Y.
Harrell Fm.
Burket Shale
Tully Ls.
Zone D
Zone A
Zone A
UPPER DEVONIAN
M. DEVONIAN
MISS.
UPPER DEVONIAN
M. DEVONIAN

FIGURE 7

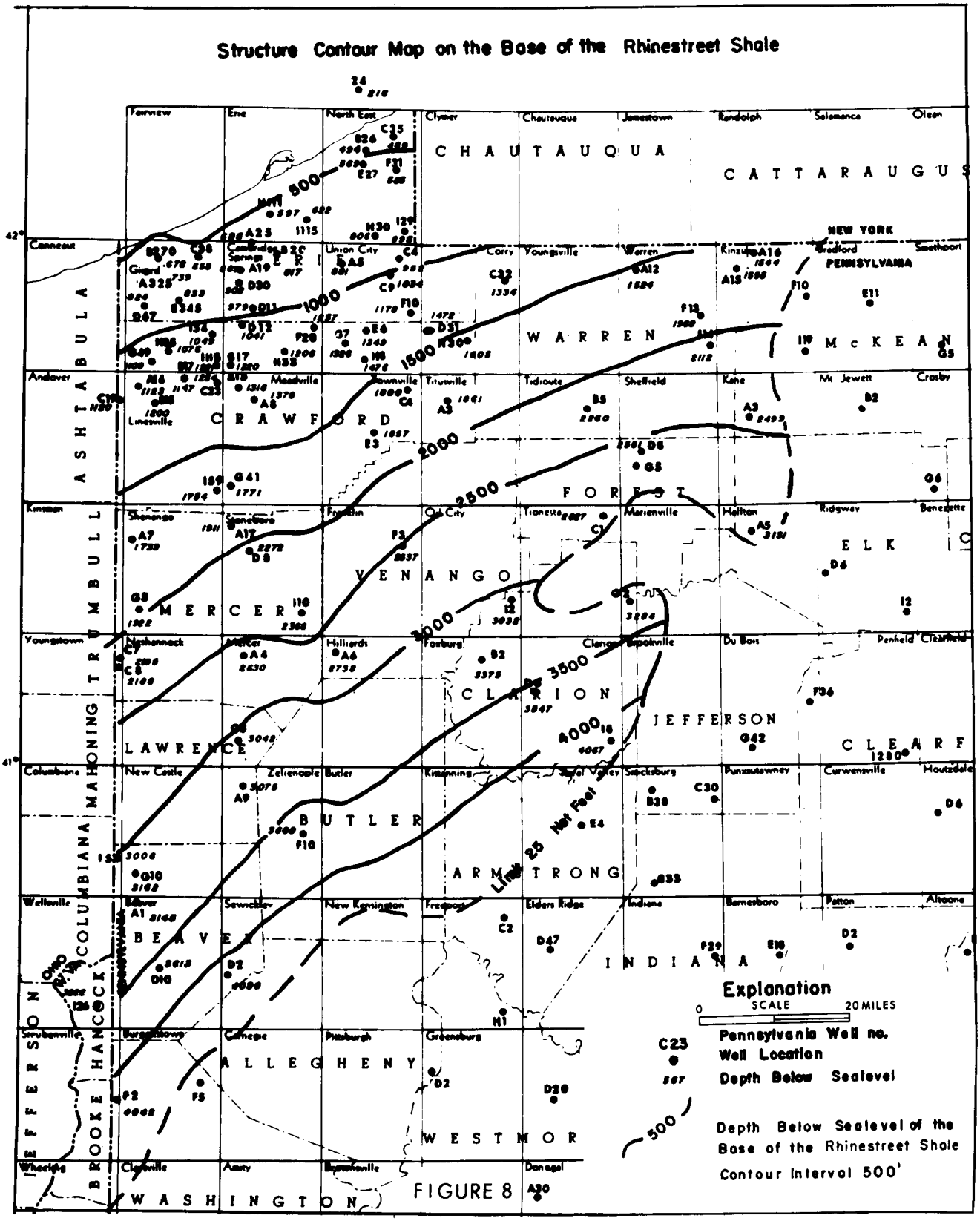
Structure Contour Map on the Base of the Rhinestreet Shale
CHAUTAUQUA
CATTARAUGUS
ASHTABULA
ERIE
WARREN
McKEAN
CRAWFORD
FOREST
TRUMBULL
MERCER
VENANGO
ELK
MAHONING
CLARION
JEFFERSON
LAWRENCE
CLEARFIELD
COLUMBIANA
BUTLER
ARMSTRONG
BEAVER
INDIANA
JEFFERSON
BROOKE
HANCOCK
ALLEGHENY
WESTMORELAND
WASHINGTON
NEW YORK
PENNSYLVANIA
500
1000
1500
2000
2500
3000
3500
4000
Explanation
SCALE 0 20 MILES
Pennsylvania Well no.
Well Location
Depth Below Sealevel
Depth Below Sealevel of the Base of the Rhinestreet Shale
Contour Interval 500'

FIGURE 8

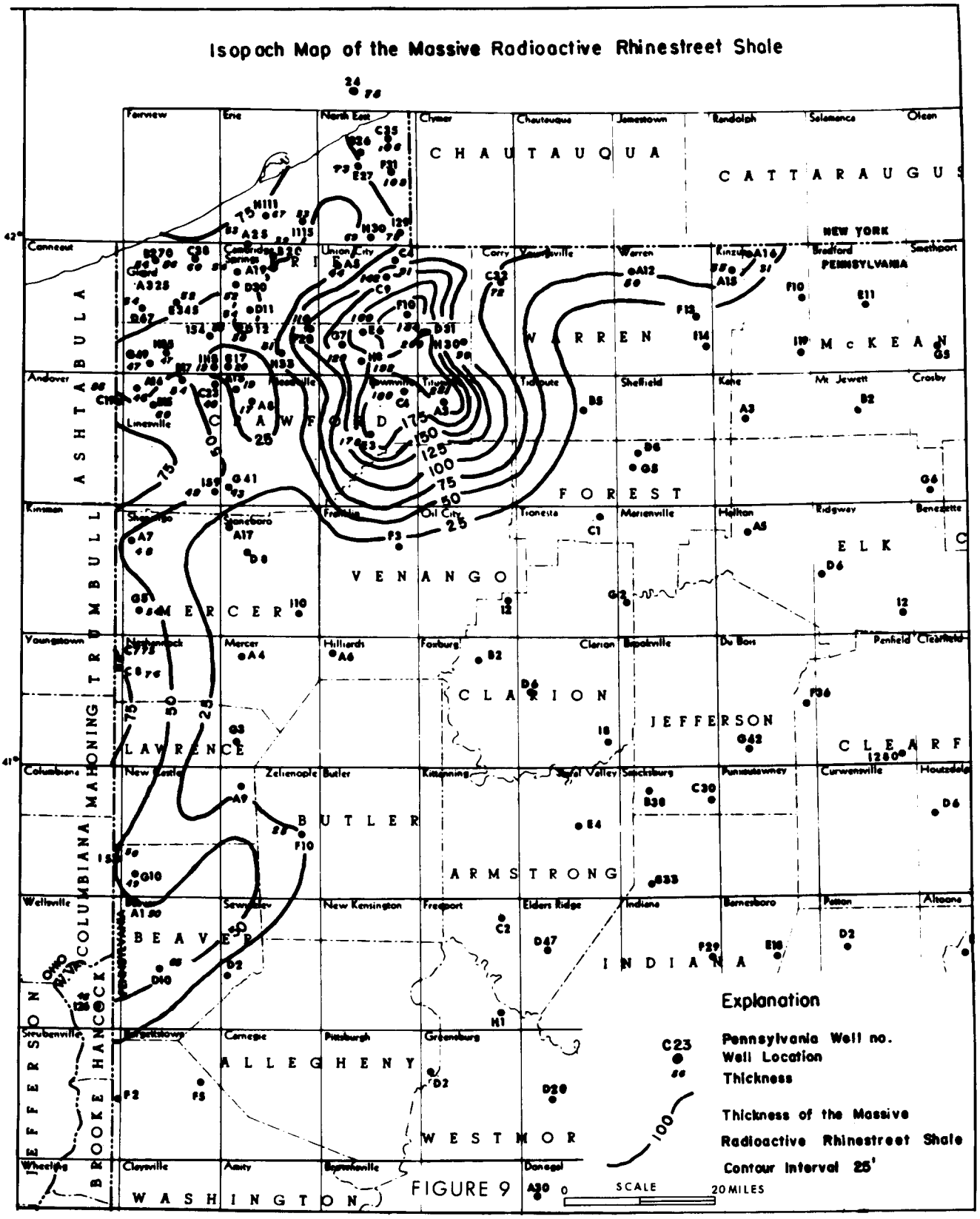
Isopach Map of the Massive Radioactive Rhinestreet Shale
CHAUTAUQUA
CATTARAUGUS
NEW YORK
PENNSYLVANIA
WARREN
McKEAN
CRAWFORD
FOREST
ELK
VENANGO
MERCER
CLARION
JEFFERSON
CLEARF
LAWRENCE
BUTLER
ARMSTRONG
BEAVER
INDIANA
ALLEGHENY
WESTMOR
WASHINGTON
ASHTABULA
TRUMBULL
MAHONING
COLUMBIANA
HANCOCK
BROOKE
JEFFERSON
Explanation
Pennsylvania Well no.
Well Location
Thickness
Thickness of the Massive Radioactive Rhinestreet Shale
Contour Interval 25'
SCALE
0
20 MILES

FIGURE 9

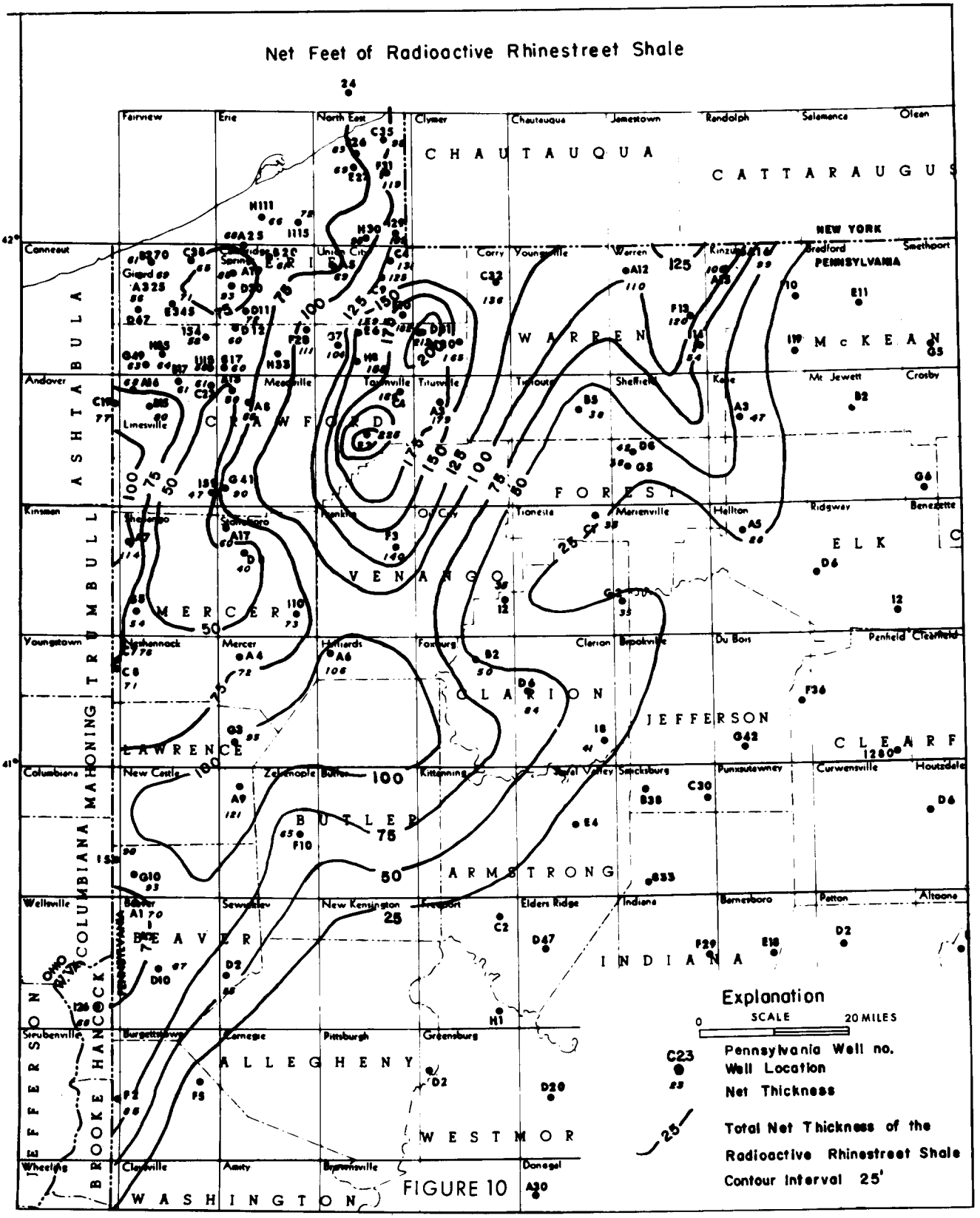
Net Feet of Radioactive Rhinestreet Shale
CHAUTAUQUA
CATTARAUGUS
ASHTABULA
TRUMBULL
MAHONING
COLUMBIANA
JEFFERSON
BROOKE
HANCOCK
WARREN
CRAWFORD
VENANGO
FOREST
ELK
CLEARF
MERCER
CLARION
JEFFERSON
LAWRENCE
BUTLER
ARMSTRONG
INDIANA
BEAVER
ALLEGHENY
WESTMOR
WASHINGTON
NEW YORK
PENNSYLVANIA
McKEAN
Explanation
SCALE 0 20 MILES
Pennsylvania Well no.
Well Location
Net Thickness
Total Net Thickness of the Radioactive Rhinestreet Shale
Contour Interval 25'

FIGURE 10

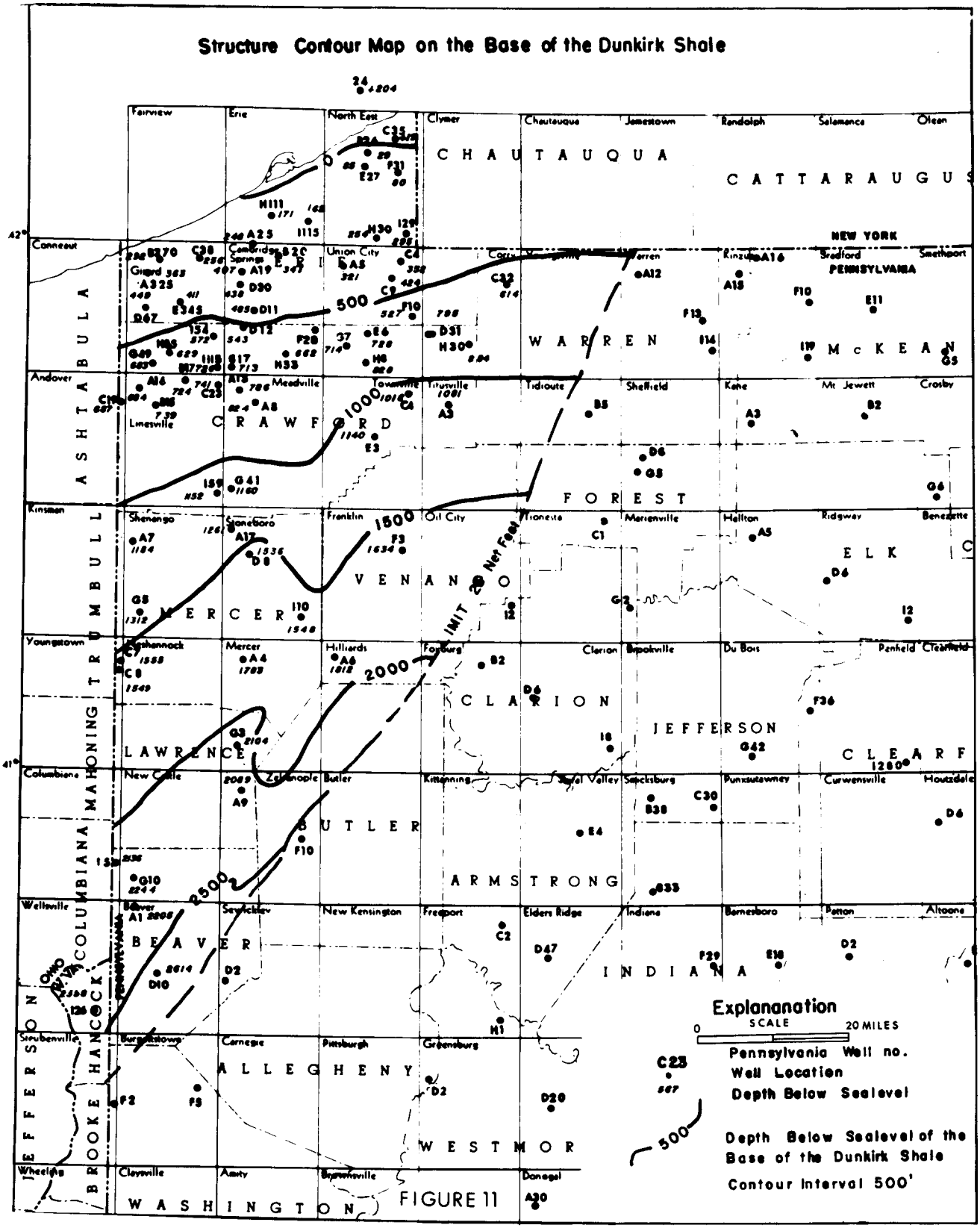
Structure Contour Map on the Base of the Dunkirk Shale
CHAUTAUQUA
CATTARAUGUS
NEW YORK
PENNSYLVANIA
ASHTABULA
TRUMBULL
MAHONING
COLUMBIANA
BROOKE
HANCOCK
WARREN
McKEAN
CRAWFORD
FOREST
ELK
VENANGO
MERCER
CLARION
JEFFERSON
CLEARFIELD
LAWRENCE
BUTLER
ARMSTRONG
BEAVER
INDIANA
ALLEGHENY
WESTMORELAND
WASHINGTON
500
1000
1500
2000
2500
Net Feet
Explanation
SCALE 0 20 MILES
Pennsylvania Well no.
Well Location
Depth Below Sealevel
Depth Below Sealevel of the Base of the Dunkirk Shale
Contour Interval 500'

FIGURE 11

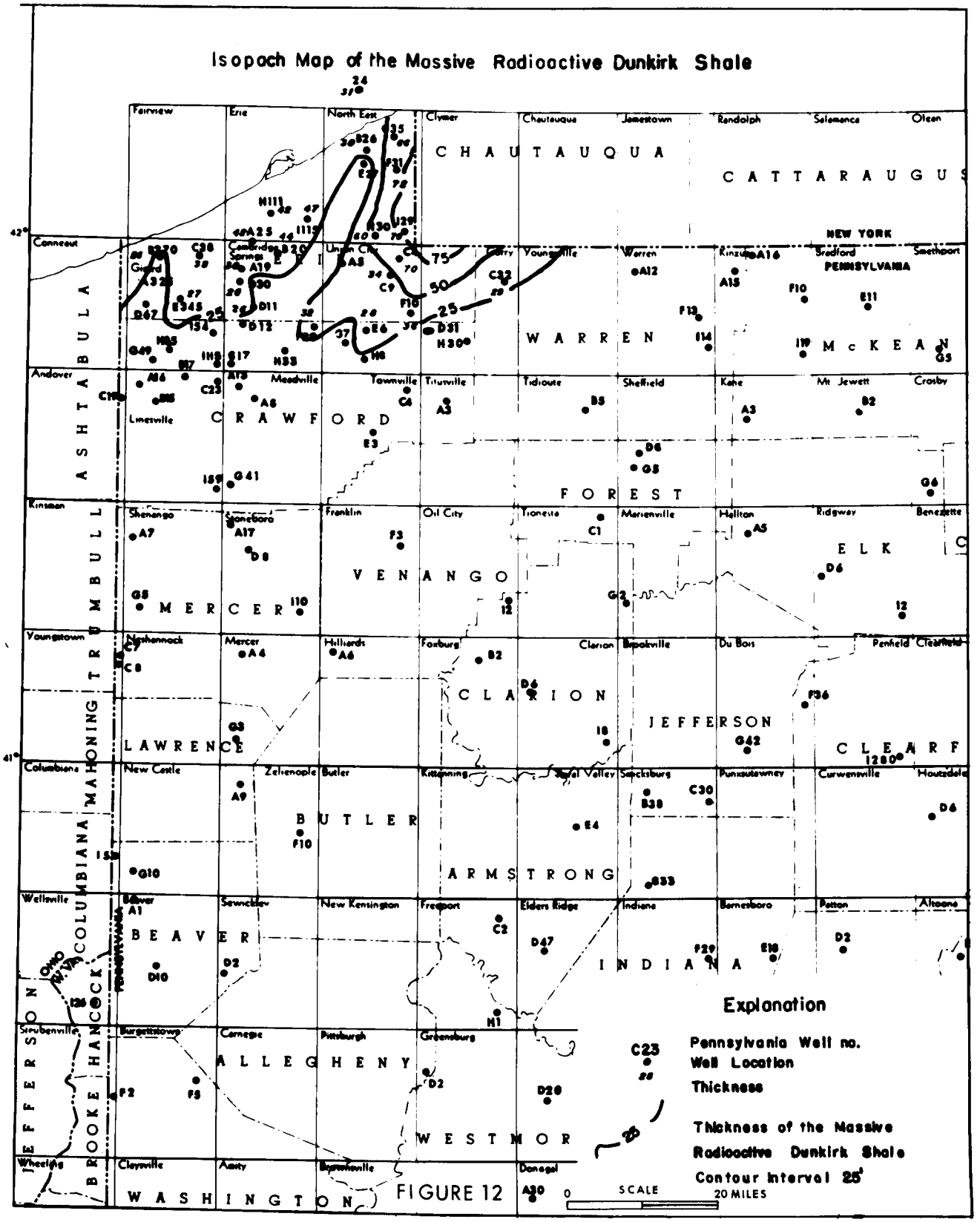
Isopoch Map of the Massive Radioactive Dunkirk Shale
CHAUTAUQUA
CATTARAUGUS
NEW YORK
PENNSYLVANIA
WARREN
McKEAN
CRAWFORD
FOREST
ELK
VENANGO
MERCER
CLARION
JEFFERSON
CLEARF
LAWRENCE
BUTLER
ARMSTRONG
INDIANA
BEAVER
ALLEGHENY
WESTMOR
WASHINGTON
ASHTABULA
TRUMBULL
MAHONING
COLUMBIANA
BROOKE
HANCOCK
JEFFERSON
Explanation
Pennsylvania Well no.
Well Location
Thickness
Thickness of the Massive Radioactive Dunkirk Shale
Contour interval 25'
SCALE
0
20 MILES

FIGURE 12

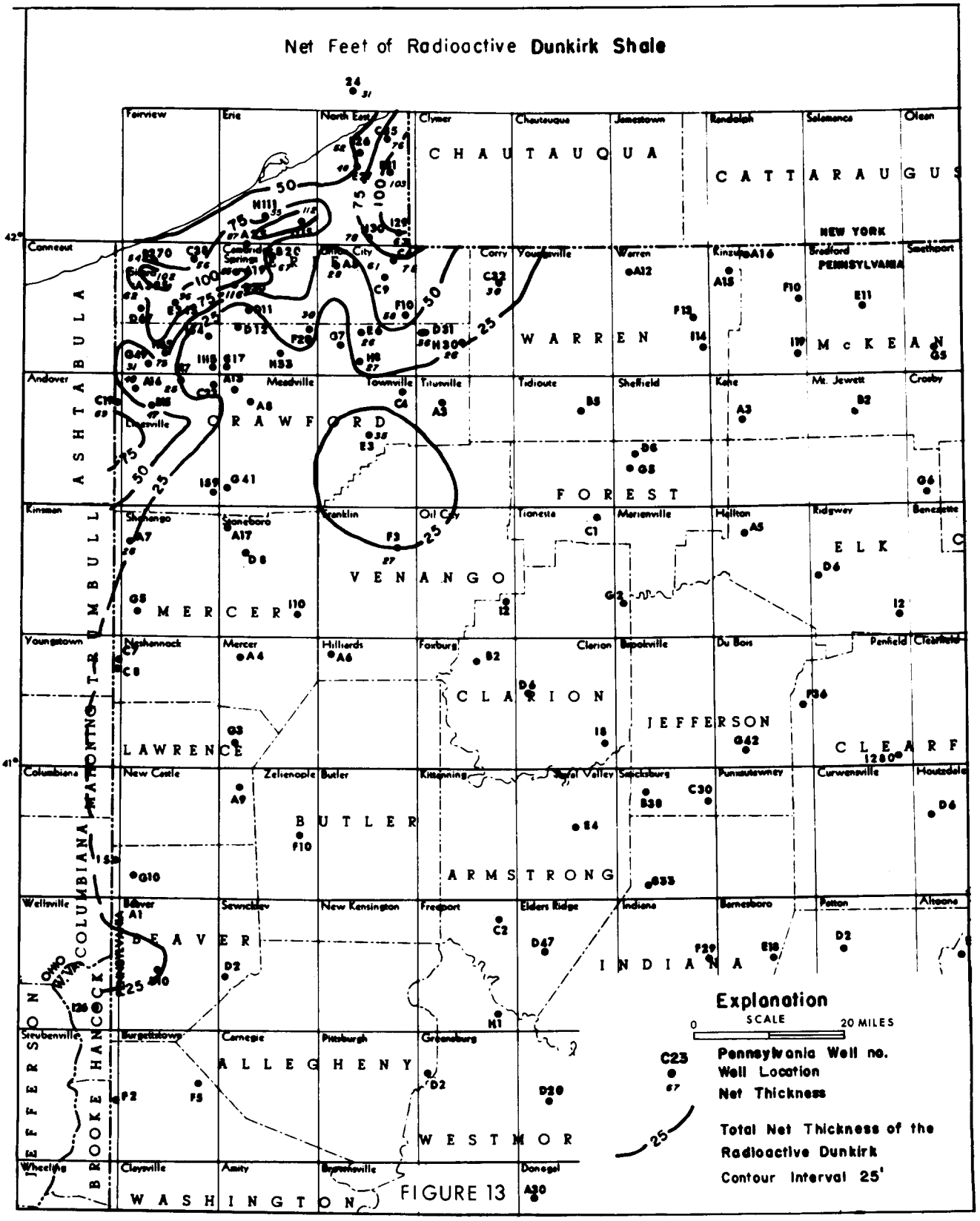
Net Feet of Radioactive Dunkirk Shale
CHAUTAUQUA
CATTARAUGUS
NEW YORK
PENNSYLVANIA
ASHTABULA
WARREN
McKEAN
CRAWFORD
FOREST
TRUMBULL
MERCER
VENANGO
ELK
CLARION
JEFFERSON
CLEARF
LAWRENCE
COLUMBIANA
BUTLER
ARMSTRONG
BEAVER
INDIANA
JEFFERSON
BROOKE
HANCOCK
ALLEGHENY
WESTMOR
WASHINGTON
Explanation
SCALE 0 20 MILES
Pennsylvania Well no.
Well Location
Net Thickness
Total Net Thickness of the Radioactive Dunkirk
Contour Interval 25'

FIGURE 13

WIRELINE LOGS AND SAMPLE STUDIES IN STRATIGRAPHY AND GAS OCCURRENCE OF THE DEVONIAN SHALES ALONG THE SOUTHERN TIE SECTION IN EASTERN KENTUCKY AND VICINITY.

by

Edward N. Wilson, Kentucky Research Foundation, University of Kentucky
Jaffery S. Zafar, Kentucky Research Foundation, University of Kentucky

ABSTRACT

A stratigraphic cross-section (the Southern Tie section) was constructed from Ross County, southeastern Ohio, through northeastern Kentucky and Wast Virginia to Scott and nearby Counties in southwest Virginia, using wireline logs (principally the Gamma Ray and Density logs) and sample studies of key wells along the section.

Stratigraphic correlation by wireline logs, although the section crosses from the craton in Ohio to the deep part of the Valley-and-Ridge, is straightforward, identifying an alternation of radioactive and relatively non-radioactive shale units (some not present at the base in the northwest) across the whole section. In the southweast, there are more units at the base; and the upper radioactive units have been replaced by a different lithology. But wireline log characteristics are not entirely consistent with lithology as apparent in samples. Radioactivity is usually proportional to organic content or dark color; but some shales and metabentonites have unusual radioactivity, and some black shales (especially those exhibiting moderate rather than low density) are only slightly radioactive.

Drillers' shows of gas (indicative of the vertical position of reservoirs) are commonly but not exclusively near the top of radioactive units (the "Berea" production of Pike County, Kentucky, being a significant exception). Very low density shales may be related to fractured or sloughing zones, possibly reservoir zones.

Intensive comparative study of sample descriptions, drillers' reports, and wireline logs may be indispensable to effective stimulation of production in the individual well and to the full development of the gas potential of the Shales.

INTRODUCTION

The coming in to general use of the normal electric log (spontaneous potential and resistivity curves) in the forties was revolutionary to mud rotary country. The driller and geologist all of a sudden had a good depth control and a check on estimated sample lag; and in addition the logs themselves were excellent clues to lithology and hydrocarbon content. Very quickly the promoter (who did not understand the electric log) invented the work "picture" to describe them to this clients; and most of us smiled on this ploy as only a slight, but reasonable, exaggeration. Subsequently, new electrode configurations, contact electrodes, and induction logging were introduced to overcome difficulties with non-conductive mud or to increase precision of interpretation and/or computation; and the geologist was more or less in business without bothering about the rocks themselves.

Cable tool country, as Appalachia, deals in casing strings and dry open hole, so the electric log does not work there; but the introduction of the gamma ray log (and shortly the neutron log), which could operate in dry open hole and see through casing, produced a similar revolution.

They were followed by more precise tools such as the Sidewall Neutron Porosity and Bulk Density. The gamma ray log is not as good a lithology detector as the electric log; but there is good correlation of sand and lime on one hand and fine-grained shale on the other, with carbonaceous and radioactive shale (such as is found in large fractions of the Devonian gas shales) being hyper-radioactive. In general, these logs do not give a clue as to hydrocarbon content (except the neutron log in cases of dry gas in a dry reservoir, and the temperature log where gas is being evolved).

The general use of wireline logs in eastern Kentucky is a post-1960 phenomenon; and even now they are omitted as a pointless expense by many traditional and/or small independent operators. But the Shale gas play is now so marginal economically that most of it is by large operators who do run at least a correlation wireline log, and often run a whole suite for analytical purposes. Often the wireline suite is the only trustworthy document, as in some air rotary wells, where the driller is unable to interpret either the rig response or rate of penetration, and the samples are of (typically) poor quality. So in some instances we may be forced to rely on wireline logs.

However, the major portion of Shale well developments predates the common use of wireline logs; so drillers logs (or Well Completion Reports, to be more precise) supplemented in some instances by sample sets with or without operator-sponsored well-sitesample description may be our only available documentation for important parts of the EGSP mission.

As we use these data (drillers logs), I think we are impressed--even astonished-- at the amount and high quality of information typically retained in them. But also we see depth measurement corrections that connot be applied reasonably up the hole, some records that are marvels of brevity and ambiguity (usually in the critical wells), and a common failure to recognize or record slight variations in lithology or rock type in the Shale which is the chief focus of our attention.

In the face of inadequacies of drillers' logs, as geologists, we are especially pleased by the correlation potential of gamma ray logs, even when the scales of radioactivity of adjacent logs are different, bed-by-bed correlations are usually possible, and significant thicker units can frequently be traced over long distances. Many of the ambiguities of the gamma ray log by itself are simply resolved by the availability of additional curves, particularly the compensated formation density log, that is, the formation density with caliper.

Wireline logs, then, lead us readilly to a preliminary stratigraphic characterization of the Devonian Shales (indeed of the whole Paleozoic sedimentary comumn) and, by their success, may mislead us into thinking we have an infallible handle on every significant fact that might come out of a hole. Also they are d--- easy to use.

It being easy to fall into the error of seeing a one-to-one correlation between wireline log and geologic property, and equally easy to discount the importance of any property which a wireline log fails to inform us about, it is wise to remind ourselves that a wireline log does no more than to measure a geophysical property of a borehole and that we understand the rocks around the borehole only by analyzing and interpreting the logs and the borehole conditions under which they were obtained.

And even assuming the highest levels of interpretive skills, we still need other data effectively to discharge our mission of characterizing the Eastern Gas Shales and enhancing their productive capacities. This paper hopes to illustrate the coordinated use of all available data toward this mission along a significant line-of-section in Ohio, Kentucky, West Virginia, and Virginia.

CLASSIFICATION OF THE UPPER DEVONIAN SHALES BY L. J. PROVO.

(Figure 1)

Working in outcrop and subsurface in northeastern Kentucky, Linda Provo (Fulton) built up a perceptive classification of the Upper Devonian shales, by dividing them into seven units alternating between bodies of black and brown organic shales with minor greenish-gray silty beds and bodies of greenish-gray silty (or calcareous) shale with subordinate dark organic shale. There is a generally good correlation between high radioactivity on gamma ray logs and high organic content of the shale.

At the beginning, Miss Provo used the Inland #537 FANNIN EST., 22-W-82, Boyd County, as her reference subsurface section. This well is on the Southern Tie Section. At this stage she was merely numbering her units. In her later dissertation, she shifted allegiance to Inland #533 FEE, 11-V-81 (also Boyd County) and correlated her units into parts of the standard Ohio nomenclature. Her

Unit #2 was tentatively correlated with Chagrin; but she identified a trio of good marker beds in outcrop which she and colleagues later formally named the Three Lick Bed, so the name Three Lick appears in the Table hereon.

In this classification, units generally thin from the basin to outcrop, and lower ones may be absent. Hence there can be a question whether Unit #7 is actually correlatable with the Marcellus, hence her question mark by that formation.

THE SOUTHERN TIE SECTION

(Figure 2)

The Appalachian Basin in late Devonian time is elongated northeast-southwest. The rocks are thickest at the southeast outcrop and thin to the northwest outcrop on the flank of the Cincinnati Arch. Stratigraphic variation longitudinally is relatively slight; but the Southern Tie section is transverse to the Basin and encounters considerable variation in that direction.

The Section begins at outcrop in Ross County, Ohio thickens southeastward, crosses the Mavity Monocline in Boyd County (monocline in Pennsylvanian rocks at the surface, but probably a fault at Ohio Shale depths), the Walbridge Fault(s) in Lawrence County, the Warfield Fault in Martin County, and the locale of the Pine Mountain Fault (perhaps here an anticline if present at all) in Buchanan County, Virginia. From Buchanan County it doglegs south in one 37-mile jump to Scott County, Virginia, which is pretty deep into the Valley-and Ridge Province and where the Siluro-Devonian carbonates are nearly pinched out. For most of its course it follows the Big Sandy River, which feature may follow a geological lineament with more than Recent significance. The apparent structural thin at 6-U-82, Lawrence County is due to the well's having been projected about six miles northeast to the line of section: the shales seem to thicken in that direction, too.

On this section, gamma ray log correlation is simple along its northwestern half over the whole interval; and is reasonably certain in the lower part (Units #5 and below) over the whole width of the Section.

The Cleveland, Three Lick, and Upper Huron can be traced, thickening gradually from Ohio across the Pine Mountain anticline. The radioactive signatures of the Cleveland and Upper Huron is inexplicably lost in 3-K-87 (Pike County), only to be regained southeast of the Pine Mt. anticline.

Unit #4 (Middle Huron) begins to thicken abruptly southeastward in Pike County. Unit #5, #6, and #7 continue all across the section, splaying southeastward. Unit #7 (Marcellus (?)) is pinched out northwest-ward within Scioto County, Ohio (between 25-Z-81 and 16-CC-79).

In southeastern Buchanan County and in Scott County, Virginia, Units #1 through #4 have lost all semblance of radioactive signature (the Brallier Formation?) but below these levels almost bed-by-bed correlation is possible.

In a qualitative way, we observe that amount of radioactivity in a shale bed is proportional to its organic content; and in turn organic content is inversely proportional to bulk density. This rough approximation allows us to postulate correlations from the bulk density curve as well as from the gamma ray curve. A very choppy density curve in a generally radioactive section (probably) does not indicate thin beds of exceptional organic content, but that the log itself is perturbed by either sloughing of walls of the hole, or by existence of fracturing, either of which might suggest loci of gas occurrence, and nearly always does portend completion problems.

A SAMPLE DESCRIPTION DETAILS A GOOD DRILLERS LOG

(Figure 3)

The advent of the good wireline log lead to poorer drillers logs; but a well-kept drillers log (the rule in the 'old days') is astonishingly useful considering its usual brevity. Color of rock and shows of gas and/or oil are routinely recorded; and neither of these can be obtained from wireline logs.

The Columbian Fuel #1 Jake SMITH, 10-M-86, Pike County, Kentucky was drilled in 1939 and has a good drillers log but no wireline log., and samples were kept. Now sample depth measurements are drillers depth measurements, but generally the intervals are shorter. Also, the geologist gets a

firsthand experience of the rock, whereas the drillers log has passed through the interpretive competences of the driller. The result is a sample description which is more detailed than the driller's, but perforce does not identify shows with certainty. Except that limestone is ground up, cable tool samples cause fewer interpretive problems than rotary samples.

Sometimes shale described as brown or brownish black or resinous is especially radioactive whereas a truly black (blackish black) is not; but commonly there may be no distinction between the colors of radioactive shales and non-radioactive shales. In this well however we have a significant discrepancy in that the sample description calls for much more black shale of the Sunbury than the driller recorded. Wireline logs in both directions do not resolve the dilemma, however, for the driller's thin Subury seems to fit the radioactive thickness in the well to the northwest, and the sample description's thick Sunbury appears to fit the radioactive thickness in the well to the southeast.

In this well, the driller was content with one call of "Corniferous", but the geologist from the samples determines a rich Siluro-Devonian stratigraphy. This latter detail is essential to reasonable exploration.

WIRELINE LOGS VERSUS MUD ROTARY SAMPLES

(Figure 4)

Mud rotary samples have the biggest chunks, allowing the geologist to observe rock textures and structures. They do, however pose an interpretational problem (depthwise) from sample lag and contamination.

In these two wells in Scioto and Lawrence Counties, Ohio, we can make pretty good wireline log correlations. Specifically, we correlate the Bedford Formation between the wells, and, knowing that the Oriskany is present in Scioto County (although the resolution of the gamma ray log leaves its position vague) we identify an Oriskany zone in the Lawrence County well. The facts are, however, that the wireline log does not record color and the "Bedford" is red and siltier and sandier--the Catskill. And the gamma ray density logs do not readily differentiate between sandstone and limestone, with the result that calling Oriskany Sandstone we actually have Bois Blanc Limestone.

In this case lithologic ambiguity was made more obscure because only poor resolution is possible for beds in thicknesses of 3 to 5 feet. But the salutary lesson is that wireline logs by themselves are insufficient for correct interpretation.

WIRELINE LOGS VERSUS AIR ROTARY SAMPLES

(Figure 5)

Air rotary drilling is very speedy and there is virtually no sample lag. The samples come up mostly as a fine powder; and often we cannot determine whether certain lithologies may have been selectively blown away: in short, sample quality is typically poor to impossible. Often it is easy to find excuse to rely on wireline logs exclusively.

It is an interesting irony, that Provo used the FANNIN well as a type. Her Unit #7 is predominately organic and radioactive, and it is identified in the FANNIN well, the only question being whether it can be correlated with the Marcellus black organic shale. The gamma ray indicates a good radioactive (ergo-organic-rich) bed in the unit.

The samples, good quality although air rotary, are unmistakable. The shale is radioactive but medium gray and silty, not organic. Let's leave this before we stratigraphers get embarrassed!

But perhaps an interpretational footnote might be in order: it may be that at diastems, unconformities, and the like radioactive detritus may accumulate--at least, sometimes the expected position of formational boundaries is occupied by a 'shale' which is more radioactive than thin shales above and below-- in eastern Kentucky the putative top of the Ohio Shale is frequently markedly radioactive.

FRACTURES AND RARE LITHOLOGIES ON WIRELINE LOGS AND SAMPLE DESCRIPTIONS

(Figure 6)

The POBST and SMITH wells are 37 miles apart on the southeast end of the Southern Tie Section.

The gamma ray logs of the upper part of the holes indicate no black or radioactive shales correlative with Units #1 and #3 further northwest. The gamma ray log is so conclusive that we are not hesitant to identify black shale in the interval 5730-5770 as misplaced and to move it down to the interval 6130-6170 where samples are missing. We then have good correlation between the wireline log and sample lithology.

Lower parts of the wells correlate readily.

There are reports of faults in the Smith well identified in a non-available dipmeter survey. We are unable to see faults in the Shale either on the gamma ray log or in the samples; apparently, unless we can spot duplication or omission of beds we can't identify faults. We can, however, identify calcite-filled fractures (but no slickensides) in Unit #7, in the samples--perhaps this is some contribution to placing gas in the hole.

When our colleagues put a scintillometer against a metabentonite in a core or on an outcrop, they get a large radioactive response. In a well, however, since the bentonite is thin the gamma ray excursion is scarcely different than for a fine grained shale; so without samples we would usually interpret the wireline log as indicating normal shale or maybe brown shale rather than bentonite. In both the Pobst and the Smith wells, bentonites were found in the samples. Because of depth measurement discrepancies it is difficult to identify the particular beds of the gamma ray logs which are the expressions of the bentonites.

We have tentatively located and identified the Tioga Bentonite in both wells. On the respective wireline logs higher bentonites found in each well (in Unit #6) look like clays in the Smith and brown shale in the Pobst.

(Lights On)

WHERE AND HOW DOES GAS OCCUR IN THE SHALE?

This question is substantive to the mission of the Eastern Gas Shales Project. The driller, of course, merely says, "I call'em as I see'em". And he does a creditable job. Scientific types have suggested three mechanisms of containment of the gas: (a) in finely silty layers with low permeability in the gray shales, (b) in fractures particularly in the organic rich parts of the shale, and (c) adsorbed on the organic constituents and feeding into fracture or intergranular porosity. It is an interesting fact that competent men from different areas of the Basin opt for different mechanism: it may well be that the actual mechanisms are locally controlled.

RECOGNIZING GAS IN THE HOLE

Usually shows of gas are not very large in the shale, and may not even be detectable. The standard measure of a gas show in cable tool practice is the Open Flow (OF) test by orifice-meter or pitot tube, and the shut-in Rock Pressure Test. Both are taken at the surface and can be invalidated by too much open hole under the last casing, thiefing by higher porous beds, leaks in casing, and the special atypical reservoir properties of the Shale itself.

The driller himself has a serious problem in observing the evolution of gas: if appreciable gas is coming out of the hole he may not be able to recognize a minor increment. But cable tool drillers are notably conscientious about shows.

Now the wireline Temperature Log, logged from the top down at first entry into the hole after it has been shut down to equilibrate, has come to aid the driller. For extremely small gas flows there is also the Differential Temperature log (which accentuates small anomalies) and the Sibilation Log (not common in Kentucky) which in effect detects minor hissing from very small flows of gas.

(Figure 7)

Temperature logs run in dry holes (holes not making gas) show a regular increase of temperature

with depth. The rate of increase per unit of depth (slope of the curve) is the geothermal gradient and it is generally higher the deeper you go. But one might also observe that there is some correlation between gradient and formation lithology: sandstones and limestones have a low gradient, shales have a medium gradient, Basement rocks have a relatively high gradient.

When gas is produced into an empty borehole at lower pressure it expands and cools adiabatically, lowering the temperature of the surrounding rock. The temperature curve has a distinctive shape beside discrete porous zones as in the Big Lime where fair volumes are being produced. In the Shale depth fixes for shows are sometimes difficult to obtain, because of vey small shows.

On these two logs, you can observe that in many instances the driller and the temperature log agree except for a depth discrepancy. But in one case a show deep in the shale was not reported by the driller. This show appears to be coming from a radioactive (and presumably organic rich) zone.

DRILLERS SHOWS AND SHOW STRATIGRAPHY IN THE SHALE

When a conscientious driller reports black or brown shale versus light gray shale and reports shows of gas as they occur, we might be able to interpret the occurrence of gas in the various units of the formation.

(Figure 8A)

The drillers in Ashland Field, Boyd County, were not very consistent: as a result it is difficult assuredly to identify Provo's units. It appears that there are no shows in either the Cleveland or the Three Lick. Several shows occur in the middle and lower parts of the U. Huron, probably in the organic rich parts.

The driller calls one or two "Gordons", possibly sands but not so identified. The upper one may include the lower parts of the Middle Huron (organic poor) and the upper parts of the Lower Huron (apparently organic rich). There are three reported shows near the base of the Lower Huron presumably in organic rich rock.

Three shows at or near the Lower Huron-Olentangy contact suggest possibly a secondary porosity at an unconformity.

Nearly all the shows are associated with organic rich rock. It is strange that shows seem to be in the lower parts of units: if fracturing were through, one would expect accumulation in the tops of units.

On the wireline log, one might note the increased bulk density in the vicinity of the top of the Silurian: this is attributed to dolomite and anhydrite in the Silurian as contrasted to Devonian limestone.

(Figure 8B)

Big Sandy drillers logs in Martin County are consistent and Provo's units are commonly ascertainable. An organic rich zone near middle of the generally organic poor Three Lick unit is commonly recognized; and two shows are reported from it.

Four shows at or near the top and one about fifty feet below the top of the organic rich Upper Huron are reported.

A show in the Middle Huron is nearly the only one documented from gray silty shale as constrasted with brown or black organic shale.

The organic rich Lower Huron is spangled with shows in the top, middle, and near the base.

(Figure 8C)

Big Sandy Drillers logs in the south part of Pike County are fair, less consistent than in Martin County, but we note that the differentiation beween organic rich and organic poor rock is not so distinct on the wireline log, either. The driller is consistent with the Cleveland, Three Lick, and Upper Huron, but is vague in distinguishing between Middle and Lower Huron.

This is Berea country, with two shows in the top of the Formation, but six in the lower part. Two shows are at top of Cleveland: this is different from Boyd and Martin County. A show in the lower part of the Three Lick may be in an organic rich body. There are shows in the middle of the Upper Huron, and a number throughout the Lower Huron.

SUMMARY AND CONCLUSIONS

(Figure 9)

When the Southern Tie section is supplemented with sample descriptions we see little striking modification to the correlations we made from the wireline logs, escept that the unlogged hole in 10-M-86, Pike County, has samples that appear to restrict the Cleveland (Unit #1) to a shorter section (reduced from the base) than the wireline correlation suggested. This change is perhaps the strongest hint not to rely exclusively on wireline logs.

The fact that we can't find black organic rich rock in Unit #7 (Marcellus (?)) reminds us that our stratigraphic work needs some revision.

(Lights up, please)

Used with caution, we conclude that wireline logs are premier stratigraphic tools and serious engineering tools for depth control. The gamma ray log by itself without resort to density or neutron logs is a good correlation tool but is ambiguous with regard to some critical lithologies as metabentonites and radioactive but non-organic shales near formation boundaries.

From temperature logs, and within the ambiguities of drillers logs, it appears that nearly all shows are in or near the brown or black organic rich and radioactive shale units at consistent stratigraphic positions. If the gas occurs only in fractures, then there are stratigraphic as well as tectonic constraints on their vertical extent.

Fractures are difficult to identify in a borehole. Possibly the caliper log and a very noisy density log indicate zones of fractures.

ACKNOWLEDGEMENTS

We acknowledge the contributions of Frank R. Ettensohn, Assistant Professor of the University of Kentucky Department of Geology, particularly in the well-to-well wireline correlations, but also for his comments on outcrop stratigraphy.

Roy C. Kepferle, United States Geological Survey, Cincinnati and assigned Technical Project Officer of the Kentucky ERDA-EGSP project, exercised broad coordination and collaborated extensively in this paper. We acknowledge with thanks his contributions, particularly of the Ohio outcrop section and of the field discussions in Virginia.

To Linda J. Provo (Fulton), now of EXXON USA, New Orleans, whose pioneer work in classifying the Upper Devonian Shales of Kentucky was highly useful in this work, we acknowledge special debt.

REFERENCES

Myung, John I., 1976, Fracture Investigations of the Devonian Shale using Geophysical Well-Logging Techniques, in Devonian Shale Production and Potential, Proceedings of the Seventh Appalachian Petroleum Geology Symposium held at Morgantown, W. VA., March 1-4, 1976, Energy Research and Development Administration, Morgantown Energy Research Center MERC/SP-76/2, pp. 212-238.

Provo, Linda J(eanne), 1977, Stratigraphy and Sedimentology of Radioactive Devonian-Mississippian Shales of the Central Appalachian Basin. (Dissert.) Dept. of Geology, University of Cincinnati, OH, pp. i-xi, 1-177.

Provo, L. J., Kepferle, R. C., and Potter, P. E., 1977, Three Lick Bed: Useful Stratigraphic Marker in the Upper Devonian Shale in Eastern Kentucky, Energy Research and Development Administration, Morgantown Energy Research Center MERC/CR-77-2, pp. ii, 1-56.

APPENDIX

Tables of wells used on Figures.

State	County	Operator-Well#-Farm Name	Carter Coord.	Elev. Datum	Total Depth	Comp. Date	Status
Figure 1--Classifications of Provo; and Figure 5--Air Rotary Samples.							
KY	Boyd	Inland Gas #533 FEE	11-V-81	862 KB	9595	04-09-1968	D&A
KY	Boyd	Inland Gas #537 FANNIN	22-W-82	708 KB	7800	12-13-1968	Gas
Figures 2 & 9--Southern Tie Section							
OH	Ross	Outcrop @ COPPERAS MT.	2-GG-76		Base not exposed		
OH	Scioto	Continental #1 SHISLER	16-CC-79	531 DF	1075	12-01-1962	D&A
OH	Scioto	USS Chemical #1 FEE	25-Z-81	557 KB	5607	06-06-1968	WD
KY	Boyd	Inland Gas #537 FANNIN	22-W-82	708 KB	7800	12-13-1968	Gas
KY	Boyd	Inland Gas #535 McKEAND	25-W-83	868 KB	9445	06-17-1968	D&A
KY	Lawrence	Inland Gas #542 YOUNG	6-U-82	884 KB	12634	05-13-1971	D&A
WV	Wayne	Columbia #20060 FEE	15-T-84	647 KB	3598	03-05-1976	Gas
KY	Lawrence	Columbia #9557 FIEGER	10-S-83	802 DF	4037	09-23-1971	Gas
KY	Martin	United Fuel #1 JAMES	19-Q-84	659 KB	13172	05-07-1959	D&A
KY	Martin	Columbia #20336 FEE	16-P-85	944 KB	3457	11-05-1976	Gas
KY	Pike	Columbian Fuel #1 SMITH	10-M-86	1068 GL	5343	11-12-1939	D&A
KY	Pike	Columbia #9697 KENTLAND	3-K-87	1293 DF	4944	12-27-1972	Gas
VA	Buchanan	Columbia #9781 PITTSTON	2-I-88	1580 KB	6803	09-17-1973	Gas
VA	Buchanan	Columbia #9722 POBST	4-H-89	1683 KB	7296	04-26-1973	D&A
VA	Scott	Tidewater #1 SMITH	6-B-87	1468 KB	7222	01-30-1964	Gas
Figure 4--Mud rotary holes in Scioto and Lawrence Counties, Ohio.							
OH	Scioto	Continental #1 SHISLER	16-CC-79	531 DF	1075	12-01-1962	D&A
OH	Lawrence	Ballard & C. #1 COLLINS	11-AA-83	963 KB	2518	01- -1972	D&A?
Figure 6--...unusual lithologies...Virginia.							
VA	Buchanan	Columbia #9722 POBST	4-H-89	1683 KB	7296	04-26-1973	D&A
VA	Scott	Tidewater #1 SMITH	6-B-87	1468 KB	7222	01-30-1964	Gas
Figure 8A--Drillers logs in Ashland Field.							
KY	Boyd	Patton #1 RALPH BROS.	24-X-83	557	2364	08-29-1929	Gas
KY	Boyd	Ohio Southern #1 RICE	23-X-83		2055	12-04-1928	Gas
KY	Boyd	Ky Fuel #K-74 POLLIT & R	23-X-83		2199	04-06-1929	Gas
KY	Boyd	Ky Fuel #97 WALKER	23-X-83		2202	12-11-1929	Gas
KY	Boyd	Ohio-Ky #1 RAY	23-X-83		2070	02-20-1929	Gas
KY	Boyd	Ky Fuel #K-79 PATTON	23-X-83		2040	05-17-1929	Gas
KY	Boyd	Inland #96 PATTON	22-X-83		2233	11-02-1929	Gas
KY	Boyd	Ohio-Ky #1 CALDWELL	2-W-83	625	2249	10-06-1930	Gas
KY	Boyd	Ohio-Ky #1 NUNLEY	2-W-83	760	2226	07-31-1930	Gas

APPENDIX (Cont.)

State	County	Operator-Well#-Farm Name	Carter Coord.	Elev. Datum	Total Depth	Comp. Date	Status
Figure 8B--Drillers logs in Big Sandy Field, Martin County, Kentucky.							
KY	Martin	Ky W.VA Gas #539 CORNETT	12-P-84	880	2800	- -1936	Gas
KY	Martin	United Fuel #4263 SMITH	11-P-84	750	3029	10-21-1930	Gas
KY	Martin	Ky W.VA Gas #5274 CARLISLE	11-P-84	835	2895	?	Gas
KY	Martin	Ky W.VA Gas #5245 PREECE	11-P-84	1130	3051	- -1938	Gas
KY	Martin	Ky W.VA Gas #5296 CARLISLE	11-P-84	990	2417	?	Gas
KY	Martin	Ky W.VA Gas #5218 PREECE	15-P-85	1135	2820	?	
KY	Martin	Warfield #3 CASSADY, A F	10-P-84	737	2762	11-22-1913	Gas
KY	Martin	Ky W.VA Gas #5276 CARLISLE	10-P-84	885	2915	- -1940	Gas
KY	Martin	Ky W.VA Gas #5284 CARLISLE	10-P-84	860	2962	04-09-1941	Gas
KY	Martin	Warfield #3 CASSADY, J E	10-P-84	740	2715	11-04-1941	Gas
KY	Martin	Warfield #4 CASSADY, J E	6-P-85	1040	3054	05-16-1946	Gas
KY	Martin	United Fuel #5 CASSADY, J E	6-P-85	865	2982	05-17-1947	Gas
Figure 8C--Drillers logs in Big Sandy Field, Pike County, Kentucky.							
KY	Pike	Columbian Fuel #B-11KY WV	1-L-86	918	3330	06-14-1941	Gas
KY	Pike	Columbian Fuel #B-3 KY WV	9-L-86	1621	3781	09-18-1945	Gas
KY	Pike	Columbian Fuel #B-5 FEE	9-L-86	1253	4242	03-29-1946	Gas
KY	Pike	United Fuel #2 ROWE	12-L-86	1626	4422	12-11-1952	Gas
KY	Pike	Columbian Fuel #B-1 KY W.VA	2-L-86	928	3795	10-28-1944	Gas
KY	Pike	Howe #H-19 KENTLAND	19-L-86	930	4305	11-16-1931	Gas
KY	Pike	Columbian Fuel #2 JUSTICE	22-L-86	761	3813	10-11-1943	Gas
KY	Pike	United Fuel #42 KENTLAND	22-L-86	1079	4167	06-14-1952	Gas

Figure 1. L. J. Provo's classification of units of the Devonian Shale with their subsurface expressions in wireline logs in Boyd County, Kentucky.

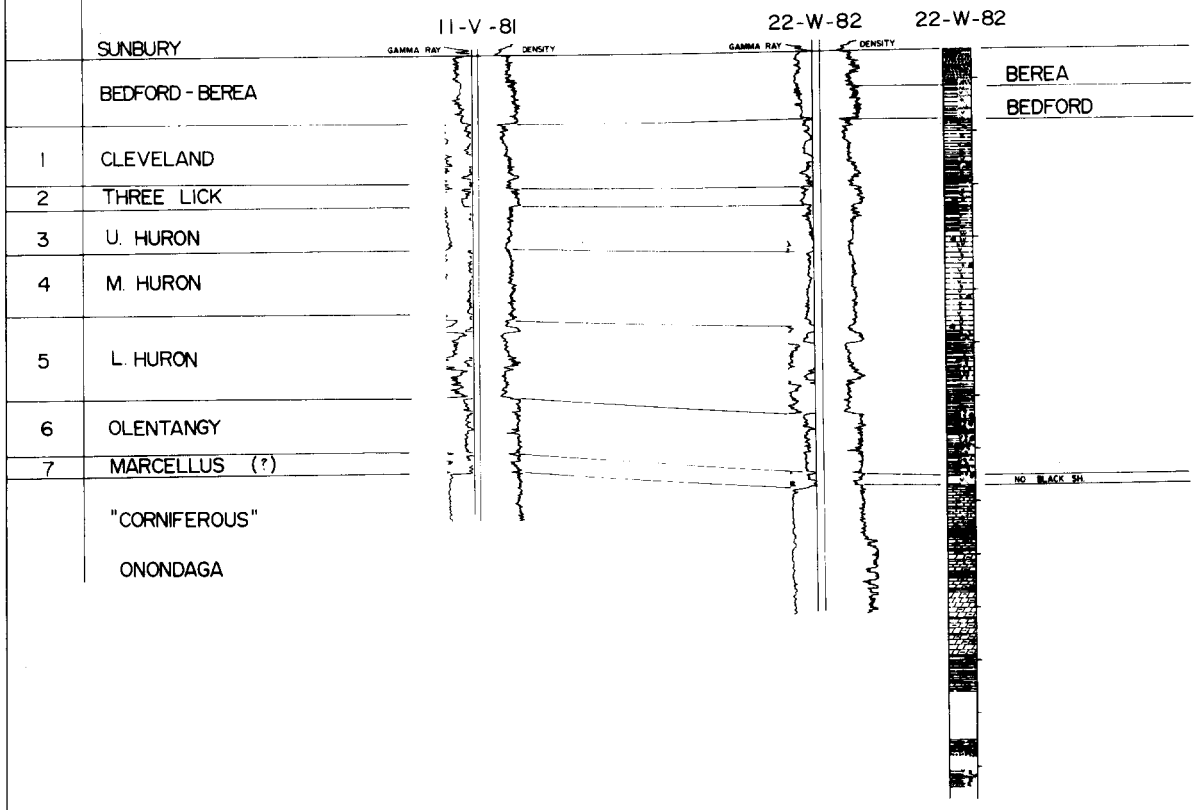

Figure 5. Wireline log stratigraphy versus sample description in Inland #537 FANNIN EST., an air rotary hole in 22-W-82, Boyd County, Kentucky.

Figure 2. Correlations, chiefly by wireline logs, along the Southern Tie Section in Ohio, Kentucky, West Virginia and Virginia.

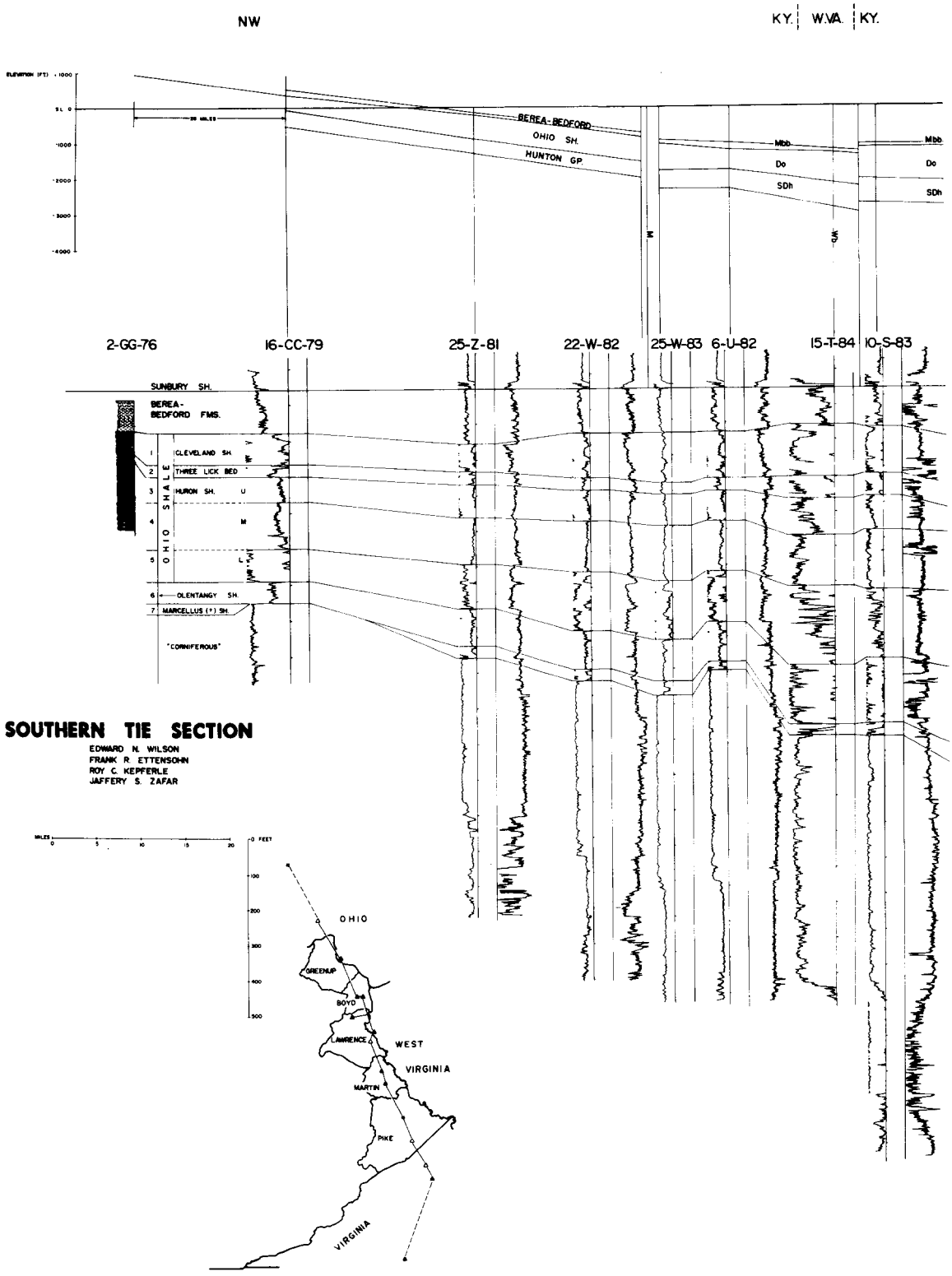

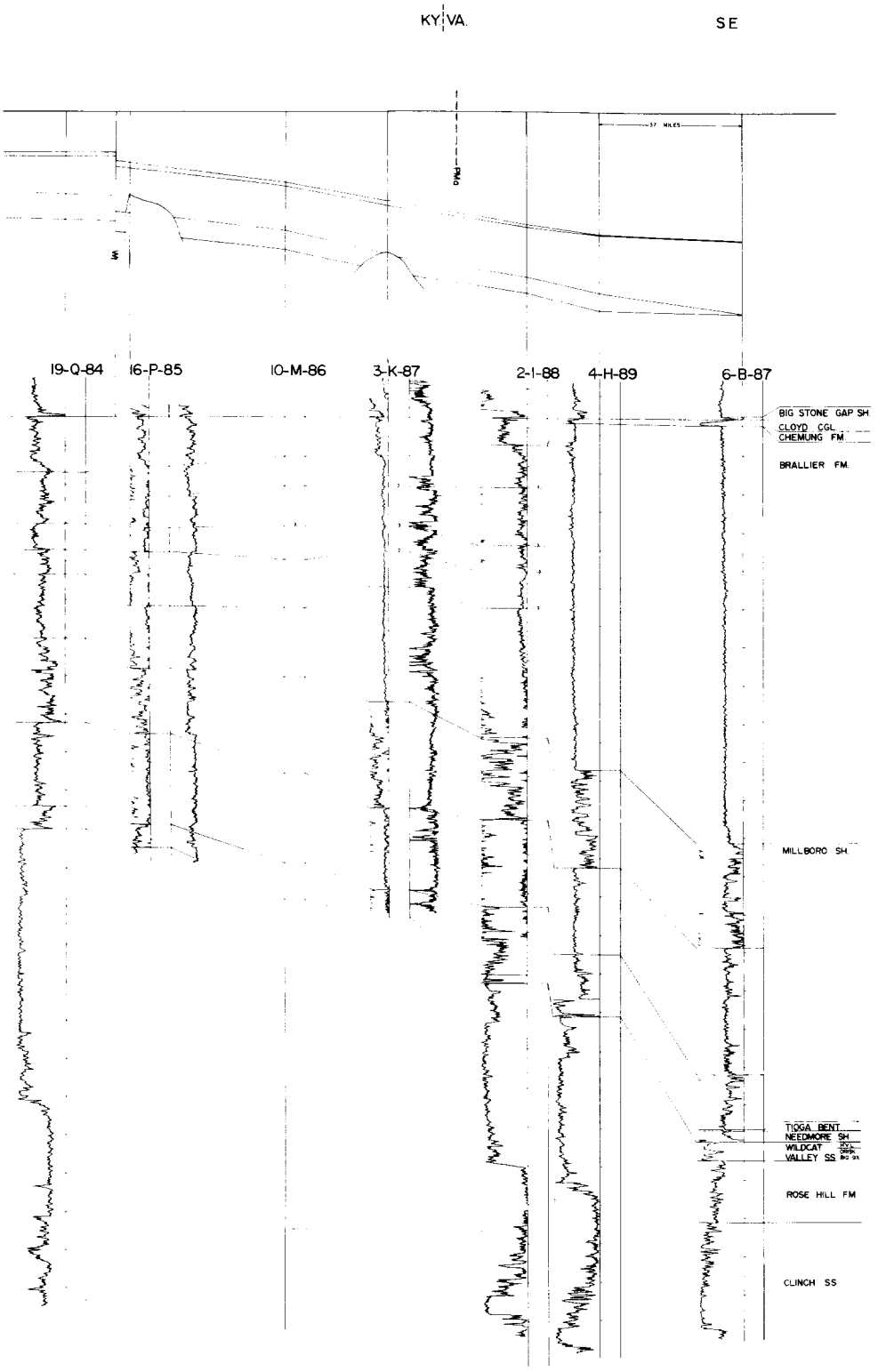
KY VA.
SE
37 MILES
19-Q-84
16-P-85
10-M-86
3-K-87
2-I-88
4-H-89
6-B-87
BIG STONE GAP SH.
CLOYD CGL.
CHEMUNG FM.
BRALLIER FM.
MILLBORO SH.
TIOGA BENT.
NEEDMORE SH.
WILDCAT
VALLEY SS.
ROSE HILL FM.
CLINCH SS

Figure 3. Comparison of drillers log and sample description in Columbian Fuel #1 J. SMITH, a cable tool hole in 10-M-86, Pike County, Kentucky, with correlations to wireline logs to the northwest and southeast.

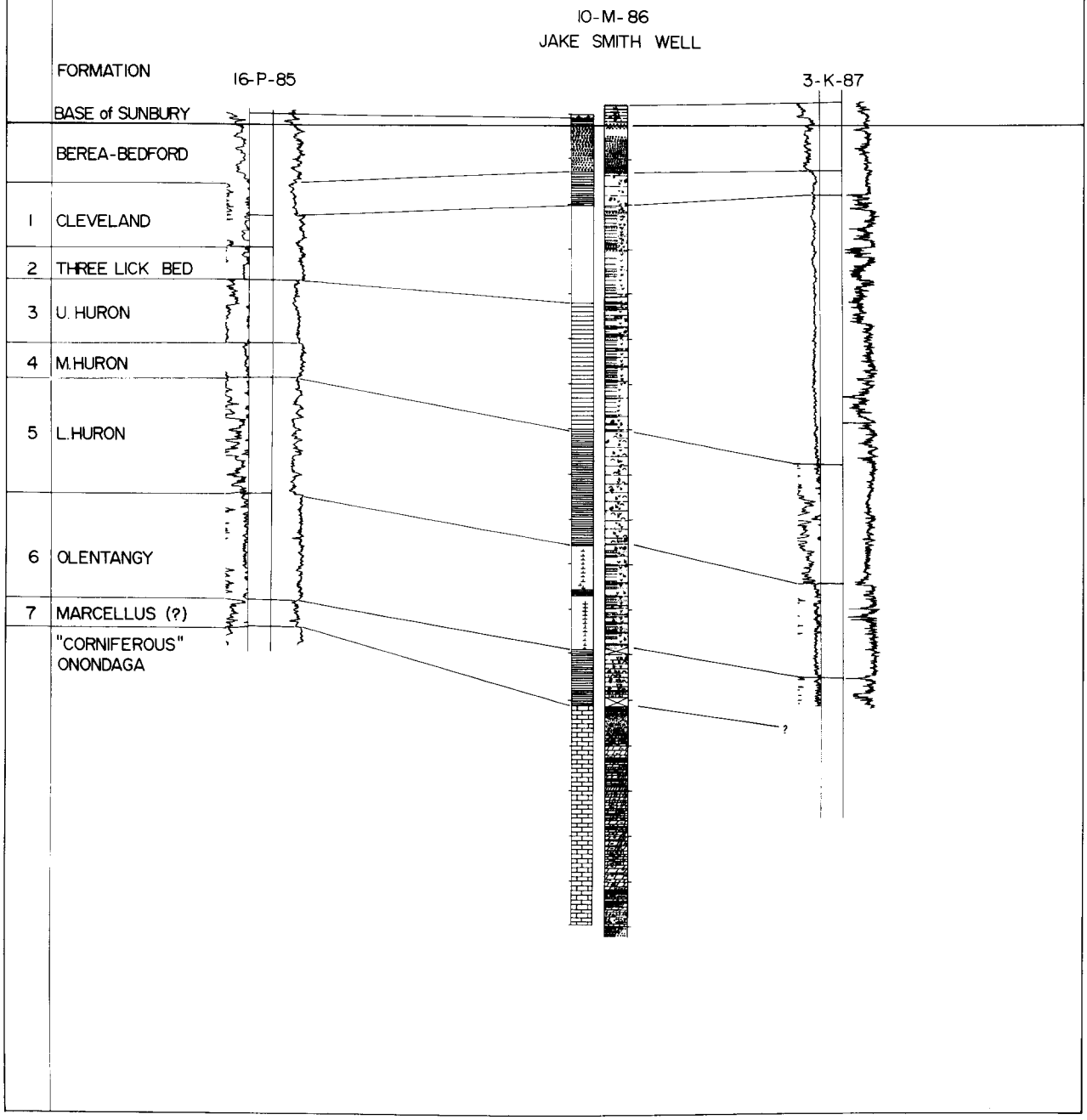

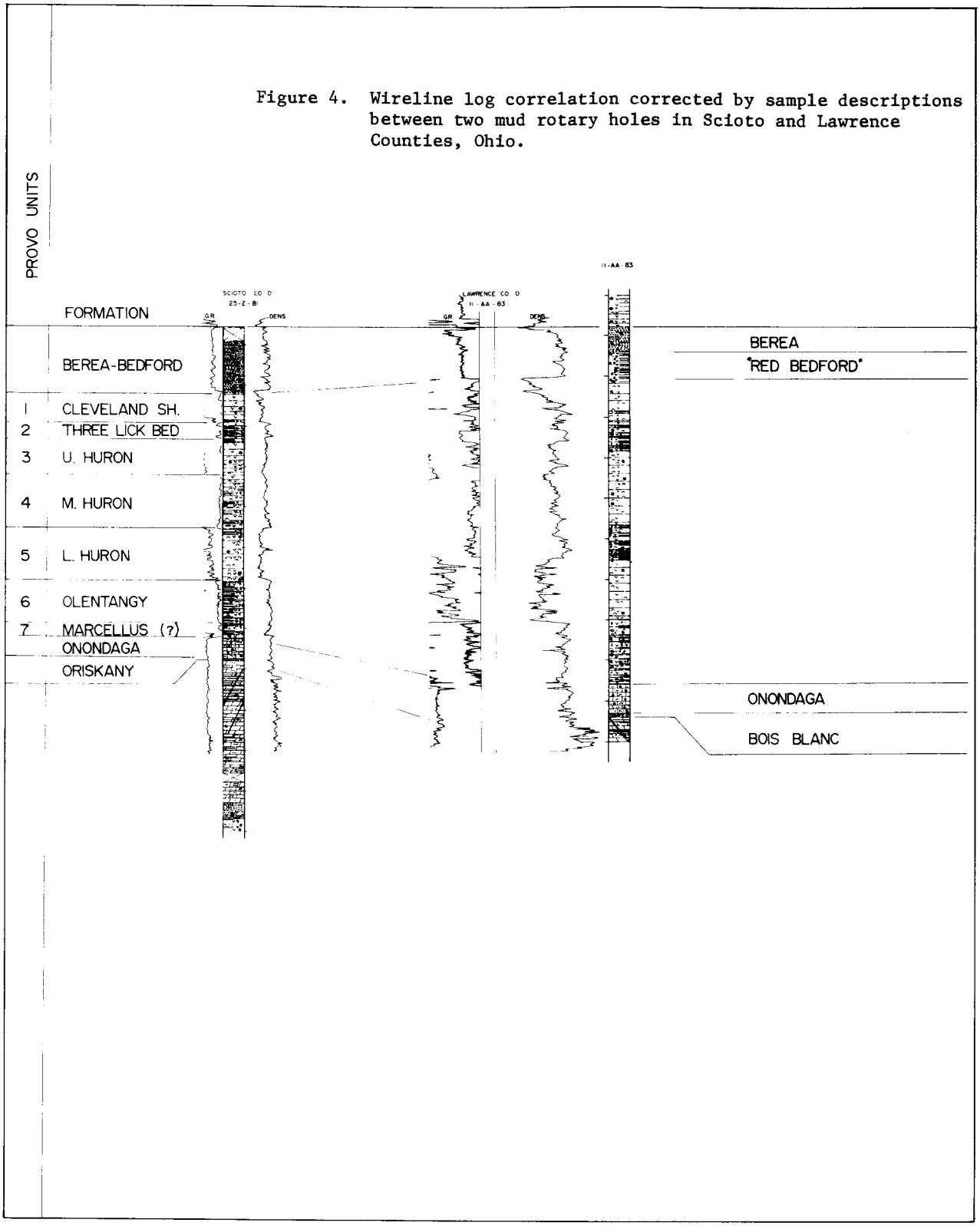

Figure 4. Wireline log correlation corrected by sample descriptions between two mud rotary holes in Scioto and Lawrence Counties, Ohio.

Figure 6. Comparison between wireline logs and sample descriptions for recognition of faulting, fracturing, and unusual lithologies in two wells in Buchanan and Scott Counties, Virginia.

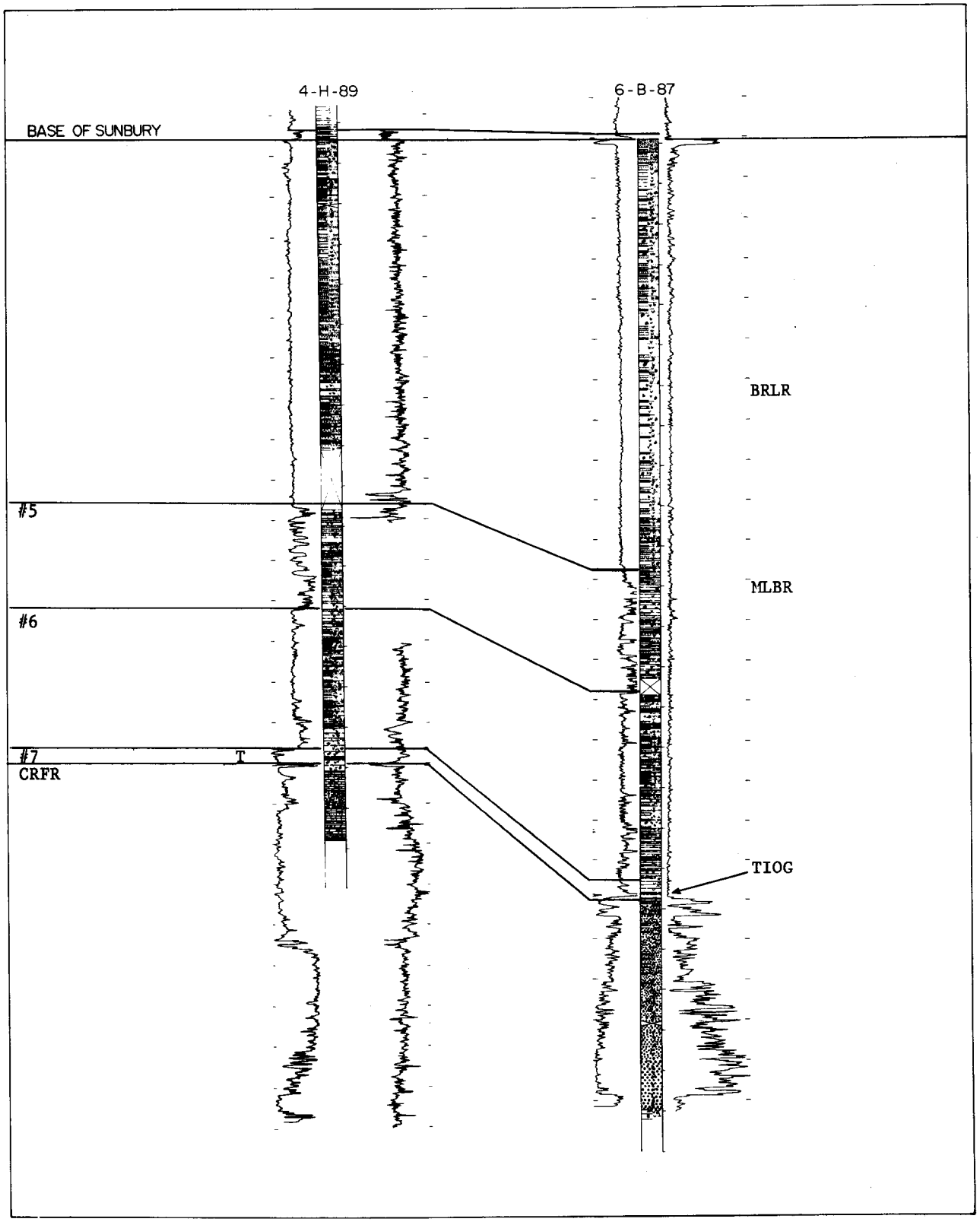

MARTIN CO., KENTUCKY 8-0-84
UNITED FUEL GAS #8946 FEDERAL GAS, OIL, & COKE

LAWRENCE CO., KENTUCKY 4-S-82
KY. W. VA. GAS #1429 COSSIN

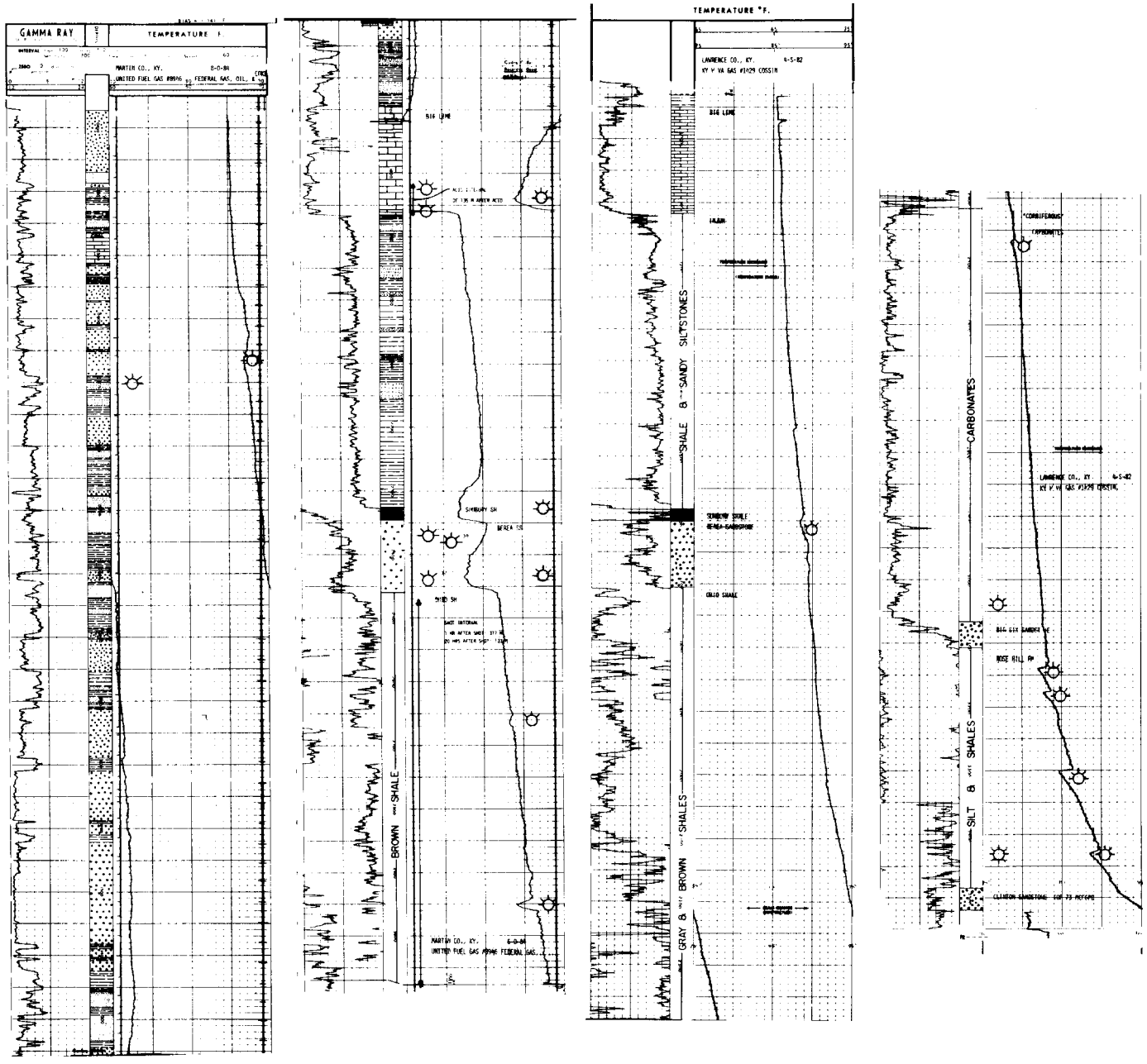

Figure 7. Recognition of shows of gas in drillers logs and temperature logs of two wells in Lawrence and Martin Counties, Kentucky.

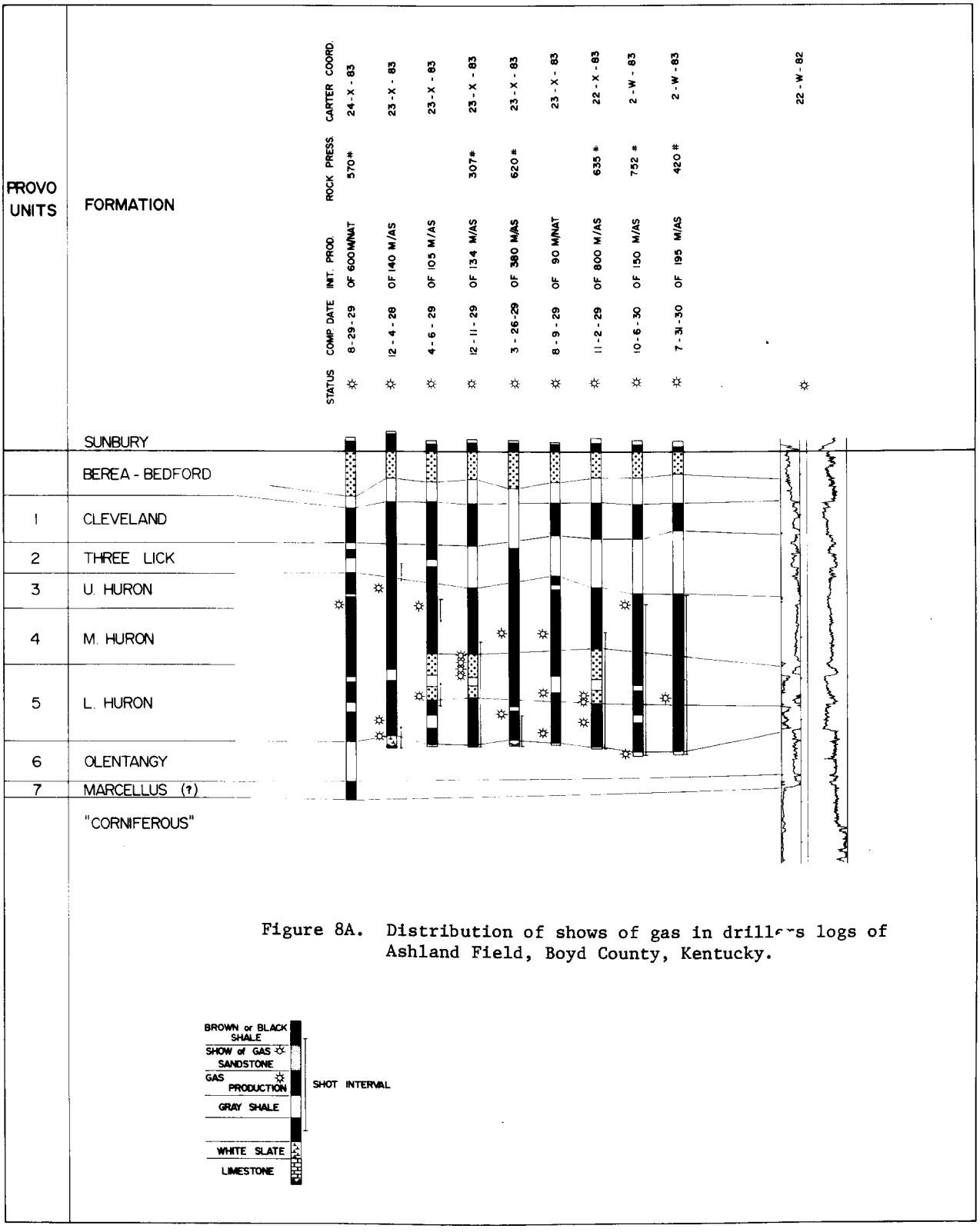

Figure 8A. Distribution of shows of gas in drillers logs of Ashland Field, Boyd County, Kentucky.

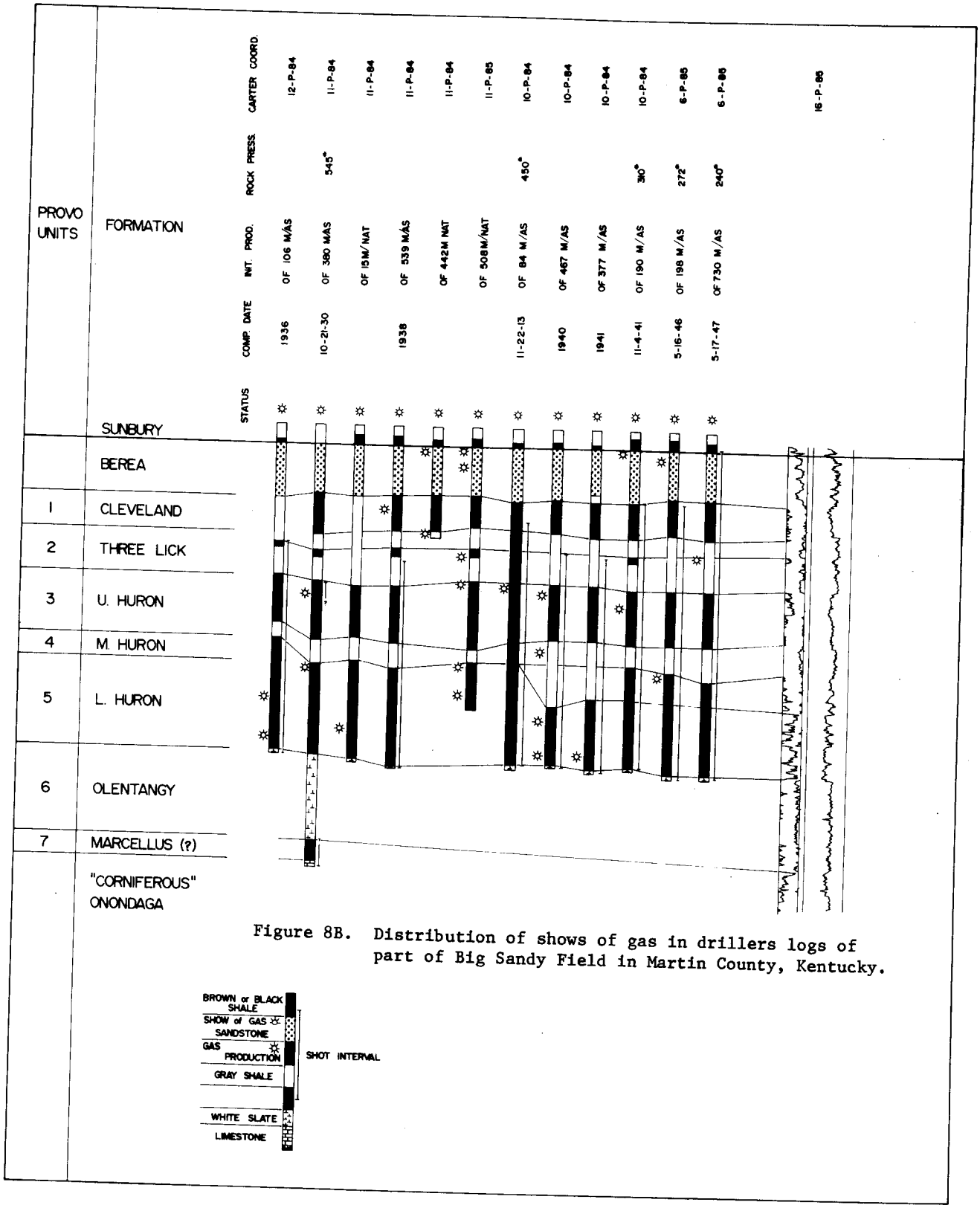

Figure 8B. Distribution of shows of gas in drillers logs of part of Big Sandy Field in Martin County, Kentucky.

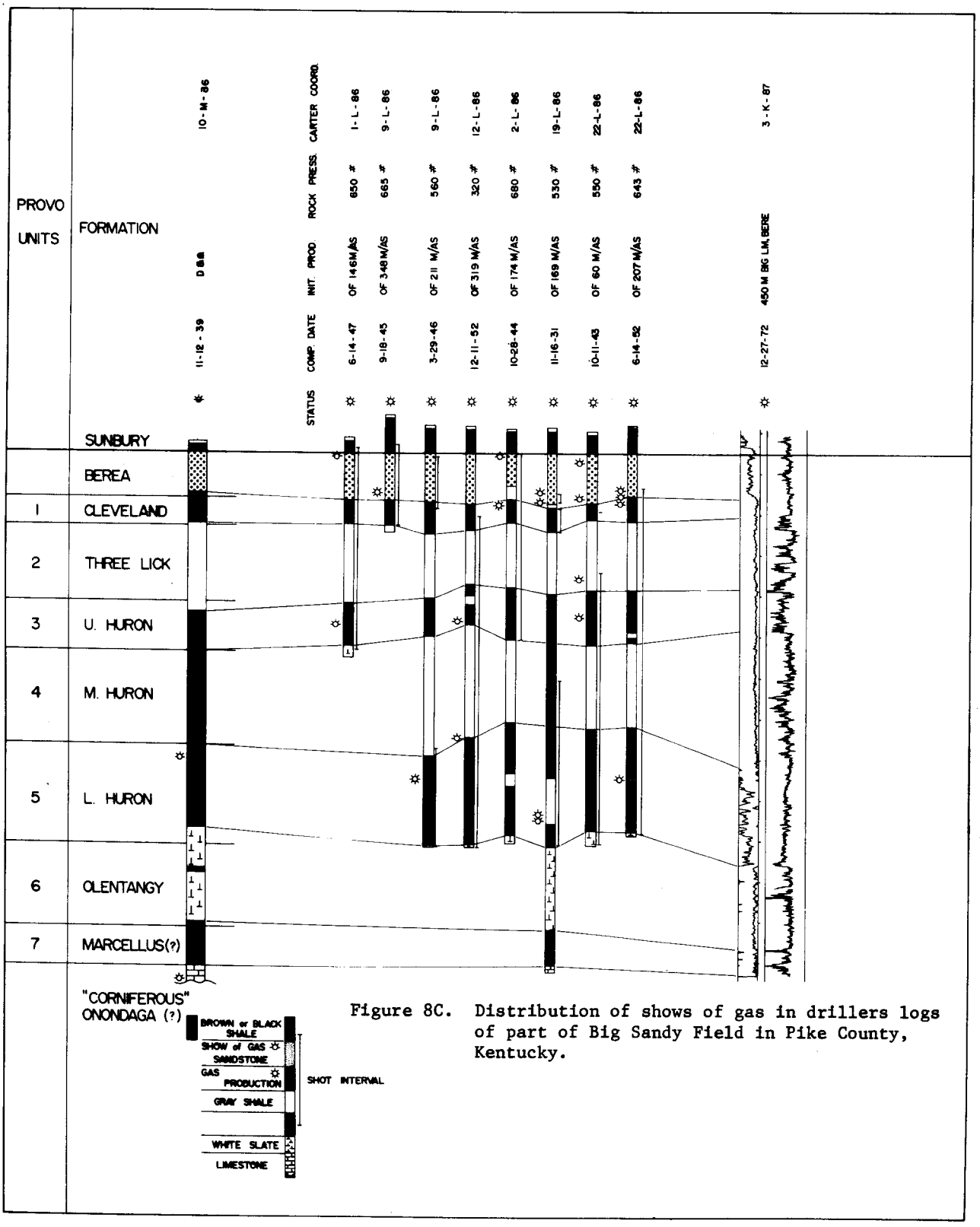

Figure 8C. Distribution of shows of gas in drillers logs of part of Big Sandy Field in Pike County, Kentucky.

Figure 9. The Southern Tie Section with sample descriptions added.

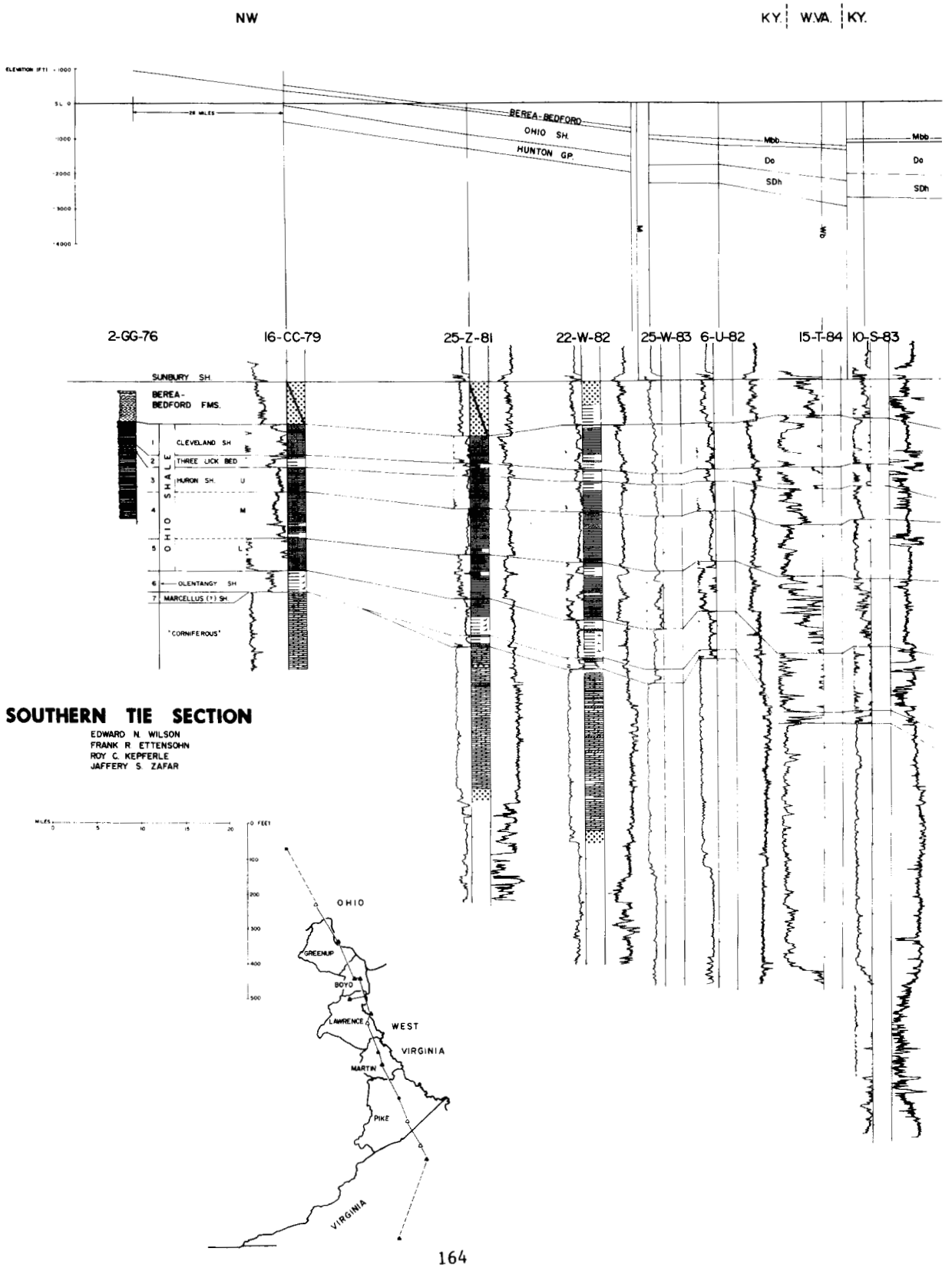

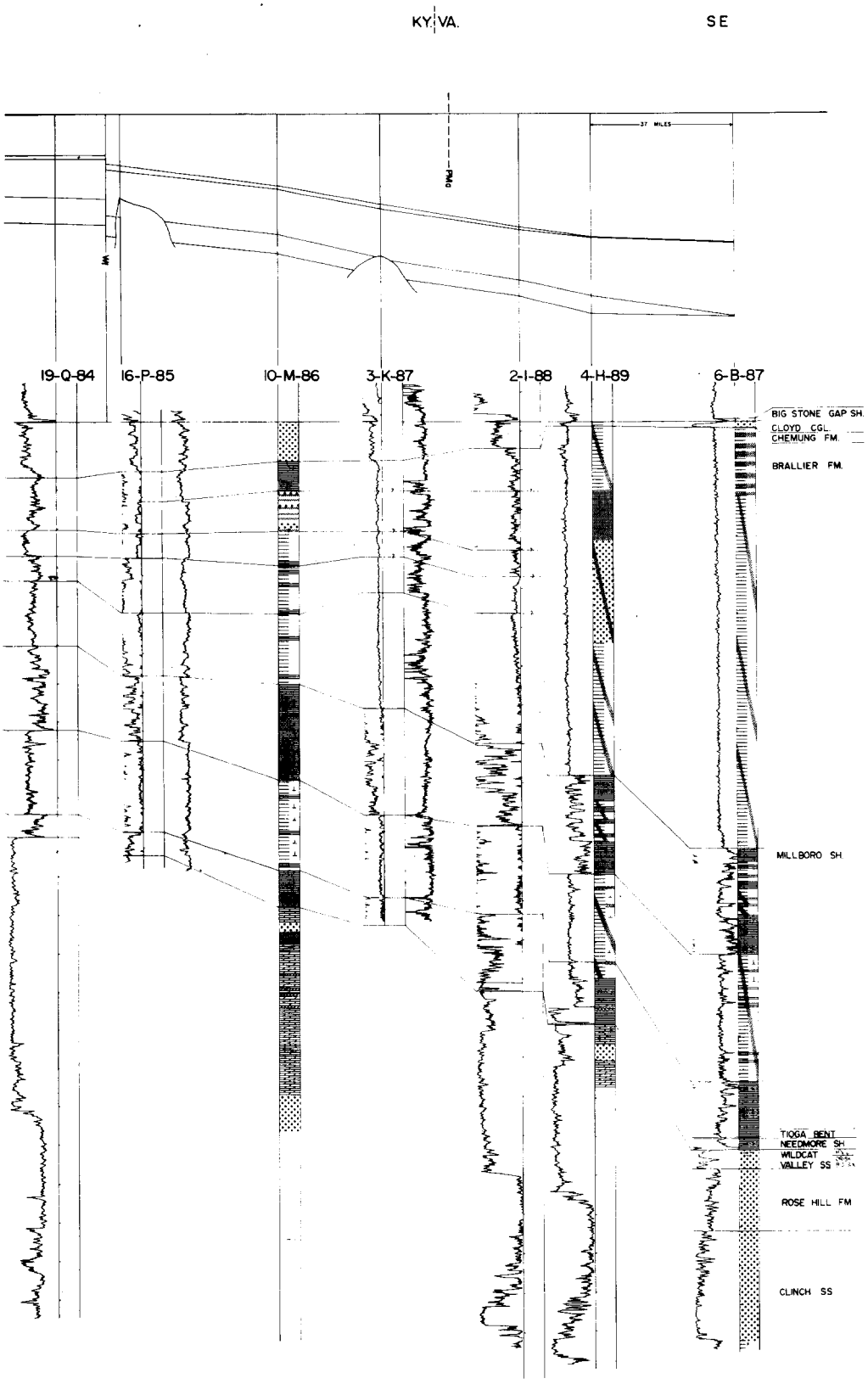
KY.
VA.
SE
37 MILES
PMD
19-Q-84
16-P-85
10-M-86
3-K-87
2-I-88
4-H-89
6-B-87
BIG STONE GAP SH.
CLOYD CGL.
CHEMUNG FM.
BRALLIER FM.
MILLBORO SH.
TIOGA BENT
NEEDMORE SH.
WILDCAT
VALLEY SS
ROSE HILL FM.
CLINCH SS

TIOGA BENTONITE TIME-MARKER ASSOCIATED WITH DEVONIAN SHALES IN APPALACHIAN BASIN

JOHN M. DENNISON AND DANIEL A. TEXTORIS
UNIVERSITY OF NORTH CAROLINA AT CHAPEL HILL
CHAPEL HILL, NORTH CAROLINA 27514

ABSTRACT

THE TIOGA BENTONITE IS AN INTERVAL UP TO 203 FT (61 M) THICK WITH SEVERAL TUFF LAYERS. THE MIDDLE COARSE ZONE OF THE TIOGA CONSISTS OF THREE TUFF BEDS WITHIN AN INTERVAL OF 2 FT (0.6 M). THE TOP OF THE MIDDLE COARSE ZONE MARKS THE TOP OF THE ONESQUETHAW STAGE THROUGHOUT 102,000 SQ MI (265,000 SQ KM). IT IS OMITTED BY OVERSTEP OF THE CHATTANOOGA-OHIO SHALE IN EASTERN TENNESSEE AND KENTUCKY.

THE BASE OF DEVONIAN SHALES IS DIACHRONOUS, ABOUT 530 FT (160 M) BELOW THE TIOGA MIDDLE COARSE ZONE IN NORTHEASTERN VIRGINIA, AND ABOUT 45 FT (14 M) ABOVE THE TIOGA IN CENTRAL OHIO.

THE BEREA PLUTON NEAR FREDERICKSBURG, VIRGINIA IS THE BEST FIT FOR AN INTRUSIVE EQUIVALENT OF THE VOLCANIC ROOT FOR THE MIDDLE COARSE ZONE.

INTRODUCTION

The Tioga Bentonite is a volcanic ash layer which, by definition, marks the top of the Onesquethaw Stage throughout its occurrence in a continuous area of about 102,000 sq mi (265,000 sq km) of the eastern and northeastern part of the Appalachian basin. The same tuff layer is also recognized in the Michigan and Illinois basins by various authors. This paper summarizes evidence, principally from the Appalachian basin, which indicates that the principal source of volcanic eruption was located in the Virginia Piedmont at about latitude 38°, beyond the limits of presently preserved Devonian strata of the Appalachian basin.

PREVIOUS WORK

The first identification in the literature of the bed now known as the Tioga Bentonite was by James Hall (1843, p. 163), who described a clay parting near the top of the Onondaga Limestone in Seneca County, New York. In 1931 Fettke (p. 8) recognized a biotite-rich layer near the base of the Devonian shales in the Tioga Gas field, located in the county by that name in northern Pennsylvania; in 1949 he proposed the name Tioga Bentonite for this subsurface marker (Ebright, Fettke, and Ingham, 1949, p. 10). Oliver (1954, 1956) identified the Tioga Bentonite bed a few feet below the bottom of the Marcellus Shale in western New York, and he found that eastward in New York the base of the Devonian Shales drops lower in the section, so that the Tioga Bentonite occurs at the base of or perhaps within the lower few feet of Marcellus Shale in the Catskill region (see correlation charts by Rickard, 1964, 1975). Flowers (1952) first identified the Tioga in wells of West Virginia, and

Fettke (1952) summarized the known occurrence of the Tioga in the subsurface of Pennsylvania. Weaver (1956) and Lounsbury and Melhorn (1964) reported on the clay mineralogy of the Tioga.

Outcrop studies of the Tioga Bentonite in the Appalachian Valley and Ridge Province were initiated by Dennison in 1958, and then he carried this stratigraphic work westward into the subsurface. Dennison (1960, 1961) recognized the importance of the Tioga as a time surface, and he designated the Tioga Bentonite zone as the top of the Onesquethaw Stage. Use of the Tioga tuff to mark the top of the Onesquethaw Stage has been followed by Rickard (1964, 1975); Oliver and others (1967, 1969).

Textoris joined Dennison in investigation of the Tioga in 1963, adding emphasis on the petrology. These authors have published two short papers summarizing the Tioga stratigraphy and petrology (Dennison and Textoris, 1970, 1971), based on much less detailed information than is now available.

Detailed studies of the Tioga revealed that there is more than one tuff layer, especially near the proposed source area, and an internal stratigraphy has emerged. Near the middle of the Tioga tuffaceous interval, there occurs a bundle of three or four readily recognizable tuff beds within a span of usually two feet (0.6 m), coarser than any other portion of the Tioga tuffaceous material. This is called the Tioga middle coarse zone, and is apparently the portion of the Tioga which forms the principal marker horizon which can be traced farthest from the volcanic source. The top of the Tioga middle coarse zone is now designated as the top of the Onesquethaw Stage (Dennison and Hasson, 1976, p. 285).

The Tioga volcanic ash was blown beyond the limits of the Appalachian basin (Fig. 1), so that the Tioga is now generally recognized in the deeper parts of the Illinois basin and on some Indiana outcrops and cores at the east edge of the basin (Meents and Swan, 1965; Collinson and others, 1967; Droste and Vitaliano, 1973; Droste and Shaver, 1975a, 1975b). The Tioga is probably the same bentonite as the Michigan basin ash fall called the Kawkawlin Bentonite by Baltrusiatis (1974, 1975), from occurrences near the top of the Lucas Formation. Droste and Shaver (1975a, 1975b) and Doheney, Droste, and Shaver (1975) maintain that the bentonite of northern Indiana (Fig. 1 of this paper) is within the Detroit River Formation and is equivalent to the bentonite of Baltrusiatis. Resolution of the present literature controversy over the Tioga Bentonite(s) of the Midwest will ultimately depend on a more detailed understanding of the Tioga stratigraphic patterns in the Appalachian basin. Swan (Meents and Swan, 1965) thought he recognized the Tioga in one Iowa outcrop, which has never been confirmed by others.

STRATIGRAPHY

Some 127 Tioga outcrops are known in the Valley and Ridge Province from Tennessee to Pennsylvania and along the north and west edge of the Appalachian basin in New York and Ohio. In addition, the Tioga is recognized in some 400 wells in this basin, from sample descriptions or from a characteristic gamma ray peak on well logs.

The Tioga Bentonite in outcrop is characterized by micaceous tuff layers up to a few inches (few centimeters) thick and by interlayers of grayish brown to brownish gray, thinly laminated, platy- to sheety-weathering, tuffaceous shales with a color contrasting with the medium dark gray to black of the enclosing Devonian shales. This brownish color persists into the subsurface, accounting for the drillers term "brown break" recognized for over 25 years near the base of the Devonian shales. In the subsurface the tuff beds are identified in well cuttings by prominent biotite flakes with abundant pyrite. The Tioga cuttings have been reported generally at only one position in the wells, but multiple bentonites are sometimes noted. These could represent more than one ash layer, or they may be well cavings from a single layer.

In outcrop, certain tuffaceous layers contain profuse Styliolina, Tentaculites, Leiorhynchus, and Ambocoelia, often with various bedding planes in a single exposure dominated by one particular genus, as if a spatfall was killed by ash from an eruption.

The general stratigraphic occurrence of the Tioga within the Devonian shales is diagrammed in Fig. 2, where the letter "T" designates an identified Tioga occurrence at the base of the Millboro or Marcellus Shale. In this cross section, at the latitude of the south border of Pennsylvania, the Tioga tuffaceous interval coarsens eastward from about 2 ft (0.6 m) in the west to 8 ft (2.4 m) in the east. The Tioga middle coarse zone occurs precisely at the basal boundary of the black Devonian shales, and separates the overlying black shales from the limy, underlying dark gray shales of the

Needmore Shale or the limy cherty beds of the upper Huntersville Formation. Just west of the left end of the cross section in Fig. 2, the base of the Devonian shales is even younger, and the Tioga occurs within limestone beneath the Devonian shales. In the Marble Cliffs quarry at Columbus, Ohio, an isolated outcrop of the Tioga has been identified at the Columbus-Delaware Limestone contact, so that in central Ohio the Tioga position at the base of the Delaware Limestone is some 45 ft (14 m) below the base of the Devonian shales.

The bottom of the Devonian shales (Needmore Shale) extends below the Tioga in eastern areas, with the maximum stratigraphic distance occurring at Seven Fountains on Massanutten Mountain, Virginia, where the base of the Needmore Shale is about 530 ft (160 m) below the Tioga middle coarse zone. Using the middle coarse zone as a time surface, the base of the Devonian shale climbs about 575 stratigraphic ft (175 m) from east to west across the Appalachian basin.

The Tioga Bentonite is omitted by overstep of the Chattanooga-Ohio Shale, where the unconformity increases westward onto the Nashville dome and Cincinnati arch. Figure 1 shows the west limit of continuous Tioga outcrops and wells on the west side of the Appalachian basin. The most southwestern outcrop, and the only outcrop certainly known in Tennessee, is where Tennessee Route 70 crosses Clinch Mountain (Dennison and Boucot, 1974). There the Tioga middle coarse zone is obliterated by weathering at the top of glauconitic sandstone of the Huntersville Member of the Wildcat Valley Sandstone, but the brownish shales and characteristic fossils of the Tioga are readily identified. At least four tuff beds are recognized there in the basal 27 ft (8.2 m) of the Chattanooga (Millboro) Shale. Tuff beds in the same part of the Millboro Shale have been recognized in outcrops as far away as Wytheville, Virginia, 112 mi (180 km) to the northeast.

In the Ohio and Kentucky subsurface there is a fairly pronounced west limit to the occurrence of the Tioga, either because of pre-Devonian shale erosion of the tuff bed, or because the tuffs were deposited in shallow water along the Cincinnati arch and were generally obliterated by wave reworking. Isolated Tioga occurrences have been reported at the top contact of the Columbus Limestone at Columbus and Sandusky, Ohio. The westward termination of continuous Tioga in Kentucky is based on westward abrupt loss of the characteristic strong gamma ray kick in well logs. The mapped termination suggests that renewed subsidence of the Rome trough permitted preservation of the Tioga beneath the Chattanooga-Ohio shale overstep several miles farther west in Kentucky within the Rome trough structural region.

There are several Tioga tuffaceous layers. The Tioga middle coarse zone is easily recognized as 3 or 4 distinct tuff beds all within an interval of generally 2 ft (0.6 m). The total thickness of the middle coarse zone, as well as the thickness and field observation of grain size of the individual tuffs within the middle coarse zone all increase toward the latitude of northern Massanutten Mountain (38° 45') in the Valley and Ridge Province. The additional tuff layers also increase in number toward Massanutten Mountain, so that at Seven Fountains there occurs a maximum of 31 silt- to sand-size tuff beds within the total Tioga interval. These extend both above and below the middle coarse zone. The middle coarse zone thins and becomes finer-grained away from Massanutten Mountain, so that at the most northern outcrop in the Valley and Ridge (Bellefonte, Pennsylvania), there is a single tuffaceous zone 0.3 ft (0.09 m) thick at the Marcellus-Selinsgrove contact, but within this lighter-colored tuffaceous zone there are three faintly-recognizable graded tuff beds; thus the middle coarse zone merges into a single lighter-colored clay parting far from the volcanic source. This is apparently the single Tioga Bentonite bed recognized in outcrops of New York (Oliver, 1954, 1956) and in the isolated outcrop within the Illinois basin (Fig. 1). About 10 ft (3 m) below the Tioga middle coarse zone in several outcrops in Pennsylvania there occurs another tuff layer, and this is probably the so-called "second Tioga" which occurs in some wells in western New York and adjacent Pennsylvania. Eastern New York and northeastern Pennsylvania are located farther from the apparent volcanic source, and only one Tioga bed (middle coarse) extends to wells located there and to outcrops in east-central New York.

The Tioga tuffaceous interval is not vertically continuous tuff or tuffaceous brownish shale in outcrops or wells. There are also intervening layers with no recognizable tuffaceous admixture. It is possible to determine from outcrop and well sample descriptions the total recognizable thickness of strata with tuff admixture. This total thickness is isopached on the map in Fig. 1, which shows a maximum of 203 ft (61 m) at Seven Fountains on Massanutten Mountain.

The Tioga middle coarse zone is an isochronous surface throughout its occurrence in the Appalachian basin. It was apparently deposited on the sea floor below wave base, since the internal stratigraphy of the middle coarse zone is always recognizable. The strata which enclose the middle coarse zone are a complex group of facies. At various places the middle coarse zone rests on Onondaga Limestone, Buttermilk Falls Limestone, Selinsgrove Limestone, Needmore Shale, Huntersville Chert,

and Wildcat Valley Sandstone. Oliver (1956) believed that the lowest Marcellus probably dropped beneath the Tioga in eastern New York, but Dennison has observed the Tioga at the precise Onondaga-Marcellus boundary in wells just west of the Catskill escarpment outcrop belt.

The Tioga middle coarse zone nearly everywhere in the Appalachian basin is overlain directly by black shale of the Marcellus, Millboro, or Ohio Shale Formations (with nomenclature usage determined by presence or absence of certain siltstone units hundreds of feet higher in the stratigraphic section), but in the northwest the middle coarse zone is overlain by limestone (in western New York by the Seneca Member of the Onondaga Limestone or by the Delaware Limestone in much of Ohio).

The geologic moment of the Tioga middle coarse zone volcanism was also the time of an abrupt sea level rise (or dropping of the sea floor) throughout the Appalachian basin (Dennison and Head, 1975). Throughout most of the basin, where the middle coarse zone is preserved, there was an abrupt transition immediately after the volcanic event to a black shale environment (Marcellus or Millboro) directly overlying Onesquethaw Stage chert or limestone or limestone and shale. It is difficult to know for certain whether this change in sedimentation was a result of sea level rise, or if the sudden incursion of euxinic shale resulted from tectonic downsinking of the basin accompanied by a sudden uplift of the terrigenous source area as the Acadian orogeny was intensified at the moment of Tioga volcanism. Evidence at several localities favors actual water depth increase following the volcanic outburst, and their distribution around the basin margin suggests a real rise in sea level. In southeastern West Virginia and part of southwestern Virginia the shallow marine Bobs Ridge Sandstone is directly overlain by the Tioga followed by black Millboro Shale (Dennison, 1961). The same lithologic sequence occurs at Clinch Mountain, Tennessee (Dennison and Boucot, 1974). In Wise County, Virginia, coral biostromal sandy limestone is overlain by black Millboro Shale, with the Tioga layer separating them (Dennison, 1961). At Seven Fountains in the Massanutten Mountain area of Virginia, the Tioga rests on probable moderate water-depth silty sandstone of the upper Needmore Formation, and the Tioga zone is directly overlain by fissile, very dark gray shale of the Marcellus Formation. At Bowmanstown, Pennsylvania, shallow marine sandy limestones and sandstones of the Buttermilk Falls Formation (Epstein, Sevon, and Glaeser, 1974) contain the lowest tuff layers of the Tioga; these are followed by the middle coarse zone of the main Tioga eruption and are immediately overlain by fissile black shales of the Marcellus. In central and eastern outcrops and in the subsurface of New York, the upper Onondaga Limestone was probably deposited slightly below wave base, but immediately after the Tioga ash fall an upward change to very fine muds of the basal Marcellus Shale probably indicates an increase of water depth (Lawrence Rickard, personal communication, 1975). All of these localities with local evidence of water depth increase combine to show a regional consistency probably implying a true sea level rise throughout the Appalachian basin.

PETROLOGY

Nearly 300 samples of the Tioga tuff and associated rocks have been studies in detail. Besides the petrography, reported in this paper, a number of other analyses have been performed such as X-ray diffraction, differential thermal analysis, Kendall Rank Correlation Coefficient test, and atomic absorption spectrometry. The results of these will be given in a lengthy subsequent paper to be published in 1978.

Besides the samples from the Appalachian basin, we studied some from outcrops and wells from southeastern Michigan, southwestern Indiana, and east-central Illinois, all of which are probably Tioga Bentonite. These areas will enter into our analyses in a subsequent paper.

The Tioga tuff ranges (in its original rock state) from coarse crystal tuffs rich in biotite and feldspars (Fig. 3) to tuffaceous shales. A large variety of diagenetic processes has altered these tuffs to rock types such as bleached biotite-rich mudstone or shale. The most widely distributed beds of the middle coarse zone range from coarse biotite-feldspar crystal tuffs near the postulated source volcano to vitric-crystal tuffs to fine vitric tuffs and finally tuffaceous shales farthest away in New York, and biotite-bearing or tuffaceous dolostones, shales, and siltstones in Ohio.

Perhaps the most unique character of the Tioga tuff, both megascopically and microscopically, is the presence of euhedral to subhedral crystals of bleached biotite (Fig. 4). In the coarse middle zone, the biotite may constitute up to 80 percent of the tuff. It lies parallel to bedding, is often graded, and occurs densely packed or scattered throughout the rock. Diameter to thickness ratios vary from 4:1 near the source to 12:1 in more distant areas. A distribution of biotite size is given in Fig. 6, and a pattern away from the probable source in northeastern Virginia is evident. Similar distribution maps for feldspar and quartz emphasize this pattern, with coarsest crystals in northern Virginia corresponding to the thickest accumulation of tuff-influenced beds (Fig. 1). The iron

leached from the biotite to produce the bleached appearance has been used to supply iron for the authigenic pyrite and limonite stain which pervades most samples. Some muscovite has been identified by X-ray, also, but has not been isolated petrographically.

Up to 35 percent of some samples of the middle coarse zone consist of euhedral and fragmented K-feldspar and Na-rich plagioclase. Included in these are microcline, albite, sanidine, and andesine. The condition of the feldspars varies considerably from very fresh unaltered types, particularly from the subsurface, to those completely replaced by kaolinite, calcite, illite, and possibly some zeolites (Figs. 5 and 11). Usually, however, even samples which have undergone extreme diagenesis display sufficient evidence that feldspars were once present, even to the point where twinning has been preserved in the clays that replaced the feldspar. The distribution pattern of the feldspar (Fig. 7) follows other crystal patterns, displaying a distinct northeast axis, and indicating that the source volcano was not far from northeastern Virginia.

Quartz, which seldom exceeds five percent of the sample, occurs in two ways in the middle coarse zone, both of which suggest a volcanic source rather than a terrigenous one (Fig. 8). It occurs as broken crystal fragments which are angular and have the elongate geometry of slivers. Less often, it occurs as euhedral crystals, some with embayed zones. Both types are very clear with non-undulating extinction. Figure 10 displays the regional size distribution, reiterating a pattern which the biotite and feldspar show. Since quartz is not very common, even in samples from near the source, it is not reasonable to expect to find microscopically discernable volcanic quartz in samples farther away, especially if terrigenous quartz had been introduced into the environment.

Vitric portions of the tuff, as great as 90 percent, make up the matrix and were probably originally fine glass dust and shards (Fig. 9). The glass has devitrified to illite with smaller amounts of smectite. Since the vitric material was finer in size than the crystals, it would have been blown farther from the volcano and form the bulk of the representative material of the coarse middle zone farthest from the volcano; thus producing clay-rich beds amongst other non-clay rocks. A few samples contain what appear to be ghost fragments of pumice or larger pieces of vitric tuff. Up to eight percent of some samples consist of these clasts, which range from 1 to 2 mm.

Euhedral zircon and apatite (Figs. 9 and 11) are the common volcanic trace minerals. Maximum dimensions are up to 0.25 mm, and the two minerals may be found intergrown. The general regional size distribution is similar in pattern to those of the major volcanic minerals.

As expected in such a porous and permeable material as a tuff, especially containing unstable ingredients such as fine glass, a multitude of minerals have replaced original material and filled voids. Major products of diagenesis are illite, kaolinite, smectite, and pyrite, followed by less abundant gypsum, basaluminite, limonite, calcite, chlorite, and zeolites.

SOURCE VOLCANO

Speculation as to the location of the volcanic source of the Tioga tuffs was not possible until an array of outcrops and wells had been examined to permit detailed stratigraphic sampling over a large geographic area. The exact location is still unknown, but improved data permit a more precise geographic location for the pluton which fed the volcano.

Based on isopach patterns of the Tioga Bentonite, Dennison (1961) concluded that the source volcano was probably located several miles southeast of the position of Lexington or Staunton, Virginia. Several critical outcrops had not yet been discovered, so that the center of thickest Tioga is now about 70 mi (110 km) farther north but still on the east side of the outcropping Devonian fold belt (Fig. 1).

More detailed study led Oliver and others (1967, p. 1019) to postulate a source volcanic area near Monterey, Virginia. This was done on the basis of general isopach data, crystal size, the geographic and stratigraphic distribution of pyroclastics, and especially the presence of apparent lava flows in the Tioga portion of the stratigraphic column.

Fullagar and Bottino (1969) obtained K-Ar and Rb-Sr dates on these apparent flows, resulting in a 47 million year age (Eocene). The apparent flows are really sills intruded into the Tioga Bentonite zone. The Tertiary age is confirmed by the presence of igneous glass along the chill margins of one of the dikes in the area (personal communication, Charles Milton, 1972), and by a Tertiary paleo-

magnetic pole position in the dikes on both limbs of the Monterey syncline (Lovlie and Opdyke, 1974).

This led us to seek another source, such as the Columbia Granite granodiorite pluton in Fluvanna County, Virginia (Dennison and Textoris, 1970, 1971). However, Fullagar (1971) obtained a much older date for the Columbia Granite, about 595 million years, compared with the expected 370 million years required for the Tioga part of the geologic time scale.

Better isopach and petrologic crystal-size control now suggest a source located near the north end of Massanutten Mountain, Virginia, somewhere to the east in the Piedmont (compare isopach and crystal-size data in Figs. 1, 6, 7, and 10 of this paper). The coarsest crystal sizes are at Wardensville, West Virginia and at Seven Fountains, and the thickest total tuffaceous strata and largest number of recognizable tuff beds both occur at Seven Fountains on Massanutten Mountain.

We suggest the Berea pluton, located 6 mi (9 km) northwest of Fredericksburg, Virginia as a very strong candidate for the actual source pluton for the Tioga eruption. It has recently been mapped by Plavides (1976), who described its petrology and obtained ages ranging from 347 to 361 million years. Plavides (personal communication, 1977) considers the 361 million years to be the more reliable cooling age for the pluton, and even this age is perhaps a few million years younger than the actual time of intrusion. The Berea pluton is a coarse-grained microcline gneissic granite with perthite, myrmekite, antiperthite, biotite, epidote, and sphene (Plavides, 1976, p. 4). Figure 12 of this report is a photomicrograph of a sample from the Berea pluton. Besides the mineral types listed in the caption, zircon and apatite are also present. Thus, the general composition and mineralogy needed to produce a tuff such as the Tioga seem to be found in the Berea pluton. The age of the Berea is a rather good fit for the expected age of the Tioga. The Berea pluton is remarkably close to the locality of maximum thickness and coarsest crystals of the Tioga tuffaceous strata, especially when a palinspastic reconstruction is made to pull the Valley and Ridge outcrops back to their Devonian depositional positions before the Alleghany orogeny (Dennison and Textoris, 1971, p. 54 shows a palinspastic map of Tioga thickness in parts of Virginia, West Virginia, and Maryland). Dennison (1976) proposed that the foreshortening of the Valley and Ridge outcrop belt resulted chiefly from gravity sliding westward from the crest of the Blue Ridge anticlinorium; the Berea pluton in the Piedmont may have shifted very little in position during the Alleghany orogeny. Such a palinspsatic reconstruction would place the Seven Fountains Tioga locality very close to the Berea pluton.

The Petersburg Granite group of plutons (Fig. 1) is also relatively a late group in the Piedmont. The 330 million year concordia age (Wright, Sinha, and Glover, 1975) is too young for the Tioga, and the location is too far south for a good fit for Tioga isopach and crystal-size data.

At present, the stratigraphic and petrologic detail do not permit the resolution of more than one geographic source for Tioga eruptions. The apparent location in the Piedmont of Virginia suggests that the Tioga eruption was a volcanic manifestation along the 38th Parallel fracture zone of an early stage of the Acadian orogeny (Dennison and Johnson, 1971), an event which signaled a sudden westward shift of Devonian shale deposition for another 100 mi (160 km) farther into the Appalachian basin at the moment of the stratigraphic boundary between the Needmore and Marcellus Shales. This was accompanied by a marked increase in Appalachian basin water depth, perhaps an eustatic sea level rise.

Other possibilities for the Tioga source volcano location is somewhere beneath the Coastal Plain sedimentary cover in or offshore from Virginia, in Africa which during the Devonian was perhaps a part of the Appalachia terrigenous clastic source area to the east of the Appalachian basin, or even at some site now swallowed by convection cells associated with spreading of the Atlantic Ocean. All of these possibilities are beyond the limits of testing for validity.

The Berea pluton seems to fit the available data strikingly well, and every effort should be made to test whether this pluton is indeed the source of the Tioga tuff which spread over a vast area of the Devonian eastern North America.

ACKNOWLEDGEMENTS

Portions of this investigation were supported by research grants from the University of Illinois, University of North Carolina, West Virginia Geological and Economic Survey, and by a contract from the Energy Research and Development Administration with the University of North Carolina.

REFERENCES

Baltrusaitis, E. J., 1974, Middle Devonian bentonite in Michigan basin: Am. Assoc. Petroleum Geologist Bull., v. 58, p. 1323-1330.

Baltrusaitis, E. J., 1975, Middle Devonian bentonite in Michigan basin: reply: Am. Assoc. Petroleum Geologist Bull., v. 59, p. 1221-1223.

Collinson, C., James, G. W., Swann, D. H. and others, 1967, Devonian of the north-central region, United States, in Oswald, D. H., ed., Internat. Devonian Symposium, Alberta Soc. Petroleum Geologists, v. 1. p. 933-971.

Dennison, J. M., 1960, Stratigraphy of Devonian Onesquethaw Stage in West Virginia, Virginia, and Maryland: Ph.D. dissert., Univ. Wisconsin, 339 p.

Dennison, J. M., 1961, Stratigraphy of Devonian Onesquethaw Stage in West Virginia and bordering states: West Virginia Geol. Survey, Bull. 22, 87 p.

Dennison, J. M., 1976, Gravity tectonic removal of cover of Blue Ridge anticlinorium to form Valley and Ridge Province: Geol. Soc. America Bull., v. 87, p. 1470-1476.

Dennison, J. M. and Boucot, A. J., 1974, Little War Gap at Clinch Mountain provides standard reference section for Silurian Clinch Sandstone and most nearly complete Devonian section in eastern Tennessee: Southeastern Geology, v. 16, p. 79-101.

Dennison, J. M. and Hasson, K. O., 1976, Stratigraphic cross section of Hamilton Group and adjacent strata along south border of Pennsylvania: Am. Assoc. Petroleum Geologists Bull., v. 60, p. 278-287.

Dennison, J. M. and Head, J. W., 1975, Sea level variations interpreted from the Appalachian basin Silurian and Devonian: Am. Jour. Sci., v. 275, p. 1089-1120.

Dennison, J. M. and Johnson, R. W., Jr., 1971, Tertiary intrusions and associated phenomena near the Thirty-eighth Parallel fracture zone in Virginia and West Virginia: Geol. Soc. America Bull., v. 82, p. 501-507.

Dennison, J. M. and Textoris, D. A., 1970, Devonian Tioga Tuff in northeastern United States: Bull. Volcanologique, v. 34, p. 289-294.

Dennison, J. M. and Textoris, D. A., 1971, Devonian Tioga Tuff: Virginia Division of Mineral Resources, Information Circ. 16, p. 64-68.

Doheney, E. J., Droeste, J. B., and Shaver, R. H., 1975, Stratigraphy of the Detroit River Formation (Middle Devonian) of northern Indiana: Indiana Dept. Natural Resources, Geol. Survey Bull. 53, 86 p.

Droste, J. B. and Shaver, R. H., 1975a, Jeffersonville Limestone (Middle Devonian) of Indiana: stratigraphy, sedimentation, and relation to Silurian reef-bearing rocks: Am. Assoc. Petroleum Geologists Bull., v. 59, p. 393-412.

Droste, J. B. and Shaver, R. H., 1975b, Middle Devonian bentonite in Michigan basin: discussion: Am. Assoc. Petroleum Geologists Bull., v. 59, p. 1217-1221.

Droste, J. B. and Vitaliano, C. J., 1973, Tioga Bentonite (Middle Devonian) of Indiana: Clays and Clay Minerals, v. 21, p. 9-13.

Ebright, J. R., Fettke, C. R., and Ingham, A. I., 1949, East Fork-Wharton gas field, Potter County, Pennsylvania: Pennsylvania Geol. Survey, 4th Ser., Bull. M30, 43 p.

Epstein, J. B., Sevon, W. D., and Glaeser, J. D., 1974, Geology and mineral resources of the Lehighton and Palmerton quadrangles, Carbon and Northampton Counties, Pennsylvania: Pennsylvania Topog. and Geol. Survey Atlas 195cd, 460 p.

Fettke, C. R., 1931, Physical characteristics of the Oriskany Sandstone and subsurface studies in the Tioga gas field, Potter County, Pennsylvania: Pennsylvania Geol. Survey, 4th Ser., Bull. 102-B, p. 1-9.

Fettke, C. R., 1952, Tioga Bentonite in Pennsylvania and adjacent states: Am. Assoc. Petroleum Geologists Bull., v. 36, p. 2038-2040.

Flowers, R. R., 1952, Lower Middle Devonian bentonite in West Virginia: Am. Assoc. Petroleum Geologists Bull., v. 36, p. 2036-2038.

Fullagar, P. D., 1971, The age and origin of plutonic intrusions in the Piedmont of the southeastern Appalachians: Geol. Soc. America Bull., v. 82, p. 2845-2862.

Fullagar, P. D., and Bottino, M. L., 1969, Tertiary felsite intrusions in the Valley and Ridge Province, Virginia: Geol. Soc. America Bull., v. 80, p. 1853-1858.

Hall, James, 1843, Geology of New York: Albany, State of New York, pt. 4, 683 p.

Lounsbury, R. W. and Melhorn, W. N., 1964, Clay mineralogy of Paleozoic K-bentonites of the Eastern United State (Part 1): Clays and Clay Mineralogy, v. 12, p. 557-565.

Lovlie, R. and Opdyke, N. D., 1974, Rock magnetism and paleomagnetism of some intrusions from Virginia: Jour. Geophys. Research, v. 79, p. 343-349.

Meents, W. F. and Swann, D. H., 1965, Grand Tower Limestone (Devonian) of southern Illinois: Illinois Geol. Survey Circ. 389, 34 p.

Oliver, W. A., Jr., 1954, Stratigraphy of the Onondaga Limestone (Devonian) in central New York: Geol. Soc. America Bull., v. 65, p. 621-652.

Oliver, W. A., Jr., 1956, Stratigraphy of the Onondaga Limestone in eastern New York: Geol. Soc. America Bull., v. 67, p. 1441-1474.

Oliver, W. A., Jr., de Witt, W. Jr., Dennison, J. M., Hoskins, D. M., and Huddle, J. W., 1967, The Appalachian basin, United States, in Oswald, D. H., ed., International Symposium on the Devonian System, Alberta Soc. Petroleum Geologists, v. 1, p. 1001-1040.

Oliver, W. A., Jr., de Witt, W., Jr., Dennison, J. M., Hoskins, D. M., and Huddle, J. W., 1969, Correlation of Devonian rock units in the Appalachian basin: U.S. Geol. Survey, Oil and Gas Investigations Chart OC-64.

Pavlides, Louis, 1976, Piedmont geology of the Fredericksburg, Virginia, area and vicinity: Guidebook for Field Trips 1 and 4, Geol. Soc. America, Northeast-Southeast Sections Joint Meeting, 43 p.

Rickard, L. V., 1964, Correlation of the Devonian rocks of the New York State: New York State Mus. and Sci. Service, Map and Chart Ser., no. 4.

Rickard, L. V., 1975, Correlation of the Silurian and Devonian rocks in New York State: New York State: New York State Mus. and Sci. Service, Map and Chart Ser. no. 24.

Weaver, C. E., 1956, Mineralogy of the Middle Devonian Tioga K-bentonite: Amer. Min., v. 41, p. 359-362.

Wright, J. E., Sinha, A. K., and Glover, L., III, 1975, Age of zircons from the Petersburg Granite, Virginia; with comments on belts of plutons in the Piedmont: Am. Jour. Sci., v. 275, p. 848-856.

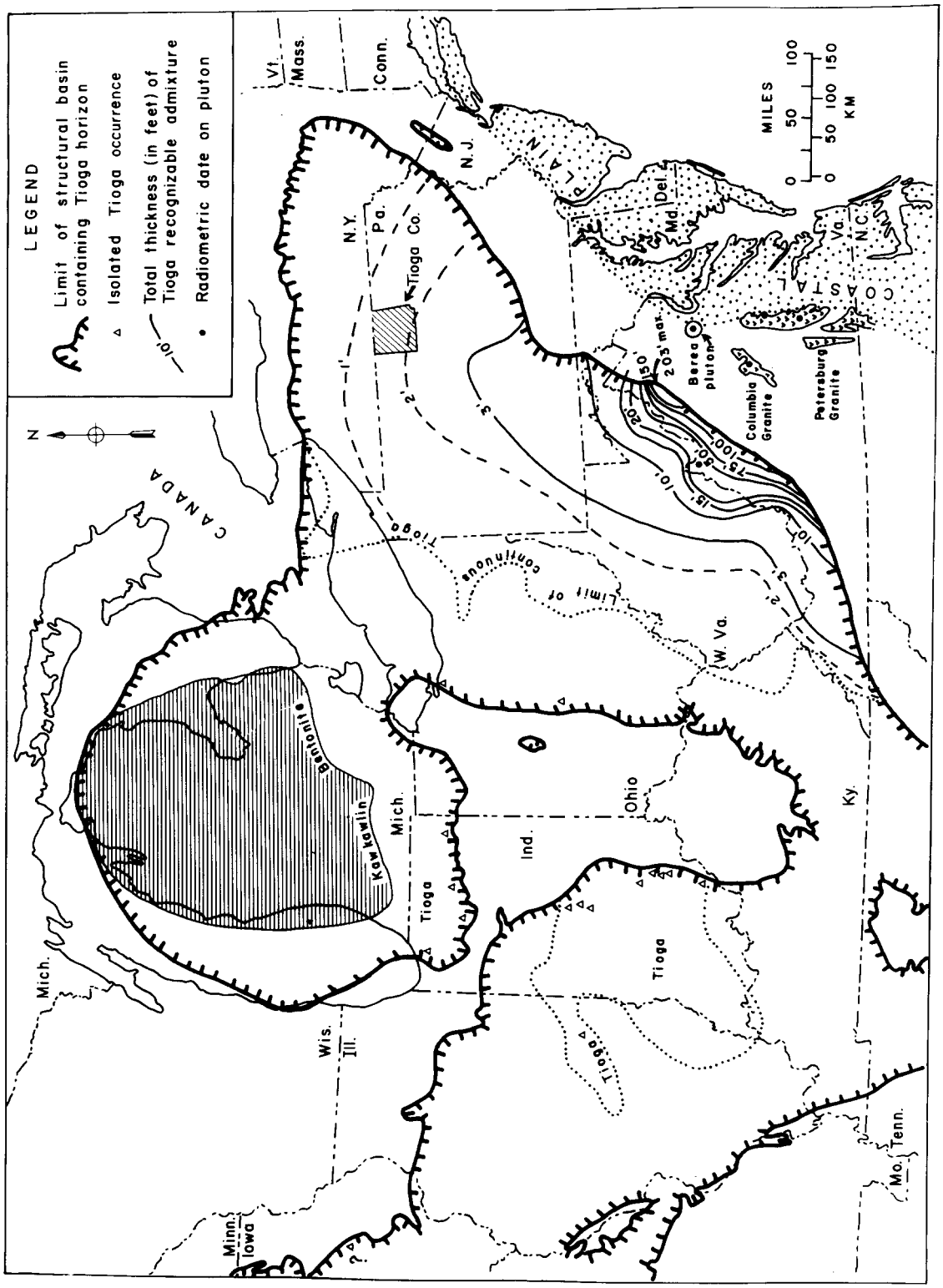

Fig. 1 Distribution and thickness of Devonian Tioga tuffaceous beds in structural basins.

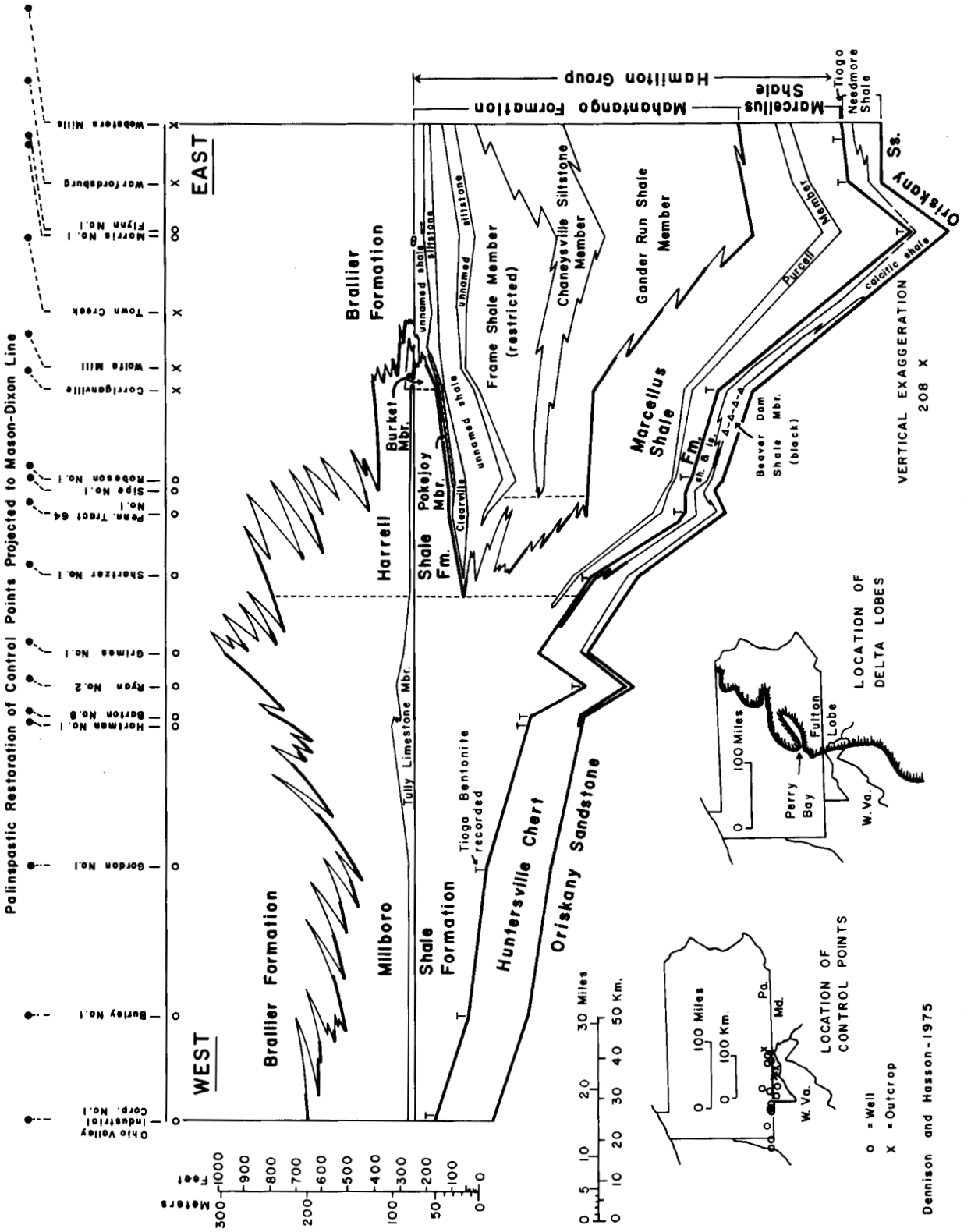

Fig. 2. Facies and recommended nomenclature of Hamilton Group and associated Devonian strata along latitude 39° 43' N in stratigraphic cross section of Fulton Lobe at the Mason and Dixon Line (after Dennison and Hasson, 1976).

Fig. 3. Photomicrograph (plain light) of a thin section of the middle coarse zone of the Tioga Bentonite, cut perpendicular to bedding. Sample is a crystal tuff from Selingsgrove Junction, Pennsylvania, 6 mi (9 km) south of Sunbury. Dark parallel flakes are euhedral biotite crystals, clear angular grains are fragmented volcanic quartz, and subhedral gray crystals accentuated with dark limonite rims are albite with some K-feldspar which have been altered slightly to clay minerals. Crystals are set in an illite-smectite matrix which was originally volcanic glass dust and shards. Black squares are authigenic pyrite.

Fig. 4. A portion of an euhedral biotite crystal, partially embayed, set in an illite matrix which was originally glass dust and shards. Other large crystals are biotite cut perpendicular to mineral cleavage. Sample is a crystal-vitric tuff, middle coarse zone, Tioga Bentonite, Allansville, West Virginia. Plain light. Length of photomicrograph is 0.9 mm.

Fig. 5. From upper left to center are three subhedral feldspar crystals. A black biotite crystal separates them from an euhedral feldspar crystal to right of center. All four have been replaced by illite/kaolinite. Sample is a crystal-vitric tuff, middle coarse zone, Tioga Bentonite, Wardensville, West Virginia. Plain light. Length of photomicrograph is 2.0 mm.

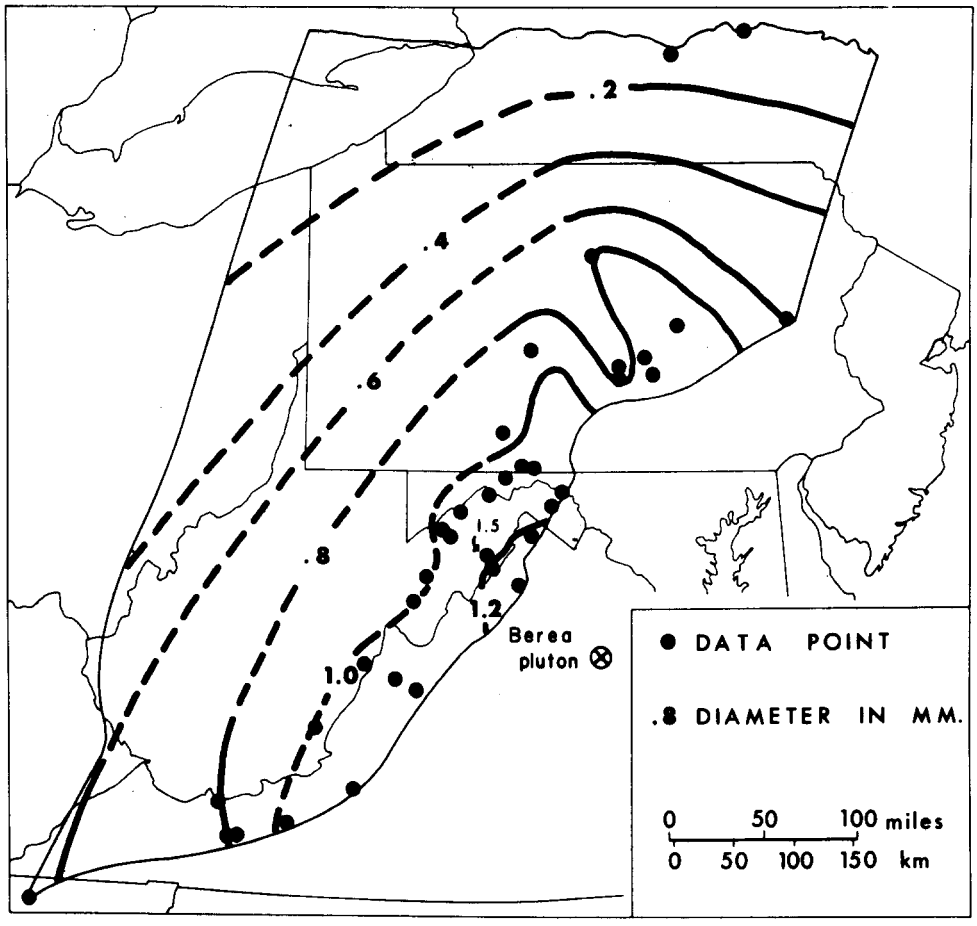

Fig. 6. Mean diameter of coarsest biotite in middle coarse zone of Tioga Bentonite, Appalachian basin. Preliminary map.

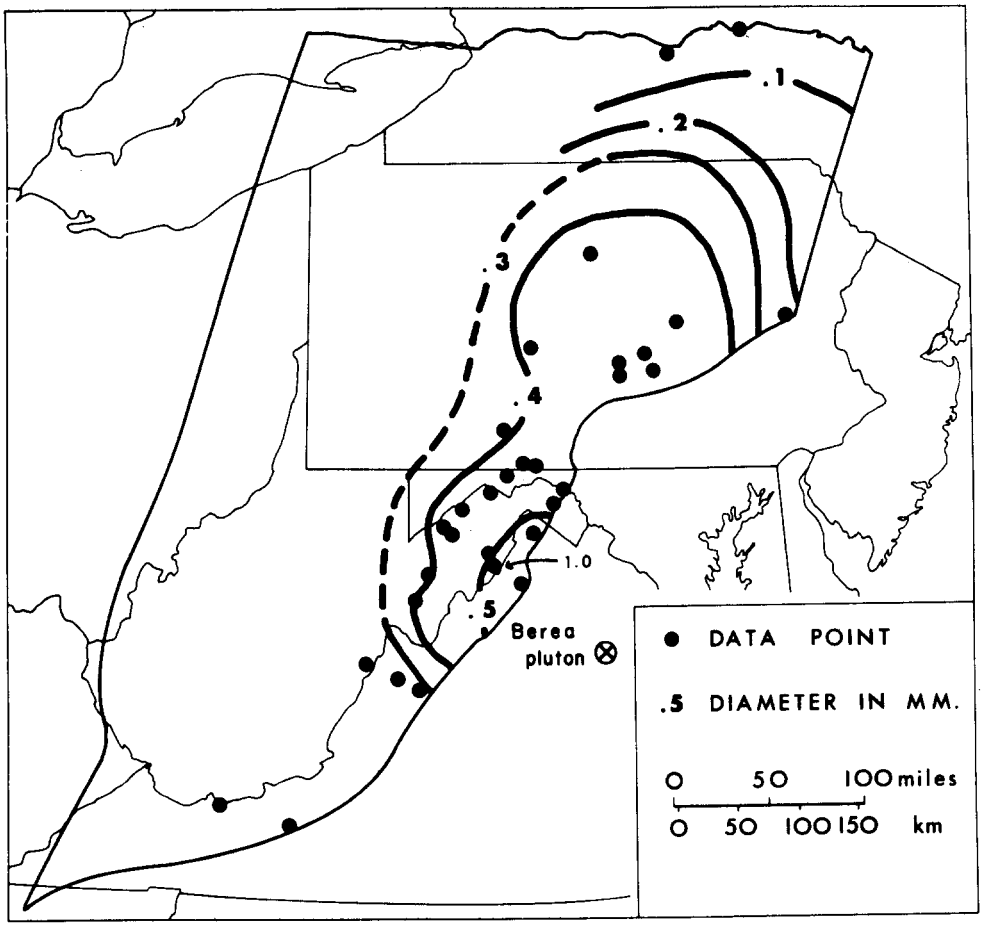

Fig. 7. Mean diameter of coarsest feldspar in middle coarse zone of Tioga Bentonite, Appalachian basin. Preliminary map.

Fig. 8. Two crystals of volcanic quartz. To the left is an euhedral, embayed crystal, and to the right is an angular and fragmented sliver of a crystal. Biotite crystals and illite matrix surround them. Sample is a crystal-vitric tuff, middle coarse zone, Tioga Bentonite, Allansville, West Virginia. Polarized light. Length of photomicrograph is 0.9 mm.

Fig. 9. In the center is an euhedral zircon crystal touching a portion of an euhedral biotite crystal to the right. Both are set in an illite matrix which was originally glass dust and shards. Sample is a crystal-vitric tuff, middle coarse zone, Tioga Bentonite, Wardensville, West Virginia. Plain light. Length of photomicrograph is 0.9 mm.

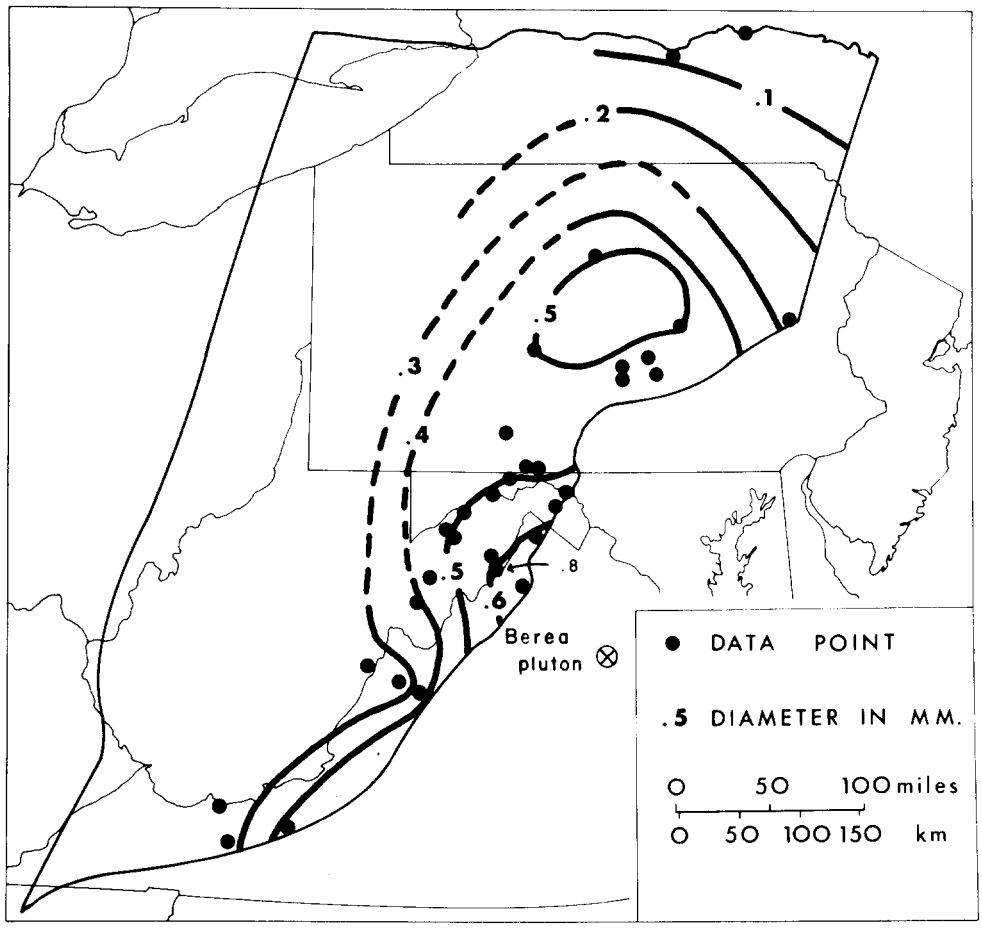

Fig. 10. Mean diameter of coarsest quartz in middle coarse zone of Tioga Bentonite, Appalachian basin. Preliminary map.

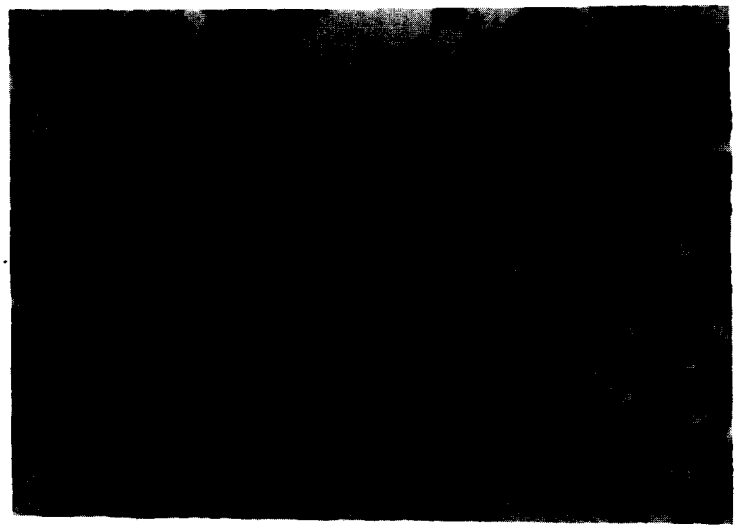

Fig. 11. Left of center is a clear euhedral apatite crystal. To its right is an anhedral sanidine crystal partially replaced by calcite. Note biotite bent over apatite and sliver of volcanic quartz in upper center. Sample is a crystal-vitric tuff, middle coarse zone, Tioga Bentonite, Allansville, West Virginia. Plain light. Length of photomicrograph is 0.9 mm.

Fig. 12. This sample is a microcline gneissic granite from the Berea pluton, Berea, Virginia, about 6 mi (9 km) northwest of Fredericksburg. Visible are microcline, plagioclase, quartz, biotite, and leucoxene. Polarized light. Length of photomicrograph is 3.0 mm.

THE NEW ALBANY SHALE AND CORRELATIVE STRATA IN INDIANA

by

John L. Bassett and Nancy R. Hasenmueller
Indiana Geological Survey
Bloomington, Indiana

ABSTRACT

The New Albany Shale has a maximum thickness of 337 feet in southwestern Indiana and thins northward and eastward to about 90 feet in the outcrop area. In the Michigan Basin, strata equivalent to the New Albany are 348 feet thick in Lagrange County. The base of the New Albany is 4,500 feet below sea level in southwestern Indiana, and the base of the Antrim Shale is 150 feet above sea level in northern Indiana (Lagrange County).

In the Illinois Basin the New Albany is divided into four members: the Hannibal, Grassy Creek, Sweetland Creek, and Blocher Shales. The lithologic equivalents of the New Albany in the Michigan Basin are the Sunbury, Ellsworth, and Antrim Shales.

The New Albany produced commercial gas from seven fields in Harrison County and one field in Martin County. Two small gas fields have been found in the New Albany in Daviess County.

OBJECTIVES

The first phase of the Eastern Gas Shale Project in Indiana has consisted of collecting drill hole data on the New Albany Shale and equivalent strata and studying the stratigraphy and structural framework of the units.

Through July 1, 1977, study has been concentrated on five principal aspects: (1) preparing a map showing location of New Albany datum points, (2) dividing the New Albany into four members in the Illinois Basin, (3) determining the structure on both the top and the base of the formation, (4) preparing a map showing the thickness of the New Albany and equivalent rocks, and (5) preparing maps showing gas shows in the New Albany and underlying Middle Devonian limestone.

INTRODUCTION

Carbonaceous shales of Devonian-Mississippian age are present in the Illinois Basin in southwestern Indiana and in the Michigan Basin in northeastern Indiana. The New Albany Shale in the Illinois Basin was once continuous with that of the Michigan Basin, but it has been removed by erosion along the northwestward-trending Cincinnati Arch (Lineback, 1970, p. 2).

The New Albany paraconformably overlies the Middle Devonian limestone southwest of the Cincinnati Arch province. The New Albany is overlain by the Rockford Limestone in southwestern Indiana except where the Rockford is not present and the New Albany is directly overlain by the Mississippian New Providence Shale (Borden Group). In the Michigan Basin strata equivalent to the New Albany overlie the Middle Devonian limestone and are overlain by the Coldwater Shale (Mississippian).

In southwestern Indiana the New Albany Shale crops out on the flank of the Cincinnati Arch, where it ranges in total thickness from 90 to 130 feet. The rocks both dip and thicken southwestward

into the Illinois Basin and attain a maximum thickness of 337 feet in extreme southwestern Indiana. In the southern part of the Michigan Basin strata equivalent to the New Albany are as much as 348 feet thick.

The two dominant lithologies of the New Albany are a brownish-black organic shale and a greenish-gray nonorganic shale. The brownish-black organic shale constitutes more than 80 percent of the New Albany in the southwestern part of the Illinois Basin (Lineback, 1970, p. 4). Elsewhere in Indiana the brownish-black organic shale constitutes only 20 to 40 percent of the New Albany Shale and equivalent strata (Lineback, 1970, fig. 2).

The counties referred to in this paper are shown in figure 1.

STRATIGRAPHY

Illinois Basin:

The name New Albany Shale was proposed by Borden (1874, p. 158) for the brownish-black shale exposed at New Albany, Floyd County, Indiana. On the basis of lithology, paleontology, and jointing, Campbell (1946, p. 835) subdivided the unit into several formations and members. On the basis of lithology, Lineback (1968, p. 1291) subdivided the New Albany into five members in the outcrop belt: Blocher, Selmier, Morgan Trail, Camp Run, and Clegg Creek (in ascending order). Becker (1974, p. 45), using lithologic samples and geophysical logs, recognized the lowermost outcrop member, the Blocher, in the subsurface in the Illinois Basin, but he did not differentiate other outcrop members in the subsurface. He (1974, p. 45, 46) also recognized and described the Hannibal Member as the uppermost member of the New Albany Shale in the subsurface of Indiana.

In the present study five north-south and six west-east stratigraphic cross sections were compiled by using geophysical logs of 109 selected wells in the Illinois Basin. Lithologic strip logs for the selected wells were examined when they were available. As a result of this study the subsurface New Albany has been subdivided into four members: Blocher, Sweetland Creek, Grassy Creek, and Hannibal (in ascending order).

Blocher Member - The name Blocher Formation was first used by Campbell (1946, p. 840) for the brownish-black organic-rich calcareous to dolomitic shale in the basal part of the New Albany. Lineback (1968, p. 1295) redefined the Blocher of Campbell by raising the upper boundary of the unit to the base of the greenish-gray shale of the Selmier Member. Collinson and others (1967, fig. 13), using geophysical data, mapped the thickness and distribution of this unit in the Illinois Basin. Lineback (1970, fig. 7), using lithologic characteristics, mapped the Blocher in southwestern Indiana slightly thicker than Collinson and others. In this report recognition and thickness of the unit are based primarily on geophysical log evidence.

On electric logs the Blocher is recognized as a high-resistivity unit at the base of the New Albany overlying Middle Devonian limestone in the Illinois Basin (fig. 2A). The Blocher is 48 feet thick in the southwestern part of the basin and thins to the north and east. North of central Vigo County the Blocher is not recognized on electric logs.

Sweetland Creek Member - The name Sweetland Creek was first used by Udden (1899, p. 65-78) for strata exposed along Sweetland Creek, Muscatine County, Iowa. The Sweetland Creek Shale as redefined by Collinson and others (1967, p. 960) is restricted to the greenish-gray shales underlying the Grassy Creek (a black organic shale) at the type section. Meents and Swann (1965, fig. 4) traced the Sweetland Creek as an "unnamed shale" from Illinois into southwestern Indiana.

In the subsurface of Indiana the name Sweetland Creek Member of the New Albany Shale is being applied to the slightly calcareous to dolomitic greenish-gray to very dark-gray shale underlying the black shales of the Grassy Creek. The Sweetland Creek overlies the Blocher in the deeper part of the basin; however, where the Blocher is not present, north of central Vigo County, the Sweetland Creek rests on Middle Devonian limestone. The shales of the Sweetland Creek are generally lighter in color and have a lower resistivity on an electric log than the Blocher or the Grassy Creek (fig. 2A).

The Sweetland Creek is 49 feet thick in Posey County and thins eastward to 13 feet in Washington County. The unit thins northward to northern Vigo County, and north of that point it thickens slightly at the expense of the overlying Grassy Creek.

Grassy Creek Member - The Grassy Creek Shale was named by Keyes (1898, p. 59-63) for exposures along Grassy Creek in Pike County, Missouri. Meents and Swann (1965, fig. 4) and Collinson and others

(1967, fig. 7) recognized the Grassy Creek in the subsurface of Illinois and traced this unit into southwestern Indiana.

In the present study the name Grassy Creek Member of the New Albany Shale is applied to the brownish-black organic-rich pyritic noncalcareous shale that overlies the Sweetland Creek and underlies the greenish-gray shales of the Hannibal. In the subsurface the high resistivity of the unit on electric logs differentiates it from the units below and above (fig. 2A). The Grassy Creek is 118 feet thick in Posey County and becomes thinner and less organic to the north and east.

Hannibal Member - The Hannibal Shale was named by Keyes (1892, p. 289) for 75 feet of sandy shale exposed at Hannibal, Missouri. The Hannibal is as much as 100 feet thick in western Illinois and thins eastward in the Illinois Basin (Willman and others, 1975, p. 130). Meents and Swann (1965, fig. 4) and Collinson and others (1967, p. 947) traced a combined Hannibal-Saverton unit into southwestern Indiana. Becker (1974, p. 48) proposed that in the subsurface of Indiana the name Hannibal Member of the New Albany Shale be applied to the greenish-gray shale that lies between the base of the Rockford Limestone and the top of the black shales of the New Albany.

The Hannibal is greenish-gray noncalcareous low-organic shale characterized by low electrical resistivity on a geophysical log (fig. 2A). This unit can be differentiated from the greenish-gray shales of the New Providence only when overlain by the Rockford Limestone. It is 48 feet thick in Posey County and thins eastward in the basin.

Michigan Basin:

In the southern part of the Michigan Basin three stratigraphic cross sections were compiled by using geophysical logs of 29 selected wells. Three units equivalent to the New Albany are recognized in northern Indiana: the Antrim, Ellsworth, and Sunbury Shales (from oldest to youngest). These units are more than 340 feet thick in Lagrange County (fig. 3) and thin to the east and west. In the western part of the Michigan Basin the New Albany equivalents are overlain by thick glacial drift, and to the east in Lagrange, Steuben, Noble and DeKalb Counties they are overlain by the Coldwater Shale (Mississippian). In general, the strata have a lower percentage of organic material than the New Albany does in the Illinois Basin (Lineback, 1970, fig. 2).

Antrim Shale - The name Antrim Shale was proposed by Lane (1901, p. 9) for an exposure of shale in Antrim County, Michigan. The Antrim in the southern part of the Michigan Basin is predominantly black organic-rich shale with greenish-gray calcareous shale in the lower part of the unit from LaPorte County eastward. The natural gamma radiation of the unit, except for the lower part, is high (fig. 2B). The Antrim ranges from about 70 to 220 feet in thickness and thickens eastward as the greenish-gray shale of the Ellsworth grades into the black organic shale of the Antrim.

Ellsworth Shale - The name Ellsworth Shale was formally proposed by Newcombe (1933, p. 49-51) for greenish-gray shale exposed in a quarry near Ellsworth, Antrim County, Michigan. The lower part of the Ellsworth Shale consists of interbedded greenish-gray nonorganic shale and black organic shale that exhibits moderate to high natural gamma radiation. The upper part of the Ellsworth is greenish-gray nonorganic shale characterized on a gamma ray log by low gamma radiation (fig. 2B). Both the upper and lower parts of the Ellsworth extend into the northern part of the Illinois Basin (Lineback, 1970, p. 32). The upper part may correlate with the Hannibal Member of the New Albany Shale.

Sunbury Shale - The Sunbury Shale was originally described as the Sunbury Black Slate by Hicks (1878, p. 216, 220) for shale exposed in Delaware County, Ohio. The Sunbury in northern Indiana is black organic shale about 10 feet thick. This unit has high gamma radiation and is recognized on gamma ray logs in Lagrange, Steuben, Noble, and DeKalb Counties. The Sunbury separates the greenish-gray shales of the Ellsworth from those of the Coldwater Shale. In areas where the Sunbury is not present, the Ellsworth cannot readily be separated from the overlying Coldwater Shale (fig. 2B).

STRUCTURE

A structure contour map on the base of the New Albany Shale and its equivalents was compiled from about 1,400 well records in the Illinois Basin and about 400 well records in the Michigan Basin. Where available, datum points were selected at a density of one well per section and contoured at a 100-foot interval. Figure 4, with a contour interval of 500 feet in the Illinois Basin, is a simplified version of the original map.

The New Albany Shale both thickens and dips into the Illinois Basin. In the outcrop belt the base of the formation is 500 to 600 feet above sea level. In extreme southwestern Indiana the base

of the shale is 4,500 feet below sea level. Within 20 miles of the outcrop belt the rocks dip 20 to 30 feet per mile to the southwest; the dip increases basinward and is about 40 to 60 feet per mile in southwestern Indiana. This generally uniform southwesterly dip of the shale is disturbed locally by the Mt. Carmel Fault and by a series of small domal structures reflected upward from Silurian reefs.

The Mt. Carmel Fault in south-central Indiana is a normal fault downthrown on the west (basinward) side about 100 feet. Rocks on the basinward side of the fault are folded into a southward-plunging anticline in Monroe, Lawrence, and Washington Counties (fig. 4).

Silurian reef structures extend in a belt from Vigo and Clay Counties southward to Dubois County. The structures are generally about one mile in diameter and are represented on the New Albany structure map by small domal areas with 100 to 150 feet of closure. The New Albany thins slightly over some of the reef structures.

The base of the Sunbury-Ellsworth-Antrim interval in the Michigan Basin dips northward at 10 to 20 feet per mile beneath thick glacial drift or Mississippian Coldwater Shale. In northern Steuben County the base of the Antrim is approximately at sea level. No major faults or reef structures interrupt the northward dip, although there are several small flexures and local variations in strike and dip.

OCCURRENCE OF GAS

Gas has been produced from the New Albany Shale from seven fields in Harrison County, one field in Martin County, and two small fields in Daviess County (table 1). All fields are now largely abandoned except the one-well Bramble Field in Daviess County. Figure 5 shows the distribution of these fields and of oil and gas shows in the selected study wells.

Of the some 1,400 study wells penetrating the New Albany Shale in the Illinois Basin, about 6 percent are reported to have had some show of gas from the shale. A clustering of gas shows is found along the Mt. Carmel Fault in Monroe, Lawrence, and Washington Counties, in western Greene County, and in Harrison County.

The random distribution of gas shows appears to have no relationship to structure. Although many gas shows have been reported in the Silurian reef belt in western Greene County, none of these shows have been correlated with a structural high over a buried reef despite the fact that there is significant oil and gas production from underlying Middle Devonian carbonates over these reef-induced structures (fig. 6).

Sorgenfrei (1952) noted the correlation of New Albany gas fields in Harrison County with "nose" or "dome" structures. Such a correlation is not seen on the scale and contour interval of the present map. The Loogootee North Field in Martin County (fig. 5) seems to have been associated with a small basin or syncline with a few tens of feet of closure (Sorgenfrei, 1952). Little correlation is seen between thickness of the shale and the occurrence of gas.

In Harrison County, gas in the New Albany has been generally produced in the upper part of the formation (Grassy Creek Member), or from a zone 20 to 30 feet above the base (Sorgenfrei, 1952). At the single-well Bramble Field in Daviess County, an initial production of 250 MCF/24 was obtained from the entire thickness of the unit. At the Glendale Field the single producing well yields gas from a zone seven feet thick near the middle of the unit.

Scattered shows have been reported from the Antrim Shale, but there are no producing wells in the Michigan Basin.

Table 1. Data on gas fields in the New Albany Shale in Indiana
[Modified from Becker and Keller, 1976]

County	Field name	Discovery year	Number of wells	Average initial production	Average depth	Present Status (1977)
Daviess	Bramble	1974	1	250MCF/24	1,700	Active
Daviess	Glendale	1940	1	750MCF/24	2,100	Abandoned
Harrison	Corydon	1923	15	110MCF/24	800	93% Abandoned
Harrison	Elizabeth	1925	1	Gas	750	Abandoned
Harrison	Laconia	1915	106	220MCF/24	700	99% Abandoned
Harrison	New Boston	1885	13	245MCF/24	450	85% Abandoned
Harrison	New Middletown	1923	26	120MCF/24	750	96% Abandoned
Harrison	Rosewood	1895	21	225MCF/24	300	90% Abandoned
Harrison	Rosewood North	----	4	Gas	300	Abandoned
Martin	Loogootee North	1902	12	780MCF/24	1,500	92% Abandoned

LITERATURE CITED

Becker, L. E.
1974 - Silurian and Devonian rocks in Indiana southwest of the Cincinnati Arch: Indiana Geol. Survey Bull. 50, 83 p.

Becker, L. E., and Keller, S. J.
1976 - The New Albany Shale and equivalent strata in Indiana, in Devonian shale production and potential: Proceedings of the Seventh Appalachian Petroleum Geology Symposium, Morgantown, W. Va., p. 162-168.

Borden, W. W.
1874 - Report of a geological survey of Clark and Floyd Counties, Indiana: Indiana Geol. Survey, Ann. Rept. 5, p. 133-189.

Campbell, Guy
1946 - New Albany Shale: Geol. Soc. America Bull. v. 57, p. 829-908.

Collinson, Charles, and others
1967 - Devonian of the north-central region, United States, in International Symposium on the Devonian System: Alberta Soc. Petroleum Geologists, v. 1, p. 933-971.

Hicks, L. E.
1878 - The Waverly Group in central Ohio: Am. Jour. Sci., ser. 3, v. 16, p. 216-224.

Keyes, C. R.
1892 - Principal Mississippian section: Geol. Soc. America Bull., v. 3, p. 283-300.

1898 - Some geological formations of the Cap-au-Gres uplift: Iowa Acad. Sci. Proc., v. 5, p. 58-63.

Lineback, J. A.
1968 - Subdivisions and depositional environments of New Albany Shale (Devonian-Mississippian) in Indiana: Am. Assoc. Petroleum Geologists Bull., v. 52, p. 1291-1303.

1970 - Stratigraphy of the New Albany Shale in Indiana: Indiana Geol. Survey Bull. 44, 73 p.

Lane, A. C.
1901 - Suggested changes in nomenclature of Michigan formations: Michigan Miner, v. 3, no. 1, p. 9.

Meents, W. F., and Swann, D. H.
1965 - Grand Tower Limestone (Devonian) of southern Illinois: Illinois Geol. Survey Circ. 389.

Newcombe, R. B.
1933 - Oil and gas fields of Michigan, a discussion of depositional and structural features of the Michigan Basin: Michigan Geol. Survey Pub. 38, Geol. ser. 32, 293 p.

Sorgenfrei, Harold, Jr.
1952 - Gas production from the New Albany Shale (M. A. thesis): Bloomington, Indiana Univ., 26 p.

Udden, J. A.
1899 - The Sweetland Creek beds: Jour. Geology, v. 7, p. 65-78.

Willman, H. B. and others
1975 - Handbook of Illinois stratigraphy: Illinois Geol. Survey Bull. 95, 261 p.

Figure 1. Map of Indiana showing counties.

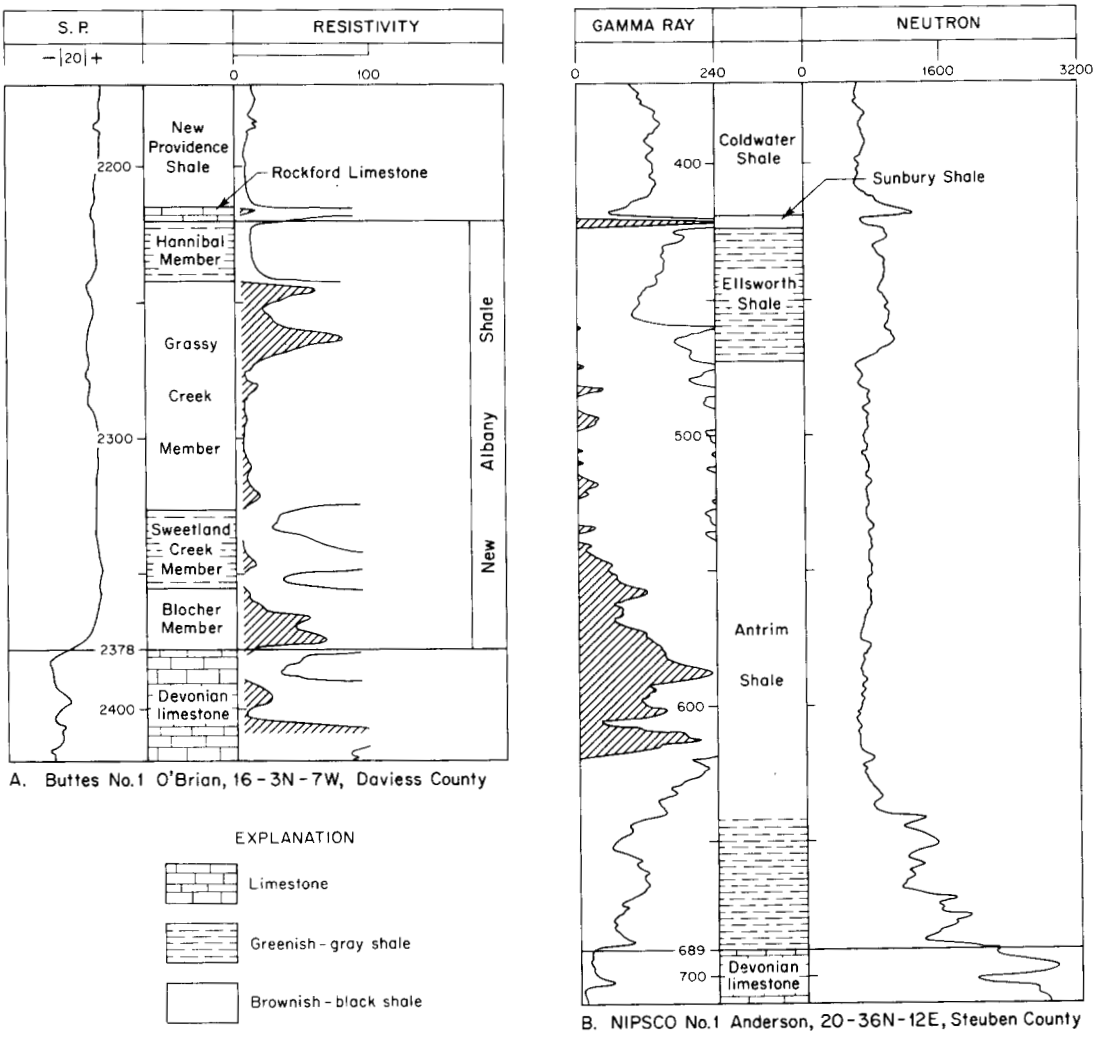

Figure 2. Geophysical log and stratigraphy of the New Albany Shale in the Illinois Basin (A) and of the equivalent strata in the Michigan Basin (B).

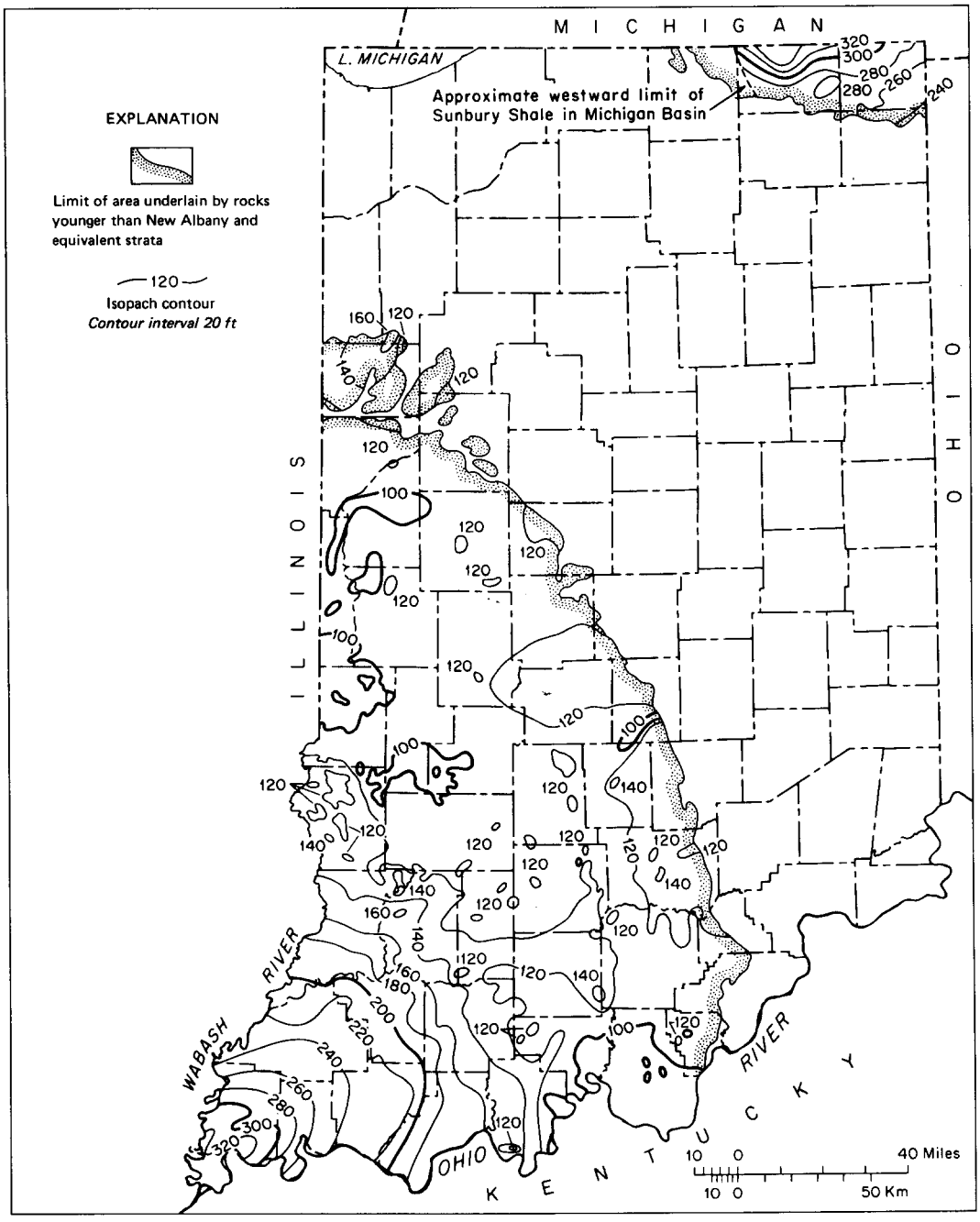

Figure 3. Isopach map of the New Albany Shale and equivalent strata in Indiana.

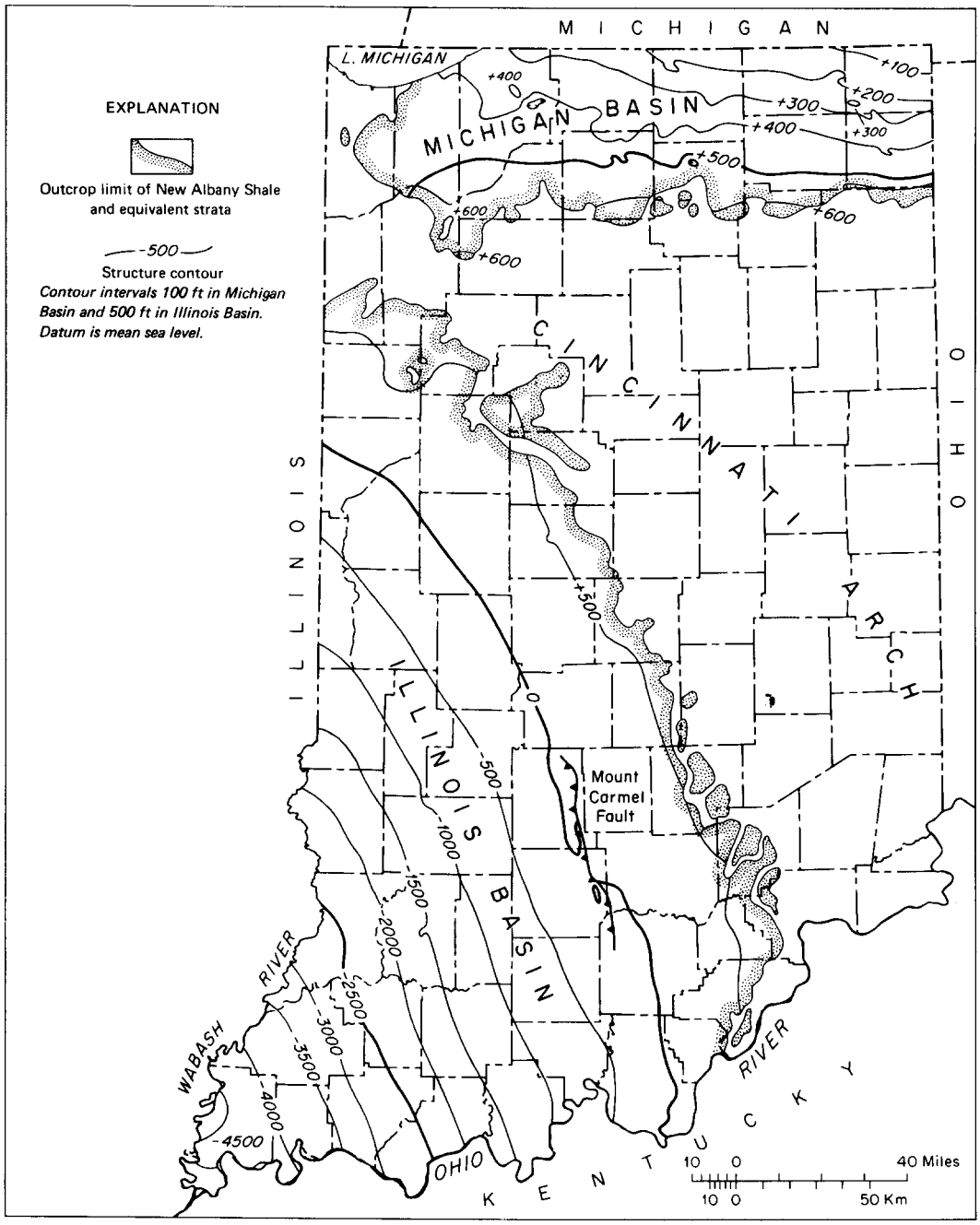

Figure 4. Map of Indiana showing structure on the base of the New Albany Shale and equivalent strata.

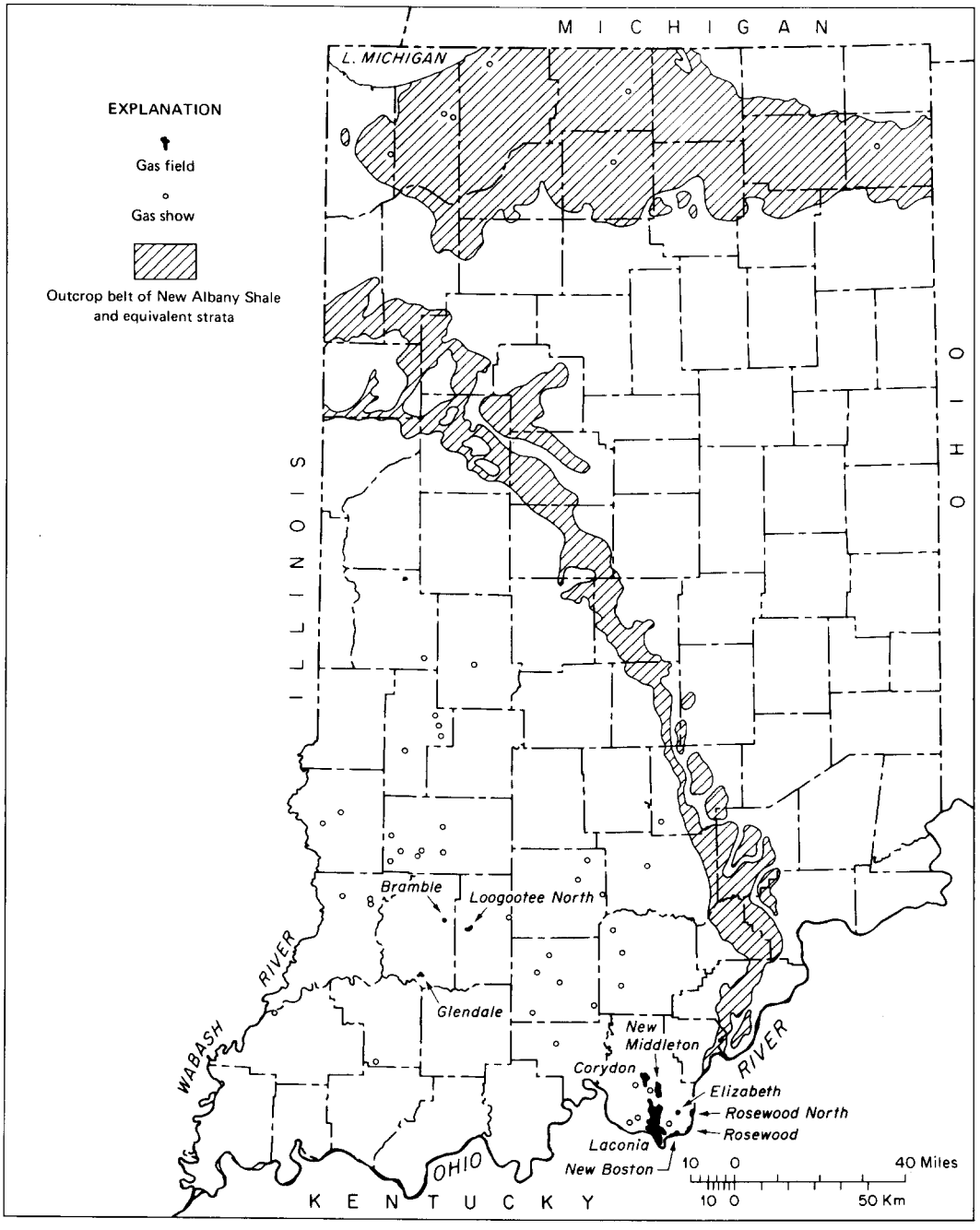

Figure 5. Map of Indiana showing gas fields and gas shows from the New Albany Shale.

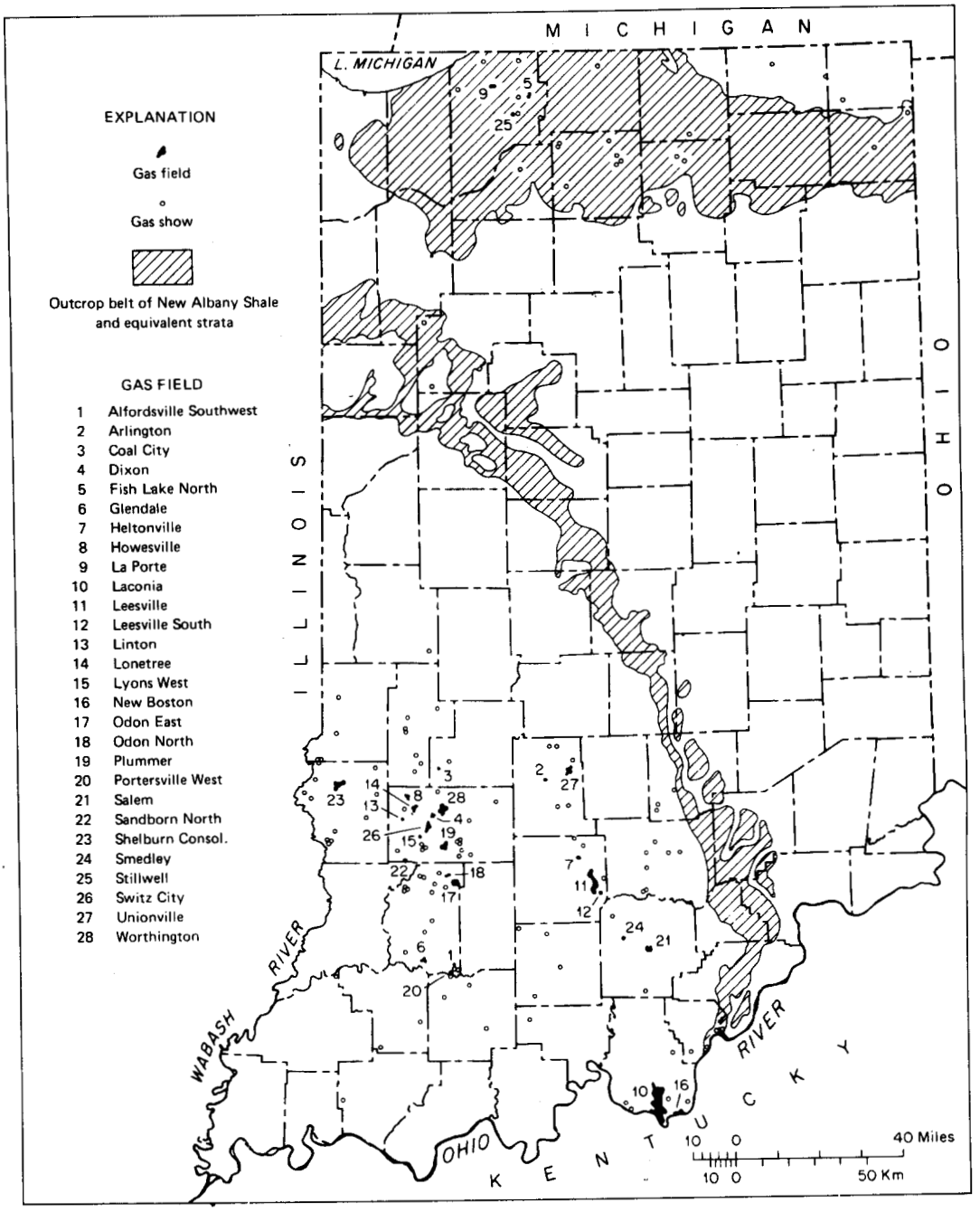

Figure 6. Map of Indiana showing gas fields and gas shows from the Middle Devonian limestone.

PRELIMINARY MODEL OF CATSKILL DELTA IN WEST VIRGINIA

by

Joesph F. Schwietering
West Virginia Geological and Economic Survey

ABSTRACT

Cross sections and diagrams will be used to illustrate a preliminary concept of the structural framework and history of the Catskill Delta and related rock units in West Virginia. In this discussion an attempt will be made to relate the growth of the delta to westward transgressions of the sea onto the craton.

In the model I am going to present I hope to show that the distribution of the lithofacies present in the Catskill Delta complex can, in part, be explained by relating the growth of the delta to transgressions of an epicontinental sea onto the interior of the craton and to simultaneous pulses of mountain building that occurred during the Acadian Orogeny.

In general terms the model consists of a delta system forming in a shallow epicontinental sea that lies between mountains along the continental margin and the interior of the continent. The delta is built out from the mountains toward the interior of the continent. Transgressions of the epicontinental sea onto the craton occur during periods of mountain building along the continental margin in the manner suggested by Johnson (1971). The sedimentary facies present within the epicontinental sea move laterally in response to periods of transgression, regression, and still stand of sea level.

Figure 1 is a diagram showing the relative position of 1) a closing ocean, 2) mountains along a continental margin, 3) an epicontinental sea, 4) delta facies, 5) prodelta facies, and 6) black mud facies. Erosion of the rising mountains along the continental margin provides sediments for the growth of the delta. The rising sea level combined with subsidence in the area of sediment accumulation provides room for the accumulation of sediments and continued growth of the delta.

If the interior of the continent supplies great quantities of sediments to the sea, then a complex delta system will form along the interior margins of the epicontinental sea. However, if little or no clastic sediments or plant material is supplied to the interior margins of the sea, then, depending on climatic conditions, evaporite or carbonate deposits will accumulate along the interior margins. If a large amount of mud is supplied to the interior margins of the sea, either by being washed in from the craton or by settling from sea water, then gray or black muds will accumulate along the interior margins of the sea. Gray mud deposits will form when only small amounts of plant material accumulates with the mud. Black mud deposits might form if large quantities of plant material accumulates with the mud. The critical factor in determining whether organic rich (black) mud will be preserved is the availability of oxygen to oxidize the plant material that accumulates with the mud. If there is not enough oxygen in the mud to oxidize the plant material that remains after the feeding and decomposition activities of organisms living in or on the mud, then black mud will accumulate. The boundary between aerobic and anaerobic environments could be at the sediment-water interface or at some horizon within the water above the mud. In essence the black mud may be analogous to very muddy marine or brackish water peat deposits. If this is the case,

then black shales, like the Ohio Shale, are analogous to very shaly marine or brackish-water coals.

Figure 2 is an attempt to show how facies in a shallow epicontinental sea might move laterally in response to a transgression and an associated orogeny. At time 1 (T1) (Fig. 2a) a delta and prodelta complex is building out from mountains along a continental margin toward the interior of a continent. Black mud is accumulating along the interior margin of the epicontinental sea. If sea level remains stationary relative to the craton and subsidence beneath the sea is not adequate to offset the rate of sediment accumulation, then the sea will slowly fill in and the delta facies will move toward the interior of the craton. Also, with the filling in of the sea, the black mud facies along the interior margin will migrate toward the central parts of the sea over earlier deposited distal prodelta deposits.

The Cleveland Shale in northeastern Ohio may represent a still stand of sea level late in the Devonian. In the vicinity of Cleveland, Ohio a zone of interbedded gray siltstone, gray shale, and black shale, called the Olmsted Member by Cushing and others (1931, p. 36) and here referred to as the Olmsted facies, is present in the basal part of the Cleveland Shale. The Olmsted facies is thought to represent the intertonguing of the black shale of the Cleveland Shale Member of the Ohio Shale with the gray shale and siltstone of the Chagrin Shale (Pepper and others, 1954, p. 16). The upper part of the Cleveland Shale Member is composed predominantly of black shale and it overlaps the Olmsted facies to the east. Farther east, in eastern Ohio, the Cleveland Shale pinches out between gray shale and siltstone of the underlying Chagrin Shale and gray shale and siltstone of the overlying Bedford Shale (Pepper and others, 1954; Lewis and Schwietering, 1971). Sedimentary structures in the siltstones in the Olmsted facies and the Chagrin Shale indicate that the silt was derived from the east (Thomas L. Lewis, oral commun.).

In view of the model presented in this paper, the interbedded black shale and gray shale and siltstone of the Olmsted facies represent the intertonguing of the shallow water black mud facies along the interior margin of an epicontinental sea with the most distal parts of the prodelta facies. The eastward extension of the upper part of the Cleveland Shale over the prodelta facies that makes up the Chagrin Shale represents the infilling of the sea and a seaward extension of the shallow-water black mud facies along the interior margins of the sea. The gray shale and siltstone of the overlying Bedford Shale represent a rise in sea level and an advance of the deeper water prodelta facies over the shallow-water black mud facies.

Assume that at some time later than time T1 a rise in sea level associated with a pulse of uplift in the mountains along the continental margins occurs. Such a rise in sea level is indicated by T2 on Figure 2b.

A rise in sea level would cause a deepening of the water in the epicontinental sea and a lateral migration of facies. The shallow-water facies in the epicontinental sea would migrate toward the mountains along the continental margins and toward the center of the craton along the interior margins of the sea. As sediments from the rising mountains were being carried into the epicontinental sea, prodelta deposits would accumulate over a much wider area, covering the earlier deposited shallow-water deltaic sediments along that part of the sea bordering the rising mountains and the shallow-water mud facies in that part of the sea along the interior of the craton. The delta facies would migrate toward the mountains along the continental margins and the black mud facies would migrate toward the interior of the continent. With a subsequent still stand of sea level, or rapid infilling of the epicontinental sea the shallow-water facies would again migrate toward the center of the sea in the manner described above.

So, depending on stratigraphic relations, a black shale layer could indicate a transgression of the sea or an infilling of a sea. If the black shale occurs in the lower part of a transgressive sequence, as is the case for the basal part of the Ohio Shale, the black shale represents a shallow-water muddy facies in a transgressive sea. If the black shale forms a wedge pinching out toward the central deeper parts of an epicontinental sea within prodelta sediments, the black shale may represent an infilling of the epicontinental sea and the shallow-water muddy facies moving toward the central parts of the sea.

I will now attempt to use this model to explain the vertical and lateral distribution of delta, prodelta, and black shale facies associated with that part of the Catskill Delta present in West Virginia. Figure 3 is a map of the Appalachian Basin and surrounding area. The distribution of the Middle and Upper Devonian outcrops around the perimeter of the basin and the location of the Catskill Delta are shown on the map. The location of the Catskill Delta clastic wedge is taken from "The evolution of North America" by Philip B. King (1959, p. 61). Much of the stratigraphic data used in the following discussion were extracted from the published works of Dennison (1961, 1963, 1970,

1971), Dennison and Naegele (1963), and Woodward (1943).

Over much of West Virginia, and the rest of the Appalachian Basin, Middle and Upper Devonian rocks that make up the Catskill Delta rest upon rocks belonging to the Middle Devonian Onesquethaw Stage. In West Virginia the Onesquethaw Stage consists of the Onondaga Limestone and the Huntersville Chert in the west and the Needmore Shale in the east. Dennison (1971, p. 1180) suggested that the oldest Catskill Delta clastics are preserved in the Needmore Shale.

Onesquethaw rocks were formed during a transgression of an epicontinental sea to the west and south from northeastern West Virginia and adjoining parts of adjacent states. In northeastern West Virginia early Onesquethaw rocks rest conformably on the Oriskany Sandstone. While in southern and western West Virginia an unconformity separates Onesquethaw rocks from the Oriskany or older rocks.

The Onondaga Limestone and the Huntersville Chert were formed in a carbonate shelf in the western and southern parts of the transgressing sea, while the calcitic gray shale and black shale that make up the Needmore Shale were formed in a shallow sea that laid between the carbonate shelf to the west and a rising land mass to the east. The clastic sediments in the Needmore Shale thicken to the east (Dennison, 1961, p. 18-25) and get coarser to the east indicating an eastern source area in the vicinity of the present continental shelf or Atlantic Coastal plain (Dennison, 1971, p. 1180).

The black shale in the Needmore Shale is called the Beaver Dam Member. This black shale is most common in the basal part of the Needmore Shale in a north-south belt that passes through northeastern West Virginia. In cross sections of Onesquethaw rocks in West Virginia, Dennison (1961) shows the Beaver Dam Black Shale Member intertonguing with carbonate and chert to the west and calcitic gray shale to the east. When we apply the model described earlier in this paper, the stratigraphic relations and the aerial distribution of the Beaver Dam Black Shale suggests that the black shale formed from organic rich mud that accumulated in relatively shallow water on the seaward side of a carbonate shelf in which lime mud and chert accumulated (Fig. 4). The black mud deposits graded eastward into deeper water prodelta calcareous mud deposits derived from an eastern source.

On cross sections Dennison (1961) shows Beaver Dam Black Shale above and within calcitic gray shale in the upper part of the Needmore Shale in west-central Virginia. He also shows calcitic gray shale of the Needmore Shale overlying the Onondaga Limestone in north-central West Virginia and a thin sandstone (Bob Ridge Sandstone Member) at the top of the Needmore Shale in southeastern West Virginia. The black shale in the upper part of the Needmore Shale in west-central Virginia and the Bob Ridge Sandstone in southeastern West Virginia may represent the development of relatively shallow water in this area as a result of the rate of sedimentation exceeding the rate of subsidence or the rise in sea level. The presence of calcitic gray shale of the Needmore Shale over the Onondaga Limestone in north-central West Virginia may indicate that sea level continued to rise (transgress) in this area and as a result prodelta sediments were deposited over the shallow-water carbonates (Fig. 5).

The Tioga Metabentonite, or its equivalents, marks the top of the Onesquethaw Stage. In eastern West Virginia the Tioga Metabentonite rests upon the Needmore Shale and it is overlain by the Marcellus Shale. In north-central West Virginia, New York, and Ohio the Tioga Metabentonite is reported to occur within the Onondaga Limestone or its equivalents (Dennison, 1961; Oliver and others, 1967, p. 1006-1007). The Marcellus Shale is a black shale with some thin limestone beds and concretions (Woodward, 1943, p. 311-316). The Marcellus is overlain by the Mahantango Formation which consists of gray to dark gray shale with interbedded gray siltstone and sandstone and locally some gray fossiliferous limestone that occurs as beds or nodular concretion zones. The Mahantango and Marcellus grade vertically and laterally one into the other. The Mahantango is thickest (about 600 feet) in the northeastern part of West Virginia, but thins to the south as a result of facies change and is not recognized in southeastern West Virginia. The gray shale, siltstone, and sandstone of the Mahantango give way to the south to black shale of the Marcellus (Dennison and Naegele, 1963, p. 15-16). Farther south the Marcellus passes into the lower part of the Millboro Shale in southwestern Virginia. The Marcellus and Mahantango in West Virginia are southern equivalents of the Hamilton Group in New York (Oliver and others, 1967, p. 1006-1007).

The Marcellus Shale and the Mahantango Formation are present in the subsurface of the northern and central parts of West Virginia. A preliminary examination of gamma-ray logs suggests that both formations are absent in southwestern West Virginia. In the subsurface the formations thin to the west, and in the western part of the state an unconformity separates the Mahantango Formation from the younger rocks that overlie it (Fig. 5).

The Marcellus Shale and the Mahantango Formation represent a continuation of the transgression

of the epicontinental sea that began during the Onesquethaw Stage. However, the rate of transgression either stopped or became very slow toward the end of the Onesquethaw Stage and early in the overlying Cazenovia Stage. As a result of the halt or slowing in the rate of transgression, the epicontinental sea became shallow throughout its extent and in the Cazenovia Stage the black muds that formed the Marcellus Shale were deposited in the shallow water present in the eastern part of the sea. A carbonate shelf that is today represented by the upper parts of the Onondaga Limestone and the Columbus and the Delaware Limestones existed in the western part of the sea.

During the Cazenovia Stage, the epicontinental sea became deeper as a result of renewed transgression, subsidence or a combination of transgression and subsidence. As the sea became deeper the sediments that formed the gray shale, siltstone and sandstone of the Mahantango Formation were carried into the epicontinental sea from a highland area rising along the eastern margin of the continent. During the early part of this transgression the principle clastic sediments carried into the West Virginia portion of the sea consisted of the mud that formed the shale in the lower part of the Mahantango Formation. As time progressed and the epicontinental sea became shallower in West Virginia, coarser sediments, silt and sand, were carried into the sea from the eastern highlands which had been rising during the transgression. These coarser sediments produced the interbedded shale, siltstone and sandstone present in the upper part of the Mahantango Formation.

Late in the Middle Devonian a regression of the sea from the interior of the continent occurred. This regression is represented by the unconformity at the top of the Mahantango Formation in western West Virginia, the unconformity separating the lower part of the Olentangy Shale from the upper part of the Olentangy Shale in central Ohio (Tillman, 1970; Gable, 1973), and the unconformity at the top of the Hamilton Group in southwestern New York (Rickard, 1964). Erosion during this regression may account for the absence of the Marcellus Shale and the Mahantango Formation in southwestern West Virginia, if indeed they are absent in this area. Apparently the sea did not completely drain from the Appalachian Basin for no unconformity is reported at this level in the eastern part of West Virginia.

Following this regression an epicontinental sea again began to transgress onto the craton. In the subsurface of north-central West Virginia the initial rock unit formed during this transgression was the Tully Limestone (Fig. 6). In south-western New York the Geneseo Shale overlaps the Tully Limestone to the west (Huddle, 1974, p. 516). A similar overlapping relation is present in the subsurface of north-western West Virginia. Here, the Harrell Shale, in part a southern equivalent of the Geneseo Shale, overlaps the Tully Limestone to the west. Stratigraphic relations between the Tully Limestone and the Harrell Shale are not clear cut in eastern West Virginia. Dennison and Naegele (1963, p. 17-18) report the occurrence of a thin zone of interbedded medium dark gray limestone and calcitic shale or limestone concretions in the middle part of the Harrell Shale in northeastern West Virginia. They tentatively correlate this zone of interbedded limestone and shale or concretions with the Tully Limestone. The Tully Limestone has not been positively identified in southeastern West Virginia.

The relations between the Tully Limestone and the Harrell Shale (Geneseo Shale to the north) appear to be similar to that between the Onondaga Limestone and the Marcellus Shale discussed above. Again, a carbonate shelf formed along the interior margin of an epicontinental sea. This carbonate shelf (Tully) passed seaward (eastward) into an area of black mud (Harrell) which accumulated in relatively shallow water. The presence of possible Tully Limestone equivalents within the Harrell Shale in northeastern West Virginia (Dennison and Naegele, 1963, p. 17-18) may represent continuous deposition in this area while the higher standing land to the west underwent erosion. As the sea continued to rise and transgress onto the craton, the relatively shallow water black mud facies moved inland (westward) and overlapped the carbonate shelf facies. With the rising sea level, prodelta sediments that now make up the Brallier Formation were deposited over the relatively shallow water black muds that formed the Harrell Shale (Fig. 7).

As the sea transgressed toward the interior of the craton an uplift (orogeny) occurred in the mountains along the continental margin. These mountains supplied the sediments that make up the Upper Devonian part of the Catskill Delta. The rising sea level and subsidence provided room for the accumulation of the delta and prodelta sediments.

Early in this transgression the water became relatively deep in eastern West Virginia. The mud and silt that formed the shales and siltstones of the Brallier Formation may have been carried into this deep water by turbidity currents flowing down slope from an eastern source area. During the deposition of the Brallier Formation the sea transgressed far to the east and the terrestrial and shallow water marine facies of the Catskill Delta were located near the rising land area to the east. At this time the epicontinental sea was also moving onto the craton to the west. Here, the initial

sediments deposited in the sea were shallow-water black and gray mud. These sediments formed the interbedded black and gray shale of the upper part of the Olentangy Shale in western West Virginia and adjacent states. As the transgression continued the water deepened in these western areas and deeper-water sediments (mud and turbidity current deposits) accumulated over the previously deposited shallow-water sediments.

In time the rate of transgression and subsidence decreased and the more shallow-water facies of the Catskill Delta complex began to prograde westward into eastern West Virginia, and the coarser sediments of the Greenland Gap Group ("Chemung") were deposited on the Brallier Formation. The sandstone and siltstone that make up the Benson Sand, a subsurface equivalent of the lower part of the Greenland Gap Group, present in the subsurface of north-central West Virginia are thought by Cheema (1977) to have been deposited by turbidity currents flowing down-slope from an eastern source area. As the sediments in the lower part of the Greenland Gap Group accumulated in eastern West Virginia the black mud facies that existed along the interior margin of the sea began to spread eastward toward the central parts of the sea as the water became progressively more shallow with the influx of sediments into the sea. These western black muds formed the Ohio Shale. Lower parts of the Ohio Shale extend eastward into southwestern West Virginia.

Variations in the rate of transgression and subsidence are reflected by the intertonguing relations between the Ohio Shale and equivalent gray shale and siltstone to the east, and the intertonguing of the gray shale and siltstone with sandstone of the Greenland Gap Group still farther east. As time went on during the Late Devonian the Catskill Delta began to build far out into the epicontinental sea toward the interior of the continent. In eastern and central West Virginia this prograding of the delta is reflected in the progressive average coarsing of the marine sediments upward through the Greenland Gap Group into the terrestrial deposits of the Hampshire Formation. To the west, prodelta sediments moved inland over the earlier deposited, relatively shallow water gray and black mud that accumulated along the interior margin as the sea transgressed onto the craton.

References Cited

Cheema, M. R., 1977, Sedimentation and gas production of the Upper Devonian Benson Sand in north-central West Virginia - a model for exogeosynclinal mid-fan turbidites off a delta complex: Univ. West Virginia Ph.D. disser. (unpub.), 116 p.

Cushing, H. P., Leverett, F., and Van Horn, F. R., 1931, Geology and mineral resources of the Cleveland district, Ohio: U.S. Geol. Survey Bull. 818, 138 p.

Dennison, J. M., 1961, Stratigraphy of Onesquethaw Stage of Devonian in West Virginia and bordering states: West Virginia Geol. and Econ. Survey Bull. 22, 87 p.

Dennison, J. M., 1963, Stratigraphy between Tioga metabentonite and Pocono Formation along Allegheny Front in Maryland and West Virginia, in Shepps, V. C., ed., Symposium on Middle and Upper Devonian Stratigraphy of Pennsylvania and adjacent states: Pennsylvania Topog. and Geol. Survey, Rept. G39, p. 213-227.

Dennison, J. M., 1970, Stratigraphic divisions of Upper Devonian Greenland Gap Group ("Chemung Formation") along Allegheny Front in West Virginia, Maryland, and Highland County, Virginia: Southeastern Geology, v. 12, p. 53-82.

Dennison, J. M., 1971, Petroleum related to Middle and Upper Devonian deltaic facies in central Appalachians: Am. Assoc. Petroleum Geologists Bull., v. 55, p. 1179-1193.

Dennison, J. M., and Naegele, O. D., 1963, Structure of Devonian strata along Allegheny Front from Corriganville, Maryland to Spruce Knob, West Virginia: West Virginia Geol. and Econ. Survey, Bull. 24, 42 p.

Gable, K., 1973, Conodonts and stratigraphy of the Olentangy Shale (Middle and Upper Devonian), central and southern Ohio: Ohio State Univ., M.S. thesis (unpub.), 90 p.

Heckel, P. H., 1969, Devonian Tully Limestone in Pennsylvania and comparison to type Tully Limestone in New York: Pennsylvania Topog. and Geol. Survey Inf. Circ. 60, 33 p.

Huddle, J. W., 1974, Middle/Upper Devonian conodont zonation in western New York (abs.): Geol. Soc. America abstracts with Programs, v. 6, p. 516.

Johnson, J. G., 1971, Timing and coordination of orogenic, epirogenic, and eustatic events: Geol. Soc. America Bull., v. 82, p. 3263-3298.

King, P. B., 1959, The evolution of North America: Princeton Univ. Press, Princeton, New Jersey, 189 p.

Lewis, T. L., and Schwietering, J. F., 1971, Distribution of the Cleveland Black Shale in Ohio: Geol. Soc. America Bull., v. 82, p. 3477-3482.

Oliver, W. A., Jr., de Witt, W., Jr., Dennison, J. M., Hoskins, D. M., and Huddle, J. W., 1967, Devonian of the Appalachian Basin, United States, in Oswald, D. H., ed., International symposium on the Devonian System: Alberta Soc. Petroleum Geologists, Calgary, Alberta, v. I., p. 1001-1040.

Pepper, J. F., de Witt, W., Jr., and Demarest, D. F., 1954, Geology of the Bedford Shale and Berea Sandstone in the Appalachian Basin: U.S. Geol. Survey Prof. Paper 259, 111 p.

Rickard, L. V., 1964, Correlation of the Devonian rocks in New York State: New York State Mus. and Sci. Service Geol. Survey Map and Chart Ser., no. 4.

Tillman, J. R., 1970, The age, stratigraphic relationships, and correlation of the lower part of the Olentangy Shale of central Ohio: Ohio Jour. Sci., v. 70, p. 202-217.

Woodword, H. P., 1943, Devonian System of West Virginia: West Virginia Geol. and Econ. Survey, v. 15, 655 p.

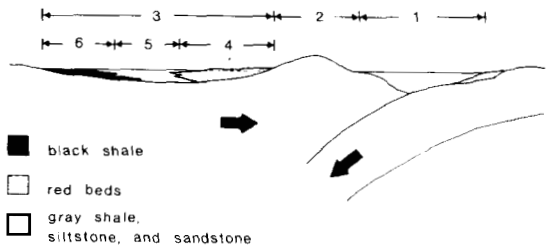

Figure 1 Diagram showing 1) closing ocean, 2) mountains along continental margin, 3) epicontinental sea, 4) delta facies, 5) prodelta facies, and 6) black mud facies.

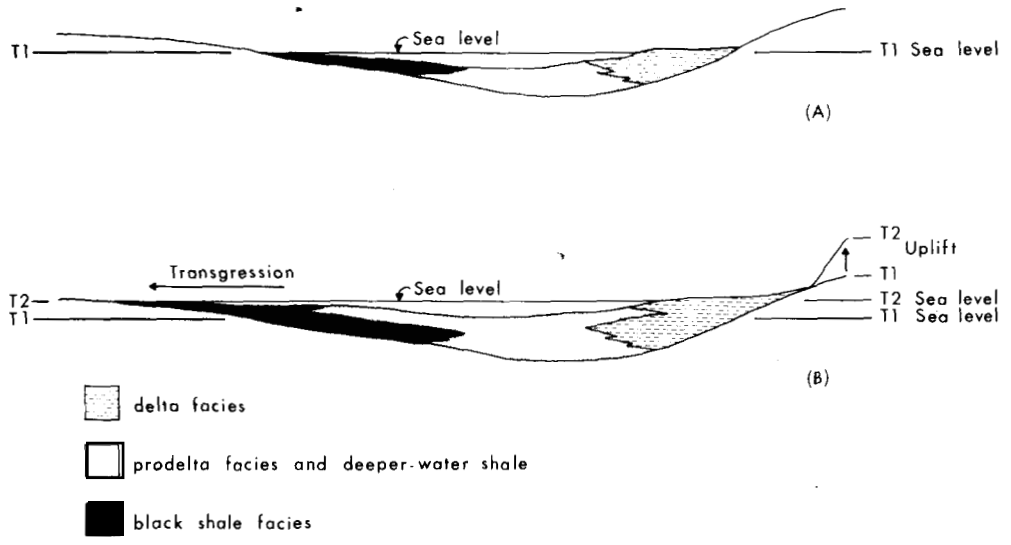

Figure 2 Diagram showing lateral movement of facies during a transgression of an epicontinental sea.

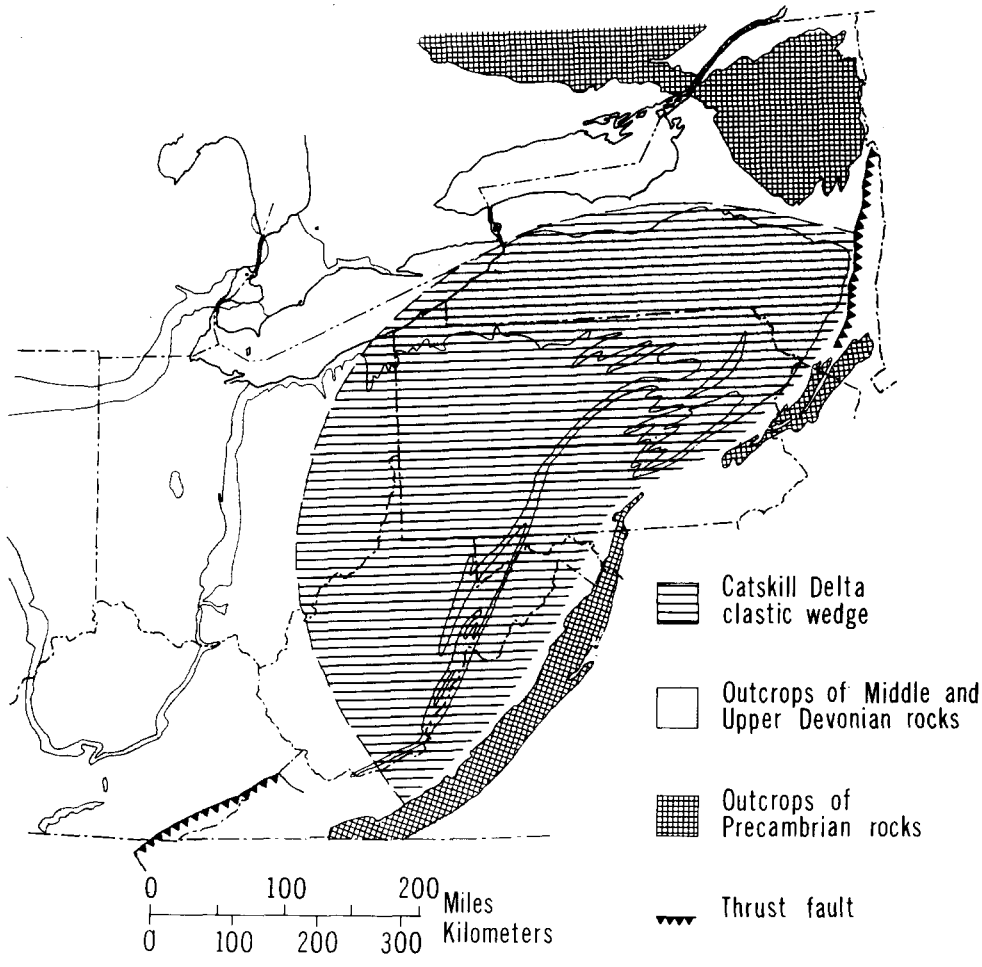

Figure 3 Map of Appalachian Basin and surrounding areas showing outcrops of Middle and Upper Devonian rocks around the perimeter of the basin and the location of the Catskill Delta clastic wedge.

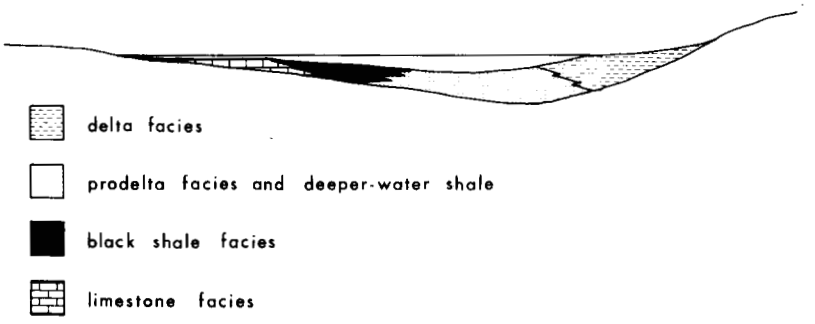

Figure 4 Diagram showing a possible distribution of facies in an epicontinental sea with a carbonate shelf along interior margin of sea.

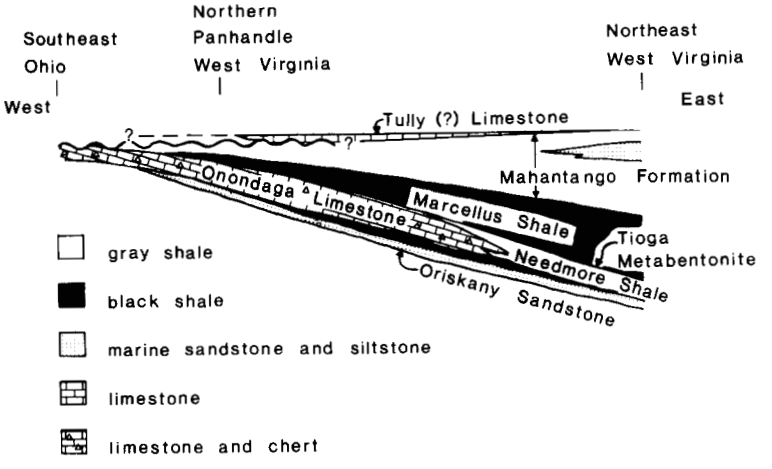

Figure 5 Diagramatic east-west cross section of Middle Devonian rocks in northern West Virginia. Diagram is not to scale.

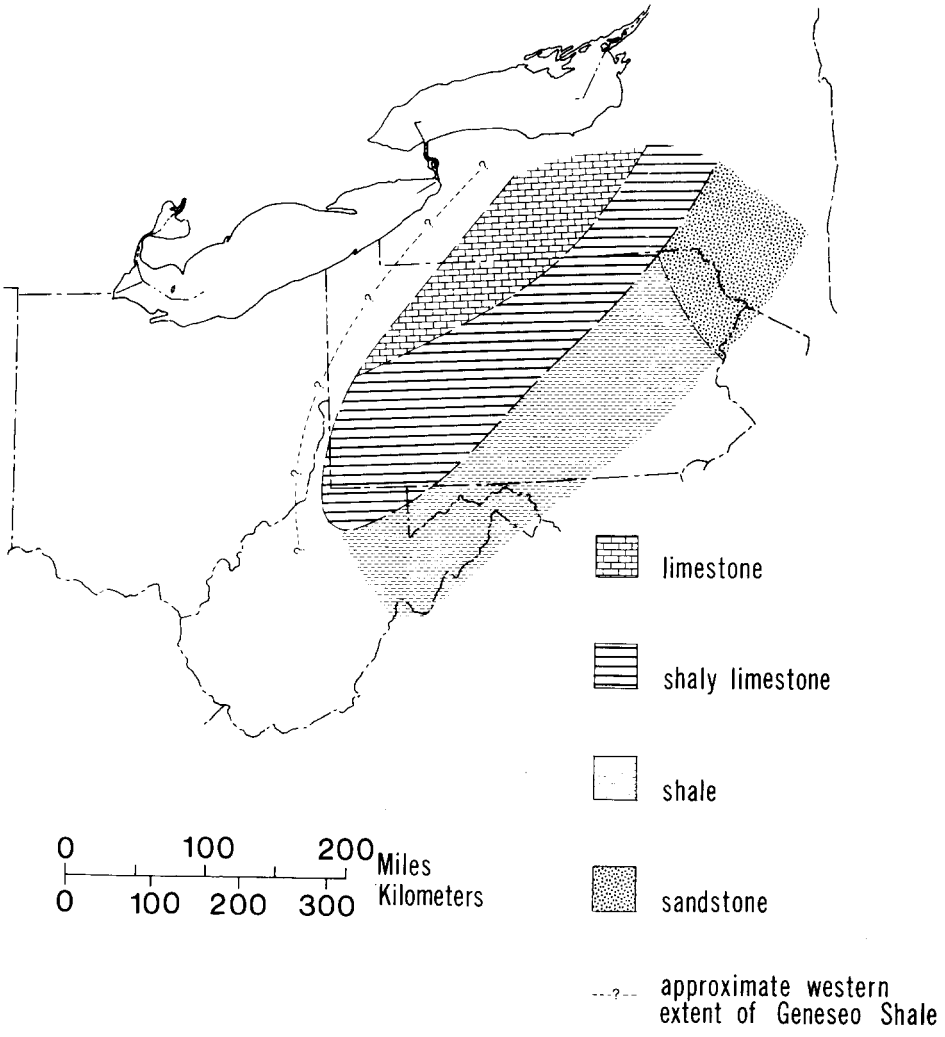

Figure 6 Map showing the distribution of facies in the Tully Limestone and its clastic equivalents and the approximate western extent of the Geneseo Shale and its equivalents. (Modified from Heckel, 1969, fig. 4, p. 22.)

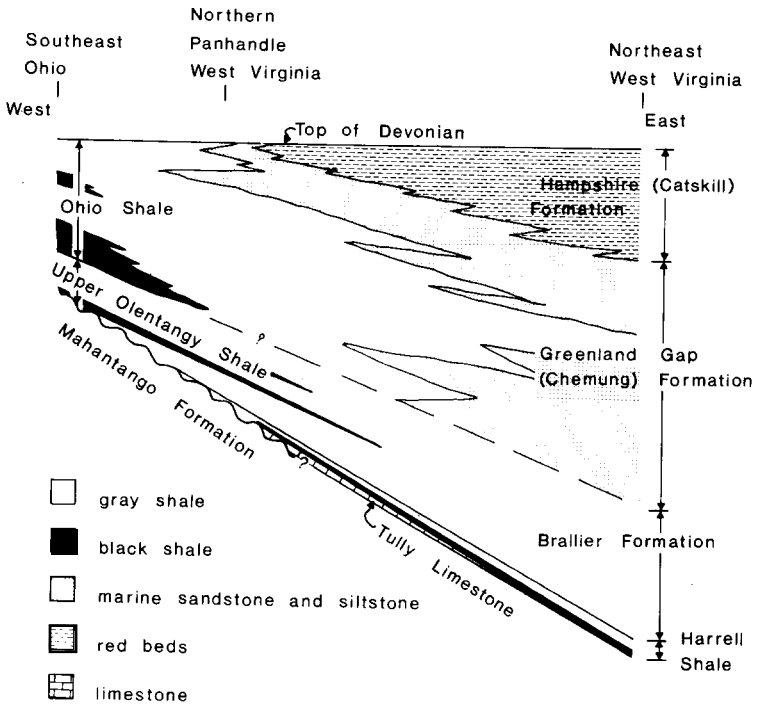

Figure 7 Diagramatic east-west cross section of Upper Devonain rocks in northern West Virginia. Diagram is not to scale.

PHYSICOCHEMICAL CHARACTERIZATION OF DEVONIAN GAS SHALE

R. E. Zielinski, A. Attalla, E. Stacy, B. D. Craft, and R. L. Wise
Monsanto Research Corporation*
Mound Facility
Miamisburg, Ohio 45342

ABSTRACT

Several physicochemical analyses are being performed to better characterize the Devonian gas shales located in the Appalachian and Illinois Basins. The results of these analysis are being integrated with the geochemical analyses to present an accurate characterization of the Devonian shales and to accurately assess their resource potential.

These studies are also providing data that are being used to evaluate the physical behavior of the shales.

*Mound Facility is operated for the U. S. Department of Energy by Monsanto Research Corporation (Contract No. EY-76-C-04-0053).

INTRODUCTION

Core samples from seven wells drilled in Illinois, Indiana, Kentucky, and Virginia have been analyzed by various physicochemical methods for the purpose of characterizing their basic structure.

Clay mineralogy, detailed kerogen assessment, pulsed NMR, dilatometry, mass spectrometry, and mechanical testing will be discussed in this paper; however, Scanning Electron Microscopy, Energy Dispersive X-Ray Analysis, and Secondary Ion Mass Spectrometry have also been used to better characterize the basic nature of the Devonian shales. Some of these analyses such as clay mineralogy and detailed kerogen assessment are directly related to the geochemical analyses, while others such as the mechanical testing and dilatometry are used primarily to characterize the physical nature of the shales and indirectly are related to the geochemistry of the shales.

The location of the seven wells is displayed in Figure 1. In most cases, the entire stratigraphic unit of Devonian shale was cored. Samples for the physicochemical analyses were taken at 30-foot intervals and stored in air tight metal containers. Shortly after arrival at the laboratory, the containers' air space was sampled either by gas chromatography or mass spectrometry. The container was opened, and the subsequent analyses were performed.

DISCUSSION AND RESULTS

Detailed Kerogen Analysis

Detailed elemental analysis of the kerogen material from the wells is currently being performed. This analysis determines the specific carbon, hydrogen, nitrogen, and oxygen content of the sample. The analytical results are used to confirm the basic structure of the kerogen and can also be used to assess the hydrocarbon potential of the material.

The results of the samples from the O-1, I-1, and KY-2 wells are shown in Figure 2, which is a plot of the Atomic H/C versus Atomic O/C. In Figure 2, Line A indicates the trend of the algal kerogens from the Green River oil shales, etc. Kerogens which produce large quantities of oil and then thermally derived gas; essentially, what would be considered the amorphous types. Line B indicates the trend of kerogens of intermediate composition. These possess the qualities of a good source rock and are essentially the herbaceous type. Line C indicates the trend of kerogens consisting of debris of higher vegetation and organic matter of terestrial origin. These kerogens produce primarily thermally derived methane and are composed of the wood-coaly type. The samples from the three wells essentially cluster around Line B.

Using the elemental composition of the kerogen, it is possible to calculate the gross heating values of the shale cores. Average values per well are listed in Table 1. The first value listed assumes that no organic sulfur is present. This assumption should be fairly accurate, since organic sulfur was detected in only one of our extraction samples. However, since specific organic sulfur determinations have not yet been performed on the samples, a second set of values was calculated assuming the 2% organic sulfur concentration that is generally accepted for the New Albany shales. As can be seen from the calculated values, the 2% sulfur increases the gross heating value by approximately 100 cal/g. In reality, though, it is felt that based upon the experimental data already accumulated, the actual values would be closer to the lower numbers and generally agree with those obtained by John Ward Smith[1].

Clay Mineralogy

Core samples from four wells were analyzed for clay mineral content. The shales were obtained from Devonian intervals in the I-1 Well, the P-1 Well, the KY-2 Well, and the VA-1 Well.

Three patterns were made for each sample: untreated, ethylene glycol, 300°C. Illite, mixed-layer illite-montmorillonite, chlorite, and kaolinite are present. Minor amounts of siderite, dolomite, and feldspar are present in some samples. Kaolinite is present in minor amounts only in well KY-2. This may be due to a difference in source material or to the shallow depth of burial

(low temperature). In KY-2, kaolinite decreases with depth; however, the mixed-layer clay tends to increase, suggesting these trends are depositional. In VA-1, the mixed layer clay decreases with depth as the illite content increases. This may be due to burial diagenesis as the sharpness ratio increases and the crystallinity index decreases with depth. As the illite peaks become narrower (due to increased crystallinity, increased grain size or loss of expanded layers) the sharpness ratio $\left(\text{S.R.} = \frac{10\text{Å}}{10.5\text{Å}}\right)$ increases and the crystallinity index (C.I. = peak width at half-height in mm) decreases.

Regionally the clay mineral suite is relatively uniform except for the kaolinite in KY-2 and a relatively low mixed-layer value for I-1. The average values are as follows:

	Illite	Mixed-Layer	Chlorite	Kaolinite
I-1	74	12	14	
P-1	70	20	10	
KY-2	69	21	7.5	2.5
VA-1	73	19	8	

The data are too limited to make any stratigraphic interpretation at this time.

The S.R. for VA-1 averages 4.01 and for KY-2 averages 4.28. The C.I. values average 1.82 and 1.65 respectively. The differences are probably not statistically significant. The P-1 samples have a higher S.R. (5.15) and lower C.I. (1.5) than those from VA-1 and KY-2. I-1 has a lower S.R. (3.34) and a similar C.I. (1.68). Though the values are too few to be significant, the date indicate the P-1 samples have probably been exposed to higher temperatures than those in the other three wells.

The amount of mixed-layer clay is calculated using the height of the 10Å peak of the ethylene glycol treated sample and the 10Å peak of the sample heated to 300°C. The increase in peak height after heating is assumed to be due to the collapse of expanded layers in the mixed-layer clay. In the untreated samples, the mixed-layer peak occurs as a shoulder on the low angle side of the 10Å illite peak. Its apex appears to be in the range of 10.5 to 11Å or less; on glycolation there is little change in the peak position. The mixed-layer clay apparently contains 10 to 20% expanded layers.

The presence of this mixed layer clay suggests the shale has not been heated to temperatures higher than 200 to 250°C. If sufficient potassium is available, the mixed-layer phase should convert to illite at 200 to 250°C. If the mixed layer (4:1) clay originally had a higher content of expanded layers, it has probably been exposed to temperatures higher than approximately 100°C. Unfortunately, little is known about the effects of time on clay diagenesis. Time should tend to lower both the temperature values given above.

Figure 3 is a plot of 10Å peak height vs. percent organic carbon. As expected, there is a good inverse linear relation for most samples. At this time, there is no apparent reason why five samples fall off the trend. The samples from well I-1 were not plotted as they were run on a different x-ray machine, and the intensities are not comparable.

Figure 4 contains plots showing the relation of the C.I. and percent mixed-layer clay with depth in KY-2. There is a large amount of scatter. The mixed-layer content appears to increase and the crystallinity decrease (C.I. increase) with depth. The interval is so short and the depth so shallow that major diagenetic effects are not apparent. Figure 5 contains a plot of the sharpness ratio vs. depth for KY-2. Also shown is a three point moving average plot of the S.R. values. The S.R. appears to decrease slightly with depth.

Figure 6 shows the results of the present study in contrast with Weaver's[2] estimate of the clay mineral composition in North America versus time.

This study is still in progress and should identify , as more data becomes available, the the quantitative relationship between burial diagenesis of clay minerals and the hydrocarbon generation.

Pulsed NMR

The main purpose of the pulsed nuclear magnetic resonance (NMR) study of Eastern Gas Shales is the development of a rapid, nondestructive, determination of their fuel content. This analytical method is base on the fact that the initial amplitude of the pulsed NMR free induction decay (FID) signal is directly proportional to the number of atoms of a particular element or isotope of an element in the sample.

Proton pulsed NMR of shale yields the total hydrogen content of the shale. Any component of shale containing hydrogen will contribute to the free induction decay signal of proton pulsed NMR. Thus, hydrogen bonded to carbon atoms in the organic species, water hydrogen, and other inorganic hydrogen will contribute to the total NMR signal. Based on the assumption that for a given type of shale the water content is constant, then the pulsed NMR signal should be directly proportional to the oil yield or organic content of the shale. Oil yield is obtained along with total gas effluent directly from the Material Balance Assay of the shale. Organic carbon is obtained from wet chemistry and elemental analysis. Correlation coefficients of 0.9395, 0.9156, and 0.8852 were obtained for the oil yield, organic carbon, and total gas effluent as a function of total hydrogen conent by pulsed NMR (Figures 7-9). Oil yield possibly correlated better than the organic carbon, and the total gas effluent because of the greater concentration of hydrogen in oil than in organic carbon or gas effluent. Inorganic gases containing no hydrogen constitute much of the effluent gas.

Dilatometry

To determine the effects of fracturing and drilling fluids on the shale, test specimens are being core drilled from large samples using an air cooled diamond core drill. The specimens are restrained under load (∿112 psi) in the axial direction, and they are placed in intimate contact with the fracturing fluid. The linear expansion is measured by means of an LVDT (Linear Variable Differential Transducer), which has been calibrated over the full range needed for these experiments.

The output signal from the LVDT is amplified and continuously recorded and converted to a digital signal, which can be used to monitor linear displacement as a function of time.

Typical results from this experiment are presented in Figure 10. Currently, only samples from the KY-2 well are being tested; however, testing on samples from the other wells will be initiated shortly. As the results indicate, samples exposed to water exhibit the greatest expansion, and those exposed to kerosene exhibit the least amount of expansion. The unexpected result was that the shale exposed to Water and 30% Methanol and 2% KCℓ expanded more than the shale exposed to only Water and 2% KCℓ.

The basic clay composition of the shale is illite which adsorbs water when an imbalance occurs between the concentration of ions held at the clay surface and the solute content of the contacting liquid.[3] The degree of hydration can theoretically be controlled by reducing the amount of water base and increasing the electrolyte content of the fluid. The fluid with the KCℓ addition should inhibit swelling by increasing the ionic level. The fluid with the KCℓ and Methanol additions should further inhibit swelling by slowing down water transfer. Since the KCℓ and Methanol additions have not inhibited swelling as much as the KCℓ addition above , additional studies are being performed in an attempt to identify this anomaly which has been consistent in all the KY-2 samples tested to date.

One of the first follow-up studies which was performed was an examination of the residue which settled out during testing. Figure 11 shows typical results from this investigation. Figure 11A is the normal secondary image of the residue. Figure 11B shows the x-ray map for potassium, and Figure 11C shows the x-ray map for chlorine. A comparison of these two maps shows some mismatches in concentration. When a x-ray map was generated for sulfur (Figure 11D) the pattern matched that

of the chlorine mismatch, indicating a sulfur-chlorine combination, a corresponding x-ray map for iron explained the potassium mismatch. These results indicate that a possible reaction is occurring with the pyrite which is present in the sample and perhaps this reaction affects the swelling characteristics of the shale. This type of elemental combination was not observed in the Water and 2% KCl residue. This has been the first post-test difference noted between the samples, and it has been consistent in the samples examined to date. To verify the effects of pyrite on the fluids and ultimately the swelling characteristics, additional studies will be performed on samples with various levels of pyrite concentrations.

Mass Spectrometry

Prior to the use of the shale core samples for the various tests, the sealed container is opened in a special test fixture. The composition of the gases in the sealed container are determined by mass spectrometry, and the internal pressure of the container is monitored by means of an automatic pressure recording device. Contrasting results for the various wells are shown in Table 2. The hydrocarbon results are supportative of the gas chromatography results and serve as verification data. The nitrogen-oxygen results are somewhat perplexing. The ratio of these gases (O_2/N_2) for normal air is approximately 0.27. An examination of the results, however, shows that this ratio is not always present in the container upon opening. One of the first explanations for these types of results would be oxidation of the interior walls of the containers, but this effect has not been observed when the containers are examined after opening. The next most logical explanation is the oxidation of the shale core. This is a somewhat feasible explanation because as the oxygen concentration decreases, the CO_2 concentration increases. To verify this result, several continuous monitoring tests have been performed. The results for two of these tests are graphically presented in Figure 12. In this figure, the initial compositions of the gas in the container is zeroed out and the mole % changes of CH_4, O_2, and CO_2 are monitored as a function of time. For Sample KY-2-48, it appeared that the depletion of oxygen occurred at a much faster rate than the in-growth of CO_2. For Sample KY-2-56, the depletion of oxygen appeared to be mirrored by the in-growth of CO_2. The basic difference between these two samples is that the kerogen content of KY-2-48 was woody-coaly, while that of KY-2-56 was herbacious. This can account for some difference in the oxygen depletion rate as the oxidation potential of woody-coaly material should be higher than that for herbaceous material. Other differences might become obvious as the samples are subjected to detailed analysis.

The mass spectrometry results in general do indicate that in certain instances oxygen is depleted from the cover gas and oxidation of carbonaceous material is one of the processes that is occurring. As more detailed analyses become available from the samples, it should be possible to explain why some samples preferentially suffer depleted oxygen levels in the cover gas.

Mechanical Testing

Mechanical tests are being performed on the shales to predict their mechanical behaviour and to correlate this behavior to the basic characteristics (geochemical, inorganic composition, etc.) of the shale.

The mechanical testing equipment is shown in Figure 13. The test specimens are prepared in a helium atmosphere and are coated with an impervious coating prior to testing. As the test progresses and cracks are generated in the specimen, the gas released from these new surfaces are characterized using the quadrupole mass spectrometer and the pressure monitoring equipment. This experimental setup permits not only the recording of the breaking strength of the material but it also identifies the gases released from the sample during test and permits the calculation of gas release rate per surface area generated.

Table 3 lists some of the results obtained to date on the mechanical test specimens. Table 4 lists typical permeation reates determined on mechanically tested specimens. The breaking strength is in the range which was expected for the shale samples; however, our data base is not large enough at this time to make valid comparisons between these data and the other characterization data available on the shale samples.

One of the extensions of the mechanical testing experiments is the determination of the effects of moisture on the mechanical properties. Table 5 lists two of the results from this study. Both samples were exposed to air at two different relative humidities for six weeks prior to test. In the case of the sample exposed to 44.4% relative humidity, there was approximately no change in its mechanical strength; however, exposure to 100% relative humidity resulted in an approximate reduction of 42% in breaking strength. This sequence of testing is currently continuing with samples exposed to 25 and 75% relative humidity also scheduled for testing. Samples are also being maintained in contact with the other fluids examined in the dilatometry study to determine the effects of these fluids on the mechanical properties of the shale.

CONCLUSION

The results of these studies are expanding the data base for Devonian gas shales. Some of the work such as the clay mineralogy and its integration with the geochemical study can only help to expand our knowledge of paleozoic shales, which at the current time is very scant. Some of the other studies such as mass spectrometry serve to verify the results of associated analysis, but they also indicate some unusual characteristics of the shale such as the oxygen depletion occurrance. The dilatometry study is perhaps indicating that variables such as pyrite concentrations can have significant effects on the behavior of the shales.

Since the study has been initiated, several correlations with other data have been made, several unexpected observations have been noted, and our data base on the Devonian shales and their fuel resources has expanded. As more data become available and they are integrated into the data base, an accurate characterization of both the Devonian shales and their fuel resources should evolve.

REFERENCES

1. Smith, John Ward and Young, Neil B., "Organic Composition of Kentucky's New Albany Shale: Determination and Uses," Chem. Geol., 2, 157-170, 1967.

2. Weaver, C.E., "Potassium, Illite and the Ocean," Geochim et Cosmochim. Acta, 31, 2181-2196, 1967.

3. O'Brien, D. E. and Chenevert, M.E., "Stabilizing Sensitive Shales with Inhibited, Potassium-Based Drilling Fluids," J. Pet. Tech., 1089-1100, September, 1973.

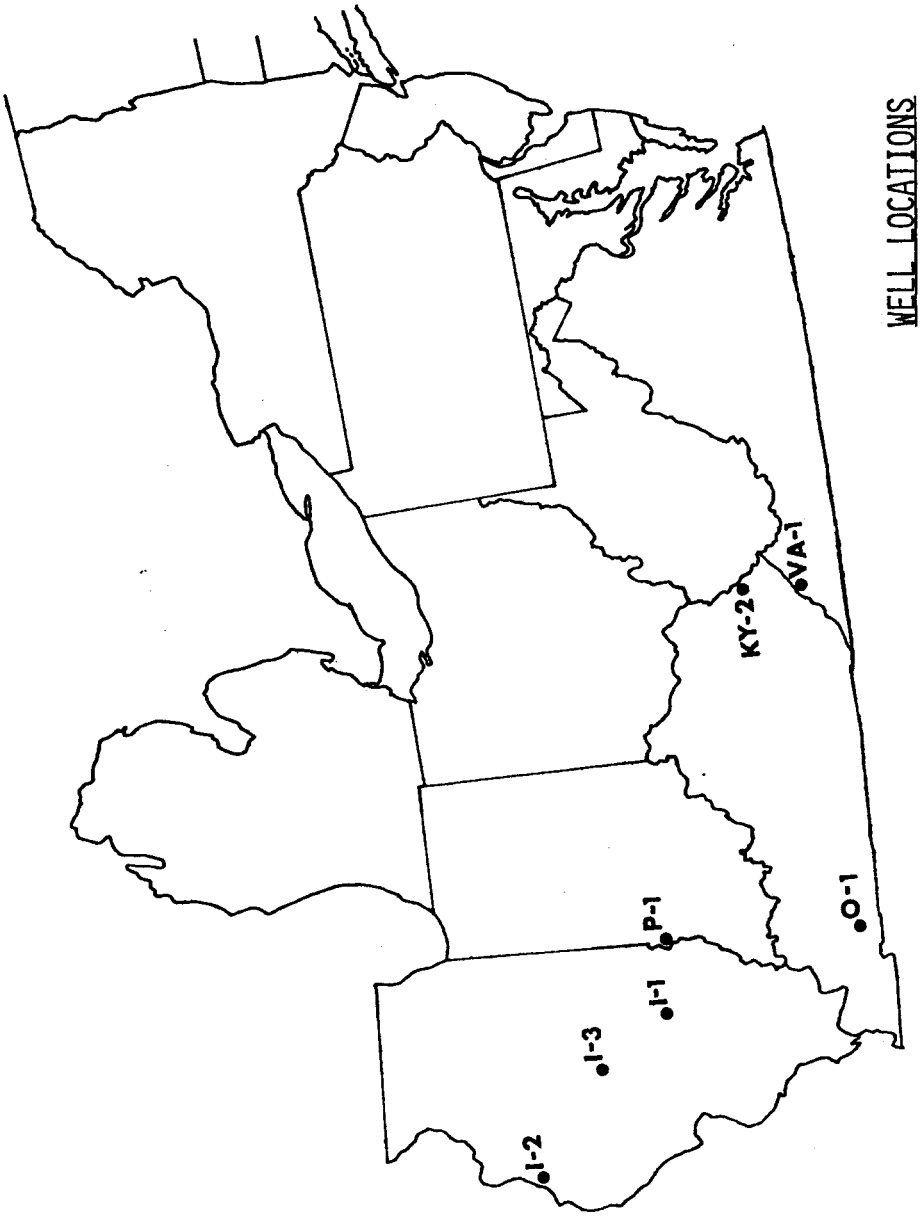

WELL LOCATIONS

I-1: Effingham County, Illinois
I-2: Henderson County, Illinois
I-3: Tazewell County, Illinois
KY-2: Martin County, Kentucky
O-1: Christian County, Kentucky
P-1: Sullivan County, Indiana
VA-1: Wise County, Virginia

FIGURE 1

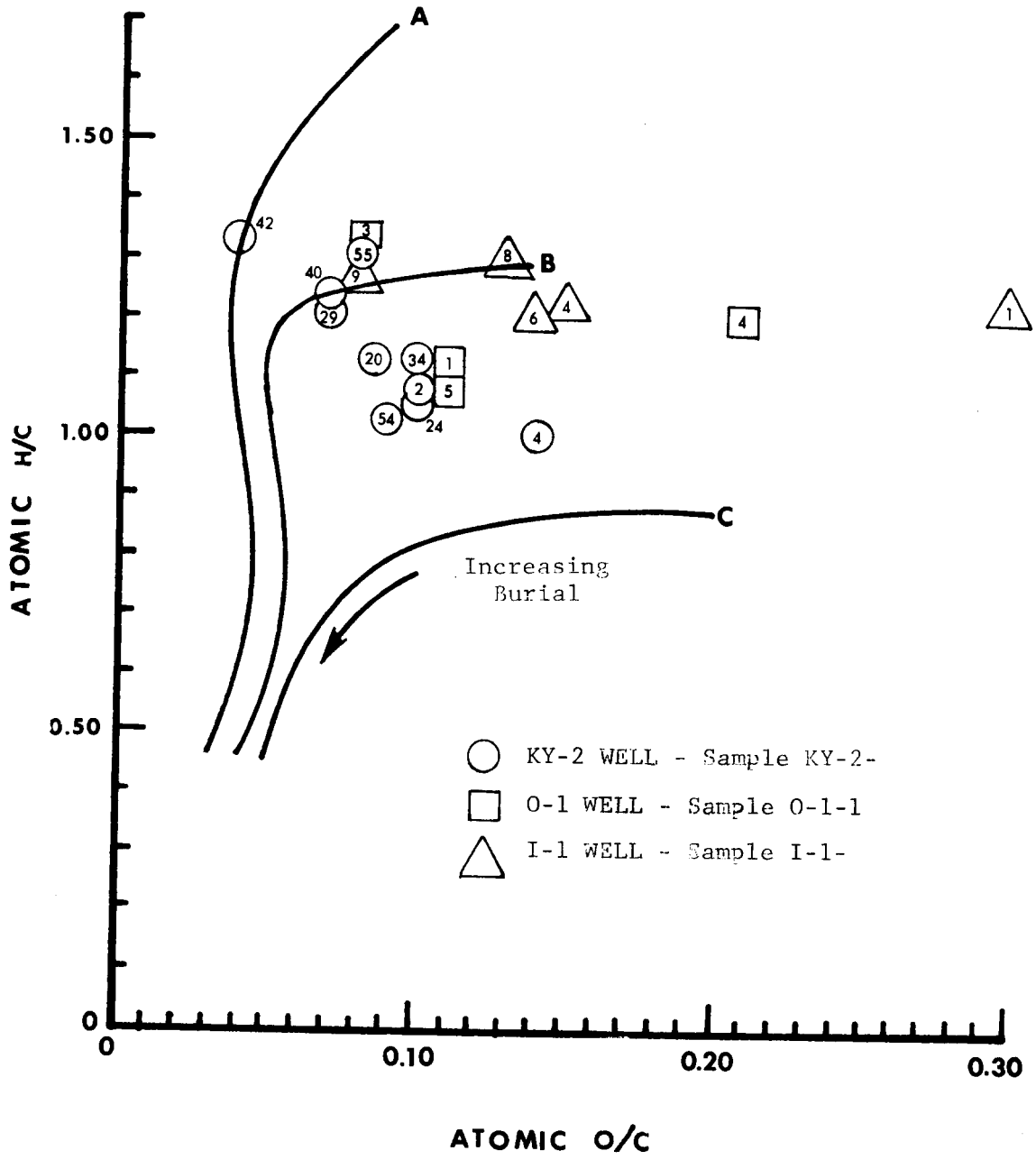

—FIGURE 2: KEROGEN COMPOSITION—

TABLE 1

CALCULATED* GROSS HEATING VALUES
BASED UPON THE KEROGEN COMPOSITION

WELL	GROSS HEATING VALUE 1* cal/g	GROSS HEATING VALUE 2** cal/g
KY-2	8256.92	8359.92
O-1	8232.08	8335.08
I-1	8093.76	8196.76

*Gross heating value (cal/g) = 8,400(C) + 27,765(H) + 1,500(N) + 2,500(S) - 2,650(O).

**Determined by assuming 2% sulfur and modifying the oxygen value. {New Oxygen Value = (Determined Value - 2%.)}

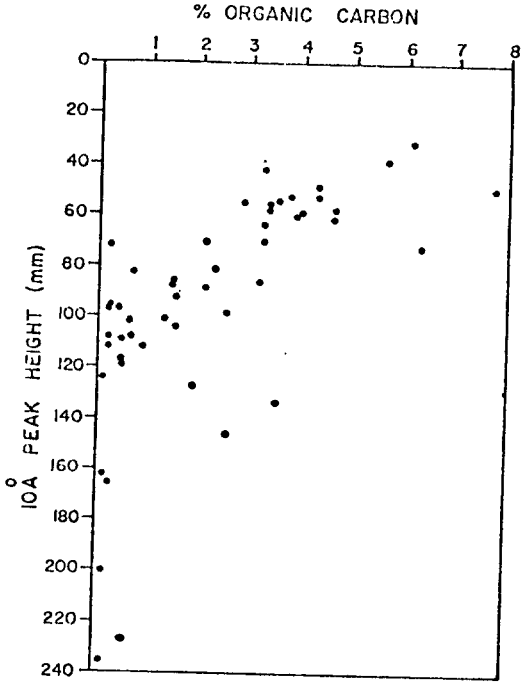
% ORGANIC CARBON
1
2
3
4
5
6
7
8
0
20
40
60
80
100
120
140
160
180
200
220
240
10Å PEAK HEIGHT (mm)

FIGURE 3

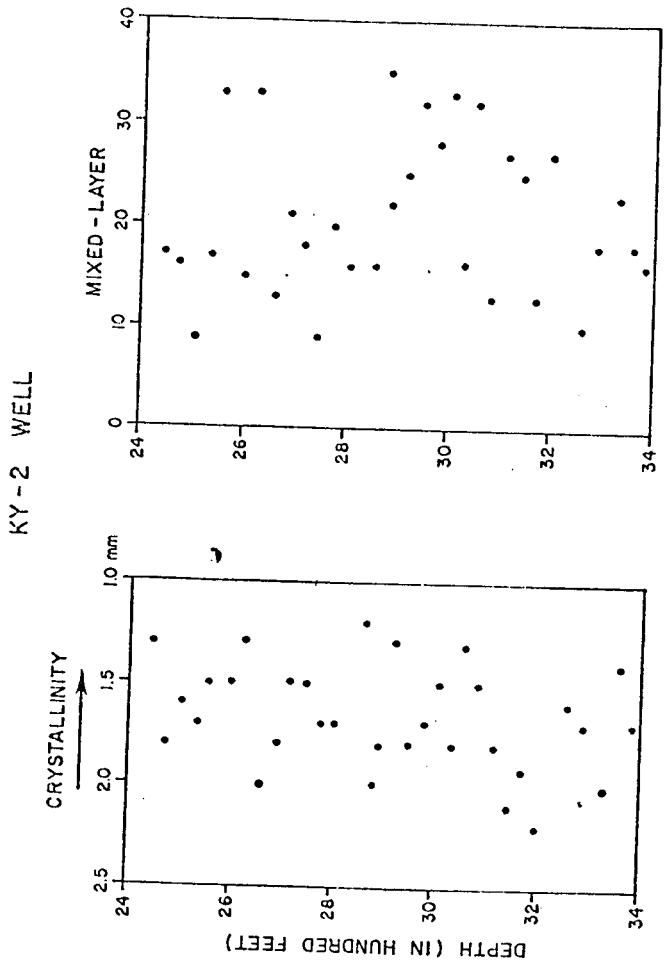
KY-2 WELL
MIXED-LAYER
0
10
20
30
40
CRYSTALLINITY
1.0 mm
1.5
2.0
2.5
24
26
28
30
32
34
DEPTH (IN HUNDRED FEET)

FIGURE 4

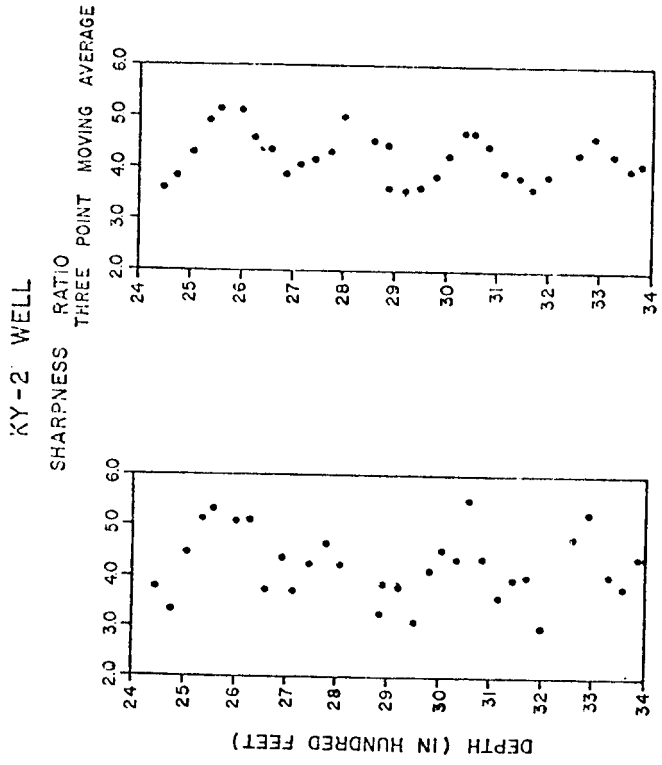
KY-2 WELL
SHARPNESS RATIO
THREE POINT MOVING AVERAGE
2.0
3.0
4.0
5.0
6.0
24
25
26
27
28
29
30
31
32
33
34
DEPTH (IN HUNDRED FEET)

FIGURE 5

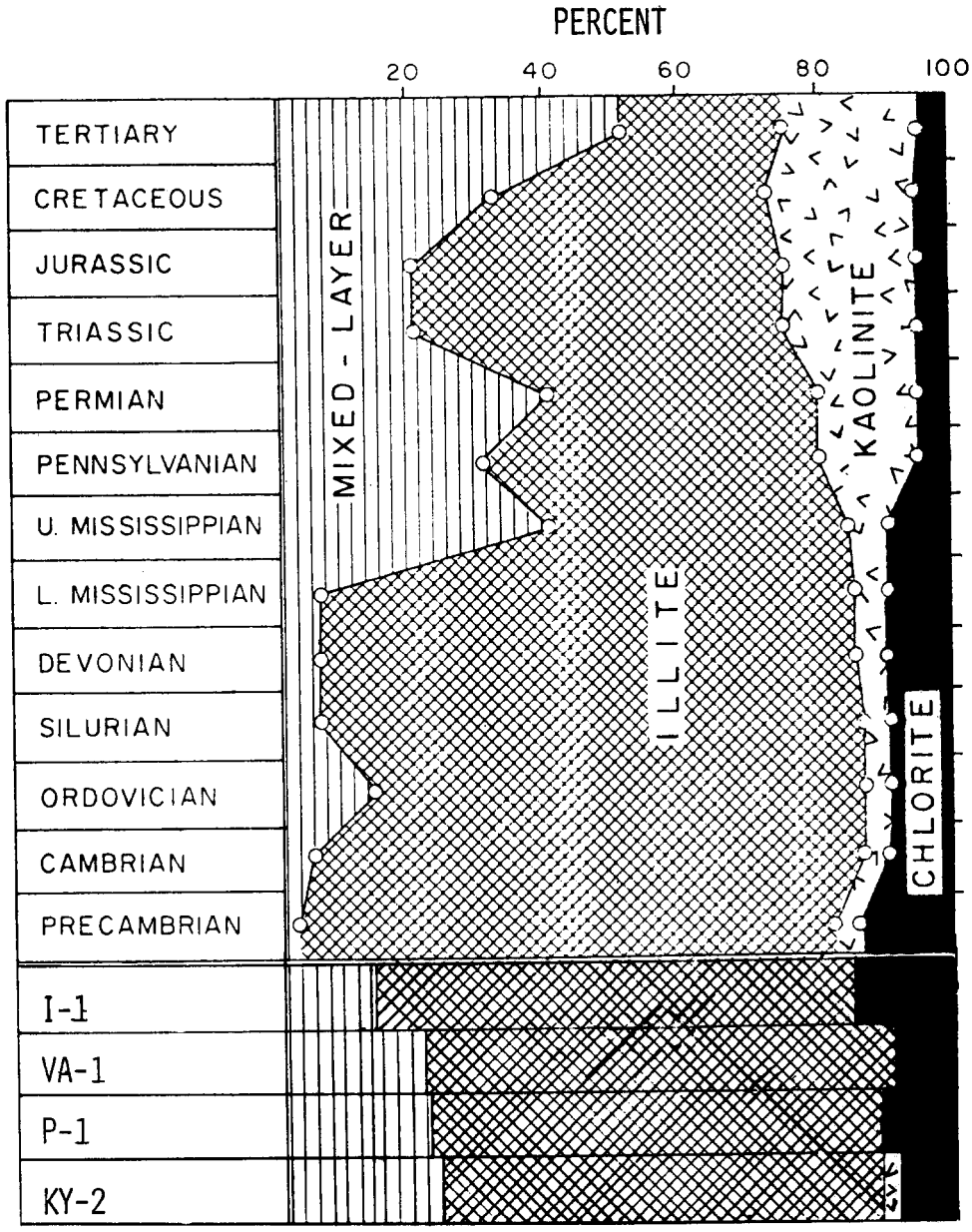

CLAY MINERALOGY RESULTS

FIGURE 6

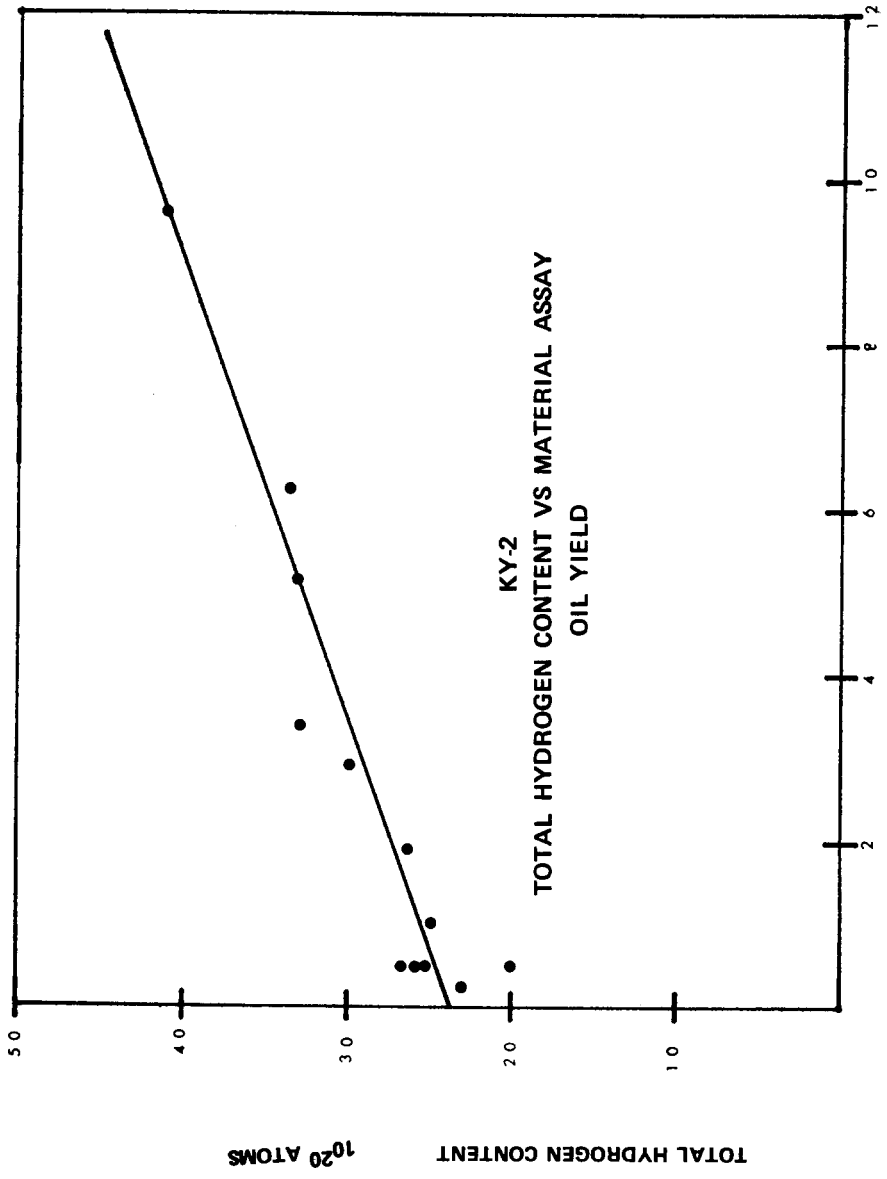
KY-2
TOTAL HYDROGEN CONTENT VS MATERIAL ASSAY
OIL YIELD
OIL YIELD, (GAL/TON)
2
4
6
8
10
12
TOTAL HYDROGEN CONTENT
10^20 ATOMS
10
20
30
40
50

FIGURE 7

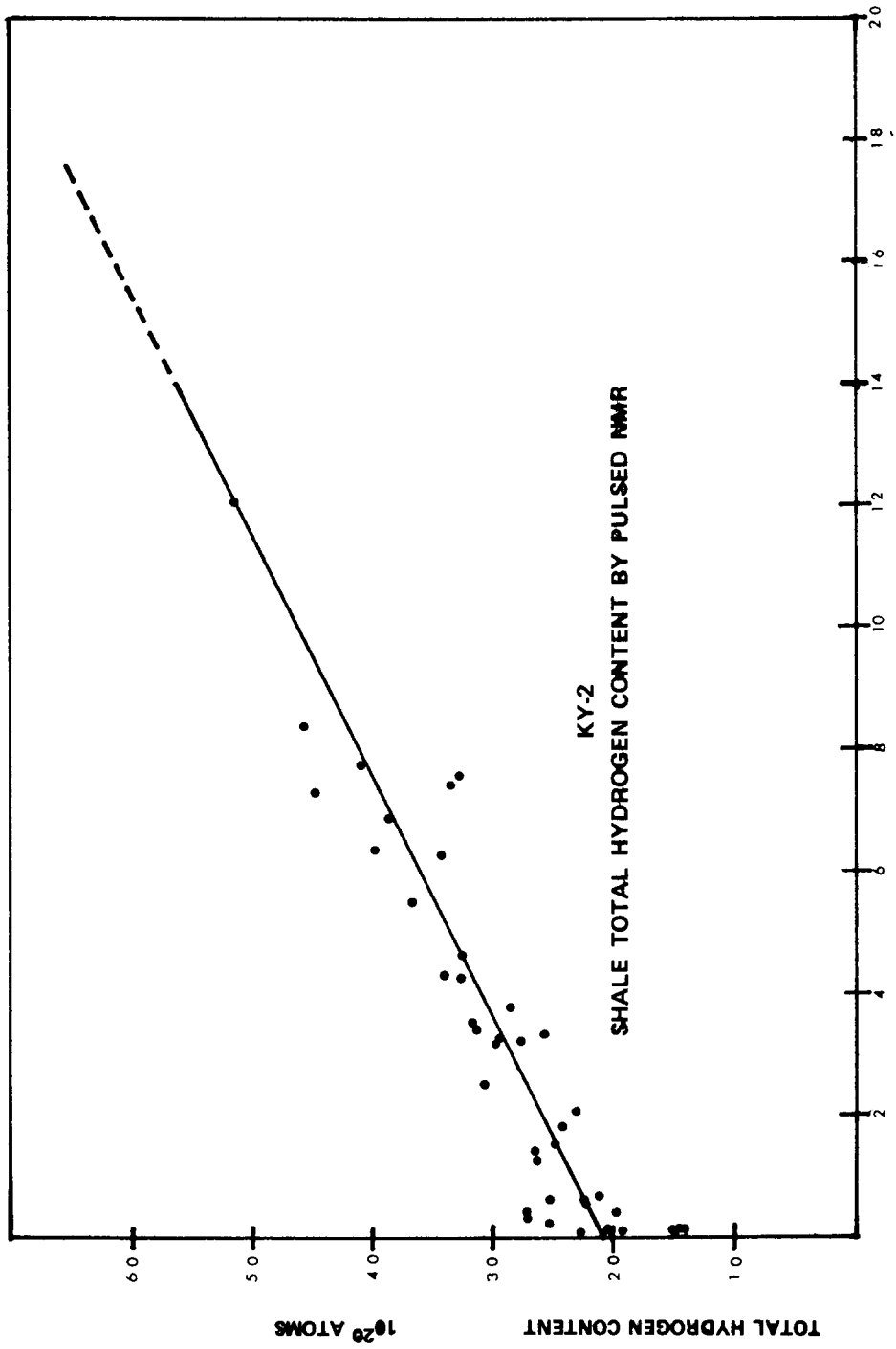
KY-2
SHALE TOTAL HYDROGEN CONTENT BY PULSED NMR
TOTAL HYDROGEN CONTENT
10^{20} ATOMS
ORGANIC CARBON, WT %

FIGURE 8

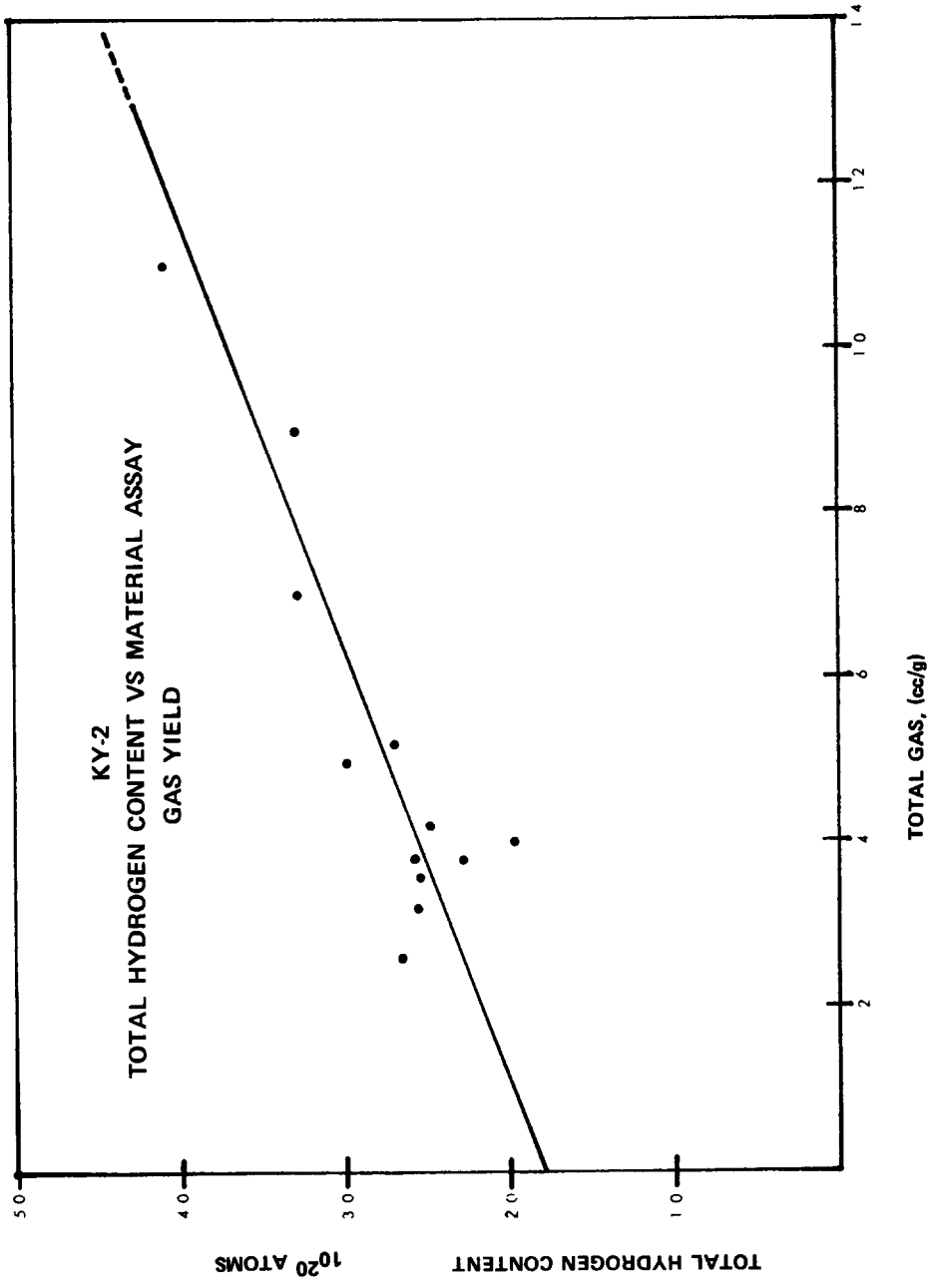
KY-2
TOTAL HYDROGEN CONTENT VS MATERIAL ASSAY
GAS YIELD
TOTAL HYDROGEN CONTENT
10^{20} ATOMS
TOTAL GAS, (cc/g)
50
40
30
20
10
2
4
6
8
10
12
14

FIGURE 9

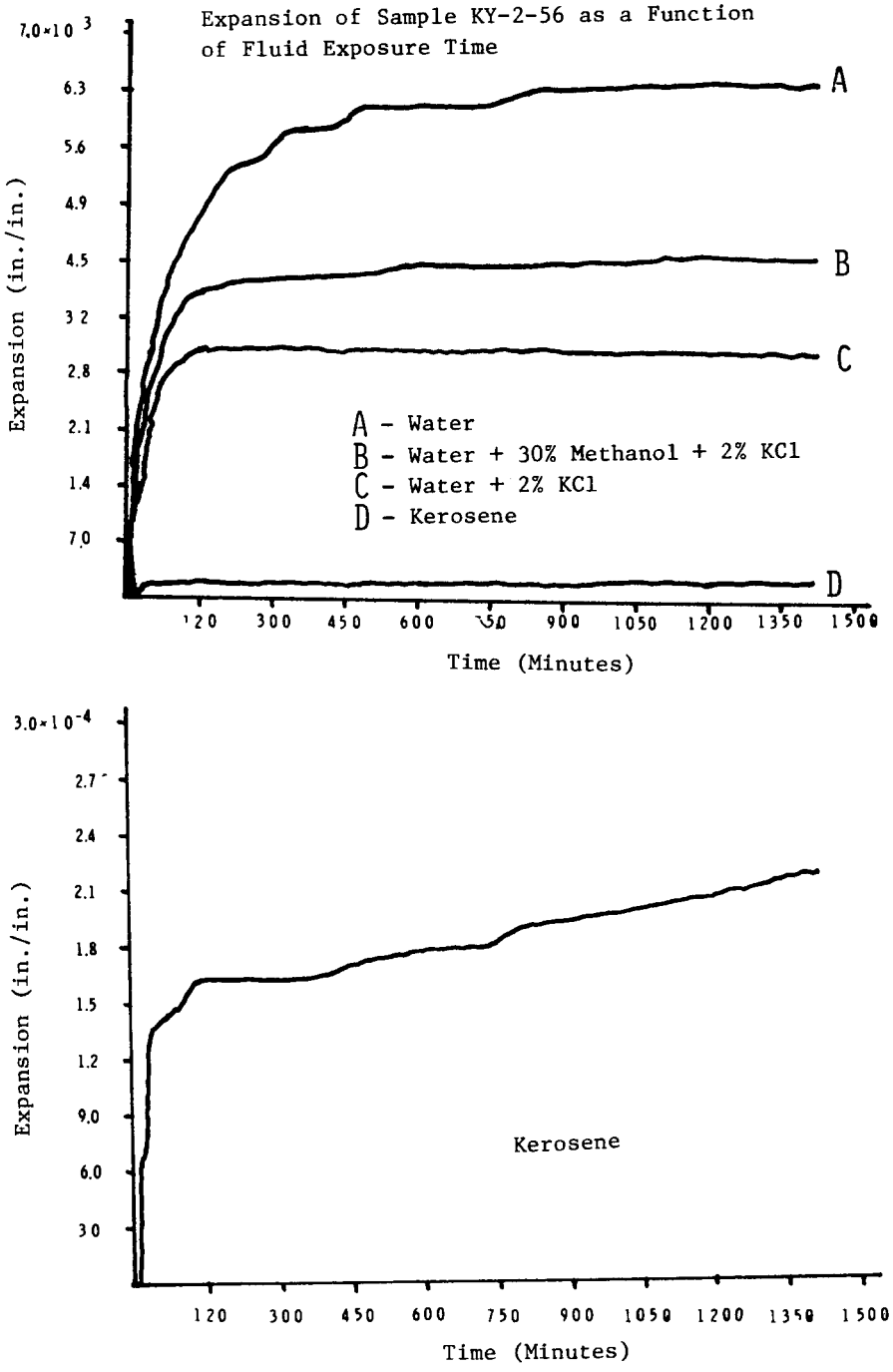
Expansion of Sample KY-2-56 as a Function of Fluid Exposure Time
7.0×10 3
6.3
5.6
4.9
4.5
3 2
2.8
2.1
1.4
7.0
Expansion (in./in.)
A
B
C
D
A - Water
B - Water + 30% Methanol + 2% KCl
C - Water + 2% KCl
D - Kerosene
120 300 450 600 750 900 1050 1200 1350 1500
Time (Minutes)
3.0×10-4
2.7
2.4
2.1
1.8
1.5
1.2
9.0
6.0
3 0
Expansion (in./in.)
Kerosene
120 300 450 600 750 900 1050 1200 1350 1500
Time (Minutes)

FIGURE 10

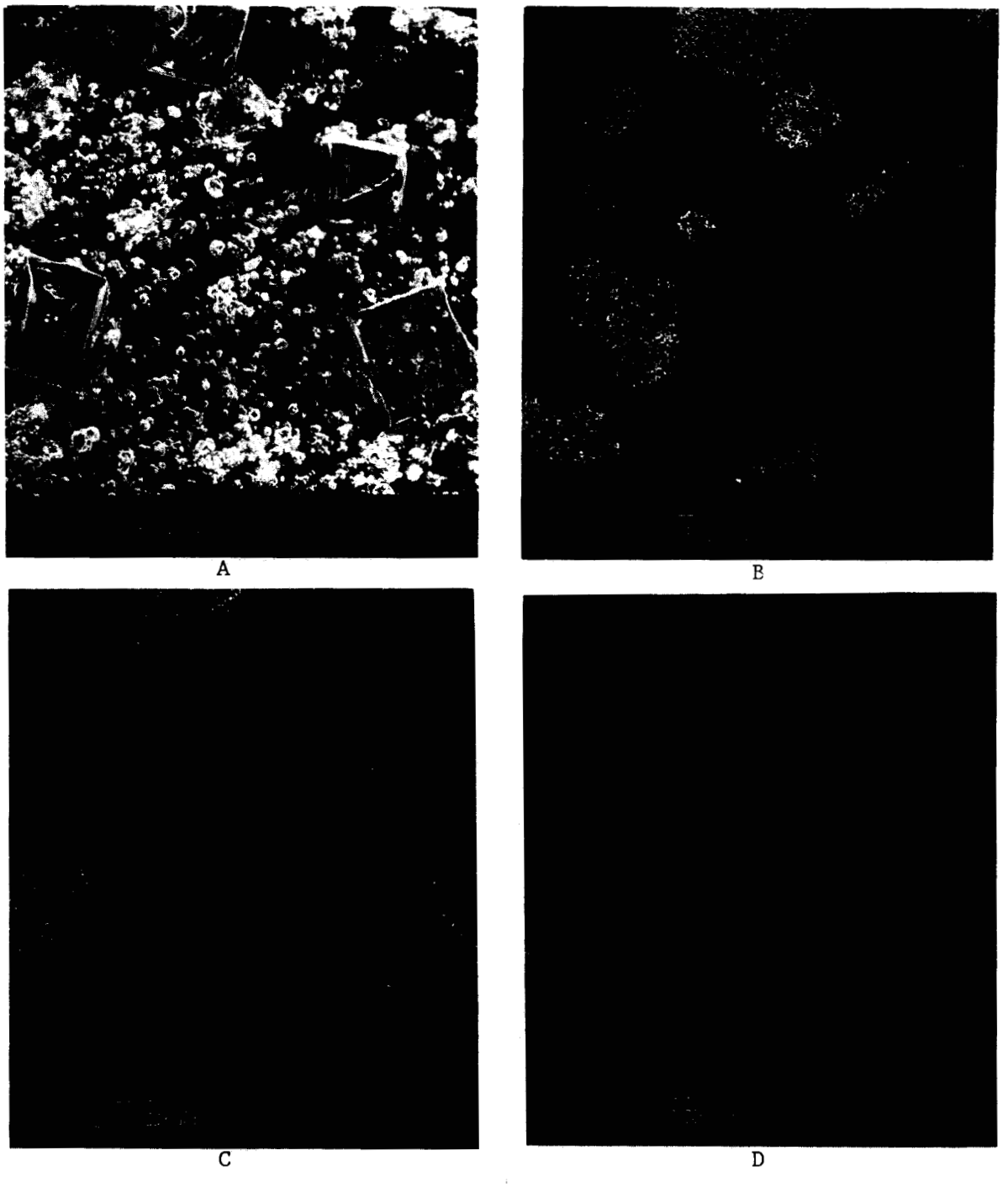

Residue from Water and Methanol and 2% KCℓ
Dilatometry Test

FIGURE 11

TABLE 2

MASS SPECTROMETRIC RESULTS FROM SELECTED SAMPLES

Components (Mole %)	KY-2-1	KY-2-14	VA-1-7	VA-1-16	I-1-2	I-2-1	I-3-3
Methane	21.18	0.39	0.21	56.70	17.53	0.08	0.48
2-H_2	0.21	0.04	0.00	0.10	0.15	0.00	0.02
4-He	0.00	0.00	0.00	0.00	0.00	0.00	0.00
18-H_2O	0.47	5.59	0.14	0.13	0.13	0.35	0.66
26-C_2H_2	0.00	0.00	0.00	0.00	0.00	0.00	0.00
28-CO	0.00	0.00	0.00	0.00	0.00	0.00	0.00
29-CO	0.00	0.00	0.00	0.00	0.00	0.00	0.00
30-CO	0.00	0.00	0.00	0.00	0.00	0.00	0.00
28-N_2	62.60	72.88	77.08	37.33	68.86	92.29	94.52
28-C_2H_4	1.76	0.02	0.01	1.14	0.95	0.00	0.00
30-C_2H_6	1.15	0.02	0.00	1.11	0.76	0.00	0.00
32-O_2	9.32	19.56	20.96	1.35	9.40	2.47	1.56
40-Ar	0.74	0.90	0.87	0.38	0.75	1.14	1.15
44-CO_2	1.20	0.56	0.07	1.58	0.85	3.55	1.53
45-CO_2	0.03	0.01	0.00	0.03	0.02	0.05	0.02
46-CO_2	0.00	0.00	0.00	0.00	0.00	0.02	0.00
47-CO_2	0.00	0.00	0.00	0.00	0.00	0.00	0.00
44-C_3H_8	1.34	0.03	0.01	0.14	0.60	0.04	0.05
29-C_2H_5							
Gas Pressure (atm)	2.578	1.111	1.037	4.420	2.023	1.741	1.478
O_2/N_2 Ratio	0.15	0.27	0.272	0.036	0.137	0.027	0.017
Ar/N_2 Ratio	0.01	0.01	0.011	0.010	0.011	0.012	0.012
Time in Can (Days)	182	251	24	113	177	56	26

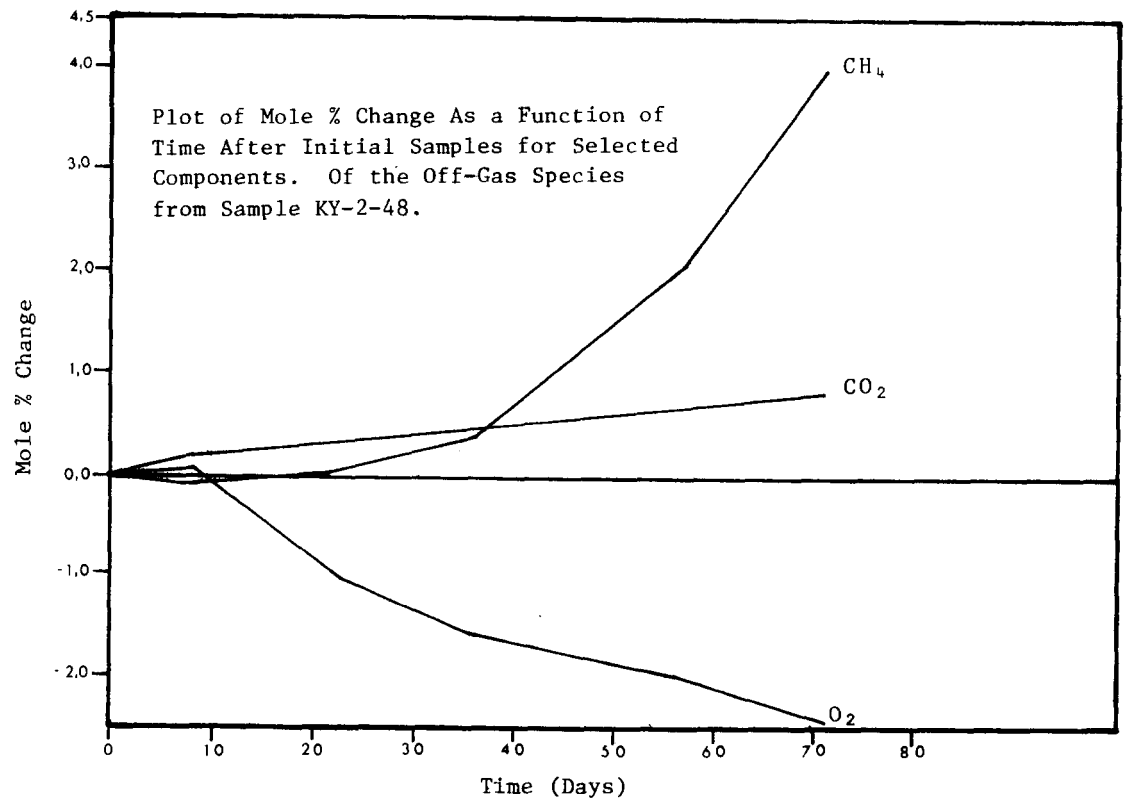
Plot of Mole % Change As a Function of Time After Initial Samples for Selected Components. Of the Off-Gas Species from Sample KY-2-48.
CH4
CO2
O2
Mole % Change
Time (Days)
4.5
4.0
3.0
2.0
1.0
0.0
-1.0
-2.0
0
10
20
30
40
50
60
70
80

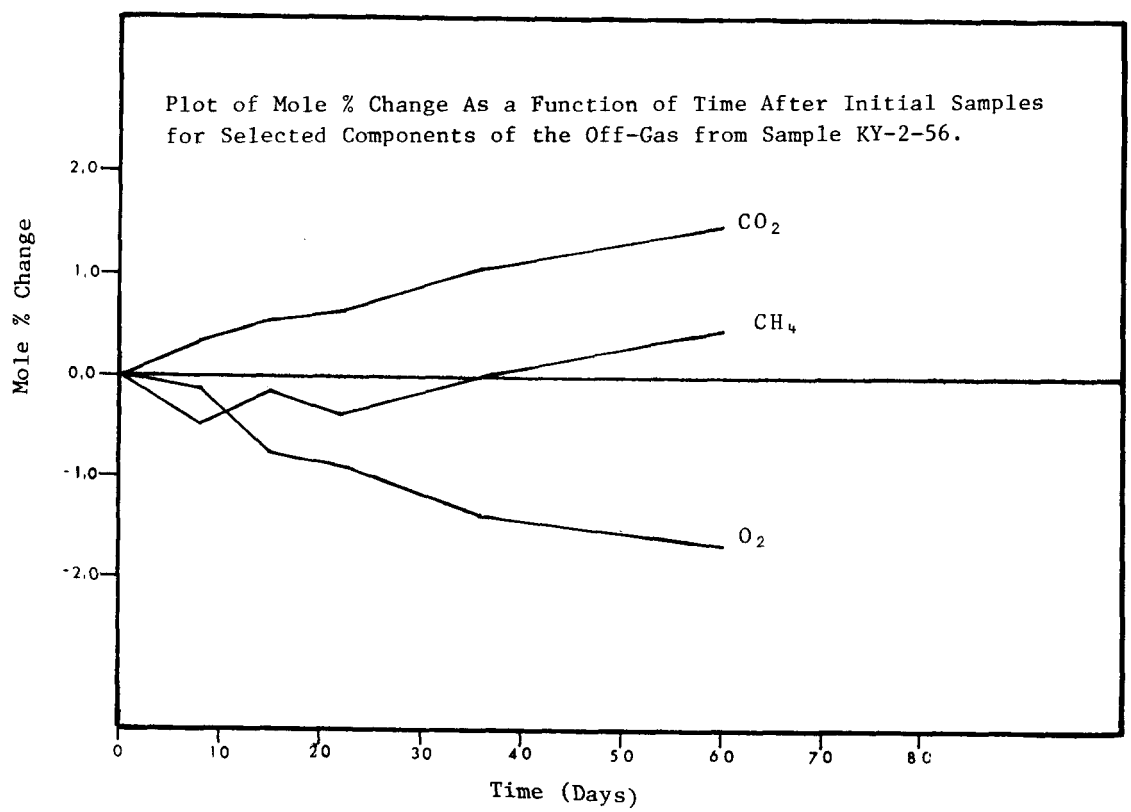
Plot of Mole % Change As a Function of Time After Initial Samples for Selected Components of the Off-Gas from Sample KY-2-56.
CO2
CH4
O2
Mole % Change
Time (Days)
2.0
1.0
0.0
-1.0
-2.0
0
10
20
30
40
50
60
70
80

FIGURE 12

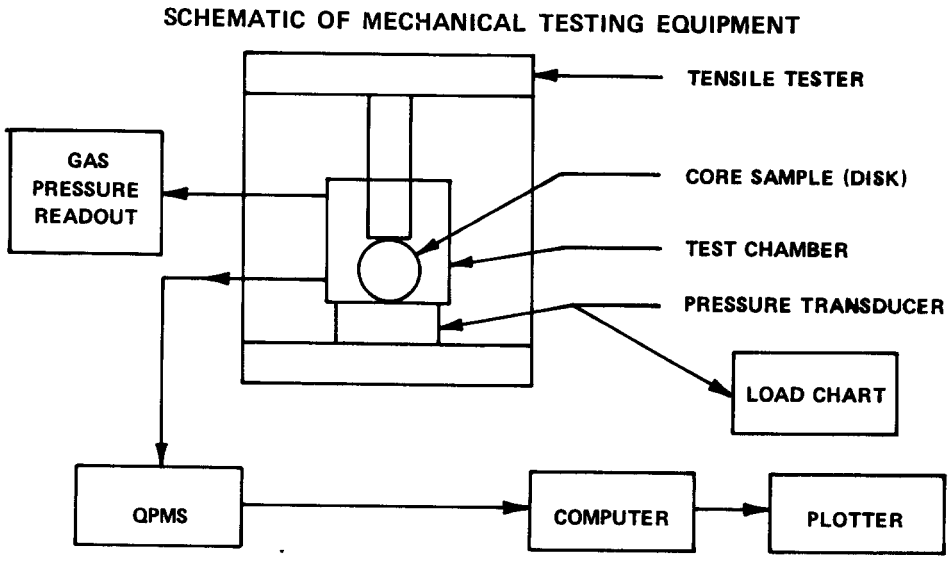
SCHEMATIC OF MECHANICAL TESTING EQUIPMENT
TENSILE TESTER
GAS PRESSURE READOUT
CORE SAMPLE (DISK)
TEST CHAMBER
PRESSURE TRANSDUCER
LOAD CHART
QPMS
COMPUTER
PLOTTER

FIGURE 13

TABLE 3

MECHANICAL TEST RESULTS

SAMPLE	SHORE HARDNESS	BREAKING STRENGTH (MPa)
KY-2-1	24.10	3.268
KY-2-3	16.30	2.031
KY-2-5	15.40	1.166
KY-2-10	13.40	1.523
KY-2-17	15.20	1.704
KY-2-22	10.65	1.384
KY-2-30	8.58	0.849
KY-2-43	15.50	1.614

TABLE 4

PERMEATION RATE OF GAS THROUGH NEW EXPOSED SURFACE

SAMPLE NO.	LINEAL AREA OF FRACTURE (cm^2)	MOLES OF GAS PER cm^2 PER SECOND
P-1-2	45.0	3.405×10^{-7}
P-1-3	72.0	1.314×10^{-6}
KY-2-1	38.1	5.452×10^{-7}
KY-2-3	42.3	9.354×10^{-7}
KY-2-10	32.6	1.840×10^{-4}
KY-2-12	42.1	1.551×10^{-4}
KY-2-17	38.0	1.407×10^{-5}
KY-2-22	36.4	2.089×10^{-4}
KY-2-43	40.2	4.377×10^{-5}
KY-2-56	54.8	2.7536×10^{-6}

TABLE 5

MECHANICAL TEST RESULTS FOR
SAMPLES EXPOSED TO MOISTURE

SAMPLE	RELATIVE HUMIDITY	STRENGTH (M PA)	RELATIVE CHANGE
1	100%	2.201	-42%
2	44.4%	3.792	~0

CHARACTERIZATION AND ANALYSIS OF DEVONIAN SHALES: I. PHYSICAL CHARACTERIZATION

R. S. Kalyoncu
W. G. Coppins
D. T. Hooie
M. J. Snyder

BATTELLE COLUMBUS LABORATORIES

ABSTRACT

Physical characterization of Eastern Devonian Shales is an important step in Battelle's Columbus Laboratories' efforts to determine the relationships between shale characteristics, hydrocarbon content, and well location. Among the physical properties to be determined are density, surface area, pore size, pore size distribution, and permeability.

Methods of physical characterization, and some characterization data, are reported and several problems are discussed. The initial findings and some possible implications about relationships with other data on the same samples are also discussed.

INTRODUCTION

Eastern Gas Shales Project (EGSP) was initiated by ERDA in July, 1976, with research contracts awarded to various universities, government laboratories, industries, and independent research laboratories. Battelle's Columbus Laboratories is presently the only independent research laboratory contracted by ERDA to establish the overall characterization of the Eastern Devonian Gas Shales. The main objectives of the program are to obtain detailed characterization data on these shales and to determine the relationships between the characteristics of the shales and their potential gas contents, ultimately leading to development and demonstration of technologically and economically viable gas recovery methods from the Devonian Shales.

Approximately 1000 core samples of Eastern Devonian Gas Shales from a number of sites in the Appalachian and Illinois basins will be examined in the program. After sufficient characterization data for individual wells have been compiled, a regression analysis for pattern recognition will be performed to establish possible interrelationships between shale properties, hydrocarbon gas content, and well locations from which the samples were obtained. Selected core samples are given in Table 1.

The statement of work for this research under contract No. E(40-1)-5205 calls for the following six major tasks to be performed:

(1) Core sampling
(2) Gas content and gas release kinetics
(3) Chemical characterization of shale
(4) Physical characterization of shale
(5) Lithology of shale
(6) Data interpretation and correlation.

Task 1. Core Sampling

In cooperation with ERDA and the appropriate State Geological Survey, Battelle participates in the selection of core samples. These samples are stored in special sealed containers - to preserve their "down-hole" state as well as possible. Core samples are also provided for Juniata College and Mound Laboratory. Battelle also is gathering the relevant information from on-site observations and well-log data for subsequent interpretation and correlation with characterization results on the selected samples.

Task 2. Gas Content and Gas Release Kinetics

This task calls for the quantitative determination of the hydrocarbon gas evolved from and surrounding the shale samples in the sealed containers and the study of gas release kinetics through thermogravimetric and gas dynamics methods. If possible, kinetic parameters, such as activation energy and reaction rate constants, will be obtained in these kinetic studies.

Task 3. Chemical Characterization of Shale

Performance of this task requires measurement of total carbon, hydrogen, and nitrogen contents on all samples along with determination of a number of trace elements by optical emission spectroscopy on selected samples from each well.

Task 4. Physical Characterization of Shale

Microstructural and physical characterization of the shale samples are accomplished through density, surface area, permeability, porosity and pore size distribution measurements.

Task 5. Lithology of Shale

This task comprises the mineralogical analysis of the shales through x-ray diffraction methods and study of thin sections and bulk shales by light and scanning electron microscopy, respectively.

Task 6. Data Interpretation and Correlation

Statistical analysis using computer techniques will be employed for this task. All the data compiled on the project, e.g., on-site observations, well-log, and laboratory characterization data will be used to determine possible trends and relationships between the potential gas contents and the physical, chemical, and other characteristics of the shale.

The tasks which are briefly described above are summarized in Figure 1 as they appear in the original statement of work. Description of the experiments and the evaluation of the data obtained under Task 4 entitled physical characterization makes up the main theme of this paper. Brief mention of the lighology, carbon contents, and free gas contents will be made, however, to establish certain correlations between the physical characterization data and gas contents of the shales.

An informative description of the methods and procedures employed in performing the physical characterization of shales follows.

Bulk, Apparent, and True Densities of Shale

Experimental Methods described in the Appendix were used to determine the three densities of the shale, namely, bulk, apparent, and true densities. Open, closed, and total porosities were calculated from the density data.

Tables 2 through 5 summarize some of the density data obtained during the last year. A wide variation in the density values of the individual samples is observed in almost all the wells studied. This is likely due to the variations in chemical composition of the shales (especially organic content) rather than porosities, as supported by the total carbon content and XRD analyses. In a few instances some samples were even found to have higher bulk and apparent densities than true densities. A possible explanation for this rests in the difficulty of obtaining representative samples for the characterization experiments. Different specimens from the same core are employed for the measurement of bulk and apparent and true density measurements. The possibility of

utilizing nonrepresentative or unlike samples is very real and is unavoidable because solid chunks are used in the bulk and apparent density measurements and powdered specimens are utilized in true density determinations. It is quite possible for a bulk density sample to contain a large amount of a high density mineral such as pyrite or siderite, in which case, the bulk density measured could be higher than the true density determined using another sample.

The measured bulk density values range from 2.3 to 2.8 g/cc with typical values around 2.6 g/cc. Typical true density values are around 2.7 g/cc. Open, closed, and total porosities calculated from the measured density values are also depicted in Figures 2 through 5. The open porosity values calculated from bulk and apparent densities range from 0.6 to 5.0 percent and closed porosities vary between 0.3 and 3.0 percent.

A significant correlation does not exist between the bulk densities and porosity, although one might expect that a low bulk density value would be accompanied by a high porosity. A reasonably good correlation between the bulk density and initial gas content appears to be the case as discussed in Part II of this paper. A very significant correlation is found between the bulk densities and the carbon contents of the shales as Figures 2 and 3 illustrate for O-1 and P-1 wells, respectively. As can be seen, the carbon contents are inversely proportional to bulk density values. As the organic matter in the shales increases, the bulk densities decrease.

Surface Areas of Shale

Some of the surface area data as obtained using the Micromeritics Model 2205 automatic surface area analyzer are reported in Tables 6 through 8 for various wells. Considerable variation also exists in the surface area values of the shales. The surface area values do not seem to bear a relationship to sample depth or porosity values contrary to expectations. Also, no distinct correlation exists between surface areas and initial gas contents of shales. From the XRD studies, however, surface areas of the shales seem to tie in well with the clay mineral contents in the shales, high surface area values indicating higher clay mineral content. This observation, however, is semiquantitative at best since no efforts were made to quantitatively determine the mineral composition of the shales. This general relationship, however, is rather unmistakable. So far there appears to be no relationship between the carbon content and surface area values. Plots in Figures 4 through 6 are intended to show possible one-to-one relationships between the surface areas and other properties of the shales. As evident from these figures, distinct correlations between the surface areas and bulk density, well depth, and porosity values are not found. The surface area values are probably governed more closely by the content of finer particle size plate-like clay minerals. Samples with higher surface areas seem to contain higher fractions of clay minerals as evidenced by x-ray diffraction analyses. Such an observation is also true for the color of the pulverized shale samples. Lighter colors are observed with higher clay mineral and lower organized contents.

The surface areas are measured in the as-received condition without any special treatment (thermal or otherwise) of the powdered shale specimens, except for 15 minutes outgassing and equilibration in the sample holder of the surface area apparatus at room temperature. These surface area values should be designated as "apparent" values, because the measured surface areas are greatly affected by the thermal and other physical conditions under which the experiments are carried out. To illustrate, for example, the importance of outgassing temperatures on the surface area values determined a series of measurements were made of the same shale sample at various outgassing temperatures. Figure 7 summarizes these findings. As is obvious from the figure, the measured surface area of sample C-1-2782 at 200 C outgassing temperature is almost an order of magnitude higher than the value obtained for the same sample outgassed at room temperature for the same length of time.

Mercury Intrusion Porosity of Shales

Presently only raw porosimeter data on about 60 samples have been obtained. Pore size and pore size distribution as a function of pressure are being calculated. The experimental difficulties initially encountered in porosity measurements have been resolved and no future problems are foreseen at the present. A computer program has just been developed for porosity and pore size distribution. Results for one specimen are summarized in Figure 8. The calculated net pore volume for this sample is 0.01995 cc/g (which is about 5 percent by volume) and the average pore diameter is 0.046 μm. These values compare reasonably well with the porosity values calculated from the density data with the calculated porosities being somewhat higher than the porosity values determined using the mercury intrusion porosimeter. This is not unexpected as the total porosity determined with the

mercury intrusion porosimeter is a function of pore size and the pressure at which the mercury is forced into the pores. Since the instrument has a limited pressure capacity (15,000 psi in this case), pores smaller than a certain size together with most of the closed pores will not be included in the measured porosity values.

Permeability of Shale

Permeabilities of shale to helium gas were determined employing the method described in the Appendix. Out of the 50 permeability runs that have been made on as-received shale samples of one-inch diameter and 1/4 inch thick discs, only a few samples showed any measurable permeability to helium. These measurements indicate that the shales in as-received state are virtually impermeable to gases. Even the samples where the gas flow was parallel to bedding planes exhibited zero to negligible permeabilities (in the order of 7×10^{-7} Darcy) to helium gas. These findings of the permeability measurements are in no way contradicted by the density and porosity data as indicated by significantly high bulk densities and relatively small porosities of the shales. Presently, some attempts are being made toward enhancing the permeabilities of the shales by chemical and thermal treatments.

CONCLUDING REMARKS

The values of the physical characterization data on the shales determined as described in this paper may be of limited value in reaching the ultimate goal of the Eastern Gas Shales Project. One-to-one correlations between physical property data and initial gas release or organic carbon content are presently either vague or nonexistent. However, at this stage of the investigation, it is not entirely unexpected that there are but few direct correlations. Many of the unresolved questions will not be answered until sufficient data have been collected to perform a multiple regression analysis leading to a pattern recognition. The number of variables and the volume of data involved in the program are far too numerous to permit any simple-type correlation.

At the time sufficient data have been compiled, a regression-type analysis will be conducted in an effort to determine the interrelationships and trends between the hydrocarbon gas content and the physical and chemical characteristics of shales both for individual wells and for basins.

As mentioned earlier in this article, some of the data being compiled from the as-received shale possibly may have limited value. What may be even more useful are property data on shales obtained before and after certain types of treatment of the shale. For example, the difference between the surface area values of as-received shale samples and samples which had been thermally treated would probably be a much more useful parameter in assessing the potential gas yields as opposed to a single surface-area measurement on an as-received sample. By the same token, the difference in permeability between an as-received specimen and a sample subjected to leaching to remove organics would be a much better measure of the organics content and the relative ease of removal than merely a single value of permeability of an as-received shale specimen. With this reasoning, therefore, a limited effort is being placed on such studies.

In much the same vein as measurement of property data solely on as-received samples is the question and importance of utilizing representatice samples for the generation of these data. Emphasis on this characterization aspect is particularly important when working with relatively inhomogeneous materials of highly variable compositions, such as shales. The wide variation in much of the characterization data to date can be attributed to the difficulty of obtaining representative samples. For example, some of the data indicate a higher bulk than true density for the same core sample. This anomoly can only be explained on the basis of sample selection and preparation. Bulk density measurements are made on a solid piece of shale, whereas powdered specimens of possibly differing compositions are used for true density measurements. It is highly conceivable that a bulk density sample may contain a large amount of a high density material such as pyrite or siderite. Pyrite, in particular, is most likely to be present because it has been observed to be present in streaks along the bedding planes.

C-H-N measurements are likewise greatly influenced by sample selection. These measurements are made with 3 to 5 mg powdered samples and because of the extremely small quantities of material being measured, extreme care must be taken in the extrapolation of these data as being representative of the core sample or as being related in some fashion to the values of the entire shale bed.

Summarily, the data generated must be utilized in an extremely careful manner until such time as sufficient numbers are available to be considered as truly representative of the particular shale. Premature evaluations based on insufficient and widely scattered data can only lead to erroneous and quite misleading conclusions.

The characterization data obtained also greatly depend on the specific experimental parameters and conditions so that the measured values of physical properties could vary greatly even when identical instrumentation and supposedly identical conditions are employed. The surface area values, for example, as discussed previously will greatly depend on outgassing temperature and time. Whenever the characterization data are presented and discussed, the experimental procedure used to obtain the data and exact physical and thermal conditions under which the data are obtained should be described in detail.

ACKNOWLEDGEMENTS

This research project was funded by the United States Energy Research and Development Administration under Contract No. E(40-1)5205. Experiments described in the text were performed by Messrs. Weaver and Roese. Their efforts in this project are gratefully acknowledged.

APPENDIX

EXPERIMENTAL METHODS

1. Sample Preparation

Following puncturing for off-gas analysis, the can is opened and the core sample removed. It is oriented as in the down-hole position and photographed. A rough drawing of the fracture segments is constructed, together with a brief description of the mineralogical and fractographic features. Total weight of the sample core is obtained, together with the weight of the empty can and lid. A weighed sample is removed for gas kinetics analysis.

To obtain adequate sample representation, portions of the core are removed from the top from the center and from the bottom. Samples, approximately 1-1/8" x 1/2" x 1/2", are retained for bulk and apparent density measurements. The remainder is ground together in a rotary mill. Following the grinding, the samples are sieve-sized using screens of 10, 20, 100, and 200 mesh. The various fractions are utilized as follows:

-10 + 20 fraction for porosity measurement

-100 + 200 fraction for true density measurement
surface area measurement

-200 fraction for C-H-N and XRD analyses.

2. Bulk and Apparent Density Measurements

Samples are cut from the top, center, and bottom of each core. A sample approximately 1-1/8" x 1/2" x 1/2" is cut from each section of the core. The procedure is as follows:

(a) Weigh (in grams) the as-cut samples before placing in the vacuum drying oven, record on computer sheet.

(b) Dry sample overnight in vacuum oven at 250 F.

(c) After samples are cooled, weigh and record on computer sheet, (W_D).

(d) Place samples in a container, then place samples and container in a vacuum set up for two hours. At the end of the two hours, cover samples to 1/2 inch above top of samples with kerosene and let stand for two hours under vacuum. After two hours in kerosene, remove container from vacuum set up. Let the container with samples in kerosene set overnight.

(e) Get suspended weight of samples and record on computer sheet, (W_{ss}). Get weight of basket in kerosene and record on computer sheet. Check basket weight with each weighing for suspended weight by placing sample on bottom of suspended weight container. If there is a difference in basket weight, record on computer sheet.

(f) With a tissue dampened with kerosene, wipe excess kerosene from sample, then get the wet weight, record on computer sheet, (W_s).

(g) Dry samples overnight in vacuum oven at 250 F. Let samples cool and then weigh, record on computer sheet.

The calculation of densities proceeds as follows:

(a) Weight of shale sample after oven drying at 250 F = W_D (gm)

(b) Weight of sample following impregnation with kerosene, i.e., saturated weight = W_S (gm)

(c) Weight of saturated sample suspended in kerosene $= W_{SS}$ (gm)

Using these data, the following calculations can be made:

(d) Bulk volume (V_B)

$$V_B = \frac{W_S - W_{SS}}{\rho \text{ kerosene}} , \quad (cc)$$

(e) Bulk density (D_B)

$$D_B = \frac{W_D}{V_B} , \quad (g/cc)$$

(f) Apparent volume (V_A)

$$V_A = \frac{W_D - W_{SS}}{\rho \text{ kerosene}} , \quad (cc)$$

(g) Apparent density (D_A)

$$D_A = \frac{W_D}{V_A} , \quad (g/cc)$$

(h) Open porosity (P_o)

$$P_o = \frac{V_B - V_A}{V_B} , \quad (\%)$$

Use of the true density permits calculation of true volume.

(i) True volume (V_T)

$$V_T = \frac{W_D}{D_T} , \quad (cc)$$

where D_T is true density

(j) Total porosity (P_{TOT})

$$P_{TOT} = \frac{V_B - V_T}{V_B} , \quad (\%)$$

(k) Closed porosity (P_C)

$$P_C = P_{TOT} - P_O , \quad (\%)$$

For all of the density measurements, the temperature of the sample and kerosene is measured and a correction applied to the density of the kerosene.

3. True Density Measurements

True density and volume need:

Pychnometers and stoppers with capillary tube.

The experimental procedure is as follows:

(a) Dry the stopper and bottle at 100°C for two hours.

(b) Weigh pychnometer and stopper (P).

(c) Fill pychnometer with kerosene to mark.

(d) Weigh pychnometer and kerosene and stopper (W_1).

Empty the kerosene, wash pychnometer with acetone and dry in oven for two hours. Weigh 4 g powdered sample in pychnometer.

(e) Dry pychnometer and sample and stopper in vacuum at 120 C overnight.

(f) Weigh pychnometer and sample and stopper (W).

(g) Fill pychnometer with kerosene to 1/3 full.

(h) Place paper between stopper and pychnometer. Place pychnometer in a plan of hot water and boil for 15 minutes.

(i) Fill the bottle to the base of the neck with kerosene and cool to room temperature.

(j) Fill the bottle the remaining distance to mark on neck of bottle and stopper.

(k) Wipe the bottle dry with a soft cloth.

(l) W_2 = final weight of pychnometer with sample, stopper, and kerosene.

Calculations:

(1) True volume

a. V_t = true volume, cc

b. $V_t = (W + W_1 - W_2 - P)/\rho$ kerosene

(2) True density

a. ρt = true density, g/cc

b. $\rho t = (W - P)/V_t$

(3) Closed porosity

a. Pc = percent closed porosity

b. $Pc = [(V_a - V_t)/V_a] \times 100$

(4) Total porosity

a. Pt = percent total porosity

b. $P_t = Po + Pc$

c. $P_t = [(V_b - V_t)/V_b] \times 100$

4. Surface Area Measurements

The surface area of powdered shale samples - ground to 100-200 mesh - is measured with a Micromeritics High Speed Surface Area Analyzer, Model 2205, by determining the quantity of gas necessary to form a single layer of gas molecules, a so-called monomolecular layer, on a representative sample. Testing is accomplished using argon gas at the temperature of liquid nitrogen (-179 C), because under these conditions, the gas molecules are strongly absorbed on most solid surfaces, and the area occupied by each adsorbed gas molecule on a solid surface is known within relatively narrow limits. The background of this technique is based on the well known B.E.T. theory.

Argon is particularly appropriate for automated instrument analysis as it has a low vapor pressure at liquid nitrogen temperature, making it possible to measure correspondingly small

adsorptions - hence, relatively low specific surface areas - with reasonable accuracy. It has a very high ionization potential because its stable electronic shells give it extreme chemical inertness. Argon has the smallest atomic dimensions of the gases generally used in adsorption work and low polarizability. It should be expected, therefore, to show little variation in its heat of adsorption from one solid to another and to be unlikely to undergo localized adsorption.

The basic construction of the instrument is shown in Figure A-1. It consists of three sample holders; three two-stage valves, two pressure sensors, one which is set somewhat below atmospheric pressure and one at the pressure of monolayer formation, a variable volume cell, three sorption pumps connected to the variable volume by a solenoid valve and the associated piping and connectors. The basic components of the system are maintained at fixed temperatures. Electronic controls and auxiliary systems are not indicated.

As the valves are arranged on the diagram, the sample on the left is being outgassed, i.e., prepared for analysis, the center sample is being analyzed, and the section on the right is closed for sample changing. Outgassing is accomplished by forcing argon through the sample at a selected temperature. Water and other vapors previously adsorbed are thus flushed from the sample. The adsorption or analysis step is carried out with the sample holder immersed in liquid nitrogen. Immediately prior to this cooling of the sample, the gas pressure in the system associated with the sample, including that of the variable volume and pressure detectors, is brought automatically by the sorption pump to the higher of the two fixed pressures. When the sample is then cooled, the gas pressure in the sample space decreases due to the change in temperature and to the gas being removed by adsorption onto the sample. The pressure in the variable volume portion of the system is brought to the lower of the two fixed pressures, again by the sorption pump. Upon shifting a valve, the variable volume shifts automatically so that the pressure is maintained at the lower of the two fixed pressure points. The magnitude of the shift is a measure of the gas adsorbed as a monomolecular layer, hence of the surface area of the sample.

5. Porosity Measurements

Pore size and pore size distribution of the shales are measured with a Carlo Erba Mercury Intrusion Porosimeter Model AG/60. The maximum operating pressure of this instrument is 15,000 psi.

The determination of pore size with the mercury penetration method is based on the behavior of nonwetting liquids in capillaries. Because of its surface tension, a liquid cannot spontaneously enter a small pore which has a wetting angle greater than 90. This resistance may be overcome by exerting a certain external pressure. The pressure necessary to force the liquid with surface tension is a function of the pore size, r.

The relationship between pore size and exerted pressure is given by the equation of Washburn.

$$pr = 2\ \sigma\cos\Theta$$

where

r = pore radius
σ = mercury surface tension
Θ = wetting angle
p = absolute pressure exerted

The relationship derives from the following consideration: In a capillary with circular section, the surface tension of the liquid operates in the contact area for a length equal to the pore circumference. This force is perpendicular to the plane of the contact surface; the force tending to push the liquid out of the capillary is:

$$2\pi r\sigma\cos\Theta$$

Against this force, the external pressure will be exerted on the area limited by the contact circumference with a value equal to

$$p\pi r^2$$

When equilibrium has been reached, these two forces have the same value

$$2\pi r\sigma\cos\Theta = p\pi r^2$$

Hence, the pore radius is inversely proportional to the pressure

$$r = 2\sigma\cos\Theta/p$$

When using mercury, and assuming surface tension 480 dynes/cm and wetting angle 141.3°, and also assuming that all pores have cylindrical shape, the following relationship between pore radius and pressure is obtained

$$r = 75{,}000/p$$

where

r = pore radius in A^o

p = absolute applied pressure in Kg/cm^2

This equation is exact only in the case of circular pores. For pores of irregular form, the ratio between the pore cross section (related to the pressure exerted) and the pore perimeter (related to the surface tension) is no more proportional to the radius, but, depending on the pore shape, will give lower values.

The value of the wetting angle (here assumed to be 141.3°) depends on the nature of the sample, and should therefore be considered as an average value only. By means of the x-rays, the mercury wetting angle has been measured on a large number of samples. Values between 135° and 142° have been found; hence, we have assumed 141.3° as average value of the wetting angle.

Surface tension should also be considered as an uncertain value. At 25°C, its value is of about 482.2 dynes/cm, while at 50°C, it is of 472 dynes/cm. It is possible to notice this parameter is rather stable to temperature changes, and 480 dynes/cm has been assumed as an average value. In spite of the presence of these errors, we presume the nature of porous substance and the pores form remain constant in the entire pore size range of a given sample. Therefore, the pressure-radius function of the pores may have a certain displacement in the absolute radius values but remains correct from a relative point of view.

6. Permeability Measurements

Permeability is measured by recording gas flow through a specimen under a pressure gradient. The apparatus consists of a vacuum supply, a manometer, a specimen holder, and the necessary plumbing for operation. A schematic diagram of the permeability assembly is depicted in Figure A-2.

Initial Operating Status:

(1) Valves 6 and 7 closed; 1, 2, 3, 4 open

(2) Roughing pump on

(3) Cold trap filled

This will supply vacuum to the system. Care should be taken not to open valve 6 as this will allow mercury to be drawn into the system. Closing valves 3 and 4 will isolate specimen holder "A" from the system allowing it to be opened for specimen insertion. After this is done, it should be resealed and valves 3 and 4 opened again to draw vacuum on this part of the system again. Specimen insertion is dealt with on Page 3. Opening valve 7 very slowly will allow helium to enter the manometer. When Hg level is near the bottom of the calibration, the valve should be closed. The apparatus is now ready for operation.

The following steps are followed in the operation of the unit:

(a) Read mercury meniscus level.

(b) When thermocouple gauge shows 100 microns, close valve 5.

(c) Using a stopwatch, time the rise of the mercury column that will begin when valve 6 is opened and end when it is closed. The best technique for this is to open the valve rather quickly, starting the stopwatch at the same time. Observe the rise of mercury column and stop gas flow (close valve 6) when it nears the top of the calibration. Also stop the stopwatch as the valve is closed. Vastly different flow rates may fill the column in as little as 2-3 seconds, so alertness is mandatory.

(d) With valve 6 closed, valve 5 should be opened to restore vacuum to the system as soon as possible.

(e) Record elapsed time and new meniscus level.

(f) Bleed more helium into the manometer by slowly opening valve 7.

Apparatus is now ready for next run.

If specimen is to be changed, in step 4, leave valve 5 open but close valves 3 and 4 before vacuum is restored. This will allow opening specimen holder "A" without losing vacuum or working against vacuum. When holder is resealed, opening valves 3 and 4 simultaneously will minimize specimen disturbance from pressure differential in the holder.

Sealing the specimen in the holder can be a problem; however, care in all the following procedures minimizes this.

After the above set up is assembled, molten latex is poured in the cup to a level approximately 1/16" above the top of the brass plug. The cup should be heated before pouring and may be heated after pouring to facilitate flowing and leveling of the rubber. Too much heat will bubble and scorch the seal, making it worthless. After cooling, seal may be peeled from the cup and the brass plug removed. Cut out hole formed by brass plug with a cork-borer of appropriate size. Insert specimen in place of brass plug, coat seal very lightly with stopcock grease, and replace in specimen holder.

One of the steps necessary in determining permeability is to ascertain the volume of the specimen holder, so that the volume of gas filling may be subtracted from the total volume flowed through the specimen. As long as the atmosphere pressure, ambient temperature, type of specimen (size) and seal do not change, a given volume may be assumed for any one series of runs.

(a) Insert an impermeable plug in the seal and load specimen holder.

(b) Evacuate system by opening valves 1, 2, 3, 4, and 5. Valves 6 and 7 should be closed.

(c) While system is evacuating, slowly bleed helium in the system through valve 7, filling the manometer to allow calibration No. (95-100 cc).

(d) Close valve 5 when 100 micron vacuum is reached and open valve 6.

(e) If mercury level rises, then stops, record new level. If mercury level does not stabilize, there is a system leak.

(f) Close valve 6, open valve 5 and re-evacuate. If repetition of this test does not yield widely varied figures, an average value for volume may be obtained. All volumes on this apparatus read out directly in cubic centimeters.

The calculation of permeability is carried out in the following manner. The experimental parameters obtained include:

(1) Sample thickness (L) (cm)

(2) Sample cross-sectional area (A) (cm^2)

(3) Atmospheric pressure (P) (atm)

(4) Inflow pressure (P'_1) (atm)

(5) Viscosity of permeating medium (μ) (poise)

(6) Amount fluid permeated at a given time (Q) (cm^3)

Calculate

(1) Volume per unit area per unit time permeated

$$q = \frac{Q}{(A)(t)}$$

(2) Total inflow pressure

$$P_1 = P + P'_1$$

(3) Outflow pressure

$$P_2 = P_1 - P'_1 = P \text{ (atmospheric pressure)}$$

(4) Calculate

$$\frac{P_1 + P_2}{2}$$

(5) Corrected volume permeated

$$\bar{Q} = z/A = 1 \div 4$$

(6) Calculate

$$\frac{P_1 - P_2}{L}$$

(7) Calculate permeability

$$P = \frac{\bar{Q}\mu L}{A(P_1 - P_2)} \quad \text{Darcys}$$

TABLE 1. IDENTIFICATION OF CORED WELLS AND SAMPLES SELECTED

Well Code Number	Location of Well	Well Operator	Date Sampled	Core Depth Interval, feet	Number of Samples
C-1	Lincoln County, WV	Columbia Gas	Jan. 1976	2746 - 4045	82
C-2	Lincoln County, WV	Columbia Gas	Jan. 1976	2655 - 3971	17
R-109	Washington County, OH	River Gas	July 30, 1976	3494 - 3705	25
P-1	Sullivan County, IN	Energy Resources of Indiana, Inc.	Sept. 1, 1976	2495 - 2595	11(a)
O-1	Christian County, KY	Orbit Gas	Sept. 18, 1976	2183 - 2319	13(b)
C-336	Martin County, KY	Columbia Gas	Nov. 6, 1976	2434 - 3405	117(c)
T-1	Effingham County, IL	Tri-Star	Feb. 13-18, 1977	3006 - 3106	15(d)
C-338	Wise County, VA	Columbia Gas	Apr. 22-30, 1977	4871 - 5469	40(e)
N-1	Henderson County, IL	No. Illinois Gas	July 13-17, 1977	319 - 620	31(f)
N-2	Tazewell County, IL	No. Illinois Gas	Aug. 16-20, 1977	898 - 1158	23(g)

(a) An additional 6 samples were selected and encapsulated for other ERDA contractors.
(b) An additional 4 samples were selected and encapsulated for other ERDA contractors.
(c) An additional 90 samples were selected and encapsulated for other ERDA contractors.
(d) An additional 16 samples were selected and encapsulated for other ERDA contractors.
(e) An additional 41 samples were selected and encapsulated for other ERDA contractors.
(f) An additional 26 samples were selected and encapsulated for other ERDA contractors.
(g) An additional 29 samples were selected and encapsulated for other ERDA contractors.

TABLE 2. DENSITY DATA OF C-2 WELL

Sample ID	Bulk Density g/cc	Apparent Density g/cc	True Density g/cc	Open Porosity %	Closed Porosity %	Total Porosity %
C-2-2655	2.731	2.770	2.770	1.414	0.664	2.077
-2710	2.708	2.770	2.805	2.220	1.406	3.626
-2761	2.705	2.776	2.882	2.565	3.604	6.169
-3000	2.737	2.757	2.827	0.714	2.799	3.513
-3025	2.708	2.727	2.653	0.679	0.000	0.679
-3050	2.716	2.733	2.835	0.643	3.566	4.209
-3101	2.737	2.755	2.712	0.634	0.000	0.634
-3303	2.810	2.825	2.841	0.539	1.024	1.563
-3328	2.821	2.835	2.887	0.496	1.869	2.366
-3378	2.581	2.589	2.663	0.298	2.766	3.064
-3428	2.630	2.638	2.677	0.290	1.756	2.046
-3478	2.757	2.783	2.936	0.946	5.202	6.148
-3528	2.616	2.625	2.561	0.363	0.000	5.534
-3896	2.642	2.683	2.745	1.510	2.245	3.755
-3922	2.575	2.592	2.577	0.664	0.082	0.747
-3961	2.550	2.559	2.560	0.317	0.383	0.700
-3971	2.559	2.568	2.702	0.335	4.926	5.261

TABLE 3. DENSITY DATA OF O-1 WELL

Sample ID	Bulk Density g/cc	Apparent Density g/cc	True Density g/cc	Open Porosity %	Closed Porosity %	Total Porosity %
O-1-2183	2.248	2.262	2.301	0.634	2.214	2.849
-2191	2.403	2.416	2.399	0.549	0.851	1.401
-2220	2.470	2.483	2.497	0.530	0.586	1.116
-2230	2.662	2.676	2.689	0.536	0.929	1.465
-2239	2.422	2.438	2.461	0.617	0.949	1.566
-2251	2.733	2.781	2.665	1.705	0.000	1.705
-2259	2.360	2.372	2.320	0.495	0.000	0.495
-2271	2.462	2.471	2.579	0.358	4.849	5.207
-2281	2.403	2.416	2.402	0.518	0.323	0.841
-2290	2.500	2.511	2.412	0.436	0.000	0.436
-2300	2.605	2.616	2.469	0.425	0.000	0.425
-2310	2.619	2.630	2.659	0.442	1.709	2.151
-2319	2.409	2.420	2.486	0.428	2.666	3.095

TABLE 4. DENSITY DATA OF P-1 WELL

Sample ID	Bulk Density g/cc	Apparent Density g/cc	True Density g/cc	Open Porosity %	Closed Porosity %	Total Porosity %
P-1-2495	2.654	2.796	2.650	5.078	0.000	5.078
-2505	2.293	2.308	2.338	0.636	2.378	3.014
-2515	2.447	2.473	2.390	1.064	0.207	1.272
-2528	2.442	2.455	2.525	0.547	2.747	3.294
-2536	2.411	2.453	2.337	1.674	0.000	9.348
-2547	2.368	2.423	2.216	2.262	2.271	4.533
-2554	2.487	2.528	2.590	1.605	2.462	4.067
-2565	2.608	2.660	2.488	1.930	0.935	2.865
-2575	2.543	2.559	2.503	0.619	0.000	0.619
-2585	2.414	2.429	2.549	0.619	4.585	5.204
-2595	2.592	2.612	2.657	0.770	4.099	4.869

TABLE 5. DENSITY DATA OF R-109 WELL

Sample ID	Bulk Density g/cc	Apparent Density g/cc	True Density g/cc	Open Porosity %	Closed Porosity %	Total Porosity %
R-109-3494	2.747	2.793	2.777	1.669	0.374	2.043
-3506	2.697	2.717	2.646	0.736	0.000	0.736
-3516	2.692	2.716	2.707	0.894	1.082	1.976
-3526	2.611	2.680	2.787	2.524	3.807	6.331
-3536	2.750	2.772	2.831	0.775	2.094	2.869
-3545	2.746	2.764	2.964	0.657	6.836	7.493
-3555	2.698	2.726	2.736	1.035	0.627	1.662
-3564	2.655	2.672	2.814	0.623	5.039	5.662
-3575	2.705	2.721	2.636	0.570	0.000	0.570
-3585	2.651	2.668	2.695	0.650	1.005	1.656
-3593	2.638	2.653	2.739	0.567	3.121	3.688
-3605	2.593	2.607	2.584	0.519	0.024	0.543
-3606A	2.550	2.566	2.541	0.609	0.000	01609
-3606B	2.606	2.621	2.655	0.550	1.495	2.045
-3616	2.634	2.651	2.657	0.649	1.254	1.903
-3626	2.743	2.769	2.824	0.937	2.731	3.668
-3634	2.699	2.713	2.630	0.527	0.000	0.527
-3644A	2.659	2.693	2.692	1.260	0.371	1.631
-3644B	2.671	2.683	2.711	0.423	1.025	1.448
-3665	2.722	2.744	2.689	0.790	0.745	1.536
-3675	2.694	2.718	2.612	0.876	0.000	0.876
-3685	2.754	2.782	2.715	1.001	0.000	1.001
-3695	2.583	2.594	2.703	0.403	4.007	4.409
-3705	2.708	2.743	2.707	1.283	0.000	1.283
-3711	2.747	2.788	2.733	1.456	0.000	1.456

TABLE 6. SURFACE AREA DATA

Sample ID	Surface Area (m^2/g)
C-1-2755	2.47
C-1-2782	1.08
C-1-2787	1.18
C-1-2802	1.27
C-1-2837	3.22
C-1-2842	2.75
C-1-2897	1.00
C-1-2947	1.21
C-1-2959	2.89
C-1-2964	2.08
C-1-2999	3.64
C-1-3039	2.02
C-1-3085	4.31
C-1-3175	2.97
C-1-3198	3.86
C-1-3218	1.04
C-1-3326	1.82
C-1-3346	1.37
C-1-3593	4.35
C-1-3651	2.89
C-1-4045	4.59

TABLE 7. SURFACE AREA DATA

Sample ID	Surface Area (m^2/g)
C-338-4882	11.94
C-338-4892	8.35
C-338-4912	8.90
C-338-4940	9.42
C-338-4950	5.93
C-338-4960	3.13
C-338-4980	2.23
C-338-5232	3.52
C-338-5283	5.54
C-338-5293	5.56
C-338-5332	2.76
C-338-5347	7.18
C-338-5357	11.20
C-338-5372	16.69
C-338-5382	11.90
C-338-5434	3.16
C-338-5394	3.89
C-338-5447	15.76
C-338-5459	18.31
C-338-5467	12.97

TABLE 8. SURFACE AREA DATA

Sample ID	Surface Area (m^2/g)
T-1-3012	8.414
T-1-3022	2.364
T-1-3043	3.60
T-1-3051	7.85
T-1-3056	7.21
T-1-3063	8.67
T-1-3067B	1.35
T-1-3074	5.37
T-1-3080	3.48
T-1-3080B	7.29
T-1-3086	10.11
T-1-3094B	7.97
T-1-3099	3.32
T-1-3106B	2.12

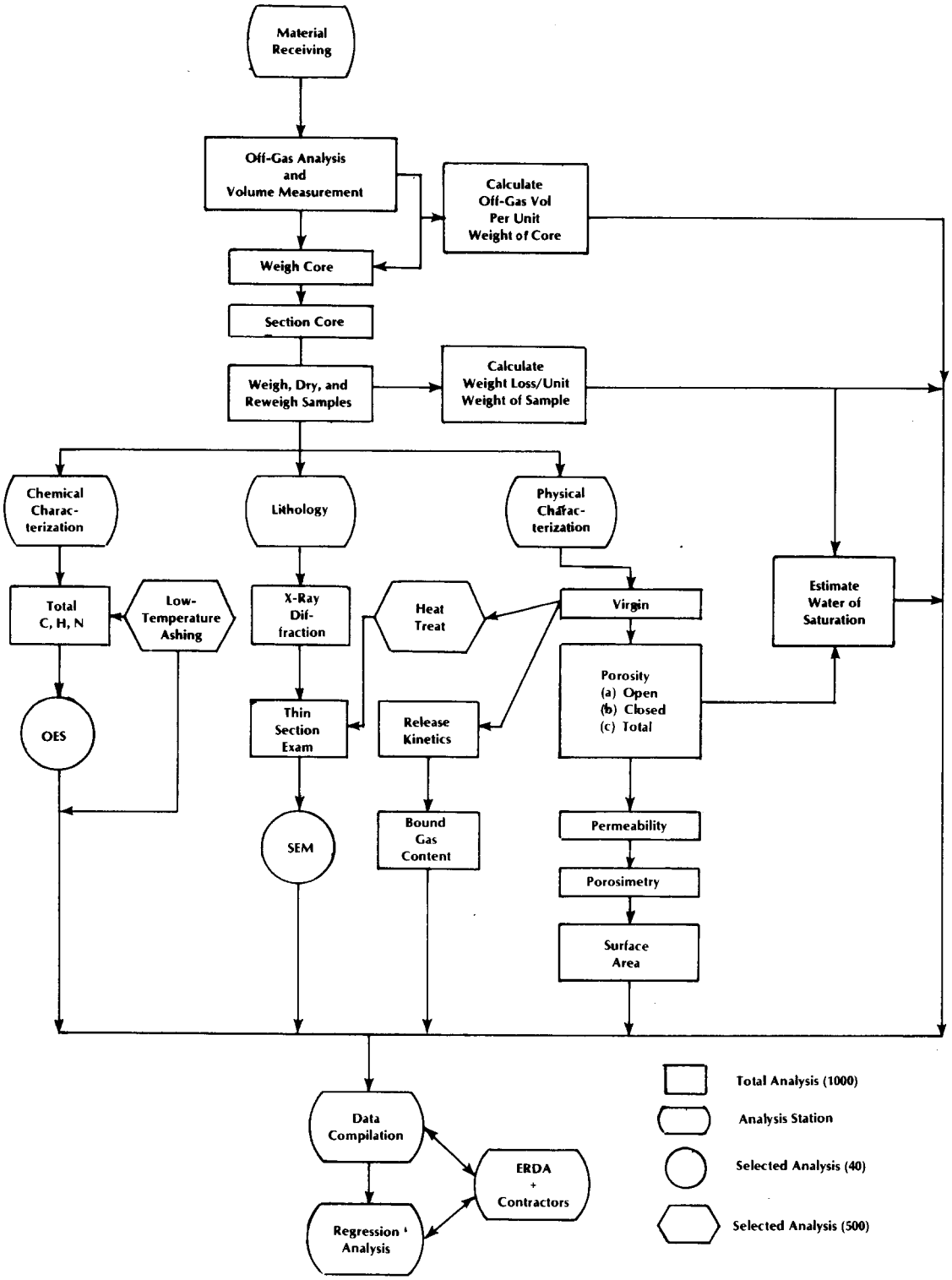

FIGURE 1. PROPOSED ANALYTICAL PLAN FOR GAS SHALE SAMPLES

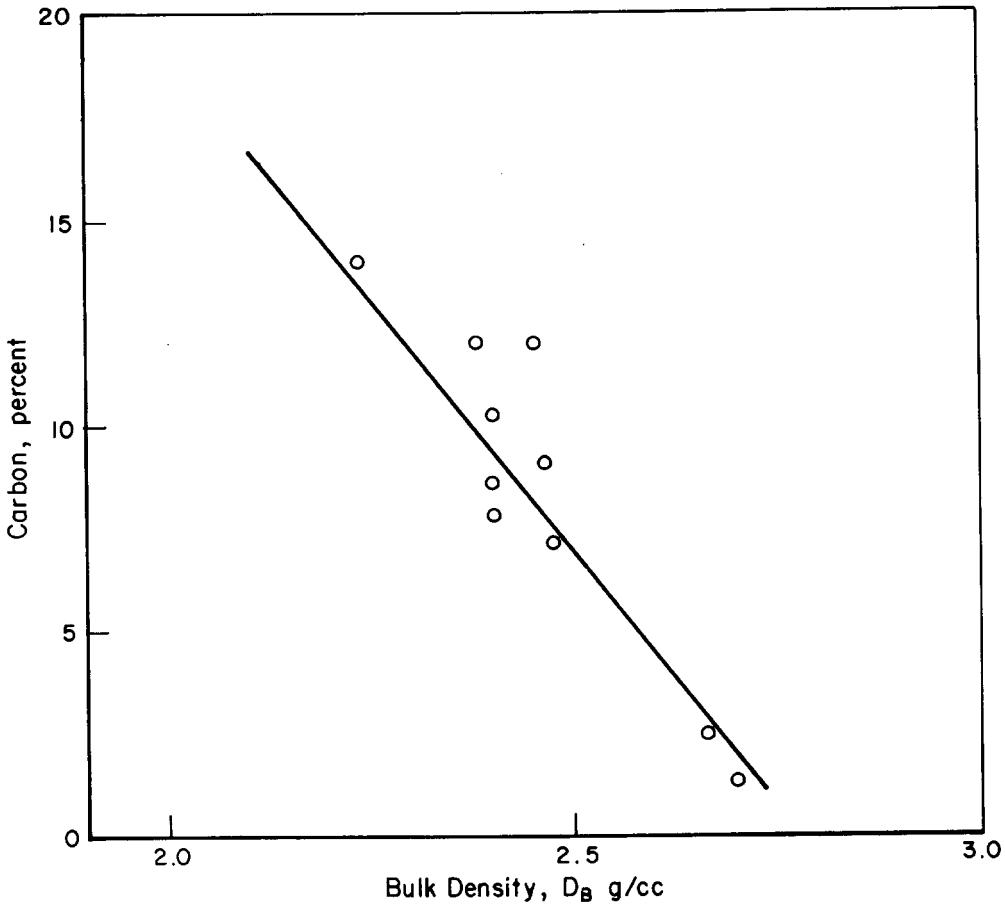

FIGURE 2. CORRELATION BETWEEN THE BULK DENSITY AND CARBON CONTENT OF 0-1 SAMPLES

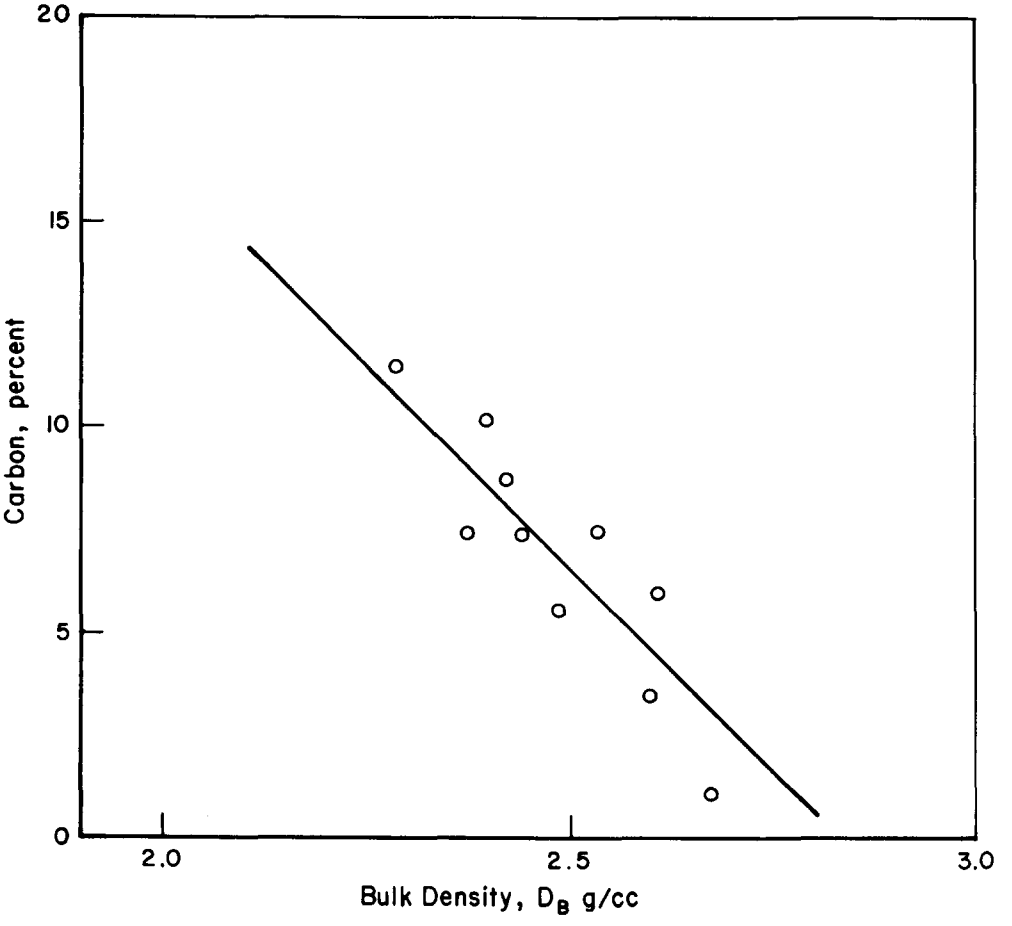

FIGURE 3. CORRELATION BETWEEN THE BULK DENSITY AND CARBON CONTENT OF P-1 SAMPLES

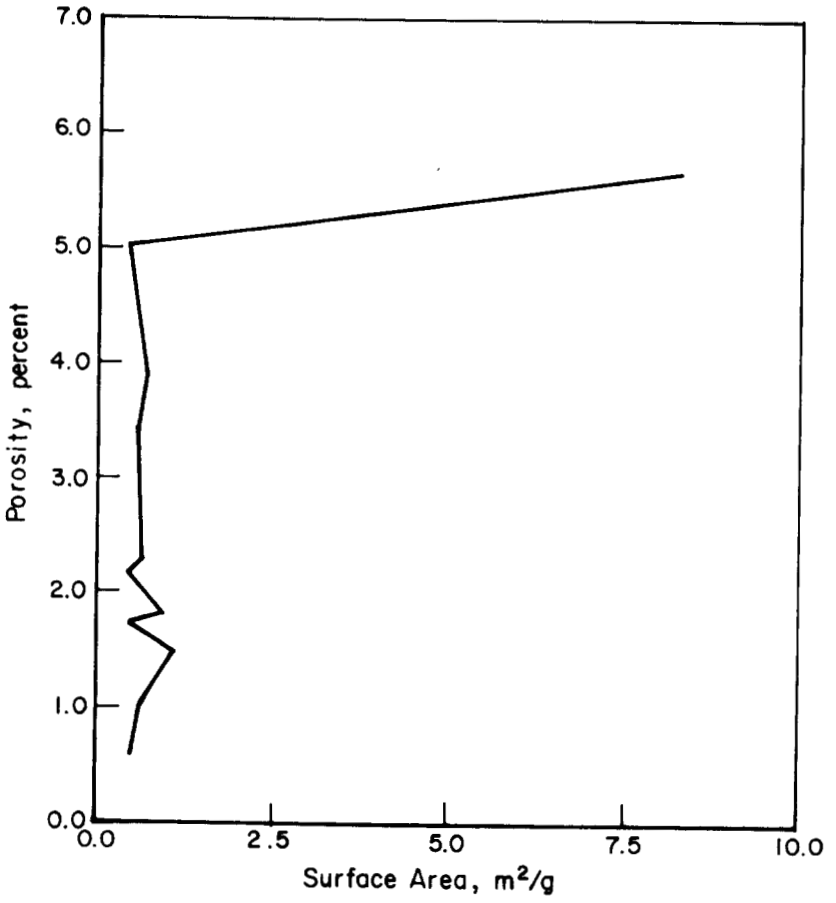

FIGURE 4. CORRELATION BETWEEN THE SURFACE AREA AND POROSITY OF P-1 SAMPLES

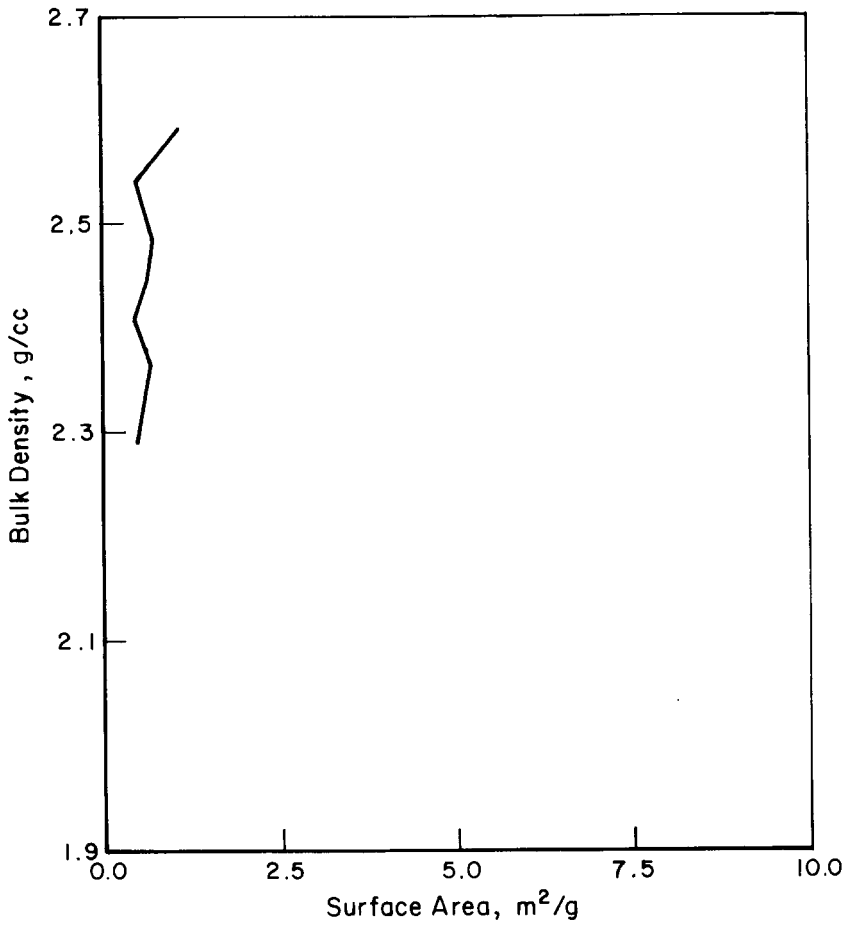

FIGURE 5. CORRELATION BETWEEN THE SURFACE AREA AND BULK DENSITY FOR P-1 SAMPLES

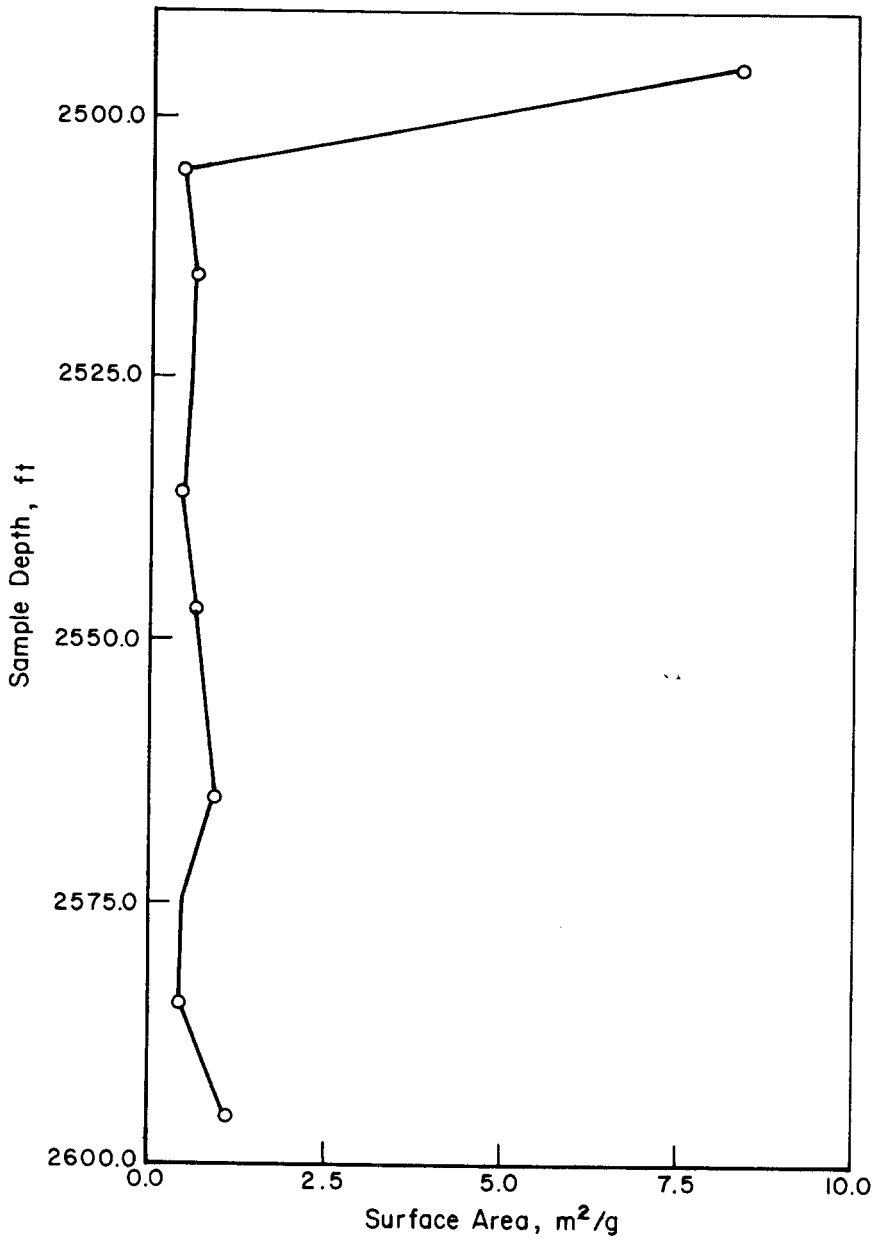

FIGURE 6. SURFACE AREAS AS A FUNCTION OF SAMPLE DEPTH FOR P-1 SAMPLES

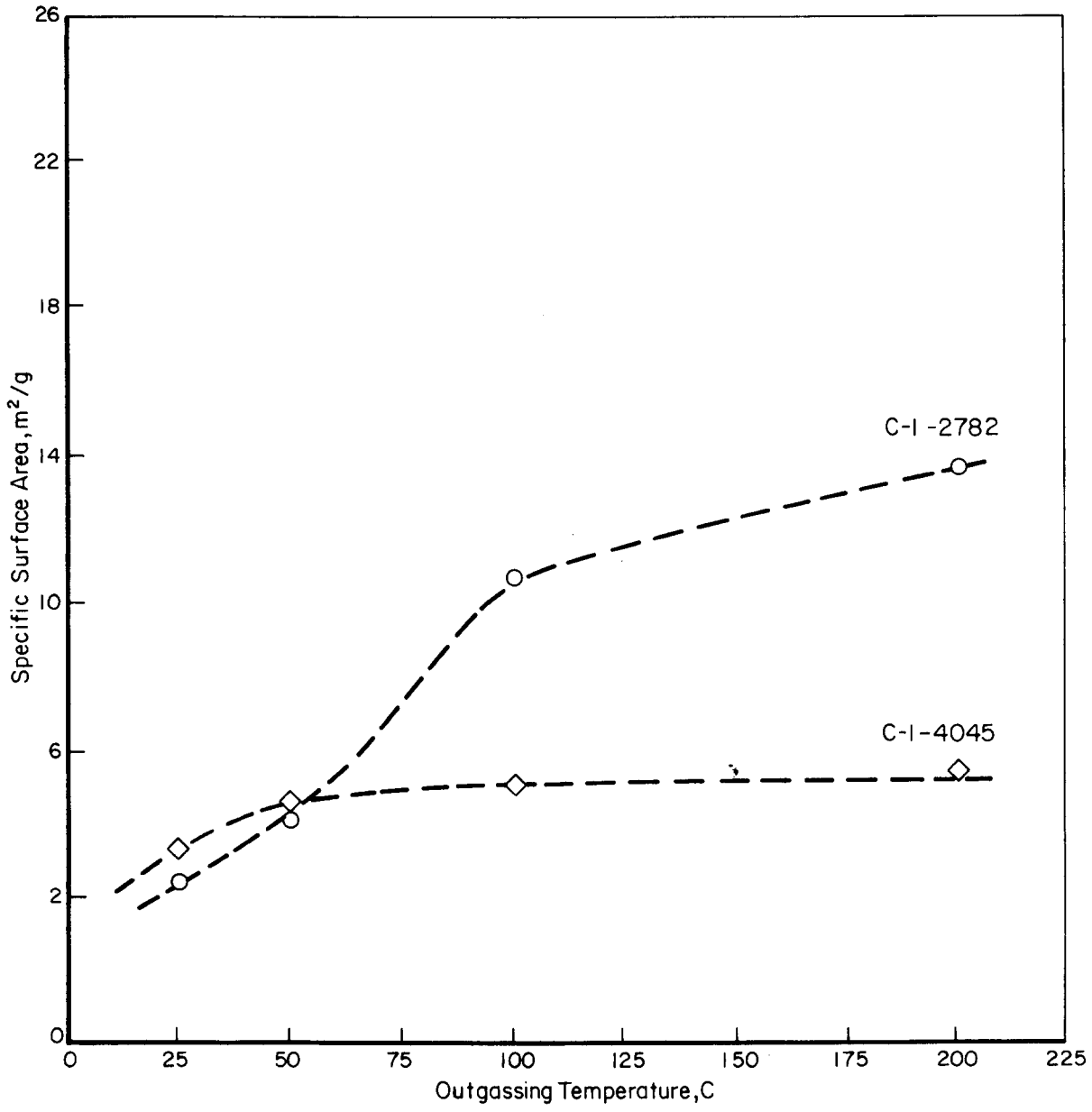

FIGURE 7. EFFECT OF OUTGASSING TEMPERATURES ON THE MEASURED SURFACE AREA VALUES OF TWO SHALE SAMPLES

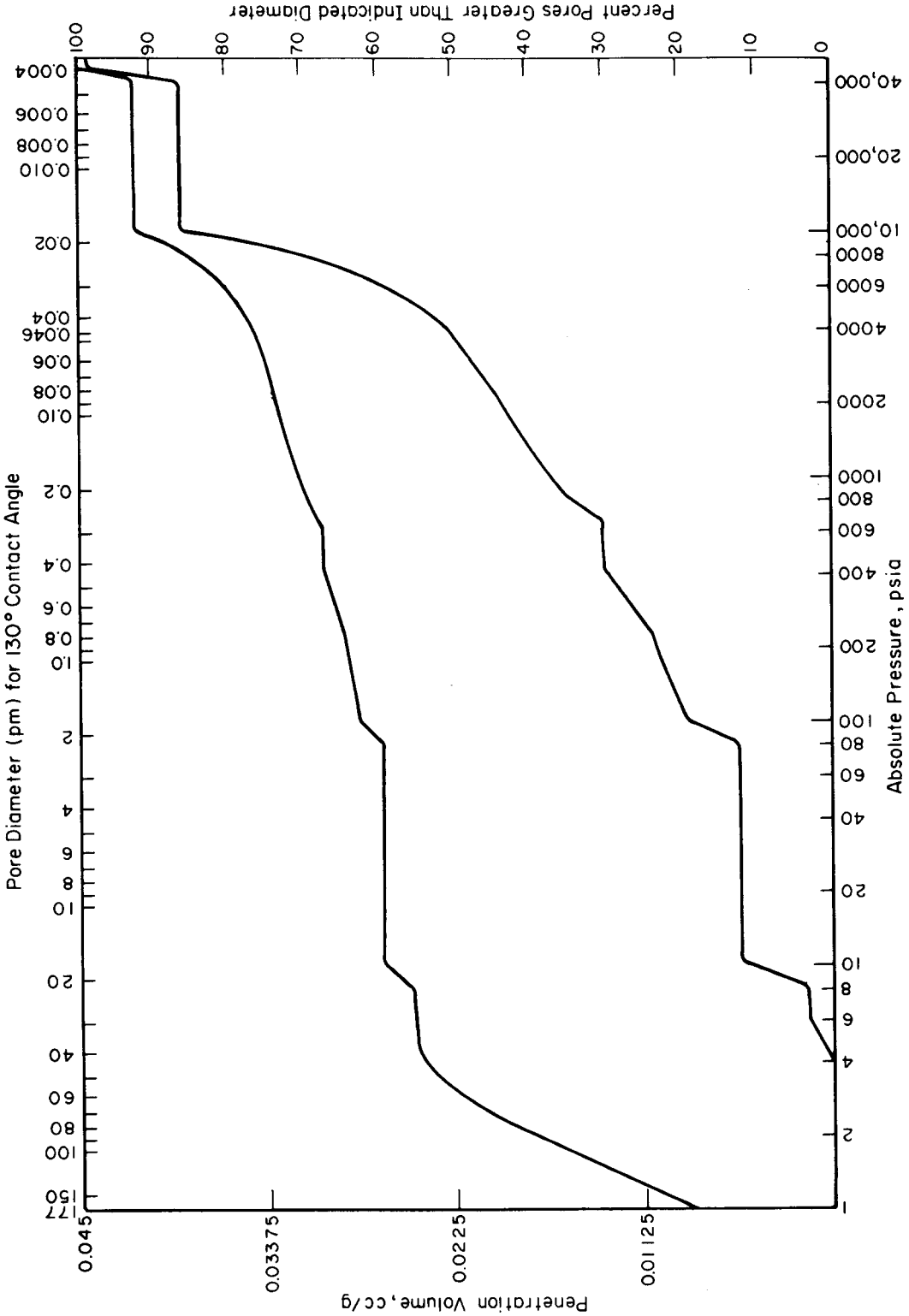

FIGURE 8. PORE VOLUME AND PORE SIZE DISTRIBUTION OF SAMPLE C-1-3651

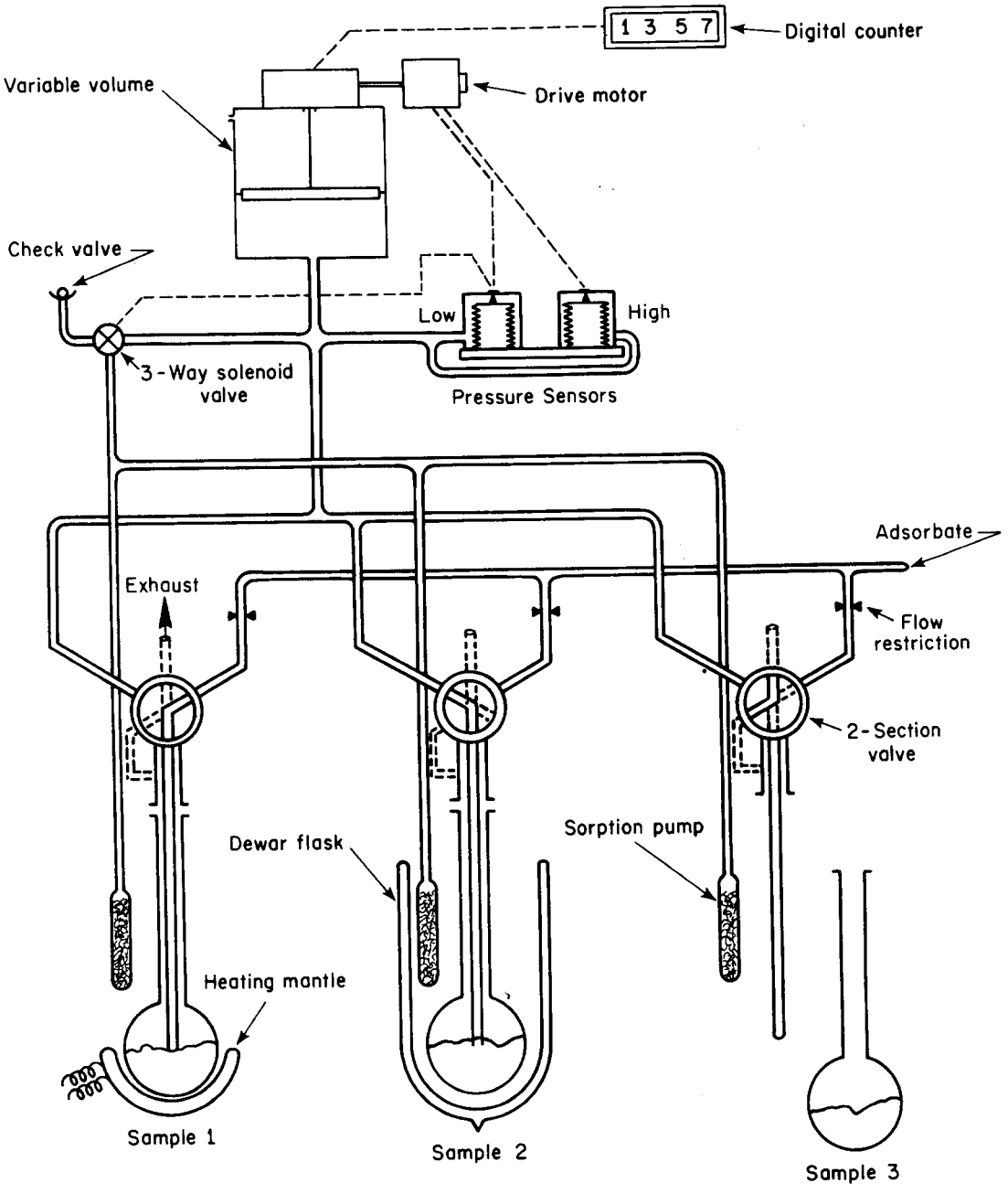

FIGURE A-1. SCHEMATICS OF SURFACE AREA ANALYZER

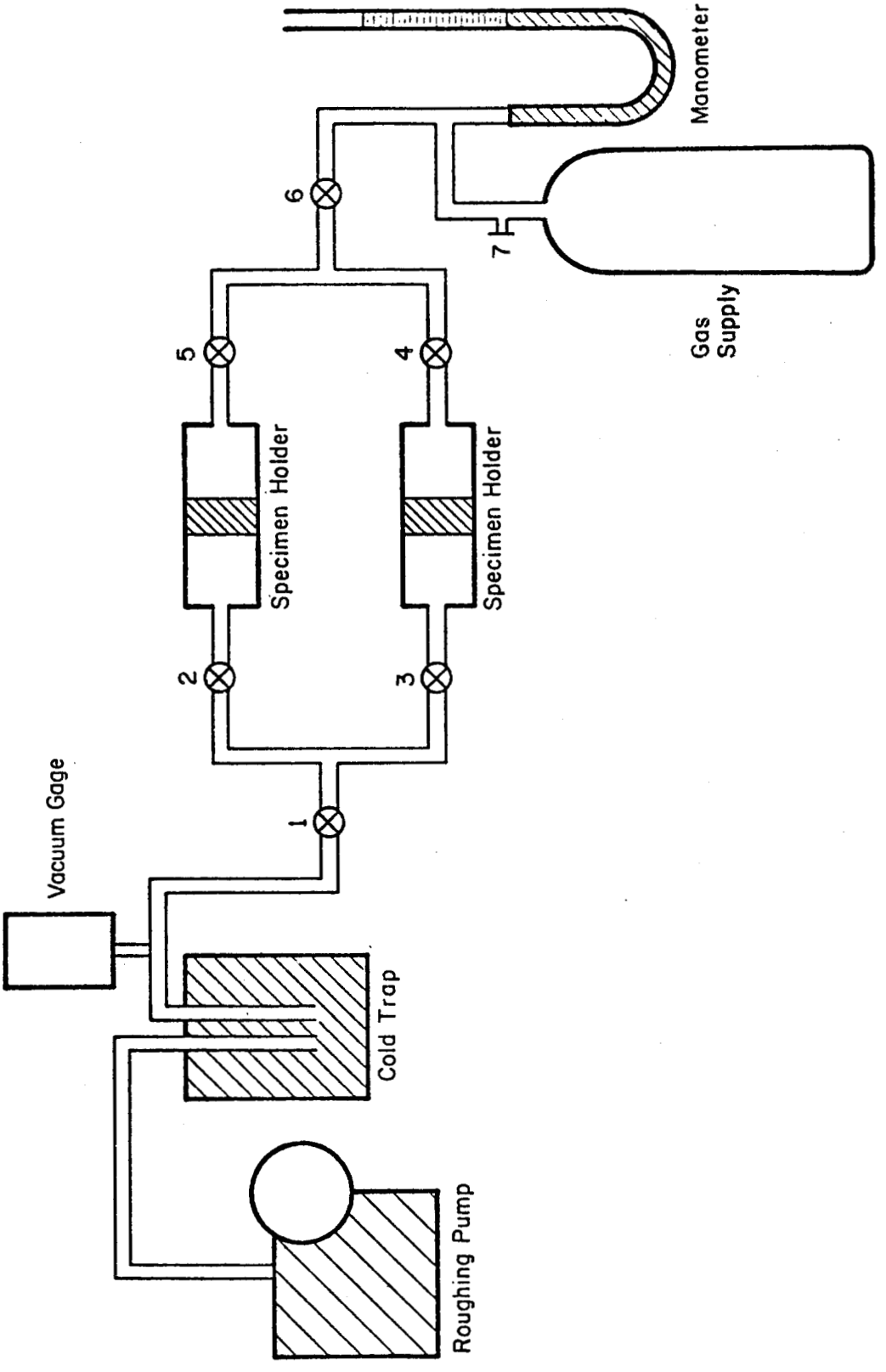

FIGURE A-2. SCHEMATIC DRAWING OF THE PERMEABILITY APPARATUS

NEW DATA FOR URANIUM, THORIUM, CARBON, AND SULFUR IN DEVONIAN BLACK SHALE, FROM WEST VIRGINIA, KENTUCKY, AND NEW YORK*

by

JOEL S. LEVENTHAL
MARTIN B. GOLDHABER
Branch of Uranium and Thorium Resources
U.S. Geological Survey, Denver, CO 80225

ABSTRACT

Data are presented for uranium, thorium, organic carbon and sulfur in Devonian Black Shale. Uranium varies between 1.5 to 38 ppm. This range in part reflects regional trends, but within a given core, values from 1.5 to 15.8 ppm, (Cattaraugus County, New York); 3.2 to 38 ppm, (Perry County, Kentucky); 3.4 to 36.6 ppm, (Lincoln County, West Virginia); 3.4 to 21 ppm, (Jackson County, West Virginia) were noted. Some large concentration changes over short (∿1 ft.) depth intervals were documented.

Thorium is much less variable than uranium with a mean value of 15 ppm, near the mean value of 12 ppm previously reported for more typical marine shale. Both uranium and carbon are generally higher than the average values quoted for shales of 3.7 ppm for uranium and 2.1 percent for carbon.

Uranium is positively correlated with organic carbon and total sulfur. The plots of the carbon, sulfur, and uranium with depth for Perry County, Kentucky, and Jackson County, West Virginia, in particular show a very good correspondence between uranium and carbon. In the Perry County core the uranium and sulfur relationship is not as closely correlated in the upper part of the shale, but becomes so, in the lower portion.

Introduction

As part of the Energy Research and Development Administration's Eastern Gas Shales effort, the U.S. Geological Survey, Branch of Uranium and Thorium Resources has undertaken a program to provide geochemical data on uranium and trace elements in Devonian Black Shale. In this initial report, data obtained from four shale cores are used to:

(1) Present comparitive results on several analytical techniques for uranium and thorium determination

(2) Present data showing the depth variability of uranium within black shale sequences on a range of depth scales of from one inch to several hundred feet

(3) Present data on the interrelationships among carbon, sulfur, uranium, and thorium in these shales.

Subsequent reports will deal with work now in progress on:

(1) Fission track maps and distribution of uranium

*Preliminary version, not edited or reviewed to conform with U.S. Geological Survey standards and nomenclature.

(2) Carbon and sulfur isotopes

(3) Trace elements as related to carbon and sulfur

(4) Types of organic material and relation to uranium

(5) Microprobe studies

(6) Assessment of quantities (geographic and geologic distribution and amount) of uranium and trace elements of economic or environmental interest.

Geologic setting. Organic rich shale deposited in widespread seas west of and marginal to the Appalachian geosyncline in Devonian time is present in the Appalachian, Illinois, and Michigan basins (Conant and Swanson, 1961). The names applied to this shale include: Chattanooga Shale, New Albany Shale, Ohio Shale, Antrim Shale, and Geneseo Shale (see fig. 1). The shale varies in thickness from 20 feet in Tennessee to more than 200 feet in Ohio. It is exposed at the surface in portions of Tennessee, Ohio, and Kentucky and presently is buried up to 5000 feet deep in Virginia and 1500 feet in New York.

These shales are gray to black in appearance with the darker colors frequently corresponding to higher organic carbon content. This darkening, however, does not continue in the range of the highest organic carbon contents ($\geq$ 6%C). Pyrite is conspicuously present as nodules up to 2 inches in diameter, as thin lenses, small euhedral crystals as well as microscopic forms (framboids and single crystals). Marcasite has also been locally noted. Fine layers of chert(?), carbonate, and organic-matter deficient sand and silt have been described. Phosphate is present at the top of the shale as nodules.

The stratigraphy of upper Devonian shales has been intensively studied in Tennessee (Conant and Swanson, 1961) and in Ohio (Hoover, 1960; Lewis and Schwietering, 1971). Recent work by Provo (1977) and Provo, Kepferle, and Potter, (1977) has been directed towards correlation of the Kentucky and West Virginia black shales into the known stratigraphy of Ohio Shale in Ohio and Chattanooga Shale of Tennessee. Of cores discussed in this report, only the Perry County, Kentucky core falls within this new stratigraphic framework. The Perry County core section is equivalent to the complete Chattanooga Shale, showing the three (3) units of the Gassaway member and the two (2) units of the Dowelltown member as follows (see results for sample depths).

Sample No.	Ohio Shale equivalent	Chattanooga Shale equivalent
1-5	Cleveland Shale	u Gassaway
6-7	Three Lick Bed	m Gassaway
8-9	u Huron Shale	l Gassaway
10-13	m Huron Shale	u Dowelltown
14-18	l Huron Shale	l Dowelltown
19-21	Olentangy Shale	----------

Analytical Techniques

Uranium and thorium were analyzed by the delayed neutron technique (Amiel, 1962; Millard, 1976), at the U.S. Geological Survey by Hugh Millard, and co-workers. A subset of these samples was analyzed for uranium and thorium by Dr. William Blackburn at the University of Kentucky by the γ-ray spectrometry method, (Adams, Richardson and Templeton, 1958) for comparison with delayed neutron determinations. Additional samples provided by Dr. A. Barry Maynard, were analyzed for uranium by fluorimetry at Energy Research and Development Administration, Grand Junction, Colorado and for uranium by delayed neutrons, at the U.S. Geological Survey, Denver.

Carbon was determined by the wet oxidation technique (Allison, 1965), at Rhinehart Laboratories, Arvada, Colorado, or by Leco induction furnace combustion by the U.S. Geological Survey, Branch of Oil and Gas Resources. Ash content used to estimate a weight loss upon combustion (WLOC) at ~550°C was measured by U.S. Geological Survey laboratories.

Sulfur was determined by the Leco induction furnace technique by Van Shaw at the U.S. Geological Survey, Denver.

Analytical precision. Analyses were made on duplicate samples to check reproducibility of the delayed neutron technique for thorium and uranium determination. Three samples were crushed and split, using a sample splitter into two separate aliquots each for analysis. Analyses were performed concurrently (table 1). The thorium difference between splits ranges from ∿9% to ∿30% with a mean difference of ±8% between samples. The uranium reproducibility is considerably better and ranges from 1% to 5% with the mean at ∿±2%.

Eleven pairs of samples were analyzed at the same time (table 2). These samples were not split in a splitter, but the 10 gram samples of rock powder and chips (¼ inch) were taken from the same core depth. These results show uranium variations between splits generally in the range of ±3%, which is the same as the quoted analytical precision from counting statistics. The thorium results show poorer agreement, generally in the range of ±10%.

Nineteen additional pairs of split samples were analyzed (table 3). These represent 10 gram portions from the same piece of core (but not homogenized splits). The analyses were performed at two different times. The results listed first for each pair represent samples analyzed in one group, and the second number corresponds to a second group of analyses.

The difference between one sample group and the other follows no systematic pattern. The thorium reproducibility within pairs is from 5% to 100%; most values in the ±15-20% range. The uranium difference is 0-20%, (one sample 30%) most falling into the ±3-5% range. Some portion of the imprecision with this suite may simply reflect minor sample heterogeneity.

The samples showing poor agreement in thorium values between splits generally occur when the thorium/uranium ratio is 1.10 or less (indicated by a √ in table 3). This is due to the uranium masking the small thorium signal (H. Millard, oral communication, 1977). This effect will be further discussed below.

Intercomparison of analytical techniques. There are several research groups measuring uranium (and thorium) in the black shales by different techniques. In order to better compare results, it is advantageous to intercalibrate among these techniques. The comparison with fluorimetry is especially significant as earlier work in the 1950's by the U.S. Geological Survey and others was done primarily by fluorimetry, whereas presently the delayed neutron technique is used by the U.S. Geological Survey. A suite of ten samples was analyzed for uranium by fluorimetry (ERDA, Grand Junction, Colorado) and delayed neutron counting (U.S. Geological Survey, Denver, Colorado) (table 4). The agreement is generally within ±10%; which we consider satisfactory.

Some analyses by γ-ray spectrometry for both thorium and uranium were made at the University of Kentucky, Department of Geology by Dr. William Blackburn. The results are compared with delayed neutron determination (table 5). The agreement for uranium is again generally within ±10%. In the case of thorium, however, there are serious discrepancies: U.S. Geological Survey sample nos. 17, 11, 6, and 2 are the only ones falling within ±20% of the γ-ray data; sample nos. 16, 13, and 9 are greater than 50% different, with the remaining samples falling within 20-50% range. The resulting thorium/uranium values, therefore, show poor agreement between the two techniques. It has been suggested that the preferred analytical technique for uranium is delayed neutrons (Stuckless and others, 1977). In these sets of samples, however, both fluorimetry and γ-ray spectrometry are satisfactory.

Problems arise in the delayed neutron analysis of thorium when the thorium/uranium value is less than 1 as noted above. Most rocks, other than uranium ores, have the thorium/uranium values near 3 and delayed neutron technique supplies adequate data although the γ-ray technique is superior.

Results and discussion

Analytical determinations of uranium, thorium, (and for selected samples) organic carbon, weight loss on combustion, and sulfur were made on samples of black shale from four localities. These results are presented below.

Perry County, Kentucky. The analytical data for Perry County (Kentucky core well no. 7239) are summarized in table 6. The 21 samples were taken at as close to 20 foot intervals as permitted by available core material. Uranium content varies widely from 3.2 to 38 ppm whereas thorium shows a more restricted range of from 11 to 22 ppm with a majority of results falling in the range of 14 ± 3 ppm. Furthermore, a number of data points at the extreme low and high end are just those which are subject to a large thorium uncertainty. The thorium/uranium ratio is dominantly influenced by

the uranium variation. Organic carbon results fall between 0.2 to 12.9%, with a mean value of 4.3%. The sulfur content ranges from 0.08% to 6.36% with a mean of 2.3%.

Figure 2 shows the uranium, carbon, sulfur, thorium, and thorium/uranium data for the Perry County core plotted versus depth. It can clearly be seen that uranium and carbon covary throughout the core, whereas for uranium and sulfur the positive relationship is well developed only below 2570 feet. The thorium data remain relatively constant, although the thorium/uranium varies considerably due to changes in uranium. Low organic carbon and high thorium/uranium values may serve as geochemical indicators of lithologies other than black shale such as the Three Lick Bed (sample 6) and the Olentangy Shale (samples 19-21).

Jackson County, West Virginia. Analyses for uranium, thorium, and carbon are summarized in table 7 and figure 3 for samples from Jackson County, West Virginia (Cottageville well 12041). Thorium values range from 12.0 to 19.0 ppm with only one sample outside the range 15 ± 3 ppm. Uranium content varies from 3.4 to 21 ppm, and carbon from 0.1 to 5.6%. Figure 3 shows the carbon, uranium, and thorium/uranium variations with depth. As with Perry County, the carbon and uranium are strongly correlated. Sulfur and (WLOC) data are given separately in table 8.

Lincoln County, West Virginia. Uranium, thorium and thorium/uranium ratio determinations are given for Lincoln County, West Virginia (well 20402) in table 9. The data represent three discontinuous shale intervals. Data for WLOC and sulfur are presented in table 8.

Cattaraugus County, New York. The results of uranium, thorium, and thorium/uranium determinations for the Cattaraugus County, New York core (West Valley NX-1, well 31-009-06740) are summarized in table 10. The data for organic carbon, WLOC and percent sulfur are given in table 11. This core is not all of upper Devonian age. A report by W. de Laguna (1972) describes the core; work in progress by Art Van Tyne (N.Y. State Geological Survey) and Wallace de Witt (U.S. Geological Survey) will help in assigning stratigraphic relations since the core probably represents more than only upper Devonian age rocks. The black shale units are in the depth intervals 920-958 and 1313 to 1520 feet (de Laguna, 1972).

Variability of uranium content over short depth intervals. To better understand the details of the uranium distribution, a sufficient number of samples must be analyzed to discern variations both stratigraphically and regionally. Early work by Swanson and Kehn (1955) reported "uniform" uranium (70-90 ppm) in forty-seven vertically spaced (3/4 to 2 1/2 inch intervals), samples from the upper Gassaway member of the Chattanooga Shale. These authors also reported a similar uranium content in samples taken over a geographic distance of approximately 1 mile. Kehn, (1955) reported a range of 6 to 110 ppm uranium for the Chattanooga Shale, the former value from the organically poor upper Dowelltown member, and the latter from the upper Gassaway member. The Gassaway member contains averages of 50-68 ppm uranium for forty-nine cores and the upper Gassaway unit shows even higher averages of 60-90 ppm uranium.

From the standpoint of resource evaluation, these data are probably satisfactory for central Tennessee (Mutschler and others, 1976). However, modern instrumental methods are capable of much better precision than the 70-90 ppm which was considered "uniform" due to ± 10 ppm error in the uranium determinations in the early 1950's.

In order to examine the question of short range uranium variability we have analyzed two types of samples; those which contain obvious short range color or textural changes, and those which appear visually homogeneous. Samples from the Cattaraugus County, New York, core were analyzed based upon the first of these criteria. The results (table 12) show that in general the uranium content changes markedly with observable lithologic transitions, as expected. The samples (table 12), that were the darker color showed higher uranium content. Variations of up to a factor of 2 between adjacent samples were noted. These larger changes typically were associated with striking color transitions.

The results for short sampling intervals in more homogeneous appearing core, intervals are contained in tables 13-16.

Several groups of samples from the West Virginia cores were taken over intervals of approximately 1 foot. Table 13 gives Jackson County, West Virginia data for two such intervals spanning 3514-15 feet and 3232-33 feet. The results in table 13 show uranium values of 10.2 to 20.4 ppm; however, only two samples (containing 10.2 and 12.1 ppm) are far from the general range observed with this sample suite of 16.6 to 20.4 ppm. The latter interval shows a jump from 11.8 to 6.3 ppm and then a gradual trend to 4.3 ppm.

Tables 14, 15, and 16 show similar suites of samples from Lincoln County. The samples beginning at a depth of 3001 feet (table 14) show a trend of decreasing uranium from 8.9 to 4.4 ppm over a depth interval of one foot. A trend of irregularly increasing uranium (from 5.2 to 8.3 ppm) with depth is suggested by results in table 15. Table 16 similarly shows systematic trends with depth. Especially interesting are samples L-3956, and L-3965. These individual samples are several feet above or below the 3961-3962 foot suite of closely spaced samples and show uranium values different by a factor of 2 from the 3961 suite.

Uranium and carbon relationship. A number of previous investigators have stressed that a positive correlation exists between uranium and organic carbon content (Swanson, 1960 and 1961; Breger and Brown, 1963). As previously discussed, our data likewise exhibit such a positive correlation (figs. 4, 5, 6, and 7). [Weight loss on combustion, WLOC, (equal to 100% -% ash) is closely related to organic carbon (fig. 8), and therefore, WLOC is also necessarily correlated with uranium (figs 9 and 10). Only Perry County samples were analyzed for both organic carbon and WLOC (fig. 8) for samples in the other cores either WLOC or organic carbon were measured but not both.]

We have fit a linear least squares regression equation to our uranium-carbon data according to the relationship, y=mx+b, where; x=carbon percentage, m=slope, y=uranium in ppm and b is the intercept (U value at zero C). The quantity r^2 is a measure of goodness of fit of the data to a straight line (perfect fit=1). A linear carbon-uranium dependance as opposed to some other formulation, was chosen on the basis of visual inspection of the plotted data.

Whole core

	b	m	r^2
Perry County, Kentucky	-6.2	5.0	0.44
Jackson County, West Virginia	3.1	3.2	0.84
Cattaraugus County, New York	2.5	3.2	0.76
Closely spaced intervals			
Jackson County, West Virginia	2.2	5.0	0.93
Lincoln County, West Virginia	2.0	4.0	0.92

Values for Jackson and Lincoln Counties, West Virginia for closely spaced samples were taken to emphasize short range uranium variation and therefore, do not necessarily reflect the entire core. The high r^2 value for these analyses is probably due to this choice of samples and illustrates the extremely close correlation of uranium and carbon in a more limited facies of the black shale.

Another type of correlation was shown in figures 2 and 3 of the Perry County, and Jackson County, where the data is displayed with depth. Here the covariance of the uranium and organic carbon down the core is striking. The two sets of data show the relationship where a change of one percent in organic carbon corresponds to a change of approximately 5 ppm in uranium.

Our data on short range variations seems to add complexity to the uranium vs. carbon relationship. The pairs (and groups) of samples from New York showed marked variation when there were lithology changes (table 12), and the uranium contents did covary with the organic carbon (table 11). The New York samples were rather low in uranium content (all but three less than 8 ppm) and organic carbon.

On the other hand, some samples in the West Virginia cores showed marked changes in uranium when no visible change in the sample lithology was obvious, but the organic carbon measurement again generally correlated with the uranium change. These effects were true for samples in the range of 5-10 ppm and 15-20 ppm uranium.

A higher value of m (slope) indicates more uranium incorporated for the same amount of carbon. Thus Perry County, Kentucky has a higher uranium/carbon ratio than the New York core. Further work (in progress) will consider these uranium/carbon ratios for other upper Devonian shales as well as modern environments to understand whether this ratio is dependent on distance from or type of source of uranium, type of organic matter, diagenesis or other variables, such as sulfur.

The carbon and sulfur data for Perry County are plotted in figure 11. As pointed out previously, these elements are related for many samples. The sulfur vs uranium data for the Kentucky West Virginia and New York samples are plotted in figures 12 and 13.

It appears that the concentration of uranium is related to both the organic carbon and sulfur contents.

Thorium content of black shales. Brown (1975) reports results of work up to 1962 which includes data on thorium in the Chattanooga Shale from east central Tennessee. The range for the Gassaway member is 6.8 to 11.0 ppm thorium and the weighted average of 24 analyses was 8.6 ppm. For the Dowelltown member, the thorium range was higher (9.5 to 12.5 ppm) and the weighted average of 18 analyses was 10.7 ppm.

Our measurements of thorium show much less variability than uranium both within and between cores. The mean value for thorium in all our samples is 15.2 ppm which is not far from the 12 ppm reported (Turekian and Wedepohl, 1961) as average for shales. The thorium/uranium ratio varies considerably in our sample from 0.4 to 5.3. Generally the higher values are not black shale facies such as the Three Lick Bed in Perry County, or the green or gray shale in the upper portion of the New York core. Figure 14 shows that the thorium/uranium ratio was related to the organic carbon. These observations seem to confirm the earlier suggestions of Adams and Weaver (1958). However, this relationship is really only a result of the uranium variation, since the thorium is relatively constant.

In view of the relative constancy of the thorium data, the large variations in thorium/uranium ratio reflect mainly the effect of uranium variations. These data are plotted, versus organic carbon in figure 14 and illustrate the systematic decrease in thorium/uranium ratio with increasing carbon (and therefore uranium) content. Thorium/uranium ratios have been used as indicators of sedimentary processes (Adams and Weaver, 1958). They used gamma-ray spectrometry to determine thorium and uranium contents of sedimentary rocks. Thorium/uranium ratios range from 0.02 to 21, when the uranium ranges from 0.1 to 250 ppm and the thorium from 0.1 to 132 ppm. Ratios in oxidized continental deposits are generally above seven, whereas marine deposits usually have ratios below seven. In earlier work, Koczy (1949) and Hurley (1956) have suggested that the thorium/uranium ratio should decrease as the distance from shore increased.

The restricted data for 18 black shales (Adams and Weaver, 1958) gives U=1.4-80 ppm (mean 10.5 ppm), Th=1.6-28 ppm (mean 13.4 ppm) and Th/U=12.0-0.07 (mean 1.28). Results from analysis of 52 green and gray shales show 1.1-12 ppm uranium (mean 3.2 ppm U), 0.2-47 ppm thorium (mean 13.1 ppm Th) with thorium/uranium values from 11 to 0.7 with a mean of 4.9. Thus the black shales do show a lower thorium/uranium ratio which is due to enrichment in uranium. The thorium content of shales varies much less than the uranium content. The uranium and thorium values depend on variable uranium contents which are controlled by the selective leaching from or enrichment into the rocks. The black shales show the enrichment of uranium to a greater degree than the green and gray shales probably as a result of the increased levels of organic matter.

Summary

Uranium, thorium, carbon and sulfur have been measured in cores of Devonian Black Shale from New York, West Virginia, and Kentucky. The average values for the entire cores are generally in the range of 10-20 ppm and 2-5 percent respectively, however, the Kentucky values are somewhat higher and the New York values lower. These values are less than half of the uranium and carbon concentrations reported for central Tennessee. These data seem to indicate lower uranium as one gets farther from Tennessee.

The covariance of uranium and carbon is observed for all samples, but the uranium to carbon ratio is not constant. Short range variations in uranium content over one foot intervals are observed. Both of the above observations indicate that our knowledge of the relationship between uranium and its source and the various types of organic matter and other reductants is incomplete.

References cited

Adams, John A. S., and Weaver, Charles E., 1958, Thorium-to-uranium ratios as indicators of sedimentary processes: example of concept of geochemical forces. Bull. Amer. Assoc. Pet. Geol., v. 42, p. 387-430.

Adams, J. A. S., Richardson, J. E., and Templeton, C. C. (1958). Determination of Th and U in sedimentary rocks by two independent methods. Geochim Cosmochim Acta, v. 13, p. 270.

Allison, L. E., 1965, Organic Carbon, in Methods of Soil Analysis. Ed. by C. A. Black, Am. Soc. Agron, Madison, Wisconsin. Monog. no. 9, 1367-78.

Amiel, S., 1962, Analytical application of delayed neutron emission in fissionable elements. Anal. Chem., v. 34, p. 1682-1686.

Bates, T. F., and Strahl, E. O., 1957, Mineralogy, petrography and radioactivity of representative samples of Chattanooga shale. Geol. Soc. Amer. Bull., v. 68, p. 1305-1314.

Breger, I. A., and Brown, A., 1962, Kerogen in the Chattanooga shale. Science, v. 137, p. 221-224.

_____, 1963, Distribution and types of organic matter in a barred marine basin. Annal. N. Y. Acad. Sci., v. 25, p. 741-755.

Brown, A., 1975, Preliminary report on the economic potential of the Chattanooga shale in Tennessee. Data as of 1962. With a section on precision of uranium determination by Irving May. U.S. Geological Survey open-file report no. 75-135, 303 p.

Conant, L. C., and Swanson, V. E., 1961, Chattanooga shale and related rocks of central Tennessee and nearby areas. U.S. Geological Survey Prof. Paper 357, 91 p.

Degens, E. T., 1965, Geochemistry of Sediments, Prentice-Hall, Englewood Cliffs, N. J., 321 p.

de Laguna, W., 1972, Hydraulic fracturing test at West Valley, New York. ORNL-4827, 64 p.

Hoover, K. V., 1960, Devonian-Mississippian shale sequence in Ohio. Ohio Geol. Surv. Inf. Circ. 27, 154 p.

Hurley, P. M., 1950), Direct radiometric measurement by gamma ray scintillation spectrometer of uranium, thorium and potassium. Bull. Geol. Soc. Amer., v. 67, p. 395-412.

Koczy, F. F., 1949, The thorium content of Cambrian alum shales of Sweden. Sveriges Geol. Unaersok, Sev C, Avhanale och Uppoat, no. 509, Arsbok 43, 12 p.

Lewis, T. L., and Schwietering, J. F., 1971, The distribution of the Cleveland black shale in Ohio. Geol. Soc. Amer. Bull., v. 81, p. 3477-3482.

Millard, H. T., Jr., 1976, Determination of uranium and thorium in U.S. Geological Survey standard rocks by the delayed neutron technique in U.S. Geological Survey. Professional Paper 840, ed. by F. J. Flanagan. p 61-66.

Mutschler, P. H., Hill, J. J., Williams, B. B., 1976. Uranium from the Chattanooga shale. Some problems involved in development. U.S. Bureau of Mines Information Circular 8700, 85 p.

Provo, L. J., 1977, Stratigraphy and sedimentology of radioactive Devonian-Mississippian shales of the central Appalachian basin. Final report U.S. Energy Research and Development Administration. Contract A8(05-1)-1650. 102 p.

Provo, L. J., Kepferle, R. C., Potter, P. E., 1977. Three Lick Bed: Useful stratigraphic marker in the Upper Devonian shale in eastern Kentucky. ERDA-MERC/CR-77-2. 55 p.

Stuckless, J., Millard, H., Bunker, C., Nkomo, I., Rosholt, J. Bush, C., Keil, R., 1977. Comparison of some analytical techniques for determining uranium, thorium and potassium in granitic rocks. Jour. Res., U.S. Geol. Surv., v. 5, p. 83-91.

Swanson, V. E., 1960, Oil yield and uranium content of black shales. U.S. Geological Survey Prof. Paper 356-A, p. 1-44.

_____, 1961, Geology and geochemistry of uranium in marine black shales. U.S. Geol. Survey Prof. Paper 356-C, p. 67-112.

Swanson, V. E., and Kehn, T. M., 1955, Results of 1952-53 sampling of Chattanooga shale in Tennessee and adjacent states. U.S. Geol. Survey, TEI, 366-98 p.

Szalay, A., 1964, Cation exchange properties of humic acids and enrichment of UO_2^{+}. Geochim et Cosmochim Acta, v. 28, p. 1605-1614.

Turekian, K. K., and Wedepohl, K. H., 1961, Distribution of elements in some major units of the Earth's crust. Geol. Soc. Amer. Bull., v. 72, p. 175-191.

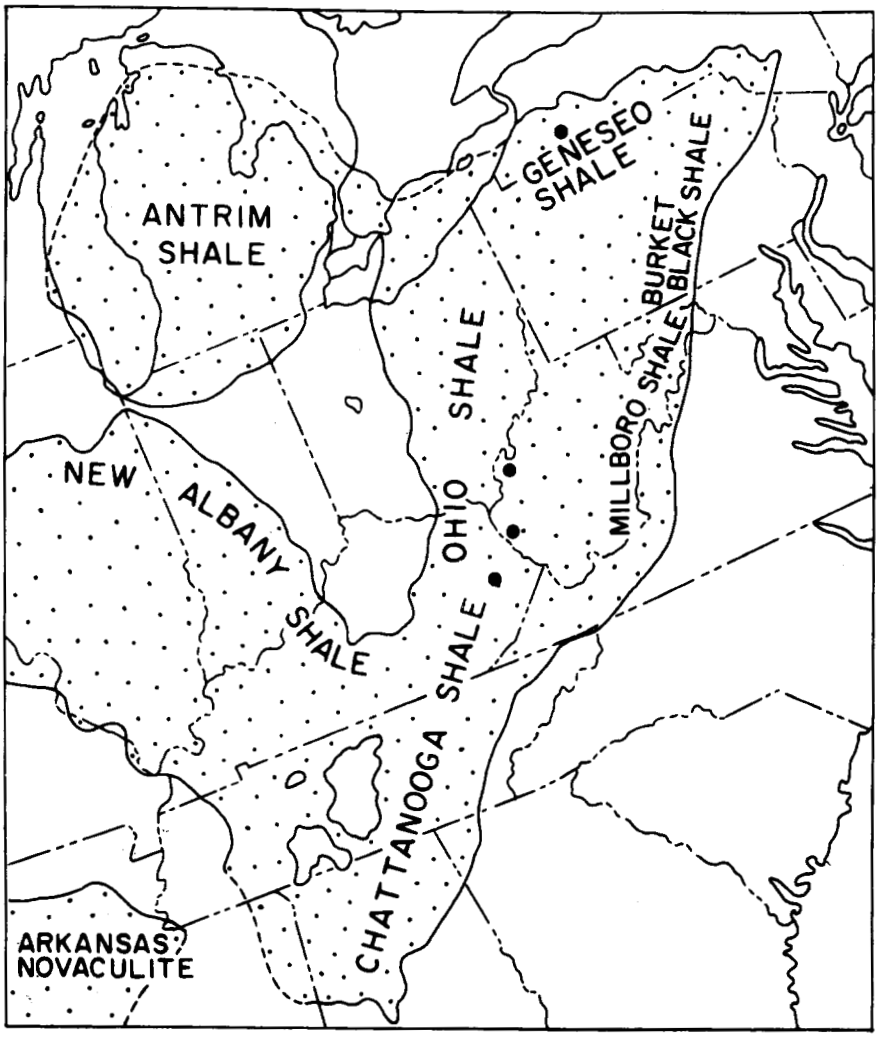

Figure 1. Map showing regional distribution of Upper Devonian black shale in eastern U.S, [after Conant and Swanson (1961) and Provo, Potter and Kepferle (1977)]

Figure 2. Chemical data (U, C, S, Th) for Perry County, Kentucky, core showing variation with depth.

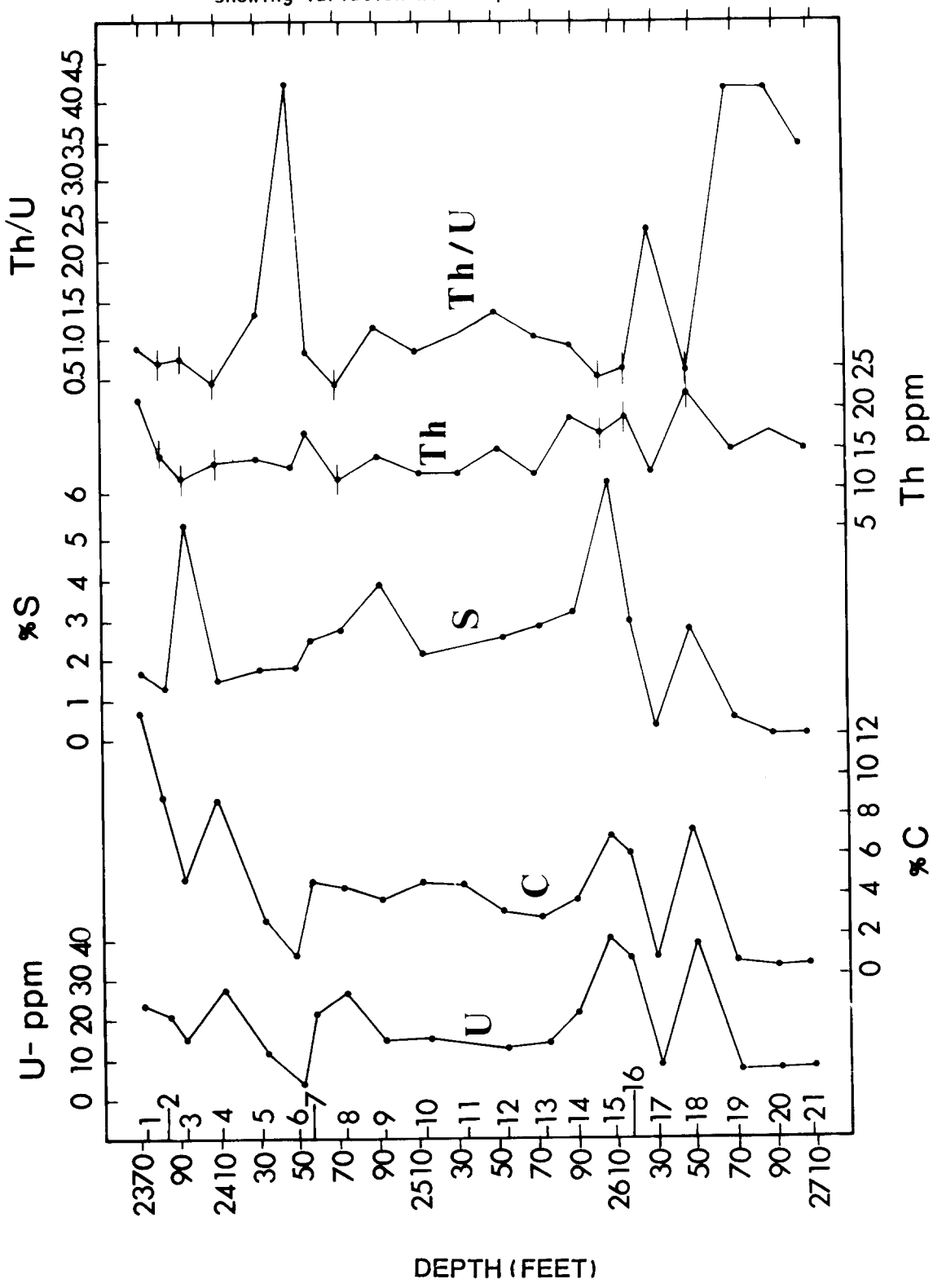

192

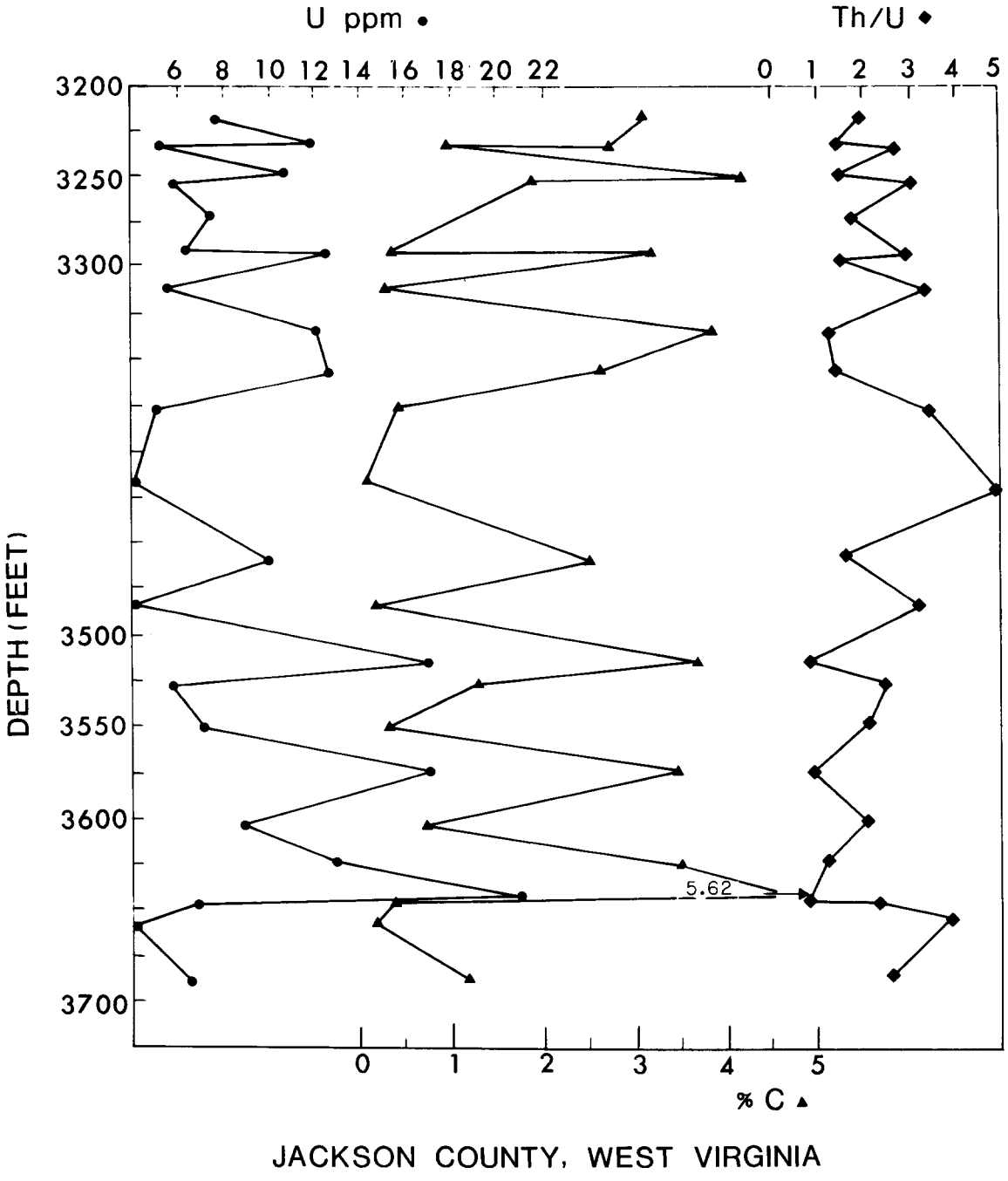

Figure 3. Chemical data (U, C, Th/U) for Jackson County, West Virginia, core showing variation with depth.

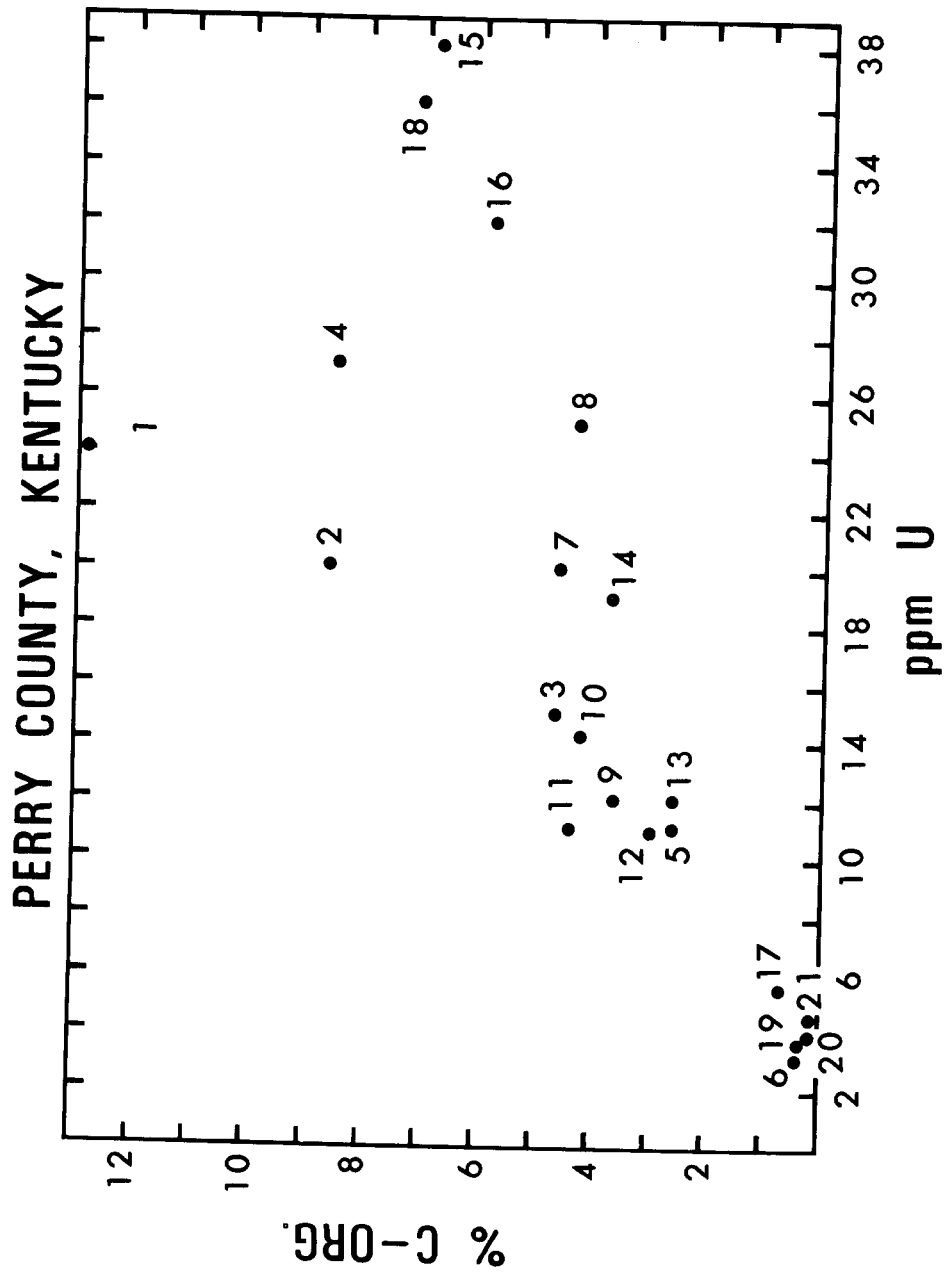

Figure 4. Perry County, Kentucky, % C vs ppm U., numbers are samples identified on Table 6.

Figure 5. Jackson County, West Virginia, % C vs ppm U, numbers are depths.

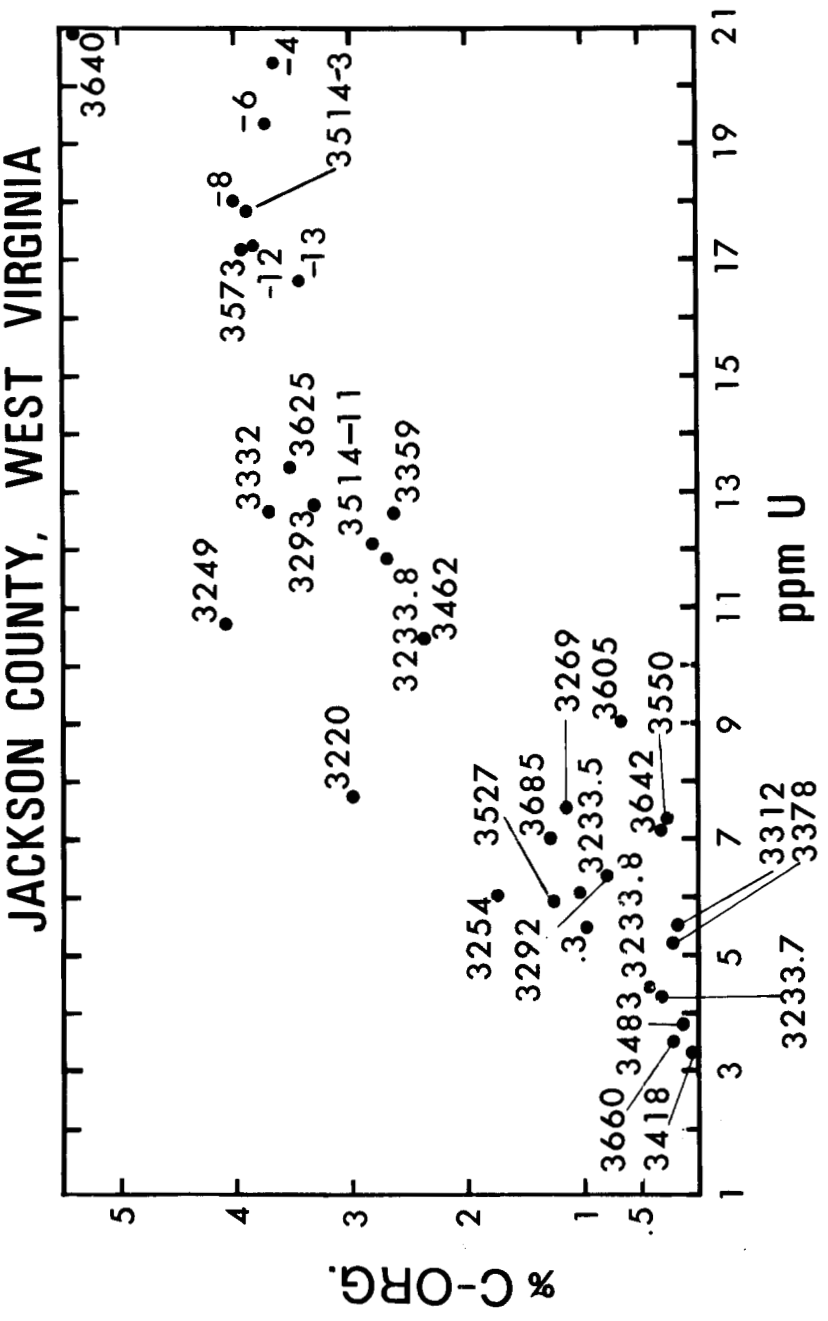

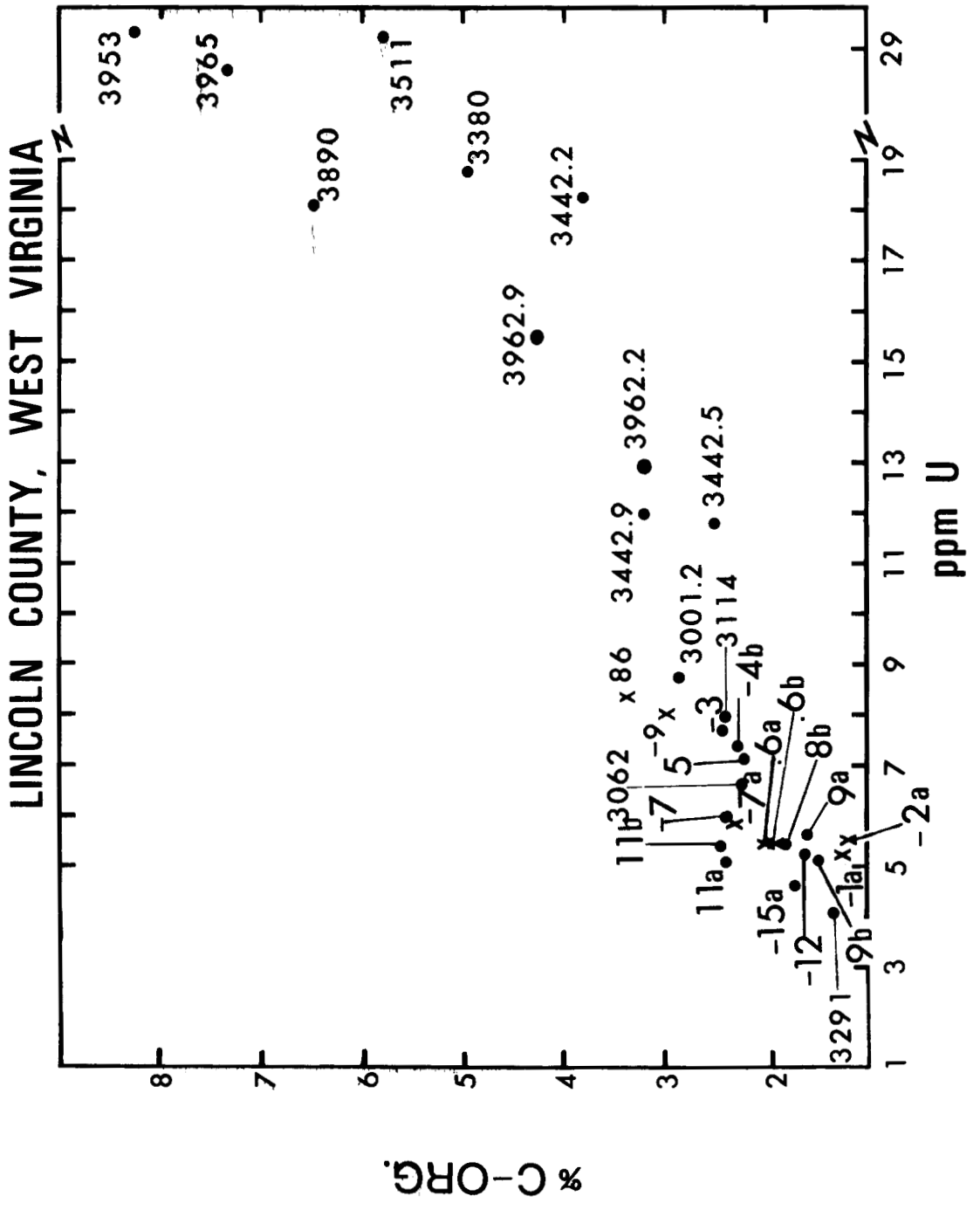

Figure 6. Lincoln county, West Virginia, % C vs ppm U, numbers are depths.

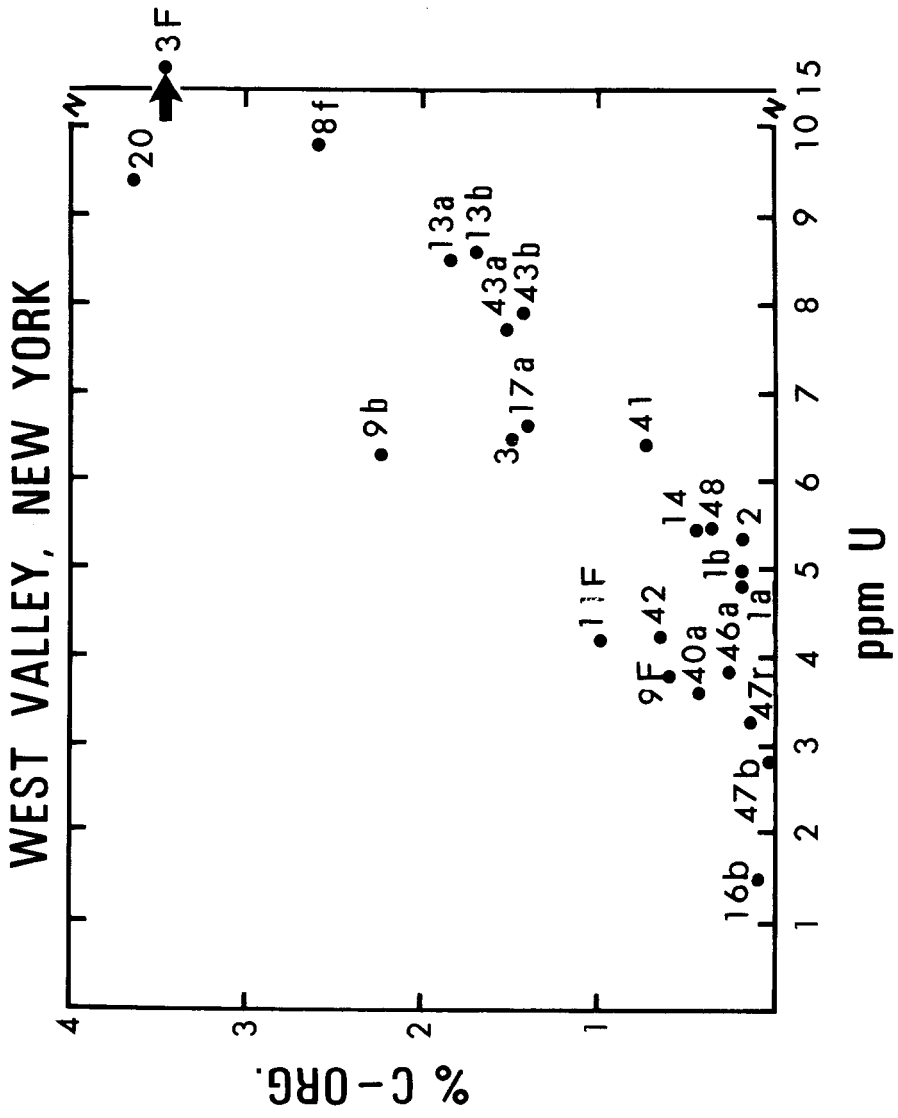

Figure 7. Cattaraugus County (West Valley) New York, % C vs ppm U., numbers refer to samples on tables 10 & 11.

Figure 8. Perry County, Kentucky, % C org. vs 100%--% Ash equivalent to Weight loss on combustion (WLOC).

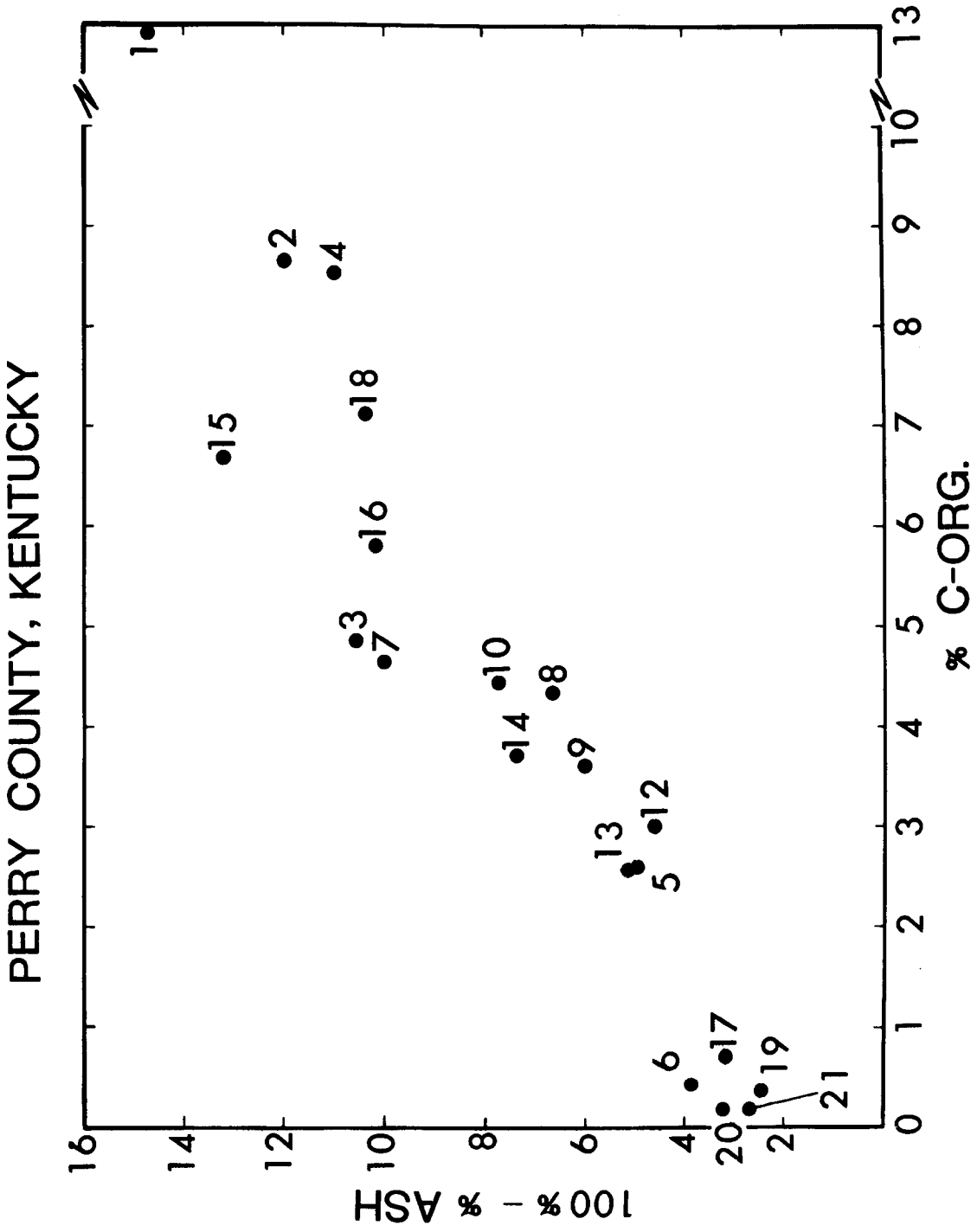

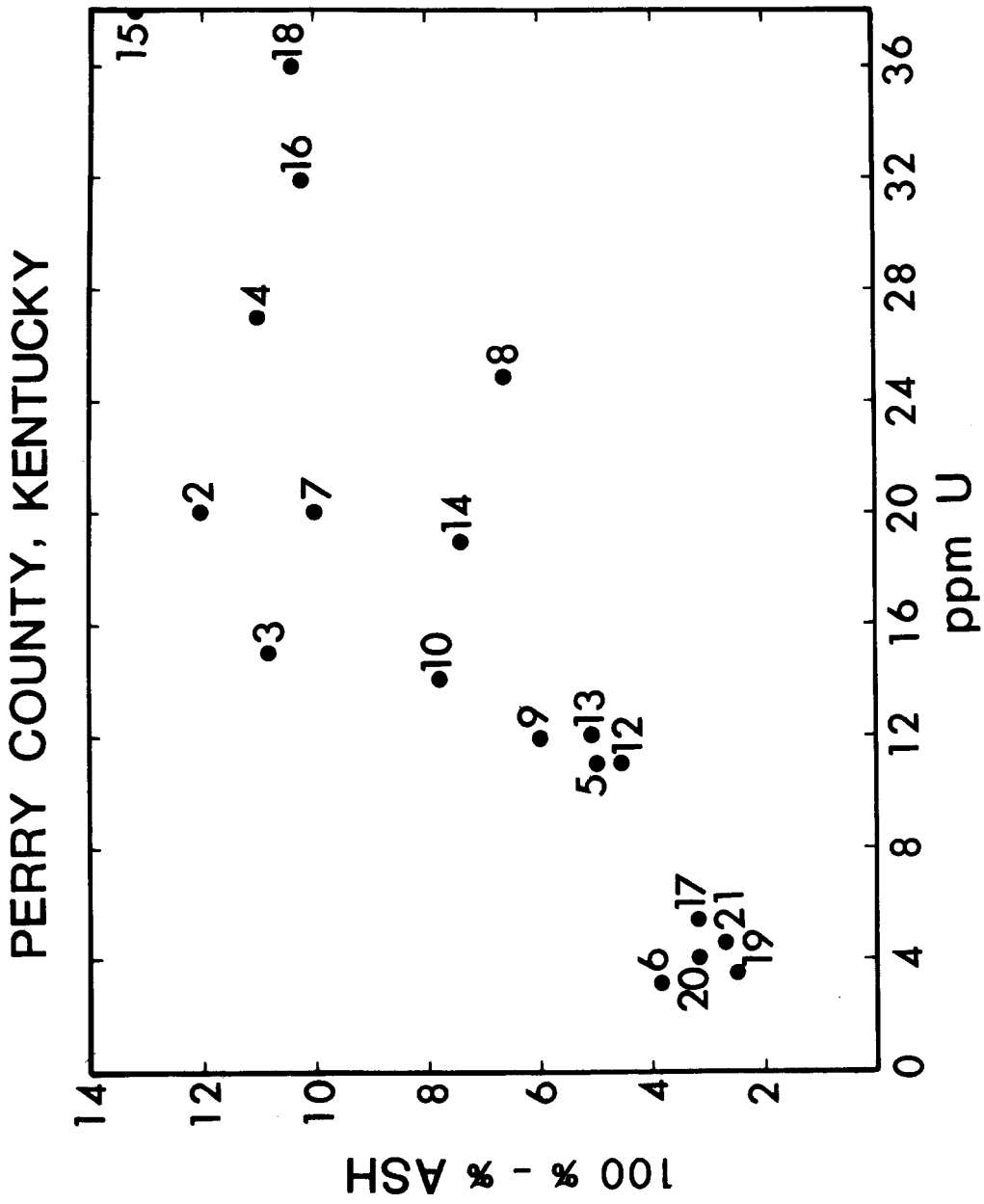

Figure 9. Perry County: ppm U vs 100%-%ash (WLOC) .

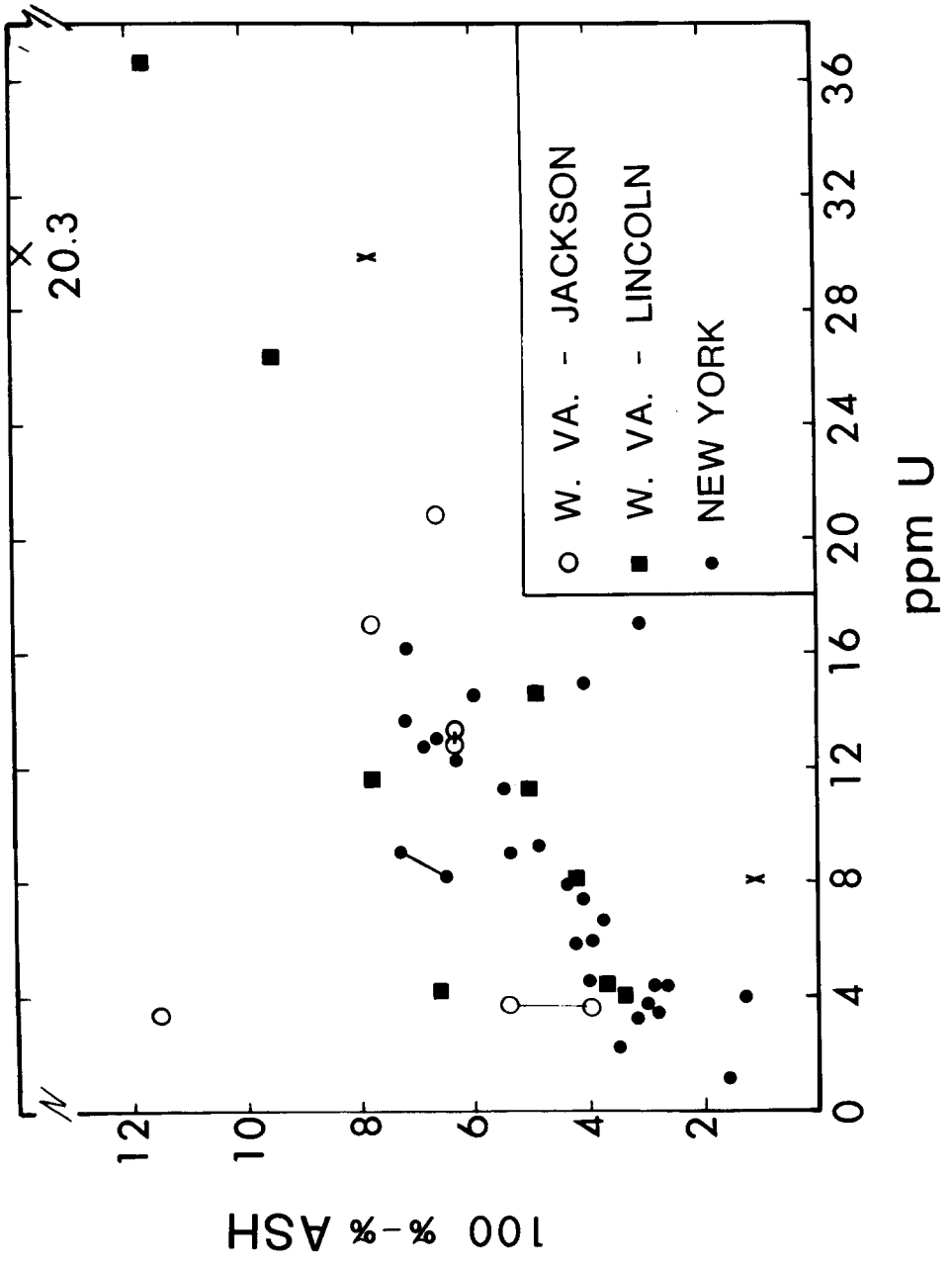

Figure 10. Data from West Virginia and New York for ppm U and 100%-% ash (WLOC).

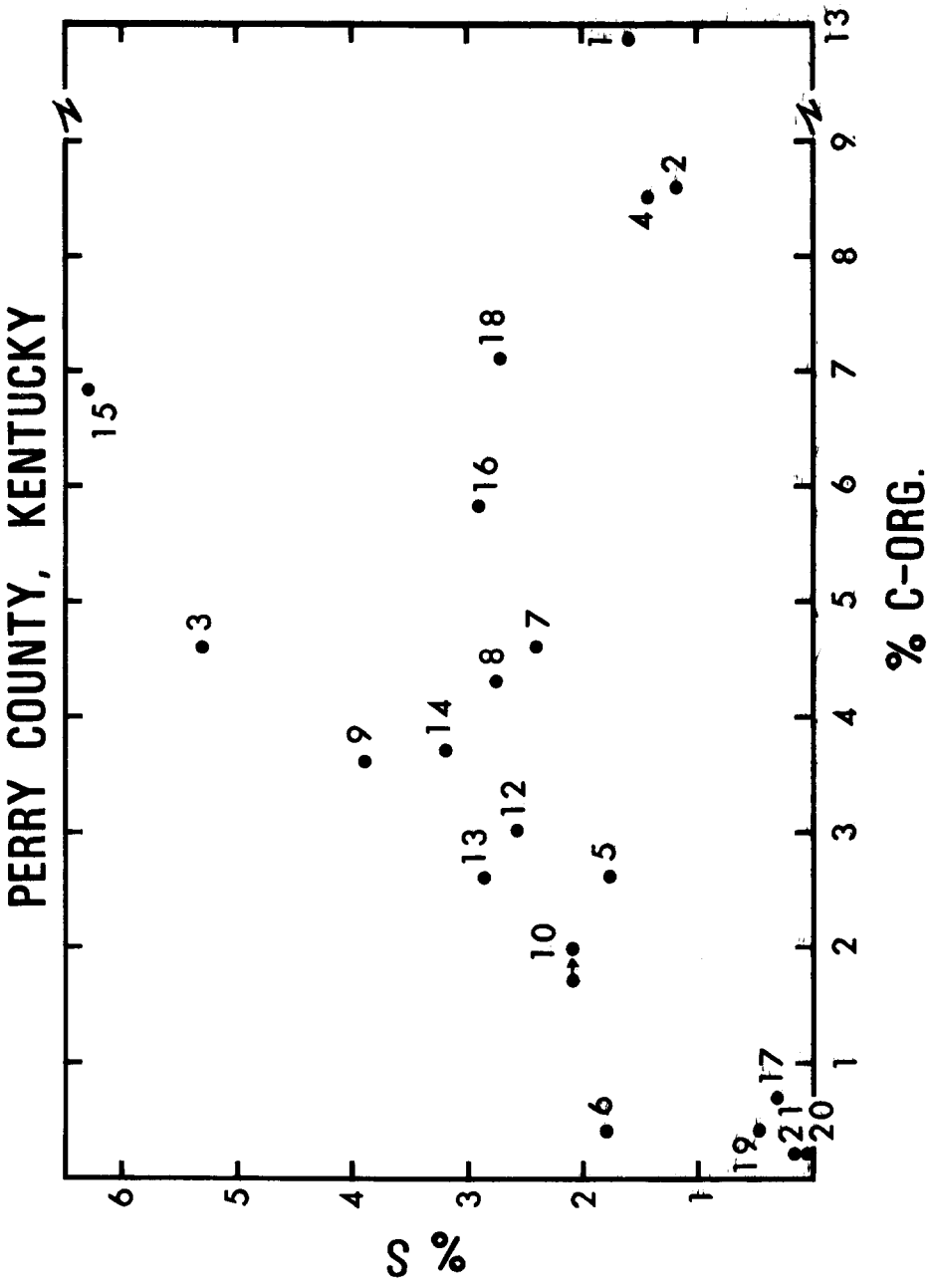

Figure 11. Perry County, Kentucky, % S vs % C org.

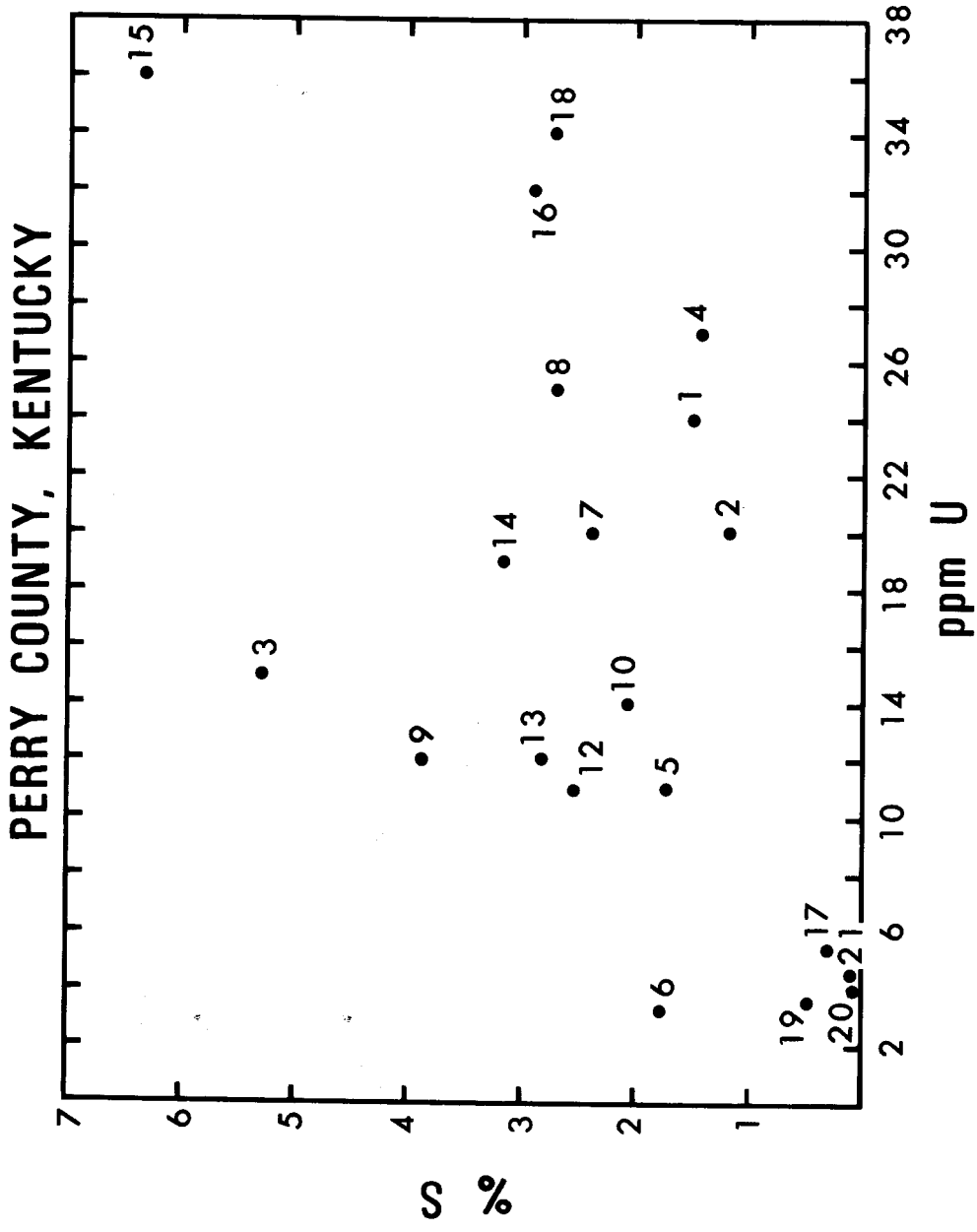

Figure 12. Perry County, Kentucky, % S vs ppm U.

Figure 13. West Virginia and New York data for % S vs ppm U.

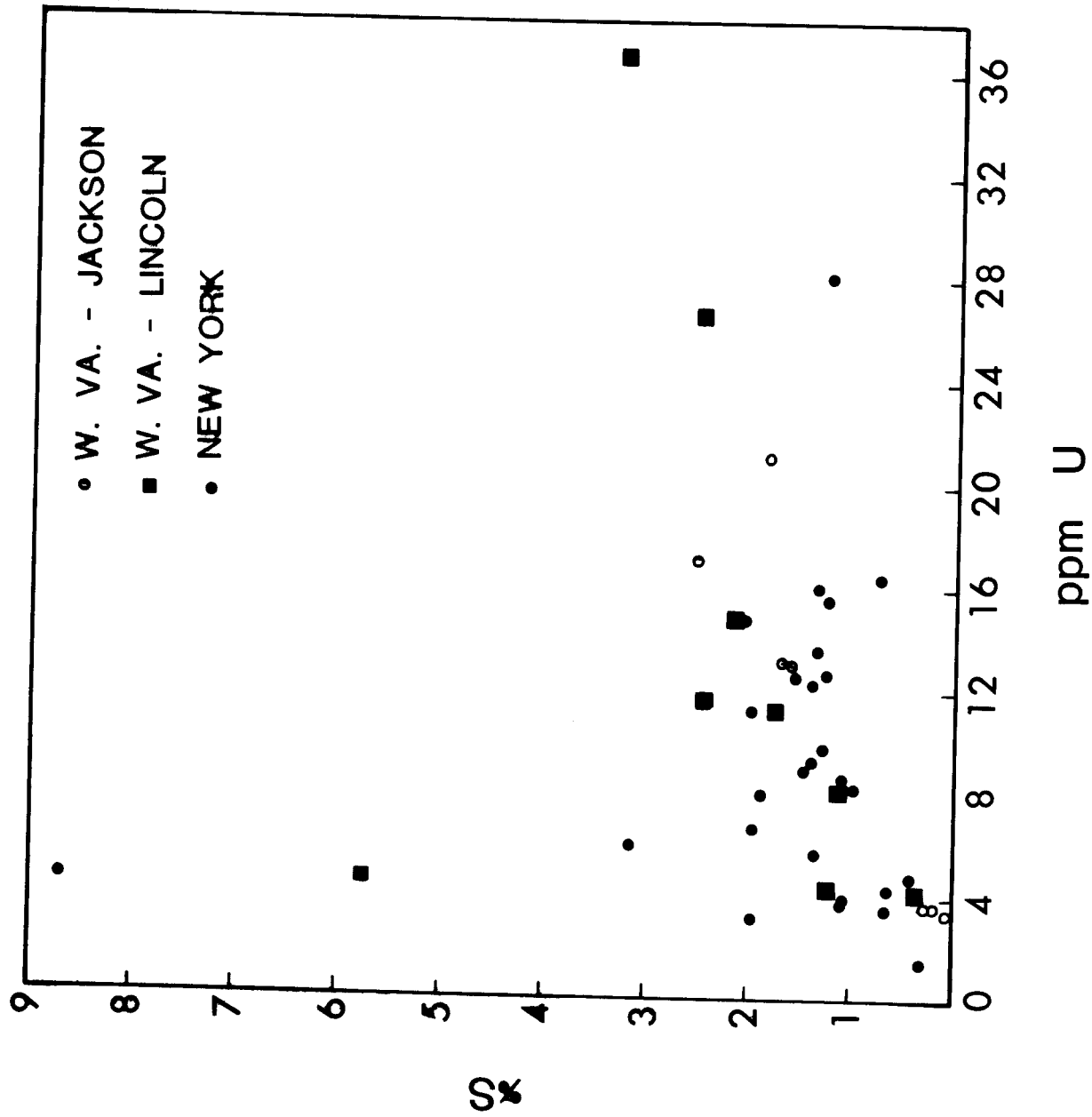

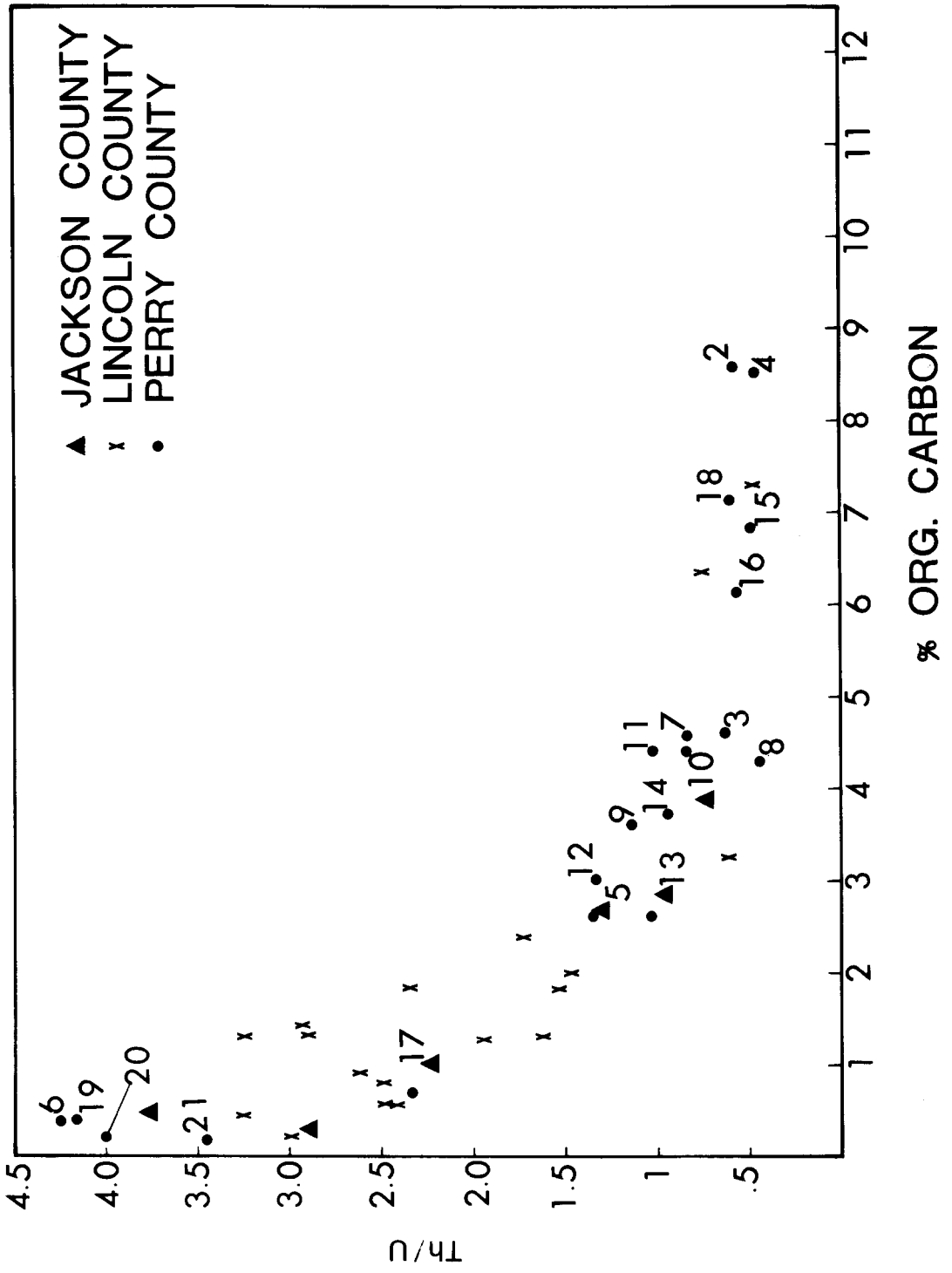

Figure 14. Data from West Virginia and Kentucky for Th/U vs % C organic.

Table 1. Results of U and Th analyses of 3 pairs of splits of black shale samples.

Sample	Th ppm	U ppm	Th/U
C-3483	13.4	3.75	3.58
C-3489	10.5	3.83	2.75
C-3625	16.20	13.12	1.24
C-3690	15.03	13.04	1.15
NY - 9	14.43	8.47	1.70
NY- 99	12.83	8.22	1.56

Table 2. Results of U and Th analysis of duplicate portions of 11 samples analyzed at the same time.

Sample	Depth, ft.	Th,ppm	U,ppm	Th/U
Ny-1a	818	16.1	4.8	3.3
1b	818	16.5	4.9	3.4
2Fa	797	12.9	5.8	2.2
2Fb	797	14.4	5.6	2.6
8a	1344	13.8	3.4	4.1
8b	1344	12.4	3.6	3.5
9a	1498	7.9	6.5	1.2
9b	1498	12.4	6.3	2.0
40a	1328	15.9	3.6	4.4
40b	1328	16.1	3.7	4.4
43a	686	14.7	7.7	1.9
43b	686	11.7	7.9	1.5
46a	313	18.5	3.8	4.9
46b	313	16.8	4.0	4.2
12a	721	15.1	5.9	2.6
12b	721	15.6	6.3	2.5
13a	1222	14.1	8.5	1.7
13b	1222	12.9	8.6	1.5
17a	1442	14.0	6.6	2.1
17b	1442	13.5	6.6	2.0
18Fa	1407	16.4	7.6	2.1
18Fb	1407	16.2	7.7	2.1

Table 3. Results of U and Th analysis of duplicate portions of 19 samples analyzed at different times.

Sample		Th ppm	U ppm	Th/U
NY-41		15.7	6.4	2.44
-41		14.8	7.4	2.0
NY-44		13.7	3.3	4.15
-44		10.2	3.5	2.89
NY-48F		19.6	11.4	1.72
-48F		13.6	12.5	1.09
NY-16L		3.2	1.0	3.2
-16L		4.2	1.5	2.78
NY-18		16.7	4.2	3.98
-18		20.1	3.7	5.44
NY-19		19.5	4.4	4.41
-19		11.1	4.3	2.61
NY-20		12.8	9.4	1.36
-20		15.0	9.0	1.66
NY-20F		18.1	12.0	1.51
-20F	✓	13.8	12.6	1.10
NY-17F		16.9	14.8	1.15
-17F		16.2	13.7	1.18
NY-15F		13.2	13.1	1.01
-15F		13.9	14.7	0.94
NY-3F	✓	15.9	16.0	1.01
-3F		22.3	15.8	1.39
NY-3		13.3	6.4	2.08
-3		16.6	8.0	2.09
NY-4F		17.0	10.5	1.62
-4F		15.1	9.2	1.64
NY-5F		14.5	10.3	1.40
-5F		16.0	9.8	1.63
NY-7		15.4	7.4	2.08
NY-7-2		10.5	6.0	1.75
NY-10F		18.1	10.5	1.73
-10F	✓	10.8	11.2	0.97
NY-11F		13.9	4.2	3.26
-11F		11.6	4.3	2.68
NY-14F		15.7	12.3	1.28
-14F	✓	8.3	12.3	0.67
NY-15		13.2	5.3	2.52
-15		11.3	5.8	1.96

Table 4. Comparison of uranium determinations by delayed neutrons and fluorimetry on 10 samples.

Perry County Depth	Delayed Neutrons	Fluorimetry
2380	20.0	20
2413	20.7	25
2449	7.1	6
2547	8.9	6
2601	37.5	38
2612	33.5	30
2664	44.5	38
2674	13.5	13
2691	12.0	10
2705	4.8	4

Delayed neutrons by USGS, Denver

Fluorimetry by Bendix Field Engrng, ERDA, Grand Junction

Table 5. Comparison of γ-ray spectromety and delayed neutron analysis of 18 samples for uranium and thorium.

U Ky Sample no. BSB-XX-76	Th ppm γs	Th dn	U ppm γs	U dn	Th/U γs	Th/U dn	USGS Sample #BB-XX
- 3-	7.0	11	15.7	15.8	0.45	0.73	-20
16	9.0	14	24.0	28.0	0.38	0.51	19
19	9.3	17	23.7	23.5	0.39	0.71	18
21	15.1	13	31.7	31.8	0.48	0.41	17
22	14.2	29	68.2	69.5	0.21	0.41	16
23	10.2	18	46.9	51.4	0.22	0.35	15
61	17.2	23	56.2	59.7	0.31	0.39	14
26	8.0	19	19.0	23.0	0.42	0.83	13
31	8.6	17	24.7	28.5	0.35	0.59	12
33	8.4	10	32.8	40.9*	0.26	0.23	11
34	9.4	15	46.6	50.9	0.20	0.30	10
35	8.0	17	44.5	47.9	0.18	0.35	9
40	9.7	13	14.3	14.9	0.68	0.85	7
46	9.4	11	19.3	14.3*	0.49	0.76	6
49	13.5	23	21.8	23.8	0.62	0.97	5
53	7.6	15	28.1	23.5	0.27	0.64	4
56	23.0	21	50.9	45.2	0.45	0.46	2
60	18.2	24	39.9	43.9	0.46	0.55	1

γs = gamma ray spectrometry, U.Ky

dn = delayed neutrons, USGS

* = outside limits of ±10% for each on U.

Table 6. Results of U, Th, organic C and S analyses for Perry County, Kentucky core.

Depth[1] (ft.)	Sample[2] No.	U[3] (ppm)	Th[4] (ppm)	Th/U[4]	% Organic Carbon	% S
2371.1	1	24	21	0.87	12.9	1.52
2383.6	2	20	(14)	(0.70)	8.6	1.20
2393.1	3	15	(11)	(0.76)	4.6	5.31
2410.4	4	27	(13)	(0.48)	8.5	1.44
2431.7	5	11	14	1.33	2.6	1.75
2449.0	6	3.2	13	4.24	0.4	1.78
2456.0	7	20	17	0.84	4.6	2.41
2471.2	8	25	(11)	(0.44)	4.3	2.71
2491.0	9	12	14	1.15	3.6	3.88
2513.2	10	14	12	0.84	(1.7)	2.07
2531.1	11	11	12	1.03	4.4	
2553.2	12	11	15	1.34	3.0	2.54
2572.2	13	12	12	1.03	2.6	2.85
2589.5	14	19	19	0.93	3.7	3.17
2605.4	15	38	(17)	(0.50)	6.8	6.36
2617.2	16	32	(19)	(0.61)	5.8	2.92
2629.8	17	5.4	12	2.34	0.7	0.32
2648	18	36	(22)	(0.60)	7.1	2.74
2670	19	3.5	15	4.17	0.4	0.49
2689.9	20	4.0	17	4.15	0.2	0.08
2706.0	21	4.5	15	3.44	0.2	0.11

[1] Depth from core boxes, interval of sample is ~0.6 ft.

[2] Used on figures

[3] Rounded off to nearest whole number, unless less than 10 ppm

[4] ( ) indicates as much as ±50% error

Table 7. Results of U, Th, and organic carbon analysis for Jackson County, West Virginia core.

Depth (Ft.)	% C Organic	Th ppm	U ppm	Th/U
C-3220	3.0	13.9	7.6	1.8
3232	2.7	15.5	11.8	1.
3233	1.0	13.7	5.3	2.6
3249	4.1	15.1	10.7	1.4
3254	1.8	17.0	5.9	2.9
3269	1.1	12.9	7.5	1.7
3292	0.9	19.0	6.5	2.9
3293	3.2	17.0	12.5	1.4
3312	0.3	17.4	5.5	3.2
3332	3.8	13.9	12.0	1.2
3359	2.6	15.8	12.6	1.3
3378	0.4	17.4	5.1	3.4
3418	0.1	17.6	3.4	5.2
3462	2.5	16.1	10.2	1.6
3483	0.2	12.0	3.8	3.2
3514	3.7	(13.6)	17.2	(0.8)
3527	1.3	14.7	5.8	2.5
3550	0.3	15.2	7.2	2.1
3573	3.9	(15.0)	17.1	(0.9)
3605	0.7	17.7	8.9	2.0
3625	3.5	16.5	13.0	1.3
3640	5.6	(16.0)	21.0	(0.8)
3642	0.4	15.8	7.1	2.3
3660	0.2	13.5	3.5	3.9
3685	1.2	17.5	6.8	2.6

Table 8.

Sulfur and WLOC data for Jackson and Lincoln Counties, West Virginia

[WLOC = weight loss in combustion at 550°C]

Sample	WLOC	Sulfur percent
	Jackson County	
C-3483	5.4, 4.0	0.28, 0.21
C-3573	7.8	2.55
C-3626	6.0, 6.3	1.72, 1.58
C-3640	6.7	1.81
C-3660	(11.6)	0.03
	Lincoln County	
L-2733	3.4	0.37
3020	3.7	1.24
3312	5.6	5.74
3398	4.2	1.07
3551	7.8	2.41
3914	5.0	1.74
3951	11.7	3.27
3956	9.5	2.51
3961.6	4.9	2.16

Table 9. Results of U and Th analysis of the Lincoln County, West Virginia core.

Sample Depth (ft.)	Th ppm	U ppm	$Th/_U$
L-2636	21.2	4.0	5.27
2655	19.7	4.1	4.81
2694	17.2	4.0	4.27
2713	17.2	3.7	4.71
2733 sp.	17.5	4.1	4.26
2756	17.6	4.4	4.04
2770	18.8	8.7	2.16
3001	14.9	6.0	2.49
3020	19.9	4.4	4.53
3041	16.0	5.2	3.08
3062	13.4	6.4	2.10
3081	14.4	6.4	2.26
3082	14.8	9.2	1.60
3114	13.1	8.0	1.63
3291	15.1	3.4	4.50
3312	9.7	4.2	2.33
3337	14.1	6.3	2.25
3358	16.2	4.6	3.72
3380	(15.0)	18.5	(0.81)
3398	17.4	8.1	2.15
3420	(16.0)	21.2	(0.76)
3442	(12.6)	14.6	(0.86)
3486	(13.4)	14.5	(0.92)
3511	(15.5)	21.4	(0.72)
3551	14.9	11.7	1.27
3572	(14.5)	17.4	(0.84)
3890	19.1	18.0	1.06
3901	14.1	7.5	1.89
3914	18.2	11.2	1.63
3928	15.4	6.5	2.35
3936	16.7	12.7	1.32
3951	(17.3)	36.6	(0.47)
3953	(14.4)	29.5	(0.49)
3956	(15.3)	26.5	(0.58)
3957	(7.1)	13.8	(0.51)
3961.6	18.8	14.7	1.28
3962	(9.3)	15.8	(0.63)
3965	(20.9)	28.8	(0.73)

Table 10. Results of U and Th analysis of Cattaraugus County, New York core.

New Number	Depth (Ft.)	Old Number	Th ppm	U ppm	Th/U
1	313*	46	17.7	3.9	4.54
2	418*	47	15.0	3.7	4.09
3	452	10	16.2	3.7	4.39
4	508	42	15.1	4.2	3.58
5	562	18	16.7	4.2	3.98
6	641	6	15.8	6.2	2.54
7	686*	43	13.2	7.8	1.69
8	721*	12	15.4	6.1	2.54
9	786	2	7.2	5.3	3.27
10	797*	2F	13.6	5.7	2.39
11	809	3A	12.2	9.2	1.33
12	818*	1	16.3	4.9	3.36
13	827	1F	13.1	6.0	2.18
14	942	11	14.0	4.0	3.5
15	962	19	19.5	4.5	4.41
16	1047	7	15.4	7.4	2.08
17	1108	45	19.0	4.2	4.53
18	1184	8F	12.3	9.6	1.28
19	1203	5F	14.5	10.3	1.40
20	1222*	13	13.4	8.5	1.57
21	1242	44	13.7	3.3	4.15
22	1255*	16F	13.4	4.0	3.37
23	1256	16L	4.2	1.5	2.78
24	1257	16B	11.7	3.3	3.59
25	1285	4	10.8	2.6	4.20
26	1297	4F	17.0	10.5	1.62
27	1315	41	15.7	6.4	2.44
28	1328*	40	16.0	3.7	4.36
29	1344*	8	13.1	3.5	3.75
30	1366	10F	18.1	10.5	1.73
31	1389	11F	13.9	4.2	3.26
32	1407	18F	16.3	7.7	2.12
33	1421	14F	15.7	12.3	1.28
34	1428	14	16.6	5.4	3.01
35	1439	17F	16.9	14.8	1.15
36	1442*	17	13.7	6.6	2.07
37	1450	15F	13.2	13.1	1.01
38	1463	15	13.2	5.3	2.52
39	1469	48	14.5	5.4	2.69
40	1470	5	14.3	5.4	2.66
41	1471	48A	12.2	8.2	1.50
42	1478	48F	19.6	11.4	1.72
43	1477	3	13.3	6.4	2.08
44	1478	3F	15.9	15.8	1.01
45	1490	20	12.8	9.4	1.36
46	1494	20F	18.1	12.0	1.51
47	1497	9F	12.3	3.8	3.23
48	1498*	9	10.2	6.4	1.60

* is average of multiple samples from that interval. Samples represent 4-7 inch interval

Table 11. Sulfur and WLOC and organic carbon data for Cattaraugus County, New York core.
[WLOC = weight loss in cumbustion at 550°C]

Sample	Percent C org.	WLOC percent	Percent sulfur
43a	1.5		
43b	1.5		
46a	0.3		
48	0.4		
9b	2.2		
1a	0.2		
1b	0.2		
2	0.2		
11f	1.0	4.0	8.7
13a	1.9		
13b	1.7		
14	0.4		
17a	1.4		
20	3.7	5.8	1.4
40a	0.4		
14	0.7		
42	0.7		
3	1.5	4.6	1.9
3F	3.6	7.2	1.4
8F	2.6		
16L	0.1	1.6	0.3
47bo	0.1		
47 red	0.2		
9F	0.6		
4F	--	4.9	1.4
5		5.0	1.3
7-2		3.9	3.2
9		6.9	1.05, 1.1
10F		5.5	2.0
12		1.3	1.1
14F		6.4	1.4
15		4.2	1.4
15F		6.0	1.3
16F	--	2.8	0.6
16		3.4	2.0
17		3.8	2.0
17F		7.2	1.4
19		2.8	0.4
20F		6.9	1.3
44		2.8	0.6
48F		6.6	1.6
18		3.0	1.3
8		3.4	0.8
41		4.1	2.1

Table 12.--Uranium and thorium data for differing lithologies in New York, core

Sample	Color	Depth, Ft.	Th/ppm	U/ppm	Th/U
9	dark	1498	10.9	6.4	1.70
9F	light	1497	12.3	3.8	3.2
3	light	1477	13.3	6.4	2.1
3F	dark	1478	15.9	15.8	1.0
16	----	1255	13.2	3.3	3.6
16L	light	1256	3.2	1.0	3.2
16F	dark	1255	13.7	4.3	3.2
16B1	dark	1257	11.7	3.3	3.6
47	gray	418	16.1	3.7	4.3
47r	red	418	18.1	3.2	5.7
47m	brown	418	10.5	2.5	4.3
47bo	gray	418	9.4	2.8	3.3
47B1	black	418	21.1	6.2	3.4

Table 13. Short range uranium and carbon variations in the Jackson County, West Virginia core.

Sample No.	% Organic Carbon	Th	U	$Th/_U$
C-3514-1		(12.7)	17.0	(0.74)
-2		(10.5	18.9	(0.55
-3	3.9	(13.1)	17.8	(0.73)
-4	3.7	(13.3)	20.4	(0.65)
-5a		19.5	18.9	1.03
-5b		(13.7)	18.8	(0.73)
-6	3.8	(17.2)	19.4	(0.89)
-7		(16.2)	18.1	(0.89)
-8	4.0	(13.2)	18.0	(0.73)
-9		(13.4)	17.3	(0.77)
-10		12.8	10.2	1.25
-11	2.8	11.8	12.1	0.97
-12	3.8	(9.9)	17.2	(0.58)
3515.1-13	3.5	(12.6)	16.6	(0.76)
3232.8	2.7	15.5	11.8	1.31
3233		13.9	6.3	2.23
3233.4		13.5	5.8	2.35
.5	1.0	13.5	6.1	2.21
.6		12.9	4.9	2.62
.7	0.33	12.2	4.3	2.87
.8	0.44	16.4	4.4	3.73

Table 14. Short range variations on uranium content in the Lincoln County, West Virginia core.

Sample No.	Th	U	Th/U
L-3001-1	15.9	8.9	1.78
-2	13.4	8.7	1.54
-3	13.7	7.6	1.81
-4a	14.0	7.4	1.90
-4b	14.4	7.3	2.00
-5	15.8	7.1	2.23
-7	16.6	5.9	2.82
-8a	13.2	5.2	2.56
-8b	13.4	5.4	2.47
-9a	13.9	5.6	2.49
-9b	16.6	5.1	3.25
-10	15.7	5.1	3.07
-11a	16.7	5.1	3.25
-11b	15.2	5.4	2.81
-12	12.6	5.2	2.44
-13	14.3	5.0	2.84
-14	17.0	4.4	3.89
-15a	13.2	4.6	2.88
-15b	16.6	4.5	3.73

Table 15. Short range variations on uranium content in the Lincoln County, West Virginia core.

Sample No.	Th	U	Th/U
L-3080.6a	14.5	5.3	2.71
6b	14.1	5.3	2.67
3081-1a	16.0	5.2	3.09
-1b	14.4	5.3	2.72
-2a	16.1	5.5	2.91
-2b	17.2	5.3	3.23
-3a	17.7	5.3	3.36
-3b	15.1	5.7	2.64
-4	14.6	6.5	2.24
-5	11.0	7.5	1.46
-6a	13.6	5.8	2.33
-6b	13.5	6.0	2.23
-7a	9.4	5.8	1.63
-7b	16.0	7.4	2.15
-8a	15.3	8.1	1.89
-8b	14.2	8.3	1.72
-9	11.9	8.0	1.47
-10	15.9	7.4	2.17
-11	14.4	8.0	1.81

Table 16. Short range variations on uranium content in the Lincoln County, West Virginia core.

Sample No.	Th	U	Th/U
L-3442.1	(12.5)	16.2	(0.77)
.2	(11.9)	18.2	(0.66)
.3	(9.0)	18.4	(0.49)
.5	13.1	11.8	1.11
.6	13.5	11.2	1.21
.9	15.5	12.0	1.29
L3953.0	(14.4)	29.5	(0.49)
L3956.8	(7.1)	13.8	(0.51)
L3961.2	(12.9)	17.3	(0.75)
.3	(9.3)	18.0	(0.52)
.5	(9.6)	16.7	(0.58)
.6	(7.5)	15.8	(0.47)
.7a	(11.5)	15.4	(0.75)
.7b	(9.7)	15.0	(0.65)
L3962.2	(8.4)	12.9	(0.65)
L3962.9	(10.6)	15.5	(0.68)
L3965	(20.9)	28.8	(0.73)

GEOCHEMICAL CHARACTERIZATION OF THE DEVONIAN BLACK SHALE FROM COTTAGEVILLE, WEST VIRGINIA: A PRELIMINARY LOOK AT MULTIVARIATE ANALYSIS

by

Stephanie J. Bialobok and Steven C. Lamey
ERDA/Morgantown Energy Research Center
and
Jojok Sumartojo, Vanderbilt University

ABSTRACT

R-mode cluster analysis of geochemical data obtained from the Cottageville wells #11940 and #12041 groups the data into nine clusters. The results indicate "key" geochemical variables which may be analyzed to characterize the Devonian shale.

Of the 43 geochemical and mineralogical parameters analyzed by regression analysis from well #11940 nine show variations with depth. Specific gravity, moisture, organic sulfur, copper, barium, Fe_2O_3, and Na_2O have negative correlations with depth; whereas boron and chlorite have positive correlations with depth.

INTRODUCTION

The Devonian black shale, known in different states under a variety of formational names (Chattanooga, New Albany, Ohio, etc.), (Cooper, et.al., 1942).has continuously been the object of geologic investigations. Since 1940, this remarkable stratigraphic unit has been studied by investigators because of its anomalous contents of radioactive minerals (Swanson, 1960; Conant and Swanson, 1961; Hickman and Lynch, 1967). Other studies on the geochemistry of black shales in the U.S. have been presented by various authors (Duncan and Swanson, 1965; Vine, 1969; Vine and Tourtelot, 1970). Recent geochemical and geological investigations of the Devonian black shale are being carried out by, among others: Renton (pers. comm., 1976), Kepferle (pers. comm. 1976), Blackburn (pers. comm., 1976), and Yen (pers. comm., 1976). At the present time, ERDA is currently involved in a major program to determine the potential of the Devonian Shale as a source of natural gas. The initial phase of this program is a resource inventory and characterization of the Black Shale, of which this study is a part.

This paper summarizes the work done at the ERDA/Morgantown Energy Research Center on the geochemical analyses of two well cores #11940 and #12041 obtained from drilling in the Cottageville West Virginia area (Byrer, et.al., 1976). A total of 43 geochemical and mineralogical variables were analyzed by various methods. The analytical results were statistically processed by means of cluster analysis and regression analysis. This procedure was performed to determine the geochemical coherence of the variables, the interrelationship among the variables; and to determine which parameters could best be used in a geochemical description of the Devonian Shales.

ANALYTICAL METHODS

The analyses of the shale samples were carried out using a variety of wet chemical and instrumental techniques. Most of the analyses were done following the procedures commonly used for the analyses of coals. (Staff, U.S. Office of Coal Research, 1967).

The shale sections were selected at five-foot intervals. Eight inch sections of the four inch diameter cores were halved, and one-half removed for petrographic analysis and archiving. The remaining half, after surface sampling, was pulverized to -8 mesh. (2380 microns) A representative portion of this sample was then ground to -60 mesh (250 microns) for elemental analyses, combustion analysis, and chemical separations. A portion of this material was McCrone-ground with ethanol for 15 minutes to -325 mesh (44 microns). This was used for infrared studies, thermal chromatography, and low-temperature ashing.

THERMAL CHROMATOGRAPHY

The determination of the relative amount of material present within the various carbon number groups was carried out using an MP-3 thermal chromatograph (Chromalytics Corp., Unionville, PA). Ground samples were heated from 60°C to 600°C at a rate of 12°C/minute. The evolved gases were captured on a trap held at room temperature and the trap was then heated to 250°C in less than one minute in order to release the adsorbed gases as a "slug." The gases were then back-flushed to a gas chromatograph. A flame ionization detector was used to measure the various organic species as they eluted. The chromatogram consisted of peaks representing a homologous series of hydrocarbons extending to C_{35}.

For analysis, the series was divided into four carbon number groups; C_{12} and below, C_{13} through C_{20}, C_{21} through C_{26}, and C_{27} to the end of the chromatogram. These correspond to approximate boiling ranges of 215°C, 216°C to 361°C, 362°C to 443°C, and above 443°C at 760 mm. The peak height of each component was then measured, and an assessment of the material present in each fraction was made.

MAJOR AND MINOR ELEMENTS

The analyses of the major and minor elements were conducted on the high-temperature ashes. The methods were essentially those of Gibson and Ode (1962) and involved the application of: (1) spectrophotometric methods for SiO_2, Al_2O_3, TiO_2 and P_2O_5, (2) EDTA titration for CaO and MgO, and (3) flame photometry for Na_2O and K_2O. The analysis of SO_3 was based on a method by U.S. Bureau of Mines (U.S. Office of Coal Research, 1967, p. 75).

Two solutions were required: the first of these prepared from a sodium hydroxide fusion of the ash was used for the silica and aluminum oxide analyses, and the second from the evaporation of the ash with hydrofluoric and sulfuric acids was used for the remaining determinations. The spectrophotmetric analyses were carried out on a Beckman DU while the flame photometric procedures used a second Beckman DU with flame attachments.

FORMS OF SULFUR

The total sulfur present in coal and shale generally occurs in three forms. Consequently, a sulfur analysis usually consists of a breakdown of the total sulfur into its various forms: (1) sulfate sulfur; as calcium or iron sulfate (2) pyritic sulfur; and (3) organic sulfur. Organic sulfur is determined by difference and requires the determination of total sulfur.

Sulfate Sulfur - Dilute HCl was added to a 2 g sample and the mixture brought to a boil. This was filtered and the residue was saved for the pyritic sulfur determination. Bromine water was added to the filtrate followed by ammonium hydroxide. A second filtration was carried out with the residue being discarded. The filtrate was made slightly acid and barium chloride added. The barium sulfate produced was filtered, dried, and weighed, and the sulfate originally present was calculated.

Pyritic Sulfur - The residue and filter paper from the sulfate sulfur determination were treated with dilute HNO_3, filtered and the residue discarded. An excess of NH_4OH was added to the filtrate and the solution was filtered. The sulfur in the filtrate was then determined by the same method as the sulfate sulfur.

Organic Sulfur - Organic sulfur is determined by subtracting the sum of the pyritic and sulfate sulfur from the total sulfur.

Total Sulfur - The analysis for total sulfur was carried out by incinerating the core sample with Eschka mixture (two parts light calcined MgO and one part anhydrous Na_2CO_3). One gram of sample was placed in a porcelain crucible, covered with the Eschka mixture and heated slowly to 800°C until complete combustion was attained. The material was then cooled, digested with water, and filtered. The filtrate was acidified and precipitated as $BaSO_4$ through the addition of $BaCl_2$.

NITROGEN

Nitrogen was determined by the Kjeldahl-Gunning method (U.S. Office of Coal Research, 1967, p. 9). A one gram sample ground to -60 mesh (250 microns) was initially digested in acid until all particles of the sample were oxidized. The digested solution was then diluted with water and made alkaline with NaOH solution. This solution was then distilled into standard H_2SO_4 and titrated with standard NaOH.

HTA (HIGH TEMPERATURE ASH)

Ashing was carried out by placing a 1 g sample in a ceramic crucible and heating to ignition at 750°C. The material was maintained at 750° until a constant weight was attained.

TOTAL CARBON AND HYDROGEN

Total carbon and hydrogen were determined by heating the sample to 850°C in an oxygen atmosphere. A sample weighing 0.2 g and ground to -60 mesh (250 microns) was combusted and at the same time aspirated to a series of U-tubes by the pressurized oxygen. The first tube was filled with granular anhydrous $Mg(ClO_4)_2$ to absorb the hydrogen generated in the form of water vapor. The increase in weight of this tube gave the percentage hydrogen present in the shale. A second tube containing NaOH -asbestos with a layer of $Mg(ClO_4)_2$ on top, absorbed the liberated CO_2. The increase in weight of this bulb gave the total carbon content.

INORGANIC CARBON

Carbonate minerals in varying amounts are usually present in shales. The carbon dioxide liberated when the above are treated with dilute HCl allows one to estimate the amount of these minerals present.

The analysis was carried out on 10 grams of sample ground to -60 mesh (250 microns). Dilute HCl was added to the sample immersed in hot water in an Erlenmeyer flask. Heat was then applied and the CO_2 released was trapped in a bulb containing sodium ascarite. The increase in the weight of the bulb was due to the CO_2 in the sample.

TRACE ELEMENTS

The analyses of trace elements B, Mn, Ni, Ba, Cr, Sr, and Cu were carried out on a Spectrametrics Incorporated Spectraspan III argon plasma emission spectrometer. Details of the techniques will be reported later by the Chemical Services Branch at MERC.

MOISTURE

Moisture content of the samples was determined by heating the rock powder in an oven at 105°C for 1 hour. The weight loss expressed in per cent is the moisture content.

SPECIFIC GRAVITY

This physical variable was determined in a pycnometer.

LTA (LOW TEMPERATURE ASH)

LTA was determined by oxidizing the ground samples in a plasma oxygen environment generated by passing commercial grade O_2 through a radio frequency field (13.56 MHz) at 1mm Hg. (Gluskoter, 1965) (Mazza and Wilson, 1977). The weight of the residue is the low temperature ash expressed in per cent.

STATISTICAL TECHNIQUES

Cluster Analysis

The cluster analysis is a relatively new technique to classify geologic samples. Originally used in taxonomic classification, it now has a growing application in geologic data reduction. (McCammon, 1968; Hidalgo, 1974). The classification is based on the assocation of each sample with every other sample on the basis of the similarity in their measured variables (in the present case, the geochemical and mineralogical variables). (Parks, 1966; McCammon, 1968; Davis, 1973).

One method of comparing each sample to every other sample is by using a coefficient of dissimilarity, for example, the distance coefficient. This coefficient is a measure of the Average Taxonomic Distance between any pair of samples in m-dimensional space, where "m" is the number of variables used.

There are two techniques of cluster analysis: the Q-mode and the R-mode. The Q-mode analysis compares sample to sample; the R-mode compares variable to variable. (Davis, 1973). This paper shows the results of R-mode analysis. The basis for linking two variables together is that each must have the highest correlation with the other. Therefore, items with the lowest dissimilarity have the highest correlation.

It should be noted that there are different ways to achieve this highest correlation between two items. In this study, the UPGMA (Unweighed Pair Group Method of Analysis) was used. UPGMA attempts to weigh each cluster proportionally to the number of objects within it during the averaging process. Some of the other methods do not; thereby allowing those objects added late in the clustering process to exert a greater influence than those linked earlier. (Davis, 1973).

All data from the two cores was standardized before being subjected to cluster analysis. The purpose of standardization is to produce a collection of data that is unitless, thereby enabling the comparison of a distribution of one variable to another when the two variables are expressed in different units of measurement.

While mineralogical analyses were performed on these samples, and subsequently added to the cluster analyses, they have been deleted from the final results. Cluster analyses performed with mineralogy data were different, in this case from cluster analyses performed without mineralogy data. The difference is partly due to the semi-quantitative nature of mineralogy by x-ray diffraction, so for this reason, the mineralogy has not been included.

Computation procedures have been presented by various authors (Sokal and Sneath, 1963; Parks, 1966); Harbaugh and Merriam, 1968; McCammon, 1968; Davis, 1973). The computer program for cluster analysis used in this paper is the NT-SYS (Numerical Taxonomy System) developed by the State University of New York at Stony Brook and adapted to the computer IBM 360/75 370/145 at West Virginia University.

There is one obvious drawback to cluster analysis. Because of the nature of the program, every variable is forced to cluster with every other variable. The result may therefore be a cluster of variables that are together not because their behavior is similar, but because they are unlike any other variables in the matrix.

RESULTS AND DISCUSSION

The Cottageville Well #11940

The dendrogram of the R-mode cluster analysis indicates the grouping of the 36 geochemical variables (Table 1) into eight clusters (Figure 1). The clusters, while exhibiting a low degree of mutual relationship among the variables, fit geochemical patterns.

Cluster 1: B and Ni cluster with total carbon, organic carbon and combustible LTA (the organic fraction). The association of these elements with organic matter in sedimentary rocks has been suggested (Goldschmidt, 1954, Couch, 1971). (Zubovic, 1966) found that in sediments rich in organic matter (such as coals) there is an affinity of boron with organic matter. The high concentrations of Ni in areas of high organic productivity (such as upwelling water) has been reported (Schutz and Turekian, 1965).

Cluster 2: The clustering of the sulfur species may be entirely genetic and may not be influenced by any geochemical factors.

Cu has been reported as sulfides in shales of Mansfeld, Germany (Goldschmidt and Peters, 1931, 1932, 1933), and Cr and Cu are considered to be elements commonly associated with the organic fractions of black shale deposits (Vine, 1966, 1970). These elements also occur in low concentrations in sea water (Vine, 1966).

There is no apparent explanation for H_2 in this cluster.

Cluster 3: The occurrence of mineral carbon, CO_2, CaO, MnO, is believed to be associated with the carbonate minerals (Vine 1969) and this cluster seems to support this belief. Ba associated with the carbonate fraction has been reported (Vine, 1970) as detrital mineral fractions.

The analysis for SO_3 (Staff, U.S. Office of Coal Research, 1967) supports the existence of $CaSO_4$ as reported by x-ray diffraction (Mazza, pers. comm., 1977). The presence of SO_3 in this cluster may be an example of this relationship. The SO_3 may also be associated with the Ba as $BaSO_4$.

Cluster 4: Because mineral matter is generally more dense than organic matter, the relationship between LTA and Specific Gravity is expected to be proportional.

There is no apparent explanation for Sr in this cluster.

Cluster 5: The occurrence of this cluster may be related to the genetic nature of the variables. This hypothesis is also supported by the tight grouping of the variables. Because all of these variables were determined in the same way, the cluster may suggest a relationship based on the method of analysis.

Cluster 6: There is no apparent explanation for this cluster.

Cluster 7: The relationship between HTA and SiO_2 reflects the genetic nature of the two variables, as HTA is largely composed of SiO_2.

The relationship between Al_2O_3 and K_2O most probably reflects the clay minerals present in the shale. The occurrence of Fe and Mg in shales has been reported (Vine, 1966, 1970) and in most cases its occurrence is attributed to detrital mineral matter. In this case, Fe and Mg may represent chlorite, which has been reported by x-ray diffraction.

The loose association of Na_2O with the other clusters may represent the substitution of Na for K into the lattices of feldspars and plagioclase. Also the loose association of moisture may reflect the ability of clay minerals to adsorb water.

Cluster 8: The clustering of these two variables may reflect their occurrence in low concentrations. The N_2 content of the shale samples from this core was usually 0.0, and the highest value ever reported for a single sample was 0.22. For P_2O_5, the average content was 0.1.

RESULTS AND DISCUSSION

The Cottageville Well #12041

The geochemical variables (Table 2) in this well are grouped into nine clusters. While some of the clusters which appeared in the Cottageville well #11940 are also present in this well, there has been a reclustering among some of the less stable variables.

Cluster 1: The tight grouping of the sulfur species again seems to support a clustering based on the genetic nature of the variables.

The clustering of H_2 with the organic carbon and total carbon reflects the hydrocarbon nature of the organic material within the shale.

The clustering of the sulfur species with the carbon fraction is not fully understood, but a close examination of the cluster reveals that the sulfur species are linked to the carbon fraction by way of the organic sulfur, a variable which in this case shows its dual nature.

There is no apparent explanation for the occurrence of LTA in this cluster.

Cluster 2: The grouping of Al_2O_3 and K_2O again supports the occurrence of clay material in the shale. The linking of moisture to this cluster is again probably due to the adsorptive ability of the clays.

The clustering of B is not fully understood, but (Vine, 1970) has concluded from statistical analyses of chemical data, that B can be associated with the detrital mineral fraction in some black shales.

Cluster 3: The occurrence of this cluster is not fully understood. While Ba and Sr usually associated with the detrital mineral fraction, Cu is usually associated with the organic fraction. The occurrence of Ba is probably as barite, which has been identified by IR (Childers, pers. comm., 1977), and Sr may be occurring as celestite, although the substitution of Sr for Ba into the barite lattice is possible (Dana, 1951). In this cluster the occurrence of Cu could possibly be as the sulfide.

Cluster 4: The clustering of Fe_2O_3 and MgO again supports the occurrence of chlorite.

Cluster 5: This cluster resembles cluster 3 of the #11940 well dendrogram, except for Ba, which has been eliminated from this cluster.

Cluster 6: There is no apparent explanation for this cluster.

Cluster 7: Again, as in the #11940 well dendrogram, the tight grouping of the organic fractions in this cluster seem to indicate the relationship is based on the analytical technique.

There is no apparent explanation for N_2 in this cluster, and its very loose association with the organic fractions seems to indicate that the amount of influence it exerts is slight.

Cluster 8: There is no apparent explanation for this cluster. Sulfate sulfur, Na_2O, and SiO_2 are usually considered to be associated with the mineral fraction, while Ni is usually associated with the organic fraction.

Cluster 9: The relationship between P_2O_5 and combustible LTA is not fully understood, although the loose relationship of Cr to this cluster supports its association with the organic fraction (Vine, 1966, 1970).

CORRELATION COEFFICIENTS

Correlation coefficients were determined on the data from the Cottageville well #11940. Correlation coefficients measure the degree of interrelationship between two variables in a way that is not influenced by measurement units (Davis, 1973). It is therefore a unitless number. The value for a correlation coefficient of plus 1 indicates a perfect linear relationship between two variables and a correlation coefficient of minus 1 indicates an inverse relationship between two variables. Any values in between plus 1 and minus 1 are possible correlation coefficients; including zero, which shows the lack of any linear relationship.

SPSS (Statistical Package for the Social Sciences) available at the Vanderbilt University Computer Center was used to process the Cottageville well #11940 data. Table 3 shows the results of processing the variables vs. depth.

As shown in the table, boron and chlorite have a positive correlation coefficient, that is, their values increase with increasing depth. The increasing abundance of chlorite with depth in argillaceous sediments has been reported (Burst, 1969). The direct relationship between boron concentration and depth has also been reported (Hills and Levinson, 1975). This may indicate a diagenetic change (or burial metamorphism) with depth, or it may support the use of boron as an environmental indicator.

SUMMARY AND CONCLUSIONS

The statistical analyses of geochemical data obtained from the Cottageville wells #11940 and #12041 indicate that, in general:

1) the clustering of the data fits geochemical patterns; and,
2) some of the clusters are controlled by the genetic nature of the variables or by the analytical technique.

The shale cores may be "grossly" characterized in terms of a few geochemical variables; but generally, the cores exhibit a heterogenous nature which would require a more detailed analysis. In addition, the results of analysis to determine correlation coefficients indicate that there are some elements with concentrations that vary with depth which may be useful in the reconstruction of the depositional environment.

Statistical analysis as attempted in this paper can be applied for regional correlation of geochemical data. The simultaneous use of Q-mode and R-mode analysis may help determine factors controlling the hydrocarbon content of the shales. The ultimate use of statistical analysis sees the clustering of geochemical data with stratigraphy and lithology to recreate the depositional environment in hopes of using it for the prediction of areas of high gas production.

ACKNOWLEDGEMENTS

The authors would like to thank the following people for their help in the successful completion of this work.

E. E. Childers, Analytical Equipment R & D Branch, Morgantown Energy Research Center, for sample preparation; the Chemical Services Branch, Morgantown Energy Research Center, for elemental analyses; the Computer/Math Branch, Morgantown Energy Research Center, especially J. Mercer, for statistical analyses; M. Vickers, West Virginia Geological Survey, for assistance in geostatistical interpretations; and J. J. Renton, West Virginia Geological Survey, R. W. Stanton, U. S. Geological Survey, and S. M. Warshauer, West Virginia University, for critically reviewing this manuscript.

TABLE 1

"STATISTICAL ANALYSIS OF GEOCHEMICAL DATA FROM COTTAGEVILLE #11940"

Variable	Number of Samples	Mean	Standard DEV	Variance	Sum	Corrected SS	Low	High	C.V. %
Totcarb	58	2.791	1.715	2.943	161.910	167.754	0.270	7.600	61.455
Orgcarb	58	2.406	1.909	3.645	139.570	207.800	0.020	7.370	70.345
Mincarnb	58	0.358	0.773	0.597	22.340	34.081	0.010	4.580	200.756
Specgra	58	2.656	0.115	0.013	154.090	0.759	2.350	2.870	4.346
Moisture	58	0.487	0.152	0.023	28.270	1.322	0.050	0.870	31.253
Hydrogen	58	0.829	0.411	0.169	48.100	9.638	0.220	2.950	49.585
Nitrogen	58	0.048	0.063	0.004	2.829	0.231	0.0	0.290	131.184
Totsulf	58	2.193	1.091	1.169	127.200	66.666	0.280	7.530	49.313
Pyrsulf	58	1.948	0.737	0.540	113.010	31.008	0.160	3.520	37.854
Orgulf	58	0.141	0.093	0.008	8.220	0.494	0.010	0.620	65.703
Sulsulf	58	0.031	0.058	0.003	1.820	0.195	0.0	0.440	186.725
CO_2	58	1.554	2.852	8.081	83.730	460.624	0.030	16.970	196.917
HTA	58	90.086	10.081	101.643	5225.020	5792.663	38.430	95.870	11.191
SiO_2	58	56.920	7.379	54.453	3301.370	3103.825	24.470	69.890	12.964
Al_2O_3	58	16.419	2.741	7.516	952.310	428.437	6.240	20.090	16.698
Fe_2O_3	58	6.583	1.283	1.646	381.830	93.834	3.610	9.380	19.490
CaO	58	1.435	2.905	8.443	83.250	481.297	0.180	17.950	202.448
MgO	58	1.538	0.356	0.125	89.220	7.231	0.610	2.210	23.155
Na_2O	58	0.678	0.181	0.032	39.330	1.867	0.230	1.390	26.694
K_2O	58	3.646	0.739	0.546	211.510	31.178	0.900	4.980	20.281
P_2O_5	58	0.012	0.060	0.003	5.960	0.207	0.0	0.190	58.724
TiO_2	58	0.715	0.261	0.068	41.480	3.899	0.180	0.250	36.572
SO_3	58	0.874	0.429	0.184	50.730	10.537	0.230	2.280	49.158
MnO	58	0.048	0.041	0.001	2.800	0.100	0.020	0.220	86.948
B	58	0.014	0.005	0.000	0.860	0.001	0.010	0.020	22.995
Cu	58	0.006	0.006	0.000	0.380	0.002	0.0	0.040	101.292
Ni	58	0.056	0.004	0.000	0.330	0.001	0.0	0.010	87.799
Ba	58	0.054	0.017	0.000	3.160	0.017	0.040	0.140	32.466
Cr	58	0.009	0.002	0.000	0.530	0.000	0.0	0.010	30.983
Sr	58	0.015	0.005	0.000	0.890	0.001	0.010	0.020	37.057
LTA	58	97.837	1.818	3.307	5674.570	188.506	92.660	99.900	1.859
Combita	58	2.142	1.834	3.363	124.250	191.732	0.020	7.340	85.613
Chlorite	58	5.144	1.351	1.826	298.400	104.123	2.400	9.000	26.270
Illite	58	53.068	6.685	44.696	3078.000	2547.724	17.400	61.600	12.598
Kaoline	58	1.958	2.347	5.512	113.600	314.240	0.0	8.100	119.879
Quartz	58	31.334	7.112	50.591	1817.400	2883.691	20.400	78.700	22.699
Ortclas	58	0.117	0.220	0.048	6.800	2.782	0.0	0.800	188.460
Placlas	58	3.112	1.341	1.799	180.500	102.561	0.0	8.600	43.103
Calcite	58	1.477	4.287	18.382	85.700	1047.780	0.0	22.900	290.165
Dolomite	58	0.817	2.341	5.480	47.400	312.402	0.0	16.800	286.464
BeloC_{12}	58	27,857	22.469	504.891	1615.750	28788.799	0.0	72.300	80.659
$C_{12}C_{20}$	58	11.491	10.271	105.501	666.500	6013.605	0.0	42.000	89.384
C_{28} Up	58	7.455	6.587	43.396	432.400	2473.583	0.0	20.400	88.363

TABLE 2

"STATISTICAL ANALYSIS OF GEOCHEMICAL DATA FROM COTTAGEVILLE #12041"

Variable	Number of Samples	Mean	Standard Dev	Variance	Sum	Corrected SS	Low	High	C.V. %
Totcarb	94	1.720	1.342	1.802	161.760	167.590	0.0	6.570	78.008
Orgcarb	94	1.433	1.396	1.949	134.790	181.282	0.0	6.470	97.366
Minicarnb	94	0.236	0.309	0.095	23.150	8.892	0.0	1.710	125.562
Specgra	94	2.707	0.085	0.007	254.480	0.681	2.470	2.900	3.162
Moisture	94	0.460	0.145	0.021	43.320	1.971	0.030	0.890	31.597
Hydrogen	94	0.703	0.160	0.025	66.140	2.393	0.350	0.270	22.799
Nitrogen	94	0.004	0.007	0.000	0.390	0.005	0.0	0.030	185.050
Tutsulf	94	1.904	0.827	0.684	178.990	63.676	0.180	3.380	43.456
Pyrsulf	94	1.687	0.777	0.603	158.650	56.156	0.010	3.110	46.041
Orgsulf	94	0.220	0.112	0.012	20.740	1.186	0.020	0.630	51.190
Sulsulf	94	0.008	0.013	0.001	0.840	0.016	0.0	0.080	148.121
CO_2	94	0.903	1.128	1.272	84.910	118.340	0.040	6.280	124.880
HTA	94	92.829	1.639	2.686	8725.990	249.889	86.930	95.780	1.766
SiO_2	94	58.386	6.064	36.775	5488.350	3420.123	5.940	66.840	10.386
Al_2O_3	94	18.503	2.137	4.569	1739.300	424.936	11.970	24.250	11.552
Fe_2O_3	94	6.447	0.753	0.567	606.050	52.758	3.130	7.920	11.682
CaO	94	0.818	0.961	0.925	76.920	86.061	0.090	7.320	117.558
MgO	94	1.700	0.500	0.250	159.880	23.331	0.180	3.600	29.448
Na_2O	94	0.469	0.216	0.046	44.140	4.356	0.0	1.300	46.090
K_2O	94	3.828	0.580	0.336	359.920	31.314	1.710	4.950	15.155
P_2O_5	94	0.142	0.378	0.143	13.350	13.316	0.0	3.650	266.441
TiO_2	94	0.699	0.282	0.079	65.720	7.425	0.0	1.410	40.417
SO_3	94	0.707	0.389	0.152	66.490	14.140	0.090	2.150	55.127
MNO	94	0.050	0.024	0.000	4.700	0.056	0.030	0.130	49.340
B	94	0.018	0.005	0.000	1.740	0.002	0.0	0.040	28.518
Cu	94	0.006	0.007	0.000	0.640	0.004	0.0	0.020	105.985
Ni	94	0.031	0.036	0.001	3.000	0.120	0.0	0.200	112.860
Ba	94	0.033	0.024	0.000	3.110	0.055	0.0	0.120	73.907
Cr	94	0.011	0.004	0.000	1.070	0.001	0.0	0.030	37.783
Sr	94	0.010	0.006	0.000	0.980	0.003	0.0	0.020	57.851
LTA	94	92.230	24.260	588.581	8669.680	54738.107	0.0	99.990	26.304
Combita	94	2.375	10.170	103.432	233.320	9619.236	0.0	99.000	428.084
Chlorite	94	5.264	1.367	1.870	494.880	173.990	0.960	9.130	25.981
Illite	94	52.181	7.882	62.134	4905.080	5778.466	4.540	64.360	15.106
Kaoline	94	2.566	5.562	30.944	241.210	2877.883	0.0	51.900	216.784
Quartz	94	32.845	7.589	57.607	3087.440	5357.516	1.140	80.330	23.108
Ortclas	94	0.650	2.046	8.682	61.190	807.467	0.0	28.720	452.656
Placlas	94	2.739	1.040	1.082	257.480	100.636	0.0	7.000	37.977
Calcite	94	0.637	1.520	2.312	59.950	215.088	0.0	11.800	238.454
Dolomite	94	0.262	1.123	1.261	24.680	117.292	0.0	8.300	427.737
BeluoC_{12}	94	17.401	22.624	511.873	1635.700	47604.249	0.0	61.000	130.019
$C_{13}C_{20}$	94	11.334	14.732	217.056	1065.400	20186.271	0.0	42.800	129.988
$C_{21}C_{27}$	94	5.959	7.876	62.033	560.200	5769.146	0.0	25.300	132.160
C_{28} UP	94	3.601	5.064	25.649	338.500	2385.449	0.0	19.000	140.641

TABLE 3. Correlation coefficients showing the variation of listed variables with depth (99% confidence level, 45 variables, significant value of r = $\pm$ 0.328)

Variables	r
Specific gravity	-0.36
Moisture	-0.43
Organic S	-0.55
Fe_2O_3	-0.47
Na_2O	-0.38
Chlorite	0.41
Boron	0.63
Copper	-0.36
Barium	-0.36

DENDROGRAM FOR THE COTTAGEVILLE WELL 11940

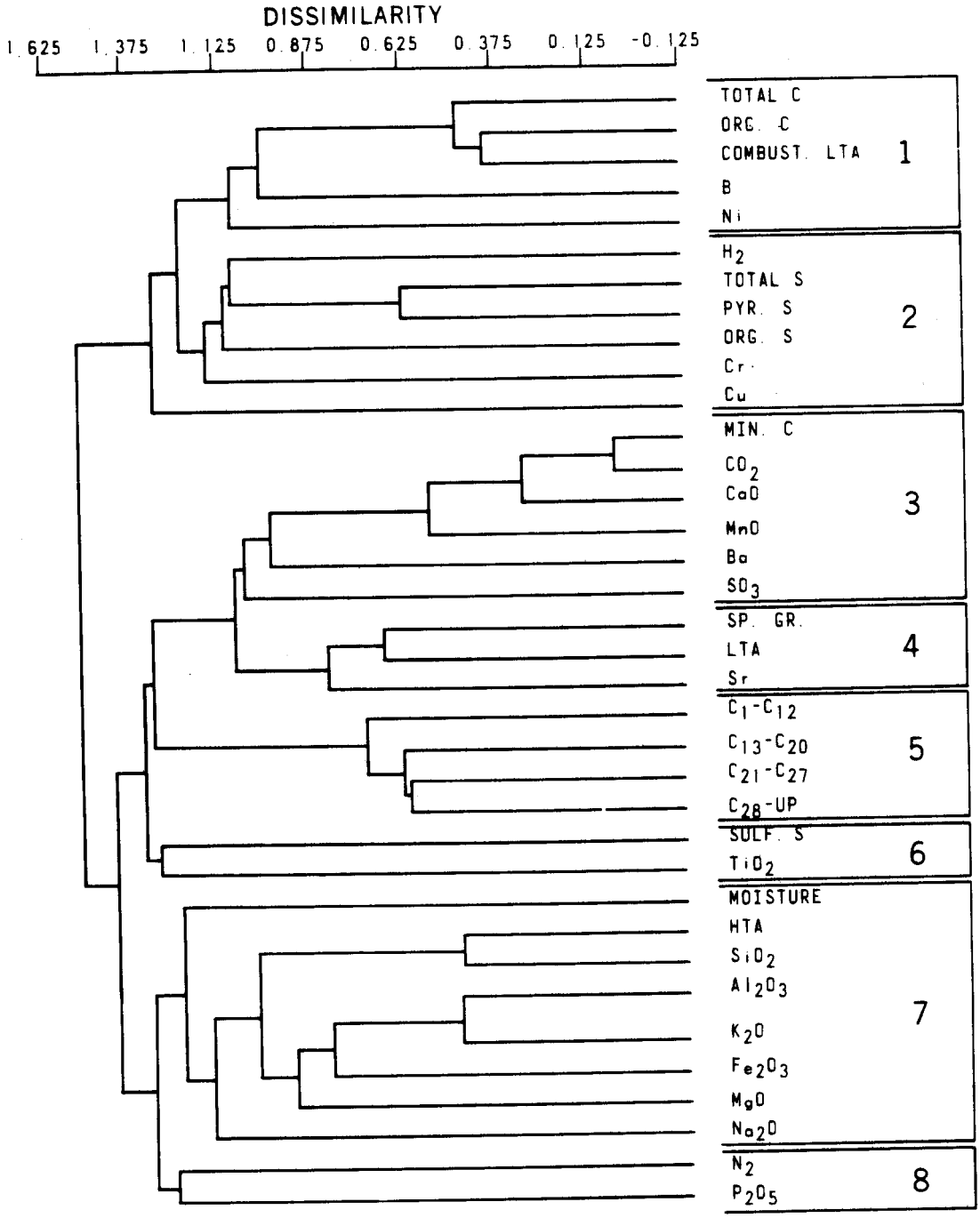

DENDROGRAM FOR THE COTTAGEVILLE WELL 12041

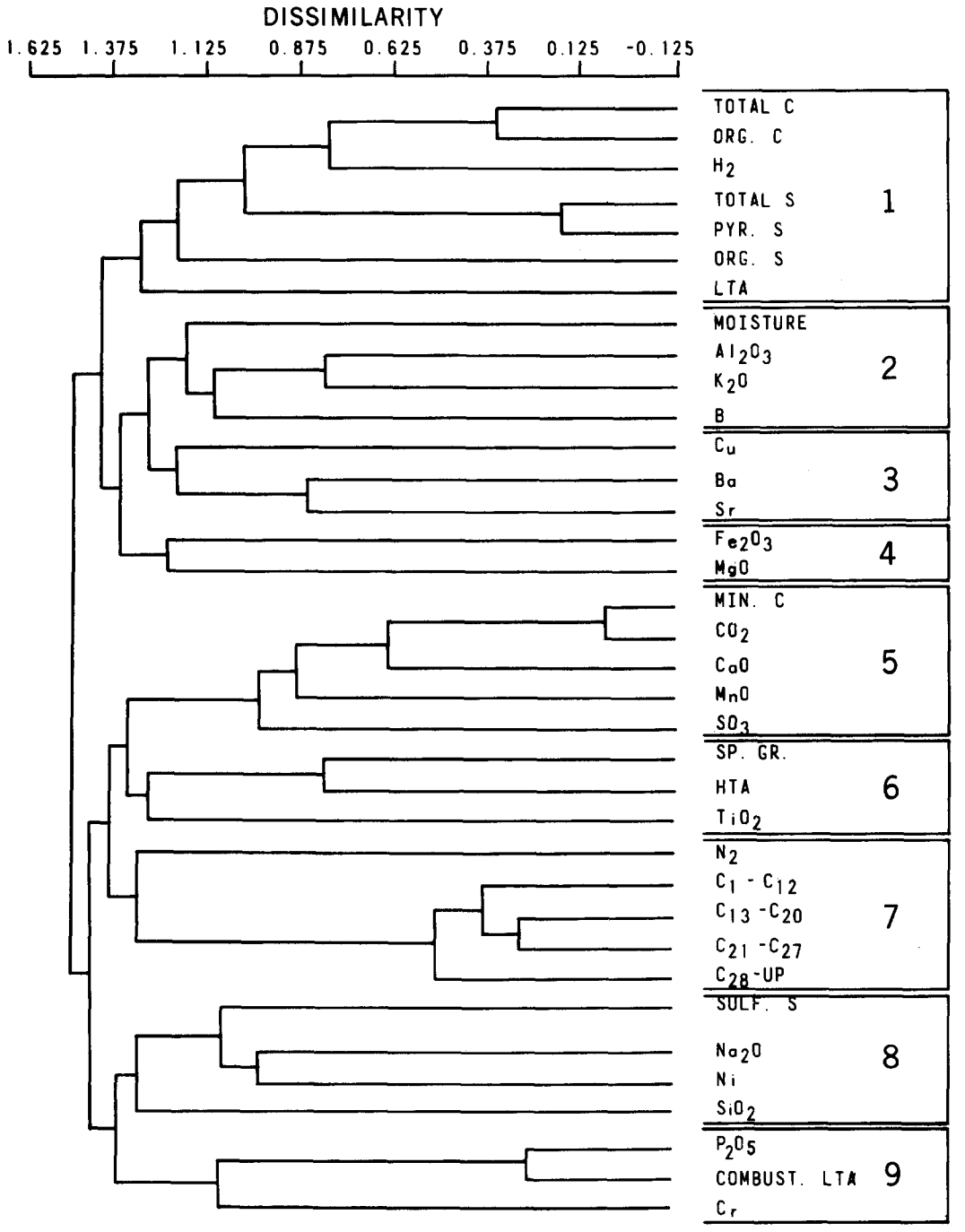

REFERENCES

1. Blackburn, W.H., 1976, Personal Communication: University of Kentucky.

2. Burst, J.F., 1969, Diagenesis of Gulf Coast Clayey Sediments, and its possible relation to petroleum migration: Amer. Assoc. Petrol. Geol. Bull. 53, 73-93.

3. Byrer, C.W., Trumbo, D.B., and Rhoades, S.J., 1976, Lithologic description of cored wells #11940 and #12041 in the Devonian Shale in the Cottageville, West Virginia area: U.S. ERDA - Morgantown Energy Research Center Techn. Rept; MERC/TPR-76/7, 22 pp.

4. Childers, E.E., 1977, Personal Communication: Morgantown Energy Research Center.

5. Conant, L.C. and Swanson, V.E., 1961, Chattanooga Shale and related rocks of Central Tennessee and nearby areas: U.S. Geol. Survey Prof. Paper, 357, 91 pp.

6. Cooper, G. Arthur, et.al., Correlation of the Devonian Sedimentary Formulation of North America, Correlation Chart No. 4, 1942, Bulletin of the Geological Society of America, 65 pp.

7. Couch, E.L., 1971, Calculations of paleosalinities from boron and clay mineral data: Amer. Assoc. Petrol. Geol. Bull., v. 55, p. 1329-1837.

8. Dana, James D. and Dana, Edward S.,1951, The System of Mineralogy, 7th ed. by Charles Palache, Harry Berman and Cliffort Frandel.

9. Davis, J.C., 1973, Statistics and Data Analysis in Geology: New York, J. Wiley & Sons, 550 pp.

10. Duncan, D.C. and Swanson, V.E., 1965, Organic-rich shale of the United States and World land areas: U.S. Geol. Survey Circ., 523, 30 pp.

11. Gibson, F.H. and Ode, W.H., 1962, Application of rapid methods for analyzing coal ash and related materials: U.S. Bur. Min. Rept. Inv., 6036, 23 pp.

12. Gluskoter, H.J., 1965, Electronic low-temperature ashing of bituminous coal: Fuel, 44, 285-291.

13. Goldschmidt, V.M., 1954, Geochemistry: Oxford, Clarendon Press, 730 pp.

14. Harbaugh, W. and Merriam, D.F., 1968, Computer applications in stratigraphic analysis: New York J. Wiley & Sons, 282 pp.

15. Hickman, R.C. and Lynch, V.J., 1967, Chattanooga Shale investigations: U.S. Bur. Min. Rept. Inv., 6932, 55 pp.

16. Hidalgo, R.V., 1974, Inorganic Geochemistry of Coal, Pittsburgh Seam, Ph.D. Dissertation, West Virginia University.

17. Kepferle, R.C., 1976, Personal Communication: U.S. Geol. Survey - University of Cincinnati.

18. Mazza, M.H., 1977, Personal Communications, Morgantown Energy Research Center.

19. Mazza, M.H. and Wilson, J.S., 1977, X-ray diffraction examination of coal combustion products related to boiler tube fouling and slagging, Advances in x-ray analysis, v. 20.

20. McCammon, R.B. 1968, The dendograph: A new tool for correlation: Geol. Soc. America Bull., 79, 1663-1670.

21. Parks, J.M., 1966, Cluster Analysis Applied to Multivariate Geologic Problems: J. Geol., 74, 703-715.

22. Renton, J.J., 1976, Personal Communication: West Virginia University.

23. Schutz, D.F. and Turekian, K.K., 1965, The investigation of the geographical and vertical distribution of several trace elements in sea water using neutron activation analysis, Geochem. Cosmochim Acta, 29, 259-313.

24. Sokal. R.R. and Sneath, P.H.A., 1963, Principles of Numerical Taxonomy: San Francisco, W.H. Freeman & Co., 359 pp.

25. Swanson, V.E., 1960, Oil yield and uranium content of black shales: U.S. Geol. Survey Prof. Paper, 356-A, 44 pp.

26. U.S. Office of Coal Research, 1967, Methods of analyzing and testing coal and coke: U.S. Bur. Min. Bull., 638, 82 pp.

27. Vine, J.D., 1966, Element Distribution in some Shelf and Eugeosynclinal Black Shales, U.S. Geol. Survey Bull., 1214-E, 31 pp.

28. Vine, J.D., 1969, Element distribution in some Paleozoic black shales and associated rocks: U.S. Geol. Survey Bull., 1214-G, 32 pp.

29. Vine, J.D., Tourtelot, E.B., and Keith, J.R., 1969, Element Distribution in some Trough and Platform types of Black Shale and Associated Rocks, U.S. Geol. Survey Bull., 1214-H, 31 pp.

30. Vine, J.D. and Tourtelot, E.B., 1970, Geochemistry of black shale deposits - A summary report: Econ. Geol. 65, 253-272.

31. Yen, T.F., 1976, Personal Communication: University of California, Los Angeles.

32. Zubovic, P., 1966, Physiochemical properties of certain minor elements as controlling factors of their distribution in coal: Adv. Chem. Ser., 55, 221-246.

A PETROLOGIC STUDY OF THE DEVONIAN SHALES FROM CENTRAL TENNESSEE AND WEST VIRGINIA

Jojok Sumartojo, Department of Geology, Vanderbilt University, Nashville, Tennessee 37235
Peter Waldstein, U.S. ERDA/Morgantown Energy Research Center, Morgantown, West Virginia 26505*

ABSTRACT

The X-ray mineralogy of the Devonian black shales collected from outcrops in central Tennessee and drillings in Kentucky and West Virginia, is simple and fairly uniform. The mineral assemblage consists mainly of chlorite, illite (muscovite), and quartz, with minor amounts of feldspars, carbonates, and pyrite.

Petrographic and scanning electron microscopic (SEM) examinations show the occurrence of organic matter (spore, kerogen, bitumen, and woody fragments) and minerals such as gypsum, pyrite, halite, albite, sphalerite, calcium phosphate. SEM observations also show the presence of spaces among the phyllosilicate platelets and the authigenic minerals, and in the fine cracks. Futhermore the size and distribution of quartz grains can be revealed by using an SEM.

INTRODUCTION

U.S. ERDA/Morgantown Energy Research Center (MERC) has an ongoing multifaceted research project on the Devonian black shales in Ohio, Kentucky, Tennessee, Illinois, and West Virginia. This black shale, which in Tennessee is called Chattanooga Shale, was the object of much investigation in the 1960's during the high activities of exploration for uranium minerals and petroleum (Swanson, 1960; Conant and Swanson, 1961; Hickman and Lynch, 1967). Attention is given now because of the association of this black shale with natural gas.

Exploratory wells have been drilled, and more will be drilled, by ERDA/MERC in the mideastern states (West Virginia, Ohio, Kentucky, and Tennessee). Apparently, the entrapment of gas in the Devonian black shale is due to the presence of fracture systems, which are either open or partly mineralized (W.K. Overbey, Jr., 1976, pers. comm.). However, the presence of these fractures is not sufficient to account for the amount of gas recovered from the shale horizon encountered during drilling.

One of the drilled wells is the Nicholas Combs well # 7239, located about 12 miles north of Hazard, Perry County, Kentucky. The lithologic log of this well has been described by Byrer and Trumbo (1976). Other completed wells are wells # 20403 drilled in Lincoln County, and # 11940 in Jackson County, near Cottageville, both in West Virginia (Byrer et al., 1976a; Byrer et al., 1976b).

The purpose of the present study is to find if there are pore spaces, other than the fractures, which may act as additional spaces for the gas entrapment. We also want to know if the clay mineral assemblage and the organic matter indicate the diagenetic stage of this remarkable shale. To answer these questions, we examined selected samples from the completed wells and from outcrops in central Tennessee using X-ray diffraction, and optical and electron microscopy, with the emphasis on the last technique.

---

* Present address: P.O. Box 33128, District Heights, Maryland 20028.

To our knowledge, only scant work has been presented in the literature on the fabric and grain-size distribution of indurated shales based on electron microscopic studies (O'Brien, 1968; 1970). Scanning electron microscopic (SEM) studies have been carried out by various investigators on other geologic materials such as quartz grains (Krinsley and Takahashi, 1962, 1964; Krinsley and Doornkamp, 1973; Margolis and Krinsley, 1974; Almon et al., 1976), clay minerals (Borst and Keller, 1969; Bohor and Hughes, 1971), etch pits on quartz (Subramanian, 1975), coals (Finkelman et al., 1976; Greer, 1977), and other rocks (Gillot, 1969; Pittman and Dischatko, 1970; Oehler, 1975).

ANALYTICAL PROCEDURES

Mineralogy and Petrography

The identification of minerals by X-ray diffraction was based on the common procedures (Brown, 1961; Warshaw and Roy, 1961; Biscaye, 1965; Carroll, 1970). Thin sections and polished sections were also prepared for petrographic examinations.

Scanning Electron Microscopy

Sample preparation for the SEM work was minimal. Rock chips of about 1 cm x 1 cm x ½ cm, broken parallel and perpendicular to the sedimentary layering, were mounted on aluminum stubs using epoxy glue or plastic cement. Fractured and polished surfaces were prepared for this study. The mounted samples were then carbon-coated in an ETEC vacuum coater-evaporator. The samples were directly examined under an ETEC "Autoscan" scanning electron microscope at an operating voltage of 20 kilovolts.

The identification of minerals was based on the X-ray fluorescence spectra detected by means of a NUCLEAR SEMICONDUCTOR Si(Li) energy dispersive crystal and a TRACOR NORTHERN NS-880 recorder.

We examined samples of the Devonian black shales from two outcrops in Central Tennessee, MERC's wells # 7239 (depth interval: 2529.47-2530.68 feet), # 20403 (depth interval: 3894.48-3895.07 feet) and # 11940 (depth interval: 3750-3750.35 feet).

RESULTS AND DISCUSSION

Petrography

Microscopic examinations of thin sections show that the black shales consist mainly of quartz (about 30-40%), illite (muscovite) and chlorite (40-60%), and organic matter (1-3%). In minor amounts, feldspars, calcite (and possibly also dolomite), heavy minerals such as zircon, rutile, and pyrite also occur in the samples.

In hand specimens as well as thin sections, the Devonian black shale is a dark, grey to black, finely laminated shale. The laminations of 0.1 to 0.5 mm are due to the proportion and variation of grain size of quartz (average diameter of about 0.02 mm) and organic matter. The organic matter occurs as black discrete particles (from less than 0.5 μm to 0.02 mm), and brownish yellow material forming stains (coating) on the groundmass (Fig. 1a). In addition, collapsed spores of about 0.2 to 0.5 mm in diameter occur throughout some samples (Figs. 1c and 1d). Reddish brown organic matter (woody ?) and thin-walled and possibly cuticular material occasionally occur in the rocks (Fig. 1b). A few of the spores are filled with authigenic minerals such as pyrite, carbonate, and quartz. Pyrite and gypsum may occur also as veinlets (Fig. 1f). Larese and Heald (1977) also pointed out that there are two kinds of spores; the thick and the thin-walled spores. In their samples, they found barite and pyrite filling the spores.

The presence of highly birefringent phyllosilicate indicates that the mineral is muscovite (rather than illite as such). This is also indicated on the X-ray diffractograms. The discrete organic particles are presumably the insoluble kerogen (Figs. 1a and 1e), whereas the brownish stain is the organic matter soluble in a benzene-alcohol mixture.

Mineralogy

The X-ray mineralogy of the minus 4 μm fraction is fairly uniform and simple. All of our samples are composed mainly of chlorite, illite, quartz, and traces of feldspars and carbonates (calcite and dolomite). Pyrite, which was identified on polished sections, was not detected on the X-ray diffractograms. Other minerals in minute amounts were detected by SEM examinations. We did not attempt to do quantitative determination of the clay minerals, because at best, the result would be only an

estimate of the relative abundance (van der Marel, 1966). However, we think that illite is present in greater abundance than chlorite because of the higher intensity of the illite basal reflections.

The similarity in the mineralogy of the samples from different localities is obvious (Fig. 2). The simple assemblage chlorite-illite (which is actually fine-grained muscovite) and quartz is typical of low-stage metamorphic pelitic rocks. However, the Devonian black shales are sedimentary rocks and do not show the characteristic slaty cleavage development, typical of true metamorphic rocks. In our samples, we did not find swelling clay minerals or kaolinite; the illite (001)-peak on the diffractograms shows a high degree of peakedness without showing any significant variation among the samples (Figs. 2 and 3). Observations led us to think that the phyllosilicates in the black shales are composed of relatively unaltered detrital muscovite and chlorite, the two phyllosilicates abundant in the metamorphic and igneous parent rocks of pre-Chattanooga time.

The high degree of peakedness of the (001) reflection is related more to the original muscovite rather than to the newly formed illite in the sediments. For this reason, we use the term muscovite interchangeably with illite. With the samples available to us, it was not possible to use the width at half-peak height as an indicator of diagenetic stage as shown by other investigators on rocks of different ages (Kubler, 1968; Weber, 1972a, 1972b; McKirdy et al., 1975).

The isolated kerogen from four samples of well # 7239 show, on the X-ray diffractograms, their non crystalline nature as indicated by the absence of diffraction peaks. Mature kerogen, i.e. kerogen which has been subject to highgrade diagenesis or some degree of metamorphism, would have shown a certain degree of crystallinity. It would be indicated by the peaks occurring at about 2θ angles of 26°, 43°, and 54° (Fig. 4). (McKirdy et al., 1975; Landis, 1971).

Scanning Electron Microscopy

Figures 5a, 5b, 5c, and 5d are the photomicrographs of a sample from well # 7239, broken at an angle of about 80° to the bedding plane. The fabric of shale with the primary preferred orientation of the phyllosilicates is shown in figure 5c; authigenic gypsum is shown at the center of figure 5c and 5d. These photographs show the presence of pore spaces among the phyllosilicates and gypsum crystals. Dean and Ross (1976) reported the occurrence of gypsum in powdered shale as a product of the reaction between calcite and pyrite which were present in their samples. However, our samples were freshly broken chips. The well developed fissility shown in figure 5c is due to the high degree in crystallinity of the phyllosilicates, especially illite. The abundance of organic matter within the shale may also promote the well developed fissility (O'Brien, 1970).

The grain and grain-size distribution, especially of quartz, can be shown on polished sections. Because of the difference in polishing hardness of quartz and other constituents, quartz grains stand out pretty well. Figures 6a to 6d give us some idea of the morphology, size, and distribution of quartz. The presence of fine cracks parallel to the sedimentary layerings is also shown in those figures. Other photomicrographs (Figs. 9f and 10d) show the general appearance of quartz distribution. The lamination due to the variation of grain size of quartz, also recognizable under petrographic microscope, is shown in figure 10e.

It is understandable that an SEM would reveal the presence of mineral constituents in shales, previously unrecognizable under an optical microscope or detectable on X-ray diffractograms. On the basis of the X-ray fluorescence and back-scattered electron photomicrographs (Figs. 7a to 7g, and 8a to 8d), we identified the presence of minerals such as pyrite (Fig. 9a), gypsum (Fig. 9b), halite (Fig. 9c), albite (Fig. 9d), ZnS (most probably sphalerite, Fig. 9e), quartz (Fig. 9f), Ca-phosphate (Fig. 9g), and inclusions in spores (Figs. 9i and 10a). Indeed, it is not possible to identify minerals with more complex formulas just on the basis of X-ray fluorescence alone; other means of identification should be carried out to identify the mineral phases (Plant, 1976, p.108; Finkelman, 1976).

The identification of organic matter (Figs. 9h, 10a, and 10c), under an SEM is not simple. Spores can be identified without too much difficulty, whereas the discrete organic particles (kerogen) or woody material can only be inferred from the back-scattered-electron photomicrographs of polished sections. In figures 8b and 10b, for example, the fine, dark, round and vermicular spots are organic matter. On unpolished broken surfaces, the dark spots may be due to the morphological features rather than the presence of organic matter (Figs. 6b and 7e).

During our SEM observations, we tried not to record just the aesthetically pleasing images, although admittedly we spent much time in looking at pyrite framboids! Other investigators, such as Greer (1977), have shown beautiful photomicrographs of pyrite in Iowa coals.

CONCLUSIONS

The results of our preliminary work on the petrology of the Devonian black shales indicate that the mineralogy of this argillaceous rock is simple and fairly uniform, being composed mainly of chlorite, illite, and quartz, with traces of feldspars, carbonates, and pyrite. Investigation is being carried out on this shale by other researchers, such as J.J. Renton of the West Virginia University, whose mineralogical results are essentially similar to ours (pers. comm., 1976). The clay mineralogy is well understood; however, we still intend to study the variation in the diagenetic stage using the reflectance of kerogen and the nature of illite as has been done on other rocks (Maxwell and Hower, 1967; Foscolos and Kodama, 1974; Foscolos et al., 1976; Diesel and Offler, 1975).

Our SEM examinations revealed petrographic features previously unobserved. We have detected the presence of minute pore spaces and minerals, and have shown the size and distribution of quartz by means of electron micrographs. It is not clear to us how to explain the presence of pyrite coexisting with gypsum; whether these minerals indicate a hypersaline environment or just the product of diagenesis, we do not know. During our SEM work, because of the high resolution of an SEM, we unwittingly may limit our observations.

ACKNOWLEDGMENTS

We wish to express our thanks to the various people who helped us in completing this work: John Kovach and Steve Lamey of MERC, for their continued interest and discussions, Edward Childers also of MERC, who patiently separated the kerogen, and Steve Caldwell of Vanderbilt University who did the busy work for sample preparation. Acknowledgment is also due to the Oak Ridge Associated Universities which granted a faculty research fellowship to one of us (J.S.) at MERC in Summer, 1976.

Support for a part of this work was defrayed by Grant No. EY-77-G-21-8122 awarded to Vanderbilt University by U.S. ERDA/MERC, and by a grant-in-aid awarded to J.S. by the Natural Science Committee of Vanderbilt University.

REFERENCES

ALMON, W.R., FULLERTON, L.B., and DAVIES, D.K., 1976, Pore space reduction in Cretaceous sandstones through chemical precipitation of clay minerals: Jour. Sed. Petrol., 46, 89-96.

BISCAYE, P.E., 1965, Mineralogy and sedimentation of Recent deep-sea clay in the Atlantic Ocean and adjacent seas and oceans: Bull. Geol. Soc. America, 76, 803-832.

BOHOR, B.F. AND HUGHES, R.E., 1971, Scanning electron microscopy of clays and clay minerals: Clays and Clay Min., 19, 59-54.

BORST, R.L. AND KELLER, W.D., 1969, Scanning electron micrographs of API reference clay minerals and other selected samples: Proc. Internatl. Clay Conf., 1, 871-901, Israel Univ. Press.

BROWN, G. (Ed.), 1961, The X-ray identification and crystal stuctures of clay minerals: London, Mineral Soc., 544 pp.

BYRER, C.W., VICKERS, M.K., RHOADES, S.J., and EASTERDAY, B.G., 1976a, Lithologic description of cored wells #20402 and #20403 in the Devonian shale in Lincoln County, West Virginia: U.S. ERDA/Morgantown Energy Research Center Techn. Rept. MERC/TPR-76/9, 58pp.

BYRER, C.W., TRUMBO, D.B., and RHOADES, S.J., 1976b, Lithologic description of cored wells #11940 and #12041 in the Devonian shale in the Cottageville, West Virginia area: U.S. ERDA/Morgantown Energy Research Center Techn. Rept. MERC/TPR-76/7, 22pp.

BYRER, C.W. and TRUMBO, D.B., 1976, Lithologic description of core material from Nicholas Combs No. 7239 well, Perry County, Kentucky: U.S. ERDA/Morgantown Energy Research Center Techn. Rept. MERC/TPR-76/2.

CARROLL, D., 1970, Clay minerals: A guide to their X-ray identification: Geol. Soc. America Spec. Paper, 126, 80pp.

CONANT, L.C. and SWANSON, V.E., 1961, Chattanooga Shale and related rocks of central Tennessee and nearby areas: U.S. Geol. Survey Prof. Paper, 357, 91pp.

DIESEL, C.F.K. and OFFLER, R., 1975, Change in physical properties of coalified and graphitised phytoclasts with grade of metamorphism: Neues Jahrb. Mineral. Mh.,9, 11-26.

DEAN, R.S. and ROSS, G.J., 1976, Anomalous gypsum in clays and shales: Clays and Clay Min., 24, 103-104.

FINKELMAN, R.B., STANTON, R.W., and BREGER, I.A., 1976, Energy dispersive X-ray analysis of in situ minerals in coal: Geol. Soc. America Abstr. Progr., 8, 865-866.

FOSCOLOS, A.E. and KODAMA, H., 1974, Diagenesis of clay minerals from Lower Cretaceous shales of northeastern British Columbia: Clays and Clay Min., 22, 319-335.

FOSCOLOS, A.E., POWELL, T.G., and GUNTHER, P.R., 1976, The use of clay minerals and inorganic geochemical indicators for evaluating the degree of diagenesis and oil generating potentials of shales: Geochim Cosmochim. Acta, 40, 953-966.

GILLOTT, J.E., 1969, Study of the fabric of fine grained sediments with the scanning electron microscope: Jour. Sed. Petrol., 39, 90-105.

GREER, R.T., 1977, Coal microstructure and the significance of pyrite inclusions, in: Om Johari, (Ed.), Scan.Electr. Microsc. 1977, 1, 79-93, Proc. 10th Ann. SEM Symp.

HICKMAN, R.C. and LYNCH, V.J., 1967, Chattanooga Shale investigations: U.S. Bur. Min. Rept. Inv., 6932, 55pp.

KRINSLEY, D.H. and TAKAHASHI, T., 1962, Surface textures of sand grains: Science, 138, 1262-1264.

KRINSLEY, D.H. and DOORNKAMP, J.C., 1973, Glossary of sand grain surface textures: London, Cambridge Univ. Press, 91pp.

KUBLER, B., 1968, Évaluation quantitative du métamorphisme par la cristallinité de l'illite: Bull. Centr. Rech. Pau-SNPA, 2, 385-397.

LANDIS, C.A., 1971, Graphitization of dispersed carbonaceous material in metamorphic rocks: Contr. Mineral. Petrol. 30, 34-45.

LARESE, R.E. and HEALD, M.T., 1977, Petrography of selected Devonian shale core samples from the CGTC 20403 and CGSS 11940 wells, Lincoln and Jackson Counties, West Virginia: U.S. ERDA/Morgantown Energy Research Center Techn. Rept. MERC/CR-77/66, 27 pp.

McKIRDY, D.M., SUMARTOJO, J., TUCKER, D.H., and GOSTIN, V., 1975, Organic, mineralogic and magnetic indications of metamorphism in the Tapley Hill Formation, Adelaide Geosyncline: Precambrian Res., 2, 345-373.

MARGOLIS, S.V. and KRINSLEY, D.H., 1974, Process of formation and environmental occurrence of microfeatures on detrital quartz grains: Amer. Jour. Sci., 274, 449-464.

MAXWELL, D.T. and HOWER, J., 1967, High-grade diagenesis and low-grade metamorphism of illite in the Precambrian Belt Series: Amer. Mineral., 52, 843-857.

O'BRIEN, N.R., 1968, Electron microscope study of black shale fabric: Naturwissensch.,10, 490-491.

O'BRIEN, N.R., 1970, The fabric of shale - an electron-microscopic study: Sedimentol., 15, 229-246.

OEHLER, J.H., 1975, Origin and distribution of silica lepispheres in porcelanite from the Monterey Formation of California: Jour. Sed. Petrol., 45, 252-257.

OVERBEY, W.K., Jr., 1976, Personal communication, U.S. ERDA/ Morgantown Energy Research Center, Morgantown, W.V.

PITTMAN, E.D. and DUSCHATKO, R.W., 1970, Use of pore casts and scanning electron microscope to study pore geometry: Jour. Sed. Petrol., 40, 1153-1157.

PLANT, A.G., 1976, Applications of microbeam techniques to mineralogy, in: D.G.W. Smith, (Ed.), Short course in microbeam techniques: Mineral. Assoc. Canada Short Course Handb., 1, 107-134.

RENTON, J.J., 1976, Personal communication, Department of Geography and Geology, West Virginia University, Morgantown, W.V.

SUBRAMANIAN, V., 1975, Origin of surface pits on quartz as revealed by scanning electron microscopy: Jour. Sed. Petrol., 45, 530-534.

SWANSON, V.E., 1960, Oil yield and uranium content of black shales: U.S. Geol. Survey Prof. Paper, 356A, 44pp.

van der MAREL, H.W., 1966, Quantitative analysis of clay minerals and their admixtures: Contr. Mineral. Petrol., 12, 96-138.

WARSHAW, C.M. and ROY, R., 1961, Classification and a scheme for the identification of layer silicates: Bull. Geol. Soc. America, 72, 1455-1492.

WEBER, K., 1972a, Notes on determination of illite crystallinity: Neues Jahrb. Mineral. Mh., 6, 267-276.

WEBER, K., 1972b, Kristallinität des Illits in Tonschiefern und andere Kriterien schwacher Metamorphose im nordöstlichen Rheinischen Schiefergebirge: Neues Jahrb. Geol. Paläont. Abh., 141, 333-363.

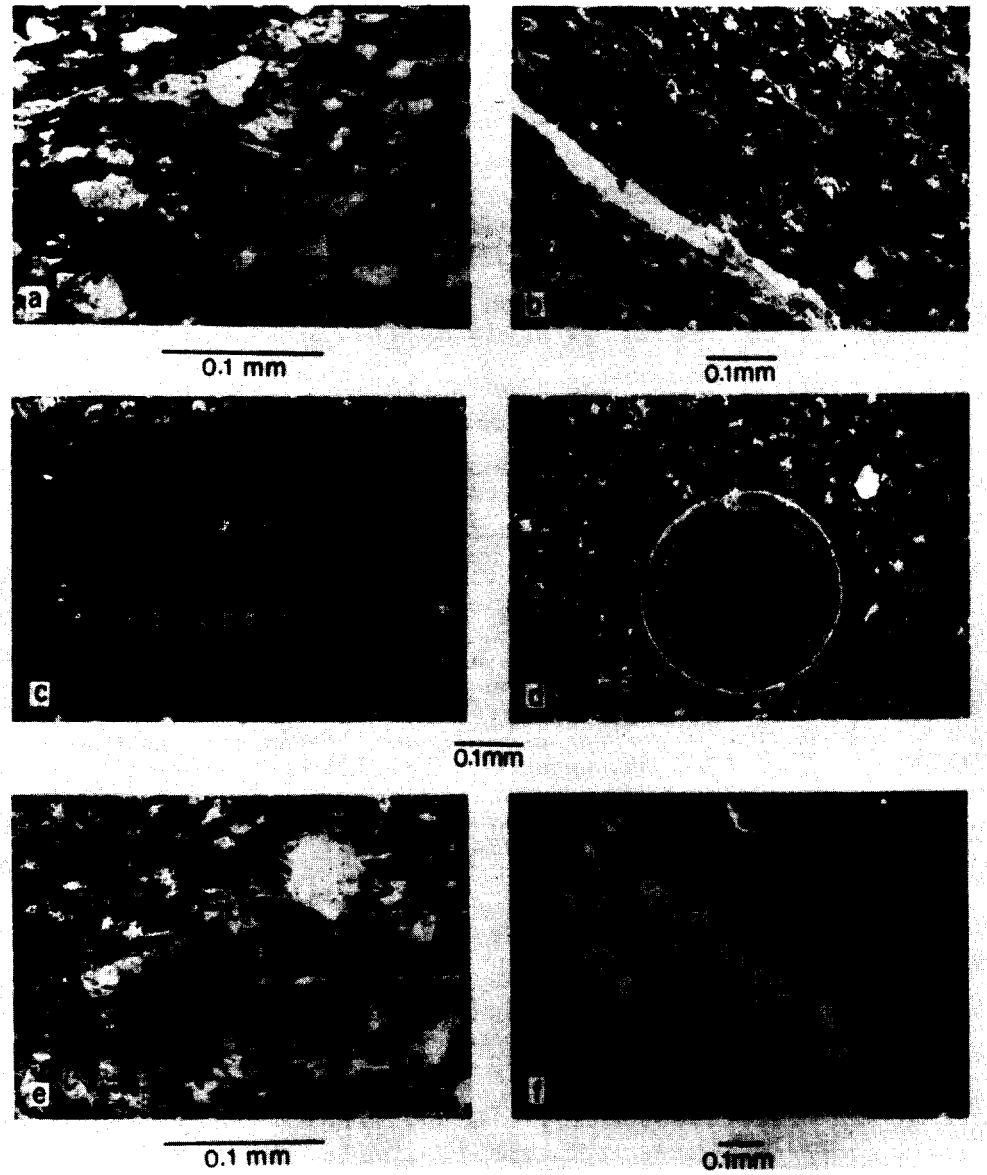

Figure 1. Photomicrographs of selected Devonian black shales.

(a) Quartz (light), phyllosilicates, and kerogen (black). Parallel polarizers. Sample collected 4 miles northeast of Nashville. Section perpendicular to bedding. (b) Thin-walled spores, cuticular matter (?), kerogen, and microcrack. Parallel polarizers; sample cut perpendicular to the bedding, from well #11940 at depth interval: 3713.78-3714.43 feet. (c) Collapsed spore (thick-walled) in sample collected 9 miles east of Nashville. Crossed polarizers; section cut perpendicular to the bedding plane. (d) Spore in sample from well #11940 at depth interval: 3750-3750.35 feet. Parallel polarizers; section cut parallel to the bedding plane. Notice the discrete organic particles (kerogen), and the general dark color of the groundmass (bitumen). (e) Pyrite (black grains at center), kerogen, detrital quartz (light), and detrital phyllosilicates (fine shreds). Sample, the same as in 1d, but cut perpendicular to the bedding plane. Parallel polarizers. (f) Veinlets of pyrite (dark) and gypsum (light) in a sample from well #7239 at depth interval: 2529.47-2530.68 feet. Parallel polarizers. Section cut perpendicular to the bedding plane.

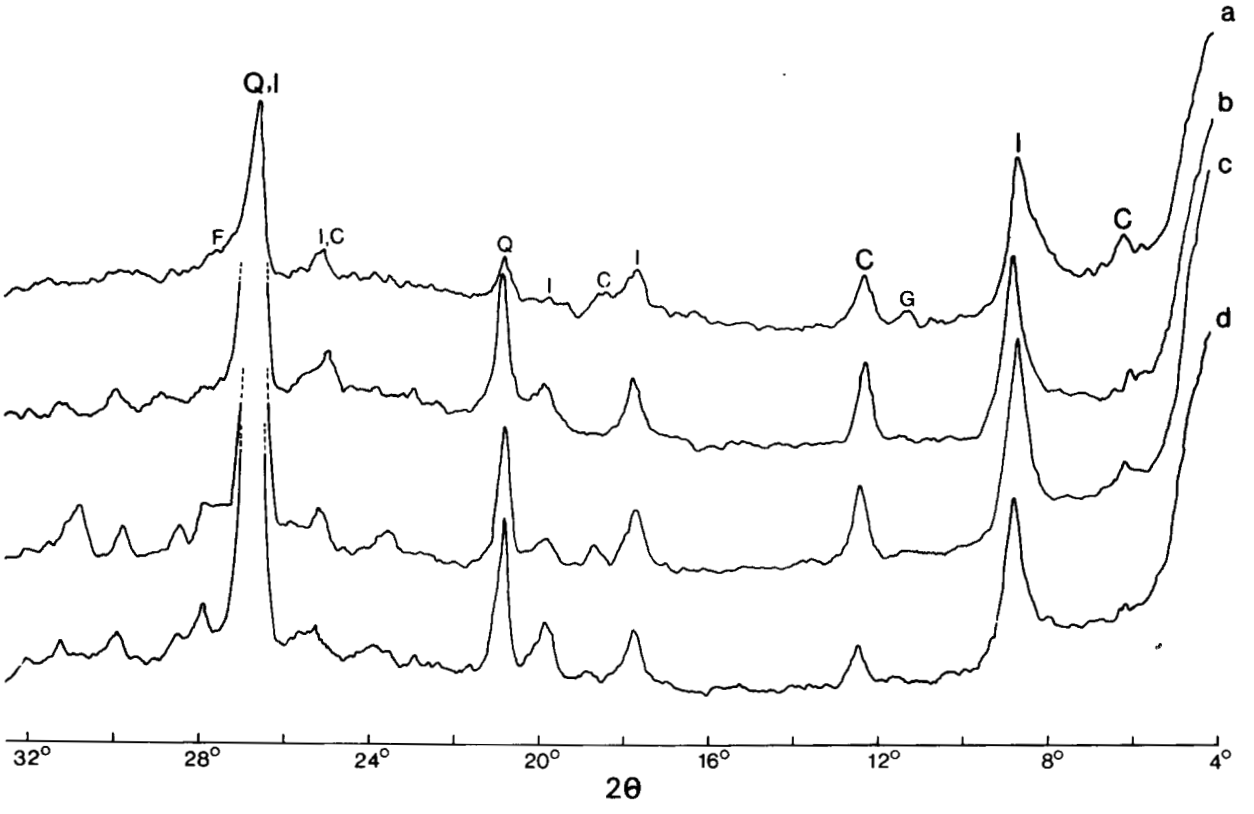

Figure 2. X-ray diffractograms of the minus 4 μm fraction.

a. Sample collected from an outcrop, 4 miles northeast of Nashville.

b. Sample from well #11940 at depth interval: 3445.1-3445.6 feet.

c. Sample collected from an outcrop, 9 miles east of Nashville.

d. Sample from well #7239 at depth interval: 2529.47-2530.68 feet.

C = Chlorite
I = Illite
G = Gypsum
Q = Quartz
F = Felspars

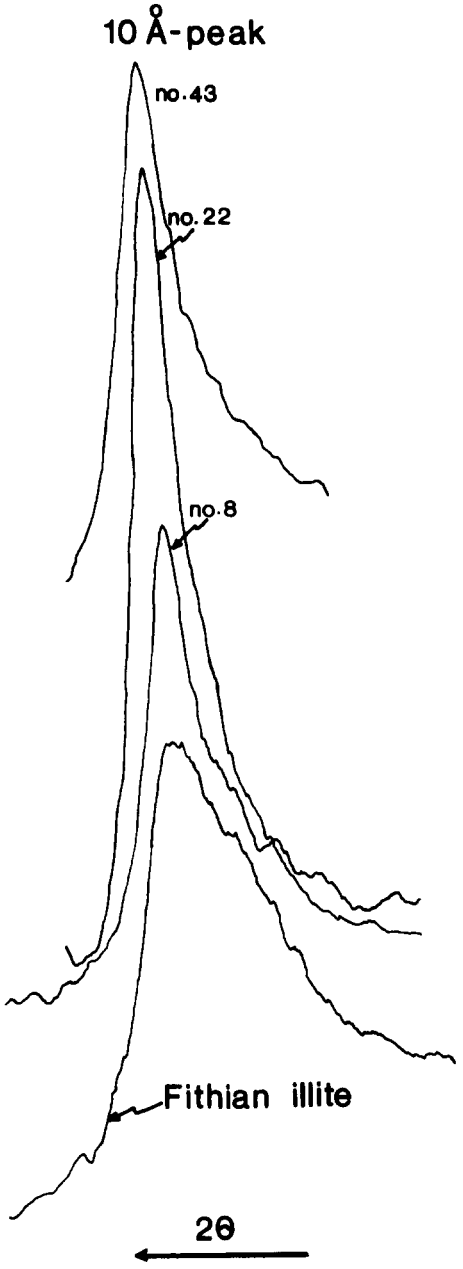

Figure 3. Comparison of the peakedness of the illite basal reflection in samples from well #11940 with that of illite from Fithian, Illinois.

Sample no. 8: Depth interval: 3445.1-3445.6 feet

Sample no. 22: Depth interval: 3610.9-3611.3 feet

Sample no. 43: Depth interval: 3713.78-3714.43 feet

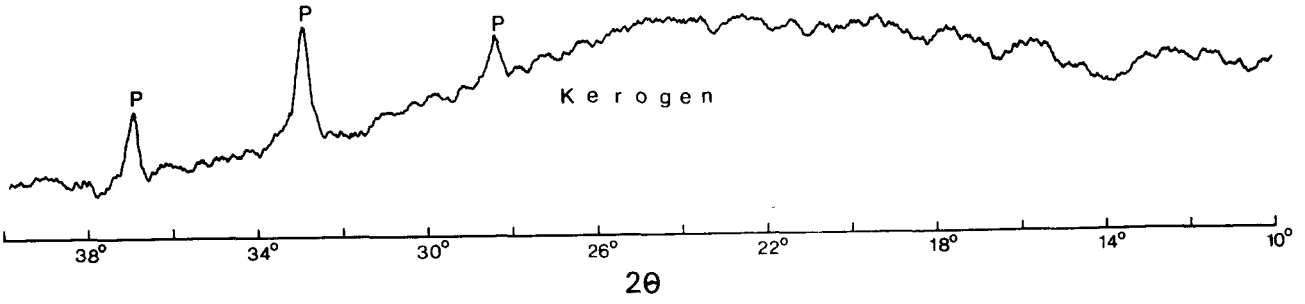

Figure 4. Typical X-ray diffractogram of kerogen isolated from 4 samples in well #7239 at depth intervals of:

2379.61-2380.77 feet
2468.58-2469.74 feet
2559.58-2560.26 feet
2599.88-2600.54 feet

Only P (=pyrite) peaks show the presence of crystalline matter. The run from 40° to 60° (2θ-angle) is not shown.

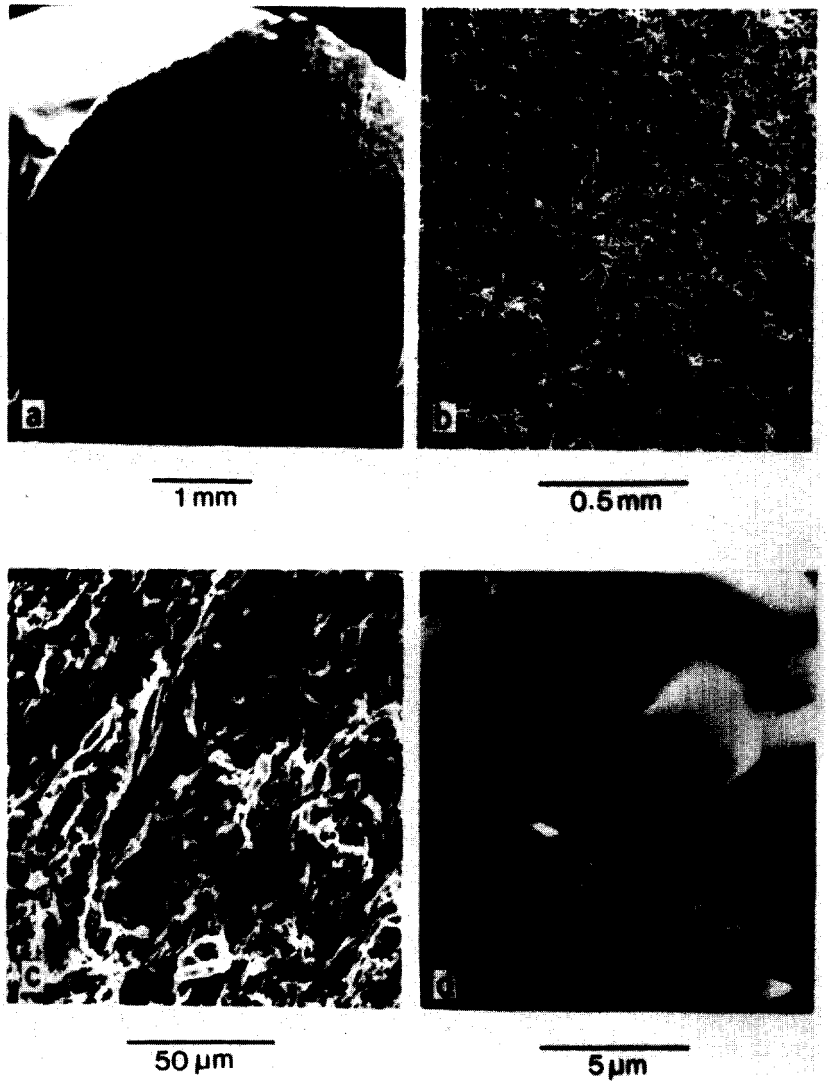

Figure 5. SEM photomicrographs of a sample from well #7239 at depth interval of 2529.47-2530.68 feet. Sample was broken approximately perpendicular to the bedding plane. Photographs were taken at different magnifications. Note the presence of gypsum shown in figures c and d. A collapsed spore is shown at the center of figure c; this same photograph shows the well developed fissility of the sample.

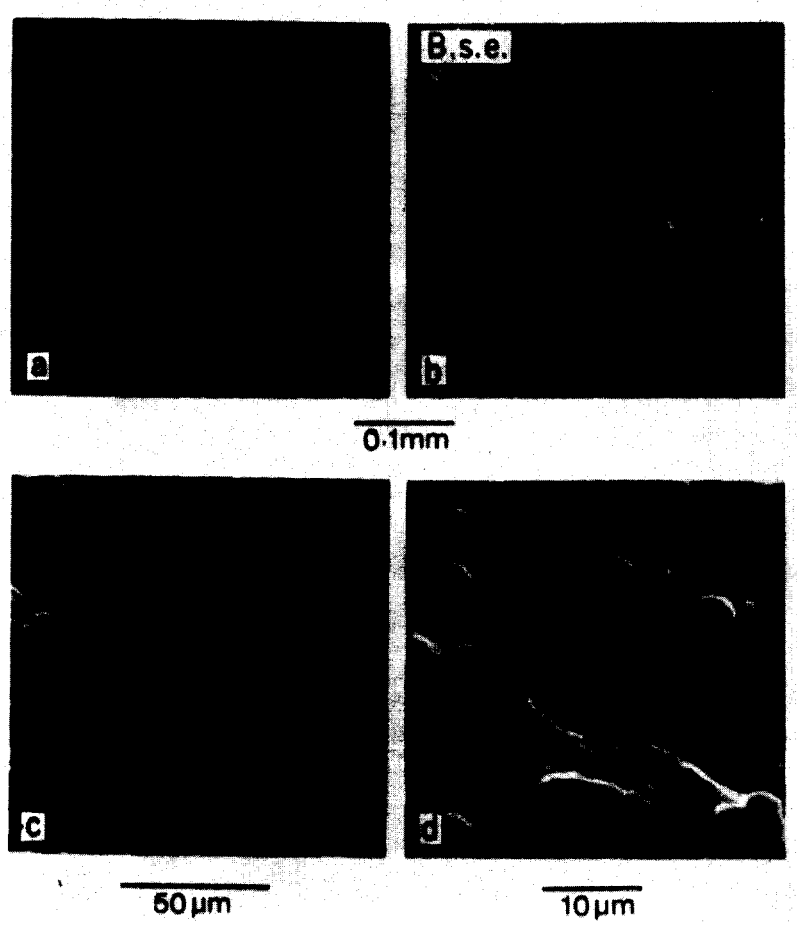

Figure 6. SEM photomicrographs of a sample from well #11940 at depth interval: 3750-3750.35 feet, at different magnifications. These photographs give some idea about the grain size of quartz and the dimension of a microcrack. Sample polished perpendicular to the bedding plane.

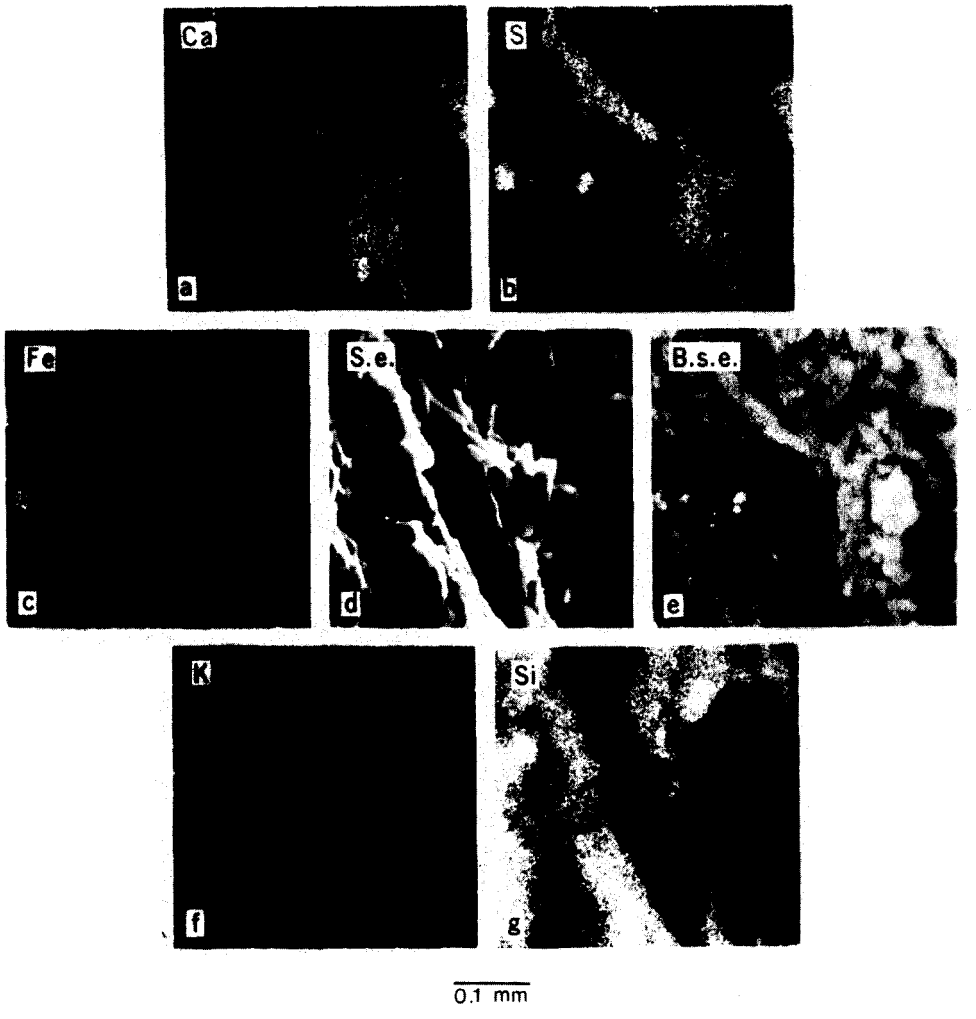

Figure 7. Method of identifying minerals by means of X-ray fluorescence (elemental mapping) and back-scattered electron imagery.

Figures a and b indicate the presence of calcium sulphate, also shown by the monoclinic crystals in figure d. Combination of figures b and c indicates the presence of pyrite, also shown by the corresponding light spots in figure e.

Figures f and g indicate the presence of illite, whereas figure g alone without the corresponding spots in figure f, indicates the presence of quartz.

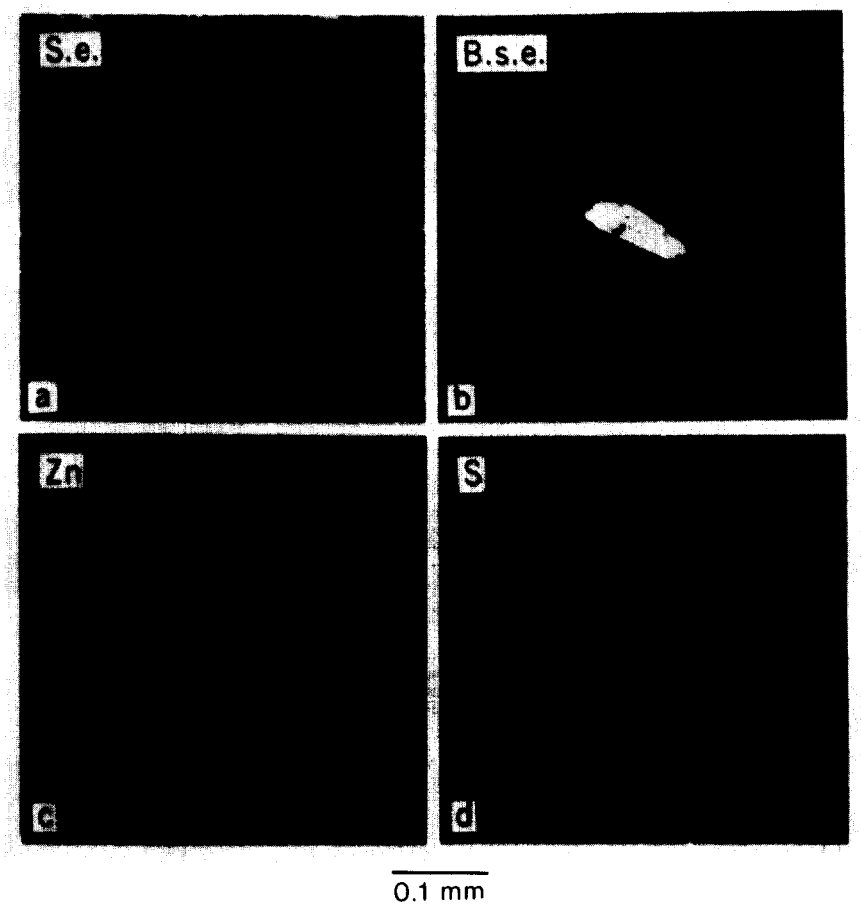

Figure 8. Method of identifying a mineral, similar to figure 7.

S.e. = Secondary electron

B.s.e. = Back-scattered electron

The mineral is probably sphalerite rather than wurtzite.

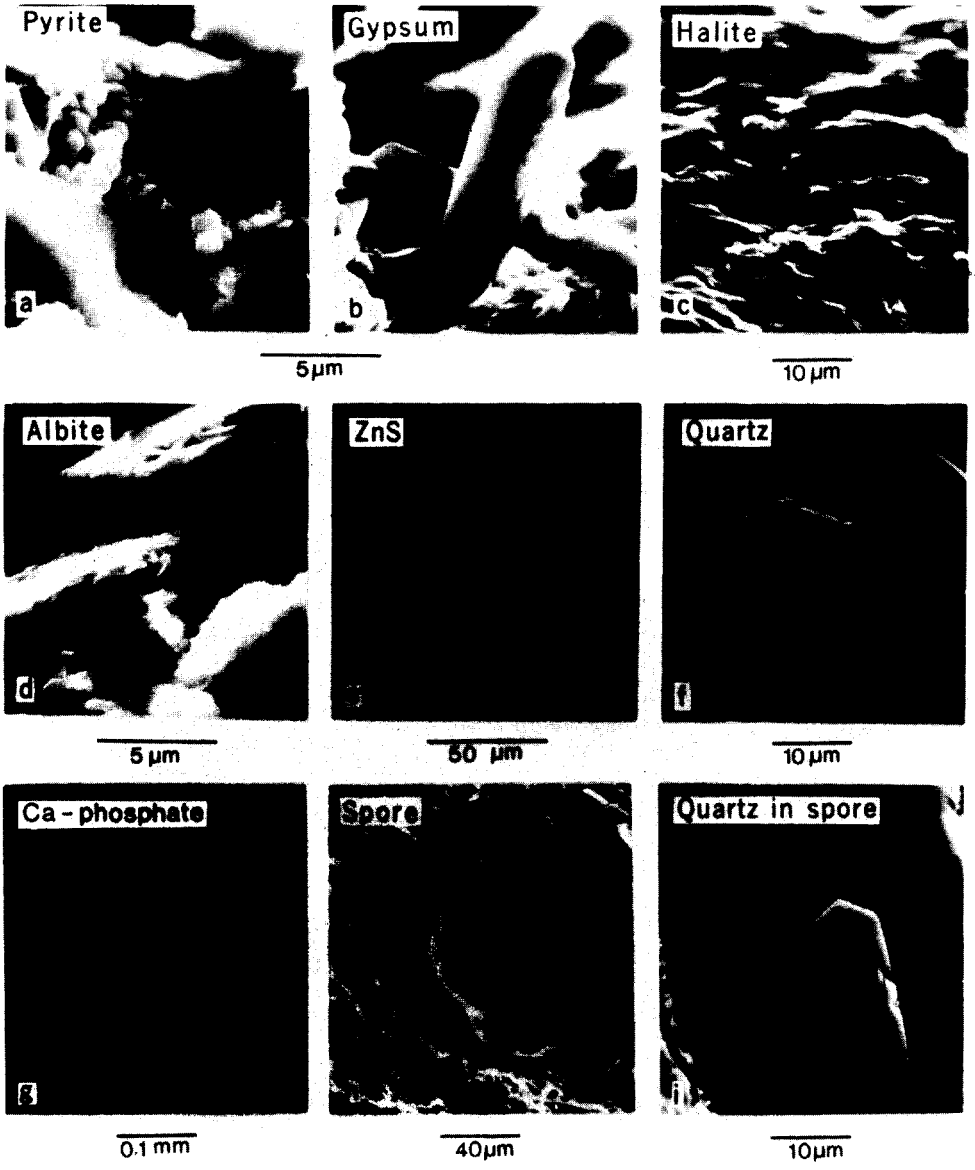

Figure 9. Minerals detected by SEM in selected samples of the Devonian black shales.

a. Pyrite in pore space among the phyllosilicate crystallites. Sample from well #20403.

b. Gypsum crystal in a sample from well #7239. Another possible mineral would be anhydrite; however, anhydrite is orthorhombic. The prismatic crystals in the figure indicate the presence of slanting (001) plane.

c. Halite in a sample from well #20403.

d. Authigenic albite in a sample from east of Nashville.

e. Sphalerite in a sample from well #11940.

f. Detrital quartz in a sample from well #11940.

g. Calcium phosphate in a sample from an outcrop, 4 miles northeast of Nashville.

h. Spore remain in a sample from well #7239.

i. Quartz inclusion in a spore in a sample from well #11940.

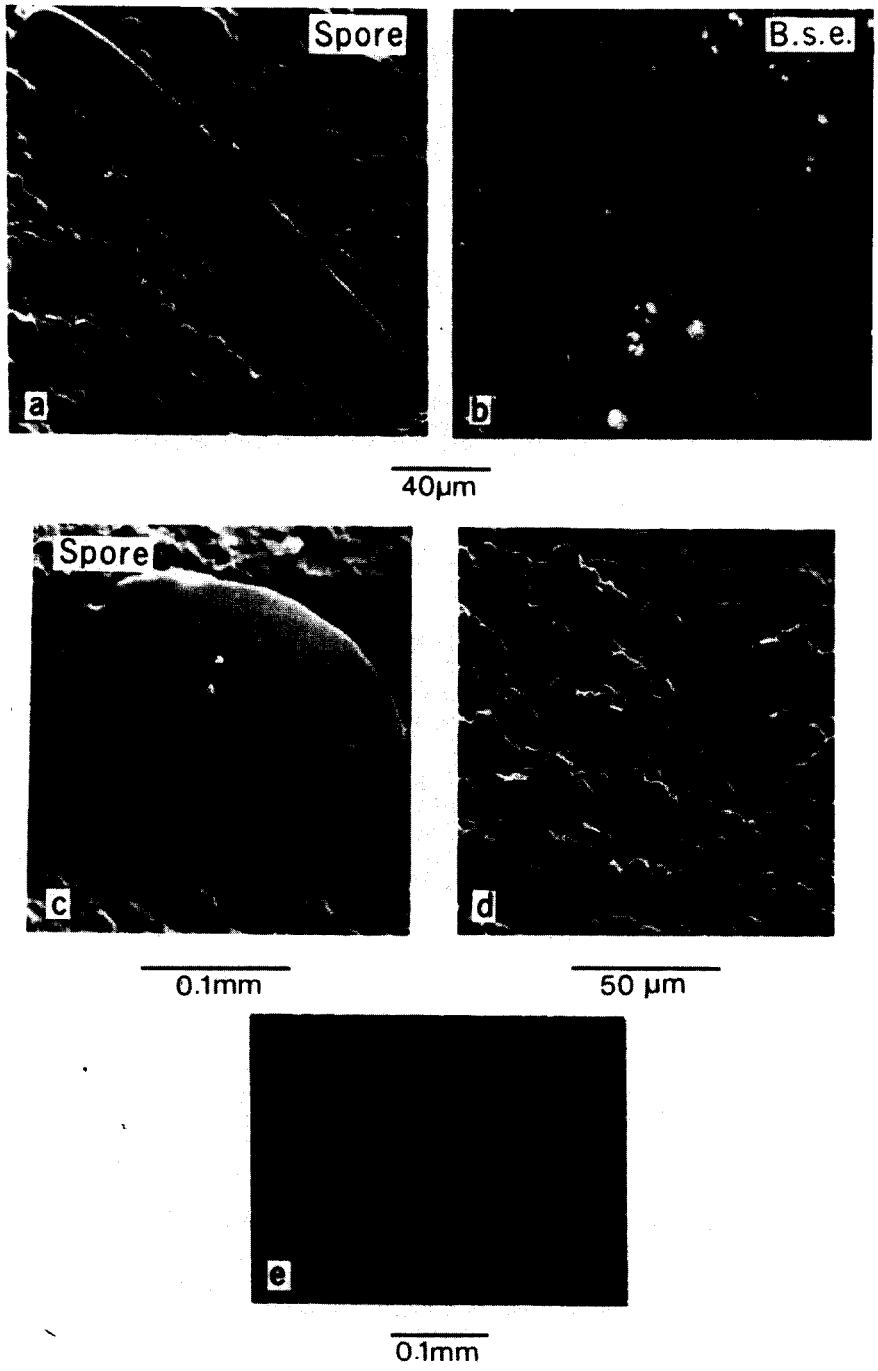

Figure 10. SEM photomicrographs of polished chips from well #11940.

a and b. Section cut perpendicular to the bedding plane. The inclusion in the spore is composed of Ca-Mg-Fe (ferroan dolomite?). Note the vermicular shape of organic matter (woody?) and discrete black spots of kerogen in b. The bright spots are pyrite.

c. Spore in a sample from well #11940 cut and polished parallel to the bedding plane. Note the space around the spore.

d. Quartz grains showing relief due to the difference in polishing hardness of quartz and phyllosilicates.

e. Sedimentary lamination due to the difference in grain size of detrital quartz. Sample cut and polished perpendicular to the bedding plane.

PETROLOGY OF NEW ALBANY SHALE GROUP (UPPER DEVONIAN AND KINDERHOOKIAN) IN THE ILLINOIS BASIN, A PRELIMINARY REPORT*

R. D. Harvey, W. A. White, R. M. Cluff,
J. K. Frost, and P. B. DuMontelle

Illinois State Geological Survey
Urbana, Illinois 61801

ABSTRACT

Studies of two cores through the New Albany Group of Upper Devonian and Kinderhookian (lower Mississippian) age in Christian County, Kentucky, and Sangamon County, Illinois, based on radiography of slabs and petrography of thin sections, permit classification of the shale strata into several distinct lithofacies. Lithofacies are defined on the basis of color, the character of laminations, synaeresis distribution and amount of pyrite, silt and carbonate constituents, spore content, and small scale sedimentary and biogenic structures. Correlations are examined between various lithofacies and the occurrence and the properties of internal surface area, the clay orientation, and other physical properties of the shales. Lithofacies provide a basis for interpreting the environments of deposition.

INTRODUCTION

The Illinois State Geological Survey, with support of the United States Energy Research and Development Administration (ERDA), has undertaken a comprehensive investigation of the extensive shale strata of the New Albany Group (Upper Devonian and Kinderhookian) in the Illinois Basin. These strata are commonly very dark gray to black because of an abundance of organic matter that occurs as an integral part of the shale material; thus they are a potential source of hydrocarbons, especially of natural gas. For this investigation, the Survey's activities are divided into two major study areas, geological and geochemical. Each major area is subdivided into four projects. The geological projects are: 1) stratigraphy and structure of New Albany in Illinois; 2) mineralogic and petrographic characterization; 3) analysis of physical properties; and 4) mineral resources evaluation system. The latter involves the development of a geologic information system designed for use on an IBM 360/75. The geochemical projects are: 1) quantitative determination of major, minor, and trace elements; 2) trace element distribution between shale inorganic and organic phases; 3) mode of occurrence and relation of distribution of hydrocarbon phases; and 4) adsorption/desorption studies of gases through shales.

Purpose of Study

The physical and chemical behavior of the bulk shale material results from the behavior of the microscopic constituents within the shale. The bulk properties of importance—porosity, permeability, nature of the fluid flow, drillability, and potential for recovery of hydrocarbons—are fundamentally dependent on the mineralogical, petrographic, and chemical properties of the shales. The bulk chemical elements in the shale occur in the form of mineral grains, dispersed organic particles and fluids, and some soluble salts. Mineralogical analyses provide data that will be helpful for evaluation of the chemical analyses and some of the physical properties of the shales. The petrographic analyses provide microstructural and textural properties needed for evaluation of certain physical and chemical

*The work reported here was done pursuant to contract number E-(40-1)-5203 with the U.S. Energy Research and Development Administration.

properties. The data generated will provide a fundamental basis for regional and local correlations of geologic data for interpretation of the sedimentology, depositional environments, and diagenetic history, and for evaluation of hydrocarbon potential.

Scope of Report and Setting

This is a preliminary report on only a part of the investigation. It deals mainly with the second geologic project, the mineralogic and petrographic characterization of the shales, and to a lesser extent with some test data of the physical properties and some of the chemical analyses that were completed during the first year of the project. Also reported are data and preliminary petrologic interpretations and evaluations of samples studied from two cores from the Illinois Basin: one from Sangamon County, Illinois, (SW¼ SW¼ NE¼ Sec. 11, T. 15 N., R. 3 W.) (API 12-167-00115) near Mechanicsburg, designated here as 01IL, and one from Christian County, Kentucky, (650 ft from North Line and 90 ft from East Line of 12-G-25) (API 16-047-31175) 2 miles east of Crofton, designated here as 01KY. The locations of these two cores, the general structure of the New Albany shales, and some regional tectonic features are shown in figure 1. The entire thickness of the New Albany is represented in both cores by samples studied, 142.6 feet in the 01KY core and 207.6 feet in the 01IL core. Tentative correlations of lithologies suggest that the upper 127 feet in the Illinois core (sample 01IL13L1 and above) are not represented in the Kentucky core, and that approximately the lower 18 feet in the Kentucky core (samples 01KY12C and below) are not present in the Illinois core.

METHODS OF ANALYSES AND PROCEDURES

Analyses

The various mineralogic and petrographic properties investigated for this project are listed in table 1, and the methods of analyses and the types of seamples needed for each analysis are also listed. Only some of these analyses will be discussed in this report. The mineralogy was determined mainly by X-ray diffraction of powders and smoothed slabs of the core segments selected for study. The X-rays were generated from a copper target and passed through a graphite crystal oriented so that only the K_α diffraction radiation passes through the crystal and into the collimator. The samples were scanned at 2 degree 2Θ per minute. The X-ray diffraction signal was set at 500 counts full scale.

Various types of microscopic techniques were used for mineralogical and other analyses—especially transmitted light microscopy of specially prepared thin sections of the shales and vertical reflected light microscopy of polished slabs and of specially prepared, particulate grain mounts.

Radiographic analyses were made of oriented slabbed samples (figs. 2 and 3) cut about ¼ × 4 × 4 inches and X-rayed with a Picker Industrial Mini-Shot apparatus. A radiograph consists of a plate of type M industrial X-ray film exposed to X-rays passing through the slab sample for 3 minutes at 38 kV. Different parts of the radiograph are exposed differently depending on the relative density, texture, and structure of different parts of the slabbed sample.

Procedure

The preparation of the samples for the various analyses made for the mineralogic and petrographic characterizations and for the chemical analyses are shown in figures 2 and 3. A clay fraction (<2 μm) was separated from a crushed sample for clay mineral analyses. The clay was dispersed in distilled water with a deflocculant (80-percent sodium hexametaphosphate and 20-percent sodium carbonate) and allowed to stand until all particles greater than 2 μm had settled. The top 40 mm were then siphoned off, flocculated, centrifuged for ten minutes, mixed, and smear (random oriented clay) slides of this material were made. These slides were allowed to dry in air and then were placed in an atmosphere of ethylene glycol for one week before X-ray diffraction analyses were made. The relative abundances of the various clay minerals in the sample were determined by the method used by Odom and Parham (1968).

The clay mineral orientation index was determined by X-ray diffraction of a smoothed slab of the sample cut perpendicular to the bedding and mounted on a glass slide. This section was placed in the X-ray holder so that the same beds (laminae) were X-rayed from 2.5 to 22.5 degree 2Θ. The areas of the peaks at 4, 8.8, 12.5, and 19.5 to 20.0 degree 2Θ were determined. The orientation index is the ratio of the area of the 19.5 to 20.0 peak to the sum of the areas determined for the other listed peaks. Depending on the intensity of the peaks (001 and hk1), adjustments for some samples had to be made for the certain clay minerals and micas present.

Oriented thin sections, prepared using kerosene lubrication during sawing and grinding stages, were ground to about 60 μm on a thin-section machine and hand ground to about 30 μm thick. They were

covered with immersion oil and a cover glass only while being examined under the microscope.

An index of the hardness of the core material on a foot by foot basis was determined with a Shore scleroscope hardness tester. This method is a dynamic rebound type of hardness test that is commonly used to determine the hardness of metals, plastics, or other uniform materials. We judged it was applicable to the needs of this project as a relative index to the hardness of the shales. The portable tester was placed firmly on the core and the hardness was determined. Twelve hardness measurements were made in an approximate square inch area of the core. The highest and lowest values were rejected, and the average of the remaining 10 tests was taken as the hardness index for that part of the core. An average hardness was determined at 1 foot intervals throughout the length of the core.

The specific gravity was determined with a Jolly Balance on irregular pieces of the core, about 3/4 inch across and from selected portions of the cores studied, and also by weight and volume measures of several of the whole core segments, about 4 inches long, that were canned for off-gas analyses. Distilled water at room temperature was used as the displacing liquid in these determinations. The value determined is the bulk specific gravity; it is equivalent to the bulk density of the sample in grams per cubic centimeter.

The methods used for the determination of the various chemical elements present in the samples are as follows:

X-ray fluorescence	- SiO_2, Al_2O_3, Fe_2O_3, MgO, CaO, K_2O, TiO_2, P_2O_5, S
Neutron activation	- Na_2O, Cr, Co, Mn, Sc, U
Photographic optical emission	- Be, Cu, Pb, Mo, Ni, V, Zn, Zr
Wet chemistry	- Total C, mineral C, organic C (by difference)
Ion selective electrode	- F

Informational and Unique Sample Numbering System

A system of sample numbering was devised by the staff of the Illinois State Geological Survey for this project, and it is used in this report. The unique sample number consists of 8 ciphers. The first four ciphers identify the core from which the sample was taken. The first two of these indicate the numerical sequence of the core as it was drilled or selected for study within any one state. The third and fourth are abbreviations of the name of the state in which the core was drilled. The fifth and sixth ciphers of the unique sample number indicate the data set. Each 10-foot interval of the New Albany in the core is identified by a data set that is numbered in order starting at the top. The seventh cipher is a letter designating the main purpose for which the sample was taken and analyzed. "L" stands for lithologic studies, and "C" stands for chemical analyses of off-gases and constituent elements. At the drilling site, the C samples were sealed in canisters for off-gas analyses. Several other letters are used on this project by other investigators at the Survey. The last cipher in the number indicates the specific number of the sample, lithologic or chemical, taken from that data set interval of the core. In the case of lithologic samples, L1 samples are selected by a geologist during examination of the core to be representative of the predominant lithology in that data set, and L2, L3, etc. are taken of accessory lithologies as needed. Thus, for example, the sample number 01IL02L2 identifies the second, or accessory lithologic sample taken from the interval 20.0 to 29.9 feet down into the New Albany from the 01IL core. In a fully computerized system, the first four ciphers can be keyed to the 9-digit API identification to identify the specific location of the core.

RESULTS

Petrography-Macrocharacterization

The macroscopic characterization of the samples from the 01IL core are listed in table 2 and from the 01KY core, in table 3. The sample numbers listed in these tables and in subsequent tables are the last four ciphers of the complete and unique sample number assigned to each. Many of the specific characteristics listed in tables 2 and 3 are abbreviated, or are listed in symbolic terms that are defined in the footnotes to table 2. The data are based on visual studies, aided with a 10-power microscope, of slabs of the samples and on studies of the radiographs.

Most of the samples are strikingly laminated; the laminations vary in thickness from fine (up to 2 mm thick) to massive (more than 25 mm thick). The 01IL samples are more commonly massive; while the 01KY samples are predominantly laminated with thickness of laminae mainly less than 10 millimeters.

Synaeresis joints are irregular polygonal systems of joints or cracks that are now filled with a secondary (diagenetic) mineral. They are recognized in radiographs and in slabs of the rocks by their linear form and predominant vertical orientation; they cross but a few beds of shale. These joints strike in a random pattern in horizontal sections. We have recognized synaeresis joints in 8 of the 16 samples of 01IL and in 16 of the 25 samples of 01KY (for example, see plate 3B). Most of the synaeresis joints are rather short, about 5 to 10 millimeters, and are crooked in vertical section. Less abundant are calcite-filled joints; these are much more planar in form and are longer than the pyritic joints. We suspect that some of the short, crooked ones contain siderite, but this has not been confirmed.

The 01IL samples are mainly dark greenish gray with a few that are olive black, or brownish black, or grayish black; the 01KY samples are predominantly brownish black with a few that are olive gray, or olive black, or gray black, or black. The 01IL samples are mostly strongly bioturbated, while bioturbation is rarely present in the 01KY samples. Pyrite nodules are generally absent or less than 5 in number in 01IL samples, while they are generally 5 to 25 in number in the 01KY samples.

Petrography—Microcharacterization

Despite the fine grain size of the samples, a number of features can be characterized with a petrographic microscope. Foremost among these features is the character of silt and fine sand-sized fraction of the rock. The relative proportions of clay, quartz, pyrite, carbonate, and coarse micas can be visually estimated within 10 percent if the thin section is ground to about 20 μm (if standard thickness sections are prepared, it is best to feather one edge slightly). Feldspars are usually indistinguishable from quartz, although within some coarse-silt laminae occasional twinned grains are visible. Accessory minerals, such as glauconite and zircon, are also occasionally present. The distribution of the various silt components is also visible. Typically, most of the silt is randomly dispersed throughout the shale. In the laminated lithologies, thin silt laminae are very common (plate 1A); in the nonlaminated lithologies, silt is sometimes concentrated within burrow fillings (plate 1B).

The average and maximum size of quartz grains (as viewed in thin section) are recorded as a rough indicator of current velocities. For nearly all of the samples studied the average size is about 25 μm and the maximum about 50 μm. Most grains are subangular to subrounded, as would be expected at these grain sizes (no significant abrasional rounding occurs at diameters below about 50 μm). One unusual occurrence of rounded silt grains segregated within a burrow fill is illustrated in plate 1C.

A variety of diagenetic features are characterized from thin-section analysis. Pyrite occasionally fills the central cavities of spores and other microfossils, and it has preserved them in an uncompressed state. Fine-grained, sparry carbonate cements are common as interparticle fillings in silt laminae and as intraparticle fillings in fossils. Micritic (calcite) shales in the upper part of the "Glen Park" Formation in the 01IL core commonly display neomorphic growth of microspar. Pressure solution and corrosion of silt-grain boundaries are also common in some samples. Compaction features, including the compression of spores and deformation of synaeresis joints, were observed in almost all samples.

A variety of microfossils and fossil fragments are present in the shale and can be identified in thin section. Spores are the only abundant fossil and two different types usually occur together: one thick-walled and the other thin-walled (plate 1D). Conodonts, phosphatic fish scales and inarticulate brachiopod fragments (plate 1E), and calcispheres (plate 1F), are rare components of the shale but occur in great numbers in a few samples. A variety of macerals, or plant-derived fragments other than spores, occur abundantly dispersed in the brownish-black shales. They are commonly about 5 μm in size and consist mainly of undifferentiated liptinite, some vitrinite, and a few inertinite particles.

Mineralogy

Analyses of the identity and relative abundance of the minerals present in the samples are essentially complete. The samples from both of the cores are rich in illite-type clay and quartz, which occurs as silt grains and as rare and irregular chalcedonic patches. Plagioclase and/or K-feldspar are silt-size grains that were detected in minor abundances in all samples but one (01IL20L1). Minerals that are minor constituents in many 01IL samples are calcite, dolomite, and pyrite; in many 01KY samples calcite is a minor constituent, usually occurring in late stage of synaeresis joints. Trace minerals that occur in several samples are apatite (or siderite) and marcasite. A strong peak observed at 9.4 Å indicates that basaluminite, ideally $Al_4SO_4(OH)_{10} \cdot 5H_2O$ (Hollingworth and Bannister, 1950), may be present in the two deepest samples from the New Albany in the 01KY core. This trace mineral constituent and its associated mineral, calcite, are the only minerals whose occurrence is related to depth in the core.

The main differences in the mineral composition of the samples of the two cores are: chlorite is relatively abundant in the 01IL core; dolomite, siderite, and/or apatite are more often present in the 01KY than in the 01IL core. Kaolinite was not detected in any of the samples. The clay mineral composition of the two cores is shown in the triangular diagram, figure 4.

Chemical Analyses

Preliminary results of the major, minor, and some trace elements for the 01IL samples are listed in table 4 and for the 01KY samples in table 5. We want to emphasize that they are preliminary values and subject to being revised. In particular, the results that were analyzed by photographic optical emission are suspected of having a high bias; restandardization of the method is currently in progress. The data are presented here only to show general trends in the concentrations.

The results indicate the trace elements are generally higher in the Kentucky core than in the Illinois core. In spite of the suspected high bias of some of the elements, including Mo, this element is especially high in several of the 01KY samples. Sample 01KY07C1 contains the highest concentration of Mo; several other trace elements are also relatively abundant in this sample (Pb, Ni, U, V, and Zn). Fluorine (F) and phosphorus, reported as P_2O_5, are especially abundant in 01KY05C1 in association with calcium. Together they occur in the abundant fossil fragments observed petrographically in the sample. Sample 01IL07L1 contains a relatively high concentration of calcium, which occurs as calcite ($CaCO_3$). Of the trace elements in the Illinois samples, the concentrations of zinc (Zn) are relatively high in 01IL10L1; lead (Pb) and nickel are relatively high in 01IL21L1 (table 4).

Physical Properties

The results of the hardness, specific gravity, and clay orientation index measurements for the 01IL core are listed in table 6 and for the 01KY core, in table 7. The Shore hardness data listed for the samples is the average value for the footage in the core closest (within one foot) to the position of the sample analyzed for petrography and chemical tests. Shore hardness data could not be obtained for many of the samples studied in the 01IL core because there were but a few large core segments available in the core, and most of these were slabbed for radiography rather than used for hardness tests. The data show a range in hardness from 20.2 to 22.7 for the 01IL samples and 21.4 to 24.6 for the 01KY samples.

The specific gravity ranges from 2.32 to 2.50 for the 01IL samples and a greater range of 2.2 to 2.70 for the 01KY samples. The clay orientation index varies from 1.0 to 5.3 in the 01IL samples to one sample from this core testing up to 7.4 at one point in the sample (01IL21L1). The clay orientation index for the 01KY samples show a much smaller range of 1.4 to 2.7.

DISCUSSION OF RESULTS

Clay Mineralogy

Analyses of the clay mineralogy are complete on too few locations within the Illinois Basin, and the stratigraphic correlations between the two cores studied are too little known to draw conclusions regarding the direction of sediment transport as was proposed by Parham (1962, 1966). However, the absence of kaolinite suggests either the shales were deposited at some considerable distance from the shoreline, or some of the feldspar and/or mica, occurring in the samples, are alteration products from kaolinite that might have been deposited in the original sediment. The former interpretation is favored because of the fineness of the grain size and the absence of significant authigenic silicate mineral grains in observations to date. According to the trends observed by Parham (1966), the relative abundance of chlorite in the samples studied suggest the Kentucky location was closer to the shoreline than was the Illinois location at the time of deposition of the New Albany.

The abundance, 2.5 parts and above, of mixed-structure clays in three of the 01KY samples might be due to the abundance of organic matter in these samples. If organic matter was absorbed on the surface of these small clay crystals, they would not be able to incorporate K or MgOH into their crystal structure as needed to form illite or chlorite respectively.

The unusual occurrence of basaluminite, a hydrous aluminum sulfate reported here in two samples at the base of the New Albany in the 01KY core, was previously observed in outcrops many miles south of this well by Milton et al. (1955). They observed the mineral to occur in a clayey residuum, which was interpreted as a zone of weathering. Our study of the samples bearing basaluminite (01KY13C1 and 01KY12C1, 13C1) does not reveal any signs of weathering, but they do contain considerable amounts of calcite, which may be associated with the basaluminite. Further work on this occurrence is needed.

Clay Orientation Index

The orientation index (tables 6 and 7) indicates how randomly the clay particles are oriented in the shale. A perfectly flocculated clay should have all the clay minerals oriented in a completely random arrangement. If some deflocculation takes place after sedimentation, some of the attractive forces between the particles will be weakened, and some of the repulsive forces will be increased. This action allows some of the plate-shaped particles to reorientate more or less parallel to the horizontal. The more perfect is the horizontal orientation, the more easily the shale splits along the bedding planes. The orientation index is a clue to the environments of deposition and early diagenesis.

In the 01IL core, the clay orientation index (table 6) is found to be relatively low, down to about the 1660-foot level, which indicates a low degree of parallel orientation of the clay platelets in these shales. This may be due to either their being deposited in a flocculated condition or to extensive burrowing of the sediment by organisms. The lower part of the 01IL core generally has a high index, indicating more preferred orientation of the platelets in the horizontal direction in this part of the New Albany.

In the 01KY samples the orientation indices generally show decreasing parallelism with depth down to about the 2280-foot level (sample 09C1, table 7), where the correlation with depth appears to reverse.

Petrography

Synaeresis

Synaeresis is a physio-chemical process in which the attractive forces between the particles of a suspension or gel are greater than the repulsive ones. This attraction between particles in the suspension produces tension in the particle network. As the chemical environment of the interstitial liquid changes, the relative strength of the attractive and repulsive forces between the particles changes, and cracks form in the sediment at or near the water interface. The forces are thought to remain throughout the diagenetic history of the sediment.

Over 90 years ago, Salisbury (1885, p. 287) recognized synaeresis polygons in Pleistocene sediments along the Wisconsin River. In 1934, Jüngst stated that synaeresis could produce such structures as pits and mounds or cones, cracks and structures similar to hail and raindrop impressions. Abromov (1961) recognized two stages of diagenesis, early and late, and that synaeresis occurred in both stages. In 1961 White found that in laboratory experiments cracks might start to develop within 30 minutes. White (1964) found that the first carbonate that was precipitated in the cracks was siderite, next ferro-dolomite, and last calcium carbonate.

We have found in the samples studied that the early synaeresis joints are filled with pyrite, and they have a very crooked form. We interpret this crookedness to have developed during compaction, but before the formation of late-stage joints. The late-stage synaeresis joints observed are filled with calcite, and they are much straighter and are nearly vertical. These are interpreted to have formed during a post-compaction stage of diagenesis.

Some joint systems in sedimentary rocks probably are a result of combined synaeresis and regional stresses. Synaeresis produces some tension in the rocks and regional stresses may have some control of the orientation of the resulting cracks. This subject is discussed further by Abromov (1961).

The occurrence of calcite-filled synaeresis joints suggests that acid treatment of wells drilled in the New Albany to dissolve the calcite might prove to be effective in creating fractures cross-cutting shale and siltstone strata, and thereby might increase the rate of flow of hydrocarbons into the well.

The concept of petrographic lithofacies and its application to shales

Sedimentary petrographers have used the microfacies concept (Textoris and Carozzi, 1964) for many years as a method of characterizing subtle variations in the fabric and the composition of sandstones and carbonate rocks. This concept has proven to be extremely valuable in interpreting the depositional and diagenetic history of these rock types, but the difficulties of the microscopic study of shales in thin section have largely prevented its application to shales. This study presents an opportunity to apply this concept to the study of shales by using a wide variety of methods of analysis. The variations in mineralogic and petrographic characteristics of the samples studied permit their subdivisions into several distinctive lithologies. Since the term microfacies most strictly applies to lithologies defined on the basis of thin-section petrography, we prefer to use the more general

term lithofacies in this report.

Studies of sedimentary fabrics in recent muds from various depositional settings (Moore and Scruton, 1957) and the interrelationships between organisms and muddy substrates (Rhoads, 1974) have greatly increased our understanding of small-scale structures in mudrocks. These studies, and others, have established several factors that control the nature of the sediment deposited in a wide variety of environments. These factors are: 1) sediment source; 2) physical process of deposition; 3) rate of deposition; and 4) reworking by sediment-ingesting organisms. The latter is, in turn, controlled by a number of other conditions, such as oxygen content and salinity of the water.

The separation of shales into lithofacies defined on the basis of texture, small-scale sedimentary structures, and biogenic structures has the potential of revealing subtle changes in oxygenation, current activity, and depth of the waters in which the rocks were deposited. Further separation by mineralogical composition and diagenetic structures (such as synaeresis joints) may reveal differences in the source area and early burial history of the sediment. Because the relations between physical and biogenic sedimentary structures and the environment of deposition are generally better understood than the controls on physical and chemical properties, this approach may provide new insights on those controls.

Lithofacies of the New Albany

The shale lithofacies defined in this paper were chosen by characterizing seven basic properties (table 8). The color of the rock and the degree of lamination form the backbone of the classification, defining four broad lithologies (types I, II, III, and IV). Each lithology has been divided into two subcategories on the basis of synaeresis, degree of bioturbation, form and distribution of pyrite, silt content and mineralogy, and the abundance of spores. The samples studied are identified as to microfacies in the last column in tables 2 and 3.

Because at this time only about 40 samples from two cores have been examined, it is almost certain that not all of the lithofacies present in the shales of the New Albany have been observed, nor perhaps have all of the features that may prove useful in defining lithofacies been recognized. Furthermore, it is recognized that the characteristics chosen to define lithofacies, and the lithofacies themselves, are partly subjective and depend upon the techniques that are used to study the shale. An example of this is the extensive development of synaeresis fractures observed in many samples, which we judged important enough to warrant their separation into distinct lithotypes. The recognition of extensive synaeresis is dependent upon routine radiography of the core samples; many synaeresis joints are invisible on the core itself and they are not very striking in thin section.

Lithofacies I: Bioturbate greenish-gray mudstones. This lithofacies is characterized by extensive bioturbation, an absence of laminations and other primary sedimentary structures, and by its very light color. Plate 2 illustrates the swirling texture, which is the result of sediment mixing by burrowing organisms. Distinct burrows are not visible on this radiograph, because the compositional difference between burrow filling and matrix is very slight. Burrows can be distinguished on the core itself by their distinctly lighter color.

Pyrite is a very minor component of this lithofacies and is essentially confined to burrow fillings and to a few synaeresis joints. Organic carbon content of the rock is quite low, the samples studied so far have ranged from 0.0 to 0.9 percent carbon. Two subcategories have been established primarily on the silt content of the mudstone:

Type I-A - under 25 percent silt and

Type I-B - over 25 percent silt (ranging up to argillaceous quartz siltstones).

The silt in all samples was dominantly quartz and feldspar, with carbonate silt being a very minor fraction of the total and largely confined to a few laminae.

Lithofacies I is typical of the Hannibal and Saverton Shales of Illinois, which comprise the upper portion of the New Albany Group. No examples of this lithofacies were present in the OlKY core. We interpret this lithofacies to have been deposited in dysaerobic waters that supported an abundant soft-bodied infauna, but that did not contain sufficient oxygen to support calcified benthic invertebrates (Rhoads and Morse, 1971). This lithofacies may also represent the shallowest and most highly agitated environment of New Albany deposition, although the absence of depositional sedimentary structures makes this somewhat speculative.

Lithofacies II: Indistinctly bedded olive-gray shales. This lithofacies is also characterized by extensive bioturbation, but the sediment was not as completely bioturbated—the general bedding is

still discernible. The color of the shale is somewhat darker than lithofacies I; it ranges from olive gray to olive black and reflects a higher content of organic matter.

Two subcategories were defined by the abundance of synaeresis and the form and distribution of pyrite:

Type II-A (plate 3A) - very few or no synaeresis joints present; abundant pyrite nodules along bedding.

Type II-B (plate 3B) - very abundant pyrite-filled synaeresis joints, with few pyrite nodules.

The difference between these lithotypes is interpreted as reflecting different diagenetic environments. Depositional structures and features in the two lithotypes are very similar, except for silt content and mineralogy, with type II-B generally containing less total silt and a greater proportion of carbonate silt.

Lithofacies II is interpreted as having been deposited in dysaerobic waters similar to lithofacies I, except that the activity of burrowers was not as intense. There are several possible explanations for this, a few of which are listed below:

1) The oxygen content of the water may have been lower than that of the environment in which lithofacies I was deposited, and thus the population of burrowing organisms was correspondingly smaller. A possible implication is that lithofacies II represents a slightly deeper, less agitated environment.

2) Some other physical restriction, such as salinity fluctuations, reduced the population of burrowing organisms. Variations in salinity and other chemical characteristics of pore waters in the sediment might also correlate with the diagenetic differences between lithofacies I, II-A, and II-B.

3) Lithofacies II might reflect a higher rate of deposition. If the burrowing population remained approximately constant, then the intensity of burrowing per volume of sediment might drop.

4) The faunal composition of the burrowers may have varied geographically and through time, with corresponding variations in the size, type, and intensity of burrowing. We do not have sufficient data on trace fossils in the shale to evaluate this possibility.

At this time we do not have sufficient data to speculate on the controls of synaeresis development and of pyrite distribution.

Lithofacies III: Poorly laminated brownish-black shales. This lithofacies is characterized by distinct but variable laminations. Finely laminated shales are interbedded with massive or very thickly laminated shales (plate 4B). Sporadic burrows are visible, but sediment mixing is minimal (plate 4A). The organic content of the shales is generally high (3 to 6 percent), and they are predominantly brownish-black.

Two subcategories were established principally on the basis of synaeresis:

Type III-A (plate 4A) - very few synaeresis joints.

Type III-B (plate 4B) - abundant synaeresis joints.

In addition, all of the samples of lithofacies III-A contain sedimentary structures such as cuts and fills, ripples, cross-bedding, and small loads. Although it is tempting to interpret this lithofacies as a high-current velocity facies of the New Albany, it seems likely that similar sedimentary structures were originally present in the sediments of lithofacies I and II, but were subsequently destroyed by extensive burrowing. (These structures do indicate greater current activity than the finely laminated brownish-black shales of lithofacies IV.)

This lithofacies is interpreted as having been deposited in marginal anaerobic/dysaerobic waters, in which only a very few burrowing organisms could survive; oxidation of organic matter in the sediment was negligible. This lithofacies was presumably deposited in deeper waters than was either lithofacies I or II. In modern euxinic basins, such as the Black Sea, the mixing of surficial waters can transfer oxygen to depths of approximately 150 meters, below which anaerobic conditions prevail (Caspers, 1957). Byers (personal communication, 1977) has suggested that 150 meters is a reasonable minimum depth for the anaerobic/dysaerobic boundary in certain ancient settings.

Lithofacies IV: Finely laminated brownish-black shales. This lithofacies is characterized by fine, evenly spaced, parallel laminations of pyrite and silt. There is no indication of disturbance

by burrowing. The uniformity of the laminations indicates that they are pelagic sediments and were not deposited by traction or density currents. Spores are abundant in most samples, and organic content is uniformly high (3 to 6.4 percent). Color ranges from brownish black to gray black to black.

Two subcategories were defined by a very striking difference in the form of pyrite in the shale; they probably reflect differences in the diagenetic environment.

Type IV-A (plate 5A) - pyrite is evenly dispersed through the shale as minute grains and as fine laminae.

Type IV-B (plate 5B) - pyrite is principally clumped into small scattered nodules, although scattered grains and pyritic laminae are also present as in Type IV-A.

This lithofacies is interpreted as having been deposited in anaerobic waters devoid of benthic organisms. It probably represents the deepest, quietest conditions of New Albany deposition. Little evidence of currents in this lithofacies environment was found, and pelagic sedimentation was probably dominant.

Relation of lithofacies to physical properties. The lithofacies classification is not a quantitative parameter, but several of the criteria used to distinguish the classes are based on qualitative descriptive properties. The classes are thought to be, most significantly, a relative measure of the oxygen content of the depositional environment, with decreasing oxygen corresponding to increasing lithofacies class number. It is therefore useful to consider the relations between the lithofacies and the results of certain physical property tests. These relations are shown in figure 5. Lithofacies class increases with increasing internal surface area ratio (fig. 5A). Because this ratio of the internal surface area measured by use of CO_2 includes the ultra-fine pores in the sample whose diameters are less than 4 to 5 Å, and the area measured by use of N_2 does not include these pores, the graph can be interpreted to indicate that the more anaerobic was the site of deposition, the more abundant are the ultra-fine pores in the final lithified shale. The relation of lithofacies with hardness is shown in figure 5B. It is apparent from this graph that the lower the lithofacies class, the softer the shale is likely to be. Although many samples of lithofacies IV tested as soft as those of I through III, several samples of each are proportionately harder with increasing class number. There is little or no relation of significance between lithofacies and clay orientation index (fig. 5C).

CONCLUDING REMARKS

Characteristics of the petrography, the mineralogic and chemical composition, and the physical properties—hardness, specific gravity, and clay orientation index—were analyzed and evaluated for samples of the New Albany from two cores in the Illinois Basin. Samples were characterized from segments of the cores taken approximately every five to ten feet through the New Albany. The core taken in western Kentucky (Christian County) was an oriented core drilled by ERDA. The New Albany was represented by 207.6 feet of mainly grayish black, finely laminated silty shales. The core taken in central Illinois (Sangamon County) was a core drilled many years ago and is stored at the Illinois State Geological Survey. Samples taken of this core represented 142.6 feet of New Albany; they consist mainly of gray, massive and bioturbated, argillaceous siltstones and silty shales.

Four distinctive lithofacies were recognized and each of these was divided into two subdivisions, based on uniquely differing petrographic and mineralogical characteristics. These lithofacies correlate in some important respects with the physical properties of the samples. We observe that the class of lithofacies increases with an increasing abundance of the ultra-fine pores (ratio of the CO_2 and N_2 measured internal surface areas, fig. 5A). With increasing class of lithofacies, we observe an increasing number of samples to be proportionately harder (fig. 5B). No significant relation has been observed to date between the lithofacies and the clay orientation index and the specific gravity of the samples. The lithofacies classification is a useful technique to be applied to the study of shales, because of the utility it provides in describing the petrography of a large number of samples and in interpreting the environments of deposition and other sedimentological features.

In the light of additional data that have been recently generated on the same samples, continued evaluation of the data presented here is in progress. In addition, four new cores of the New Albany in Illinois have now been made available for study, and petrographic and other analyses of samples from these cores are in various stages of completion.

REFERENCES

Abromov, S. P., 1961, Factors determining consolidation of argillaceous sediments in the process of diagenesis: Acta Universitatis Carolinae, Geologica Supplementum 1, 2nd Conference on Clay Mineralogy and Petrography in Prague, Universita Karlova, Praha, p. 263-275.

Caspers, H., 1957, Black Sea and Sea of Azov: Treatise on Marine Ecology and Paleoecology, Geological Society of America Memoir 67, v. 1, p. 801-890.

Hollingworth, S. E., and F. A. Bannister, 1950, Basaluminite and hydrobasaluminite, two new minerals from North Hamptonshire: Mineralogical Magazine, v. 29, no. 208, p. 1-17.

Jüngst, H., 1934, Geological significance of synaeresis: Geologische Rundschau, v. 25, p. 312-325.

Milton, Charles, L. C. Conant, and V. E. Swanson, 1955, Sub-Chattanooga residuum in Tennessee and Kentucky: Geological Society of America Bulletin, v. 66, p. 805-810.

Moore, D. G., and P. C. Scruton, 1957, Minor internal structures of some recent unconsolidated sediments: American Association of Petroleum Geologists Bulletin, v. 41, p. 2723-2751.

Odom, I. E., and W. E. Parham, 1968, Petrology of Pennsylvanian underclays in Illinois and their application to some mineral industries: Illinois State Geological Survey Circular 429, 36 p.

Parham, W. E., 1962, Clay mineral facies of certain Pennsylvanian underclays: Ph.D. thesis, University of Illinois, Urbana, 122 p.

Parham, W. E., 1966, Lateral variations of clay mineral assemblages in modern and ancient sediments: Proceedings International Clay Conferences: Jerusalem, Israel, v. 1, p. 135-145.

Rhoads, D. C., and J. W. Morse, 1971, Evolutionary and ecologic significance of oxygen-deficient marine basins: Lethaia, v. 4, p. 413-428.

Rhoads, D. C., 1974, Organism-sediment relations on the muddy sea floor: Oceanography and Marine Biology Annual Review, v. 12, p. 263-300.

Salisbury, R. D., 1885, Columnar structure in subaqueous clay: Science, v. 5, p. 287.

Swann, D. H., and A. H. Bell, 1958, Habitat of oil in the Illinois Basin, in Weeks, L. G., editor, Habitat of oil: American Association of Petroleum Geologists, Tulsa, p. 447-472.

Textoris, D. A., and A. V. Carozzi, 1964, Petrography and evolution of Niagaran (Silurian) reefs, Indiana: American Association of Petroleum Geologists Bulletin, v. 48, no. 4, p. 397-426.

Thomas, Josephus, Jr., and R. R. Frost, 1977, Internal surface area and porosity in eastern gas shales from the sorption of nitrogen, carbon dioxide, and methane, in Proceedings First Eastern Gas Shales Symposium: Morgantown, WV, ERDA, Morgantown Energy Research Center (this publication).

White, W. A., 1961, Colloidal phenomenon in sedimentation of argillaceous rocks: Journal of Sedimentary Petrology, v. 31, p. 560-570.

White, W. A., 1964, Origin of fissure fillings in a Pennsylvanian shale in Vermilion County, Illinois: Transactions Illinois Academy of Science, v. 57, p. 208-215.

TABLE 1 - MINERALOGIC AND PETROGRAPHIC ANALYSES, METHODS AND TYPES OF SAMPLES

Property	Method of analysis	Type of samples
I. Mineralogy		
A. Silt (>2 μm)	X-ray diffraction and microscopy	Powders and slabs
B. Clay (<2 μm)	X-ray diffraction	Clay fraction of powders
C. Trace constituents	Microscopy	Slabs and thin sections
II. Petrography		
A. Macrocharacterization	Visual, microscopy and radiography	Oriented slabs
1. Structure a. Lamination b. Synaeresis		
2. Color		
3. Bioturbation		
4. Sedimentary features		
5. Fossil occurrences		
B. Microcharacterization	Microscopy	Thin sections
1. Constituents and distribution		
2. Texture: grain size, shape, orientation, sorting, etc.		
3. Structure: laminations, x-bedg.		
4. Paleontology: abundance, bioturbation, orientation, etc.		
5. Diagenetic features		
C. Directional properties		
1. Clay orientation index	X-ray diffraction	Oriented slabs
2. Particle orientation	Microscopy	Oriented thin sections
D. Disbursed organic matter		
1. Total organic matter	Low-temperature ashing	Powders
2. Reflectance of vitrinite	Microscopy	Particle mounts
3. Maceral analysis	Microscopy	Particle mounts and thin sections

TABLE 2 - PETROGRAPHY—MACROCHARACTERIZATION, SANGAMON COUNTY, ILLINOIS, CORE SAMPLES (01IL)

Sample number	Depth* (ft)	Laminations†		Synaeresis joints**		Color#	Bioturbation	Pyrite nodules††			Other sedimentary features@	Litho-facies
		Thickness	Contrast	Early stage	Late stage			Size range (mm)	Number	Occurrence		
01L2	1576.0	ms	pr	—	—	5GY4/1	very strongly	—			—	I-B
03L1	1589.4	ms	pr	—	few	5GY4/1	very strongly	—			—	I-B
04L1	1602.0	ms	pr	several	—	5GY4/1 & 5Y2/1	very strongly	2-16	few	sc	—	I-B
05L1	1615.1	ms	pr	several	—	5GY5/1	very strongly	2-16	few	sc	—	I-B
06L1	1619.5	ms	pr	several	—	5GY4/1	very strongly	<1-1	few	sc	—	I-B
07L1	1631.6	ms	pr	—	—	5GY4/1	very strongly	—			—	I-B
07L2	1633.6	ms	pr	—	—	5GY5/1 & 5Y6/1	completely	—			—	I-A
09L1	1647.4	ms	pr	few	—	5GY4/1	very strongly	2-4	several	sc	—	I-A
09L2	1656.2	ms	fr	few	—	5GY4/1	strongly	2-4	few	sc	—	I-A
12L1	1678.6	ms	pr	few	few	5Y2/1	strongly	2-4	few	bg	—	II-A
13L1	1688.0	ms	fr & pr	—	—	5Y2/1	medium	<1	several	bg	—	II-A
14L1	1698.2	cs	fr & pr	—		5YR2/1 & 5GY4/1	weakly	<1	several	bg	b	II-A
16L1	1723.4	fn & med	fr & gd	—	—	N2	—	<1-16	few	bg	—	IV-A
18L1	1740.2	fn & med	fr & gd	—	—	5YR2/1	—	2-16	few	bg	—	IV-A
19L1	1753.5	med	fr & gd	—	—	N2	—	—			—	IV-A
20L1	1763.3	med & ms	fr & gd	several	—	5GY5/1 & 5YR2/1	very strongly	2-16	few	bg	—	I & III-A

*Depth below reference level of 595.9 ft above MSL.
†Abbreviations for thickness: ms = massive (nonlaminated or over 25 mm), fn = fine (up to 2 mm), med = medium (2 to 10 mm), cs = coarse (10 to 25 mm); for contrast: pr = poor, fr = fair, gd = good.
**Early stage joints are filled with pyrite and/or siderite. Late stage joints are filled with calcite. Dash (—) = not detected, few = 1 to 4, several = 5 to 25, abund = over 25.
#Geological Society of America rock color chart: N1 = black, N2 = grayish black, 5YR2/1 = brownish black, 5Y2/1 = olive black, 5Y4/1 = olive gray, 5Y6/1 = light olive gray, 5GY4/1 = dark greenish gray, 5GY5/1 = med dark greenish gray.
††Dash (—) = not detected, few = 1 to 4, several = 5 to 25, sc = scattered throughout, bg = only on bedding planes.
@a = pyrite veinlet ending in large pyrite nodule, b = near vertical natural fracture, c = large pyrite-rich area, d = soft sediment deformation, e = cut and fill structure, f = cross laminated silt layer.

TABLE 3 - PETROGRAPHY—MACROCHARACTERIZATION, CHRISTIAN COUNTY, KENTUCKY, CORE SAMPLES (01K1)

Sample number	Depth* (ft)	Laminations†		Synneresis Joints**		Color#	Bioturbation	Pyrite nodules††			Other sedimentary features@	Litho facies
		Thickness	Contrast	Early stage	Late stage			Size range (mm)	Number	Occurrence		
01L1	2181.0	fn	gd	—	—	N1	—	2-10	few	sc	—	IV-A
01C1	2182.3	fn	gd	—	—	5YR2/1	—	1-25	few	bg	—	IV-A
02L1	2188.6	fn	gd	—	several	5YR2/1	—	1-1	several	sc	—	IV-A
02C1	2191.2	fn	gd	—	—	5YR2/1	—	1-20	several	bg	a	IV-B
03L1	2210.7	fn & med	fr	few	few	5YR2/1	—	1-8	several	bg	—	IV-B
03C1	2220.3	fn	fr	few	few	5YR2/1	—	1-20	several	bg	b	IV-B
04C1	2230.2	ms	fr	several		5YR2/1 & 5Y4/1	medium	1-16	several	sc & bg	b	II-B
04L1	2231.1	fn & med	fr	—	—	5YR2/1	sporadic?	1-4	several	bg	—	III-A
05C1	2240.1	fn & cs	fr & pr	few	few	5YR2/1	—	2-16	several	bg	c	IV-B
05L1	2244.1	med	fr	—	—	5YR2/1	—	1-2	several	bg	—	IV-B
06C1	2250.0	ms	fr	abund	—	5Y4/1	strongly	1-4	several	sc	—	II-B
06L1	2255.4	ms	fr	abund	—	5Y4/1	strongly	1-8	several	sc	—	II-B
07C1	2260.3	fn & med	fr	few	—	5YR2/1	—	1-20	several	bg	—	IV-B
07L1	2263.7	fn & cs	fr & pr	—	few	5YR2/1 & N1	—	1-8	several	bg	d	III-A
08C1	2270.3	med & cs	fr	several	—	5YR2/1	sporadic	1-4	several	bg & sc	e	III-A
08L1	2273.5	fn	pr	abund	—	N2	sporadic	1-4	abund	sc	b	III-B
09C1	2280.0	med & cs	gd	several	few	5YR2/1	sporadic?	1-4	several	sc	—	III-A
10L1	2287.8	med	fr	few	few	5YR2/1	—	1-4	several	bg	—	IV-B
10C1	2290.8	fn & med	fr	abund	—	5Y2/1	—	1-4	abund	bg	—	III-B
11L1	2293.0	fn & ms	pr & gd	abund	—	5YR2/1	—	1-4	abund	sc & bg	—	III-B
11C1	2299.8	fn & cs	gd	few	—	5YR2/1	—	1-4	several	bg	e & f	IV-B
12C1	2310.5	fn & med	pr & gd	—	—	5YR2/1	—	1-4	several	bg	—	IV-B
12L1	2311.1	fn	fr	—	—	5YR2/1	—	1-4	several	bg	—	IV-B
13L1	2312.7	fn & med	pr & gd	—	—	5YR2/1	—	1-4	several	bg	—	IV-B
13C1	2318.8	fn & med	pr & fr	—	—	N2	—	1-22	few	bg	f	IV-B

*Depth below reference level of 548.0 ft above MSL. All other footnotes are given in footnotes to Table 2.

TABLE 4 - CONCENTRATION OF MAJOR, MINOR, AND SOME TRACE ELEMENTS, SANGAMON COUNTY, ILLINOIS, CORE SAMPLES (01IL)

Sample number	SiO_2 (wt %)	Al_2O_3 (wt %)	Fe_2O_3 (wt %)	MgO (wt %)	CaO (wt %)	Na_2O (wt %)	K_2O (wt %)	TiO_2 (wt %)	P_2O_5 (wt %)	S (wt %)	C (wt %)	Org. C (wt %)
01L2	64.5	10.4	4.31	2.25	1.04	0.98	3.91	0.87	0.08	0.02	0.88	0.43
03L1	71.8	8.54	2.61	1.84	2.03	1.25	2.98	0.93	0.33	0.05	0.96	0.29
04L1	74.0	9.19	2.20	1.13	0.32	1.41	3.81	0.95	0.03	0.07	0.97	0.80
05L1	70.4	9.77	2.88	1.48	0.39	1.24	3.47	0.99	<0.01	0.06	0.44	0.28
07L1	51.7	6.81	2.07	2.59	15.4	0.94	2.35	0.56	0.31	0.07	3.88	0.15
09L1	58.8	12.7	4.01	2.70	1.35	1.05	4.08	0.93	0.02	0.09		
09L2	65.4	12.1	4.72	1.62	0.30	1.14	4.26	1.00	0.05	0.25		
10L1	65.3	11.7	5.84	1.64	0.06	1.03	3.85	0.87	0.01	0.89		
11L1	57.9	14.9	5.00	1.90	0.01	0.74	5.40	0.84	0.06	0.27		
12L1	60.2	15.0	5.01	2.63	0.43	0.84	5.32	0.89	<0.01	0.18		
13L1	58.8	16.1	5.09	2.74	0.36	0.81	5.63	0.81	0.02	0.31		
14L1	56.5	14.1	5.20	2.22	0.52	0.74	4.69	0.77	<0.01	0.54		
15L1	51.5	13.2	5.19	2.17	0.18	0.61	4.96	0.66	0.05	0.92		
16L1	53.8	11.7	5.35	2.04	0.71	0.74	3.78	0.68	0.03	1.28		
17L1	57.1	12.2	4.62	1.54	0.61	0.84	3.74	0.66	0.04	1.10		
18L1	62.5	11.7	4.15	1.27	0.47	0.86	3.48	0.64	0.08	0.92		
19L1	55.0	12.2	5.62	1.67	0.56	0.74	3.86	0.62	0.10	1.36		
20L1	58.0	12.3	4.37	2.22	2.26	0.92	3.87	0.69	0.08	0.84		
21L1	56.4	14.8	4.83	2.15	0.77	0.74	4.88	0.67	0.03	0.71		

Sample number	F (ppm)	Be (ppm)	Cr (ppm)	Co (ppm)	Cu (ppm)	Pb (ppm)	Mn (ppm)	Mo (ppm)	Ni (ppm)	Sc (ppm)	U (ppm)	V (ppm)	Zn (ppm)	Zr (ppm)
01L2	920	4.3	88	8.9	14	5.6	220	<2	81	13	5	380	92	490
03L1	810	2.6	79	5.9	24	4.4	280	<2	30	10	7	110	120	730
04L1	370	2.5	88	6.2	12	6.7	120	<2	40	11	7	120	120	660
05L1	500	3.8	57	10	10	7.2	150	<2	41	10	6	170	94	540
07L1	570	2.2	49	6.2	11	6.6	1010	<2	35	9	5	85	50	620
09L1	560	5.1	130	14	21	6.2	330	7.3	72	20	6	220	88	520
09L2	600	4.8			23	11	250	7.0	78		4	180	170	500
10L1	600	4.3	130	71	35	10	200	40	78	19	6	160	700	400
11L1	970	5.4	150	18	36	8.0	250	13	100	24	6	250	130	350
12L1	820	5.5	110	15	30	10	290	11	92	24	3	230	140	380
13L1	940	5.7	170	20	37	7.8	270	20	95	27	7	240	140	300
14L1	810	5.0	140	17	46	9.2	230	53	110	22	11	310	180	330
15L1	940	5.0	88	23	63	19	240	180	120	20	21	300	310	280
16L1	670	5.0	96	44	120	18	260	210	120	21	31	340	140	300
17L1	1000	4.6	110	29	68	13	210	92	72	19	17	220	92	310
18L1	640	3.9	60	20	58	9.6	180	84	70	15	14	220	120	260
19L1	860	4.3	77	25	68	19	270	130	99	16	31	220	68	240
20L1	810	3.8	84	18	48	16	320	38	66	15	6	160	62	340
21L1	1070	4.8	88	11	74	34	340	60	140	17	10	510	130	230

TABLE 5 - CONCENTRATION OF MAJOR, MINOR, AND SOME TRACE ELEMENTS, CHRISTIAN COUNTY, KENTUCKY, CORE SAMPLES (01KY)

Sample number	SiO_2 (wt %)	Al_2O_3 (wt %)	Fe_2O_3 (wt %)	MgO (wt %)	CaO (wt %)	Na_2O (wt %)	K_2O (wt %)	TiO_2 (wt %)	P_2O_5 (wt %)	S (wt %)	C (wt %)	Org. C (wt %)
01C1	53.2	10.1	6.85	0.74	0.14	0.73	3.06	0.56	0.10	2.42	14.13	14.03
02C1	59.3	9.65	5.40	1.21	1.63	0.66	2.71	0.50	0.06	1.84	10.86	10.29
03C1	57.8	9.93	7.31	1.08	1.60	0.66	2.76	0.54	0.10	1.93	7.78	7.03
04C1	62.8	15.0	3.91	1.49	0.56	0.88	4.22	0.71	<0.01	0.35	2.24	1.64
05C1	48.0	10.0	7.74	1.69	7.30	0.77	2.61	0.45	4.25	2.27	7.01	5.81
06C1	59.0	16.4	4.40	1.98	1.25	0.99	4.31	0.83	0.07	0.22	1.69	0.66
07C1	49.9	13.5	6.20	1.05	0.26	0.78	3.93	0.70	0.07	1.74	12.61	12.30
08C1	57.9	14.4	3.37	2.10	2.03	0.90	4.23	0.73	0.13	0.53	6.00	5.04
09C1	51.9	11.5	3.60	3.59	4.81	0.81	3.49	0.71	0.01	0.62	7.51	5.39
10C1	53.0	11.5	2.64	2.83	3.69	0.77	3.81	0.68	0.05	0.64	10.56	9.23
11C1	45.0	9.77	4.28	4.75	7.50	0.83	2.99	0.52	0.19	1.38	10.16	7.43
12C1	51.6	8.44	3.16	4.31	7.51	0.61	2.87	0.43	0.15	1.00	8.32	5.67
13C1	46.0	7.07	3.09	4.08	11.7	0.48	2.61	0.35	0.19	1.18	10.38	7.30
08L1	55.0	14.5	5.05	1.82	1.69	0.87	4.14	0.71	0.12	0.89		
10L1	54.3	11.9	2.90	3.62	5.67	0.77	3.62	0.71	0.03	0.42		
11L1	51.8	10.9	3.42	3.47	5.58	0.78	3.53	0.63	0.04	0.78		
12L1	49.8	8.07	2.62	4.25	10.3	0.55	2.64	0.37	0.19	0.90		
13L1	49.8	7.59	3.05	4.19	9.32	0.54	2.63	0.36	0.25	1.02		

Sample number	F (ppm)	Be (ppm)	Cr (ppm)	Co (ppm)	Cu (ppm)	Pb (ppm)	Mn (ppm)	Mo (ppm)	Ni (ppm)	Sc (ppm)	U (ppm)	V (ppm)	Zn (ppm)	Zr (ppm)
01C1	640	5.5	66	39	94	12	110	350	150	12	61	280	82	230
02C1	630	5.4	57	29	67	10	310	340	120	12	43	220	140	190
03C1	500	4.1	58	23	87	16	250	200	120	13	24	200	180	220
04C1	900	5.1	68	11	52	11	270	11	67	17	14	210	86	210
05C1	2930	3.2	62	32	60	18	410	77	94	14	37	120	170	210
06C1	890	4.1	90	12	35	8	350	5	44	19	6	170	99	240
07C1	740	5.9	87	23	240	31	160	450	450	17	40	820	420	290
08C1	880	5.3	102	14	280	14	190	11	150	20	7	310	280	320
09C1	770	5.2	84	11	150	7	360	16	110	17	7	210	70	360
10C1	800	5.9	95	12	260	10	200	45	170	18	6	290	180	270
11C1	860	4.7	64	13	160	14	400	35	120	15	8	250	270	270
12C1	920	3.8	54	11	170	7	320	46	140	10	11	320	100	200
13C1	920	3.7	85	13	290	10	360	150	220	13	22	480	500	180
08L1	950	5.4	120	13	210	14	190	39	140	20	13	390	340	250
10L1	870	3.9	75	6	76	5	360	5	77	14	6	170	110	240
11L1	770	4.0	83	8	180	6	330	13	110	16	6	180	320	230
12L1	970	3.3	67	10	160	8	370	43	140	11	12	290	190	170
13L1	860	3.3	71	11	210	7	360	75	190	12	13	420	180	180

TABLE 6 - PHYSICAL PROPERTIES, SANGAMON COUNTY, ILLINOIS, CORE (01IL)

Sample number	Depth (ft)	Shore hardness*	Specific gravity*	ISA, CO_2/N_2†	Clay orientation index
01L2	1576.0	—	2.45	~1.0	1.0
03L1	1589.4	21.1	2.38	~1.0	1.7
03L2	1592.9	~25	2.50	—	—
04L1	1602.0	22.7	2.44	~1.0	1.7
05L1	1615.1	22.3	—	0.93	1.3
06L1	1619.5	—	2.47	—	2.0
07L1	1631.6	—	2.46	1.2	1.1
09L1	1647.4	—	2.48	~1.0	1.1
09L2	1656.2	—	2.49	~1.0	1.4
10L1	1657.7	—	2.42	1.3	1.0
11L1	1667.6	—	2.42	1.5	2.0
12L1	1678.6	—	2.46	1.2	2.4
13L1	1688.0	—	2.38	1.2	3.7
14L1	1698.2	—	2.36	1.7	2.0
15L1	1710.2	—	2.35	2.9	2.7
16L1	1723.4	—	2.26	4.1	1.9-2.2
17L1	1730.8	—	2.32	4.7	2.7
18L1	1740.2	20.2	2.35	3.4	2.5-4.3
19L1	1753.5	—	2.40	4.1	5.3
20L1	1763.3	—	2.45	1.7	3.0
21L1	1776.3	—	2.44	~2.0	2.4-3.2

*Data taken on core segments within one foot of depth indicated.
†Ratio of internal surface area as measured with CO_2 and N_2. Data taken from Thomas and Frost (1977).

TABLE 7 - PHYSICAL PROPERTIES, CHRISTIAN COUNTY, KENTUCKY, CORE (01KY)

Sample number	Depth (ft)	Shore hardness*	Specific gravity*	ISA, CO_2/N_2†	Clay orientation index
01L1	2181.2	26.4	—	—	2.4
01C1	2182.4	26.9	2.21	26.2	—
02L1	2188.8	30.9	—	—	2.0
02C1	2191.3	31.8	2.37	20.4	—
03L1	2216.9	29.7	—	—	2.2
03C1	2220.4	32.1	2.50	16.2	—
04C1	2230.3	23.8	2.64	2.8	—
04L1	2231.2	26.1	—	—	2.0
05C1	2240.3	24.6	2.63	13.2	—
05L1	2244.3	27.6	—	—	2.0
06C1	2250.2	29.4	2.70	1.67	—
06L1	2255.6	27.5	—	—	1.8
07C1	2260.3	21.4	2.31	20.6	—
07L1	2263.9	23.7	—	—	1.8
08C1	2270.5	24.4	2.49	8.5	2.7
08L1	2273.7	21.5	—	13.6	—
09C1	2280.2	22.7	2.50	10.6	1.4
10L1	2288.0	—	—	8.2	—
10C1	2290.9	—	2.38	13.6	1.7
11L1	2293.2	24.0	—	11.4	—
11C1	2300.0	22.2	2.47	13.8	1.6
12C1	2310.6	29.5	2.52	9.6	2.5
12L1	2311.2	33.6	—	9.4	—
13L1	2312.8	29.8	—	10.0	—
13C1	2319.0	34.6	2.46	17.4	2.7

*Data taken on core segments within one foot of depth indicated.
†Ratio of internal surface area as measured with CO_2 and N_2. Data taken from Thomas and Frost (1977).

TABLE 8 - LITHOFACIES CHARACTERISTICS

	Color				Laminations				Synaeresis			Bioturbation				Pyrite				Silt				Spores		
Lithofacies	gray	green-gray	olive-gray	brown-black	massive	indistinct	medium to thick	fine	extensive	minor	absent	very strongly	strongly	moderately	none	rare	synaeresis fillings	scattered nodules	thin laminae	abundant	minor	quartzose	carbonate	absent	common	abundant
I-A	X	X			X					X		X				X					X	X		X		
B	X	X			X					X		X				X				X		X		X		
II-A			X			X				X	X		X					X		X		X			X	
B			X			X			X			X					X				X		X	X		
III-A				X			X			X	X			X				X		X		X	X		X	
B				X			X		X					X			X	X		X		X	X		X	
IV-A				X				X			X				X				X	X		X				X
B				X				X			X				X			X		X		X	X			X

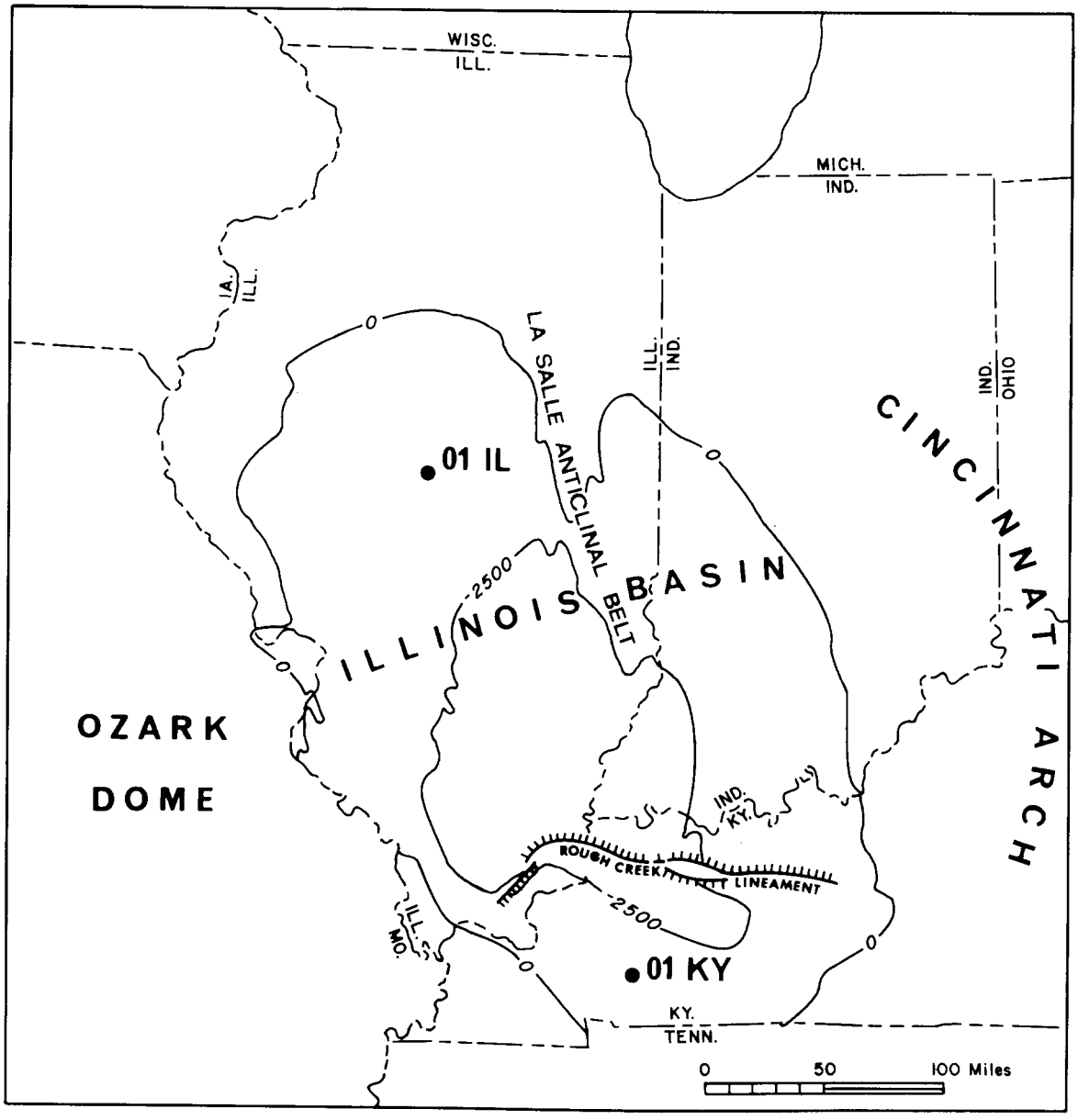

Fig. 1 - Tectonic setting and location of cores studied. Contours show elevation (in feet) of the base of the New Albany Group shales (after Swann and Bell, 1958, fig. 2).

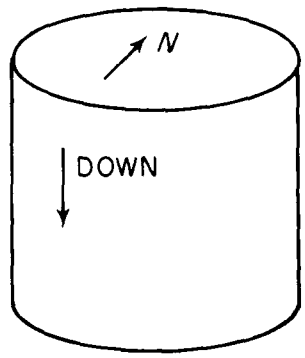

A. Orientation of the core segment.

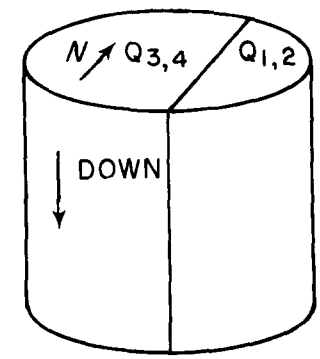

B. The core segment is soaked in distilled water prior to sawing with tap water lubrication. The two pieces, $Q_{1,2}$ and $Q_{3,4}$, are cleaned, then rinsed in distilled water. After drying, $Q_{1,2}$ is crushed and pulverized for various tests. $Q_{3,4}$ is cast in epoxy to hold it together during subsequent sawing.

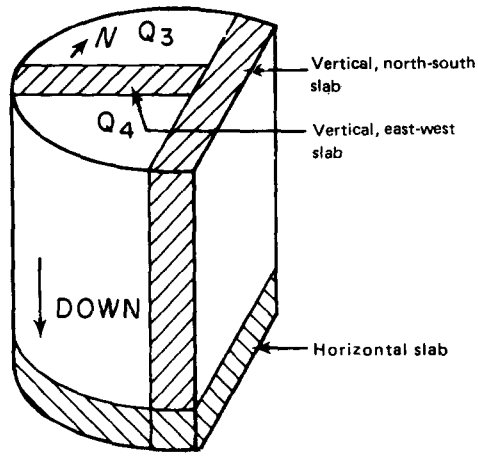

C. Three oriented slabs are cut for petrographic analyses. Saw cuts are made with kerosene lubricant. Q_3 is returned to archive storage.

Illinois State Geological Survey

Fig. 2 - Diagram showing the procedures used to obtain samples for mineralogic, petrographic, and chemical analyses from the core segments of New Albany Shale.

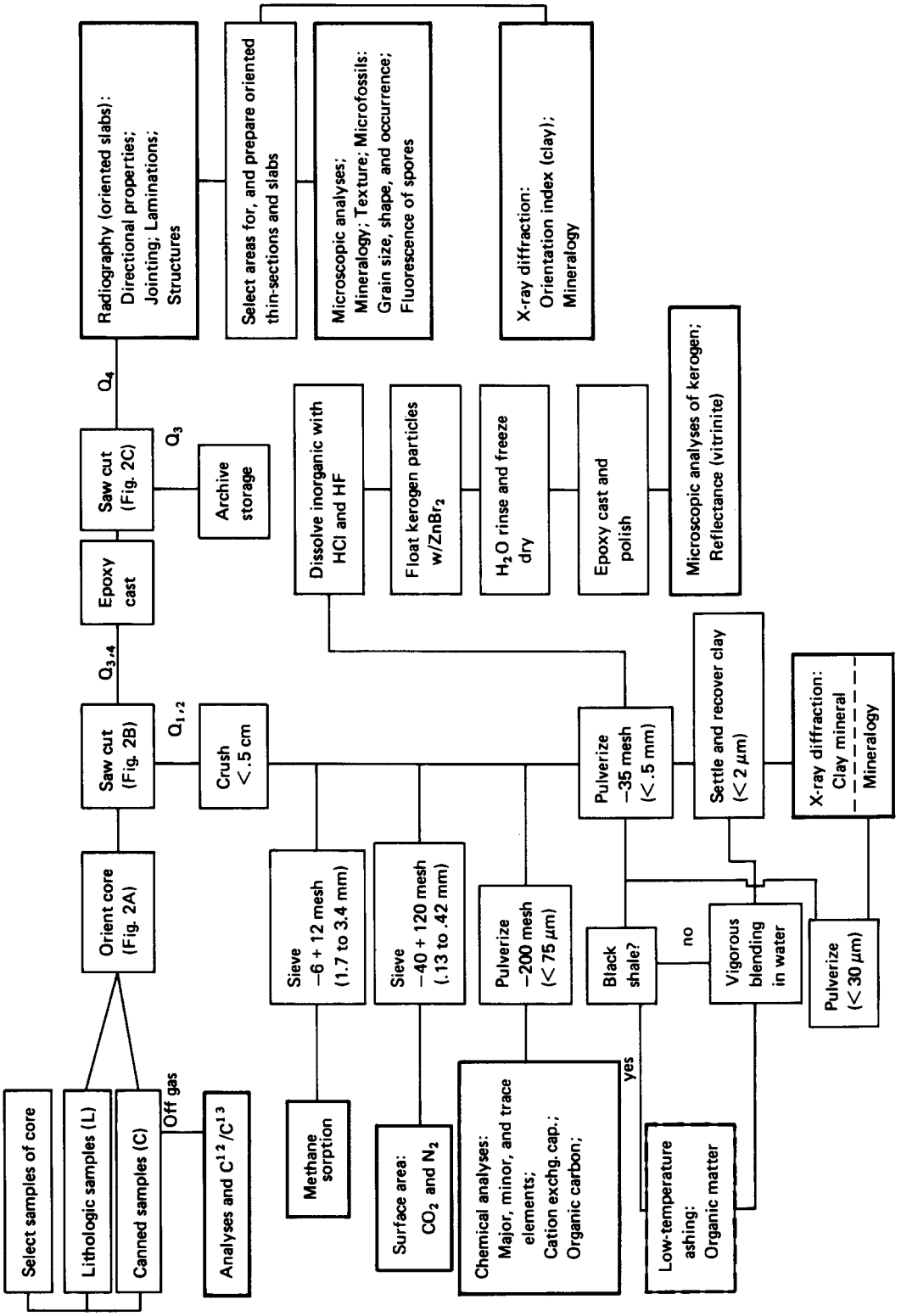

Fig. 3 - Diagram of processing and preparation of samples of New Albany Shale for mineralogic, petrographic, and geochemical analyses at the Illinois State Geological Survey. Sample preparation steps are in thin lines and analyses are in wide lines.

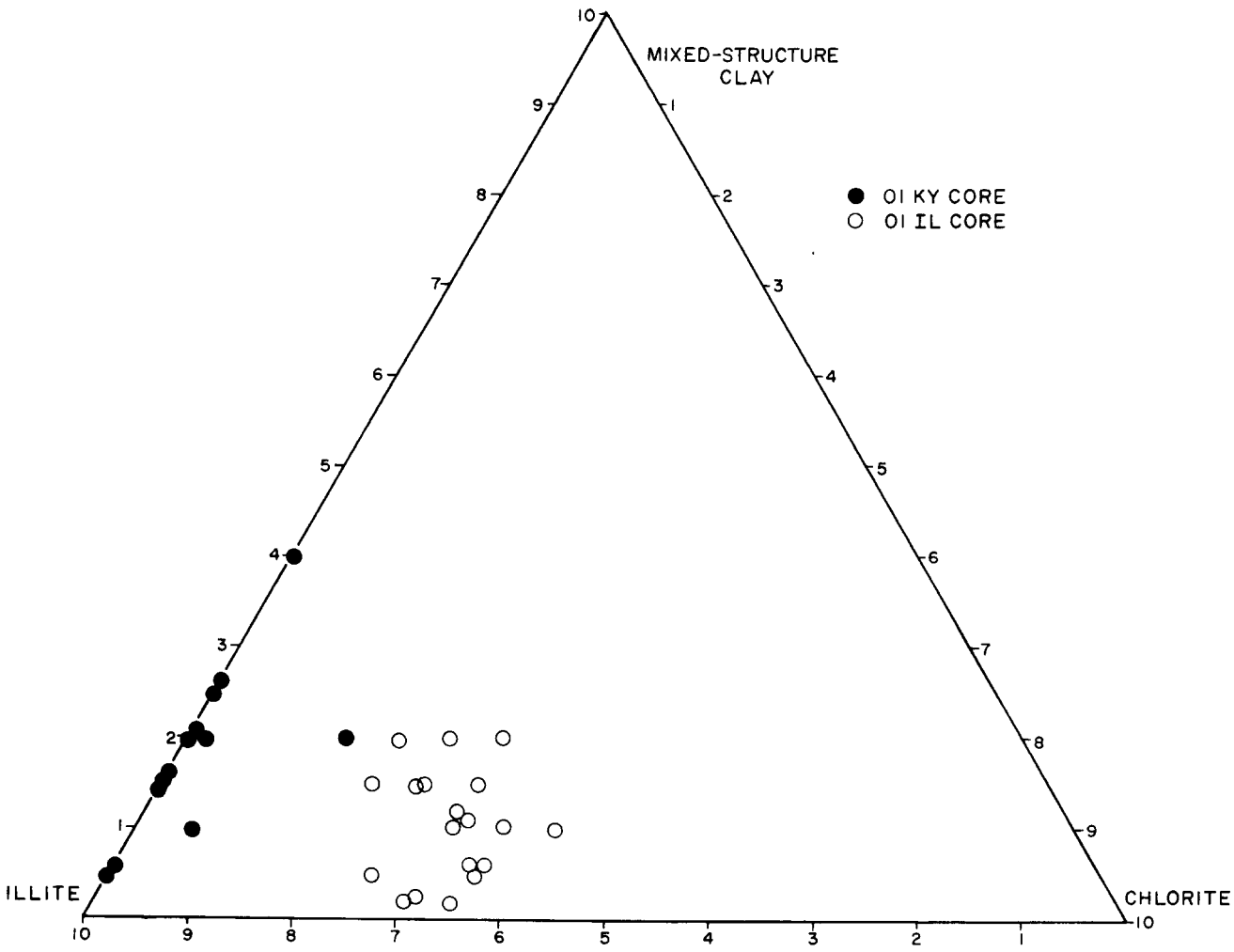

Fig. 4 - Clay mineral composition of samples taken from the Kentucky and Illinois cores. Kaolinite was not detected in the samples.

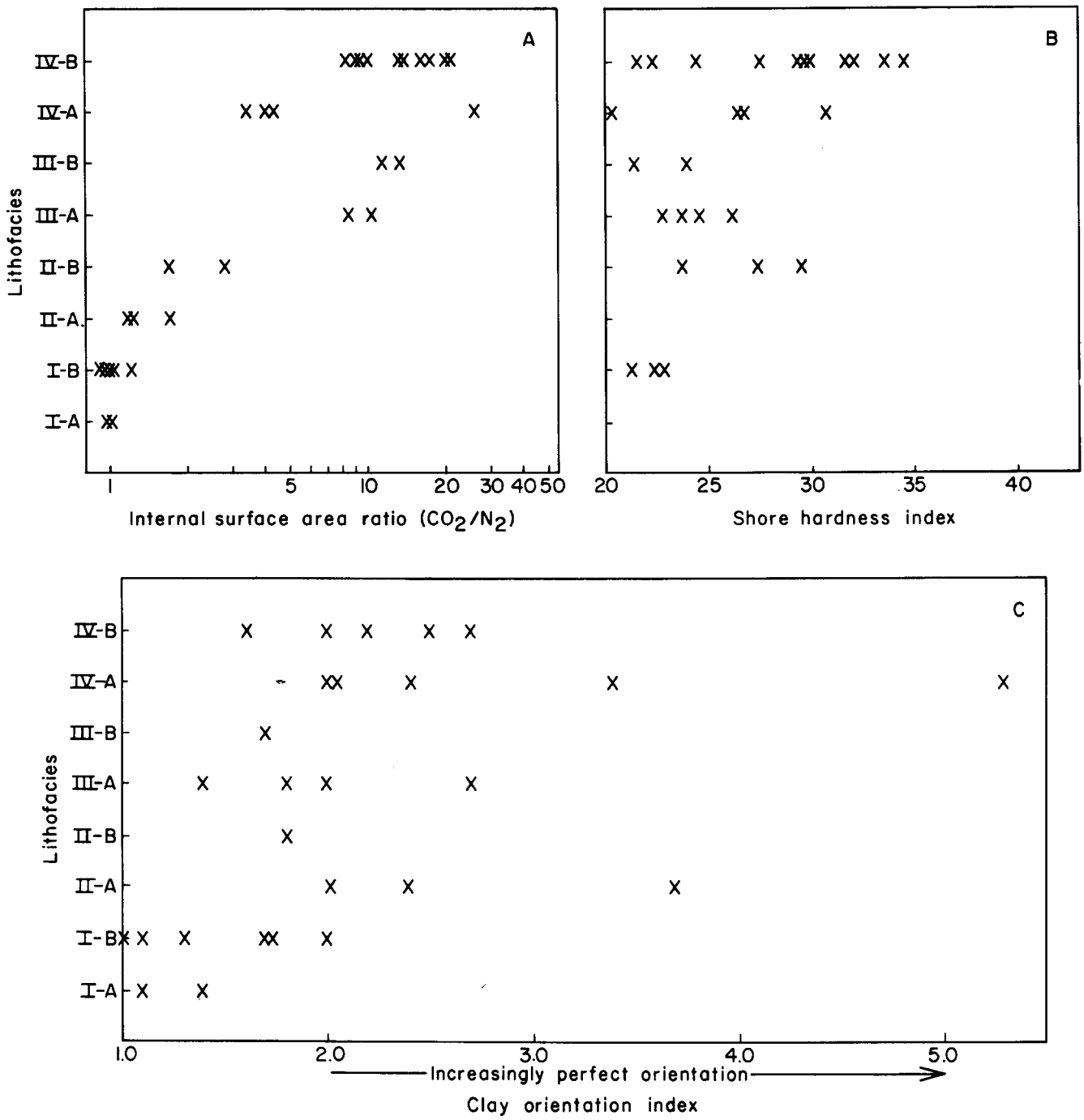

Fig. 5 - Relation of lithofacies classification to (A) internal surface area ratio, (B) shore hardness index, and (C) clay orientation index.

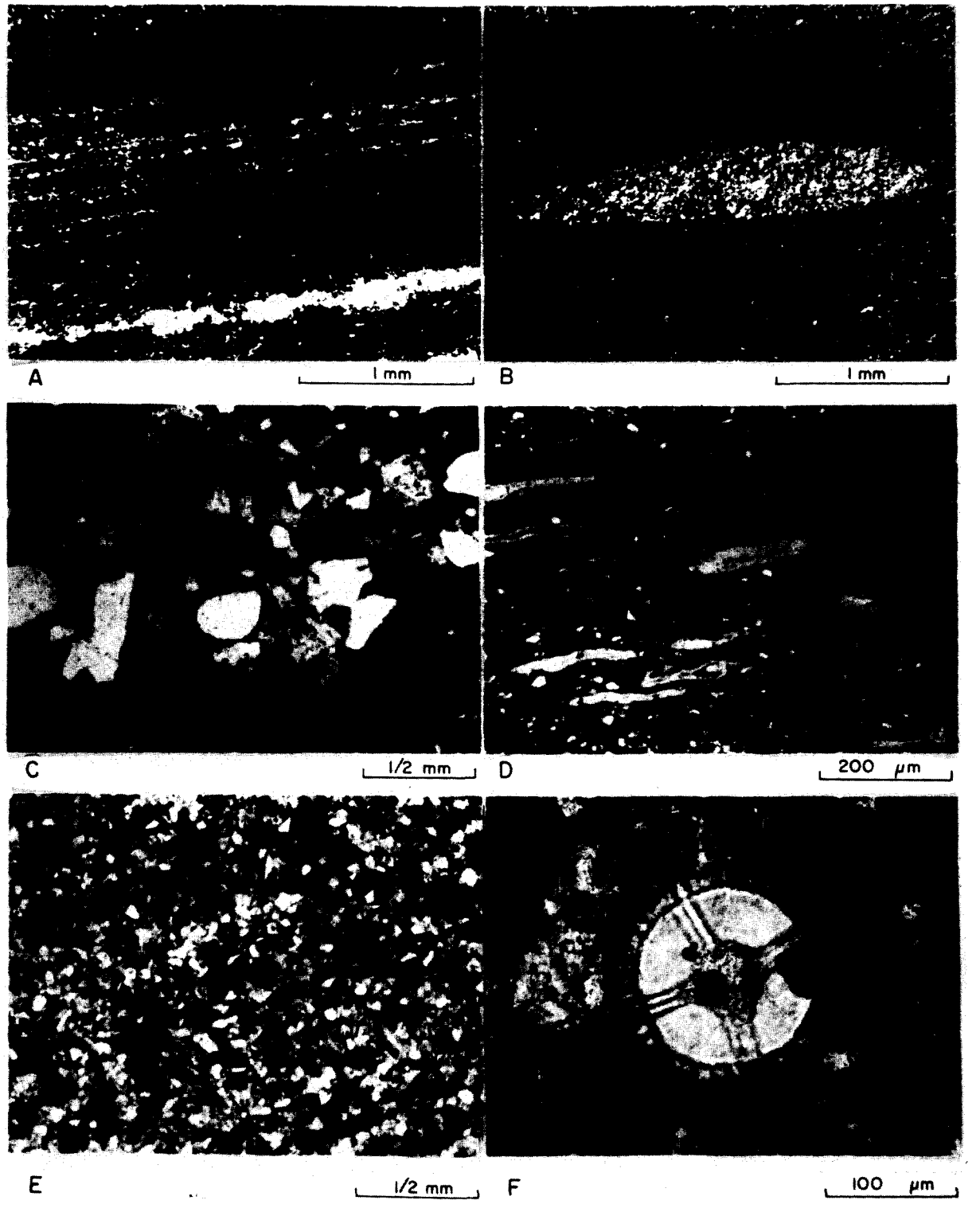

PLATE 1. (A) Fine silt laminae in brownish-black shale. Sample 01KY08C1. (B) Compressed burrow with silt-rich filling. Clay is well oriented in area surrounding but poorly oriented within burrow. Sample 01KY08C1. (C) Rounded fine sand grains concentrated within a burrow filling. Sample 01KY08C1. (D) Flattened spores. Note the difference between thin-walled and thick-walled types. Sample 1KY03L1. (E) Several phosphatic fossil fragments scattered in a silt layer. The fragments are shown here as needle-shaped, about 0.1 to 0.2 mm long, and oriented more or less NE-to-SW on this micrograph. Sample 01KY07L1. (F) Calcisphere (probably *Radiina* Reitlinger). Note the inner perforate capsule and the thick spines projecting from the outer wall, and the pyrite grains (black) within and around the calisphere. Sample 01KY04L1.

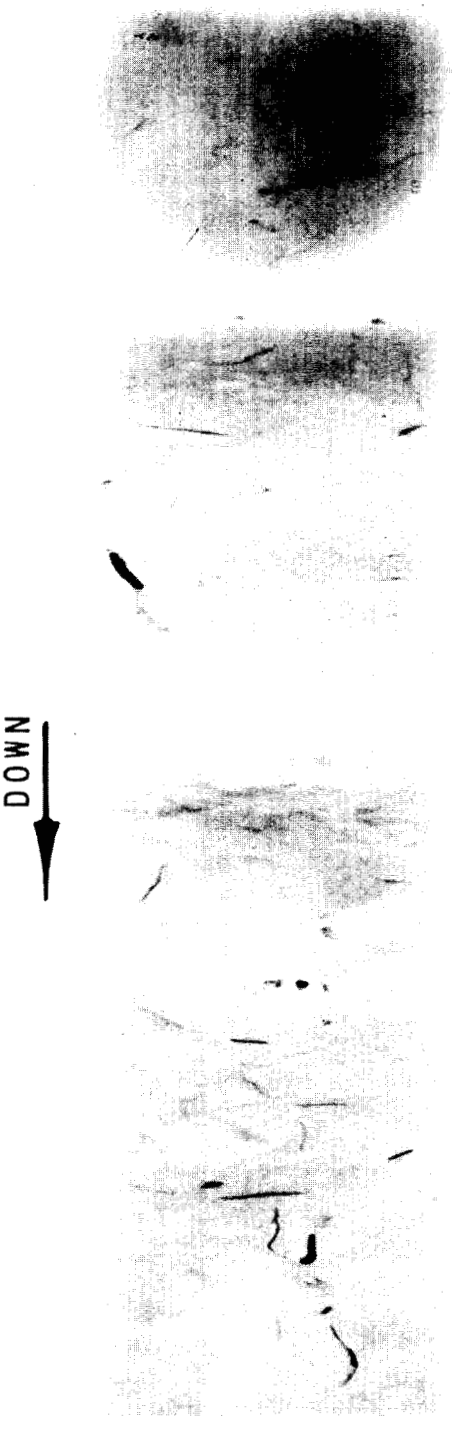

PLATE 2. Bioturbate greenish-gray mudstone. Lithofacies I-B characterized by a swirling texture due to the mixing action of burrowing organisms in the sediment. Short black streaks are pyrite-filled burrows and short synaeresis joints. Lithofacies I-A is similar in megascopic appearance to that shown here of I-B, but is generally finer grained. Sample 011L04L1.

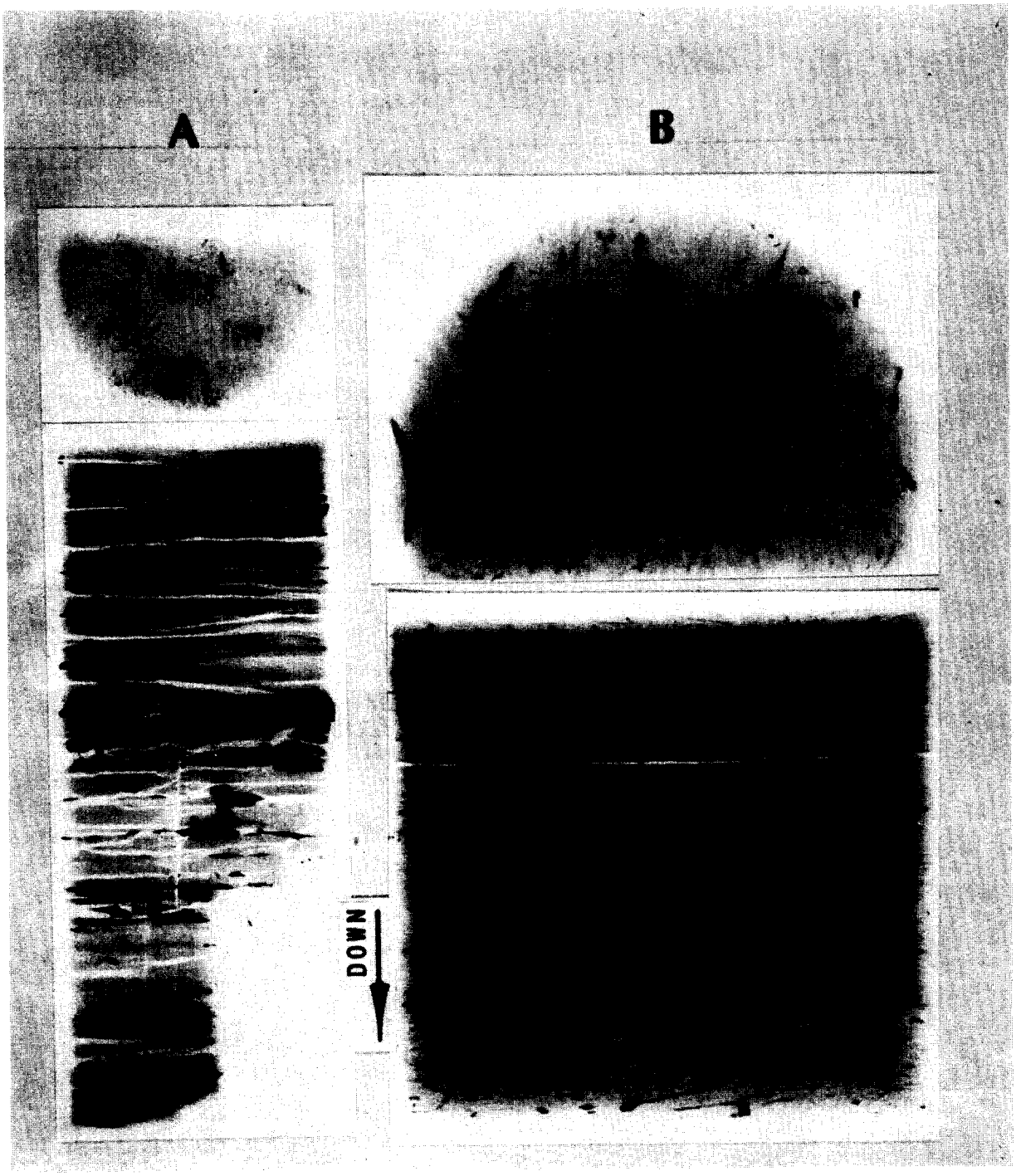

PLATE 3. Indistinctly bedded olive-gray shales. (A) Lithofacies II-A, characterized by indistinct bedding (massive) and abundant pyrite nodules and lenses. Sample 01IL14L1. (B) Lithofacies II-B, characterized by extensive bioturbation and synaeresis joints. The joints are pyrite-filled and were deformed into their crooked form by compaction. Bedding is visible but very indistinct. Sample 01KY06C1.

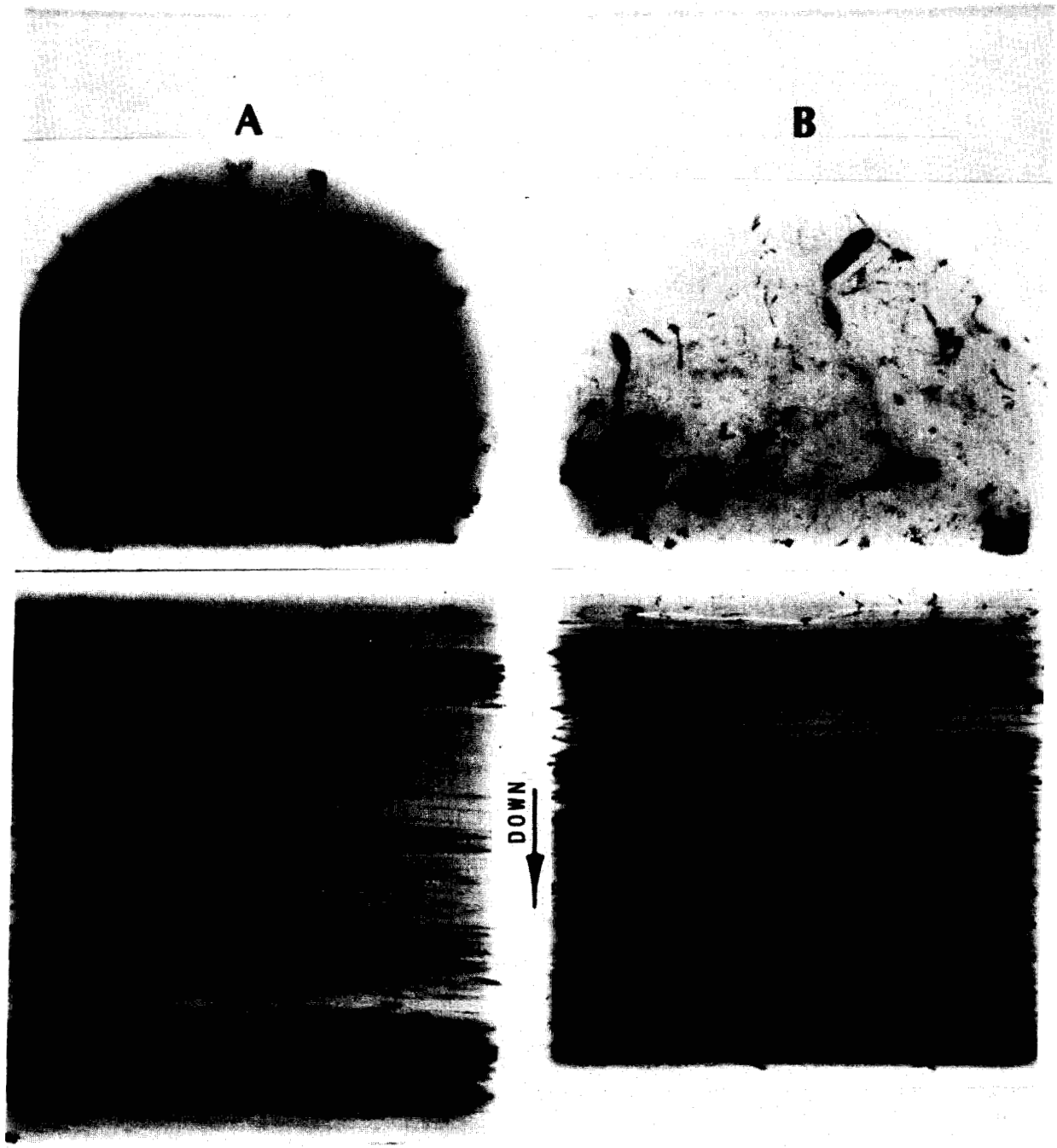

PLATE 4. Poorly laminated brownish-black shales. (A) Lithofacies III-A, characterized by medium to coarse laminations. Few synaeresis joints, sporadic burrowing, and few primary sedimentary structures such as ripples and cross-bedding are present. Sample 01KY08C1. (B) Lithofacies III-B, also characterized by medium to coarse laminations and weak bioturbation, but with much more extensive synaeresis development. Primary sedimentary structures, other than laminations, are absent. Sample 01KY11L1

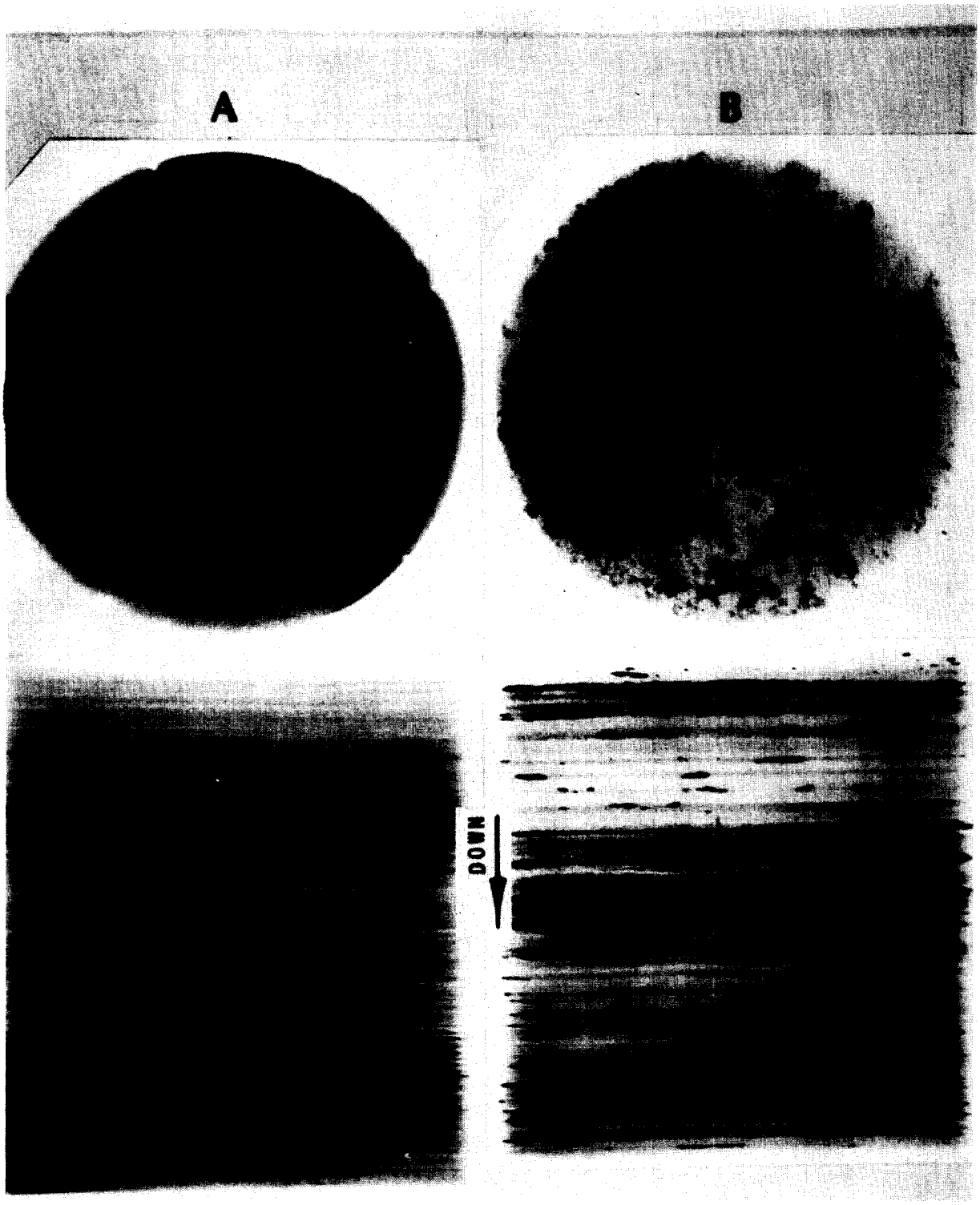

PLATE 5. Finely laminated, brownish-black shales. (A) Lithofacies IV-A, characterized by very fine and closely spaced pyritic laminae and an occasional large pyrite nodule (as at lower left). Sample 01KY01L1. (B) Lithofacies IV-B, characterized by slightly thicker and more irregular laminae and by numerous small pyrite nodules. Short vertical lineation at the center of the radiograph is a late stage (post-compaction) synaeresis joint filled with calcite. Sample 01KY03L1.

THE RELATIONSHIP BETWEEN DENSITY AND GAMMA-RAY INTENSITY IN THE DEVONIAN SHALE SEQUENCE, LINCOLN COUNTY, WEST VIRGINIA

James W. Schmoker
Geophysicist, U. S. Geological Survey, Denver, Colorado

ABSTRACT

The crossplot of density versus gamma-ray intensity from the Devonian shale sequence penetrated by three wells in Lincoln County, West Virginia, is linear. Geochemical data predict a linear crossplot if it is assumed that organic content is the only variable producing changes in formation density. Factors other than organic content appear to have only a second-order effect upon density changes. The gamma-ray log can be used to distinguish lithologic and stratigraphic units in the Devonian shale sequence in this area and to estimate their density to $\pm$ 0.017 g/cm^3 (68% confidence level). The crossplot between density and gamma-ray intensity can be used to identify intervals where factors other than organic content may contribute to density changes.

INTRODUCTION

The in situ bulk density of the Devonian shales of western West Virginia responds directly to variables of possible hydrocarbon-exploration interest such as matrix mineralogy, organic content, porosity, and pore-fluid type. Of these variables, organic content exerts the greatest influence on formation density. Organic material is commonly occurring and has a specific gravity of 1.0 g/cm^3, whereas the average grain density of the shale minerals is about 2.7 g/cm^3 (Smith and Young, 1964). In this study, logs from three wells in Lincoln County, West Virginia, were used to investigate the degree to which changes in organic content account for density variations in the shale, and to quantify the relationship between organic content, gamma-ray intensity, and density.

EXPERIMENTAL APPROACH

Independent measurements of formation density and organic content were necessary to determine the contribution of organic material to observed density changes. The density of the Devonian shales was measured with the compensated density log. The intensity of naturally occurring gamma radiation was used as a measure of the organic matter in the rocks.

Gamma-Ray Intensity and Organic Content

The dark, organic-rich Devonian shales of the Appalachian basin have higher gamma-ray responses than the lighter colored shales which contain less organic matter. The radioactivity is primarily due to uranium and its daughter products (Schwietering, 1970; Swanson, 1956). The uranium is not randomly distributed but is associated with organic matter (Conant and Swanson, 1961; McKelvey and Nelson, 1950), which explains the positive correlation between gamma-ray intensity and organic content. Moore (1954) has shown that organic materials such as peat, lignite, and subbituminous coal are effective in extracting uranium from aqueous solution. The uranium in the Devonian shales was probably precipitated from normal sea water by organic matter (Conant and Swanson, 1961). The gamma-ray log, by responding to uranium associated with organic material, should provide a quantitative measure of the organic content of the Devonian shales.

Gamma-Ray Intensity and Density

The gamma-ray intensity is assumed to be a linear function of organic content, based on the geochemical evidence cited and specific data given by Beers (1945):

$$\gamma = k_o V_o + \gamma_B \quad (1)$$

where γ is the gamma-ray intensity in API units, γ_B the baseline gamma-ray intensity unrelated to organic matter, V_o the volume-percent organic content, and k_o a constant.

V_o has a direct influence on formation density, because the specific gravity of the organic material is low compared to that of the shale minerals. An increase in V_o lowers the density of the formation. Organic content may also have a less direct effect upon density. The heavy mineral pyrite, with a density of 5.0 g/cm^3, is most abundant in the organic-rich black shales. Organic content apparently controls the pyrite distribution, and laboratory data (Brown, 1956; Strahl and others, 1955) indicate an approximate linear relationship between the two:

$$V_p = k_p V_o \quad (2)$$

where V_p is the volume-percent pyrite content and k_p a constant. Increasing organic content lowers the density of the formation, but the effect may be somewhat modified by increasing amounts of pyrite.

The formation density, ρ, can be written in terms of the density of organic matter ρ_o, the pyrite density, ρ_p, and the average density of all other constituents, ρ_a:

$$\rho = V_o\rho_o + V_p\rho_p + (1-V_o-V_p)\rho_a \quad (3)$$

Substituting for V_o and V_p using equations 1 and 2, and combining the various constants leads to the equation:

$$\rho = k_1\gamma + k_2 \quad (4)$$

where k_1 and k_2 are constants.

The crossplot of gamma-ray intensity and formation density should be linear if organic content is the only factor causing changes in the formation density.

DATA

The gamma-ray and density logs studied were from the Columbia Gas Transmission Corp. 20401, 20402, and 20403 wells, located within 1 mile (1.6 km) of each other near Ranger, Lincoln County, West Virginia. The wells were drilled to evaluate technical and economic aspects of massive hydraulic fracturing in the Devonian shales.

Stratigraphic Setting

The Devonian shale sequence at this location is about 1,360 ft (415 m) thick, nearly flat lying, and covered with about 2,700 ft (823 m) of younger Paleozoic sedimentary rocks. It is bounded at the top by the Berea Sandstone of Mississippian age and at the base by the Onondaga Limestone of Middle Devonian age. In the study area, the sequence can be subdivided into a dark, basal unit, equivalent to the Marcellus Shale of Middle Devonian age, overlain by gray shales and siltstones of Late Devonian age for which no formal stratigraphic name is completely appropriate. Two dark-shale zones interfinger with the gray shales and siltstones. Locally, drillers call these the upper and middle brown shales, and call the basal unit the lower brown shale. The combined thickness of the three brown shales is about 400 ft (122 m). A lithologic description of the Devonian shales encountered in the 20402 and 20403 wells is given by Byrer and others (1976).

Digitized Data

The wells were open and air-filled when logged, and log corrections were not required. In general, however, the quantitative interpretation of gamma-ray logs should include corrections for factors such as hole diameter, mud density, and casing and cement thickness (Rhodes and Mott, 1966). The density and gamma-ray logs were digitized at 2 ft (.61 m) intervals. Digitized data were entered into computer storage, from which crossplots and calculations were generated.

CROSSPLOTS

Figure 1 is the crossplot of density and gamma-ray intensity from the Devonian shale section penetrated by the Columbia Gas 20401, 20402, and 20403 wells. Digitized data were smoothed by averaging 20 ft (6.1 m) intervals. A linear correlation is evident, and a least-squares fit to the data evaluates the constants k_1 and k_2 of equation 4:

$$\rho = -.00120\gamma + 2.877 \quad (5)$$

The correlation coefficient between density and gamma-ray intensity is -.932. The standard deviation of density values about the regression line is .020 g/cm^3.

For the crossplot of figure 2, the same data were smoothed by averaging intervals of relatively constant physical properties. There were eighteen intervals, ranging in thickness from 20 to 170 ft (6.1 to 51.8 m). The least-squares fit to the data of figure 2 is given by:

$$\rho = -.00129\gamma + 2.896 \quad (6)$$

The correlation coefficient is -.962, and the standard deviation is .017 g/cm^3.

The two regression lines do not differ significantly. However, the data smoothed over lithologic intervals (figure 2) are better represented by the regression line, as is evident to the eye and demonstrated by a smaller standard deviation and a more negative correlation coefficient.

DISCUSSION

At a confidence level of 68%, the density of a 20 ft (6.1 m) interval in the Devonian shale section can be estimated to ± .020 g/cm^3 from the gamma-ray intensity alone. The density of a given lithologic unit can be estimated to ± .017 g/cm^3. These results imply that organic content is the primary variable causing changes in shale density.

The density difference between organic-rich and organic-poor shales is large compared to the error in gamma-ray density estimates of about ± .02 g/cm^3. The two rock types can be confidently distinguished using the gamma-ray data. In fact, the accuracy of gamma-ray density estimates is roughly equivalent to that of compensated density logs. In the three wells studied, the gamma-ray log can be used quantitatively to determine formation density.

Deviations from Regression Lines

Deviations from the regression lines are due to factors not taken into account by equation 4. Such factors might include:

1) Errors in the gamma-ray and density data.
2) Inappropriate assumptions relating organic content to pyrite and uranium.
3) Changes in formation density due to variations in the mineral matrix, pore fluid, or porosity.

Points on figure 1 with gamma-ray intensities greater than 300 API units are grouped above the regression line defined by the remaining data. A similar distribution is not obvious on figure 2, perhaps because of fewer data points. Although the compensated density log can give erroneous results when pyrite is present (Clavier and others, 1976), the trend observed on figure 1 is opposite the expected effect and cannot be explained by an anomalous density-log response. Possibly either the pyrite or uranium concentration increases nonlinearly when organic content reaches some threshold level.

Data points falling more than two standard deviations from the regression line are denoted by solid black symbols on figures 1 and 2. The number of such points does not exceed that expected from a normal distribution, but the points are not randomly arrayed. Seven of eight occur below the regression line, with densities lower than predicted by the gamma-ray log, and represent brown shale intervals. Densities lower than expected could imply increased porosity or the presence of gas, but a direct correlation to gas shows was not found. Hydraulic-fracturing experiments, which may provide additional information on gas-productive zones, have not been completed and evaluated. As this example illustrates, the crossplot of density and gamma-ray intensity might identify zones where factors other than organic content contribute to density changes.

Regional Validity

The crossplots and regression equations are based on data from one location. They are assumed valid over some larger, but at present undefined, area. A linear relationship between density and gamma-ray intensity should exist where the depositional environment of the Devonian shales was similar to that of the study area.

Patchen (1977) observes that the brown shales become less radioactive to the east, although retaining the same dark color. McKelvey and Nelson (1950) note that the ratio of uranium to organic matter may vary in the same shale formation. Thus some evidence suggests that the slope of the regression line might change from area to area, perhaps because of regional differences in the sedimentation rate, the nature of the organic matter, or the chemical composition of the sea water at the time of deposition.

SUMMARY

Crossplots of density and gamma-ray intensity from Devonian shales in three wells in Lincoln County, West Virginia, show a linear relationship between increasing gamma-ray intensity and decreasing density. For intervals of relatively constant physical properties, the correlation coefficient between density and gamma-ray intensity is -.962, and the standard deviation of density values about the least-squares fit is .017 g/cm^3. Geochemical data predict a linear crossplot if organic content is the only variable producing changes in formation density. The results imply that factors other than organic content have only a second-order effect upon density variations.

The gamma-ray log, properly corrected for borehole conditions, can be used quantitatively:

1) To distinguish lithologic and stratigraphic units in the Devonian shale section and to estimate their density with a precision approaching that of the compensated density log.
2) To identify, by crossplotting with density, intervals where factors other than organic content are contributing to density changes.

Further work is needed to determine the regional validity of the approach, the possible dependence of crossplot slope upon location, and the range of density and gamma-ray values over which the linear relationships hold.

ACKNOWLEDGEMENTS

This work was performed under the auspices of the U.S. Energy Research and Development Administration under Interagency Agreement EX-76-C-01-2287. The cooperation of the Columbia Gas Transmission Corp. is gratefully acknowledged.

REFERENCES

Beers, R. F., 1945, Radioactivity and organic content of some Paleozoic shales: Am. Assoc. Petroleum Geologists Bull., v. 29, no. 1, p. 1-22.

Brown, A., 1956, Uranium in the Chattanooga Shale of eastern Tennessee: U.S. Geol. Survey Prof. Paper 300, p. 457-462.

Byrer, C. W., Vickers, M. K., Rhoades, S. J., and Easterday, B. G., 1976, Lithologic description of cored wells #20402 and #20403 in the Devonian shale in Lincoln County, West Virginia: Morgantown Energy Research Center TPR-76/9, 58 p.

Clavier, C., Heim, A., and Scala, C., 1976, Effect of pyrite on resistivity and other logging measurements: SPWLA Seventeenth Annual Logging Symposium, June 9-12, 1976, 34 p.

Conant, L. C., and Swanson, V. E., 1961, Chattanooga shale and related rocks of central Tennessee and nearby areas: U.S. Geol. Survey Prof. Paper 357, 91 p.

McKelvey, V. E., and Nelson, J. M., 1950, Characteristics of marine uranium-bearing sedimentary rocks: Soc. Econ. Geologists Bull., v. 45, no. 1, p. 35-53.

Moore, G. W., 1954, Extraction of uranium from aqueous solution by coal and some other materials: Soc. Econ. Geologists Bull., v. 49, no. 6, p. 652-658.

Patchen, D. G., 1977, Subsurface stratigraphy and gas production of the Devonian shales in West Virginia: Morgantown Energy Research Center CR-77/5, 35 p.

Rhodes, D. F., and Mott, W. E., 1966, Quantitative interpretation of gamma-ray spectral logs: Geophysics, v. 31, no. 2, p. 410-418.

Schwietering, J. F., 1970, Devonian shales of Ohio and their eastern equivalents: The Ohio State Univ., Ph.D. thesis, 79 p.

Smith, J. W., and Young, N. B., 1964, Specific-gravity to oil-yield relationships for black shales of Kentucky's New Albany formation: U.S. Bur. Mines Rept. Inv. 6531, 13 p.

Strahl, E. O., Silverman, E. N., O'Neil, R. L., and others, 1955, An investigation of the mineralogy, petrography and paleobotany of uranium-bearing shales and lignites. Scope A-shales. Fourth Annual Report. Period of April 1, 1954 to March 31, 1955: U.S. Atomic Energy Comm. NYO-6068, 79 p.

Swanson, V. E., 1956, Uranium in marine black shales of the United States: U.S. Geol. Survey Prof. Paper 300, p. 451-456.

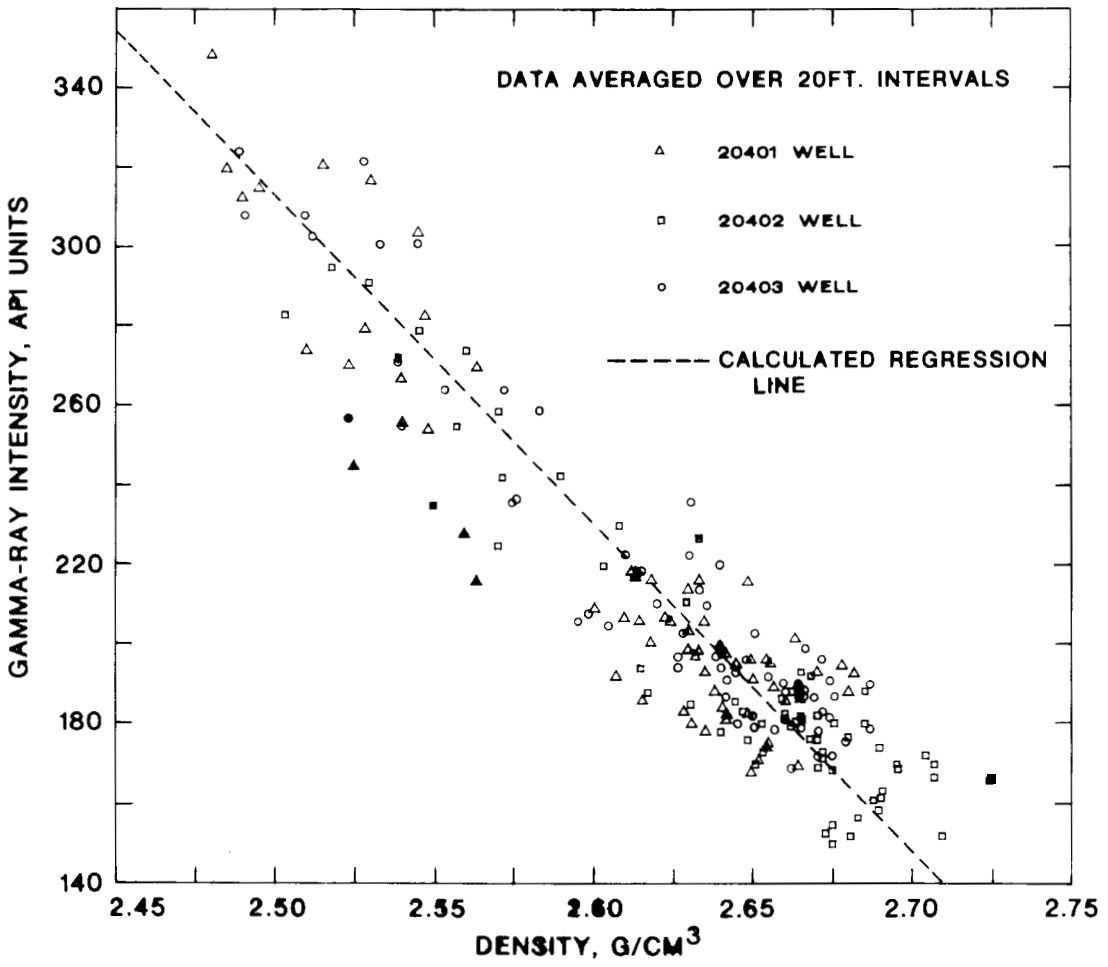

Figure 1. -- Crossplot of density and gamma-ray intensity with digitized data smoothed by averaging 20 ft (6.1 m) intervals. Solid black symbols denote points more than two standard deviations from the regression line.

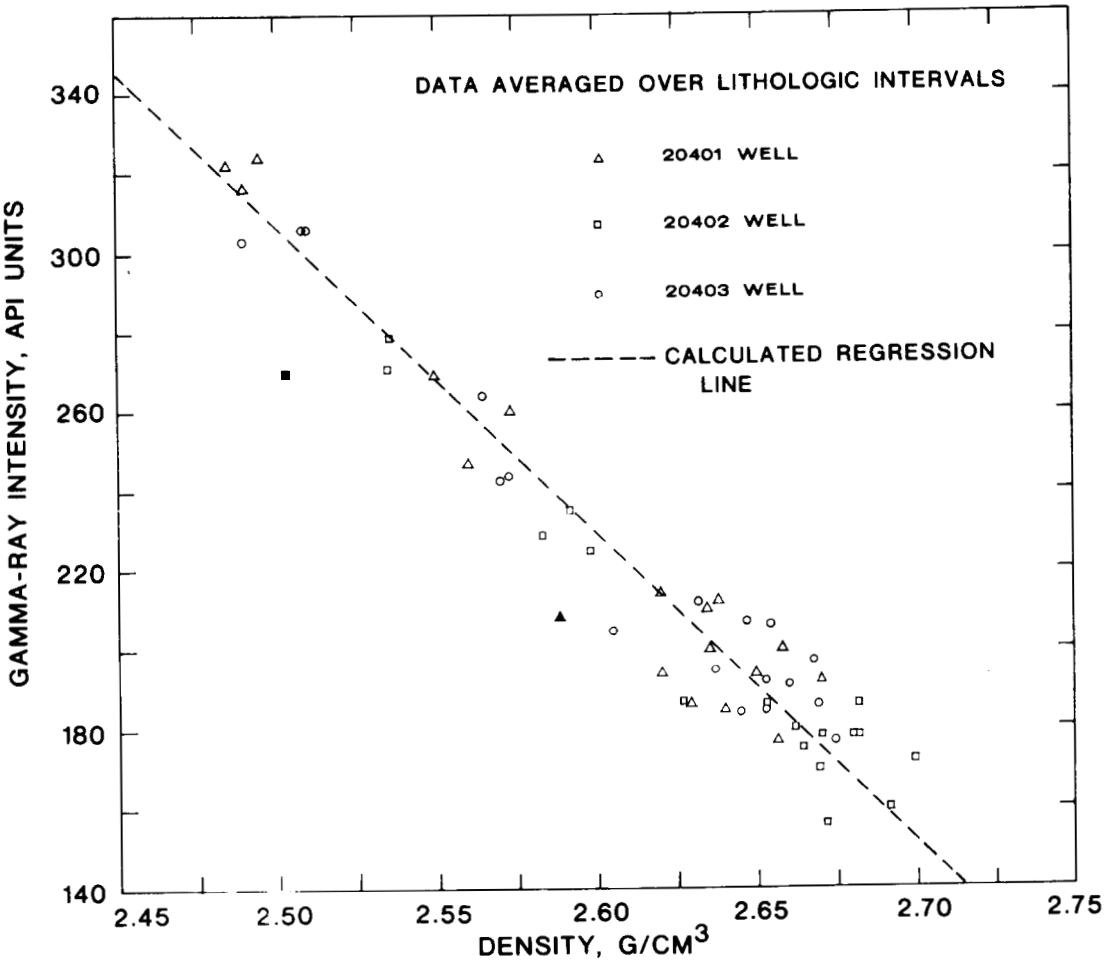

Figure 2. -- Crossplot of density and gamma-ray intensity with digitized data smoothed by averaging intervals of relatively constant physical properties. Solid black symbols denote points more than two standard deviations from the regression line.

AMEX/VESCORP DEVONIAN SHALE PROJECT
LAWRENCE & SCIOTO COUNTIES, OHIO

by

John N. Cochrane
F. Daniel Ryan
Steven H. Alkire

ABSTRACT

Amex/Vescorp in conjunction with U.S.E.R.D.A., Ohio E.R.D.A., and National Petroleum Corporation, is conducting a field demonstration test to provide information on the Devonian Shales, in Lawrence and Scioto Counties, Ohio which can be used in the immediate and surrounding areas to increase gas production from the shale.

The general objectives of this program are to establish the effectiveness of remote sensing imagery as a tool in picking shale well site locations, to determine the benefit of advanced stimulation techniques, and to determine if a scaled up version of the fracture technique deemed to be the better of the two above would be a cost-effective method of improving production rates and reserves.

Analysis of the remote sensing imagery was completed on May 24, 1977. Nine primary and twelve alternate well locations have been selected as a result of this work. The drilling of these wells will commence in the near future at which time coring and logging will be used to help determine which zones should be stimulated.

Prepared for the Energy Research and Development administration, under Contract No. E(40-1)-5253.

INTRODUCTION

The devonian Shale underlies more than 100,000 square miles in the Appalachian area including such states as Kentucky, West Virginia, Michigan, Indiana, New York, Pennsylvania, Ohio and others. This Devonian Shale formation is the subject of much speculation because of large estimates of natural gas reserves. The U.S. Energy Research and Development Administration and the Ohio Energy and Resource Development Agency have both gone on record as estimating gas in place in the Devonian Shale to be in the quadrillions of cubic feet in the continental United States. The Ohio ERDA has estimated that with existing technology, seventy (70) trillion cubic feet of gas could be produced in Ohio alone.

Even with the impressive reserve estimates, the low field price for natural gas prevents the Shale from receiving any more than nominal attention from independent producers.

The potential of the Devonian Shale is not a newly discovered horizon of productivity. Several thousand wells have and are producing natural gas from Shale. Most shale wells in the Appalachian area are contained in the Big Sandy Field of Kentucky and West Virginia in addition to several Ohio counties such as Lawrence, Scioto, Meigs and Licking.

It is generally recognized that the average shale well will outproduce the average sandstone well in Appalachia, but it takes several decades for the shale production to occur. The economics favor sandstone over shale because of cash flow considerations related directly to rate of production. Independent producers are economically attracted to the lower gross production of sandstone because of the more acceptable rate of return it provides. In contrast, while containing much larger recoverable reserves, the shale presently produces at so slow a rate of return as to deem it financially unacceptable. This generalization would be more aptly applied to less fractured shale areas such as found in Ohio than to the highly fractured Big Sandy Field of Kentucky and West Virginia.

The primary problem area with shale is stimulation. Shale is generally very tight, having porosities of 4 to 5%, or less. The consensus of opinion for Appalachian Shale is that large production is a direct result of communicating with natural fracture systems either in the drilling operation or through stimulation. Therefore, if a well can be drilled into a natural fracture system and then be efficiently stimulated, economics resembling sandstone wells will hopefully result.

The initial stimulation of Devonian Shales consisted of employing liquid nitroglycerine to explosively stimulate a small zone of the borehole. The zone of stimulation was usually no greater than 50 feet in thickness. The Shale section becomes several thousand feet thick in some areas of the Appalachian Basin. Liquid nitroglycerine proved very dangerous to use over a large interval.

Eventually liquid nitro gave way to black powder and desensitized nitroglycerine. The majority of shale wells have been treated with 80% gel which is desensitized nitro. This form of stimulation allowed producers to treat thick zones of shale at a time. Zones as thick as 1200 feet have been treated with 80% gel.

The introduction of hydraulic fracturing in the Appalachian Basin eventually led to a comparison between "shooting" 80% gel and "water fracing" in the shale. Kentucky West Virginia Gas Company and others have compared these two stimulation methods in similar shale areas and have generally concluded that hydraulic fracturing with water was superior to shooting.

In recent years, several revolutionizing concepts in stimulation have been examined in the Devonian Shale. The U.S. ERDA, Columbia Gas System Service Corporation and others have examined stimulation methods such as stiff foam, cryogenic fracs, and liquid explosives. Results to date do not appear conclusive regarding the merits of these new concepts in stimulation because of a limited number of treatments for each type of stimulation and little direct comparison between the new stimulation techniques in the same shale field.

This proposal seeks to make a direct comparison between stiff foam stimulation and cryogenic stimulation in Lawrence and Scioto Counties, Ohio. The State of Ohio has considerable shale history but very little in the way of new stimulation techniques have been examined in Ohio Shales. None of the new methods have been employed in Lawrence and Scioto Counties which have been the most prolific shale production areas in the State.

In addition to direct stimulation comparison, the program proposes to provide information concerning the Devonian Shale in Southern Ohio that is presently not available. Although many shale wells have been produced in the subject area, very little is known about the stratigraphy or physical properties of this shale.

Figure 1 indicates the townships from which productive shale wells have been recorded in the State of Ohio. The target area for this program is circled.

PROPOSED PROGRAM AND OBJECTIVES

The general objectives of the proposed program are to identify natural fracture systems in the shale by use of remote sensing imagery and also to establish the quantitative benefit of advance stimulation techniques compared to historic stimulation techniques in the Ohio Devonian Shale. The historic stimulation treatment in Southern Ohio has been nitroglycerine or desensitized nitroglycerine. The proposed program will evaluate the effectiveness of stiff foam and cryogenic fracturing.

The initial period of the program will be concerned with geologic study of the area including the interpretation of the available well information and remote sensing. With respect to remote sensing, the objective will be to extract geologic fracture/lineament patterns in the area of question through use of the LANDSAT satellite and high altitude aircraft imagery available from the United States Geological Survey (USGS) Eros Data Center. Similarly, recent low altitude and radar imagery (SLAR), will be collected and analyzed.

A comprehensive evaluation of stimulation alternatives in the Lawrence and Scioto County area would be of immediate benefit to the State of Ohio and the producers of the Appalachian area in providing relief to Ohio's natural gas shortage. Equally important, however, is the base case data available from the currently producing wells in that area. Only six (6) shale wells were drilled in Ohio in 1975. A successful stimulation program would substantially increase the number of shale wells drilled and produced.

In this program, we will be comparing stiff foam hydraulic stimulations with cryogenic stimulations. The questions we shall attempt to answer are:

1. Are the stimulation treatments technically and economically feasible?
2. What basic data relative to the shale is necessary before the techniques will be commercially viable?
3. Can we identify the zones where the treatment should be applied?
4. What are the basic formation characteristics of this area which have made it a good producer?

Although this area has historically been a good producer, very little factual shale data exists. We will establish through cooperation with the Ohio Geological Survey, a comprehensive set of shale data. Although we know this area to be a prolific gas producing area, there is no data to relate gas producing potential with basic shale characteristics.

In researching new techniques, we should first concentrate on the historically proven areas and then expand into the unknown areas. Our proposed program takes such an approach and is, therefore, aimed at providing maximum probability of success.

Foam, used as a fracturing fluid is a mixture of fluid, gas, a foaming surfactant and the propping agent. The liquid phase can be fresh water, diluted and concentrated acids, lease crude, etc. The surfactant is chosen to combine with this liquid and form foam when mixed with the gas. Currently, nitrogen is the gas used in foam fracturing due to its availability and other desirable qualities that make it acceptable to the oil field; however, many other gases could be used in FOAM-FRAC$_{TM}$.

Foam made with only these materials possess superior fluid-loss control, excellent proppant carrying capacity, and high viscosity. Chemical additives are not required to enhance either the viscosity or the fluid leak-off characteristics of the foam.

Application of foam fracturing has had impressive, but limited, success.

Minerals Management attributes the high deliverability increases in wells after stimulation with foam to the following:

1. The low natural fluid loss of foam limits invasion of the fracturing fluid to approximately one-half inch. Once production is initiated, the small amount of fluid is quickly returned to the fracture, and thus out of the well.

2. Absence of solid or chemical fluid-loss additives to control fluid leak-off during treatment leaves both the formation face and the proppant bed clean and thus maximum proppant-bed transmissivity can be utilized.

3. The liquids in the foam constitute only 10% to 30% of the total foam volume. In field applications of the technique, approximately 90% of the liquids have been returned indicating that the formation does not become saturated with fluid.

4. Clean-up time to date has been less than 12 hours on an average 20,000 gallon job. Well testing has usually commenced on the second or third day after fracturing. The short time the fluid is on the formation limits the amount of chemical reaction with the formation and clay absorption of the water.

Cryogenic treatments in the shale have heretofore been limited. At least three such treatments, two by Columbia Gas and one by Kentucky West Virginia Gas have been carried out. The results of the cryogenic treatments appear to be very positive. However, substantial additional work remains to be done to evaluate cryogenic treatment results and provide a quantitative basis of comparison.

LOGGING PROGRAM

The following logging operations will be carried out on each well:

7-7/8 inch empty hole:
Temperature (1400 Feet to TD)
Sibilation (Optional)

7-7/8 inch fluid-filled hole:
Compensated Formation Density (1400 feet to TD)
Compensated Neutron Log (1400 feet to TD)
Gamma Ray (Surface to TD)
Borehole Compensated Sonic (1400 feet to TD)
Dual Laterlog (1400 feet to TD)

5-1/2 inch casing:
Cement Bond (1400 feet to TD)
Perforating Depth Control-Gamma Ray (1400 feet to TD)

Post Stimulation
Temperature
Spinner Survey
Gamma Ray - Beads

FRACTURE DESIGN

The fracture would consist of one projected fracture treatment in the selected shale interval. The maximum fracture interval has been chosen to be 150 feet. The actual interval to be treated would be determined upon completion of the well logging, coring and reservoir analysis.

CORING PROCEDURE AND ANALYSIS

The entire shale interval of the first well would be cored with foam after drilling to the top of the Shale section as determined by drill cuttings analysis. It is estimated that 150 feet will be cored in each of the next two wells. All core will be oriented. A 7-27/32 inch diamond core cutter with a 6-1/4 inch external diameter barrel would be used to cut a 4 inch diameter core.

Immediately after each barrel of core is surfaced, it would be removed from the barrel, packaged and shipped to the U.S. ERDA in Morgantown, West Virginia for core orientation.

WORK STATEMENT

Nine wells are proposed to be drilled in the general area of Lawrence and Scioto Counties in Ohio. Pipelines are available near the project acreage.

Geological evaluation of the area in Lawrence and Scioto Counties including remote sensing will be used to determine specific well locations. Every effort will be made to provide the stiff foam and cryogenic treatments with as similar conditions for test as possible, thus minimizing any bias that could occur through stimulating preferred wells with one type over the other. In the first six wells the stimulation designs will attempt to maintain the fracture radius per unit pay section constant for all treatments.

Three of the initial six wells in the program will be stimulated with foam, the second three will be cryogenic treatments. Wells seven through nine will await the results of the first six wells.

The specific stimualtion designs must await downhole information. However, as a minimum the treatments are expected to be at least comparable in volume to the hydraulic stimulation presently being used in Devonian Shale. At this time, it is estimated that 140,000 gallon foam fractures and 40,000 gallon cryogenic fractures will be used on the first six wells.

The remaining three wells could be stimulated with larger treatments than wells one through six depending upon initial results.

DRILLING PROGRAM

Upon selection of the first three well sites, an 11" hole would be drilled to 1400 feet using air as the circulating medium to the bottom of the Berea Formation. The 8-5/8" casing would be set and cemented to surface. Coring would then commence using foam as the fluid system. The first well would be cored throughout the entire interval and selective coring of approximately 150 feet is projected for each of the two wells that follow. Samples would be obtained from 1400 feet to total depth at 10 foot intervals on those wells not cored.

Upon completion of logging and preliminary reservoir testing, 5-1/2" casing would be set at total depth and cemented. A 3000 psi working pressure wellhead would be installed and the rig moved to the next location.

There would be a gas detector unit on the well from the time the 8-5/8" casing is drilled out until total depth is attained. Information about total combustible gas and methane, liquid hydrocarbons and oil florescence in drill cuttings and lithology would be provided.

The core would then be shipped to Core Laboratories, Inc. in Mt. Pleasant, Michigan for the following analysis: (1) Gamma Surface Log (2) Color Photo (3) Full Diameter Analysis, including porosity, grain density, fluid saturations, vertical permeability, oriented horizontal permeability in 45° quadrants (4) Gas Volume Test on Native State Core (5) Hydrocarbon Analysis (6) Core Slab (7) Fracture Analysis, and (8) Full Diameter Accoustic Velocity Test at 5 Overburden Pressures.

Core samples will also be sent to Cardinal Chemicals for Core Flow Tests and Foam Evaluation. Representative samples of the core will be sent to Halliburton and Dowell for chemical analysis, fluid compatability and basic fracture treatment design.

The Ohio Geological Survey plans a comprehensive evaluation of the Ohio Shale. To the extent possible, our program will compliment the OGS project and we shall extract the maximum information from the OGS project for application in our testing program. We will maintain constant liason with the OGS.

RESERVOIR TESTING

A consulting engineer will design the detailed well testing package for this program. It is anticipated that reservoir properties will be obtained from analysis of the logs and core where available. Drill stem tests will be run if significant shows of gas are encountered.

Open flows will be monitored throughout the coring and/or drilling phase of each well.

Each well will be tested after total depth is attained after the breakdown operation and after the stimulation in order to describe the capacity for production of the well.

Modified isochronal four point deliverability tests and pressure draw down or build up tests will be conducted for sufficient amounts of time to obtain an optimum of information.

PROJECT PROGRESS

Phase I of our project, the geologic analysis of the area, has been completed. Dr. B. R. Henniger of Ashland College collected and analyzed Landsat and High Altitude Imagery, Side Looking Airborne Radar Imagery, and Infrared Imagery. By visual analysis, Dr. Henniger has identified and mapped the major natural fracture systems that occur on the surface in the project area. He then went into the area on foot to verify these fractures. Dr. Henniger could not cover the entire area that had been studied, but he did spend four days verifing the fracture systems that he had access to. Therefore, it is believed that the entire area studied has been accurately analyzed.

Dr. Henniger also measured surface fracture dips while in the area. Out of 255 fracture dip measurements, only one was in excess of 15° from vertical. Thus by drilling wells at intersections or zones of surface fracture systems, we should be able to encounter these same fracture systems at ±2000' in a shale well. If these systems are not encountered by the wellbore itself, due to the almost vertical dip, we should easily encounter them upon fracturing the well.

After compiling this data, Dr. Henniger recommended 9 primary and 12 alternate well locations on acreage within and surrounding the project area. Title surveys are now being done on these locations. Drilling of the first well should commence in September, 1977.

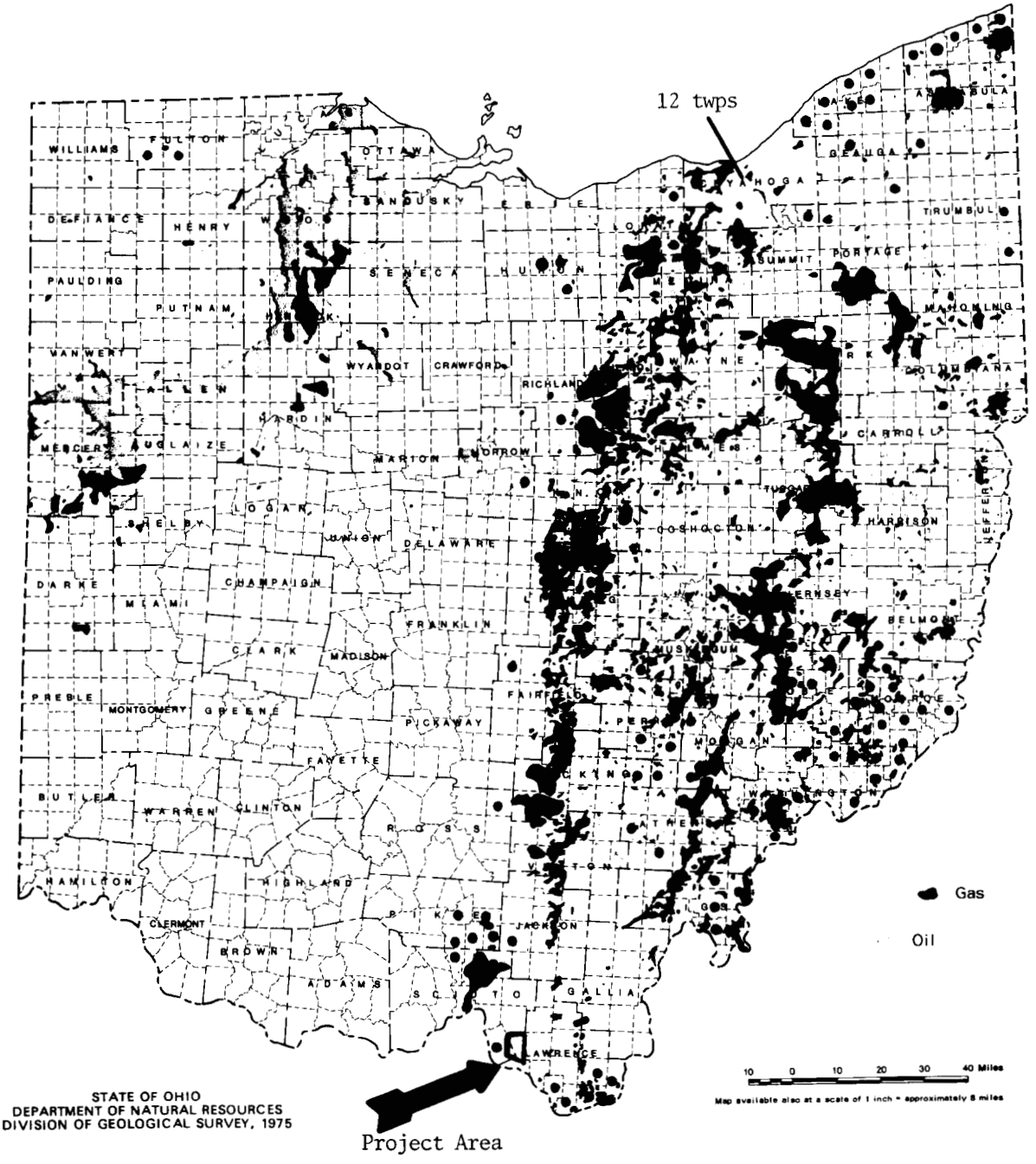

OIL AND GAS FIELDS OF OHIO

Figure 1 Townships from which productive (domestic and largely marginal commercial)shale wells have been recorded. Indicated by dot (•).

CHEMICAL EXPLOSIVE FRACTURING OF EIGHT TIGHT GAS WELLS

by

S. J. LaRocca, Petroleum Technology Corporation
Arthur M. Spencer, Petroleum Technology Corporation
Redmond, Washington

ABSTRACT

The objective of this joint ERDA/industry program is to evaluate the potential of chemical explosive fracturing using up to 30,000 pounds of explosives to stimulate and enhance recovery of gas from tight reservoirs. Six of the eight wells are in the Devonian Shale: three in Kentucky and three in West Virginia. The remaining two wells are in the Canyon Sands of southwest Texas.

A general description of the on-site explosive manufacturing, placement and detonation techniques is presented. Details of the pre-shot and post-shot testing and production are given on wells worked on and stimulated to date. The program is continuing.

INTRODUCTION

During the fall of 1976 the United States Energy Research and Development Administration (ERDA) and Petroleum Technology Corporation (PTC) completed negotiations and contracts to stimulate eight tight gas wells, in a joint ERDA/industry program, using chemical explosive fracturing. The objective is to evaluate the potential of chemical explosive loads, up to 30,000 lbs., to stimulate and enhance recovery of gas from tight reservoirs.

Three contracts cover the eight-well program. Key features of the program are presented in Table 1 The industry participants provide the test wells and/or technical assistance, equipment and leases. A brief description of the explosive manufacturing and placement process precedes the summary of the field work accomplished to date under the three contracts.

EXPLOSIVE MANUFACTURING AND PLACEMENT PROCESS

Petroleum Technology Corporation's technique of explosive stimulation of oil/gas wells is inherently safer than other methods presently employed. This is due to the unique on-site, downhole manufacturing process. No explosives (except for 1/2 lb. used in the detonator/booster) are handled on the surface. A fuel and an oxidizer are pumped down into the well some 100 ft. below the surface to a mixer, where they combine to form a high energy liquid explosive. The explosive is then displaced down the tubing to the formation to be fractured. The usual deployment of the equipment for the remote explosive manufacturing and displacement process is illustrated in Figure 1. Additional details will be found in the Proceedings of the Second ERDA Symposium on Enhanced Oil and Gas Recovery, Volume 2 - Gas, page C-7.

Prepared for the Energy Research and Development Administration under Contract Numbers EY-76-C-08-0685, EY-76-C-08-0686 and EY-76-C-08-0687.

TECHNICAL PROGRESS

Kentucky Program (EY-76-C-08-0685

Five criteria were established as guides for the selection of an existing well to be stimulated by chemical explosive fracturing. This well should be one which: (1) had been previously shot with conventional 80% gel explosive; (2) is offset by hydraulically fractured wells; (3) produces at a rate below average for the area; (4) has sufficient reservoir potential and/or gas reserves to warrant a re-stimulation attempt and, (5) is in the vicinity of surface lineaments determined from ERTS and U-2 photographs. After examining files for several wells combined with on-site inspections, well number 6810 located in Perry County, Kentucky, emerged as the best candidate. PTC purchased this well from Kentucky West Virginia Gas Company for use in this program. For contract identification it is known as well 685-1.

Thirteen years ago the well came in at 60 MCFPD, following a 4225 lb 80% gel shot. Gas production had declined to a rate of 9 MCFPD by late 1976 when the well was selected for treatment. Offset wells had been successfully hydraulically fractured, and the well was in the vicinity of surface lineaments determined from remote sensing imagery. Following a recent 17 day shut-in period, the surface pressure was 337 psig and the bottomhole (3200') pressure was 454 psig. Later surface pressure readings, after being shut-in 60 days, were up to 393 psig, about 150 psi less than the original pressure and the current pressure of an offset hydraulically fractured well. The pressure survey also indicated the presence of about 250 ft. of liquid in bottom of the well, which must have entered the wellbore through the open hole section above the shale. The liquid, later found to be oil, while creating an unnecessary back pressure of the shale, probably caused reservoir skin damage which could account for the poor producing performance of this well. A wellbore diagram, Figure 2, illustrates the downhole situation prior to cleanout of the rubble from the original shot hole.

Initial cleanout operations were begun in mid-March, 1977. Approximately two barrels of light green oil, heavy oil and grease-like substance were recovered from the well by venting and swabbing operations. Gas flow rates, as measured to atmosphere with a pitot tube-manometer after the oil was recovered, varied from 60 to 125 MCFPD. Gas production ceased almost immediately when the packer and tubing were pulled from the well. Evidently water had been leaking through the casing for some time and filled the annulus above the packer. Thus, when the packer released, the water fell to the bottom and halted all gas flow. The shale continued caving in the hole at such high rates that the hole began to fill up in spite of drilling and bailing efforts. In fact, after five days, the hole actually filled up 213 feet to 2877 feet.

Water flow increased from 20 to 70 gallons per day and caused continual sluffing from the formation wall. Cavings were cleaned out to 3030 ft., some 230 ft. above the original TD, and efforts were commenced to halt or reduce the leaks by squeeze cementing and tightening the casing. These efforts failed and water influx actually increased to 240 gallons a day through holes in the casing. The water influx was finally halted by running a full 7" x 5 1/2" tapered liner inside the old casing and cementing it in place.

Cleanout was accomplished using 5" tools. Some sluffing still occurred until a sodium silicate solution was spotted in the well at regular intervals. By June 23 the well was cleaned out to 3244 ft, which, according to the original drilling records, was 14 feet below the base of shale.

The GR logging tool picked up two "hot spots" at 3218 feet to 3196 feet and 2900 feet to 2892 feet, which tend to be characteristic of the Devonian Shale; while the dual pad caliper tool indicated the diameter of the open hole below the 5-1/2 inch liner ranged from just under 7 inches to in excess of 18 inches. The temperature log showed cooling effects at approximately 2835 feet, 2985 feet and 3070 feet, indicating possible gas entry points into the wellbore.

Following interpretation of the logs, preparation for the production and reservoir tests began by running the production equipment in the well. A Lynes PI inflatable packer was run into the well on 2-3/8 inch steel tubing and set in the open hole at 2627 feet (tubing measurement). Figure 3 illustrates the existing downhole configuration of the well as it is prepared for the testing.

After the tubing was landed in the wellhead on June 30, the gas flowing through the tubing was meausred with a 2-inch pitot gauge at 60 MCFPD. The well was shut-in overnight and the surface tubing pressure increased to 150 psig in 13½ hours. The well pressure was bled down and a bottom hole pressure gauge was run into the well and positioned at 3150'. The well was shut in on July 1 for an extended pressure buildup test. These data are tabulated in Table 2.

After 40 days of pressure buildup, a 4-point modified isochronal test was run. Selected data from this test is presented in Table 3. Both surface and bottomhole pressure measurements are shown. The well is currently on long term stabilized flow test. The data gained from the pressure buildup, modified isochronal and stabilized flow tests should provide an insight into such reservoir parameters as maximum reservoir pressure, pressure drawdown, gas deliverability, Kh and skin damage effects. These pretreatment parameters would then be compared to similar characteristics obtained after the shale section is subjected to chemical explosive fracturing.

Explosive placement is dictated by the information gained from the logs. Five possible gas zones were indicated by the gamma ray and temperature logs. They are scattered over the entire Devonian Shale section. Hole size can be determined from the caliper log. From the top of the shale to TD the hole diameter varies; 50 feet of hole is 18" or more, 80 feet of hole is between 15" and 18", with 280 feet between 8 and 15 inches (average 11.75"). A 30,000 lb. load of PTC-4 explosive will fill this large borehole and permit simultaneous treatment of all of the indicated gas zones.

This well is scheduled for CEF by the 1st of December 1977. Following treatment of this existing well, two new wells will be drilled to the Devonian Shale in Eastern Kentucky for this program. The locations selected will be governed primarily by the presence of lineaments determined from remote sensing imagery studies prepared by MERC personnel. These two wells will be drilled, logged and completed open hole through the Devonian Shale formation. The actual treatments will be designed to permit injection of a large quantity of the explosive into the formation prior to detonation. Post shot production testing will be carried out before and after rubble removal in order to ascertain the effect of wellbore rubble on gas production.

West Virginia Program (EY-76-C-08-0686

The three wells for this program are located on a 1258 acre parcel of land in Lincoln County, West Virginia, obtained as a farmout from Columbia Gas System. The site is roughly 8 miles west of Branchland, W.Va. The first well 686-1, has been drilled, chemically explosive fractured and is now on production. Two downhole gas-air explosions in the casing during workover operations prevented cleanout of the rubble zone after treatment and almost caused the well to be abandoned. Ray Resources Rig No. 7 moved on location October 8, and it is expected that both wells 686-2 and 686-3 will be drilled and cased by October 21. This site is traversed by many lineaments determined from remote sensing imagery analysis which was used to select the drilling locations. Figure 4 shows the location of the wells relative to the area joint strike data. Also, in this region are several Devonian Shale wells which have been completed with various hydraulic fracturing techniques. Production and flow test data will be used to compare the effectiveness of this chemical explosive fracturing technique.

The location for the first well was prepared in Jan and Feb 1977 during a let up of the severe winter weather experienced in the eastern U.S. Eight days were required by the rotary rig to air drill the Well No. 1 to TD, 3795 ft. Drilling, cementing and casing the well were accomplished using conventional techniques and equipment. The production string consisted of 7", 20 lb. J-55 casing set at 2505 feet and cemented back to 1500 feet. A 6¼" diameter hole extended nearly 1300 feet through various shale sections. No measureable gas show was encountered in the Devonian shale section prior to treatment. The open hole section was logged using gamma ray, compensated density, caliper, induction and neutron tools. Following the logging operation the fiberglass tubing, packer, mixer, dual oxidizer and fuel tubing strings and Command Fire Detonator were run into the well. As a backup to the Command Fire Detonator, a mechanical type 1" O.D. timebomb detonator was run into the well through the tubing using a wireline prior to mixing and injecting the explosive. Refer to Figure 5.

The explosive manufacturing process took place without incident. Oxidizer and fuel were pumped into the well down to the mixer and explosive was manufactured and displaced into the open hole and formation at rates up to 55GPM (620 lb/min.). Wellhead pressure were zero throughout the entire manufacturing process. A total of 29,400 lbs, or roughly 2700 gallons, of PTC-4 explosive was manufactured prior to displacing the explosive from the tubing.

Treated fresh water was employed to displace the wiper plug and explosive from the tubing. Aside from separating the explosive and water, the wiper plug is designed to trigger the Command Fire Detonater when it seats in the baffle located below the packer. However, the plug failed to seat after pumping approximately 200 gallons more water than calculated to reach the baffle. Subsequent investigations indicated the fiberglass tubing had apparently split somewhere above the baffle and below the packer, which permitted the displacing water to escape from the tubing and thus prevented displacement of the plug to the baffle. A sinker bar and wireline was run into the well and encountered the plug about 8' above the baffle. While tagging the plug with the sinker bar, the plug was pushed into the baffle,

which activated the Command Fire Detonator. Detonation of the explosive occurred immediately, trapping the wireline in the tubing. The wireline and debris plugged the tubing and prevented the release of the detonation gases up the tubing.

The wireline and tubing were cut at about 2000 feet and pulled from the well. A rock bit was used to cleanout the hole to about 2080' where a tight spot in the casing was encountered. After pulling the drill string and bit it was noted that the well was producing gas through the vent line. Measurements made using a manometer-type gauge revealed the well was flowing gas at the rate of 265MCFD. The gas was flared to confirm that it was not detonations products which are non-combustible.

Subsequent efforts to mill through the tight spot in the casing using air resulted in two down-hole gas-air explosions and fires. The drill string parted leaving 18 feet of junk (oil jars, bumper jars, subs and tapered mill) in the casing. Gas production declined from 265MCFPD to 133MCFPD after the fire. A 2 3/8" tubing string with a packer were run into the well and set above the junk to complete the well for production.

Flow tests and pressure build up surveys were run after the well was connected to the pipeline. Gas flow rates against pipeline pressure of 20 psi ranged from 18 to 66 MCFPD. The maximum surface pressure reached during the buildup survey was 425 psig which translates to a bottom hole pressure at 3108 feet of 472 psig. Although quantitative analysis of the pressure buildup and drawdown data is not possible due to the debris and junk in the well, production from the well will continue to be monitored and compared to the results achieved on Wells Nos. 686-2 and 686-3.

The 7" casing points in wells Nos. 686-2 and 686-3 will be slightly below the Injun Sand instead of below the Berea Sand as was the case in well No. 686-1. An inflatable packer will be set in the shaley Berea Sand interval to isolate the 1300 foot open hole section in the Devonian Shale for treatment with 30,000 pounds of PTC-4 explosive. Approximately 100 - 150 feet of frac sand and cement will be employed to backup the packer. The high casing points plus use of inflatable packers backed with a solid tamp should eliminate the possibility of damage to the 7" casing when the in situ explosive is detonated. Considering the gas production increase (0 to 265 MCFPD, open flow) realized from treatment of well 686-1 prior to the gas/air explosion, it is believed these well completion changes will enhance greatly the chances of successfully stimulating the shale in this area. In addition, all tubing will be carefully inspected and pressure tested prior to running it in a well to be treated.

Texas Program (EY-76-C-08-0687)

This two well program is to demonstrate the technical and economic feasibility of CEF in the tight lenticular Canyon Sands of the Val Verde-Kerr Basin in Sutton County, Texas. A detailed lineament analysis from LANDSAT and aerial photographic mosiacs, combined with more conventional geological factors, such as contours of the base of the Canyon Sands and elevated structural terrain, were used to define favorable drilling sites. Nearby producing wells were also desired for post stimulation comparisons. Following a review of these data, concurrence on the location was reached by the three participants; Union Oil of California, ERDA and PTC. The well location is some 20 miles southwest of Sonora and is identified as W.E. Sawyer "4" Well No. 1 by Union Oil, but is designated Well No. 687-1 for purposes of contract association.

Drilling was done with air and mist with a rotary unit to 7337 ft. The 7 inch 23 lb casing was set at 5966 ft and the 5 7/8 inch open hole section extends 1371 feet more to TD. Borehole audio tracer survey and differential temperature logs were run. The temperature survey indicated major gas entry regions are at 7150 - 7158 ft and 7188 - 7196 ft, with some gas coming from the bottom of the well. Prestimulation pressure build up and flow tests have been run and are currently being analyzed by Union's Research Department in Brea, California. After being shut in 42 days, the bottom-hole pressure built up to 1380 psig. The gas flow rate stabilized at 12 MCFPD during drawdown tests.

It was originally proposed to treat the entire 1371 foot open hole interval in two stages using a total of 60,000 pounds of explosives. Since the temperatures and acoustical logs show the gas is entering the wellbore near the bottom of the hole, the treatment design has been altered to use 30,000 pounds over the bottom 600 - 800' of open hole.

If the test programs in Kentucky and West Virginia go as scheduled, the PTC rigs could move on this Sutton County well during the first half of 1978. The actual treatment should take between 7 and 10 days to complete, after which the well will be flow tested and cleaned out as necessary to fully evaluate the treatment.

CONCLUSIONS AND SCHEDULE

Although progress in conducting field tests under these three contracts has not been as rapid as anticipated, the results obtained in treating the first well in West Virginia indicate CEF can be an effective means of stimulating tight gas wells completed in the Devonian Shale if mechanical and placement problems can be solved. Problems associated with the test on well 686-1 have been analyzed and steps are being taken to prevent reoccurence on future tests.

Cleanout and remedial techniques employed in preparing the previously shot well in Kentucky could point the way to preparing other similarly completed shot wells if CEF is successful in revitalizing the gas production. The use of a cable tool rig instead of an air rotary rig for this type of work is dictated by the mountainous terrain and small drill site locations of these old wells.

Modifications are currently being made in PTC's downhole equipment as a result of a premature detonation in a 7500 foot deep oil well in south Texas. That particular program is geared to evaluating CEF in the Austin Chalk Formation and is being carried out under a separate industry contract. While these changes are aimed at preventing similar early detonations in these deep, high temperature wells, the modifications should improve the PTC process and will be employed in the shallower Devonian Shale wells. It is anticipated that these equipment modifications will be completed and field tested in a well by the first of November.

Field testing of the PTC CEF process is expected to be underway by the first week of November. Wells 686-2 and 686-3 in Lincoln County, West Virginia are expected to be treated by the middle of November. The PTC rigs will then move to Perry County, Kentucky to test the process in well 685-1 by the first of December. The results of these tests, as well as performance of the revised downhole equipment, will be evaluated prior to moving the rigs to Texas for treatment of the 7500 foot deep well in Sutton County. Allowing for these evaluations and inclement weather, it is expected that well 687-1 will not be treated before March 1978.

ACKNOWLEDGEMENTS

We wish to thank the many individuals and organizations who have contributed their time, talent and means to this new approach to explosive stimulation. Particularly we thank C.A. Komar of ERDA, Morgantown, for his positive assistance in technical direction, especially his timely decisions in response to field problems which occurred during cleanout and drilling operations. Also from ERDA, Morgantown, Al Yost has assisted us in setting up and evaluating the flow, buildup and production tests. We also extend our appreciation to R.T.Stearns of ERDA, Las Vegas, for his capable assistance in administration of the contracts and industry subcontracts. From industry, we wish to thank Ernest B. Jenkins and Dewayne Dials of Kentucky West Virginia Gas Company for their counsel and cooperation in the eastern Kentucky program. John Foster, Walter Chapman and Paul Hyde, and John Hennings of Columbia Gas Transmission Company have assisted in many ways, from program planning to the day-to-day supply and maintenance activities at the location in West Virginia. Also Bob Forrest, Lou Cook and Gordon Owens of Columbia Research, have assisted with the lineament analyses and provided valuable criticism of the process following treatment of well 686-1. From Union Oil, we are indebted to Steve Pye, John Hawkins and Jimmy Hughes, whose efforts in getting the Texas program underway are appreciated. Special recognition is also due Walter Fillippone, Union Oil of California, Clyde Pierce, ERDA Morgantown, and Gordon Owens, Columbia Gas System for their interpretation of ERTS and aerial photographs used in the preparation of lineament maps.

Finally, we appreciate the efforts of the many unnamed suppliers, engineers, drillers and field hands, whose interest, dedication and work have brought the program this far.

TABLE 1

EXPLOSIVE FRACTURING EIGHT-WELL PROGRAM

Contract No.	No. of Wells New	No. of Wells Existing	Formation	Depth (Ft.)	Location	Industry Participants*
EY-76-C-08-0685	2	1	Devonian Shale	2800-3500	Eastern Ky.	PTC/KWV
EY-76-C-08-0686	3	0	Devonian Shale	2500-3800	Lincoln Co., WV	PTC/CGS
EY-76-C-08-0687	2	0	Canyon Sands	6000-7500	Sutton Co., TX	PTC/Union

*PTC is Petroleum Technology Corporation
KWV is Kentucky West Virginia Gas Company
CGS is Columbia Gas System
Union is Union Oil Company of California

TABLE 2

WELL 6810 BOTTOMHOLE PRESSURE DATA

Time (Days)	Pressure (psi)
0	108
.1	138
.2	157
.3	170
.4	182
.5	191
.7	209
1.0	224
1.5	248
2.0	267
2.5	280
3.0	293
4.0	310
5.0	326
6.0	341
8.0	357
10.0	373
14.0	387
17.0	397
21.0	407
28.0	420
33.0	432
40.0	436

TABLE 3

WELL 6810 FLOW TEST RESULTS

Time (Hrs.)	Well Condition	Flow Rate (MCFPD)	Bottom Hole Pressure (psig)	Surface Pressure (psig)
0	Shut in	--	435.7	410
0	Flowing	42.94	435.7	410
3	Flowing	38.89	399.3	370
3	Shut in	--	399.3	370
6	Shut in	--	419.6	390
6	Flowing	90.70	419.6	390
9	Flowing	72.29	336.7	310
9	Shut in	--	336.7	310
12	Shut in	--	381.1	328
12	Flowing	143.29	381.1	328
15	Flowing	106.50	246.7	240
15	Shut in	--	246.7	240
18	Shut in	--	322.7	290
18	Flowing	292.57	322.7	290
21	Flowing	119.73	115.3	110
21	Shut in	--	115.3	110

TYPICAL EQUIPMENT DEPLOYMENT AT WELLSITE

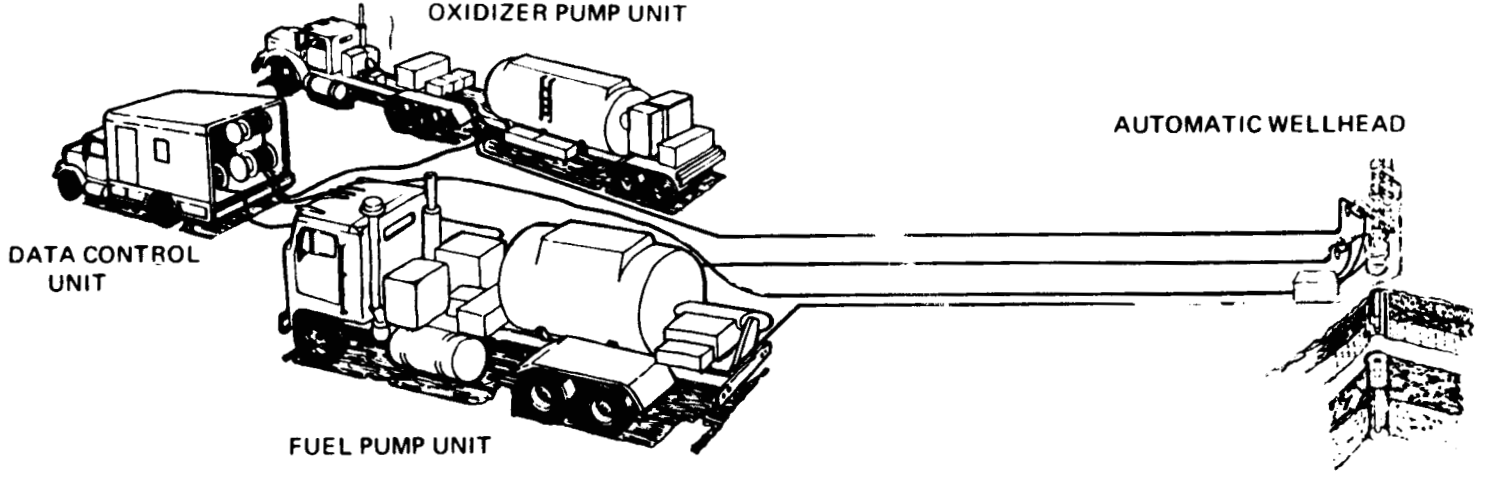

IN THE ASTRO-FLOW II PROCESS, THE CHEMICALS THAT FORM THE EXPLOSIVE ARE TRANSPORTED AS TWO NONDETONABLE COMPONENTS -- A FUEL AND AN OXIDIZER. THE COMPONENTS ARE PUMPED INTO THE WELL USING THE FUEL AND OXIDIZER PUMP UNITS AND BLENDED TOGETHER DOWNHOLE TO FORM THE EXPLOSIVE. IN THIS MANNER, SURFACE FACILITIES AND PERSONNEL ARE NOT EXPOSED TO EXPLOSIVE HAZARDS. BOTH PUMPING UNITS, AS WELL AS THE AUTOMATIC WELLHEAD ASSEMBLY, ARE CONTROLLED FROM THE DATA CONTROL UNIT. ONCE THE EXPLOSIVE IS IN PLACE AT THE BOTTOM OF THE WELL, IT IS DETONATED TO STIMULATE THE PRODUCTION OF THE WELL.

FIGURE 1

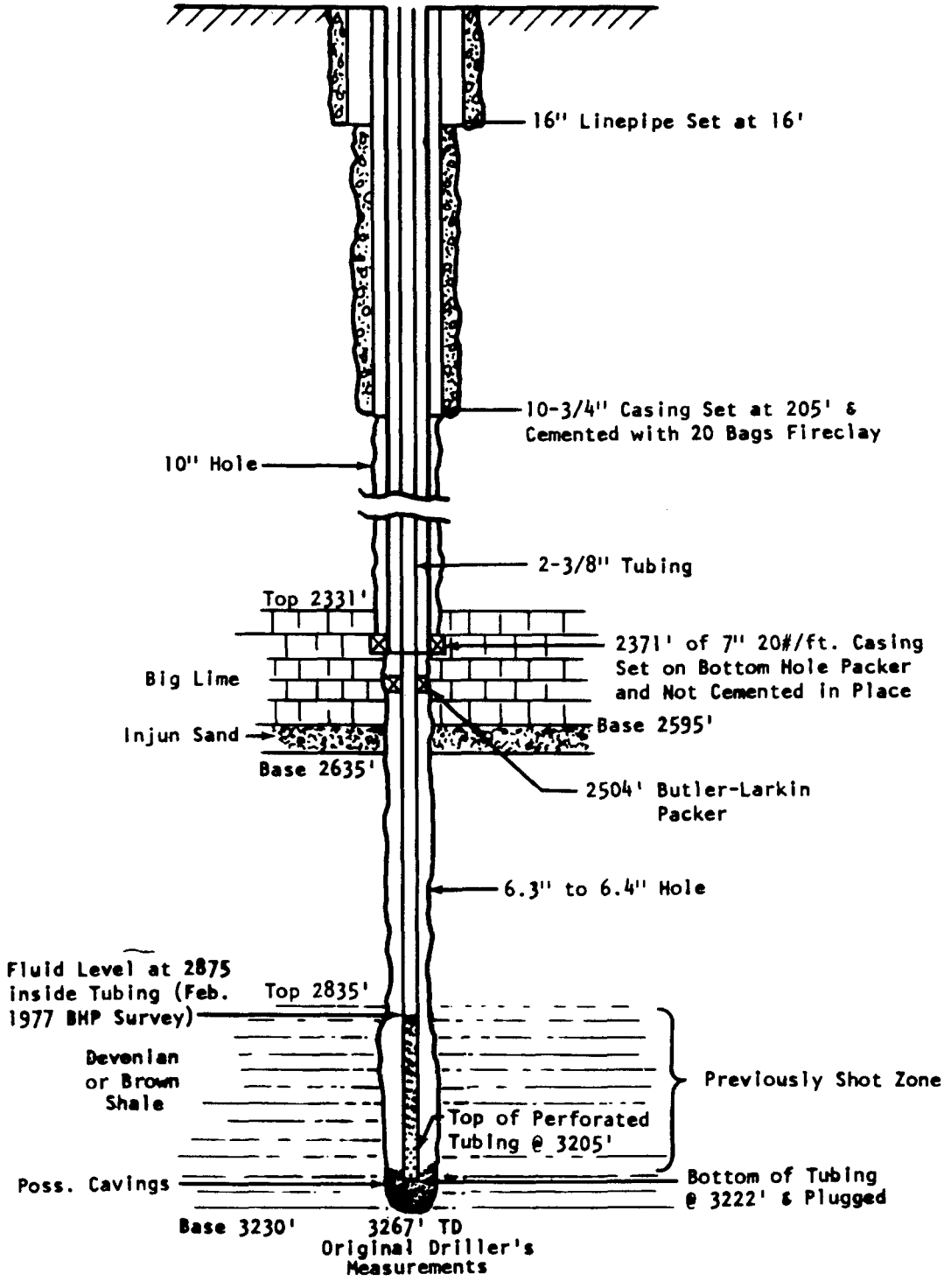

FIGURE 2

WELL NO. 685-1 PERRY COUNTY, KENTUCKY

WELL BORE DIAGRAM PRIOR TO WORKOVER

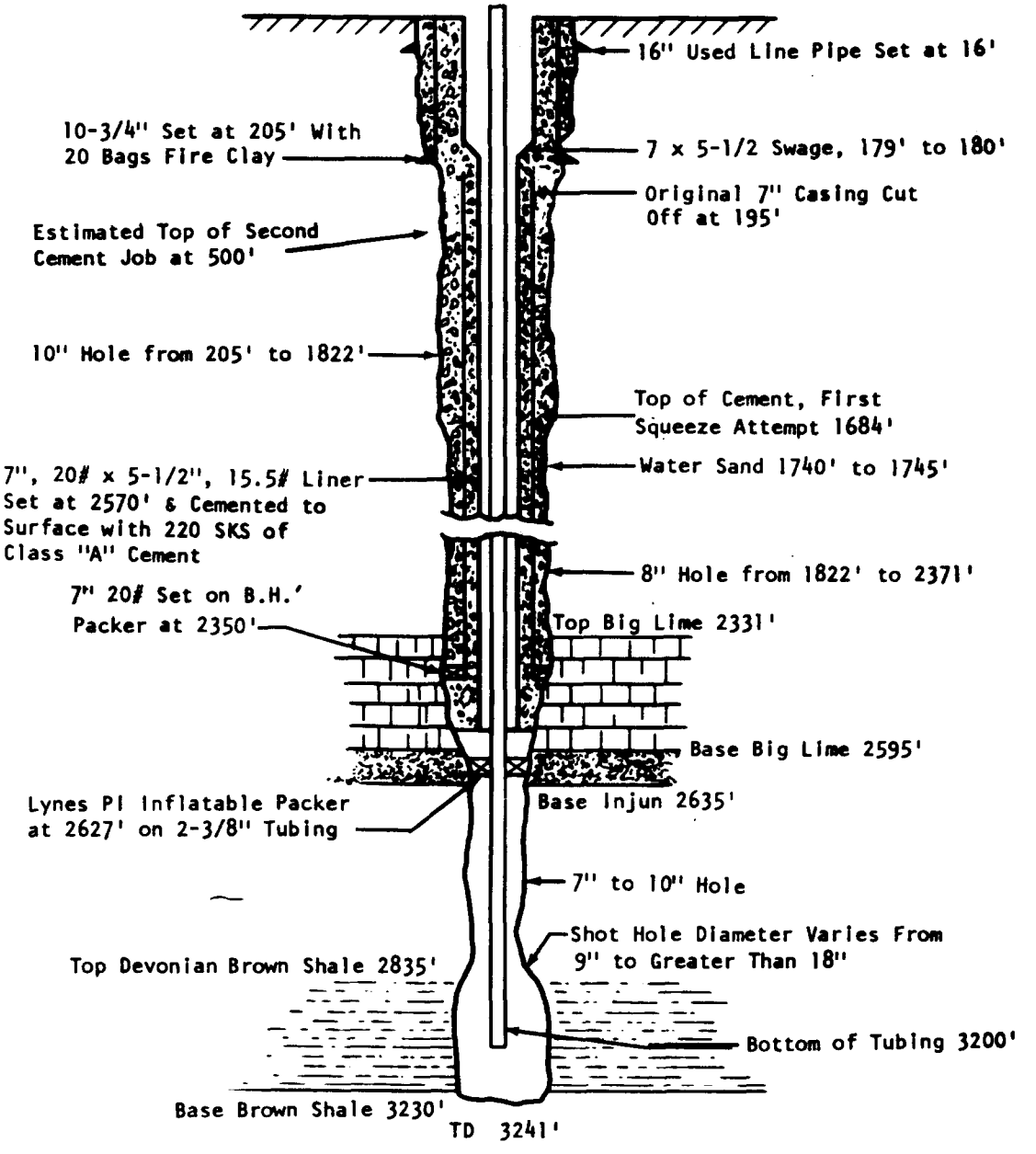

FIGURE 3

WELL NO. 685-1 PERRY COUNTY, KENTUCKY
COMPLETED FOR PRODUCTION TESTING

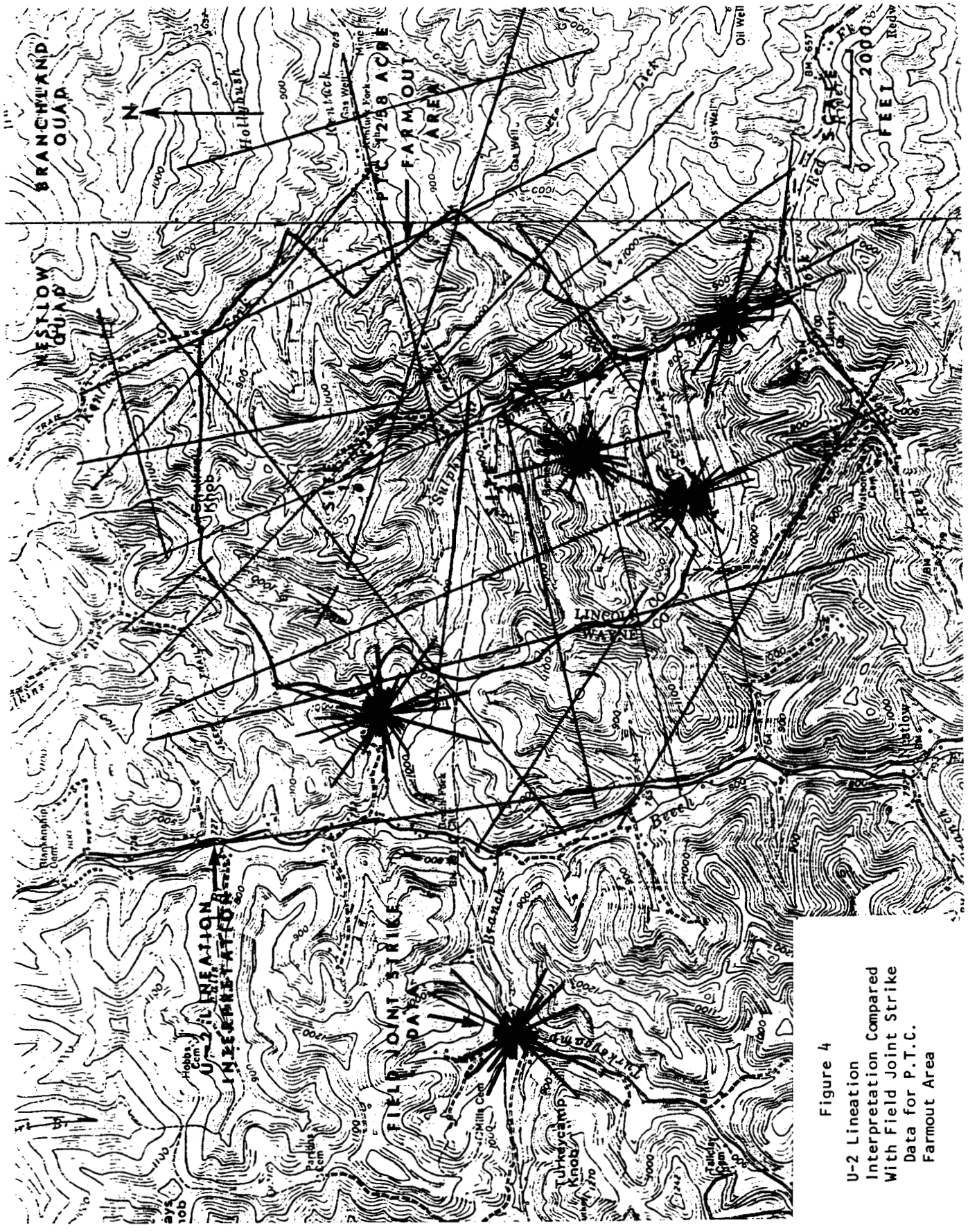

Figure 4
U-2 Lineation
Interpretation Compared
With Field Joint Strike
Data for P.T.C.
Farmout Area

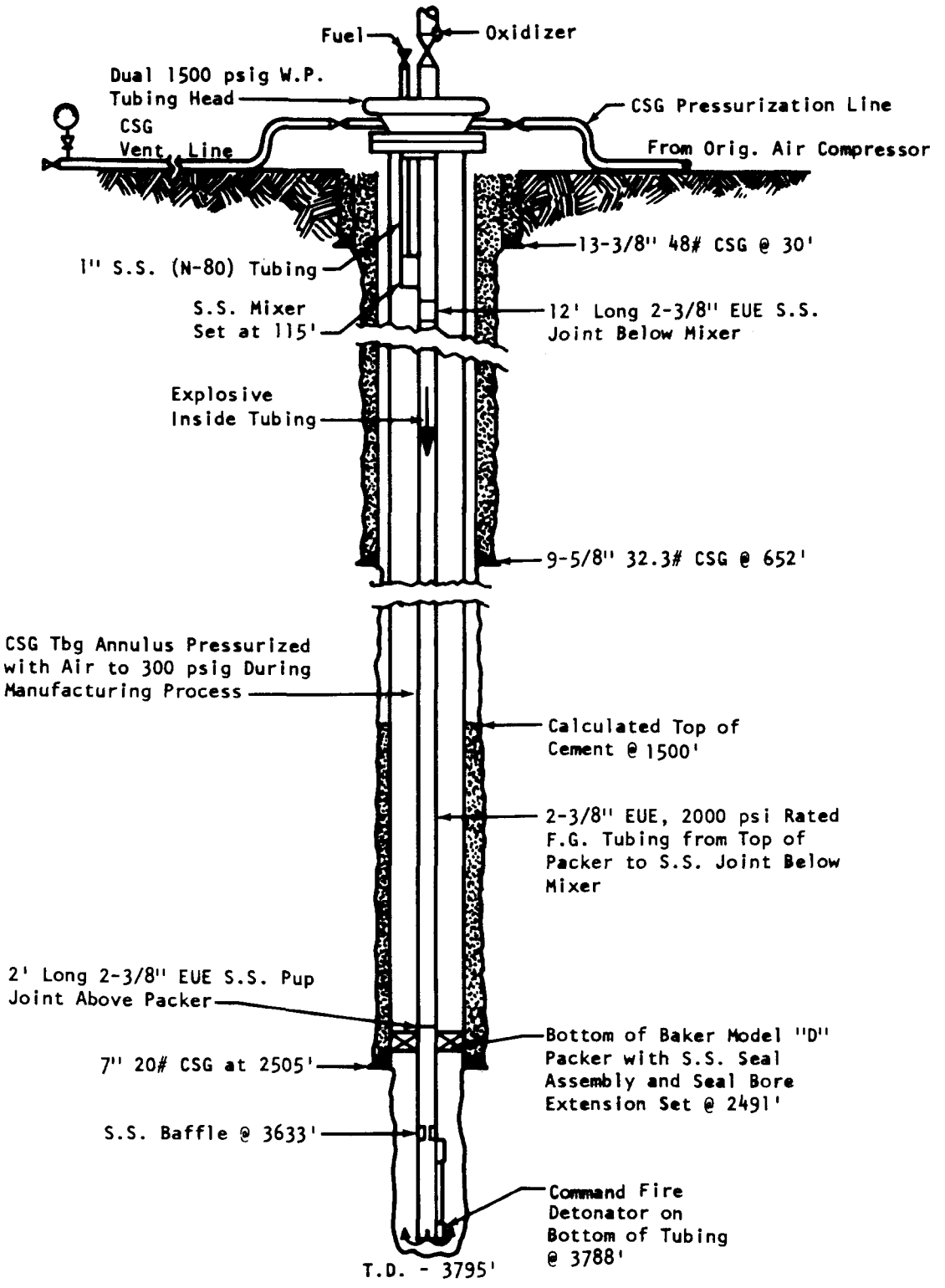

FIG.5
WELLBORE DIAGRAM OF
WELL NO.686-1 WITH TREATING
EQUIPMENT IN PLACE.
LINCOLN COUNTY, WEST VA.

DYNAMIC PROPERTIES OF DEVONIAN SHALES

by

W. J. Carter
B. W. Olinger
Los Alamos Scientific Laboratory
Los Alamos, N.M. 87545

ABSTRACT

Successful prediction and optimization of explosive effects in geologic materials requires a thorough knowledge of the constitutive relations governing the rock response to impulsive loading. Such constitutive relations must include descriptions of both wave propagation and fracture phenomena under dynamic stress. The initial phase of our program therefore has been directed toward acquiring these basic data. Here, some of the dynamic properties of gas shales and the techniques used to determine them are discussed.

ELASTIC PROPERTIES

The first step towards understanding both static and dynamic stress response is determination of the elastic constants. The samples whose dynamic properties are presented here were obtained from two pieces of core from Columbia Gas Well No. 20402, one from approximately 1040 m and the other from 1092 m below the surface. X-ray diffraction patterns showed both to be common illite shales, where the composition is very fine silica or quartz grains and a minor amount of anhydrous clay minerals. The densities of the two pieces were 2.7 g/cm^3 (1040 m in depth) and 2.4 g/cm^3 (1093 m). These densities span a commonly accepted average bulk density of 2.55 g/cm^3 for eastern gas shales.

The elastic properties of the samples investigated appear to have transversely isotropic symmetry. This means that there is an elastic symmetry axis of rotation perpendicular to the bedding and an elastic axis of two-fold symmetry in the bedding planes.

The samples were prepared for sound speed measurements by cutting them into plates 30 to 60 mm in diameter and 2.0- to 7.5-mm-thick at angles 0°, 45°, and 90° to the bedding. Densities were determined by immersion. The sound speeds were determined from the difference in transit time for an ultrasonic pulse traversing an aluminum plate and the combination of the same aluminum plate and a sample plate. Because of interferences of the ultrasonic pulses at the shale bedding interfaces, only first pulse arrivals were measured. Specifically, an aluminum plate is set between the transmitting and receiving 22-mm-diameter transducers (10 MHz x-cut quartz for longitudinal modes and 5 MHz y-cut quartz for shear modes). The first signal arrival through the plate is set to a fiducial on the screen of a Tektronix 454 oscilloscope. The received pulse is amplified by a Tektronix 461A wideband amplifier. The gas shale specimen plate is placed between the transducers along with the aluminum plate. A suitable oil or resin is used to bond all sample-plate-transducer interfaces. The first signal arrival is again reset to the fiducial using the delay-time-multiplier dial of the oscilloscope. The delay or time difference was determined using a time interval meter of nanosecond accuracy and the two gate pulses generated by the oscilloscopes.

We have assumed that the elastic wave velocities are a linear function of density over the range studied here. The linear equations for the five different propagation modes measured are listed below with a description of each.

$$V_1 = +1.679 + 1.277\ \rho \quad (1)$$

V_1 is the longitudinal velocity directed parallel to the shale bedding.

$$V_3 = -1.003 + 1.808\ \rho \quad (2)$$

V_3 is the longitudinal velocity directed perpendicular to the shale bedding.

$$V_4 = -1.332 + 1.438\ \rho \quad (3)$$

V_4 is both the shear velocity directed perpendicular to the bedding of the shale, and the shear velocity directed parallel to the bedding with particle motion perpendicular to the bedding.

$$V_5 = +1.151 + 1.245\ \rho \quad (4)$$

V_5 is a quasi-longitudinal velocity directed at 45° to the bedding.

$$V_6 = -1.416 + 0.627\ \rho \quad (5)$$

V_6 is the shear velocity directed parallel to the bedding with the particle motion also parallel to the bedding.

The velocities are converted to the elastic moduli of a transverse isotropic solid by the following relations:

$$C_{11} = \rho V_1^2$$

$$C_{33} = \rho V_3^2$$

$$C_{44} = \rho V_4^2$$

$$C_{66} = \rho V_6^2$$

$$C_{12} = C_{11} - 2C_{66}$$

$$C_{13} = [(.5C_{11} + .5C_{44} - \rho V_5^2)(.5C_{33} + .5C_{44} - \rho V_5^2)/.25]^{1/2} - C_{44}$$

$$B \text{ (bulk modulus)} = (C_{33} + 2C_{13})^2/(C_{33} + 2C_{11} + 2C_{12} + 4C_{13}).$$

The elastic moduli and bulk sound speed for the two density shales studied here and the average bulk density shale are listed in Table 1.

DYNAMIC TENSILE STRENGTHS

Divergent propagation of a shock wave in either spherical or cylindrical symmetry results in an initial positive axial compression which rapidly converts into tension. This dynamic tensile hoop stress is a major cause of radial fracture in the surrounding rock. In addition, spalling or slabbing occurs when the rarefaction or release wave from a free surface and the rarefaction wave following the shock interact and form a spreading tension wave. Thus, the dynamic tensile strength of rock is an important property to be determined when attempting to predict the fracture pattern of a rock. Here a technique is described for determining the dynamic tensile strength of materials and the results of studies using this technique for gas shales are presented.

The technique involves impacting samples of known shock impedance and bedding orientation with a thin driver of known shock impedance, thus generating a well-defined shock in the sample. The impedance of the impactor plate is chosen so that the interface between the impactor and the sample separate after passage of the rarefaction wave from the rear free surface of the impactor. The rarefactions from the impact surface of the sample and the front free surface interact in the middle region of the samples creating a tension wave. The target plate in which the shale samples are mounted is recovered and the shales are removed and examined for spall. The experimental configuration is shown and described in Fig. 1.

The impactor plate used is polymethylmethacrylate (PMMA), ρ_o = 1.186, its thickness chosen to cause interaction of the rarefactions midway through the sample. Since the shock velocities in shales are within a few percent of the elastic longitudinal velocities at these stress levels, it was assumed the stress induced in the gas shale samples is approximately

$$P = \rho\, C_L\, u_p \qquad 6)$$

where ρ is the density of the shale, C_L is the measured elastic longitudinal velocity, and u_p is the particle or interface velocity between the PMMA and shale. Since the stress levels were only of the order of 100 MPa (0.1 GPa), the stress induced in the PMMA impact plate is approximately

$$P = \rho\, C_B\, (u_D - u_p) \qquad 7)$$

where ρ is the density of the PMMA, C_B is the bulk elastic velocity as determined from the Hugoniot (C_B = 2.598 km/s), u_D is the particle or interface velocity before impact and u_p is the particle or interface velocity. At impact, both the stress and the interface velocity in the gas shale and the PMMA at the interface has to be identical. If the shock wave in the shale sample is not overtaken by the release wave, and the thickness of the impact plate is such as to prevent this, the magnitude of the maximum tension induced in the gas shale should nearly equal the maximum stress induced in the gas shale.

$$\text{Tension} = -u_D\, \frac{(\rho\, C_L)_s\, (\rho\, C_B)_p}{(\rho\, C_L)_s\, (\rho\, C_B)_p} \qquad 8)$$

where the s subscript denotes gas shale and p denotes PMMA. Both the density and elastic longitudinal velocity of each shale sample are determined before each impact experiment, and the impact plate velocity is determined during the experiment (Fig. 1), thus the tension induced in each sample can be readily calculated.

The diagnosis of an impact experiment is straightforward. The target plate is recovered and each shale is examined for spalling. It was found that shales having a density of 2.69 g/cm^3 would not spall under tension as high as 66 MPa (0.66 kbars) if the tension waves propagated along the bedding, but shales of a similar density, 2.57 g/cm^3, spalled as low as 45 MPa (0.45 kbars) if the tension waves propagated perpendicular to the bedding. For shales having a density of 2.40 g/cm^3, the tensile strengths were less than 40 MPa for both propagation directions. The stress rates involved in these experiments are of the order of 1 GPa/μs (10 kbars/μs) and regions under tension remain so for only about 2 μs if they do not spall. Experiments involving lower stress rates and longer tension durations would find the tensile strengths of the shales to be smaller.

RESPONSE TO PLANE STRESS IMPULSES

Properties of gas shales in response to dynamic stress can best be determined from the analysis of the degradation of finite stress impulses as they pass through the shales. Various techniques and analyses are currently used by various laboratories, including those originating at the Stanford Research Institute and the Sandia Laboratories, Albuquerque.

The technique used here is to measure the stress history of an impulse at several depths in a sample. The sample assembly consists of a stack of four plates, all 40-mm in diameter, of thicknesses 2, 4.5, 4.5, and 5 mm respectively. The impactor plate is usually 3-mm-thick. The density, elastic properties, and orientation of all plates are matched. Between the plates of the sample assembly are 50-ohm grids of 0.01-mm-thick Manganin foil covering an area of 40 mm^2 in the central region. The resistance of the grids are well defined as a function of stress under impact conditions. The resistance is deduced from the voltage generated at the null point of a pulsed Wheatstone bridge caused by the change in resistance of the manganin grid. The sample-manganin gage stack is placed in a target plate and surrounded by velocity pins. The entire assembly looks much like that in Fig. 1 except that the 6 small samples are replaced by the stack, and the PMMA plate mounted on the hollowed aluminum projectile is replaced with copper for high stress levels and aluminum for low stress levels.

In the upper left diagram of Fig. 2 is a stress history typical of those recorded in a number of experiments on the gas shales. The differences between the experiments are the orientation of the bedding to the direction of planar shock propagation, the densities, and the stress levels. The response to the shock loading and unloading was calculated using the computer code GUINSY2.[1] The analysis requires the stress histories, a correlation of regions on the stress profiles, the initial

density of the shales and the initial gage locations. From the analysis the specific volume, the particle velocity, and internal energy of the shales are correlated with the stress as a function of time at each location. In the remaining sections of the figure is plotted particle velocity as a function of the loading and unloading stress, strain as a function of the loading and unloading stress, and the loading and unloading wave velocity as a function of particle velocity.

HUGONIOTS OF EASTERN GAS SHALES

Response of the shales to large amplitude shocks, between 10 and 100 GPa, was determined from simultaneous measurements of the shock wave velocities through shale samples and through a standard material whose Hugoniot is well known. From these measured shock velocities, the mass or particle velocities in the shales are deduced. The experimental technique is described elsewhere [2]by the impedance match method.

The equilibrium Hugoniot equation of state is completely defined by knowing only the initial density (ρ_o), the shock velocity (u_s), and the particle velocity (u_p). The pressure (P), compression ($1-V/V_o$), and change in internal energy (ΔE) are derived from the above three parameters using the conservation relations

$$P = \rho_o u_s u_p \tag{9}$$

$$V/V_o = (u_s - u_p)/u_s \tag{10}$$

$$\Delta E = P(1-V/V_o)/2\rho_o \tag{11}$$

The u_s, u_p locus for material not undergoing transitions in structure or bonding is linear,

$$u_s = c + s\, u_p. \tag{12}$$

The data such as plotted in Fig. 3 for a typical shale can be fit satisfactorily with two linear fits with a break between them at approximately u_s = 5.75 km/s. This indicates that there is a discrete reduction in the volumes of the shales at the pressure associated with that shock velocity, 20 GPa. The volume reduction at that pressure between the two Hugoniots is 6% for the 2.4 g/cm^3 shales and 7% for the higher density shales. Since the major component of the Devonian shales is quartz (30% to 60% by volume), the change in volume can probably be attributed to the α-quartz to stishovite phase transformation. The transition pressure found here is 6 to 10 GPa above the quartz-stishovite transition pressure extrapolated from high temperature, static high pressure data. There are several explanations for this difference. The first is that the quartz, floating in a matrix of kerogen and other minerals, requires time to reach an equilibrium pressure and to transform, resulting in a shock wave immediately followed by a transition relaxation wave. Below 20 GPa the shock wave is not overrun by the relaxation wave for sample thicknesses used here. The other explanation is that because of shock heating caused by pore collapse and compression of the kerogen, the normal equilibrium transition pressure for quartz is shifted to higher pressures. The knowledge of which explanation is correct may be important since the first explanation would mean that the shales may be able to absorb large amounts of energy at pressures as low as 10 to 14 GPa.

In addition to lack of equilibrium of the phase transformation process, the lower phase Hugoniots themselves are also not at equilibrium. For equilibrium, the Hugoniot intercept of the lower phase should also be the bulk sound speed. Comparing the bulk sound speed values in Table I with the intercepts one finds the intercepts to have much higher values. The Hugoniots determined for these shales at low pressures are a combination of equilibrium compressions of the shale constituents and strong elastic components. The elastic influence is evident in a comparison of the longitudinal elastic wave velocities of the higher density shales and their u_s, u_p intercepts.

The high pressure Hugoniots such as the upper linear u_s, u_p fit in Fig. 3 all agree well. However, all the data seem to show systematic upward curvature. This probably indicates transitions in one or more of the minor components of the shales masked by the monotonic compressions of the remainder of the components.

REFERENCES

1. Seaman, L., Lagrangian analysis for multiple stress or velocity gages in attenuating waves, J. Appl. Phys. 45, 4303-4314, 1974.

2. McQueen, R. G., Marsh, S. P., and Fritz, J. N., Hugoniot equation of state of twelve rocks, J. Geophys. Res. 72, 4999-5036, 1967.

TABLE I

ELASTIC MODULI OF EASTERN GAS SHALE

Density (Mg/m^3)	2.40	2.55	2.70
C_{11} (GPa)	54	62	71
C_{33} (GPa)	26	33	41
C_{44} (GPa)	11	14	18
C_{66} (GPa)	20	23	26
C_{12} (GPa)	13	16	19
C_{13} (GPa)	17	17	16
Bulk Modulus (GPa)	16	17	18
Bulk Sound Speed (km/s)	2.60	2.61	2.61

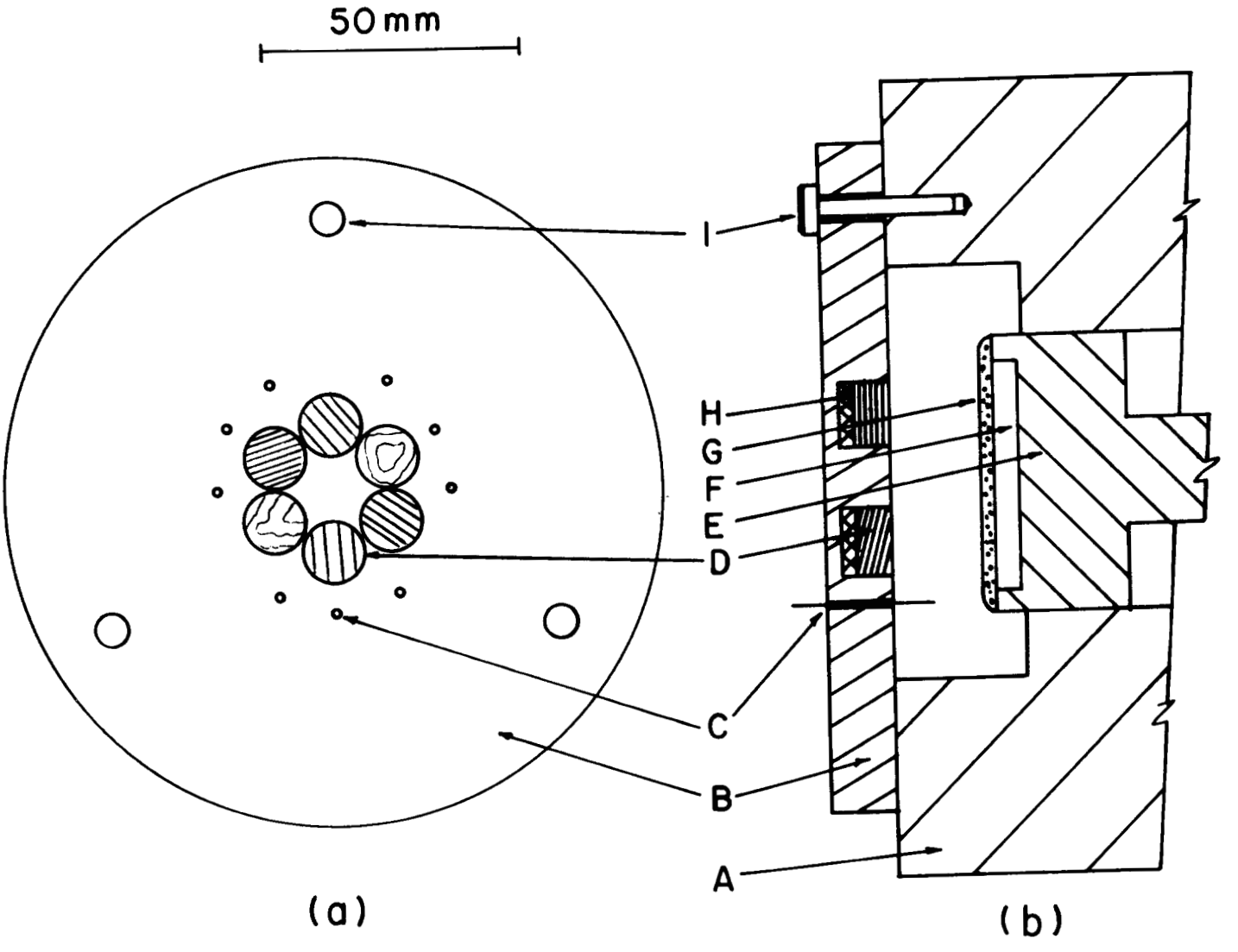

Fig. 1. A front view of a target plate (a) and a cross-sectional view of an impact experiment (b). The view, (a), shows the arrangement of the shale samples in the target plate, machined from Al. Six samples, D, of different densities and orientations are mounted in the target plate, B. Each sample is backed with low density (0.015 g/cm^3) plastic foam, H, to facilitate mounting the specimens' impact surfaces flush with the target plate's surface. The specimens are held in the plate with a thin layer of epoxy. Shorting pins, C, of various lengths are used to determine the velocity of the impact plate, G. The front surface of the impact plate is covered with a 0.01 mm thick Al foil shorted to the projectile, E. A pulse is generated on a repetative time-marked oscilloscope sweep as each charged pin is shorted. The muzzle of the 3 m long, high pressure gas gun used to drive the projectile is labeled A, the target plate mounting screws are labeled I, and the unsupported area behind the impact plate is labeled F.

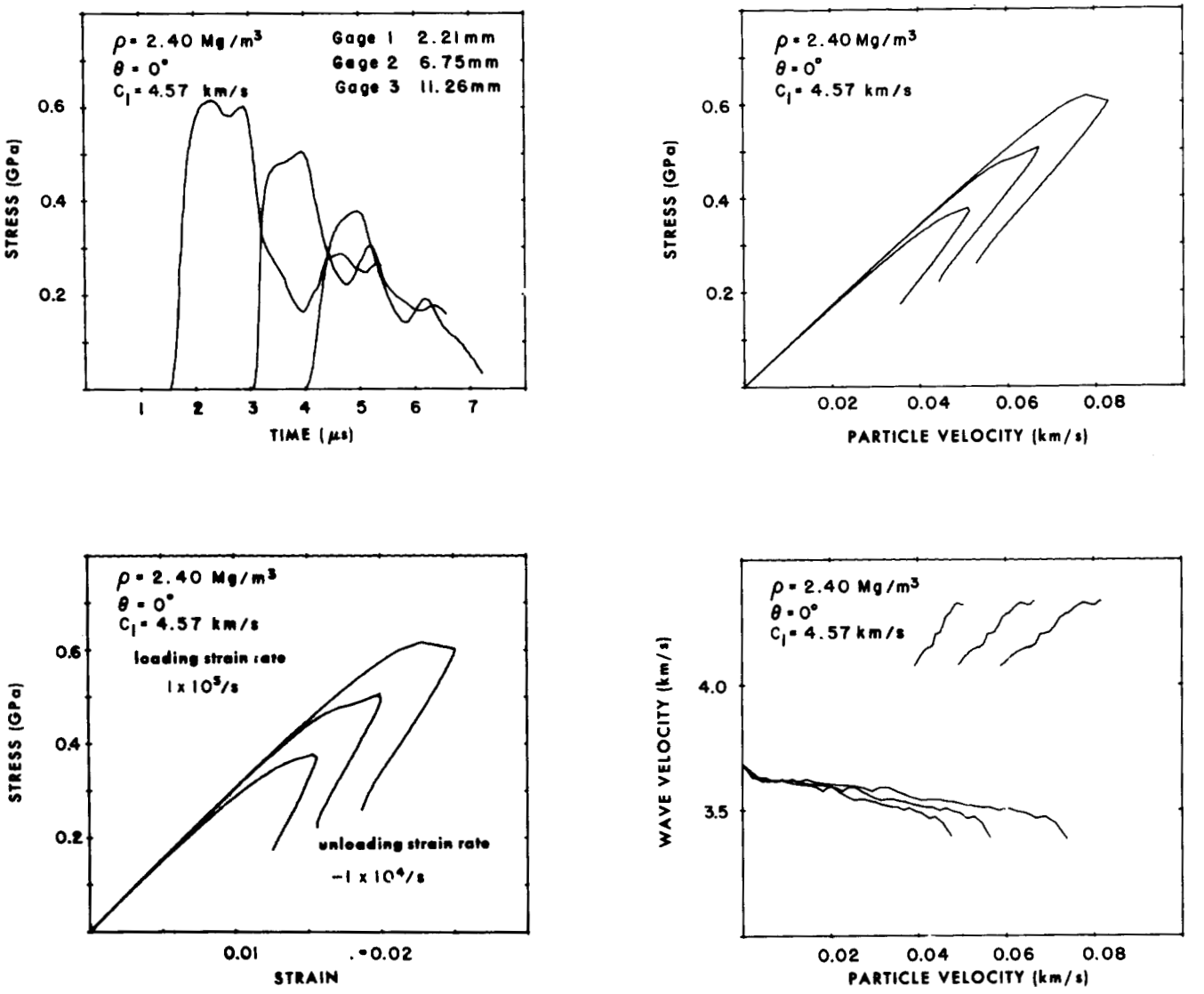

Fig. 2. Response of gas shale (ρ = 2.40 Mg/m^3, θ = 0°, C_L = 4.57 Km/s) to low stress planar shock loading and unloading.

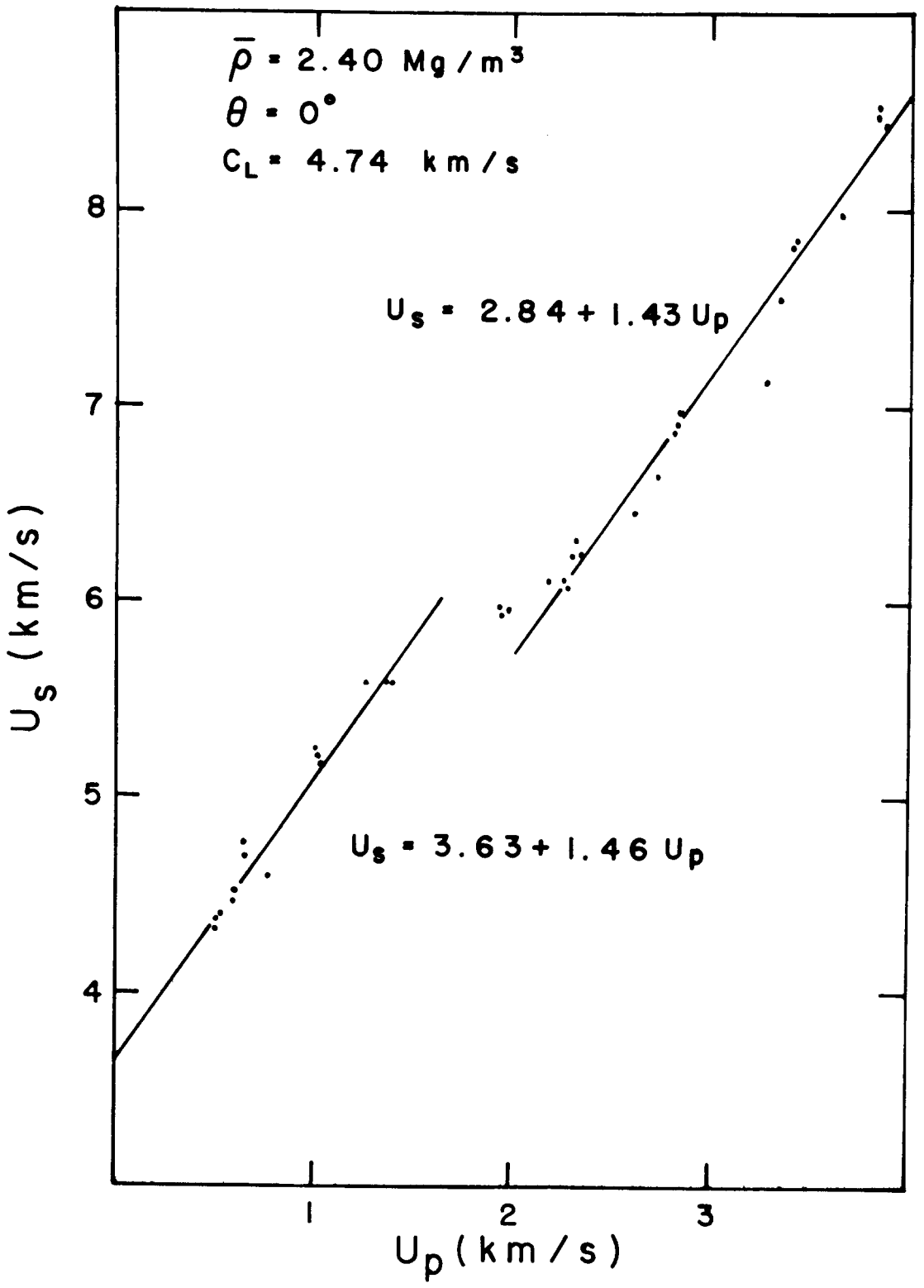

Fig. 3. Hugoniot of gas shale (ρ = 2.40 Mg/m^3, θ = 0°, C_L = 4.74 Km/s) to 80 GPa.

NOVEL FRACTURING TREATMENTS IN THE DEVONIAN SHALE

by

Stephen P. Cremean, Columbia Gas System Service Corporation

ABSTRACT

COLUMBIA GAS, IN TWO PROGRAMS BEING CONDUCTED IN CONJUNCTION WITH THE U.S. ENERGY RESEARCH AND DEVELOPMENT ADMINISTRATION (USERDA), IS CURRENTLY INVESTIGATING THE TECHNICAL AND ECONOMIC EFFECTIVENESS OF MASSIVE HYDRAULIC FRACTURING (MHF) AND CRYOGENIC FRACTURING TECHNIQUES FOR ENHANCED GAS RECOVERY IN THE UPPER DEVONIAN SHALES OF THE EASTERN UNITED STATES.

THREE SHALE WELLS TO BE MASSIVELY FRACED UNDER ERDA CONTRACT NO. E(46-1)-8014 ARE LOCATED IN A 5,000 ACRE UNDEVELOPED TRACT IN WESTERN LINCOLN COUNTY, WEST VIRGINIA. IN EACH OF THE THREE WELLS, SELECTED WITH REMOTE SENSING IMAGERY FOR PROXIMITY TO SURFACE FEATURES (LINEAMENTS), THE TOTAL DEPTH ENCOMPASSES THE ENTIRE UPPER DEVONIAN SHALE; A SEQUENCE WHICH CONTAINS FOUR PRIMARY ZONES OF INTEREST. THE SCOPE OF THIS INVESTIGATION IS TO INDIVIDUALLY STIMULATE THESE TWELVE ZONES OF INTEREST WITH VARIOUS MHF TECHNIQUES. SINCE INCEPTION, SIX MHF STIMULATION TREATMENTS HAVE BEEN PERFORMED USING FOAM AND MODIFIED WATER IN TWO OF THE WELLS. THE THIRD WELL IS BEING PRESERVED TO UTILIZE INFORMATION LEARNED FROM THE FIRST TWO.

FOUR SHALE WELLS TO BE CRYOGENICALLY FRACED UNDER ERDA CONTRACT NO. EF-76-C-05-5303 ARE LOCATED IN MARTIN COUNTY, KENTUCKY (2 WELLS), WISE COUNTY, VIRGINIA (1 WELL), AND TRUMBULL COUNTY, OHIO (1 WELL). IN THE FIRST THREE WELLS, SELECTED WITH REMOTE SENSING IMAGERY, THE TOTAL DEPTH ENCOMPASSES THE ENTIRE UPPER DEVONIAN SHALE; A SEQUENCE WHICH CONTAINS FOUR PRIMARY ZONES OF INTEREST IN THE AREAS STUDIED. TWO ZONES OF INTEREST WILL BE INDIVIDUALLY FRACTURED USING CRYOGENIC FLUIDS IN EACH OF THESE WELLS. THE FOURTH WELL WAS CHOSEN TO TEST THE TECHNICAL AND ECONOMICAL FEASIBILITY OF STIMULATING THE SHALE IN A WELL CURRENTLY PRODUCING FROM A DEEPER HORIZON. THERE ARE FOUR ZONES OF INTEREST IN THE DEVONIAN SHALE IN THIS WELL, OF WHICH TWO WILL BE INDIVIDUALLY STIMULATED. NONE OF THE SHALE WELLS IN THIS PROGRAM HAVE YET BEEN STIMULATED.

ONCE COMPLETE, THESE TESTS CAN BE USED TO ASSESS THE PROMISE OF LARGE STIMULATION TREATMENTS AND/OR THE USE OF CRYOGENIC FLUIDS IN STIMULATING THESE SHALES AND DESIGNING FUTURE TREATMENTS.

INTRODUCTION

The increasing demand for all energy forms and particularly natural gas, and its decreasing supply has attracted attention from industry and the Government to explore new and large historic and non-historic sources of natural gas.

The thick, hydrocarbon-bearing Upper Devonian Shales (hereafter referred to as simply Devonian Shales), which underlie much of the Eastern States, have become a specific target of this exploration (Figure 1). The gas reserves locked in these shales, estimated to exceed by several times the current proven gas reserves of the nation, have made them a primary interest. Unfortunately, these shales, formed from muds deposited approximately 350 million years ago, are fine-grained with very low permeability; making it difficult to economically produce large quantities of gas from them to meet the natural gas demands.

The objectives of two jointly sponsored Columbia Gas-USERDA cost-sharing programs, initiated in June, 1975 and in July, 1976, respectively, are to assess the technical and economic effectiveness of obtaining these large accumulations of gas with a stimulation technique known as massive hydraulic fracturing (MHF)[1], and with a stimulation technique known as cryogenic fracturing.[2]

This paper specifically presents the shale portion of these programs and the research and field operations that have transpired since their initiation. Because of basic differences in the two programs, they are presented separately below.

3-WELL MHF PROGRAM

Background of Program

The purpose of this joint Columbia Gas-USERDA program is to determine if the Devonian Shales of the eastern United States can be economically developed with massive hydraulic fracturing (MHF) treatments. Since the concept of MHF is based on existing knowledge employing existing field equipment, it represents an expedient technical solution to releasing these large gas reserves.

The scope of this program is to drill, core and log (for characterization) and stimulate, with MHF techniques, the Devonian Shales in three wells.

The first well for the program will be used as a MHF test-bed requiring a maximum of four (4) MHF treatments designed for effective treatment of each zone. The selection of these zones will be based on the physical limitations of injecting the fluid and the knowledge gained from the coring and logging program on the reservoir rocks.

The intent of the second well in this program is to create longer fracture extensions from a smaller shale thickness zone. These smaller zones will be selected in regions of secondary porosity (natural fractures) in the Devonian Shales as found with core and log data. In this second well, a maximum of four of these zones are to be hydraulically stimulated.

The third well in the program will incorporate the results from the first two wells, which will provide design optimizations for the stimulation and target zone selections. For this well, a maximum of four treatments have also been allocated.

This program, therefore, calls for twelve MHF stimulation treatments to be performed in the Devonian Shales in three wells selectively chosen.

Criteria Used for Selecting the Wells

Since this program entails the investigation of a new technique in the Devonian Shales, Columbia Gas believed that the MHF program well sites would have to be close to an area of proven Devonian Shale production. This, it was felt, was the best way to allow a comparison of the new MHF technique's capabilities of increasing gas production. Also, this area selected would have to be near existing gas gathering lines to allow extensive production testing to make this comparison. The area chosen,

[1] Massive hydraulic fracturing is defined as a hydraulic fracturing method utilizing at least 200,000 gallons of fluid and 200,000 pounds of sand.

[2] Cryogenic fracturing is defined as a hydraulic fracturing method utilizing primarily fluids which are introduced into the well as liquids and flow back as gases, resulting in rapid clean-up times.

based on these criteria, was the "Big Sandy" field of southwestern Virginia, western West Virginia and eastern Kentucky (noted on Figure 1).

After the selection of this general area, the criteria used to more specifically locate the well sites were:

1. Selection of a relatively large undrilled area so that maximum pressures would be encountered. This area would be indicative of a virgin Devonian Shale area and thus could be used as a model for other undrilled shale areas of the Appalachian Basin.

2. The area should have production indicative of a fractured reservoir. Traditionally, better producing Devonian Shale wells are thought to be associated with the occurrence of natural fracture systems.[1,2] The large induced fracture achieved by an MHF should communicate with a maximum number of these gas-containing natural fractures, and also offer an increased efficiency of producing matrix-bound gas through the induced fracture.

3. The area would have to be suited for the complicated logistics involved with MHF treatments. Since these treatments require a large number of pumping equipment and storage tanks, ample space for their placement was needed.

With considerable analysis of the available field data, three tracts were selected in the "Big Sandy" field based on the above criteria. Detailed production histories and special geologic maps were prepared covering a 36 square-mile range around each of these areas.

At the same time each of the three tracts were being analyzed for reservoir pressure, production and geologic data, Columbia was reviewing remote-sensing imagery in these areas. This imagery (primarily LANDSAT, with some U-2 and SKYLAB) was used to distinguish surface fractures (lineaments). The assumption in this analysis is that these surface expressions are manifestations of underground fracture patterns. With this imagery, the wells could be located in proximity to these surface lineaments to intersect the natural fracture systems downhole.

After analyzing this imagery data and field checking the three potential areas, an undeveloped tract in western Lincoln County, approximately 40 miles southwest of Charleston, West Virginia was selected for the location of the three test wells (Figure 2). This selected area was then submitted to the USERDA at the Morgantown Energy Research Center (MERC) in Morgantown, West Virginia for review. The three sites selected were approved and drilling operations commenced in early 1976.

Preliminary Field Operations

Drilling of the first project well (Well No. 20403) began in early January, 1976. By the end of March, 1976, all three project wells were drilled and cased. The total depth of each well, which encompassed the entire Devonian Shales, were 3,920 feet (Well No. 20401), 4,066 feet (Well No. 20402) and 4,067 feet (Well No. 20403). The wells are located approximately one mile from each other.

In order to fully characterize the Devonian Shales for resource delineation and treatment design, Columbia felt it very important to core, in at least one well, the entire Devonian Shale column. Also, it was felt, this core should be supplemented with a complete suite of logs in all three project wells. Well No. 20403 was cored throughout the entire Devonian Shale column. In this well a total of 1,335 feet (from 2,720 feet - 4,055 feet) of shale was cored. The second project well drilled (Well No. 20401) was not cored due to the excessive shale thickness encountered in Well No. 20403; which was almost twice as thick as originally budgeted for. Lastly, the third project well drilled (Well No. 20402) was selectively cored for a total of 610 feet in the shales where additional detailed information was believed important (higher gas content zones). These high gas content zones were based upon off-gassing tests from the core taken in Well No. 20403.

All of the cores extracted from both wells were oriented every two feet for correlation to natural surface fracture orientation obtained from remote sensing interpretation. Coring time, with orientation, averaged about 100 feet every 24 hours. Stiff foam was used as the coring medium

because of the apparent water sensitivity of the Devonian Shales.[3] With the use of this fluid, minimal problems were encountered.

After the respective wells were drilled and cored, logs were run for further Devonian Shale evaluation. The basic logging program for the three wells was designed around both dry-hole and wet-hole logs. Table I illustrates the type of logs run in the three wells.

MHF Treatments

Since this joint Columbia Gas-USERDA program began, six operationally successful MHF stimulation treatments have been performed in the Devonian Shales in two of the project wells. Rather than laboriously state the types and volumes of fluid and sand used in these treatments, Tables II (Well No. 20403) and III (Well No. 20401) are presented to illustrate these values along with other information found.

The procedures for performing each of these treatments included: evaluating the log and core information available for zone selection; perforating the zones as selected; breaking down the zones with HCl acid for wellbore damage removal; obtaining pre-treatment open flows; pre-frac reservoir testing the zones (to obtain initial values of flow capacity, reservoir pressure and assess wellbore damage); treatment design, execution and clean-up; obtaining after treatment open flows; and lastly, post-frac reservoir testing of each zone (to obtain final flow capacity, reservoir pressure and wellbore damage values to compare to pre-frac test values).

In Table II, the volumes of fluid and the treatment application parameters found in three MHF foam type treatments performed in three separate zones in Well No. 20403 are illustrated. The three zones treated were selected based on log and core data depicting gas containment zones. The specific depths selected and perforated are also given in Table II.

The use of foam as a fracturing fluid in Well No. 20403 came about after reviewing various frac proposals prepared by the Service Companies from both a technical and economic viewpoint. In view of the potential clean-up problems in this low pressure reservoir, it was decided to try foam-fracing because of its beneficial "energy-assist" mechanism. Also, it was decided to use foam in the stimulation of all four zones in Well No. 20403, because, by utilizing essentially the same frac fluid and the same design on all four zones, direct comparisons of production results with our in-place free-gas measurements from the cores could be accomplished.

In Table III, the volumes of fluid and the treatment application parameters found in two types of MHF treatments performed in three separate zones in Well No. 20401 are illustrated. Since the basic program scheduled one well for treatments to extend induced fractures from a smaller treatment zone (100 feet) to intersect natural fractures, the three zones in this well were selected with this criterion from log information. Resistivity cross-plots were used to determine the probable higher permeable zones; i.e., zones of natural fracture concentrations, which produce secondary porosity zones. The specific depths of the zones selected and perforated are also given in Table III.

The first MHF treatment of the lowermost shale zone (Lower Brown Shale) in Well No. 20401 utilized a frac fluid consisting of gelled (guar gum) water. The choice of using a gelled water type treatment in the shales was based upon: (1) the need for a comparison of its effectiveness as measured against the results of the foam-type treatments and, (2) its present popularity with producers using it in other reservoirs throughout the industry, because of its attractive economics and past effectiveness. However, due to an excessive clean-up time experienced after this first gelled-water treatment (5 months to recover only 38% of the fluid used), the treatment type used on the second zone in this well (Middle Brown Shale) was modified. This second treatment included a foam spearhead component followed by a gelled water component, with nitrogen pumped throughout the treatment for an additional "energy-assist" mechanism for faster recovery. The volume ratio of the gelled water component to foam component was about 7 to 1. The third treatment involved two cycles of foam followed by gelled water, again with nitrogen pumped throughout. The gelled water to foam volume ratio in this treatment was about 8 to 1.

The sand schedule for the six treatments performed thus far utilized the injection of 80/100 mesh sand, to seal-off microfractures believed present in the Devonian Shales and thus minimizing

fluid leakoff,[4] followed by the injection of 20/40 mesh sand for maximum propped frac height. The volumes of sand and the peak concentrations, in pounds per gallon (ppg), emplaced in each treatment are given in Tables II and III.

Also included in Tables II and III are the clean-up times required for the frac fluid recovery of each treatment and the percentages recovered after these treatments. The most immediate effectiveness of a fracturing treatment that can be monitored for comparison is the clean-up time; that is, the amount of time after turnaround necessary for gas production. In the case of the treatments performed in the program, this time was cut-off when the gas was flowing free of fluid and also, the gas was flowing at a sufficient rate, without drowning out, to allow a constant terminal rate pressure analysis (on the order of 20 Mcfd because of flow gauge limitations).

Production Results

For preliminary comparisons, measurements of gas volume open flows before and after the MHF treatments were obtained. It should be noted here that Columbia does not recommend using these "initial" pre- and post-frac open flows as indicators of the MHF's effectiveness in increasing gas production. However, these initial open flows do serve as preliminary indicators of the presence of gas in the shales or, as we have recently found, as indicators of possible fracture communication in the shales. Therefore, these pre- and post-frac open flows are presented for illustration in Figure 3.

In Well No. 20403, there was no measurable open flow before the MHF foam treatment on its first zone, which includes all of the Lower Brown Shale and a portion of the Lower Gray Shale (refer to Figure 3 for perspective of location in shale column). After the foam treatment, the total hydrocarbon flow rate rose to 110 Mcfd, after the production of the nitrogen used in the treatment ceased. Therefore, this open flow indicated to us that gas is present in these lower sections of the Devonian Shales, which in this portion of the Basin have never been a primary target for stimulation.

Upon perforating and breaking down the second zone in this well (Middle Brown Shale), an open flow of 95 Mcfd was measured. Because this open flow was suspiciously close to the first zone's open flow (110 Mcfd), a pressure interference test was conducted to investigate for communication (fracture migration) between the two zones. The interference test proved that communication existed between the two zones, and it was evident that the MHF foam treatment conducted on the first zone propagated some 199 feet vertically, into the untreated second zone. Therefore, during the MHF foam treatment on the second zone that followed, a diverting agent (benzoic acid) was used in the treating fluid to bridge-off the downward growth of the fracture into the lower zone already treated. The initial open flow recorded from this second zone after its treatment and subsequent clean-up was 200 Mcfd, which indicated additional gas production due to the second treatment but did not pinpoint the zone of production.

Subsequently, the third zone in this well (including a portion of the Middle Gray Shale and all of the Upper Brown Shale) was perforated and broken down and an initial open flow of 103 Mcfd was gauged, which is substantially low enough that communication was not suspected. However, based on the experience of the lower zones, a pressure interference test was conducted. The results showed that communication wasn't present, indicating this open flow of gas to be "virgin" from this section of the shale. Nevertheless, as a safeguard, during the foam treatment of the third zone, a diverting agent was used to prevent fracture migration downward in the zones previously treated. The initial open flow recorded from this third zone after its treatment and subsequent clean-up was 107 Mcfd, indicating no production increase resulting from the third treatment.

In the other project well (No. 20401), there was no measurable open flow prior to the MHF gelled water treatment performed on this well's first zone (Lower Brown Shale; refer to Figure 3). After this treatment and an extended clean-up time of 5 months, the open flow was gauged at 110 Mcfd. Upon perforation and breakdown of the second zone (Middle Brown Shale), there was also no appreciable flow; leading us to believe there was no fracture induced communication between the two zones. Subsequently, a pressure interference test conducted reinforced this belief. After the treatment and subsequent clean-up of this zone, an initial open flow of 111 Mcfd was measured.

Upon perforation and breakdown of the third zone (Middle Gray and Upper Brown Shale), there was no measurable flow. Because of the lack of gas flow and also low rock pressure measured in the zone (48 psi), we assumed no communication and treated the third zone. As of the time this paper was written, this third zone was still cleaning up and approximately 32% of the water used has been recovered. The open flow after eight days of clean-up was gauged at 30 Mcfd.

Reservoir Testing Results

In an attempt to define the improvement of the MHF treatments on each zone, pre- and post-frac reservoir tests were conducted to establish flow capacity (kh), permeability (k), skin effect (S) and effective fracture length ($2x_f$) for comparison. These tests consisted of approximately one week of draw-down (flowing the well at a constant rate) and two weeks of buildup (shutting the well in).

The data obtained from Well No. 20403 was compiled and submitted to H. K. van Poollen and Associates of Littleton, Colorado (sub-contracted reservoir engineering consultant in the program) for their analysis. Table IV presents their test analysis results for the first two zones in Well No. 20403. Several types of analyses were used to calculate these results, which included the interpretation of linear, spherical and pseudo-radial flow regimes during the tests. The data obtained from Well No. 20401 is being analyzed in a similar manner by the Depletion Department of Columbia Transmission Corporation.

As illustrated in Table IV, pre- and post-frac data for the first zone in Well No. 20403 were not adequate because of a failure in the pressure recording device, and a complete analysis could not be performed. However, analysis of the flow test suggests the possibility of a permeability (k), in the range of 0.05 to 0.10 md after the treatment of this zone.

As mentioned earlier, interference testing indicated that the fracture generated by the first foam treatment migrated vertically into the second perforated interval (3,409 feet to 3,651 feet), resulting in communication between the sets of perforations. Therefore, the contributing interval during the pre- and post-frac testing of the second zone was not exactly known. In order to distinguish this uncertainty, van Poollen and Associates examined two limiting cases. Case I (as illustrated) assumes gas production during the testing was coming only from the second perforated zone (h = 205 feet). In Case II, they assume that the gas production is coming from both perforated zones and the interval in between (3,409 feet - 4,031 feet, h = 622 feet).

The results from the testing of the second zone show, from both cases, that the effective permeability, (k), of the portion of the shale reservoir investigated is in the range of 0.03 to 0.44 md. Also, from the Horner plot of the pre-frac pressure test data, the negative skin effect(s) values of -4.3 (Case I) and -4.1 (Case II) indicate improvement of near wellbore conditions. These improvement indicators are probably due to the vertical extent of the fracture from the first zone moving up into this second zone and removing its wellbore damage. After the second treatment, these wellbore conditions were only slightly improved to -4.9 (Case I) and -4.75 (Case II).

Another important purpose of these test analyses is to determine the effective fracture length ($2x_f$) created by these MHF treatments. Once again, looking specifically at the Horner plot analysis, the pre-frac test data in Table IV indicate that the effective fracture length ($2x_f$) is 72-86 feet. Once again, this frac length probably represents the lateral extent of the first fracture in Zone 1. Subsequently, after the MHF treatment of the second zone, this effective frac length grew to 136-156 feet, as illustrated by the post-frac test data. Accordingly, this resulted in almost twice the effective surface area available for gas flow from the reservoir. In the second zone, the observed increase in open flow, from 95 Mcfd before the treatment to 200 Mcfd after the treatment, reflects this increase in effective surface area. However, these effective frac length values obtained, according to the test results, are significantly lower than the predicted 760 feet from the Carter equation used by the Service Companies to determine the areal extent of a fracture.[5]

The test results for the third zone stimulated in Well No. 20403 and the three zones treated in Well No. 20401 were not available for presentation in this paper.

13-WELL MHF PROGRAM - SHALE WELLS

Background of Program

The purpose of this joint Columbia-USERDA program is to determine whether massive hydraulic fracturing, dendritic fracturing, or cryogenic fracturing techniques can be used to economically recover the gas reserves in tight sandstones and shales of the eastern United States. This paper presents only the portion of that program directly pertaining to the stimulation of the Devonian Shales by cryogenic fracturing techniques. Since the concept of cryogenic fracturing is based on existing knowledge employing existing field equipment, it represents another expedient solution to releasing the large gas reserves in the Devonian Shale.

The scope of the program (pertaining to shale tests only) is to drill, core, and log (for characterization) and stimulate, with cryogenic techniques, the Devonian Shales in four wells, one of which is to be a dual completion in a well currently producing from a deeper horizon. These wells will be spread throughout the Appalachian Basin so that the results can be used as being representative of different portions of the Basin. Four gas-bearing zones were expected in each of the shale wells in this program. Two treatments (covering two of the zones of interest in each well) are proposed for each one of these wells. The selection of these zones will be based on the physical limitations of the ability to pump the fluid and the knowledge gained from the coring and logging program on the reservoir rocks.

The shale portion of this program, therefore, calls for eight cryogenic stimulation techniques to be performed in the Devonian Shales in four wells selectively chosen throughout the Appalachian Basin.

Criteria Used for Selecting the Wells

Unlike the three-well MHF program, two of these wells were located outside of the "Big Sandy" field so that cryogenic fracturing could be tested in extreme locations of the Appalachian Basin in addition to historic producing areas. Where possible, the wells were also to be located near existing gas gathering lines for extensive production testing. The criteria used to locate these wells more specifically were:

1. Selection of a relatively large undrilled area for each well so that maximum pressures would be encountered, assumed to be indicative of production from other undrilled areas in the same portion of the Basin.

2. The area for each well would have to be suited for the complicated logistics involved with cryogenic treatments. These treatments require at least as much space for equipment as an MHF.

3. Where possible, the area should have production indicative of a fractured reservoir, for the same reasons as cited for the MHF well location.

With considerable analysis of the available field data, four tracts were selected in three general areas for more detailed study. Detailed production histories and special geologic maps were prepared covering a 36 square-mile range around each of these areas.

At the same time each of the three areas were being analyzed for reservoir pressure, production, and geologic data, Columbia was reviewing remote-sensing imagery in two of these areas, similar to that used to locate the MHF well sites in the 3-well program. With this imagery (primarily LANDSAT, with some U-2 and SKYLAB), three well sites in these two areas were selected in proximity to these surface lineaments to intersect the natural fracture systems downhole. In the northernmost area studied, remote imagery was inadequate for interpretation because of glacial deposits overlying the terrain obstructing imagery manifestations.

Two of the wells (No's. 20336 and 20337) located by remote sensing are approximately six miles apart in Martin County, Kentucky, a productive shale area in the "Big Sandy" field. One well (No. 20338-T), also located by remote sensing, is in Wise County, Virginia, near the southern extreme of the Appalachian Basin. The last well (No. 11236 - dual completion) is a producing Clinton well in Trumbull County, Ohio, which is in the northern portion of the Basin. These well

locations are depicted in Figure 2. The selected well sites were submitted to the USERDA at the Morgantown Energy Research Center (MERC) in Morgantown, West Virginia for review. These well sites (and existing well) selected were approved and drilling operations commenced in late 1976.

Preliminary Field Operations

Drilling of the first project shale well (Well No. 20336, Martin County, Kentucky) began in October, 1976. By the end of May, 1977, all of the three new shale wells were drilled and cased. The total depth of each of these wells, which encompassed the entire Devonian Shales, were 3457 feet (Well No. 20336), 3602 feet (Well No. 20337), and 5740 feet (Well No. 20338-T). The total depth of the Clinton well in Trumbull County (Well No. 11236) to be dually completed in the Shale was 4743 feet, with the base of the Devonian Shale at 2701 feet.

Well No. 20336 was cored throughout the entire Devonian Shale column. In this well, a total of 988 feet (from 2432 feet to 3420 feet) of shale was cored. The second project shale well drilled (Well No. 20337) was not cored. Well No. 20338-T was selectively cored for a total of 386 feet in the shales where additional detailed information was believed important (higher gas content zone). The zones to be cored were the high radioactive zones determined from logs run in nearby wells. All of the cores extracted from both wells were oriented every two feet, as in the 3-well MHF program.

After the respective wells were drilled and cored, logs were run for further Devonian Shale evaluation. The logs run on these shale wells are summarized in Table V. The logs were run in dry holes in Wells No. 20336, 20337, and 20338 to minimize fluid damage to the shale, and in a fluid filled hole in Well No. 11236. The logs in the shale interval in Well No. 11236 were run in 1973 when this well was completed in the Clinton. A temperature log was rerun in this well in 1977 to determine the potential gas-bearing zones in the shale which is presently behind casing.

Cryogenic Treatments

None of the shale wells in this program have yet been stimulated as of the writing of this paper. However, the proposed stimulation treatment parameters for the four wells are summarized in Table VI. The figures shown are based on preliminary proposals from the Service Companies, and are subject to change. The same general procedures discussed in the 3-well MHF program for performing each of these treatments will be used in stimulating the shale wells in this program.

The proposed treatment intervals are illustrated in Figure 8. These intervals were generally selected based on log and core data depicting gas containment zones. As observed in the figure, the proposed eight treatments in these four wells encompasses all of the "Brown Shale" zones.

Production and Reservoir Testing

Although no testing has yet been done on any of these wells, the same general evaluation procedures will be used as in the 3-well MHF program. Measurements of gas volume open flows before and after the cryogenic treatments will be used as preliminary indicators of the treatment effectiveness and possible fracture communication. Pre- and post-frac pressure transient tests will be conducted by Columbia to establish flow capacity (kh), permeability (k), skin effect (S), effective fracture length ($2x_f$), and possible turbulence effects.

An isochronal test will be conducted on each of these wells, which is expected to take one to two weeks, after the well has been shut in long enough for pressure stabilization. Each test will consist of three draw down-buildup cycles, with measurement of flow rates and both bottom-hole and well-head pressures.

Test data will be analyzed by Intercomp Resource Development and Engineering, Inc. of Houston, Texas (reservoir engineering consultants subcontracted by Columbia for this project). Intercomp will use both conventional plotting techniques and numerical simulation[6] to interpret the data.

ASSOCIATED RESEARCH INVESTIGATIONS

In association with Columbia Gas, other organizations have been incorporated into these programs. Figure 4 presents these other organizations and their functions in the programs. It is beyond the scope of this paper to discuss their specific functions in any detail. However, in general, the majority of these organizations are involved in Devonian Shale core studies. These core studies include examining the cores for mineralogy, organic carbon content, trace element composition, maturation, physical properties (including rock mechanics), stimulation design, etc. The final outcome of these investigations will be an assessment of the characterization and resource delineation of the Devonian Shales.

In conjunction with these organizations, Columbia is also performing core studies on the Devonian Shales. Our endeavors in these studies have centered around free-gas measurements of the shale (off-gassing experiments). These data are presented in Figures 5 and 6 for Wells No. 20403 and 20336 respectively. From these graphs, it can be seen that almost all of the shale has some free gas evolving, with the higher values in the rich organic sections (black shales from lithology description). These results are very important from the standpoint of potential free gas reserve estimates and original gas in place estimates.

Figures 7 and 8 illustrate another aspect of the Devonian Shales Columbia has been involved with. Figure 7 summarizes the geologic findings of the three Devonian Shale MHF wells, as prepared by Columbia's geologists, while Figure 8 summarizes the geologic findings of the four Shale wells in the 13-well project. The cross sections of each well were primarily based on log information, with some core information (as indicated) used to define the zones of vertical fractures.

From the preliminary log analysis, Figure 7 shows that six separate zones (Upper-Middle-Lower Gray Shales and Upper-Middle-Lower Brown Shales) exist in the Devonian Shales in the area of Lincoln County, West Virginia. Also, it illustrates that although these separate zones remain of the same thickness in the offset wells (approximately one mile apart) the gas distribution (from sibilation logs) and the vertical fracture distribution (observed from cores extracted) vary from one offset well to the other. This clearly demonstrated to Columbia the need and importance of a complete analysis of each Devonian Shale well in the program to enable selective stimulation treatments.

The nomenclature used in Figure 7 is slightly different than that used in Figure 8. Log analysis of the four shale wells in Figure 8 indicated four or five high radiation zones in these wells, which were generally found to contain darker shales from core analysis. Subsequent reanalysis of the logs in Wells 20401, 20402, and 20403 indicate another high radioactive zone in the Middle Gray Shale not previously thought to be significant. In general, zone 1 in Figure 8 was found to correlate with the Upper Brown Shale zone in Figure 7; zone 2 with the previously undefined radioactive zone in the Middle Gray Shale zone in Figure 7; zone 3 with the Middle Brown Shale zone in Figure 7; and zone 4 (and zone 5) with the Lower Brown Shale zone in Figure 7. In Well No. 11236 (northern part of Basin), zones 4 and 5 are thought to represent the Harrell and Marcellus Shales, respectively. In the other wells investigated, these shales are not separated. Also observed in Well No. 11236 is the lack of a distinct interval corresponding to zone 1 (Upper Brown Shale) in the other wells. As Figures 7 and 8 indicate, log and core data from many more wells are needed to define the Devonian Shales throughout the Appalachian Basin.

SUMMARY

Since the initiation of these Columbia-USERDA programs, three Devonian Shale wells have been selected for massive hydraulic fracturing, and four Devonian Shale wells have been selected for cryogenic fracturing. These wells were selected using various areal topography and production criteria, and the wells have been drilled, cored (selectively) and logged.

From the cores extracted, off-gassing experiments were performed which indicate free gas is present throughout the entire Devonian Shale column in the geographical areas cored. Continued research on the cores by Columbia and other organizations is being conducted for characterization and resource delineation of the Devonian Shales.

With the suite of logs run in the three MHF wells, cross-sections of the Devonian Shales in this geographical area have been prepared. These cross-sections depict six lithologically different sections (zones) in the Devonian Shale in this area. Subsequent reanalysis of these logs and the suite of logs run on the four wells to be cryogenically fraced indicates that up to eight different zones are possible in some parts of the Appalachian Basin.

Based on available core and log data, six zones in two wells have been selected and stimulated with MHF techniques. Three zones in one well were stimulated with the same fluid, namely, foam. The three zones in the other well were stimulated using gelled water in one zone and a foam-gelled water type in the other two zones. Six more zones remain to be selected and massively fraced, four of which will be optimized treatments in the third well.

None of the four wells to be cryogenically fraced have yet been treated. Eight zones in these four wells will be cryogenically fraced.

Production resulting from the zones that have been massively fraced to date indicate that gas is definitely present in zones of the Shale that have not been historically produced before. Furthermore, reservoir testing of two zones in one well indicates this production has resulted from vertical fractures extending laterally from 136 to 156 feet. This effective fracture length is on the order of five times smaller than predicted with the use of these massive volumes of fluid.

NOMENCLATURE

BPM = barrels per minute
h = height
ISIP = instantaneous shut-in pressure
k = permeability
kh = flow capacity
Mcfd = thousands of cubic feet per day (gas flow)
md = millidarcy
N_2 = nitrogen
ppg = pound per gallon
S = skin factor
Scf = standard cubic feet
Sg = gas saturation, in percent
xf = fracture length on one wing
$2x_f$ = effective fracture length
ϕ = porosity, in percent

ACKNOWLEDGEMENTS

The author wishes to thank Steve McKetta for much of the information presented herein and the Columbia Gas System Service Corporation management for permission to publish this paper.

REFERENCES

1. Patchen, D.G.: "Subsurface Stratigraphy and Gas Production of the Devonian Shales in West Virginia" in Eastern Gas Shales Project, Morgantown, West Virginia, Morgantown Energy Research Center, March, 1977, pp. 14-15.

2. Ryan, W.M.: "Remote Sensing Fracture Study - Western Virginia and Southeastern Kentucky" in Devonian Shale Production and Potential, Proc. of Seventh Appalachian Petroleum Geology Symposium, Morgantown, West Virginia, March 1-4, 1976, Morgantown Energy Research Center, pp. 94-95.

3. Ray, E.O.: "Shale Stimulation - A New Approach", Proc. of the Technical Sessions - Kentucky Oil and Gas Association, Thirtieth and Thirty-first Annual Meetings 1966 and 1967, Lexington, Kentucky, Kentucky Geological Survey, 1968, p. 41.

4. Miller, B.D., and Warembourg, P.A.: "Prepack Technique Using Fine Sand Improves Results of Fracturing and Fracture Acidizing Treatments", SPE Paper 5643, 50th Annual Fall Meeting, SPE, Dallas, Texas, September 28 - October 1, 1975.

5. Howard, G.C., and Fast, C.R.: Hydraulic Fracturing, Dallas, Texas, SPE of AIME, 1970, pp. 33-34.

6. Dowdle, W.L., and Hyde, P.V.: "Well Test Analysis of Hydraulically Fractured Gas Wells", SPE Paper 6437, 1977 Deep Drilling and Production Symposium, SPE, Amarillo, Texas, April 17-19, 1977.

TABLE I

LOGGING PROGRAM FOR 3 TEST WELLS
IN COLUMBIA GAS/USERDA
DEVONIAN SHALE-MHF PROGRAM

Dry-Hole Logs Consisted of:	Wet-Hole Logs Consisted of:
Formation Density Compensated Log (FDC) Sidewall-Neutron-Porosity Log (SNP) Dual Induction Log Temperature Log - Absolute Temperature Log - Differential Sibilation Log	CORIBAND Series - Composed of Gamma Ray Log, Formation Compensated Density Log (FDC), Compensated Neutron Log (CNL), Compensated Sonic Log, Dual-Induction-Laterolog, and Micro-laterolog 3-D Velocity Log Seisviewer Thermal Decay Time Log (TDT)

TABLE II

VOLUME AND TREATMENT PARAMETERS
OF MHF FOAM FRACS
PERFORMED ON WELL NO. 20403

ZONE	ZONE 1	ZONE 2	ZONE 3
FORMATION PERFED INTERVAL (FT.)	Lower Brown Lower Gray Shale 3858-4031	Middle Brown Shale 3409-3651	Upper Brown - Middle Gray Shale 2954-3230
TREATMENT DATE	6/21/76	11/15/76	5/23/77
TREATMENT TYPE/QUALITY	Foam/77%	Foam/81%	Foam/82%
TREATMENT SIZE (GALLONS) Foam Water SAND VOLUME (LBS.) 80/100 Mesh/Peak Conc. 20/40 Mesh/Peak Conc. NITROGEN VOL. (Scf)	 250,000 58,480 299,000 19,000/1 ppg 280,000/1.5 ppg 2,458,200	 319,750 59,750 439,000 29,400/1 ppg 410,000/2 ppg 2,500,000	 345,944 62,270 340,000 60,000/3 ppg 280,000/1.5 ppg 3,229,088
AVG. RATES (BPM)	37.5	40	9.6
AVG. TREATING PRESS. (PSIG) MAX. TREATING PRESS. (PSIG)	1930 2250	1550 1710	1390 1480
ISIP ISIP/MINUTES	1950 1070/5 min.	850 770/5 min.	1190 1150/5 min.
CLEAN-UP TIME (DAYS) % RECOVERED	29 44-water 52- N_2	17 14-water 80-N_2	32 20-water 93-N_2

TABLE III

VOLUME AND TREATMENT PARAMETERS
OF MHF FRACS
PERFORMED ON WELL NO. 20401

ZONE	ZONE 1	ZONE 2	ZONE 3
FORMATION	Lower Brown Shale	Middle Brown Shale	Middle Gray Shale
PERFED INTERVAL (FT.)	3788-3860	3272-3410	2988-3092
TREATMENT DATE	8/3/76	5/17/77	8/15/77
TREATMENT TYPE/QUALITY	MHF	MOD-MHF	MOD-MHF
TREATMENT SIZE (GALLONS)	517,014	104,160	100,590
Foam	--	12,684	11,424
Water	517,014	91,476	89,166
SAND VOLUME (LBS.)	930,000	321,762	352,380
80/100 Mesh/Peak Conc.	190,000/3 ppg	59,178/6 ppg	84,252/8 ppg
20/40 Mesh/Peak Conc.	740,000/3 ppg	262,584/8 ppg	268,128/8 ppg
NITROGEN VOL. (Scf)	120,000	741,000	790,000
AVG. RATES (BPM)	25.4	30	30
AVG. TREATING PRESS. (PSIG)	1758	800	800
MAX. TREATING PRESS. (PSIG)	5000	950	1500
ISIP	1200	250	700
ISIP/MINUTES	250/15	0/5	500/2
CLEAN-UP TIME (DAYS)	116	20	8*
% RECOVERED	38	54	32*

* Preliminary Data

TABLE IV

RESERVOIR TESTING RESULTS
WELL NO. 20403

	TEST DESCRIPTION	CASE I* kh md. ft.	CASE I* k md.	CASE I* Skin	CASE I* x_f ft	CASE II* kh md. ft.	CASE II* k md.	CASE II* Skin	CASE II* x_f ft
Zone 1	Pre-Frac Flow Test	No Analysis				No Analysis			
	Pre-Frac Buildup Test	No Analysis				No Analysis			
	Post-Frac Flow Test	--	.05 → .10	--	--	--	.05 → .10	--	--
	Post-Frac Buildup Test	No Analysis				No Analysis			
Zone 2	Pre-Frac Flow Test								
	1/q Equivalent Plot	37	0.180	-2.60	8	37	0.059	-2.50	7
	Spherical Plot	29	0.140	--	--	68	0.110	--	--
	Linear Plot	--	0.179	--	22	--	0.088	--	9
	Pre-Frac Buildup Test								
	Horner Plot	22	0.109	-4.30	43	21	0.034	-4.10	36
	Spherical Plot	20	0.120	--	--	58	0.094	--	--
	Linear Plot	--	0.109	--	38	--	0.034	--	34
	Post-Frac Flow Test								
	1/q Equivalent Plot	91	0.445	-2.80	5	91	0.146	-2.70	8
	Linear Plot	--	0.130	--	306	--	0.042	--	290
		--	0.445	--	166	--	0.146	--	144
	Post-Frac Buildup Test								
	Log-Log Curve Match	66	0.320	--	142	66	0.106	--	124
	Horner Plot	26	0.128	-4.90	78	26	0.042	-4.75	68
	Spherical Plot	18	0.090	--	--	37	0.060	--	--
	Linear Plot	--	0.128	--	84	--	0.042	--	72

*Assumed ϕ = 2.438%; Sg = 77.3%; h = 205 feet
**Assumed ϕ = 1.804%; Sg = 45.8%; h = 622 feet

TABLE V

LOGGING PROGRAM FOR 4 SHALE TEST WELLS
IN COLUMBIA GAS/USERDA
13-WELL PROGRAM

Well No. 20336 (Dry-Hole)	Well No. 20337 (Dry-Hole)	Well No. 20338 (Dry-Hole)	Well No. 11236 (Wet-Hole)
Gamma Ray Temperature Induction Compensated Formation Density Sidewall Neutron Porosity	Gamma Ray Temperature Induction Density Borehole Compensated Epithermal Neutron Porosity Wellbore Sibilation Comp-Pro (Production Index)	Gamma Ray Temperature Induction Density Borehole Compensated Epithermal Neutron Porosity Wellbore Sibilation	Gamma Ray Temperature Dual Induction Laterolog Compensated Formation Density Sidewall Neutron Porosity

TABLE VI

PROPOSED VOLUME AND TREATMENT
PARAMETERS OF CRYOGENIC FRACS

WELL	20336		20337		20338		11236	
Perfed Interval	2968-3122	2666-2712	3526-3574	3100-3250	5450-5480	4890-4910	2410-2545	1915-2000
Treatment Size (Gallons)	42,000[1]		42,000[1]		100,000[1]		100,000[1]	
CO_2	12,600		12,600		35,000		35,000	
Water	29,400		29,400		65,000		65,000	
Sand Volume (Lbs.)	90,000		90,000		270,000		270,000	
80/100 Mesh/Peak Conc.	30,000		30,000		45,000/4		45,000/4	
20/40 Mesh/Peak Conc.	160,000		60,000		225,000/4		225,000/4	
CO_2 Vol. (Mscf)	945		945		2,625		2,625	
Avg. Rate (BPM)	25		25		30		30	
CO_2	7.5		7.5		10.5		10.5	
Water	17.5		17.5		19.5		19.5	

[1]Proposed Treatment Parameters per Zone (2 Zones per Well)

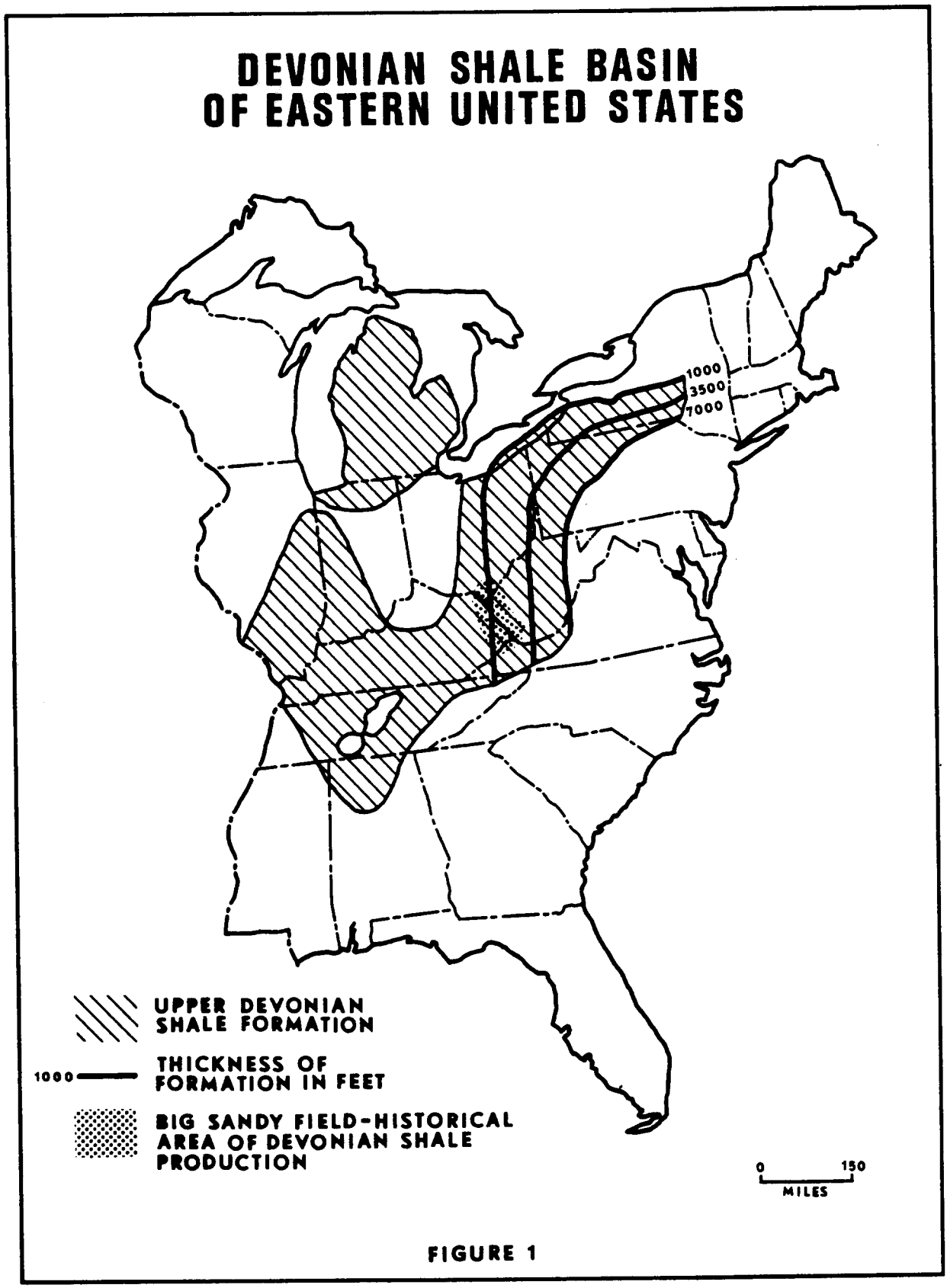
DEVONIAN SHALE BASIN
OF EASTERN UNITED STATES
1000
3500
7000
UPPER DEVONIAN
SHALE FORMATION
1000
THICKNESS OF
FORMATION IN FEET
BIG SANDY FIELD-HISTORICAL
AREA OF DEVONIAN SHALE
PRODUCTION
0
150
MILES

FIGURE 1

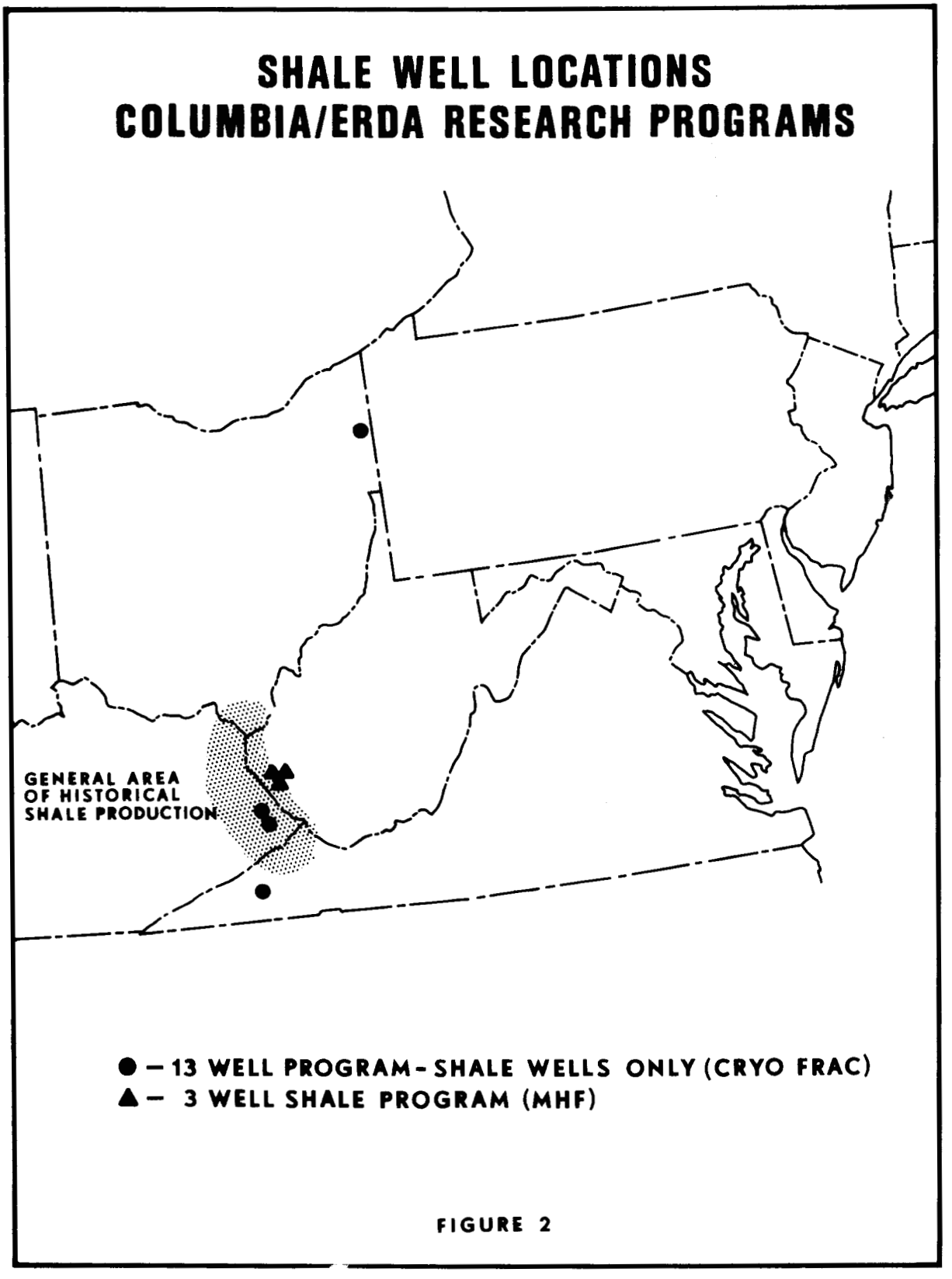
SHALE WELL LOCATIONS
COLUMBIA/ERDA RESEARCH PROGRAMS
GENERAL AREA
OF HISTORICAL
SHALE PRODUCTION
● — 13 WELL PROGRAM - SHALE WELLS ONLY (CRYO FRAC)
▲ — 3 WELL SHALE PROGRAM (MHF)

FIGURE 2

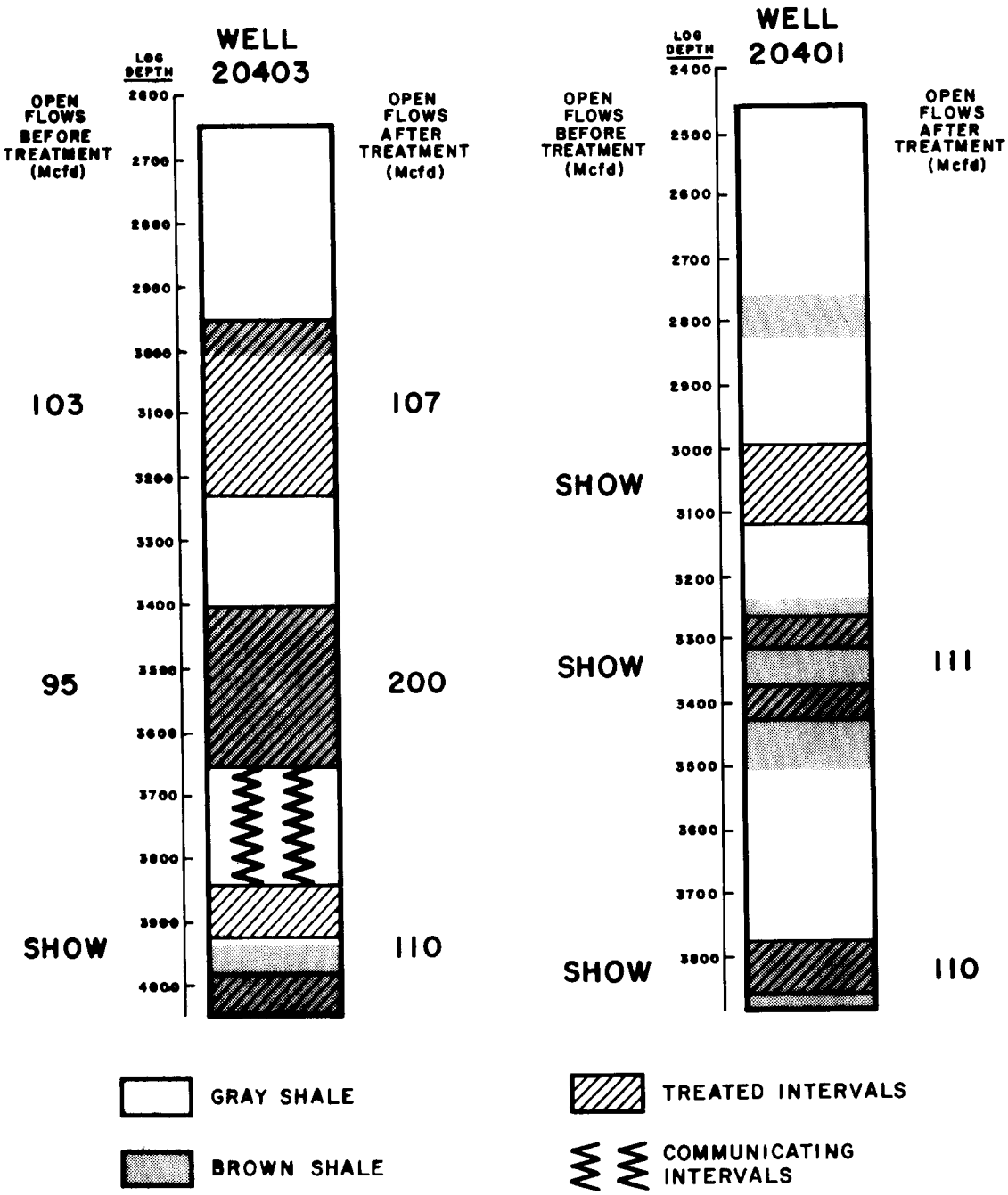
OPEN FLOWS
WELLS NO. 20403 & 20401 (MHF)
WELL 20403
LOG DEPTH
OPEN FLOWS BEFORE TREATMENT (Mcfd)
OPEN FLOWS AFTER TREATMENT (Mcfd)
2600
2700
2800
2900
3000
3100
3200
3300
3400
3500
3600
3700
3800
3900
4000
103
95
SHOW
107
200
110
WELL 20401
LOG DEPTH
OPEN FLOWS BEFORE TREATMENT (Mcfd)
OPEN FLOWS AFTER TREATMENT (Mcfd)
2400
2500
2600
2700
2800
2900
3000
3100
3200
3300
3400
3500
3600
3700
3800
SHOW
SHOW
SHOW
111
110
GRAY SHALE
BROWN SHALE
TREATED INTERVALS
COMMUNICATING INTERVALS

FIGURE 3

ASSOCIATED ORGANIZATIONS INVOLVED IN
COLUMBIA GAS/USERDA PROGRAMS

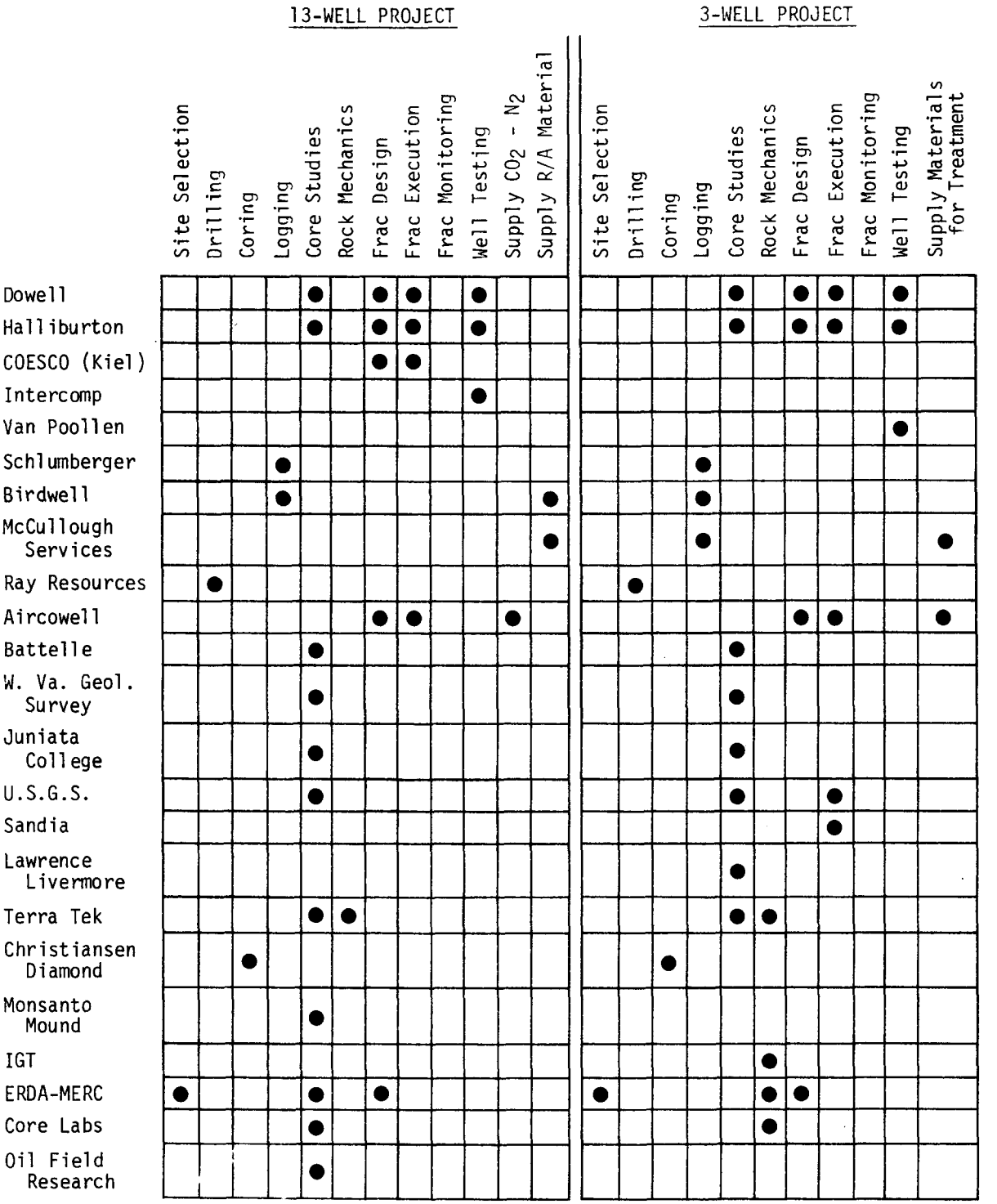

FIGURE 4

FREE-GAS MEASUREMENT FROM CORES ON WELL NO. 20403

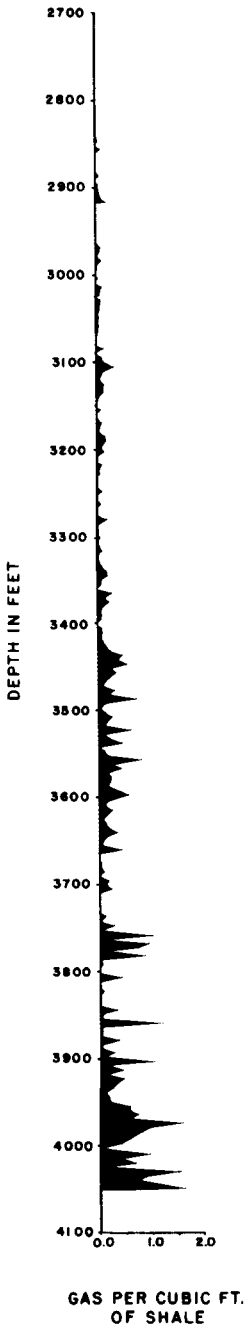

FIGURE 5

FREE-GAS MEASUREMENT FROM CORES ON WELL NO. 20336

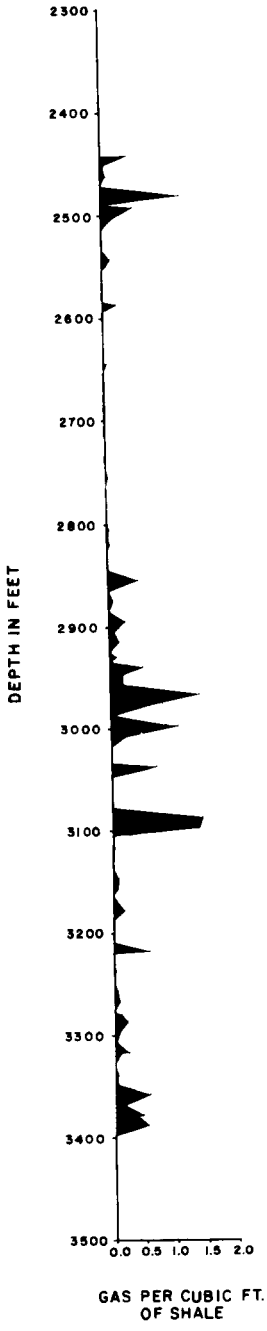

FIGURE 6

SUMMARY OF GEOLOGICAL FINDINGS

(COLUMBIA MHF WELLS, LINCOLN CO., W.VA.)

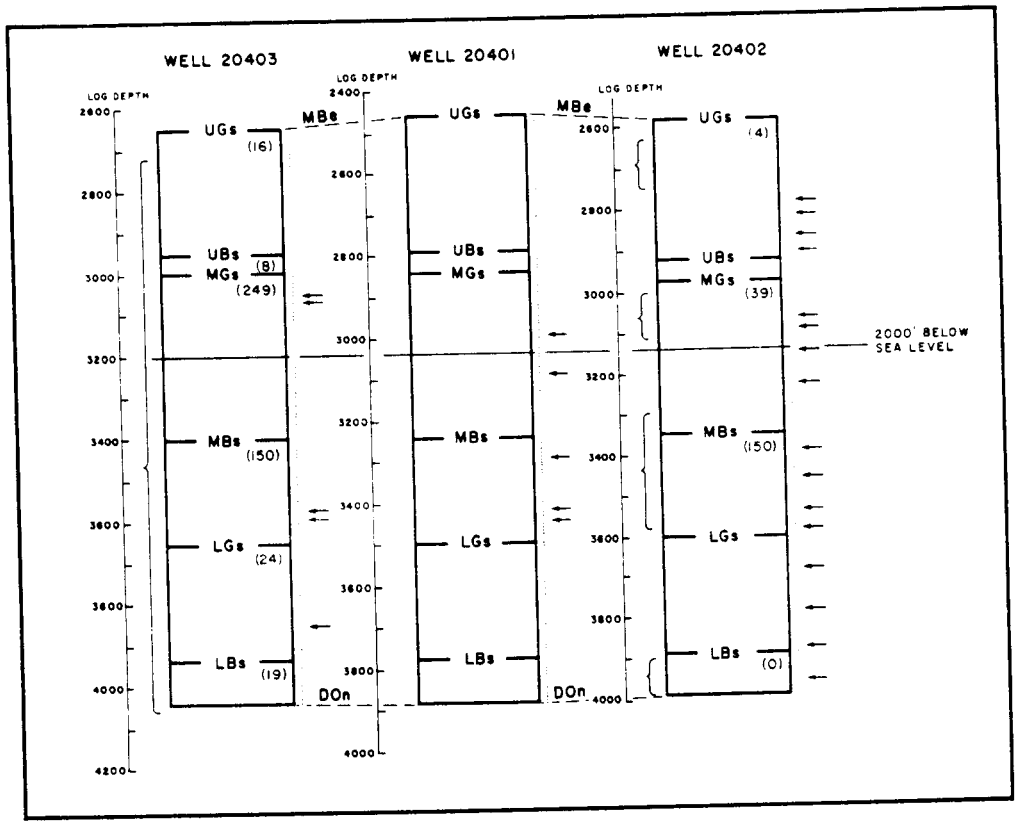

LEGEND

MBs – BASE OF BEREA SANDSTONE

UGs – TOP OF UPPER GRAY SHALE AND SILTSTONE

UBs – TOP OF UPPER BROWN SHALE

MGs – TOP OF MIDDLE GRAY SHALE

MBs – TOP OF MIDDLE BROWN SHALE

LGs – TOP OF LOWER GRAY SHALE

LBs – TOP OF LOWER BROWN SHALE

DOn – TOP OF CORNIFEROUS (ONONDAGA) LIMESTONE

⟵ – GAS SHOW FROM SIBILATION LOG

⋮ – PROBABLE PERMEABLE INTERVAL FROM RESISTIVITY CROSS PLOTS

(5) – FEET OF OBSERVED VERTICAL FRACTURES

{ – CORED INTERVAL

FIGURE 7

SUMMARY OF GEOLOGICAL FINDINGS SHALE WELLS–13 WELL PROGRAM

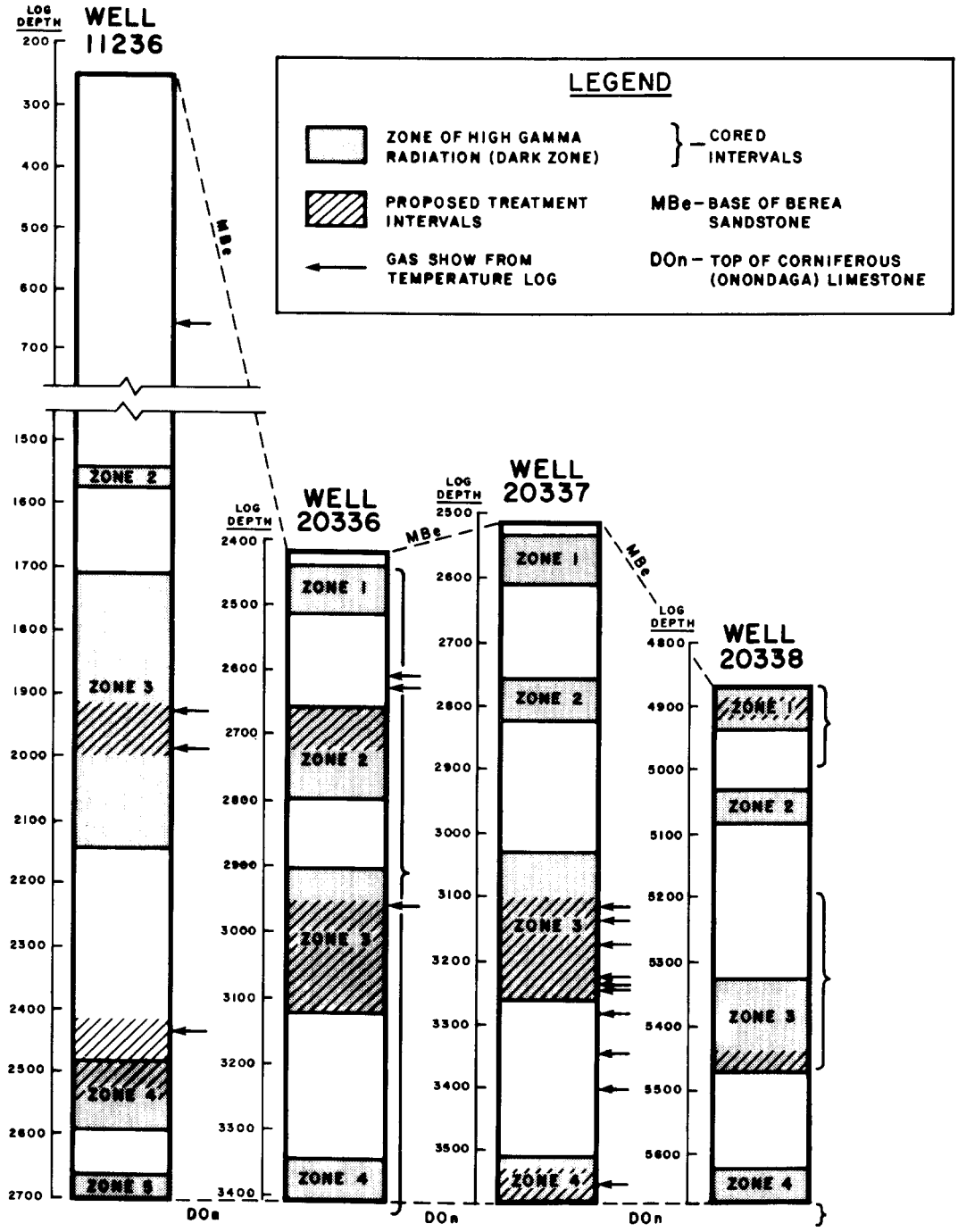

FIGURE 8

ROCK MECHANICS ASPECTS OF MHF DESIGN IN EASTERN DEVONIAN SHALE GAS RESERVOIRS

by

A. H. Jones
A. S. Abou-Sayed
L. A. Rogers

Terra Tek, Inc.
Salt Lake City, Utah

ABSTRACT

As part of an ERDA/OGST program, rock mechanics considerations are used to help design deeply penetrating hydraulic fractures in Devonian shale at Columbia Gas System Service Corporation wells in Lincoln County, West Virginia. Rock properties of the pay zone were considered in relation to the barrier formations. Formation properties ... specifically, elastic moduli, critical stress-intensity factor and the minimum *in situ* stresses ... were determined from laboratory core measurements and field tests. Analyses using formation properties suggest that the Middle Brown Shale zone is the layer (in the Devonian shale) that is most likely to "contain" a deeply penetrating hydraulic fracture. Fracture containment analyses indicated that the gray shales on either side of the Middle Brown would act as barriers to fracture growth, provided the fracture fluid is injected at a pressure that does not exceed the naturally occurring stress in the Middle Brown Shale by more than 400 psi. The Lower Brown Shale and the Upper Brown Shale are also preferred zones for fracturing but at less favorable conditions. Fracture fluid injection pressure in the Lower and Upper Brown Shales should exceed the naturally occurring stress in the reservoir rock by no more than 250 psi and 200 psi, respectively. Fracture initiated in the gray shales would be expected to move out of zone.

INTRODUCTION

The eastern Devonian shales represent a potential gas reservoir of enormous size [Ranostaj, 1976]. Unfortunately, the reservoir consists of tight formations that require stimulation before economic gas production can be achieved. Massive hydraulic fracturing represents a possible stimulation technique for these formations. Under contract from the Energy Research and Development Administration, Columbia Gas System Service Corporation has been assigned the task of:

1) Determining the technical and economic feasibility of hydraulic fracturing in Devonian shales, and

2) Identifying the fracture distribution, gas distribution and ways to achieve economic production by application of stimulation research findings.

To accomplish these objectives, a three-well program [Ranostaj, 1976] was planned in Lincoln County, West Virginia; see Figure 1. Different hydraulic fracture treatments were planned for the first two wells in order to obtain data necessary to optimize the stimulation treatment in the third well. Terra Tek, under subcontract from Columbia Gas, was to determine mechanical characteristics of the formations to better design and interpret the results of the massive hydraulic fracturing (MHF) tests. The Devonian shale in the area of the three-well test program consists of several layers of brown and gray shales, as shown in Figure 2. Natural gas is found in all of the layers with the Middle

Prepared under Contract No. E(46-1)-8014.

and Lower Brown Shale layers having the best potentials. Since the bedding is nearly horizontal and there are no major tectonic displacements in the area of the test program, the shale layers are expected to be similar in the 20401, 20402 and 20403 wells. Data from all three wells are thus combined to form a composite picture of the area.

In hydraulic fracturing of surface rock formations, the rock is subject to:

1) The fracturing fluid pressure which tends to open the crack.
2) The far field *in situ* stresses acting to close the crack.

During a hydraulic fracture treatment, the forces from the treatment fluid need to overcome both the *in situ* stress and the fracture toughness of the rocks, a material property similar to the tensile strength that represents the resistance of rock to fracturing. In a layered subsurface formation such as the Devonian shale, the separate layers may have different fracture toughness, and/or elastic moduli along with different natural occurring stresses in the ground. Fracture containment analyses is accomplished by evaluating these factors as they apply to the particular zone of the gas reservoir being stimulated. To determine whether a layer is a barrier or not, it is thus necessary to determine its properties in relation to the adjacent layers. A particular layer may be a barrier in some instances and not a barrier in other instances, depending on the relative relationships of the stresses and mechanical properties.

CONTAINMENT CRITERIA

When a fracture is initiated in rock, the fracture will extend when the stress-intensity factor at its tip reaches a critical value. Whether a fracture moves up, down or out depends on the relative values of the critical stress-intensity factors for the various materials and the stress-intensity factors along the fracture perimeter as generated by the loading conditions and fracture geometry. Hence, a fracture analyses require the determination of the stress-intensities and comparing them to the critical values [Simonson, *et al.*, 1975]. The following data are used in such analyses:

1) The elastic moduli in the pay zone and bounding layers.
2) The *in situ* stress field and, in particular, the minimum principal stresses in the pay zone and the bounding layers above and below the pay zone.
3) The fracture toughness or critical stress-intensity factors for the pay zone and bounding layers.
4) Fracturing fluid and the pump schedule.

Knowledge of the elastic moduli and the *in situ* stresses for the pay zone and both of the bounding layers is needed to determine whether or not the bounding layers are barriers to crack extension outside the pay zone.

Hydraulic fracture analysis is inherently a three dimensional problem: the mathematical solutions of which are extremely complicated. The present work will be limited to treating two-dimensional cracks. Such a simplified analysis provides considerable insight into understanding the parameters and conditions which influence hydraulic fracture propagation [Simonson, *et al.*, 1976].

The basic concept of containment analyses is illustrated in Figure 3. The fluid is moving such that the pressure near the well-bore is higher than the pressure near the tip. Estimates of the stress-intensity factor at the edges and tip of the propagating fracture can be made if the pressure profile, *in situ* stresses and elastic moduli along the crack shape are known. These estimates are then compared to the critical stress-intensities. The fracture will propagate when the stress-intensity factors reach the critical values. In the special case where the stress-intensity factor would be equal to the critical value at all points of the perimeter around the crack, the fracture would propagate in all directions at the same time. On the other hand, if the stress-intensity factor reaches a critical value only at the tip and not at the upper and lower edges, the fracture is then confined to the pay zone.

For this discussion, we will consider a long, narrow crack in infinite material. This model is representative of a hydraulic fracture with a shorth height and a long length. The plane strain mathematical model gives the following equation for the stress intensity factor at the upper crack edge

$$K_I = \frac{1}{\sqrt{\pi \ell}} \int_{-\ell}^{+\ell} \left(P_y - S_y\right) \sqrt{\frac{\ell+y}{\ell-y}}\, dy$$

where

P_y = Pressure profile in crack

S_y = Far field horizontal stress profile

y = Position along crack

ℓ = Height from the crack center to the tip

S_y represents the minimum principal *in situ* stress since fracture will be normal to this stress. Note in this equation that the stress-intensity factor is dependent upon the profile of the stress difference between the pressure inside the fracture and native *in situ* stresses across the fracture. Different combinations of fluid pressures and *in situ* stresses will give different values of K_I and, in turn, different results for a prediction of the final fracture geometry.

(i) Influence of Elastic Moduli:

The above equation for K_I is for the hypothetical case where the elastic moduli of the pay zone and the bounding layer are equal. If the elastic moduli of the several layers were different, then there is an additional influence on the stress-intensity factor as a result of the difference in the moduli. Figure 4 illustrates the qualitative behavior of the stress-intensity factor for a crack that moves perpendicular to an interface between two materials with different moduli when plane strain conditions across the bounding layers prevail. If the elastic modulus in the pay zone is higher than that of the bounding layer, then as a fracture propagates toward the boundary the stress-intensity factor increases such that it will reach the critical value and the fracture will "snap" into the bounding layer. On the other hand, if the modulus in the pay zone is lower than the moduli in the bounding layers, then a fracture which is propagating from the pay zone toward the bounding layers will find the stress-intensity at its tip nearest the interface decreasing as the boundaries are approached such that the critical value is not reached and the fracture is contained within the pay zone.

(ii) Influence of *In Situ* Stress:

Difference in *in situ* stresses between the pay zone and the barrier layers have a distinct influence on fracture propagation. Consider the hypothetical case, shown in Figure 5, in which a hydraulic fracture has extended by some mechanism or other, into adjacent layers with similar elastic moduli but different *in situ* stresses. Figure 6 shows a plot of the distance the crack will advance into the region of high stress (the barrier layers) in terms of the pressure, P, within the fracture and P_o, the fracture fluid pressure required for the fracture to reach the interface. The curves in this figure are for a crack height of 200 feet, a fracture toughness of 1,000 psi$\sqrt{\text{in}}$ and for parametric values of the *in situ* stress difference $S_2 - S_1$. For a stress difference of 1,000 psi, for example, an over pressure of 500 psi would be expected if the fracture were to propagate a distance of 100 feet into the region of higher *in situ* stress. Finally, if the *in situ* stress in the barrier layers (S_2) were less than the *in situ* stress in the pay zone (S_1), a situation would exist where it requires less pressure to propagate the fracture in the barrier than in the pay zone.

It is these principles that will be used to design deep penetrating hydraulic fractures in Devonian shale in the next section.

SUMMARY OF ROCK MECHANICS DATA

Ultrasonic velocities and elastic moduli were determined for cores taken from several layers in wells 20402 and 20403 [Lingle and Abou-Sayed, 1976]. The effect of confining pressure on the measured velocities was very small, on the order of 2 percent for pressures ranging from atmospheric to 4,000 psi. Also, the changes in velocity with temperature over the range encountered in these wells (approximately 100° F) was less than 1 percent for the P-wave and within the accuracy of the measured system for the S-wave. Figure 7 shows the comparison of laboratory data with data obtained from logs. Densities and P-wave velocities are, in general, in good agreement, with the exception of the sample from 3910 feet. The laboratory S-wave velocities (measured with the same polarization as the logs) are consistently 10 to 12 percent higher than the log value at identical depth. This is possibly the result of the logs detecting the arrival of a surface wave and not the S-wave [Lingle and Jones, 1977]. With this assumption, the revised S-wave velocities shown in Figure 7 agree very well (within 0.5 percent) on the average with the laboratory measured S-wave velocities.

Young's modulus has been calculated using the measured bulk densities, P-wave velocities and the revised S-wave velocities. For the purpose of these calculations, the material was assumed isotropic and homogeneous. Figure 8 illustrates the general trend of the data. Also shown are static moduli from triaxial compression of the Upper Brown and Lower Gray Shales. As expected, the static moduli are lower than the sonic moduli; for the samples tested the difference is on the order of 20 to 30 percent.

Critical stress-intensity factors were determined experimentally for the Gray Shales by internal pressurization of cylindrical samples with two radial prenotches. This method was developed by Clifton, *et al.*, (1976). In this method a sample of the core about two to three inches long has a small diameter hole drilled along the axis and notches placed in the walls of the small hole to specify the fracture initiation points. A bladder is placed in the hole to prevent fluid from entering the sample or the notches and then pressure is applied in the bladder until the sample bursts. Figure 8 summarizes the results for the Gray Shales.

In situ stresses, especially the difference in *in situ* stresses between the pay and barrier formations, are the most critical parameters to MHF containment. Unfortunately, this is the parameter for which the least amount of data is available. A single mini-hydraulic fracturing test was performed by Terra Tek at the 2745 foot level (Upper Gray Shale) in well number 20402 [Abou-Sayed, *et al.*, 1977]. These results were as follows:

Minimum Horizontal Stress	2360 psi, N 40° W to N 45° W
Maximum Horizontal Stress	4390 psi, N 45° E to N 50° E
Overburden Stress	3210 psi
Pore Pressure	~ 250 psi

The measured principal stress directions agree well with the prevailing geological structure in the region and with the principal stress directions reported by Overbey (1976) from a series of measurements in West Virginia. A basement structure map of the region in which the reported tests were conducted is shown in Figure 9. The map, adapted from Harris (USGS Map I-919D, 1975) by Overbey (1976), shows a projection of the Rome Trough through the northwestern edge of West Virginia. Schumaker (1976) describes the Rome Trough as a graben bounded by high-angle, normal faults. This structure lies within an area which is a junction of three distinct geological provinces [Werner, 1976]:

1) Central Appalacian Fold Belt,
2) Southern Appalacian Thrust Fault Belt, and
3) Appalacian Plateau with Basement Faults.

Although it is not known whether or not basement faults penetrate into the Devonian shales in this area, Overbey's measurements (1976) suggest a correlation of principal stress directions with the basement structure. At locations which fall outside the projection of the Rome Trough, the measured direction of σ_{HMAX} are oriented generally east-west and are normal to the predominantly north-south strike of the thrust faults and folds of the Appalacian Mountains. Measured directions of σ_{HMAX} which fall within the projection of the Rome Trough are N 45° E to N 50° E, or parallel to the strike or the basement faults and in agreement with the directions reported here.

An estimate of the minimum horizontal stresses in the other shale layers was made on the basis of elastic theory. Data from the Upper Gray Shale was analyzed for determination of applied boundary displacements in both horizontal directions as might be imposed through normal faulting on the boundaries of the Rome Trough. These same displacements were applied to the other shale layers and the resulting minimum *in situ* stress in these layers were estimated using moduli derived from corrected logs. Figure 8c shows a plot of the estimated minimum horizontal principal stresses in the different formations. These estimates correlate with two independent observations. Swolfs, *et al.*, (1977), based on strain relaxation data, estimated the minimum *in situ* stress gradients from the surface of 0.52 psi per foot for the Middle Brown Shale and 0.76 psi per foot for the overlying Middle Gray Shale. These stress gradients coincide with the data shown in Figure 8c at the Middle Gray Shale/Middle Brown Shale interface. Field engineers contend that either the Lower Gray or the Lower Brown Shale will breakdown under a hydrostatic head of water. The estimated minimum *in situ* stress shown in Figure 8c for the Lower Brown Shale would also predict this behavior.

DATA INTERPRETATION

Although the tests were minimal, sufficient data was gleaned from available information to perform a containment analyses. Both Figure 8a and 8c indicate that the gray shales and Onondaga Limestone will act as barriers to the fracture growth in the brown shales. The gray shales are not strong barriers (moduli contrast is less than 30 percent and the largest *in situ* stress difference is less than 800 psi), however, and can also be broken down if fluid pressures are too high. The brown shales will not form barriers to fractures in the gray shales. This interpretation correlates with field results reported by McKetta (1977). A fracture initiated in the Lower Gray Shale in well 20403 propagated upwards into the Middle Brown Shale. Communication was noted on perforating and breaking down the Middle Brown Shale.

A significant factor in successful completion of MHF treatment in reservoirs with marginal barrier formations is the control of fracturing-fluid flow rate and the maximum allowable bottom hole treatment pressure (BHTP). There are other factors, besides containment of the induced fracture, that might impose certain bounds on both flow rate and BHTP. These are proppant transport, created crack width, strength of casing, location of perforation and the like. However, the calculated value of BHTP that would prevent the fracture penetration into barrier zones would prove instrumental in achieving a contained fracture geometry. An estimate of the maximum BHTP for a given treatment can be obtained following the arguments presented earlier. For a pay formation height of 2c, and a pumping pressure of P, the fracture will extend a length ℓ' into the barrier layer such that [Simonson, *et al.*, 1976]:

$$P - S_1 = \frac{1}{\sqrt{\pi(c+\ell')}} \left[K_{Ic} - \frac{2(S_2-S_1)(c+\ell')\cos^{-1}\left(\frac{c}{c+\ell'}\right)}{\sqrt{\pi(c+\ell')}} \right]$$

where K_{Ic} is the critical stress-intensity factor for the barrier layer and S_1 and S_2 are the minimum *in situ* stresses for the pay and barrier zones, respectively. Penetration of the fracture initiated in the Middle Brown Shale into the Middle Gray Shale is shown in Figure 10. For excess pumping pressure in the fracture ($P-S_1$) less than 400 psi, the penetration is kept within 50 feet. To maintain fracture intrusion into the Middle Gray Shale within this limit, the bottom hole treatment pressure during hydraulic fracturing of the Middle Brown Shale layer should not exceed the minimum horizontal stress in that zone by more than 400 psi, plus any expected drop in pressure across the perforation. Corresponding considerations for the Lower Brown and Lower Gray Shales (the Onondaga Limestone forms a strong barrier due to its large elastic moduli) leads to a BHTP of 250 psi in excess of the minimum horizontal stress for the Lower Brown Shale. For the Upper Brown Shale, the Upper Gray and Middle Gray Shales will form weak barriers. Following similar considerations as outlined above, this leads to a BHTP of 200 psi in excess of the minimum horizontal stress for the Upper Brown Shale.

In treating the Middle Brown Shale first, the fracture will propagate into both the Middle Gray and Lower Gray Shales. There is, therefore, the possibility that later fractures initiated in the Upper Brown and in the Lower Brown Shales will interact with the earlier fracture created in the Middle Brown Shale. In a multi-stage MHF it is important that the better reservoir formation be fractured first.

NOMENCLATURE

c = Half the pay formation height

K_I = Stress-intensity factor for Mode-I cracks (opening mode)

K_{Ic} = Critical stress-intensity factor (fracture toughness)

ℓ = Half the crack height

ℓ' = Length of fracture extension in the barrier layer

P_o = Fracturing fluid pressure needed to achieve a fracture height of 2c

P = Fracturing fluid pressure

P_y = Fracturing pressure profile in the vertical direction

S_1 = Minimum far-field horizontal stress in the pay zone

S_2 = Minimum far-field horizontal stress in the barrier layer

S_y = Minimum far-field horizontal stress profile in the vertical direction

y = Vertical distance along fracture surface

σ_{HMAX} = Maximum far-field horizontal stress

ACKNOWLEDGMENTS

It is a pleasure to acknowledge the assistance of Columbia Gas System Service Corporation personnel who cooperated on this project. The authors appreciated greatly the assistance and many discussions with Mr. C. Komar, USERDA, Morgantown, during the course of the work. Contributions to the program were made by several other Terra Tek personnel, in particular, Dr. H. Swolfs and Messrs. C. Brechtel and R. Lingle.

REFERENCES

Abou-Sayed, A. S., C. E. Brechtel and R. J. Clifton; "*In Situ* Stress Determination by Hydrofracturing - A Fracture Mechanics Approach," Accepted for Publication in the Journal of Geophysical Research, 1977.

Clifton, R. J., E. R. Simonson, A. H. Jones and S. J. Green; "Determination of the Critical Stress-Intensity Factor K_{Ic} in a Circular Ring," Exp. Mech., Vol. 16, pp. 233-238, 1976.

Lingle, R. and A. S. Abou-Sayed; "Comparison of Log with Laboratory Measured Data for Columbia Gas System Service Corporation Weel #20403," Fourth Progress Report, Terra Tek, TR 76-45, September 1976.

Lingle, R. and A. H. Jones; "Comparison of Log and Laboratory Measured P-Wave and S-Wave Velocities, Terra Tek, TR 77-19. Published in Proceedings of Eighteenth Annual Logging Symposium, Houston, 1977.

McKetta, S. F.; "Massive Hydraulic Fracturing of the Devonian Shale in Lincoln County, West Virginia," Proceedings of ERDA Enhanced Oil, Gas Recovery & Improved Drilling Methods Symposium, Tulsa, Oklahoma, August 30-31, September 1, 1977.

Overbey, W. K., "Effect of *In Situ* Stress on Induced Fractures," Proceedings of Seventh Appalachian Petroleum Geology Symposium, USERDA," Morgantown, MERC/SP-76-2, March 1-4, pp. 182-211, 1976.

Ranostaj, E. J., "Massive Hydraulic Fracturing Eastern Devonian Shales," ERDA Symposium on Enhanced Oil, Gas Recovery, Tulsa, Oklahoma, Vol. 2, p. C-3, September 9-10, 1976.

Shumaker, R. C., "A Digest of Appalachians Structural Geology," Proceedings of Seventh Appalachian Petroleum Geology Symposium, USERDA," Morgantown, MERC/SP-76-2, March 1-4, pp. 75-93, 1976.

Simonson, E. R., A. H. Jones and A. S. Abou-Sayed, "Experimental and Theoretical Considerations of Massive Hydraulic Fracturing," Terra Tek, TR 75-39, December 1975.

Simonson, E. R., A. S. Abou-Sayed and R. J. Clifton, "Containment of Massive Hydraulic Fracture," Society of Petroleum Engineers Journal, 1977, in Press.

Swolfs, H. S., R. Lingle and J. M. Thomas, "Determination of the Strain Relaxation and their Relation to Subsurface Stresses in Devonian Shale," Terra Tek, TR 77-12, February 1977.

Werner, E., "Remote Sensing Studies in the Appalachian Plateau for Applications to Fossil Fuel Extractions," Proceedings of ERDA Symposium on Enhanced Oil, Gas Recovery, Tulsa, Oklahoma, Vol. 2, p. C-2, September 9-10, 1976.

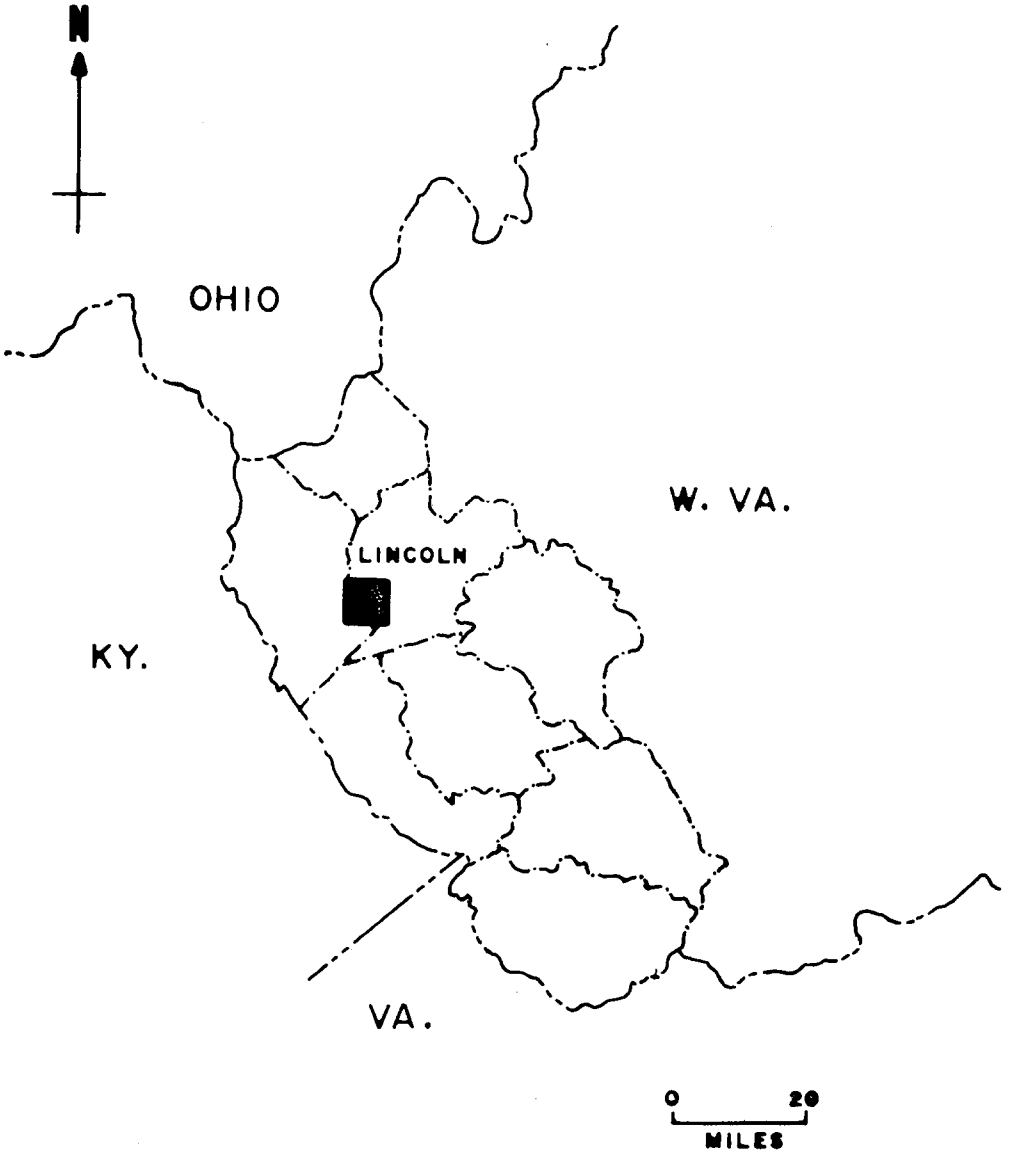

Figure 1. Location of wells in Lincoln County, West Virginia.

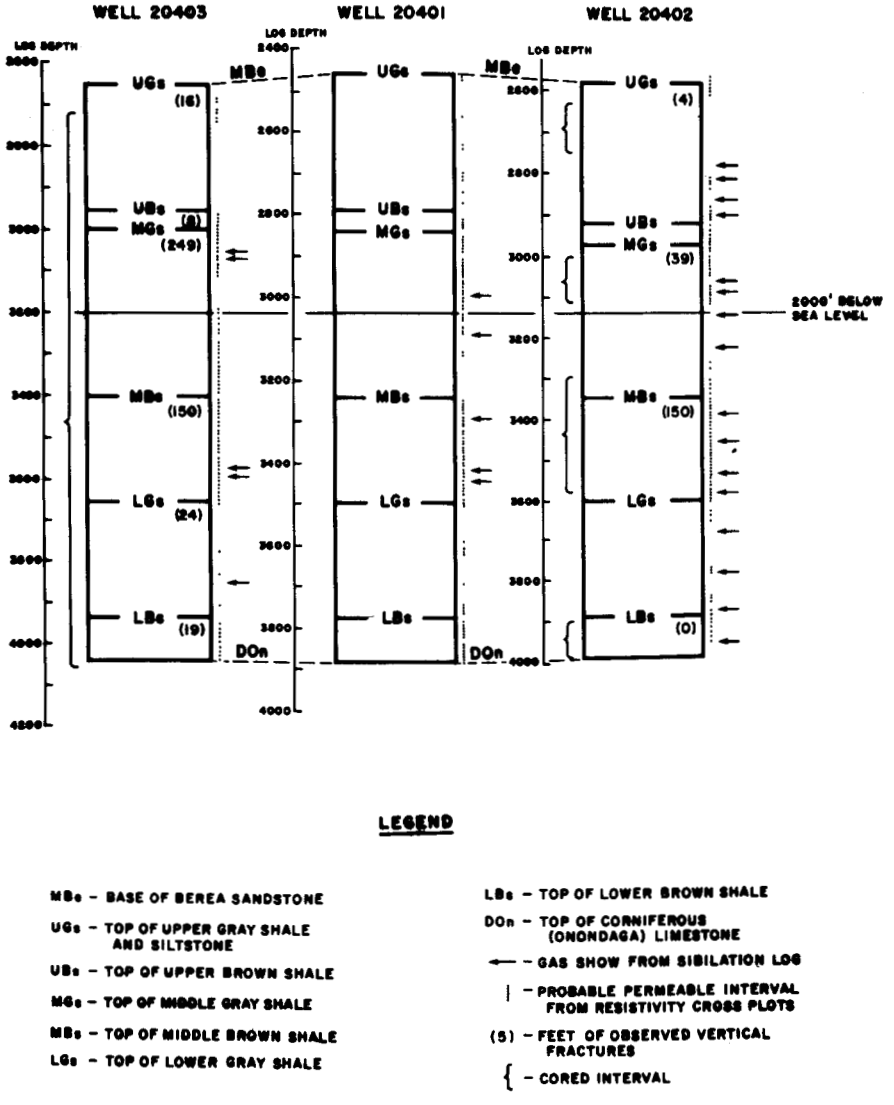

Figure 2. Summary of geological findings [from Ranostaj, 1976].

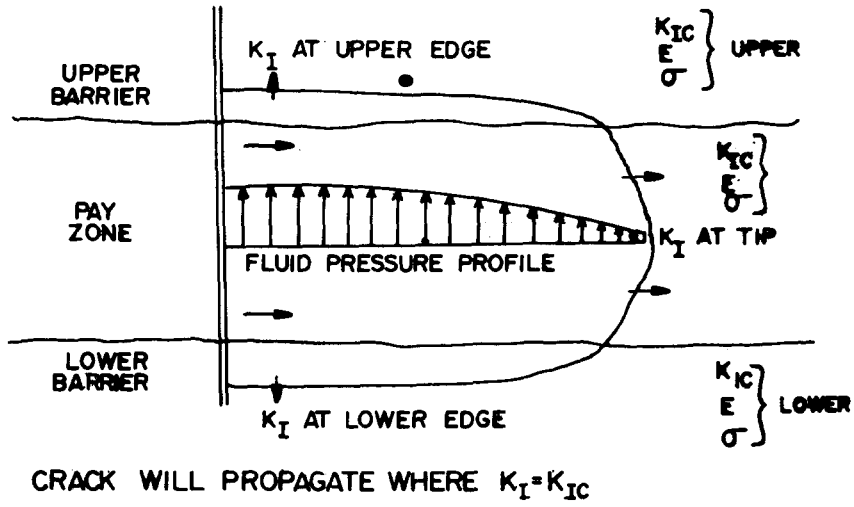

Figure 3. Schematic diagram to illustrate fracture containment analysis.

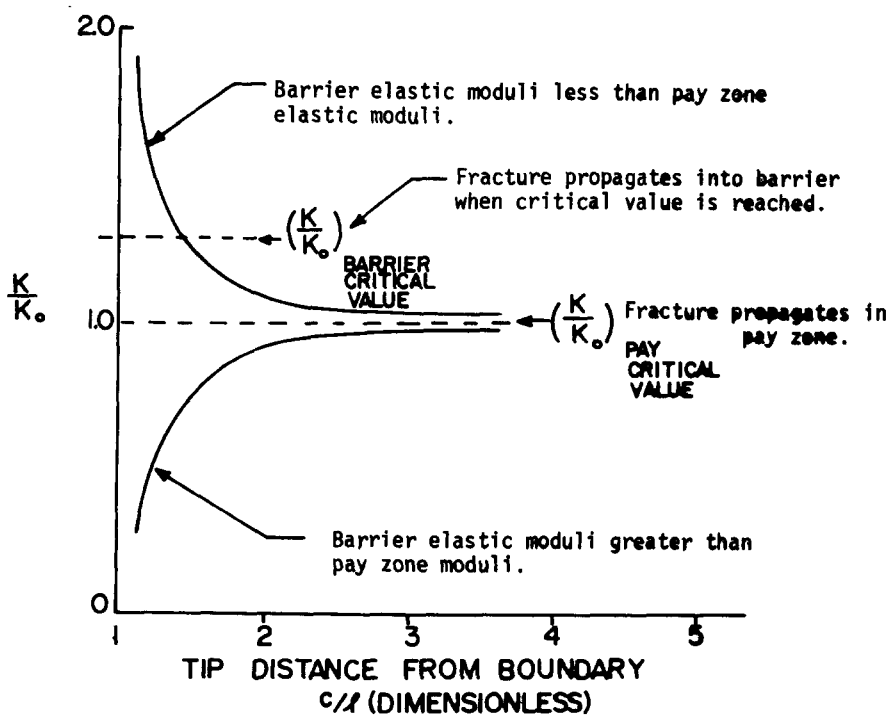

Figure 4. Qualitative behavior of the stress-intensity factor as a crack of length 2a approaches the boundary of an adjacent layer with different elastic moduli. (c is distance from fracture center to boundary).

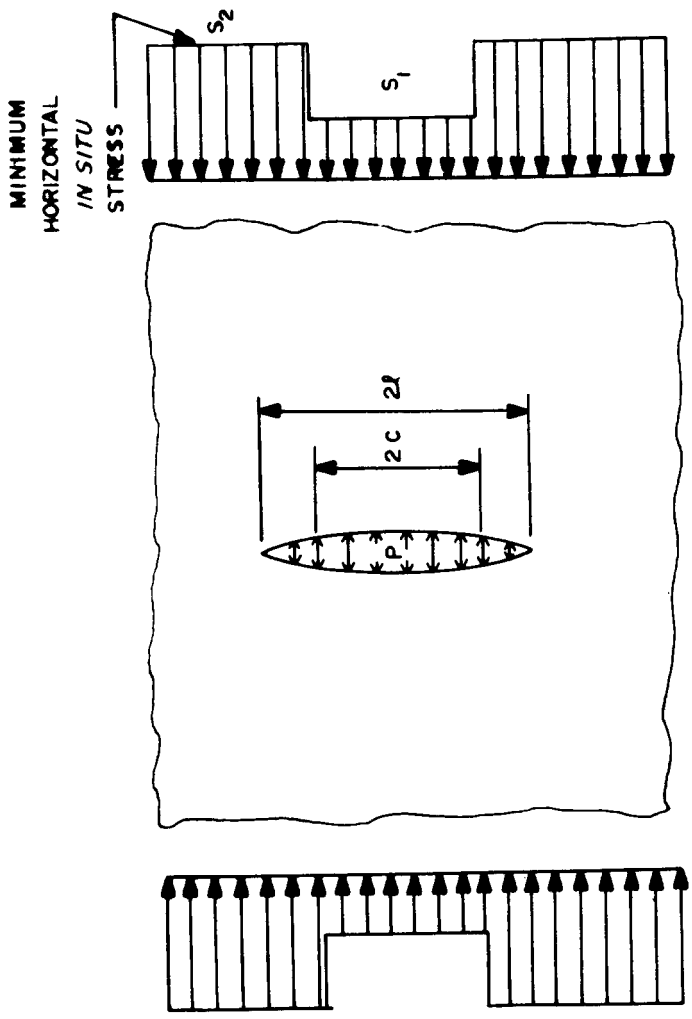

Figure 5. Vertical hydraulic fracture loaded under uniform pressure (P) with differing minimum horizontal stress in pay zone & barriers.

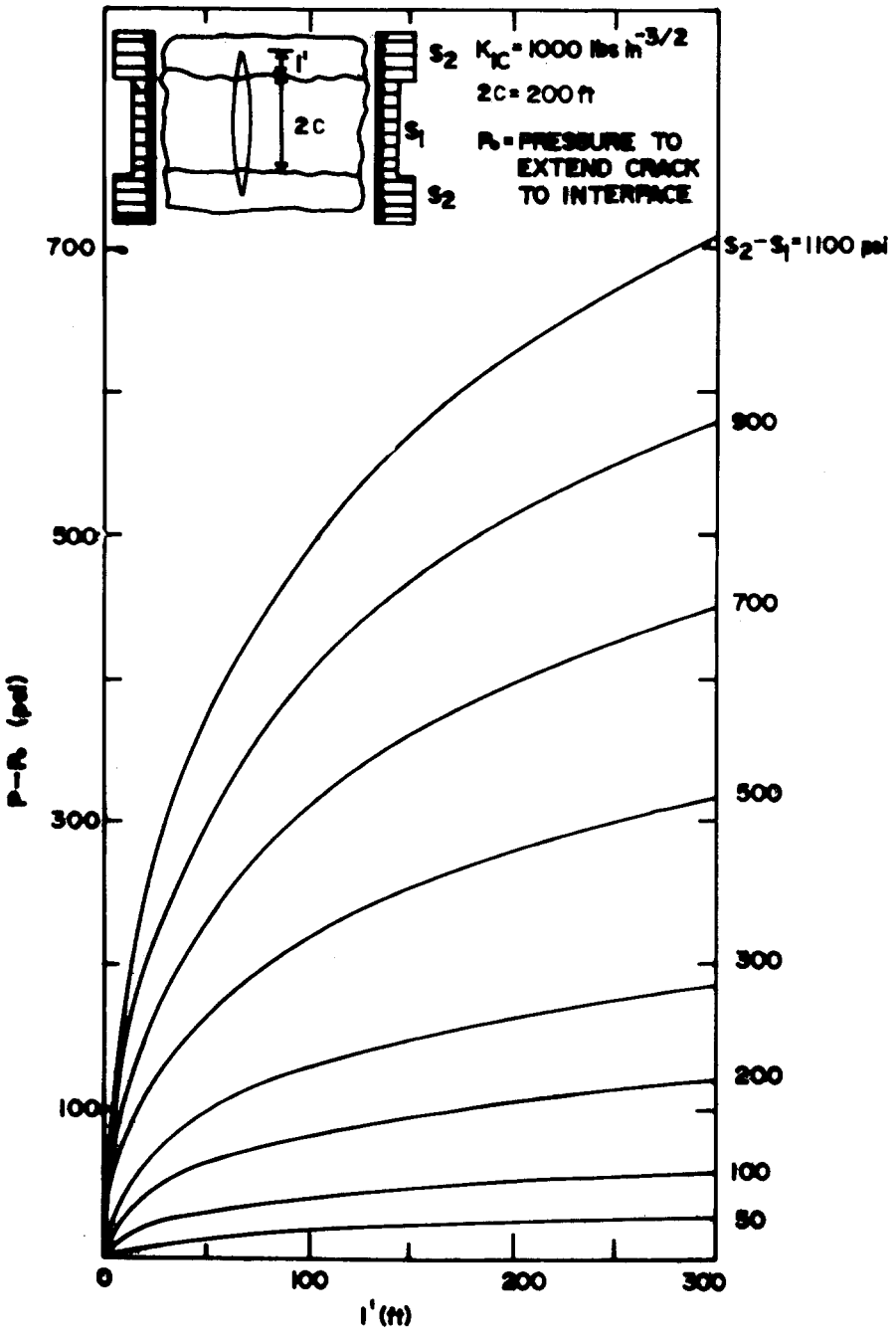

Figure 6. Estimate of fracture migration into the barrier layers. [From Simonson, *et al.*, 1976].

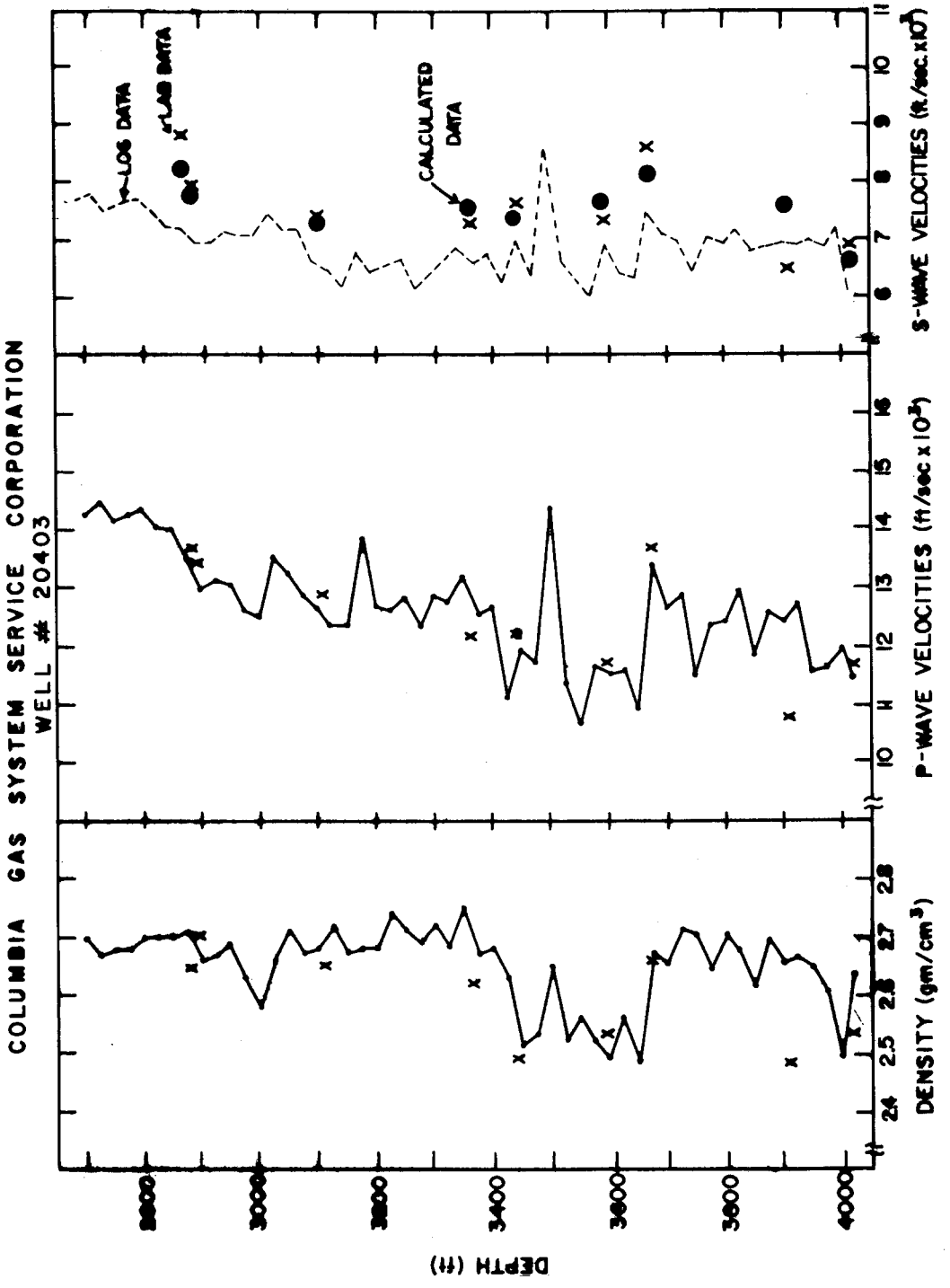

Figure 7. Comparison of laboratory data with log data. Correction to S-Wave assuming that the log detected surface waves is also shown.

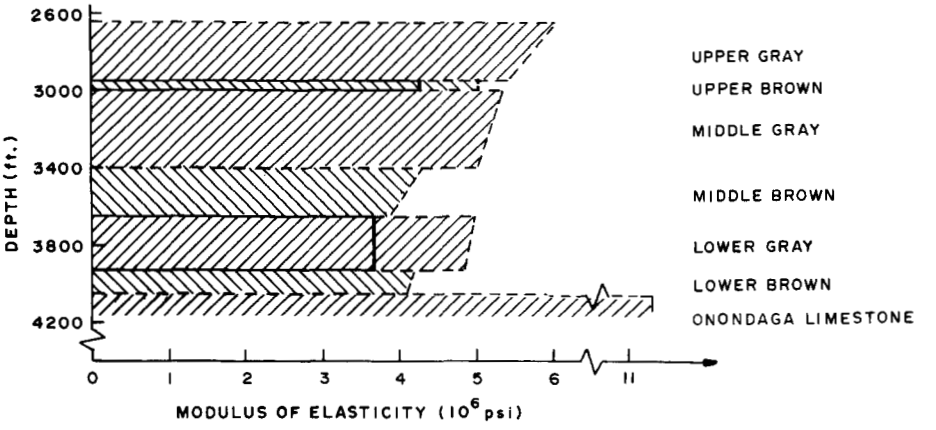

Figure 8a. Log derived (dotted lines) and laboratory measured (solid lines) modulus of elasticity.

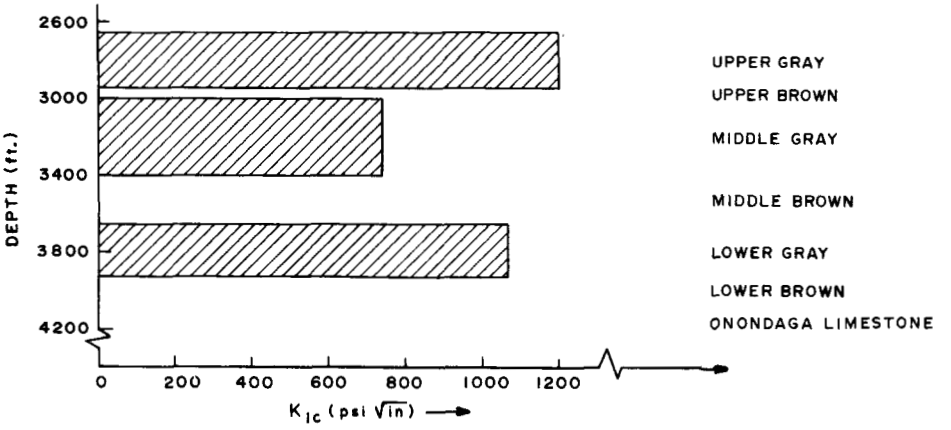

Figure 8b. Critical stress-intensity factor for the barrier shales only.

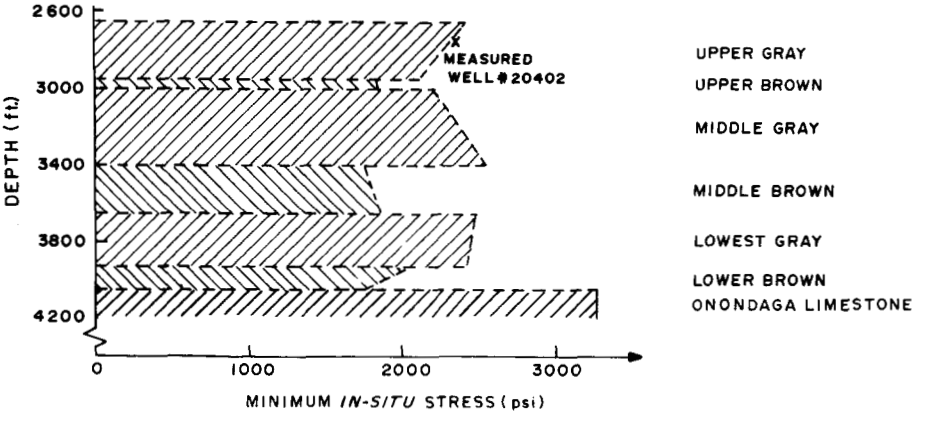

Figure 8c. Derived minimum *in situ* stresses correlated to measured stresses (x) at 2745 ft. in Well 20402.

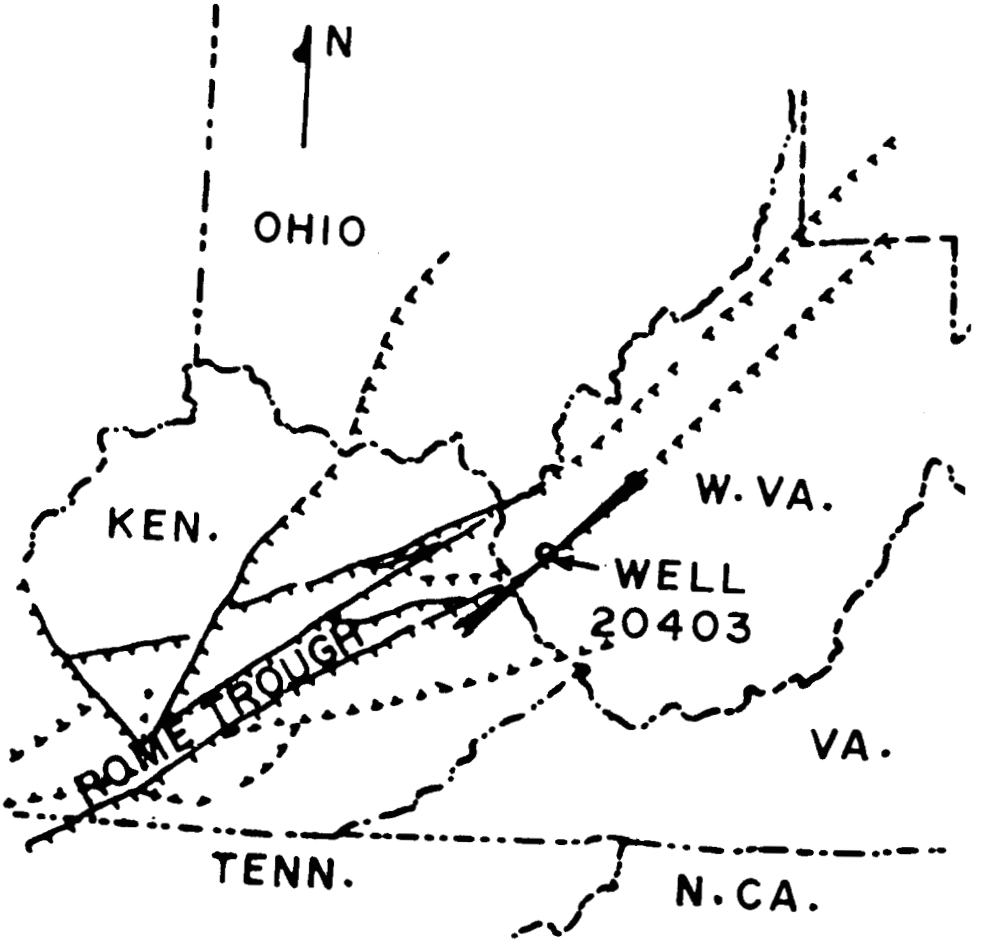

Figure 9. Basement structure of Kentucky-West Virginia adapted from Overbey (1976) with the direction of maximum horizontal stress at well 20403.

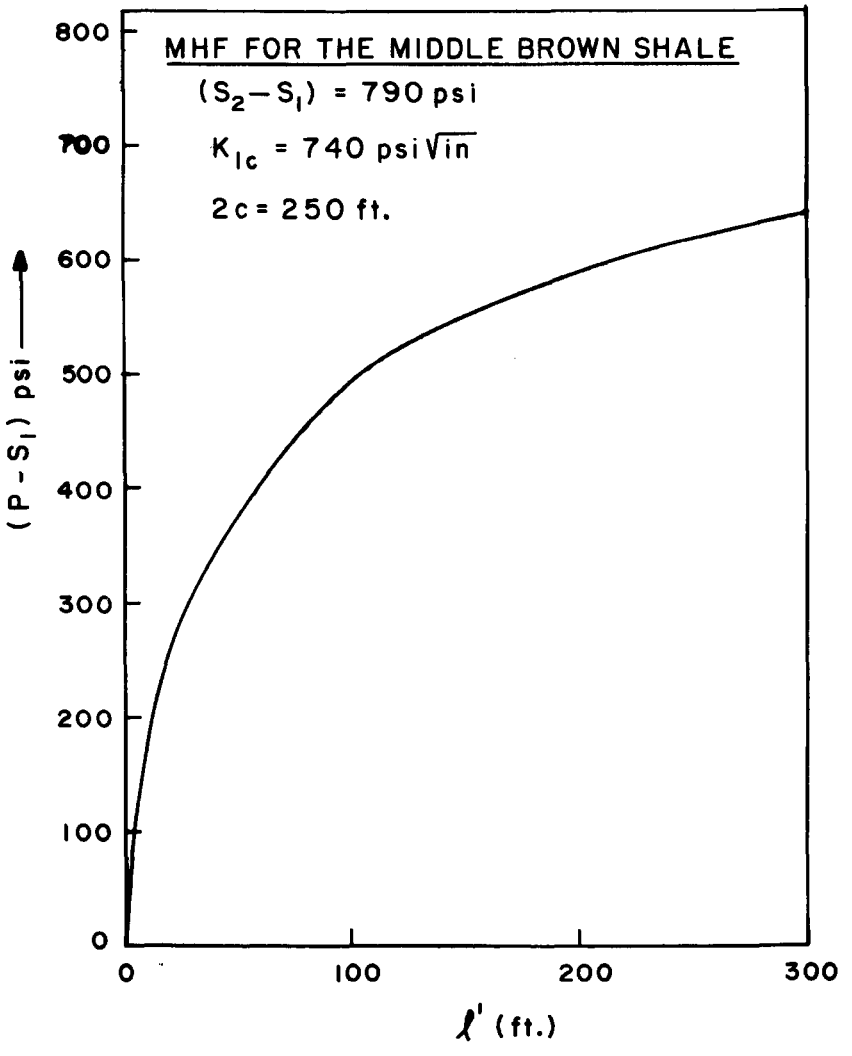

Figure 10. Fracture penetration into the Middle Gray Shale for fracture in the Middle Brown Shale.

TILT MONITORING OF MASSIVE HYDRAULIC FRACTURE EXPERIMENTS IN DEVONIAN SHALE OF WEST VIRGINIA

by

M. D. Wood, U.S. Geological Survey

ABSTRACT

Several Massive Hydraulic Fracture (MHF) experiments have been monitored with surface tiltmeter arrays in a variety of geologic settings. The principal objective of these experiments is to develop a useable technique for determination of azimuth and extent of hydraulic fractures. Signals from three MHF experiments in the Wattenberg, Colorado gas field at depths approaching 10000 feet have been reasonably explained by a simple dislocation model. Determinations of the spatial geometry were in accord with other available information. Comparable results are lacking from three MHF experiments monitored at half the depth in a Devonian shale section in West Virginia. Neither the shape of the response curves nor their amplitudes agree with a simple model of a biwinged, propagating fracture yet there are signals that correlate with variations of injection rates and driving pressures. Lack of well-defined signals across the tiltmeter array for all these experiments suggests that the fracture failed to attain significant design length and/or a preexisting fracture system was encountered that permitted disposal of the fracture fluid and proppant without sufficient deformation to generate a tilt signal. Synthesis of these data with other surface monitoring experiments, post-fracture evaluation and measurements in the wellbore may resolve this uncertainty.

*Paper not available at time of publication

RESULTS FROM A MHF SURFACE ELECTRICAL POTENTIAL MAPPING EXPERIMENT

Carl L. Schuster
Leon J. Keck
Sandia Laboratories
Albuquerque, New Mexico

ABSTRACT

Sandia Laboratories has developed a surface electrical potential system for remotely determining the azimuthal orientation of massive hydraulic fractures. The basis of the system is to use the fracture well as a current electrode which changes geometry as the conductive fluid is pumped out into the formation. This results in a changing electric potential field at the surface which is measured radially around the well. The system was deployed for a MHF experiment with Columbia Gas in the Devonian Shale during August 1976 in Lincoln County, West Virginia. Several operational problems during the two days of fracturing somewhat impaired the data. Potential changes during the pumping did indicate fracture growth; however, the data did not give a clear indication as to its orientation. A screen-out that occurred at the end of the first day's pumping did produce some interesting potential changes.

INTRODUCTION

Several papers presented at the Devonian Shale Production and Potential Symposium indicate a large recoverable natural gas supply could be established from the Devonian shale if an economic means of stimulation could be developed.[1] Several methods of developing these reserves are being attempted with one technique being the use of massive hydraulic fracture stimulation. The development of these reservoirs will require that the fracturing techniques be understood and an accurate knowledge of their dimensions, orientations, and characteristics be measured. Early attempts were made by Sandia Laboratories to determine fracture parameters in the Pinedale field in Wyoming.[2] These early experiments indicated the value of the surface electrical mapping technique and resulted in the system being developed and fielded by Sandia for obtaining fracture data. The system was developed over the 1974-1975 time frame and completed early in 1976 with a completely redesigned and improved electronic system. This improved system was deployed for a Devonian shale MHF experiment in July and August of 1976. Data were recorded for two days of a MHF experiment and the analysis of these data are presented in this paper. Additional experiments have been conducted in the western tight gas sands using this system with good results. Fracture growth period and fracture orientation have been detected on several experiments. The results from the Devonian shale experiment conducted in Lincoln County, West Virginia however do not give a clear indication of fracture orientation probably because of a much shorter horizontal fracture length.

ELECTRICAL DATA SYSTEM

The electrical potential data system contains three sub-systems: 1) a current generator, 2) the surface potential measurement system, and 3) the computer and data control system. The current generator system contains the necessary equipment for

generating current pulses that are injected between the fracture well and a remote well casing. The fracture well acts as one of the current electrodes which during the course of the fracturing experiment will change its geometry. This change in geometry is reflected in a changing potential pattern at the surface. The potential measurement system consists of 24 sub-systems for measuring the potential on radials located every 15° around the fracture well. These potentials are multiplexed together and brought into the computer system which records the potentials for each of the 24 locations. Figure 1 is a layout of the surface potential system that was used in Lincoln County, West Virginia for the fracture on Columbia's 20401. For this experiment the radial locations were 500 ft. and 3000 ft. on 15° spacings. The current return well was located approximately two miles north, 30° east from the frac well. Data were collected approximately every two minutes starting from before fracture initiation until an hour after the shut-down on the first frac day. A complete electrical description of the system will not be given here as it is contained in reference 3.

MATHEMATICAL ANALYSIS

An extensive effort has taken place to model the well casing and fluid-filled fracture as a current electrode with the resulting electrical potential field and changes that occur at the surface. Initial modeling effort was to assume the well casing and fluid to be perfectly conductive and to act as line sources for current in an infinite, homogeneous medium. The potential changes at the surface were then calculated based upon the changing geometry of the current electrode. Because of the limitations imposed by this constrained model, a second effort was undertaken that utilized the Green's function integral approach.[4,5] Since these have been reported on extensively, this paper will only summarize the results from those papers. The schematic layout used for the model is shown in Figure 2. The fracture length, height, and depth can all be adjusted in the model as well as the radius for the two potential measuring points. Figure 3 shows the results of the potential changes around the frac well for four different fracture ratios. Curve A is for a fracture that is perfectly asymmetrical; that is, both wings are of equal length and curve C is for a 25%-75% fracture where one fracture length is 75% of the total. As can be seen in Figure 3 the asymmetric nature of these curves allows for both the fracture orientation to be determined and also the asymmetry of the fracture. Data that are basically two cycles in nature going around the fracture well indicate a symmetrical fracture. When these data become one cycle then it indicates a fracture that is more asymmetrical. Both types of data have been collected on other experiments.[6]

EXPERIMENT DESCRIPTION

On August 3 and 4, Sandia participated in a MHF experiment with Columbia Gas in Lincoln County, West Virginia. The fracture well was Columbia's well 20401 and was to be fractured as part of a jointly funded ERDA/industry project with the Morgantown Energy Research Center being the technical project office. Sandia's participation was directed at evaluating the surface electrical potential technique for determining fracture orientation in a Devonian shale experiment.

The surface array was installed with the inter-radials located at 500 ft. and the outer radials at 3000 ft. radially every 15° around the fracture well. Figure 4 shows the topography of the area and the wells of interest. Well 5420 was the current return well and was located approximately two miles to the north-northeast. Installing the array was most tedious as can be seen by the extreme hilly topography. The site was occupied by several herds of cattle and also several roads had to be crossed for the installation which caused considerable trouble with the potential wires being broken. During the course of the experiment several wires were broken and had to be replaced causing loss of data during these periods.

EXPERIMENT RESULTS

On August 3, the main fracture treatment was started. Fourteen perforations had been emplaced between 3788 ft. and 3860 ft. of depth and the formation had been broken down prior to the main frac date. Two percent KCl had been added to the frac fluid to increase its conductivity for the electrical potential test. After approximately 460,000 gallons of fluid had been pumped, a screen-out occurred which

terminated pumping on August 3. On August 4, additional perforations were placed and pumping was resumed. A total of 506,000 gallons and 930,000 pounds of proppant was placed into the fracture well in the two days of pumping.

The surface electrical potential data collected during the fracture has been thoroughly analyzed. An example of how the fracture orientation has been determined on previous experiments in the Western Tight Gas Sands Program is illustrated in Figure 5.[7] This data was collected during an AMOCO experiment in the Wattenberg area northeast of Denver, Colorado. The data demonstrates the progressive growth of a fracture oriented primarily in the northwest direction with the minor fracture axis extending to the southeast. The four curves indicate the fracture growth for each one-fourth of the pumping interval. An analogous type of presentation cannot be made for the data collected during the Devonian shale experiment. Throughout the entire test day there were major changes in the potential field as illustrated by the data plotted from one of the radials as shown in Figure 6. (However, these major changes were not consistent enough to show the fracture orientation. The man-made and natural hazards i.e., cows and cars causing broken radial wires precluded obtaining sufficient data to see any asymmetry in the data being plotted around the fracture well.) Changes that did occur in the potential field were essentially uniform around the fracture well and could not be discerned above the noise level that was present. This lack of determination is probably caused by the lack of extensive horizontal growth in the fracture. This could be caused by the fracture obtaining a greater vertical dimension or by filling of existing fractures close to the wellbore.

The fracture growth that was recognized did occur during the first three to four hours of pumping. The phenomena of early fracture growth had been seen on several previous experiments. The decreasing potential indicates that the fracture area is growing. As can be seen on Figure 6 the potential decreases from the start of pumping at 8:00 until approximately 12:00 at which time the fracture growth seems to level out and remain constant until 15:00. The potential changes that occurred between 15:00 and 16:00 hours are a direct result of the screen-out that occurred. All radials showed similar types of potential changes during the screen-out. The potential changes for one of the radials are shown in Figure 7 in an expanded time and voltage scale. In Figure 7 the region A is the time of increasing pressure and decreasing flow resulting from the original screen-out. Region B is a period of temporary shut-down in the fracturing operation and Region C is a period of pressure surging in an attempt to reestablish flow into the formation. The increase in the potentials during the screen-out could indicate that the fracture tip had closed when fluid flow in the main fracture was stopped. Several attempts were made to reinitiate flow into the fracture by pressure surges (Region C) at the wellhead. These surges evidently resulted in the tip being opened and closed and the potential increasing and decreasing during that time.

The potential change caused by this fracture tip phenomena when examined radially around the fracture well could also give an indication of the fracture orientation. The percentage change in potential from before-to-after screen-out was approximately 4-1/2%. Figure 8 shows the normalized percentage change from before-to-after screen-out plotted radially around the fracture well. The asymmetrical change around the well is a little over ±1%. It is not clear whether this change is due to fracture geometry changing or as a result of the electrical noise. The loss of data on the radial at zero degrees also causes some uncertainity. If the change that is seen is a result of the fracture orientation, then major axis would apparently be towards the west with the minor fracture axis oriented to the east.

One method of enhancing the surface potential data that has produced the results previously discussed in the Wattenberg experiments was to have an open hole completion with a downhole current probe in the fracture well. This technique allows for the current to be introduced directly into the frac fluid and enhance the changes seen at the surface. Future experiments in the Devonian shale should probably rely upon this method for enhancement of the surface potential data.

CONCLUSIONS

The surface electrical potential technique did show fracture growth being created as it is reflected on the surface by a reducing potential. However, the reducing potential did not show an asymmetrical shape which would indicate fracture orientation. The screen-out which occurred at the end of the first day of pumping caused some rather unique potential changes at the surface probably caused by the fracture tip closing. These changes, however, were not asymmetrical enough to allow the fracture orientation to be determined. Evidently the fracture length to depth ratio was not large enough for the fracture to appear as a horizontal line. This could be caused by the fracture growth extending vertically or downward and causing the fracture to appear more as a sphere from the surface than as a line source.

REFERENCES

1. Devonian Shale Production and Potential Proceedings of the Seventh Appalachian Petroleum Geology Symposium, Morgantown, West Virginia, March 1-4, 1976.
2. Power, D. V., Schuster, C. L., Hay, R. G., and Twombly, J.: "Detection of Hydraulic Fracture Orientation and Dimensions in Cased Wells," SPE 5626, presented at the SPE 50th Annual Fall Meeting, Dallas, Texas, September 28-October 1, 1975.
3. Keck, L. J. and Seavey, R. W.: "Instrumentation System for Massive Hydraulic Fracture Mapping," SAND-77-0195, Printed April 1977.
4. Bartel, L. C., McCAnn, R. P., and Keck, L. J.: "Use of Potential Gradients in Massive Hydraulic Fracture Mapping and Characterization," SPE 6090, presented at the SPE 51st Annual Fall Meeting in New Orleans, Louisiana, October 4-6, 1976
5. Bartel, L. C.: "Model Calculations of the Potential Gradients Used in Massive Hydraulic Fracture Mapping and Characterization," presented at the 46th Annual International Meeting of the Society of Exploration Geophysicists, Houston, Texas, October 24-28, 1976.
6. McCann, R. P., Hay, R. G., and Bartel, L. C.: "Massive Hydraulic Fracture Mapping and Characterization Program: First Annual Report - August 1975 through July 1976," SAND-77-0286, Printed June 1977.
7. McCann, R. P., Bartel, L. C., and Keck, L. J.: "Massive Hydraulic Fracture Mapping and Characterization Program - Surface Potential Data for Wattenberg '75-'76 Experiments," SAND-77-0396, Printed August 1977.

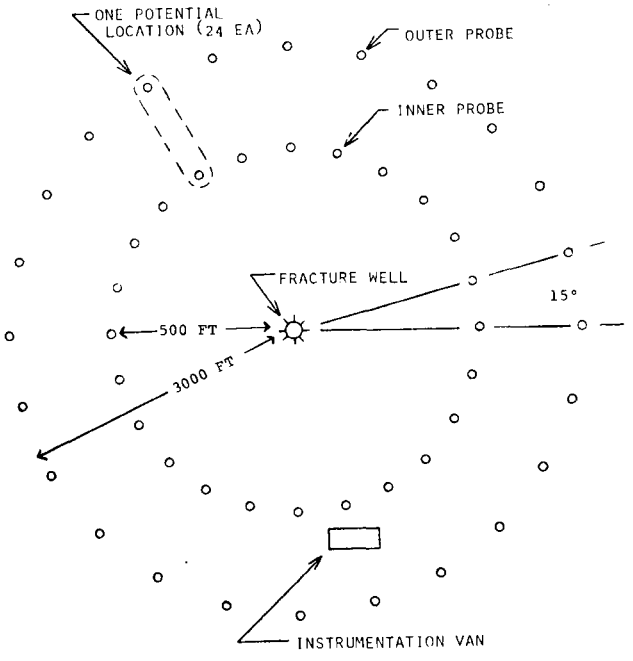

Figure 1. Layout for Surface Potential Instrumentation

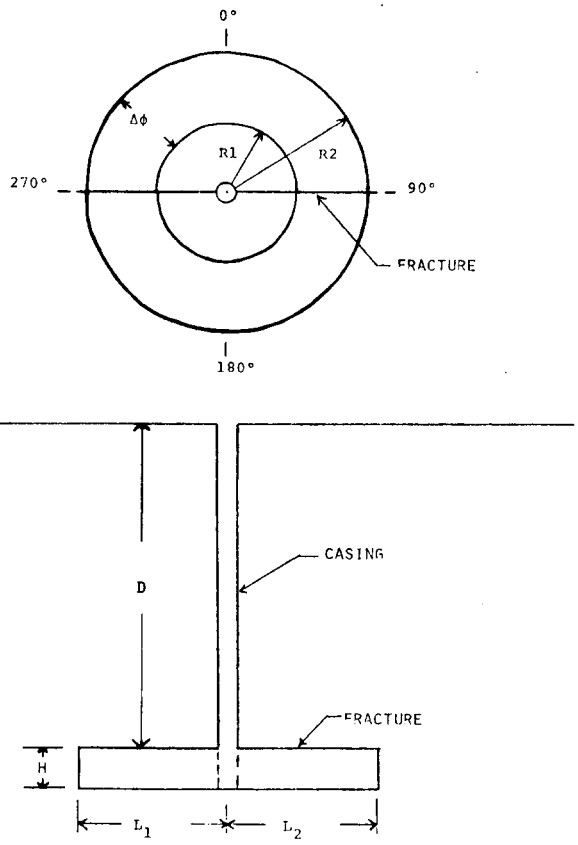

Figure 2. Schematic Layout for Model

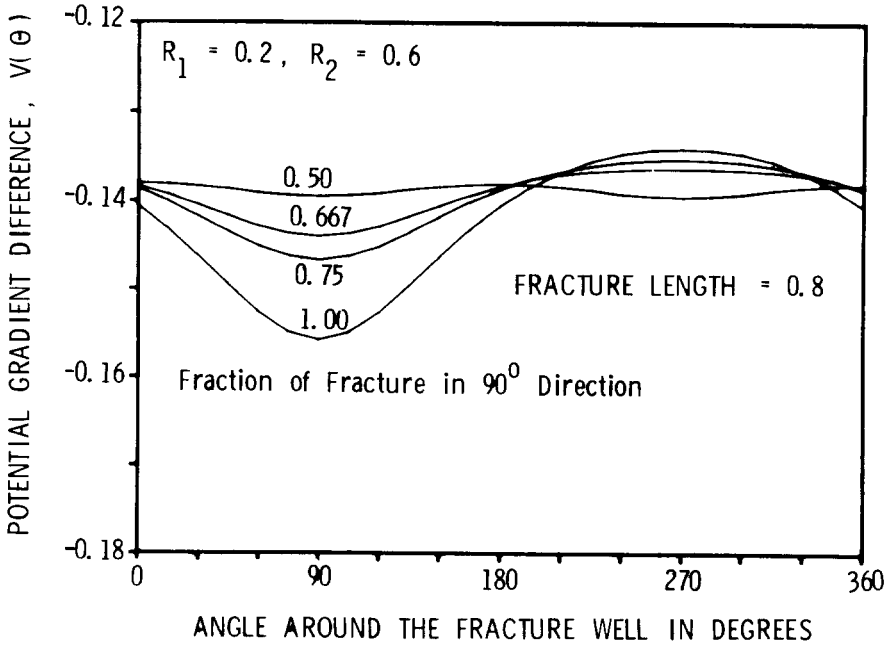

Figure 3. Potential Changes for Asymmetric Fractures

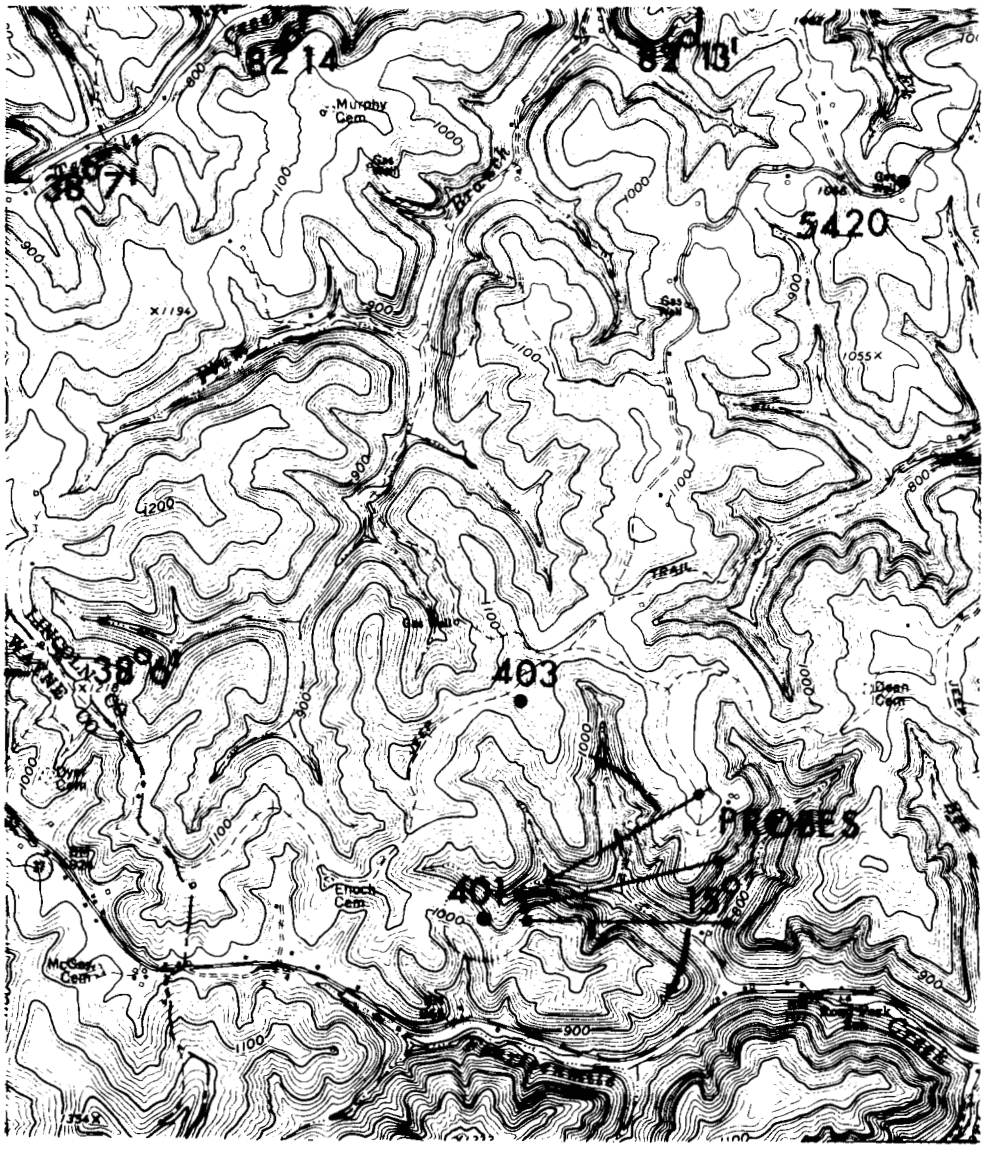

Scale 1 inch = 2000 feet

Figure 4. Columbia MHF Experiment Layout.

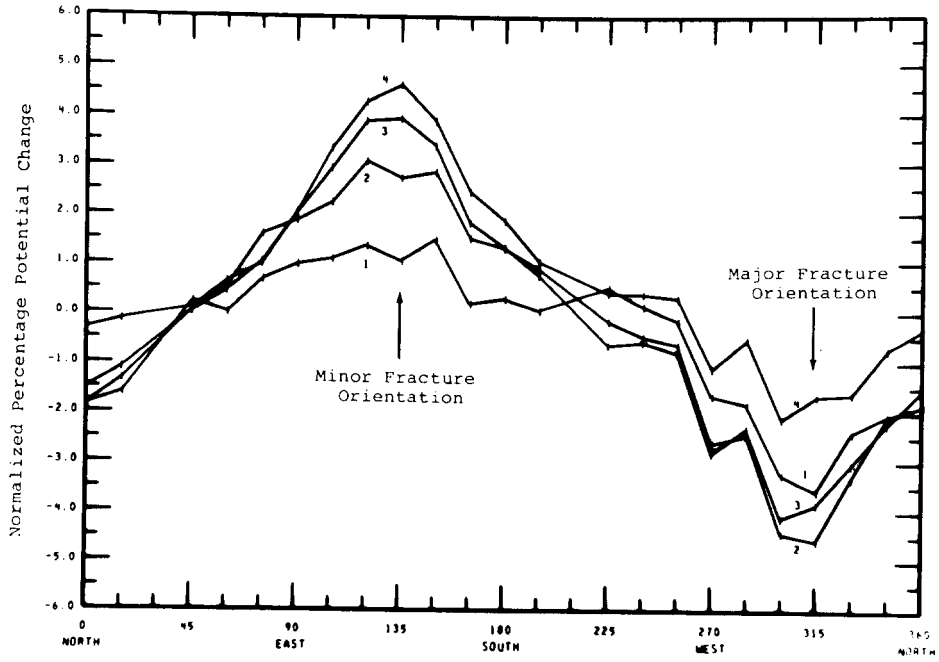

Figure 5. Progressive Growth of Fracture as a Function of Direction for a Wattenberg Fracture

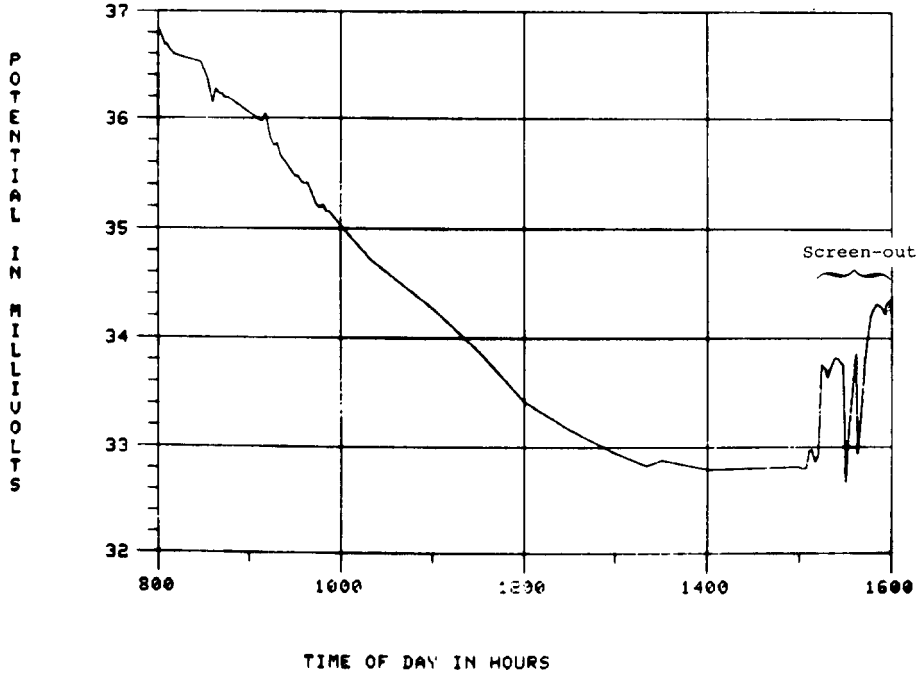

Figure 6. Potential for Radial A-3 on August 3

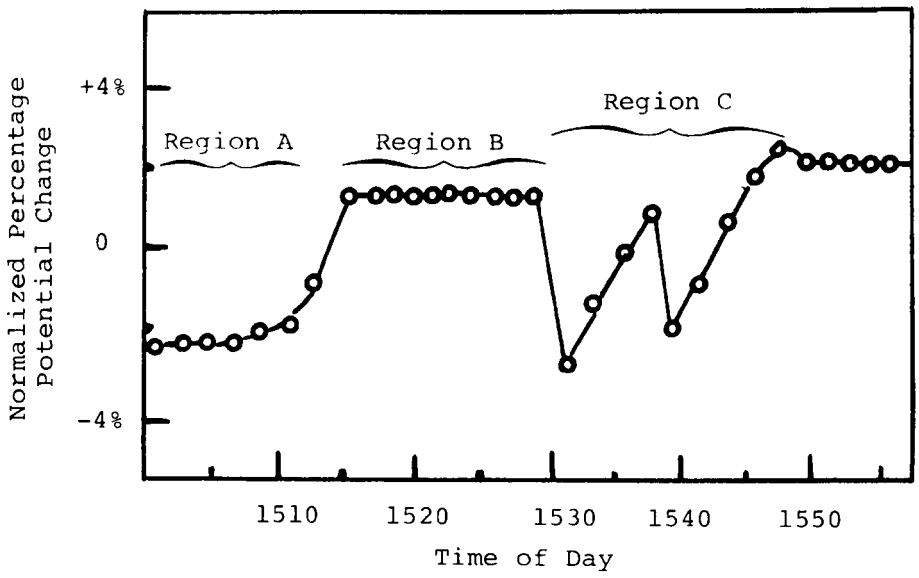

Figure 7. Potential Changes During Screen-Out

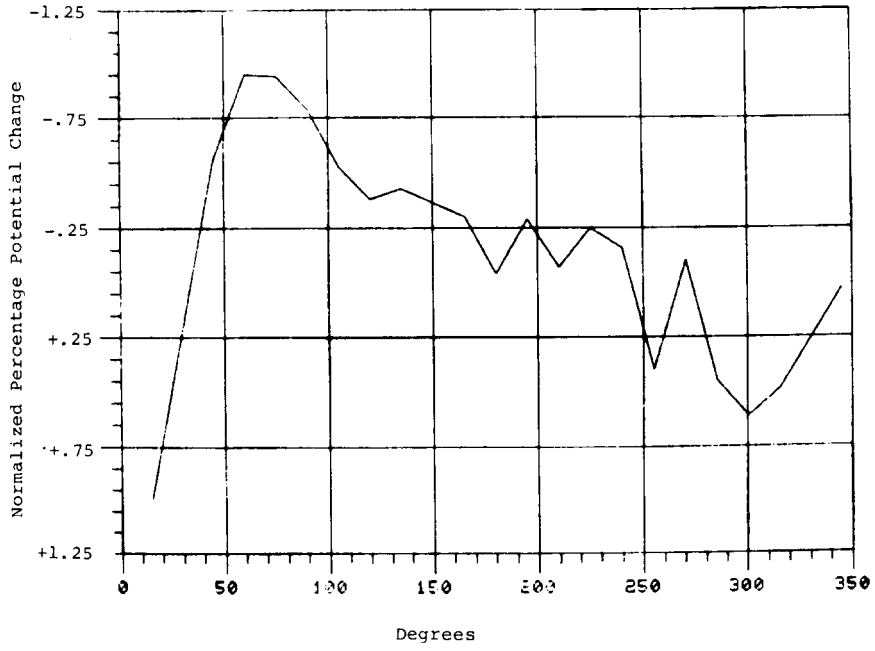

Figure 8. Potential Change Resulting from Screen-out

PALEOCURRENT SYSTEMS IN SHALY BASINS: PRELIMINARY RESULTS FOR APPALACHIAN BASIN (UPPER DEVONIAN)

by

R. C. Kepferle[1], Paul Lundegard[2],
J. B. Maynard[3], Paul Edwin Potter[4],
W. A. Pryor[4], Neil Samuels[2],
and Frederick J. Schauf[2]

ABSTRACT

Studies of paleocurrent systems in shaly basins have been very few; they can be made (1) by examining the paleocurrent structures of the siltstones, sandstones, and carbonate deposits that are minor constituents of most shaly basins; (2) possibly by studying shale fabrics as seen by the Scanning Electron Microscope and other methods; and (3) by mapping scalar variables such as the C_{13}/C_{12} ratio (marine versus terrestrial carbon) within the shale itself.

Once the methodology for such studies has been improved, we can in turn expect improvements in:

(1) relating one argillaceous subfacies to another,
(2) relating argillaceous mineral associations to another,
(3) explaining textural gradients within the basin,
(4) locating shorelines and inlets and defining overall basin shape and its paleocirculation,
(5) defining environments of deposition, and
(6) explaining possible variation of terrestrial to marine carbon (gas versus oil) within a basin.

A summer's fieldwork studying outcrops and oriented cores of the Upper Devonian shale sequence of the Appalachian basin illustrates many of the above dividends that result from paleocurrent studies of shaly basins--one of sedimentology's unexploited fields.

INTRODUCTION

Paleocurrent maps have become common tools for basin analysis. From these maps one can determine the probable source of sediments and the manner in which the basin was filled. In combination with stratigraphy, petrology and paleontology, a reasonable depositional model can be constructed for the basin. This model, in turn, can be used to help predict the location and trend of the different facies within a basin.

Examples of paleocurrent studies in shaly basins are few because paleocurrent markers in shaly basins are both less abundant and more subtle than in most terrigenous and carbonate basins. However, shaly basins commonly contain sufficient coarser grained siltstone and sandstone interbeds and fossil debris to infer paleocurrent directions for the more competent currents. In addition, fabric studies are needed to evaluate the paleocurrent significance of oriented mineral grains, nodules, microfossils, and plant debris such as the disc-like microfossil Tasmanites, and fine carbonaceous shreds.

---

[1]U. S. Geological Survey, Cincinnati, Ohio
[2]Graduate Student, University of Cincinnati
[3]Associate Professor of Geology, University of Cincinnati
[4]Professor of Geology, University of Cincinnati

PURPOSE AND METHOD

This paper describes some of the methods we used and the problems we have met, presents some of the results, and suggests some conclusions. This is part of an ongoing analysis of the depositional patterns in the Devonian shale sequence in the Appalachian basin.

In a search of the published literature we found that paleocurrent trends in the Appalachian basin have been combined with facies analyses for part of the Silurian sequence (Yeakel, 1959, fig. 58) and the Lower Mississippian sequence (de Witt, 1951; Pepper and others, 1954; Pelletier, 1958, fig. 16). Devonian alluvial paleocurrents have been studied by McIver (1961, 1970) and Burtner (1963) in the Catskill facies. Devonian paleocurrents from marine rocks have been published for New York (Colton, 1967), Pennsylvania (Nagle, 1967, figs. 5-7) and northeastern Tennessee and Virginia (Jones and Dennison, 1970).

Serious gaps in available data are readily apparent. A field program to fill these gaps was carried out in the summer of 1977. The main participants of this part of the program were Neil Samuels, Paul Lundegard, and Fred Schauf.

The objective of the study for the summer was to map paleocurrent indicators in Devonian outcrops of western New York, western Pennsylvania, Ohio, eastern Kentucky, northeastern Tennessee, and most of Virginia and West Virginia. Samuels and Schauf covered the northern part of the outcrop belt; Lundegard, the southeastern part. Normally, one to three exposures per 7-1/2 minute quadrangle were sampled along the outcrop belt. Also inspected for paleocurrent indicators were five cores available at the Morgantown Energy Research Center. These included cores from wells drilled in Carrol and Washington Counties, Ohio; Martin County, Kentucky; Wise County, Virginia; and Lincoln County, West Virginia.

In the field, we described the outcrop, emphasizing the lithologies present, their sequence, and the paleocurrents of each, and transferred each day's work to a standard form. At each outcrop, the checklist of questions included:

(1) How many paleocurrent indicators are present?

(2) How do they correlate with one another?

(3) How do the different structures correlate with different lithologies, fossil and/or concretions?

(4) What controls fossil orientations?

(5) Can we recognize the stratigraphic unit of previous workers?

In the office the results were plotted on the AMS one- by two-degree sheets (scale 1:250,000). Statistical treatment and grouping of data followed the procedure outlined by Potter and Pettijohn (1963, Ch. 10).

RESULTS

In spite of the variety of paleocurrent indicators present, the most common and most reliable are sole marks on the bottom of siltstone and sandstone beds found within the shale sequence. The most commonly used of these sole marks are flutes and grooves. Flutes give a vectoral sense to the current that formed them, whereas grooves give merely a line of movement.

The data gathered in the course of reconnaissance, stratigraphic and areal mapping studies by all participants are summarized in figures 1 through 4. Detailed maps (figs. 1, 2, and 3) show the general uniformity of the paleocurrent system both at the northern side of the basin in New York, Pennsylvania, and Ohio (figs. 1 and 2) and along its southern side in Virginia, West Virginia (fig. 3) and northeastern Tennessee. These results harmonize well with the earlier study by McIver (1961, 1970) of the very sandy Upper Devonian in Pennsylvania, Maryland and south-central New York. Here, and where we studied the paleocurrents in western New York, Pennsylvania and northern Ohio, as well

as in West Virginia, Virginia and Tennessee (fig. 4), the paleocurrents are oriented normal and "down-dip" to Upper Devonian isopachs shown by de Witt and others (1975). Our outcrop studies are also generally in accord with the data we have collected from the oriented cores, although much more work needs to be done on the cores.

SIGNIFICANCE

The Upper Devonian rocks, based on the studies of McIver and our own, were deposited by a very uniform system of paleocurrents when viewed basin-wide. The flow from east to west is uniform for all the sandy and silty facies of the Upper Devonian. The currents are indicated by crossbedding in far eastern Pennsylvania and New York and by solemarks in turbidites distal to the west, well into West Virginia and Ohio. Because the distal turbidites are interbedded with the black (gas producing) and gray shale of the Upper Devonian sequence, these shales most probably had a similar pattern of west-trending paleocurrents. Evidence supporting this inference is provided by Jones and Dennison (1970), who measured fossil orientation in the Chattanooga Shale in northeastern Tennessee.

Additional studies of paleocurrents from oriented cores, combined with careful facies mapping of the internal stratigraphic units of the Upper Devonian in western Pennsylvania, eastern Ohio, West Virginia and eastern Kentucky should help us better predict and understand gas-producing trends in the Upper Devonian, especially if these trends are related to primary deposition rather than later fracturing. The present paleocurrent studies should also be most helpful in understanding the distribution of both marine and terrestrial carbon in the shale.

For the future we plan to:

(1) better relate the fossil and clay mineral fabrics of the shales to the paleocurrents of their interbedded siltstones and sandstones, and
(2) study the paleocurrent system of the "pure shale" facies where it is thinner and more distal in central Ohio and along the outcrop in parts of Kentucky and Tennessee.

NOMENCLATURE

Fabric -- The spatial arrangement of the constituents (grains, fossils, clay minerals, etc.) of a rock.

Lingula -- A small marine bivalve with a smooth phosphatic shell, locally common in the Devonian shale.

Paleocirculation -- The inferred circulation system of an ancient sedimentary basin.

Paleocurrent -- A current direction recognized in ancient rocks from sedimentary structures, fossil orientation, or fabric.

Sedimentology -- The study of the origin and economic potential of sediments, modern and ancient.

Tasmanites -- The generic name given resinous, very small, semispherical spore-like organic remains, usually flattened to discs less than 1 mm in diameter, locally abundant in Devonian shale.

REFERENCES

Burtner, R. L. Sediment Dispersal Patterns within the Catskill Facies of Southeastern New York and Northeastern Pennsylvania. Pennsylvania Geol. Survey, General Geology Rept. G39, 1963, pp. 7-23.

Colton, G. W. Orientation of Carbonate Concretions in the Upper Devonian of New York. U.S. Geol. Survey Prof. Paper 575-B, 1967, pp. B57-B59.

de Witt, W., Jr. Stratigraphy of the Berea Sandstone and Associated Rocks in Northeastern Ohio and Northwestern Pennsylvania. Geol. Soc. America Bull., v. 62, 1951, pp. 1347-1370.

de Witt, W., Jr., W. J. Perry, Jr., and L. G. Wallace. Oil and Gas Data from Devonian and Silurian Rocks in the Appalachian Basin. U. S. Geol. Survey Misc. Inv. Map I-917-B, 1975, 4 sheets.

Jones, M. L. and J. M. Dennison. Oriented Fossils as Paleocurrent Indicators in Paleozoic Lutites of Southern Appalachians. J. Sediment. Petrology, v. 40, 1970, pp. 642-644.

McIver, N. L. Sedimentation of the Upper Devonian Marine Sediments of the Central Appalachians. Unpub. Ph.D. Thesis, Johns Hopkins Univ., 1961, 530 pp.

_____. Appalachian Turbidites, Chapter 4. In G. W. Fisher and others, Editors, Studies of Appalachian Geology: Central and Southern. New York, John Wiley and Sons, Inc., 1970, pp. 69-81.

Nagle, J. S. Wave and Current Orientation of Shells. J. Sediment. Petrology, v. 37, 1967, pp. 1124-1138.

Pelletier, B. R. Pocono Paleocurrents in Pennsylvania and Maryland. Geol. Soc. America Bull., v. 69, 1958, pp. 1033-1064.

Pepper, J. F., W. de Witt, Jr., and D. F. Demarest. Geology of the Bedford Shale and Berea Sandstone in the Appalachian Basin. U. S. Geol. Survey Prof. Paper 359, 1954, 111 pp.

Potter, P. E., and F. J. Pettijohn. Paleocurrents and Basin Analysis. Heidelberg, Springer-Verlag, 1963, 296 pp., 30 pls.

Rowe, L. Sedimentary Environments of the Java Group (Upper Devonian) - A Three Dimensional Study. Unpub. Ph.D. Thesis, Univ. of Rochester, 1976, 192 pp.

Yeakel, L. S., Jr. Tuscarora, Juniata and Bald Eagle Paleocurrents and Paleogeography in the Central Appalachians. Geol. Soc. America Bull., v. 73, 1962, pp. 1515-1540.

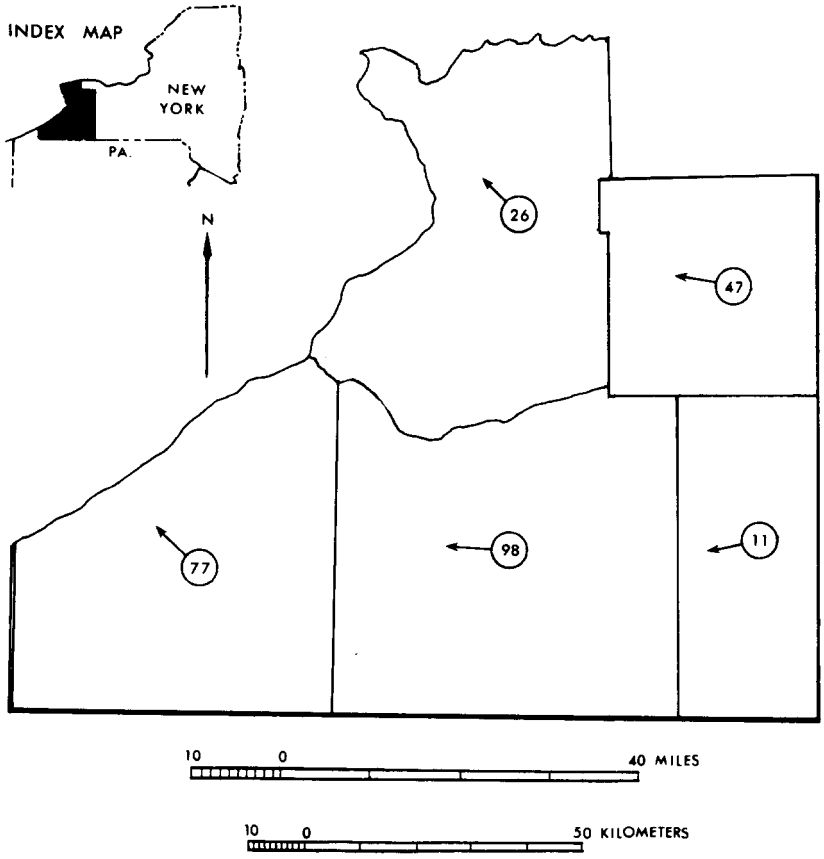

Figure 1.--Map showing vector means by county of Devonian paleocurrent data, western New York. Arrow indicates vector mean calculated for number of readings indicated by circled number. Two hundred fifty-nine observations.

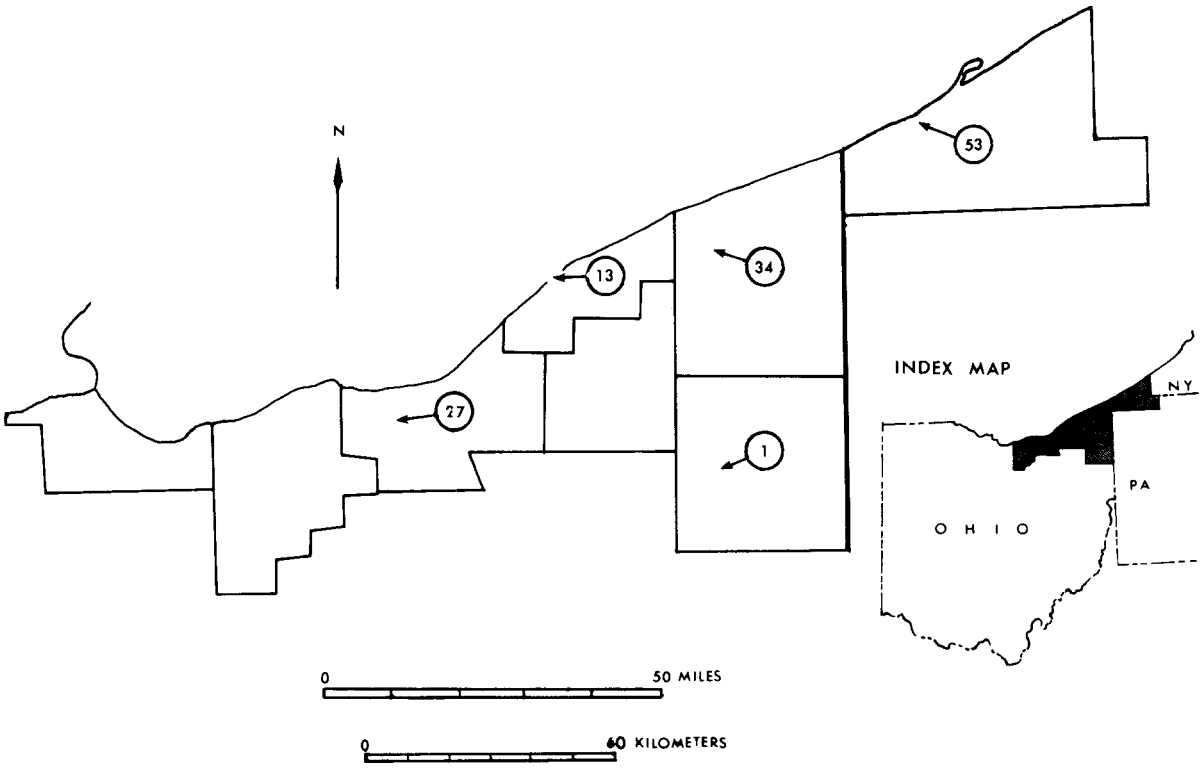

Figure 2.--Map showing vector means, by county, of Devonian paleocurrent data, northeast Ohio and Erie County, Pennsylvania. Arrow indicates vector mean, calculated on number of readings indicated by circled number. One hundred twenty-eight observations.

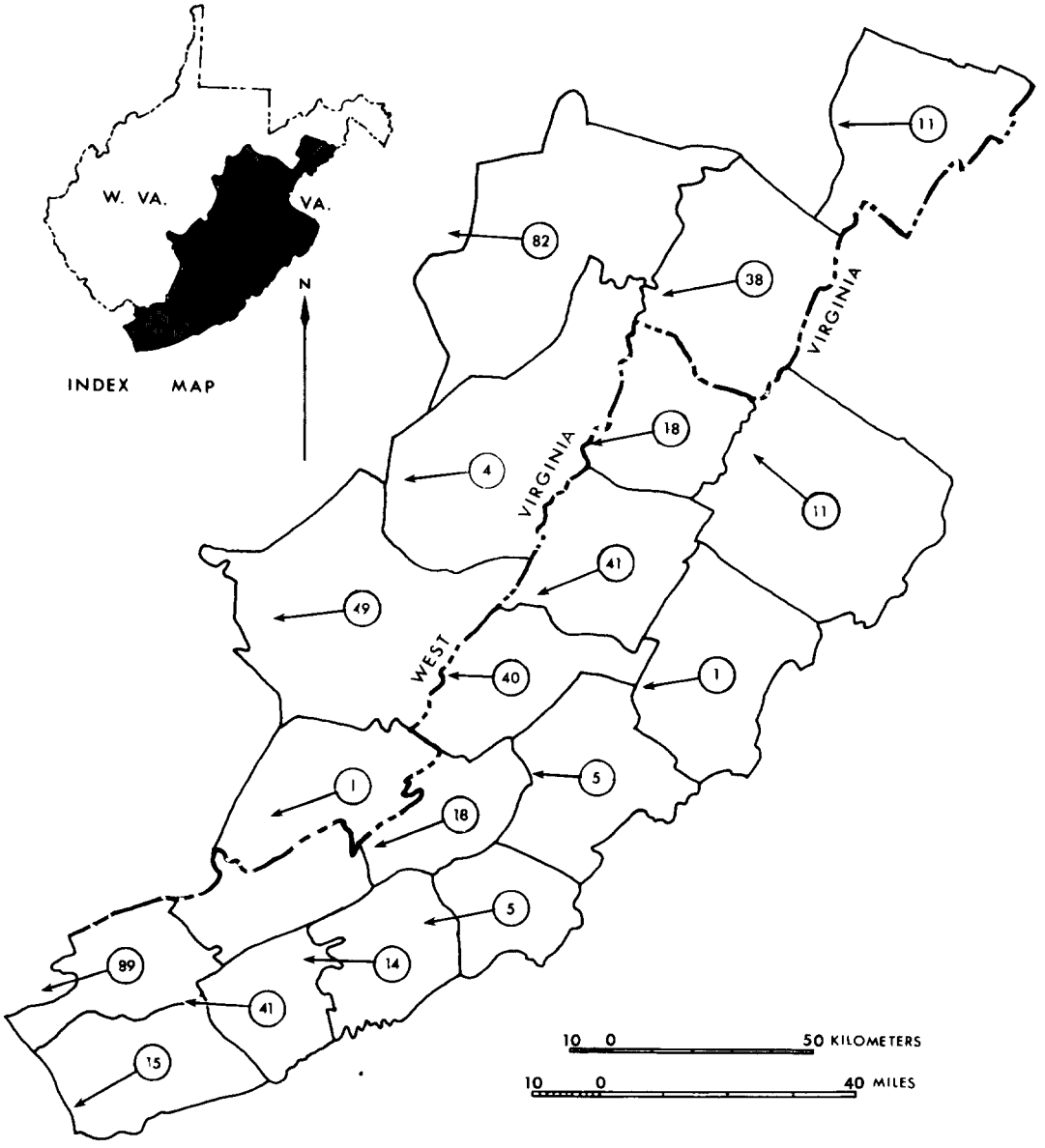

Figure 3.--Map showing vector means by county of Devonian paleocurrent data, western Virginia and adjacent West Virginia. Arrow indicates vector mean calculated for number of readings indicated by circled number. Four hundred eighty-three observations.

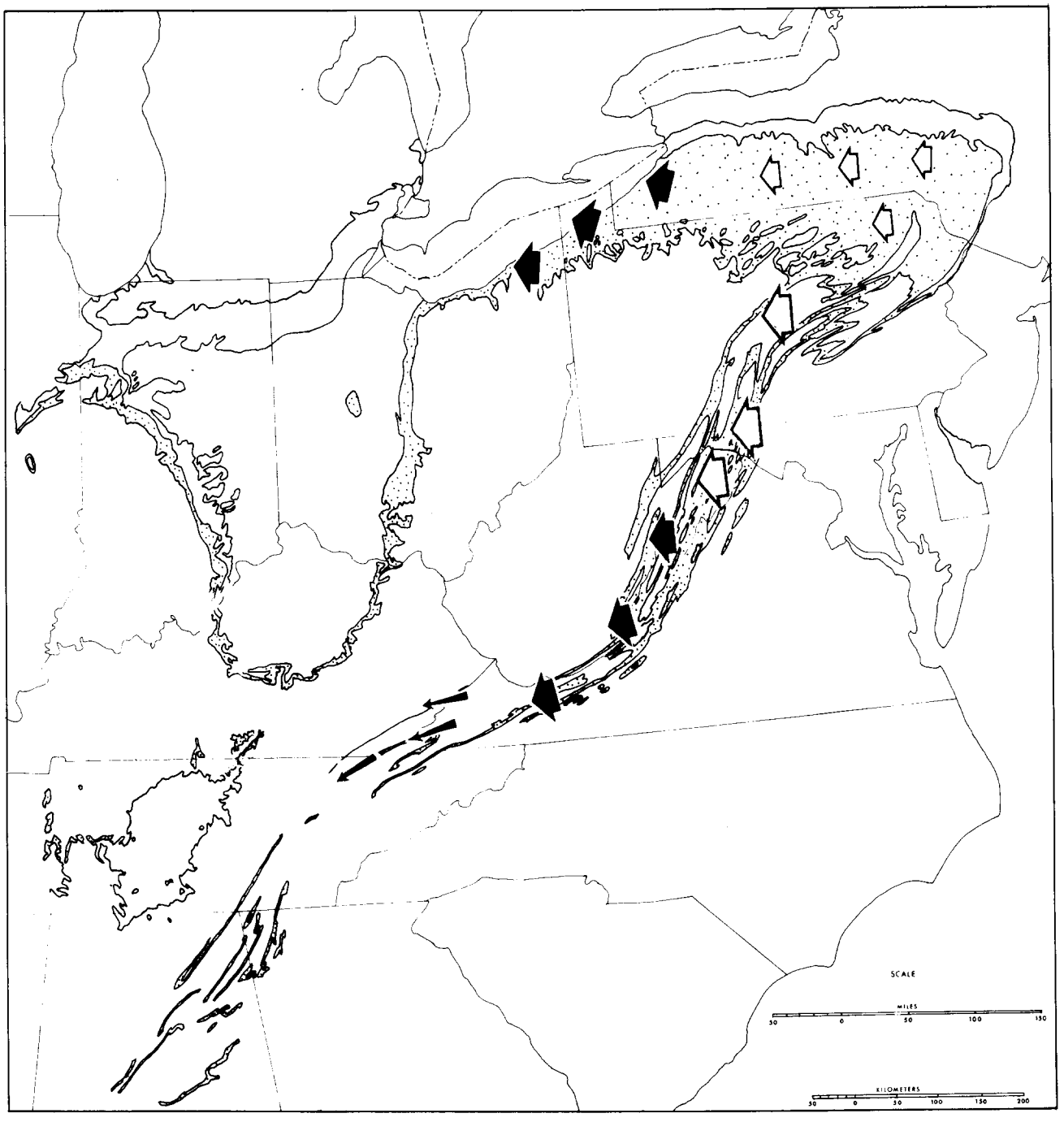

Figure 4.--Map of Appalachian Basin showing Upper (stippled) and Middle Devonian outcrop belt and summary of Devonian paleocurrents. Large solid arrows summarize data shown on figures 1, 2 and 3; open arrows summarize data from McIver (1970); slender arrows show paleocurrent data in southern Virginia.

STRESS TRAJECTORY SIMULATIONS ACROSS THE APPALACHIAN PLATEAU PROVINCE IN WEST VIRGINIA

Sunder H. Advani, West Virginia University
Hota V.S. GangaRao, West Virginia University
H. Y. Chang, West Virginia University
Claude S. Dean, Morgantown Energy Research Center
William K. Overbey, Jr., Morgantown Energy Research Center

ABSTRACT

Finite element model formulations for the simulation of stress trajectories across the Appalachian Plateau Province in West Virginia are given. Pertinent mechanisms responsible for re-orientation of the East-West principal stress pattern over the Rome Trough region are reviewed. In addition, numerical results delineating the effect of sub-structure properties on surface stresses and field stresses for the "buttress" and "slip" model formulations are presented. Finally, the applicability of the results to the identification of natural Devonian shale fracture zones and preferential zones for induced fracturing is discussed.

INTRODUCTION

Extensive research and development efforts are currently being devoted to stimulate the production of natural gas from Devonian and Mississipian Shales in the Appalachian, Illinois, and Michigan basins [1]. As an integral part of this effort, the Morgantown Energy Research Center is conducting the Eastern Gas Shales Project. The program elements of this project include (i) natural gas resource and recoverable reserve characterization and evaluation, (ii) development of improved recovery technology, and (iii) promotion of expanded commercial production. Several pertinent papers dealing with these elements were presented at the Seventh Appalachian Petroleum Geology Symposium [2].

Since gas production can be correlated with the extent and frequency of fracture systems, the determination of regional in situ stresses is imperative. The magnitudes of these stresses serve as fundamental diagnostic indicators of natural fracture zones and preferential zones for hydraulic or explosive fracturing. In this paper, the mechanism(s) responsible for re-orientation of the East-West principal stress pattern and stress magnitudes over the Rome Trough region are investigated by use of the finite element method.

MODEL FORMULATIONS

The postulated trajectory directions for the maximum surface in situ stress, from bore hole strain gage measurements and hydraulic fracturing, are revealed in Figure 1 [3]. The direction of the maximum principal stress, in the belt of the Rome Trough, is found to be parallel to the belt direction. This phenomenon, therefore, appears to be related to the basement faulting which formed the Rome Trough and the basement-cover interaction. The basement depth map of West Virginia provided by Kulander and Dean [4] is illustrated in Figure 2a with the Rome Trough region presumably forming a belt in the N40E direction across the Western Central region of West Virginia. A corresponding schematic of the basement faults and detached structure is shown in Figure 2b [5]. Two plane strain finite element models are formulated based on these considerations. Model I, shown in Figure 3a, simulates a generalized basement-cover system with one major step. The cover material is assumed to be homogeneous and isotropic for this model. Figure 3b illustrates Model II which

conforms to the actual stratigraphic detail of the formation and fault system (Figure 2b). The cross section of this model corresponds to Section AA in Figure 2a. Figure 4 reveals the selected stratigraphic distribution and material properties [6] for Model II.

The normal displacement at the basement-cover interface is assumed to be zero. The gravitational loading is taken to act vertically at each joint of the finite element structure. The normal horizontal stress specified on the selected vertical boundaries of the models includes the in situ tectonic stress and the Poisson effect $\sigma_{HORIZONTAL} = \sigma_{OB}\ \nu/(1-\nu)$.

Two fundamental types of boundary conditions, based on the assumed stress re-orientation mechanism, are chosen to investigate the stress responses for Models I and II. The first basic boundary condition representation is referred to as the "buttress" model formulation (Case A) with the specified horizontal stress being resisted, to a large extent, by the step(s). Figures 5a and 5b illustrate this case and boundary conditions for Models IA and IIA respectively. The second distinct boundary condition representation is designated as the "slip" formulation (Case B) since a specified vertical displacement is prescribed at the dominant basement fault region. The resulting stress re-distribution forms a basis for the mechanism governing re-orientation of the stresses. The slip model formulations Models IB and IIB are illustrated in figures 6a and 6b respectively.

MODEL SIMULATIONS, RESULTS, AND DISCUSSION

The NASTRAN computer program [7] is employed for the stress response computations. Since both models I and II are subjected to in-plane loading, membrane elements (CQDMEM) are used with total degrees of freedom of 462 and 1978 respectively. The in-situ tectonic stress, specified on the right hand of the vertical boundary, is taken arbitrarily to be 1000 psi (6.9 MPa) (Figures 5 and 6). The vertical slip magnitude for Models IB and IIB is selected to be 100 ft. (30.48m) and 10 ft (30.48m) respectively. The choice of the lower slip value for Model IIB is dictated by the unrealistic result trends obtained for this case when the value of 100 ft (30.48m) is used. The following results and discussion are based on the isotropic (Model I) and layered (Model II) finite element model simulations for the buttress (case A) and slip (case B) mechanistic formulations. Particular attention is devoted toward characterizing the horizontal stress values at the surface and stress concentrations and/or reliefs resulting from the fault zones. The stress contour magnitude can be converted to psi by multiplying the values by 6944.

MODEL I

Figures 7a and 7b reveal the simulated maximum horizontal stress contours for Models IA and IB. The general stress distribution trend for the two cases is defined in terms of the significantly influenced regimes in Figure 8. Zone A, at the surface (right of the fault), is subjected to a high compressive stress. A low tensile stress is developed in Zone B and Zone C is tectonically relaxed. The horizontal stress field on the top layer computed for both the cases reveals that its direction changes from N50°W on the right hand side of the step to N40°E on the left hand side. Zones D and E are under the influence of moderately high compressive stresses due to the fault discontinuity. Vertical stresses at different locations are generally distributed as a linear function of the depth except at Zones D and E in which low and high vertical stresses respectively are computed. The magnitude of the horizontal stresses at the base of the step for Models IA and IB differ by a factor of three. In Zone H, however, both models yield the same magnitude of stresses. A tensile zone is evident in region G for Model IB only.

Model II

Regional horizontal stress magnitudes (in the element I.D. region 501 to 2901)* for Models IIA and IIB are characterized in Figures 9 and 10 respectively. As expected, the numerical values (in regions removed from the fault zone) for the horizontal force components due to the tectonic action and overburden Poisson effect are proportional to the layer Young's Modulus and $\sigma_{OB}\ \nu/(1-\nu)$ respectively. Qualitative trends similar to those obtained in Model I are revealed. Zones A and B in Figure 11 are subjected to high horizontal stresses and region C developes a tensile stress for both cases. In addition, Zone D also manifests a tensile region for the slip Model IIB. Zone E to the right of the faults has a high horizontal compressive magnitude for Case A. For Case B, however, these stresses are relatively increased at the top of region E and relieved near the basement. The

*The I.D. region refers to the co-ordinate system in Figure 3b. For example, the last two digits correspond to the vertical co-ordinate and the first digit(s) corresponds to the horizontal co-ordinate.

portion to the left of the maximum slip point apparently acts as a cantilevered beam with tensile stresses increasing at the top and enlarging the tensile zone.

The maximum horizontal stress directions at the surface change by 90° at the basement fault 1 in Model IIA and basement fault 2 in Model IIB.

CONCLUSIONS AND RECOMMENDATION

The results of the finite element model simulations for Models I and II illustrate the pronounced effects of the buttress and slip mechanisms in altering the surface stress magnitudes and field stress trajectories. The re-orientation of the maximum surface in situ horizontal compressive stress, resulting from the tensile zones and relaxed stress states, is demonstrated for all the selected models in the region West of the Rome Trough. These results and concepts can therefore be applied to exploration areas such as the Cottageville site (lying West of the major fault) and thrust fault development sites such as the Burning Spring anticline where a wedge shaped lubricated salt zone is present.

The stress magnitudes for the litho-stratigraphic Model IIB are sensitive in terms of the prescribed vertical slip. A slip magnitude of 10 ft (3.048 m), for the Model II geometry and fault dimension, appears to be realistic. Computation of the relative stress contributors resulting from the buttress and slip mechanisms and delineation of the governing mechanism(s) requires additional geological field data and model simulations.

The stress responses computed here, when coupled with field data, serve as preliminary identifying high density natural fracture zones and/or zones for induced fracturing. For example, the tensile zones may be conducive to explosive fracturing techniques. The use of the finite method as a tool for computing in situ stress magnitudes and orientations for various geologic systems and induced fractures (coring, massive hydraulic fracturing) appears promising. These analytical investigations are currently in progress at West Virginia University.

ACKNOWLEDGMENTS

This work was performed for the Morgantown Energy Research Center under Contract No. EY-77-X-21-0368. Computer services were provided by the West Virginia Network for Educational Teleprocessing.

REFERENCES

1. "Research Progress Reviews," Morgantown Energy Research Center, U.S. ERDA, Morgantown, WV, June 1976.

2. "Devonian Shale Production and Potential," Proceedings Seventh Appalachian Petroleum Geology Symposium, Editors Shumaker R. C. and W. K. Overbey, Jr., MERC/SP-76/2, 1976.

3. Overbey, W. K., Jr., "Effect of in situ Stress on Induced Fractures," Proceedings Seventh Appalachian Petroleum Geology Symposium, MERC/SP-76/2, 1976.

4. Kulander, B. R. and S. L. Dean, "Gravity, Magnetics, and Structure of Allegheny Plateau - Western Valley and Ridge, West Virginia and Adjacent States," West Virginia Geological Survey Publication, 87 pages, In Press.

5. Shoemaker, R. C., Private Communications, 1977.

6. "Handbook of Physical Constants," Editor Clark, S. P. Jr., Memoir 97, Geological Society of America, 1966.

7. McNeal, R. N., "NASTRAN Theoretical Manual,"NASA CR NA SJ-10049, 1969.

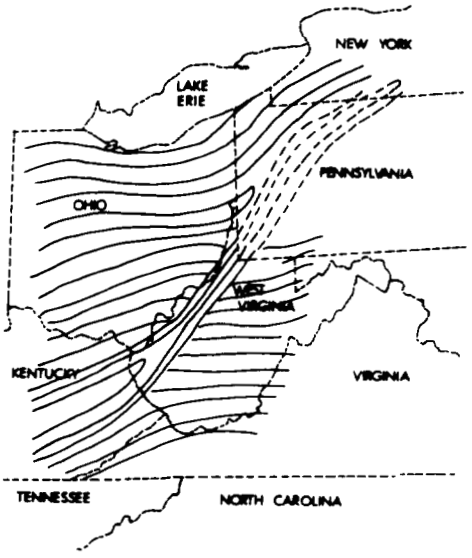

Figure 1. Postulated Stress Trajectories for the Central Appalachian Region [3].

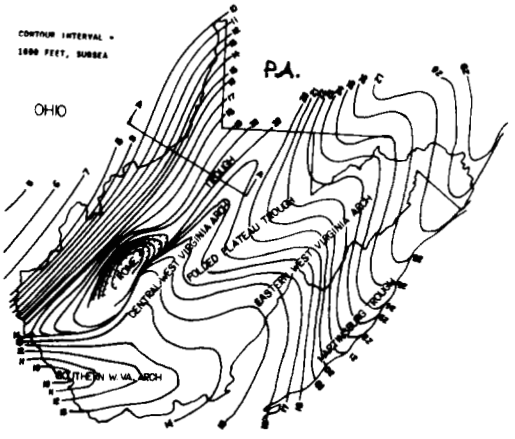

Figure 2a. Basement depth map of West Virginia [4].

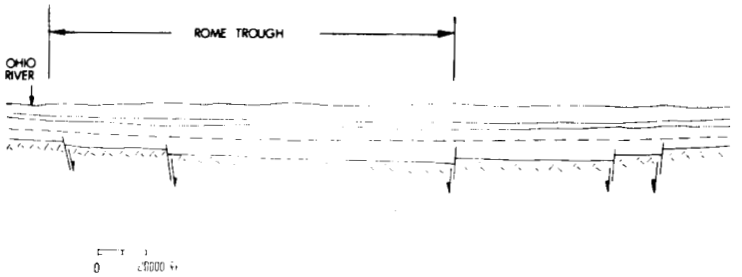

Figure 2b. Schematic of Rome Trough tectonics [5]

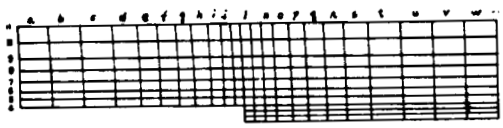

Figure 3a. Finite element model (Model I) for single basement faulting analysis.

Figure 3b. Finite element model (Model II) simulating detached structure across Rome Trough in West Virginia.

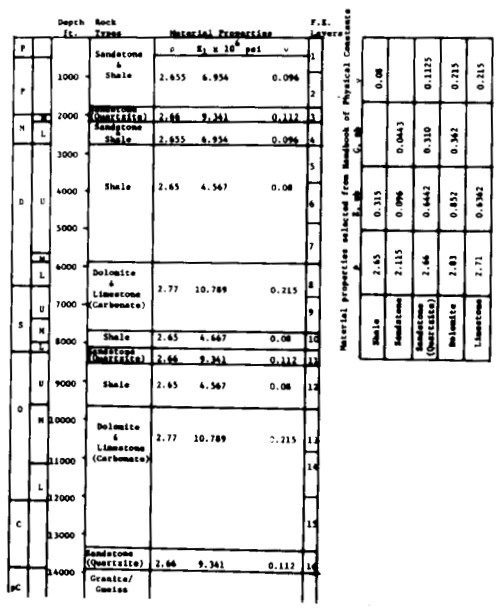

Figure 4. Generalized chart illustrating stratigraphic and material proties near Parkersburgh, WV.

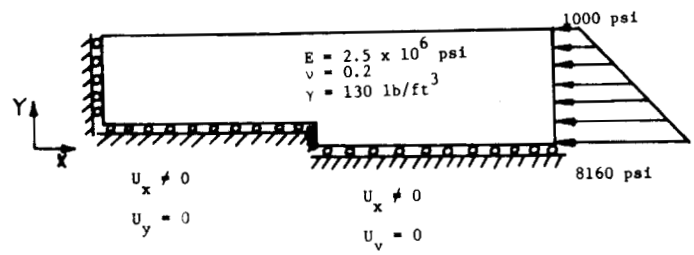

Figure 5a. Boundary conditions, loading configuration and material properties for Model IA.

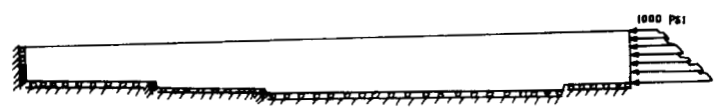

Figure 5b. Boundary conditions and loading configuration selected for Model IIA.

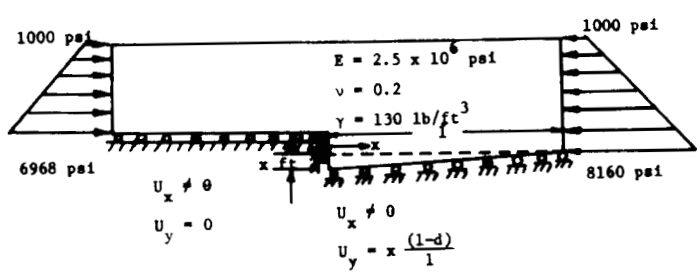

Figure 6a. Boundary conditions, loading configuration and material properties for Model IB.

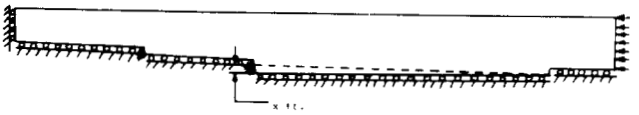

Figure 6b. Boundary conditions and loading configuration for Model IIB.

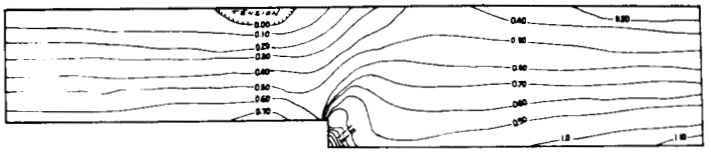

Figure 7a. Horizontal stress contours for Model IA.

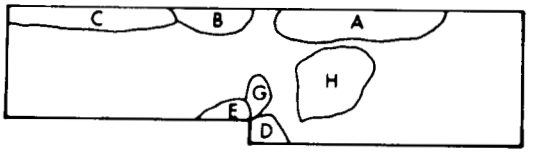

Figure 8. Sketch of significantly influenced stress distribution regions for Model I.

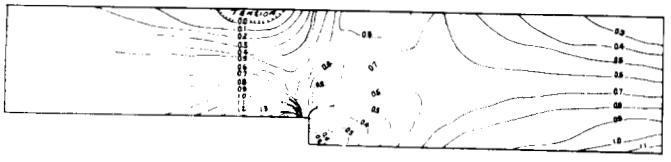

Figure 7b. Horizontal stress contours for Model IB.

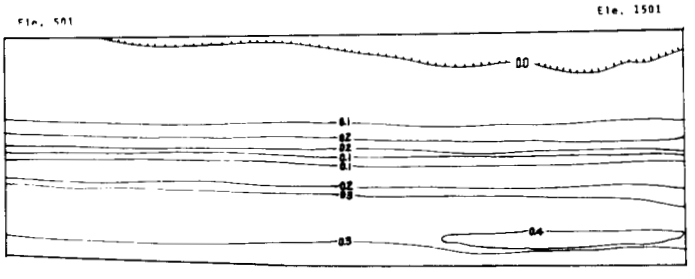

Figure 9a. Horizontal stress contours for Model IIA.

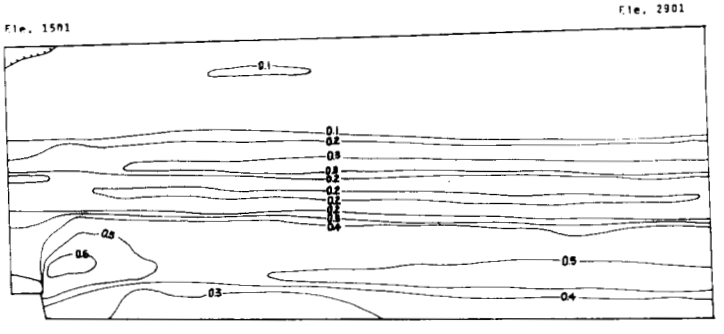

Figure 9b. Horizontal stress contours for Model IIA.

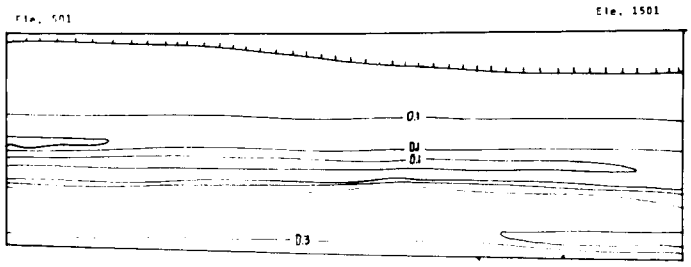

Figure 10a. Horizontal stress contours for Model IIB.

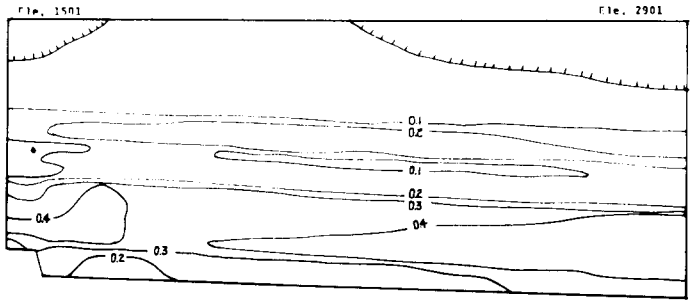

Figure 10b. Horizontal stress contours for Model IIB.

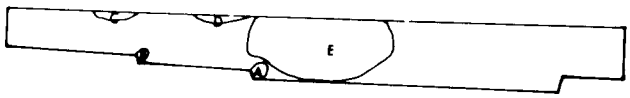

Figure 11. Sketch of significantly influenced stress distribution regions for Model II.

SEISMIC MODELLING OF COMPLEXLY DEFORMED FOLD-AND-THRUST-BELT ROCKS, CENTRAL APPALACHIANS*

WILLIAM J. PERRY, JR.[1]
GERALD SMITH[2]
MYUNG W. LEE[2]

[1]U.S. Geological Survey, Reston, Virginia
[2]U.S. Geological Survey, Denver, Colorado

ABSTRACT

BY MEANS OF NORMAL RAY-PATH SEISMIC MODELLING TECHNIQUES, BALANCED GEOLOGIC CROSS SECTIONS OF COMPLEXLY DEFORMED ROCKS MAY BE CORRELATED WITH SEISMIC-RECORD SECTIONS WITHIN THE SAME AREA. THESE TECHNIQUES PROVIDE A BETTER RESOLUTION OF COMPLEX SUBSURFACE STRUCTURE WHERE LARGE-SCALE LITHOTECTONIC UNITS ARE DEFINED AND WHERE THEIR INTERVAL VELOCITIES ARE KNOWN OR CAN BE APPROXIMATED. A SIMPLIFIED FOUR-LAYER STRUCTURAL MODEL IN THE CENTRAL APPALACHIANS INVOLVES (1) MIDDLE AND UPPER DEVONIAN SHALES AND SILTSTONES (LITHOTECTONIC UNIT 1, INTERVAL VELOCITY 15,000 FT/SEC), (2) MIDDLE ORDOVICIAN THROUGH LOWER DEVONIAN CLASTIC AND CARBONATE ROCKS (CONBINED LITHOTECTONIC UNITS 2, 3, 4, AND 5, INTERVAL VELOCITY 17,000 FT/SEC), (3) CAMBRIAN AND ORDOVICAIN CARBONATE ROCKS, CHIEFLY DOLOSTONE (LITHOTECTONIC UNIT 6, INTERVAL VELOCITY 22,000 FT/SEC), AND (4) BASAL CLASTIC ROCKS (LITHOTECTONIC UNITS 7 AND 8, ESTIMATED INTERVAL VELOCITY 18,500 FT/SEC). VELOCITY CONTROL TO A DEPTH OF 13,000 FT IS PROVIDED BY THE NEARBY RAY SPONAUGLE WELL. LITHOTECTONIC UNITS 5 AND 7 CONTAIN MAJOR DÉCOLLEMENTS. NORMAL RAYPATH ANALYSIS OF THE CHIEFLY FOLDED UPPER LAYERS ABOVE TECTONICALLY STACKED SLABS OF THE HIGH-VELOCITY LITHOTECTONIC UNIT 6 PROVIDE A QUANTITATIVE MODEL OF ACTUAL RAY PATHS THROUGH THE HIGHLY DEFORMED, YET POTENTIALLY GAS-BEARING ROCKS. NORMAL RAY-THEORY SOLUTIONS OF GEOLOGIC CROSS SECTIONAL MODELS SHOW THAT COMPLEX RAY PATHS ARE OBTAINED FROM THE STRUCTURAL GEOMETRY OF UNITS HAVING HIGH VELOCITY AND DENSITY CONTRAST. THE GEOLOGIC CROSS SECTIONAL MODELS ARE CONSTRAINED (1) BY GOOD SURFACE AND SPARSE WELL CONTROL, (2) BY THE SIMPLIFYING ASSUMPTION THAT STRAIN TRAJECTORIES WERE PARALLEL TO THE PLANE OF SECTION, (3) BY THE IMPERATIVE OF MASS BALANCE DURING DEFORMATION, AND (4) BY MODELLED SUBSURFACE GEOMETRY CONSISTENT WITH KNOWN STRUCTURAL BEHAVIOR OF THE VARIOUS LITHOTECTONIC UNITS AND QUALITATIVELY CONSISTENT WITH THE SEISMIC DATA.

THE TRUE POSITION OF SEISMIC REFLECTORS, WHERE NORMAL RAY-PATHS ARE COMPLEX, WILL NOT BE RESOLVED BY MIGRATION DURING NORMAL SEISMIC PROCESSING OF RECORD SECTIONS FROM FOLD AND THRUST BELTS. SEISMIC MODELLING AIDS IN AN EVALUATION OR REJECTION OF PROSPECTIVE "CLOSURES" BENEATH DÉCOLLEMENT STEP-UPS (RAMPS) AND APPARENT FAULTS AND OTHER DEEP-SEATED STRUCTURES THAT MAY BE GENERATED BY COMPLEX, REFRACTED RAY PATHS THROUGH VERTICAL TO OVERTURNED HIGH-VELOCITY LITHOTECTONIC UNITS OVER NEARLY FLAT BASEMENT. THE SPATIAL CONFIGURATION AND MAGNITUDE OF PROBABLE STRUCTURAL TRAPS CAN BE MORE REALISTICALLY EVALUATED BY INTERGRATING GEOLOGICAL AND SEISMIC MODELLING TECHNIQUES.

*Paper not available at time of publication

REGIONAL SEISMIC INVESTIGATIONS IN EASTERN-TENNESSEE

by

Edward R. Tegland
Lloyd Johnson

GEOPHYSICAL SERVICES INC.

ABSTRACT

During February and March of 1977 two regional seismic lines were collected for Tennessee State Department of Conservation under a grant from ERDA. The purpose of these lines was to evaluate the sedimentary section in Eastern Tennessee in general and, in particular, to establish the regional extent of the Mississippian-Devonian shales in that area.

In addition to conventional reflection seismic control collected with the Vibroseis* technique along State Highway 32 and State Highway 70, three refraction studies were made for shallow velocity control. Two of these refraction studies were located on strike on a shale outcrop and one on an older carbonate outcrop section.

Surface geologic control was provided by the state geologist's office for all quadrangles traversed by the lines and was tied into the profiles.

The data has been worked into profile and regional map form.

INTRODUCTION

In February, 1977 a seismic program consisting of two regional multifold Vibroseis* lines and three shallow refraction profiles was collected for the Department of Conservation of the State of Tennessee. The purpose of this program was to promote an improved understanding of the geology of Eastern Tennessee in general and to improve the knowledge of the occurrence of the Devonian-Mississippian shales in particular.

FIELD PROGRAM

Figure 1 shows the field program and how it relates to available surface geologic information. Table 1 provides pertinent information concerning the geologic quadrangles traversed by the lines.

The northern segment of line TC-1 was filled in from the town of Tazewell to the Kentucky border by a segment of existing data (K-1 south) purchased from Geophysical Service Inc. and re-processed to be consistent with TC-1. This line segment was collected using a 24 channel DFS III recording system.

---

*Trademark of Continental Oil Company

The group interval and source interval were 330 feet (100 meters) yielding a "nominal" 12 fold CDP stack with a subsurface interval of 165 feet (50 meters). Figure 2A shows the "split spread" configuration employed in collecting K-1.

Figure 2B shows the "assymetric split spread" used in collecting lines TC-1 and TC-2. In this case the instrumentation was 48 channel DFS IV system with CFS-1 field computer. The group interval was 220 feet (70 meters) and the shot interval was 440 feet (140 meters) yielding a 110 feet (35 meter) subsurface spacing with a nominal 12 fold CDP coverage.

The assymetric arrangement used in the new work not only yields a greater subsurface trace density but provides a greater range of shot-to-detector offsets with which to work in measuring velocities. The split spread configurations are particularly valuable in dealing with crooked lines because they provide an added set of near offset traces which improve the shallow data coverage in selective stacking.

Figure 3A shows the source pattern used in collecting the data and its wavenumber response. Figure 3B shows the geophone array used in collecting the data and its wavenumber response. Figure 3C shows the combined wavenumber response of the source and receiver systems used.

Also shown on figure 3C are the frequency limits of the data as imposed by the 14-56 Hz. sweep and the frequency/wavenumber plots of noise and refraction arrivals as estimated from the three refraction profiles (figures 5A-5C). The attenuation indicated for these events is only realized when the line is perfectly straight. Generally speaking, the observed attenuation will be somewhat less. The surface noise exhibited by the refraction spreads appears to have been attenuated well since little evidence of it can be found on the production reflection data.

REFRACTION STUDIES

Figure 4 shows the field layout used to gather the refraction data. A single vibrator taking 10 sweeps which were summed and correlated provided the source of signal. The geophones for each group were bunched to maximize output and minimize attenuation of horizontally traveling energy. These refraction studies were collected for two purposes:

1. To estimate the velocity and thickness (if possible) of the near surface.
2. To evaluate the surface noise conditions.

The data recorded for these studies is shown in figures 5A, 5B and 5C. A review of the noise aspect of the studies was presented earlier.

Initial estimates of velocity trends were made by fitting straight lines to correlative event patterns on the sections themselves. Then events of interest were accurately timed using large scale "wiggle trace" records and plotted in time-distance format as shown in figures 6A, 6B and 6C. Line segments were then fitted with care to each observable velocity unit. The direct velocity wave in the most near surface unit was generally not easily picked due to other surface propagation modes created by the vibrators. The velocity of this unit was estimated in all cases by evaluation of secondary events at the larger offsets. These secondary arrivals were extrapolated back to zero offset. Thickness of the shallowest unit was estimated from the critical distance equation below:

$$Z_0 = \frac{XC}{2} \left(\frac{V_1 - V_0}{V_1 + V_2} \right)^{\frac{1}{2}} \qquad \text{(Eq. 1)}$$

Where: Z_0 = thickness of layer 0

XC = distance at which velocity trends 0 and 1 intersect. i.e., critical distance

V_0 = velocity of upper unit

V_1 = velocity of lower unit

$V_0 < V_1$

Table 2 lists the pertinent data from the three studies. Studies 2 and 3 were designed to evaluate the target shale sections. The results confirmed the feeling that velocity would fall near 14,000 feet per second in the shale. Study 1 looked at an older carbonate outcrop and verified the high velocity section expected there. An intermediate velocity zone was found to exist in the carbonate section with velocity close to that of the shales. Since the study was located on an Eggleston-Hardy Creek outcrop area, it is possible that the shallow exposure was argillaceous. L. D. Harris (1965) indicates up to 60 feet of Bentinite near the top of the Eggleston section. All refraction studies were sited to eliminate structural and dip effects; however, the assymetric velocity picture of study no. 1 indicates dip and possible faulting. Accurate geologic description of the field sites is unavailable. In all cases the lowest velocity "weathered" material was rather thin and of moderate velocity. This information coupled with independent tests conducted on the reflection data lead to utilization of a 10,000 fps (3049 m/s) velocity for calculating datum corrections to remove weathering and elevation effects.

SEISMIC DATA PROCESSING

The processing used for handling the reflection data is outlined below:

Field Processing

1. Diversity vertical stack - 15 sweeps per pattern.
2. Vibroseis* correlation and display.

Office Processing

3. a. Preprocess coordinate data and generate subsurface coverage map (printer map), figure 7.
   b. Reformat field data.
4. a. Initialize CDP gather specification tables for X-Y selective gathers according to specified "stack track", figure 7.
   b. Trace conditioning
      1) gain recovery
      2) deconvolution
      3) trace edit
5. Normal moveout with "ball park" velocity.
6. Brute stack, filter and display.
7. Evaluate data and choose events for residual static estimation.
8. a. Residual static calculation.
   b. Velocity analysis at suitable locations. Display results.
9. Interpret velocity and evaluate static run.
10. Submit new velocity data for final moveout, static correction, CDP stack, filter and display.
11. Fine tune velocity control and depth convert sections.
12. Interpret profiles in light of known and estimated geology.

TRACE GATHERING FOR CDP STACK

Whenever the path of the seismic line is not straight, one no longer has common depth point stack. The nature of the subsurface scatter to be expected and a processing method to more properly treat these situations was presented by Tegland (1974).

Two steps are employed. First, the coordinates of all shots and receivers are preprocessed and the theoretical reflection point of each pair is calculated. A printer map is then prepared showing the distribution of subsurface coverage defined by all reflection points for a line. Symbols A thru X are used to indicate redundancy (fold) 1 thru 24. Figure 7 is a segment of such a map from Line TC-1.

The second operation commences with an interpretation of where the stack line should follow through the available coverage and how large a window either side of the line should be used in accepting traces into the stack. A 220 foot window was used in processing the current data. Figure 7 shows the track of the stack line. Generally, an attempt is made to fulfill three criteria:

1. Maximum fold.
2. Complete offset range with preference to short offsets.
3. Minimum number of direction changes.

The reflection point coordinates of each contributor are averaged to yield a final position for that stacked trace. These positions have been plotted to provide base map control for the line. Each stacked trace is given an identifying number which is posted periodically on the base map.

DATUM CORRECTIONS

One has several approaches available for applying datum corrections. In this case since the existing topography was often related to geologic structure directly, a floating datum was chosen which was generally a smoothed version of the minimum elevations along the lines. Datum corrections should then reflect largely a stripping of the lower velocity material. As indicated earlier, a correctional velocity of 10,000 fps (3048 m/s) was used as per equation 2.

$$TC = \frac{DE - DS}{10{,}000} \qquad \text{(Eq. 2)}$$

TC = correction time in sec.
DE = datum elevation in feet
DS = surface elevation in feet

Since datum was generally at or below the surface, these corrections were generally zero or negative. i.e., representing removal of excess time.

In an experimental mode, tests using correctional velocities from 8000 fps (2438 m/s) to 16,000 fps (4876 m/s) in five even increments were made. Only marginal differences could be seen between these correctional velocities.

Subsequently residual statics are calculated automatically to improve the stack response within each trace collection. The deeper event sequences associated with the Cambrian clastic section and the pre-Cambrian were chosen for scanning by the computer in formulating these residual corrections. The automated corrections are calculated in a surface consistent manner. Each time a particular surface location is occupied by a receiver the resulting trace has a receiver correction applied for that location. Similarly, each trace from a particular source location is corrected with a unique correction for that location.

VELOCITY ANALYSIS

Since the CDP trace collections resulting from the crooked line selective gather contain generally variable fold and offset ranges, one must be selective and choose which have high fold and a good range of offsets from longest to shortest with a few, if any, missing. Using the "brute stacks" as a guide locations were also chosen based on the quality of the data. Since residual static correction normally preceeded velocity analysis, one should expect that even better data would be presented to the analysis.

The form of analysis used employs two types of calculations and displays. The first method uses a series of user-defined "trial" velocities to form stacked output over several CDP sets. The results are displayed as a panel (left half of figure 8) for visual interpretation. The second method utilizes a combination of moveout scans and dip scans over the same trace collections followed by automatic picking of the results.

Time, amplitude, velocity and dip parameters of each detected event are plotted as shown in the right half of figure 8. The interpreter's job then is to marry the information into a geologically feasible time-velocity function for that location. The primary concern at data processing time is to arrive at the velocity which maximizes the response of the stacked output for those events deemed desirable. i.e., primary reflections. This velocity is generally referred to as V_S or stacking velocity. In simply layered situations it can be related to RMS velocity as described by Dix (1955) by equation 3.

$$V_{RMS} = (V_S)\ (\cos \phi) \qquad \text{(Eq. 3)}$$

where ϕ = dip angle

One can then calculate the interval velocity for a given subsurface unit bounded in time by T_1 and T_2 according to equation 4. This relationship is referred to as Dix's equation in the literature.

$$V_I = \left(\frac{T_2\ V^2_{RMS_2} - T_1\ V_{RMS}}{T_2 - T_1} \right)^{1/2} \qquad \text{(Eq. 4)}$$

As dips become divergent and the geology more complicated, equations 3 and 4 become poorer estimations.

An average velocity, i.e., one that relates vertical time to depth, can be calculated by integrating the intervals determined from equation 4. This result is given by equation 5.

$$V_{avg} = \frac{\sum_{i=1}^{N} V_{I_i} \left(DT_i \right)}{\sum_{i=1}^{N} DT_i} \qquad \text{(Eq. 5)}$$

where DT_i = time interval across a given layer

VI_i = interval velocity through that layer

The average velocity as indicated in equation 5 is used to depth convert the seismic traces such that the final display profiles have a linear vertical depth scale.

INTERPRETATION

The interpretation of the reflection data basically contains two tasks:

1. Determine the structural profile.
2. Identify geologic units.

To assist in these tasks the surface geology was transferred from the various quadrangles involved to the CDP map. This was accomplished by simply overlaying the documents and manually tracing contacts and other features. Since the various source documents were of different vintage and authorship, exact boundary ties were a small problem and nomenclature changes were even a larger problem. Figure 9 shows one of the seismic-geologic index maps derived in this fashion.

With the seismic-geologic map to work from the interpreter can easily position significant boundaries in their proper surface location along the record section. Zero depth corresponds closely with the surface topography in this case because of the floating datum used.

Pertinent subsurface cross sections accompanying the various geologic maps are also identified for reference on the seismic-geologic index maps. Table 1 summarizes the available knowledge. In addition, a description of L. S. Bales well in western Virginia, approximately four miles (6.7 km) northwest of the start of Line TC-2, was available. According to Harris (1967) the well is located at Virginia coordinates 140,075 N and 575,900 E which would place it in the NW extremity of the Kyles Ford quadrangle. Projections of the geologic section in this well were made using a scaled up version of Harris' plate.

The interpreted results are expected to be the depth converted sections with visible reflection contacts identified geologically and structural shape outlined where reliable velocity and other supporting information is available it will be annotated. Projections of fault planes and geologic contacts which are not marked by notable reflections will be made where possible using combined surface dips, seismic dips and estimated thicknesses

CLOSING REMARKS

At the time of this writing, interpretation had not been completed on this data. The details of the interpretation will be shown where possible in the oral presentation and will be available later this year from the Tennessee Department of Conservation, Division of Geology in Nashville, Tennessee.

The author wishes to express his gratitude to Mr. Statler and Mr. Millici for providing incentive for the project and the complete surface geology coverage provided.

BIBLIOGRAPHY

DIX, 1955, Seismic velocities from surface measurements: Geophysics, Vol. 20, No. 1, pp. 68-86.

FAUST, 1951, Seismic velocity as a function of depth and geologic time: Geophysics, Vol. 16, pp. 192-206.

HARRIS, 1967, Geology of the L. S. Bales Well, Lee County, Virginia - a cambrian and ordovician test: Kentucky Geological Survey, Ser. X, Special Publication 14.

TEGLAND, 1967, CDP techniques and crooked traverses: 44th International Meeting of the Society of Exploration Geophysicists, Dallas, 1974.

TABLE NO. 1

QUADRANGLE	SEIS LINE	AUTHORS	AGENCY	STATUS - YEAR	SUPPLEMENTAL	
					GEOL. COL. + ECON. GEOL.	PROFILES
MIDDLESBORO SOUTH	K-1	K. J. ENGLAND	U. S. G. S.	COMPLETE #GQ-301 1964	YES	YES
WHEELER	K-1	L. D. HARRIS	U. S. G. S.	COMPLETE #GQ-435 1965	YES	YES
TAZEWELL	K-1/TC-1	L. D. HARRIS	U. S. G. S.	COMPLETE #GQ-465 1965	YES	YES
HOWARD QUARTER	TC-1	L. D. HARRIS R. B. MIXON	U. S. G. S.	COMPLETE 1970 #GQ-842	YES	YES
AVONDALE	TC-1	R. C. MILLICI	TENN. DEPT. CONSERVATION	WORK MAP NO DATE	GEOL. COL.	NO
BEAN STATION	TC-1	R. C. MILLICI	TENN. DEPT. CONSERVATION	SKETCH ON TOPO MAP	NO	NO
MORRISTOWN	TC-1	R. L. ODER R. C. MILLICI G. D. SWINGLE	TENN. DEPT. CONSERVATION	COMPLETE 1965 GM 163-NE MRS 163-NE	YES. RESOURCES SUMMARY	YES
KYLES FORD	TC-2	R. C. MILLICI	TENN. DEPT. CONSERVATION	WORK MAP PLUS GEOLOGIC WRITE UP	YES	NO
PRESSMENS HOME	TC-2	R. C. MILLICI	TENN. DEPT. CONSERVATION	SKETCH ON TOPO MAP	GENERALIZED SECTION	NO
BUREM	TC-2	R. C. MILLICI	TENN. DEPT. CONSERVATION	SKETCH ON TOPO MAP	NO	NO
MC CLOUD	TC-2	R. C. MILLICI	TENN. DEPT. CONSERVATION	SKETCH ON TOPO MAP	ROUGH	NO
MOSHEIM	TC-2	R. C. MILLICI	TENN. DEPT. CONSERVATION	SKETCH ON TOPO PLUS WORK MAP STRATEGIC MIN. INVEST.	YES	NO
GREENVILLE	TC-2	R. C. MILLICI	TENN. DEPT. CONSERVATION	WORK MAP	NO (REFER TO BAILY-TOWN MAP)	NO
DAVY CROCKETT LAKE	TC-2	R. C. MILLICI	TENN. DEPT. CONSERVATION	SKETCH ON TOPO MAP	ROUGH	NO
HOT SPRINGS	TC-2	R. C. MILLICI	TENN. DEPT. CONSERVATION	SKETCH ON TOPO MAP	ROUGH	NO

TABLE NO. 2

REFRACTION STUDY RESULTS

STUDY NO.		V_{LEFT}	V_{RIGHT}	V_{AVG}	X_{CL}	X_{CR}	X_{CAVG}	THICKNESS		COMMENTS
								ESTIMATED WEATHERING	MIN. M-D SHALE	
1	V_0	10,000	10,000	10,000	NA	NA	NA	144	NA	
	V_1	13,250	14,285	13,767	650	800	725	NA	NA	Dipping
	V_2	16,875	21,250	19,067	No Est.	825	No Est.	No Est.	No Est.	Faulted
2	V_0	7,500	7,500	7,500	NA	NA	NA	120	NA	
	V_1	14,000	15,000	14,500	475	375	425	NA	443	Slight dip. Offset variance in long halves.
3	V_0	7,500	7,500	7,500	NA	NA	NA	184	NA	
	V_1	15,000	15,000	15,000	700	575	637.5	NA	417	Possible slight dip. Delay time variance.

THICKNESS ESTIMATES BASED ON AVERAGED VELOCITY VALUES (V_{AVG}) AND CRITICAL DISTANCE (X_{CAVG})

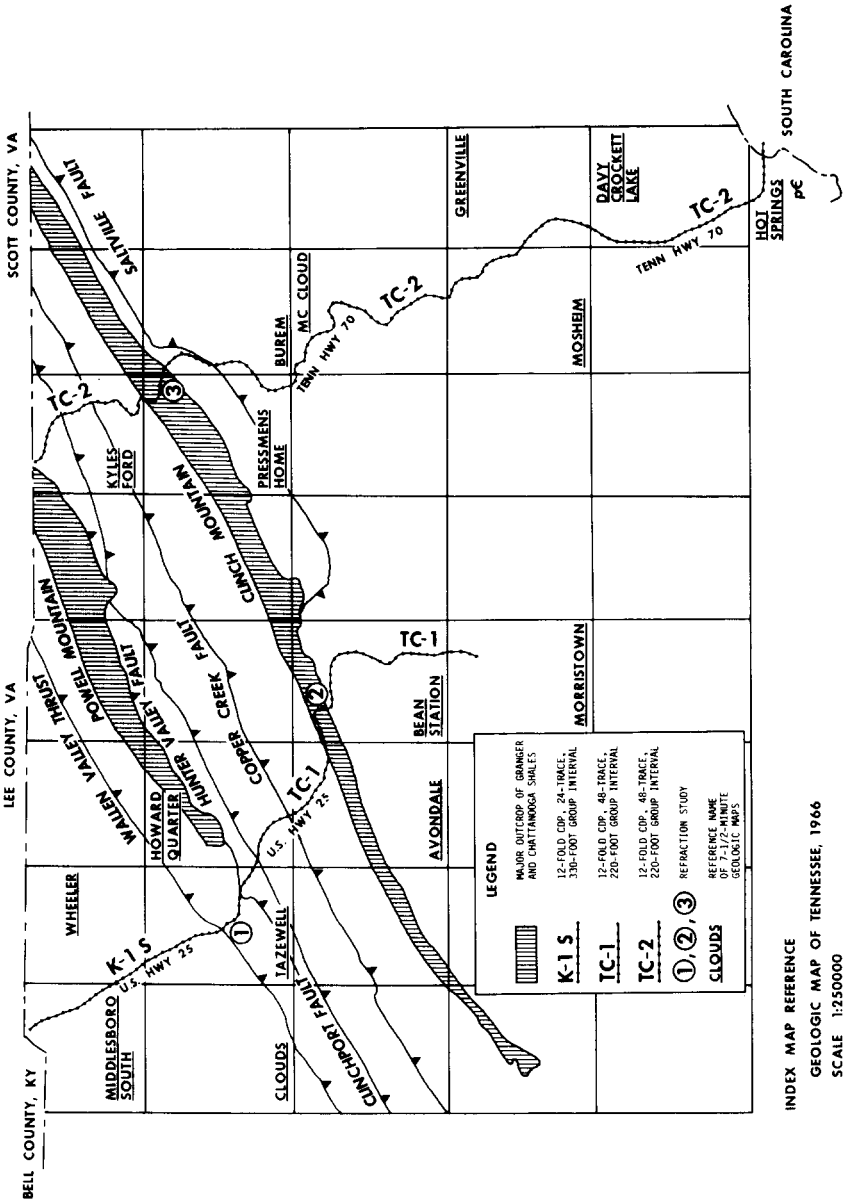
TENNESSEE DEPARTMENT OF CONSERVATION
DIVISION OF GEOLOGY
EASTERN TENNESSEE SEISMIC PROGRAM
BELL COUNTY, KY
LEE COUNTY, VA
SCOTT COUNTY, VA
SOUTH CAROLINA
MIDDLESBORO SOUTH
WHEELER
CLOUDS
TAZEWELL
BEAN STATION
AVONDALE
MORRISTOWN
MOSHEIM
GREENVILLE
DAVY CROCKETT LAKE
HOT SPRINGS
BUREM
MC CLOUD
PRESSMENS HOME
KYLES FORD
HOWARD QUARTER
WALTEN THRUST
POWELL MOUNTAIN
VALLEY FAULT
HUNTER
COPPER CREEK FAULT
CLINCH MOUNTAIN
SALTVILLE FAULT
CUNCHORT FAULT
K-1 S
TC-1
TC-2
U.S. HWY 25
TENN HWY 70
pC
LEGEND
MAJOR OUTCROP OF GRANGER AND CHATTANOOGA SHALES
K-1 S 12-FOLD CDP, 24-TRACE, 330-FOOT GROUP INTERVAL
TC-1 12-FOLD CDP, 48-TRACE, 220-FOOT GROUP INTERVAL
TC-2 12-FOLD CDP, 48-TRACE, 220-FOOT GROUP INTERVAL
①, ②, ③ REFRACTION STUDY
CLOUDS REFERENCE NAME OF 7-1/2-MINUTE GEOLOGIC MAPS
INDEX MAP REFERENCE
GEOLOGIC MAP OF TENNESSEE, 1966
SCALE 1:250000

FIGURE 1

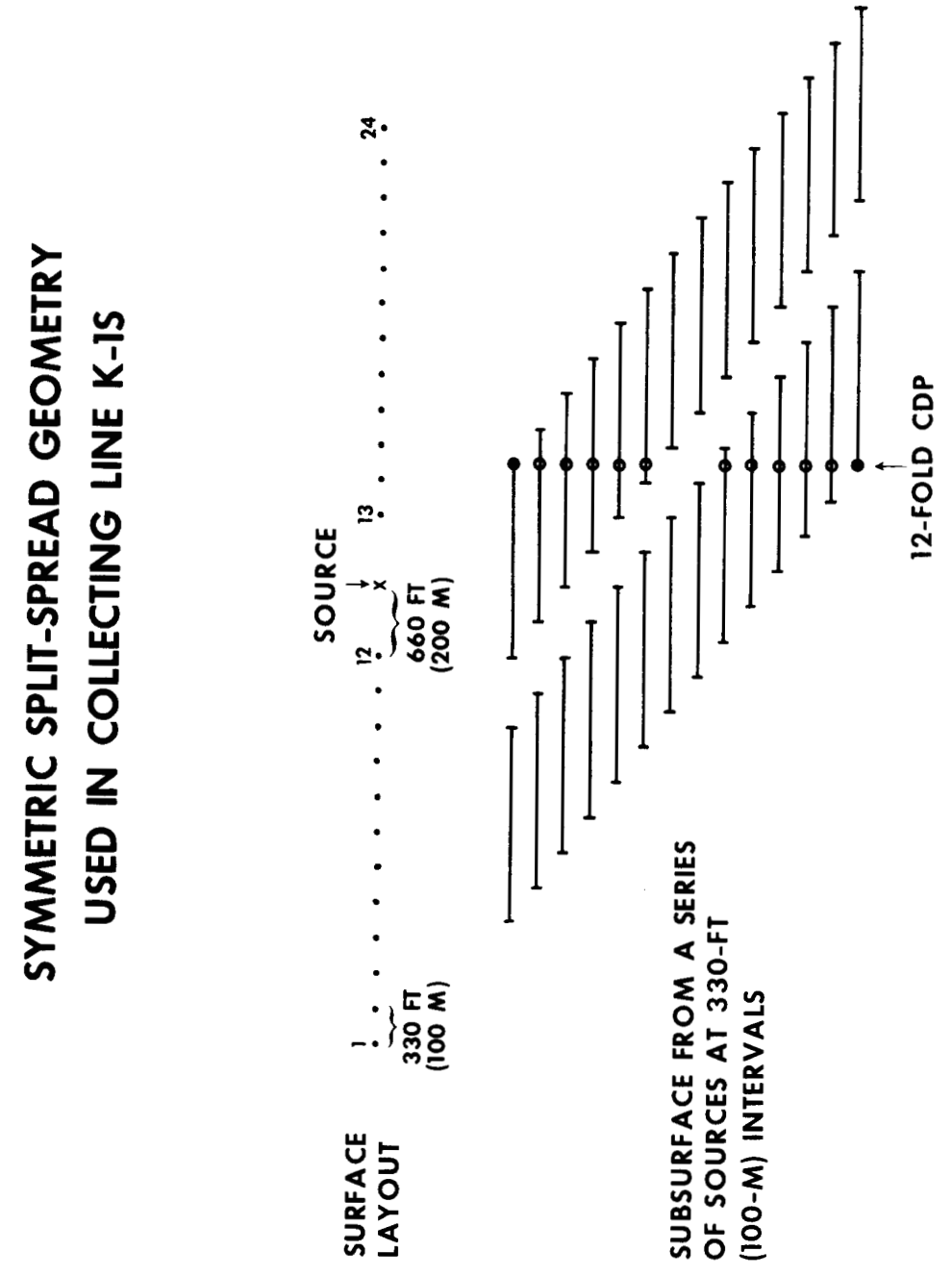
SYMMETRIC SPLIT-SPREAD GEOMETRY
USED IN COLLECTING LINE K-1S
SURFACE LAYOUT
1
330 FT (100 M)
SOURCE
12
13
24
660 FT (200 M)
SUBSURFACE FROM A SERIES OF SOURCES AT 330-FT (100-M) INTERVALS
12-FOLD CDP

FIGURE 2A

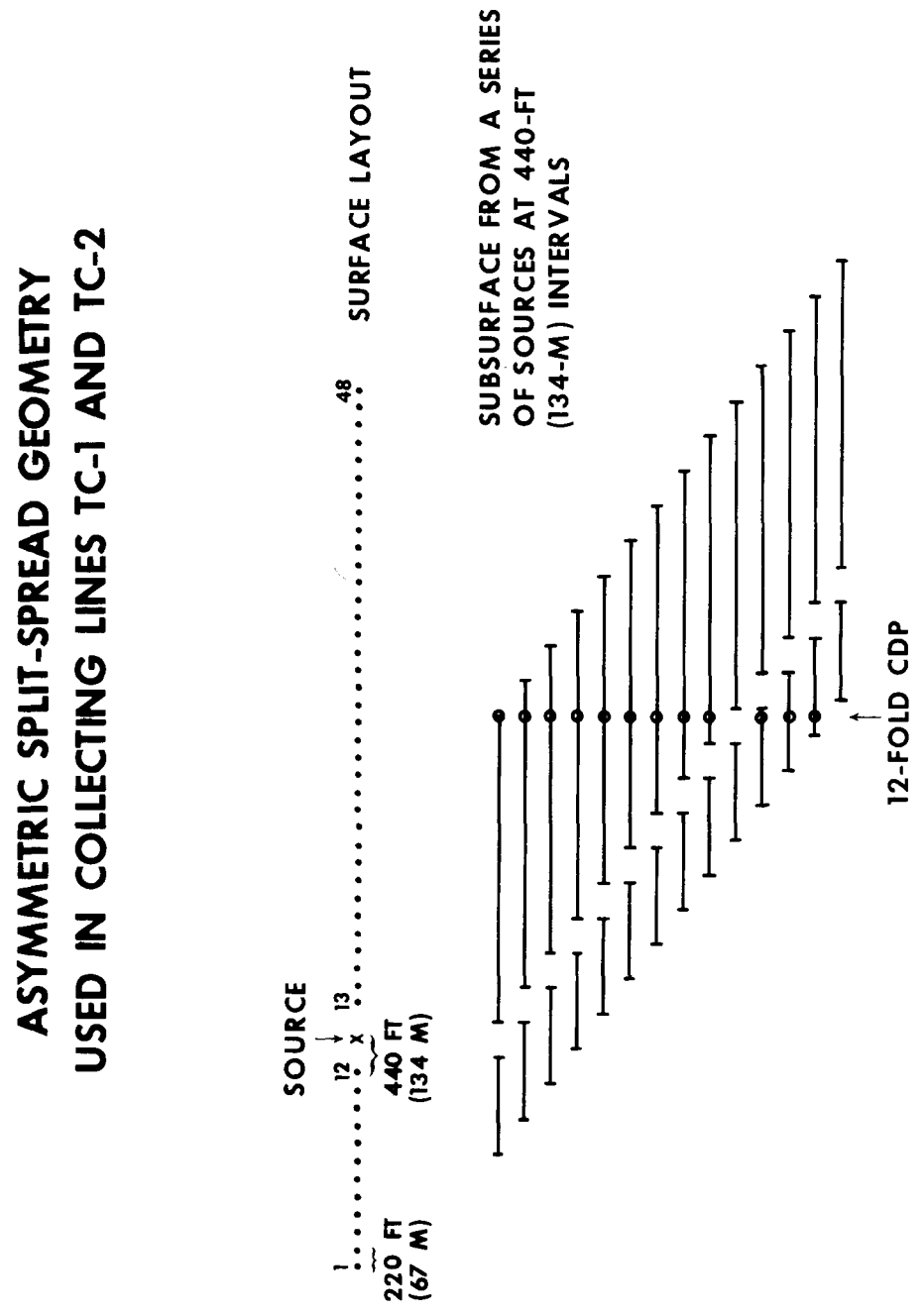
ASYMMETRIC SPLIT-SPREAD GEOMETRY
USED IN COLLECTING LINES TC-1 AND TC-2
SURFACE LAYOUT
SOURCE
1
12
13
48
220 FT
(67 M)
440 FT
(134 M)
SUBSURFACE FROM A SERIES
OF SOURCES AT 440-FT
(134-M) INTERVALS
12-FOLD CDP

FIGURE 2B

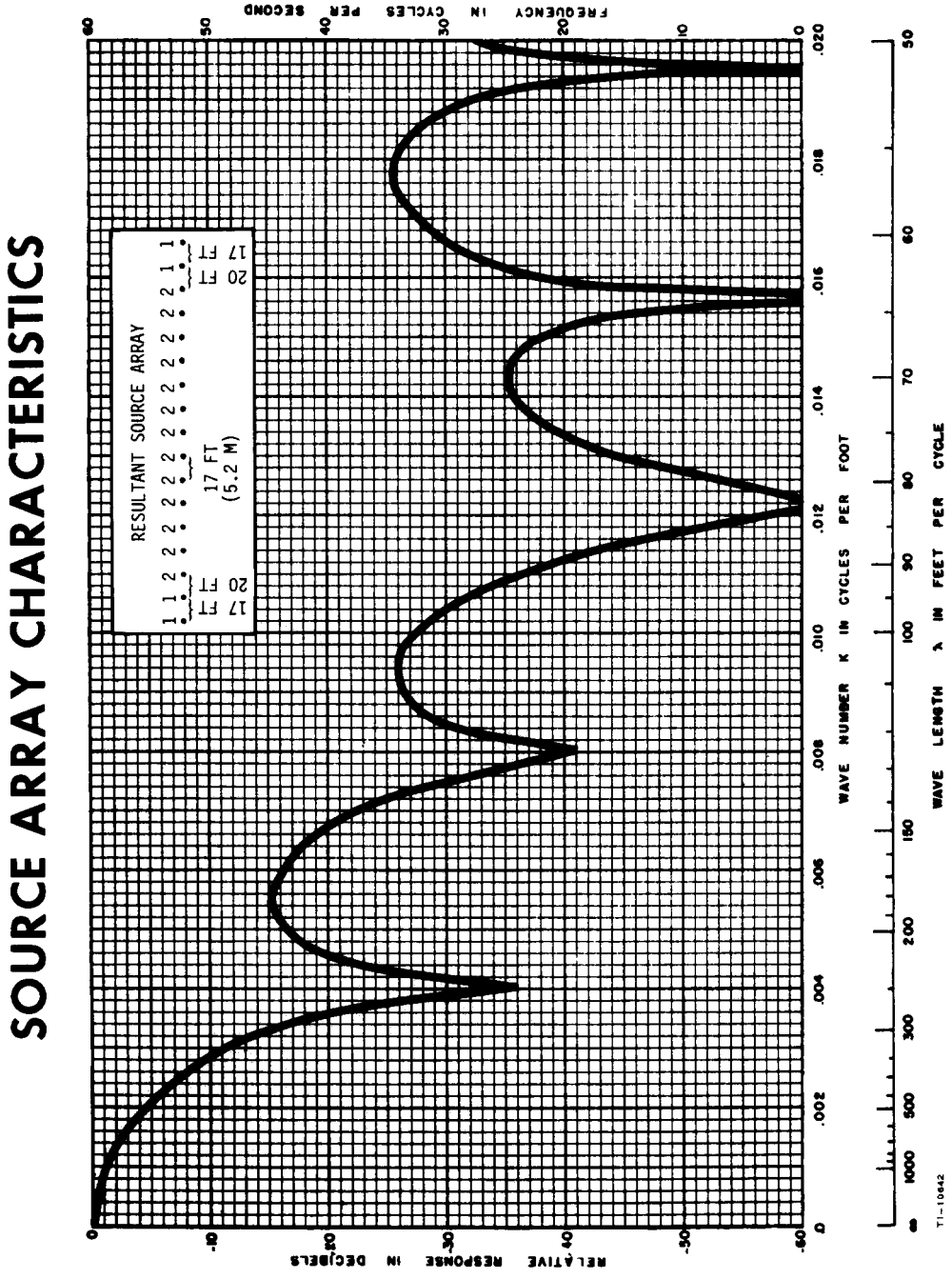
SOURCE ARRAY CHARACTERISTICS
RESULTANT SOURCE ARRAY
17 FT
20 FT
17 FT
20 FT
17 FT
(5.2 M)
FREQUENCY IN CYCLES PER SECOND
RELATIVE RESPONSE IN DECIBELS
WAVE NUMBER K IN CYCLES PER FOOT
WAVE LENGTH λ IN FEET PER CYCLE
TI-10442

FIGURE 3A

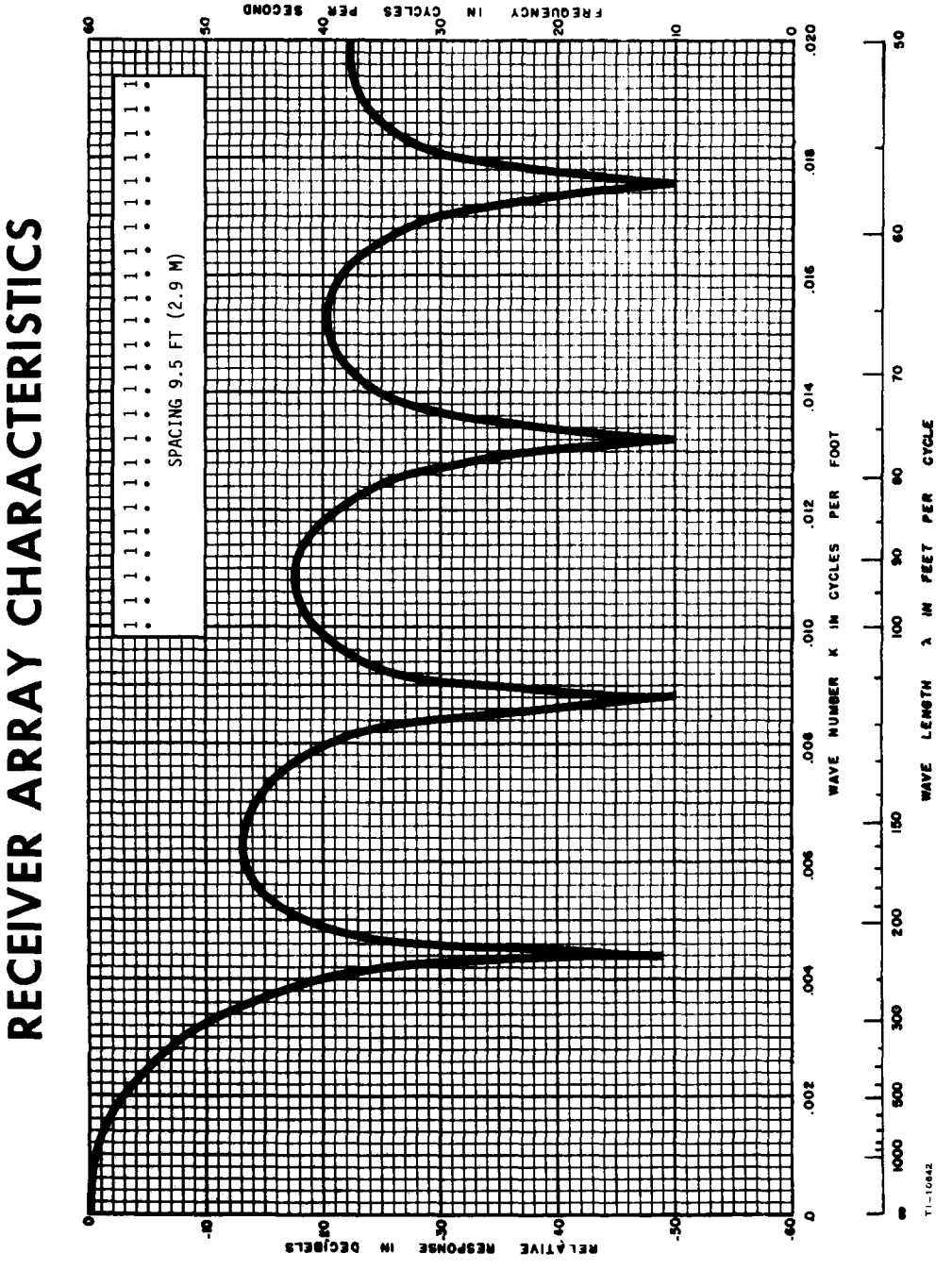
RECEIVER ARRAY CHARACTERISTICS
SPACING 9.5 FT (2.9 M)
FREQUENCY IN CYCLES PER SECOND
RELATIVE RESPONSE IN DECIBELS
WAVE NUMBER K IN CYCLES PER FOOT
WAVE LENGTH λ IN FEET PER CYCLE
TI-10642

FIGURE 3B

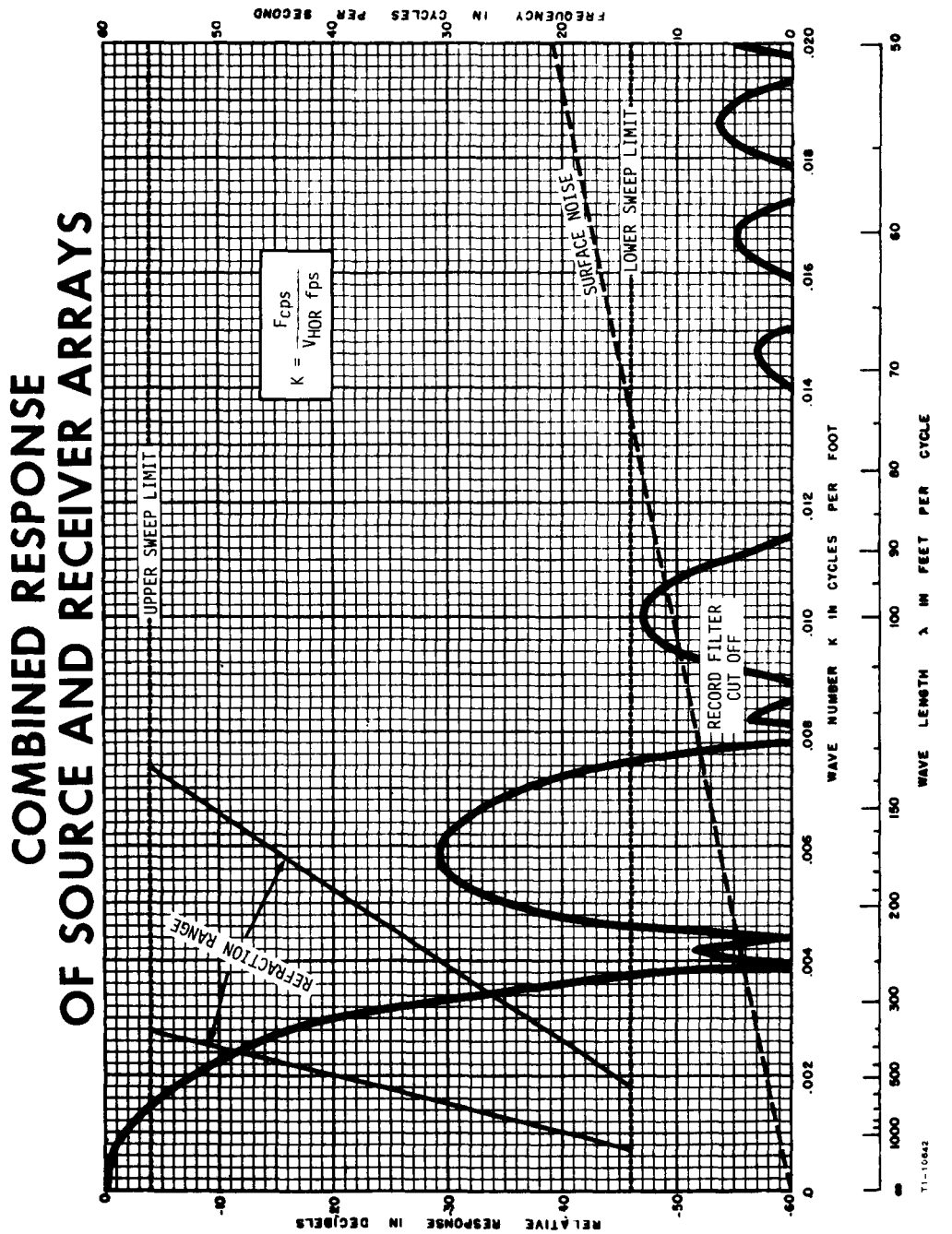
COMBINED RESPONSE
OF SOURCE AND RECEIVER ARRAYS
UPPER SWEEP LIMIT
REFRACTION RANGE
$K = \frac{F_{cps}}{V_{HOR}\ fps}$
SURFACE NOISE
LOWER SWEEP LIMIT
RECORD FILTER CUT OFF
FREQUENCY IN CYCLES PER SECOND
RELATIVE RESPONSE IN DECIBELS
WAVE NUMBER K IN CYCLES PER FOOT
WAVE LENGTH λ IN FEET PER CYCLE
T1-10642

FIGURE 3C

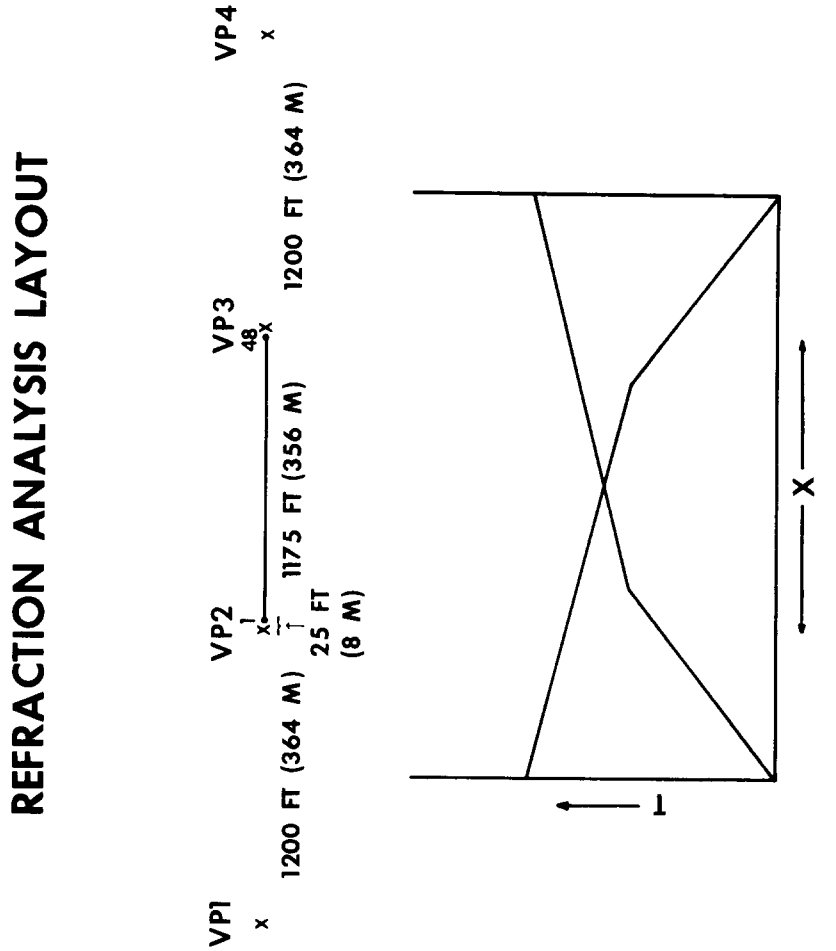
REFRACTION ANALYSIS LAYOUT
VP1
VP2
VP3
VP4
48
1200 FT (364 M)
1175 FT (356 M)
25 FT
(8 M)
1200 FT (364 M)
T
X

FIGURE 4

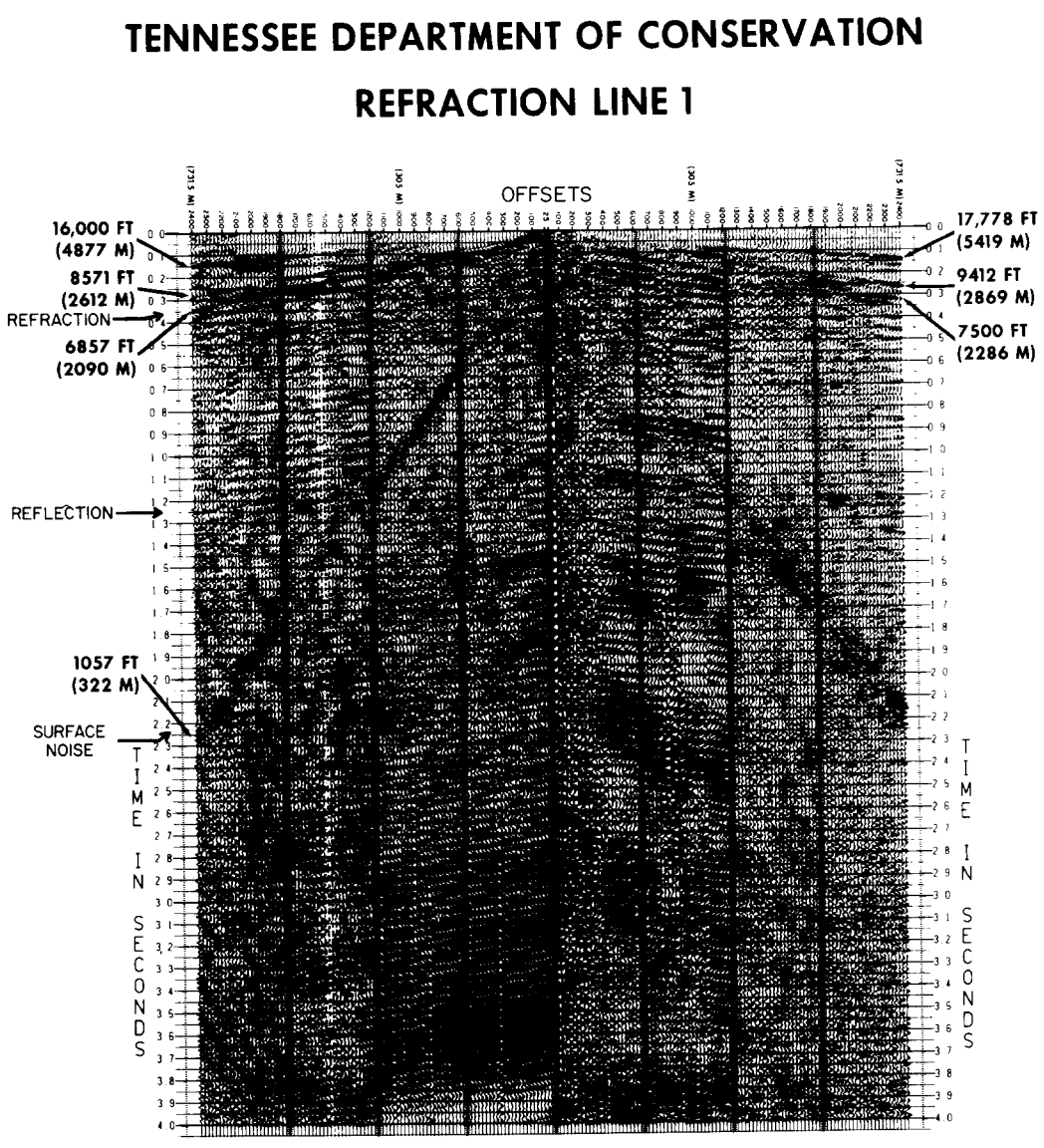
TENNESSEE DEPARTMENT OF CONSERVATION
REFRACTION LINE 1
OFFSETS
16,000 FT
(4877 M)
8571 FT
(2612 M)
REFRACTION
6857 FT
(2090 M)
REFLECTION
1057 FT
(322 M)
SURFACE
NOISE
17,778 FT
(5419 M)
9412 FT
(2869 M)
7500 FT
(2286 M)
TIME IN SECONDS
TIME IN SECONDS

FIGURE 5A

TENNESSEE DEPARTMENT OF CONSERVATION

REFRACTION LINE 2

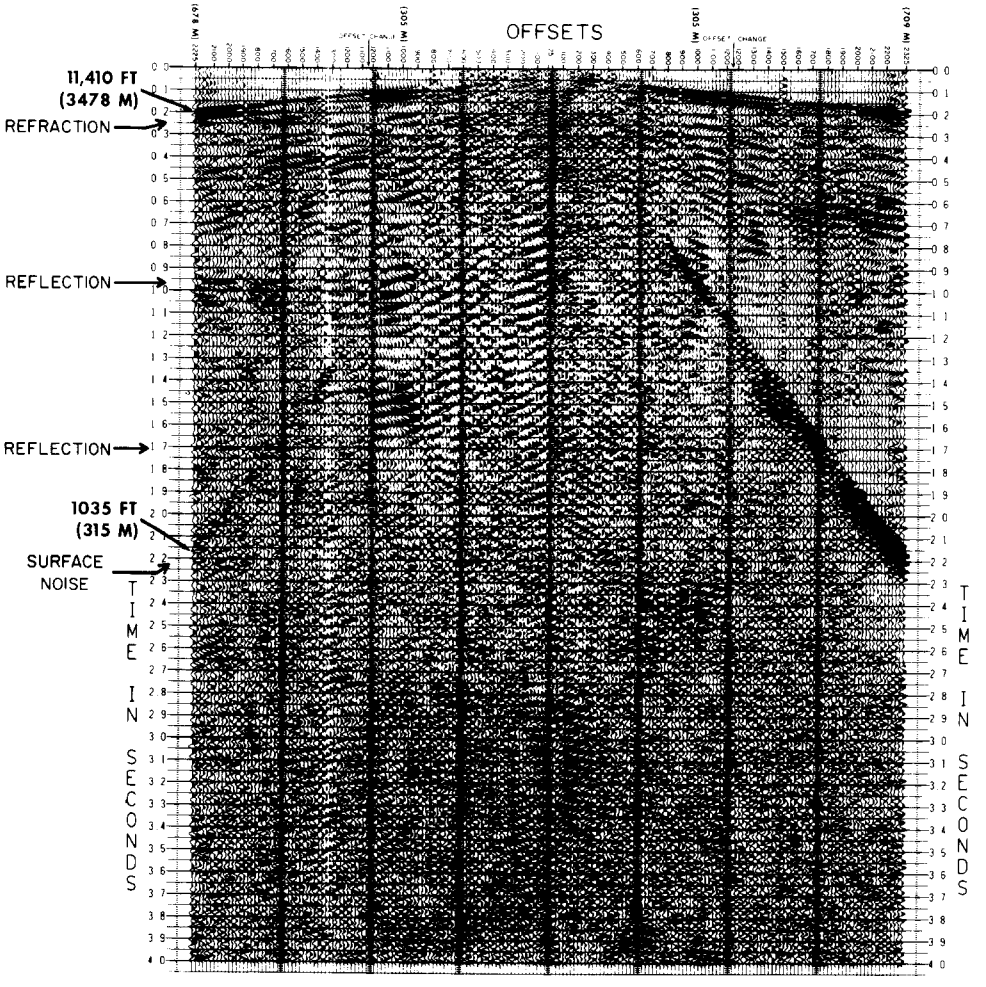

FIGURE 5B

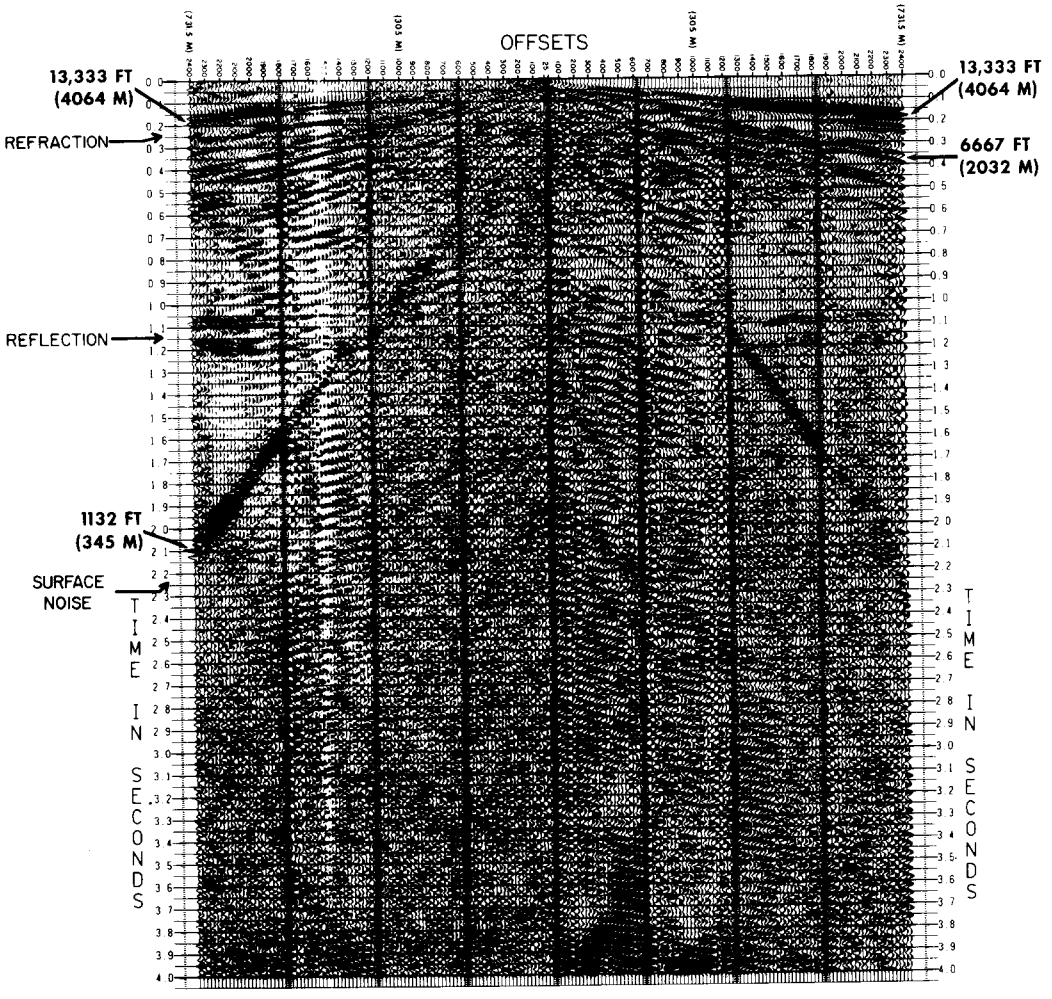
TENNESSEE DEPARTMENT OF CONSERVATION
REFRACTION LINE 3
OFFSETS
13,333 FT
(4064 M)
REFRACTION
REFLECTION
1132 FT
(345 M)
SURFACE
NOISE
TIME IN SECONDS
13,333 FT
(4064 M)
6667 FT
(2032 M)
TIME IN SECONDS

FIGURE 5C

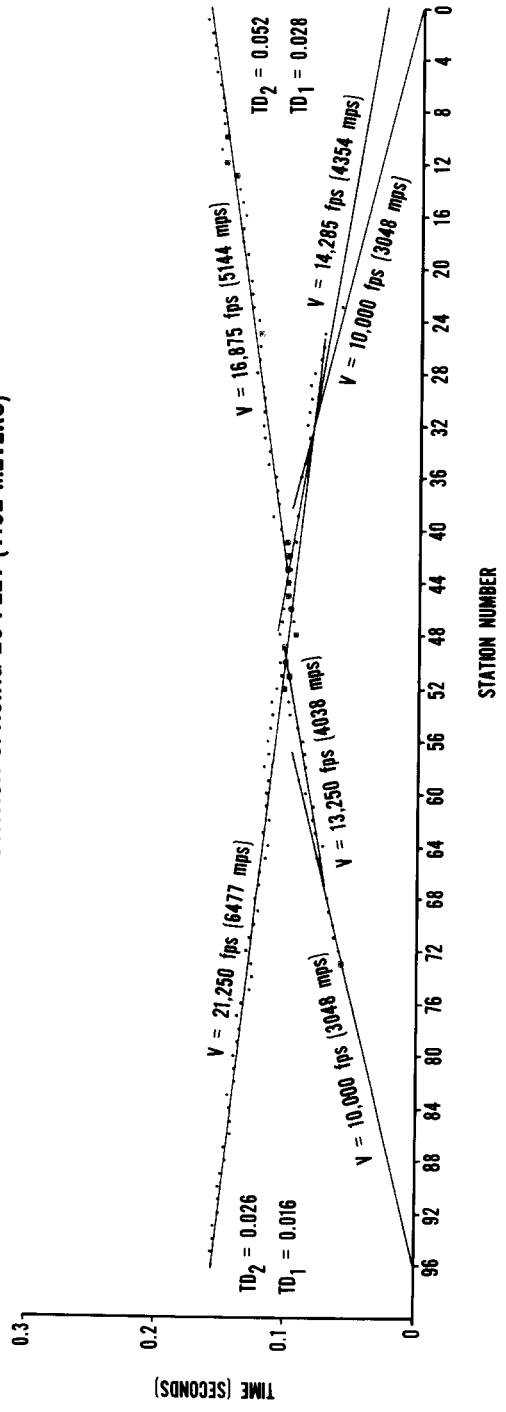
REFRACTION STUDY NO. 1
TENNESSEE DEPARTMENT OF CONSERVATION
STATION SPACING 25 FEET (7.62 METERS)
V = 16,875 fps (5144 mps)
V = 14,285 fps (4354 mps)
V = 10,000 fps (3048 mps)
V = 21,250 fps (6477 mps)
V = 13,250 fps (4038 mps)
V = 10,000 fps (3048 mps)
TD2 = 0.052
TD1 = 0.028
TD2 = 0.026
TD1 = 0.016
TIME (SECONDS)
0.3
0.2
0.1
0
STATION NUMBER
96 92 88 84 80 76 72 68 64 60 56 52 48 44 40 36 32 28 24 20 16 12 8 4 0

FIGURE 6A

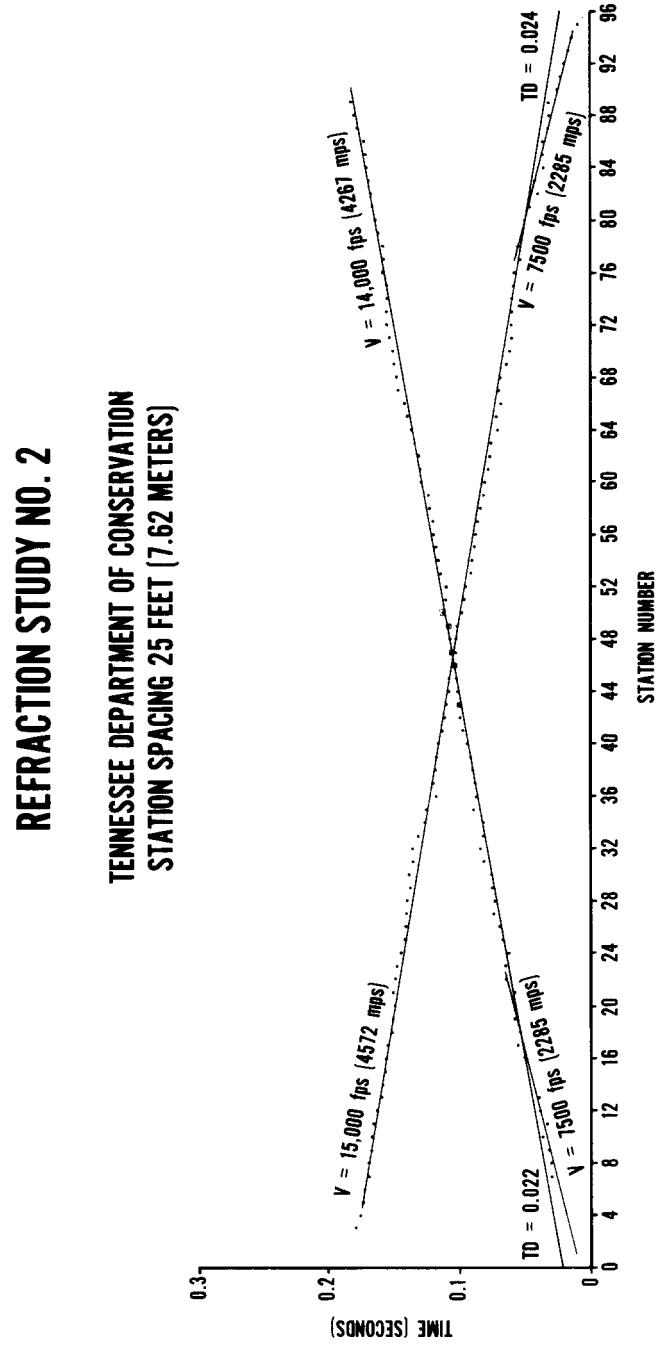
REFRACTION STUDY NO. 2
TENNESSEE DEPARTMENT OF CONSERVATION
STATION SPACING 25 FEET (7.62 METERS)
V = 14,000 fps (4267 mps)
V = 7500 fps (2285 mps)
TD = 0.024
V = 15,000 fps (4572 mps)
V = 1500 fps (2285 mps)
TD = 0.022
TIME (SECONDS)
0.3
0.2
0.1
0
0 4 8 12 16 20 24 28 32 36 40 44 48 52 56 60 64 68 72 76 80 84 88 92 96
STATION NUMBER

FIGURE 6B

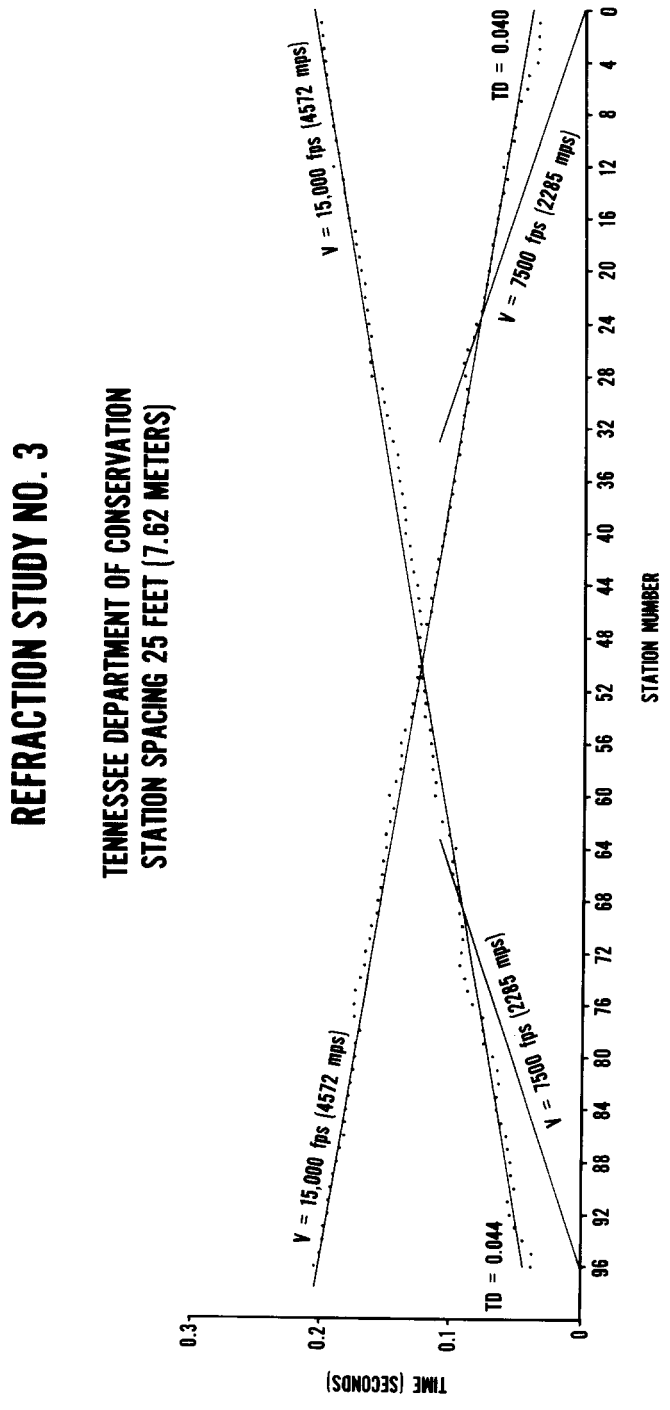
REFRACTION STUDY NO. 3
TENNESSEE DEPARTMENT OF CONSERVATION
STATION SPACING 25 FEET (7.62 METERS)
V = 15,000 fps (4572 mps)
V = 7500 fps (2285 mps)
TD = 0.040
V = 15,000 fps (4572 mps)
V = 7500 fps (2285 mps)
TD = 0.044
TIME (SECONDS)
0.3
0.2
0.1
0
STATION NUMBER
0 4 8 12 16 20 24 28 32 36 40 44 48 52 56 60 64 68 72 76 80 84 88 92 96

FIGURE 6C

SUBSURFACE DISTRIBUTION FOR SEGMENT OF LINE TC-1

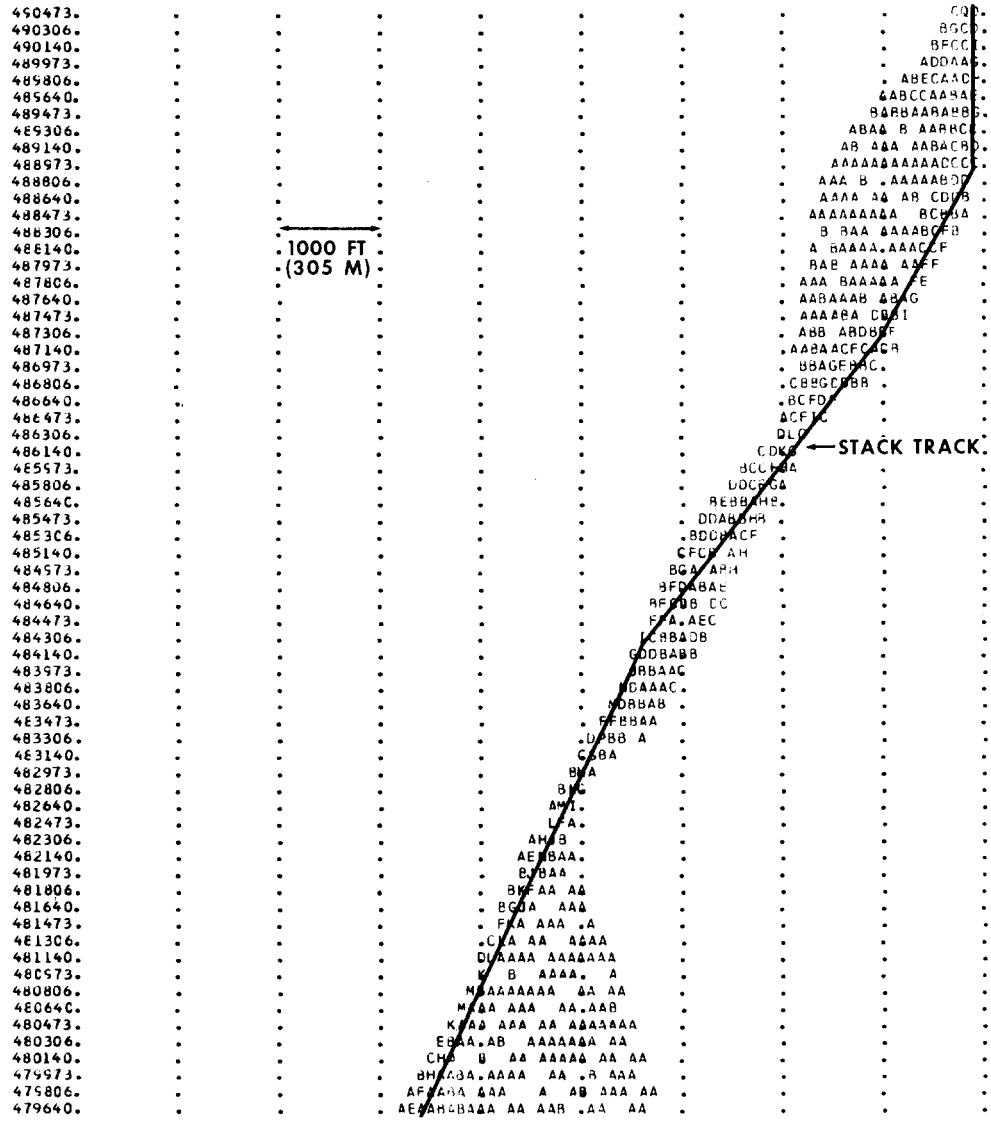

FIGURE 7

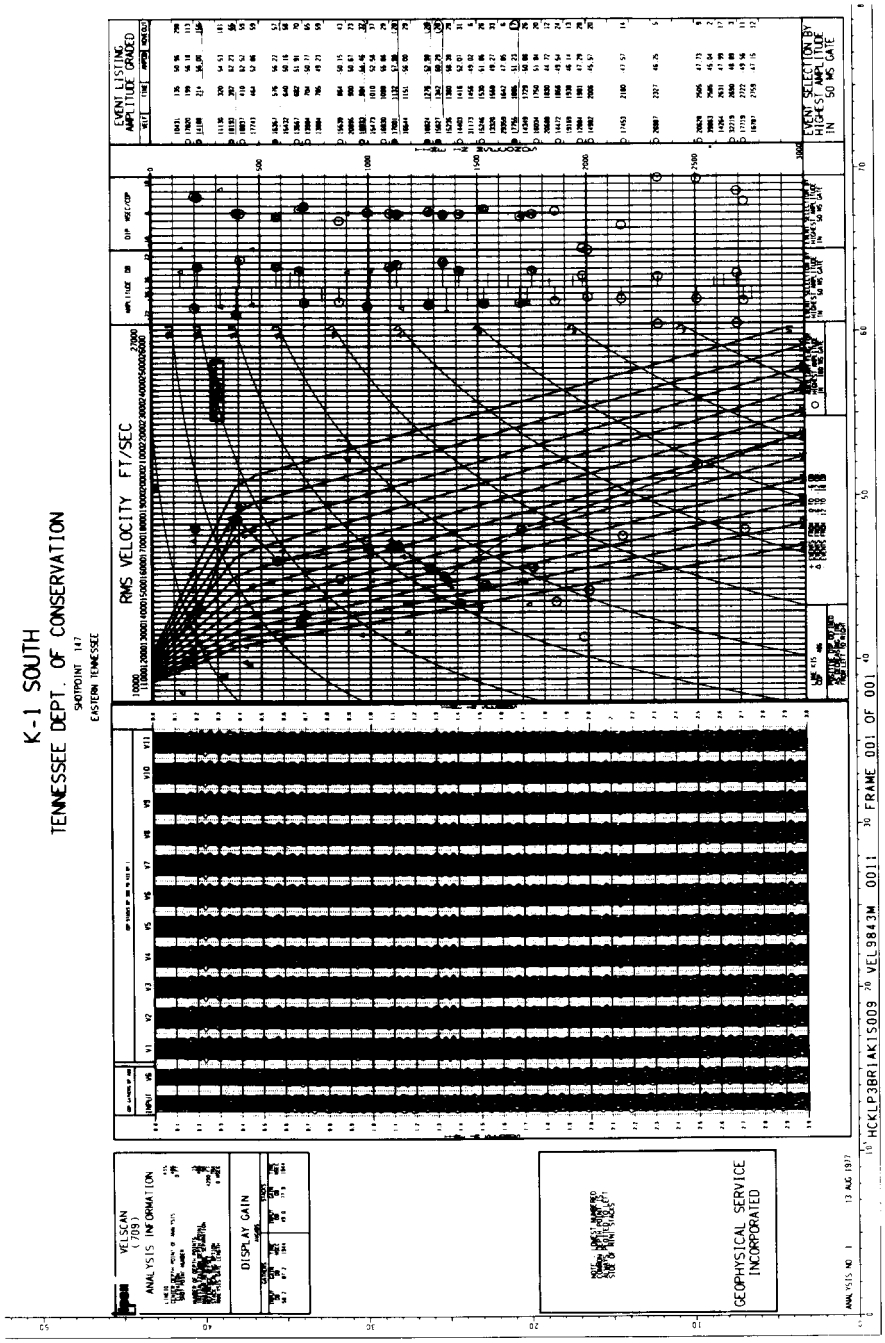
VELOCITY ANALYSIS EXAMPLE
K-1 SOUTH
TENNESSEE DEPT. OF CONSERVATION
SHOTPOINT 147
EASTERN TENNESSEE
RMS VELOCITY FT/SEC
EVENT LISTING
AMPLITUDE ORDER
EVENT SELECTION BY
HIGHEST AMPLITUDE
WELSCAN
(709)
ANALYSIS INFORMATION
DISPLAY GAIN
GEOPHYSICAL SERVICE
INCORPORATED
HCKLP3BRIAK1S009 70 VEL9843M 0011 30 FRAME 001 OF 001

FIGURE 8

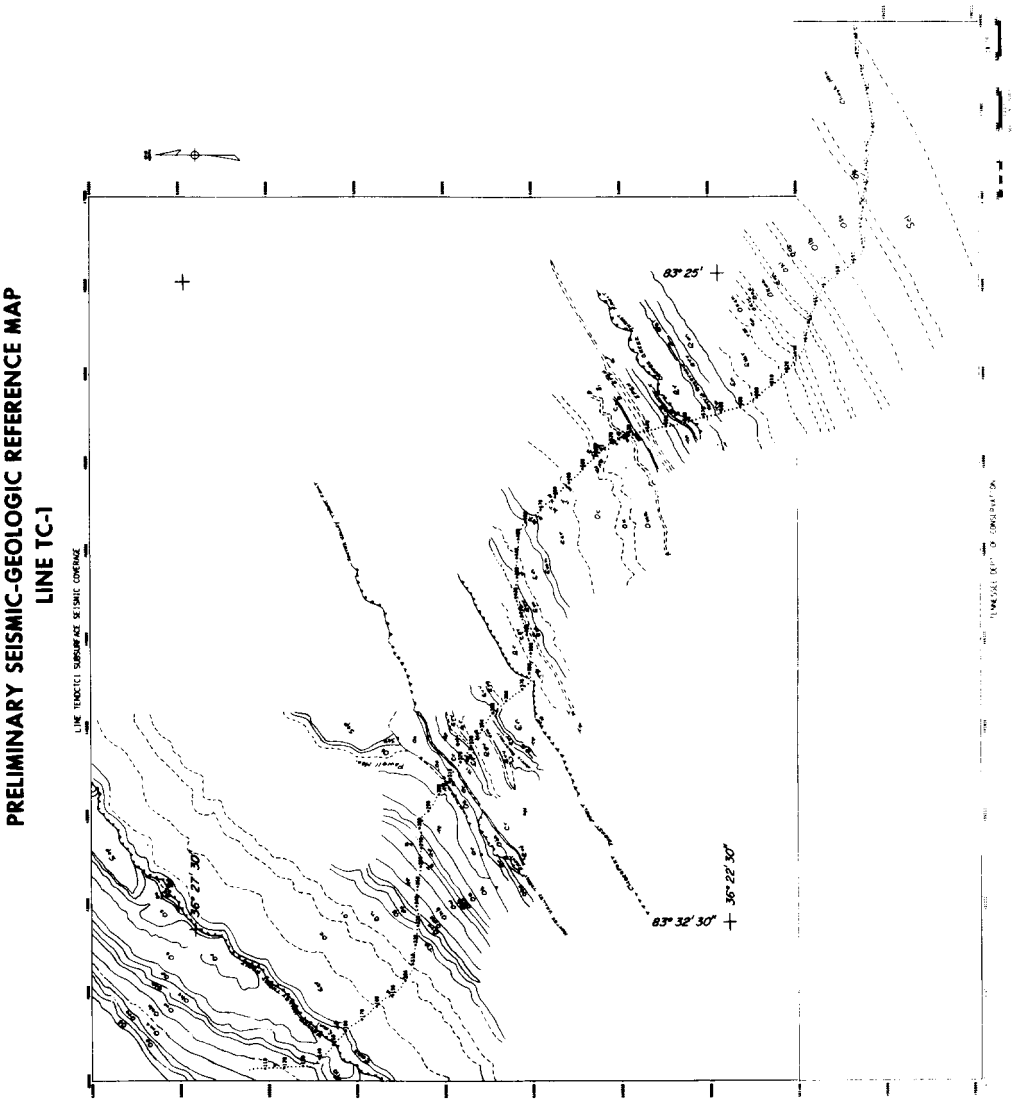
PRELIMINARY SEISMIC-GEOLOGIC REFERENCE MAP
LINE TC-1
LINE TENOCTC1 SUBSURFACE SEISMIC COVERAGE
83° 25'
83° 32' 30"
36° 22' 30"
36° 27' 30"

FIGURE 9

INTERRELATIONSHIPS OF PHOTOLINEAMENTS, GEOLOGICAL STRUCTURES, AND FRACTURE PRODUCTION OF NATURAL GAS IN THE APPALACHIAN PLATEAU OF WEST VIRGINIA

by

Eberhard Werner, Department of Geology and Geography,
West Virginia University, Morgantown, WV 26506

ABSTRACT

Natural gas production from the Devonian black shales of the Appalachian Basin is mainly from fracture permeability. Wells which intersect many natural or induced fractures are expected to be better producers than wells intersecting few or no fractures. Natural fracture zones often appear as photolineaments on various types of remote sensing imagery. In some areas, photolineaments have been demonstrated to be loci of improved production of hydrocarbons. Photolineaments are also often related to surface and subsurface fractures and stress fields. The various relationships of all these features in the Devonian shale gas production areas of western West Virginia were investigated during this project. Photolineaments were mapped from satellite and aircraft imagery; surface fractures were measured at outcrops; subsurface fractures were measured on cores; and natural gas initial open flow data were obtained from driller's logs. Fractures were found to relate to the primary directions of nearby photolineaments; however, there was considerable scatter in this data. Wells of high initial open flows are usually found between rather than on or near photolineaments.

INTRODUCTION

A significant fraction of all hydrocarbon production is from wells which either have intersected natural fractures or which have had fractures artificially produced in them. Such production comes from formations which, although "tight", have considerable hydrocarbons trapped in intergranular porosity. These formations have such low intergranular permeability that hydrocarbons, even natural gas, can only be produced economically from fractures. The Middle and Upper Devonian black shales of the Appalachian Basin which underlie the Plateau and eastern Continental physiographic provinces are excellent examples of the fractured hydrocarbon reservoir. It has been estimated that as much as 460 quadrillion cubic feet of gas - potentially 200 to 300 years supply - may be in these shales; of this, about 285 trillion cubic feet could be extracted under expectable conditions of technology and economics [1]. Since most of the wells are presently only marginally profitable, any exploration technique which decreases the ratio of low- to high-producing wells would increase the ultimate recovery.

The aim of the present project is to ultimately develop a technique for planning wells which uses low-cost remote sensing methods. Mapping of fractures and use of such maps in planning well fields has been a routine procedure in many areas. Normally photolineaments are mapped from air photos, satellite imagery, and any other type of imagery available. *Photolineaments* are continuous linear or curvilinear features or alignments of discrete features which can be detected on aerial photographs or other imagery [2]. Such procedures have been found to be of significant aid in some arid terrains such as those of northern Africa or southwestern Asia. In the United States, photolineament mapping has been successfully used as an exploration tool by Columbia Gas in their Haysi Field in western Virginia and southeastern Kentucky. Here it was found that for wells producing from the rather tight Berea siltstones, those wells drilled on or near photolineaments produced at about

twice the rate of the other wells [3]. The potential usefulness of the photolineament mapping procedures in fractured reservoirs is not restricted specifically to siting of wells. A relationship has been demonstrated among the orientation patterns of photolineaments, surface fractures, subsurface fractures, and regional stress fields [4]. Thus, even if specific siting cannot be done, the techniques can still be used for predicting induced fracture orientations in various stimulation procedures.

METHOD OF STUDY

Regional photolineaments were mapped from satellite imagery at scales of 1:1,000,000 and 1:5,000,000. Local patterns were mapped at various scales, but most commonly at 1:250,000 (the standard scale of the Eastern Gas Shales Project). Surface fractures (joints) were measured on outcrops in selected areas; orientation patterns were plotted; and preferred orientation directions determined. Subsurface data are scarce, and only that data derived from a core in Jackson County, West Virginia, was used in this study (published in [5], p. 16-17). Initial open flow figures were obtained from driller's logs on file with the West Virginia Geological and Economic Survey.

The area chosen for this study consists of portions of West Virginia and eastern Kentucky with small adjacent portions of Virginia and Ohio also included (figure 1). The reasons for choosing this area have been outlined previously [6]. Briefly, this area is of interest for two chief reasons: it is geologically or topographically different from other areas where remote sensing methods have been applied in the past; and it is underlain by the Devonian gas shales. Two areas of West Virginia were chosen for detailed study: 1) the Jackson-Mason County area, which contains the Cottageville (Mount Alto) Gas Field and has been the scene of intensive investigations by personnel of the Morgantown Energy Research Center of ERDA and others; 2) Wayne County, which has passing through it several major photolineaments associated with the 38th Parallel Lineament and also has available a considerable amount of initial open flow data for Devonian shale gas wells.

RESULTS AND CURRENT STATUS

This is the third and final year of this project. A full discussion of this project will be available in the final contract report and only a summary will be presented here. Results of previous years have already been reported [6]; only brief summaries of the current year will be given here.

Data Analysis Procedures

One of the major tasks of this project has been the evaluation and development of procedures and research tools. Among these are the statistical techniques used to test the similarity or dissimilarity of sets of orientation data. Last year it was discovered that the Wald-Wolfowitz Runs Test could be used to compare orientation data distributions. Subsequently, other tests were evaluated and one, Kuiper's modification of the Kolmogorov-Smirnov Test [7] was adopted for use in some of the statistical analyses. A computer program to plot orientation diagrams and to provide the statistical analyses of the data distributions was completed. Additionally, a general mapping computer program to aid in the analysis of the various types of data utilized by this project was completed. A discussion of the characteristics of these programs is beyond the scope of this report, but they will be fully described in the contract final report.

Relationship of Photolineaments to Geological Features

This year's effort in terms of this phase of the project consisted of collecting data on joints and comparing this with large-scale photolineament maps. Measurements of orientation and other properties of fractures in outcrops are the primary field data utilized in this project. A relationship between orientation of fractures in surface outcrops and fractures in subsurface hydrocarbon reservoirs has been established for some areas [8]. There is also a relationship between surface fractures and photolineaments in some areas [9, 10]. In the final report of this contract, there will be a more extensive discussion of these relationships; only a brief example of problems encountered and results obtained will be given here.

Problems encountered. In Jackson County (figure 1 shows location), the surface rocks are of the Permo-Pennsylvanian Dunkard Group which is primarily a deltaic sequence consisting of gray and red mudstones, siltstones, and channel and bar sandstones. The most prevalent rocks in outcrop are

the sandstones. There are several reasons why fractures measured on these sandstones may not be reliable indicators of regional fracture patterns. The sandstones tend to be relatively small patches surrounded by the mudstones. This leads to two conditions. First, regional fractures may not be propagated through the mudstones into the sandstones. Thus, fractures seen in the sandstones may well be due to fracturing of a brittle mass only poorly supported by the surrounding, rather weak mudstones and breaking up under its own weight. Second, the irregular shapes of the sandstone bodies can cause refraction of a propagating fracture and so change its orientation by twisting the propagating wave front about an axis parallel to the direction of propagation. In this case, although the fractures are related to regional fracture patterns, the directions found tend to differ from that pattern.

The effects of these problems are partially reduced by a regional analysis employing several thousand measurements. With this quantity of data, errors introduced by factors active in small areas are eliminated or greatly attenuated. In any case, however, any analysis done cannot depend on a *small* error margin.

Results. Figure 2 shows the most important preferred orientations at outcrops in the general area of the Cottageville Gas Field. Figure 3 is a summary of the more prominent photolineaments of the same area as the joint measurements. A comparison of figures 2 and 3 shows that several of the trends are coincident. The major preferred directions on both diagrams are approximately the same. There is, however, clearly not complete agreement between the two patterns. Assuming a relationship between the two types of features, the disagreement between the two sets of orientations could be caused by either 1) the distortions of joint directions by sand lenses as outlined above, or 2) a difference in reaction of the short (joints) and long (photolineaments) features to regional stresses which may have varied in direction. There is, however, too much coincidence of the orientations of the two sets of data for it to be ignored entirely. Thus, it appears that the photolineament maps may serve to at least partially predict surface outcrop fracture directions.

Predicting subsurface fracture orientation from photolineaments is less certain. It is difficult to evaluate this relationship mainly because of the lack of data. However, in the vicinity of the core from which the subsurface orientation measurements were taken is one outcrop site. The relationship between the two sets of orientation measurements is not clear-cut, but at least one of the major directions of the surface outcrop matches the chief subsurface fracture orientation. From this meager evidence, one may postulate a relationship between surface and subsurface fractures, and indirectly between subsurface fractures and photolineaments. Such a relationship needs extensive testing, however, before it can be applied as a predictive tool. The additional step of predicting subsurface fractures induced during stimulation of wells is even less certain because of additional restrictions placed on their formation by conditions under which they form.

Relationship of Initial Open Flows and Photolineaments

A considerable amount of raw data has been gathered. About 400 wells in Wayne County and 160 wells in the Jackson-Mason County area were found which included gas yield data for the Devonian shales. Most of the data is after-shot initial open flows although some natural open flows and underway gas tests were also found.

Problems encountered. Both the photolineament and the gas initial open flow data presented problems. The gas production figures were derived from driller's logs on file with the West Virginia Geological and Economic Survey. The information on such logs is of variable quality. Often it difficult to determine the source formation of the gas produced. It is possible also that some of the gas ascribed to the Devonian shale may come from another formation. Despite attempts to eliminate errors of this nature, it is possible that some errors nevertheless remain in the data.

Photolineament mapping presents many problems. Affecting the analysis most is the choice of imagery type and scale which in turn affects the type of photolineament mapped. If too large a scale is chosen, the map which results will have have far too many lines for usefulness in most cases. Almost any point would be on or near a photolineament and any kind of analysis depending on relative locations would probably be meaningless. (This type of map is not totally useless, however, since orientation patterns can still be obtained from it.) In this particular study, for example, it would be useless to have a map on which the photolineaments are closer together than the wells. In such a case, all wells would be "near" photolineaments.

It is also apparent that photolineaments mapped from different scales (and types) of imagery do not necessarily represent the same type of features. Literature reports of the width of the influ-

ence zone of photolineaments range from 40 feet to 1 mile. Most of this difference is probably due to imagery scale choices which result in photolineament maps which preferentially depict certain types of photolineaments. There is, however, no evidence that the influence zone width of photolineaments is always related to imagery scale. Thus, any test made for the relationship of proximity of a well to a photolineament and hydrocarbon production will have the uncertainty related to influence zone width.

Results. Test analyses were done for Wayne County and for the Jackson-Mason County area. The photolineament maps for both areas (figures 4, 5, 6, and 7) were prepared in a similar manner. Individual maps were produced for each of the types of imagery available (8 maps for Jackson-Mason, 4 maps for Wayne). These were then superimposed and those photolineaments which appeared on two or more maps were extracted and are shown on figures 4-7. Superimposed on these photolineament maps are the before- and after-shot open flow data.

The results for Wayne County seem to indicate that the natural open flows are less on or near photolineaments. After-shot open flows are not clearly related to photolineaments. Although some of the wells with high after-shot flows do fall on or near the photolineaments, even more fall between them. There are no high natural open flows on or near photolineaments (except possibly for one case).

The picture for the Jackson-Mason County area is similar. An additional photolineament map was produced from imagery at a scale of 1:65,000 for the Cottageville Gas Field because of the close spacing and generally higher yields of those wells. The results were no different than those above. The wells with high initial open flows were not near photolineaments.

These results are not entirely unexpected in light of the probable characteristics of the features represented by photolineaments. Such features are generally zones of undetermined (but ranging at least from 40 feet to 1 mile) width in which the rocks differ from those around them, and in particular, where the rocks are more fractured than the surrounding rock. If no secondary mineralization has caused sealing of the fractures, such zones should be much more permeable than the country rock. However, since photolineaments, by the fact that they can be seen on aerial imagery, must represent conditions at the surface of the earth, and if these conditions (i.e., fracturing) exist to the depth of the gas reservoir, then it is entirely reasonable that the gas has been vented to the surface through the fracture permeability. The only conditions under which one might expect better production due to such fracture zones would be if they were very well sealed above the gas reservoir.

Thus, it appears that the locations of photolineaments are poor choices for gas wells in the area investigated. Several possible explanations exist for the apparent discrepancy of findings of this study and that referenced for the Haysi Field [3]. First, the lithologies of the producing formations are different. The producing horizon in the Haysi Field is the Berea siltsone; the producing horizon in western West Virginia is the Devonian shale. The two rock types behave differently under stresses which produce fracturing. Second, the Haysi Field is located in an area of Appalachian thin-skinned tectonics, where the areas of this study are probably not.

CONCLUSION

Photolineament maps may be used to predict surface fracture orientations, and indirectly may also be useful to predict subsurface fracture orientations. Both of these relationships must be further tested, particularly in areas of different lithologies and different tectonic histories. Natural open flows of gas wells in the study area appear to be low on photolineaments, with high open flows occurring only between photolineaments. High values of after-shot open flows appear to be more uniformly distributed. Chances of good wells appear to be slightly enhanced by avoiding locations near photolineaments seen on small-scale imagery.

ACKNOWLEDGEMENTS

The work in this project was supported initially by U.S. Bureau of Mines Grant G0155011 and later by U.S. ERDA Contract E-(40-1)-8040. Thanks are due Robert C. Shumaker and Russell L. Wheeler of the Department of Geology and Geography of West Virginia University and William K. Overbey, Jr. and Clyde Pierce of the Morgantown Energy Research Center, ERDA, for their advice throughout this project.

REFERENCES

1. Brooks, Kenneth: "Devonian Shale Gas Study", presented at Devonian Shale Symposium, Columbus, Ohio (1972).
2. Werner, Eberhard: "Photolineament Mapping in the Appalachian Plateau and Continental Interior Provinces - A Case Study", *Proc. 5th Remote Sensing of Earth Resources Conf.* (in press).
3. Ryan, William M.: "Remote Sensing Fracture Study - Western Virginia and Southeastern Kentucky", *U.S. ERDA MERC/SP-76/2* (1976), 94-95.
4. Overbey, W. K. Jr., W. K. Sawyer, and B. R. Henniger: "Relationships of Earth Fracture Systems to Productivity of a Gas Storage Reservoir", *U.S. Bureau of Mines RI 7952* (1974), 133 p.
5. Patchen, Douglas G. and Richard E. Larese: "Stratigraphy and Petrology of the Devonian 'Brown' Shale in West Virginia", *U.S. ERDA MERC/SP-76/2* (1976), 4-19.
6. Werner, Eberhard: "Remote Sensing Studies in the Appalachian Plateau for Application to Fossil Fuel Extraction", *Second ERDA Symposium on Enhanced Oil & Gas Recovery, Proceedings* (1976) 2, C-2/1 - C-2/10.
7. Kuiper, Nicolaas H.: "Test Concerning Random Points on a Circle", *Indag. Math.* (1960) 22, 38-47.
8. Komar, C. A., W. K. Overbey, Jr., R. L. Rough, and W. S. Lambert: "Factors that Predict Fracture Orientation in a Gas Storage Reservoir", *J. Pet. Tech.* (May 1971) 23, 546-550.
9. Werner, Eberhard: "Long Lineaments in Southeastern West Virginia", *Proc. W. Va. Acad. Sci.* (1975) 47, 113-118.
10. Kowalik, W. S.: "Comparison of Skylab and LANDSAT Lineaments with Joint Orientations in Northcentral Pennsylvania", The Pennsylvania State University, *ORSER-SSEL Technical Report 12-75* (1975) 12 p.

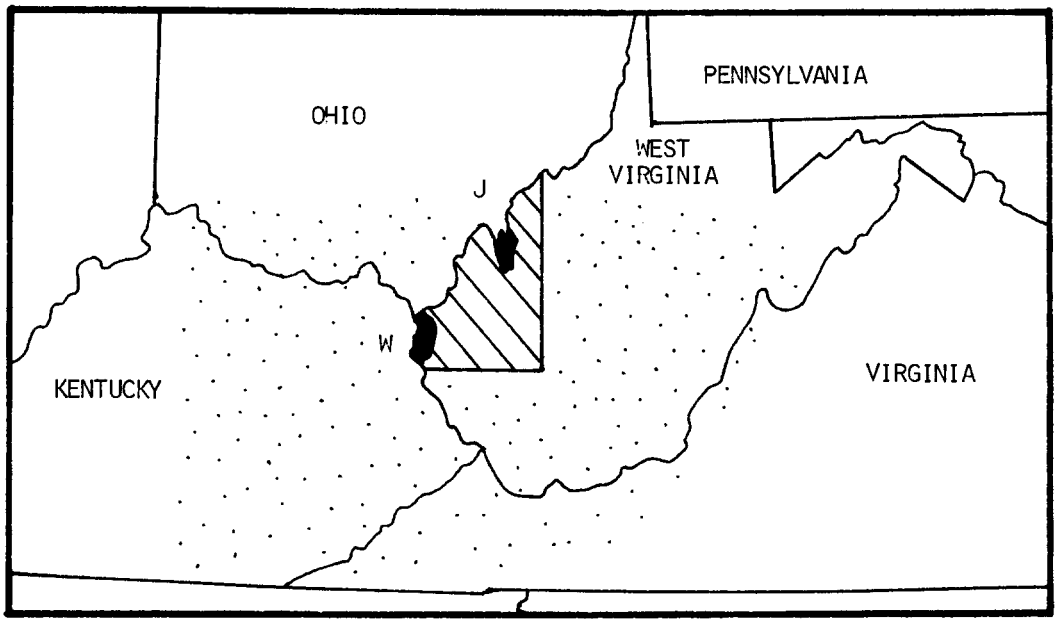

Figure 1. Area of study. The overall photolineament study covers the area shown in stipple pattern. The area of West Virginia underlain by the Devonian gas shales is approximated by the shaded area. J - Jackson County, W - Wayne County.

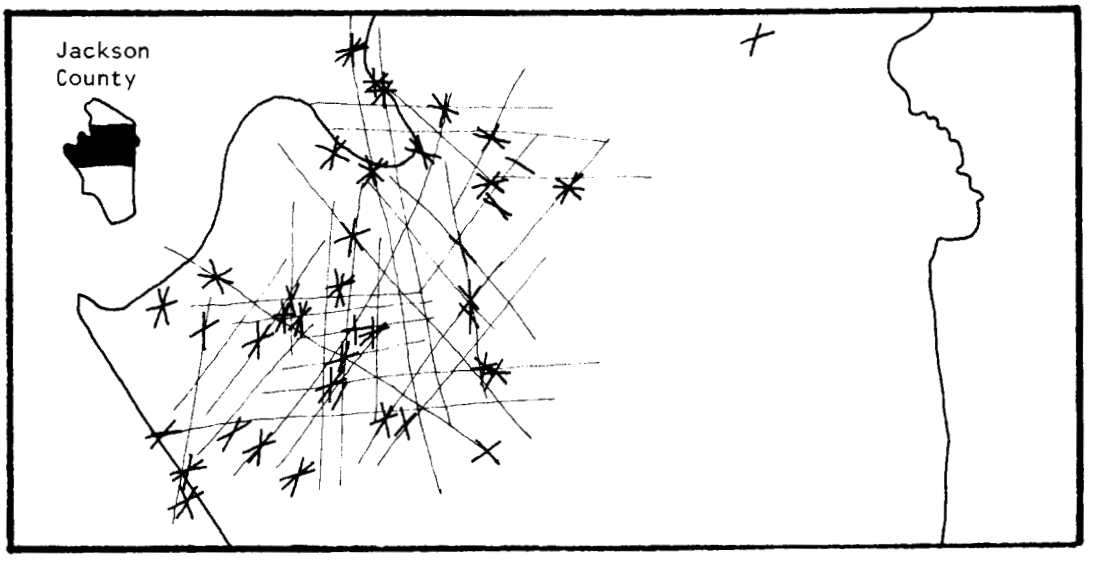

Figure 2. Joint patterns in part of Jackson County, West Virginia. The rosettes indicate the orientation peaks at individual outcrops. Light lines are interpolations of these directions between outcrops and are probably indicative of the regional trends.

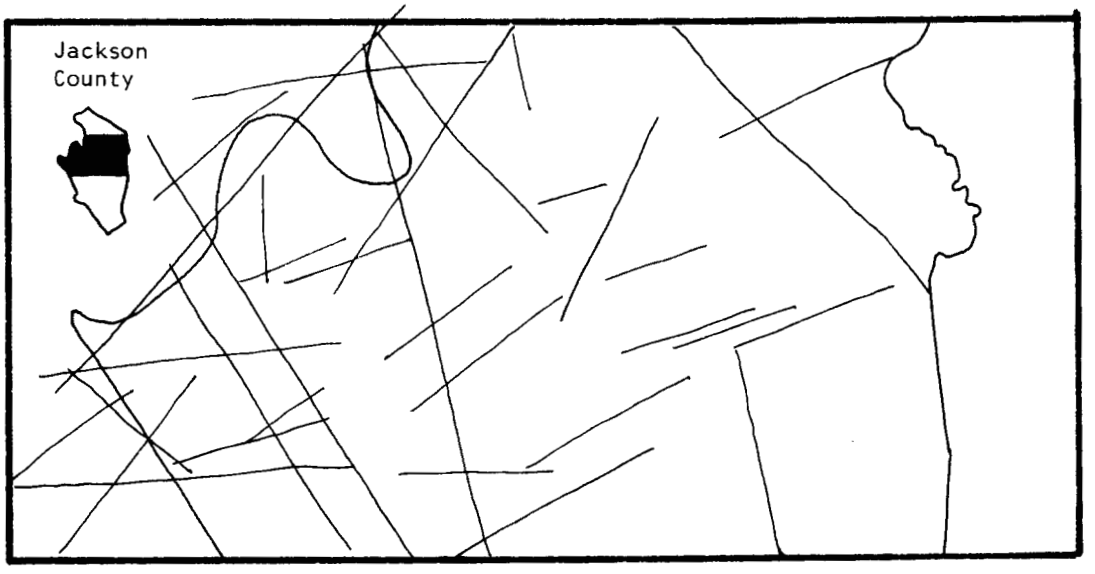

Figure 3. Major photolineaments in the portion of Jackson County for which joint data is shown in figure 2. Photolineaments are derived from LANDSAT, Skylab, and high-altitude aircraft imagery. Photolineaments shown are visible on two or more of the eight images used.

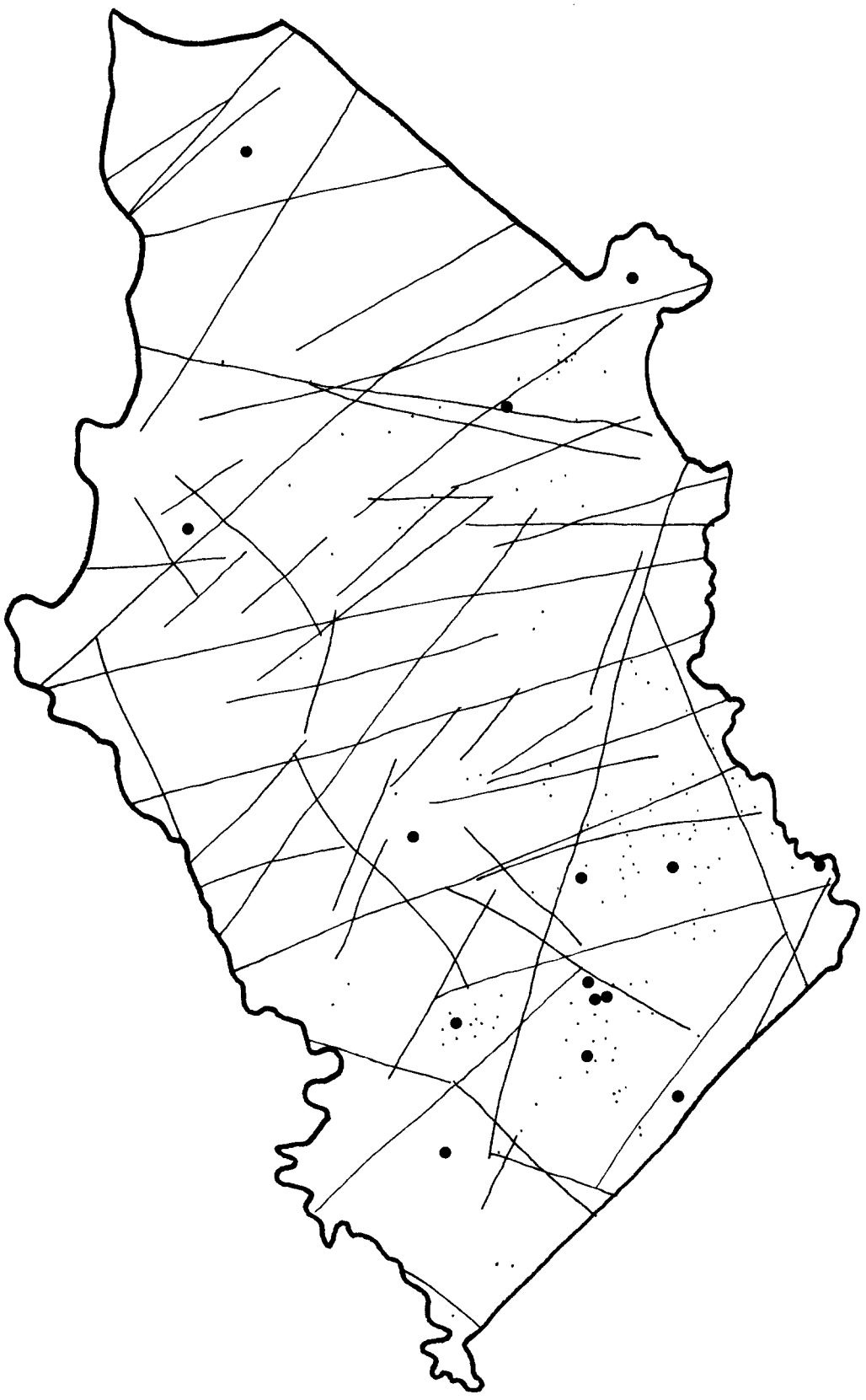

Figure 4. Map of Wayne County, West Virginia showing major photolineaments (those visible on two or more of the four images used) and natural initial open flows of gas wells. Small dots indicate relatively poor wells, large dots relatively good wells.

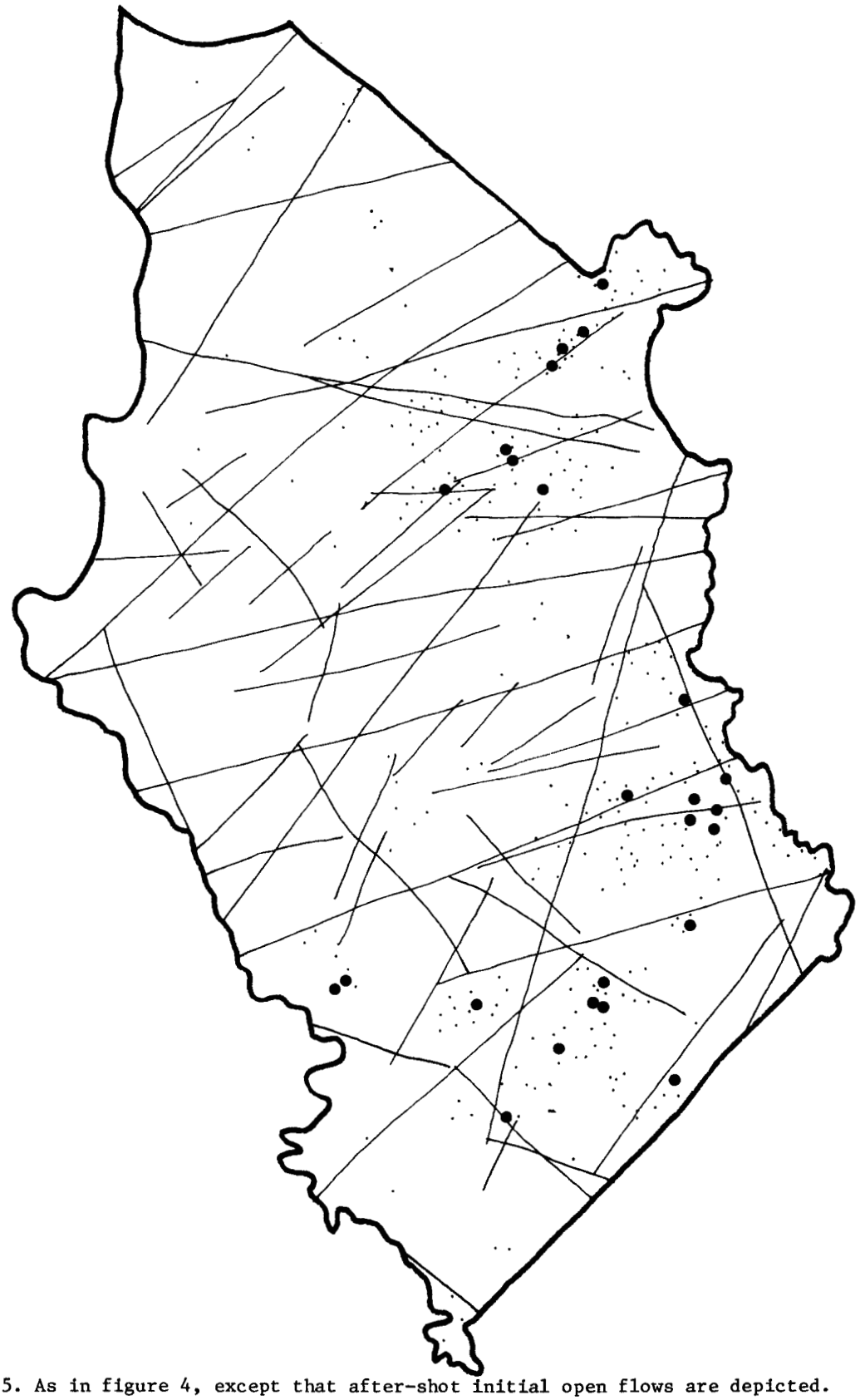

Figure 5. As in figure 4, except that after-shot initial open flows are depicted.

Figure 6. Map of Jackson County and a portion of Mason County, West Virginia, showing major photolineaments (those visible on two or more of the eight images used) and natural open flow of gas wells. Large dots indicate good wells, small dots relatively poor wells.

Figure 7. As in figure 6, except that after-shot initial production is depicted.

CORRELATION BETWEEN OUTCROP FRACTURES, GEOPHYSICS AND ROME TROUGH STRUCTURE IN KANAWHA COUNTY, WEST VIRGINIA

by

BYRON R. KULANDER, ALFRED UNIVERSITY
STUART L. DEAN, UNIVERSITY OF TOLEDO
RICHARD E. WILLIAMS, JOHNS HOPKINS UNIVERSITY

ABSTRACT

The eastern flank of the Rome trough through Kanawha County, West Virginia, is steepened by pronounced faulting. Normal faults, down to the west, produce a maximum vertical separation of approximately 7000 feet within a horizontal distance of several miles. Total relief along the eastern margin of the trough in Kanawha County is approximately 10,000 feet from the trough axis to the crest of the eastward-lying Central West Virginia arch. The western trough margin is also undoubtedly faulted. However, geophysical data suggest that fault activity, particularly vertical offsets of the scale attributed to large eastern margin faults may be diminished. Total intensity residual magnetic relief over the pronounced basement faults, from the Central West Virginia arch in Clay and Fayette Counties to the trough axis totals 450 gammas. The sharp residual gradient slopes northwest, is convex upward in profile over the basement faults, and regionally corresponds with the eastern margin of the Rome Trough throughout West Virginia. A Bouguer gravity map, uncorrected for terrain effects, shows a west-dipping steepened gravity gradient of 10 (mgal) milligals in Kanawha County over the eastern trough margin. A pronounced 7 mgal gravity gradient exists over the fault-steepened sector of the trough margin. Regionally, a linear gravity low and high, including the intervening steepened western dipping gradient, correspond with the Rome trough and Central West Virginia arch basement features respectively. The Rome trough and Central West Virginia arch are also geologically differentiated on a regional and local scale. A zone of increased low amplitude folds in Paleozoic strata lies between the trough and arch axes. A coal form-line structure map compiled by R. Shumaker (1974, West Virginia Geological Survey) shows an abrupt increase in structural complexity from west to east over the eastern trough margin. Southward in Mingo and Logan Counties, West Virginia, the Warfield fault outcrop trace corresponds with the pronounced eastern trough margin basement faulting. In Kanawha County, the Cabin Creek Syncline lies over the basement fault zone. Most interesting, however, is the observation that the basement faults, including related structural style changes and geophysical anomalies, separate two major systematic fracture domains. Regionally consistent systematic and nonsystematic fractures in coal (face and butt cleat) change trend immediately over the basement faults delineating the eastern margin of the Rome Trough. The abrupt coal fracture trend change occurs generally within two to four miles. Coal systematic fractures west and east of the basement fault zone trend N45°W and N75°E respectively. At many outcrops within the fracture trend change zone, both systematic-nonsystematic fracture sets are present. At some outcrops within this zone the coal appears to be chaotically fractured, and locally formed fracture sets obscure regionally developed fracture trends.

GENERAL GEOLOGY

Exposed bedrock within the area under investigation ranges in age from the Lower Pennsylvanian New River Formation to the Permian Dunkard Group (Figure 1). The region lies entirely within the Allegheny plateau and is traversed by the low amplitude folds characteristic of this structural province. Two distinct fold trends are evident. The predominant and subordinate axial trace trends are N40-45E and N-S, respectively. The Warfield anticline displays dips on either limb recognizable at a single outcrop, and is the predominant structure crossing the area. A form-line map of surface coals in West Virginia, compiled by Shumaker (1), accurately depicts the surface rock configuration (Figure 2) and compliments structural data obtained from the West Virginia geological map (2).

Structural contour maps of the Mississippian age Greenbrier Limestone (3), and the Lower Middle Devonian Onondaga limestone (4), show subsurface folding at least through Middle Devonian strata. Major surface fold trends can be generally correlated with subsurface folding. Onondaga structural contours are more closely spaced on the east limb of the northeastward plunging Warfield anticline indicating structural asymmetry toward the east. Values of total structural relief on the western and eastern flank of the Warfield structure at the Onondaga level are 500 and 1200 feet respectively along the southern Kanawha County boundary. Structural contours on the Onondaga and Greenbrier formations show vertical northeastward plunge component of 1000 feet and 300 feet respectively. The 300 foot vertical plunge component corresponds with the surface plunge shown on the form-line map. The 1000 foot vertical plunge component corresponds approximately with the northeastward Rome Trough basement deepening in Kanawha County. Part of the 700 foot plunge difference may be attributed to the fact that Greenbrier rocks rise regionally to the northeast in contrast to Onondaga rocks which plunge regionally northeastward. However, northeastward stratigraphic thickening and/or a structural discontinuity may exist between the Greenbrier and Onondaga levels to account for the apparent discrepancies in the vertical plunge components. This interval (Middle Devonian to Middle Mississippian) contains the Devonian gas shales that are of primary importance to the eastern gas shales project.

Figure three shows that Precambrian surface structure within the investigation area is dominated by sections of the Rome Trough and eastward lying central West Virginia arch (5). Evidence to date suggests that the deepest section of the Rome Trough lies in Kanawha County. The Rome Trough's eastern flank and the western limb of the central West Virginia arch are accentuated by a narrow zone of pronounced normal faulting. Normal faults within this zone have a maximum combined throw of 7000 feet within a horizontal distance of two miles. The Rome Trough's western margin is also undoubtedly faulted. However, to date the authors have not had access to seismic data to corroborate this assumption. Magnetic and gravity data do not indicate faulting of the magnitude evident on the eastern flank of the trough.

Several spatial correlations can be drawn between proposed basement structure and surface geology if Figures 1, 2, and 3, and a regional tectonic map are compared.

(1) The surface expressions of shallow north-to-northeast trending folds show an increase in frequency over the Rome Trough. This is especially evident if the basement map and a tectonic map are regionally compared.

(2) Basement structure and subsurface geology regionally show an increase in the number of fold axial traces over the central West Virginia arch.

(3) Isopach maps by Ping Fan Chen (6) of the Cambrian-Ordovician Conococheague, Stonehenge, Chazy and Chambersburg formations show depoaxes corresponding generally with the Rome Trough.

(4) The axis of the Warfield anticline corresponds generally with the deepest portions of the Rome Trough.

(5) The Warfield fault surface trace in northern Mingo County, immediately south of the map area, lies over the projected zone of basement faulting. Fault movement through Pennsylvanian time may be attributed to continued basement movement and/or differential compaction over the trough. If fracturing throughout the sedimentary column is related to the basement fault zone the Devonian shales in this region may possess increased fracture porosity.

TOTAL INTENSITY RESIDUAL MAGNETIC MAP

The total intensity residual magnetic map taken from a previous regional map compiled by the authors (5) illustrates magnetic anomalies that can be directly related to basement features (Figure 4). The Rome Trough axis corresponds with a linear Rome magnetic low, and the central West Virginia arch possesses a distinct linear positive magnetic signature (5). Zietz and King (7) have shown that these magnetic features are continuous from New York to Alabama. The westward dipping magnetic gradient separating the Central West Virginia anomaly from the Rome Trough magnetic low is the most pronounced in the region with a maximum magnetic relief within the mapped area of 840 gammas. This convex and pronounced magnetic gradient corresponds almost exactly with the zone of Rome Trough basement faulting.

The pronounced +300 gamma elongate magnetic anomaly through southernmost Kanawha County was used to calculate burial depth and a minimum susceptibility contrast for the anomaly producing body (5). An averaged depth of -18,400 below ground surface was obtained by the Vacquier method (8) utilizing total magnetic intensity, magnetic curvature, and aeromagnetic analog tapes supplied by the United States Geological Survey. Depths by all methods ranged between -18,040 and -18,800 feet. These depths are too low for the upthrown Rome Trough fault block surface, and the basement depths shown in Figure 3, are based on seismic profiles and stratigraphic projections. The calculated minimum susceptibility contrast obtained from the magnetic studies is .0017 cgs units. If the basement is assumed to be predominantly granodiorite, this susceptibility contrast indicates a mafic anomaly generating body, perhaps approximating gabbro or anorthosite in composition. If the trough is an extensional feature, its association with mafic or ultramafic rocks would not be surprising. Well data from Kentucky Geological Survey files list three wells in eastern Kentucky (Boyd County), on the northwest flank of the Rome Trough, that penetrated basement anorthosite. A deep well in Mingo County also drilled into basement rock of this composition.

The maximum residual magnetic relief of 840 gammas over the buried fault zone cannot be attributed to basement faulting alone. A two dimensional total intensity magnetic curve was calculated assuming (1) vertical fault with a displacement of 7000 feet, (2) burial depth to the upthrown block surface of -15,000 feet (subsea), (3) susceptibility contrast of .0025 cgs units between mafic basement and overlying sedimentary rocks, (4) vertical rock magnetization. The calculated maximum magnetic relief for the profile proved to be 200 gammas. It is emphasized that the 200 gamma figure is a maximum value for the fault-induced component of the total 840 gamma observed magnetic anomaly. This is so because the susceptibility contrast was assumed for fault offset mafic rocks. The susceptibility contrast and resulting anomaly would be less if basement rocks were more granitic and the propounded mafic intrusion top was located beneath the Precambrian surface. In any case the major component of the magnetic anomaly must be attributed to an intra-basement susceptibility contrast. To illustrate this, a total intensity magnetic curve was calculated over the fault area assuming a susceptibility contrast within the basement. The model assumed (1) no basement fault, (2) the previously calculated susceptibility contrast of .0017 cgs units (mafic intrusion into granodioritic host rock, (3) width for the vertical tabular intrusion of 15 miles (obtained from magnetic curvature map), (4) tabular intrusion extending 25 miles to the base of the earth's crust, (5) tabular intrusion top at -18,500 feet (subsea). The calculated magnetic profile produced a maximum anomaly of 600 gammas.

The two dimensional fault and intrusion models can be viewed as approximate at best. However, they do indicate the necessity for the major magnetic influence of an intra-basement mafic intrusion.

BOUGUER GRAVITY

A Bouguer gravity map of the area under investigation was contoured from Bouguer gravity data obtained from the National Defense Mapping Agency (Figure 4). The map, uncorrected for terrain effects, shows good correlation of a pronounced linear gravity high and low with the Central West Virginia arch and the Rome Trough basement features respectively. Maximum total relief along the northwestward-sloping gravity gradient across the fault zone, from gravity high to gravity low, is 19 mgals. The steepest section of this gravity gradient (5 to 9 mgals) generally lies immediately west of the fault zone. No residual Bouguer gravity map was constructed. However, a calculated gravity profile over the steepest gradient and fault intersection in the north-central map sector, produced a maximum difference of 15 milligals in a distance perpendicular to gradient of 14 miles.

This compares with the observed Bouguer anomalies and would approximate residual gravity values if they were derived. The profile assumed (1) a basement fault with burial depths and dimensions as described in the magnetic section, (2) a density contrast of 0.1 gm./cm^3 (sedimentary rocks = 2.65 gm./cm^3, basement rocks = 2.75 gm./cm^3). The gravity model is much oversimplified. Until more density and gravity data are obtained only these tentative observations can be made. However, preliminary treatment of available gravity data do indicate a faulted basement and an intra-basement intrusion (2.75 gm./cm^3 density). If more gravity data were obtained, corrected for terrain effects, and residual anomalies isolated, a more accurate gravity model could be derived.

SYSTEMATIC AND NONSYSTEMATIC FRACTURES IN COAL.

The terminology utilized in the coal outcrop fracture analysis is essentially that adopted by Hodgson (9, 10). Coal systematic fractures (face cleat) are those that are repeatedly found in a common orientation. Those of any specific orientation are considered to be in the same set. Systematic fractures in most cases are vertical, exhibit planar or gently curved surfaces, and are typically regional in nature. However, local systematic fracture sets can be related to various nearby structures. Nonsystematic coal fractures (butt cleat) generally display a more curviplanar surface and typically terminate at systematic fractures. The nonsystematic coal fractures show a greater variation in strike at any given station. The term "cross joint" used by Hodgson for a particular type of nonsystematic fracture has not been adopted by the authors because of possible confusion with fractures in igneous rocks (11,12) and those perpendicular to fold axes (13) that have been given the same designation by other investigators.

A regional fracture pattern for any given rock type can generally be broken down into distinct fracture domains. Fracture domains, especially in coal, are generally, but not always, distinguished by the presence of a predominant fracture direction. However, several fracture sets can persistently occur in the same domain. Fracture domain boundaries, marking zones where regional fracture trends change, can be abrupt (2 to 10 miles) or gradual.

Regional systematic and nonsystematic fractures in coal are well-developed in the investigation area. Furthermore regional fracture studies in other sections of the Allegheny plateau indicate that systematic fractures in a given fracture domain possess a singular trend with little variation for thousands of square miles (14). This may be true for any rock type and particularly so for coal and Mississippian age sandstone and shale.

Fracture frequencies in coal as a rule proved to be more highly variable at a single outcrop than over an entire fracture domain. Fracture frequency in glossy vitrain layers was greater than in dull fusain or durain coal layers. Fracture frequencies in bone coal were lowest of all, and bone coal fractures often differed in trend from associated coal beds.

Two coal fracture domains are evident within the area under investigation (Figure 6). Systematic fractures over the Rome Trough trend N45W with few exceptions. In contrast the predominant fracture trend within the domain occupying the southeastern map sector over the central West Virginia arch is N70E. Another domain boundary trending east-west and lying between 38°15' and 38°30' latitude may transect the map area. North of this probable boundary fracture trends change from N70°E to EW. Ongoing fieldwork will better delineate these fracture trend changes.

The boundary separating the two major fracture domains is marked and abrupt. Fracture trends common to one domain change within two to ten miles to fracture trends characteristic of the adjoining domain. Within this domain boundary, fracture trends common to both domains may occur together and local systematic fracture sets are present. At many outcrops within the domain boundary the coal is chaotically fractured by both regional systematic fracture sets and superimposed local sets. A critical result of multiple fracture set occurrences within the domain boundary is that fracture permeability is increased even though the range of fracture frequencies at a given outcrop may not change appreciably.

The most casual appraisal of the major domain boundary position reveals a remarkable spatial relationship. The fracture domain boundary coincides exactly in the studied area with the zone of predominant basement faulting and related geophysical anomalies that accentuate the eastern Rome Trough margin. To the authors' knowledge, this is the first regional fracture domain boundary in the Allegheny plateau in West Virginia that can be geometrically related to a marked and proven basement structure and resulting magnetic and gravity anomalies.

A comprehensive interpretation attempting to explain the origin of the coal fractures would be premature at this time. Data accumulated to date is incomplete and is not available for all rock types. However, the following preliminary observations can be made.

(1) Coal fractures were initiated in the brittle fracture mode and propagated perpendicular to the local maximum principal tension.

(2) Systematic and nonsystematic coal fractures are not geometrically related to fold axes. Evidence from other parts of the plateau indicates that systematic-nonsystematic fractures in all rock types predate and are unrelated to folding (14,15).

(3) Regional fracture sets in the mapped area change trend abruptly over the basement fault zone. Also, no well-formed fracture sets differing from regional trends are persistent everywhere along and within the domain boundary. If it is assumed that all systematic fractures formed at approximately the same time, then the basement fault zone would have served as a boundary separating different stress fields responsible for the fracturing. It follows that the fault zone may have in some way attributed to the two distinct stress fields. Spatial relationships strongly support this premise.

(4) If domain boundaries for systematic fractures in other rock types lie over the basement fault zone, photolineaments related to fracture trends and resulting topography could change orientations in this location. However, no discrete lineaments parallel to the buried fault zone need be present.

CONCLUSIONS

The geological and geophysical relationships and implications discussed in previous sections could prove to be extremely important. Increased fracture frequency and permeability in coal is produced by the presence of overlapping regional and additional local fracture sets within the investigated fracture domain boundary. If increased fracture permeability is present in underlying strata, the gas bearing Devonian shale and other reservoir rocks above the basement fault zone may prove to be an area of high exploration potential.

ACKNOWLEDGEMENTS

The authors express their appreciation to Richard Borst and Frank Secondo, academic and operations managers at the Alfred University Computing Center, for assisting with data reduction and map printing. The authors would also like to thank Mr. and Mrs. H. R. Kulander for their hospitality during the field work phase of this project.

REFERENCES

(1) Shumaker, Robert, 1974, Coal form-line structure map, W. Va. Geol. and Econ. Survey, Morgantown, WV, 26505, open file report.

(2) Cardwell, D. H., Erwin, R. B., and Woodward, H. P., editors, 1968, Geologic map of West Virginia, W. Va. Geol. and Econ. Survey, Morgantown, WV, 26505.

(3) Haught, Oscar, 1968, Structural contour map of the Greenbrier Limestone in West Virginia, W.Va. Geol. and Econ. Survey, morgantown, WV, 26505.

(4) Cardwell, D. H., 1973, Deep well and structural geologic map of West Virginia, W.Va. Geol. and Econ. Survey, Morgantown, WV, 26505.

(5) Kulander, B. R., and Dean, S. L., in press, Gravity, Magnetics, and Structure of the Allegheny Plateau-Western Valley and Ridge in West Virginia and adjacent states, W.Va. Geol. and Econ. Survey, Morgantown, WV, 26505.

(6) Chen, Ping Fan, 1972, unpublished isopach maps of select Cambrian and Ordovician rock units, W. Va. Geol. and Econ. Survey, Morgantown, WV, 26505.

(7) Zietz, I., and King, E. R., 1977, The New York-Alabama Lineament: a possible plate boundary, in abs with programs, Geol. Soc. Amer., v. 9, No. 3, p. 333.

(8) Vacquier, V., Steenland, N. D., Henderson, R. G., Fietz, I., 1951, Interpretation of Aeromagnetic maps, Geol. Soc. Amer., Mem. No. 47, 151 p.

(9) Hodgson, R. A., 1961, Regional Study of Jointing in the Comb Ridge-Navajo mountain area, Arizona and Utah, Bull. Am. Ass. Petrol. Geol., v. 45, pp. 1-39.

(10) Hodgson, R. A., 1961, Classification of Structures on Joint Surfaces, Am. J. Sci., v. 259, pp. 493-502.

(11) Balk, R., 1937, Structural behavior of igneous rocks, Geol. Soc. Amer. Memoir 5, 177 pp.

(12) Hutchison, R. M., 1956, Structure and petrology of the Enchanted Rock batholith, Llanc and Gillespie Counties, Texas, Geol. Soc. Amer. Bull., v. 67, pp. 763-806.

(13) Badgley, P. C., 1965, Structural and Tectonics Principles, Harper, New York, NY, 521 pp.

(14) Dean, S. L., Kulander, B. R., Williams, R. E., 1977, (in press), Regional Tectonics, systematic fractures, and photolinears in Southeastern West Virginia, in Proceedings of the Second International Conference on Basement Tectonics, ed. Melvin Podwysocki, Nat. Aeronaut. and Space Admin., U.S. Geol. Survey.

(15) Dean, S. L., Kulander, B. R., 1977, Kinematic Analysis of Folding and Prefold Structures on the Southwestern Flank of the Williamsburg anticline, Greenbrier County, West Virginia, in Abstracts with Programs, Southeastern Section, Geol. Soc. Amer., v. 9, No. 2, pp. 132-133.

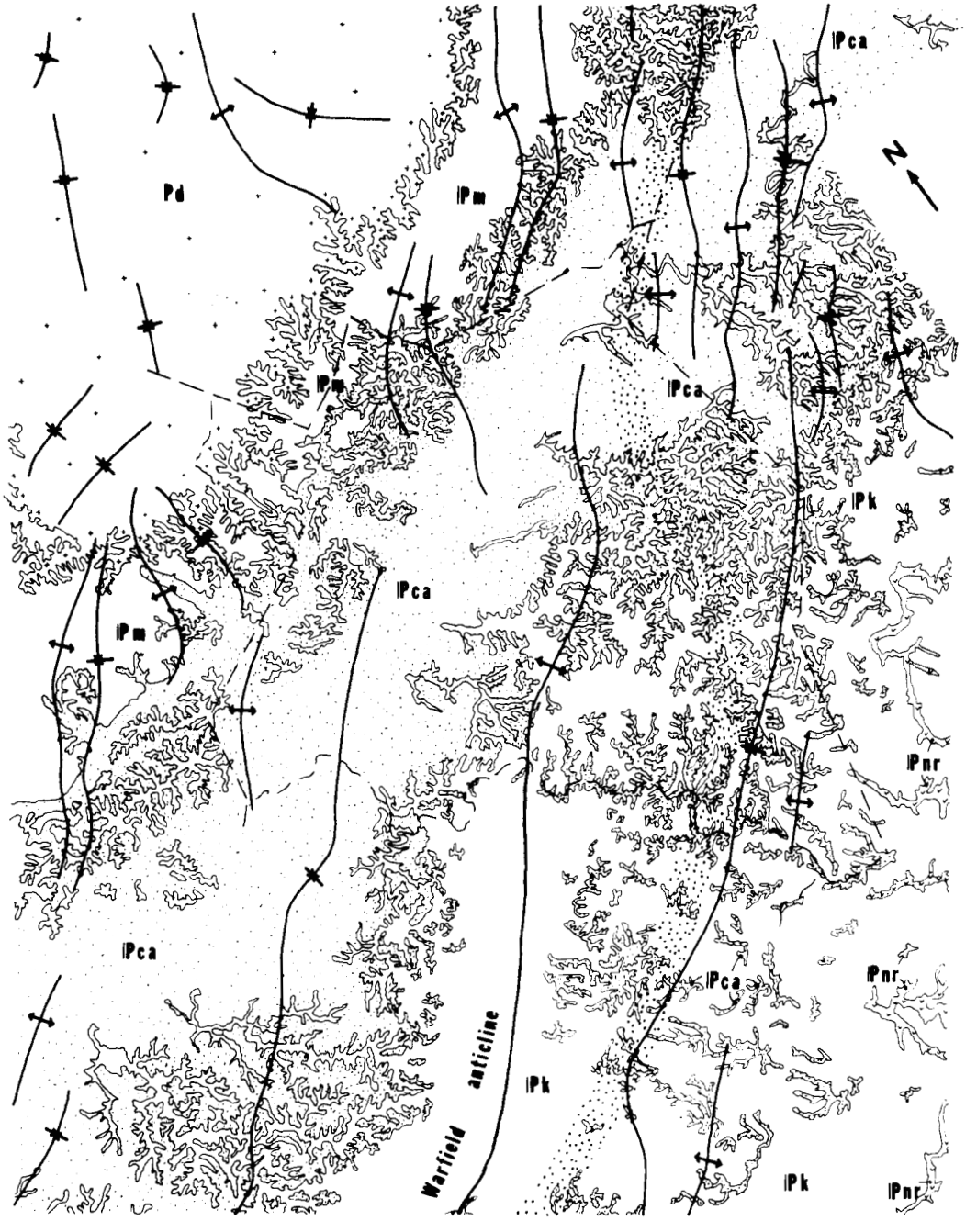

Figure 1, geologic map of Kanawha County (dashed) and surrounding regions. Pd = Dunkard Group (crossed), IPm = Monongahela Group (blank), IPca = Conemaugh Group and Allegheny Formation (stippled), IPk = Kanawha Group (blank), IPnr = New River Group (checked). Stippled band indicates zone of subsurface basement faulting. Geology from Geological map of West Virginia, Cardwell, et al., 1968. Scale = 1:560,000.

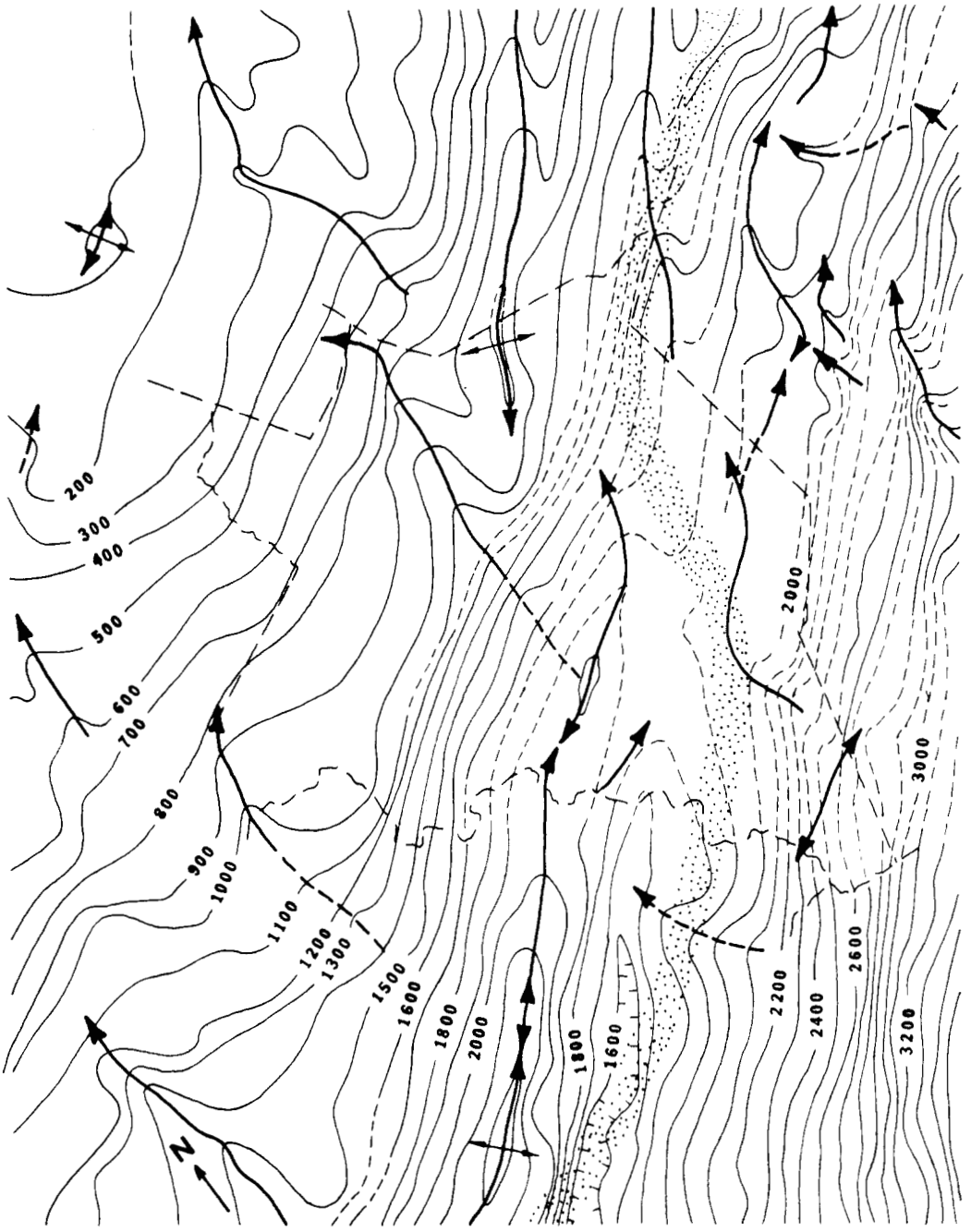

Figure 2, Coal form-line structure map of the area under investigation, after Shumaker, 1974, West Virginia Geol. and Econ. Survey, open file report. Stippled band indicates zone of basement subsurface faulting. Kanawha County boundary is dashed. Kanawha Co. W. Va. Scale = 1:560,000.

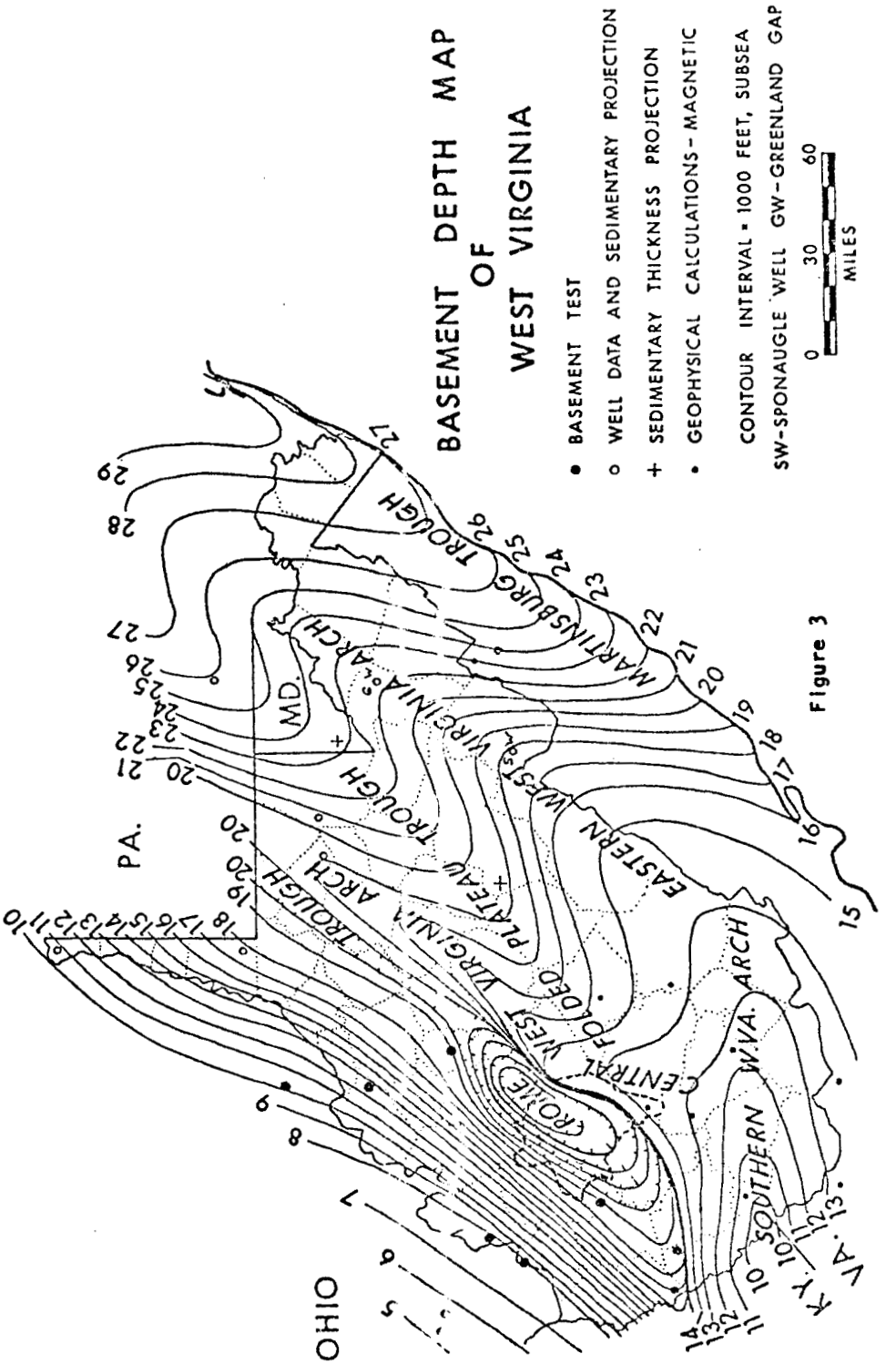
BASEMENT DEPTH MAP
OF
WEST VIRGINIA
BASEMENT TEST
WELL DATA AND SEDIMENTARY PROJECTION
SEDIMENTARY THICKNESS PROJECTION
GEOPHYSICAL CALCULATIONS - MAGNETIC
CONTOUR INTERVAL = 1000 FEET, SUBSEA
SW-SPONAUGLE WELL GW-GREENLAND GAP
0 30 60
MILES
OHIO
PA.
MD.
KY.
VA.
MARTINSBURG TROUGH
WEST VIRGINIA ARCH
EASTERN WEST VIRGINIA ARCH
PLATEAU TROUGH
CENTRAL WEST VIRGINIA TROUGH
FOLDED
CROME
SOUTHERN W.VA. ARCH

Figure 3

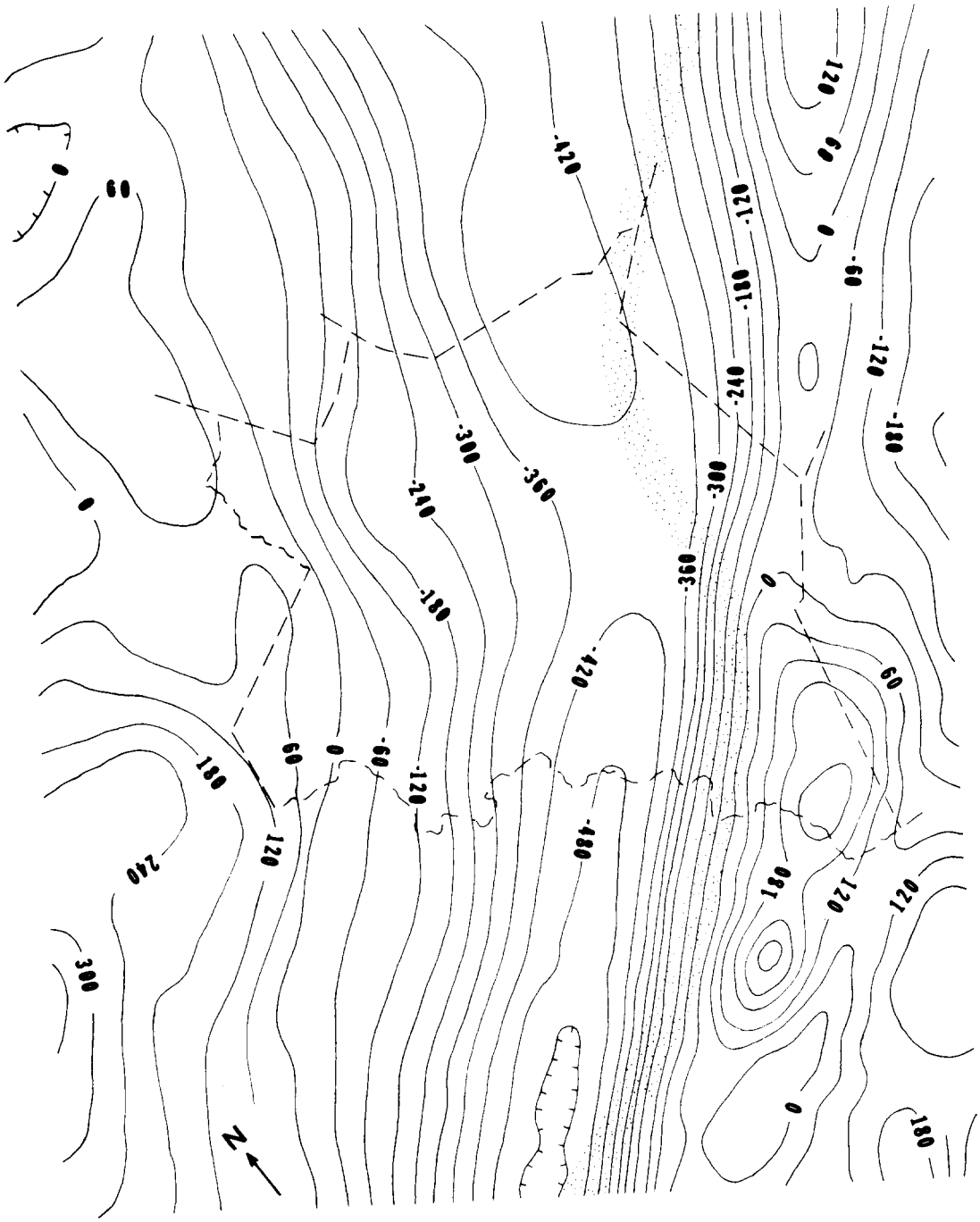

Figure 4, total intensity residual magnetic map of the area under investigation (from Kulander and Dean, in press). Stippled band indicates zone of subsurface faulting. Kanawha County boundary is dashed. Contour interval, 60 gammas. Scale = 1:560,000.

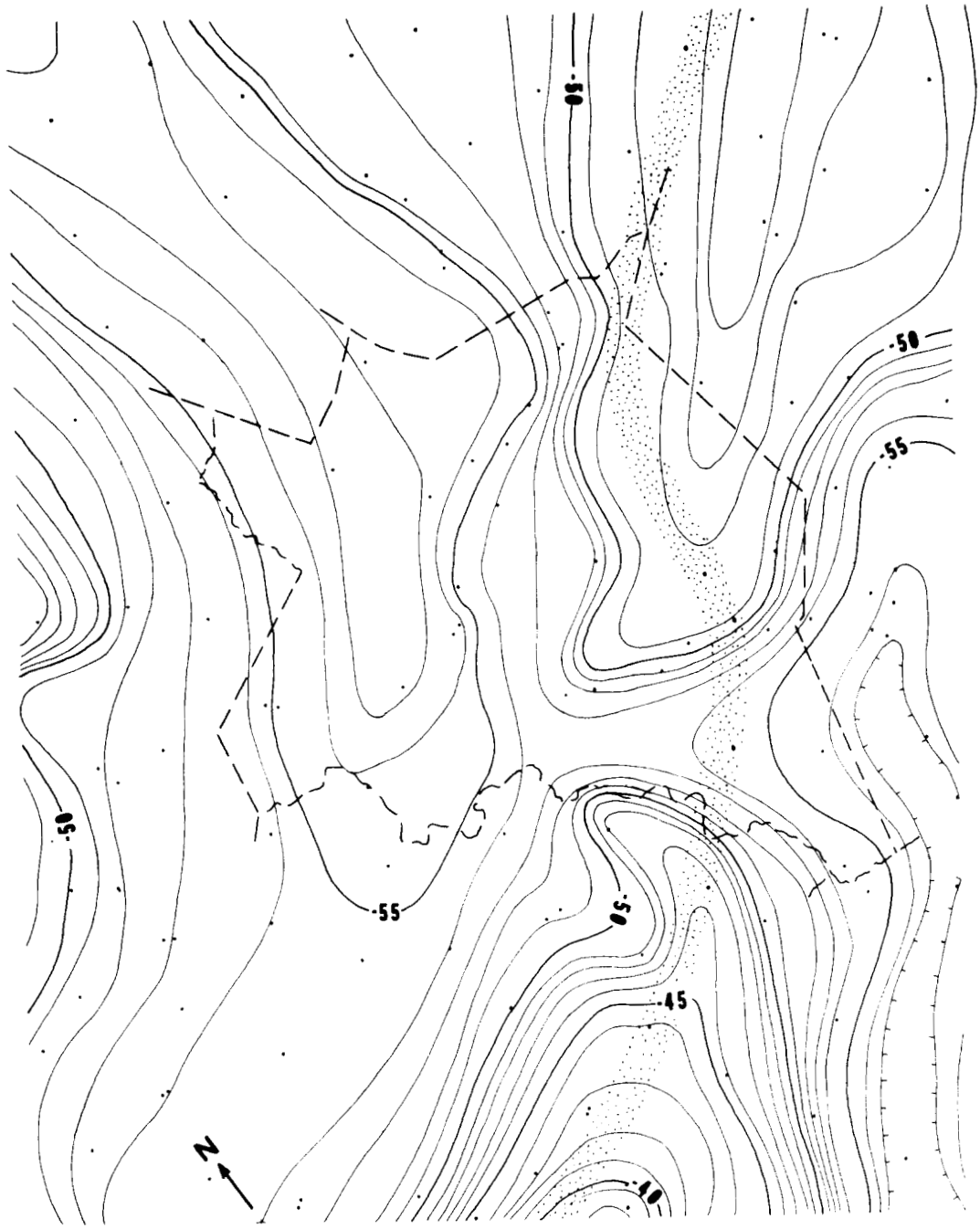

Figure 5, Bouguer gravity map of the area under investigation. Gravity data was obtained from the National Defense Mapping Agency. Heavy dots mark gravity stations. Stippled band indicates zone of subsurface basement faulting. Kanawha County boundary is dashed. Contour interval, one milligal. Scale = 1:560,000.

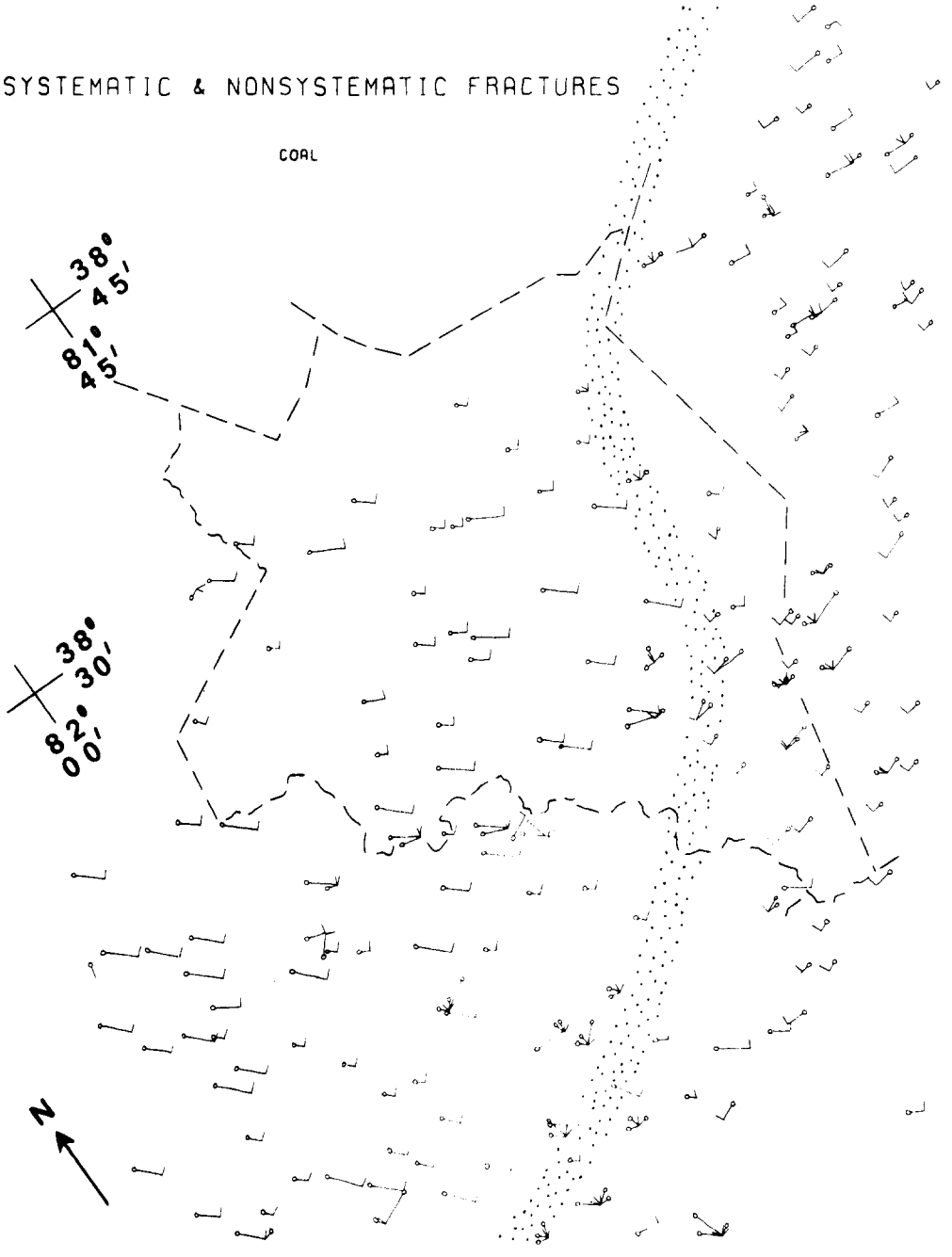

Figure 6, systematic - nonsystematic fracture trends in coal. Barb with ball indicates mean systematic fracture trend. Naked barb indicates mean nonsystematic trend. Systematic barb length is inversely proportional to the standard deviation of ten fracture set azimuth bearings taken over each outcrop extent. Systematic-nonsystematic barbs originate at station locations. Stippled band indicates zone of subsurface basement faulting. Scale = 1:560,000.

ANALYSIS OF STRUCTURAL GEOLOGICAL PARAMETERS THAT INFLUENCE GAS PRODUCTION FROM THE DEVONIAN SHALE OF THE APPALACHIAN BASIN

by

Robert C. Shumaker
Keith G. Kirk
E. B. Nuckols III
Brian R. Long

West Virginia University

ABSTRACT

The Department of Geology and Geography at West Virginia University is studying the structural parameters that may affect gas production from the Devonian shale in southwestern West Virginia and eastern Kentucky. The project is designed to (1) document fracture patterns and structural deformation within and around areas of Devonian shale production; (2) evaluate inexpensive geophysical and remote sensing techniques to locate potentially productive fracture zones; and (3) study production within producing fields for comparison with adjacent non-productive areas to assess the influence of structure on production.

Work was initiated this year on: (1) regional analysis of basin structure, (2) compilation of surface fractures from eastern Kentucky and West Virginia, (3) shallow high frequency seismic and resistivity studies to locate fracture zones and (4) groundwater studies above the Cottageville Devonian shale gas field for comparison with a production study of that same field.

INTRODUCTION

The intent of this paper is to introduce our project to other scientists interested in developing gas reserves from the Devonian shale, to explain the goals of our grant, to report our scientific progress, and finally, to solicit the assistance of other individuals in obtaining structural data for the vast area covered by our project (Figure 1). Our intent is to provide the most accurate and up-to-date structural background for co-workers in the Eastern Shale Gas Project but while our efforts are directed toward that end, we realize that your advice, assistance and criticism is required if our project is to fully reach that goal.

OBJECTIVES

The general objective of our project under contract E(40-1)-5194 is to study the structural parameters of the Devonian shales that effect gas production in eastern Kentucky and West Virginia.

To that end our program is specifically designed to:

1. Collect, compile, and analyze geologic data to construct regional structure maps of eastern Kentucky and West Virginia.

2. Determine if structural types and styles affect production and determine if minor structures as mapped in outcrop could influence production characteristics.

3. Determine if shallow seismic surveys can detect near-surface faults and fracture zones, and if

such structures can be detected, to further determine how fractures related to both production from the shale and to lineations observed on remotely sensed data.

4. Determine if a relationship exists between groundwater movement and shale gas productivity.

Through the integration of our work with others it is our ultimate goal to discover if relationships exist between Devonian shale gas production and geologic structure. If such a relationship is established, we will attempt to develope a method or methods for selecting favorable sites to drill shale wells that have a greater potential for gas production than the norm for that region.

ORGANIZATION

In order to attain the stated objectives we have designed several tasks which have been organized into five study groups. Four of these groups: regional structure studies, fracture studies, structural type studies, and production studies, are carried under ERDA's Resource Inventory Tasks. One study group, geophysical studies, is carried under Shale Characterization Tasks.

Regional structure and fracture studies will provide a structural background for the basin and entire project. The structural type studies seek to document, by analytical field work, details of structures which are either producing gas at the present time or which we feel are prospective. The production records are available that permit thorough analysis and documentation of geologic parameters that influence gas production from the shale. The geophsyical studies are charged with the task of developing inexpensive geophysical techniques that can locate shallow fracture zones of high permeability.

TECHNICAL PROGRESS

A major part of our effort during the first year of this comprehensive study has been spent in recruiting and hiring qualified personnel, accumulating structural and production data for analysis, and ordering and designing seismic and remote sensing equipment.

Technical progress was achieved on regional structure, regional fracture, production, and geophysical studies during the first year of the project. Delay of certain tasks was necessary to integrate and coordinate our work with that of other contractors. Also certain tasks are dependent on data compiled by other contractors and certain of our own tasks. In addition, we have been slightly delayed by problems in recruiting experienced technical personnel who are qualified, not only for the position, but who are qualified to return to school for an advanced degree.

A general summary of progress for each of the study groups is given below. Because of the general interest in shale gas production in the Cottageville field, the principal investigator, Mr. E.B. Nuckols, III has expanded that portion of the report, and Mr. Keith Kirk has written a more detailed report on general procedures utilized in our geophysical studies because of interest in his work.

Regional Structural Studies - R.C. Shumaker and Brian R. Long

The primary task of this group is to collect data and construct maps that will provide a regional structural framework for eastern Kentucky and West Virginia (Figure 1). This task is important to the project in that the regional structural framework is provided for all contractors in the primary producing area of the Devonian shale gas. Such maps are absolutely necessary in order to evaluate the importance that geologic structure has on production, and in order to compare regional structure with results of other regional geologic, geochemical, and engineering research. The standard map scale of 1:250,000 for these maps will facilitate comparisons.

Results of regional structure studies as of August 1977 are as follows: (1) Preliminary structure maps (1:250,000) have been compiled for the top of the Precambrian basement, the base of the Onondaga, the top of the Berea, and the top of the Mississippian Lime for part or all of the study area (Figure 2). Maps (1:250,000) showing the general outline of production for the Devonian shale have also been compiled for eastern Kentucky and West Virginia. Most of the data for these maps comes from publications or data supplied by the West Virginia Geologic and Economic Survey and the Kentucky Geologic Survey. Dudley Cardwell of the West Virginia Geologic and Economic Survey and Ed Wilson of the Kentucky Geologic Survey have been particularly helpful to our work. (2) Compilation of joints, lineaments, and in-situ stress measurements has begun and field work to collect fracture data has been initiated in eastern Kentucky. As fractures and lineaments are delineated, in part under contract E(40-1)-8040, comparison will be made with the production data being compiled in another study group (see production

studies below). As a part of this program we are mounting a multi-spectral camera in a low-altitude aircraft to obtain imagery from producing areas to use the imagery in fracture trace analysis. We would like to acknowledge the assistance of NASA/Johnson Space Center, Clear Lake, Texas and particularly Ben Hand for his assistance in obtaining the camera and viewer to be used in this project.

Structural Type-Style Studies

Outcrop studies of specific structures and specific stratigraphic units within the Devonian shale will be undertaken with similar studies planned for adjacent states by the U.S. Geological Survey. These studies will be initiated in the fall of 1977, and will be under the direction of Dr. Russell L. Wheeler.

Production Studies - E.B. Nuckols III and D. Scott Jones

It is our feeling that the compilation and analysis of production data from shale gas fields is of paramount importance to the success of the entire Devonian shale project. Detailed analysis of producing fields must be available for use by all workers within the ESGP project when evaluating the results of their analysis against the practical yardstick of shale gas production.

The Mount Alto Field (Figure 1, Cottageville) was selected as the initial study area because the primary operator within this field, the Consolidated Gas Supply Company, had initiated a study of the field and has established close working relationships with ERDA and ERDA contractors. We found a very cooperative attitude prevalent so that most production data is available and is being compiled from the files of several gas companies operating in the field.

We have also initiated a groundwater investigation under the direction of Dr. Henry Rauch in the Mount Alto gas field area. The possibility that a relationship exists between groundwater yields and deep gas production from the shale is based on the premise that fracture porosity, which often enhances groundwater production, may also affect production from the underlying shale. Perhaps just as likely is the possibility that an inverse relationship exists between groundwater production and production of the shale. This is particularly true if the fracture zone that produces enhanced groundwater recoveries extends through the entire stratigraphic section to the shale. Under these conditions the gas may be slowly escaping to the surface. While the possibilities of an interrelationship may be small, it should be evaluated, and if the production characteristics from the two different reservoirs are related, then groundwater production could be used as a method for locating productive shale gas wells. During this summer we have sampled over sixty wells. Twenty additional wells in the Cottageville area will be sampled this fall. Included in the evaluation are such parameters as the temperature of the groundwater, the depth to water, yield, and conductivity.

Geophysical Studies - Keith G. Kirk

Several geophysical methods have the potential to locate shallow fracture zones. In the case of shale gas, any geophysical method adopted by operators to locate fractures must not be expensive because the marginal economics of shale gas production demands frugality in exploration expenditures.

Our research program investigates the possibility of using inexpensive (approximately $30,000 of equipment) shallow-penetration resistivity and seismic devices to readily locate fracture zones.

Three areas of investigation (Figure 1) have been selected to test resistivity and seismic equipment against known shallow fracture zones. We have modified standard low-frequency seismic equipment to the high-frequency range with the purpose of more precisely defining bed boundaries in order to determine if fractures and faults with minor offsets can be identified by any one of the several methods to be tested. If results at the test sites are encouraging, we intend to study the Mount Alto (Cottageville) shale gas field and selected lineaments within the Devonian shale gas producing area to determine if a correlation exists between fractures, lineaments and shale gas production.

GEOPHYSICAL METHODS USED TO LOCATE ZONES OF SECONDARY POROSITY

by

Keith G. Kirk
Department of Geology and Geography
West Virginia University
305 White Hall
Morgantown, WV 26506

ABSTRACT

It is important to develop a program to evaluate the influence of fractures on production from Devonian shales since areas of secondary porosity along fractures and lineaments have the highest producing wells. As part of the development of such a program at West Virginia University, geophysical methods are under development to map fractures and to rapidly ground truth fracture zones located by aerial photo lineament analysis.

The tri-potential electrical resistivity and high frequency/high resolution seismic profiling with horizontal polarized shear wave analysis are being tested for their applicability in locating fractures. Initial results show the tri-potential survey is capable of rapidly accessing fracture zones at shallow depth. Preliminary evaluation is still underway with the seismic techniques and should be complete by mid August 1978. Theoretically, much greater depth may be investigated with the seismic methods used.

INTRODUCTION

It is widely accepted that most of the production from the Devonian shale is a result of secondary porosity, and that such secondary porosity should be greatest along fracture zones and faults. While there has not been a detailed study of the effects of faulting on shale production, there is no obvious increase of gas from wells located near the Warfield fault (see test site in Figure 1). In the past decade photo lineament analysis has been developed in an attempt to locate fracture zones that show little or no displacement. Water wells located in or near these lineaments often have great increase in production of water volume. However, there are also many occasions when wells located in this manner have shown no significant increase in production. Since problems of shale gas production are similar to those encountered in locating water wells in fracture zones, we are developing geophysical methods that can rapidly access whether or not a given photo lineament is associated with a fracture zone, and more importantly, whether or not the fracture zone is associated with an increase in porosity. This paper will briefly outline two geophysical methods that are being tested at West Virginia University to accomplish the task of evaluating photo lineaments for their potential zones of higher production of natural gas in the Devonian shales.

The two techniques that are being tested at WVU are the tri-potential electrical resistivity method (TPER) and a seismic technique called shallow high-resolution reflection profiling (SHRRP).

THE TPER METHOD

The TPER is a method of resistivity survey in which three different electrode configurations are used. These three electrode configurations are shown in Figure 3 . Resistivity is measured for each of these configurations.

Profiling Tri-Potential Survey

In the tri-potential profiling survey the four electrodes are kept at a constant interval, and they are moved in a line across the surface. In this way, a large area is covered at a relatively constant depth of investigation in a short time. This type of survey is designed to locate anomalies associated with lateral variations in resistivities such as buried ore bodies, faults, fracture zones, cavities, and filled sinkholes.

Fracture Zones

In the field, a fracture can take on one of three resistivity distributions. These are the following

cases: where the fracture is of a lower resistance than the country rock, where the fracture is of higher resistance than the country rock, and where there is no appreciable difference between the country rock and the fracture. In the first two instances the fracture will show up either as a peak or a trough on a profile plot of distance versus resistivity. In as much as a resistivity contrast is necessary to locate the fracture, only the first two cases are of importance and will be discussed.

The case in which the fracture resistivity is higher than in the surrounding rock generally occurs in areas where the parent rock is of low resistivity (0-450 ohm-ft) and where the fluid in the porous zone along fractures is of a higher resistance than the surrounding rock. This can also occur in areas where the fracture zones have been cemented, for instance, by calcite cement; such cemented layers act as insulators when compared to the more conductive surrounding rock.

Theoretically, this situation can be modeled by use of a thin vertical insulating sheet in a conducting medium. This was done by Carpenter (1955). In this theoretical example three cases were examined. These are:

(i) the case in which all four electrodes are on one side of the insulating sheet,

(ii) the case in which one of the electrodes is on the opposite side of the insulating sheet from the other three, and

(iii) the case in which two electrodes are on each side of the sheet.

For case (i), using image theory, Carpenter has shown that for the electrode arrangement $C_1P_1P_2C_2$ the apparent resistivity between the two potential electrodes can be expressed by the equation:

$$\rho_{\alpha_{cppc\text{-}i}} = \rho\{1+1(2t+2)+/(2t-2)-1/(2t+1)-1/(2t-1)\}$$

Similarly, for the $C_1C_2P_2P_1$ configuration,

$$\rho_{\alpha_{ccpp\text{-}i}} = \rho\{1+3\ 1/t-1/(2t-1)-1/(2t+1)\}$$

and for the electrode configuration $C_1P_1C_2P_2$,

$$\rho_{\alpha_{cpcp\text{-}i}} = \rho\{1+3(1/(2t+2)+1/(2t-2)-1/t)\}$$

For case (ii), Carpenter has shown that for the electrode arrangement $C_1P_1P_2C_2$,

$$\rho_{\alpha_{cppc\text{-}ii}} = \rho\{1/2 +1/(2t+2)-1/(2t+1)\}$$

for the $C_1\ C_2P_2P_1$ arrangement,

$$\rho_{\alpha_{ccpp\text{-}ii}} = \rho\{3/2+(3/2)t-3/(2t+1)\}$$

and for the electrode arrangement $C_1P_1C_2P_2$,

$$\rho_{\alpha_{cpcp\text{-}ii}} = -3\rho\{1/2t-1/(2t+2)\}/2.$$

Note that in the last case, $\rho_{\alpha_{cpcp\text{-}ii}}$ is negative.

For case (iii) and the electrode arrangement $C_1P_1P_2C_2$,

$$\rho_{\alpha_{cpcp\text{-}iii}} = \rho\{2+1/(2t+2)+1/(2-2t)\}$$

$C_1P_1C_2P_2$ array:

$$\rho_{\alpha_{cpcp-iii}} = \rho[3+3(1/(2t+2)+1/(2-2t)0/2]$$

where:

t = d/s
s = electrode spacing
d = distance between the center of the array and the insulating sheet
p = resistivity of surrounding media

From the above eight equations, one can plot apparent resistivity versus distance to obtain the theoretical plot of the resistivity distribution of traverses over a fracture for each of the three electrode arrays. Figure 4 shows the normalized plot of these relationships. As one can see, the curve is discontinuous at the critical points where the bounds of the equations representing these curves overlap. In actuality, this theoretical curve is not encountered in nature because the assumptions of nonconductance and infinitesimal thickness of the insulating sheet in the theoretical model are not met in the field. In the field one must account for the actual resistivity and the width of the fracture zone. A fourth variable, known as the delta percent, is present when the three resistances measured for each electrode configuration are related. This variable is a measure of the lateral heterogeneity caused by the fracture zone. This variable is represented by the equation:

$$+ \frac{R_{cppc}-R_{cpcp}-R_{ccpp}}{R_{cppc}} \times 100$$

where

Rcppc = Resistance of CPPC Array
Rcpcp = Resistance of CPCP Array
Rccpp = Resistance of CCPP Array

Field results using the TPER method confirm the theoretical calculations.

Karst Terrain Sites

Profiling surveys were used in selected sites of karst terrains to delineate the presence of fracture zones, caverns, and filled sinkholes. The areas chosen are in Monroe County, West Virginia and Centre County and Bedford County, Pennsylvania.

Several survey profiles were run across the known fractures associated with Miller's Cave in Centre County, Pennsylvania. In this survey a ten foot electrode spacing was used to keep the cave (occurring at a 40 ft depth) from influencing the resistivity values. Past research by Ebau (1973) has shown that the fracture above the cave transmits surface water underground. Figure 5 shows plots of resistivity and residual resistivity versus distance from the fracture for one of the traverses. In this case the CPPC resistivity and the delta percent residual are plotted. The anomaly associated with this fracture and filled sinkhole causes a decrease in resistivity over the fracture. This is logical since the limestone in this area has a higher resistivity than the water percolating through the fracture. The delta percent values increase near the cave verifying the presence of this fracture. In each of the traverses across this fracture the CPCP array showed the greater response to the presence of the fracture.

TPER profiling surveys were also performed for the United States Bureau of Mines at their Underground Coal Gasification (UGC) site in Wetzel County, West Virginia (Kirk 1976). These surveys were run across areas where photo lineament analysis indicated the presence of suspected fracture zones. The same general response was encountered here as at the Miller's Cave site in Pennsylvania.

Resistivities typically encountered at the UGC site were in the range of 90 to 300 ohm-ft, and were predominantly below 200 ohm-ft. This is consistent with the bedded sand and shales encountered at or near the surface at the site. At the UGC site the soils are clay-rich, formed from grey acid shales and fine-grained dirty sandstones. The resistivity range encountered at the UGC site, therefore, seems to be realistic for this terrain.

For each traverse at this site two electrode spacings were utilized: a 10 foot spacing and a 40 foot spacing. The 10 foot spacing was chosen because it was believed that this would be the minimum electrodes spacing required to detect fractures below the typically two to four foot thick, highly

compacted soil zone. The 40 foot spacing was chosen because it was estimated that any longer array of cables and electrodes would be unmanageable in the heavily vegetated areas where a number of the surveys were to be run.

This site had been logged approximately 40 years ago and, therefore, the old abandoned logging roads that ran parallel to the hill contours were used for three of the profile lines. The remainder of the profiles were run in the valley bottom areas at the site. Approximately two weeks were required to clear the old logging roads and portions of the valley before the resistivity profiles could be run. All of this field data was collected using a Soil Test model R-40 Terra Scout resistivity meter that had been modified by the installation of a switching circuit to facilitate the rapid change from one electrode array to another.

Figure 6 shows the results of a TPER profiling survey run across the two lineaments that were mapped by using low altitude imagery. The response of the TPER method to these fractures would indicate that they are shallow because of the delta percent residual drop off with depth at the 40 ft electrode spacing. No precise determination of the fracture depth can be made since only two different surveys were run across the fracture zone.

The delta percent plot for the ten foot electrode spacing is of interest since it responds at two points along the traverse. Theoretically this type of response would result as one passes across a vertical resistivity boundary or zone. The distance between the two maximum points for the ten foot spacing along the traverse suggests that the fracture zone is approximately fifty feet wide. A similar response was obtained at traverse C-C' as it passed across the fracture bearing 115°.

This fracture zone was associated with a lineament that was mapped using high altitude infra red photography. It is important to note that even though both resistivity and aerial photography indicate the presence of this fracture zone the well data available at the site does not show any displacement across this fracture zone.

THE SHRRP METHOD

In the past ten years advances in digital electronics and digital data processing have led to a new generation of seismographs. These signal-enhancement dynamic digital seismographs have a greatly increased capability to resolve bed boundaries. Using the best technology and under ideal conditions beds as thin as six inches can be detected. Unlike their analog counterparts these new digital instruments are capable of investigating shallow as well as deep structures. This capability opens up new areas of seismic investigations. These include mining applications to the coal industry in locating sand channels and abandoned workings, applications to engineering geology for site evaluation, and seismometric mapping in unconsolidated sediments for the hydrogeologist. Most important in regards to our research project, we believe that this technique has the potential to define fracture zones and faults of very small displacement.

In the SHRRP technique, it is important that the highest possible frequency seismic waves be used. This is true because resolution, defined as the thinnest detectable bed is inversely proportional to frequency. This can be expressed by the empirical equation:

$$R = V/(4 \cdot \pi \cdot f)$$

where: R = resolution
V = velocity
f = frequency

At the common velocities (7000 to 15,000 ft/sec) of sedimentary rocks, the 20hz wave can only resolve at best those beds greater than 28 feet thick. For the same velocity the 400hz signal can resolve beds as thin as 1.4 feet. This is a 20 fold increase.

Figure 7 shows a plot of the same equation with frequency as the independant variable, and the interrelationship between resolution and frequency can be readily observed.

Most of the investigations using the SHRRP technique are still in the developmental stage at West Virginia University, and therefore, no specific field test results can be described. Preliminary results do show that the technique has great promise for better definition of fracture zones. Recent discussions with Dr. Farr from Western Geophysical and Dr. Coan from Continental Oil Company, who have been investigating similar techniques over the past several years, show comparable encouraging results. The proprietary nature of their research does not permit disclosing the specific results of their tests.

Conclusion

The TPER and SHRRP techniques are being used at West Virginia University to investigate fracture zones that can be initially located by photo lineament analysis. The TPER technique has been evaluated in previous research at the University,and it has been proven capable of locating fracture zones at depths of up to one hundred feet from the surface. The SHRRP technique is in the early developmental stage. Our theoretical investigations and initial tests, and independent preliminary test by Farr and Coan (personal communication) suggest that the SHRRP techniques has similar capability. As designed in our program this technique should be inexpensive when compared to other seismic programs designed for locating fracture zones. It should have wide applications for solving other geologic problems encountered in the search for energy resources, and it should have the additional advantage of presenting data in the form of geologically realistic sections.

PRODUCTION CHARACTERISTICS OF DEVONIAN ORGANIC SHALES IN THE COTTAGEVILLE FIELD NEAR RIPLEY, WEST VIRGINIA

by

E. B. Nuckols III
Department of Geology and Geography
West Virginia University
305 White Hall
Morgantown, WV 26506

ABSTRACT

Exploration for and development of upper Devonian organic shales ("Brown Shales") in the Cottageville Field started in the late 1920's. Continued development has lead to the drilling of over one hundred shale wells with accumulative production of more than 10 billion cubic feet of natural gas. Data indicates primary production from zones of organic shales in the Huron member of the Ohio Shale Formation. Due to the extremely low porosity and permeability of these shales, production of gas is considered to be through natural fractures.

Historically, production of gas was either natural or by stimulation with gelled ammonium nitrate. Wells with meager gas flows were normally stimulated through "shooting", but success in reaching natural fracture reservoirs,and thus reaching production,has varied. Production trends, trends of wells which have the largest natural flows, flow after stimulation, gas shows, and structural maps, all indicate an orientation of approximately N 40° E for the field with definite limits to it's aerial extent.

INTRODUCTION

Upper Devonian shale deposits underlie a major portion of the Appalachian, Michigan and Illinois Basins (Figure 8). Within the Appalachian Basin, the major Devonian shale gas producing states are Kentucky, Ohio, Virginia and West Virginia. Within these states a total of more than 9,600 productive shale gas wells have been drilled. Within existing shale production of northwestern West Virginia (Figure 9), the Cottageville Gas Field may be the only true "shale" producing field. Other fields found within this general area are producing from middle and upper Devonian siltstone and sand-siltstone lithologies. The Cottageville Gas Field is located near the West Virginia-Ohio border in the West Virginia counties of Mason and Jackson. Figure 10 shows the general location and configuration of the gas field with Oriskany and "Newburg" gas wells flanking the shale wells on the east and north.

GEOLOGIC SETTING

The Devonian age formations that underlie the Cottageville Gas Field are approximately 2,300 feet thick. The middle and upper Devonian shales comprisong the upper 2,100 feet of the total section. The upper contact of the Devonian shales is placed at the base of the Mississippian Age Berea sandstone, and the lower contact is with the Onondaga limestone. Within this predominantly shale section are found light grey to brown-black shales, light to medium grey siltstones and very rarely white to light grey sandstones. Of these different lithologies, the dark organic rich shale zones occupy approximately 350 feet or 15 percent of the entire shale section. These highly organic shale zones

occur in three stratigraphically distinct portions of the shale section, and they are easily recognizable on gamma-ray and density logs (Figure 11). The upper two organic zones (Zones II and III) are found within the Huron shale member of the Ohio Shale Formation. These two zones are mainly composed of dark brown-black organic rich shales, but occasionally they have light to medium grey shale and siltstone interbeds. Separating the lower and upper organic rich shale zones of the Huron are lithologies of shale and siltstone with an occassional thin organic shale bed. Within the Cottageville Gas Field, these two zones have an average combined thickness of 250 feet, and they are the main reservoirs of Devonian shale gas production. Below these two organic zones found in the Huron is a third organic zone found in the Olentangy Formation. Like the younger shales found in the Huron Shale, this organic rich shale has interbeds of light to medium grey shale and siltstones. This organic rich shale has an average thickness of 100 feet, and has rarely produced any gas within the Cottageville area.

Regional east-west correlations of the Devonian shale sequence (Figure 12) indicated the absence of deposition of the Huron organic rich shale zones just to the east of the Cottageville field. The gradual facies change of the organic shales to the east seems to coincide with the western edge of the Rome Trough, thereby indicating a change in the depositional environment. The western edge of the trough is a basement fault or fault zone (Shumaker unpublished map) that may have created the stress fields (Figure 13) that would create or open the fractures in the shale that are necessary to the production of natural gas.

PRODUCTION CHARACTERISTICS

Drilling for shale gas in the Cottageville area began October 9, 1929, when Cities Service drilled their first "shale" well. This well proved to be a meager beginning for the shale field as their well had a natural open flow of only 4.6 Mcf and a 213 Mcf final flow after stimulation by "shooting". At that time, a well with such a small flow could hardly compete with the shallower "plays" in the Berea and Injun sands which annually produced wells with natural flows of several million cubic feet of gas. However, as the field developed, wells with open flows up to 3.4 million cubic feet of gas we drilled, and this encouraged additional developmental drilling.

The primary target for drilling has been the highly organic shale zones (Zones II and III) of the Huron shale member of the Ohio Shale (known in Ohio as the Big and Little Cinnamon). A typical drilling program involves setting a string of casing just below the Berea sandstone. The Berea sandstone and shallower Salt sands of this area produce large volumes of saltwater, and therefore, they must be cased off to insure a completion in the Devonian shale section. After the casing is set, the well is usually drilled to a point just below the lower organic shale zone (Zone II) of the Huron shale. At that depth, the formation is usually tested and a decision is made whether to produce the well naturally, if there is sufficient natural flow, or to stimulate the well by shooting if there is no flow of gas or a flow up to several hundred thousand cubic feet of gas. Shooting a well means that canisters of 80% gelled nitroglycerine are lowered into the bore hole and then detonated. Historically, this has proved to be the best method of stimulating shale wells with small natural flows. Some variation in shooting techniques such as "tamping" the shot with pea gravel to contain the explosion, thereby hopefully retaining more energy to fracture the shale, have been tried. Until the late 1960's, drilling within the field was done exclusively by cable tool drilling rigs. This meant that wells which were stimulated by shooting (open hole without tamping the shot) ran the risk of being clogged by rubble from the shot or if the shot went smoothly the hole would "blow" itself clean. This clean-up aspect of production stimulation was very critical, because a shot that did not clean the hole stood the chance of losing a part or even all of it's production potential. With the adoption of air rotary drilling, wells could either be "tamped" or shot naturally, and then careful reentry techniques could be used to successfully clean out the remaining rubble.

After some fourty-eight years of in-field drilling, over one hundred shale wells have been drilled in the Cottageville Field. Consolidated Gas Supply Corporation has drilled more wells than any company (43); Columbia Gas Transmission Corporation and Cities Service have drilled 17 and 16 respectively. The highest natural flow encountered was 3480 Mcf with the highest stimulated flow being 1981 Mcf (this well had only a natural flow of 36 Mcf). With the passage of time, rock pressures have generally decreased as the number of wells drilled to the reservoir increased. The highest initial rock pressure taken was 1000 pounds per square inch early in the history of this field. Several wells have good production histories, but one in particular has produced over 952,500 Mcf in twenty-six years and is still producing. Found below are a few statistical averages concerning production within the field:

NATURAL OPEN FLOWS (81 wells)	188.2 Mcf
FLOWS AFTER SHOT STIMULATION (90 wells)	355 Mcf
ROCK PRESSURE TEST (lbs/psi)	639.6
ACCUMULATIVE PRODUCTION (77 wells)	10.08 Bcf
AVERAGE ACCUMULATIVE PRODUCTION PER WELL	137.7 Mcf

EFFECT OF RESERVOIR FRACTURING

Of the three organic rich shale zones within the Devonian shale section, only the Huron organic shales have been extensively drilled and stimulated. The primary gas reservoir in the Cottageville Gas Field is the lower organic shale zone of the Huron (Martin and Nuckols, 1974). Stimulation of this organic shale zone by shooting has greatly increased the volume of gas produced from this field. However, the gas probably comes from naturally occuring open fractures that were either penetrated by drilling or that were interconnected to the well bore by shooting.

In 1975, Consolidated Gas Supply Corporation and the Energy Research and Development Administration entered into an agreement to core and analyze the shale section for two wells in the Cottageville Field. The first core was taken in a well near the Jackson-Mason County line. Coring of the lower Huron shale was interrupted when an initial gas flow of approximately 3.5 MMcf was encountered (this flow finally stabilized at 1007 Mcf). Close inspection of the core revealed natural fractures with secondary deposits of dolomite and calcite along the fracture plane just above the zone that encountered the large gas flow. A core was taken in a second well drilled in the northwest portion of the field. Unlike the first core, there were few natural fractures in the organic shales, and the well tested no natural open flow. Detailed laboratory analysis of both cores revealed very low matrix porosities (less than 3% average) and permeabilities (less than .01 millidarcy). In as much as the rock of both cores are lithologically similar, we presume that the main difference in permeability relate directly to the fractures. This was the first direct evidence that fracturing is critical to production, a conclusion that most geologists and engineers had presumed to be true. Formation evaluation of fractured reservoirs is always difficult. Evaluation of the organic shales through electrical logs has proved effective to some degree, but not conclusive by any means. A major drawback is that almost all shale wells in the Appalachian Basin are drilled by air rotaries, and the bore holes are logged air-filled. Gamma-ray logging has proved very useful for stratigraphic correlation as the organic shale is naturally radioactive, and Density logs permit discrimination of less dense zones that are usually characteristic of the organic shales. The last few years has seen the development of acoustic tools for the detection of gas. The coupling of gamma ray, temperature and acoustic logs has enabled the log analysis to pinpoint (within 1 to 2 feet) gas entry into the well bore from the organic shales. This procedure only locates the fracture by inference, and it does not in any way determine the orientation of the fracture. Only through coring has the orientation of the fracture patterns been delineated.

Production characteristics of the field may indirectly indicate fracture trends in the reservoir. It would be expected that the trend of open fractures would be reflected by linearity of many producing parameters. To test this assumption preliminary isopressure, isoflow and isoproduction maps were drawn to see if there were any prominent linear trends.

The isopressure map (Figure 14) was constructed from well-head pressures taken immediately after completion of the well but prior to the wells initial production. There are two important modifying factors that complicate interpretation of the data and resulting map. First, the well-head pressures were taken at various times after completion of the wells. Shut-in times ranged from a few hours to fourteen days. Secondly, registration of true formation pressure (wells that were shut-in for only a few hours probably did not reach their full potential rock pressure) may be altered by rubble in a well bore from the shot or caving shortly after the withdrawal of drilling equipment. This rubble may block off some production, reduce the initial rock pressure test.

A less important factor in analyzing initial rock pressure test is the possibility that not all of the gas is being produced from the zone of interest, and the gas could be coming from a shallow zone with less pressure. From the isopressure map (Figure 14) an obvious linear trend of approximately N 40° E can be seen. A general linear trough of low pressures trends through the axis of the field, but there are two areas of high pressure in the north central portion of the field. Flanking this trough on either side are areas that are interpreted to be at their "virgin" rock pressures. The two high pressure areas in the north central portion of the field were drilled early in the development of the field. The figures in these two areas may be virgin rock pressures if pressure tests on the outer limits of the field are accurate. Low "bulge" areas of low rock pressures normal to the axial trend of the field are thought to reflect the more recent fate of drilling in these areas. Preliminary inspection of initial rock-pressure data indicates a linear relationship between rock pressure

and time. As wells are drilled rock pressures decline. At the present time, drilling encounters pressures that are only 35 to 40 percent of original field pressures. We intend to more thoroughly investigate the relationships between field production and declining reservoir pressure. Of major interest will be the extent of linearity with the passage of time.

An isoflow map (Figure 15) was constructed from final open flow data. The data on this preliminary map does not discriminate as to whether the well produced naturally or whether it has been stimulated Open flow tests should also be effected by the amount of time permitted between the test and the time the well was completed. Natural open flow tests on several wells were taken immediately after the well was stimulated by shooting (less than three hours). Other tests were taken several days after completion. Again, we hope to normalize the data for more accurate comparison between wells. The area of highest flow is in the southern part of the field just north of the Jackson-Mason county line These northeast-southeast linear trends may again reflect the trend of open fractures in the reservoir.

An isoproduction map (Figure 16) was drawn based on production records that were obtained from Consolidated Gas Supply Corporation, Columbia Gas Transmission Company and Cities Service. Certain of the wells have been abondoned while others have just been completed so that the amount of data may vary greatly from well to well. We are still compiling data on these wells as of this date. This map, like the isopressure and isoflow maps, shows a general linear trend of N 40° E. Unlike the other map configurations, there are two definite areas of good production, one area being in the southern end of the field, near the Jackson-Mason County line, and the other to the north. The exact significance of this observation is not known. We can only presume that there wells encountered more open fractures.

Comparison and analysis of the three maps suggests the following observations:

A) There is similarity between accumulative production and open flow trends.

B) There is a northeast-southwest linear trend to the accumulative production and open flow maps.

C) Linear trends normal to the northeast trend of the field are apparent on the open flow and initial rock pressure maps.

REFERENCES

1. Bagnall, William D., and Ryan, William M., "The Geology, Reserves, and Production Characteristics of the Devonian Shale in Southwestern West Virginia," paper presented in the 7th Annual Appalachian Petroleum Geology Symposium on "Devonian Shale Production and Potential", sponsored by the West Virginia Geologic and Economic Survey, WVU Department of Geology and Geography, and U.S. Energy Research and Development Administration (Morgantown), March 1-4, 1976, Morgantown.

2. Brown P., "Energy from Shale - A little Used Natural Resource," in "Natural Gas from Unconventional Geologic Sources," National Research Council, (NTIS), 1976.

3. Dennison, J.M., 1971, Petroleum related to Middle and Upper Devonian deltaic facies in central Appalachians: Am. Assoc. Petroleum Geologist Bull,. v. 55, p. 1179-1193.

4. Foster, J.M., "A 'New Gas' Supply - The Devonian Shales," 1975 Eastern Regional Meeting of the Society of Petroleum Engineers of AIME, Charleston, West Virginia, November 6-7, 1975. Paper No. SPE 5451.

5. Martin, P.M., and Nuckols III, E.B., "Geology and Oil and Gas Occurrence in the Devonian Shales: Northern West Virginia," paper presented in the 7th Annual Appalachian Petroleum Geology Symposium on "Devonian Shale Production and Potential," sponsored by the West Virginia Geologic and Economic Survey, WVU Department of Geology and Geography , and U.S. Energy Research and Development Administration (Morgantown). March 1-4, 1976, Morgantown.

6. Oliver, W.A., Jr., de Witt, W., Jr., Dennison, J.M., Haskins, D.M., and Huddle, J.W., 1977, Devonian of the Appalachian Bssin, United States, in Oswald, D.H., ed., International symposium on the Devonian System: Alberta Soc. Petroleum Geologists, Calgary, Alberta, v. I, p. 1001-1040.

7. Oliver, W.A., Jr., de Witt, W., Jr., Dennison, J.M., Koskins, D.M., and Huddle, J.W. 1967, Isopach and Lithofacies maps of the Devonian in the Appalachian Basin: Pennsylvanian Topog. and Geol. Survey Progress Rept. 182, 7 sheets.

8. Overbey, Jr., William K., Effect of In-Situ Stress on Induced Fractures, paper presented in the 7th Annual Appalachian Petroleum Geology Symposium on "Devonian Shale Production and Potential", sponsored by the West Virginia Geological and Economic Survey, WVU Department of Geology and Geography, and U.S. ERDA (Morgantown), March 1-4, 1976, Morgantown.

9. Patchen, Douglas G., and Larese, Richard E., "Stratigraphy and Petrology of the Devonian "Brown" Shale in West Virginia," paper presented in the 7th Annual Appalachian Petroleum Geology Symposium on "Devonian Shale Production and Potential," sponsored by the West Virginia Geologic and Economic Survey, WVU Dept. of Geology and Geography, and U.S. ERDA (Morgantown), March 1-4, 1976, Morgantown.

10. Shumaker, R.C., "A Digest of Appalachian Structural Geology," paper presented in the 7th Annual Appalachian Petroleum Geology Symposium on "Devonian Shale production and Potential," sponsored by the WV Geologic and Economic Survey, WVU Dept. of Geology and Geography, and U.S. ERDA (Morgantown), March 1-4, 1976, Morgantown.

11. TRW, "Economic Analysis of Natural Gas Stimulation Applied to the Eastern Devonian Shales," technical report prepared for the Division of Oil, Gas and Shale Technology, the US ERDA, Contract No. (49-18)-2041, January 1977.

12. Woodward, H.P., 1943, Devonian System of West Virginia: West Virginia Geol. and Econ.Survey, Vol. 15, 655 p.

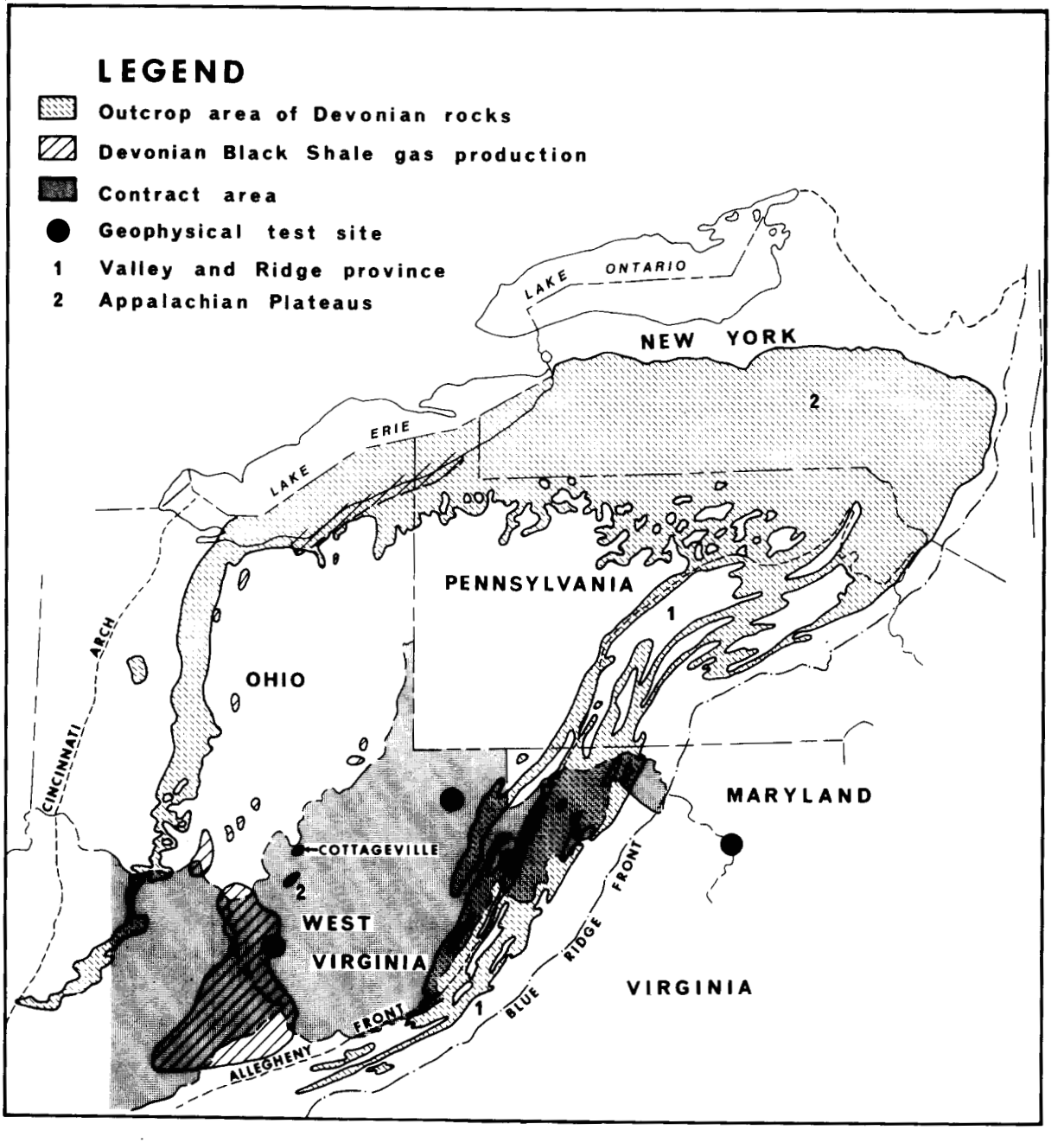

FIGURE 1
PROJECT LOCATIONS

	Dev - oil/gas	Linears	Joints	Drainage	Surface Form Line	Surface Tectonic	Greenbrier	Berea	Dev. Shale	Shale Outcrop	Penetration Shale	Tully	Onondaga	Newburg	Conasauga - ?	Precambrian
Clarksburg NJ 17-2	P			C	R	C	P				PI		P		C	P
Cumberland NJ 17-3	N				R		P				PI		P		C	P
Huntington NJ 17-4	P		C	R	R	C	P	P		R	PI		P		C	P
Charleston NJ 17-5	P			R	R	C	P	P			PI		P		C	P
Charlottesville NJ 17-6	N						P						P			P
Jenkins NJ 17-7	P		C			C	P	P			PI		P		C	P
Bluefield NJ 17-8	P			R	R	C	P	P			PI		P		C	P
Louisville NJ 16-6					R*	C*										
Winchester NJ 16-9					R*	C*										
Corbin NJ 16-12					R*	C*										
Johnson City NJ 17-10					R	C										

N = Formation or Production not present
C = Compiling data
R = Rough copy completed
P = Preliminary map completed
X = Final draft completed
* = Not within area of responsibility but available upon request
PI = Petroleum information map on hand

Regional Structure
MAP STATUS

scale 1:250,000

R.C. Shumaker (304) 293-5603

LOCATION DIAGRAM

FIGURE 2

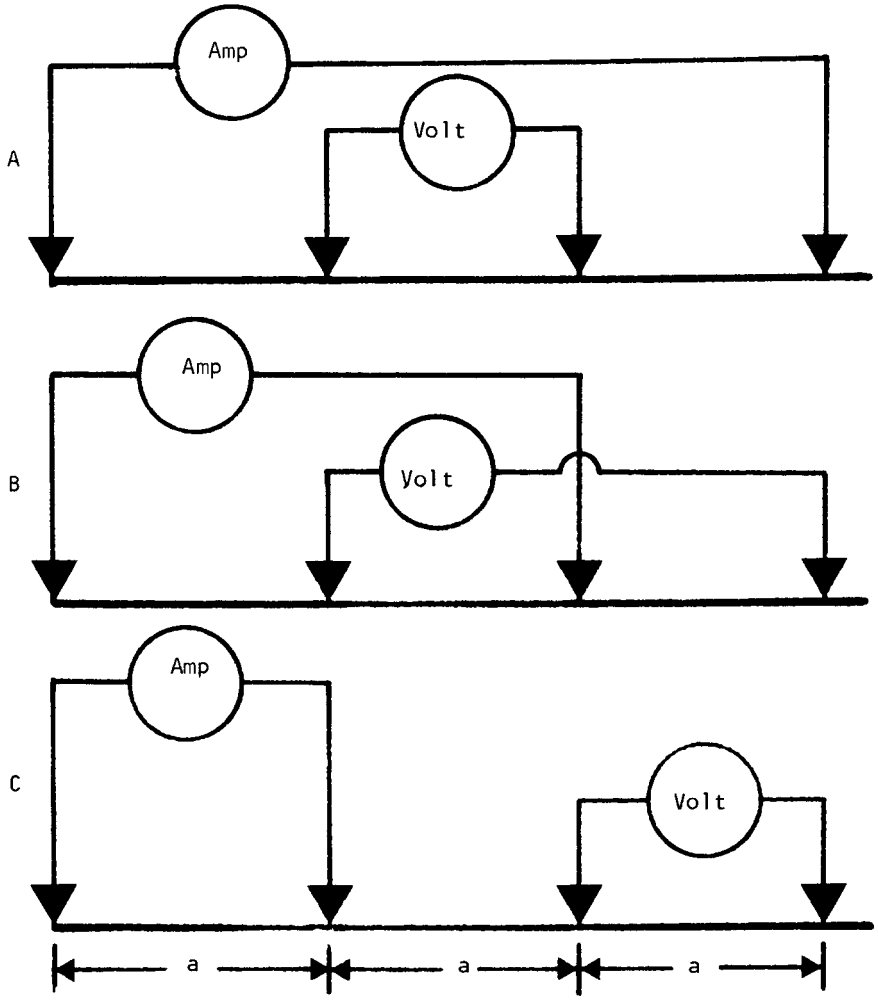

FIGURE 3
TRIPOTENTIAL ELECTRODE CONFIGURATION
A=CPPC, B=CPCP, C=CCPP

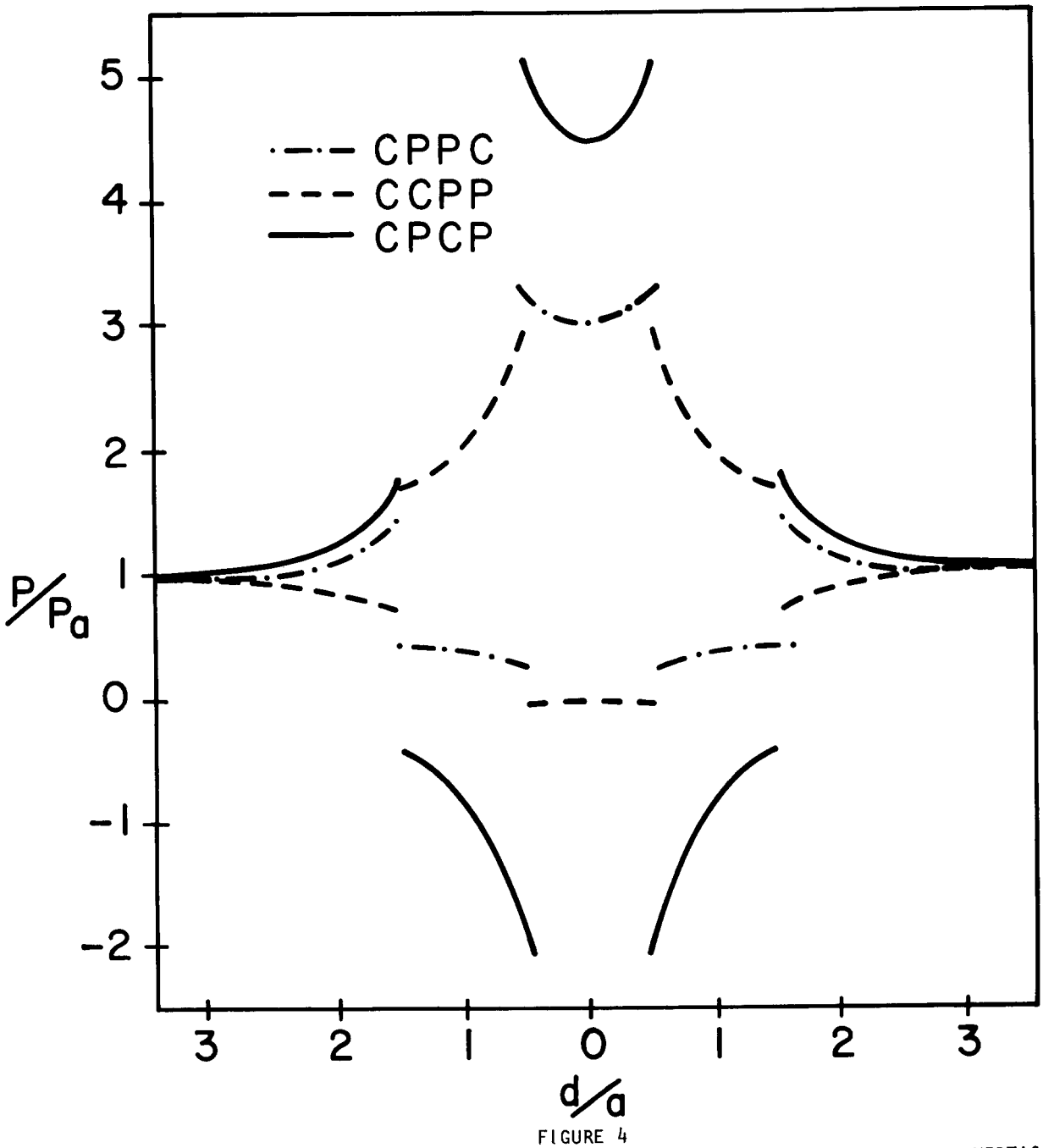

FIGURE 4
THEORETICAL TRI-POTENTIAL RESPONSE PASSING OVER A FRACTURE ZONE MODELED BY A VERTICAL INSULATING PLANE

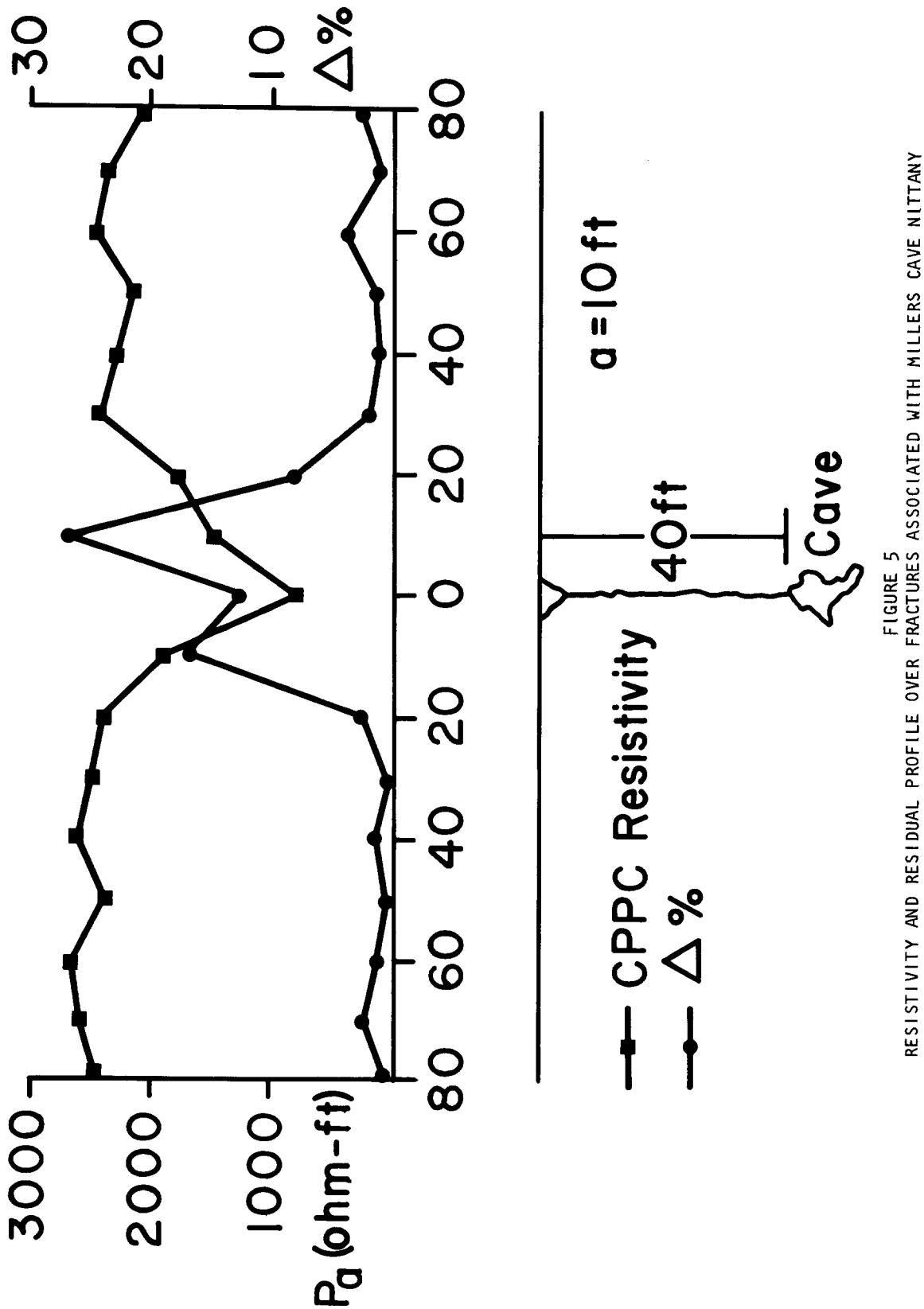

FIGURE 5
RESISTIVITY AND RESIDUAL PROFILE OVER FRACTURES ASSOCIATED WITH MILLERS CAVE NITTANY VALLEY, PENNSYLVANIA

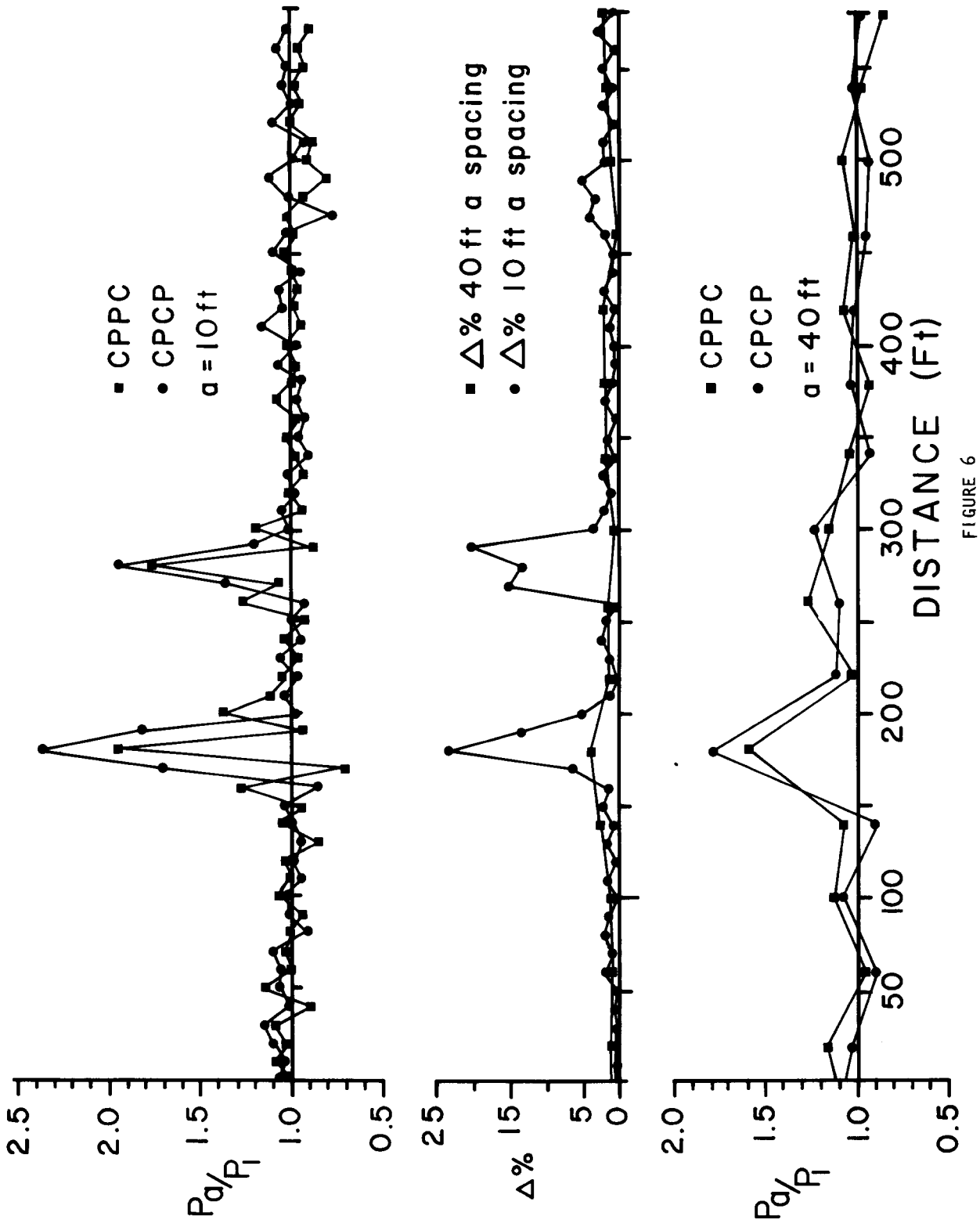

FIGURE 6
RESPONSE OF TPER SURVEY TO PRESENCE OF A "SHALLOW" FRACTURE ZONE

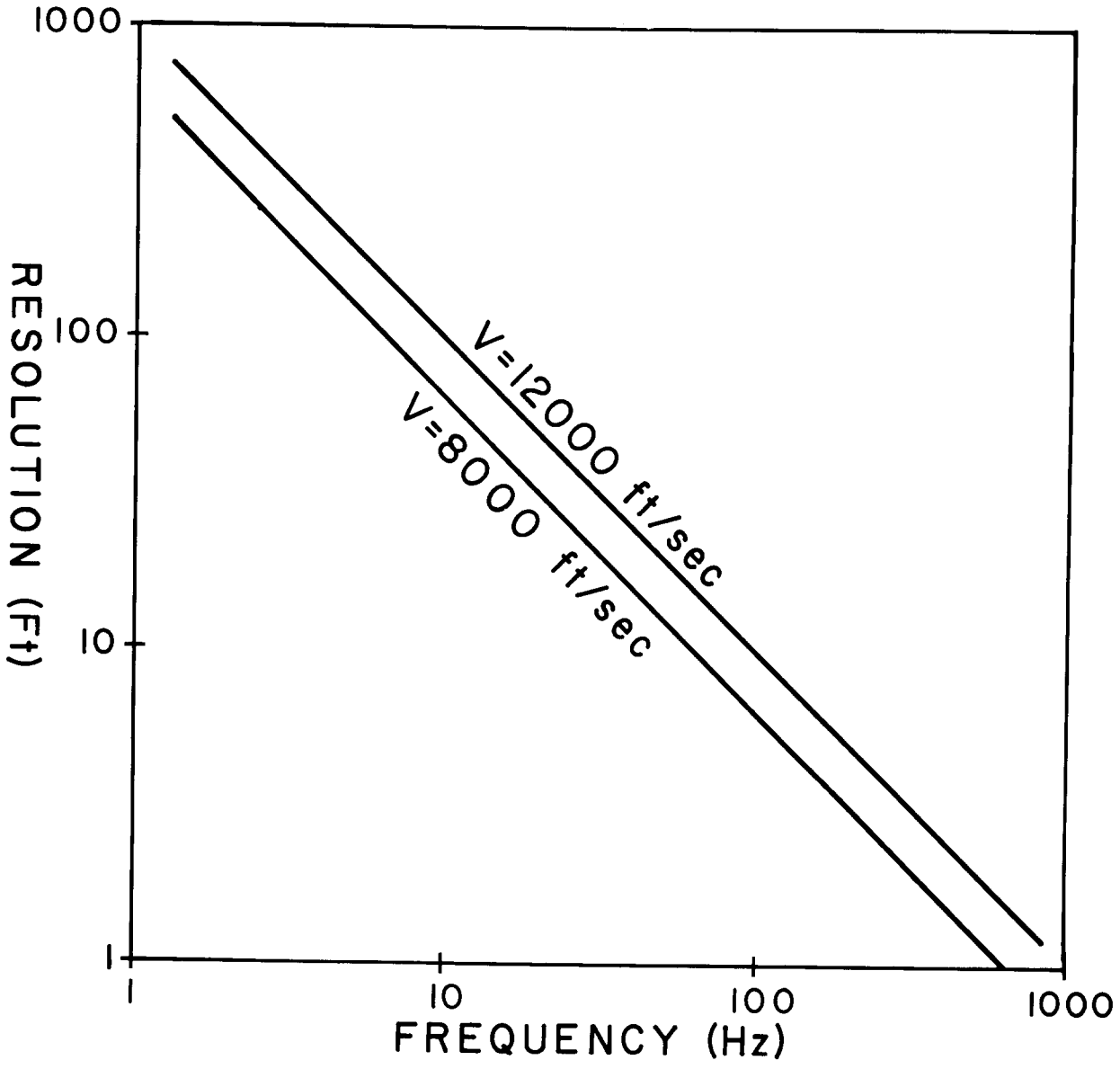

FIGURE 7
PLOT OF RESOLUTION vs FREQUENCY FOR COMMON SEISMIC VELOCITIES

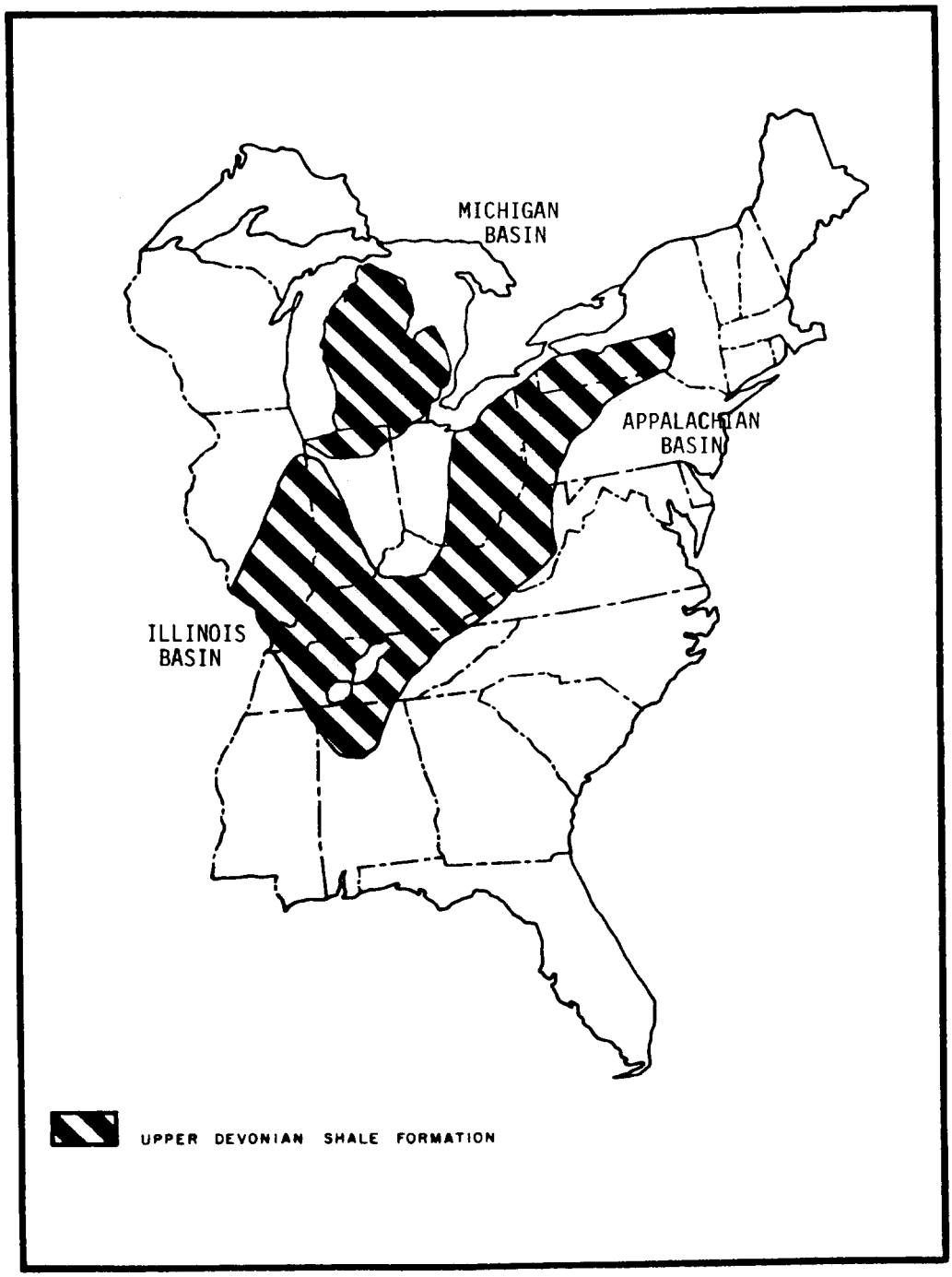

FIGURE 8

DEVONIAN SHALE BASIN. (Foster, 1975).

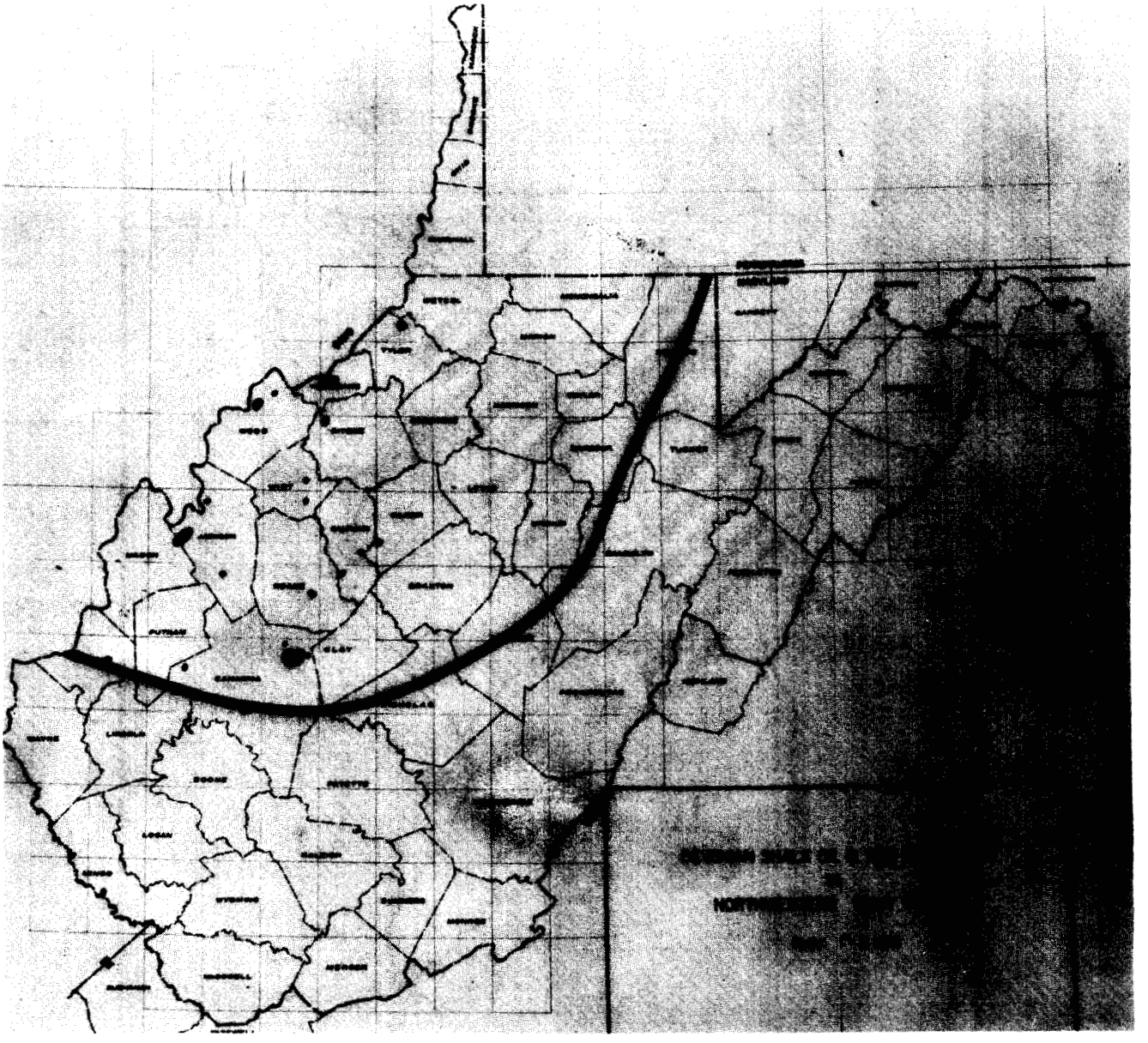

FIGURE 9
EXISTING DEVONIAN SHALE OIL AND GAS PRODUCTION IN NORTHWESTERN WEST VIRGINIA.
(Martin and Nuckols, 1976).

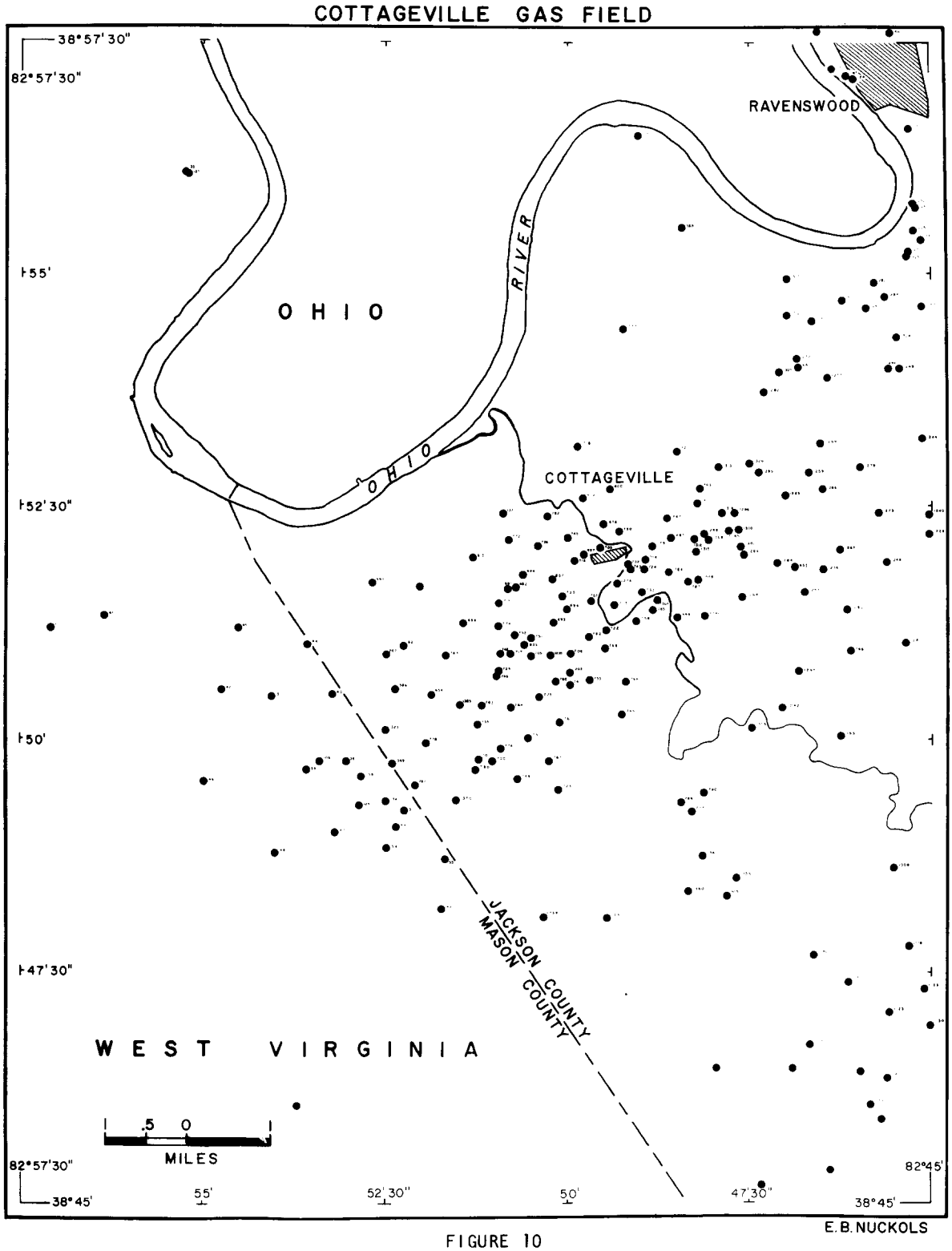

FIGURE 10

COTTAGEVILLE GAS FIELD WITH FLANKING DEVONIAN ORISKANY AND SILURIAN "NEWBURG" WELLS TO THE EAST.

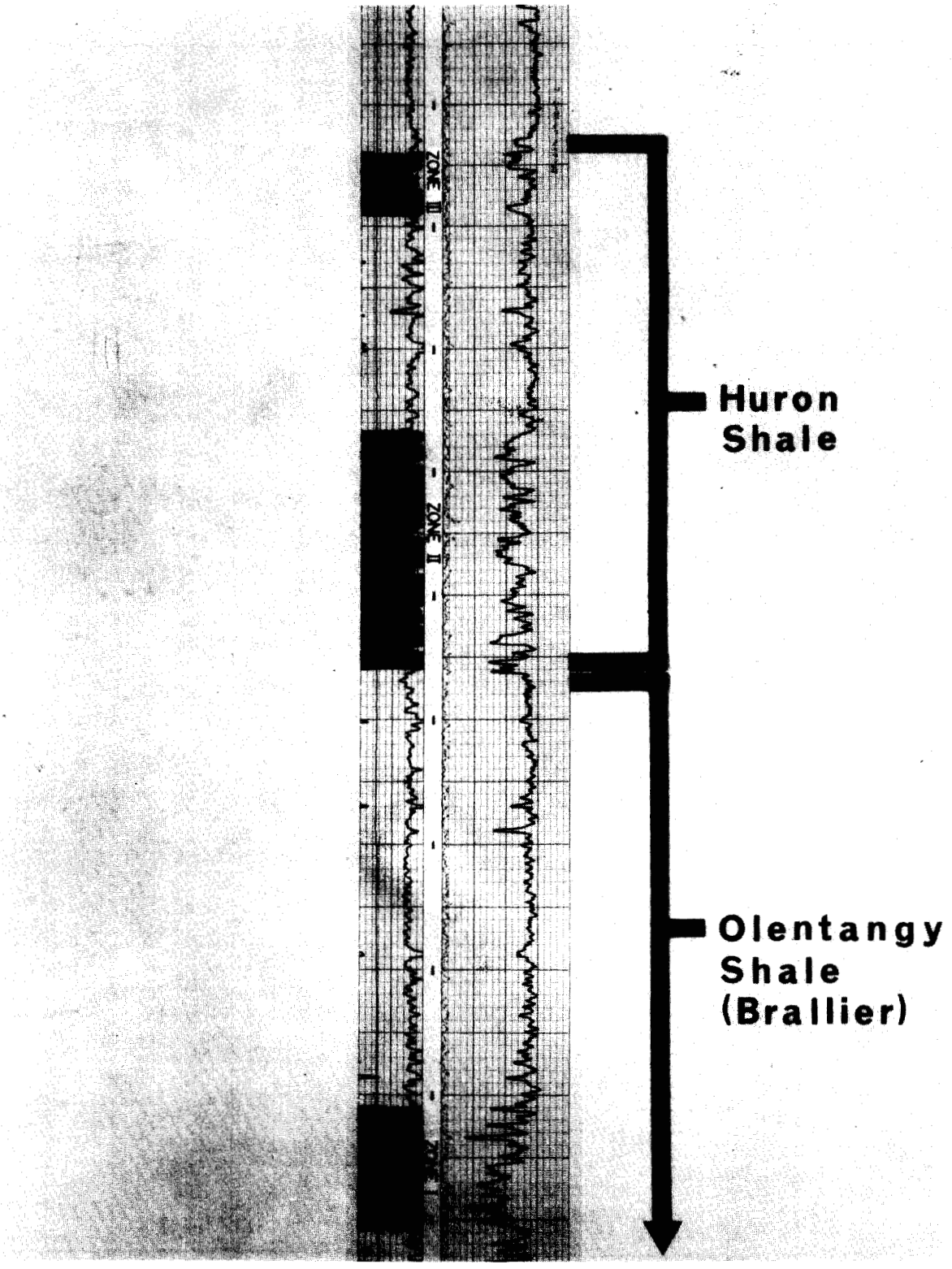

FIGURE 11
GAMMA RAY AND DENSITY LOGS PORTRAYING ORGANIC SHALE CHARACTERISTICS IN THE COTTAGEVILLE GAS FIELD, WEST VIRGINIA.

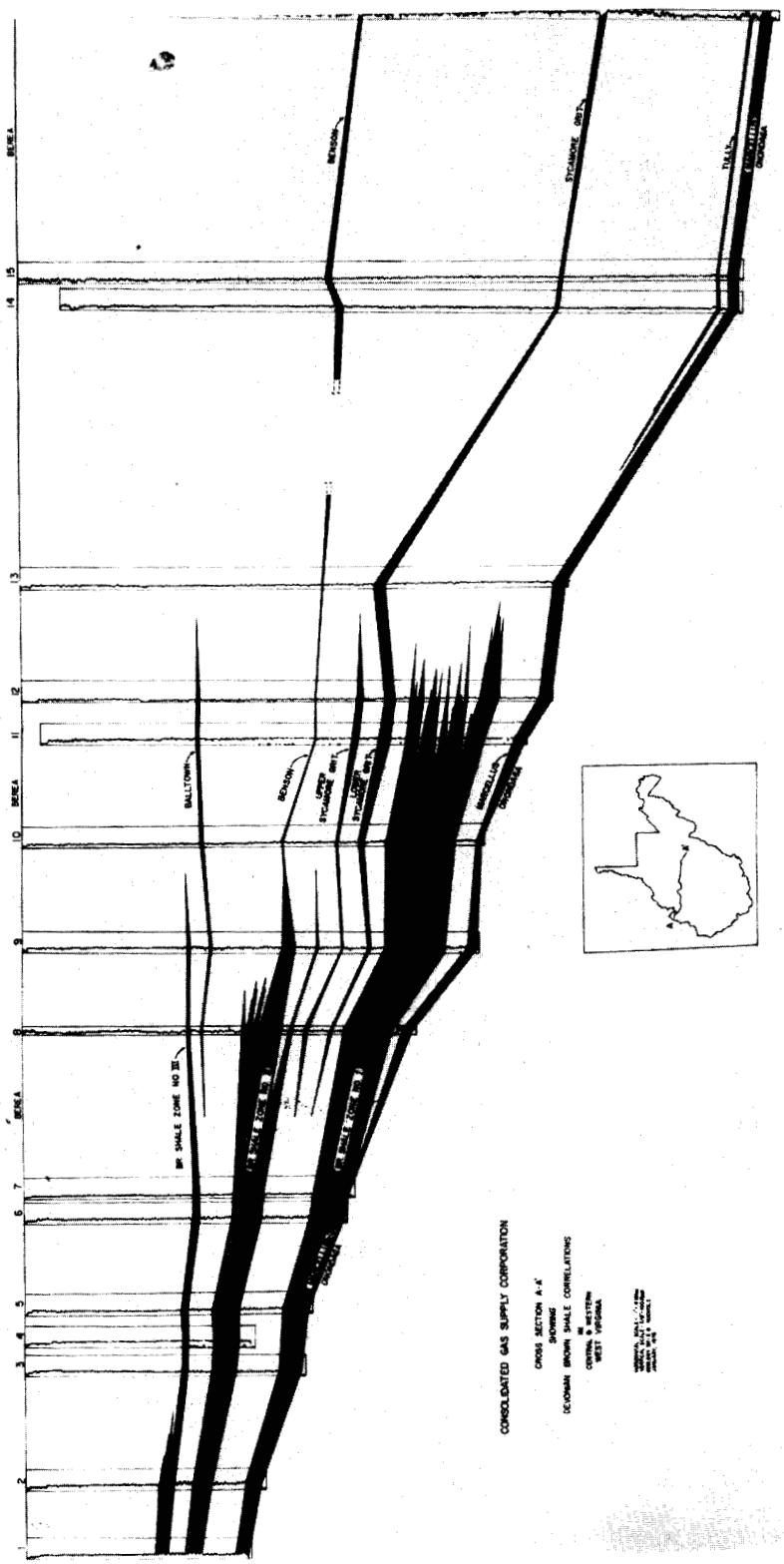

FIGURE 12
CROSS SECTION OF DEVONIAN SHALE CORRELATIONS FROM MASON TO RANDOLPH COUNTYS, WEST VIRGINIA. (Martin and Nuckols, 1976).

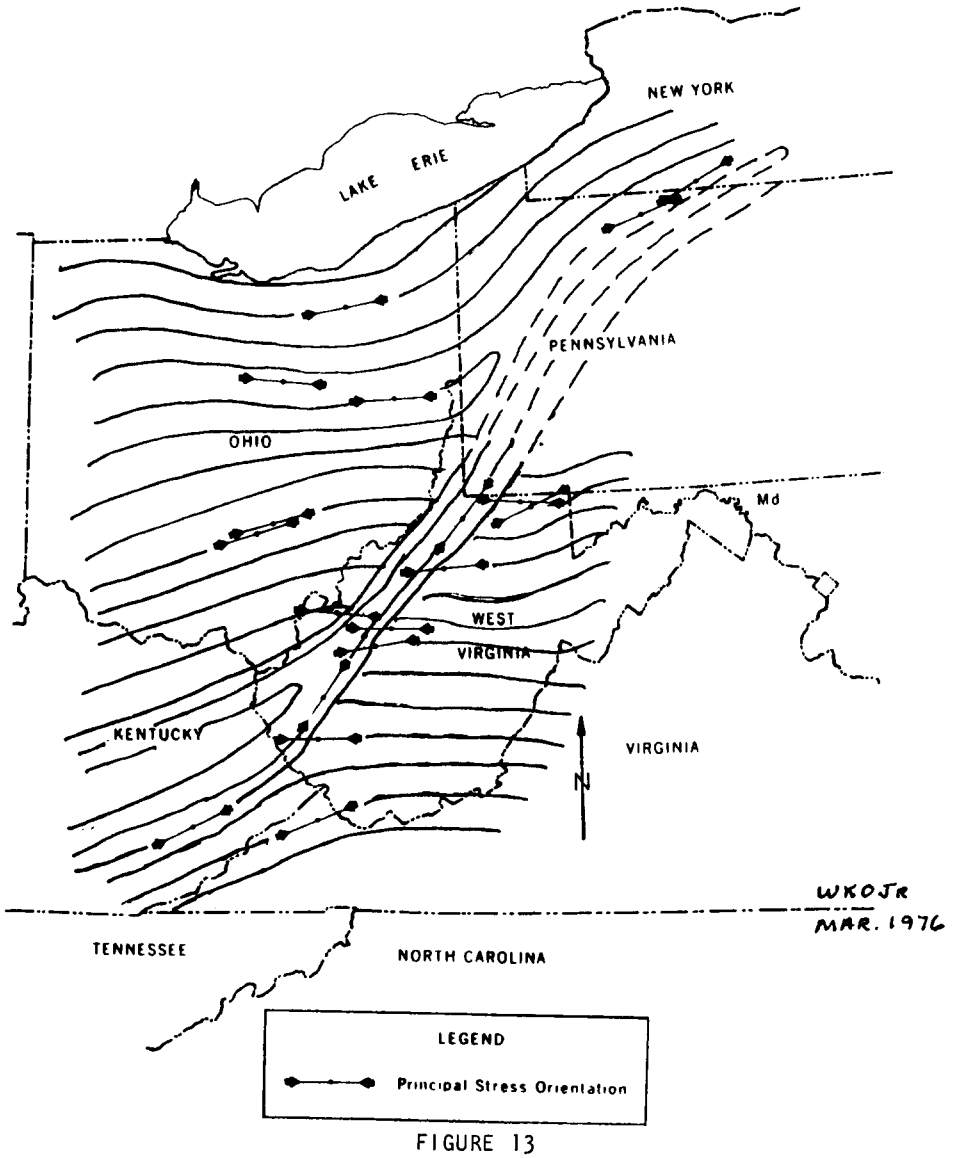

FIGURE 13

POSTULATED STRESS TRAJECTORIES FOR THE CENTRAL APPALACHIAN REGION. (Overbey, 1976).

FIGURE 14

ISOPRESSURE MAP: ROCK PRESSURE TESTS TAKEN AFTER COMPLETION OF WELLS BUT PRIOR TO PRODUCTION. CONTOUR INTERVAL: 100 lbs/sq.in.

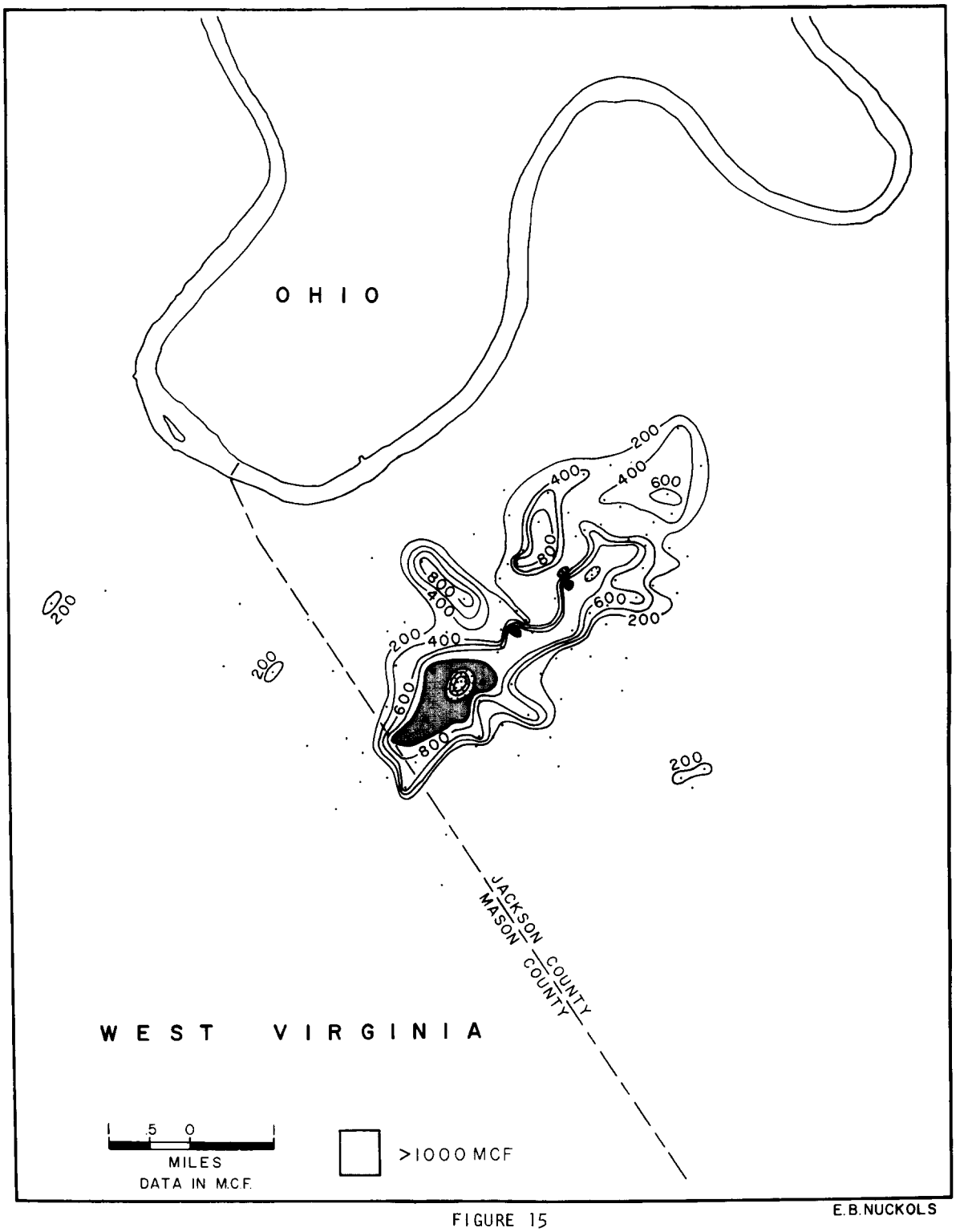

FIGURE 15

ISOFLOW MAP: FINAL OPEN FLOWS REGARDLESS OF NATURAL OR STIMULATED PRODUCTION.
CONTOUR INTERVAL: 200 Mcf (0-1000 Mcf) 1000 Mcf (1000-3000 Mcf).

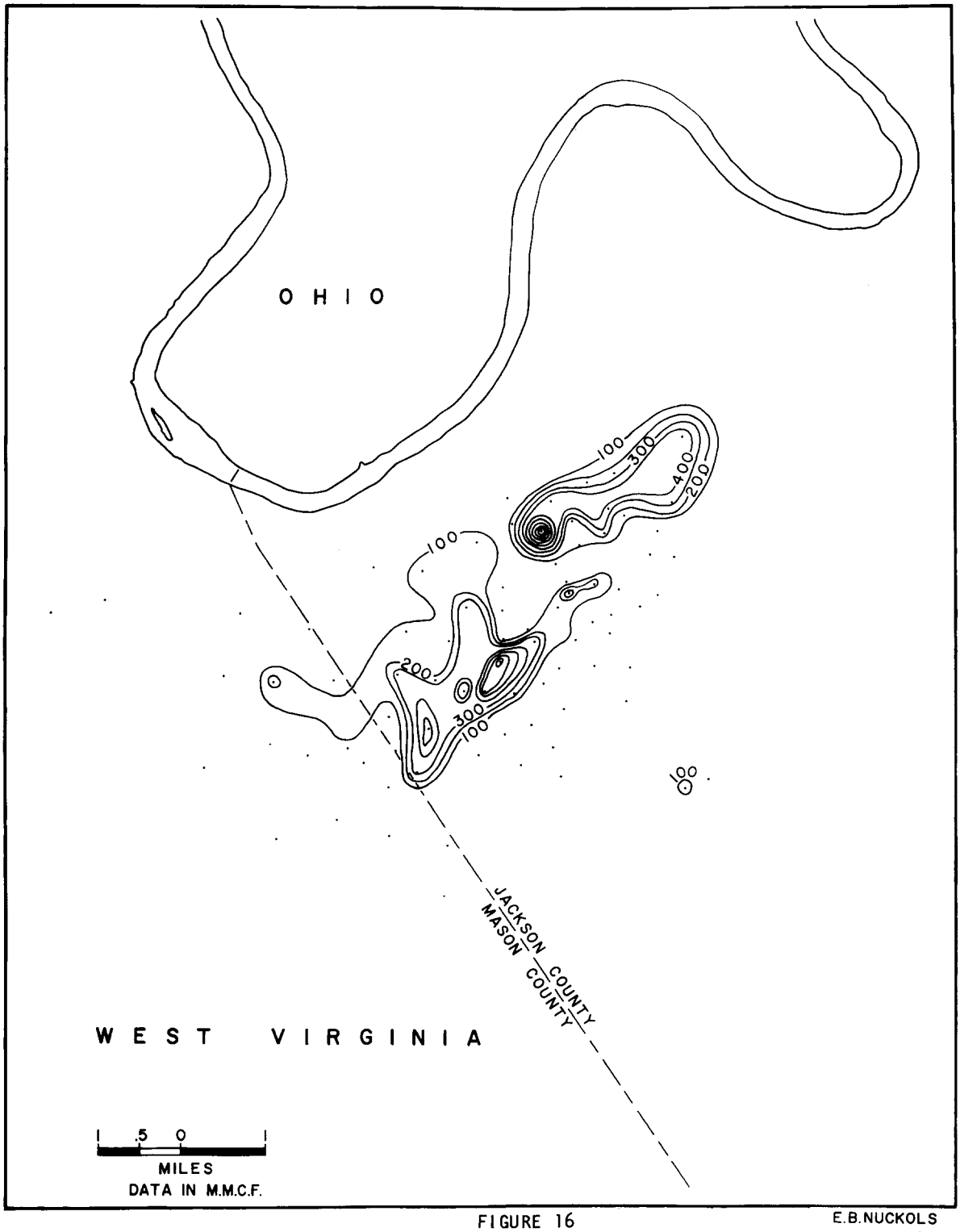

FIGURE 16 E.B.NUCKOLS

ISOPRODUCTION MAP: TOTAL ACCUMULATIVE PRODUCTION PER WELL AS OF DECEMBER 31, 1976.
CONTOUR INTERVAL: 200 MMcf.

CHARACTERIZATION AND ANALYSIS OF DEVONIAN SHALES: GAS COMPOSITION AND RELEASE RATES

M. Jack Snyder
M. P. Rausch
J. S. Ogden
R. W. Coutant

BATTELLE COLUMBUS LABORATORY

ABSTRACT

As part of the Resource Inventory and Shale Characterization subprojects of ERDA's Eastern Gas Shales Project, Battelle's Columbus Laboratories is conducting a program to determine the relationships between shale characteristics, hydrocarbon gas content, and well location. Ultimately, about 1000 core samples of gas bearing Devonian shales will be selected and sealed in special containers to preserve their approximate "down-hole" condition, and the gas-release characteristics and various chemical, physical, and lithologic characteristics will be determined.

Hydrocarbon distributions and release rates of these hydrocarbons from selected Devonian shale samples are being determined as a major effort on the program. Procedures employed involve the use of gas chromatography for composition analysis; recording microbalance and continuous-flow FID total-hydrocarbon systems for kinetics measurements; and modified Fischer Assay procedure for determination of residual heavy hydrocarbons.

Preliminary measurements of these types have now been completed for approximately 20 percent of the projected total of 1000 samples from various well sites in the Appalachian and Illinois basins. Results of these measurements and preliminary conclusions are discussed.

INTRODUCTION

This program was initiated in July 1976 as a part of ERDA's Eastern Gas Shales Project (EGSP). The objective of the program is to determine the relationships between shale characteristics, hydrocarbon gas content, and well location to provide a sound basis for defining the productive capacity of the Eastern Devonian shale deposits and for guiding research, development, and demonstration projects to enhance the recovery of natural gas from the shale deposits. The program includes a number of elemental tasks as a part of the Resource Inventory and Shale Characterization subprojects and is designed to provide large quantities of support data for the EGSP.

Approximately 1000 core samples of gas bearing Eastern Devonian shale will be examined in the program. After the characterization data for individual wells have been compiled, a regression-type analysis for pattern recognition will be performed to establish the interrelationship between the shale characteristics, the hydrocarbon gas content, and well locations from which the samples were obtained.

The work involves six tasks: core sampling, gas content and gas release kinetics, chemical characterization of the shale, physical characterization of the shale, lithology of shale, and data interpretation and correlation. Each of these tasks were briefly described in a previous paper[1].

The project was initiated in July 1976 and active laboratory work was started in September 1976. Approximately 350 core samples have now been selected and encapsulated from 10 wells, 5 in the Appalachian Basin and 5 in the Illinois Basin. The well locations are given in Table 1. Partial data are now available on 350 samples from 9 of the wells and some patterns and relationships are becoming apparent. In this paper emphasis will be on the relationships among the initial gas release data, well location, and chemical characteristic of the shale.

Core Sampling and Encapsulation

Core sampling for the EGSP is done by a team, under the supervision of the West Virginia Geological Survey, including in addition to the supervising geologist, representatives from the appropriate State Geological Survey, from the producing company, and from Battelle's Columbus Laboratories. After the core has been retrieved, reassembled, oriented, marked, and described, samples are taken by the Battelle representative for use in experiments and characteriztions being conducted at Battelle, Mound Laboratories, and Juniata College. The standard sampling sequence involves the collection of core samples at 10-foot intervals for Battelle, at 30-foot intervals for Mound Laboratories, and at 50-foot intervals for Juniata College.

The selected samples are placed in fruit juice cans and lids are applied and sealed with a canning machine for subsequent transport to the various laboratories.

Analytical Procedures for Initial Gas Release

The canned core samples are logged in and normally are stored for a minimum period of 3 weeks after canning to allow them to come to equilibrium. Some of the sealed cans bulge and distort during this equilibrium period. Many of the core sections from the recent well in Wise County, Virginia exhibited considerable outgassing during the initial examination prior to canning and many of the cans bulged noticeably within a few hours after sealing. Because of the rapid and excessive bulging, the cans were checked for possible leaks approximately 2 weeks after canning. Leaks were detected in 16 out of 72 samples checked. Gas analyses were made on these and other bulged, but not leaking, cans as quickly thereafter as possible. Subsequent checks on sealed cans from earlier wells that had not yet been analyzed revealed that some of them also were leaking and, as will be discussed later, the gas composition data suggest that some of the other cans probably had leaked before the analyses were made. Sturdier sample cans are being secured for future wells and procedures are being planned for monitoring the release of gas from the time the sample is canned.

The canned samples after the standard equilibrium period are tapped using the can sampling device shown in an exploded-view in Figure 1. The can sampler is evacuated after it is clamped to the can and the metal punch is then driven through the can top, thereby connecting the gauge and sampling volume to the free space surrounding the shale samples within the can. Two gauges are used for pressures within the cans; an Ultec gauge for pressures less than 1500 torr and an Ashcroft gauge for pressure up to 60 psig. The observed can pressure is reported in torr (mm Hg). A valving system allows a gas sample to be withdrawn from the sampler and entered into a 1 cc constant temperature sample loop. A solenoid valve controls the injection of samples into the chromatograph.

An Aerograph 1520B gas chromatograph is used for species identification. Thermal conductivity detection is employed. The carrier gas is helium at 50 psig. An Altech CTR column separates the gaseous species; the CTR is essentially a column within a column--a molecular sieve surrounds a Porapak mix. With this column it is possible to separate O_2, N_2, CO_2, and light hydrocarbons (through C_6). The detector signal is fed to a Hewlett Packard 3380A integrator and species are identified by their retention times. A standard gas mixture was prepared and includes all major species found in shale cans to date. The standard consists of (v/o):

N_2	51.11	CH_4	29.51
O_2	3.76	C_2H_6	8.50
CO_2	5.61	C_3H_8	1.52

The standard is run daily; shale gas concentrations are determined by the external standard method. Butanes and pentanes, when present, are calculated from their specific response factors. These have been previously determined for this particular experimental set up. All values are reported in volume percent.

In addition to the routine free gas analysis performed for each as-received shale can, random samples are selected for additional gas analysis. An Aerograph 2800 gas chromatograph is used. Flame ionization detection is employed and species are separated with capillary columns. The 2800 has been calibrated for identification of over 100 hydrocarbons and detects species in parts per billion concentrations. To date, traces of propylene, 2-methyl-pentane, 2-methyl 2-butene have been identified; however, the major species remain as reported: CO_2, O_2, N_2, methane, ethane, propane, butanes and pentanes.

After the initial gas analyses are completed, the can is opened, the shale sample is removed, weighed, photographed and described, and samples are taken for the various characterizations and analyses that are to be made. The bulk volume of the shale sample is subsequently calculated from the measured bulk density and the free gas space in the can is calculated by difference from the known volume of the can. The data from the gas analyses, from the various characterizations and analyses are keypunched onto computer cards for subsequent calculations, statistical analyses, and comparisons.

Tables 2 and 3 contain data illustrative of the variations in initial gas release as a function of depth of sample and location of well.

Analytical Procedures for Chemical Characterization

The direct determination of organic carbon, hydrogen and nitrogen is accomplished by controlled combustion using a Perkin-Elmer Model 240 elemental analyzer. Inorganic carbonates are not pyrolyzed if the combustion temperature is maintained under 500 C.

The Perkin-Elmer 240 elemental analyzer operates on the principle of thermal conductivity differences in the combustion products. After combustion, carbon is analyzed as carbon dioxide and hydrogen as water.

In brief, the operating procedure of the instrument is as follows: An appropriate size pulverized sample of fairly uniform particle size ($\sim$ 170 mesh)-in the case of Devonian shales 3 to 5 mg-is introduced into the cool position of the combustion column. The first cycle involves a helium purge for de-airing the shale sample. After helium purging, the system is filled with oxygen and the sample is introduced to the hot zone of the combustion column. Upon the completion of the combustion process, the helium flow resumes and the combustion products are swept through the combustion and the reduction columns. Gaseous products of no interest are screened by the special packing materials in the combustion and reduction columns. Vapors of sulfur and halogens and some other gases are removed from the stream by the packing in the combustion column and oxygen is removed by the reduction column. Only the combustion products of interest, CO_2 from carbon, H_2O from hydrogen, and elemental nitrogen are retained in the gas stream. The quantitative measurement of the three gases CO_2, H_2O, and nitrogen is made by means of thermal conductivity cells, and read-out as microvolts on a strip chart recorder. The k factor for the instrument, which relates the microvolt values to quantity of the elements analyzed, is determined using standard reference material.

Gas Content of Shale and Initial Release of Gas

As is evident from the data in Table 2 and the plot of part of that data in Figure 2, the gas content and the composition of the gas released from canned shale samples from Well P-1 varies substantially and apparently randomly with depth. A comparison of Figures 2 and 3 reveals that there are substantial differences between wells in the gas content per unit volume of shale. For Well C-2 (Figure 3), the unit gas content ranges mostly between about 0.1 and 0.5 cu ft per cu ft of shale, with a general trend of increasing gas content with increasing depth. For Well P-1 (Figure 2), on the other hand, the unit gas content is much greater and generally falls between 1 and 3 cu ft per cu ft of shale and there does not appear to be any general trend with respect to depth.

The composition of the gas also varies substantially with depth and between wells. Figure 4 is a plot of the methane content (as percentage of the total hydrocarbon gas released) versus depth for Well P-1 and Figure 5 is a similar plot for Well C-2. Again, for Well C-2 a general trend with depth is evident whereas for Well P-1, there is no clear trend. For C-2, the relative methane percentage generally decreases with depth and ranges between about 60 and 80 percent. For P-1, the methane content (with the exception of the shallowest sample), ranges between about 85 and 95 percent irrespective of the depth.

These two wells were selected as examples illustrative of the kinds of differences observed initially between the Appalachian and Illinois Basin wells. Plots of relative methane content versus the total hydrocarbon content of the released gas for these two wells are remarkably different (Figures 6 and 7). For the Appalachian Well (C-2, Figure 7), the methane content clearly is an inverse function of total hydrocarbon gas. For the Illinois Well (P-1, Figure 6), the methane content is either independent of total hydrocarbon or is a direct function of it. Gas release data from three additional Appalachian Wells and two additional Illinois Basin Wells showed the same direct relationship between methane and total hydrocarbon for Illinois Basin Wells and the same inverse relationship for Appalachian Wells (except for a few isolated samples). However, the gas release data from the most recent Appalachian Basin Well (C-338) fit the Illinois Basin pattern both in gas composition (i.e., high methane content) and amount of gas released, between 1 and 3 cu ft per cu ft of shale. The clear distinctions seen between Appalachian Basin Wells and Illinois Basin Wells are blurred somewhat by these new data and plots of methane content versus total hydrocarbon that incorporate all of the available data do not show an obvious relationship for Appalachian Basin Wells (Figure 8) although the direct relationship still appears to hold for Illinois Basin Wells (Figure 9).

A further complicating factor in attempting to assess the gas resources of the Devonian shales from gas analysis data on canned samples is the fact that some of the cans have leaked unknown amounts of hydrocarbon gas. As indicated earlier, leaking was detected in a substantial number of canned samples from one of the wells within two weeks after canning and checks on other cans have shown some of them to be leaking months after canning. An examination of the gas analysis data on other samples suggests that many of the cans may have leaked between the time they were sealed and the time that they were tapped for analysis. For example, the gas analysis results for one sample showed the total hydrocarbon content in the free space to be 90.4 percent and the nitrogen content to be 8.56 percent. If we assume that the free space contained only air at the time of canning (i.e., the gas composition was essentially 80 percent nitrogen and 20 percent oxygen) and the pressure at the time of sealing was close to one atmosphere (760 torr), the pressure at the time of tapping should have been about 7100 torr. The measured pressure was 740 torr, about an order of magnitude low, suggesting that appreciable leakage had occurred or that the sample was outgassing sufficiently during the time it was being canned to displace most of the air in the free space before it was sealed. In either case, a calculation of the gas content per unit volume of shale based on the observed pressure and gas composition at the time of tapping, underestimates the gas content in the shale in-situ by an unknown amount, perhaps as much as a factor of 10. Thus, extrapolation of current gas analysis data to produce estimates of the gas recoverable from the Devonian shales result in very shaky numbers at best. Steps that are being taken to eliminate leakage and to monitor gas composition and gas release from the time of canning will decrease the uncertainty in the future and will provide more reliable information on the areal and depth variations in the gas content of the shale.

Chemical Composition of Shale

Chemical analyses for carbon (total and organic), hydrogen, and nitrogen have been completed on selected samples from all except the most recent wells. The inorganic carbon content (derived from carbonate minerals) was determined to be a negligible fraction of the total carbon on the basis of both low-temperature ashing analyses and analyses after acid leaching on about 50 samples. Accordingly, the total carbon contents determined by combustion are considered to be a reasonably accurate measure of the organic content of the shale.

Data on the total carbon, hydrogen, and nitrogen are reported in Tables 4 through 9. The data reveal that the carbon content of the shale varies over a wide range both within a given well and between different wells. For example, the carbon content varies with depth from a low of 0.8 percent to a high of 11.5 percent in Well P-1 (Table 8) and from a low of 1.3 to a high of 14.7 percent in Well O-1 (Table 7). For Well R-109 (Table 9) the variation with depth is significantly less and the average carbon content is significantly lower than for either P-1 or O-1. As will be discussed later, the carbon content correlates reasonably well with the initial gas release from those samples.

Some of the optical emission spectroscopic data on various shale samples from several wells are given in Table 10. The spectroscopic analysis results do not reveal any unexpected or significant differences in the contents of the major elements or in the trace elements present in the shale samples taken from wells in both the Illinois and Appalachian Basins.

Gas Release and Carbon Content

As discussed in the earlier paper by Kalyoncu, et al., on Physical Characterization the initial gas release volume is inversely proportional to the bulk density of the shale but does not appear to be relatable to the porosity of the shale. This observation suggests that the density of the shale may be more a function of organic content than of pore volume and that initial gas release volume might be proportional to the carbon content.

Figure 10 is a plot of the total carbon content versus the initial gas release volume for three different wells, two in the Illinois Basin (O-1 and P-1) and one in the Appalachian Basin (C-2). Although there is appreciable scatter in these data points it is clear that higher carbon content generally is associated with higher initial gas volume. Two different regression lines are shown on the graph, one fitting the points for the P-1 well, the other fitting the points for the O-1 well. It is interesting that those samples from the C-2 well having the lowest carbon contents (below 2 percent) appear to fit the line for the P-1 well, whereas the samples having higher carbon contents fit the line for the O-1 data points.

CONCLUSIONS

The most important conclusions to be drawn from the gas release data so far is that each well is unique and that generalizations about relationships for one well or for wells within a given area may not be valid for other wells or other areas. A corollary is that a valid assessment of the gas resources of the Devonian shales requires data from many wells throughout the entire deposit.

It should be pointed out that the observed relationships (or lack of them) between gas content and shale characteristics or well locations are based on a relatively small number of samples and may be peculiar to the wells sampled.

FUTURE WORK

The coring and sampling of additional wells throughout the Eastern Devonian shales is continuing and data are now being gathered at a rate of about 25 samples per month. As more experience is gained and additional data are accumulated, the level of uncertainty will decrease and more reliable and, hopefully, more meaningful conclusions about the gas content and the relationships among gas release characteristics, shale characteristics, and well location will emerge.

TABLE 1. IDENTIFICATION OF CORED WELLS AND SAMPLES SELECTED

Well Code Number	Location of Well	Well Operator	Date Sampled	Core Depth Interval, feet	Number of Samples
C-1	Lincoln County, WV	Columbia Gas	Jan. 1976	2746 - 4045	82
C-2	Lincoln County, WV	Columbia Gas	Jan. 1976	2655 - 3971	17
R-109	Washington County, OH	River Gas	July 30, 1976	3494 - 3705	25
P-1	Sullivan County, IN	Energy Resources of Indiana, Inc.	Sept. 1, 1976	2495 - 2595	11[a]
O-1	Christian County, KY	Orbit Gas	Sept. 18, 1976	2183 - 2319	13[b]
C-336	Martin County, KY	Columbia Gas	Nov. 6, 1976	2434 - 3405	117[c]
T-1	Effingham County, IL	Tri-Star	Feb. 13-18, 1977	3006 - 3106	15[d]
C-338	Wise County, VA	Columbia Gas	Apr. 22-30, 1977	4871 - 5469	40[e]
N-1	Henderson County, IL	No. Illinois Gas	July 13-17, 1977	319 - 620	31[f]
N-2	Tazewell County, IL	No. Illinois Gas	Aug. 16-20, 1977	898 - 1158	23[g]

(a) An additional 6 samples were selected and encapsulated for other ERDA contractors.
(b) An additional 4 samples were selected and encapsulated for other ERDA contractors.
(c) An additional 90 samples were selected and encapsulated for other ERDA contractors.
(d) An additional 16 samples were selected and encapsulated for other ERDA contractors.
(e) An additional 41 samples were selected and encapsulated for other ERDA contractors.
(f) An additional 26 samples were selected and encapsulated for other ERDA contractors.
(g) An additional 29 samples were selected and encapsulated for other ERDA contractors.

TABLE 2. INITIAL GAS RELEASE DATA: WELL P-1

Sample ID	Pressure Torr	Free Volume cc	Core Volume cc	Open Porosity %	Gas Composition, Volume Percent									Gas Released Per Unit Volume of Shale
					CH_4	C_2H_6	C_3H_8	C_4H_{12}	C_5H_{12}	Total Hydroc.	N_2	O_2	CO_2	
P 1-2495	900	887	563	5.08	21.47	4.61	3.53	1.72	.63	31.96	65.87	.91	1.27	.60
P 1-2505	1345	801	649	.64	66.41	3.60	.22	0.00	0.00	70.23	21.06	2.18	6.53	1.53
P 1-2515	1900	950	500	1.06	58.46	4.19	.26	.05	0.00	62.96	29.95	2.68	4.41	2.99
P 1-2528	2104	797	653	.55	60.60	2.59	0.00	0.00	0.00	63.19	28.14	1.88	6.79	2.14
P 1-2530	1770	720	730	1.67	54.60	2.27	1.65	0.00	0.00	58.52	31.29	2.31	7.92	1.35
P 1-2547	1700	735	715	2.26	61.32	6.01	.20	0.00	0.00	67.53	27.72	.54	4.22	1.55
P 1-2554	1900	647	803	1.61	62.95	5.42	.34	.07	.03	68.81	27.23	.65	3.31	1.38
P 1-2565	1390	708	742	1.93	52.58	5.04	1.63	.59	.29	60.13	35.62	.74	3.52	1.05
P 1-2575	1970	780	670	.62	62.81	4.60	0.00	0.00	0.00	67.41	27.33	.12	5.14	2.04
P 1-2585	1340	741	709	.62	45.00	3.30	0.00	0.00	0.00	48.30	40.40	4.10	7.20	.89
P 1-2595	2030	573	877	.77	59.01	4.95	2.36	.98	.30	67.60	26.68	.56	5.51	1.18

TABLE 3. INITIAL GAS RELEASE DATA: WELL C-2

Sample ID	Pressure Torr	Free Volume cc	Core Volume cc	Open Porosity %	Gas Composition, Volume Percent									Gas Released Per Unit Volume of Shale
					CH_4	C_2H_6	C_3H_8	C_4H_{12}	C_5H_{12}	Total Hydroc.	N_2	O_2	CO_2	
C 2-2655	740	516	934	1.41	8.47	.81	.28	0.00	0.00	9.56	85.33	1.95	3.16	.05
C 2-2710	750	440	1016	2.22	11.87	1.36	.63	.04	0.00	13.90	82.60	1.36	2.15	.06
C 2-2761	740	363	1087	2.57	12.69	1.81	.99	.10	0.00	15.59	81.15	1.37	1.88	.05
C 2-3000	925	523	927	.71	25.88	3.36	1.84	.53	.20	31.81	64.57	.83	2.78	.22
C 2-3025	920	346	1104	.68	23.08	4.31	3.81	.77	.17	32.14	63.72	.72	3.42	.12
C 2-3050	890	703	747	.64	22.63	3.15	1.56	.38	0.00	27.72	67.86	1.05	3.38	.31
C 2-3101	1100	561	889	.63	32.88	5.98	2.54	.66	.34	42.40	54.70	.73	2.16	.39
C 2-3303	750	535	915	.54	19.58	4.09	2.92	.54	.21	27.34	68.50	.99	3.17	.16
C 2-3328	720	446	1004	.50	23.98	5.88	3.42	.74	.16	34.18	58.95	2.60	4.31	.14
C 2-3378	830	478	972	.30	54.10	15.10	13.05	3.11	.76	86.12	12.67	.35	.88	.46
C 2-3428	780	484	966	.29	47.29	10.47	6.31	2.07	.47	66.61	32.17	.67	.61	.34
C 2-3478	845	711	739	.95	16.34	2.87	1.56	.51	.12	21.40	69.99	7.12	1.46	.23
C 2-3528	760	296	1154	.36	57.76	15.82	10.01	2.75	.78	87.12	11.05	.98	.85	.22
C 2-3896	990	637	813	1.51	47.48	13.59	7.72	1.77	.48	71.04	26.98	.46	1.53	.72
C 2-3922	750	622	828	.66	46.33	20.46	13.27	3.96	.99	85.01	13.64	.69	.65	.63
C 2-3961	955	424	1026	.32	65.19	18.39	9.79	2.05	.44	95.86	3.69	.10	.36	.50
C 2-3971	775	516	934	.34	59.08	17.99	11.27	2.10	.33	90.77	7.38	1.54	.32	.51

TABLE 4. CHEMICAL CHARACTERIZATION DATA

Sample ID	Carbon	Hydrogen	Nitrogen
C 1-2927.A	1.1	0.6	0.2
C 1-2999	2.1	0.5	0.1
C 1-3085	1.9	0.6	0.1
C 1-3175	0.9	0.5	0.1
C 1-3198	1.9	0.7	0.1
C 1-3396	1.3	0.6	0.1
C 1-3426	4.8	0.7	0.2
C 1-3573	5.5	0.8	0.2
C 1-3593	1.5	0.6	0.1
C 1-3651	5.2	0.8	0.1
C 1-3701	7.2	1.0	0.2
C 1-3869	2.9	0.6	0.1
C 1-3998	2.8	0.6	0.1
C 1-4045	5.8	0.8	0.2

TABLE 5. CHEMICAL CHARACTERIZATION DATA

Sample ID	Carbon	Hydrogen	Nitrogen
C 2-2655	0.2	0.5	0.1
C 2-2710	0.3	0.4	0.1
C 2-2761	0.7	0.4	0.1
C 2-3000	1.0	0.5	0.1
C 2-3025	0.6	0.6	0.1
C 2-3050	1.4	0.6	0.1
C 2-3101	1.4	0.6	0.1
C 2-3303	0.7	0.5	0.1
C 2-3326	1.4	0.5	0.1
C 2-3378	4.8	0.7	0.2
C 2-3428	3.1	0.6	0.1
C 2-3478	0.7	0.5	0.1
C 2-3528	5.1	0.8	0.2
C 2-3896	1.4	0.5	0.1
C 2-3922	4.1	0.7	0.1
C 2-3961	7.1	0.9	0.2
C 2-3971	5.1	0.7	0.1

TABLE 6. CHEMICAL CHARACTERIZATION DATA

Sample ID	Carbon	Hydrogen	Nitrogen
C-338-4892	4.7	0.5	0.1
C-338-4922	3.2	0.4	0.1
C-338-5232	0.8	0.5	0.1
C-338-5322	1.8	0.5	0.2
C-338-5357	1.9	0.4	0.1
C-338-5362	6.2	0.6	0.2
C-338-5372	4.7	0.5	0.2
C-338-5404	3.8	0.5	0.2
C-338-5414	5.3	0.6	0.2
C-338-5424	5.0	0.5	0.2
C-338-5444	6.2	0.6	0.2

TABLE 7. CHEMICAL CHARACTERIZATION DATA

Sample ID	Carbon	Hydrogen	Nitrogen
O 1-2183	14.7	1.5	0.5
O 1-2191	10.5	1.1	0.4
O 1-2220	7.1	0.9	0.2
O 1-2230	2.2	0.5	0.2
O 1-2239	8.8	1.0	0.3
O 1-2251	1.3	0.4	0.1
O 1-2259	12.6	1.3	0.5
O 1-2271	9.0	0.8	0.2
O 1-2281	8.9	0.9	0.4
O 1-2290	9.8	0.8	0.3
O 1-2300	9.3	0.8	0.3
O 1-2310	8.9	0.8	0.2
O 1-2319	12.6	1.0	0.3

TABLE 8. CHEMICAL CHARACTERIZATION DATA

Sample ID	Carbon	Hydrogen	Nitrogen
P 1-2495	0.8	0.5	0.1
P 1-2505	11.5	1.3	0.3
P 1-2515	6.1	0.8	0.2
P 1-2528	8.6	1.0	0.2
P 1-2536	10.3	1.1	0.2
P 1-2547	7.1	0.9	0.2
P 1-2554	5.4	0.8	0.3
P 1-2565	3.2	0.6	0.1
P 1-2575	7.5	1.0	0.2
P 1-2585	8.7	1.0	0.2
P 1-2595	6.1	0.8	0.1

TABLE 9. CHEMICAL CHARACTERIZATION DATA

Sample ID	Carbon	Hydrogen	Nitrogen
R-109-3506	1.5	0.5	0.1
R-109-3516	1.6	0.6	0.1
R-109-3526	3.2	0.7	0.1
R-109-3536	2.2	0.6	0.1
R-109-3555	1.3	0.6	0.1
R-109-3593	2.8	0.6	0.1
R-109-3605	3.1	0.7	0.1
R-109-3606A	5.0	0.8	0.1
R-109-3606B	3.9	0.7	0.1
R-109-3665	2.4	0.5	0.1
R-109-3685	1.7	0.5	0.1
R-109-3695	3.5	0.7	0.2
R-109-3705	0.5	0.5	0.1
R-109-3711	0.5	0.5	0.1
R-109-3494	0.4	0.5	0.1
R-109-3536	2.0	0.6	0.1
R-109-3545	1.3	0.6	0.1
R-109-3585	2.2	0.6	0.1
R-109-3606B	4.0	0.7	0.1
R-109-3626	0.9	0.6	0.1
R-109-3634	2.3	0.6	0.1
R-109-3644B	2.5	0.6	0.1
R-109-3675	1.8	0.6	0.1
R-109-3695	3.3	0.6	0.1

TABLE 10. RESULTS OF OPTICAL EMISSION SPECTROSCOPIC ANALYSES

Sample Number	Elements Detected, Approximate Weight Percent																
	Si	Fe	Al	Mg	K	Na	Ca	Ti	Ni	Mo	Mn	Ba	B	Pb	V	Cu	Zr
C-1-3573	10-20	4-8	5-10	.5-1	3-5	.5	.4	.3	.005	.005	.02	.03	.01	< .01	.01	.01	.01
C-1-3651	10-20	4-8	5-10	.5-1	3-5	.5	.3	.3	.005	.005	.02	.03	.02	.01	.01	.03	.01
C-1-3701	10-20	4-8	5-10	.5-1	3-5	.5	.1	.3	.01	.01	.02	.03	.01	.01	.02	.03	.01
C-1-4045	10-20	4-8	5-10	.5-1	3-5	.5	1.	.3	.01	.005	.02	.02	.02	< .01	.03	.01	.01
C-2-3528	10-20	4-8	5-10	.5-1	3-5	.5	.4	.3	.005	.005	.02	.03	.01	< .01	.01	.01	.01
0-1-2259	10-20	4-8	5-10	.5-1	3-5	.5	1.	.3	.02	.02	.02	.02	.03	< .01	.04	.01	.01
0-1-2271	10-20	6-10	5-10	1-3	3-5	.5	4-8	.3	.005	<.005	.03	.02	.01	< .01	.01	.02	.01
P-1-2205	10-20	4-8	5-10	.5-1	3-5	.5	.3	.3	.01	<.005	.01	.02	.01	< .01	.04	.02	.01
P-1-2515	10-20	4-8	5-10	.5	3-5	.5	.1	.3	.005	<.005	.005	.02	.01	< .01	.02	.01	.01
P-1-2536	10-20	6-10	5-10	1.	3-5	.5	3-5	.3	.005	.01	.03	.02	.01	< .01	.01	.01	.01
P-1-2554	10-20	4-8	5-10	1.	3-5	.5	1.	.3	.005	<.005	.02	.03	.01	< .01	.01	.01	.01
R-109-3606A	10-20	4-8	5-10	.5-1	3-5	.5	.4	.3	.005	<.005	.02	.03	.01	< .01	.01	.01	.01

B.C.L. CAN SAMPLER

FIGURE 1.

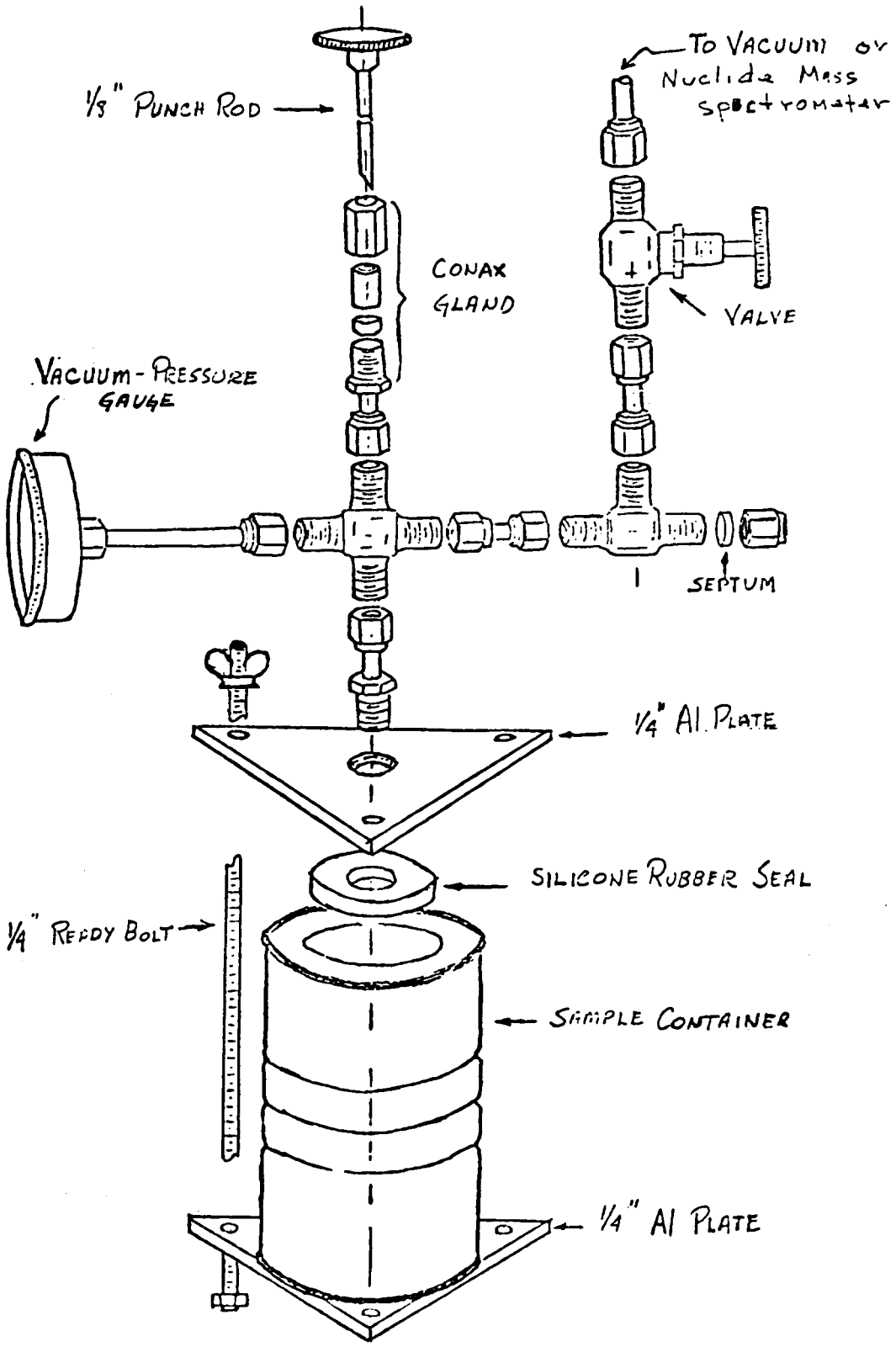

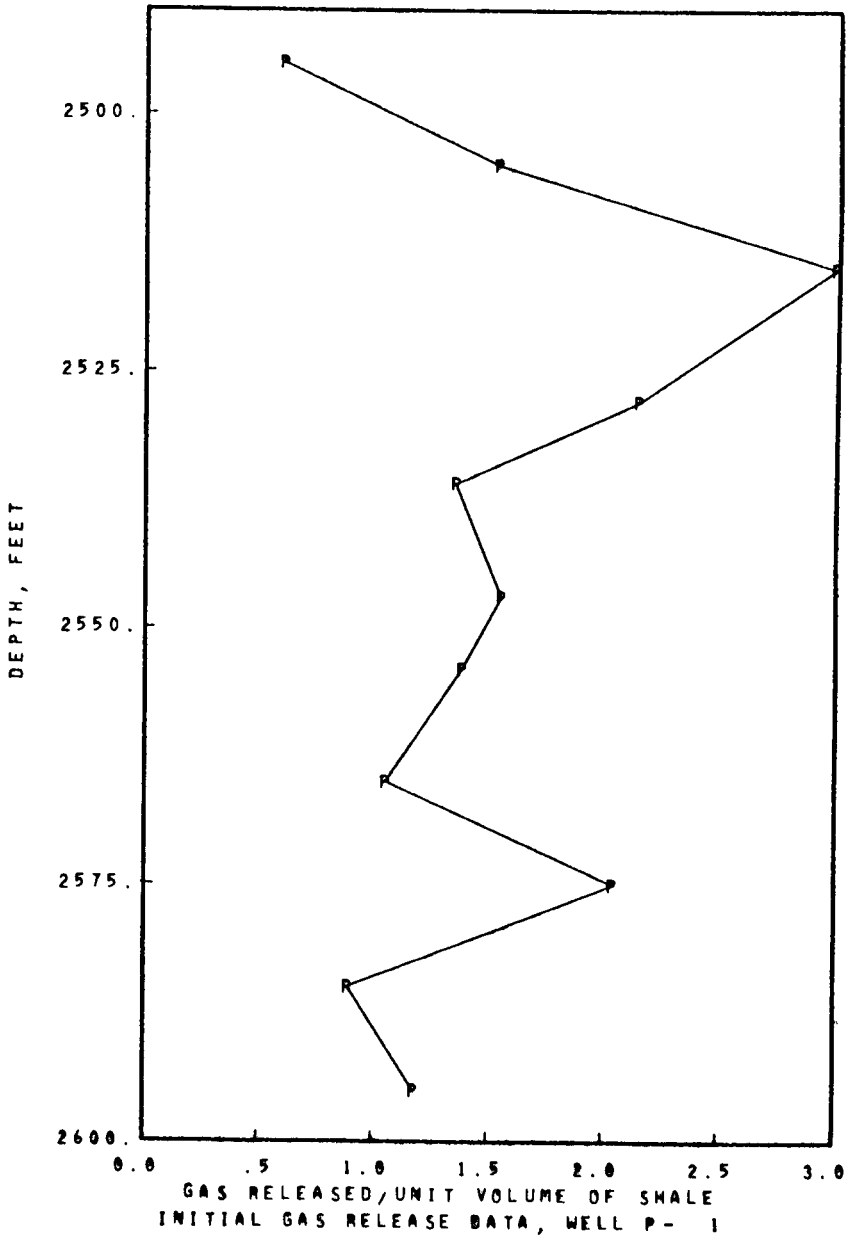
2500.
2525.
2550.
2575.
2600.
DEPTH, FEET
0.0
.5
1.0
1.5
2.0
2.5
3.0
GAS RELEASED/UNIT VOLUME OF SHALE
INITIAL GAS RELEASE DATA, WELL P- 1

FIGURE 2.

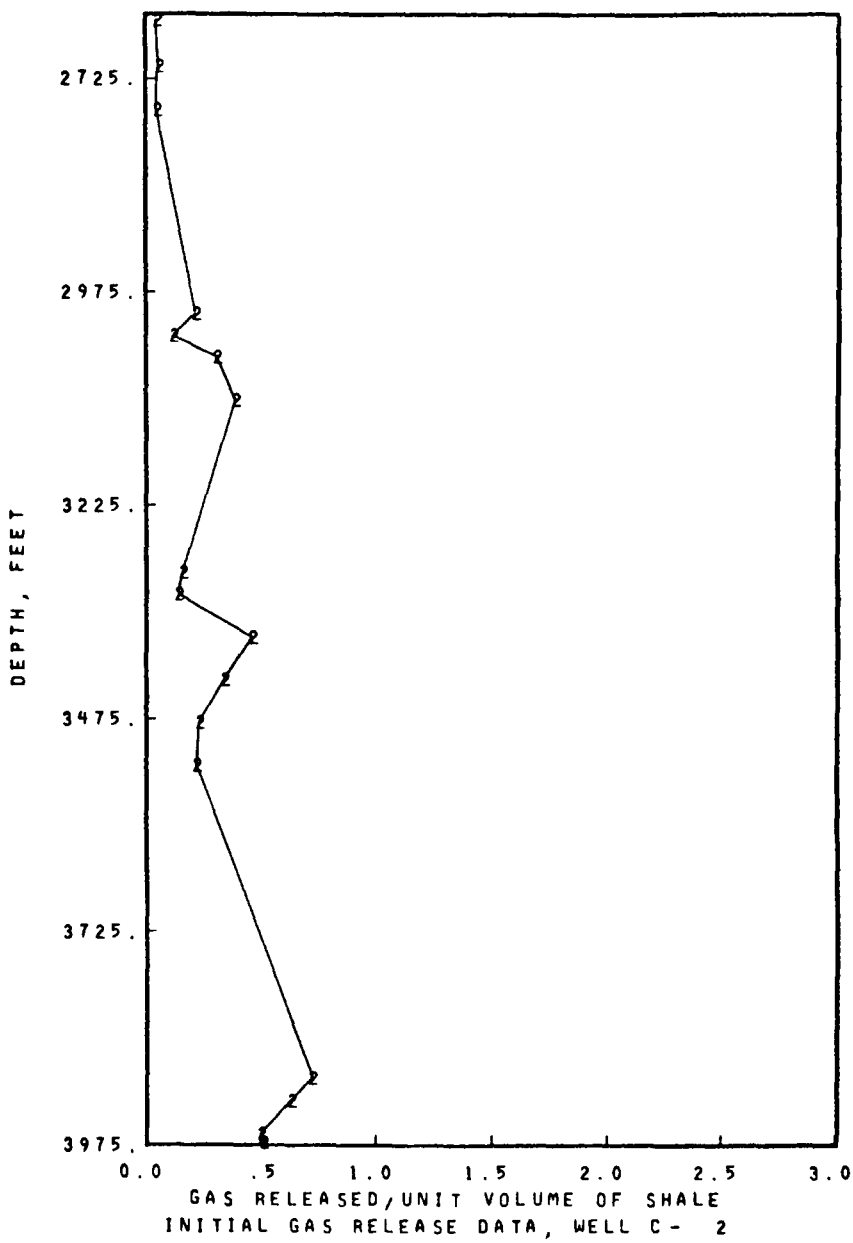
2725.
2975.
3225.
3475.
3725.
3975.
DEPTH, FEET
0.0
.5
1.0
1.5
2.0
2.5
3.0
GAS RELEASED/UNIT VOLUME OF SHALE
INITIAL GAS RELEASE DATA, WELL C- 2

FIGURE 3.

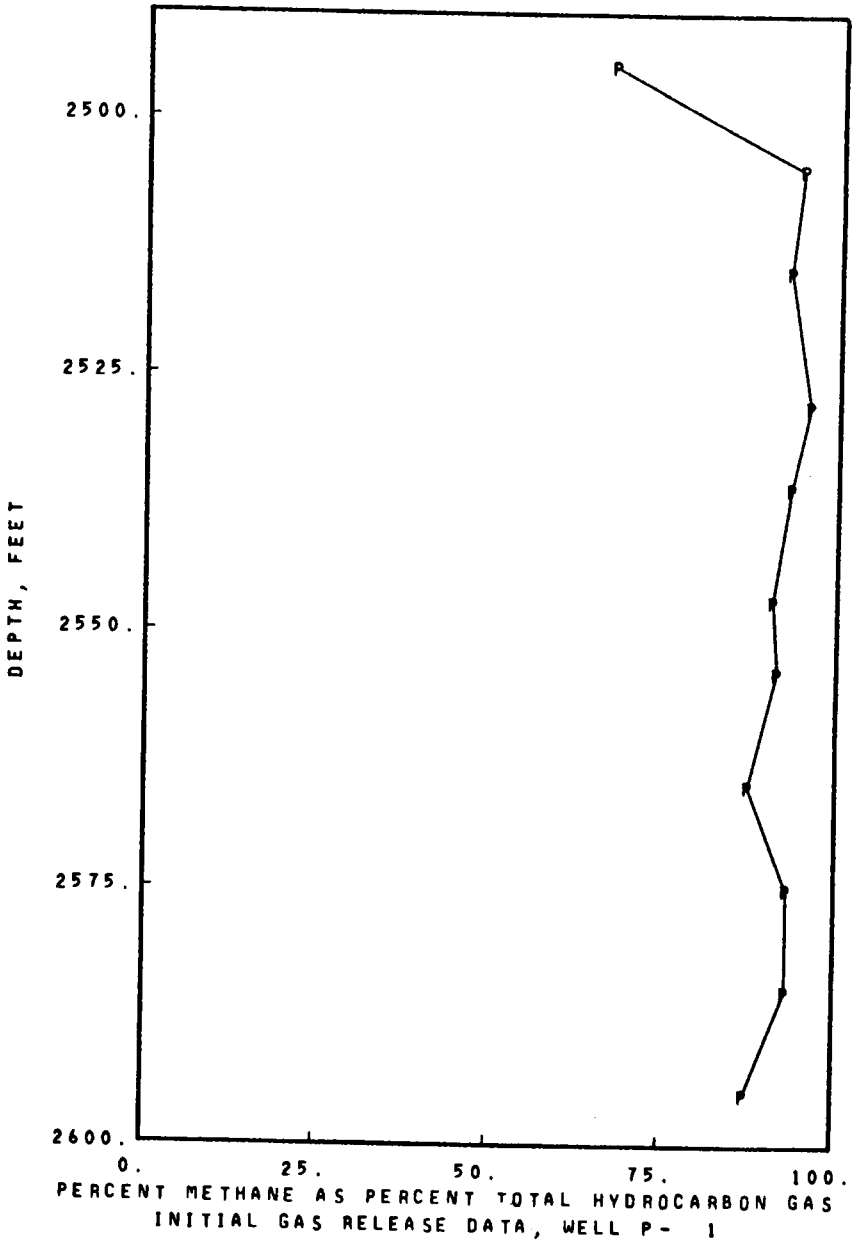
2500.
2525.
2550.
2575.
2600.
DEPTH, FEET
0.
25.
50.
75.
100.
PERCENT METHANE AS PERCENT TOTAL HYDROCARBON GAS
INITIAL GAS RELEASE DATA, WELL P- 1

FIGURE 4.

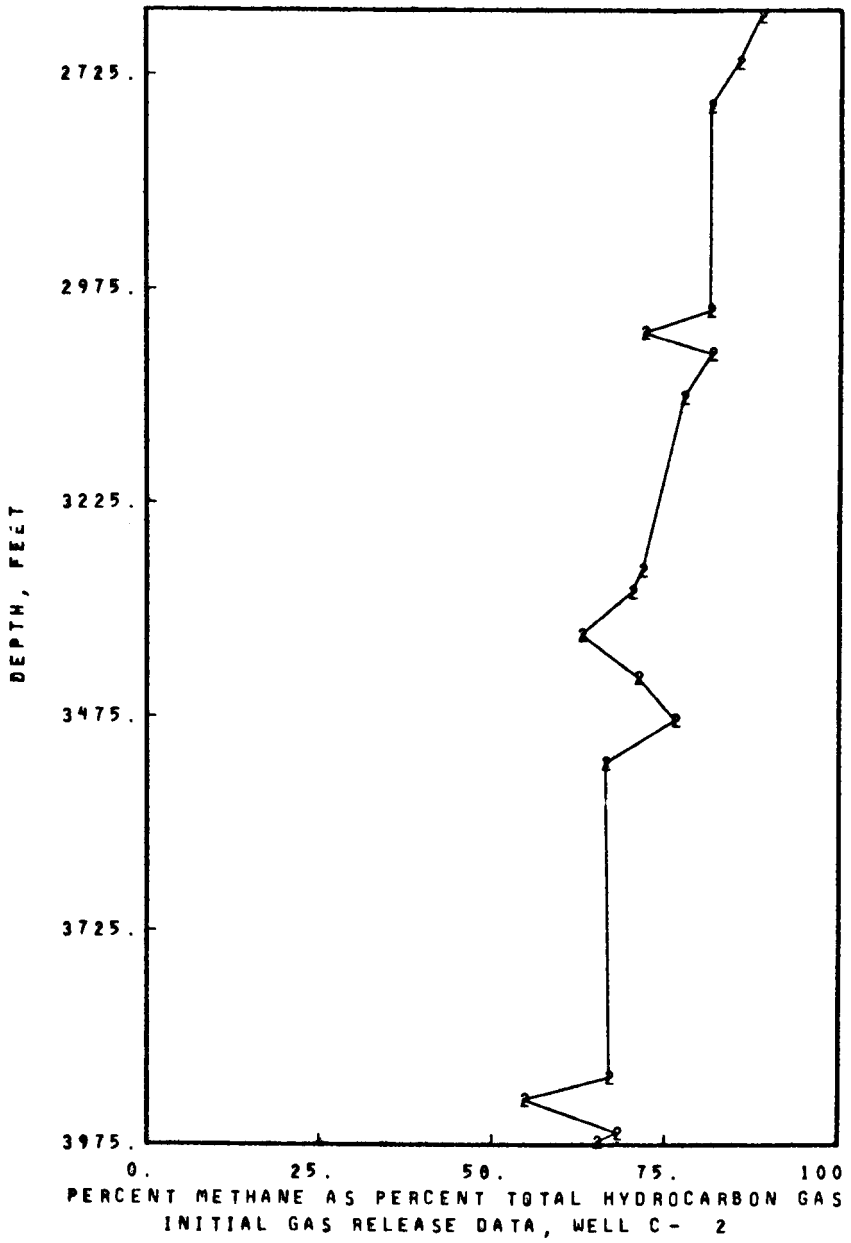
2725.
2975.
3225.
3475.
3725.
3975.
DEPTH, FEET
0.
25.
50.
75.
100.
PERCENT METHANE AS PERCENT TOTAL HYDROCARBON GAS
INITIAL GAS RELEASE DATA, WELL C- 2

FIGURE 5.

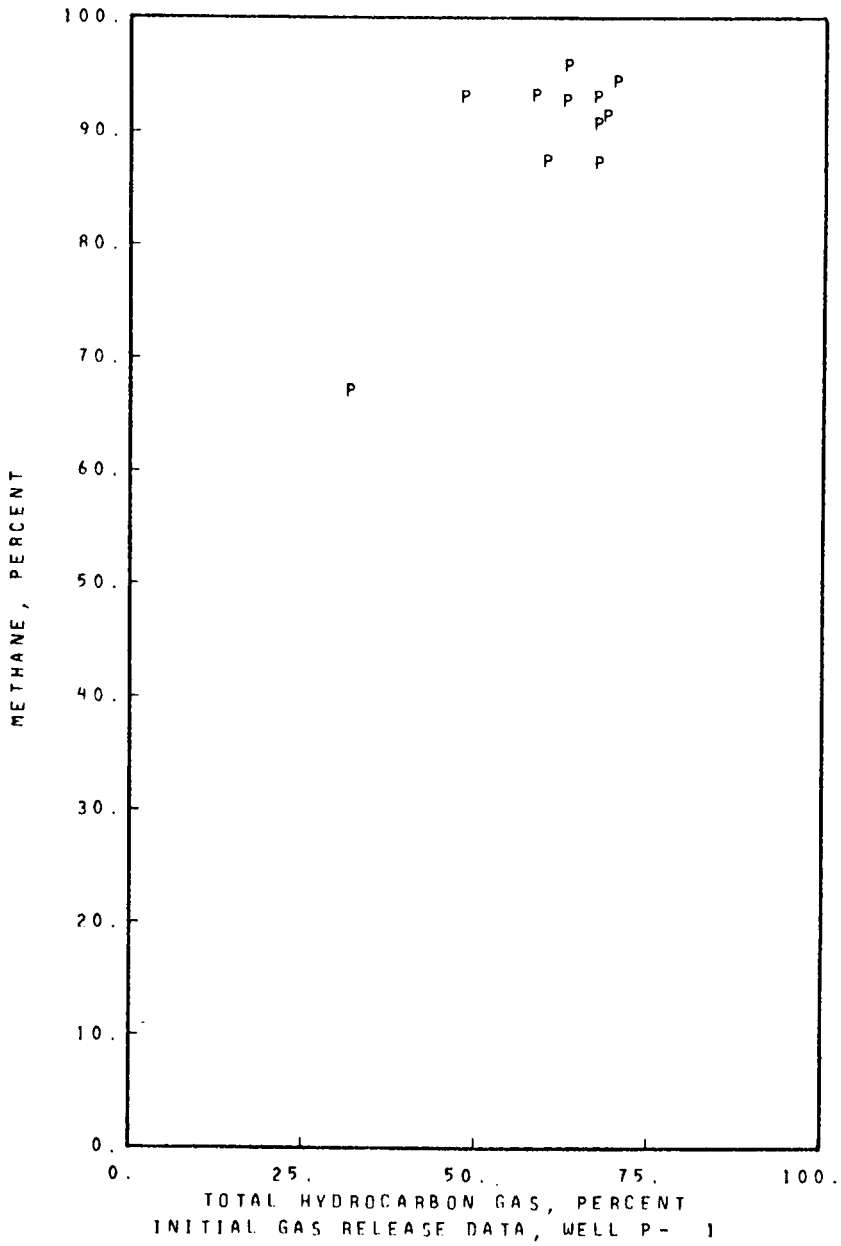
100.
90.
80.
70.
60.
50.
40.
30.
20.
10.
0.
METHANE, PERCENT
0.
25.
50.
75.
100.
TOTAL HYDROCARBON GAS, PERCENT
INITIAL GAS RELEASE DATA, WELL P- 1

FIGURE 6.

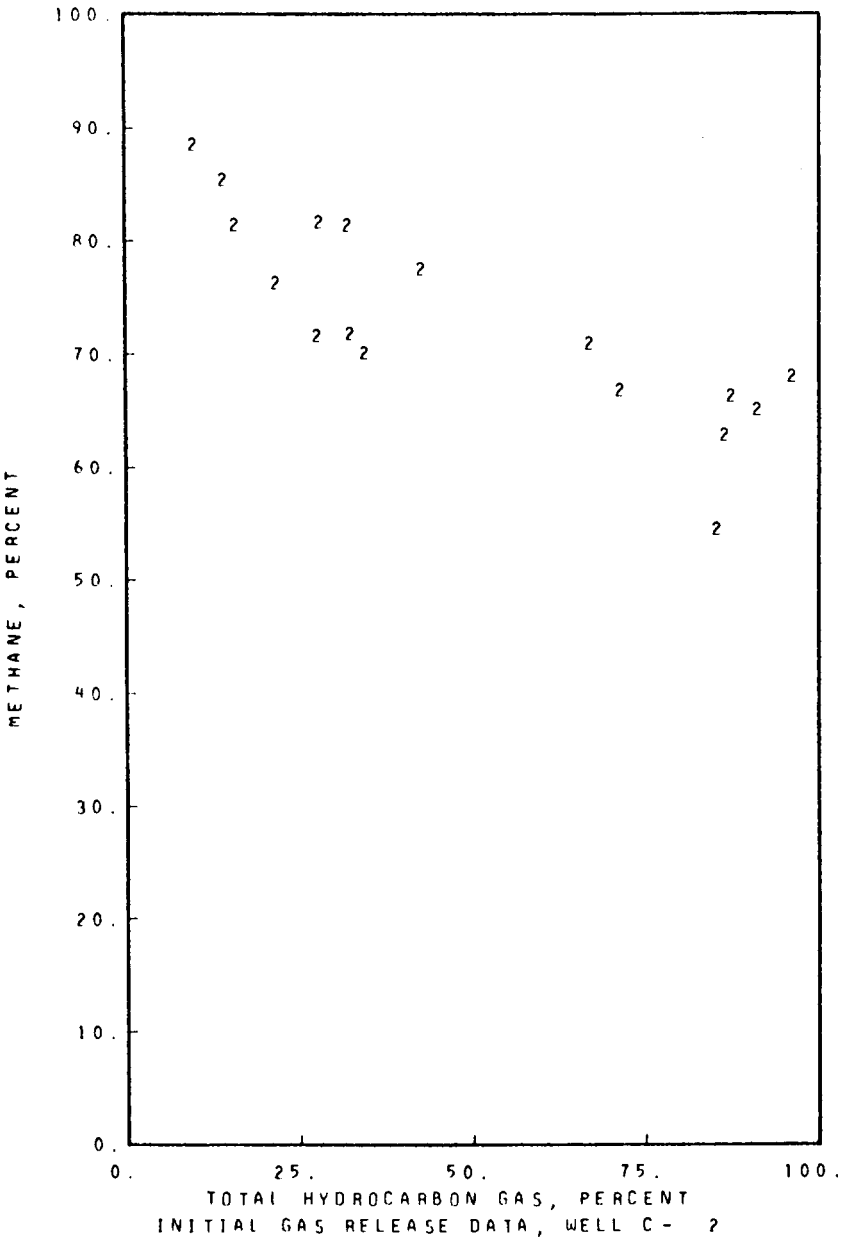
100.
90.
80.
70.
60.
50.
40.
30.
20.
10.
0.
METHANE, PERCENT
0.
25.
50.
75.
100.
TOTAL HYDROCARBON GAS, PERCENT
INITIAL GAS RELEASE DATA, WELL C- 2

FIGURE 7.

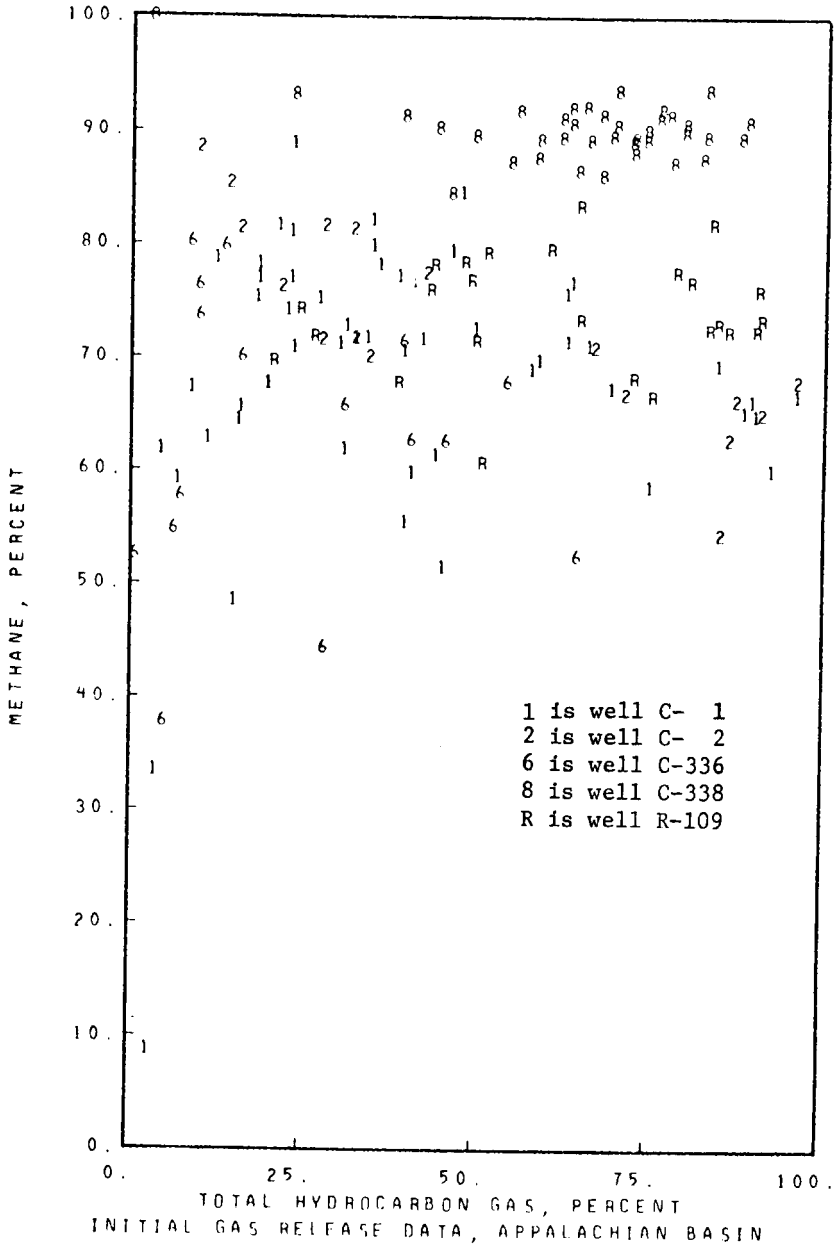
METHANE, PERCENT
100.
90.
80.
70.
60.
50.
40.
30.
20.
10.
0.
0.
25.
50.
75.
100.
TOTAL HYDROCARBON GAS, PERCENT
INITIAL GAS RELEASE DATA, APPALACHIAN BASIN
1 is well C- 1
2 is well C- 2
6 is well C-336
8 is well C-338
R is well R-109

FIGURE 8.

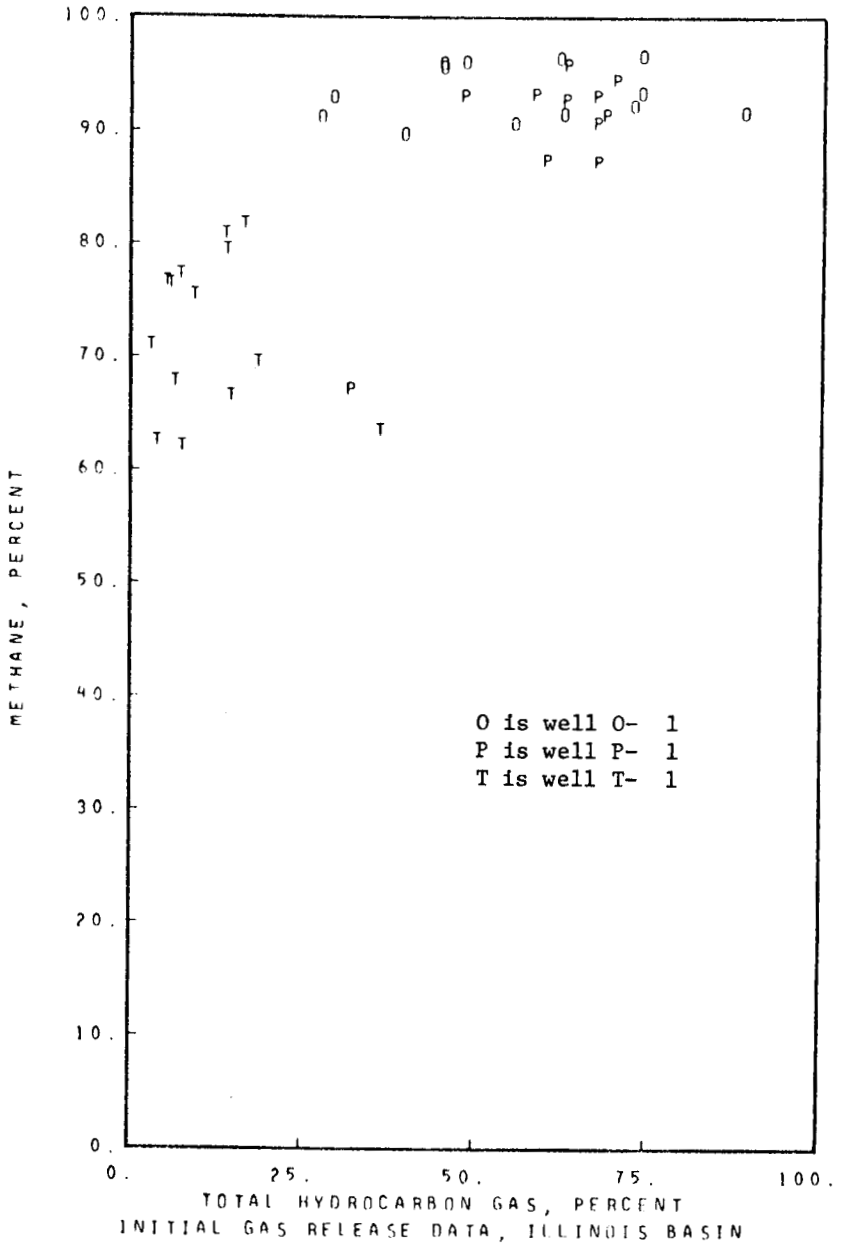
100.
90.
80.
70.
60.
50.
40.
30.
20.
10.
0.
0.
25.
50.
75.
100.
METHANE, PERCENT
TOTAL HYDROCARBON GAS, PERCENT
INITIAL GAS RELEASE DATA, ILLINOIS BASIN
O is well O- 1
P is well P- 1
T is well T- 1

FIGURE 9.

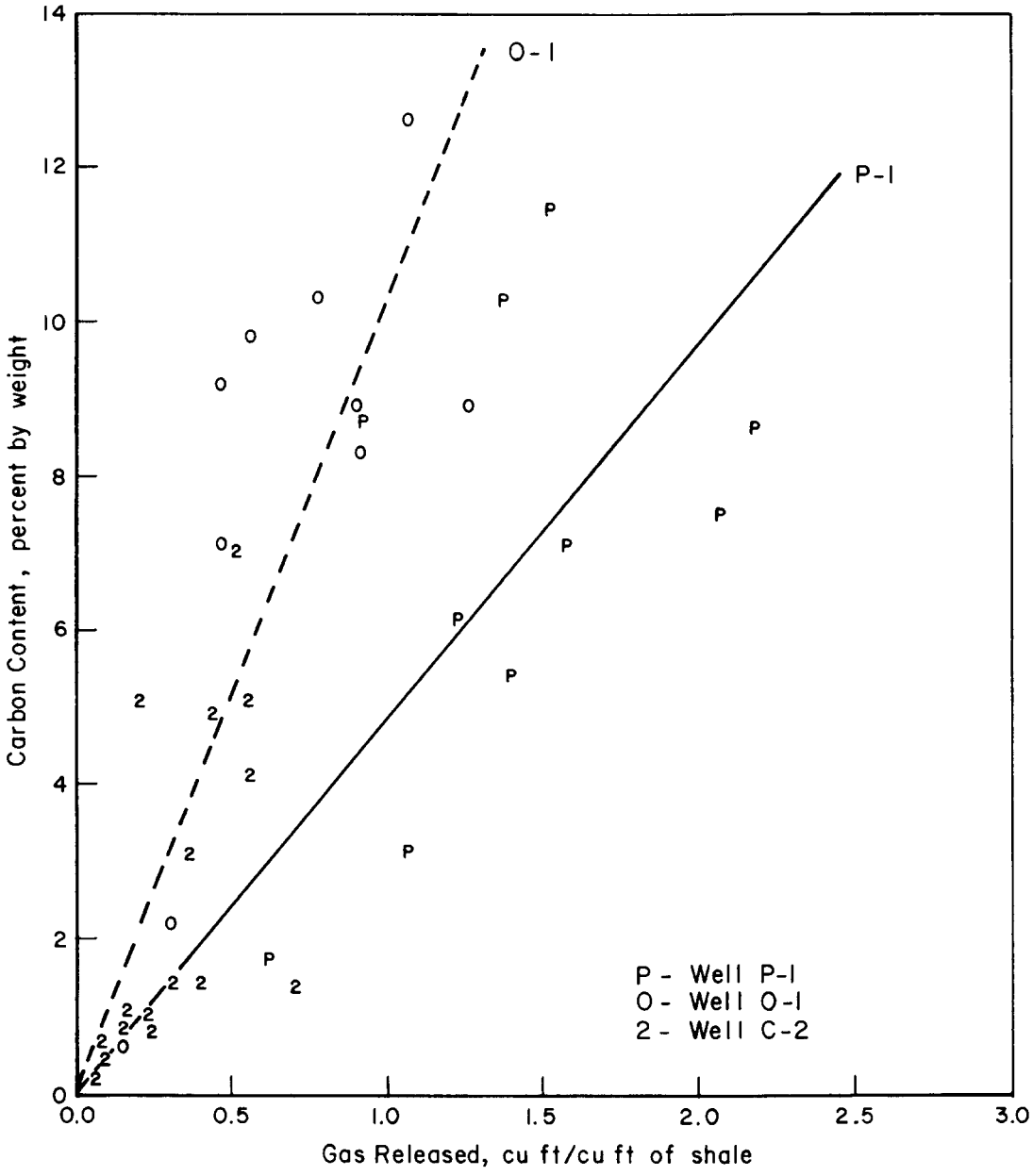
O-1
P-1
Carbon Content, percent by weight
Gas Released, cu ft/cu ft of shale
P - Well P-1
O - Well O-1
2 - Well C-2
0
2
4
6
8
10
12
14
0.0
0.5
1.0
1.5
2.0
2.5
3.0

FIGURE 10.

GEOCHEMICAL CHARACTERIZATION OF DEVONIAN GAS SHALE

RONALD E. ZIELINSKI
MONSANTO RESEARCH CORPORATION*
MOUND FACILITY
MIAMISBURG, OHIO 45342

ABSTRACT

Detailed geochemical analyses are being used to provide an accurate assessment of the oil and gas resources present in the Devonian shales in the Appalachian and Illinois Basins. The suite of geochemical analyses is designed to evaluate the organic richness, the hydrocarbon potential, the type of organic matter and the thermal maturity of the organic matter.

Laboratory techniques such as pyrolysis gas chromatography and mass balance thermal extraction were also employed to measure thermally derived oil and gas yields from the Devonian shales.

Stable carbon isotope geochemistry has also been initiated. The first phase of this study involved the determination of stable carbon isotope values for shale core samples.

*Mound Facility is operated for the U. S. Department of Energy by Monsanto Research Corporation (Contract No. EY-76-C-04-0053).

INTRODUCTION

Core samples from seven wells drilled in Illinois, Indiana, Kentucky and Virginia have been analyzed geochemically for the purpose of assessing their fossil energy resource potential. Organic geochemical data have been obtained for a better definition of the oil and gas contained in the Devonian shales.

The hydrocarbon source potential of fine-grained sediments from various worldwide locations has been studied by many researchers [1,2]. The hydrocarbon source rock studies were performed to investigate the organic richness, type (oil, condensate or gas), and state of thermal maturity of the hydrocarbon source rocks, and to determine their areal and stratigraphic distribution.

The location of the seven wells is displayed in Figure 1. In most cases, the entire stratigraphic unit of Devonian shale was cored. Samples for geochemical analyses were taken at 30-foot intervals and stored in air-tight metal containers. Shortly after arrival at the laboratory, the containers air space was sampled for methane to heptane hydrocarbons. The container was opened and additional geochemical analyses were performed.

TECHNIQUES

The geochemical analyses performed on the Devonian shale samples are shown in Figures 2A and 2B. The abundance of methane through heptane hydrocarbons (C_1-C_7) was measured by summing the contents of the air space and core material stored in an air-tight container. Organic carbon was analyzed by combustion of the carbonate-free sediment. The kerogen was examined visually for morphological classification after being isolated from the inorganic matrix. Dried core material was crushed and extracted with a benzene-methanol solvent. The soluble extract was weighed, then separated into fractions by adsorption and liquid chromatography. The normal paraffin distribution was determined by gas chromatography. Vitrinite reflectance was measured using modifications of procedures described by Landes[3], and Hacquebord and Donaldson[4].

The pyrolysis gas chromatography involves the heating of a powdered sample of core material at a constant rate. The hydrocarbons produced during the pyrolysis process are analyzed using a flame ionization detector (FID) gas chromatograph.

The material balance assay is performed in a closed system under a cover of either helium or nitrogen. The condensable hydrocarbons formed during the pyrolysis process are collected along with water in a sidearm collector. The noncondensable products are carried over into a gas collection bottle. Following the pyrolysis event, the gaseous, liquid and solid products are characterized by additional analyses.

The stable carbon isotope studies performed to date have been performed only on the organic portion of the shale core. Prior to analysis, the inorganic carbon was removed by acidification.

DISCUSSION AND RESULTS

Abundance of C_1-C_7 Hydrocarbons

Gas and gasoline-range hydrocarbons are generated from organic matter at different levels of thermal maturity. Initially, at low temperature, microbial degradation forms methane or "dry" gas. With increasing time, temperature, and depth of burial, heavier hydrocarbons are generated. In the early stages of petroleum formation, gas-oil range hydrocarbons predominate with associated amounts of "wet" gas (C_2-C_4 hydrocarbons) and gasoline-range hydrocarbons. The content and distribution of C_1-C_7 hydrocarbons is primarily dependent on three geochemical parameters; namely, the organic richness, the type of organic matter, and its level of thermal maturity.

Shales from each of the wells analyzed to date, contained large quantities of C_1-C_7 hydrocarbons (Figure 3). The average C_1-C_7 values are listed in Table 1. For the I-1, O-1, P-1 and VA-1 wells, the dry gas, wet gas and gasoline-range hydrocarbons were uniformly distributed. The gas-

oline-range hydrocarbons in VA-1 are exceptionally low, but the lithology of the samples from this well indicated that coal was present in most of the samples. In the KY-2 well, however, the hydrocarbons varied significantly throughout the entire well profile. Also listed in Table 1 are the values of C_1-C_7 hydrocarbons released to the headspace of the sample canisters. These values indicate that most of the C_1-C_4 hydrocarbons are released from the samples and are not retained in the matrix. For well O-1, however, this was not true. Other investigators[5] have indicated that samples from well O-1 contain ultramicroporous networks which inhibit the diffusion of hydrocarbon gases from the material.

The hydrocarbon concentrations listed in Table 1 are minimum values. The core samples are removed from the well and are exposed to the atmosphere for approximately 1 to 2 hours prior to being stored in the sample containers. This exposure time allows a significant amount of hydrocarbon gases to diffuse from the core. Although for most samples, the maximum exposure time is 2 hours, the P-1 samples were exposed to air for several weeks prior to canning for geochemical analysis.

Organic Carbon

The organic carbon content of fine-grained argillaceous sediments such as the Devonian shales is an indicator of organic richness. Organic matter comprised mostly of organic detritus is preserved by rapid burial. Alteration processes such as microbial degradation and thermal diagenesis transform the organic matter to the complex heterogeneous material called "kerogen." Kerogen is presumed to be the major precursor for oil and gas. As the sediments become thermally matured, oil and gas are generated. The amount of kerogen, expressed as the organic carbon content, shows the abundance of organic matter which may be altered to form hydrocarbons. The lower limit of organic carbon in shales from productive basins is 0.4 percent[6]. The worldwide average of organic carbon in shales and siltstones is 1.14 percent[7].

The amount of organic carbon in Devonian shales varies from location to location (Figure 4). In general, the average organic carbon content of sediments from the I-1, O-1, P-1, KY-2 and VA-1 wells is 6.77, 8.75, 4.73, 2.04, and 1.96 percent, respectively. The organic matter appears to be more uniformly distributed in the I-1, O-1 and P-1 wells. However, to the east, the KY-2 and VA-1 shales vary considerably in organic carbon from a low of 0.16 to a high of 7.75 percent.

Using the average organic carbon contents and the Mott Factor (1350 ft^3-gas/ton of organic matter), the predicted indigenous gas per unit volume (1 mile x 1 mile x 1000 feet) can be calculated. The existing indigenous gas can also be calculated using the experimentally determined average C_1-C_4 hydrocarbon contents. The results of these calculations are shown in Table 2. The existing indigenous gas values are very conservative. This conservatism is the result of the previously discussed loss of hydrocarbon during sample preparation at the well site. If the values were also corrected for downhole pressure and temperature they would be significantly higher.

Type of Organic Matter

The solid organic matter contained in fine-grained sediments visually reflects its source of deposition. Composed mostly of organic detritus, the kerogen is related to its depositional environment by the proportions of marine and continental organic matter it contains. Kerogen identified visually can be classified as amorphous, herbaceous, woody, or coaly (inertinite). After maturation by thermal diagenesis, the marine (amorphous) type is prone to generate abundant gaseous and liquid hydrocarbons. The nonmarine (woody-coaly) type is prone to produce mostly gaseous hydrocarbons[8,9].

Of the five wells completed to date, the type of organic matter in the I-1, O-1 and P-1 wells is primarily herbaceous and amorphous kerogen (Figure 5). This liquid rich material (if present in sufficient quantities) has the potential to generate abundant oil and associated gas. In contrast, shales from the KY-2 well contain predominant amounts of either the herbaceous-amorphous kerogen or the woody-coaly kerogen. The VA-1 well contains organic matter that is predominantly herbaceous-woody. The high organic carbon content appears to be associated with the kerogen type. In most cases, the herbaceous-amorphous kerogen is present in shales which contain abundant organic carbon. The shales containing primary or secondary amounts of woody-coaly kerogen are lean in organic matter.

C_{15+} Extract

Core material was extracted with organic solvent to yield the C_{15+} extract or "bitumen." The bitumen is composed of hydrocarbon and nonhydrocarbon material. The bitumen in recent sediments is impoverished in hydrocarbons and contains mostly nonhydrocarbon material. As the sediments become thermally matured, increasing amounts of hydrocarbons are formed. The average worldwide concentrations of hydrocarbons in shales was found to be 96 ppm(7).

Shales from four of the wells were found to contain bitumen composed mostly of hydrocarbons. The distribution of hydrocarbon and nonhydrocarbon material extracted from the Devonian shales is shown in Figure 6. The hydrocarbon portion consists of paraffin-napthene (P-N) and aromatic (AROM) fractions. The nonhydrocarbon material is separated into asphaltene (ASPH) and nitrogen-sulfur-oxygen containing compounds (NSO's). In the I-1, O-1, and P-1 wells, the average hydrocarbon content was 2159 ppm, 2463 ppm, and 3332 ppm, respectively. The average hydrocarbon content was 1469 ppm for the KY-2 shales and approximately zero for the VA-1 shales. The hydrocarbon content appears to be related to the organic carbon content and the kerogen type. In general, shales characterized by herbaceous-amorphous kerogen, and a high organic carbon content contain abundant C_{15+} hydrocarbons. Sediments with low organic carbon content and primary or secondary amounts of woody-coaly kerogen contain low amounts of C_{15+} hydrocarbons.

Thermal History

In order to assess the hydrocarbon generating capacity of potential source rocks, the thermal history and its diagentic effect on petroleum generation must be evaluated. Two methods, kerogen coloration and vitrinite reflectance, were used to measure the thermal alteration of the Devonian shales. The kerogen coloration of the plant cuticle and spore-pollen debris is measured in transmitted light. The state of thermal alteration (Thermal Alteration Index or TAI) ranges from light greenish yellow at Stage 1 for unaltered kerogen to black at Stage 5 for severely altered kerogen. The thermal zone of oil generation corresponds to a moderately mature to mature kerogen of Stage 2 to 3 (Figure 7). The kerogen in the zone of oil generation is characterized by yellow-orange to light brown color. Vitrinite reflectance (R_o) is also used to measure the degree of thermal alteration. This technique has several advantages over other thermal maturation classifications. It is an absolute measurement; it is a rigorous analytical evaluation; and it is a universally accepted technique. R_o values ranging from 0.2 to 0.6 indicate that the sediments are too immature for oil generation. The zone of petroleum generation is usually interpreted to range from 0.6 to 1.2. R_o from 1.2 to 3.0 indicate a thermal history sufficient to form wet gas and methane. The severely altered or metamorphised organic matter represented by R_o values greater than 3.0 is considered as a nonsource for hydrocarbons.

The thermal history of the Devonian shales analyzed in this study exhibit a small amount of variation (Figure 8). The organic matter in shales from the five wells is characterized by its yellow to orange-brown color. This coloration is consistent with a thermal alteration index of Stage 1+ to 3-. The average value of Stage 2 corresponds to a thermal history equal to the early stages of petroleum generation. The mean average vitrinite reflectance value in both the I-1 and O-1 wells is 0.45. In the P-1 well, a slightly higher value of 0.50 was measured. The value for KY-2 was 0.52, while that for VA-1 approached 1.0. Based on the vitrinite reflectance date, it appears likely that the Devonian shales will be increasingly more mature in an east-south easterly direction.

Material Balance Assay

Material Balance Assays (MBA's) are being performed on all the geochemical samples. For the assays approximately 100 grams of well-riffled, representative 4 to 8 mesh material are heated and destructively distilled at a maximum temperature of 500°. The assay is performed in a closed system and either helium or nitrogen is used as the flush gas. Oil and water are condensed in a centrifuge tube and noncondensable gases flow into an evacuated receiver. Following the pyrolysis process, the products are weighed and further analyzed.

The analyses performed on the pyrolysis products include oil, gas and water yield; gas compositional analysis; detailed oil and water analysis; percent post-assay organic carbon; and percent ash. These studies are designed to correlate the geochemical analyses with pyrolysis yield.

The average MBA product yields obtained to date are shown in Table 3. Table 4 lists the average gas analyses obtained for the samples from the three wells. These data support the previously determined geochemical data which indicated that the samples from the O-1 and I-1 wells would yield more hydrocarbon products than the samples from KY-2. The MBA of the KY-2 well samples also exhibited the same variations that characterized the other geochemical analyses. This is best indicated by the oil yields which varied from 0.1 to 4.6 gal/ton.

The other analyses are currently in progress on these samples, but a preliminary analysis of the oil product from the O-1 well produced the results shown in Table 5.

Pyrolysis-Gas Chromatography

To date, core samples from the I-1 well and the P-1 well have been analyzed by pyrolysis gas chromatography. Approximately 100 mg. of powdered sample was heated under helium from ambient temperature to 550°C at a constant rate of 30°C/min. The heating of the organic matter in the shale produces hydrocarbons which are swept by the carrier gas to a flame ionization detector. The amount of hydrocarbons generated vs. the temperature of generation is displayed on a recorder. The areas under the curves are computed by a digital integrator. The test data are listed in Table 6 and 7, and are shown in Figures 9 and 10.

A preliminary evaluation of the pyrolysis data from the analysis of I-1 and P-1 samples shows the following.

1. The total hydrocarbon yield is directly proportional to the C_{15+} bitumen concentration and the organic carbon content.

2. The total amount of organic carbon available for hydrocarbons is less than the total organic carbon.

3. The Fischer Assay oil yields calculated by this method are similar to the yields obtained by the modified material balance method.

4. In order to obtain optimum hydrocarbon yields during the gas production of these shales, a heating process will be required not only for extraction, but also for pyrolytic cracking.

Stable Carbon Isotope Geochemistry

Samples of shale core from five wells have been analyzed by mass spectrometry for stable carbon isotope values. Prior to analysis, the inorganic carbon was removed by acidification. The total organic carbon was converted to CO_2 and its delta^{13}C was measured relative to PDB. The delta^{13}C results show a strong correlation to the organic matter type. In general, the samples classified as gas prone, restricted marine or nonmarine are characterized by delta^{13}C values ranging from -24.6 to about -28. The oil prone, more marine type of organic matter composed mostly of herbaceous and amorphous kerogen is characterized by isotopically lighter delta^{13}C values (-27 to -31). Four of the five wells have been exposed to a similar thermal history. The organic matter from the VA-1 is more thermally mature (Table 8). Delta^{13}C values from the nonmarine shales (gas prone) from VA-1 appear to be isotopically lighter than the nonmarine shales in the other four wells. Increasing thermal maturation on kerogens of similar type usually produces a kerogen which becomes increasingly heavier relative to $^{13}C/^{12}C$. The data indicate that the opposite effect has taken place, namely the organic matter has become slightly lighter. Previous studies performed on crude oils and kerogens have shown that delta^{13}C values of -23 to -29 are indicative of marine derived organic matter. Values of -29 to -33 usually indicate marine organic matter. The initial results obtained on selected Eastern gas shales seems to show an inverse relationship when compared to previous carbon

isotope studies.

More samples from other wells are currently being analyzed to establish if this inverse relationship does exist and why it does occur. Stable carbon isotope work is also currently in progress on both the C_1-C_7 gas species and the Material Balance Assay oil product.

CONCLUSIONS

The Devonian shales are evaluated as a potential source of oil and gas based upon the type of kerogen present, its degree of thermal alteration, the nature of hydrocarbons which it has been generated and the hydrocarbons produced by pyrolysis. A preliminary evaluation of the geochemical data obtained from the core material seems to indicate that the samples from the western region have the greatest organic richness and contain the more abundant oil prone organic matter. The VA-1 well contained the most C_1-C_4 hydrocarbon gases, a minimum of 46 B Cu.ft./unit volume.

The degree of thermal alteration has been sufficient to initiate the hydrocarbon forming process in the Devonian shales in all the wells examined to date. Shales from the wells in the western region are at approximately the same level of maturation. The shales from the KY-2 and VA-1 wells are slightly more mature.

ACKNOWLEDEMENT

The author wishes to express his sincere appreciation to the staff of GeoChem Laboratories and the Analytical Department at Mound Facility for their high quality results. Special thanks are due to Mr. S. J. Martin of GeoChem Research who made significant contributions to the analyses and interpretations of the data.

REFERENCES

1. Bailey, N. J. L., Evans, C. R., and Milner, C. W. D., "Applying Petroleum Geochemistry to Search for Oil: Examples from Western Canada Basin," Am. Assoc. Petroleum Geologists Bull., 58, 2284-2294, 1974.

2. Welte, D. H., "Petroleum Exploration and Organic Geochemistry," J. Geochem. Explor., 1, 117-136, 1972.

3. Landes, K. K., "Eometamorphism, and Oil and Gas in Time and Space," Am. Assoc. Petroleum Geologists Bull., 51, 828-841, 1967.

4. Hacquebord, P. A., and Donaldson, J. R., "Coal Metamorphism and Hydrocarbon Potential in the Upper Paleozoic of Atlantic Provinces, Canada," Can. J. Earth Sci., 7, 1139-1163, 1970.

5. Thomas, J. and Frost, R. R., "Internal Surface Area and Porostiy in Eastern Gas Shales From the Sorption of Nitrogen, Carbon Dioxide, and Methane - A Status Report," Proceedings of the Third ERDA Symposium on Enhanced Oil and Gas Recovery and Improved Drilling Methods, The Petroleum Publishing Company, Tulsa, Oklahoma, August, 1977.

6. Ronov, A. B., "Organic Carbon in Sedimentary Rock (in relation to the presence of petroleum)," Gokhim., 5, 510-536, 1958.

7. Gehman, H. M., "Organic Matter in Limestone," Geochem. Cosmochim. Acta, 26, 885-897, 1962.

8. Staphin, F. L., "Sedimentary Organic Matter, Organic Metamorphism, and Oil and Gas Occurrence," Bull. Can. Pet. Geol., 17, 47-66, 1969.

9. Tissot, B. et. al., "Influence of Nature and Diagenesis of Organic Matter in Formation of Petroleum," Am. Assoc. Petroleum Geologists Bull., 58, 499-506, 1974.

WELL LOCATIONS

I-1: Effingham County, Illinois
I-2: Henderson County, Illinois
I-3: Tazewell County, Illinois
KY-2: Martin County, Kentucky
O-1: Christian County, Kentucky
P-1: Sullivan County, Indiana
VA-1: Wise County, Virginia

FIGURE 1

MOUND LABORATORY

FLOW DIAGRAM FOR ORGANIC GEOCHEMICAL ANALYSIS

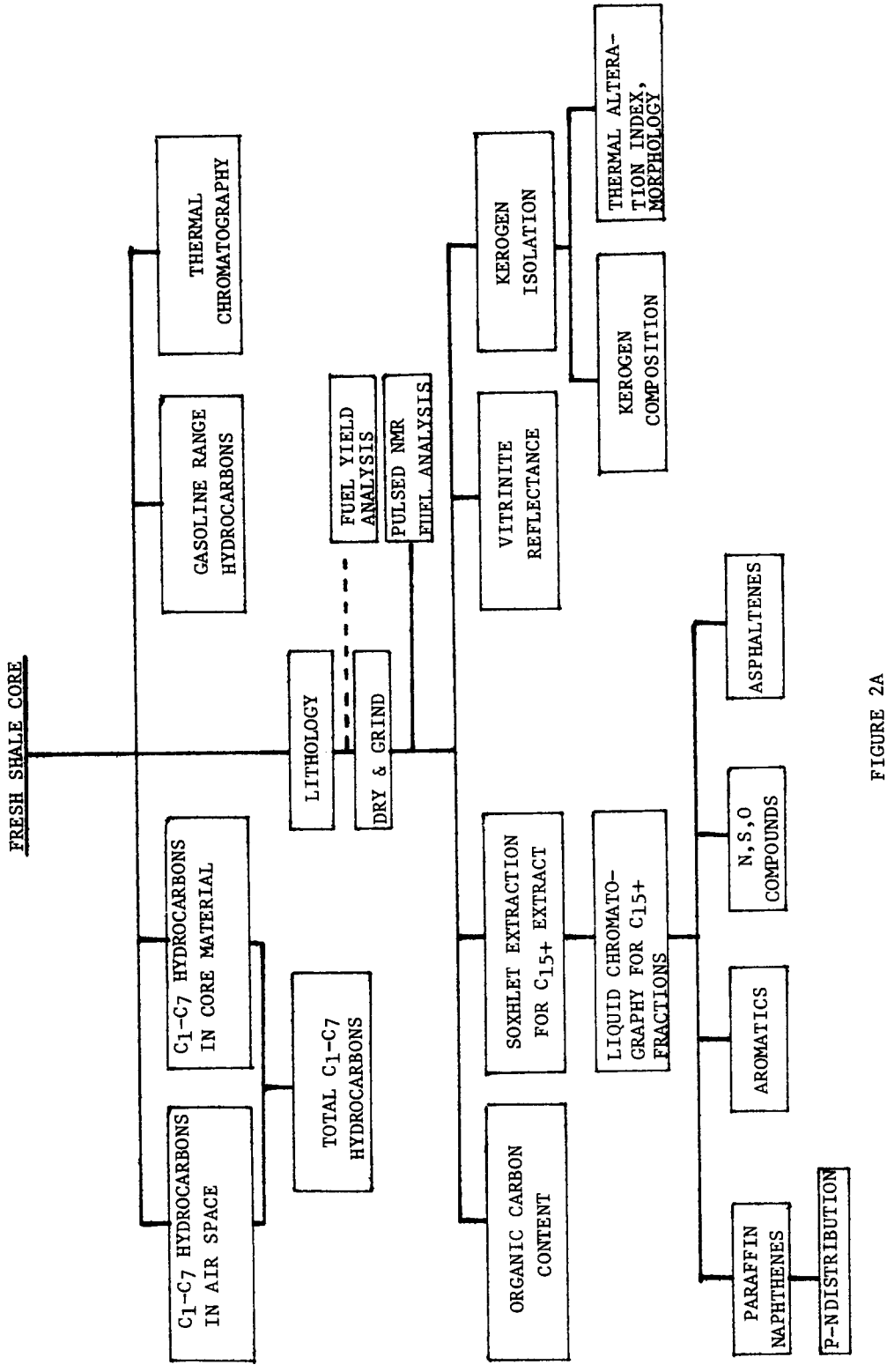

FIGURE 2A

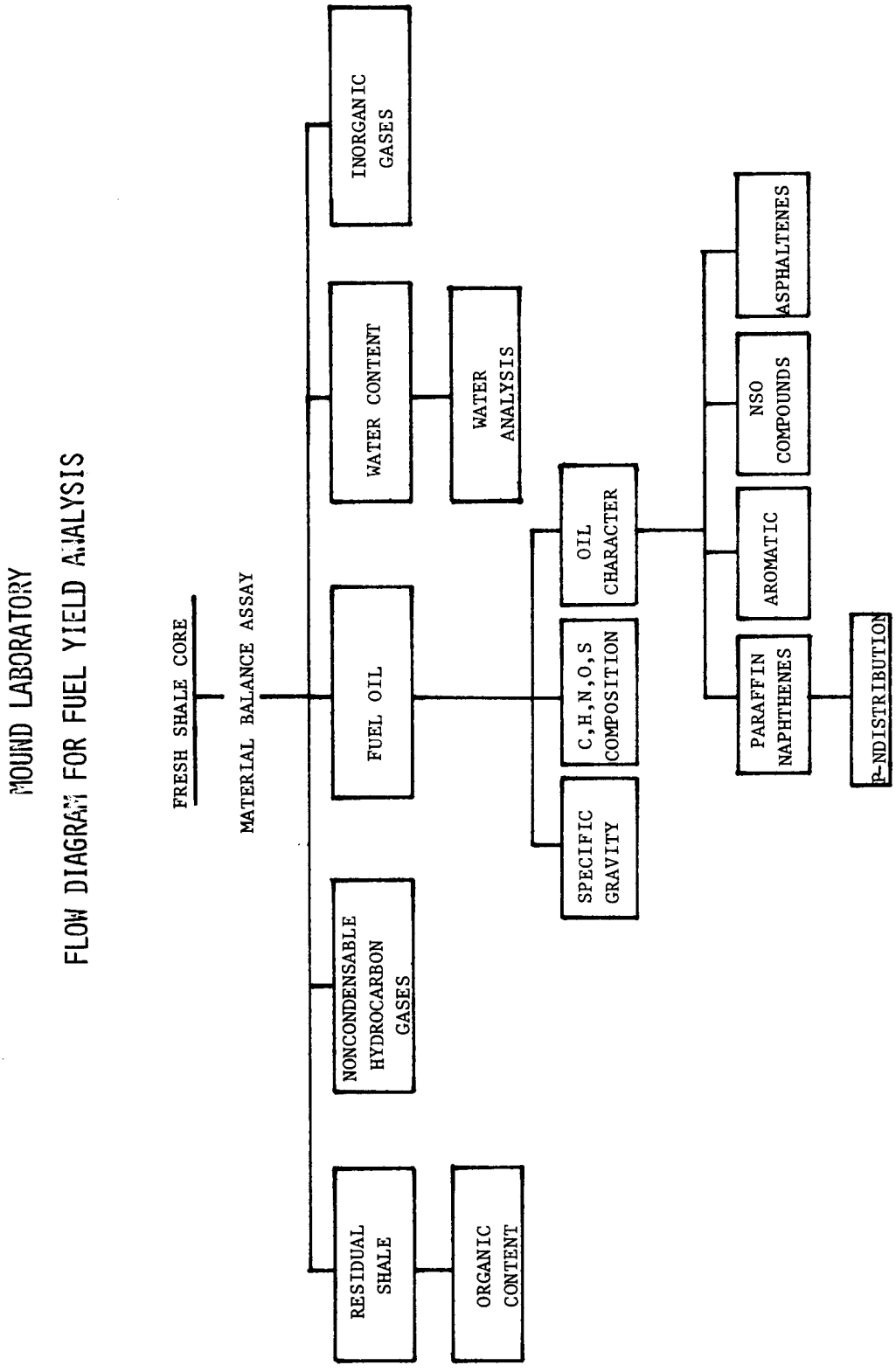
MOUND LABORATORY
FLOW DIAGRAM FOR FUEL YIELD ANALYSIS
FRESH SHALE CORE
MATERIAL BALANCE ASSAY
INORGANIC GASES
WATER CONTENT
WATER ANALYSIS
FUEL OIL
OIL CHARACTER
C,H,N,O,S COMPOSITION
SPECIFIC GRAVITY
ASPHALTENES
NSO COMPOUNDS
AROMATIC
PARAFFIN NAPHTHENES
P-NDISTRIBUTION
NONCONDENSABLE HYDROCARBON GASES
RESIDUAL SHALE
ORGANIC CONTENT

FIGURE 2B

TABLE 1

AVERAGE C_1-C_7 HYDROCARBON ANALYSES

WELL NUMBER:	KY-2	I-1	O-1	VA-1	P-1
$\overline{C_1}$ (PPM) HEAD SPACE	139227	254529	110625	1392646	59989
$\overline{C_1}$ (PPM) HEAD SPACE AND CORE	152049	291438	236505	1415673	70509
% RELEASED TO HEAD SPACE	92	87	47	98	85
$\overline{C_1\text{-}C_4}$ (PPM) HEAD SPACE	235955	338082	150602	1569960	78065
$\overline{C_1\text{-}C_4}$ (PPM) HEAD SPACE AND CORE	313779	433160	311233	1642424	104384
% RELEASED TO HEAD SPACE	75	78	48	96	75
$\overline{C_5\text{-}C_7}$ (PPM) HEAD SPACE	6704	4329	213	32	3809
$\overline{C_5\text{-}C_7}$ (PPM) HEAD SPACE AND CORE	15939	7500	1283	116	6689
% RELEASED TO HEAD SPACE	42	58	17	28	57

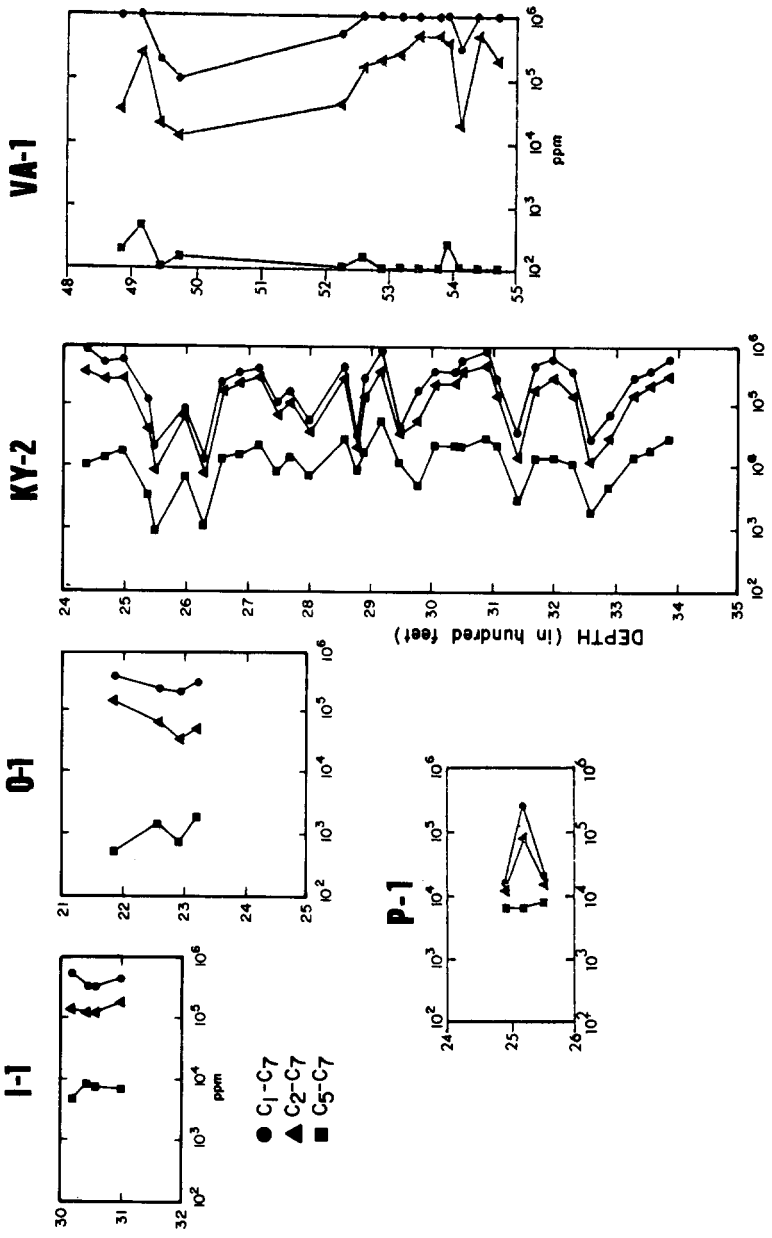

C_1-C_7 Hydrocarbon Data
for Core Samples

FIGURE 3

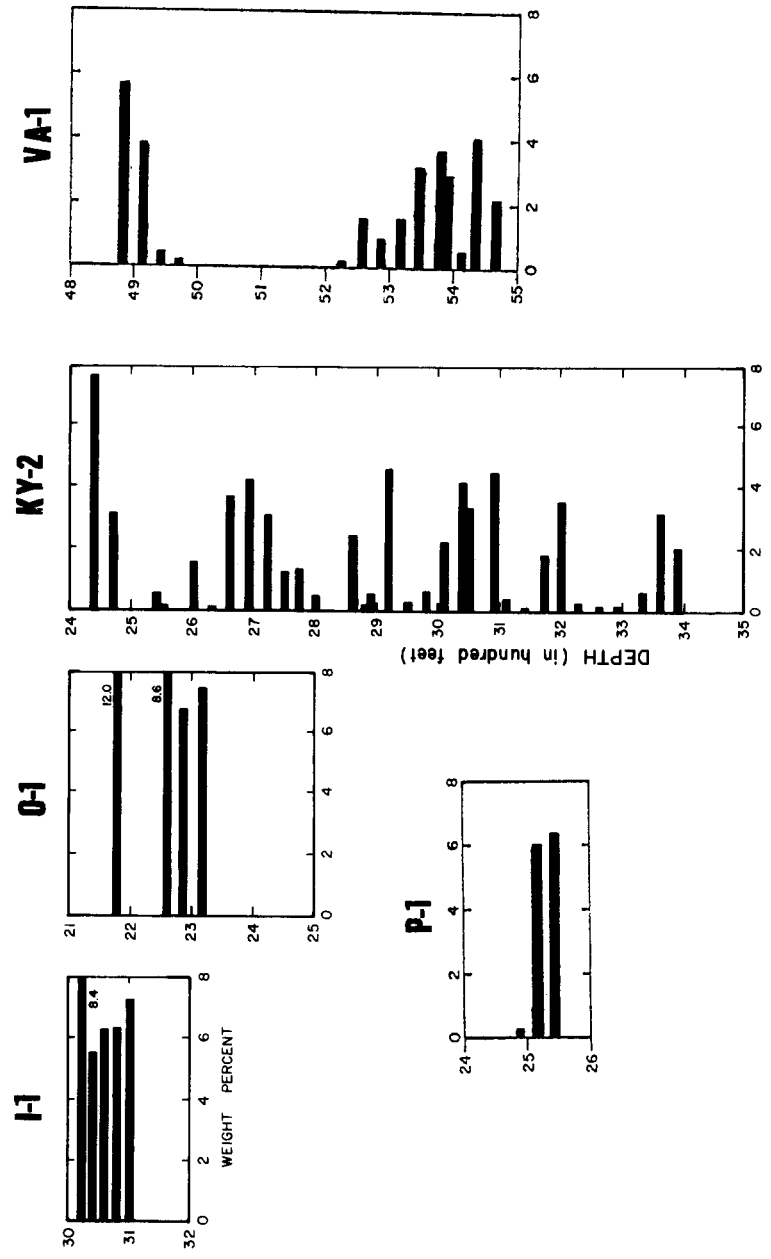

ORGANIC CARBON DATA
FOR CORE SAMPLES

FIGURE 4

TABLE 2

ESTIMATED INDIGENOUS GAS CONTENT

WELL:	I-1	O-1	KY-2	VA-1
PREDICTED INDIGENOUS GAS (B CU. FT./UNIT)	237	306	71	69
EXISTING INDIGENOUS GAS (B CU. FT./UNIT)	12	9	9	46

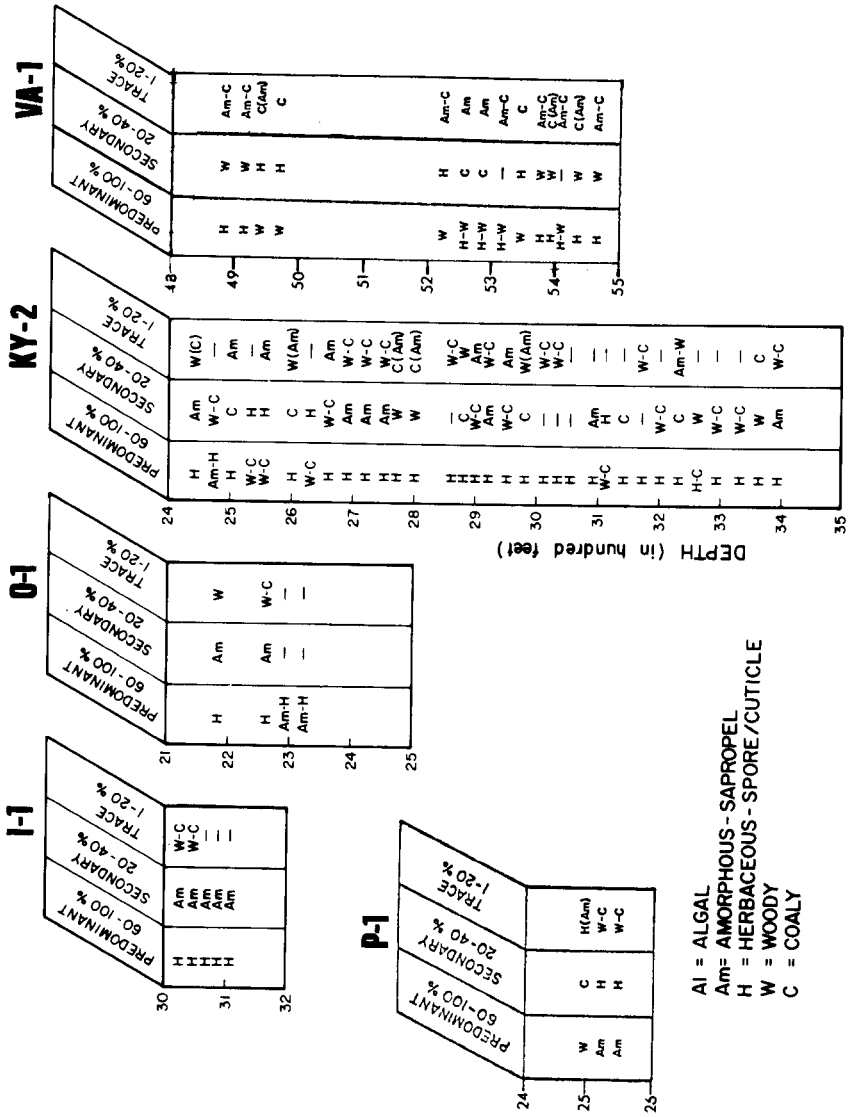

VISUAL KEROGEN DATA
FOR CORE SAMPLES

FIGURE 5

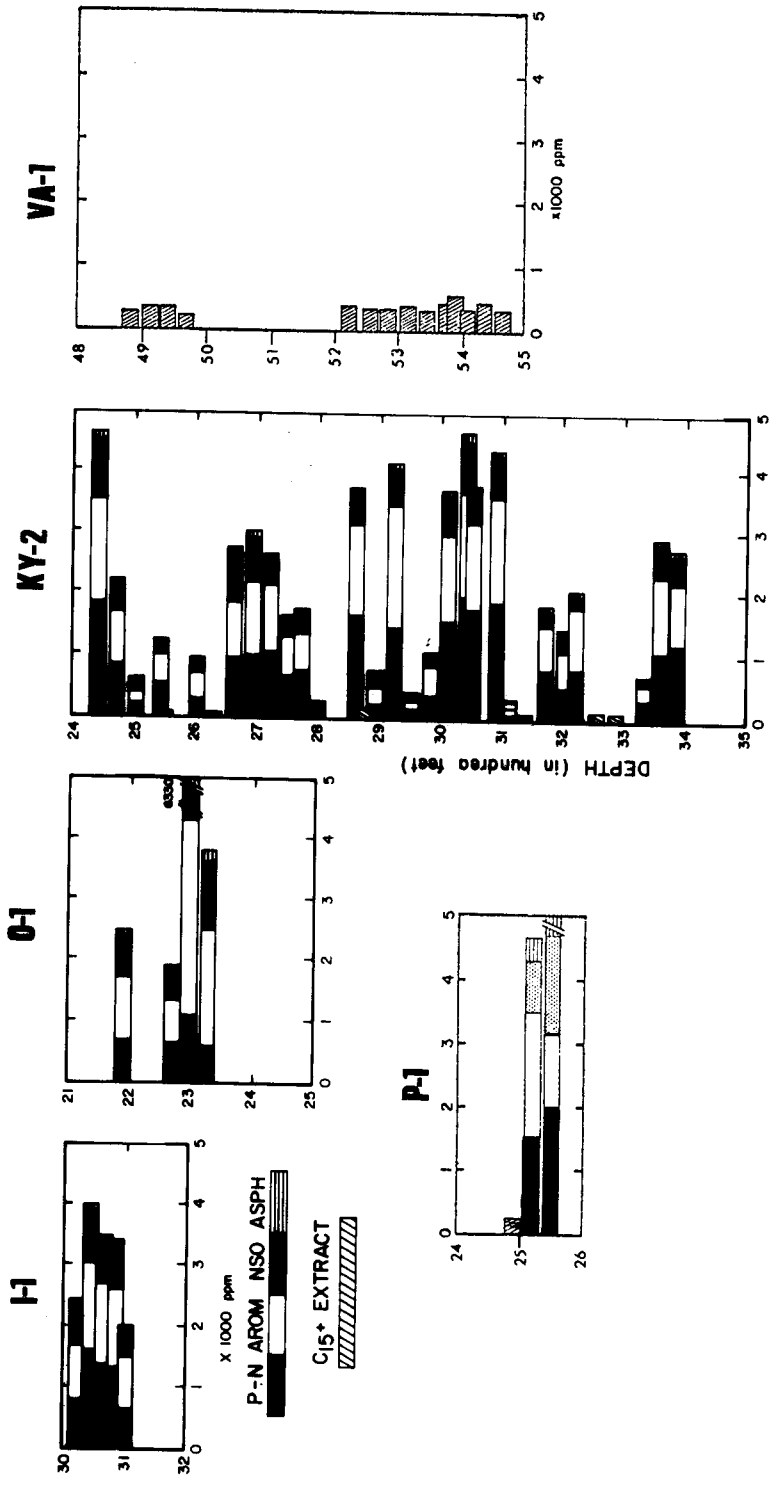

C_{15}^{+} Extract Data
for Core Samples

FIGURE 6

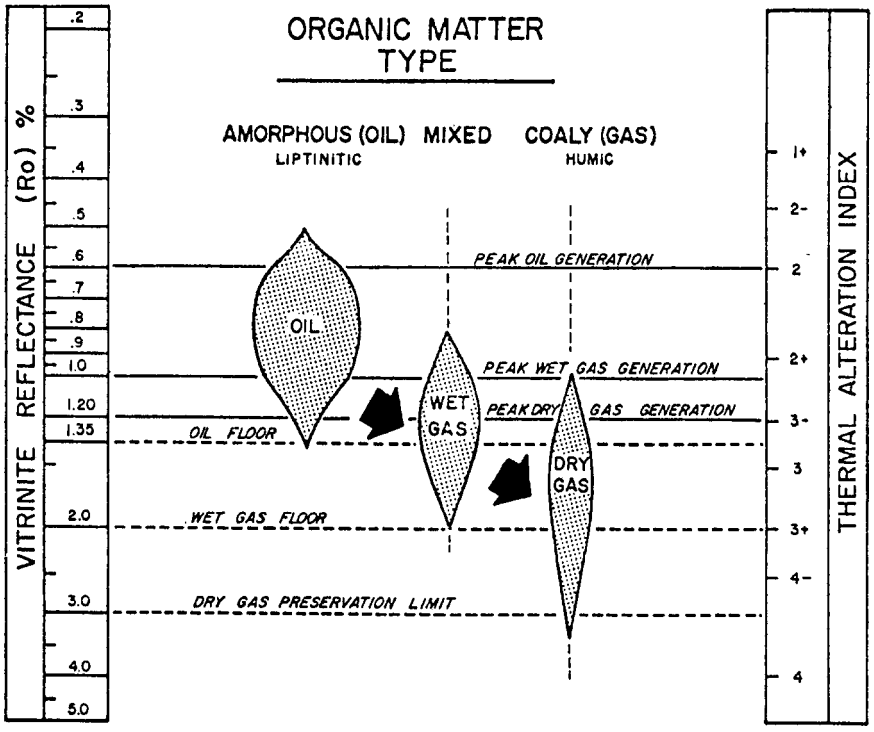
ORGANIC MATTER TYPE
AMORPHOUS (OIL) MIXED COALY (GAS)
LIPTINITIC HUMIC
VITRINITE REFLECTANCE (Ro) %
.2
.3
.4
.5
.6
.7
.8
.9
1.0
1.20
1.35
2.0
3.0
4.0
5.0
PEAK OIL GENERATION
PEAK WET GAS GENERATION
PEAK DRY GAS GENERATION
OIL FLOOR
WET GAS FLOOR
DRY GAS PRESERVATION LIMIT
OIL
WET GAS
DRY GAS
THERMAL ALTERATION INDEX
1+
2-
2
2+
3-
3
3+
4-
4

FIGURE 7

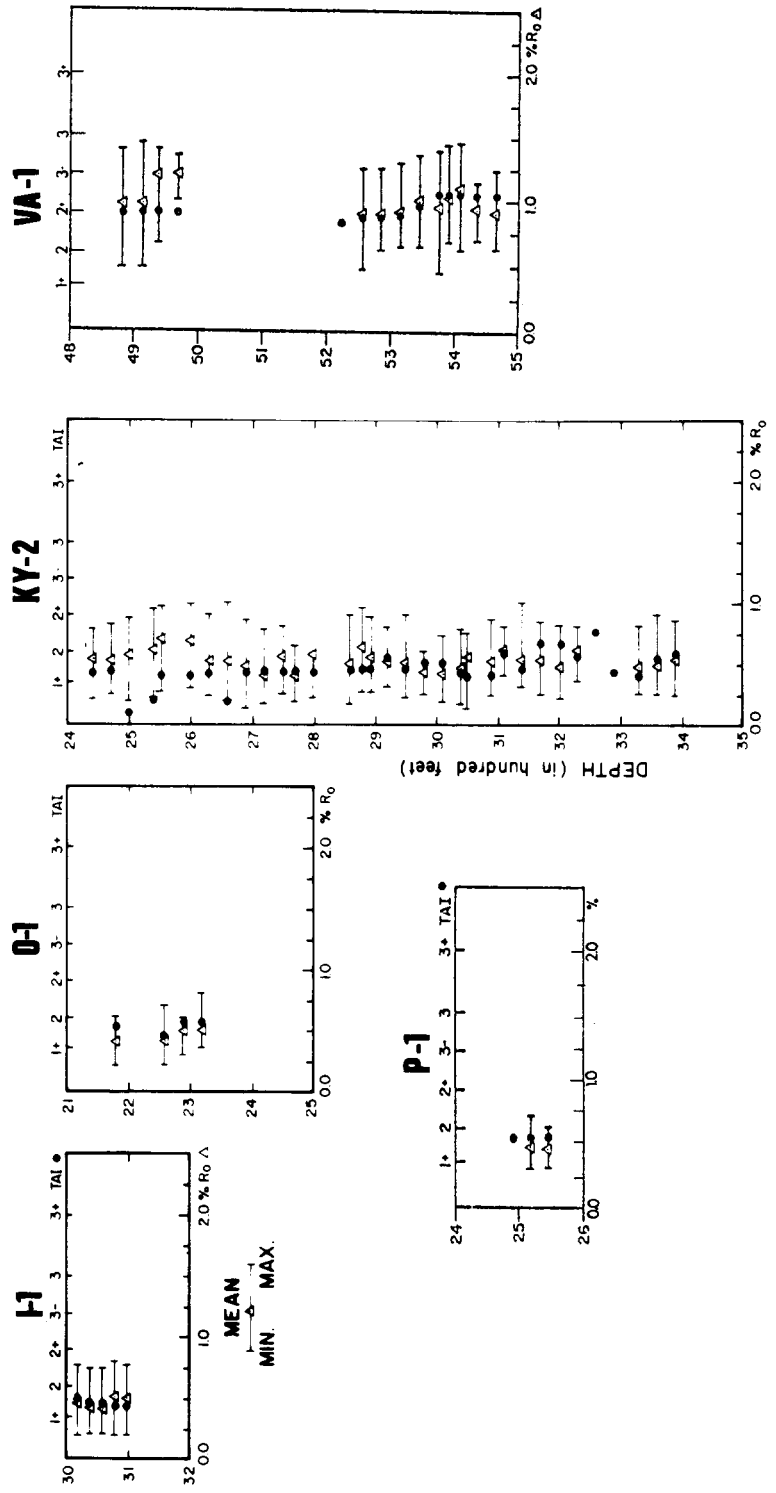

THERMAL ALTERATION INDEX AND VITRINITE REFLECTANCE FOR CORE SAMPLES

FIGURE 8

TABLE 3

MATERIAL BALANCE ASSAY

PRODUCT YIELD

WELL	O-1	I-1	KY-2
OIL YIELD (GAL./TON)	12.75	9.04	1.63
SPECIFIC GRAVITY ($60/60$)	0.910	0.907	0.866
°API-OIL GRAVITY	24	25	32
WATER YIELD (GAL./TON)	2.224	4.134	4.130
PH	9.3	9.2	9.3
HYDROCARBON GAS YIELD ($FT.^3/TON$)	224.33	166.20	31.50

TABLE 4

MATERIAL BALANCE ASSAY

GASEOUS YIELD

WELL	O-1	I-1	KY-2
HYDROCARBONS (CM^3/G)			
METHANE	3.577	2.798	0.580
ETHANE	1.191	0.649	0.177
ETHYLENE	0.208	0.147	0.023
PROPANE	0.594	0.477	0.090
PROPYLEN	0.309	0.241	0.043
I-BUTANE	0.048	0.046	0.013
N-BUTANE	0.267	0.261	0.049
BUTENE-1	0.135	0.103	0.017
T-BUTENE-2	0.041	0.033	0.015
C-BUTENE-2	0.027	0.022	0.016
I PENTANE	0.037	0.045	0.018
N-PENTANE	0.105	0.117	0.019
PENTENE-1	0.035	0.036	0.005
NON-HYDROCARBONS (CM^3/G)			
HYDROGEN	2.747	3.129	0.638
HYDROGEN SULFIDE	4.917	4.275	1.389
CARBON MONOXIDE	0.133	0.152	0.017
CARBON DIOXIDE	1.277	2.030	1.316

TABLE 5

ANALYSIS OF PYROLYSIS OIL

FROM WELL O-1

C_{15}+ OIL COMPOSITION

HYDROCARBONS	
PARAFFIN-NAPHTHENE (P-N)	19.6%
AROMATIC (AROM)	32.0%
NON-HYDROCARBONS	
ASPHALTENE (ASPH)	5.5%
ELUTED NSO	24.6%
NON-ELUTED NSO	18.3%

DETAILED COMPOSITION OF C_{15}+ P-N HYDROCARBONS

NC_{15}	7.2%
NC_{16}	15.5%
NC_{17}	18.4%
NC_{18}	16.6%
NC_{19}	13.1%
NC_{20}	10.0%
NC_{21}	7.1%
NC_{22}	4.7%
NC_{23}	3.4%
NC_{24}	2.2%
NC_{25}	1.2%
NC_{26}	0.5%
NC_{27}	0.0%
% NORMAL PARAFFIN	7.9%
% NAPHTHENE	92.1%

TABLE 6

PYROLYSIS - GAS CHROMATOGRAPHY

I-1 WELL - EFFINGHAM COUNTY, ILLINOIS

Depth	3023'	3044'	3057'	3075'	3099'
Total Hydrocarbon Yield (ppm)	49015	34171	34077	38833	39783
Gallons Per Ton	13.05	9.10	9.08	10.34	10.59
Peak I					
Temperature (°C)	272°	242°	200°	260°	--
Percent of Hydrocarbons	7.2%	8.4%	10.3%	7.7%	6.0%
Concentration (ppm)	3511	2883	3521	2985	2391
Peak II					
Temperature (°C)	450°	458°	498°	461°	470°
Percent of Total Hydrocarbons	92.8%	91.6%	89.7%	92.3%	94.0%
Concentration	45504	31288	30556	35848	37392

TABLE 7

PYROLYSIS - GAS CHROMATOGRAPHY

P-1 WELL - SULLIVAN COUNTY, INDIANA

Depth	2492'	2521'	2549'
Total Hydrocarbon Yield (ppm)	605	35115	37779
Gallons Per Ton	0.16	9.35	10.06
Peak I			
Temperature (°C)	290°	--	266°
Percent of Total Hydrocarbons	63.1%	10.3%	11.2%
Concentration (ppm)	382	3624	4239
Peak II			
Temperature (°C)	455°	464°	470°
Percent of Total Hydrocarbons	36.9%	89.7%	88.8%
Concentration (ppm)	223	31491	33540

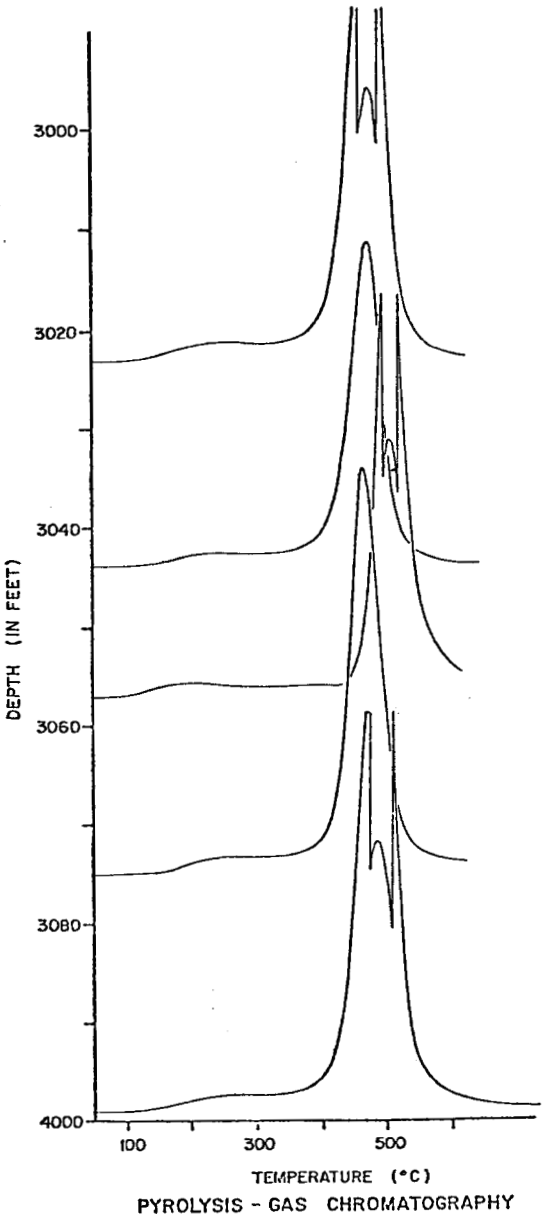
3000
3020
3040
3060
3080
4000
DEPTH (IN FEET)
100
300
500
TEMPERATURE (°C)
PYROLYSIS - GAS CHROMATOGRAPHY
WELL I-1

FIGURE 9

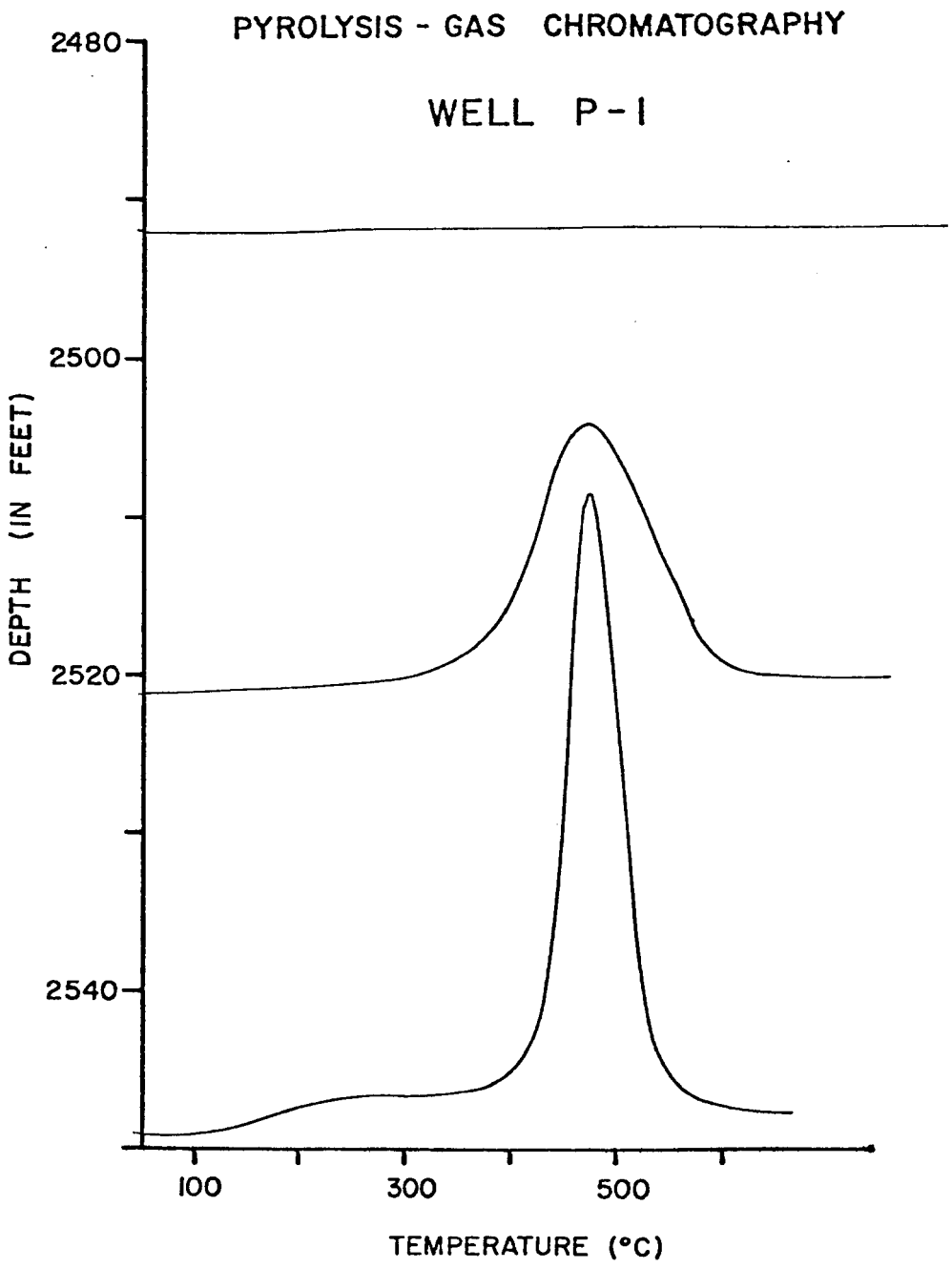
PYROLYSIS - GAS CHROMATOGRAPHY
WELL P-1
2480
2500
2520
2540
DEPTH (IN FEET)
100
300
500
TEMPERATURE (°C)

FIGURE 10

TABLE 8

DELTA^{13}C OF ORGANIC CARBON IN WHOLE ROCK

WELL	DEPTH	ORGANIC MATTER TYPE*	DELTA^{13}C PDB OF ORGANIC CARBON IN WHOLE ROCK
KY-2	2443'	H;Am;W(C)	-30.2
	2535'	W-C;H;-	-27.5
	2715'	H;Am;W-C	-30.0
	3085'	H;Am;-	-28.9
	3288'	H;W-C;-	-26.7
VA-1	4885'	H;W;Am-C	-27.9
	4945'	W;H;C(Am)	-25.6
	5319'	H-W;-;Am-C	-28.1
	5393'	H;W;C(Am)	-29.3
	5469'	H;W;Am-C	-28.7
P-1	2492'	W;C;H(Am)	-24.6
	2549'	Am;H;W-C	-28.0
O-1	2184'	H;Am;W	-31.6
	2317'	Am-H;-;-	-30.3
I-1	3044'	H;Am;W-c	-29.0
	3075'	H;Am;-	-28.9

*Organic Matter Type

Marine	Al	=	Algal
Marine	Am	=	Amorphous
Restricted Marine	H	=	Herbaceous
Nonmarine	W	=	Woody
Nonmarine	C	=	Coaly (Inertinite)

STRUCTURAL CHARACTERIZATION OF BITUMEN AND KEROGEN FROM DEVONIAN SHALE

T. F. Yen, C. S. Wen, J. I. S. Tang, J. T. Kwan, D. K. Young, and Edith Chow

University of Southern California
University Park, Los Angeles 90007

ABSTRACT

Both the bitumen and kerogen concentrates from a Cottageville Devonian Marine shale core sample have been isolated. The bitumens are further fractionated into hydrocarbons, polar resins, and asphaltic material. Each fraction has been individually characterized. Carbon preference index (CPI) was used as a parameter for the correlation of the maturation of shales. The structure of kerogen has been elucidated by physical as well as chemical methods. The molecular structure was compared with that of the lacustrine shale of the Green River Formation.
(Supported by ERDA-MERC under contract no. EY-77-9-21-8104)

INTRODUCTION

The study of the organic components of the gas- and oil-bearing shale is essential, since both the bitumen (solvent extractable) and the kerogen (insoluble) play an important role in exploration as well as production. We have recently studied the cored sample of the Devonian series from wells near Cottageville in Jackson County, West Virginia. The sample represents both Zone II and Zone III of the Brown Shale which includes the Hampshire and Chemung Groups as well as the Marcellus shale. Cored wells with depth of ca. 3400-3800 ft. are numbered 11940 and 12041 respectively.

Isolation of Bitumen

Ground shale samples (~200 mesh) were used for both the Soxhlet extraction (continuous mode at refluxing temperature of solvent) and hot soaking (stationary mode at 85° C) to achieve the highest extraction efficiency. The solvent systems in general were benzene, benzene-methanol, acetonitrile, ethylene diamine, 1 methyl-napthalene as shown in Table 1. In order to make a comparison, they were applied over a chosen period of 10 hours. From the date it is evident that increase in polarity of the solvent system facilitates the extraction. The system that used benzene-methanol as an azeotrope composition appears to be the best one.

Elemental analyses of some Devonian shale bitumens are listed in Table II. The H/C atom ratio is a good indicator of the extent of saturated carbon content and aromatic carbon content of the given fractions. The range of Devonian shale bitumens in 1.52-1.56 indicates that they are most likely to have small amounts of aromatic molecules. The Green River oil shale bitumen has a H/C value of 1.68, which indicates that it has an even more saturated carbon content. The average molecular weights of the Devonian bitumens were 378 (No. 8), 395 (No. 43) and 760 (No. 25) by vapor pressure osmometry, and probably contain molecules ranging from 100 to 900 in molecular weight.

Carbon Preference Index

Gas chromatography has been used to characterize Devonian shale bitumens. The example shown in Fig. 1 is derived from No. 8 of Core No. 11940. The column used is 3% Dexsil 300 on chromosorb Q. n-Alkanes are found to be predominant.

In this manner, the carbon preference index (CPI) has been calculated for correlation with maturation. Usually, maturation causes a more random distribution of n-alkanes, as shown in Table III where CPI is expressed as the ratio of the amount of odd carbon-numbered n-alkanes to that of even carbon-numbered ones [1,2]. Three samples (#8, #43, and #55,56, Core #11940) fall between the geological ages of Chattanooga shale (Devonian, 300 x 10^6 years) and Appalachian shale (Ordovician, 400 x 10^6 years). The low value of CPI obtained for the #25 sample (CPI 0.70) could be due to the non-uniform distribution of hydrocarbons in the sample, since the organic carbon content of this sample is only 0.16% (wt.).

The distribution of n-alkanes in #43 bitumens extracted by different benzene methanol solvent systems is shown in Fig. 2. Effects of the solvent systems on the distribution of dominant components in bitumen are investigated by using the solubility parameter. The solubility parameter, δ, is defined as the square root of the potential energy per millimeter of material. The effective solubility parameter of the mixture of components 1 and 2 with υ_1 and υ_2 volume fractions can be estimated from the following formula:

$$\delta_{mixture} = \upsilon_1\delta_1 + \upsilon_2\delta_2$$

In the benzene methanol systems, the effective solubility parameter is increased by increasing the amount of methanol. Table IV lists the dominant n-alkane components of bitumen at different ratios of benzene to methanol. The higher the solubility parameter is, the larger the carbon number in dominant components that is obtained.

Fractionation of Bitumens

The benzene-extracted bitumen was precipitated with excess n-hexane to recover the asphaltene. The deasphaltened bitumen was loaded onto a silica gel column and a neutral oil fraction was first recovered. Subsequently, benzene-n-hexane, as well as tetrahydrofuran (THF), was used as an eluate to obtain the polar materials. The product distribution was as follows: neutral oil (58%), benzene-hexane (50:50) cut (12%), THF cut (18%), asphaltene (2%). The elemental analyses of these fractions are listed in Table II. The H/C ratio decreases from 1.69 to 1.36 and then to 1.32. As can be seen from the NMR spectrum in Fig. 3, the asphaltene fraction is the most aromatic. This is supported by the evidence of C-H out of plane bending vibrations in the infrared spectra (Fig. 4). In contrast to the Green River bitumen asphaltene, the Devonian shale bitumen asphaltene is quite aromatic. The 731_{cm}^{-1} polymethylene band in the infrared spectrum of the Green River bitumen asphaltene is unique (Fig. 4B). The long-chain methylene structure in Green River kerogen is known [3]. The aromaticity value of Devonian shale bitumen asphaltene as determined by the x-ray method is 0.49, in contrast to the low value of that from Green River bitumen asphaltene, which is 0.23.

The straight chain hydrocarbons were removed from the neutral oil fraction by urea adduction. The paraffin-free neutral oil was analyzed by gas chromatography-mass spectrometry (GC-MS). This fraction contains largely 2- and 3-ring condensed aromatics substituted with mono-, di-, tri-, and tetra- C_1 to C_3 alkyl substituents with the highly substituted ones as major components (Fig. 8) Nuclear magnetic resonance spectra have been obtained for all fractions, and the structural parameters have also been determined.

The geochemical significance of the asphaltenes is essential. The Green River bitumen asphaltene is less aromatic; Devonian shale bitumen asphaltene is more aromatic. Thus, the nature of the asphaltene may be an useful indicator for maturation studies.

Isolation of Kerogen Concentrates

Kerogen concentrates were prepared under an acid leaching method which was modified from the method used for Green River oil shales [4]. The removal of particular types of minerals in Devonian shales is possible. A summary of the results of kerogen concentrates is shown in Table V, in which about 9% (by weight) of the kerogen concentrate was obtained from #43 (approximately 3714 ft.) sample, 8% from #8 (approximately 3445 ft.) sample, and 0.5% from #25 (approximately 3625 ft.) sample.

Devonian raw shale contains 1-3% (by weight) of pyrite. Pyrite is extremely difficult to separate from the shale organic material. This can be seen clearly from the infrared data of kerogen concentrates (Fig. 7) or from the x-ray powder pattern (Fig. 9).

Three different approaches are being worked upon to effect the removal of pyrite in order to minimize the ash content. They include the electrolytic treatment [5], the reduction method with lithium aluminum hydride [6], and bioleaching with Ferobacillus ferooxidans [7].

Currently, both the lithium aluminum hydride reduction and the electrolytic treatment have been successful in completely removing the pyrite from kerogen concentrates. Using the far infrared pyrite peak as a semiquantitative point of reference, as indicated in Fig. 7A, -B, and -C, progressively the peak disappears. A typical Devonian shale kerogen concentrate exhibits an ash incomplete at this time.

Structural Characterization of Kerogen Concentrate

The recently developed x-ray diffraction method for mesomorphic substance [8] was used to study the Devonian shale kerogen concentrate. The low-ash kerogen sample #43 (core #11940) was subjected to x-ray studies. A reduced intensity plot of this kerogen is presented in Fig. 10. The aromaticity value was computed to be f_a=0.37. It should be noted that the kerogen concentrate from Green River oil shale is f_a=0.15 [9]. Both the x-ray method [8] and the solid state nuclear magnetic resonance method [10] yield identical results. Also in this instance, the Appalachian black shale has an aromaticity value of f_a=0.50. We verified that the aromaticity value is a good maturation parameter.

Oxidative degradation of the kerogen concentrate has also been studied. The method is similar to the one applied to Green River oil shale kerogen [11] where smaller quantitites of aqueous alkaline permanganate were used for the stepwise, controlled oxidation of the kerogen molecule. The same method has also been applied to lignite with success [12]. During the course of the degradative studies, the larger molecules appeared to be released in the intermediate steps. For example, in Fig. 5, the gel permeation chromatogram from high pressure liquid chromatography indicates that in Steps 4-6, larger molecules are fragmented in a 7-step oxidation process. The molecules released are closer to those from coal than those from the Green River oil shale kerogen. A gas chromatogram (Fig. 6) of the derivitized acids from ether precipitation of a middle oxidized fraction of the Devonian shale kerogen concentrate indicates a similarity to the humic- or subhumic-like components derived from the chemical oxidation of many coals [13]. There are numerous substituted aromatic acids in that fraction.

Conclusion

The organic components from Devonian shale are definitely different from those of the Green River oil shale. For the first time, the bitumen and kerogen from Devonian shale are found to be quite aromatic. The asphaltene (from bitumen) and the kerogen concentrate can be used as maturation indicators within the shale deposits in different locations, as well as in different formations. Asphaltenes from Devonian shales are similar to that from petroleum, whereas the kerogen from Devonian shale is close to coal. These findings suggest that there could be extremely serious environmental problems from the contamination when Devonian shale is explored by drastic means after fracturing.

Acknowledgement

The project was supported by the Morgantown Energy Research Center through ERDA by contract no. EY-77-9-21-8104. We are appreciative of the technical advice from John Kovach and Steve Lamey of MERC, the editorial help from Keith Manasco, and the techical services of GC-MS by Paul E. Kelly.

References

(1) E.E. Bray and E.D. Evan, Geochim. Cosmochim. Acta, 22, 2 (1961).

(2) T.F. Yen, ACS Symposium Series, 18, 231 (1975).

(3) T.F. Yen in Oil Shale, Development in Petroleum Science (T.F. Yen, G.V. Chilingarian, ed.). Elsevier, Amsterdam, 1976, Chapter 7.

(4) W.E. Robinson in Organic Geochemistry (G. Eglinton, M.T.J. Murphy, ed.) Springer-Verlag, New York, 1969, Chapter 6.

(5) C.S. Wen, J. Kwan and T.F. Yen, Fuel, 55, 75 (1975).

(6) D. L. Lawlor, J.I. Fester and W.E. Robinson, Fuel, 42, 239 (1963).

(7) M.P. Silverman, J. Bact., 94, 1046 (1967).

(8) J.T. Kwan and T.F. Yen, ACS, Div. Fuel Chem., Preprint, 21 (7), 67 (1976).

(9) D.K. Young and T.F. Yen, Geochim. Cosmochim. Acta, 41, Oct. 1411 (1977).

(10) V.J. Batuska and G.E. Maciel in Preprints of 1976 Coal Chemistry Workshop, Stanford Research Institute, 1976, p. 220.

(11) T.F. Yen, Paper presented at 8th International Congress on Organic Geochemistry, Moscow, USSR, Vol. 1, p. 146, 1977.

(12) D.K. Young and T.F. Yen, Energy Sources, 3, 39 (1976).

(13) J. Bimer, P.H. Given and S. Raj, ACS, Div. Fuel Chem., Preprint, 22 (5), 169 (1977).

Table I. Extraction of Bitumens from Devonian Shale

Sample No.	Extraction Method	Solvent Composition	Bitumen[i] (%, wt.)
8	Soxhlet	Benzene, 100%	1.5
"	"	Azeotrope of Benzene/Methanol	1.8
"	"	Acetonitrile, 100%	1.8
"	Hot Soaking	Benzene, 100%	1.4
"	"	Benzene 80% - Methanol 20%	1.7
"	"	Benzene 75% - Methanol 25%	1.9
"	"	Benzene 67% - Methanol 33%	3.1
"	"	Benzene 50% - Methanol 50%	1.4
25[a, d]	Soxhlet	Benzene, 100%	1.1
"	"	Azeotrope of Benzene/Methanol	1.7
"	"	Acetonitrile, 100%	1.0
"	Hot Soaking	Benzene, 100%	1.3
"	"	Benzene 80% - Methanol 20%	1.7
"	"	Benzene 75% - Methanol 25%	1.5
"	"	Benzene 67% - Methanol 33%	1.2
"	"	Benzene 50% - Methanol 50%	1.9
43[a, c]	Soxhlet	Benzene 100%	1.2
"	"	Azeotrope of Benzene/Methanol	2.2
"	"	Acetonitrile, 100%	1.3
"	"	Ethylene diamine, 100%	3.4
"	Hot Soaking	Benzene 100%	1.4
"	"	Benzene 80% - Methanol 20%	2.1
"	"	Benzene 75% - Methanol 25%	2.3
"	"	Benzene 67% - Methanol 33%	2.3
"	"	Benzene 50% - Methanol 50%	1.5
"	"	1 Menthyl-Naphthalene	2.7
55-56[a, f]	Soxhlet	Benzene, 100%	1.0
5-6[b, g]	"	Benzene, 100%	1.0
50-51[b, h]	"	Benzene, 100%	1.4

[a] From Core No. 11940
[b] From Core No. 12041
[c] 3445.10-3445.60 ft.
[d] 3624.80-3625.23 ft.
[e] 3713.78-3714.43 ft.
[f] 3773.68-3782.35 ft.
[g] 3240.15-3245.55 ft.
[h] 3464.95-3470.35 ft.
[i] The amount of bitumen was based on weight loss.

Table II. Elemental Analysis of Organics of Shale and Related Materials[a]

Substance	Org.C (wt%)	H (wt%)	H/C	N (wt%)	S (wt%)	Ash (wt%)
#8 Bitumen	82.0	10.5	1.54	0.9	0.2	2.6
#43 Bitumen	82.8	10.5	1.52	0.5	0.1	N.D.[b]
#43-EDA-Bitumen[c]	81.4	8.9	1.31	3.2	0.8	2.5
#55-56 Bitumen	87.2	11.3	1.56	0.4	0.1	0.1
Green River Bitumen	79.4	11.1	1.68	0.9	0.7	6.8
Green River Shale Oil (Paraho)	85.8	11.3	1.58	1.4	0.5	0.01
Green River Shale Oil (TOSCO II)	85.1	11.6	1.64	1.9	0.9	N.D.
Paraho Shale Oil Asphaltene (Green River)	75.6	7.5	1.19	3.4	0.7	6.0
#55-56 Bitumen Hexane Eluate	87.5	12.3	1.69	0.1	0.1	N.D.
#55-56 Bitumen Benzene Eluate	86.2	9.8	1.36	1.0	0.1	0.2
#55-56 Bitumen THF Eluate	81.8	9.0	1.32	0.5	0.7	0.3
#8 Kerogen Concentrate	43.1	3.9	1.09	0.5	19.5	32.5
#25 Kerogen Concentrate	19.0	2.0	1.28	0.2	18.5	62.0
#43 Kerogen Concentrate	59.3	6.4	1.30	0.6	14.6	21.0
#55-56 Kerogen Concent.	27.7	2.6	1.13	0.3	16.9	49.4
Appalachian Shale Kerogen	64.1	5.5	1.03	1.8	6.2	N.D.
Green River Kerogen	68.6	8.42	1.47	3.48	2.41	9.76

[a] Other than specified, the shale is Cottageville Devonian shale.
[b] N.D. = No Determination.
[c] Solid bitumen extracted by ethylene diamine (EDA).

Table III. Maturation of Various Oil Shales[a, b]

Shale	Geological Age	Years (10^6)	CPI
Green River	Eocene	60	1.63
Kentucky	Pennsylvanian	200	1.43
Chattanooga	Devonian	300	1.17
#8 Cottageville	Devonian	—	1.09
#43 Cottageville	Devonian	—	1.04
#55-56 Cottageville	Devonian	—	0.91
Appalachian Black Shale	Ordovician	400	0.80
#25 Cottageville	Devonian	—	0.70

[a] Bitumen was extracted by Soxhlet extraction with 100% benzene.
[b] Core number is 11940 for Cottageville Devonian shale.

Table IV. Effect of Solubility Parameter on Bitumen[a]

Solvent System	Effective Solubility Parameter	Dominant Components[b] in Bitumen	CPI
Benzene 100%	9.15	C_{11}, C_{12}, C_{13}	1.10
Benzene 80%-Methanol 20%	10.22	C_{11}, C_{12}, C_{15}	0.98
Benzene 75%-Methanol 25%	10.49	C_{15}, C_{12}, C_{13}	1.01
Benzene 67%-Methanol 33%	10.93	C_{13}, C_{14}, C_{15}	1.02
Benzene 50%-Methanol 50%	11.83	C_{20}, C_{17}, C_{15}	1.01

[a] Bitumen was extracted by hot soaking from 43 sample (Core No. 11940).
[b] The first three major components from GC analysis were selected to represent the dominant components in the bitumen.

Table V. Stepwise Preparation of Kerogen from Raw Devonian Shale (Percentage Distribution totalling 100% for each sample.)

Sample no.	% Bitumen	% Wt. Loss from HCL Leaching	% Wt. Loss from HF/HCL Leaching	% Wt. Loss of Pyrite from LiAlH Reduction	% Wt.[a] Kerogen	% Mineral Residue
8	1.7	5.0	84.5	-	5.9	2.9[b]
25	1.2	17.8	80.6	-	0.3	0.2[b]
43	2.3	6.0	82.0	1.4[d]	7.1	1.1[c]

[a] Ash-free kerogen (organic only)

[b] Including pyrite

[c] Pyrite-free

[d] Original pyrite for #43 is 1.8%

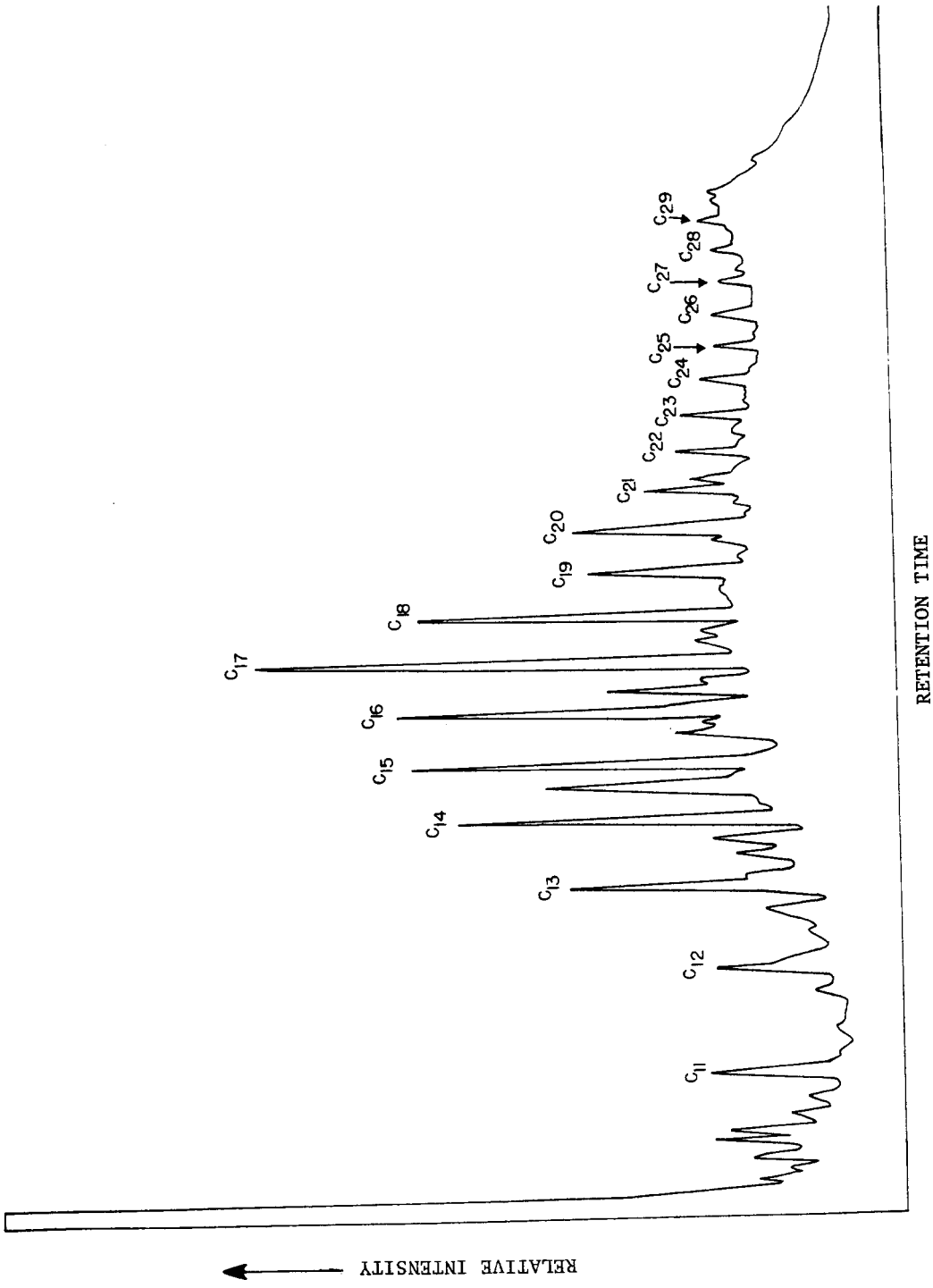

FIG. 1.
NORMAL ALKANE DISTRIBUTION IN THE BITUMEN OF DEVONIAN SHALE NO. 8 FROM CORE 11940.

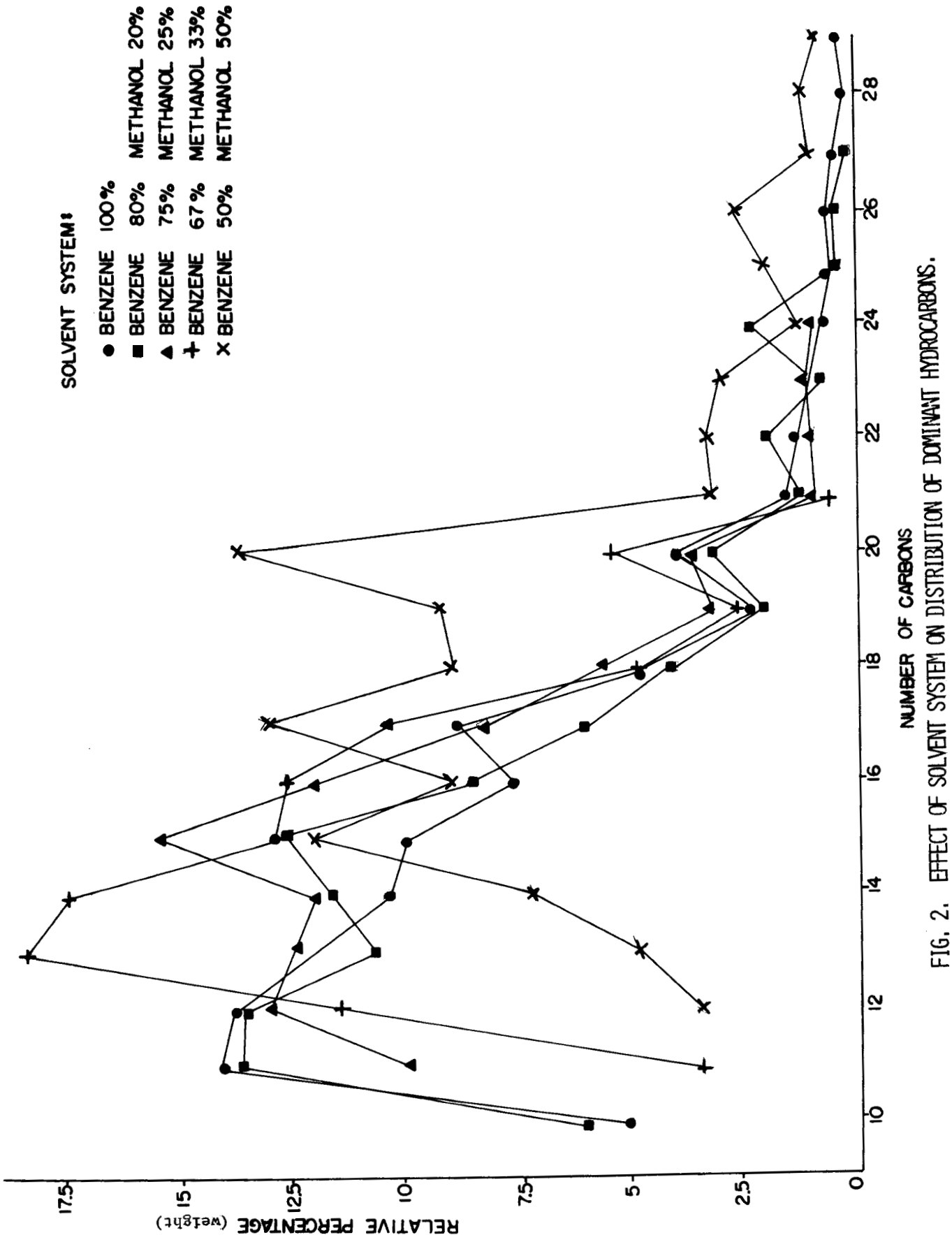

FIG. 2. EFFECT OF SOLVENT SYSTEM ON DISTRIBUTION OF DOMINANT HYDROCARBONS.

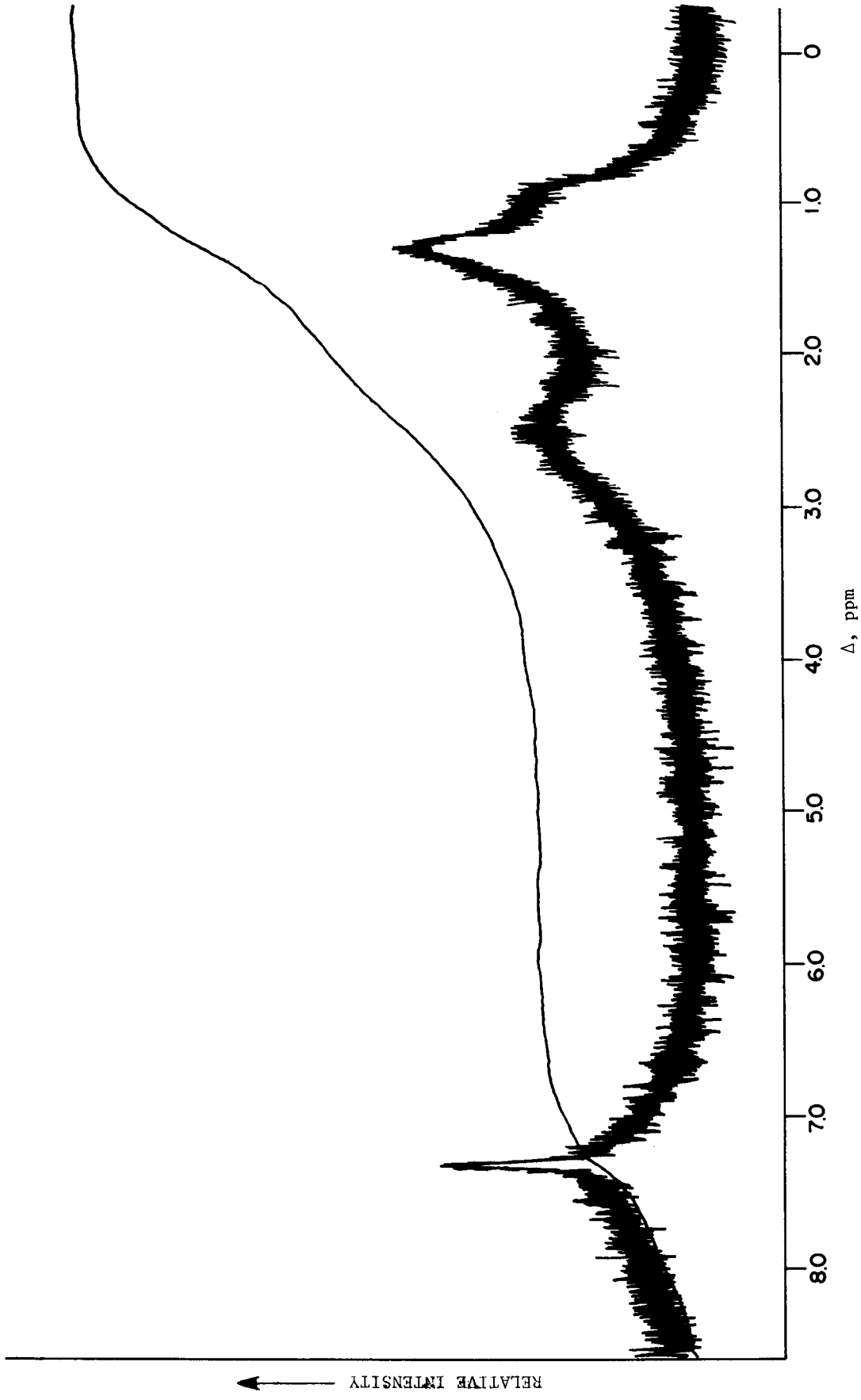

FIG. 3. NUCLEAR MAGNETIC RESONANCE SPECTRUM OF AN ASPHALTENE FRACTION FROM BITUMEN.

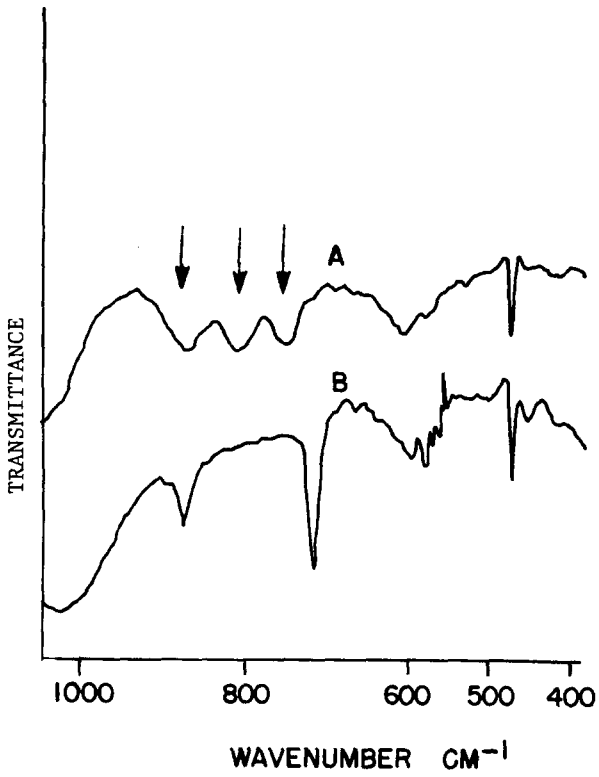

FIG. 4.

INFRARED BENDING REGIONS OF ASPHALTENES

A. DEVONIAN SHALE BITUMEN ASPHALTENE

B. GREEN RIVER SHALE BITUMEN ASPHALTENE

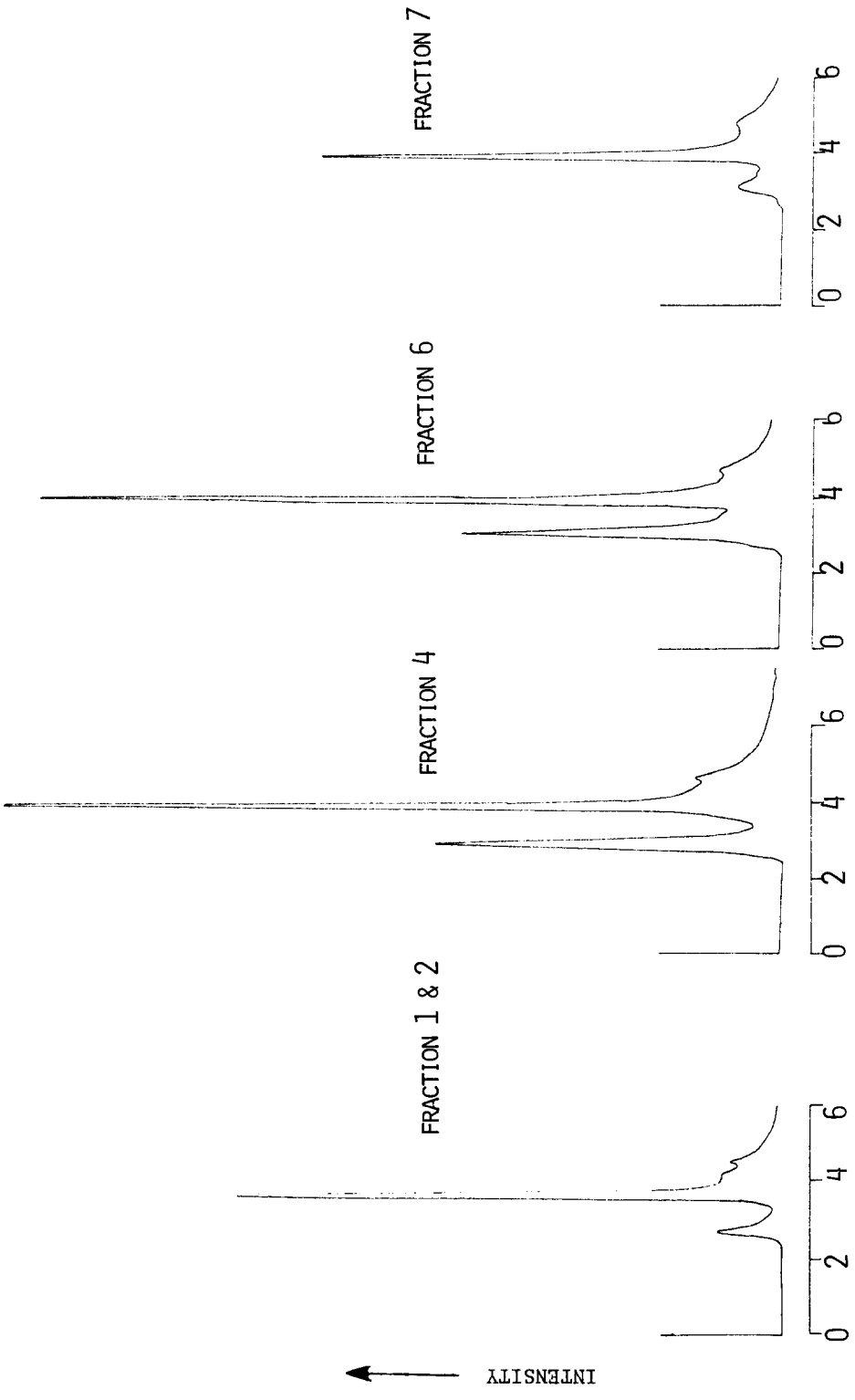

FIG. 5. GEL PERMEATION CHROMATOGRAMS OF THE OXIDIZED PRODUCTS FROM DEVONIAN SHALE KEROGEN CONCENTRATE.

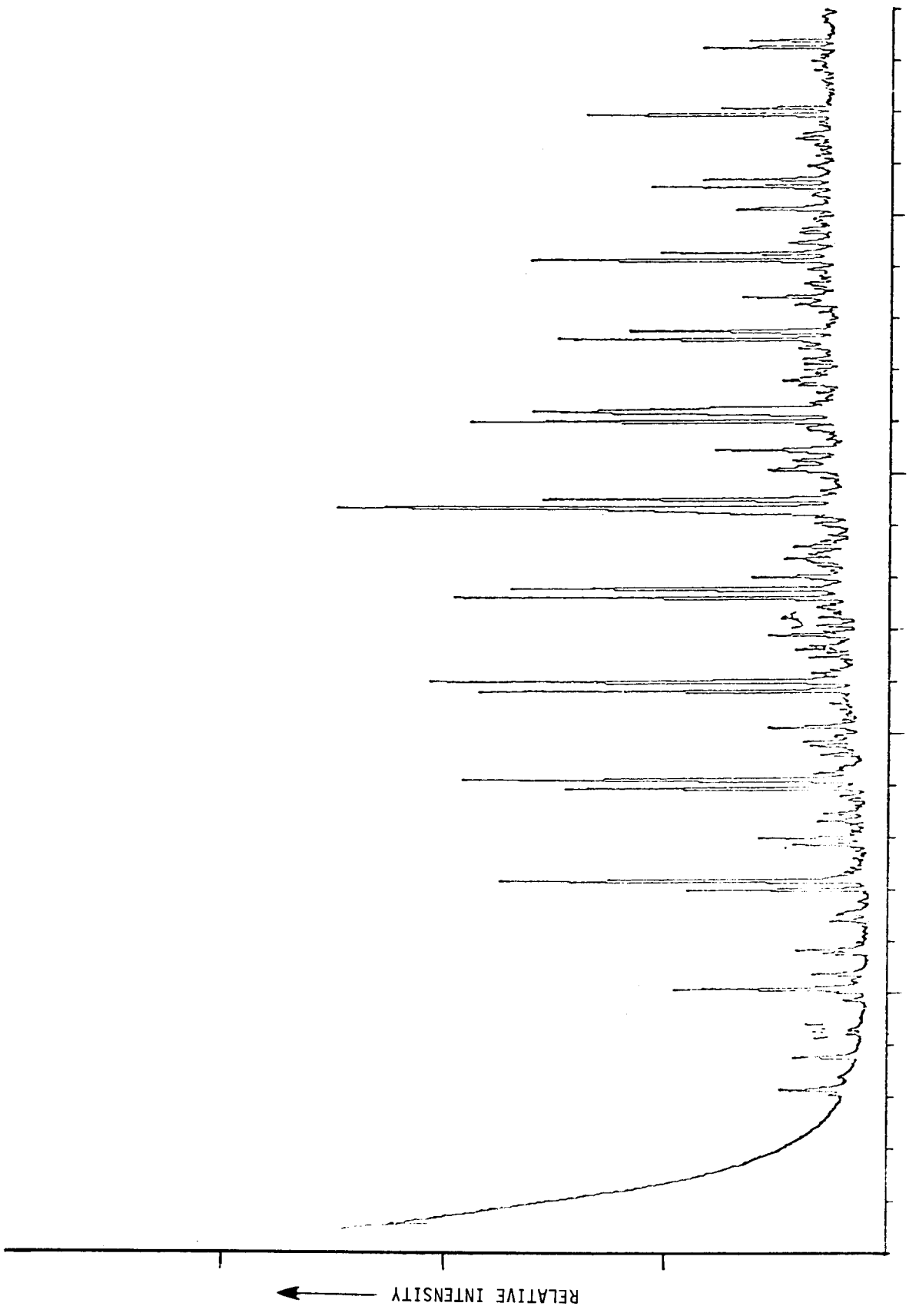

Figure 6: Oxidized Products from Devonian Shale Kerogen (Reconstructed gas Chromatogram) Pronounced peaks are due to mono and di-carboxylic acids, weak peaks are due to aromatic carboxylic acids.

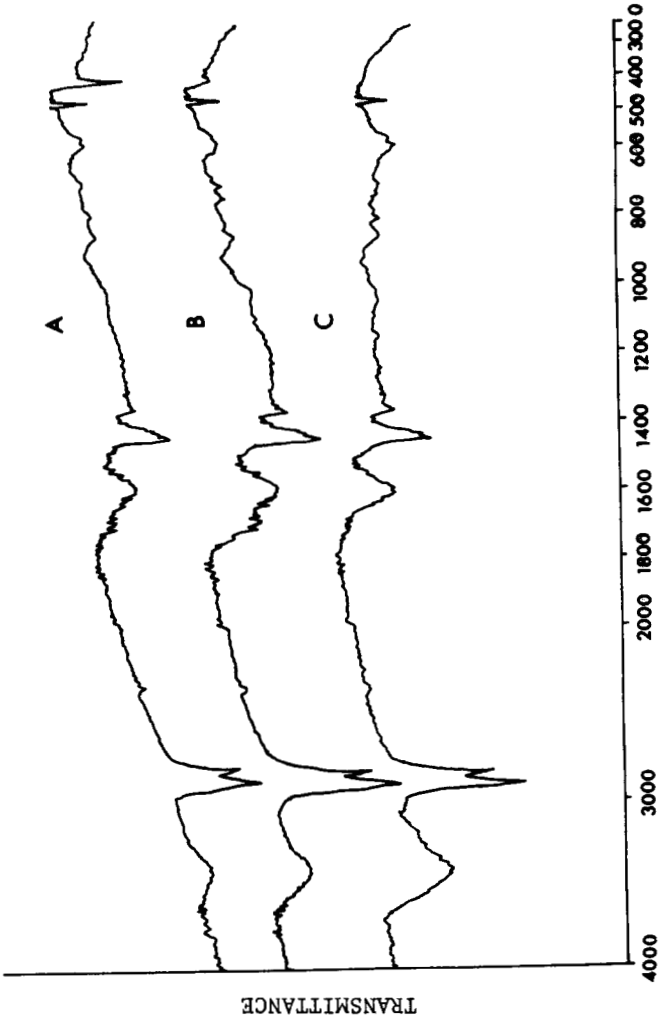

FIG. 7.

INFRARED SPECTRA OF KEROGEN CONCENTRATES AT DIFFERENT STAGES (PYRITE PEAK AT 420 CM^{-1} GRADUALLY DECREASED). A: ORIGINAL KEROGEN CONCENTRATE. B: PARTIAL BIOLEACHING. C: BY L_1AlH_4 REDUCTION.

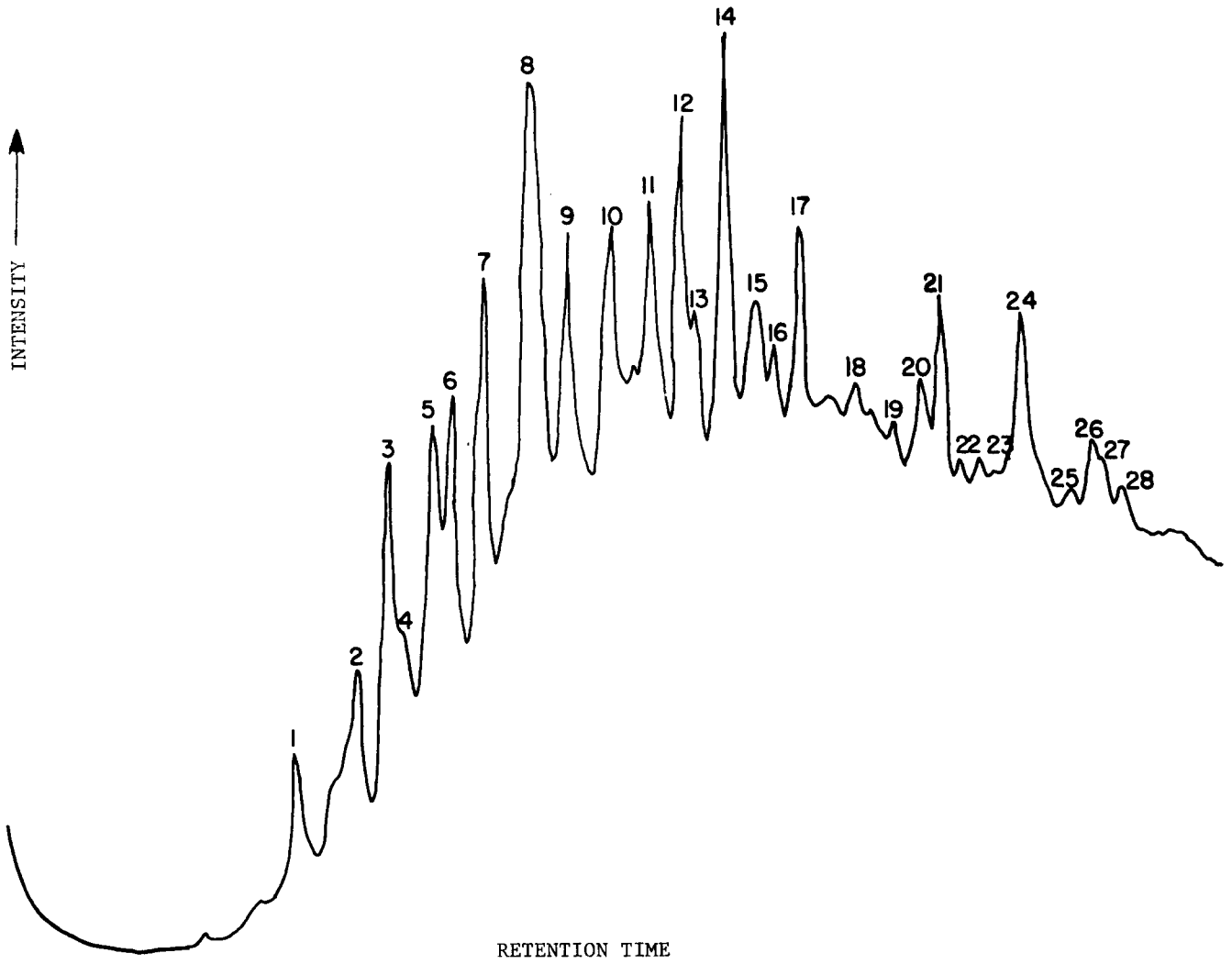

FIG. 8. SUBSTITUTED AROMATIC HYDROCARBONS FROM THE PARAFFIN-FREE NEUTRAL OIL OF DEVONIAN SHALE BITUMEN.

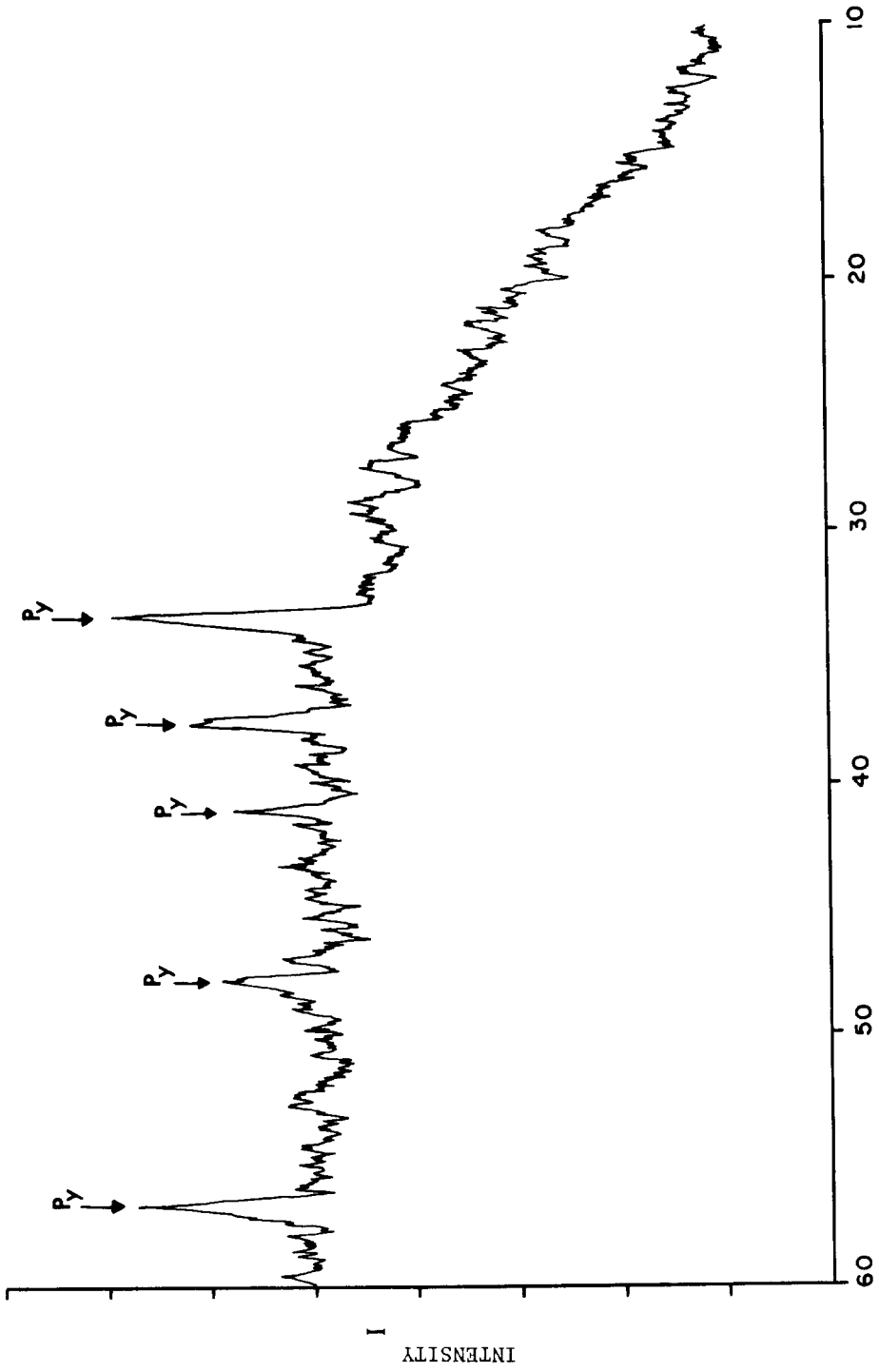

FIG. 9. X-RAY POWDER PATTERN OF KEROGEN CONCENTRATE BEFORE REMOVAL OF PYRITE.

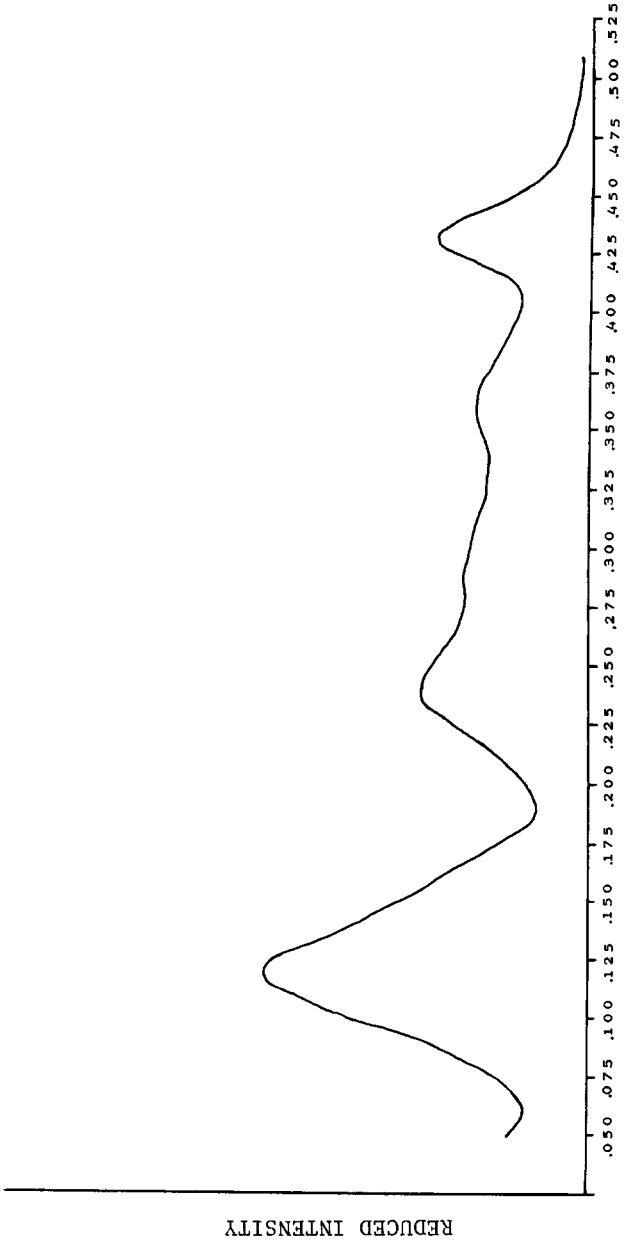

FIG. 10. REDUCED INTENSITY X-RAY DIFFRACTION SPECTRUM OF A LOW-ASH DEVONIAN SHALE KEROGEN CONCENTRATE.

INTERNAL SURFACE AREA AND POROSITY IN EASTERN GAS SHALES FROM THE SORPTION OF NITROGEN, CARBON DIOXIDE, AND METHANE—A STATUS REPORT

by

Josephus Thomas, Jr., and Robert R. Frost
Illinois State Geological Survey
Urbana, Illinois

ABSTRACT

The adsorption of N_2 at -196°C and of CO_2 at -77°C on eastern gas shales reveals significant differences in their micropore structures. Owing to differences in the activated diffusion of the two gases at their respective adsorption temperatures, as studies on molecular sieves and coals have shown, CO_2 is able to penetrate pores less than 4 to 5 Å in diameter, whereas N_2 is unable to do so. One measure of this difference is in the internal surface area (ISA) estimated from the BET method. For example, shale samples from a Kentucky core, with CO_2 as the adsorbate, have ISA values ranging from 10 to 39 m^2/g, whereas the ISA values from N_2 adsorption on the same samples range from 0.8 to 8.7 m^2/g. The diffusion rate of a gas initially contained within such an ultramicroporous network will be greatly decreased in comparison with the diffusion rate from shales containing larger pores.

High-pressure (up to 80 atmospheres) methane sorption isotherms near room temperature are shown for selected shale samples. These isotherms provide supplemental information with regard to total porosity and the gas-holding capacity of shales at depth of burial.

INTRODUCTION

The determination of the nature and extent of porosity in a polycrystalline material is often very difficult. Void spaces 1 to 2 angstrom units (Å) in diameter along grain boundaries are so small that they may not be considered pores in a practical sense; even so, the porosity of polycrystalline aggregates is generally underestimated.

In closed-pore structures the pores are almost completely isolated, which results in low permeability of the material to gases and liquids. In most limestones, for example, slight solubilization of sediments, recrystallization, and cementation of grains under compaction isolate the pores. The porosity of sintered metallic and ceramic compacts is also of this type.

Special-shaped micropores exist between the lamellae of layer-lattice structures in which van der Waals' forces predominate. Gases or liquids that can overcome the van der Waals' forces can penetrate, or intercalate, these structures. The clay mineral montmorillonite, easily permeated by polar gas and liquid molecules, is the classic example of this type. Partially-ordered carbon blacks and even graphite can be intercalated to some extent by certain inorganic compounds.

Interconnecting pore structures are best exemplified by those in zeolites and synthetic molecular sieves, in which the rigid silica skeletal frameworks yield rather well defined pores that have a fairly narrow range of size. A similar pore structure, with a not-so-well-defined range of pore size, is present in coals [1], in which rather tortuous channels of molecular dimensions (less than 10 Å in diameter) result from a partial filling or lining of pore space with nongaseous organic matter. As data in the present report will show, black shales have a similar partially interconnecting pore

structure. The presence of these ultramicropores is of special significance; the pores are large enough to contain appreciable quantities of certain gases of small molecular dimensions (e.g., methane, ethane, and other longer-chain hydrocarbons possessing little side branching), yet the pores are so small that they markedly influence the diffusion rates of the contained gases.

A direct study of porosity can be made with an electron microscope, although during study of the smallest pores (those less than 10 Å in diameter) the operating conditions must be favorable, and the field of view, which is necessarily small, prevents accurate statistical evaluation of the pore sizes. Total porosity can be evaluated by the low-angle scattering of X-rays and by the use of helium and mercury in density determinations. These methods, however, provide little information regarding variations of pore size. Mercury porosimetry, which involves the intrusion of mercury under increasing pressure into pores, provides information about pore size variations in open-pore structures, but with commercial apparatus the method has a lower limit of pore-diameter penetration of about 30 Å. Thus, much of the porosity in coals and the black shales cannot be studied by this method.

The only experimental approach that provides useful information with regard to these ultramicropores involves gas adsorption (sorption) methods. Studies by Breck et al. [2] and Lamond [3] on molecular sieves and by Walker and Geller [4] and Anderson et al. [5, 6] on coals have established that carbon dioxide as an adsorbate at -77°C can penetrate pores having diameters less than about 4 to 5 Å, whereas nitrogen, the adsorbate usually used at -196°C in the classic BET method [7], fails to do so. Although there is an apparent paradox here in that N_2 is a smaller molecule than CO_2, and a greater diffusion rate is generally associated with smaller molecules, the role of temperature is of great significance with pores of molecular dimensions, producing large differences in the activation energies of diffusing gases. Nitrogen has a much higher activation energy for diffusion than does CO_2 at their respective adsorption temperatures. Thus, CO_2 is a valuable molecular probe in evaluating pores less than about 4 to 5 Å in diameter. A measure of this porosity is the internal surface area estimated by the BET method [7]. Although the theory upon which this method is based has some shortcomings (as do other gas sorption theories) when applied to pores of molecular dimensions, the relative adsorption values obtained are reproducible and useful for correlative purposes. The use of CO_2 as an adsorbate for this purpose has been reviewed recently by Thomas and Damberger [1].

Methane as a sorbate near room temperature and at increased pressures yields isotherms that provide additional information regarding the relative total porosities of shale samples and their gas-holding capacities at depths of burial.

EXPERIMENTAL PROCEDURES

Data for internal surface area (ISA) measurements with N_2 and CO_2 as adsorbates at -196°C and -77°C, respectively, were obtained by a dynamic sorption method. This method is commonly called the gas chromatographic method, as the principles involved in the measurements are similar to those used in gas chromatography. Apparatus is basically that first described by Nelsen and Eggertsen [8] and later refined by Daeschner and Stross [9].

For the high-pressure (1 to 80 atmospheres) methane sorption isotherms, apparatus similar to that described by Dubinin et al. [10] was constructed with slight modifications for improved readout of pressure.

Shale samples were crushed and screened. The 40-×-120-mesh (about 425 to 125 μm) sieve fractions were used for the internal surface area measurements with N_2 and CO_2 as adsorbates. The 6-×-12-mesh (about 3.4 to 1.7 mm) sieve fractions were used for the high-pressure methane sorption isotherms.

For the ISA determinations, shale samples of 0.5 to 1.0 g were outgassed at 110°C in a stream of helium for 3 hours. Three-point BET plots were used with N_2 as the adsorbate at -196°C. A check on two different samples showed that no additional N_2 was adsorbed after 4 hours above that adsorbed in 10 minutes at a constant relative pressure. Thus, an equilibrium time of 10 minutes was suitable for each point. With CO_2 as the adsorbate at -77°C, however, an equilibrium time of 16 hours was necessary because of the slow activated diffusion. A single-point BET plot passing through the origin was used as a measure of the ISA. A relative pressure (p/p_o) of about 0.15 was used for CO_2; the saturation vapor pressure was 1450 mm. The area occupied by the CO_2 molecule under these conditions is 22.1 $Å^2$, based on calibration with standards of known surface areas [1].

For the high-pressure methane sorption isotherms, approximately 50 to 60 g of sample were weighed into a high-pressure cell, and outgassing was conducted under vacuum until a pressure of less than 10^{-3} mm was attained. The dead space was determined with helium. Known increments of methane were transferred to the cell, and pressure differences were determined at constant temperature as a measure of the uptake of methane by the sample.

Samples from only two cores have been studied extensively. Both were from the Illinois Basin. The more recent core is designated Orbit #1 Clark Well from Christian County, Kentucky (near Crofton). The older core (1939) is designated Miller #1 Sample from Sangamon County, Illinois (near Mechanicsburg). From a simple visual examination, and as organic carbon analyses have shown, the samples from the Kentucky core were generally darker and obviously contained more organic material than samples from the Illinois core.

RESULTS AND DISCUSSION

Internal surface area values are given in tables 1 and 2 for samples from the Kentucky and Illinois cores. Since the external surface area of 40-×-120-mesh porous particles is an insignificant fraction (less than 0.1 m^2/g) of the total measured surface, it is included in each of the ISA values.

A surface area value for a shale sample, either from CO_2 or N_2 adsorption data, will be governed to some extent by the heterogeneity of the sample (i.e., the presence of silica, carbonates, and other inorganic components and variations in the clay minerals ratio) and by the crystallite sizes of the components. Accordingly, until chemical and mineralogical analyses of the samples are completed, too much significance should not be attached to the ISA values shown within either the third or fourth columns of tables 1 and 2. Of more significance are the CO_2/N_2 ISA ratios shown in the fifth column of each table.

The larger this ratio, the greater the proportion of the porosity that is contained in pores less than 4 to 5 Å in diameter. CO_2 at $-77^{\circ}C$ penetrates these pores, whereas N_2 at $-196^{\circ}C$ does not. When the ratio is large, the sample has a more compact pore structure, and the diffusion rates of contained gases will be lower than diffusion rates of contained gases from samples having lower ISA ratios. With the latter samples, it is readily ascertained from the data that N_2 at $-196^{\circ}C$ reaches a greater proportion of the internal surface. In those cases where the ISA ratio is essentially 1, there is little porosity associated with pores less than 4 to 5 Å in diameter.

The ISA ratios for the shale samples from the Kentucky core (table 1) are, for the most part, appreciably larger than the ISA ratios for samples from the Illinois core (table 2). The organic carbon contents of samples from the Kentucky core are, in general, greater than the organic carbon contents of the Illinois core. The higher ISA ratios correlate closely with the organic carbon contents. Thus, the first two samples and the seventh sample (01C1, 02C1, and 07C1) in table 1, which have large CO_2/N_2 ISA ratios also contain the most organic carbon. A similar situation prevails for the samples in table 2.

ISA values from CO_2 adsorption range from about 10.0 to 39.3 m^2/g for samples from the Kentucky core and cover about the same range (10.1 to 34.4 m^2/g) for samples from the Illinois core. ISA values from N_2 adsorption are much lower (0.9 to 8.7 m^2/g) for samples from the Kentucky core in comparison with those (5.5 to 27.4 m^2/g) for samples from the Illinois core. Thus, it would appear that much of the organic matter occupies and lines the pores and effectively reduces pore diameters such that N_2 can no longer permeate the porosity but CO_2 can.

As a further check on the concept of occupation of pore space by organic matter, sample 01C1 from the Kentucky core, which had the largest CO_2/N_2 ISA ratio (26.2), was selected for outgassing at higher temperatures to study the influence of this treatment on the ISA values. Data are summarized in table 3.

Although the ISA from CO_2 adsorption does not change markedly after outgassing at $230^{\circ}C$ and $340^{\circ}C$, the ISA from N_2 adsorption increases about fourfold after outgassing at $340^{\circ}C$. The weight loss also increases sharply. As this outgassing temperature is not sufficiently high to cause a breakdown of the inorganic matter or to cause dehydroxylation of the clay minerals, the weight loss is from loss of organic matter. The organic material migrates from the pores at the higher outgassing temperature, thus opening up some of the ultramicropores and producing higher N_2 ISA values.

The measurements with N_2 and CO_2, important as they are in gaining an understanding of the differences in ultramicroporosity that influence the rates of diffusion of contained gases, do not reveal sufficient information about the total porosity or the gas-holding capacities of the shales. The ultramicropores provide more surface area but not necessarily more pore volume. The gas-holding capacity of a given shale will be governed by any additional larger pores in the shale that do not contribute greatly to the ISA values. The high-pressure methane sorption isotherms provide supplemental information in this regard.

Although data are as yet insufficient to permit extensive interpretation, it would appear that the lighter, grayer shales are capable of holding more gas than the darker shales. Since the porosity in the darker shales is partly occupied by nongaseous organic material, this is not an unexpected result. Whether the gray shales actually hold more gas at depth of burial than the darker shales in the stratigraphic unit is another issue.

Table 4 shows density and porosity values for three samples selected from the Illinois core. The first sample (01L2), which had the lowest CO_2/N_2 ISA ratio (about 1.0), yielded a density in helium of 2.73. The density in mercury, which is the particle density without significant pore penetration, was 2.37. The porosity of this sample thus was 13.3 percent. By the same methods, sample 15L1, which had a CO_2/N_2 ISA ratio of 2.9, was found to have a porosity of 10.5 percent, and sample 17L1 (CO_2/N_2 ISA = 4.7), which was the darkest sample in the core, had a total porosity of 9.7 percent.

Methane sorption isotherms at 28°C for these three samples are shown in figure 1. Two sets of curves are shown for the three samples; the upper set shows total methane sorbed by the three samples, and the lower set represents the physically adsorbed component of the total sorption capacity. The adsorbed component should reflect the presence or absence of ultramicroporosity, reaching a limiting value rather quickly when there is restriction in the build-up of the adsorbed layer.

As a rule of thumb, every foot of depth of burial in sediments increases the pressure 1 psi [11]. At 1700 feet burial depth, the pressure is approximately 115 atmospheres. As expected from its total porosity, sample 01L2 had the greatest gas-holding capacity of the three shales studied. Extrapolation of the uppermost curve, representing sample 01L2, to 115 atmospheres would yield approximately 10cc/g, or 320 ft^3/ton shale as its methane-holding capacity at depth of burial. It is recognized, of course, that moisture and other gases occupy some of the pore volume. The high-pressure methane sorption isotherms serve mainly to help characterize the relative porosities in the shales. Samples from various geographical locations will be examined similarly in the future to cover the gamut of expected lithologies.

REFERENCES

1. Thomas, Josephus, Jr., and Heinz H. Damberger, 1976, Internal surface area, moisture content, and porosity of Illinois coals: variations with coal rank: Illinois State Geological Survey Circular 493, 38 p.
2. Breck, D. W., W. G. Eversole, R. M. Milton, T. B. Reed, and T. L. Thomas, 1956, Crystalline zeolites. I. The properties of a new synthetic zeolite, type A: Journal of the American Chemical Society, v. 78, p. 5963-5977.
3. Lamond, T. G., 1962, The sorption of gases on carbons: Ph.D. thesis, University of Durham, Durham, England.
4. Walker, P. L., Jr., and Irwin Geller, 1956, Change in surface area of anthracite on heat treatment: Nature, v. 178, p. 1001.
5. Anderson, Robert B., W. Keith Hall, James A. Lecky, and Karl C. Stein, 1956, Sorption studies on American coals: Journal of Physical Chemistry, v. 60, p. 1548-1558.
6. Anderson, R. B., J. L. Bayer, and L. J. E. Hofer, 1965, Determining surface areas from CO_2 isotherms: Fuel, v. 44, p. 443-452.
7. Brunauer, Stephen, P. H. Emmett, and Edward Teller, 1938, Adsorption of gases in multimolecular layers: Journal of the American Chemical Society, v. 60, p. 309-319.
8. Nelsen, F. M., and F. T. Eggertsen, 1958, Determination of surface area: Adsorption measurements by a continuous flow method: Analytical Chemistry, v. 30, p. 1387-1390.
9. Daeschner, H. W., and F. H. Stross, 1962, An efficient dynamic method for surface area determinations: Analytical Chemistry, v. 34, p. 1150-1155.
10. Dubinin, M. M., B. P. Bering, V. V. Serpinsky, and B. N. Vasil'ev, 1958, The properties of substances in the adsorbed state: Studies of gas adsorption over a wide temperature and pressure range, *in* Surface phenomena in chemistry and biology, Pergamon Press, New York, p. 172-188.
11. Hubbert, M. K., and D. G. Willis, 1957, Mechanics of hydraulic fracturing: Transactions of the Society of Petroleum Engineers of AIME, v. 210, p. 153-168.

TABLE 1—INTERNAL SURFACE AREA VALUES FOR SHALE SAMPLES FROM CHRISTIAN COUNTY, KENTUCKY (CORE 01KY)

Sample number	Depth to top of sample (ft)	ISA CO_2 (m^2/g)	ISA N_2 (m^2/g)	CO_2/N_2	Organic C (%)
01C1	2182.25	39.3	1.50	26.2	14.03
02C1	2191.15	27.0	1.33	20.4	10.29
03C1	2220.30	20.4	1.26	16.2	7.03
04C1	2230.20	13.8	5.00	2.8	1.64
05C1	2240.10	13.8	1.04	13.2	5.81
06C1	2250.00	14.5	8.71	1.7	0.66
07C1	2260.30	31.3	1.52	20.6	12.30
08C1	2270.30	11.8	1.43	8.5	5.04
09C1	2280.00	11.1	1.05	10.6	5.39
10C1	2290.75	14.7	1.08	13.6	9.23
11C1	2299.75	12.7	0.92	13.8	7.43
12C1	2310.50	10.0	1.04	9.6	5.67
13C1	2318.80	14.3	0.82	17.4	7.30

TABLE 2—INTERNAL SURFACE AREA VALUES FOR SHALE SAMPLES FROM SANGAMON COUNTY, ILLINOIS (CORE 01IL)

Sample number	Depth to top of sample (ft)	ISA CO_2 (m^2/g)	ISA N_2 (m^2/g)	CO_2/N_2	Organic C (%)
01L2	1576.0	27.3	27.4	~1.0	0.43
03L1	1589.4	12.7	12.1	~1.0	0.29
04L1	1602.0	11.8	11.8	1.0	0.80
05L1	1615.1	16.6	17.8	0.93	0.28
07L1	1631.6	10.1	8.4	1.2	0.15
09L1	1647.4	22.8	23.5	~1.0	0.32
09L2	1656.2	23.3	23.4	~1.0	0.55
10L1	1657.6	16.4	12.6	1.3	1.28
11L1	1667.5	30.2	20.3	1.5	2.90
12L1	1678.6	30.8	25.7	1.2	1.72
13L1	1688.0	31.2	25.7	1.2	2.90
14L1	1698.2	31.5	19.0	1.7	4.26
15L1	1710.0	34.4	11.8	2.9	7.54
16L1	1723.4	34.0	8.3	4.1	9.59
17L1	1730.6	25.9	5.5	4.7	6.50
18L1	1740.2	20.5	6.0	3.4	5.57
19L1	1753.5	25.1	6.2	4.1	6.28
20L1	1763.3	19.3	11.5	1.7	3.09
21L1	1776.2	22.6	11.5	~2.0	3.79

TABLE 3—INTERNAL SURFACE AREA VALUES AFTER DIFFERENT OUTGASSING TEMPERATURES FOR SAMPLE 01C1

Temperature (°C)	ISA CO_2 (m^2/g)	ISA N_2 (m^2/g)	ISA CO_2/N_2	Weight loss (%)
110	39.3	1.50	26.2	~1.0
230	44.3	1.57	28.2	~2.0
340	35.8	6.46	5.5	~6.0

NOTE: Duration of outgassing was 3 hours.

TABLE 4—DENSITY AND POROSITY VALUES FOR SELECTED SHALE SAMPLES FROM SANGAMON COUNTY, ILLINOIS

Sample	ISA CO_2/N_2	Helium density (g/cc)	Mercury density (g/cc)	Porosity (%)
01L2	~1.0	2.73	2.37	13.3
15L1	2.9	2.56	2.29	10.5
17L1	4.7	2.49	2.25	9.7

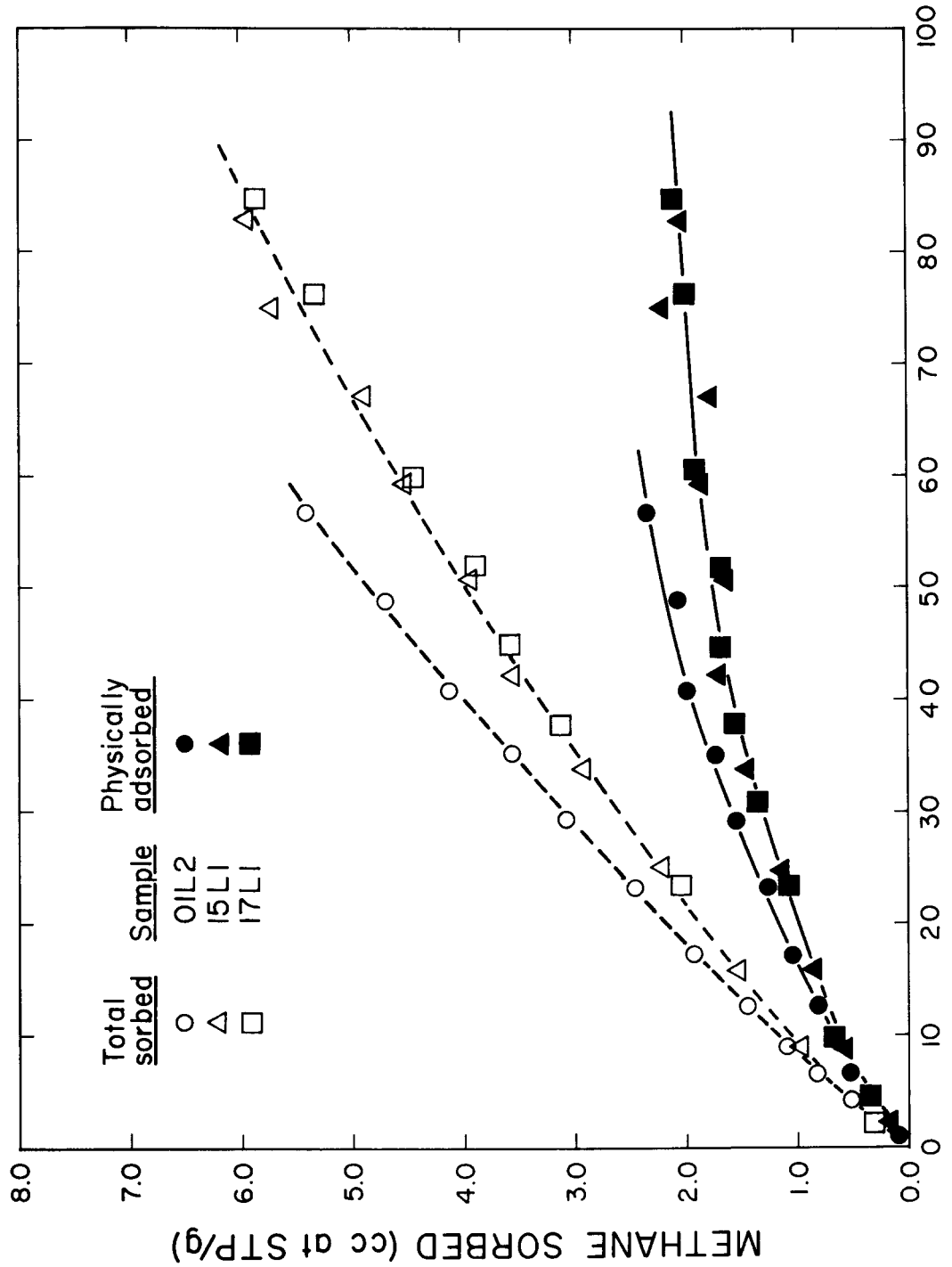

FIG. 1 - METHANE SORPTION ISOTHERMS AT 28°C

CHEMICAL AND ISOTOPIC COMPOSITION OF GAS FROM DEVONIAN BLACK SHALE CANNED CORE SAMPLES, MARTIN COUNTY, KENTUCKY AND WISE COUNTY, VIRGINIA[1/]

George E. Claypool and Charles N. Threlkeld
U. S. Geological Survey
Denver, Colorado

ABSTRACT

Core samples of Devonian Black Shale from Martin County, Kentucky and Wise County, Virginia were canned at the well-site. After outgassing in the cans for periods of 3 to 4 months, the amount and chemical composition of the gas, and the stable carbon isotope ratio of the methane in the gas was measured.

The Black Shale interval in Martin Co., KY yields from 0.03 to 0.6 ft^3 (STP) of methane per ft^3 of rock, with an average of 0.25 ft^3/ft^3. At Wise Co., VA the same rock unit yields from 0.1 to 2.2 ft^3/ft^3 of methane, with an average of 1.2 ft^3/ft^3. The gas from the Martin County core contains about 35 percent of the heavier hydrocarbon homologs (ethane, propane, butanes, etc.) in the hydrocarbon phase, and has isotopically lighter methane (weighted average $\delta^{13}C$= -52 per mil vs. PDB). The gas from the Wise County core contains only about 10 percent heavy hydrocarbons and has methane with average $\delta^{13}C$ of -43 per mil. Gas produced from wells completed in the Devonian Black Shale at nearby localities has the same isotopic composition of methane, but systematically lower contents of heavy hydrocarbons.

These differences in the amounts and compositions of the gases are due to the marked difference in temperature history at the two localities. This difference in temperature history is suggested by present depth of burial and published conodont alteration and coal rank studies in the overlying rocks. The difference in thermal maturity is confirmed by geochemical analyses such as thermal analysis which indicates that the solid organic matter (kerogen) has evolved to an early post-mature stage at Wise County, while it is just mature at Martin County. The original nature of the organic matter at these localities is believed to have been the same.

INTRODUCTION

Core samples of dark gray, black, and brown shales of middle to upper Devonian age have been obtained for study by the U. S. Geological Survey from the localities in Martin County, Kentucky and Wise County, Virginia, shown in Figure 1. The objective of this study is to understand the distribution and occurrence of natural gas and other petroluem originating in the Devonian Black Shale sequence, in terms of the geological processes responsible for the original nature and chemical transformation of sedimentary organic matter in these rocks. The approach employed in this study is to determine relationships between solid organic matter and gas and liquid hydrocarbons, in terms of the physical, chemical and isotopic composition of the various carbonaceous phases. The immobile, solid organic matter is more easily studied than the ephemeral gases and light liquids. If the relevant qualitative and quantitative relationships between solid and gaseous organic matter can be determined in a limited number of cases representing a sufficient range of geological

[1/] This report is preliminary and has not been edited or reviewed for conformity with U. S. Geological Survey standards and nomenclature.

circumstances, then the regional distribution of the type and amount hydrocarbons can be more reliably inferred on the basis of measurements of the solid organic matter alone. In this paper we report the results of analyses of gas and solid organic matter in originally similar rocks from two localities which have undergone different thermal histories. We believe that these localities represent intermediate and high degrees, relative to the thermal history of the entire Devonian Black Shale sequence in the Appalachian basin.

Core samples were canned at the well-site, shortly after removal from the core barrel, core reassembly and initial description. The Martin County samples were sealed in cans during the period October 25 to November 4, 1976 and opened for analysis during the period February 7-14, 1977. The Wise County samples were canned during April 22 to 30, 1977 and opened on June 29 and 30, 1977.

Sampling was random at fixed intervals (50 ft) over the cored part of the sequence at Martin County. Darker shales were preferentially selected at Wise County, where the sample interval was most frequently about 30 feet, but ranged from 11 to 70 feet within the cored intervals.

ANALYTICAL PROCEDURES

The canned core samples were analyzed according to the general procedure outlined in Figure 2. The cans were punctured and the pressure measured by a pressure gauge and a mercury manometer. About 30 ml of gas was withdrawn from the cans and used to fill a 25.0 ml sample loop, by which the gas was valved into a gas chromatograph. The gas was separated on a 0.64 cm x 8.7 m column (packed with Chromosorb 102) into the components air, CO_2, and C_1-C_5 alkanes, and measured by a thermal conductivity detector. The methane (and occasionally ethane) peaks were collected in a gas-tight syringe as they exited from the detector, and injected into a high vacuum combustion system where the hydrocarbons were quantitatively converted to CO_2. The stable carbon isotope ratio ($^{13}C/^{12}C$) was measured and calculated as $\delta^{13}C$, per mil relative to the PDB standard. The possibility of fractionation during gas chromatographic separation was checked and eliminated by repeat analyses of 99+% pure tank methane, with and without preparative gas chromatography.

After chemical and isotopic analysis of the free gas, the cans were weighed and average can weights, volumes, and rock density (2.62 g cm^{-3}) were used to estimate volumes of gas given off by the rock under these conditions. The cans were opened and the core samples subdivided as shown in Figure 2. Of the other analyses shown in Figure 2, only the organic carbon and thermal evolution analysis (TEA-FID) are discussed in this report.

For organic carbon and thermal analysis, a clean piece of core weighing about 200 g was crushed to about 1 cm in a jaw crusher, and a 10 g aliquot of this material was crushed to a nominal 100 mesh grain size in a Bico pulverizer. The finer crushed rock was analyzed for organic carbon by a wet oxidation technique [Bush, 1970]. TEA-FID was performed in the manner described by Claypool and Reed (1976), except that the response of the flame ionization detector (FID) was calibrated by analysis of known amounts of eicosame (n-C_{20}) coated at 4.24 per cent on alumina.

RESULTS

The computed amounts of the common gaseous compounds present in the canned core samples are given in Table 1, in STP gas volume: rock volume ratios (i.e., ml/ml, ft^3/ft^3, etc.). Also given are the qualitative measurements-- $\delta^{13}C$ of methane and the fractional proportion of methane relative to total hydrocarbons in the gas.

In general, about five times as much gas was recovered from the Wise County core samples, compared to those from Martin County. The typical quantities of methane correspond to 1.3 and 0.26 ft^3/ft^3, respectively. Within each core there is a fairly wide range of gas contents (0.1 to 2.2 ft^3/ft^3 at Wise County, 0.03 to 0.6 ft^3/ft^3 at Martin County).

There is a distinct difference in the isotopic and chemical composition of gas in core samples from the two localities. In Wise County $\delta^{13}C$ values for methane range from -36 to -45 per mil and the weighted average is -43 per mil. In Martin County $\delta^{13}C$ ranges from -35 to -54 per mil and the weighted average is -52 per mil. The gas from Wise County is distinctly drier, or lower in ethane and heavier hydrocarbon homologs, compared with the gas from Martin County. Weighted average methane contents relative to total hydrocarbons are 89% at Wise County and 65% at Martin County.

Gas samples were also collected from flowing wells producing from the Devonian Black Shale sequence in the same region. Results of analyses of these samples are shown in Table 2. The isotopic composition of methane in the gas produced from wells is nearly identical to that of representative canned core samples from nearby localities (location of wells sampled shown in Figure 1). However, the gas from the wells has much lower contents of heavy hydrocarbons.

In addition to analysis of gas given off by freshly sealed core samples, we have also made preliminary analysis of the bulk organic constituents of the rock. These results are given in Table 3 for core samples from the Martin County and Wise County wells. The following measurements are reported: (1) organic carbon, in weight percent (a measure of the total organic matter content of the rock); (2) pyrolytic hydrocarbon yield, in weight percent (the total integrated response of the flame ionization detector when the sample is heated in a flowing stream of helium at 40 °C/ min from room temperature to 700 °C); (3) volatile hydrocarbon content, weight ppm (the portion of the integrated detector response during the heating period from room temperature to 320°C); (4) the ratio of pyrolytic hydrocarbon yield to organic carbon, in percent (a measure of the convertability of the organic matter to hydrocarbons); (5) temperature of maximum pyrolysis yield, in °C (the heating temperature at which the maximum in the second peak occurs, representing the pyrolysis of solid organic matter).

The basic interpretation of this type of thermal analysis is illustrated in Figure 3, a typical TEA-FID thermogram. The three basic parameters quantified are total area, area from 0 to 8 min (30 to 320°C), and the temperature of maximum pyrolysis yield or the position of peak II with respect to heating temperature.

The variability in terms of organic richness for the entire Devonian Black Shale sequence is illustrated in Table 3. From a resource standpoint we are primarily interested in the richer shale intervals, i.e. those which contain one percent or more organic carbon. If samples containing less than one percent organic carbon are eliminated from consideration, the average organic carbon content of the Devonian Black Shale sequence is the same (3.0 percent) at the two localities. In effect, limiting consideration to samples with greater than one percent organic carbon compensates for the bias introduced when lighter-colored rocks were selected against in the sampling of the Wise County core.

The results of thermal analysis show that Martin County samples have higher absolute organic richness in terms of both pyrolytic hydrocarbons and volatile hydrocarbons. In contrast, the Wise County samples, although similar in terms of organic carbon richness, have lower contents of pyrolytic and volatile hydrocarbons.

When pyrolytic hydrocarbon yield is normalized by organic carbon content, a numerical expression is obtained for the degree of convertability of organic matter to hydrocarbons upon pyrolysis. This relative hydrocarbon yield is a function of the elemental chemical composition of the organic matter, primarily hydrogen content. This expression, pyrolytic hydrocarbon/organic carbon ratio, is plotted against the temperature of maximum pyrolysis yield in Figure 4.

In terms of relative hydrocarbon yields more of the organic matter can be converted to hydrocarbons in the Martin County samples (average 41%) than in the Wise County samples (4%).

DISCUSSION

The uniform nature of organic-rich intervals of the Devonian Black Shale sequence in terms of clay mineralogy, presence of authigenic minerals such as pyrite and siderite, and other properties indicate that these rocks are the product of depositional conditions which were quite similar over a widespread area. Similarly, it is likely that the original nature of the organic matter was also highly uniform throughout the part of the Appalachian basin under consideration. We believe that the observed differences in terms of the amounts and composition of the gas, and the behavior of the solid organic matter upon pyrolysis are almost entirely due to differences in depth of burial, which presumably controlled the thermal history. Present depths of burial are given in Table 3. The deepest samples are 3379 feet at Martin County and 5471 feet at Wise County. Maps published by deWitt (1975) indicate that the overburden rocks are of upper Paleozoic (post-Devonian) age. Maximum depth of burial probably took place at the end of the Paleozoic.

These depths suggest that the Wise County locality was buried deeper than the Martin County locality, with an overburden of about 6500 ft. of sedimentary rock of upper Paleozoic age. The Martin County core has about 3000 ft. of upper Paleozoic overburden. Other indicators of temperature history confirm the regional variation of thermal maturity suggested by overburden

thickness. A map of isocarbs (lines of equal fixed carbon content) for coals in the Appalachian basin [Postley, 1935] shows that the Martin County and the Wise County localities are on the 58% and 65% isocarbs, respectively. More recently, Epstein and others (1977) have published conodont alteration maps which show the same general pattern of variation as fixed carbon in coals. These regional differences in thermal maturity are consistent with the geochemical variations observed between the two localities.

In Figure 4, a proposed pathway of thermochemical evolution of organic matter in Devonian Black Shales is shown as a stippled pattern. This diagram can be used to evalute the general composition and thermal maturity of the bulk organic matter in sedimentary rocks. With increasing depth of burial (temperature-time) a given type of organic matter would evolve along the pathways shown in Figure 4, in terms of the thermal analysis parameters.

We assume that the original nature of the organic matter in the Devonian Black Shales was about the same at the two localities. However, because of differences in depth of burial and temperature history, the samples from Martin County still have hydrocarbon-generating potential remaining, while this potential at Wise County is largely spent. The difference in hydrocarbon yield upon pyrolysis could be due to differences in the original nature of the organic matter, however the higher temperatures of maximum pyrolysis yield observed for the Wise County samples reflect greater degrees of burial metamorphism, which is the most likely cause of the lower hydrocarbon yields. These interpretations have been confirmed by other physical and chemical measurements, such as vitrinite reflectance and analysis of gasoline-range hydrocarbons. The samples from Martin County and Wise County are thus end-members in the spectrum of thermal maturity, for the part of the Appalachian basin studied thus far.

The chemical and isotopic composition of the gas obtained from core samples is also consistent with the observed differences in thermal maturity. The general relationship between composition of natural gas and the maturity of organic matter in sedimentary rocks of Mesozoic and Cenozoic age has been outlined by Stahl (1974, 1975). In general, this relationship is that (1) dry gas containing isotopically light methane (~ -60 ‰) occurs at relatively shallow depths in thermally immature sediments, (2) wet gas with methane of intermediate $\delta^{13}C$ (-45 ‰) occurs at intermediate depths in thermally mature sediments, (3) dry gas with heavy methane (~ -35 ‰) occurs at greater relative depths in thermally post-mature sediments. The gas produced from the Devonian Black Shale sequence is isotopically lighter (enriched in ^{12}C) by about 5 to 10 per mil than natural gases in Cenozoic sediments with the same hydrocarbon composition. The correlation between $\delta^{13}C$ of methane and chemical composition of the gas with the maturity of the organic matter proposed by Stahl (1975) is not strictly applicable in the Devonian Black Shale sequence of the Appalachian basin. Similarly, the "oil deadline" is apparently associated with isotopically lighter methane (about -45 ‰) in this basin, compared with other basins where it has been placed between -38 ‰ and -28 ‰. The "oil deadline" is a concept derived from the carbon-ratio theory (White, 1915) in which there is a degree of thermal maturity above which conditions are unfavorable for the occurrence of liquid hydrocarbons.

As previously noted, the quantities of gas given off by the canned samples from the Wise County locality are about five times greater, on the average, than those from Martin County. The average organic carbon content of the Devonian Black Shale sequence is about the same at the two localities when only samples containing one percent or more organic carbon are considered. The higher yield of gas at the Wise County locality is probably due to a greater degree of conversion of organic matter to methane. If other factors controlling production of gas are equal, the Devonian Black Shale sequence should yield more gas in the areas which have undergone the greatest depth of burial and been exposed to the highest temperature. Conversely, consideration of the Devonian Black Shale for retorting or hydroretorting should be focused on those areas where the rocks have not been deeply buried, and the organic matter retains the potential for generating hydrocarbons when heated.

It is important to note that the gas produced from wells is isotopically identical and chemically similar to the gas given off by the canned shale samples from the same general locality. The increased content of heavy hydrocarbons in the canned rock samples compared to the gas produced from wells is probably an artifact of the different sampling procedures. This similarity indicates that gas produced from the shale originates in those rocks, and has not migrated from some area of more abundant gas generation, such as downdip in the foredeep of the Appalachian geosyncline. This same generalization may not apply to gas produced from sandstone reservoirs with wide lateral continuity.

CONCLUSIONS

The amount and composition of gas given off by canned samples of the Devonian Black Shale sequence has been measured at two localities (Martin County, Kentucky and Wise County, Virginia) and related to the chemical nature of the bulk solid organic matter in the rock. On the basis of these analyses, we conclude:

1. Because of relatively shallow depth of burial and lower temperatures, the organic matter in the Devonian Black Shale at Martin County has undergone only partial conversion to methane and other hydrocarbons.

2. The Devonian Black Shale sequence was subjected to deeper burial and higher temperatures at Wise County, and consequently the organic matter (including heavy hydrocarbons) show more complete conversion to methane.

3. Gas content per volume of rock is about five times higher at Wise county than it is at Martin County because of this more complete conversion of organic matter (including hydrocarbons) to methane.

4. If other factors regarding the commercial occurrence and production of gas are about equal, that part of the Black Shale sequence which has undergone higher temperature history should be given preference in attempts to discover or stimulate natural gas production.

5. That part of the Black Shale sequence which has not undergone deep burial is most favorable as a raw material for the retorting or hydro-retorting of hydrocarbons.

6. Gas produced from the Devonian Black Shale sequence is indigenous (i.e., not migrated); however, gas produced from sandstone reservoirs above and below the Black Shale may be the product of extensive lateral migration.

REFERENCES

Bush, P. R., 1970, A rapid method for determination of carbonate carbon and organic carbon: Chem. Geol., v. 6, p. 59-62.

Claypool, G. E., and Reed, P. R., 1976, Thermal-analysis technique for source-rock evaluation--Quantitative estimate of organic richness and effects of lithologic variation: Am. Assoc. Petroleum Geologists Bull., v. 60, no. 4, p. 608-611.

deWitt, W., Jr., 1975, Oil and Gas data from the upper Paleozoic rocks in the Appalachian basin: U. S. Geol. Surv., Invest. Series, Map I-917A (1:250,000).

Epstein, A. G., Epstein, J. B., and Harris, L. D., 1977; Conodont color alteration--an index to organic metamorphism: U. S. Geol. Survey Prof. Paper 995, 27 p.

Postley, O. C., 1935, Natural gas developments and possibilities east of the main oil and gas fields of Appalachian region: Am. Assoc. Petroleum Geologists Bull., v. 19, no. 6, p. 853-875.

Stahl, W., 1974, Carbon isotope fractionations in natural gases: Nature, v. 251, no. 5471, p. 134-135.

Stahl, W., 1975, Kohlenstoff-Isotopenverhaltnisse von Erdgasen--Reifekennzeichen ihrer Muttersubstanzen: Erdol und Kohle, v. 28, p. 188-191.

White, David, 1915, Some relations in origin between coal and petroleum; Washington Acad. Sci. Jour., v. 5, no. 6, p. 189-212.

Table 1. Gas volume, composition, and stable carbon isotope ratio of methane in hydrocarbon gas accumulated in canned core samples, Devonian Black Shale sequence, Wise County, Virginia and Martin County, Kentucky.

Depth feet	Sample net weight grams	Air	CO_2	CH_4	C_2H_6	C_3H_8	i-C_4H_{10}	n-C_4H_{10}	C_5H_{12}	C_1/C_{1-5}	$^{13}C_{CH4}$ ‰ v. PDB
		← volume gas (STP)/volume rock →									
					Columbia Gas Well #20338, Wise Co., Va. 1/						
4887	1631	0.107	0.002	0.841	0.180	0.029	0.002	0.001	0.000	0.799	-39.6
4906	2031	0.225	0.008	1.640	0.172	0.024	0.001	0.001	0.000	0.892	-45.3
4934	1808	0.720	0.019	2.186	0.228	0.029	0.002	0.002	0.000	0.894	-44.9
4968	2212	0.557	0.005	0.107	0.007	0.001	0.000	0.000	0.000	0.930	-44.4
5241	1509	0.933	0.500	1.558	0.109	0.010	0.001	0.001	0.000	0.928	-44.6
5252	1801	0.679	0.035	0.947	0.087	0.008	0.000	0.000	0.000	0.909	-44.0
5282	2067	0.485	0.040	1.557	0.130	0.011	0.001	0.001	0.000	0.916	-44.1
5312	1682	0.622	0.018	1.044	0.163	0.016	0.001	0.001	0.000	0.853	-40.6
5341	2058	0.080	0.003	1.010	0.106	0.009	0.000	0.000	0.000	0.898	-43.2
5372	1704	0.047	0.005	0.847	0.129	0.011	0.000	0.000	0.000	0.858	-38.3
5401	1448	0.127	0.009	1.239	0.149	0.012	0.000	0.000	0.000	0.885	-40.7
5471	1806	0.027	0.002	0.823	0.124	0.010	0.000	0.000	0.000	0.859	-36.4
					Columbia Gas Well #20336, Martin Co., Ky. 2/						
2479	1650	1.07	0.012	0.207	0.068	0.020	0.002	0.005	0.002	0.683	-52.4
2529	1532	1.39	0.008	0.104	0.023	0.012	0.000	0.002	0.001	0.734	-51.5
2579	1827	0.81	0.008	0.025	0.009	0.005	0.001	0.001	0.001	0.582	-36.7
2629	2218	0.48	0.007	0.041	0.018	0.013	0.001	0.005	0.005	0.503	-41.9
2679	2043	0.54	0.009	0.073	0.029	0.018	0.001	0.004	0.002	0.570	-34.6
2739	2123	0.28	0.012	0.218	0.071	0.038	0.002	0.008	0.005	0.640	-48.7
2779	1841	----	-----	-----	-----	-----	-----	-----	-----	-----	-----
2829	1362	1.32	0.018	0.056	0.022	0.014	0.001	0.003	0.002	0.572	-48.8
2879	1522	0.70	0.029	0.295	0.097	0.055	0.003	0.014	0.009	0.623	-50.1
2979	1362	1.05	0.032	0.532	0.162	0.096	0.006	0.028	0.019	0.632	-53.5
3029	1679	0.89	0.003	0.483	0.142	0.076	0.005	0.020	0.012	0.655	-53.1
3079	1241	1.43	0.028	0.592	0.176	0.093	0.005	0.023	0.014	0.657	-52.6
3129	1156	2.06	0.081	0.178	0.045	0.024	0.001	0.005	0.004	0.694	-50.6
3179	1545	1.04	0.050	0.072	0.010	0.004	0.000	0.001	0.000	0.825	-52.2
3229	1716	1.09	0.006	0.028	0.005	0.003	0.002	0.001	0.001	0.689	-51.6
3279	1613	0.72	0.018	0.203	0.075	0.045	0.002	0.010	0.007	0.593	-48.7
3329	1548	1.01	0.012	0.592	0.171	0.092	0.004	0.021	0.012	0.664	-54.6
3379	1210	1.16	0.011	0.531	0.169	0.098	0.005	0.022	0.013	0.633	-53.9

Constants used for all calculations:
can volume = 1450 ml
rock density = 2.62 g/ml
ambient temp = 298°K
----- = not analyzed

1/ location: 37°00'38"N 82°41'15"W

2/ location: (Carter Grid coordinates) 16-P-85, 2750' F.N.L., 1650' F.W.L.

Table 2. Chemical and isotopic composition of gas produced from Devonian Black Shale sequence, Martin County, Kentucky and Dickenson County, Virginia.

Locality	Chemical composition volume percent									
	Air	Co_2	CH_4	C_2H_6	C_3H_8	$i\text{-}C_4H_{10}$	$n\text{-}C_4H_{10}$	C_5H_{12}	$C_1/C_{1\text{-}5}$	$^{13}C_{CH4}$ o/oo
Dickenson Co., Va.[1/]	1.68	0.26	95.53	2.43	0.09	0.003	0.003	0.000	0.974	-43.8
Martin Co., Ky.[2/]	1.35	0.06	77.62	13.35	5.91	0.32	0.92	0.48	0.787	-53.0

1/ The Pittston Co. #32, Well #9759, Dickenson Co., Va., depth = 5,356 feet.

2/ Columbia Gas Co., Martin Co., #107, E. B. Paine Farm; depth = 2,723 feet.

Table 3. Organic carbon and thermal analysis of core samples, Devonian Black Shale sequence.

Depth ft.	Organic Carbon wt. %	Pyrolytic Hydrocarbon Yield wt. %	Volatile Hydrocarbon Content ppm	Pyrol. HC / Org. C. %	$T_{peak\ II}$ °C
		Wise Co., Virginia			
4887	6.17	0.45	1,000	7.3	520
4906	3.61	0.16	470	4.5	500
4934	3.35	0.15	470	4.5	506
4968	0.21	0.010	20	4.8	560
5241	1.08	0.013	40	1.2	502
5252	1.03	0.015	50	1.5	500
5282	1.45	0.035	110	2.4	528
5312	1.85	0.050	150	2.7	534
5341	2.59	0.057	150	2.2	512
5372	3.77	0.11	270	2.9	496
5401	3.61	0.14	230	3.9	538
5471	4.92	0.18	360	3.7	520
		Martin Co., Kentucky			
2479	2.89	1.22	1,130	42.3	476
2529	0.43	0.055	52	12.8	479
2579	0.54	0.11	140	19.6	474
2629	0.22	0.012	20	6.1	480
2679	2.96	1.20	1,430	40.5	473
2739	1.14	0.47	790	40.8	474
2779	1.40	0.65	1,070	46.3	472
2829	0.23	0.027	30	12.0	476
2879	2.48	1.19	2,040	48.1	474
2979	3.75	1.75	2,710	46.7	472
3029	4.35	1.88	3,330	43.1	472
3079	4.19	1.72	2,660	41.1	472
3129	0.41	0.052	77	12.9	472
3179	0.19	0.004	6	2.3	488
3229	0.12	0.005	7	4.5	483
3279	1.48	0.43	570	29.1	466
3329	4.24	1.46	1,530	34.5	470
3379	3.82	1.54	2,710	40.4	472

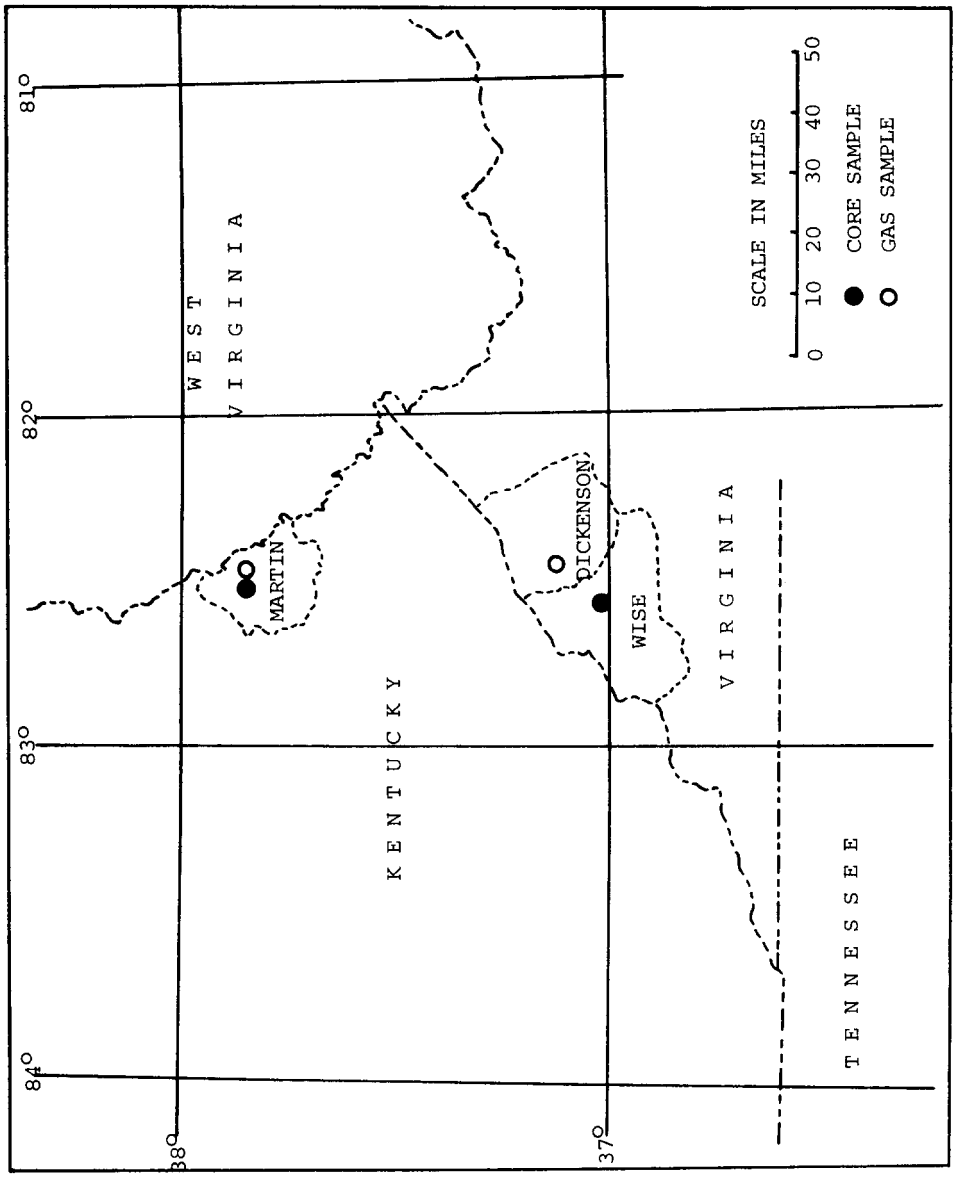

Figure 1. Map showing location of wells where core samples of Devonian Black Shale were collected and canned, and where gas samples from flowing wells were obtained.

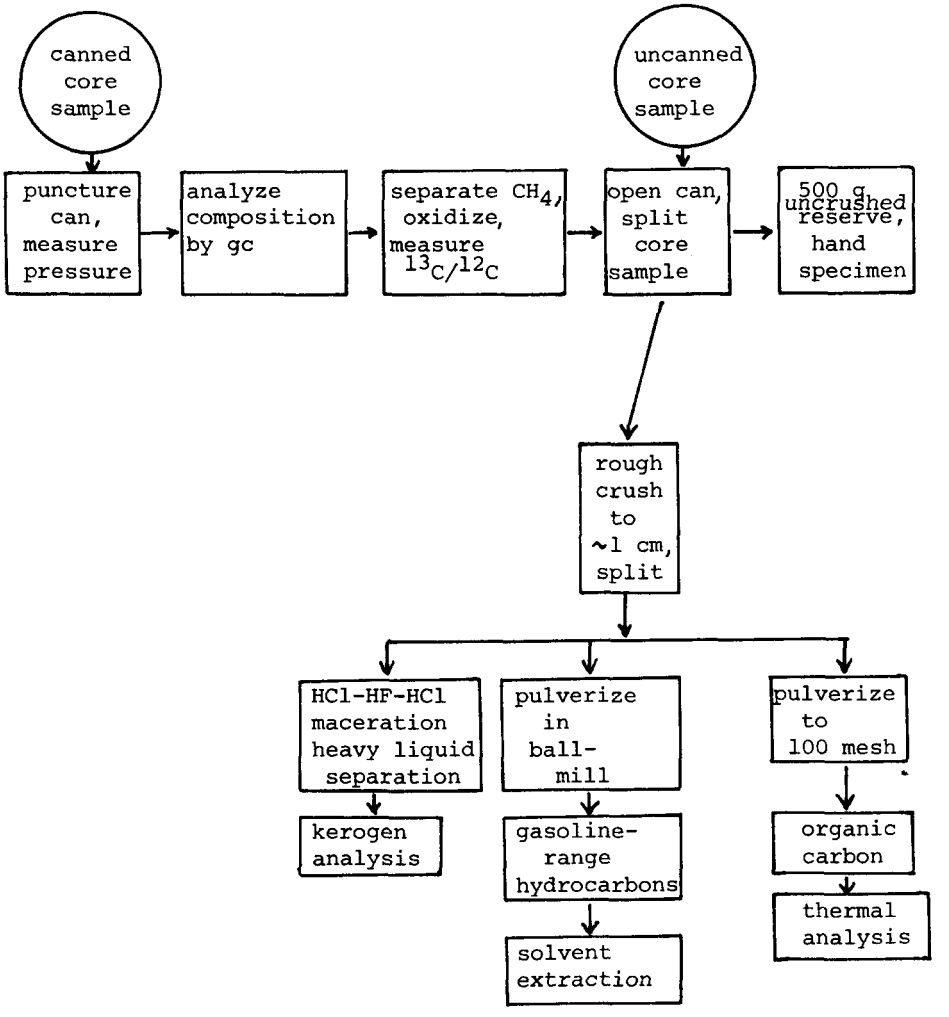

Figure 2. Flow chart illustrating scheme of analytical operations performed by U. S. Geological Survey on samples of Devonian Black Shale.

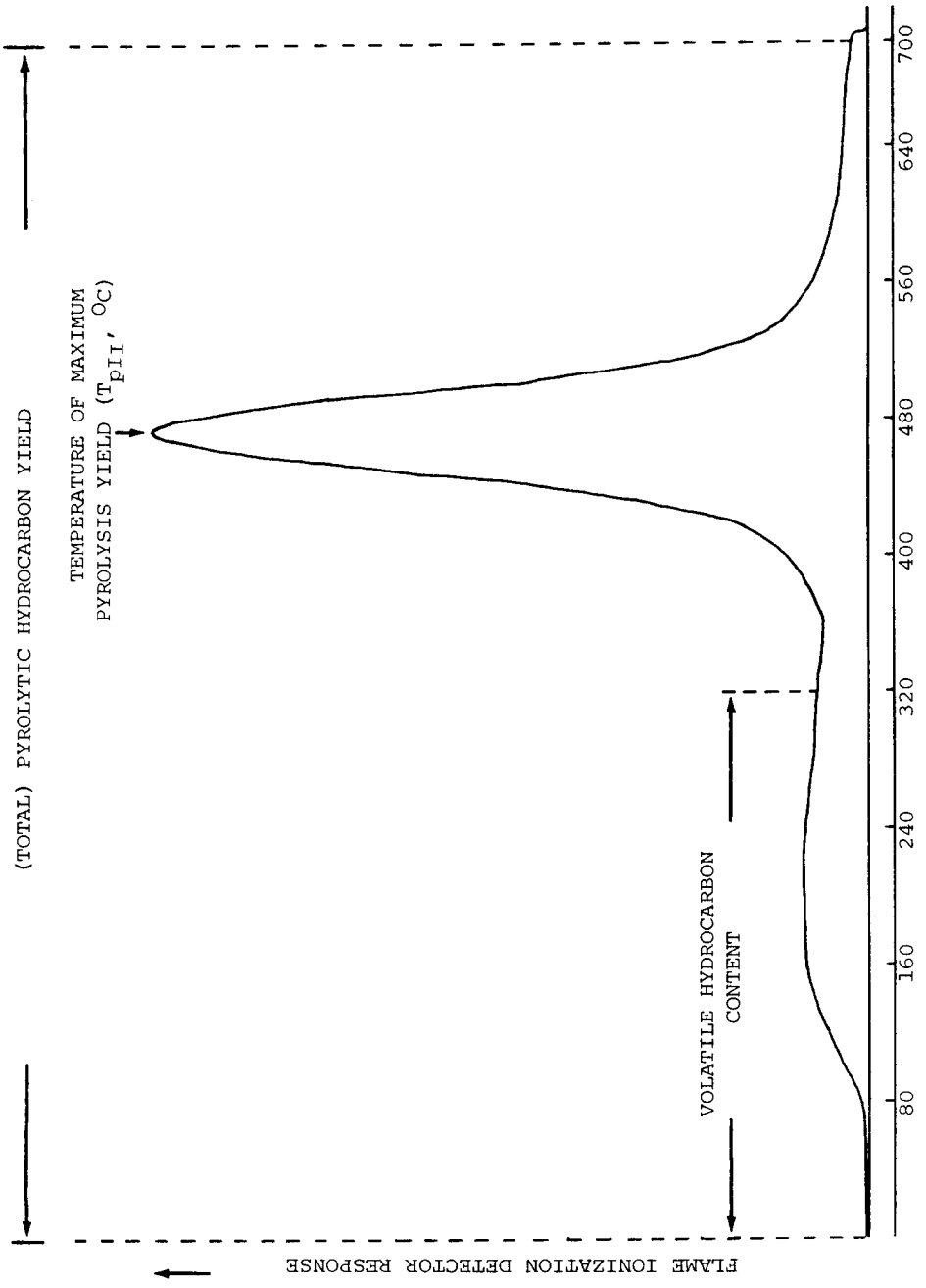

Figure 3. Typical thermogram produced by thermal evolution analysis-flame ionization detector (TEA-FID), with the three numerical parameters (two areas, one temperature) which are extracted from analysis indicated as labeled.

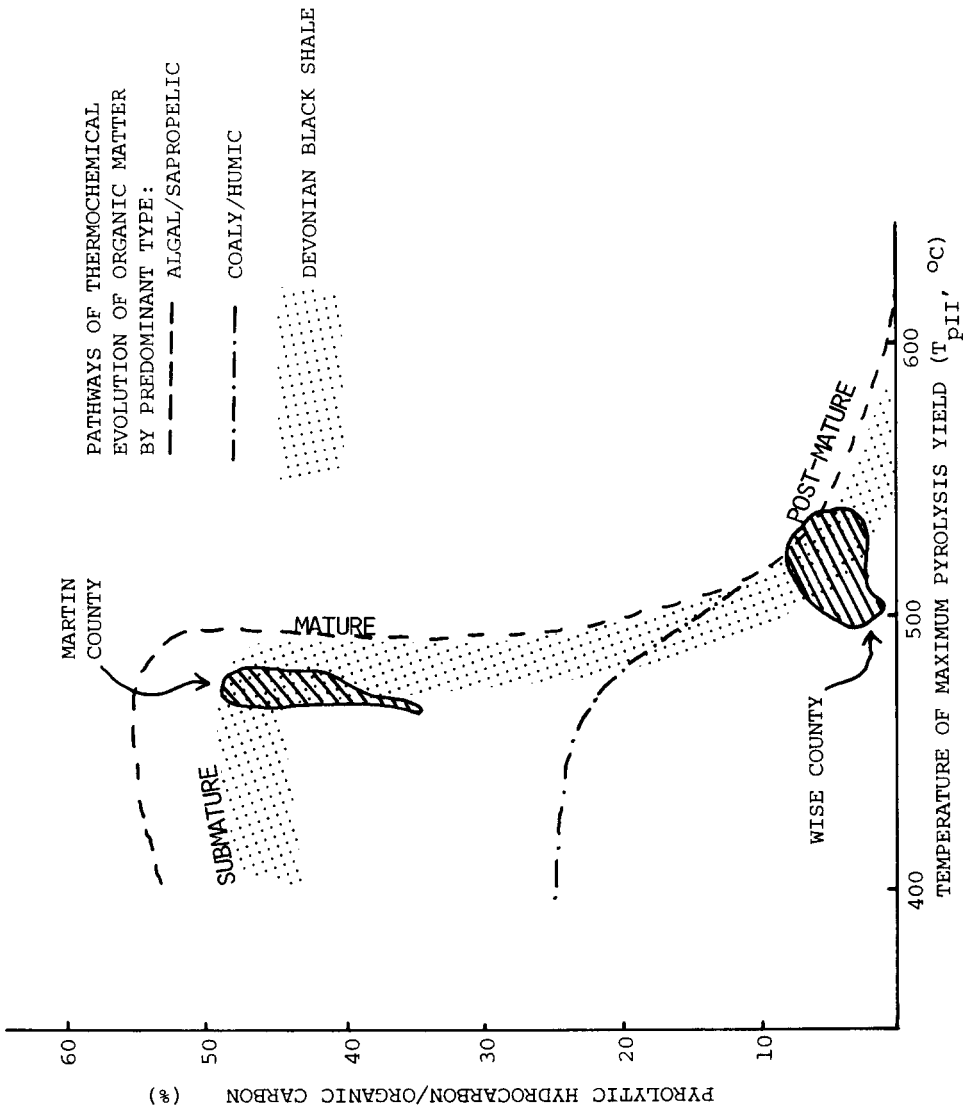

Figure 4. Diagram illustrating the interpretation of the type of organic matter and thermal maturity based on TEA-FID and organic carbon analysis. Pathways of thermochemical evolution of different types of organic matter are indicated.

THE RELATIONSHIP OF THERMODYNAMIC AND KINETIC PARAMETERS TO WELL PRODUCTION IN DEVONIAN SHALE

by

Paul D. Schettler, Jr.
Dale L. Wampler
Philip J. Sipling
Donald J. Mitchell

Juniata College
Huntingdon, Pennsylvania 16652

ABSTRACT

A mathematical model describing production of gas from wells in Devonian shales is introduced, and the extent of agreement with existing productivity data is discussed. Parameters needed for this model include the diffusion constant of gas through the rock and the sorption isotherms of gas within the rock. Methods and results of measurements of these important parameters made in our laboratories are described and discussed.

INTRODUCTION

This paper reports the results of efforts to model in the laboratory the process by which natural gas is released from tight formations (such as Devonian shales). The instrument for these studies is an apparatus in which a shale sample is initially equilibrated at some constant gas pressure; after equilibrium is reached, the pressure on the sample is suddenly changed and the rate and amounts of gas produced are monitored. The conceptual similarity of this laboratory process to the degassing of an underground reservoir is reflected in the similarity of gas loss curves produced in the laboratory with production rate curves of actual wells, except for differences in gas evolved and the time scale of evolution.

It is generally accepted that optimum production occurs in wells drilled into highly fractured areas. These fractures serve as conduits between the gas-producing rocks and the well bore. Initially, the gas in the fractures is in equilibrium with gas sorbed in the source rock; however, upon intersection of the fracture system by a well bore, the pressure in the fractures drops discontinuously, and the source rock evolves gas until equilibrium is re-established at the new pressure. The mathematical treatment of the rate of diffusion into the well bore as a function of time is thus similar to that of laboratory samples undergoing a discontinuous pressure decrease, the differences lying primarily in questions of geometry, magnitude of rock involved, and size of initial pressure drop.

This paper deals with three main topics. First, the ideas discussed above are presented in quantitative form. It is shown that the diffusion constant of methane in shale and the extent and frequency of fractures collectively are the determining parameters of well production. Of these three factors, the first two are particularly amenable to laboratory measurement; the second and third sections of this paper deal with efforts in this regard.

THEORETICAL

The purpose of this section is, first, the mathematical description of the underground processes that lead to gas production from tight formations and, second, the comparison of that description to the mathematical description of the degassing of rock in laboratory configurations.

2 THE RELATIONSHIP OF THERMODYNAMIC AND KINETIC PARAMETERS TO WELL PRODUCTION IN DEVONIAN SHALE EGS-39

Production from wells in relatively impermeable formations depends upon drilling into highly fractured areas and/or creating them artificially after the well has been drilled. These fractures serve primarily as conduits from the gas-bearing source rock to the well bore. The amount of gas diffusing out of a shale into a fracture (held at a low pressure) is given by [1,2]

$$1) \quad M_T = 2(C_2 - C_0)A\left(\frac{Dt}{\pi}\right)^{\frac{1}{2}}$$

$$\frac{dM_T}{dt} = (C_2 - C_0)A\left(\frac{D}{\pi t}\right)$$

where

A is the area of rock degassing.

C_2 is the initial concentration of gas in the rock.

C_0 is the concentration of gas in the rock as $t \rightarrow \infty$.

D is the diffusion constant.

t is the time.

Over a ten year period, for reasonable values of parameters for Devonian shale ($D - 5 \times 10^{-7}$ cm^2/sec, $C_2 - C_0 = 3$ cm^3 gas/cm^3 rock), 40 cm^3 gas (STP) would be produced for each square centimeter of fissure wall area. This amount of gas is clearly much larger than the amount of gas contained between the walls of the average fracture, thus lending support to the concept that the rock is the source of the gas and that fractures serve as conduits. It is interesting to note that the production curve predicted by equation 2) is high production over a relatively short period followed by a long tail. In fact, 32% of the total gas produced over a 20-year period is produced in the first two years, in agreement with some qualitative reports of well production from some producing wells by Roth [3] and Torrey [4]. Whereas initial well production is large, the inverse square root dependence on time implies that after the initial large production reduced production will occur unabated for many years, again in agreement with many reports of the longevity of gas shale wells.

The upper curve of Figure I shows some actual production data points [5] and an inverse square root fit versus time as the solid line. Although the fit for that well is good, it is clear that not all wells display such a simple relationship. In particular, as the lower three curves show, the initial high production rate may, to a variety of degrees, be missing.

Flattened production curves result from a mathematical viewpoint if it is assumed that an additional constriction exists at the surface of a fracture or along the fracture to the well bore that impedes the diffusive process of gas from the bulk rock. Such surface modification would be expected to occur at slickensides wherein an impermeable-looking, glaze-like finish is formed on the rock. Alternatively, mineralization may occur within the fracture, plugging the microporous surface structure of the shale. Constrictive effects along the fracture would be expected when a narrow fracture is "overloaded" by a large gas flow. All of these effects, which might be expected to be common occurrences in actual situations, should result in flattened (and decreased!) well productivity curves.

The lower curves in Figure I are fits taking in account constrictive effects of varying degrees of importance. The equation of fit is

$$2) \quad \frac{dM_T}{dt} = \frac{D(C_2 - C_0)}{g} \exp(z^2)\,\mathrm{erfc}(z)$$

$$z = \frac{D^{\frac{1}{2}}}{g} t^{\frac{1}{2}}$$

Equation 2) has been discussed in detail elsewhere [6].

Briefly, g is a constrictive parameter corresponding to some kind of impermeable coating on the fracture surface. The more impermeable the coating, the larger g is; conversely, for decreasing constrictive effects g approaches zero and equation 2) approaches equation 1). Figure II shows this effect explicitly.

The middle curve is simply the lower curve of Figure I with g = 6.318. The upper and lower curves are with identical parameters (same fracture area, same bulk rock diffusion constant and gas concentration) except that g = 0 and 30 cm for the upper and lower curves respectively. It is clear from Figure II that the effect of constrictions is to decrease markedly total production and flatten it in respect to time.

In contrast to the flattening observed in wells, most laboratory samples will give somewhat steeper curves than predicted by a simple $t^{-\frac{1}{2}}$ law; specifically experimental points will follow equation 1) closely at low t but fall below the theoretical curve at large times. This feature may not be limited to laboratory samples; in fact the points of the most productive curve of Figure I form a slightly steeper curve than the fit shown. The explanation for this phenomenon lies in the geometry of the fractures in the case of a well and the particle shapes in the case of laboratory samples; in fact the applicability of equations 1) and 2) is limited to the case where the depletion zones [6] associated with each fracture do not interfere. As a surface degases, the rock behind the surface becomes depleted to an ever-increasing extent, this zone of depletion initially extending only a short way into the rock but the extension increasing with time. Specifically

$$3) \quad d \cong \sqrt{Dt}$$

where d is the depletion zone mentioned above. When d is much smaller than the dimensions associated with rock fragments or distances between fractures, equations 1) and 2) can be expected to be obeyed. However, as time increases, d increases until it eventually becomes of the order of the fracture or particle dimensions. At this point the depletion zone from one fracture starts to move into areas already depleted by another fracture, and gas production tapers off below that predicted by the $t^{-\frac{1}{2}}$ law.

Exact functions exist and have been utilized for several laboratory degassing situations, as is discussed elsewhere [6,7,8]. Although it would appear from Figure I that geometric effects are not important in wells, they may nevertheless sometimes be detectable. As discussed elsewhere [6] the anomalous steepness of the top curve of Figure I corresponds to a mean distance between fractures of 65 cm. Anomalous steepness and large productivity may thus be linked together as both are indications of production from highly fractured zones.

DIFFUSION CONSTANTS

Diffusion constants and permeability constants are closely related.

$$D = P/K$$

where D is the diffusion constant, P is the permeability constant, and K is the solubility of gas in the rock,

$$C = KP$$

where C is the equilibrium concentration of gas in the rock, and P is the applied pressure. Diffusion (and/or permeability constants) can be measured by determining the rate that gas passes through a cut slab of sample or alternatively it can be deduced from the rate a sample of rock degases. The latter method has the advantages that it is quicker, often taking only a few minutes to get a measurement, and is more closely related to the actual underground degassing process.

In our procedure, we first equilibrate the sample at a constant pressure. For sieved samples, this typically takes less than an hour and is done on the measuring apparatus. For slabs equilibrated to 1 atm methane, the equilibration takes several days and is done before placing the sample on the measuring apparatus. As shown in Figure III, the cell is separated from a carefully calibrated volume [9] by a valve. After measuring the initial equilibrium pressure, the valve is closed, and the volume associated with the buret, etc., changed to a new pressure (typically evacuated). An automatic data-taking routine associated with a NOVA 1220 laboratory computer is started which takes pressure readings from the Datametrics Barocel. Then the valve between the cell and the calibrated volume is opened. The pressure changes resulting are monitored at a data collection rate of 25,000 readings/second for a period of several minutes for particles and about one-half hour for slabs. The pressure changes which occur after the initial pressure drop are due to the degassing of the sample. The amount of gas given off follows (initially) a $t^{\frac{1}{2}}$ law whose slope is interpretable in terms of the diffusion constant as discussed earlier for wells. The detailed procedures for slabs and particles are somewhat different, and the details are discussed elsewhere [7,8].

Table I shows results obtained at a variety of depths from Well #20403 drilled by Columbia Gas Corporation in conjunction with the Eastern Gas Shales Project. The average methane diffusion constant is 6.56×10^{-7} cm^2/sec with a standard deviation of $\pm 4.18 \times 10^{-7}$ cm^2/sec. This range represents the approximate range of diffusion constants within the Devonian shale sequence (at the Lincoln County well, etc.). There is a dependence of the diffusion constant upon the temperature and/or type of gas used. For example, our 77°K N_2 diffusion constants average 2.3 times the ice temperature methane constants although individual comparisons can deviate from this figure. There is a dependence of diffusion constant upon particle size. For data reported elsewhere [8], N_2 diffusion constants at 77°K for 500-700 μ averaged 4.5 times the value for 175-350 μ mesh size. As a general rule, work on slabs supports this contention. A sample at 3886' 2-4" gave a diffusion constant of 2.5×10^{-7} cm^2/sec for 175-350 μ mesh size, 15.4×10^{-7} cm^2/sec for 500-700 μ mesh size, and 116.1×10^{-7} cm^2/sec for a slab of shale at 3886' of dimensions 27.88 cm^2 by .72 cm thick. This size effect can be accounted for by two possible mechanisms. It may be that highly impermeable components of shale fracture more easily into material of smaller mesh size. The second possibility is that the grinding process decreases the number of microfractures or other zones of weakness associated with high diffusivity by cleaving along, hence eliminating them. Our data supports the second hypothesis; the first hypothesis would suggest that slab diffusion would be intermediate between large and small particles, an effect which has not been observed to date. Further, there is no obvious difference between the large particles and the small ones as observed under an optical microscope.

The effect of manner of sample preparation may have some effect upon results. Table II shows an increase of diffusion in samples prepared by percussion mortar. Optical examination suggests that the samples prepared by ball mill are abraded more than samples prepared by percussion mortar. If this is the case, diffusion of samples prepared by percussion mortar ought to be more representative of "bulk shale" than those prepared by ball mill. Table III shows a very interesting effect observed with slabs. The first and third samples show a methane diffusion for slabs that is some 4.5 times larger than for particles from the same shale. However, the second sample of Table II shows a slab diffusion that is only 15% of the particle diffusion. This surprising result may be understood in terms of surface preparation. Before making the measurements, the slab surfaces are ground down by peeling the surface down with a chisel. Whereas usually this results in a dull-looking surface, for the anomalous result in question a shiny, impermeable-looking, slickenside-like surface resulted. We believe that the effect of rubbing with a chisel on this sample was to produce a thin impermeable layer that lowered the rate of outgassing by about a factor of 40 over that produced from surfaces split by a percussion mortar. Work on this tantalizing but speculative area is continuing.

ISOTHERMS

The value of the determination of isotherms is at least twofold. First, it allows the estimation of concentration of gas in the rock surrounding a well given only the initial wellhead pressure. In this sense an isotherm plays the same role as porosity in standard oil technology. However, the concept of an isotherm is more general because it is a measure of all gas in the rock, that in open pores, that adsorbed on the surface of minute clay particles, and that dissolved in some kerogen or other material entrained in the rock. Some practical implications of this have been discussed elsewhere [10]. The second value of an isotherm is that it permits, at least to some degree, the determination of which of these mechanisms of entrainment are operative--open porosity, adsorption, or solution. More discussion on this point has been made elsewhere [11].

Figure IV shows some typical isotherms, showing the degree of entrainment of ethane, methane, argon and helium, all on the same sample. It should be noted that these isotherms are all straight lines within this region and hence can be associated with a "porosity." However, the porosity calculated from each gas is different, corresponding to 40%, 13%, 7%, and 3%, for C_2H_6, CH_4, An, and He respectively. As this makes no physical sense for open pores, one can only conclude that what is measured is an "effective porosity" which includes substantial amounts of adsorption and/or solution. A corollary to this is that the most appropriate measure of porosity to be associated with natural gas production is "methane porosity" obtained by direct measurement of amount of methane sorbed as a function of pressure.

In addition to the data reported in Reference 14, we have measured room temperature isotherms for the 17 samples in Table I. If it is assumed that helium sorption is due only to penetration of the open pores, the straight line He plots can be reinterpreted in terms of a helium density (wt. of sample/volume of unpenetrated samples). Helium densities average ~.04 g/ml higher than bulk densities corresponding to an average porosity of 1%. The vol. gas/ vol. rock/torr for methane given in

Table I is that in excess of that associated with the pore volume (as determined by the He isotherms). It is useful to note that the methane isotherms slopes are grouped around 3.27 x 10^{-4} vol. methane/vol. rock/torr (±42%) even though an effort was made to include a variety of lithologies in the 17 samples included in Table I.

In addition to room temperature isotherms, we have also determined isotherms of N_2 determined at liquid nitrogen temperatures. The value of this measurement is several-fold. First, if one assumes that the kerogen freezes to an impermeable solid at liquid nitrogen temperatures, then any sorption that takes place must be adsorption on the various surface areas associated with the small particles of clay minerals. Under these conditions a standard BET analysis is possible [13]. We find good fits to the BET isotherm which lends support to the adsorption model (at least at low temperatures) and results in a determination of the surface area available for adsorption. For shale samples that we have measured, this varies from a few tenths to several meters squared per gram [14]. This is a small fraction of the surface area associated with clay minerals (illite is 92 m^2/g [15]), but nevertheless sufficient to show that sufficient adsorptive capacity exists within Devonian shales to account for the amounts of methane observed.

In Table I, we have shown the nitrogen BET surface areas in terms of the volume of gas that would be required to cover the available surface area with a monolayer. This should represent the maximum amount of methane that can be adsorbed onto surface areas within the rock, as significant multilayer adsorption of methane would not be expected at temperatures present in the ordinary well.

A major point of interest concerns the degree of correlation between the isotherm parameters of Table I and the amount of gas found in the rock. We received the 17 samples reported in Table I in sealed cans along with about 213 other samples taken at 10-foot intervals down the well. After a wait of 142-156 days, the atmosphere in the cans was analyzed for O_2, N_2, CH_4, C_2H_6, C_3H_8, CO_2, H_2, and H_2S by gas thromatography [17,18]. The results for the 17 samples of Table I is summarized in Table IV. Several features are worthy of note. First, there is no close correlation between the parameters of Table I and gas content. In particular, gas content ranges over several orders of magnitude from sample to sample wherein the parameters of Table I are relatively constant. This may be expected because the isotherms of Table I essentially measure the capacity for gas content as a function of pressure. Since these remain relatively constant from strata to strata and gas content varies, it is concluded that the original gas pressure in the rock must vary considerably in various parts of the well. A consequence that follows from this is that even over geologic time the thermodynamic equilibrium of methane does not seem to be reached even in strata as close together as about 50 feet.

Several other features of Table IV include the observation that often the desorption of hydrocarbons is closely correlated with approximately equimolar adsorption of nitrogen and oxygen originally present in the can at sealing time so that the total pressure remains constant. Oxygen nitrogen ratios vary from can to can and are generally too high to account for the loss of air by can leakage; this suggests some kind of molecule-for-molecule displacement mechanism. Methane, ethane, and propane usually appear in decreasing amounts in concordance with the observations of other investigators [19,20]. Finally, gas production seems relatively well correlated with the appearance of black shale as noted by the well site core description, although this is certainly not a hard and fast rule.

CONCLUSIONS

A major conclusion would seem to be that the isotherm and diffusion parameters are not sensitive functions of depth or lithologic type of Devonian shale at least in the vicinity of the #20403 well. If this holds for other locations as well, this means that averaged parameters can safely be used in well modeling studies of the type discussed in the introduction -- a great simplification.

Apparently even relatively close layers of rock within the Devonian shale sequence are not in equilibrium with each other in respect to the chemical potential of hydrocarbon gases. More work needs to be done in this area; in particular we are interested in measuring the diffusion constants of slabs cut parallel to the bedding planes. A practical consequence of non-equilibrium is that the well bore becomes a mechanism by which equilibrium can be obtained. Gas from an outgassing region can be trapped by an adsorbing region; thus it is lost to production. The possible magnitude of this effect is under study in our laboratories.

Finally it seems possible to reach some speculative conclusions pinpointing the slickenside nature of many natural fractures as a source of slow well production. Fits to at least some available production data point to the presence of slickensides or some similar localized constriction in the

passage of gas from the source rock to the well bore. This correlates with comments of various personnel involved with cataloging natural fractures [21] that most natural fractures are slickensided or mineralized. At the moment, pinpointing slickenside formation as a major culprit in the observed constrictive effects is supported by a single laboratory measurement. This is not to imply that slickensided fractures are detrimental to production (total production is the sum of the production from each fracture), but rather that the removal of constriction from existing fractures will itself raise production significantly. Work on the role of slickensides in well constriction and their possible removal is continuing.

ACKNOWLEDGMENT

The authors wish to thank the Energy Research and Development Administration under whose auspices this work was accomplished under Contract No. E(40-1)-5197. In addition, the authors wish to thank D. Steven Hench, Eugene Boden, Martha Linton, Jay Nelson, Eric Jensen, Sharon Steckbeck, and Linda Hoeflich, who collected much of the data.

REFERENCES

1. Schettler, P., Wampler, D., Mitchell, D., and Russey, W., "Degasification of Devonian Shales," ERDA Symposium on Devonian Shales, Morgantown, W. Va., 1976.
2. Crank, J., The Mathematics of Diffusion, Oxford Press, London, 1956.
3. Roth, E. E., "Natural Gases of the Appalachian Basin," in Natural Gases of North America, Beebe, B. W., Ed., AAPG, 1968.
4. Torrey, P. D., "Summary of Natural Gas Fields of New York and Pennsylvania," in The Geology of Natural Gas, Ley, H. A., Ed., AAP, 1935.
5. Bagnall, W. D., and Ryan, W. M., "Geology, Reserves, and Production Characteristics of the Devonian Shales," Morgantown, W. Va., 1976.
6. Schettler, P., "Gas Production in Shale Wells; Constrictive and Geometric Effects," ORO-5197-1, prepared by Juniata College under Contract No. E(40-1)-5197 for USERDA, 1976.
7. Jensen, E., Steckbeck, S., Schettler, P., "Diffusion Constants in Devonian Shale," in ORO-5197-1 (see Ref. 6).
8. Schettler, P., "The Measurement of Diffusion Constants Associated with Sorption/Desorption from Slabs of Shale," in ORO-5197-2, Study of Hydrocarbon-Shale Interaction, Progress Report #2, prepared by Juniata College under Contract No. E(40-1)-5197 for USERDA, 1976.
9. Jensen, E., Schettler, P., "Calibration of the Sorption Studies Apparatus," in ORO-5197-1 (see Ref. 6).
10. Schettler, P., "The Relationship of Methane Isotherms to Well Production," in ORO-5197-3, Study of Hydrocarbon-Shale Interaction, Progress Report #3, prepared by Juniata College under Contract No. E(40-1)-5197 for USERDA, 1977.
11. Jensen, E., "Comparative Adsorption Isotherms of Gas-Bearing Devonian Shales," in ORO-5197-2 (see Ref. 8).
12. Jensen, E., Schettler, P., "Room Temperature Isotherms as a Function of Gas and Temperature on Core Samples from Well #20403 in Lincoln County, West Virginia," in ORO-5197-3 (see Ref.10).
13. Brunauer, S., Emmett, P. H., and Teller, E., J. Am.Chem. Soc., 60, 309 (1938).
14. Jensen, E., Schettler, P., "Isotherms of Devonian Shales," in ORO-5197-1 (see Ref. 6).
15. Nelson, R. A., and Hendricks, S. B., "Specific Surface Areas of Some Clay Minerals, Soils, and Soil Colloids," Soil Sci., 56, 285 (1944).
16. Hoeflich, L., Jensen, E., Wampler, D., Schettler, P., "Analysis of Hydrocarbon Gas from Cores of Well #20403, Lincoln County, West Virginia," in ORO-5197-1 (see Ref. 6).
17. Jensen, E., Schettler, P., "Analysis of Hydrocarbon Gases from Cores of Well #20336, Martin County, Kentucky, and Tristar #1 Well in Effingham County, Illinois," in ORO-5197-3 (see Ref. 10).
18. Schettler, P., Wampler, D., Mitchell, D., Sipling, P., ORO-5197-4, Study of Hydrocarbon-Shale Interaction, Progress Report #4, prepared by Juniata College under Contract No. DY-76-S-05-5197, 1977.
19. Snyder, J., Schorr, J. R., "3rd Technical Progress Report," Battelle Laboratories, ORO-5203-3, prepared under Contract No. E(40-1)-5205 for USERDA (1977).
20. Zielinski, R. E., "Physical and Chemical Characterization of Devonian Gas Shale," Mound Laboratory, prepared under U. S. Government Contract No. EY-76-C-04-0053, 1977.
21. Private communication, Eric Smith, Columbia Gas Service Corporation, for example

TABLE I. DIFFUSION AND ISOTHERM PARAMETERS, Well #20403, Lincoln County, West Virginia

Sample I.D.	Corrected Depth	Bulk Density (g/cm^3)	He Density (g/cm^3)	Isotherms: Initial Slope 0°C (Vol Gas/Vol Rock/Torr x 10^{-4}) CH_4	Isotherms: Surface Area (Vol Gas/Vol Rock) N_2 @ 77°K	Diffusion Constants (cm^2/sec x 10^{-7}): CH_4 @ 0°C	Diffusion Constants (cm^2/sec x 10^{-7}): N_2 @ 77°K	Well Site Core Description
2736' 2-4"	2736' 2-4"	2.75	2.53	4.70	6.20	3.98	12.8	Med. gray-green laminated silty shale
2806' 2-4"	2808' 2-4"	2.61	2.57	6.12	3.15	4.95	15 6	Med. dark gray silty shale
3096' 2-4"	3101' 2-4"	2.51	2.68	2.84	1.63	14.1	7.75	Med. to dark gray shale
3136' 2-4"	3141' 2-4"	2.70	2.70	3.28	5.90	3.35	11.5	Dark gray shale
3156' 2-4"	3161' 2-4"	2.61	2.70	3.52	4.94	9.87	12.9	Dark to med. gray shale
3281' 2-4"	3291' 2-4"	2.85	2.91	1.72	4.45	14.4	14.1	Med. to dark gray shale
3396' 2-4"	3407' 2-4"	2.68	--	3.32	--	5 06	8.19	Med. gray shale with black shale bands
3416' 2-4"	3428' 2-4"	2.65	2.56	3.35	.730	2.90	12.7	Very dark gray & black banded shale
3426' 2-4"	3438' 2-4"	2.37	2.56	3.82	1.30	3.90	8.72	Black shale
3446' 2-4"	3458' 2-4"	2.46	2.667	3.46	.690	3.25	22.0	Black shale
3456' 2-4"	3468' 2-4"	2.58	2.59	3.01	1.53	11.5	10.0	Med. gray shale
3496' 2-4"	3509' 2-4"	2.40	2.57	2.18	.71	6.91	11.5	Black shale
3716' 2-4"	3733' 2-4"	2.67	2.73	1.81	5.51	5.36	20.1	Blue gray & black laminated shale
3836' 2-4"	3855' 2-4"	2.60	2.73	1.66	4.90	3.61	28.9	Blue gray shale
3896' 2-4"	3914' 2-4"	2.68	2.58	2.02	4.69	5.05	30.0	Med. gray & dark gray laminated shale
4006' 2-4"	4026' 2-4"	2.67	2.62	2.53	5.21	10.7	18.2	Laminated dark gray and gray green shale
4026' 0-2"	4046' 0-2"	2.41	2.47	6.30	.559	1.35	12.6	Black shale

TABLE II. COMPARISON OF TYPE OF GRINDING

	Ball Mill	Percussion Mortar
Sample I.D.	3446' 2-4"	3446' 2-4"
Corrected Depth	3458' 2-4"	3458' 2-4"
Bulk Density (g/cm^3)	2.46	2.46
Isotherms--		
He Density (g/cm^3)	2.47	2.67
Initial Slope 0°C		
(Vol Gas/Vol Rock/Torr x 10^{-4}) CH_4	3.31	3.46
Surface Area (Vol gas/Vol Rock) N_2 @ 77°K	1.40	.690
Diffusion Constants (cm^2/sec x 10^{-7})--		
CH_4 @ 0°C	2.59	3.25
N_2 @ 77°K	6.91	22.0
Well Site Core Description	Black shale	Black shale

TABLE III. DIFFUSION OF CH_4 IN SLABS AT 0°C

Sample I.D.	Corrected Depth	Diffusion Constant (cm^2/sec x 10^{-7})	Well Site Core Description	Slab Surface Description
2736' 2-4"	2736' 2-4"	12.5	Med. gray-green laminated silty shale	Dull
3426' 2-4"	3438' 2-4"	.589	Black shale	Shiny
3836' 2-4"	3855' 2-4"	22.0	Blue gray shale	Dull

TABLE IV. OUTGASSING RESULTS, Volume of Gas Per Unit Volume of Rock

Sample I.D.	V_{CH_4}	$V_{C_2H_6}$	$V_{C_3H_8}$	V_{CO_2}	V_{O_2}	V_{N_2}
2736' 2-4"	.028	0	0	0	-.06	.08
2806' 2-4"	0	0	0	0	-.06	.07
3096' 2-4"	.127	.04	0	0	-.135	-.03
3136' 2-4"	.09	.03	0	0	-.09	.02
3156' 2-4"	.08	.04	0	0	-.1	0
3281' 2-4"	.06	.02	0	0	-.05	.05
3396' 2-4"	.200	.05	.02	0	-.15	-.11
3416' 2-4"	.740	.246	.154	.157	-.473	-.53
3426' 2-4"	.565	.215	.139	0	-.26	-.65
3446' 2-4"	.704	.242	.158	0	-.29	-.54
3456' 2-4"	.270	.078	.040	0	-.14	-.15
3496' 2-4"	.12	.047	.016	0	-.072	-.11
3716' 2-4"	.004	0	0	0	-.04	.02
3836' 2-4"	0	0	0	0	.005	-.005
3896' 2-4"	.265	.073	.02	0	-.12	-.001
4006' 2-4"	.37	.12	.025	0	-.24	-.01
4026' 2-4"	1.37	.523	.239	0	-.30	-.18

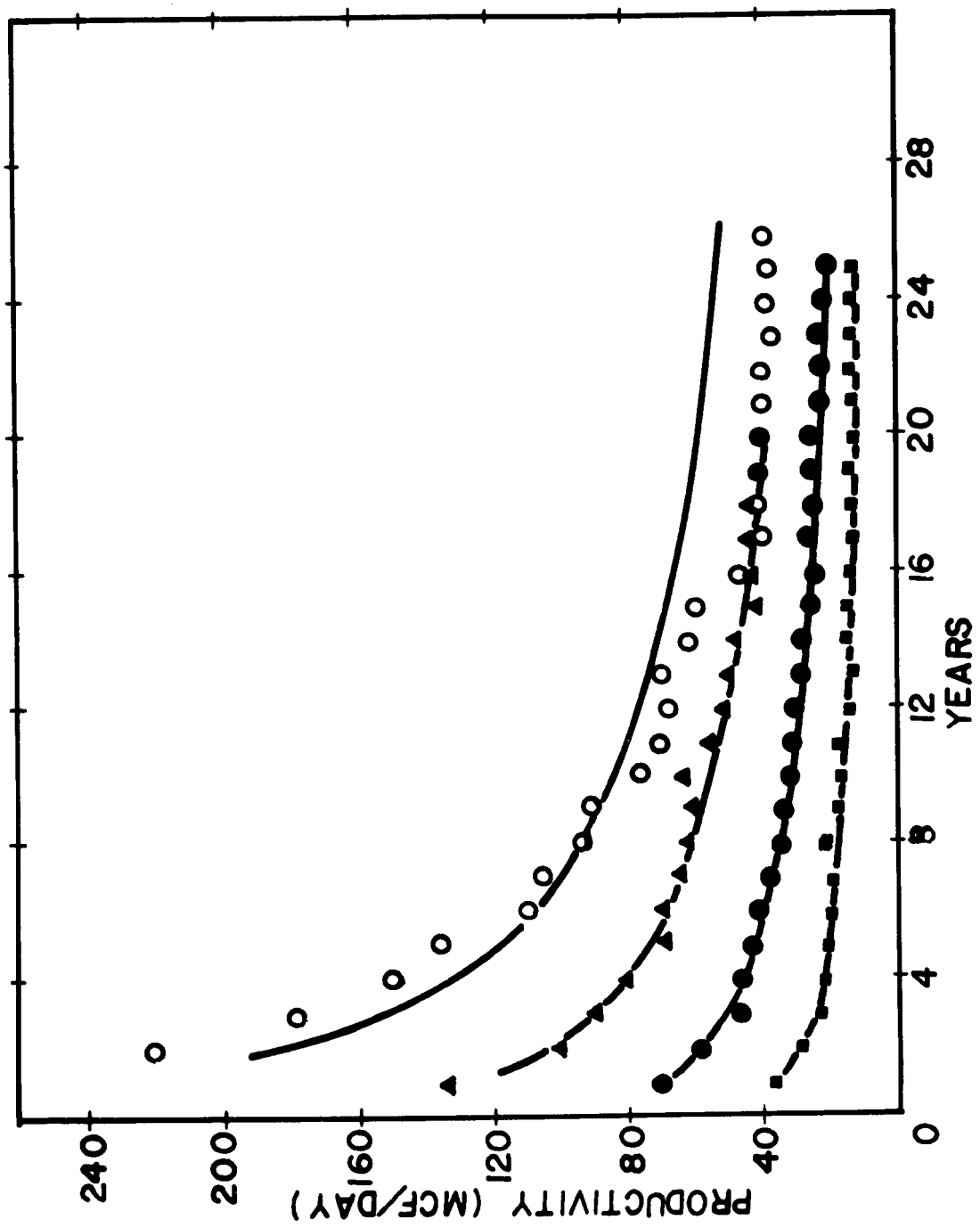

Size (meters^2) x 10^{11}	g (cm)
1.21	0
.845	4.79
.506	6.02
.254	6.32

FIGURE 1. Flow rate (million cubic ft/da.) is plotted against time (years). Data is from Ref. 5. The lines are fits as described in the text. Values of the parameters are as follows from upper to lower curves:

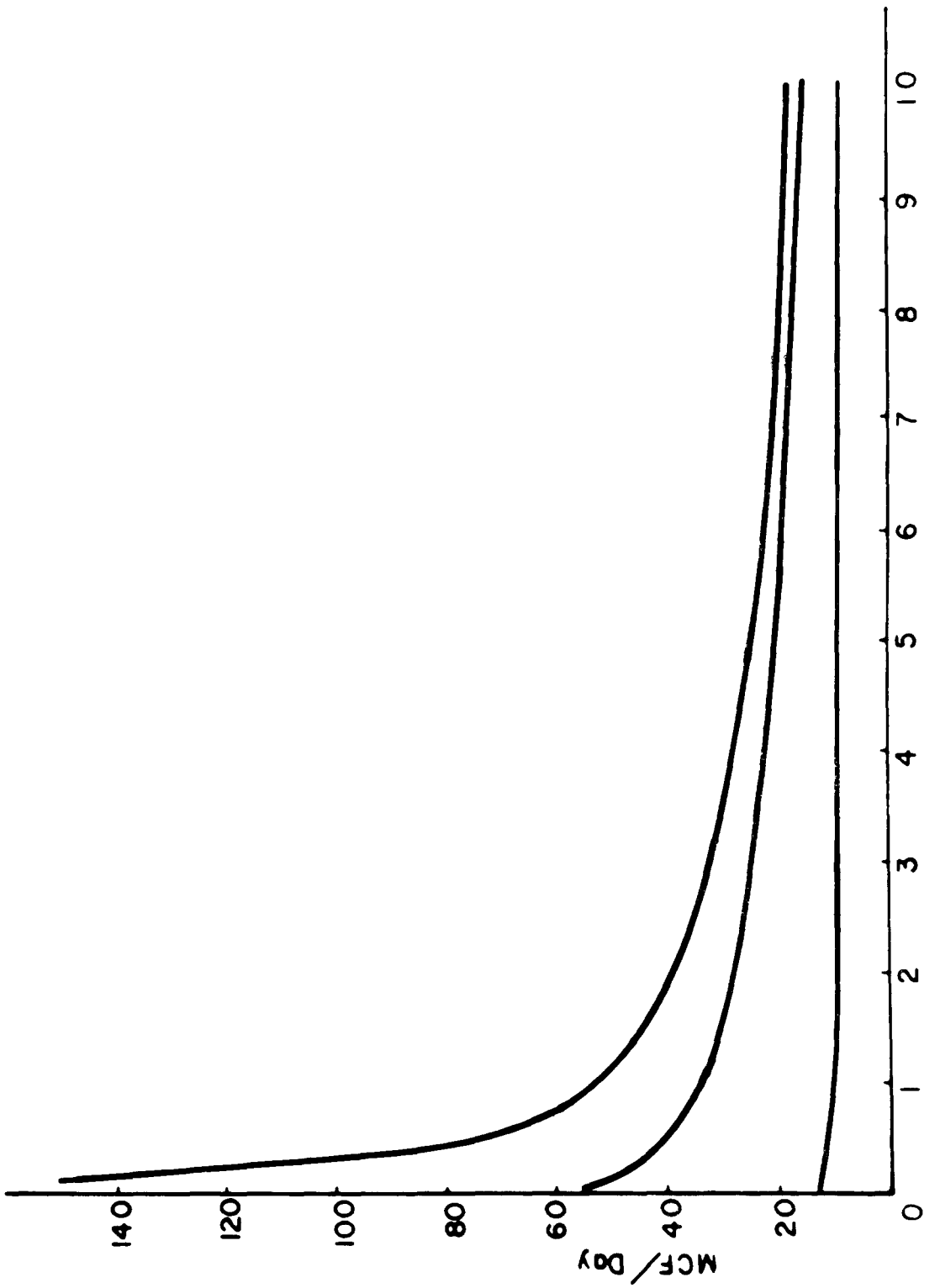

FIGURE II. The effect of localized constrictions on well production. The lower curve shows production from a well with a high degree of localized construction. In the upper curves these constrictions are progressively removed. Note that production increases and shifts to lower times.

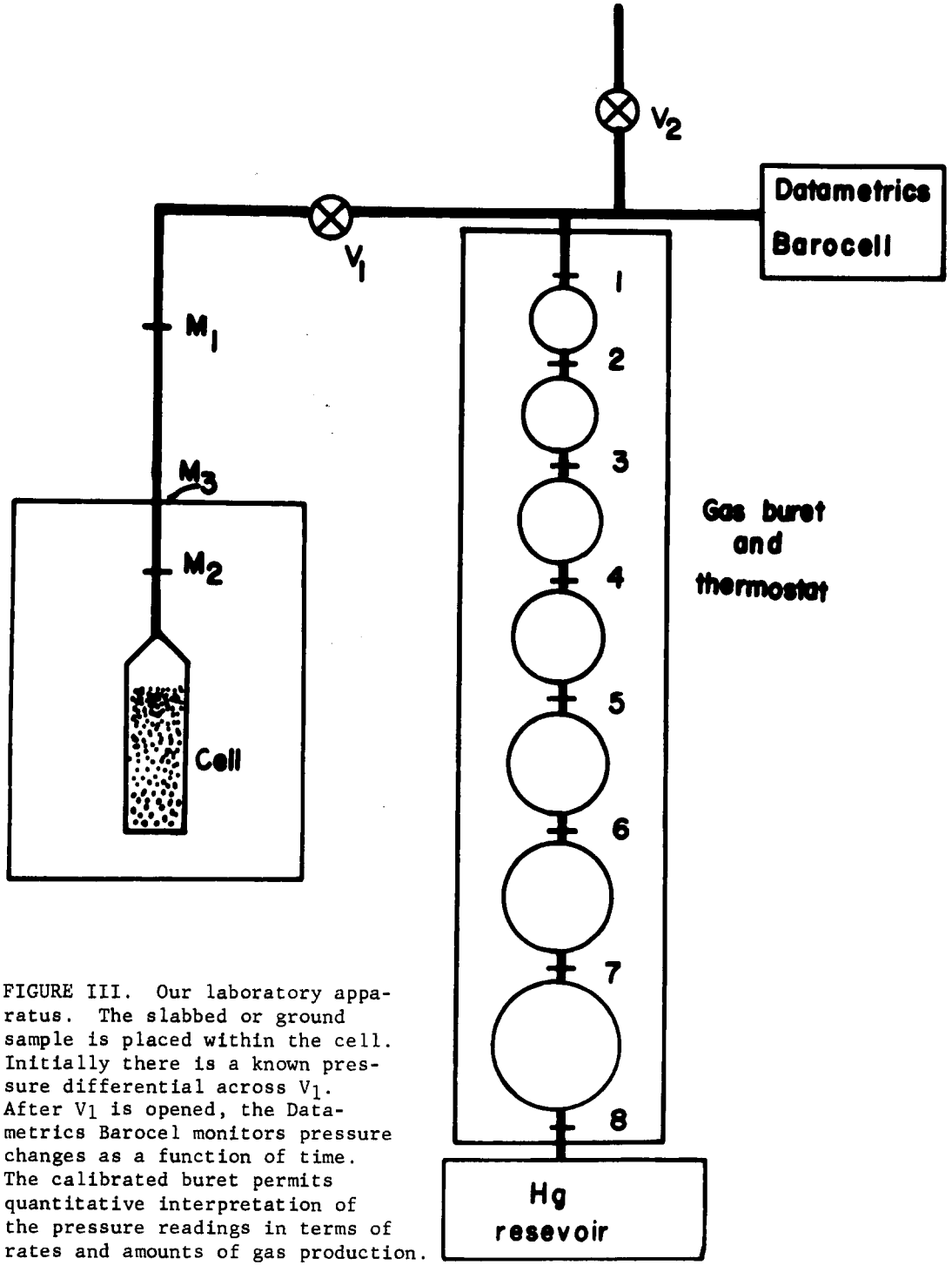

FIGURE III. Our laboratory apparatus. The slabbed or ground sample is placed within the cell. Initially there is a known pressure differential across V_1. After V_1 is opened, the Datametrics Barocel monitors pressure changes as a function of time. The calibrated buret permits quantitative interpretation of the pressure readings in terms of rates and amounts of gas production.

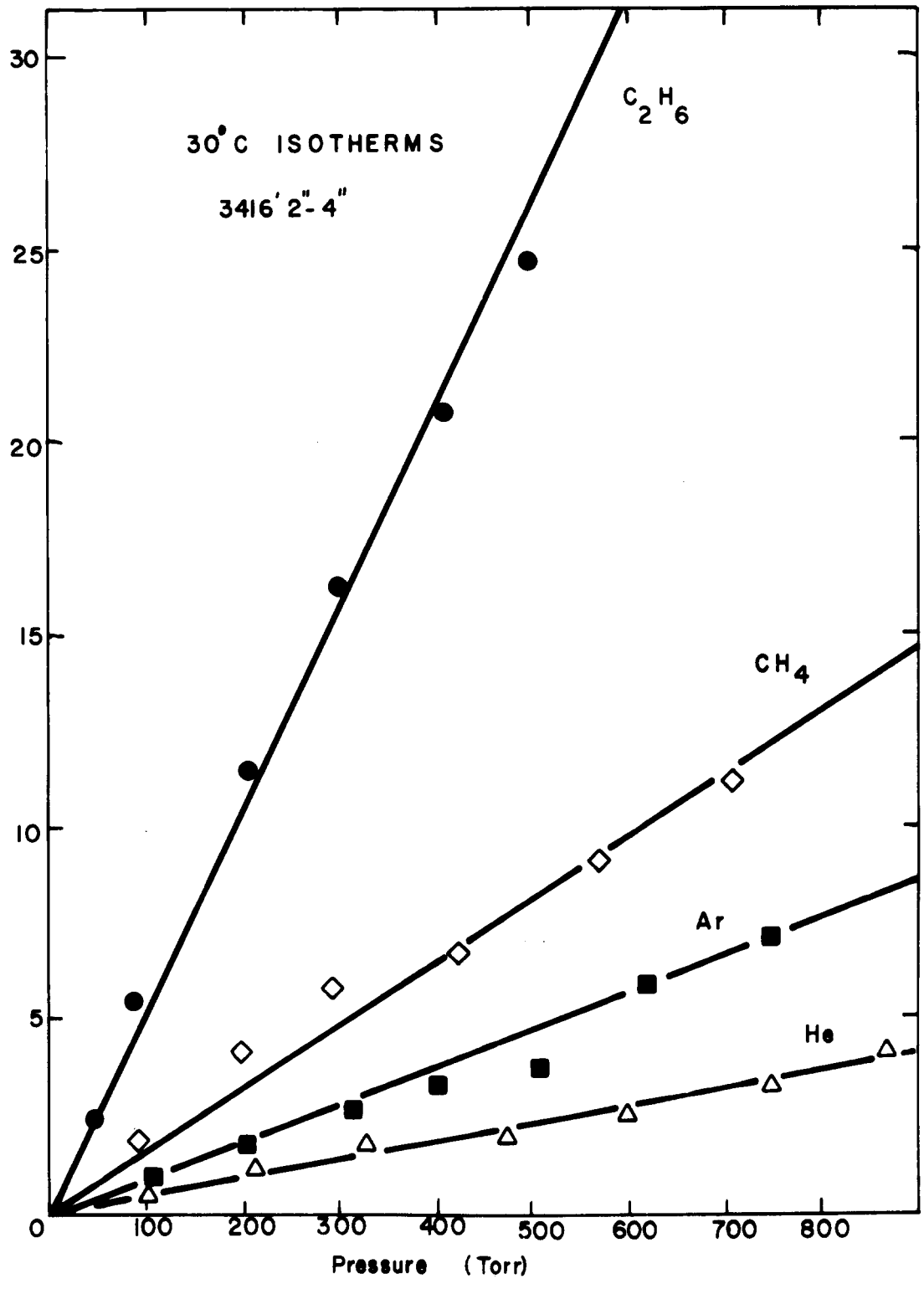

FIGURE IV. Moles of various gases sorbed on a 5.6 gram sample as a function of pressure at 30°C. The slopes correlate well with the molecular polarizabilities suggesting a simple adsorption mechanism for entrainment of gas in the rock.

CONODONT COLOR ALTERATION, AN ORGANO-MINERAL METAMORPHIC INDEX, AND ITS APPLICATION TO APPALACHIAN BASIN GEOLOGY

by

ANITA G. HARRIS

ABSTRACT

Conodonts are apatitic marine microfossils of Cambrian through Triassic age. During incipient metamorphism (50°-300°C) they change color from pale yellow to brown to black due to carbon-fixing within the trace amount of organic matter in their skeletons. As thermal metamorphism continues (300°-550°C), conodonts change from black to gray to white to crystal clear as a result of carbon loss, release of water of crystallization, and recrystallization. The conodont color alteration technique provides a unique link between mineral and organic indexing of thermal metamorphism and is best suited for carbonate rocks.

Conodont color alteration index (CAI) isograd maps for three stratigraphic intervals in the Appalachian basin show: 1) Conodont color alteration is directly related to the depth and duration of burial and the geothermal gradient. 2) Tectonics affect color alteration only where folding and faulting act to significantly increase depth of burial. 3) Isograds and overburden isopachs are conformable throughout most of the northern half and in the western part of the southern Appalachian basin; in these areas, isograd values gradually increase eastward except for a major disruption in the area of the Rome trough. 4) South of central Virginia, isograds are disrupted and irregular because late Paleozoic thrusting has severed and telescoped original burial metamorphism isograd patterns. 5) Basin restoration using conodont CAI isograds indicates a maximum shortening in northeast Tennessee of about 115 miles (185 km). 6) The CAI 2 isograd (=brown conodonts) for each stratigraphic interval lies near the eastern limit of oil production for that interval; this limit shifts eastward for each successively younger stratigraphic interval concomitant with decreasing overburden. 7) Gas production is less related to isograds and depends mostly on primary and (or) secondary porosity and permeability. The CAI 4 isograd (=brownish-black conodonts), however, approximates the eastern limit of gas production because the temperature (depth of burial) necessary to produce this high level of organic metamorphism concurrently produces mineral metamorphism that reduces porosity and permeability and the likelihood of commercial reservoirs.

INTRODUCTION

The thermal level of diagenesis or metamorphism of a rock can be evaluated from its mineral and (or) organic constituents. Incipient to high-grade metamorphic mineral assemblages (50° to +800°C) have been determined for pelitic sedimentary and volcanogenic rocks (Hower, 1976; Turner and Verhoogen, 1960). Identification techniques for determining incipient to high-grade metamorphic mineral facies range from X-ray diffraction analysis of clay minerals to megascopic field identification of porphyroblasts, respectively. The equivalent of incipient to low-grade mineral metamorphic indices (30°-300°C) have been determined for organic materials such as kerogen, vitrinite, and palynomorphs (see Bostick and Damberger, 1971, table 1). Indexing of organic materials is accomplished by means of chemical analysis, spectral fluorescence, reflectance or transluscence photometry, or visual color comparison. Organic indices are generally used for assessing temperatures of less than 300°C, whereas mineral indices are used for higher temperatures. It is noteworthy that the mineralogy and

the depositional and post-depositional environments of pelitic rocks have made them the chief source of most organic and mineral metamorphic indices. For the same reasons, carbonate rocks have been, until now, unsuitable for assessing thermal metamorphism.

A unique link between mineral and organic indexing of thermal metamorphism is provided by the conodont color alteration technique which combines both mineral and organic indexing in one element. This technique is applicable in the temperature range of 50° to 550°C and is best suited for carbonate rocks.

Although most of the earlier work concerning conodont color alteration indexing (Epstein, 1976; Epstein and others, 1977) dealt with the experimental laboratory data that justify the technique, this report deals chiefly with its application, as the experimental data are now published.

Conodonts

Conodonts (fig. 1) are apatitic marine microfossils (generally 0.1-1 mm) that contain trace amounts of organic matter. They are the hard parts of an unknown organic group of worldwide distribution in Cambrian through Triassic rocks and are valuable index fossils for biostratigraphic correlation throughout most of their geologic range. Because of their mineral composition (carbonate apatite according to Pietzner and others, 1968), conodonts are readily recovered from carbonate rocks by organic-acid treatment and are then further concentrated by heavy-liquid and (or) magnetic separation. They readily persist into greenschist metamorphic terranes and have been recovered from marbles interbedded with garnet-mica schists (Schönlaub and Zezula, 1975). Conodonts are most abundant in slowly deposited and (or) hydraulically reworked carbonate or clastic sediments. Though in the laboratory they are most easily extracted and concentrated from carbonate rocks, in the field they are most easily recognized in black shales because of the color contrast between the dull black shale and the vitreous lighter colored conodont (and even more noticeable if the conodonts are weathered and thus chalky white).

Conodont Color Alteration

Unweathered conodonts are pale yellow (fig. 1a-d), light to dark brown (fig. 1e-j), black (fig. 1k, l), opaque white (fig. 1m), and crystal clear (fig. 1n, o); if unweathered and thermally unweathered and thermally unaltered, they are pale yellow (fig. 1a-d). Using controlled time-temperature-pressure experiments with and without water, Epstein and others (1977) have shown that:

1. The sequence of color change from pale yellow to black to white conodonts found in field collections is the same as that produced by heating alone.
2. Conodont color alteration is progressive, cumulative, and irreversible.
3. Color alteration is time and temperature dependent.
4. Pressure neither retards nor accelerates color alteration.
5. In an open system, water neither retards nor accelerates color alteration, but in a sealed system, water in combination with pressure and heat retards color alteration by 50 percent.
6. Color alteration from pale yellow to black probably results from a carbon-fixing process within trace amounts of organic matter in the apatitic conodont. Progressive color alteration from black through gray and opaque white, to crystal clear is the result of carbon loss, release of water of crystallization, and recrystallization.
7. Eight distinct levels of color alteration (termed indices) can be discriminated visually.
8. An Ahrrenius plot of the experimental data and field data indicate that conodont color alteration begins at about 50°C and continues into garnet-grade metamorphism (about 550°C).

In addition, conodont color alteration has been correlated with other optical organic indices and with percent fixed carbon (Epstein and others, 1977; table 1).

APPLICATIONS OF THE CONODONT COLOR ALTERATION INDEX (CAI) IN THE APPALACHIAN BASIN

Conodont CAI as a Geothermometer

The CAI of a conodont sample can be determined by comparing unindexed conodonts with a set of laboratory-produced or field-assembled conodont standards or with a conodont color chart or soil color chip chart. These techniques are described in Epstein and others (1977).

Once a sample is indexed, a temperature range can be determined using an Ahrennius plot of the experimental data of Epstein and others (1977, fig. 3; fig. 2). For example, late Middle Ordovician conodonts from Monterey, Va., in the Valley and Ridge province of the Appalachians, have a CAI value

of 4 to 4.5. The age of the conodonts gives a maximum possible time for burial and heating of 470 m.y., but this can be further refined from a knowledge of Appalachian geology. In this part of the Appalachians, the latest possible time for beginning of unloading by erosion is Middle Triassic. Therefore, 270 m.y. is the maximum possible time for burial and heating, thus providing the lowest possible temperature for conodonts of CAI 4-4.5 (fig. 2, heavy solid lines). Using figure 2 and projecting the 4-4.5 field segment of the 270 m.y.-line to the X axis yields a temperature range of 185°-220°C for these conodonts. If, however, unloading began in the late Pennsylvanian, which is the earliest possible time for unloading in this part of the Appalachians, the maximum time for burial and heating is 210 m.y. (fig. 2, dashed lines), thus a maximum temperature range of 190°-230°C. The total possible temperature range for this samples therefore is 185°-230°C.

This temperature range is compatible with other geologic data. In the vicinity of Monterey, at least 14,300 feet (4,359 m) of rock is known to overlie the Middle Ordovician (fig. 2). If we assume an average geothermal gradient of 1°C per 100 feet, known overburden alone can account for a temperature of 160°C. Thickening and (or) duplication of section by folding and faulting combined with restoration of section missing by erosion could easily account for the additional 30°-70°C. Moreover, Paleozoic rocks in the Monterey area are cut by Cenozoic intrusions which could also indicate a higher than average Cenozoic geothermal gradient.

Conodont CAI Isograd Maps

Conodont CAI isograd maps aid in basin analysis of thickness of overburden, structural history, and oil and gas potential.

The Appalachian basin is an ideal area to test and apply conodont CAI because 1) most of the bedrock is of Paleozoic age, 2) fairly abundant geologic data are available in a basin where geologic investigation has been going on for more than a century, 3) a variety of structural settings are available from near horizontal beds on the north and west to increasingly folded and faulted terrane on the east and south, 4) post-Paleozoic deposits are negligible, 5) igneous activity is negligible, and 6) more than a century of hydrocarbon exploration has broadly outlined the limits of oil and gas production.

Isograd maps were compiled for the Appalachian basin using U.S. Geological Survey collections and many specimens and samples provided by colleagues in universities, state surveys, and the petroleum industry. All collections are from carbonate rocks and almost all are from limestone. Conodonts from noncarbonate rocks were not used, so that variation in host-rock lithology could be neglected.

Because depth (temperature) and duration of burial affect color alteration, conodont CAI isograd maps were compiled for three stratigraphic intervals--Ordovician, Silurian through Middle Devonian, and Upper Devonian through Mississippian. These intervals were chosen because each contains at least one widespread marine carbonate unit.

The best analysis of a conodont CAI isograd map is achieved when used in conjunction with an overburden isopach map. Such maps were compiled for each isograd interval (not shown in this report, but available in Harris and others, in press) using data given in de Witt (1975), de Witt and others (1975), and Miller (1975). In general, in the Appalachian basin, overburden and CAI increase eastward for almost all stratigraphic intervals in post-Middle Ordovician rocks. CAI 1 is in areas having a history of minimal burial, which are along the western edge of the basin. CAI isograd and isopach trends are conformable throughout most of the basin, especially in western and central areas where most of the Paleozoic section is preserved and deformation was minimal.

CAI isograd map for Ordovician rocks (fig. 3).--Conodonts from 60 Lower Ordovician, 318 Middle Ordovician, and 29 Upper Ordovician samples, for a total of 407 localities, were indexed (sample localities are shown in Harris and others, in press). Wherever possible, lower to middle Middle Ordovician collections were used in order to provide as uniform a stratigraphic position as possible. Isograds are drawn on the first occurrence of an index value, so that the 2 isograd passes through localities having conodonts with index values of 1½ to 2.

The consistent westward bulge of Ordovician isograds in Pennsylvania reflects the composite effect of eastward-thickening Silurian through Permian clastic wedges that are superimposed in that area. Here too, as in much of the western and central part of the basin, the relatively even spacing of isograds indicates that the original post-Ordovician overburden patterns are not tectonically disrupted. One major isograd disruption occurs within the central Appalachian basin, in the Rome trough area. Well data indicate higher CAI and isopach values in the trough than to the east or west.

Although data are meager, I have taken the liberty of presenting one possible interpretation of this area, rather than continuing the regional isograd trend through it with most of the data points appearing as anomalous hot spots. Interestingly, isograds in the Rome trough mimic Silurian isopachs (de Witt and others, 1975) as well as structure contours on the top of the Ordovician (Miller, 1975).

South of central Virginia, in the southeastern part of the Appalachian basin, isograds are disrupted and irregular, because late Paleozoic thrusting has severed and telescoped original metamorphic isograd patterns. In some areas tectonic burial by overriding thrust sheets appears to have had little influence on organic metamorphism levels in underlying autochthonous rocks indicating that the allochthonous sheet(s) was not thick enough to raise the metamorphic level of the autochthonous plate. In Tennessee, for example, along the present eastern limit of the basin where surface control is good, isograd trends in Ordovician rocks and the strike of the overriding Great Smoky thrust sheet (carrying older rocks of chlorite to biotite grade along its western edge) are discordant. Thrusting from the east can and does place more thermally mature strata over less thermally mature strata to the west. As a consequence, isograds on the surface of a thrust sheet do not necessarily characterize the organic maturity of rock in the autochthonous plate. This relationship is illustrated by the fact that autochthonous rock exposed in windows through the Blue Ridge thrust sheet in Tennessee and in the Pulaski thrust sheet in Virginia are thermally less mature than the overlying allochthonous sheet. Even more striking is the fact that conodonts from a window in the Great Smoky thrust sheet have a CAI of only 2, indicating that these Ordovician carbonate rocks could not have been buried as deeply or reached the same degree of thermal maturity as correlative rocks 10-15 miles (16-24 km) to the west which are exactly the same age but contain conodonts having a CAI of 4. The conodonts that have anomalously low CAI may be from rocks representing the eastern edge of the Appalachian basin, which were thrust westward during a late tectonic event and are now near the depocenter of the basin. Similar anomalies are found in the thrusted terranes east of the main Ordovician outcrop belt in New Jersey and New York.

The isograd map also provides a guide for basin restoration. The CAI 2 and 5 isograds are about 175 miles (280 km) apart in New York (A-A', fig. 3) in an area of little deformation. These isograds bound an area that contained a minimum of 8,000 feet (on the northwest) to 25,000 feet (on the southeast) (2,440-7,625 m) of fill. Depositional patterns and strike appear to have been reasonably consistent throughout most of the basin during the Paleozoic. The distance between the 2 and 5 isograds remains remarkably consistent southward to central Virginia at which point the 5, 4½, and 4 isograds disappear the reappear beneath the Blue Ridge thrust sheet and eastern isograd bands narrow. In the Appalachian basin, the shortest distance between the 2 and 5 isograd is 60 miles (95 km), in northeast Tennessee (B-B', fig. 3), indicating a maximum shortening of the basin in this area of 115 miles (185 km). Using different methods of basin reconstruction, Dennison and Woodward (1963) show a minimum late Paleozoic shortening of 65 miles (105 km) in this same area. Still another estimate of shortening for part of this area is given by Harris (1974). His restoration of an Upper Cambrian stromatolite bank edge indicates 40 miles (64 km) of shortening in the less tectonically disturbed west half of the Valley and Ridge province in northeast Tennessee.

If the geothermal gradient was reasonably consistent throughout the basin (isopach and isograd maps indicate it was), then overburden isopachs could be restored from isograd values in areas of erosion. The 4½ isograd area in eastern Pennsylvania now contains a minimum of 24,000 feet (7,880 m) of overburden which can be used as a base value. Table 1 gives minimum overburden ranges for Ordovician CAI values in the Appalachian basin.

CAI isograd map for Silurian through Middle Devonian rocks (fig. 4).--Conodonts from 43 Silurian and 111 Lower and Middle Devonian localities, a total of 154 points, were indexed (sample localities are shown in Harris and others, in press). Most points are for uppermost Silurian and lowermost Devonian limestones. Isograds do not extend south of southern Virginia because carbonate rocks of this age are generally absent in the outcrop belt.

The Silurian through Middle Devonian isograd map readily shows the correlation of conodont color with thickness of overburden regardless of tectonic setting. In western New York overburden is relatively thin (4,000-8,000 ft; 1,220-2,440 m) and conodonts are only slightly altered (CAI 1.5-2). Devonian rocks are virtually flat lying across New York. Only the easternmost part of the outcrop belt, just west of Albany, N.Y., is within the folded and faulted Valley and Ridge province. Conodont color gradually darkens across New York and no abrupt color change occurs at the tectonic front. The color alteration in New York conforms to an eastward-thickening wedge of Upper Devonian clastic rocks. Conodonts in south-central Pennsylvania, in the western part of the folded and faulted Valley and Ridge province, are the same color as conodonts in flat-lying rocks having comparable overburden in east-central New York. The darkest conodonts are in outliers east of the main outcrop belts and adjacent to the anthracite fields in eastern Pennsylvania, where Mississippian and Pennsylvanian rocks

are thickest. These data demonstrate that tectonics do not affect color alteration in conodonts.

Comparison of the same isograd value at different stratigraphic levels provides information on the thickness of intervening strata. Near coincidence of two such isograds indicates a thin intervening section, an unconformity, and (or) tectonic superposition. Figure 5 shows the relationship between the CAI 4 isograd in chiefly lower to middle Middle Ordovician rocks and the same isograd in Upper Silurian-lowermost Devonian rocks in the northern half of the Appalachian basin. The two isograds are nearly coincident from their northern limit to central Pennsylvania at which point they abruptly spread 60 miles (95 km) apart. They begin reconvergence at the Pennsylvania-Maryland border and finally merge in central Virginia. This configuration results from regional variation in erosional, depositional, and structural patterns. From central Pennsylvania to northeastern New York (near Albany), Upper Ordovician and Silurian rocks thin and are gradually cut out along a post-Middle Ordovician unconformity (Taconic unconformity), so that near Albany, uppermost Silurian rocks lie on Middle to Upper Ordovician rocks. Thus overburden for both units is nearly identical and isograds are nearly coincident. A Middle and Upper Ordovician chiefly clastic marine sequence thickens from 2,000 to about 15,000 feet (610-4,575 m) southeastward across Pennsylvania and thins gradually southwestward and rapidly northeastward (fig. 5A). A much thinner series of Silurian rocks follows nearly the same regional pattern (compare fig. 5A with 5B). Both intervals combine to produce the isograd pattern shown on figure 5. The reversal in isograd position (Upper Silurian-lowermost Devonian isograds west of Middle Ordovician isograds) in southern Virginia results from westward thrusting of more thermally mature younger strata over less thermally mature older strata.

CAI isograd map for Upper Devonian through Mississippian rocks (fig. 6).--Conodonts from 143 Upper Devonian through Mississippian and from 14 Pennsylvanian localities were indexed. Pennsylvanian localities were used only as a guide to contouring. Pennsylvanian-Permian rocks probably represent most of the post-Mississippian deposits in the Appalachian basin because younger deposits were very thin or absent.

A comparison of Upper Mississippian isograds and Pennsylvanian isopachs (fig. 7) in the central Appalachian basin shows:

1. The westward-projecting lobe of the CAI 1.5 isograd at the Kentucky-Tennessee border may conform to a lobe of Pennsylvanian rocks that at one time extended farther westward. Significantly the CAI 1.5 isograd outlines an area of oil and gas production from Mississippian rocks in Tennessee and Kentucky (de Witt, 1975, sheet 4).
2. The CAI 2 isograd in West Virginia encompasses the 2,500-foot-thick (762-m-thick) outlier of Pennsylvanian rock that must have at one time been part of a much thicker continuous northwest-trending clastic wedge.
3. The northwest-trending area of CAI 2 to 3.5 in southeast West Virginia coincides with anomalous Ordovician CAI highs and with an area of modern hot spring activity. The high heat flow in this area possibly results from a buried pluton (see Dennison and Johnson, 1971).

Assessment of Hydrocarbon Potential from CAI Isograd Maps

Because organic maturity within conodonts is related to depth of burial, more than one isograd map is needed to assess oil and gas potential. Accordingly, the three isograd maps were produced (figs. 3, 4, and 6). Figure 8 shows the eastern limit of commercial oil (fig. 8A) and gas (fig. 8B) production in the Appalachian basin for three stratigraphic intervals and the CAI isograd that best approximates this boundary. It is important to note that the cutoff for oil production for different stratigraphic intervals is not geographically coincident. The limit for oil production for each successively younger stratigraphic interval generally shifts eastward concomitant with decreasing overburden values (indicated by the eastward shift of the associated CAI 2 isograd). In figure 8A, the CAI 2 isograd lies near the eastern limit of oil production for each stratigraphic interval. It appears that the CAI 2 isograd which correlates with a fixed carbon value of 65 percent (table 1) marks the cutoff for commercial oil and condensate production (Bostick and Damberger, 1971, table 1). Gas production (fig. 8B), on the other hand, shows less relation to isograds. The eastern limit of Silurian through Middle Devonian production broadly meanders across the basin and across isograd trends. Gas generation occurs below, within, and well above the thermal limits for oil generation (from soon after burial into chlorite-grade metamorphism; from CAI 1 to +4). Gas production depends mostly on primary and (or) secondary porosity and permeability for accumulation in structural and stratigraphic traps. Thus it appears odd that the CAI 4 isograd approximates the eastern limit for gas production over large areas of the Appalachian basin. However, the temperature (depth of burial) necessary to produce this high level of organic metamorphism (CAI 4) concurrently produces mineral metamorphism that reduces porosity and permeability and the likelihood of commercial reservoirs.

From the standpoint of organic diagenesis, the entire Paleozoic section provides potential target horizons for oil production only in the westernmost part of the northern Appalachian basin and throughout the western half of the southern Appalachian basin. However, younger Paleozoic rocks within this terrane may not have even reached the thermal threshold for oil generation. Conodont color alteration begins near the upper thermal limit for oil generation, so that this technique can only be used for assessing the thermal cutoff, not the thermal threshold for oil generation.

The requirements for natural gas production are far less restrictive than those for oil. Gas can be generated from a greater variety of organic materials and can be generated and preserved through a much larger thermal range than oil. As a consequence, almost the entire Appalachian basin has a thermal potential for gas production. But the increase in thermal metamorphism and tectonic deformation eastward in the basin decreases the potential for gas production in that area for the following reasons. Although gas generation continues into the high levels of thermal metamorphism found in the eastern part of the basin, mineral metamorphism simultaneously acts to reduce porosity and permeability. In this same area, major and minor tectonic fractures can produce permeability and serve as channelways and traps for gas migration and accumulation. These same channelways, however, can contribute to the loss of gas from otherwise suitable traps. Therefore, exploration in the eastern part of the basin must be preceeded by detailed geologic investigration to identify appropriate targets.

REFERENCES CITED

Bostick, N. H., and Damberger, H. H., 1971, The carbon ratio rule and petroleum potential in NPC Region 9: Illinois Petroleum, v. 95, p. 142-151.

Dennison, J. M., and Johnson, R. W., Jr., 1971, Tertiary intrusions and associated phenomena near the thirty-eighth parallel fracture zone in Virginia and West Virginia: Geol. Soc. American Bull., v. 82, p. 501-508.

Dennison, J. M., and Woodward, H. P., 1963, Palinspastic maps of central Appalachians: Am. Assoc. Petroleum Geologists Bull., v. 47, no. 4, p. 666-680.

De Witt, Wallace, Jr., 1975, Oil and gas data from the upper Paleozoic rocks in the Appalachian basin: U.S. Geol. Survey Misc. Geol. Inv. Map I-917 A, 4 sheets, scale 1:2,500,000.

De Witt, Wallace, Jr., Perry, W. J., Jr., and Wallace, L. G., 1975, Oil and gas data from the Devonian and Silurian rocks in the Appalachian basin: U.S. Geol. Survey Misc. Geol. Inv. Map I-917 B, 4 sheets, scale 1:2,500,000.

Epstein, A. G., 1976, Conodont color alteration--an index to incipient through garnet-grade metamorphism [abs.]: Geol. Soc. America Abstracts with Programs, Northeastern-Southeastern Section Mtg., Arlington, Va., v. 8, no. 2, p. 167.

Epstein, A. G., Epstein, J. B., and Harris, L. D., 1977, Conodont color alteration--an index to organic metamorphism: U.S. Geol. Survey Prof. Paper 995, 27 p.

Harris, A. G., Harris, L. D., and Epstein, J. B., Oil and gas data from Paleozoic rocks of the Appalachian basin: maps for assessing hydrocarbon potential and thermal maturity (conodont color alteration isograds and overburden isopachs): U.S. Geol. Survey Misc. Geol. Inv. Map I-917 E, scale 1:2,500,000 (in press).

Harris, L. D., 1974, Cambrian facies trends--tool for estimating shortening in the southern Valley and Ridge province [abs.]: Am. Assoc. Petroleum Geologists Bull., v. 58, no. 9, p. 1892.

____1975, Oil and gas data from the Lower Ordovician and Cambrian rocks of the Appalachian basin: U.S. Geol. Survey Misc. Geol. Inv. Map I-917 D, 3 sheets, scale 1:2,500,000.

Hower, John, 1976, The determination of diagenetic and metamorphic temperatures using clay mineral assemblages [abs.]: Geol. Soc. America Abstracts with Programs, Northeastern-Southeastern Sec. Mtg., Arlington, Va., v. 8, no. 2, p. 201.

Miller, R. L., 1975, Oil and gas data from the Upper and Middle Ordovician rocks in the Appalachian basin: U.S. Geol. Survey Misc. Geol. Inv. Map I-917 C, 2 sheets, scale 1:2,500,000.

Pietzner, Horst, and others, 1968, Zur chemischen Zusammensetzung und Mikromorphologie der Conodonten: Palaeontographica, v. 128, pt. A, p. 115-152.

Schönlaub, H. P., and Zezula, Gerhard, 1975, Silur-Conodonten aus einer Phyllonitzone im Muralpen-Kristallin (Lungau/Salzburg): Verh. Geol. B.-A., no. 4, p. 253-269.

Turner, F. J., and Verhoogen, John, 1960, Igneous and metamorphic petrology: New York, McGraw-Hill Book Co., 694 p.

Vlissides, S. D., and Quirin, R. A., 1964, Oil and gas fields of the United States exclusive of Alaska and Hawaii: Washington, D.C., U.S. Geol. Survey, scale 1:2,500,000.

TABLE 1.--Correlation of three organic metamorphism indexes (all are optical techniques), percent fixed carbon, and overburden ranges for conodont color alteration indexes (CAI) in the Appalachian basin for Middle Ordovician rocks

CONODONTS			PALYNOMORPHS[1]		VITRINITE[1]	PERCENT FIXED CARBON
CAI[2]	Temperature °C[3]	Approx. overburden, in ft. (m) (values for Ordovician rocks in Appalachian basin)[4]	Translucency index (AMOCO)[5]	Weight percent carbon in kerogen	Reflectance	
1	<50-80	< 4,000 (< 1,220)	1-5	<82	< 0.8	< 60
1½	50-90	4,000-8,000 (1,220-2,440)	5-up. 5	81-84	0.7-0.85	60-65
2	60-140	8,000-12,000 (2,440-3,660)	5-6	81-87	0.85-1.3	65-73
3	110-200	12,000-18,000 (3,660-5,490)	up. 5-6	83-89	1.4-1.95	74-84
4	190-300	18,000-26,000 (5,490-7,930)	6	84-89	1.95-3.6	84-95
5	300-400	begins at 26,000-30,000 (7,930-9,150)	up. 6-7	+90	+3.6	+95

[1]Palynomorph translucency and vitrinite reflectance determinations were made on the same rock samples from which conodont CAI had been determined.

[2]Data for CAI >5 are not given because CAI values >5½ have not been found in the Appalachian basin. Several localities in North America (chiefly in Idaho, central-easternmost California, and Arizona) and Europe do have high CAI values that can be correlated with mineral indices.

[3]The temperature ranges for conodonts are from an Ahrrenius plot of experimental data (Epastein and others, 1977) and represent heating durations of 500 million to million years (lower temperature (500 m.y.-value) is applicable to heating durations of greater than about 50 million years).

[4]Overburden ranges are minimum estimates and were read from a post-Ordovician overburden isopach map (Harris and others, in press) in areas where most of the post-Ordovician section is intact and deformation is minimal.

[5]The translucency indexes are mean range values and are visual comparison estimates and not photometric determinations.

FIGURE 1.--A selection of conodont element of diverse form, age, and color. Even though this is a black and white photograph, some concept of the color change in conodonts can be appreciated. Letter symbols are explained in text.

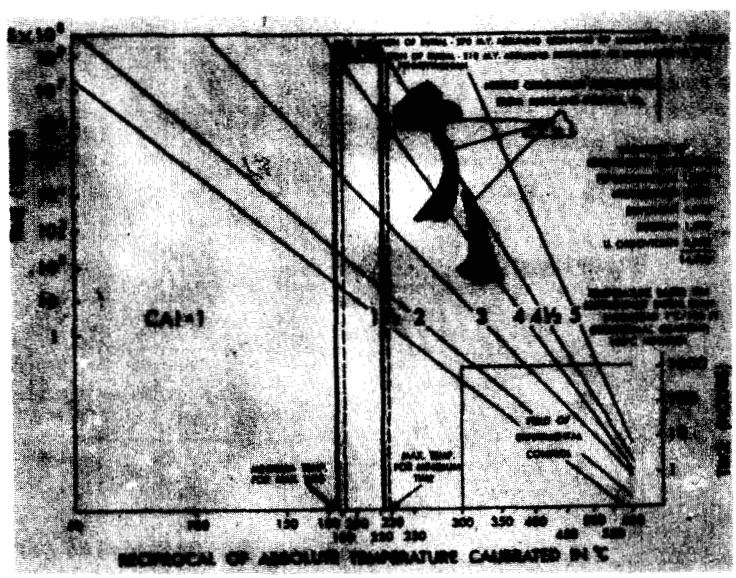

FIGURE 2.--Ahrrenius plot of data from conodont open-air heating runs of Epstein and others (1977, fig. 3) showing best color fit for late Middle Ordovician conodonts from the Valley and Ridge province near Monterey, Va. The CAI of these conodonts was determined by comparing them with index standards. Use of this plot for determination of minimum and maximum temperature ranges of conodont samples is explained in the text.

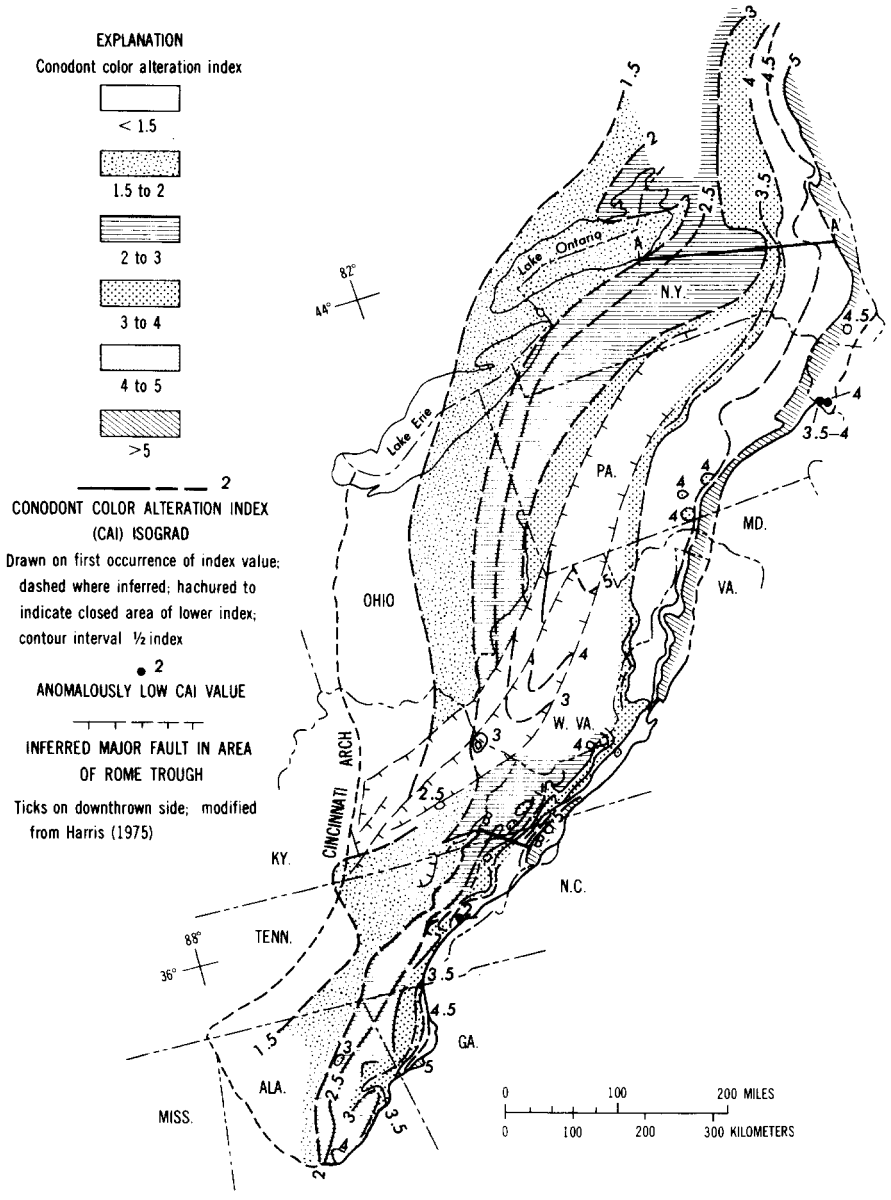

FIGURE 3.--Conodont color alteration isograd map for Ordovician carbonate rocks, chiefly limestone, in the Appalachian basin. Lettered lines are explained in text.

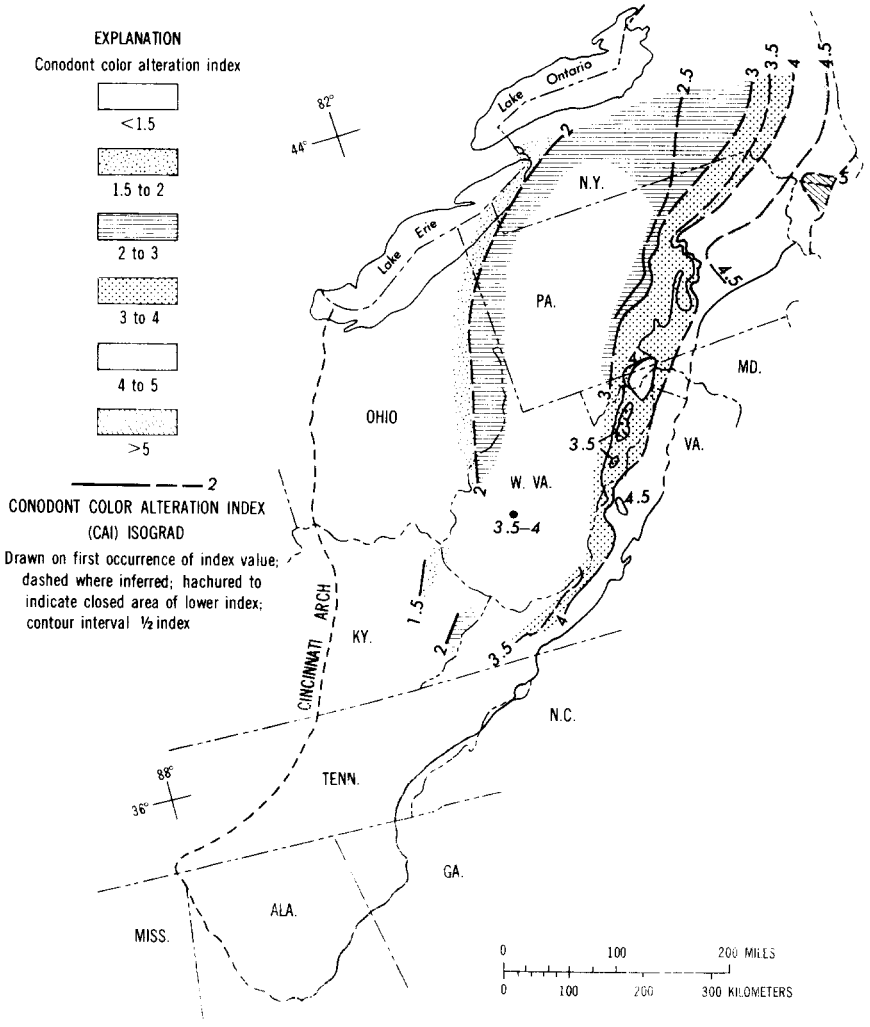

FIGURE 4.--Conodont color alteration isograd map for Silurian through Middle Devonian limestones in the Appalachian basin.

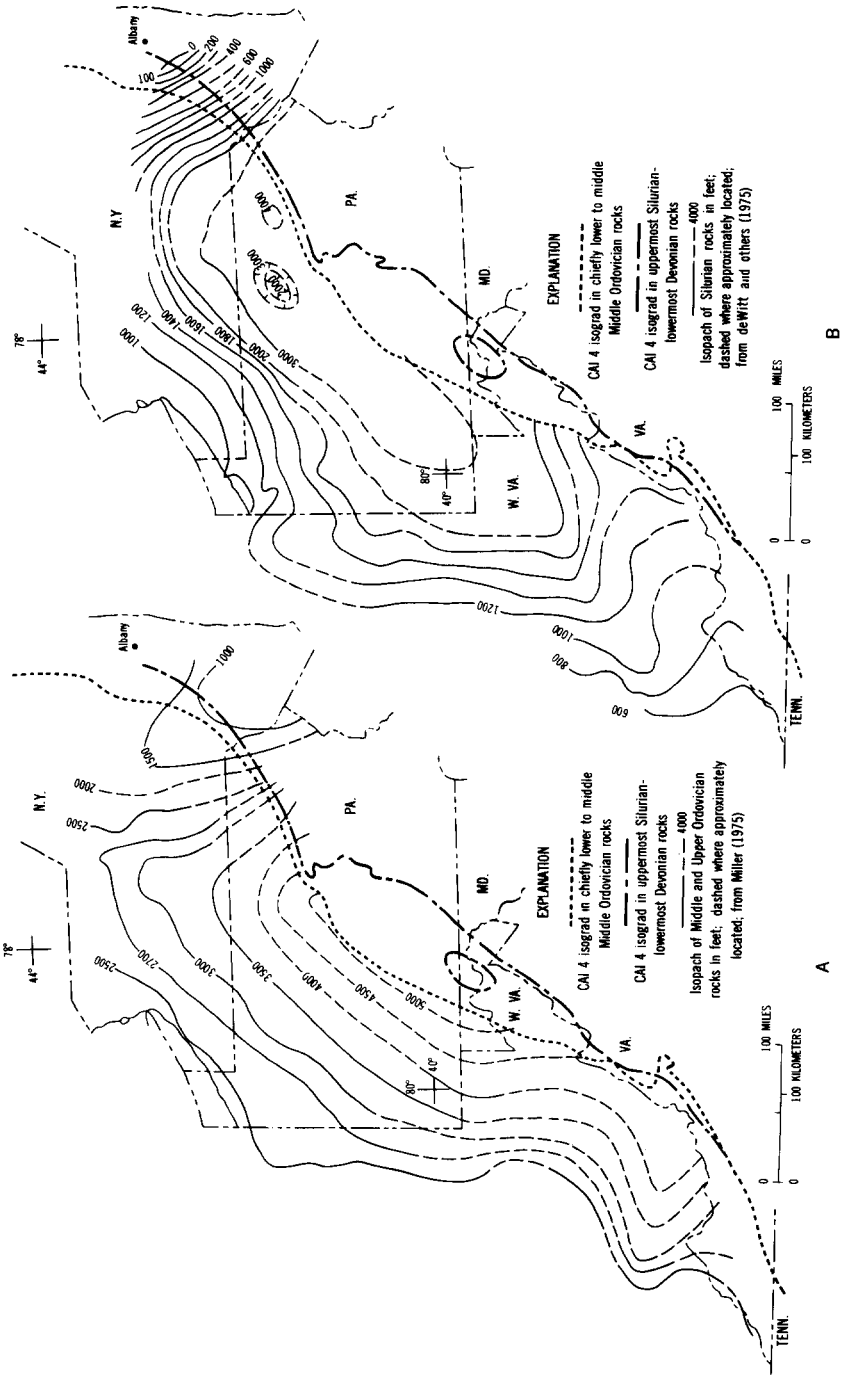

FIGURE 5.--Maps showing the relationship of the same isograd in two stratigraphic intervals to the thickness of intervening strata (see text for detailed explanation).

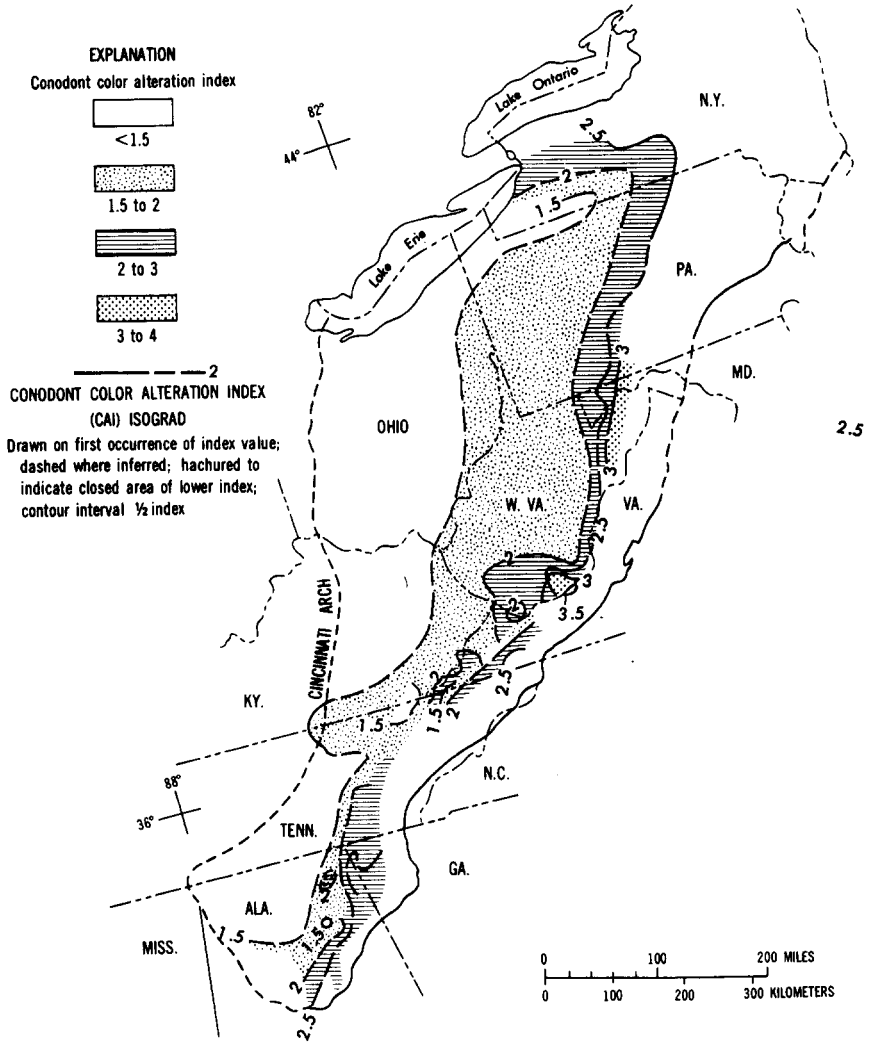

FIGURE 6.--Conodont color alteration isograd map for Upper Devonian through Mississippian carbonate rocks in the Appalachian basin (sample localities are shown in Harris and others, in press).

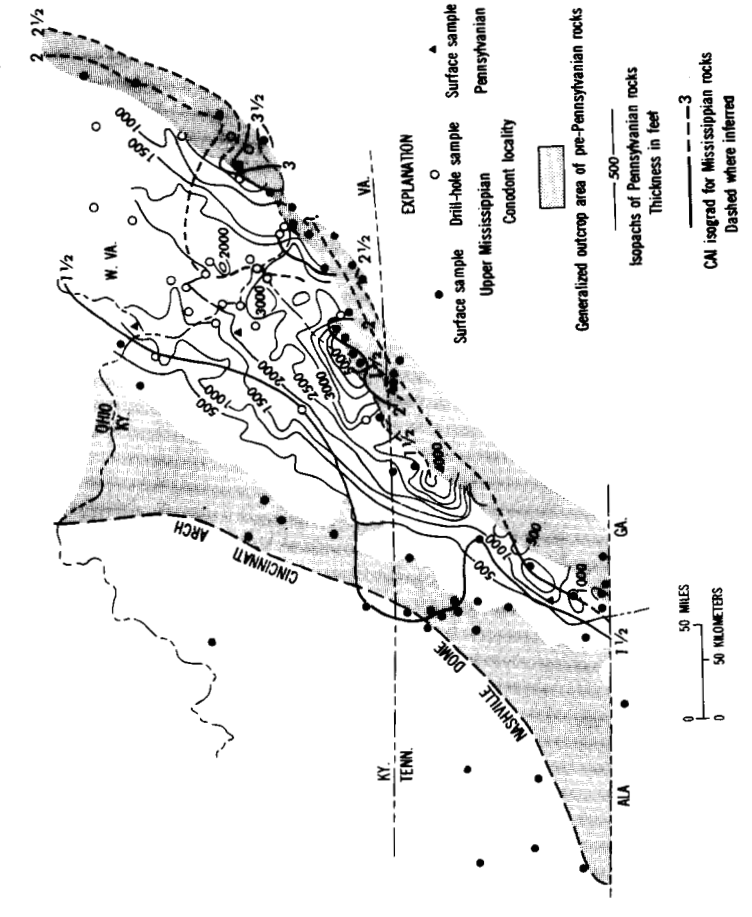

FIGURE 7.--Part of the Appalachian basin showing Upper Mississippian CAI isograds superimposed on isopachs for Pennsylvanian rocks (from Epstein and others, 1977, fig. 18).

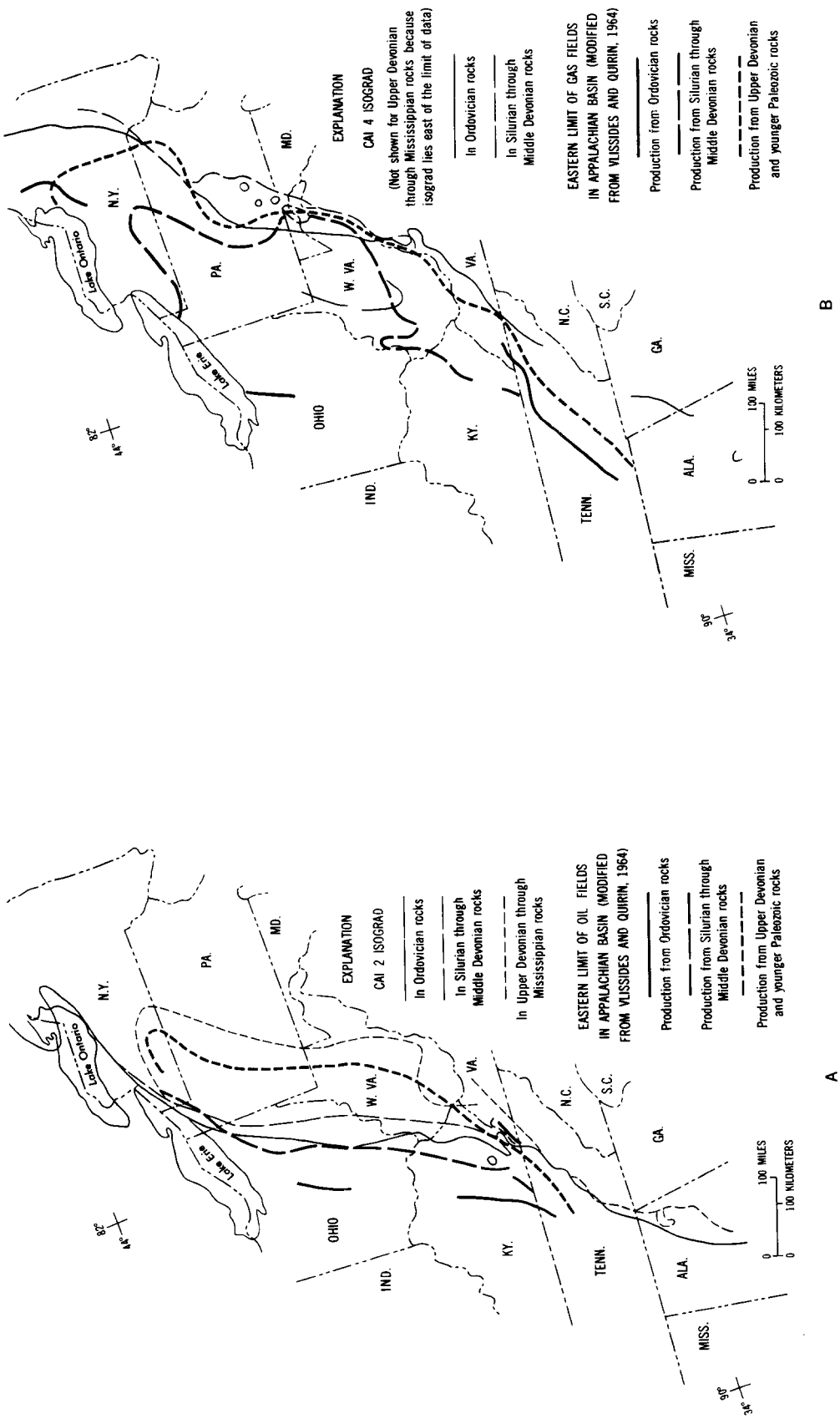

FIGURE 8.--Maps showing the eastern limit of oil (A) and gas (B) production for three stratigraphic intervals in the Appalachian basin.

DEVONIAN HARRELL AND MILLBORO SHALES IN PARTS OF PENNSYLVANIA, MARYLAND, WEST VIRGINIA AND VIRGINIA

by

Kenneth O. Hasson, Environmental and Regional Research Associates

John M. Dennison, The University of North Carolina

ABSTRACT

The Grayish Black Millboro Shale occupies the Tioga to Brallier interval west of a line between Cambria County, Pennsylvania and Rockingham County, Virginia. East of this line, the mass of black shale is split by a wedge of silty gray shale (Mahantango Formation) which becomes quite coarse eastward. This wedge separates the Millboro into the Grayish Black Marcellus Shale below and the Dark Gray Harrell Shale (with its Lower Black Burket Member) above.

The Purcell Member forms a convenient marker zone in both Marcellus and Millboro formations. The Tully limestone is present in Harrell or Burket outcrops as well as in the Millboro Shale.

INTRODUCTION

The purpose of this paper is to present some preliminary results of a stratigraphic investigation of the Harrell and Millboro Shales in parts of Pennsylvania, Maryland, West Virginia, and Virginia. The project area covers approximately 11,000 square miles (28,000 sq. km.) in these states (Figure 1). The data on which the interpretations are based consist of detailed measured sections in the Ridge and Valley area and well logs west of the Allegheny Front.

STRATIGRAPHY

Because of regional facies changes, most formations do not extend across the entire study area; thus, the stratigraphic sequence and nomenclature differ according to geographic location. The units involved will be considered in order from youngest to oldest.

Brallier Formation

The Brallier Formation (Butts, 1918) was named for exposures near Brallier Station, Bedford County, Pennsylvania. The formation consists of a monotonous sequence of medium dark gray, light olive gray-weathering silty shale with considerable interbedded siltstone. The shale is thickly laminated and chippy weathering. The siltstone is distinctly bedded in beds up to about one foot (0.3 m.) thick.

The Brallier everywhere overlies the Harrell or Millboro, and in outcrops the contact can be seen to be gradational. The lowest distinct siltstone underlain by uninterrupted shale is taken as the base of the unit both in outcrop and subsurface. In easternmost outcrops the very distinctly bedded Brallier siltstones overlie the more irregularly bedded olive silty shales or shaly siltstone of the Mahantango Formation.

Harrell Shale

The Harrell Shale (Butts, 1918) is a fissile, medium to dark gray shale which is about 260 feet (64 m.) thick in the type section. Here, the upper 180 feet (55 m.) constitute the gray portion of the formation; the lower 80 feet (24 m.) are black, fissile shale which comprise the Burket Member (Butts, 1918). A detailed description of the type section is given by Hasson (1966).

The contact with the overlying Brallier is gradational; the gray shale becomes siltier, but lacks definite siltstones and takes on an olive cast. The lowest distinct siltstone is taken as the Harrell-Brallier contact.

The transitional zone between the Harrell and Brallier is recognizable all along the Allegheny Front outcrop belt, at least from the type section to Millboro Springs, Virginia. Silt content of the zone increases upward and the shales become more thickly laminated, resembling siltstones in their flaggy appearance.

Below the transitional zone and above the grayish black shales of the Burket Member, the Harrell is very dark gray, thinly to thickly laminated shale which weathers to plates and sheets.

The Burket Member is a grayish black, fissile, platy-weathering shale. At the type Harrell the Burket rests on the Tully Limestone; at other localities the Tully is absent, and the Burket rests directly on the olive shales of the Mahantango.

The Harrell and Burket thin to the southwest and pass laterally into the Millboro Shale near Mouth of Seneca, West Virginia. To the east the upper Harrell changes facies into Brallier lithology, so that near the Virginia-West Virginia border the Harrell Shale is virtually unrecognizable, and for mapping purposes the Brallier rests on the Mahantango. In this area the Harrell is medium gray and interbedded with Brallier-type siltstones. Burket black shales are replaced eastward by siltier shales of the Mahantango. Westward into the subsurface the Harrell Shale is extended only to the limit of recognizable Mahantango.

Tully Limestone

The Tully Limestone occurs as a concretion zone from southern Pennsylvania southward. The concretions occur at the base of the Harrell Shale or within the Burket Member of the Harrell. Large concretions at the Tully position have been recognized in the Millboro Shale as far south as Bath County, Virginia. The Tully is bedded limestone to the west in the subsurface.

Mahantango Formation

The term Mahantango Formation was introduced by Willard (1935) for post-Marcellus - pre-Tully strata in central Pennsylvania. The name was taken from the North Branch of Mahantango Creek in Snyder and Juniata Counties, Pennsylvania. The reason for introducing the name was the difficulty involved in recognizing units of the Hamilton Group of New York in Pennsylvania. Mahantango is now accepted nomenclature of the West Virginia, Maryland, and Pennsylvania geological surveys.

The Mahantango consists of thickly laminated, usually silty shale with much siltstone and some limestone. The formation has several named members, some details of which were discussed in a previous paper (Dennison and Hasson, 1976). In the northeastern part of the study area these members, in upward succession, are: Gander Run Shale, Chaneysville Siltstone, Frame Shale, unnamed siltstone, unnamed shale, Clearville siltstone, Pokejoy Member, unnamed shale.

The Pokejoy Member (Hasson and Dennison, 1974) is locally a coral biostrome (Dawson, Maryland; Burlington, West Virginia) which exhibits an upward zonation somewhat similar to that described by Oliver (1951) in central New York. The corals built on the firm substrate provided by the Clearville siltstone in waters cleared by a sea level rise which caused an eastward shift of the shore line. Increased detrital sedimentation destroyed the coral environment (Hasson and Cocke, 1973).

Unfortunately, stratigraphic details of the Mahantango Formation are known only slightly, and this unit should be the subject of a major study.

Another limestone in the Mahantango is the Landes Limestone (Reger, 1924), with its type section at Landes, Grant County, West Virginia. This bedded limestone and concretion zone is almost 400 feet (122 m.) below the top of the Mahantango Formation (Hasson, 1966). In the Allegheny Front outcrop belt a limestone concretion zone occurs in the Gander Run Shale and extends laterally into the Millboro Shale. This zone is probably correlative with the Landes (Dennison and Hasson, in press).

Marcellus Shale

The Marcellus Shale is the basal unit of the Hamilton Group and consists of grayish black, thinly laminated shale. Its upper contact with the Gander Run Member of the Mahantango is diachronous. The contact is placed where the grayish black, platy shale changes upward into the siltier, more thickly laminated shales of the Gander Run.

Within the Marcellus, 28-91 feet (8.5-28 m.) above the base, occurs a zone of bedded to concretionary limestone interbedded with calcitic, thickly laminated, dark gray shale. This zone has informal status as the Purcell limestone (Cate, 1963) and provides an excellent marker horizon in the Millboro and Marcellus, traceable from Virginia to New York. Many outcrops of Purcell contain golf ball-like concretions which X-ray analysis shows to be composed of barite (Dennison and Hasson, in press).

Millboro Shale

The Millboro Shale was proposed by Butts (1940) as a mapping unit to include what is now recognized as the Tioga Bentonite-base of Brallier interval because the Marcellus and Naples shales could not be readily separated and mapped. The name Millboro is applied only in areas where the Mahantango is not recognizable.

In the type section at Millboro Springs, Virginia, the formation is about 1800 feet (550 m.) thick and contains recognizable Harrell, Mahantango and Marcellus elements, but these are too poorly developed to be considered as mappable units. The only detailed description of the section is given by Hasson (1966). A generalized column of the section is shown in Figure 2.

Lithosomes peculiar to the Harrell and Mahantango are recognizable in the section, and are labeled in Figure 2 as Harrell or Mahantango "influence." The term "influence" is used to describe lithosomes too feebly developed to map separately, so the use of Millboro as the mapping unit is quite suitable.

We use the term Millboro west of a line extending from Rockingham County, Virginia to West Virginia southwest of the Grant-Pendeleton County border in the Allegheny Front outcrop belt, and passing north along the western border of Maryland to Cambria County, Pennsylvania.

Tioga Bentonite

The Tioga Bentonite is typically brownish, tuffaceous shale which contains abundant small fossils. The middle coarse zone of the Tioga contains three sand-size tuffs within 2 feet (0.6 m.); the middle coarse zone tuffs mark the boundary between the Needmore and Marcellus in the north and the boundary between the Needmore and Millboro Shales in the south.

Needmore Shale

The Needmore Shale is divisible into three members: an upper calcitic shale and limestone, a middle calcitic shale member, and a black, basal Beaver Dam Shale Member. Stratigraphy of the Needmore has been described by Dennison (1960, 1961).

DISCUSSION

Figure 3 is a cross section drawn perpendicular to structural strike between the easternmost outcrop at Wheatfield, Frederick County, Virginia and the Morris E-1 well in Monongalia County, West Virginia. These sections and wells show that the Harrell Shale interfingers eastward with both the Brallier and the upper, unnamed shale of the Mahantango Formation. The section also shows the westward thinning of the Mahantango.

Also indicated are the western limits of recognizable Marcellus Shale (and limit of Millboro). The thinning of the section results from stratigraphic convergence as the Mahantango edge changes from siltstone to silty shale to black shale.

Figure 4, from Dennison and Hasson (in press), shows the regional facies relationships along Allegheny Front. The most obvious emphasis of the section is the southwestward thinning of the shales. Both the Marcellus and Mahantango thin and merge with the Millboro, in a manner not unlike that in Figure 3.

Southwest of Hopeville Gap, West Virginia, the name Millboro Shale must be applied to the black shales between the Tioga and Brallier Formation, because these shales cannot be divided without the presence of the intervening silty shales of the Mahantango. This unit thins to the southwest, not by unconformity but by stratigraphic convergence, as coarser prodelta muds change over to finer, distal, deeper water muds.

The post-Mahantango strata (Harrell and Burket) are characterized by a black, euxinic, probably deeper water facies (Burket) and a gray, shallower water facies (Harrell). The deepening occurred in the early phase of the Taghanic overlap when the shoreline was shifted eastward. This deepening also favored lime precipitation (Tully) locally in the shales (Hasson and Dennison, 1973).

REFERENCES CITED

Butts, C., 1918, Geologic section of Blair and Huntingdon Counties, central Pennsylvania: Am. Jour. Sci., 4th ser., v. 46, p. 523-537.

_____, 1940, Geology of the Appalachian Valley in Virginia: Virginia Geol. Survey Bull. 52, pt. I, 568 p.

Cate, A. S., 1963, Lithostratigraphy of some Middle and Upper Devonian rocks in the subsurface of southwestern Pennsylvania: Pennsylvania Topog. and Geol. Survey General Geology Rept. G39, p. 229-240.

Dennison, J. M., 1960, Stratigraphy of Devonian Onesquethaw Stage in West Virginia, Virginia, and Maryland: Unpub. Ph.D. dissert., Univ. of Wisconsin, 339 p.

_____, 1961, Stratigraphy of Onesquethaw Stage of Devonian in West Virginia and bordering states: W. Va. Geol. Survey Bull. 22, 87 p.

_____ and K. O. Hasson, 1976, Stratigraphic cross section of Hamilton Group (Devonian) and adjacent strata along south border of Pennsylvania: Am. Assoc. Petroleum Geologists Bull., v. 60, p. 278-287.

_____ and _____, (in press), Stratigraphic cross section of Devonian shales along the Allegheny Front from Maryland to Highland County, Virginia: W. Va. Acad. Sci. Proc.

Hasson, K. O., 1966, Lithostratigraphy and paleontology of the Devonian Harrell Shale along the Allegheny Front in West Virginia and adjacent states: Master's thesis, Univ. Tennessee, 89 p.

_____ and J. M. Cocke, 1973, A Middle Devonian coral-bearing unit in Maryland and West Virginia: Abstracts with Programs, Geol. Soc. America, v. 5, p. 402-403.

_____ and J. M. Dennison, 1973, Eustatic sea level rise over Fulton Lobe of Catskill Delta in Pennsylvania during Upper-Middle Devonian transition: Abstracts with Programs, Geol. Soc. America, v. 5, p. 175-176.

_____ and _____, 1974, Pokejoy Member, a new subdivision of the Mahantango Formation (Middle Devonian) in West Virginia, Maryland, and Pennsylvania: West Virginia Acad. Sci. Proc., v. 46, p. 78-86.

Oliver, W. A., Jr., 1951, Middle Devonian coral beds of central New York: Am. Jour. Sci., v. 249, p. 705-728.

Reger, D. B., 1924, Mineral and Grant Counties: West Virginia Geol. Survey, 866 p.

Willard, B., 1935, Hamilton Group of central Pennsylvania: Geol. Soc. America Bull., v. 46, p. 195-224.

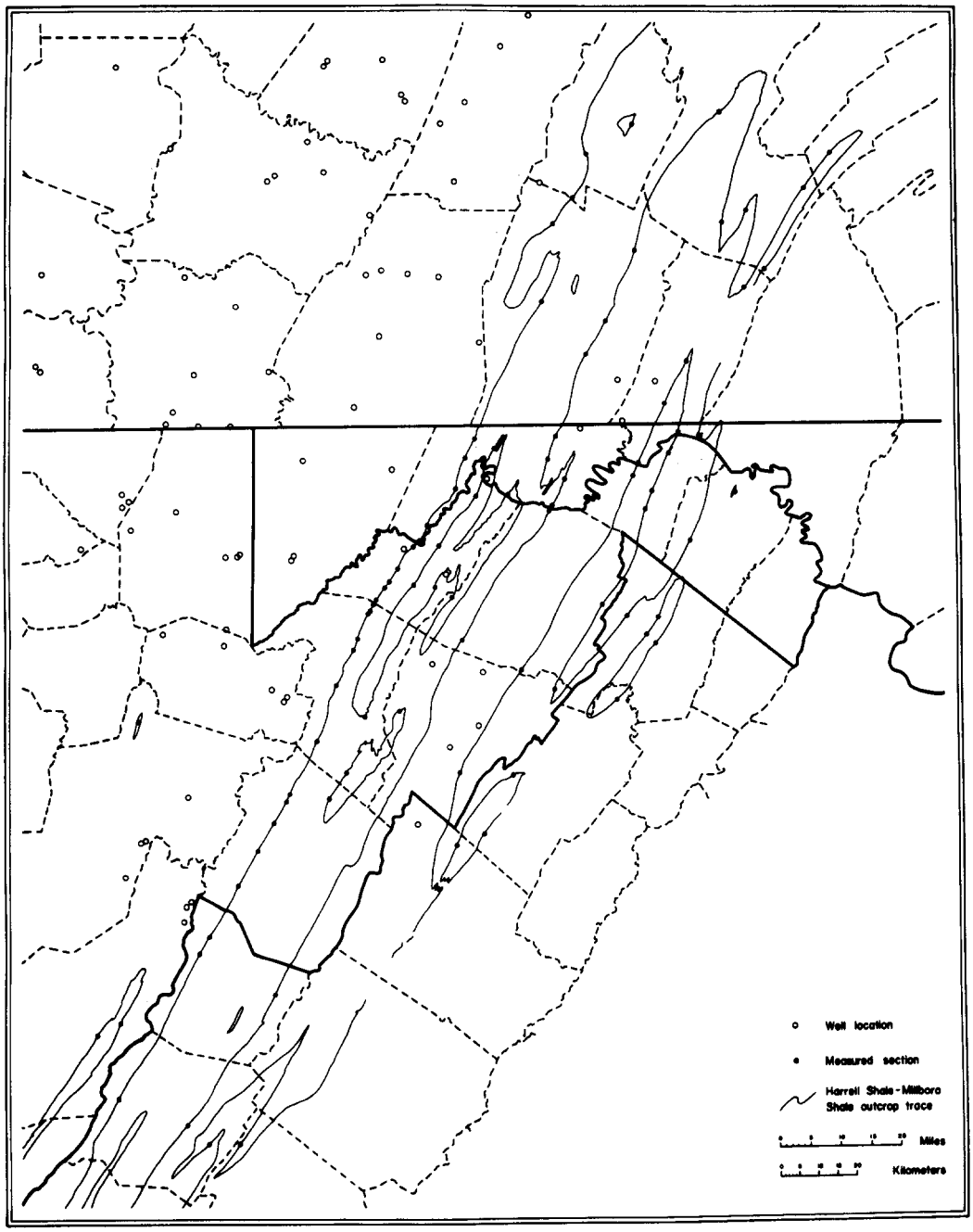

Figure 1: Map of project area showing locations of data points and Harrell-Millboro outcrop trace.

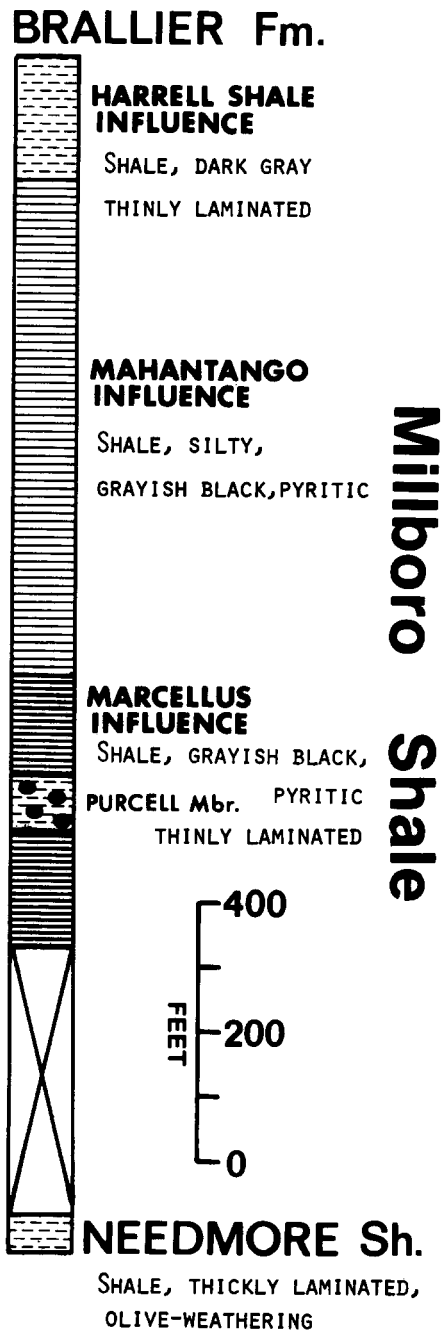

Figure 2: Columnar section of the type Millboro Shale at Millboro Springs, Virginia. The section is generalized from the detailed section by Hasson (1966).

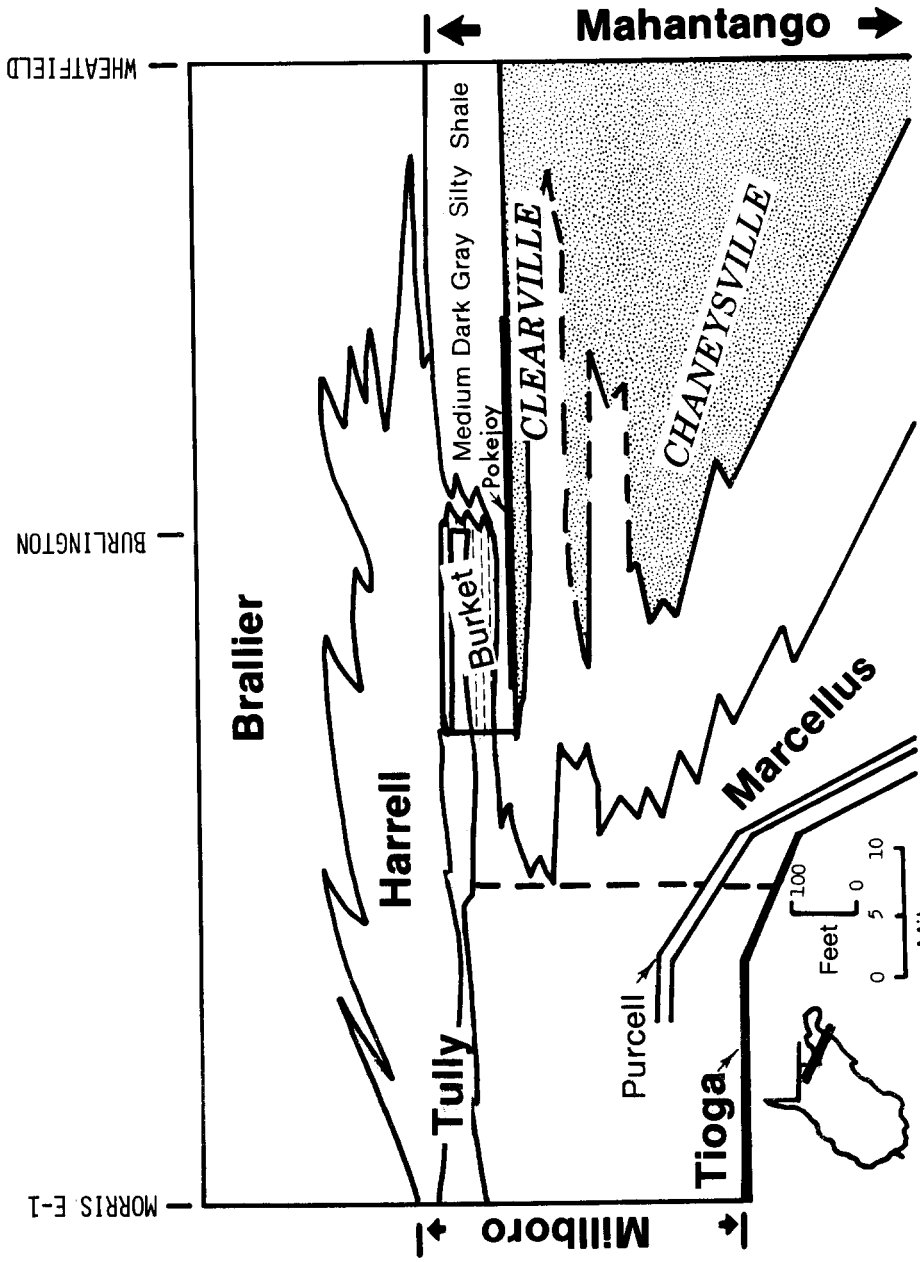

Figure 3: Stratigraphic cross section perpendicular to structural strike from eastern most outcrops north westward into the subsurface. The line of section parallels U.S. Route 50 in West Virginia.

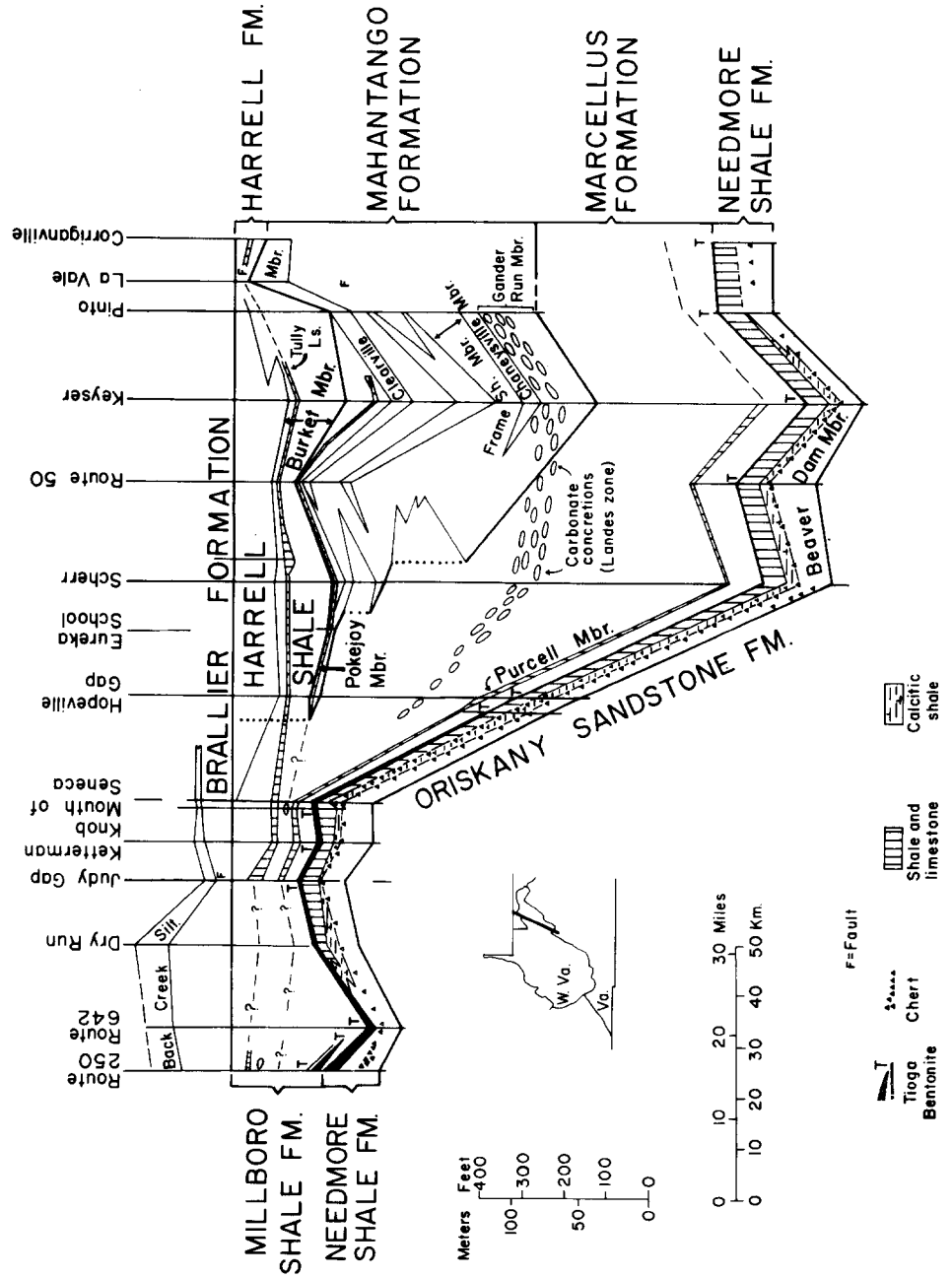

Figure 4: Stratigraphic cross section along Allegheny Front from Maryland to Highland County, Virginia. This figure is taken from Dennison and Hasson, 1977, (in press).

PETROLOGY OF LOWER HURON DEVONIAN SHALE, COLUMBIA GAS TRANSMISSION CO. WELL #20403, LINCOLN COUNTY, WEST VIRGINIA

by

Robert J. Vinopal
West Virginia Geological and Economic Survey
PO Box 879
Morgantown, West Virginia 26505

ABSTRACT

Petrographic analyses indicate that the seemingly homogeneous Lower Huron "brown shale" consists of several distinguishable units based upon composition, density, and fabric. Organic constituents occur as structured bodies (spores, shreddy material, cuticles) and as fine-grained amorphous matter which commonly coats grains and contributes to the rock matrix. Quartz, illite, and kaolinite comprise in excess of 90 percent of the total mineral constituents. Pyrite, dolomite, and calcite are common authigenic minerals. Bulk densities determined on core samples commonly differ from values on the density log. Parameters to explain these differences remain under investigation. Thin parallel laminae defined by changes in composition, texture, and color are the most abundant primary sedimentary structures. Fabric elements include orientation of clay laths, silt lenses, and interspersed silt grains which disrupt packing of the clay laths. Increasing amounts of silty lenses might be expected to produce increased permeability in the bulk rock, but compaction or authigenic mineral growth may alter this simple relationship.

INTRODUCTION

The Lower Huron Shale member is the principal gas producing interval of the Devonian shale sequence in southwestern West Virginia. This basal member of the Ohio Shale is defined in the subsurface by high API gamma ray values and aggregate thickness (Figure 1). A diamond drill core from Columbia Gas Transmission Company #20403, located in Lincoln County, West Virginia, served as the sample source for this study (Figure 2). In this well, the Lower Huron is approximately 250 ft. thick, covering the log interval from 3400-3650 ft. Previous investigators of the core include Larese and Heald (1977), who provide initial descriptions from thin-section microscopy and Bryers et. al. (1976) who provide megascopic descriptions. Thirty-nine samples were analyzed incorporating stero-microscopy, light microscopy, x-ray diffraction, x-radiography and measurements of bulk density on whole rock samples.

COMPOSITION

Shale composition was determined by x-ray diffraction and thin-section microscopy. The mean composition of the subject interval as determined by relative x-ray intensities and by thin-section point count is shown in Table 1. As can be seen illite, quartz and kaolinite comprise in excess of 90% of total mineral constituents. Various minerals reported by x-ray such as chlorite, orthoclase, and iron sulfates were not evident in thin section. Whole rock petrography of shales based on light microscopy cannot be expected to be as dinfinitive as in coarser clastic, but silt-size components are identifiable and useful information on mineral distribution and fabric elements can be obtained.

Mineral Components

Clay Thin section determined clay includes all clay size components that contribute to the

rock matrix. These include phyllosilicates (chlorite, illite, kaolinite) and other unresolved material such as fine chert, quartz, feldspar, carbonate, sulfate, and organic matter. Also included are clay constituents larger than four microns. Much of the clay is illite as indicated by its high birefringence and appears as optically continuous bundles that are commonly silt size.

Quartz-Feldspar Silt-sized grains of quartz, plaigioclase, and K-feldspar occur as disseminated grains and in lenses. Typically the quartz is angular to subangular, mono-crystalline and shows no overgrowths. Some quartz and feldspar is clay sized and cannot be resolved in thin section. This material is included in the clay matrix category for light microscopy. Chert lenses up to 0.2 mm in length are common and may represent early concentrations of silica or replacement of organic matter or the clay matrix. Chert can be seen partially replacing spores.

Sulfides Pyties is the major authigenic sulfide observed in thin section. Sphalerite was observed in trace amounts commonly as irregular masses with some euhedral forms. Pyrite occurs as: a) disseminated grains in the matrix, b) as replacement of coarse organic material which is often concentrated in specific laminae and c) as large lentoid masses (1 cm in width) with laminae bent around them. Specific forms seen in these occurrences include framboids, rare polyframboids, anhedral grains and euhedral cubic and pyritohedric forms. Some spores were replaced by pyrite prior to compaction (Larese and Heald, 1977) indicating early pyritization. Compacted spores with varying amounts of pyrite replacement were noted which along with the euhedral forms would seem to indicate at least one later period of pyritization.

Carbonate-Sulfate Dolomite is the principal carbonate component and occurs as: a) anhedral to euhedral crystals which are disseminated throughout the matrix, b) as cement in silt lenses, c) as fibrous, elliptical bodies with longitudinal symmetry which might possibly suggest replacement of organic matter. Clacite is rare and occurs as anhedral crystals. Sulfates are present as a) spore replacements (barite), b) as lentoid bodies parallel to bedding (gypsum) and c) as anhedral masses associated with pyrite aggregates (gypsum and anhydrite).

Organic Components

Organic matter consists of spores, cuticles (rare) and shreddy particles which are seen to have a red-orange tone in transmitted light. Other organic matter includes opaque grains with a dull, non-metallic luster in reflected light. These are interpreted as large vitrinite fragments. Finely divided organic material contributes to the clay matrix imparting a red-brownish tone in transmitted light. This material cannot be resolved within the limits of light microscopy and thus could not be quantified. As a matter of practicality, only silt size organic materials are counted.

Analysis

Although the limited number of samples did not reveal any definitive vertical trends, they do indicate the range of variability encountered (Figure 3). In all samples, quartz-feldspar as determined by relative percentage units from uncorrected x-ray data was consistently higher than the thin section quartz-feldspar percentage implying that clay-size quartz-feldspar is present in the Lower Huron. Clay-size quartz was determined by the difference between x-ray derived quartz and quartz percentages determined from thin section point counts. Both x-ray quartz and clay-sized quartz are expressed in relative percentage units. These are probably a reasonable approximation of absolute values, but because better quantification by using standards or known addition methods was not done, the values cannot be taken as absolute percentages. Blatt (1976) determined that of the total quartz in the average shale, 1/8 is clay size. Such quartz may be detrital or diagenetic. Correlations which relate components to one another and with gamma-ray density log responses are given in Table 2. Poor correlations exist between illite, thin section quartz, x-ray quartz and the gamma ray log. Apparently, the range of illite variation and potassium content is not sufficient to change the log response. A probable correlation may exist between organic matter determined in thin section and the gamma ray log.

The poor correlation between x-ray quartz and thin section quartz indicate that quartz in thin section cannot be well quantified with the petrographic microscope in fine-grained materials. While the thin section data is precise (reproducible), it is, however, not considered accurate with respect to total quartz. Suspended sediments from some recent lakes reveal over 40% quartz as quantified by known addition methods using x-ray diffraction, yet none of the quartz is identifiable under the petrographic microscope (E. B. Nuhfer, 1977, personal comm.). The low birefringence of quartz simply renders it black in transmitted light at such small particle sizes and thus it is not seen under crossed nicols. Higher birefringent minerals (calcite, dolomite, illite-muscovite) more visible under crossed nicols, are able to transmit light and thus particle size is a less restrict-

ing factor in quantifying these materials.

Fabric Elements

Within the samples studied, fabric elements include grain size, shape, sorting, orientation, and larger features defined by these basic elements. The largest scale fabric element is bedding. From observations of slabs at 10x under the binocular microscope, the Lower Huron is seen to contain two distinct bedding units: 1) light gray shale (5GY6/1, 5GY4/1, N5) and dark gray-black shale (N1, N2, N3). Color terminology is based on Geological Society of America Rock Color Chart. Dark shales comprise the bulk of the interval, but no quantification of the amounts of light and dark shale was made. Only horizontal parallel bedding was observed. Beds ranged in thickness from 1 cm to over 2 meters. The dark shales are typically finely laminated (Fig. 4), but also rarely laminations are lacking (Fig. 5).

Laminations are defined by varying amounts of organic matter, clay, and silt. Two readily visible types of laminae are present in the dark shales (Fig. 6). The first type contains abundant silt grains and coarse organics in a matrix of clay and fine organic material. The second type contains less silt and coarse organics and the matrix is commonly lighter in color. Contacts between the laminae are fairly sharp. Such laminations are the most abundant primary sedimentary structures. Laminations and other megascopic features are readily visible in radiographs (Fig. 7). The laminae are defined by varying radiographic density with darker tones being more opaque to x-rays. Interpretation of the tones is difficult as they reflect subtle mineralogical, chemical, and textural differences.

Smaller fabric elements within laminae include dispersed silt, silt lenses and clay orientation. Most silt is dispersed, but silt lenses are common in specific samples (Fig. 8). It is possible that such dispersed grains might disrupt the packing of clay laths and thus affect porosity. Silt lenses are commonly .15-.35 mm wide and perhaps represent starved ripples. Many lenses were seen to contain dolomite cement and clays squeezed between silt grains which may reduce permeability (Fig. 9). An indication of clay mineral orientation can be made in thin section by observing the maximum or minimum apparent clay birefringence. In the dark shales, the clay matrix shows distinct positions of extinction and illumination parallel to bedding (Fig. 10).

The light gray-green shale beds comprise a minority of the Lower Huron. They have a massive appearance and show no megascopic laminations. Silt lenses are rare, and grain size appears to be finer, but textural parameters have not been quantified (Fig. 11). Some coarse organics, typically, dark-shreddy material with occasional spores occur parallel to bedding. These have frequently been partially pyritized. Equant pyrite bodies are common. Many of the light shales are burrowed which may account for lack of laminations in those samples. Contacts between the dark and light shales are sharp (Fig. 12, 13) or show burrowing at the base of the light zones (Fig. 14).

Bulk Density

Bulk densities of coated core samples approximately twenty-five to thirty grams in weight were measured. The measured bulk densities commonly differ from the density log value. Parameters to explain these differences remain under investigation.

Acknowledgements

The writer is grateful to the Energy Research and Development Administration for making samples available. Thanks are due to Edward Nuhfer, Milton Heald and Richard Larese for helpful advice throughout the investigation. Jeff Clagett and Jim Florence greatly aided in sample preparation.

References

Blatt, H., and Schultz, D., 1976, Size distribution of quartz in mudrocks: Sedimentology, v. 23, p. 857-866.

Byrer, C. W., et. al., 1976, Lithologic description of cored wells #20402 and #20403 in the Devonian shale in Lincoln Co., West Virginia: U.S. ERDA-Morgantown Energy Research Center Technical Report, MERC/TRP/-76/9, 59 p.

Larese, R. E., and Heald, M. T., 1977, Petrography of selected Devonian shale core samples from the CGTC 20403 CGSC 11940 wells, Lincoln and Jackson Cos., West Virginia: U.S. ERDA-Morgantown Energy Research Center Technical Report, MERC/CR-7716.

Nuhfer, E. B., 1977, personal communication: West Virginia Geological and Economic Survey, Morgantown, West Virginia.

Rock-Color Chart Committee, 1975, Rock-color chart: Geological Society of America, Boulder, Colorado.

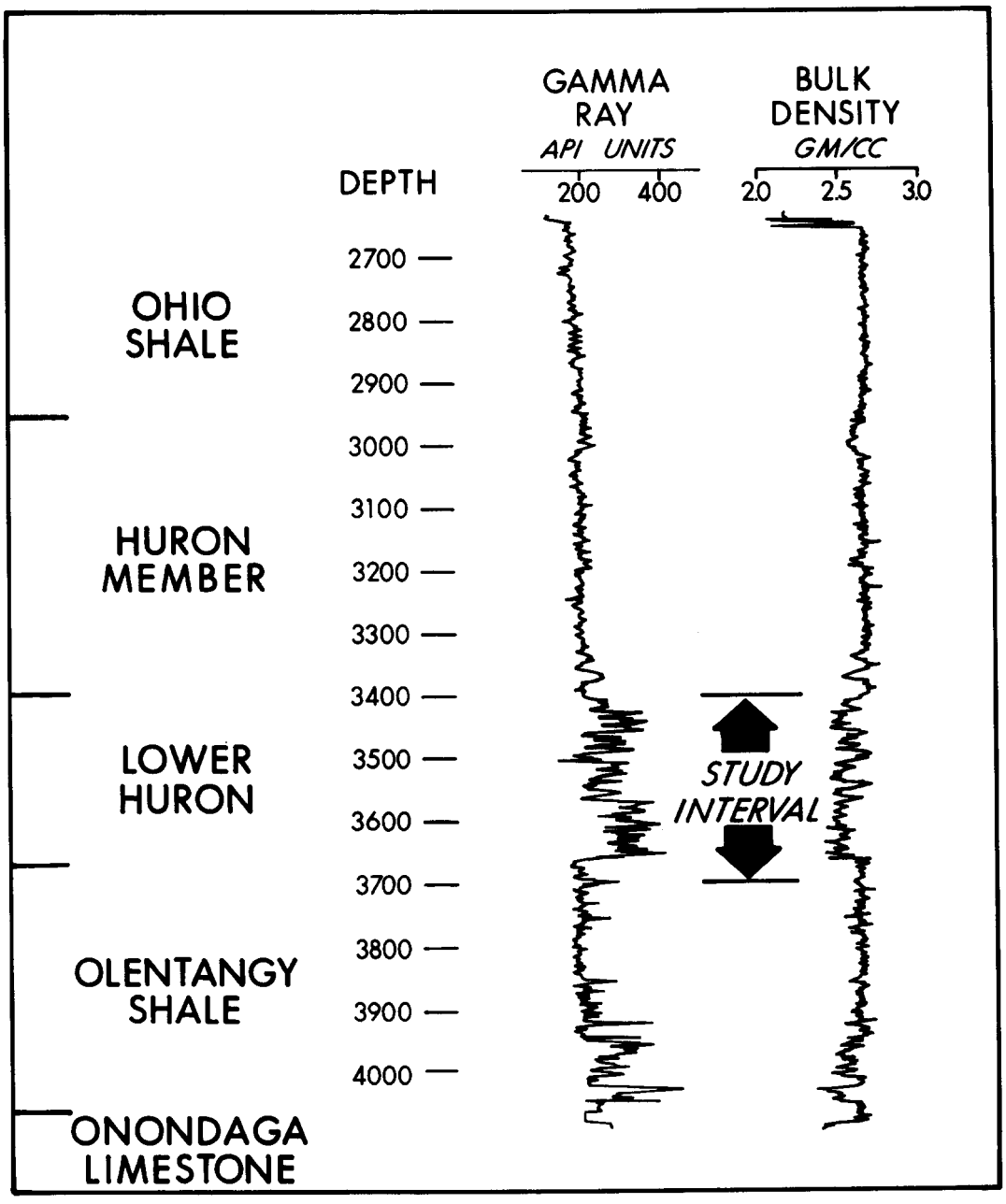

Figure 1. Stratigraphic subdivisions of the Devonian shale interval as interpreted from the CGTC #20403 core. Lower Huron is defined from 3400 to 3650 feet using USGS criteria.

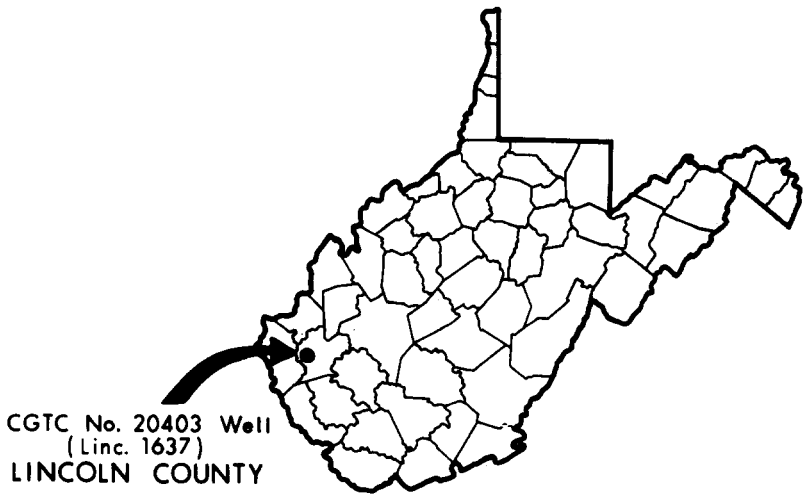

Figure 2. Index map of West Virginia showing location of cored well (CGTC #20403) utilized in this study.

X-Ray Relative Percentages

	Mean	Maximum	Minimum
Illite	45.19	56.21	29.42
Quartz	36.71	60.99	21.68
Kaolinite	8.54	22.16	.61
Pyrite	3.15	6.47	.41
Plaigioclase	1.47	3.28	.33
Dolomite	.82	3.25	0
$14^{o}A$	.75	3.82	0
$CaSO_4 \cdot \frac{1}{2}H_2O$	.44	2.20	0
Siderite	.43	.91	0
Gypsum	.28	1.09	0
Orthoclase	.20	2.01	0
Calcite	.15	.87	0
$Fe_2(SO_4)_3 \cdot 9H_2)$	.13	1.09	0

Thin Section Composition

"Clay"	65.36	76.33	54.00
Quartz-Feldspar	19.67	23.67	12.00
Sulfide	5.46	8.33	1.67
Carbonate-Sulfate	2.05	3.67	0
Organic	7.08	14.00	.33

Table 1. Compositional parameters of the Lower Huron is determined by x-ray diffraction and thin section point counts.

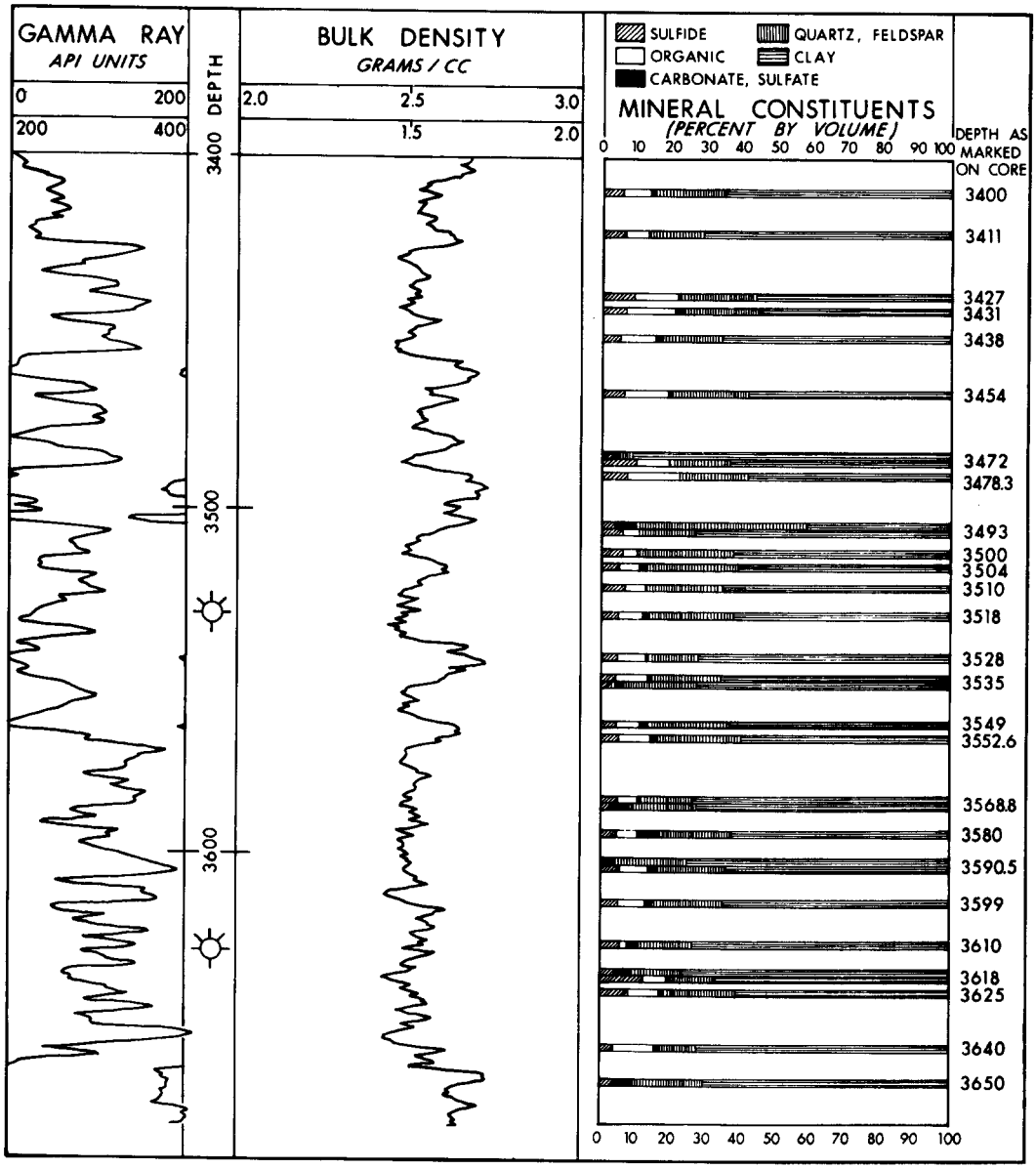

Figure 3. Geophysical and compositional characteristics of the Lower Huron. Compositional data are based on thin section analyses. Core depths are corrected to corresponding geophysical log.

Test	Correlation Coefficient	Prob R Under H_0: RHO=0
X-ray Quartz vs. API Units	-.082	.620
X-ray Illite vs. API Units	-.106	.536
Thin Section Quartz vs. API Units	-.183	.351
Thin Section Organic vs. API Units	.435	.023
Thin Section Quartz vs. Clay Size Quartz	-.402	.040
X-ray Quartz vs. Clay Size Quartz	.835	.001

Table 2 Correlations of relative components with one another and geophysical logs.

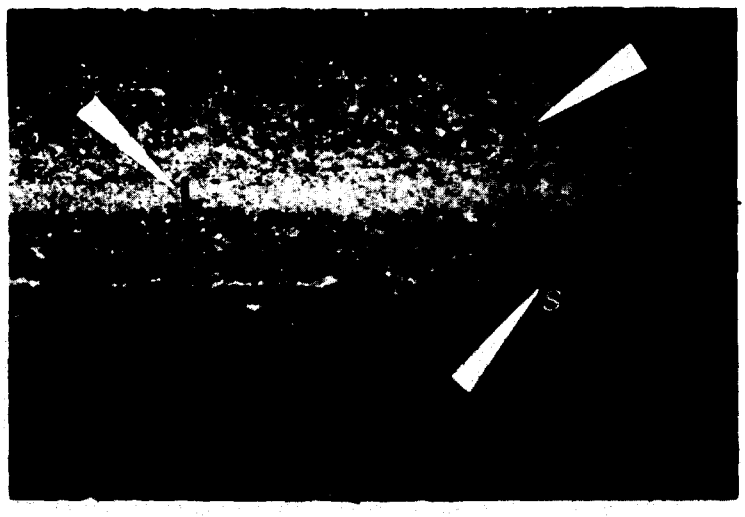

Figure 4. **Variations of laminae in organic-rich shale.** Light lamina (L) contains little silt and organic matter. Overlying lamina (I) contains some organic matter and silt. Silt lenses (S) are present in lower dark lamina. **Magnification 26.5 x. Plain light. 3478.3' depth.**

Figure 5. **Silty organic-rich shale possessing ill defined laminae.** Coarse organic material (arrow) parallel to bedding and clay orientation are principal linear features. Figure 13 shows radiograph of this slab. Magnification 26.5 x. Plain light. 3618' depth.

Figure 6. Common laminae types in organic-rich shale. Lighter lamina (L) contains less organic matter and silt than enclosing darker laminae (D). Such laminae are common in the Lower Huron, but variations in composition exist. Magnification 133 x. Plain light 3478.3' depth.

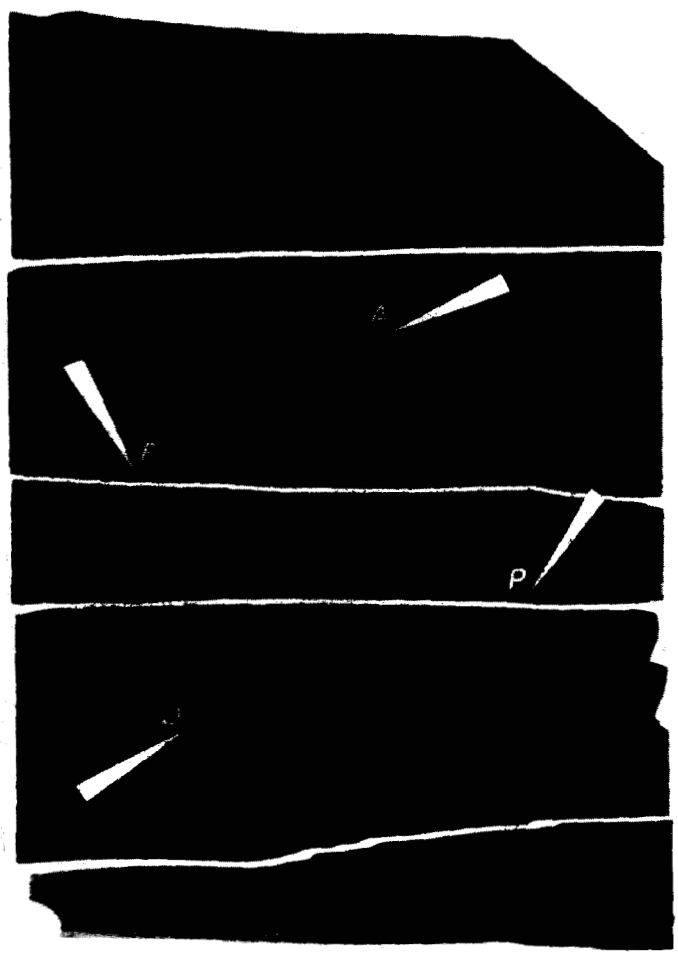

Figure 7. Radiograph of typical dark organic-rich shale from Lower Huron. The slab consists of approximately 70% grayish black (N2) laminae and 30% medium dark gray laminae (N4). Note unbroken nature of laminae showing lack of burrowing fauna. Many laminae (D) pinch and swell and are discontinuous. Micro cross lamination (A) indicates current activity. A 5mm band of light clay (N4) contains large pyritic framboids (dark equant bodies -F). Intense pyritization in laminae is shown at P by the thin black band. Organic-rich laminae commonly appear as darker tones due to pyritization, but exact interpretation of finer laminae is difficult. 1 x. 3411' depth.

Figure 8. Silt occurrences in dark shale. Most silt is dispersed (D). Silt lens (S) may increase rock permeability if not cemented. Magnification 26.5 x. Plain light. 3478.3' depth.

Figure 9. **Silty lens in dark shale. Dolomite cement (D) and authigenic** pyrite (P) may decrease porosity and permeability of lens. **Magnification 133 x. Polarized light. 3400' depth.**

Figure 10 **Preferred orientation of clay laths. Stage is rotated 45°** to bedding. Magnification 285 x. Polarized light. 3504' depth.

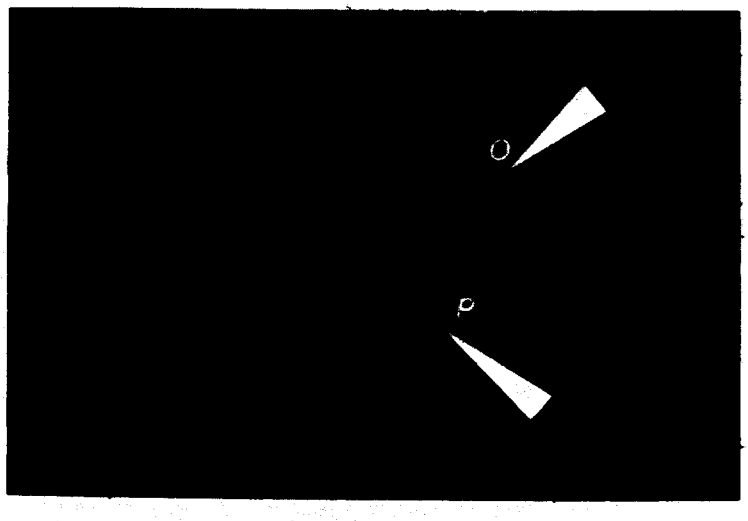

Figure 11. **Light colored shale from Lower Huron. Note coarse organic** matter (O) aligned parallel to bedding. Large pyrite aggregates (P) are replacing clay matrix. Magnification **26.5 x. Plain light. 3472.3' depth.**

Figure 12. **Contact between light and dark shale beds.** Note sharp contact (C) and pyrite (P) in light shale. See figure 13 for radiograph of slab.

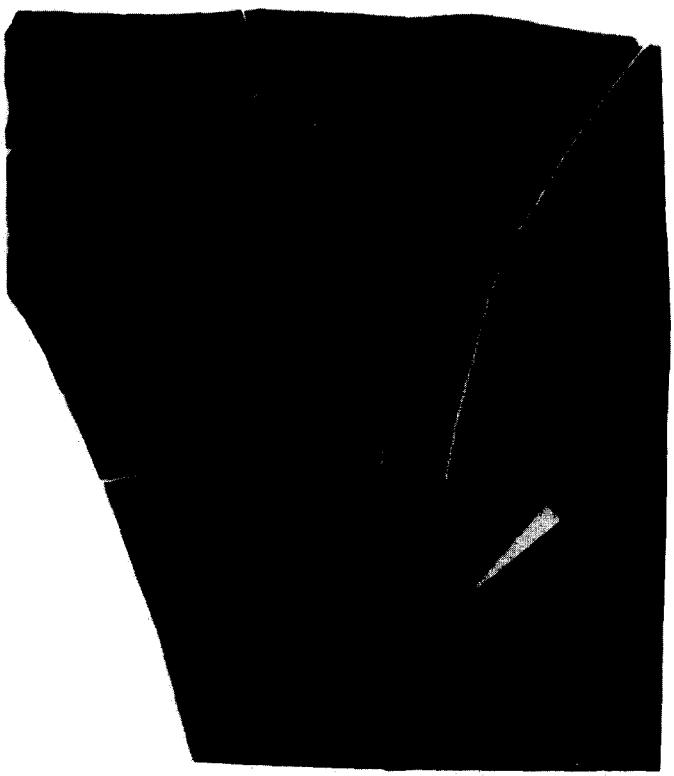

Figure 13. Radiograph of light (5Y4/1) and dark (N2) organic-rich shale showing sharp contact between bedding types. Light shale (L) shows evidence of bioturbation and lacks megascopic directional fabric elements. Note pyrite (darkest tone particles) whose distribution appears to be controlled by burrows. Contact with dark shale (D) is sharp and undulatory. The dark shale possesses poorly developed lamination in contrast to sample 3411 (fig. 7). Lens shaped areas of entensive pyritization in dark shale are shown at (P). 1 x. 3618' depth.

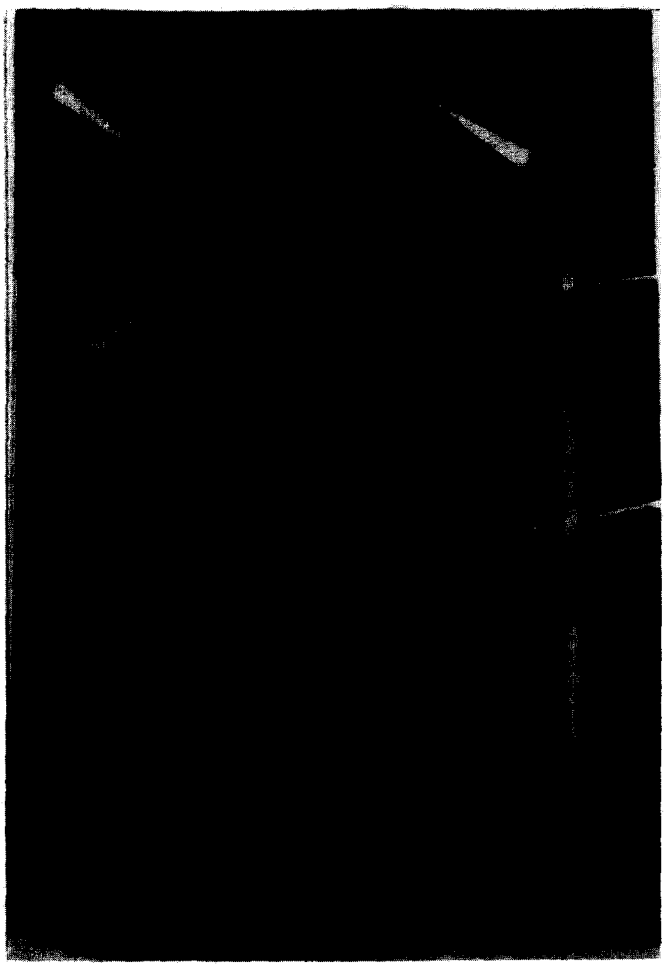

Figure 14. Radiograph of thin interbeds of light (5Y4/1) shale (white vertical bars) in dark (N-2) shale. The light shale zones are burrowed (B). Commonly the top of the light colored beds are smooth which is in contrast to the burrowed base. Isolated pyrite bodies occur at (F) with lenticular aggregates of pyrite prevalent in burrowed horizons. Dark organic shale zones are finely laminated and the laminae are commonly discontinuous. Lensoid aggregates of pyrite (P) and quartz lenses (Q) are common fabric elements. 1 x. 3510' depth.

PROCEDURES FOR THE CHARACTERIZATION OF DEVONIAN SHALES

by

W. E. Brownell
Alfred University
New York State College of Ceramics
Alfred, New York 14802

ABSTRACT

Elemental, mineralogical, and physical characterization of Devonian eastern gas shales is being done at Alfred University. In order to obtain the best data possible, several new procedures have been developed, especially in the area of mineralogical analysis. Forty-one elements are being determined quantitatively using conventional chemical procedures, specific ion electrode technique, atomic absorption, and Leco gas analyzers. A computerized X-ray diffraction procedure has been developed for qualitative analysis and quantitative determinations of the major minerals present in the shales. X-ray diffraction is also being used for measuring the preferred orientation of the disilicate minerals with respect to the core axis. Trace minerals are being identified and the sizes of the quartz grains are being measured by optical microscopy. A special disaggregation and mounting technique has been developed for the determination of the quartz particle-size distributions. Physical characterization is being done by measuring density, pore-size distribution, sonic velocity, directional tensile strength, point load strength with fracture patterns noted, and air permeability. A special apparatus and technique has been developed for the permeability measurements.

A. SCOPE OF CHARACTERIZATION

This contract is involved with elemental, mineralogical, and physical characterization of the Devonian eastern gas shales. Forty elements are being determined and, in addition, the sulfur is being determined as sulfide and sulfate, and carbon is being determined as organic carbon and carbonate carbon. Qualitative and quantitative mineralogical analyses are being made. The quartz particle-size distribution is being measured, and the angle and direction of the preferred orientation of disilicate minerals is being measured with reference to the core axis. Special techniques have been developed for the quantitative mineralogical analyses, quartz particle-size distribution, and the measurement of preferred orientation. Physical tests are being performed for sonic velocity, hardness, density, point load strength, directional tensile strength, pore-size distribution, and air permeability. Special equipment and procedures have been worked out for measuring the air permeability. The sonic velocity apparatus was built similar to that used at the Morgantown Energy Research Center.

B. ELEMENTAL ANALYSES

A list of the elements being determined together with an indication of the methods being used is given in Table 1. The major elements are being done by rather conventional silicate analysis. A flow diagram that shows the techniques used is presented as Figure 1. Boron is being determined colorimetrically by means of a curcumin complex.

The sample decomposition procedure for the determination of halides by the specific ion electrode method is to flux a 2-gram sample with sodium carbonate and zinc oxide. The fusion is dissolved in halide-free water and the residue discarded. Concentrated nitric acid is then used to expel

the carbonates, and the useful solution is diluted to a 50 ml. volume.

Three decomposition procedures are used in preparation for analyses by the atomic absorption spectrographs. Samples of shale for the determination of Se, As, Sb, Te, Tl, Ga, Ge, and Sn are treated with warm concentrated nitric acid to oxidize and remove hydrocarbons. (It has been found unnecessary to remove lignitic or pure carbon.) After the oxidation of organic matter in this way, the sample is decomposed by treatment with HF, drying, and dissolving the residue in HCl. A portion of this solution is used directly for the determination of thallium (Tl), and the rest is used in a hydride generator for the introduction of gaseous hydrides of Se, As, Sb, Te, Ge, and Sn into the spectrograph. The second procedure is used for the determination of mercury. In this procedure, the carbonaceous matter is removed by treatment with concentrated sulfuric acid followed by a treatment with a 50% H_2O_2 solution. After oxidation, $KMnO_4$ is added to the suspension and the mercury is reduced to the metallic state by adding a zinc sulfate solution. From this point, the cold vapor technique is used where the mercury vapor is conducted through a quartz-glass cell on the atomic absorption spectrograph. For all other elements determined by atomic absorption, carbonaceous matter is removed from a sample by ignition (ashing) to 1000°C in a muffle furnace. The sample is then put into solution by treatment with nitric acid, hydrofluoric acid, and perchloric acid, dried, and the residue dissolved in dilute hydrochloric acid. This solution is then ready for the atomic absorption measurements.

C. MINERALOGICAL ANALYSES

The detection of montmorillonite clay in the Devonian black shales is being done by a special technique for X-ray diffraction. This procedure starts with the removal of carbonaceous material from a pulverized sample with 15% H_2O_2. The material is then deflocculated with sodium hexametaphosphate and slowly concentrated by evaporation to form an oriented clay film. The film is removed and mounted on a glass microscope slide. After drying in ambient conditions, the (001) reflection is examined by X-ray diffraction; then the sample is treated with ethylene glycol and reexamined by X-ray diffraction. The extension of the (001) lattice spacing from about 11 or 12Å to about 17Å as a result of the glycol treatment establishes the presence of montmorillonite.

The detection of kaolinite in the presence of chlorite, as might occur in the Devonian black shales, presents a special problem. A procedure has been developed for this purpose [1]. It involves the production of a kaolinite-dimethylsulfoxide (DMSO) complex. In this procedure, 8.5 grams of finely ground shale is wetted thoroughly with DMSO liquid. A 100 ml. distillation flask is used for this purpose, and the mixture is refluxed on a hot plate at medium heat for 4 hours. After cooling the excess DMSO is removed by vacuum filtering on a sintered glass crucible. The resulting sticky mass is packed into the sample holder for the X-ray diffraction spectrometer.

The DMSO treated sample is examined by X-ray diffraction for reflections in the region of 16Å to 4Å. If kaolinite is present, most of the 7.15Å reflection is expanded to 11.18Å. The chlorite remains unaffected by the DMSO; so, if after treatment part of the 7Å reflection appears at 11Å, kaolinite is present. It has been found that the detection limit for kaolinite is about 2% which is about as good as the detection limit for most crystals by X-ray diffraction.

The quantitative mineralogical analyses of the major minerals present in the shales is being done by X-ray diffraction. In order to avoid preferred orientation of the minerals, spray drying is being used to prepare the samples and standards for X-ray diffraction measurements. Spray drying of finely pulverized materials creates hard, hollow spheres about 30 microns in diameter as shown in Figures 2 and 3. The spheres are aggregates of mineral particles and, if cleavage is present, the mineral particles are located at all possible orientations around the spheres. At first, it was thought that this technique was only necessary for the mica-like disilicate minerals, but experiments have now shown that even feldspars must be spray dried to avoid preferred orientation within the sample.

The qualitative and quantitative X-ray analyses for minerals is being done by computer control of the X-ray diffractometer, direct input of intensities and angles into the computer, and computer calculation of the desired results. Figure 4 gives a flow diagram of the computer controlled X-ray diffractometer analysis. The scheme for qualitative analysis is on the left and the scheme for the quantitative analysis is on the right. In the center of the diagram, the procedure for handling the unknown sample of Devonian shale is given. With the computer charged with the program and relevant data in storage, all of the analyses are made on one prepared sample of shale. All major minerals, certainly those present in greater amounts than 4%, will be determined quantitatively. The other minerals that show on the X-ray diffraction pattern but have intensities too low to be reliable for quantitative measurement are being reported qualitatively.

In order to measure the angle of preferred orientation relative to the core axis, a 3 mm core is being cut parallel to the core axis. This specimen is, then, in the form of a small cylinder with the north direction still identified on it. This specimen is mounted on a goniometer attached to an X-ray diffractometer. The angle for a basal spacing peak is set and the goniometer adjusted until the maximum intensity is obtained. When this is achieved, the inclination and direction is read directly off the goniometer. The data are being reported as the number of degrees inclination in a compass direction expressed in degrees from North through East.

Optical microscopy is being used, after sample disintegration with a Polytron and density separation using a linear density gradient column, to identify as many trace minerals as possible. These minerals are providing an explanation for the findings of the trace element analyses and for the geochemical conditions existing in the shale environment.

The procedure developed for measuring the quartz particle-size distribution employs a unique method of mounting the grains. The sample is first crushed to pass a 100 mesh sieve; then the carbonaceous material is removed by treatment with 15% H_2O_2. After washing and drying the sample, it is disaggregated with a solution of 3 parts fluosilicic acid (H_2SiF_6) and 2 parts of concentrated sulfuric acid (H_2SO_4). After disaggregation and partial solution of undesirable minerals, the residue containing quartz grains is washed and dried. A microscope slide and a cover glass are coated with an elastomeric silicone resin (Sylgard 182). The above residue is mixed with a warm melt of 60% camphor and 40% napthalene to disperse the individual grains, and the suspension is allowed to solidify by cooling. The solid suspension of quartz particles in camphor-napthalene is placed on the coated slide and the camphor-napthalene vehicle is removed by vacuum sublimation. Now the coated cover glass is placed over the grains with its coated side down. The assembly is sealed together in a vacuum oven leaving the center of each grain, regardless of size, in the same plane for easy focus with a microscope. Martin's diameters of a large number of grains are measured microscopically. The data on the size distribution of quartz grains are mean, median, mode, 1st quartile and 3rd quartile. All of these data are calculated with respect to volume.

D. PHYSICAL TESTS

Density measurements are being made by the method of suspension in light oil. We have determined that consistent dry weights can be obtained on the shale pieces only after drying in an oven at 100°C for about 7 days.

Pore-size distribution is being measured by a mercury intrusion porosimeter, and it has been found that the complete distribution of pores in the shales tested so far cannot be obtained by this method. Unless the method is changed to gas adsorption or some samples have a larger open-pore structure, the mean, mode, median, standard deviation, 1st quartile, and 3rd quartile will not be available. In lieu of these data, the total specific pore volumes are being tabulated for all open pores greater than 1.00 micron and greater than 0.02 micron. The distribution curves are also being submitted in written reports.

The sonic velocity measurements are being made on an apparatus similar to that at the Morgantown Energy Research Center. A pneumatic pressure system has been designed to hold the transducers tightly against the core specimen. The signal transducer is being driven by 1600 volts, and the response output is being amplified.

Directional tensile strengths and point-load strengths are being made in the usual manner. Sketches are being made of the fracture patterns obtained in the point-load test.

An apparatus has been designed to measure air permeability of one-inch diameter, subcored specimens. Measurements are being made both perpendicular and parallel to the core axis, and the results calculated in millidarcies. The thickness of the specimen is about 3/8 inch. As shown in Figure 5, a schematic drawing of the apparatus, the specimen is placed in a gasketed cell, and 60 pounds of air pressure applied to one side. The flow of air through the specimen is collected in a volumetrically calibrated tube. In the calculation of the results, a correction is applied for the backpressure created by the collection liquid. Satisfactory results are being obtained within one half to one hour's time in the test.

REFERENCES

1. S. Gonzales Garcia and M. Sanchez Camazano, "Differentiation of Kaolinite from Chlorite by Treatment with DimethylSulphoxide," Clay Miner., 7, 477 (1968)

TABLE 1 Elements Determined (ppm)

Element	Procedure	Element	Procedure
Silicon	gravimetric	Tin	atomic absorption
Aluminum	gravimetric	Mercury	atomic absorption
Iron	titration	Rubidium	atomic absorption
Magnesium	gravimetric	Zinc	atomic absorption
Calcium	gravimetric	Copper	atomic absorption
Lithium	flame photometry	Nickel	atomic absorption
Sodium	flame photometry	Cobalt	atomic absorption
Potassium	flame photometry	Manganese	atomic absorption
Titanium	colorimetric	Chromium	atomic absorption
Phosphorus	colorimetric	Vanadium	atomic absorption
Boron	colorimetric	Beryllium	atomic absorption
Fluorine	specific ion electrode	Gallium	atomic absorption
Chlorine	specific ion electrode	Lead	atomic absorption
Bromine	specific ion electrode	Barium	atomic absorption
Selenium	atomic absorption	Cadmium	atomic absorption
Arsenic	atomic absorption	Silver	atomic absorption
Germanium	atomic absorption	Molybdenum	atomic absorption
Tellurium	atomic absorption	Strontium	atomic absorption
Antimony	atomic absorption	Sulfur	Leco + gravimetric
Thallium	atomic absorption	Carbon	Leco + gravimetric
		Nitrogen	Leco

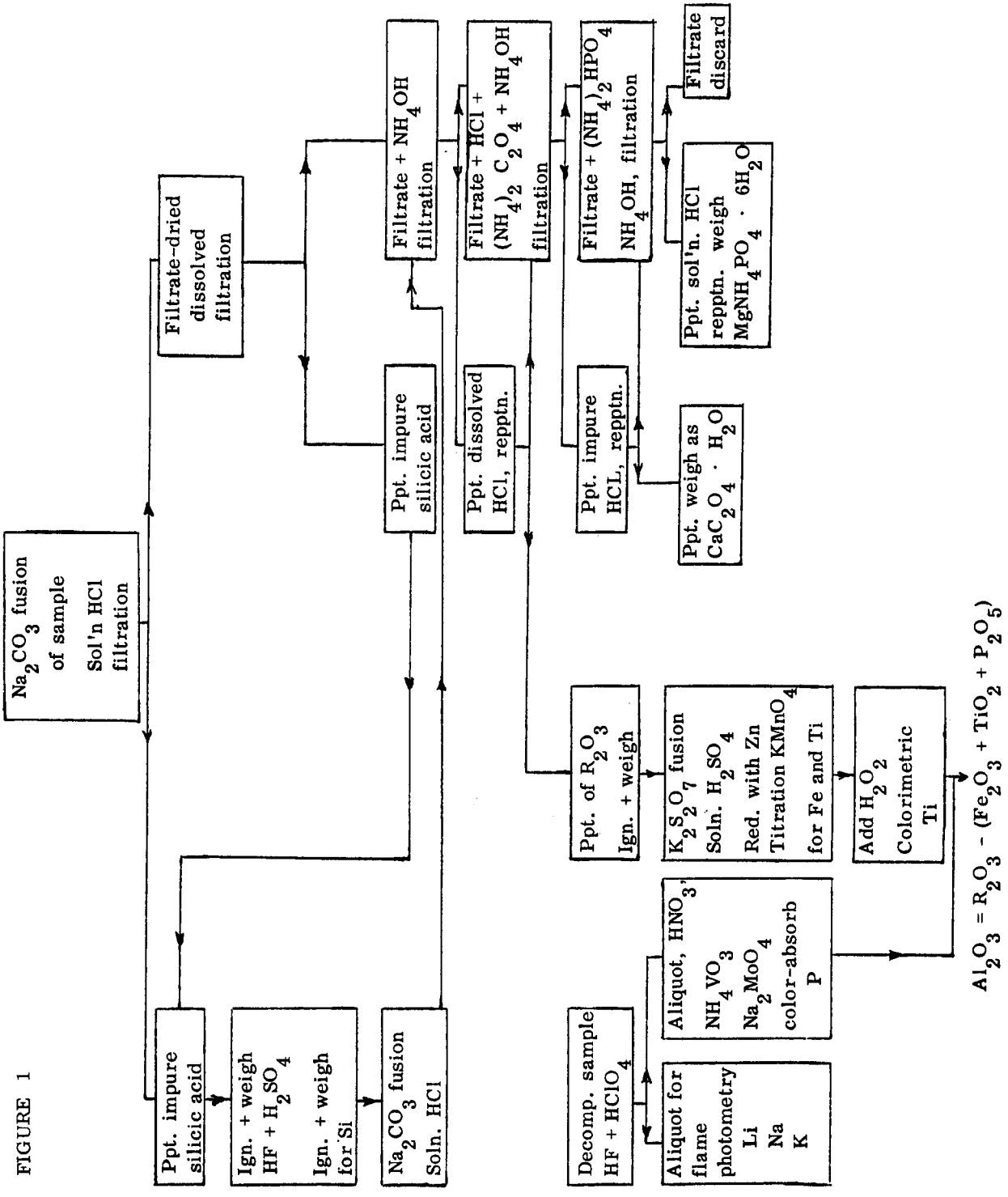
Na_2CO_3 fusion of sample
Sol'n HCl filtration
Filtrate-dried dissolved filtration
Ppt. impure silicic acid
Filtrate + NH_4OH filtration
Ppt. impure silicic acid
Ign. + weigh HF + H_2SO_4
Ign. + weigh for Si
Na_2CO_3 fusion Soln. HCl
Ppt. dissolved HCl, repptn.
Filtrate + HCl + $(NH_4)_2C_2O_4$ + NH_4OH filtration
Ppt. impure HCL, repptn.
Filtrate + $(NH_4)_2HPO_4$ NH_4OH, filtration
Ppt. weigh as $CaC_2O_4 \cdot H_2O$
Ppt. sol'n. HCl repptn. weigh $MgNH_4PO_4 \cdot 6H_2O$
Filtrate discard
Ppt. of R_2O_3 Ign. + weigh
$K_2S_2O_7$ fusion Soln. H_2SO_4 Red. with Zn Titration $KMnO_4$ for Fe and Ti
Add H_2O_2 Colorimetric Ti
Decomp. sample HF + $HClO_4$
Aliquot, HNO_3, NH_4VO_3 Na_2MoO_4 color-absorb P
Aliquot for flame photometry Li Na K
$Al_2O_3 = R_2O_3 - (Fe_2O_3 + TiO_2 + P_2O_5)$

FIGURE 1

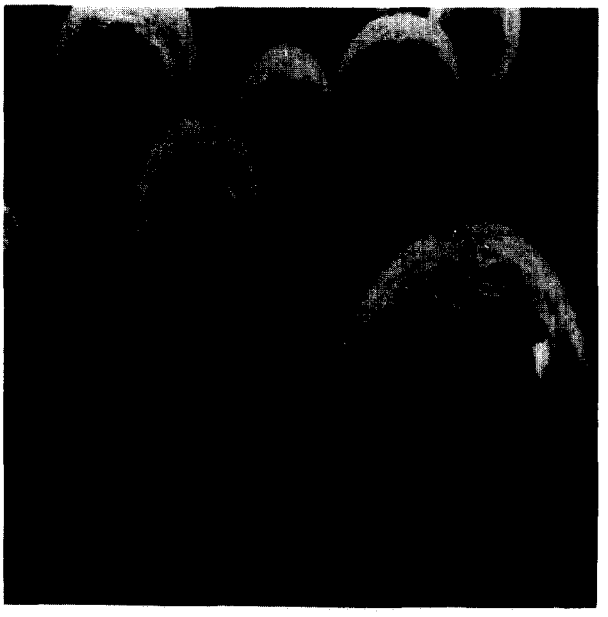

FIGURE 2 Spray dried aggregates of pure illite (SEM at 640X).

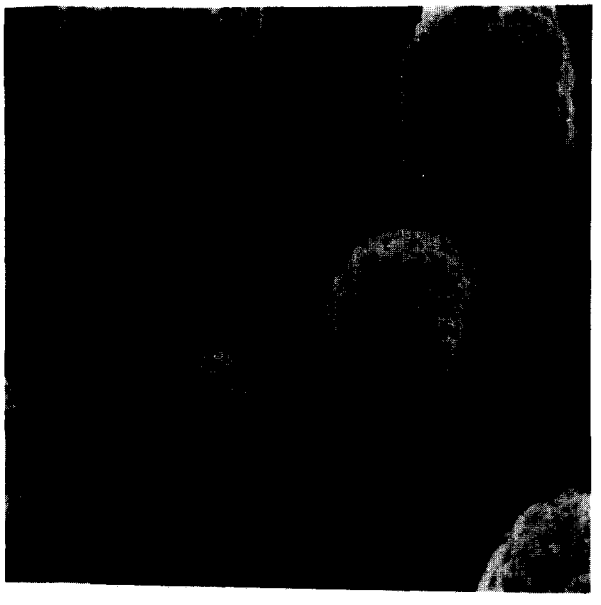

FIGURE 3 Spray dried aggregates of Chittenango shale (SEM at 640X).

FIGURE 4

Scheme for Mineralogical Analysis by X-ray Diffraction

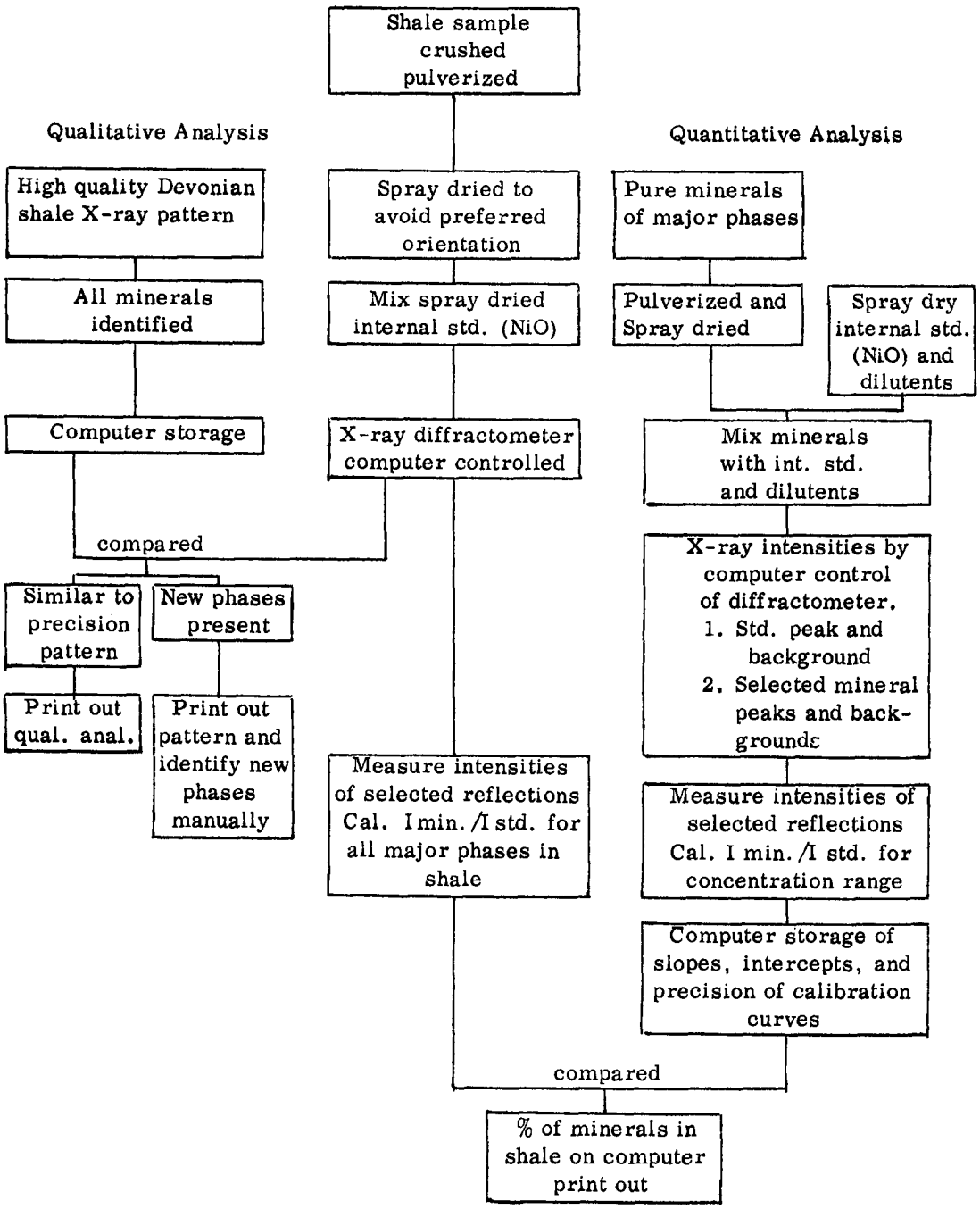

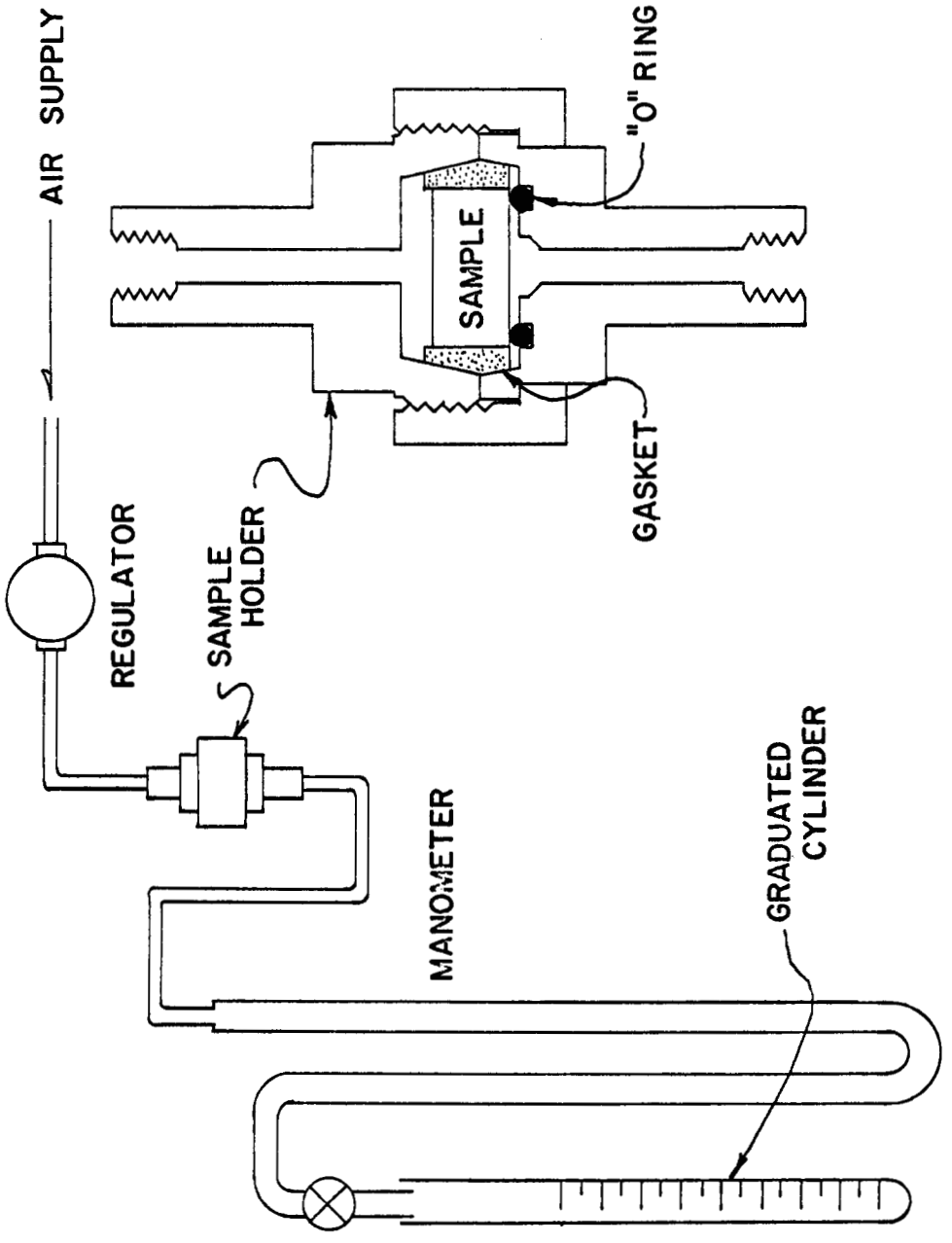
AIR SUPPLY
"O" RING
SAMPLE
GASKET
REGULATOR
SAMPLE HOLDER
MANOMETER
GRADUATED CYLINDER

FIGURE 5

A REPORT ON VARIATIONS OF STIMULATION TREATMENTS ON THE ERDA SHALE PROJECTS

by

J. L. Norton, Regional Engineer
Dowell Division of the Dow Chemical Company

ABSTRACT

This discussion covers eleven "11" treatment on the Shale and their variations in the Appalachian Basin. The basic treating fluids have been gelled water, foam and combinations of these two. The additives have been changed to improve Rheyology properties of the fluids, with the introduction of 80/100 sand to improve fracture penetration.

The laboratory data presented describes the physical & chemical composition of the Shale. Also, the S.E.M. furnishes a closer look at the Shale than previously available.

*Paper not available at time of publication

PROGRESS REPORT ON CHARACTERIZATION OF THE DEVONIAN BLACK SHALES IN OHIO

by

Frank L. Majchszak
Ohio Division of Geological Survey
Columbus, Ohio

ABSTRACT

Preliminary maps showing thickness of the Devonian shales, top and base elevations of the shales, elevation of the top of the Devonian shales radioactive facies, and thickness of the radioactive facies have been published by Janssens and De Witt. Maps showing wells producing from Devonian shales in eastern Ohio and indicating reported shows in Devonian shales in northeast and southeast Ohio are available from the Ohio Division of Geological Survey.

Research in progress focuses on identification of widespread mapping units and radioactive shale facies from borehole geophysical log cross sections. Gamma ray log control permits rapid identification of the Cleveland Shale member and of the Olentangy Shale. Maps showing the elevation of the base of the Huron member of the Ohio Shale (top of the Olentangy Shale), the thickness and distribution of the radioactive facies of the lower Huron member, and the radioactive facies of the Rhinestreet Shale equivalent (New York state terminology) within the lower Olentangy Shale are included in this progress report.

Ascertaining details of the stratigraphy of the nonradioactive Devonian shale units will be a formidable task requiring a comprehensive investigation which combines borehole geophysical log studies and detailed sample and core descriptions.

INTRODUCTION

The Devonian shales of the Appalachian Basin are the subject of an extensive research program aimed at providing information to facilitate the production of natural gas. In Ohio, the resource potential of the Devonian shales is estimated to be 67 trillion cubic feet of gas (Janssens and DeWitt, 1976).

Figure 1 shows the generalized occurrence of the Devonian shales, which in Ohio have been defined as the rocks between the base of the Berea Sandstone (Lower Mississippian) and the top of the Onondaga Limestone (Middle Devonian). Current interest is focused on the extensive shale body in eastern Ohio. This clastic wedge thickens from a featheredge at the outcrop in central Ohio to more than 4,000 feet along Ohio's eastern border with the panhandle of West Virginia.

A recent publication by Janssens and DeWitt (1976) incorporates a great deal of pertinent background material on the Devonian shales of Ohio and provides a foundation for more detailed investigations. Included is a short history of Devonian shale production, which began about 1860 and continues at the present time. Four separate periods of drilling activity have accounted for more than 1,500 productive Devonian shale wells.

On the basis of a limited number of control points (43), Janssens and DeWitt mapped the generalized thickness of the Devonian shales. They also included a brief discussion of the type locality

of each of the rock units under consideration. The stratigraphic and geographic distribution of three major radioactive shale facies within the Ohio Shale and one within the Olentangy Shale are discussed and illustrated with the aid of three cross sections. Natural gas production associated with each of the four major radioactive facies is included in the discussion. Significant quantities of oil and gas also have been produced from siltstone reservoirs within the Chagrin Shale member of the Ohio Shale. More than 100 wells have produced hydrocarbons from the Chagrin member in Monroe, Noble, and Washington Counties.

Preliminary maps showing thickness of the Devonian shales, top and base elevations of the shales, elevation of the top of the Devonian shales radioactive facies, and thickness of the radioactive facies are included in Janssens and DeWitt's report.

Janssens and DeWitt's research, as well as the present paper, is based almost entirely upon borehole geophysical log studies. This approach facilitates rapid acquisition of geologic data for preliminary mapping. More importantly, with the exception of the Chagrin siltstone production, there appears to be an empirical relationship between established production or shows of gas and high radioactivity (greater than 160 A.P.I. units) as seen on a gamma ray log. The higher than normal gamma ray readings probably reflect above-average concentrations of uranium, which, according to Swanson (1961, p. 103), result from preferential precipitation of uranium from sea water in the presence of organic matter.

A great deal of additional information and supporting data also are included in the Janssens and DeWitt report. However, because this information is both recent and is readily available in published form, it will not be repeated in this progress report.

A map showing wells producing from the Devonian shales (which includes sandstones and siltstones within the Ohio Shale) has been compiled by Janssens (1975) and has been updated by the staff of the Subsurface Geology Section. More than 140 wells and an additional 52 pool or field locations are shown. Individual wells are assigned to five categories according to reported initial production, which ranges from less than 50 MCFPD to more than 500 MCFPD.

Additionally, a map illustrating reported oil and gas shows in the Ohio Shale of eastern Ohio has been compiled and posted by Gearheart and Grapes (1977). More than 400 wells are shown by individual well symbols or by outlines which represent a cluster of wells. At least twice this number of wells have been reported to have had shows of gas in the Ohio Shale, but most of these cannot be documented by well records.

PURPOSE AND BENEFITS

One of the principal reasons for this preliminary mapping effort is to coordinate and standardize the investigative techniques and mapping units among ERDA Eastern Gas Shales Project stratigraphers so that a basin-wide interpretation can be developed. These results, although preliminary, provide a framework for correlation between known producing areas and zones and can be utilized to select sites for additional data acquisition or production-stimulation tests. In addition, interested producers can utilize reconnaissance data to focus their exploration activities in areas that are most likely to yield favorable results.

Furthermore, a rapid regional study of this scope allows the investigator to view the entire spectrum of data in the study area and to evaluate the effectiveness of predetermined mapping methods in depicting observed geologic conditions. Previewing the data in this manner may disclose inadequacy in mapping methods or may suggest techniques suitable for segregating and characterizing Devonian shale units which appear to contrast very subtly, if at all, with adjacent rocks.

SCOPE

The scope of this research is limited both in content and methodology. The two most readily mappable radioactive facies of the Devonian shales were selected for this gamma ray log investigation. With the exception of some fairly detailed correlations on three of the six regional cross sections upon which this report is based, the remainder of this study was conducted in July and August.

The structure and isopach maps in this report are based upon 197 control points. A fairly significant part of the available time was expended in selecting representative borehole geophysical logs from the files. No time was available to adequately resolve internal inconsistencies which invariably crop up in regional investigations.

Although the results of this study require qualification because they are preliminary in nature, they should be quite useful for the purpose for which they are intended.

METHODS OF INVESTIGATION

One of the most reliable and widespread of the gamma ray log picks is the top of the Olentangy Shale (base of the lower Huron member of the Ohio Shale). Throughout most of the area of investigation, the "normal" natural radioactivity of the Olentangy Shale contrasts sharply with the highly radioactive facies of the lower Huron Shale. Even where this is not the case, the gamma ray log signature of the Olentangy is sufficiently diagnostic to permit its identification.

After establishing the base of the Huron Shale throughout eastern Ohio, the next step was to map the radioactive facies of the lower Huron. To accomplish this task, it was necessary first to define on the gamma ray log a threshold value which could be used to distinguish between radioactive and nonradioactive shale. The method decided upon for this preliminary investigation involved establishing a "normal shale" base line predicated upon the gamma ray log response of shale units observed to be fairly consistently nonradioactive. A shale base line for each well in Ohio was established on the basis of the natural radioactivity levels of the Bedford, Chagrin, nonradioactive Huron, and nonradioactive Olentangy Shales. Although differing greatly because of differences in equipment, calibration procedures, hole conditions, etc., this value commonly was 140 A.P.I. units. Radioactive shales then were defined as those shales having a gamma ray log response 20 A.P.I. units (or the equivalent in the case of the older logs) to the right of the shale base line. This method, although not completely objective because of the attenuation effect of different numbers of casing strings, proved to be a pragmatic approach to the problem.

In a few areas of the state, the upper contact of the lower Huron radioactive facies is sharp and unequivocal. Typically, however, the upper contact is transitional and interbedded. In this case, for isopach purposes the top of the mapping unit was defined as the top of the uppermost radioactive tongue which was not preceded by a nonradioactive tongue of greater thickness. In a few cases, where the literal application of this criterion would exclude thick radioactive tongues genetically related to underlying units, an exception was made in the interest of providing a geologic interpretation which would more accurately represent existing local conditions. By convention, the minimum size of a unit for mapping purposes was set at 25 feet. The isopach value for the radioactive facies was arrived at by subtracting the depth of the top of the unit from the depth of its base. No adjustment was made for the thickness of interbedded nonradioactive units.

The base of the Rhinestreet Shale equivalent in Ohio was determined by tracing the unit from New York state through Pennsylvania and into Columbiana County, Ohio, on a series of regional cross sections. Correlations in New York and Pennsylvania were established by stratigraphers from the respective state surveys involved in the ERDA Eastern Gas Shales Project. The radioactive facies of the Rhinestreet Shale equivalent in Ohio was mapped in a manner similar to that described for the lower Huron Shale.

RESULTS OF INVESTIGATIONS

Figure 2 shows the elevation of the base of the Huron member of the Ohio Shale (top of the Olentangy Shale). As is the case with most regional structure maps of eastern Ohio, the map on the base of the Huron member shows homoclinal southeasterly dip into the Appalachian Basin. As expected, this map is quite similar to Janssens and DeWitt's (1976, fig. 5) regional structure map on the base of the Devonian shales (base of the Olentangy Shale) and provides structural control on a reliable mapping horizon within the Devonian shale sequence. Also, in the event that the lower Huron radioactive facies proves to be the most exploitable zone commercially, a detailed map on the base of this horizon will materially aid in predicting drilling depths.

Figure 3 illustrates the tentative relationships among the formations and members which lie between the Berea Sandstone and Onondaga Limestone. The Cleveland Shale, which has been mapped by Lewis and Schwietering (1971), is the uppermost radioactive unit within the Devonian shales sequence. As illustrated in Figure 3, the Cleveland Shale thins and pinches out eastward, probably by depositional thinning. Where the Cleveland Shale no longer is present, the overlying Bedford Shale and the underlying Chagrin Shale, which are similar lithologically, cannot be differentiated with assurance because their gamma ray log characteristics also are very similar. Possibly additional research will provide criteria which will establish a mappable contact between the Bedford and the Chagrin beyond the eastern limits of the Cleveland Shale.

As depicted in Figure 3, the contact between the Chagrin Shale and the Huron Shale is picked

easily from the gamma ray logs as far east as the border between Wayne and Stark Counties. At this point, the upper Huron radioactive facies, which is separated from the massive lower Huron radioactive facies in the Wayne County area by a westward-thinning tongue of nonradioactive shale, gradually loses its characteristic appearance on the gamma ray log. To the east, the gamma ray log appearance of the nonradioactive facies equivalent of the upper Huron Shale is indistinguishable from that of the Chagrin Shale above it and the nonradioactive tongue of the Huron Shale below it. As a result, the Chagrin-Huron contact probably will be very difficult or impossible to establish with certainty eastward of the upper Huron facies change.

The radioactive facies of the lower Huron Shale continues considerably farther eastward. However, it too undergoes a facies change to nonradioactive shale. This occurs in two stages. First, the upper half of the lower Huron gradually loses its distinctive gamma ray log appearance as interbedded nonradioactive shale beds increase in thickness to the east, by facies change, to displace the radioactive beds. Figure 3 illustrates this facies change near the Stark County-Columbiana County line. A similar change takes place in the case of the lower half of the lower Huron, except that the radioactive facies persists slightly farther east.

As shown by Figure 3, the Olentangy Shale thickens substantially to the east. A radioactive shale facies within the lower Olentangy Shale has been tentatively correlated, on the basis of regional cross sections, with the Rhinestreet Shale member of the West Falls Group (New York state terminology). The stratigraphic relationship of the radioactive facies of the Rhinestreet equivalent to surrounding rocks is shown in Figure 3.

Figure 4 shows the distribution and thickness of the radioactive facies of the Rhinestreet equivalent. At least two wells currently produce from this unit in Ohio. These are located in Columbiana County in Fairfield and Franklin Townships. Reported initial daily productions are 65 MCF after frac and 31 MCF after frac, respectively. Each of these wells was drilled to a deeper objective and plugged back for Devonian shale production. It probably is more than coincidental that these producing wells are located in an area of thick radioactive Rhinestreet and that the higher reported initial production is located in an area of thicker Rhinestreet. On the basis of this preliminary investigation, it appears as though the greatest opportunity to establish gas prodution from the Rhinestreet will be in areas where the radioactive facies has a thickness greater than 125 feet. Because Figure 4 is preliminary and generalized, additional geologic research will be required to pinpoint sites which would be likely to produce gas from this interval. Figure 4 does suggest, however, that the greatest opportunity for Rhinestreet production should be in the Columbiana-Mahoning County area where the radioactive facies appears to be the thickest.

Figure 5 shows the distribution and thickness of the radioactive facies of the lower Huron Shale. This facies of the Devonian shales probably will offer the greatest potential for large-scale gas production because of its areal extent and thickness. With the possible exception of the siltstone facies of the Chagrin Shale member, this unit is the one from which most of the established Devonian shales production has been obtained. Throughout most of eastern Ohio the radioactive facies of the lower Huron is consistently 200 to 400 feet thick. In general, this unit thins to the west by depositional thinning and to the east by facies change to nonradioactive shale. The major exception to this trend is the thick area shown in Monroe and Belmont Counties; mapping of this area is based on control from a single well. The reproducibility of the data from this well is questionable, and additional research may prove this interpretation to be inaccurate.

CONCLUSIONS

The radioactive shale units of the Devonian shales, the Cleveland Shale, the radioactive facies of the upper and lower Huron member, and the radioactive facies of the Rhinestreet equivalent within the lower Olentangy Shale can be readily and accurately mapped using gamma ray logs. Since an empirical relationship exists between gas production and the highly radioactive shale facies, mapping of the structure, thickness, and distribution of these potentially productive units should be a practical approach to subsurface stratigraphic investigations or exploration for natural gas.

Hydrocarbon production from the siltstone facies of the Chagrin member is from a conventional, albeit marginally commercial, reservoir. The question which remains to be answered concerns the productive potential of the Devonian shale units of normal radioactivity. Details of the stratigraphy of these units will be difficult, if not impossible, to ascertain by gamma ray log studies. A comprehensive investigation combining borehole geophysical log investigations and detailed sample and core examination will be required to accomplish this task.

ACKNOWLEDGMENTS

The writer would like to acknowledge the sponsorship of the U.S. Energy Research and Development Agency and the excellent cooperation and contributions of fellow researchers on the Eastern Gas Shales Project. The author also wishes to thank Charles R. Grapes II for his assistance in selecting some of the gamma ray log control.

REFERENCES CITED

Gearheart, L. C., and Grapes, C. R., 1977, Gas and oil shows in the Ohio Shale in eastern Ohio: Ohio Geol. Survey Open File Map 101.

Janssens, A., 1975, Map showing wells producing from the Ohio Shale in eastern Ohio; includes sandstones and siltstones within the Ohio Shale: Ohio Geol. Survey Open File Map 77.

Janssens, A., and de Witt, Wallace, Jr., 1976, Potential natural gas resources in the Devonian shales in Ohio: Ohio Geol. Survey Geol. Note 3, 12 p., 1 plate.

Swanson, V. E., 1961, Geology and geochemistry of uranium in marine black shales, a review: U.S. Geol. Survey Prof. Paper 356-C, p. 67-110.

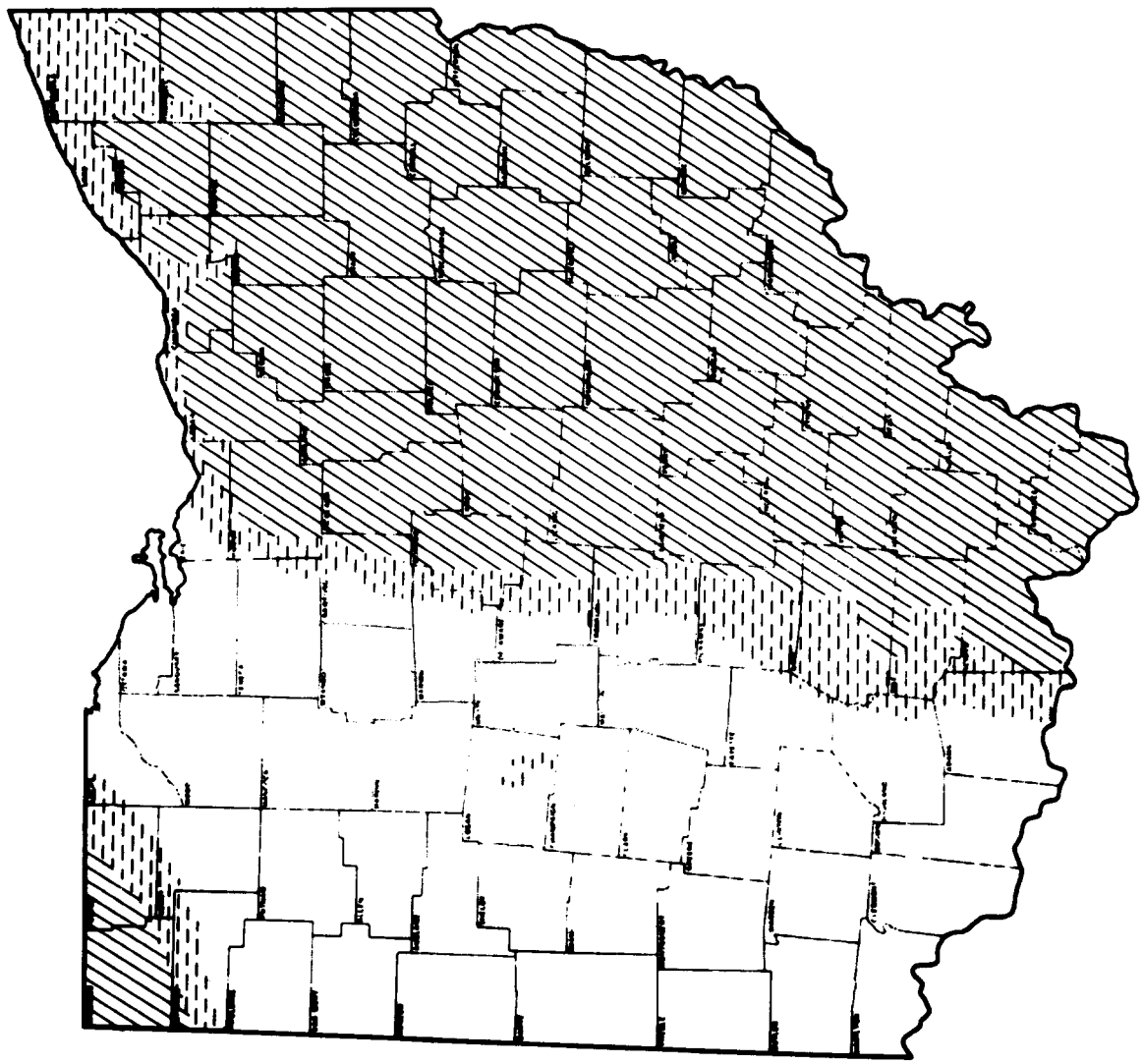

FIGURE 1. - Generalized occurence of the Devonian shales in Ohio (from Janssens and DeWitt, 1976, fig. 1)

FIGURE 2. - Preliminary regional structure map of the base of the Huron member of the Ohio Shale (top of the Olentangy Shale)

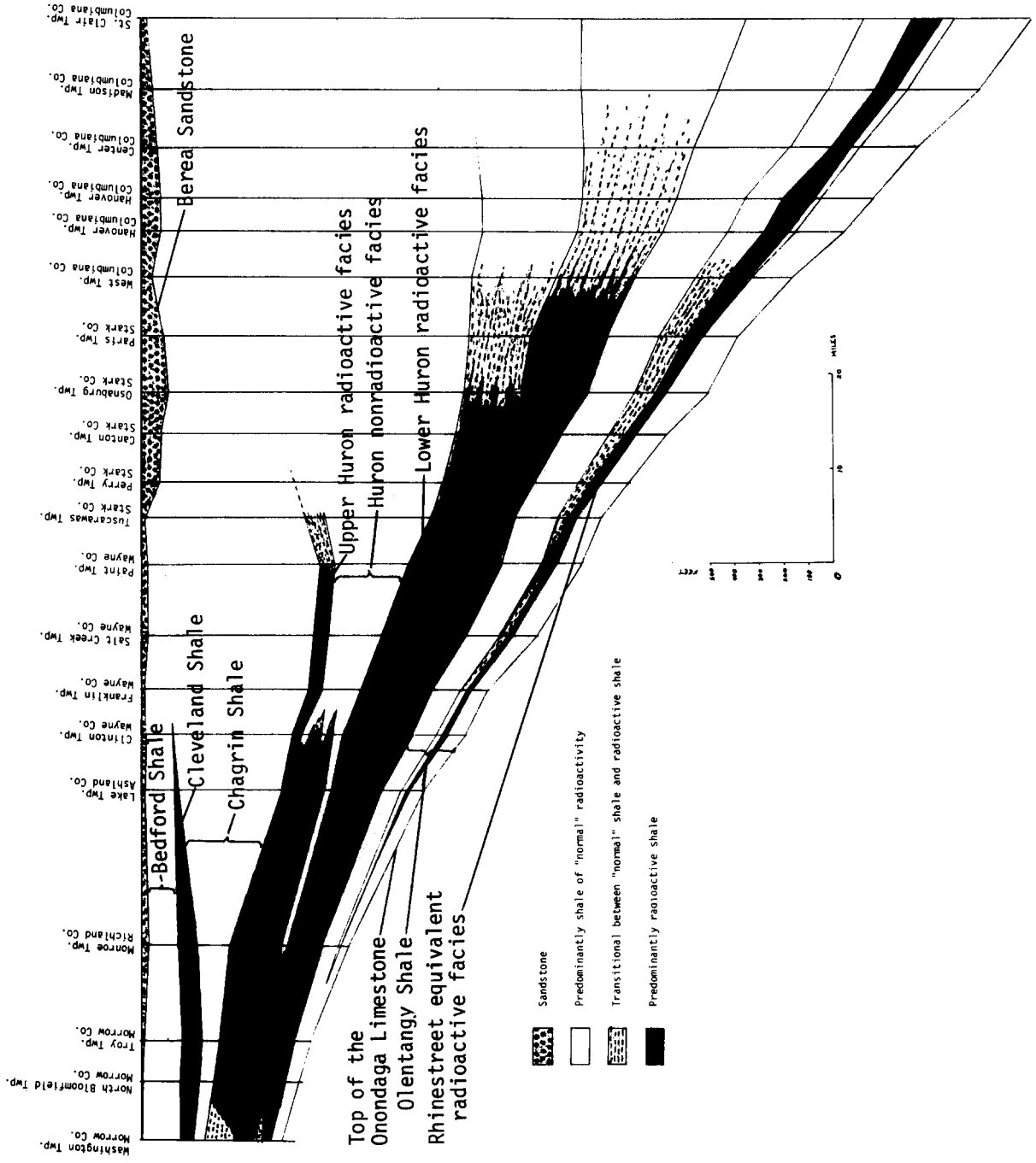

FIGURE 3. - Generalized cross section illustrating the stratigraphic relationships of the geologic units and radioactive facies comprising the Devonian shales sequence in Ohio

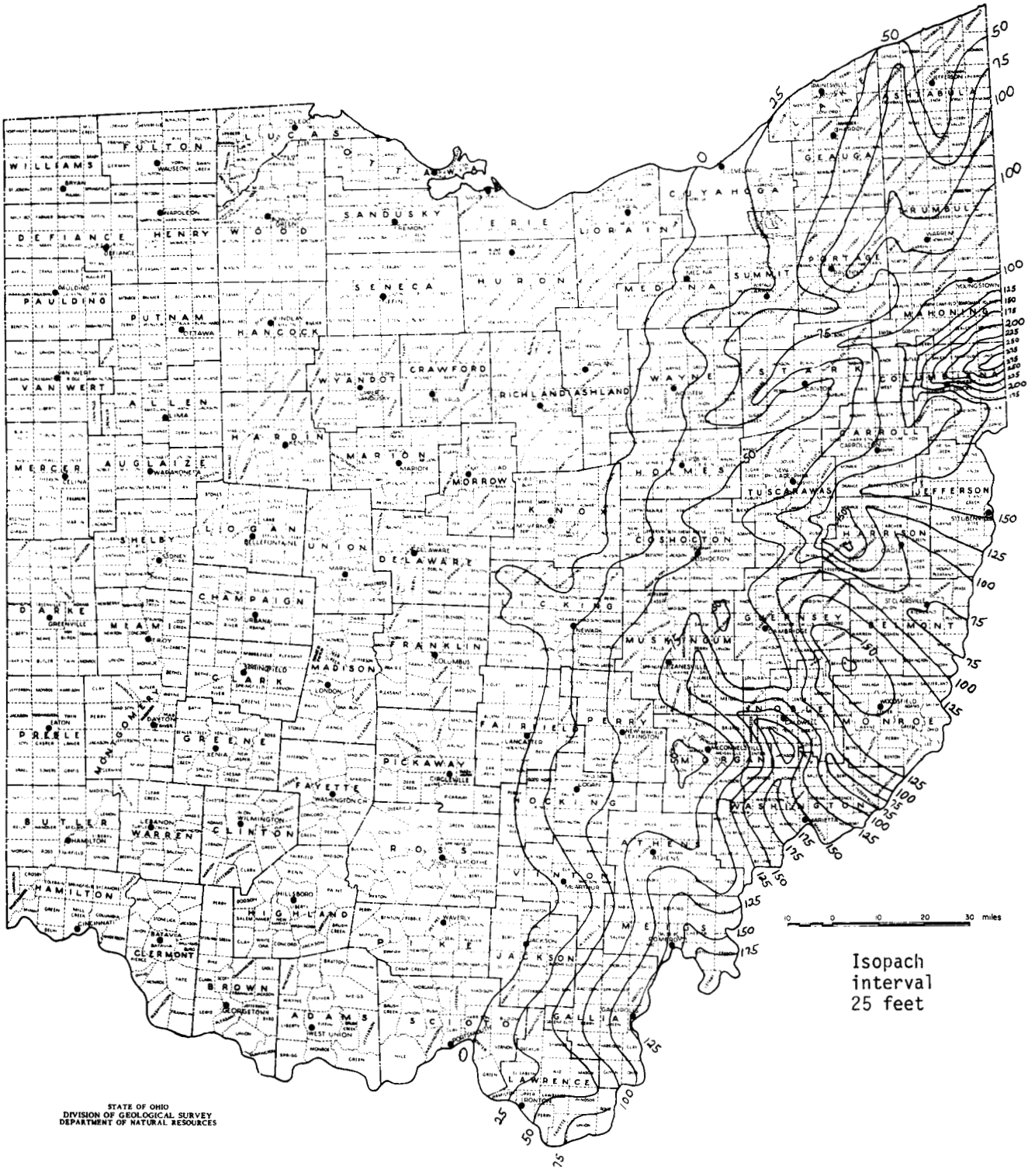

FIGURE 4. - Generalized thickness of a radioactive shale unit within the lower Olentangy Shale (approximate equivalent of the Rhinestreet Shale member of the West Falls Group of New York state)

FIGURE 5. - Generalized thickness of the radioactive shale facies of the lower Huron member of the Ohio Shale

USE OF THE SCINTILLOMETER AND GAMMA-RAY LOGS FOR CORRELATION FROM THE SUBSURFACE TO THE SURFACE IN BLACK SHALE

by

Frank R. Ettensohn, Department of Geology, University of Kentucky
Linda Provo Fulton[1], Department of Geology, University of Cincinnati
Roy C. Kepferle, U.S. Geological Survey, University of Cincinnati

ABSTRACT

Stratigraphic studies of the Devonian and Mississippian Ohio, Sunbury, New Albany, and Chattanooga Shales (consisting primarily of black, organic-rich shale) in the eastern portions of Ohio, Kentucky and Tennessee indicate that radioactive units evident on subsurface gamma-ray logs from oil and gas wells penetrating these formations can be distinguished in outcrops and in cores by using a scintillometer. Measurements of gamma radiation made with a portable scintillometer at close vertical intervals along the surface of a black-shale exposure or core are found to produce radioactivity profiles that closely resemble gamma-ray curves from the same formation in the subsurface. Because the units of the scintillometer profiles and gamma-ray curves are not identical (counts/second vs. API units), the curves are not comparable on a quantitative basis, although their patterns are qualitatively similar enough to allow good correlation.

Except for thin green-shale beds distributed throughout the black shale, exposures of the Ohio, New Albany, and Chattanooga Shales are lithologically homogeneous. Use of this technique has shown, however, that these black-shale formations contain seven major radioactive units, which can now be correlated with named surface and subsurface units. With a scintillometer, the presence or absence and thickness of these units can be determined in otherwise homogeneous-appearing exposures of the black shale or in cores from wells lacking gamma-ray logs. Use of this scintillometer technique together with gamma-ray logs has proved useful in defining an internal basin-wide stratigraphy for the Devonian and Mississippian black shales.

Key ideas: Devonian and Mississippian Ohio, Sunbury, New Albany, and Chattanooga Shales, black shale, radioactive units, gamma-ray logs, scintillometer, radioactivity profiles, correlation, stratigraphy.

INTRODUCTION

The Ohio, Sunbury, New Albany, and Chattanooga Shales (upper Devonian and lower Mississippian) consist almost wholly of black, organic-rich shale. Exposures of these black-shale formations appear to be homogeneous except for thin beds of greenish-gray shale distributed locally throughout the black-shale sequence. These black shales comprise as much as one-fourth of the Devonian sedimentary sequence in the Appalachian basin, yet because stratigraphic and paleontologic control is lacking, these shales locally defy all but the coarsest subdivision. The Devonian and Mississippian black

[1]Present address: Exxon Company, U.S.A., New Orleans, LA 70161

shales of Ohio and Tennessee have been divided (Campbell, 1946, Hass, 1956; Hoover, 1960; Conant and Swanson, 1961). In the subsurface, moreover, drillers have used informal and highly variable subdivisions based on lithology, color, and texture. In eastern Kentucky exposures, however, the Ohio, New Albany, and Chattanooga Shales have not been subdivided because of their apparent homogeneity, thus impeding comparison and correlation with black-shale units in the subsurface and in adjacent states.

Examination of many gamma-ray logs, drillers' logs, and subsurface samples from eastern Kentucky and immediately adjacent areas (Figure 1) has revealed that readily apparent and persistent radioactive units can be distinguished on gamma-ray logs from these subsurface black-shale formations (Figure 2) (Provo, 1977a, b). Although these units are related primarily to changes in the amount of radioactivity, some of the changes in radioactivity are also accompanied by changes in lithology.

These radioactive units, it seemed, should be recognizable also in outcrops and cores in the Ohio, New Albany, and Chattanooga Shales. A vertical sequence of gamma-radiation measurements was recorded at close intervals on the surfaces of black-shale exposures and cores using a scintillometer. Plotting these measurements produced radioactivity profiles which are qualitatively similar to gamma-ray curves from the same formation in the subsurface (Figure 2). The presence of radioactive units revealed by this technique in black-shale exposures and cores has greatly facilitated correlation with similar radioactive units described from the subsurface.

This paper apparently represents the first reported stratigraphic use of scintillometer-generated radioactivity profiles for correlating between the surface and subsurface in black shales. Somewhat similar techniques have been used in searching for high concentrations of uranium in black shales. Conant and Swanson (1961, Figure 18) compared the uranium content in well samples from five subunits of the Chattanooga Shale in Tennessee with a gamma-ray log from the same well. Closer yet to our technique, is the work of Glover (1959, Figure 20) in which a scintillometer-generated radioactivity profile was compared with uranium content and degree of weathering in exposures of the Chattanooga Shale in Tennessee.

PROCEDURES

The technique we have used most successfully involves a minimum of three people. Using a telescopic Jacob's staff mounted with an Abney level, two people measure a succession of five-feet vertical intervals on the face of an exposure. The measuring interval on the Jacob's staff is set at five feet, but its telescopic nature allows for easy adjustment to lesser intervals. Although the beds in most black-shale exposures throughout eastern Kentucky are nearly horizontal, the inclinometer on the Abney level can be adjusted to match the dip of the beds. One person sights through the Abney level parallel to dip, while a second person marks the line-of-sight intersection on the outcrop with a brightly colored piece of engineer's tape (Figure 3). The cumulative thickness above the base of the unit is recorded on each successive piece of tape. A third person records scintillometer measurements at two-and-one-half feet intervals using the five-feet interval markers as guides (Figure 3), describes the outcrop, and collects samples with reference to the five-feet markers. It is important that the scintillometer be placed on the flattest surface available, because depressions on the outcrop surface tend to concentrate natural radioactivity, resulting in higher-than-normal values. On exposures with nearly vertical faces, a tape must be used to measure intervals, and scintillometer measurements were recorded by rappelling down the face of the exposure (Figure 4). We have found that readings at two-and-one-half feet intervals work well when the black-shale formation is greater than 50 feet in thickness. On and near the Cincinnati Arch, however, where the entire black-shale sequence thins to less than 50 feet (Figure 5), our data indicate that measurements should be recorded at one-foot intervals. Scintillometer measurements and the lithology are plotted at the proper elevations above the base of the unit (Figures 2 and 5). The resulting radioactivity profile can then be interpreted and compared with gamma-ray logs from nearby wells (Figure 2).

Generating radioactivity profiles from cores is considerably easier. The core is laid out, and the scintillometer is placed on the core at intervals of one to two-and-one-half feet. The measurements are recorded and plotted against depth below the surface (Figures 7 and 8). Radioactivity profiles from cores provide a means of comparing core profiles with various wireline logs from the same well (Figures 7 and 8).

IMPLICATIONS

In an analysis of gamma-ray logs and sample sets from eastern Kentucky and adjacent regions, Provo (1977a, b) demonstrated that seven radioactive units can be distinguished in the Ohio, New Albany, and Chattanooga Shales of the subsurface (Figure 2). Scintillometer-generated radioactivity profiles from outcrops and cores are similar enough to gamma-ray curves from nearby wells (Figure 2)

that five to six of the radioactive units distinguished in the subsurface can also be identified in the outcrop belt and in cores. This has enabled correlation with surface units from adjacent states and with some drillers' units in the subsurface (Provo and others, 1977).

Because gamma-ray logs are continuous curves in contrast to the sequence of connected points composing radioactivity profiles, gamma-ray logs and radioactivity profiles will not be identical (Figure 7). Furthermore, because the units of radioactivity profiles and gamma-ray curves are not the same (counts/second vs. API units), the curves are not exactly comparable on a quantitative basis. Nonetheless, their patterns are qualitatively similar enough to allow good correlation. Figure 8 also shows good correlation between a resistivity log and a radioactivity profile of core from the same well. It should be noted, however, that the radioactive units do not necessarily reflect changes in lithology, but rather changes in the amount of radioactive material present. In Figure 9, the general similarity between the curve for U_3O_8 content and the radioactivity profile from Tener Mountain, Ohio, clearly illustrates this relationship.

Throughout eastern Kentucky, this largely Devonian black-shale sequence is identified under three stratigraphic names, the Chattanooga, New Albany, or Ohio Shale. The Chattanooga Shale of south-central Kentucky and the Ohio Shale of north-eastern Kentucky are entirely Devonian in age, whereas the uppermost portion of the New Albany Shale in east-central Kentucky is Mississippian in age (Figure 10). In northeastern Kentucky, the black, organic-rich Sunbury Shale of Mississippian age is separated from the Ohio Shale of Devonian age by the Berea Sandstone and Bedford Shale of Devonian and Mississippian age (Figure 10). The Berea Sandstone and Bedford Shale, however, thin to the south, and both units pinch out before reaching central Kentucky (Peck, 1967; Weir, 1976), so that Mississippian black shales equivalent to the Sunbury conformably overlie Devonian black shales equivalent to the Ohio Shale. At the point in central Kentucky where Mississippian and Devonian black shales can no longer be separated, the stratigraphic nomenclature changes from the Ohio and Sunbury Shales to the New Albany Shale (Figure 10). Except for paleontologic discrimination by conodonts (Weir, 1967), no easy means exist for differentiating Devonian and Mississippian parts of the New Albany Shale. Comparison of radioactivity profiles and gamma-ray logs from areas where the Berea-Bedford interval is present and from areas where this interval is absent revealed that Devonian and Mississippian black shales can usually be differentiated in outcrops where the Berea-Bedford interval is absent. The Mississippian Sunbury Shale and its equivalents in central Kentucky are far more radioactive than most parts of the underlying Devonian black-shale sequence. Radioactivity in the Sunbury Shale usually exceeds 300 API units and may range higher than 400 API units, creating a prominent positive deviation which is easily recognized in gamma-ray logs (Figure 2). The same positive deviation is also easily recognized in radioactivity profiles (Figure 2), even where the Berea-Bedford interval is absent (Figure 3). Hence, in Figure 11, the strong positive deviation at the top of the New Albany Shale is interpreted to be the equivalent of a similar deviation in the Mississippian Sunbury Shale. Moreover, the absence of this prominent positive deviation in some radioactive profiles from Chattanooga Shale of south-central Kentucky (Figure 5) must indicate that the Mississippian Sunbury Shale equivalent is absent in this area.

SUMMARY

Except for thin greenish-gray shale beds distributed locally throughout the Devonian and Mississippian black shales, exposures of the Ohio, New Albany, and Chattanooga Shales in east-central Kentucky appear homogeneous. The need for comparing outcrop stratigraphy in these apparently homogeneous black-shale units with the subsurface stratigraphy interpreted from gamma-ray logs prompted the development of a technique for making radioactivity profiles or synthetic gamma-ray logs from outcrops and cores. A series of readings from a portable scintillometer taken at close vertical intervals on the outcrop or on core was found to produce radioactivity profiles which closely resemble gamma-ray logs from the same formation in the subsurface. Although the radioactivity profile and gamma-ray curves are not identical and the units on each are different, patterns from the two curves are qualitatively similar enough to allow good correlation.

Examination of gamma-ray logs from wells in Devonian and Mississippian black-shale formations indicates that seven major radioactive units can be distinguished. Using a scintillometer-generated radioactivity profile, these same units can now be distinguished in otherwise homogeneous-appearing exposures of the black shale and in cores. Use of this technique facilitates correlation between the surface and subsurface and has proved especially useful for differentiating the Mississippian Sunbury Shale equivalents from the underlying Devonian black shales where the Berea Sandstone and Bedford Shale are absent.

ACKNOWLEDGMENTS

The authors thank Dennis Swager, Michael Miller, and Les Booth of the University of Kentucky for

assistance in measuring, describing, and profiling the sections and core. Les Booth drafted the figures used in this paper. We also thank Wallace de Witt, Jr., John Roen, and William MacQuown, who reviewed various stages of the manuscript. Mr. E. N. Wilson of the Kentucky Geological Survey provided access to wireline logs. The uranium analyses in Figure 9 were provided by the Nuclear Fuels Branch of the U.S. Energy Research Development Administration (operated by Bendix Field Engineering Corporation), Grand Junction, Colorado under contract number AT(05-1)-1650. This work was largely supported under ERDA contracts AT(05-1)-1650 and EY-76-C-05-5202.

REFERENCES

Campbell, F. New Albany Shale. Geol. Soc. America Bull, v. 57, 1946, pp. 829-908.

Conant, L. C., and V. E. Swanson. Chattanooga Shale and Related Rocks of Central Tennessee and Nearby Areas. U.S. Geol. Survey Prof. Paper 357, 1961, 91 pp.

Glover, L. Stratigraphy and Uranium Content of the Chattanooga Shale in Northeastern Alabama, Northwestern Georgia and Eastern Tennessee. U.S. Geol. Survey Bull. 1987-E, 1959, pp. 133-168.

Hass, W. H. Age and Correlation of the Chattanooga Shale and the Maury Formation. U.S. Geol. Survey Prof. Paper 286, 1956, 47 pp.

Hoover, K. V. Devonian-Mississippian Shale Sequence in Ohio. Ohio Geol. Surv., Inf. Circ. 27, 1960, 154 pp.

Peck, J. H. Geologic Map of the Tollesboro Quadrangle, Lewis and Fleming Counties, Kentucky. U.S. Geol. Survey Geol. Quad. Map GQ-661, 1967.

Provo, L. J. Stratigraphy and Sedimentology of Radioactive Devonian-Mississippian Shales of the Central Appalachian Basin. U.S. Energy Research and Development Administration, Grand Junction, Colorado. Open File Report under contract AT(05-1)-1650, 1977a, 102 pp.

_____. Stratigraphy and Sedimentology of Radioactive Devonian-Mississippian Shales of Central Appalachian Basin. Unpubl. Ph.D. Dissert., Univ. Cincinnati, 1977b, 177 pp.

_____, R. C. Kepferle, and P. E. Potter. Three Lick Bed: Useful Stratigraphic Marker in Upper Devonian Shale in Eastern Kentucky and Adjacent Areas of Ohio, West Virginia, and Tennessee. U.S. Energy Research and Development Administration, Morgantown Energy Research Center, MERCE/CR77-2, 1977, 56 pp.

Weir, G. W. Geologic Map of the Berea Quadrangle, East-Central Kentucky. U.S. Geol. Quad. Map GQ-649, 1967.

_____. Geologic Map of the Means Quadrangle, East-Central Kentucky. U.S. Geol. Survey Geol. Quad. Map GQ-1324, 1976.

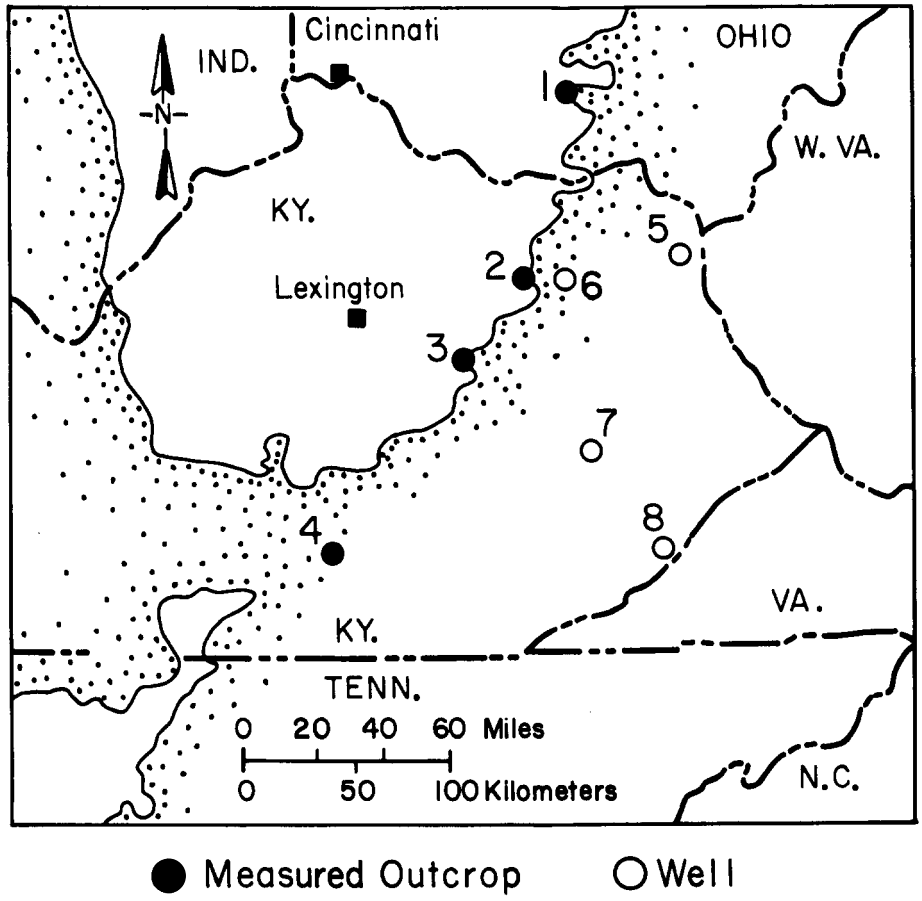

Figure 1.--Location map showing the distribution of Devonian and Mississippian black shale in eastern Kentucky and adjacent regions (stippled) and the location of outcrops, core material, and wells used in this study (after Provo, 1977a).

1. Tener Mountain Section, on Ohio Highway 32 near Peebles, Adams County, Ohio.
2. Morehead Section near Morehead Interchange on Interstate 64, Rowan County, Kentucky, 5-T-72.
3. Mountain Parkway Section near Clay City, Powell County, Kentucky 11-Q-67.
4. Big Clifty Section on Ringgold Road northwest of West Somerset, Pulaski County, Kentucky, 19-H-58.
5. Island Gas No. 533 Fee (Coalton), Boyd County, Kentucky, 11-V-81.
6. Pennzoil No. 1 Jones, Rowan County, Kentucky, 4-T-75.
7. Kentucky-West Virginia Gas Company 7239 Combs, Perry County, Kentucky, 19-K-76.
8. Pine Mountain Tunnel Project, Core Hole No. 5, Core Call No. C-247, Letcher County, Kentucky, 14-G-80.

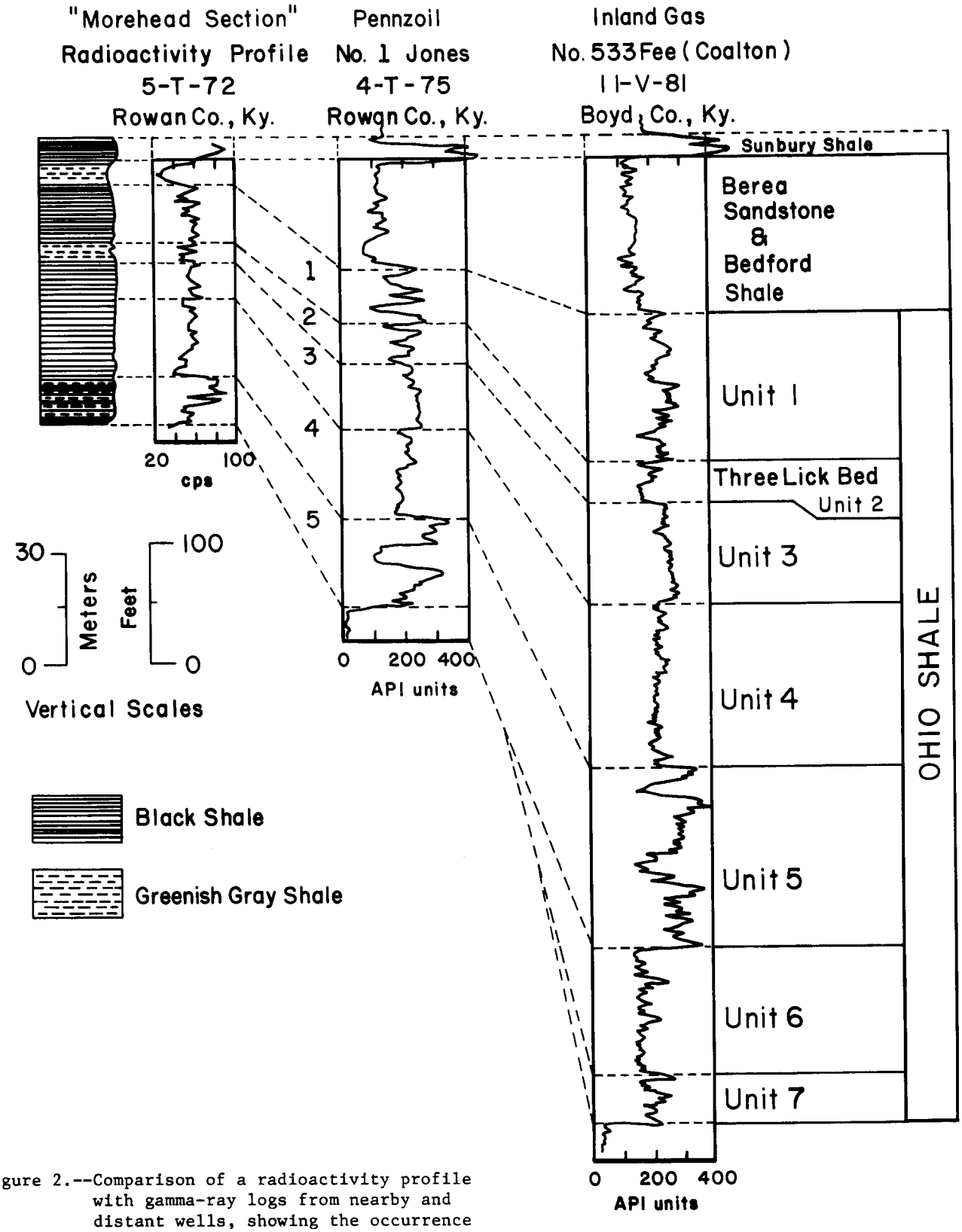

Figure 2.--Comparison of a radioactivity profile with gamma-ray logs from nearby and distant wells, showing the occurrence of radioactive units.

Figure 3.--Three students measuring, describing and profiling a black-shale section near Vanceburg, Kentucky. The upper two students are measuring and marking five-feet intervals with Jacob's staff and Abney level. The lower student is recording scintillometer readings.

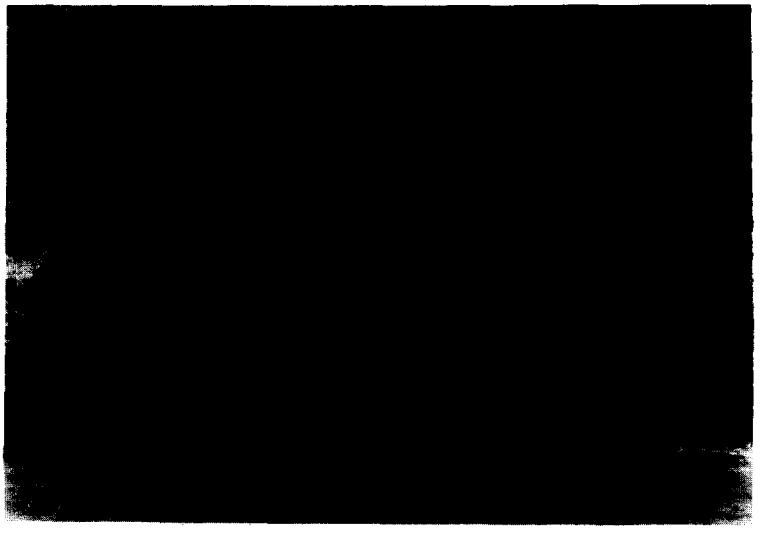

Figure 4.--Student rappelling down the nearly vertical face of a black-shale exposure to record scintillometer readings.

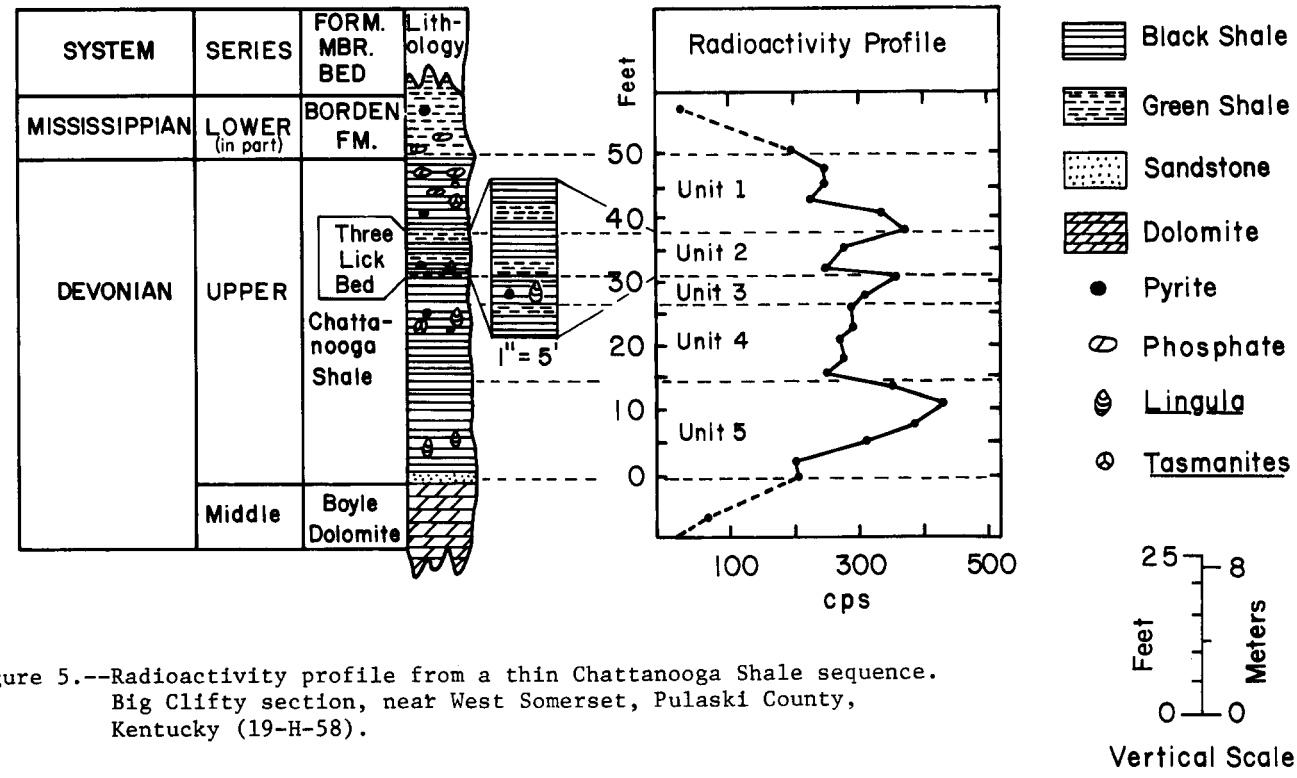

Figure 5.--Radioactivity profile from a thin Chattanooga Shale sequence. Big Clifty section, near West Somerset, Pulaski County, Kentucky (19-H-58).

Figure 6.--Use of a scintillometer on black-shale core from the Pine Mountain Tunnel Project.

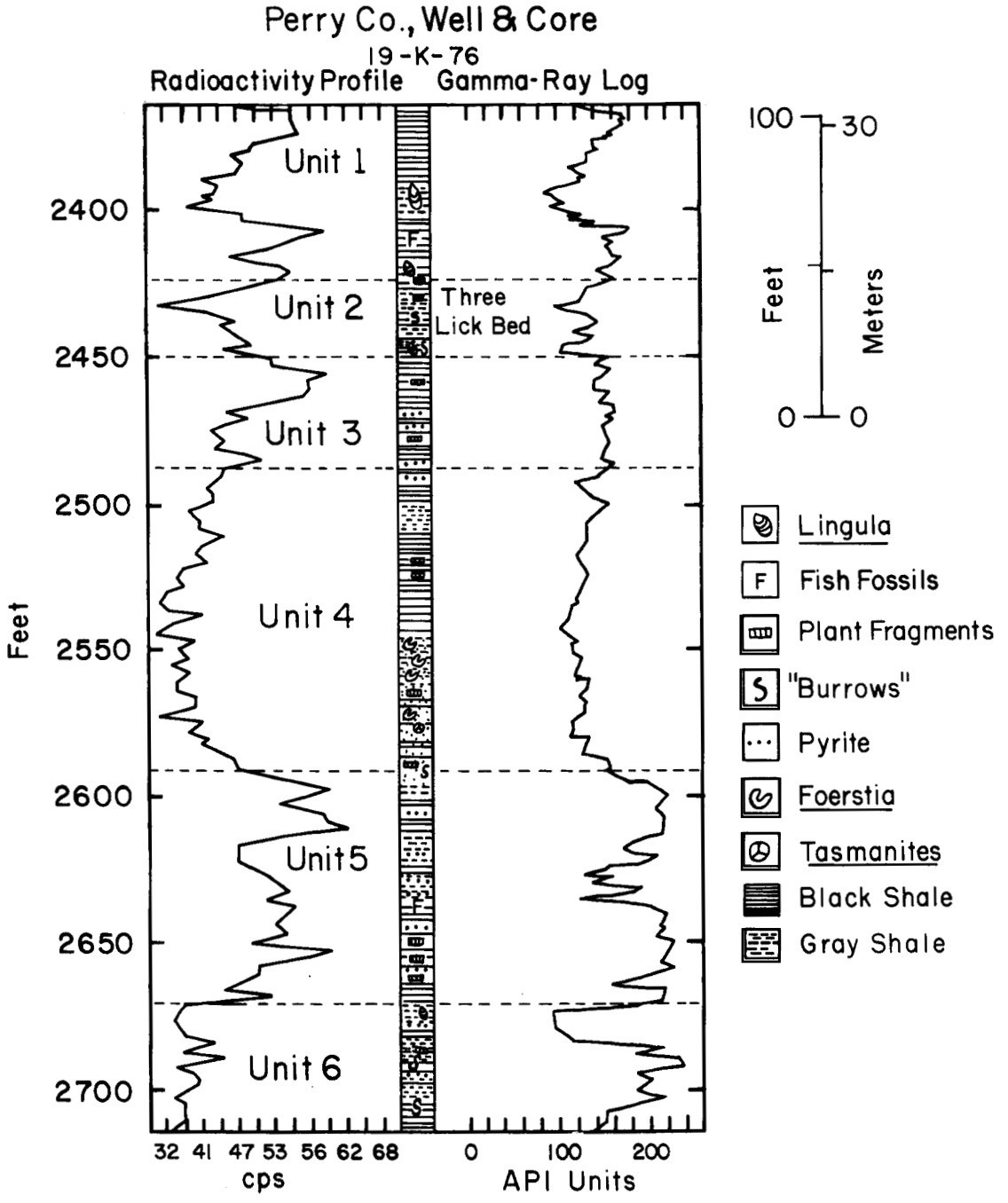

Figure 7.--Comparison of a gamma-ray log of the Ohio Shale from the Kentucky-West Virginia Gas Co. 7239 Combs Well with the radioactivity profile of core from the same well.

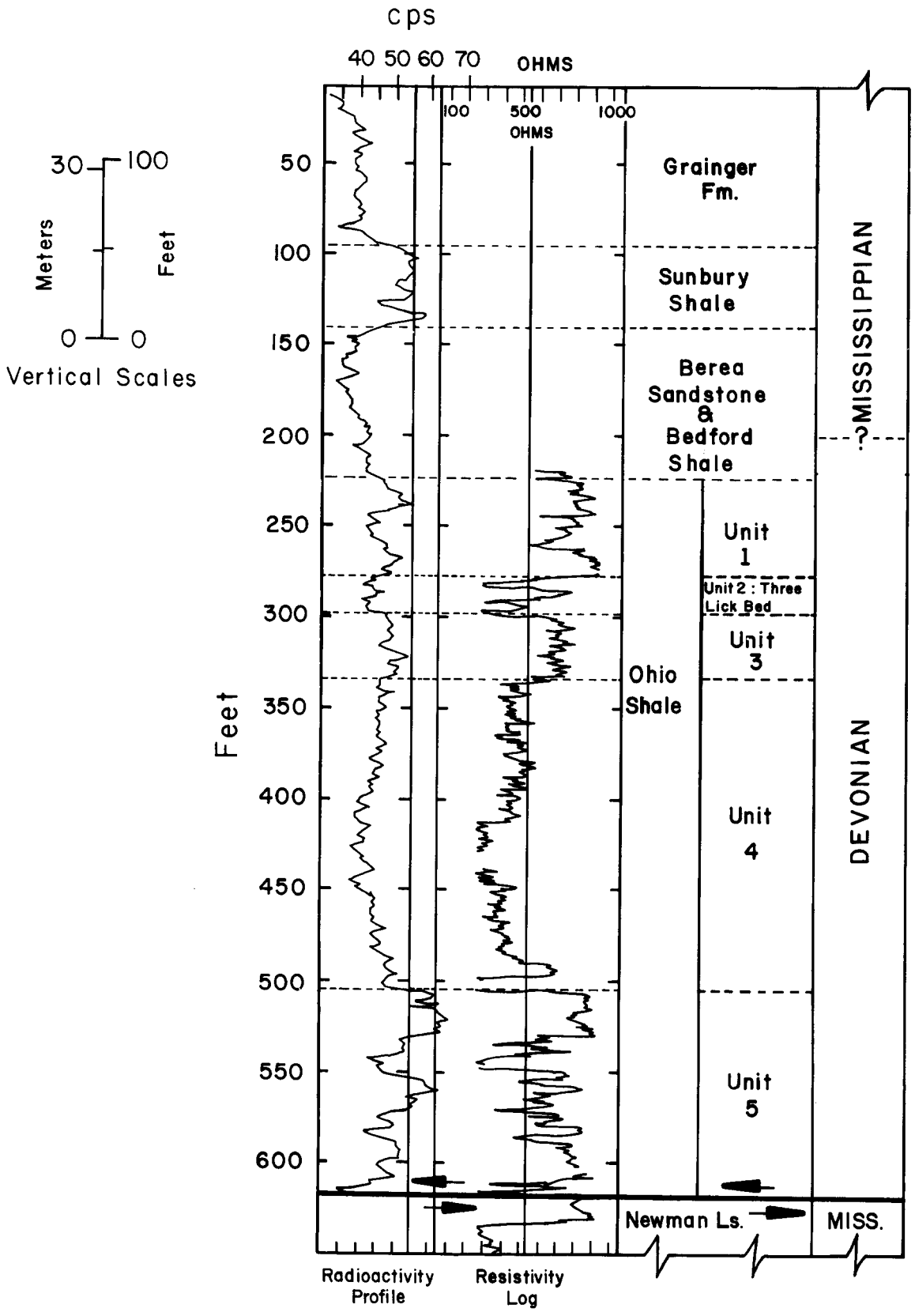

Figure 8.--Comparison of resistivity log from Pine Mountain Tunnel Project well with the radioactivity profile of core from the same well.

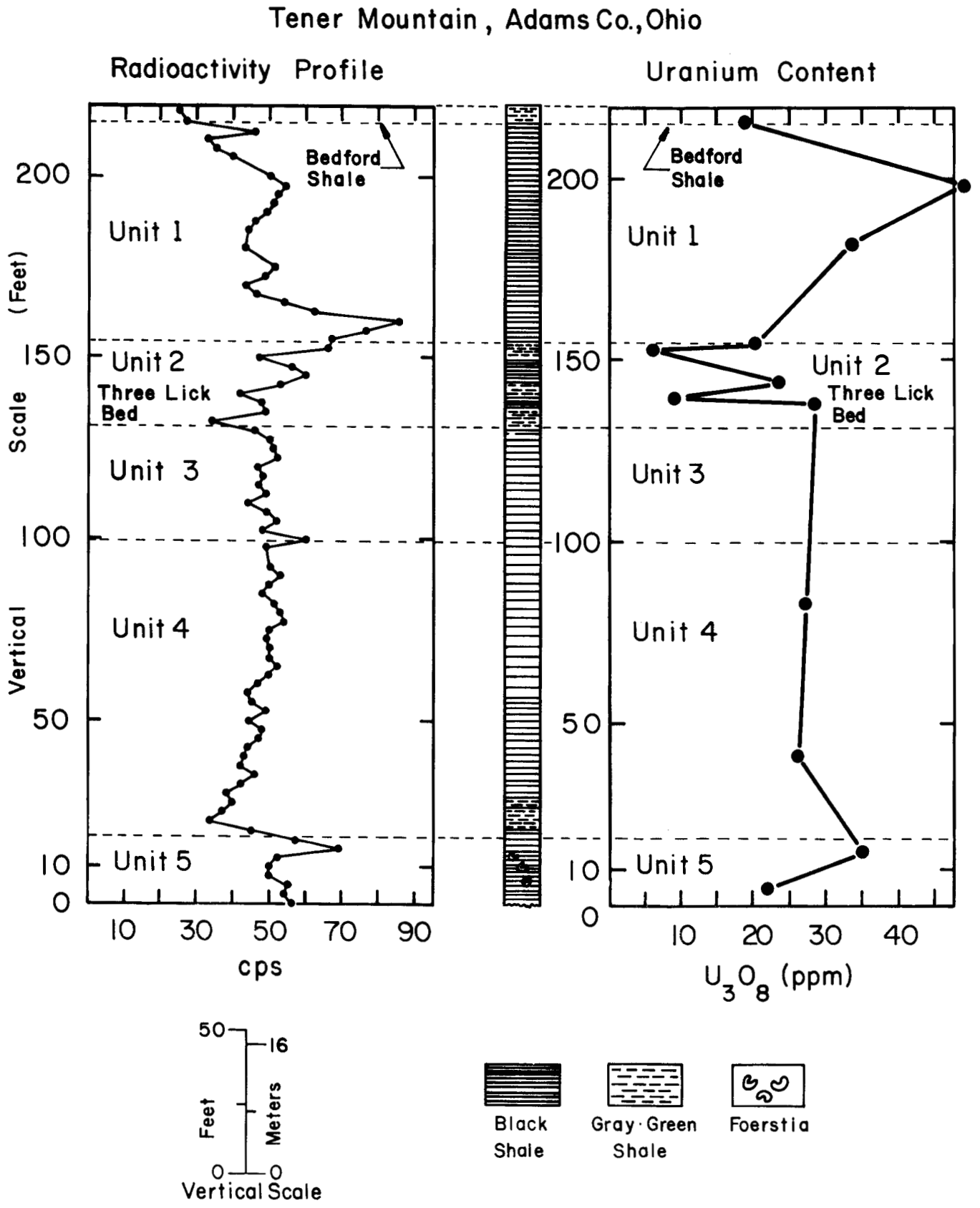

Figure 9.--Comparison of the uranium content and the radioactivity profile of the Ohio Shale from the Tener Mountain exposure, Adams County, Ohio.

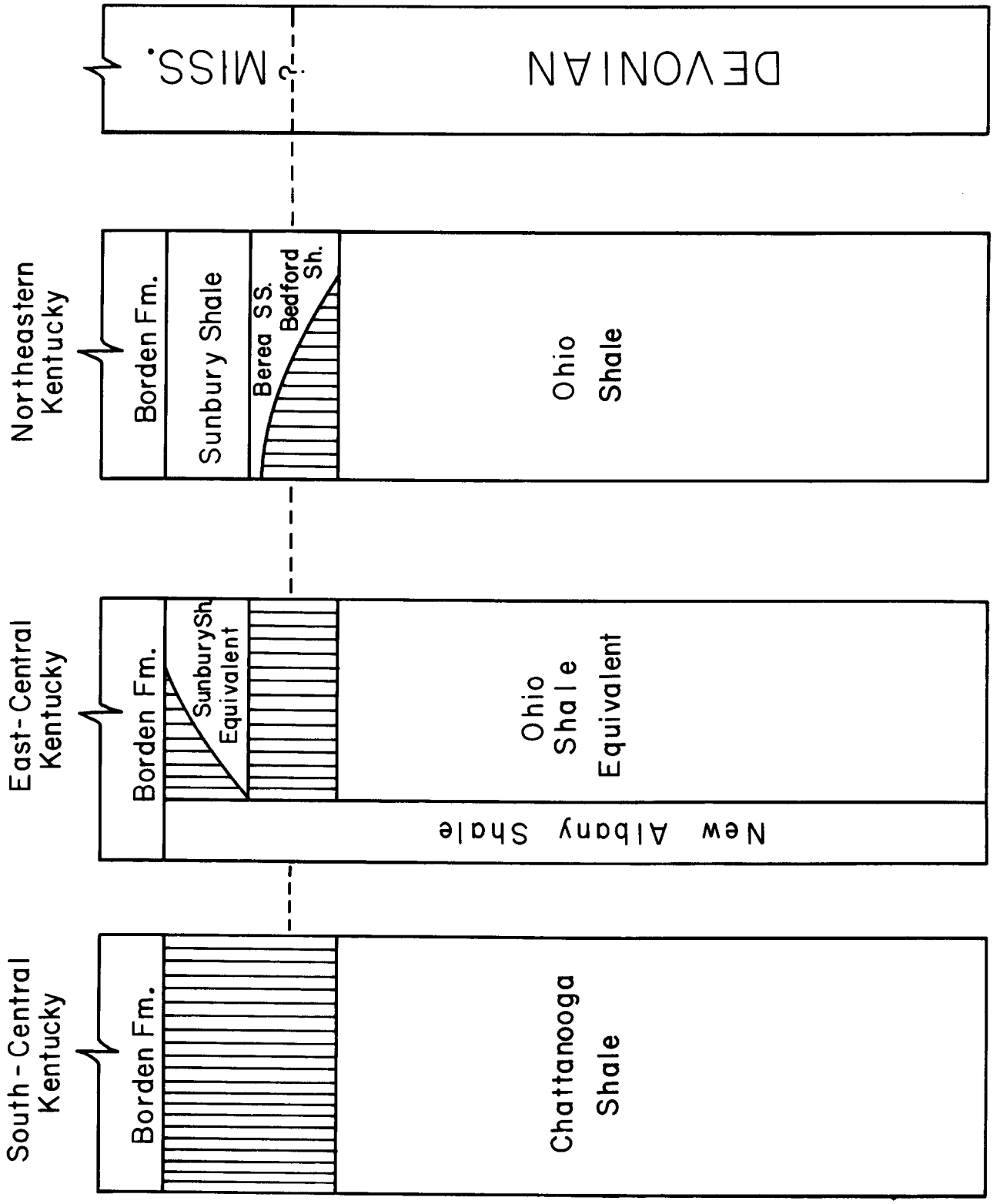

Figure 10.--Stratigraphy of the upper Devonian-lower Mississippian black-shale sequence along the outcrop belt in eastern Kentucky.

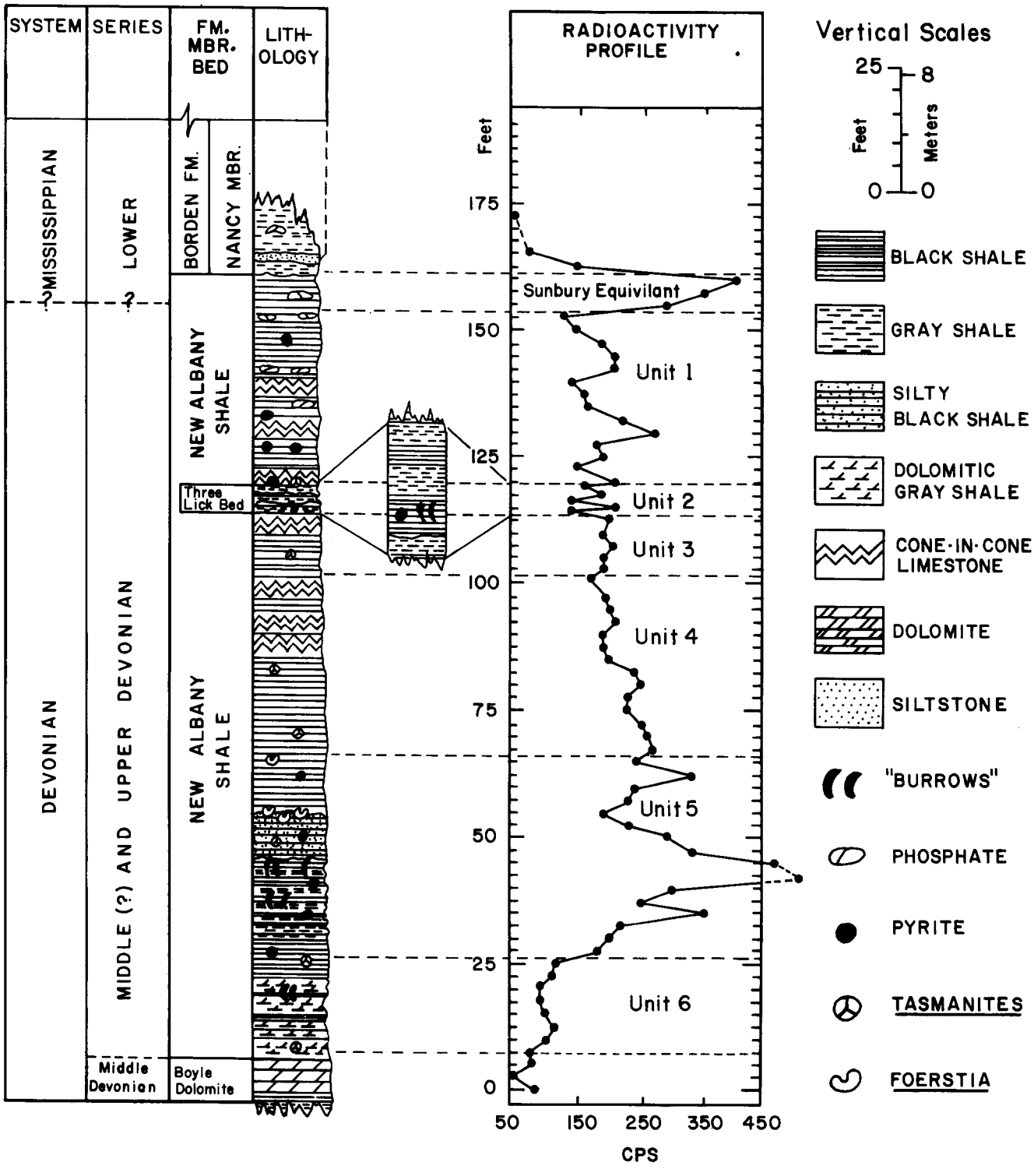

Figure 11.--Radioactivity profile from the Mountain Parkway section near Clay City, Powell County, Kentucky (11-Q-67), showing the Mississippian Sunbury Shale equivalent directly overlying Devonian black shale where the Berea Sandstone and Bedford Shale are absent.

HYBRID COMPUTERS FOR SIMULATION OF GAS DIFFUSION IN FRACTURED SHALE

by

Thomas E. Springer

Los Alamos Scientific Laboratory
Los Alamos, New Mexico 87545

ABSTRACT

To stimulate gas recovery from Devonian shales, extraction technologies may include hydraulic, explosive, and natural fractures, chemical leaching, and gas displacement. Described here is a computational technique using a hybrid (analog and digital) computer whose ultimate objective will involve simulation of experiments based on proposed extraction technologies to establish optimum economic stimulation methods. The technique has the potential use of determining expected values of production when only statistical distributions of crack densities, permeabilities, and other geophysical properties are known.

INTRODUCTION

In order to evaluate the induced change in gas production from Devonian shales caused by interconnecting existing fractures, by forming new fractures, and by modifying the region around the well bore, we have been increasing our capability for simulation of gas flow through non-isotropic porous media. While reservoir flow problems are normally solved on a digital computer, some particular characteristics of simulating gas flow in Devonian shale have indicated that a hybrid computer utilizing both analog and digital computing elements may prove more cost effective.

The purpose of this paper is to point out these characteristics and to discuss the hybrid computer model we have been implementing. With either a hybrid computer or a digital computer, diffusion flow is modeled as a one-, two-, or three-dimensional mesh of pressure nodes interconnected by transmissibilities whose values are adjusted to represent fractures, well bores, spatially varying permeabilities and porosities, and the like. The digital calculation must use discrete time steps and solve in sequence the difference equations of the mesh at each time step using such techniques as successive overrelaxation, special structure matrix solving, etc. [1,2,3,4]. The analog computer can, in principle, solve the many ordinary differential equations of the mesh in parallel. Because the problem variables exist continuously and simultaneously (instead of at discrete time steps only) throughout the analog circuits, integration is always a stable process. To realize the full potential of the hybrid computer, one wants to time-share the available hardware to be able to solve large meshes [5]. Although the existing hybrid computing facility at the Los Alamos Scientific Laboratory is not large enough for three-dimensional gas diffusion problems, the two-dimensional problem can effectively compete with the digital computer when thousands of solutions are envisioned. Since no oil or water, but only gas comprises the diffusing fluid,

the amount of analog hardware required to represent a single pressure node is considerably reduced from that required for multi-fluid flow. With our hybrid computer there is enough hardware to represent 20 pressure nodes simultaneously in a two- dimensional 5 by 4 array of nodes. To solve an effective two--dimensional problem requires many more pressure nodes, so these are time--shared three times in each dimension providing a 15 by 12 array, 180-node model. Storage limitations in the digital computer have prohibited further time sharing.

HYBRID COMPUTING

This facility is comprised of two Electronics Associates Inc. (EAI) 7800 and two EAI 680 analog consoles interfaced to an 8192-word 16-bit digital computer (Honeywell DDP-116), plus the usual printer, plotter, magnetic-tape units, disks, typewriter, card reader, and paper tape. The analog computing elements such as integrators, summers, squarers, switches, digital-to-analog multipliers (DAMs), digital-to-analog converter (DACs), and analog-to-digital converters (ADCs) are connected together to make the voltages in the circuit represent the pressures and flows at various points in the gas shale. The EAI computers contain 52 DAMs (which may be used as DACs) and 48 ADCs. The facility also has a McNeal-Schwendler Function Input Output Processor (FIOP), without which the diffusion simulation would have been impossible. This device contains 64 analog-to-digital input channels and 64 digital-to-analog output channels each with multiplying analog inputs.

The FIOP is a large one-, two-, and three-dimensional analog function generator that linearly interpolates between tabular values stored in the 4096-word memory of its hard-wired digital processor. In this application the FIOP is controlled from the digital computer. The function generation capability of the FIOP makes it possible to handle real fluid properties like viscosity and compressibility which can vary with pressure. Without its 64 DAM output channels we would not have been able to represent all the transmissibilities necessary to make the simulation effective.

As a problem solving tool for the evaluation of enhanced recovery techniques for natural gas, the hybrid computer program has some good features when compared to other types of hybrid computer programs as well as to digital computer gas diffusion codes. To the user describing a set of problems and receiving the results, the program appears to be purely digital. Data is input via punched cards or magnetic tape and results may be returned to a printer, plotter, or magnetic tape. While we can observe the internal workings of the solution, i.e., time solutions of internal pressures and flows both during and after solution convergence, for the large number of solutions planned, one simply does not have the time to examine all the internal action. Rather, one may look at only the single flow from a reservoir for many solutions for which different parameters have been varied. The set of these flows alone will determine the conditions for maximum reservoir production or will determine the expected value and standard deviation in reservoir production for a known probability distribution of parameters.

A digital program needs to be thoroughly debugged once and then it remains reliable. The analog computer, on the other hand, can fail gradually and only in selected hardware units. It must be checked on a continuing basis. Fortunately, the row-column structure of the interconnections of equipment in this model allow automatic testing to be performed regularly and systematically.

Except during maintenance, the analog interconnections for the diffusion model remain untouched. All problem changes with the model are performed digitally. Scaling of variables, a worrisome task for the fixed point analog computer, can be done automatically by digital preprocessing.

If we compare the production time, cost, and availability of the hybrid computer to the CDC 7600 digital computer for the 180-node diffusion model, advantages of the hybrid for this application become apparent. Based on some preliminary tests on a one-dimensional model [6], a single problem may be solved in about 15 seconds, which is comparable to the central processing time of the same problem on the CDC 7600. If production runs on the hybrid computer were run only one-half shift per day, the operating costs per computing time are less than one-tenth the digital computer costs, which are figured on almost three shifts of production per day. If the used hybrid computer time were to be quadrupled, the cost per unit time probably would only halve, since more maintenance would be required. More important than the reduced cost per solution is the availability of a computing tool. Where CDC 7600 available time per day is measured in minutes, the available hybrid computer time, being applica- ble for only special classes of problems, is measured in hours.

PROBLEM DESCRIPTION

In the eastern Devonian shales, the free gas present is mostly methane at pressures under 40 atmospheres and at temperatures around 38°C. The reservoir model contains a single-fluid, isothermal, compressible, real gas. The instantaneous pressure at every point in the reservoir may be described [7] by the equation

$$\frac{\partial}{\partial t}\left[\frac{P(x,y,t)}{z(P)}\right] = \frac{1}{\phi}\nabla\cdot\left[\frac{P}{z(P)}\right]\left[\frac{k(x,y)}{\mu(P)}\right]\nabla P = \frac{1}{\phi}\nabla\cdot\left[\frac{P}{z}\right]\left[\frac{k(x,y)}{\frac{\mu(P)}{z(P)}\left(1-\frac{P}{z}\frac{dz}{dP}\right)}\right]\nabla\left[\frac{P}{z}\right] \quad . \qquad [1]$$

The variables are defined under Nomenclature. The porosity, μ, and the permeability, k, are only functions of the x and y coordinates. The pressure P is a function of x, y, and time t. Since temperature is constant, the compressibility factor, z, and the viscosity, μ, are only functions of pressure. Gravity forces have been neglected.

Note that everywhere pressure appears it is divided by z. For simplicity in the rest of the paper we will consider that z is unity but will keep the pressure dependence in viscosity. Thus by letting P represent P/z and μ represent

$$\frac{\mu}{z}\left(1-\frac{P}{z}\frac{dz}{dP}\right)$$

we can treat a non-ideal gas with perfect generality. Figure 1 shows that, for methane at 38°C, this pressure dependent term varies about 19% over a 60 atm pressure range.

The pressures in the diffusion model are represented on a rectangular mesh of 15 by 12 points with any spacing Δx_j and Δy_j allowed. This mesh can represent a cartesian geometry or by multiplying both permeability and porosity by the radial distance from the axis can represent a cylindrical geometry. The differential equation at each mesh point is

$$\frac{dP_{i,j}}{dt} = B_{i,j}\Big[A_{i+\frac{1}{2},j}(P^2_{i+1,j} - P^2_{i,j}) - A_{i-\frac{1}{2},j}(P^2_{i,j} - P^2_{i-1,j}) + A_{i,j+\frac{1}{2}}(P^2_{i,j+1} - P^2_{i,j}) - A_{i,j-\frac{1}{2}}(P^2_{i,j} - P^2_{i,j+1})\Big] \quad . \qquad [2]$$

$$\text{where } A_{i+\frac{1}{2},j} = \frac{\Delta y_j}{\left[\frac{\Delta x_i}{k_{i,j}} + \frac{\Delta x_{i+1}}{k_{i+1,i}}\right]}\,\mu\left(\frac{P_{i,j}+P_{i+1,j}}{2}\right) \qquad [3]$$

$$A_{i,j+\frac{1}{2}} = \frac{\Delta x_i}{\left[\frac{\Delta y_j}{k_{i,j}} + \frac{\Delta y_{j+1}}{k_{i,j+1}}\right] \mu\left(\frac{P_{i,j} + P_{i,j+1}}{2}\right)}$$

$$B_{i,j} = \frac{1}{2\phi_{i,j}\, \Delta x_i\, \Delta y_j} .$$

The $A_{i+\frac{1}{2},j}$ and $A_{i,j\pm\frac{1}{2}}$ are called flow coefficients rather than transmissibilities since they represent the gas flow per unit difference in pressure squared. The $B_{i,j}$ are called volume coefficients. Unlike the digital computer, the analog computer is a fixed point machine and each of the quantities in the above equation must be scaled to range between zero and unity. Fortunately the scaling calculations can be performed automatically on a digital computer and the results transferred automatically to the hybrid computer.

The analog implementation of the pressure node of Eq. (1) is shown in Fig. 2. The four surrounding shadowed integrators represent either integrators from an interior neighboring node or a DAC from a boundary. The total problem has 180 interior nodes plus 54 boundary pressures; however, the analog implementation has only 20 interior nodes plus 18 boundary pressures.

The integrator operates by means of a capacitor whose voltage is the integral of its current. The integrator can be switched by "logic" signals in two microseconds from an initial condition mode to an integrate mode. The flow coefficients are set in the digital to analog multipliers from values stored in the digital computer. The analog voltage into the DAM is then attenuated by the fraction set in the digital word. Figures 3 and 4 help to illustrate how the 20-node section of the reservoir is used to solve the complete reservoir. The implemented section is used to represent one-ninth of the reservoir at a time. The 20-node section is connected to the particular part of the reservoir it is currently simulating by the 18 DACs surrounding it. These DACs are represented by the X marks along the section boundaries. They supply to the analog section model the boundary pressures previously computed as a function of time. At the same time the newly computed pressures on the outside nodes of the analog section are recorded by ADCs for later play-back to a neighboring section. In Fig. 3 all the DACs not on the outside edge of the large rectangle enclosing the complete reservoir supply "fictitious" boundary pressures to the analog model. The term "fictitious" is used to describe these internal boundary pressures which are required only because of the time-sharing nature of the solution. The outside DACs supply "real" boundary pressures. If the boundary condition, is a no-flow condition then the flow coefficient to that boundary is set to zero. Of course the hardware DACs (in Fig. 4) supply either "fictitious" or "real" boundary conditions depending on which of the nine sections is currently being represented.

The DDP-116 digital computer must control the operation of the analog computer from the time the problem-defining parameters are given to the digital computer until the analog solutions through the nine shared sections repeat those of the previous iteration and the desired output is recorded. By means of data or control lines to each analog console, the digital computer can place initial conditions on all the integrators, set all the flow and volume coefficients, and set the initial boundary pressures. To provide greater range in problem parameters, the individual time constants (capacitors) on each integrator can be changed over several orders of magnitude and an extra gain of 11.0 can be switched in series with each of the DAMs representing the flow and volume coefficients. This is useful because the volume of a node near a well bore may be four orders of magnitude smaller than one at the far end of a reservoir and some transmissibilities may be over a thousand times larger than others.

When a particular section has been set up, the digital computer issues an integrate command. A timing signal every 1.2 milliseconds tells the digital computer to update the pressures on the 18 boundary DACs and to sample the pressures on the outer analog nodes. This updating of the boundary pressures and sampling the outer analog nodes must be done one at a time. As each outer analog node is sampled, the corresponding boundary pressure on the opposite side is updated. Figure 4 shows the order in which the sampling and updating takes place. The row boundaries are done before the column boundaries. The lower left node is sampled first, indicated by the number 1, followed by an update of the corresponding lower right pressure boundary, also indicated by a 1. The sampling and updating that follow are indicated by the numbers 2, 3, etc. This ordering insures that boundary pressures are always updated at the same time from the beginning of the sample period as they were sampled. Note that the corner nodes are sampled twice to prevent any timing skew. Updating and sampling the section boundaries occur in slightly less than the 1.2 millisecond timing signal interval.

There are 40 sampling periods during each integration period. The 108 boundary pressures of all nine sections, indicated by X's in Fig. 3 must be stored for all 40 time periods. This requires 4320 words. In addition 873 words are required to store the flow and volume coefficients and initial conditions for the complete problem. If the number of time points or number of shared sections were increased, storage would increase until use of the disk would be required. Since this would slow the computation, the diffusion problem was limited to 180 pressure nodes and to 40 time periods. For the method to be efficient, the ratio of the number of boundary pressures to the number of node pressures should be as small as possible. If one node were used the ratio would be 4 : 1; for this problem the ratio is 18 : 20. No storage is required for the 6 inside nodes.

The flow coefficients, defined in Eq. (3), are functions of spatial position in the reservoir with a small dependence on the pressures of the two surrounding nodes. The average of these two pressures is used to evaluate μ or strictly, to evaluate

$$\frac{\mu}{z}\left(1 - \frac{P}{z}\frac{dz}{dP}\right)$$

A single two-dimensional table of this function of P_1 and P_2 is used in the FIOP. It is created from the one-dimensional function of Fig. 2 evaluated at the pressure

$$\frac{P_1 + P_2}{2} \quad .$$

The FIOP has the capability of multiplying each of its DAM outputs by an Output Scale Factor (OSF). The 49 OSFs of the flow coefficient DAMs are set to the spatially dependent part of the coefficient before each of the nine sections are integrated. During the integration phase the FIOP is sampling the 20 node pressures, using 49 pairs of these pressures to look up in the table the pressure dependent part of the 49 flow coefficients. At 10 microseconds per input and 20 microseconds per function evaluation, the FIOP can update the pressure dependence in all the flow coefficients every 1.2 milliseconds at the same time the digital computer is updating the boundary pressures. The FIOP is shown schematically in Fig. 5. The rest of the DAMs in the simulation representing the volume coefficients, are set before each integration phase but remain with a fixed digital setting during the integration.

The integration time for a single section requires about 50 ms. To complete the reservoir requires 450 ms. A one-dimensional diffusion model in which 6 nodes were time-shared to solve a 12-node problem required 15 iterations for the pressures to converge. We have not been able to measure the number of iterations required for convergence of this two-dimensional model in time for inclusion in the symposium proceedings, but we estimate it will require from 15 to 30 iterations. Thus a solution should be completed within 15 seconds. As with any diffusion problem, the simulated times of interest may range from a few hours to many years. Time scaling the problem determines the

number of days represented by the 50 milliseconds of analog computing time. If one is interested in the initial pressure distribution forming around a fracture, well bore, or explosive jet hole, a time scaling of 1 day/ms might be used. If one is interested in the reservoir flow over a 55-year period, a scaling of 500 days/ms might be used. A second problem can be started using a different time scale and initial conditions from the end of the first problem.

CONCLUSION

We have determined that the hybrid computer is a cost effective simulation tool for two-dimensional gas diffusion problems. It can provide accuracies of a few per cent, more than sufficient for the knowledge of the actual reservoir parameters, and can produce the large quantities of solutions necessary to do large parameter studies, probable production estimation, and optimization.

As soon as the final testing of this model is complete, one of the first uses will be the optimization of lengths, diameters, and spacing of jet-penetrated holes off a well bore. Figure 6 shows a potential use of the holes formed perpendicular to the well bore at various depths to increase gas flow. This problem, while three-dimensional, can be broken into several two-dimensional problems. Since it is an optimization problem, the complete study will require a large number of solutions which the hybrid computer can handle easily.

Precisely because the hybrid computer can produce copious solutions, an obvious problem arises: How to supply it meaningful data as fast as it can use it. Thus our immediate plans include the development of software to transform geophysical descriptions of a reservoir including uncertainties, probability distributions, and optimization parameters into many sets of data scaled for the hybrid computer model to obtain the set of flow solutions necessary to answer a particular problem.

NOMENCLATURE

Variable	Name	Description	Units
P	pressure		atmosphere
z	compressibility factor	real to ideal gas density ratio	
ϕ	porosity	pore void fraction	
k	permeability		meter^2 = 10^{12} darcy
μ	viscosity		atm day = 8.64 x 10^{12} centipoise
x,y	space coordinates		meter
t	time		days
i,j	indices on x and y		
$\Delta x_i, \Delta y_j$	node spacing along x and y		meter
P_1, P_2	pressures affecting a flow coefficient		atm
$A_{i\pm\frac{1}{2},j}, A_{i,j\pm\frac{1}{2}}$	flow coefficients		m^2/atm-day
$B_{i,j}$	volume coefficient		m^{-2}

ACKNOWLEDGEMENTS

The author is indebted to Man T. Ung for suggesting to us the basic method of solving the diffusion problem on the hybrid computer. For checking the hybrid computer model, Walt Sawyer of the Morgantown Energy Research, was most kind to supply and help us with his three-dimensional digital diffusion code, SIMPAC [8].

REFERENCES

1. D. W. Peaceman and H.H. Rachford, Jr., "The Numerical Solution of Parabolic and Elliptic Differential Equations," J. Soc. Ind. Appl. Math., 3, No. 1 (1955).
2. J. Douglas, Jr., "On the Numerical Integration of $(\partial^2 u/\partial x^2) + (\partial^2 u/\partial y^2) = \partial u/\partial t$by Implicit Methods," J. Soc. Ind. Appl. Math, 3, No. 1 (1955).
3. David M. Young, Iterative Solutions of Large Linear Systems (Academic Press, New York, 1971).
4. Reginald P. Tewarson, Sparse Matrices (Academic Press, New York, 1973).
5. G. A. Bekey and M. T. Ung, "On the Hybrid Computer Solution of Partial Differential Equations with Two Spatial Dimensions," Fall Joint Computer Conference, Las Vegas, Nevada, 1971.
6. W. J. Carter, "Gas Stimulation Studies at LASL," Proc. of ERDA Enhanced Oil, Gas Recovery and Improved Drilling Methods, Tulsa, Oklahoma, 1971.
7. M. Muskat, Flow of Homogeneous Fluids Through Porous Media, (J. M. Edwards, Ann Arbor, Michigan, 1946).
8. W. K. Sawyer and J. C. Mercer, "A Diffusity Model for Fluid Flow and Heat Conduction in Porous Media," Morgantown Energy Research Center Report MERC-SP-77/2 (1977).

FIGURE CAPTIONS

FIGURE 1. Plot of $\frac{\mu}{z}(1 - \frac{P}{z}\frac{dz}{dP})$ vs. P for methane illustrating the pressure dependent term.

FIGURE 2. Analog implementation of a pressure node.

FIGURE 3. Illustration of the 9 reservoir sections which are time-shared by the 20-node analog implementation represented in Fig. 4. The X marks represent the DACs that supply boundary pressures.

FIGURE 4. Representation of the 20 implemented pressure nodes, one of which is shown in Fig. 2. The X marks represent those in Fig. 3. The numbers pointing to the outside pressure nodes and the surrounding DACs show the order of sampling and updating the 18 pressures as time progresses.

FIGURE 5. Diagram of the FIOP, used to supply the pressure dependent parameter $\frac{\mu}{z}(1 - \frac{P}{z}\frac{dz}{dP})$ to all the flow coefficients.

FIGURE 6. Jet penetrated holes from well bore into gas shale. Optimum spacing, length, and diameters to be determined.

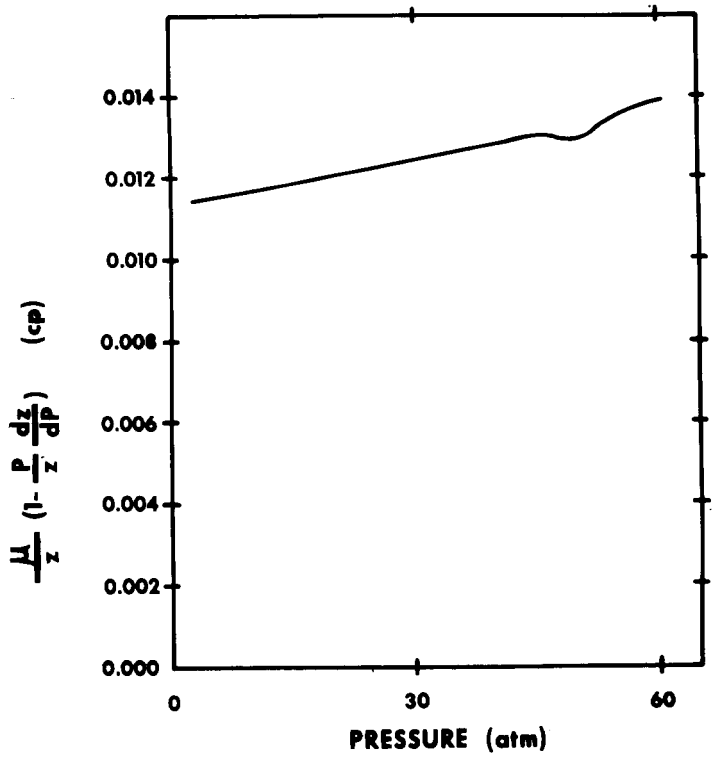

FIGURE 1

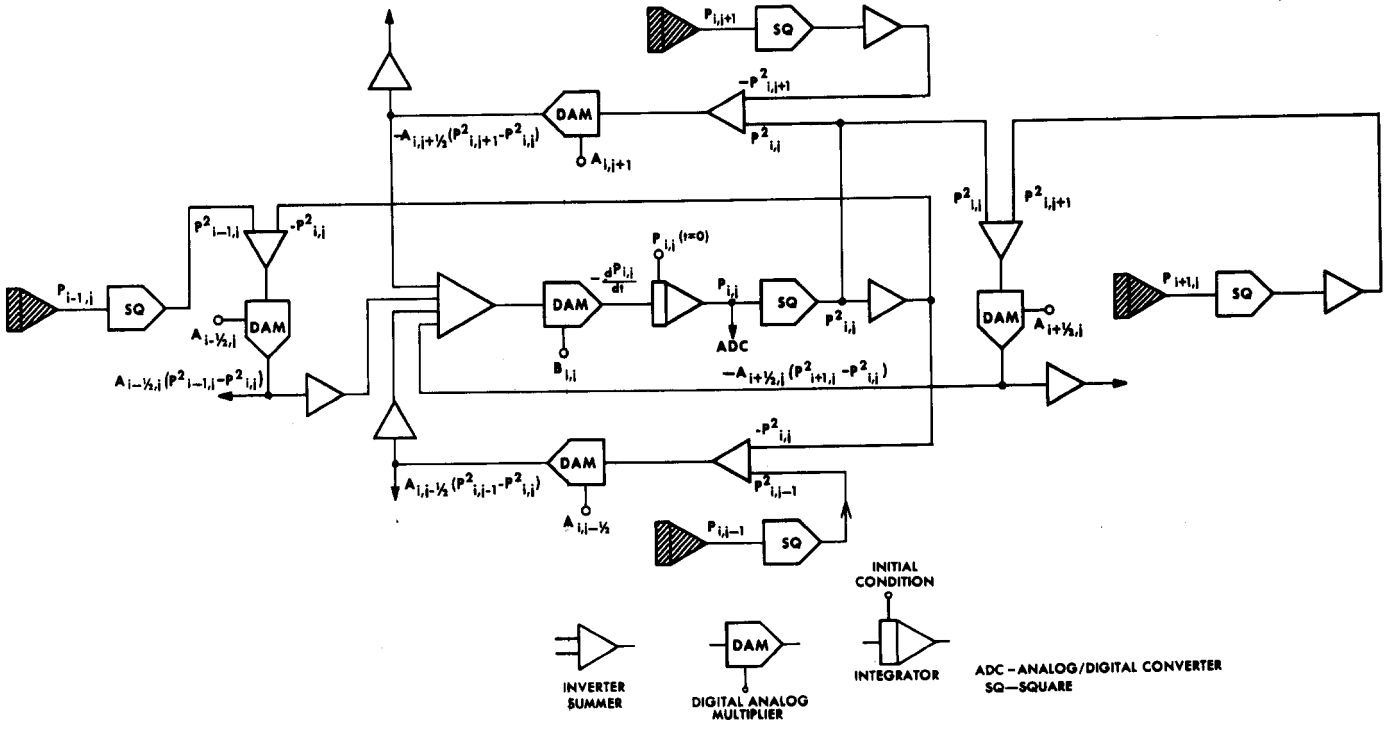

FIGURE 2

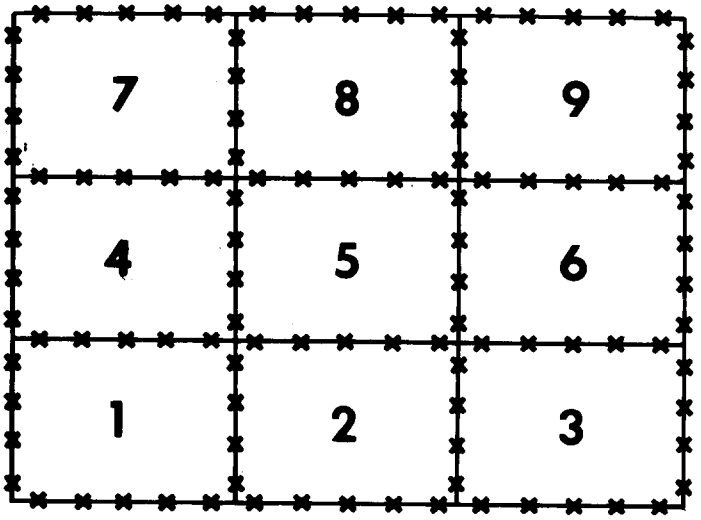

FIGURE 3

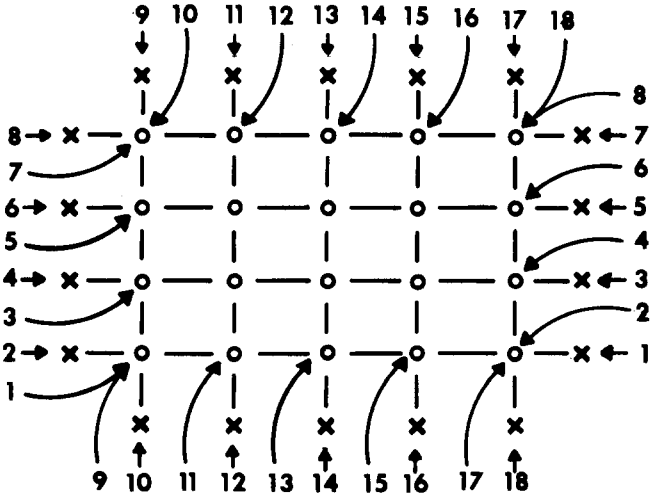

FIGURE 4

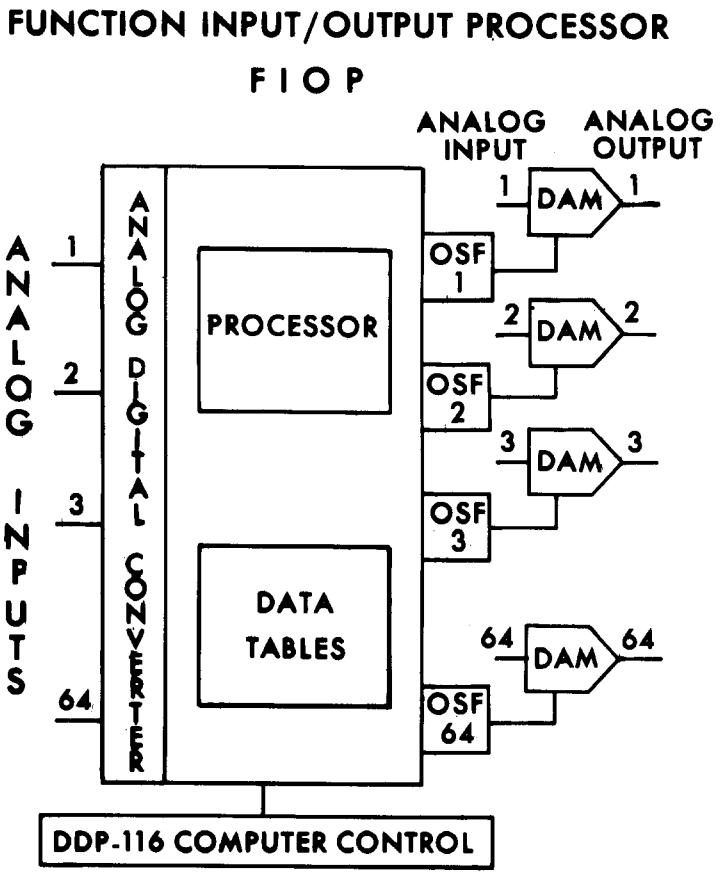

FIGURE 5

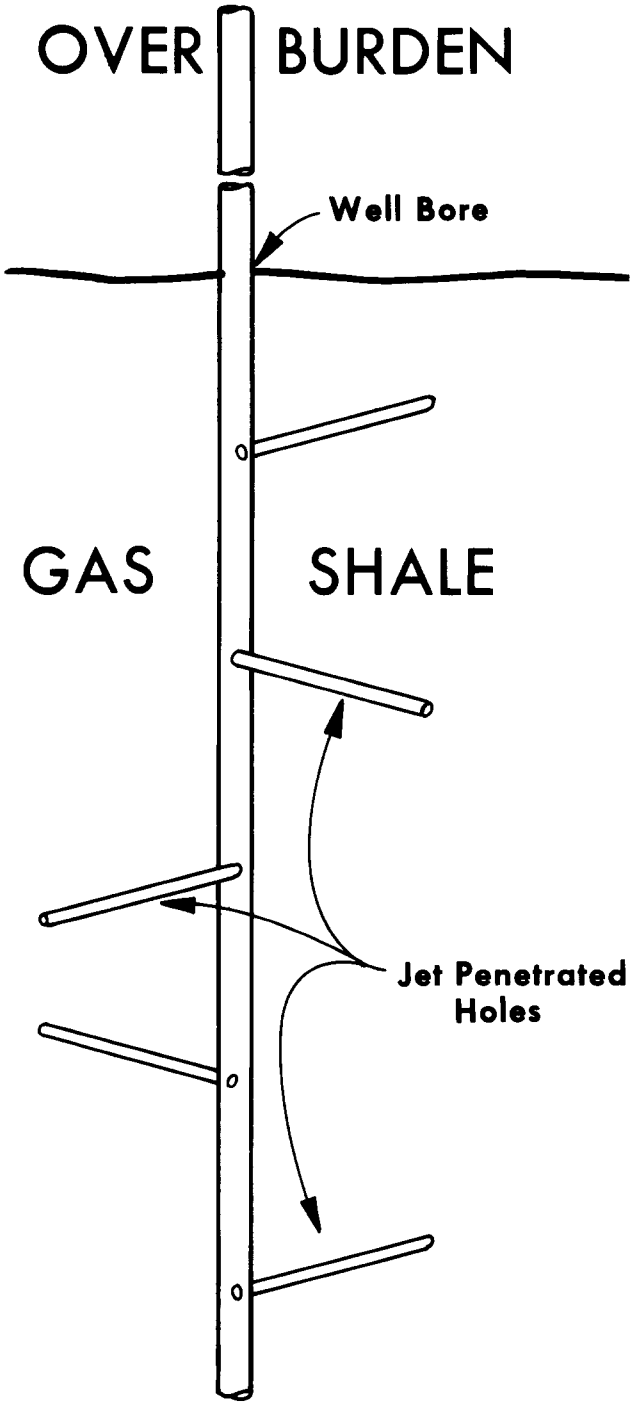

FIGURE 6

DEVONIAN SHALE EVALUATION IN STIMULATION FLUID RECOMMENDATIONS*

D. E. Simon and A. R. Jennings, Jr.
Halliburton Services

ABSTRACT

With the current emphasis on stimulation treatments in the Devonian Shale, much concern has arisen involving the compatibility of the Shale and the fluids used for stimulation. It has been determined by laboratory tests that the Shale has considerable amounts of clays dispersed throughout the formation. However, aqueous base fluids used with or without foam are the most economically feasible fluids to use for Devonian Shale stimulation.

Due to the low reservoir permeability and other characteristics of the Shale, large volume treatments appear necessary to effectively achieve economic results in the Devonian Shale. These large volumes emphasize the importance of formation compatibility with the selected treating fluid.

Petrographic analysis of Devonian Shale samples and scanning electron microscope (SEM) examination of core pieces subjected to various aqueous fluids provide information concerning the water sensitivity of the Devonian Shale in Wayne County, West Virginia. Similar tests can be conducted as Shale samples from other areas become available.

*Paper not available at time of publication.

CARBONACEOUS SHALES OF INDIANA AS SOURCES OF ENERGY, PETROCHEMICALS, AND CERAMIC MATERIALS: FIRST ANNUAL PROGRESS REPORT

by

John B. Patton
Indiana Geological Survey
Bloomington, Indiana

ABSTRACT

The Indiana Geological Survey's resource project has made these first-year contributions regarding Indiana to the overall Eastern Gas Shale Project: (1) map of 3,400 locations of wells providing data for stratigraphic studies; (2) three maps of oil and gas shows in about 1,400 wells above, in, and below the New Albany Shale; (3) 11 cross sections of New Albany Shale and equivalents; (4) structure maps on the base and the top of the New Albany Shale; (5) an isopach of the New Albany interval; (6) descriptions and some physical tests on one ERDA-sponsored oriented core and two new Survey cores; (7) one lineament map of area underlain by the New Albany Shale; and (8) tooling-up with personnel and equipment for geochemical, petrographic, mineralogic, and physical characterizations of carbonaceous shales.

GENERAL GEOLOGY

A major effort, the foundation for all the stratigraphic studies of the New Albany Shale in Indiana, was the preparation of a map showing the locations of 3,400 wells giving information useful to the total study. From this data base, 109 geophysical logs were selected to prepare five north-south and six east-west stratigraphic cross sections that subdivide the New Albany into four members, in ascending order: the Blocher, the Sweetland Creek, the Grassy Creek, and the Hannibal (Bassett and Hasenmueller, 1977).

Based on 1,400 well records in the Illinois Basin and 400 well records in the Michigan Basin, structure contour maps were prepared on the base and top of the New Albany, as well as an isopach map. The New Albany ranges from about 90 feet in thickness along its outcrop in south central Indiana to a known maximum of 337 feet in southwestern Indiana. The formation dips southwestward 20 to 30 feet per mile near the outcrop, but the dip increases basinward to 40 to 60 feet per mile. In the Indiana part of the Michigan Basin, strata equivalent to the New Albany reach a thickness of at least 348 feet in Lagrange County; the beds dip northward about 20 feet per mile beneath a cover of glacial drift and Mississippian Coldwater Shale.

Gas shows were reported for about 6 percent of the 1,400 wells that penetrate the New Albany Shale in Indiana, but only 10 gas fields have resulted from drilling activity. Nearly all fields are now abandoned except for a one-well field in Daviess County. Three maps have been prepared of oil and gas shows above, in, and below the New Albany. No correlation has been found between gas production and structure.

LINEAMENT ANALYSIS

Both high-altitude photography and LANDSAT imagery are being used to define linear features at the surface in Indiana within the area underlain by the New Albany Shale. The locations of the endpoints of each lineament are being digitized so that their orientations can be calculated by computer program.

The lineament mapping is not completed, but the lineaments mapped within the part of Indiana contained on the Danville, Indianapolis, and Vincennes 1° X 2° quadrangle maps show remarkably similar bimodal orientations, with the principal modes being oriented 90° apart at 45° - 225° and 135° - 315° (Fig. 1). Histograms comparing lineament length to frequency of occurrence show a log normal distribution (Fig. 2). The orientations of fractures measured on the one oriented core drilled in Indiana, the Energy Resources of Indiana, Inc., Phegley Farms No. 1, show a strong unimodal orientation, which differs from one mode of the lineaments by only about 10 degrees (Fig. 1). The difference is small enough to be within the error of measurement of the fractures.

PHYSICAL CHARACTERIZATION

Shore hardness, bulk specific gravity, porosity, and sonic velocity measurements have been made on samples from the Phegley No. 1 oriented core, Sullivan County. Additional physical testing will be completed after construction of necessary jigs for a testing machine.

MINERALOGY AND PETROGRAPHY

Mineralogic and petrologic characterizations of newly acquired cores and samples from quarries have been initiated. Notable results include detailed descriptions based on binocular microscopic study of one core each from Marion and Sullivan Counties and preliminary descriptions of two additional cores from Marion County. The four stratigraphic members recognized in Indiana, western Kentucky, and Illinois in descending order are the Hannibal, Grassy Creek, Sweetland Creek, and Blocher.

Although the chosen members are recognized on the basis of differences observed in geophysical logs, the members can be differentiated generally on the variable contents of the two distinct lithotypes that comprise the major part of the formation, namely brownish black mudstone or shale rich in organic material and a softer greenish gray mudstone or shale poor in organic content. Both types vary in silt and clay contents within a vertical section and from place to place. Alternating with them also are numerous thin graded or sharply defined laminae composed of minor minerals. The components of the two types are the same except for organic matter that may comprise 20 percent or more of the black type.

Texturally the New Albany ranges from massive to laminated and fissile. Although porosity is generally less than one percent, fractures and some of the thin but relatively coarse laminae provide locally increased porosity. The fractures are generally oriented NW-SE (Fig. 1) and many are healed with carbonates. Some fractures are slickensided. Contacts between silty beds and finer clayey shale are usually sharp, but some show load casts and irregularities. Many contacts between brownish beds and black shale are highly irregular. Discrete thin layers of coarse material comprising light colored beds, lenses, or laminae 1 to 30 mm thick may be sparse or abundant, but rarely make up more than 10 percent of any meter of thickness. A few relatively thick coarse-grained beds exhibit graded bedding and rarely show small scale scour features. Several types of coarse beds have been recognized: round white to clear quartz sand; a combination of pyrite and quartz sand, with or without organic matter; a combination of pyrite and carbonate grains and quartz sand; and coarsely crystalline carbonate (sparite) that may be dominantly dolomite (possibly ankerite) or calcite or a mixture. The last type is most common near the base of the New Albany Shale.

X-ray diffraction analyses of whole, unashed bulk samples (Fig. 3) reveal that the black mudstones contain the clay minerals illite (2M polymorph) and chlorite in a weight ratio roughly 2:1 and accessory mixed-layer clay minerals and kaolinite; also X-ray analysis reveals the non-clay minerals to be quartz, pyrite, marcasite, dolomite, and minor calcite and feldspar. Quartz is the dominant mineral. Pyrite and marcasite are closely associated with each other. The greenish gray mudstones are similarly composed mineralogically but contain relatively more mixed-layer clay minerals.

Pyrite and marcasite are the most common accessory minerals, comprising a high percentage of some thin beds or laminae. These minerals are also present as tiny disseminated crystals, irregular blebs, nodules, and as a cementitious component of some coarse-grained beds. Very minor amounts of barite, fluorite, apatite, and sphalerite have been noted. Part of the iron sulfide may have formed in the early stages of sedimentation, but part was formed by post-depositional diagenetic processes. The force of the crystal growth of diagenetic pyrite in some instances pushed surrounding laminated sediments outward into small dome-like structures. One large pyrite nodule was seen to be bounded by banded calcite laminae and corrugated calcite veinlets.

Fossils are generally sparse throughout the formation and may be found individually disseminated or more frequently as assemblages confined to thin beds. The fossils are dominated by amber discoidal resinous spores (Tasmanites) but also include plant fragments (commonly vitrainized) and conodonts, linguloid brachiopods, conulariids, and gastropods. Burrows and trace fossils are rare; the burrows observed are usually filled with green fine-grained materials, and some are replaced by iron sulfides. Green galuconite pellets are found, though sparsely, especially in the upper parts of the formation.

A sample of approximately 20 kilograms of chunks of the Blocher Member exposed at the Harding Street quarry of the American Aggregates Co. in Indianapolis was collected and processed as a reference sample for mineralogic and geochemical studies.

Studies of thin sections have just begun, but, interestingly, observation of some thin sections with cathodoluminescence has disclosed a surprising amount of feldspar in some coarse laminae. The method also readily reveals microfractures and other structures. Some scanning electron micrographs have been obtained.

GEOCHEMICAL CHARACTERIZATION

Analyses to determine the major components of our reference sample of high organic-content New Albany Shale from the Harding Street quarry, Indianapolis, have revealed that mixing was probably adequate for the major minerals but some variability may exist for carbonates and sulfides. This might have been anticipated because splits were made at particle size of 100 percent less than 8 mesh to provide samples for Fischer assay. Averages in weight percent, on the as-prepared basis, of duplicate determinations for each of six splits of our reference samples are as follows: SiO_2, $50.34 \pm .15$; TiO_2, $0.88 \pm .01$; Al_2O_3, $14.38 \pm .08$; Fe_2O_3, $3.83 \pm .04$; MnO, $0.034 \pm .002$; MgO, $2.59 \pm .04$; CaO, $3.06 \pm .05$; Na_2O, $0.55 \pm .02$; K_2O, $4.56 \pm .02$; P_2O_5, $0.102 \pm .001$; CO_2, $3.77 \pm .18$; H_2O-, $1.27 \pm .06$; S, $1.56 \pm .03$; C, $9.0 \pm .1$; H, $1.34 \pm .06$; total Fe is as Fe_2O_3; variations are for $\pm$ one standard deviation.

Several techniques of sample digestion have been investigated to provide an adequate solution to be used with an inductively-coupled-plasma, optical-emission-spectrometer that has been received but as of this writing has not been installed. A new type of Teflon (TM) bomb was designed to provide for wet-ashing and refluxing in the same vessel as for hydrofluoric-aqua-regia dissolution. Experiments on yields with the vessel have proved encouraging.

Standard solutions of elements to be determined have been prepared for use with the spectrometer and for atomic absorption spectrometry. Some of these solutions will be used to investigate interferences by elements to be determined by other means.

Tabulation of material resources for the study has revealed that about 640 samples from 23 cores are already available in addition to those to be obtained from three newly drilled cores (Fig. 4). Two of these cores were drilled by the Indiana Geological Survey. Gas samples collected in valved surplus Navy powder cans from one of the Survey's cores are under study by the Organic Geochemistry Group at Indiana University. Results of this and other organic geochemical studies will be reported separately.

REFERENCES

Bassett, J. L. and Hasenmueller, N. R.
1977 - The New Albany Shale and Correlative Strata in Indiana: Published in these Proceedings.

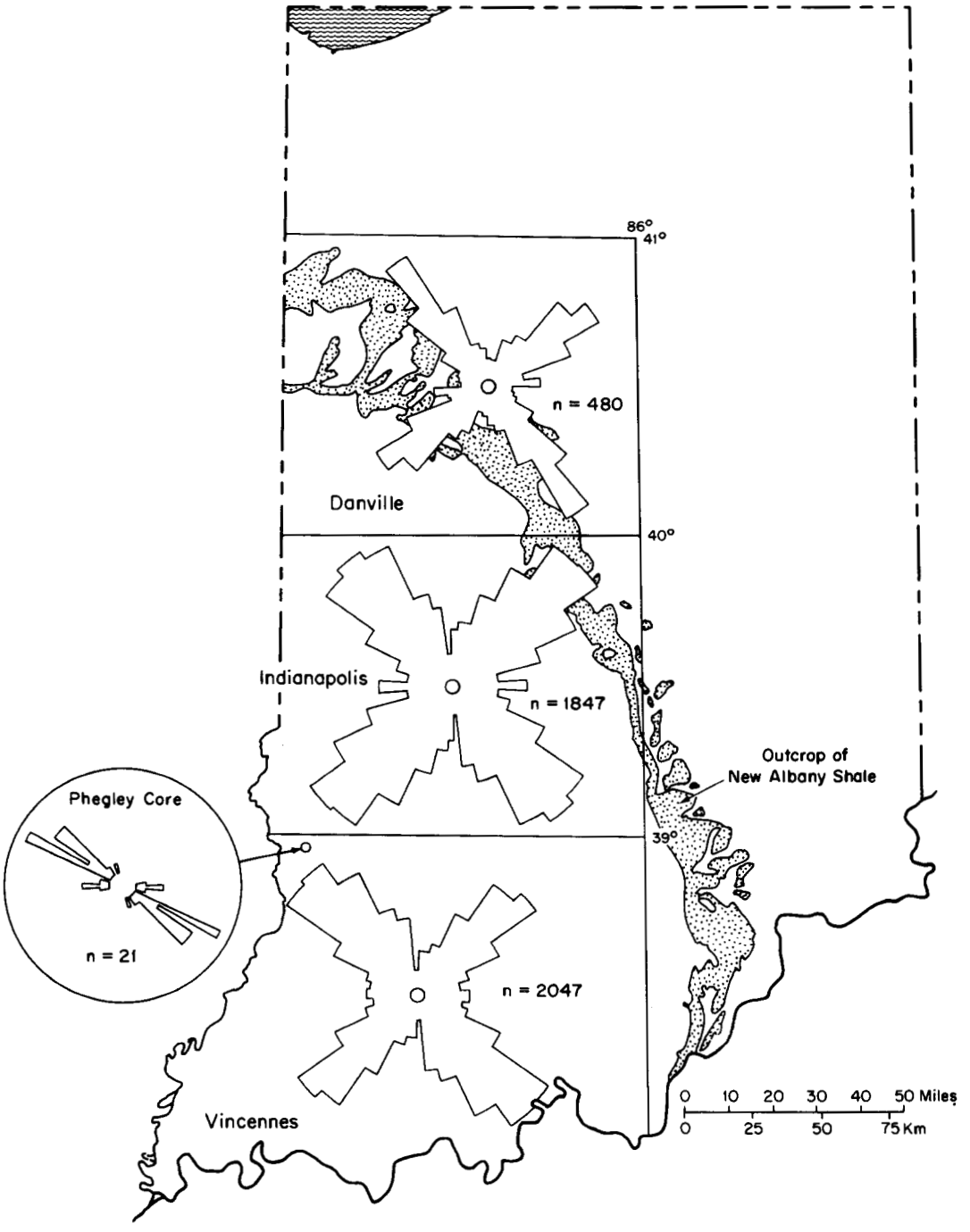

Figure 1. Map of Indiana with rose diagrams showing orientations of lineaments for the Danville, Indianapolis, and Vincennes 1° X 2° quadrangles.

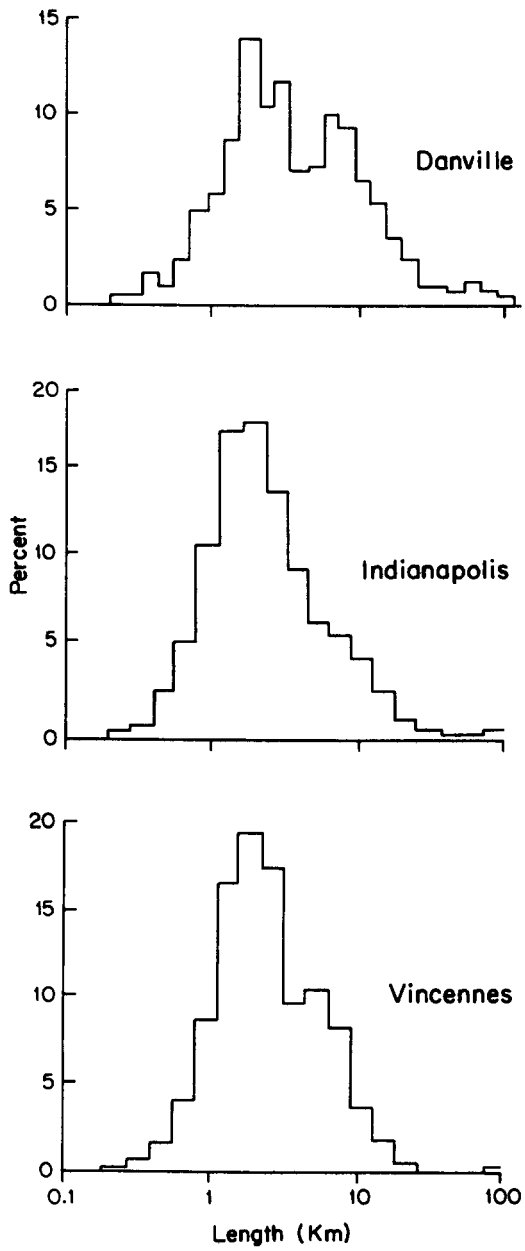

Figure 2. Histograms showing logarithm of lineament length versus percent of occurrence for the Danville, Indianapolis, and Vincennes 1° X 2° quadrangles.

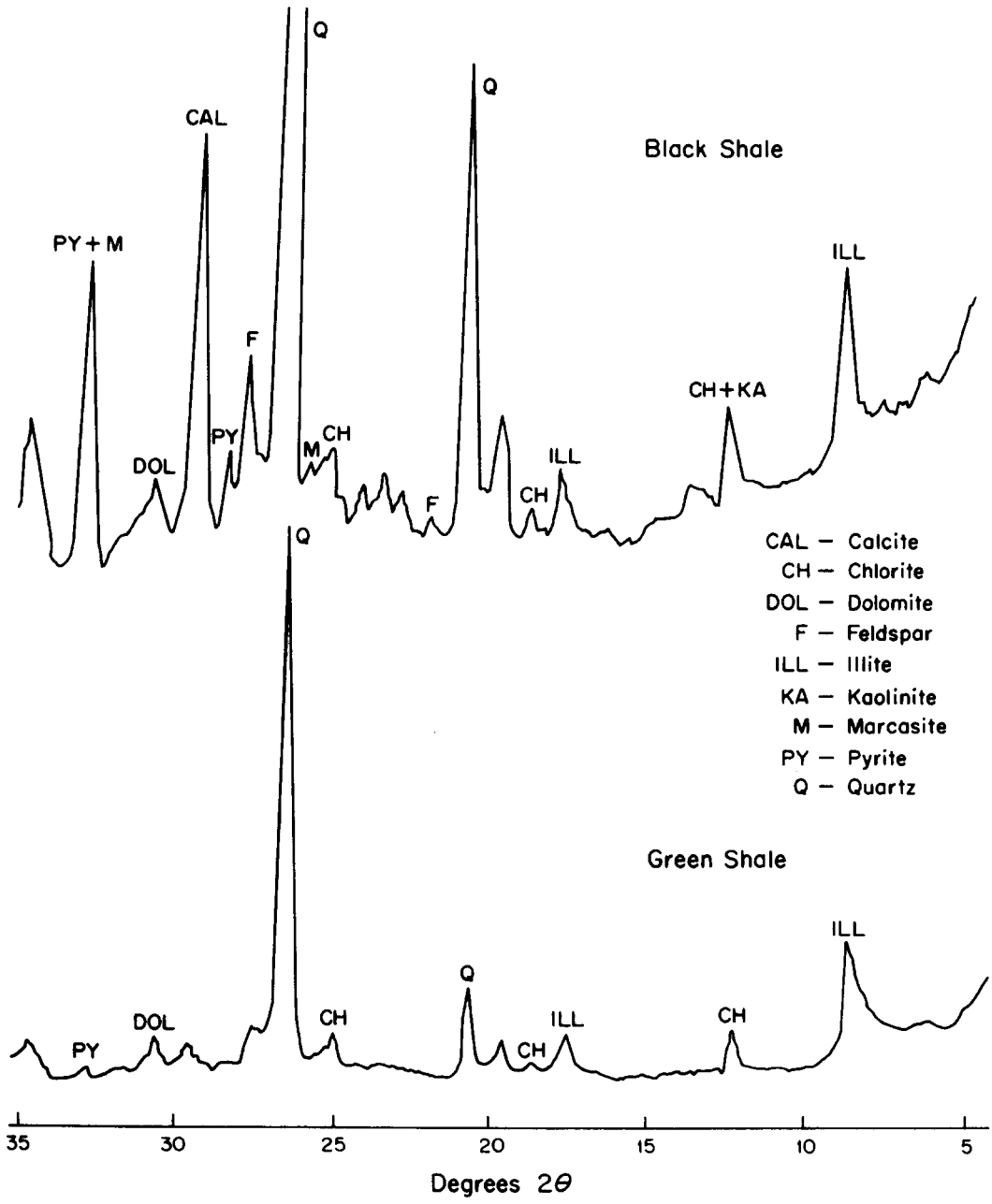

Figure 3. Powder diffractometer traces comparing mineralogy of the green and black shales of the New Albany.

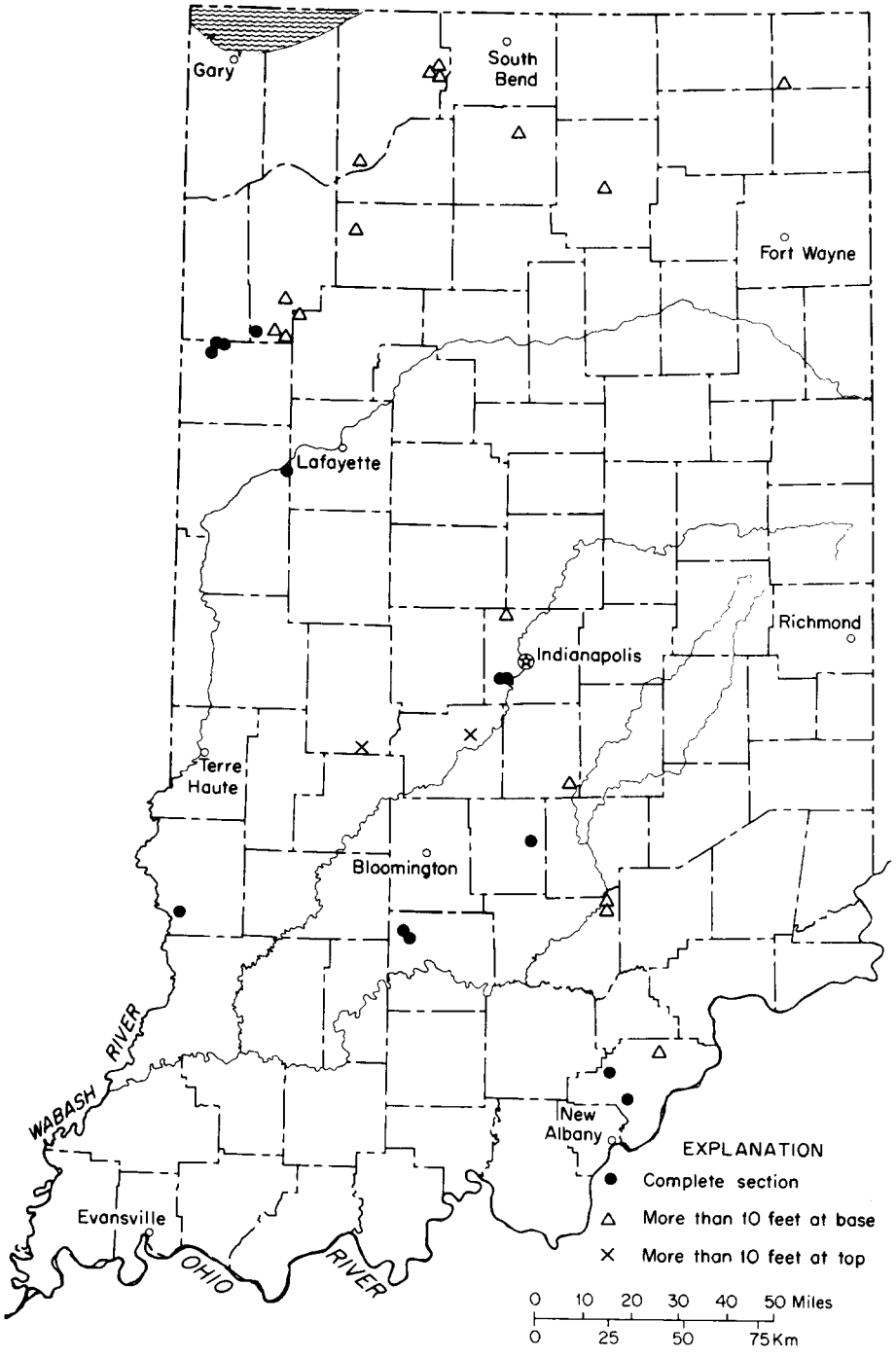

Figure 4. Map of Indiana showing locations of cores of the New Albany Shale on file at the Indiana Geological Survey.

CHARACTERIZATION OF DEVONIAN SHALES USING LASER PYROLYSIS-GAS CHROMATOGRAPHY

by

Nicholas E. Vanderborgh, J.M. Williams,
E.M. Wewerka and J.P. Bertino

Los Alamos Scientific Laboratory
University of California
Los Alamos, NM 87545

TECHNICAL UTILIZATION OF THE DEVONIAN SHALE RESOURCE FOR HYDROCARBON SUPPLIES REQUIRES INCREASED UNDERSTANDINGS OF THE SOURCE ROCKS AND OF MECHANISMS THAT LEAD TO GAS AND/OR OIL PRODUCTION. ALTHOUGH SOME CONCEPTS NOW ACCOUNT FOR THE PRODUCTION OF METHANE FROM THESE MATERIALS, LESS IS KNOWN ABOUT THE NATURE OF THE SOLID ORGANIC CONSTITUENTS AND THE BEHAVIOR OF THESE MATERIALS DURING THERMAL PROCESSING.

PULSED LASER HEATING RESULTS IN A RAPID DEPOSITION OF PRECISE QUANTITIES OF THERMAL ENERGY INTO SELECTED SHALE VOLUME SEGMENTS. THE LASL PROGRAM, PART OF MERC'S EGSP, TO UTILIZE LASER INDUCED PYROLYSIS FOR THE RAPID DETERMINATION OF THE TYPES AND AMOUNTS OF ORGANIC CONSTITUENTS IN VARIOUS SHALE SAMPLES WILL BE DESCRIBED

INTRODUCTION

Enhanced technical utilization of the natural gas resource contained with the Devonian shales underlying much of the Eastern United States requires new understandings of these source rocks and of mechanisms that eventually lead to gas and oil production. It is generally agreed that these formations consist of an organic fraction, thought to be a coaly type material(1), dispersed throughout a silicate matrix. Methane and other low-molecular weight gases are contained, probably dissolved, in the organic fraction. Drainage of gas from this type of system may require not only the creation of new flow paths, but also methods to promote gas dissolution. Because of this fact, studies of the organic constituents of these shales have begun using the method of laser pyrolysis(2).

Pyrolysis chromatography, heating a solid material to degrade it into smaller fragments and then separating these using chromatographic techniques, is a well described approach to analyzing samples which exhibit low vapor pressures at usual temperatures. Pyrolysis processes of large organic moities are complicated. Typically, during pyrolysis, different regions of the sample experience different temperatures. These temperature variances lead to different product distributions emanating from discrete regions at distinct temperatures. The overall result is a highly complicated fragmentation pattern. The distributions of various pyrolysis fragments depend markedly upon sample size and geometry. To circumvent this type of problem, several analytical pyrolysis approaches have been proposed(3). Laser pyrolysis is one of these newer methods(2).

Pulsed lasers offer a convenient power source to deliver intense, short bursts of power into well defined sample regions. In the experiments described here, a focused laser beam is used to rapidly heat a small volume of sample. This heating (the pulse width of the laser event is, approximately 10^{-3} s.) leads to a rapid temperature rise and, then, a high temperature degradation.

Depending upon the degree of focus, very high temperatures can be obtained. If these elevated temperatures are reached (temperatures in excess of 5,000K), part of the sample is converted into a high temperature plasma. Such a high temperature ensemble mirrors the atomic composition of the sampling volume(4). Upon the termination of the laser event, this atomic ensemble quenches into a series of low molecular weight gases. Those components of the pyrolysis pattern are called the plasma products. Other parts of the sample see less vigorous conditions. Products emanate from those regions through several processes. Probably the most important of these is degradation resulting from the acoustical shock wave generated by the laser burst. Attenuation of this wave results in the rupture of certain bond types. This bond rupturing process then leads to a series of higher-molecular weight products. This portion of the pyrolysis pattern is called the thermal shock products. It should be emphasized that this type of thermal processing is quite different from more conventional pyrolysis-chromatography(2).

The technique of laser heating leads to several different possibilities. First, sampling is far simplified since thin sections and solution-deposited films, required for contemporary hot-wire pyrolysis, are not necessary. Also, sampling can be done in a variety of differing sampling environments. Measurements could be made down-hole, for instance. Second, analysis of surface conditions is straightforward. In fact, unless special care is taken to penetrate the surface, this technique emphasizes chemical states of surfaces of solids(2). Third, one can examine unique regions through regions of known inhomogenities of a geological sample. For instance, one can investigate the nature of organic material either along a core section or into a core sample. None of these possibilities exist with more conventional pyrolysis-GC.

EXPERIMENTAL

A schematic of the apparatus designed for these Devonian shale studies is shown in Figure 1. The pyrolysis is done using a pulsed laser device (shown in the center of the Figure) that deposits energy into a sample contained within a chamber connected directly to the necessary analytical instrumentation. This " on line" configuration permits the direct recovery of very small amounts of pyrolysis fragments. The laser event serves as a rapid injection of the sample into the chromatograph. Following separation on the chromatographic column, analysis is completed by a mass spectrometric determination of each component. This system will give both qualitative (identification of the type of fragment) and quantitative (identification of the amount of fragment) information. Also, the mass spectrometer will permit measurement of similar chemical species that contain different isotopic composition. For instance, normally occurring methane could be readily distinguished from methane containing the carbon isotope of mass number 13. This type of distinction will be important in experiments that examine adsorption-dissolution phenomena.

Initial studies, reported here, utilize much of this instrumentation. A photograph of the experimental arrangement is shown in Figure 2. The laser power supply is shown to the left of the laser-gas chromatograph. Laser light, generated with a Nd pulsed laser, is directed through a quartz focusing lens (50 mm focal length) and onto a sample contained in the sampling chamber. (The laser is positioned horizontally, unlike the vertical orientation shown in Figure 1.) The pyrolysis products are then led into the gas chromatograph. This instrument utilizes a digital data analysis system (not shown).

Figure 3 shows the focusing lens holder. This device positions the quartz lens to steer the beam onto a discrete region of the sample. The lens can be moved precisely and reproducibly in three dimensions. The location of the sampling volume (to within a spatial distinction of 0.05 cm) is indicated by using a second, low-power laser. This source, 3.0 mw, HeNe, CW, is positioned to the rear of the main laser optical train. Generated light is fed through the optics of the main laser optical train and then through the focusing lens. In this way a focused spot illuminates the exact region that will be interrogated by the pulsed laser beam. It is this aspect of sampling that makes laser-induced pyrolysis a unique technique.

The sampling chamber for these initial studies consists of a short segment of quartz tubing. (Quartz is more resistant to fracturing than is glass.) A photograph of the sample assembly is shown in Figure 4. This top view shows the same lens assembly (Figure 3) to the left of the quartz tube. Carrier gas enters the chamber through the 1/8 in. tubing (top of figure) and exhausts into the gas chromatograph through the 1/16 in. stainless steel tubing (bottom). Specially modified fittings are utilized to minimize the dead volume of the chamber. The 1/16 in. transfer line is normally heated to 250°C during measurements to prevent the condensation of pyrolysis fragments within the transfer line. (Heat tapes have been removed for this photograph.)

Analysis consists of packing a sample fragment into the quartz tube. Either fragments (chips) or

consolidated powders can be utilized. The hydraulic connections are re-established; leaks are readily determined by the absence of pressure in the sampling chamber. The laser is then prepared for firing. Final focusing and power adjustments are made and required safety procedures are carried out. Simultaneously, the laser is fired, the chromatographic data system is initiated and the temperature programming is begun. Using valving, not shown, the carrier gas can be routed around the sample chamber so that another sample can be made ready for analysis while the first is still being processed.

Pyrolysis products consist of a wide range of differing-molecular-weight products. These can range from H_2 (2) or CH_4 (16) to high molecular weight fragments (>300), limited by the requisite vapor pressure need for chromatographic separation. Analysis has been successful using a high performance column of C_{18} on Porasil C. This column is first maintained at -10°C for the separation of low molecular weight compounds and then temperature programmed to 220°C for the eventual separation of higher molecular weight fragments. Presently the analysis system does not include mass spectrometric instrumentation. That will be added during the coming months.

RESULTS AND DISCUSSION

The sampling of complex geological material such as Devonian shales for organic compounds is not straightforward. Assuming one is dealing with core samples, two techniques are generally possible. One can grind and blend a sample, and then, after pressing to obtain a uniform density, pyrolyze the pelletized sample. This method has certain advantages, the principal of these is that a more representative sample may be available since various averaging procedures can be utilized during preparation. However such extensive sample handling could lead to a severe loss of low molecular weight compounds. The other method is to work with segments removed from larger samples (cores, for instance) using a minimum amount of grinding and, in general, using conditions that would lead to the smallest removal of potentially labile organic species. Both of these approaches are under investigation and additional work will be necessary to define adequate sampling procedures.

A representative laser pyrogram obtained by the deposition of 5 J of laser energy into a small section of Devonian shale is shown in Figure 5. The sample was taken from a core removed from Lincoln County, W.Va. at a depth of 1093 m. (Columbia Gas Well 20402). These data were taken with a flame ionization detector and consequently emphasize hydrocarbon products. The experimental conditions are listed in the legend to Figure 5.

There is strong evidence that other compounds (CO and CO_2, for example) do result from the laser degradation of these shales. Data taken under somewhat similar conditions using a thermal conductivity detector showed a variety of products. This product distribution included only a small fraction of the total as hydrocarbon compounds. Although the qualitative nature of each of the thermal-conductivity-pattern fragments is not certainly known, one can deduce that these species must consist of CO, CO_2, H_2, H_2O and, possibly, hydrosulfur compounds. Consequently, it must be emphasised that Figure 5 only shows hydrocarbons resulting from laser pyrolysis in these shale samples. We shall return to investigate the exact nature of these other compounds when mass spectrometric instrumentation is operational.

It is possible to determine the nature of several of the peaks shown in Figure 5. The first represents the quantity of methane produced by the pyrolysis event. Thermodynamic predictions suggest (6) that little methane should be produced from the quenching of a plasma with the expected carbon to hydrogen ratio. Consequently, we assume that this methane most probably results as a thermal blow off product which is thermally degraded from the shale volume under consideration. This quantity of gas could result from both the release of desorbed methane and from methane produced by several pyrolysis products.

The major peak, Peak 3, contains approximately 1/2 of the total integrated area and represents a C_2 hydrocarbon. We tentatively assign this peak to ethane although, at this writing, we cannot completely eliminate the possibility that this peak may also contain some ethene (ethylene). The second peak, Peak 2, apparently represents ethyne (acetylene). (All of these assignments are made from the comparison of measured retention times with those found using standard compounds under the same conditions. Mass spectrometric measurements will lead to less ambigious assignments.) One predicts that acetylene would be the dominant plasma product since a high temperature ensemble containing carbon and hydrogen should result in a distribution rich in C_2H_2 over wide ranges of carbon/hydrogen ratio. Clearly, in these studies acetylene is not the dominant low molecular weight gas. We must initially conclude that the elevated ethane yield results from thermal penetration into the sampling volume. Additional experimentation is needed to verify this assumption although

laser defocusing experiments tend to support this theory.

As one, maintaining constant laser energy, defocuses the laser beam, a smaller fraction of high-temperature products result. One, therefore, can change the thermolysis product distribution from one that is dominated by plasma products (high degree of focus) to one that is dominated by thermal shock products (low degree of focus). Typically, a fine degree of focus (enhanced power density) results in a more emphasised distribution of lower molecular weight compounds. Data in Table 1 illustrate this type of behavior. Here we see 11 significant peaks, peaks accounting for less than 1% of the total area are ignored. The first three peaks represent methane, acetylene, and ethane-ethene, respectively. One can readily see that focusing the beam leads to a rapid increase in Peak 3. This most probably results from a deeper penetration into the sample with a focused beam. It this were not the case, a higher temperature should produce larger relative quantities of acetylene. This data also show that methane does not increase at the same time as one sees significant increases in ethane concentration. This may suggest that methane is preferentially depleted within the sample volume. This behavior is entirely different from that found with coal samples (5).

CONCLUSIONS

1. Pulsed Nd pyrolysis with minimum sample pretreatment generates adequate quantities of products for analytical determinations.
2. Significant quantities of pyrolysis products apparently result from methane and ethane released by thermal degradation.
3. Focused power deposition leads to increased ethane production. This may result from a deeper penetration into the sample exploring regions removed from the surface that are less depleted in naturally occurring low molecular weight gases.
4. Higher molecular weight components are readily apparent. These compounds may serve both as useful chemical markers and as component sections of the larger molecular weight species that contain the candidate gaseous fuels.

ACKNOWLEDGMENT

This work performed under the auspices of the U.S. Energy Research and Development Administration

REFERENCES

1. W.K. Overbey, MERC, private communication; I.A. Breger, USGS, Reston, private communication; I.A. Breger, "Geochemical Interrelationships Among Fossil Fuels, Marsh, and Landfill Gas", in The Future Supply of Nature-made Petroleum and Gas, Technical Reports, Pergamon Press, New York, 1977.

2. N.E. Vanderborgh, Laser Induced Pyrolysis Techniques, in Analytical Pyrolysis, edited by C.E. R. Jones and C.A. Cramers, Elsevier Scientific Publishing Company, Amsterdam, 1977.

3. C.J. Wolfe, R.J. Levy and J.Q. Walker, Industrial Research, Jan. 1971, p. 40.

4. W.T. Ristau and N.E. Vanderborgh, Anal. Chem., 44, 359 (1972).

5. R.L. Hanson, N.E. Vanderborgh and D.G. Brookins, Anal. Chem., 49, 390 (1977).

TABLE 1

Devonian Shale Pyrolysis- Effects of Defocusing Nd Laser Beam Maintaining Constant Five J Pulse

PEAK NUMBER	DEFOCUSED BEAM T_R	%	PARTIALLY FOCUSED T_R	%	FOCUSED BEAM T_R	%
1	0.24	2.00	0.25	2.54	0.25	3.66
2	0.45	2.10	0.46	2.46	0.46	3.25
3	0.61	24.0	0.62	26.5	0.59	47.1
4	8.71	1.30	8.57	1.21	8.51	2.97
5	10.40	1.77	10.36	1.59	10.32	0.80
6	12.02	11.4	11.98	14.2	12.02	9.60
7	12.57	1.03	12.55	1.96	12.56	0.53
8	13.75	26.3	13.74	25.3	13.73	13.4
9	15.25	4.51	15.24	3.66	15.22	2.13
10	16.58	1.20	16.61	0.29	16.60	0.22
11	18.28	15.3	18.26	16.6	18.26	15.5

Retention times, T_R, are given in minutes.

Chromatographic Conditions- Column, 1 m, 120-150 mesh, C_{18} on Porasil C;
Temperature, -10°C for 4 minutes, then 16°/minute to 220°C.
Nitrogen carrier, 20 ml/min.

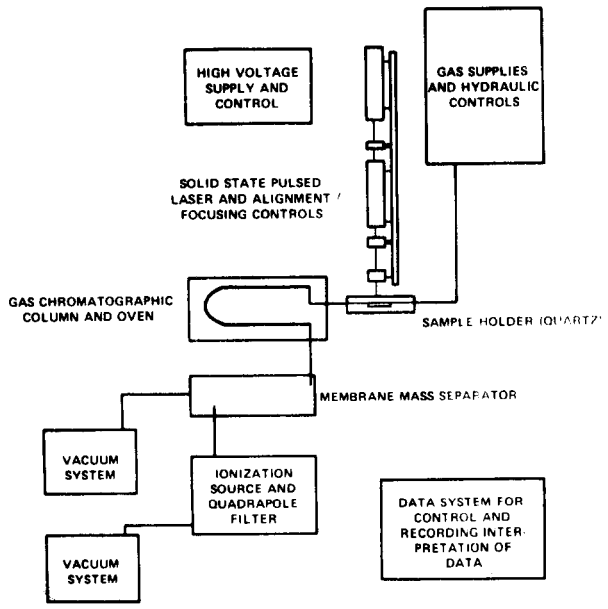

Figure 1: Laser Pyrolysis-Gas Chromatographic-Mass Spectrometric Instrumentation for Rapid Characterization of Devonian Shales

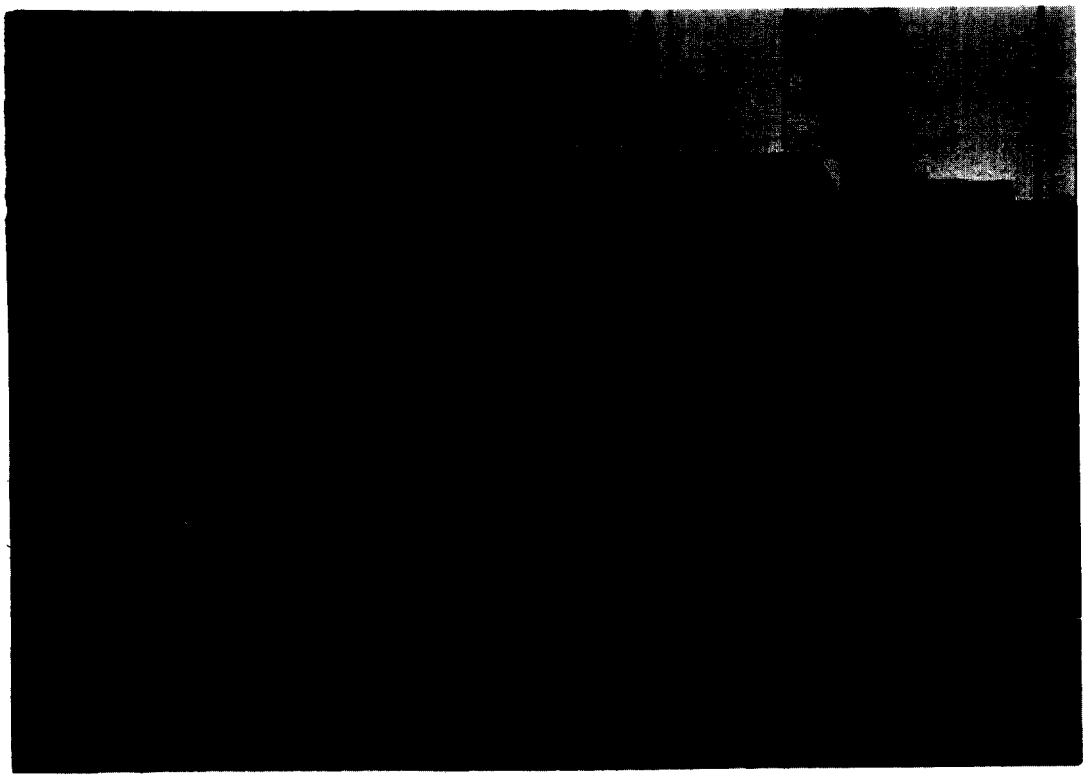

Figure 2: Overall view of laser pyrolysis-gas chromatographic instrumentation. The pulsed laser (Apollo Lasers) deposits energy into the sample contained on an assembly mounted on top of the gas chromatograph (Hewlett Packard).

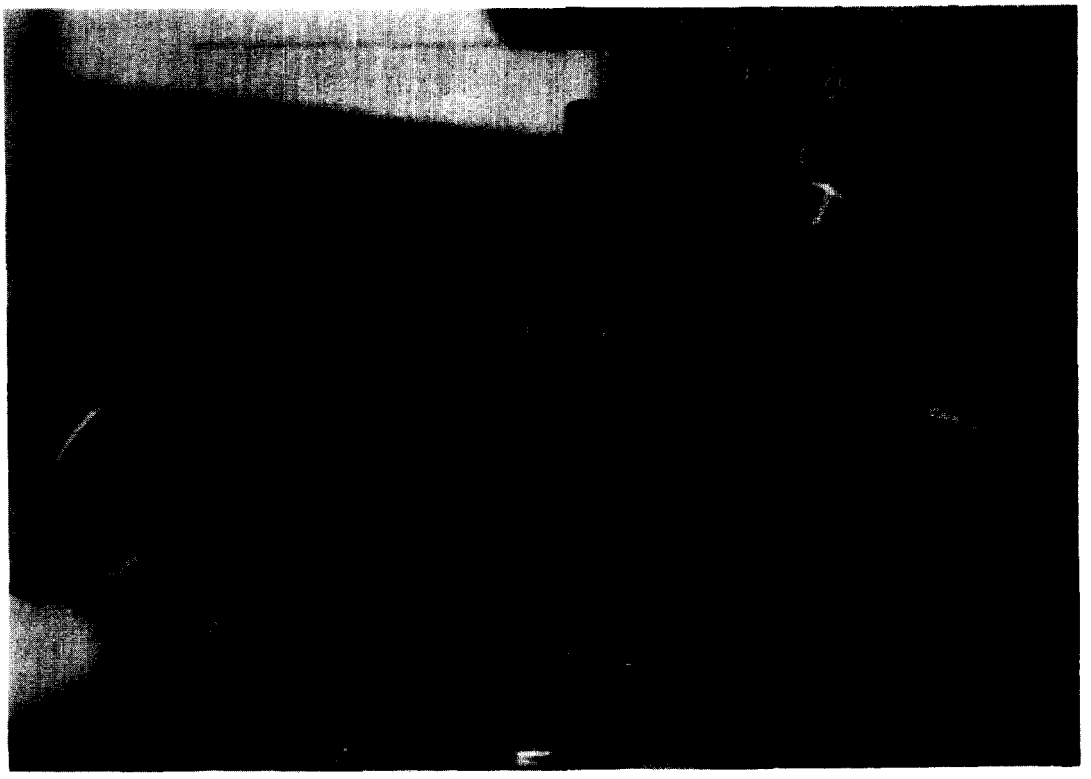

Figure 3: Close-up view of focusing lens. Quartz lens (2.54 cm diameter, 50 mm FL) is used to steem beam onto sample located in chamber behind lens.

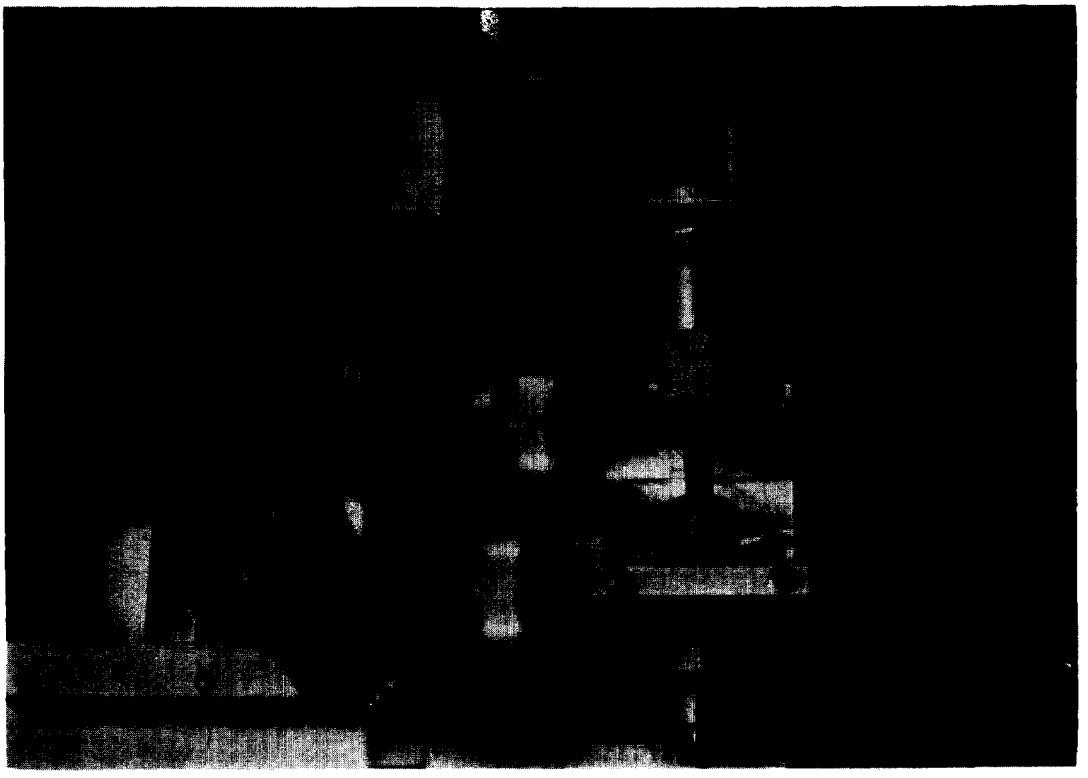

Figure 4: Sample chamber. Tube(6 mm OD) is connected to the gas hydraulic system using Vitron O-rings. Sample in place is a polymer calibration standard.

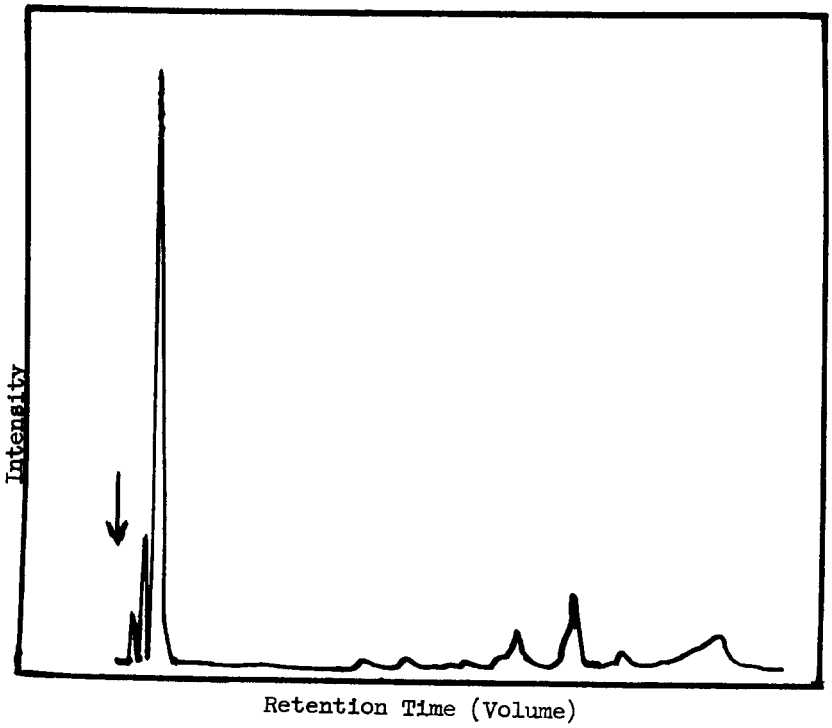

Figure 5: Laser Pyrogram emanating from a 5 J Deposition into a Devonian Shale Sample. Time of firing is shown by the arrow- time then moves from left to right. Chromatographic conditions are listed under Table 1.

SRI INTERNATIONAL'S COMPUTATIONAL FRACTURE MODEL AND ITS APPLICATION TO DEVONIAN SHALES

by

S. L. McHugh
L. Seaman
D. R. Curran
D. A. Shockey

SRI International
Menlo Park, CA

INTRODUCTION

During the past few years, research at SRI International has resulted in the development of a computational fracture model, based on observed stress-wave-induced activation, growth, and coalescence of inherent flaws in rock and other materials. The model, called NAG (for Nucleation And Growth), has shown promising predictive capabilities in studies with Arkansas novaculite and basalt (Shockey et al., 1974, 1975). The input parameters for the NAG model include inherent flaw size and orientation distributions as well as the material properties that govern flaw activation and growth.

In this model, cracks nucleate at inherent flaws and grow until they intersect other cracks or until the stress vanishes. When the cracks intersect, fragments are formed and the fragment size distribution can be calculated from the crack size distribution at the time of intersection. If the stress vanishes before crack intersection, the material acquires a population of cracks but no fragments. The extent of fracture or the degree of fragmentation resulting from a given loading pulse depends on the number of inherent flaws that are activated by the stress and the rate at which the cracks grow. The fracture-controlling parameters can be determined by either (1) performing plate impact experiments on small specimens or (2) detonating a charge of high explosive in the material (e.g., a springing experiment), quantifying the resulting fracture damage, and correlating the damage with computed stress histories (Curran et al., 1977).

To carry out one- and two-dimensional finite-difference calculations for predicting material fracture, it is necessary to know the constitutive relations that control stress wave propagation as well as the fracture parameters. A constitutive model may be developed from a Lagrangian analysis (Cowperthwaite and Williams, 1971) of stress records obtained in plate-impact experiments and from dynamic yield strength data. This constitutive model, together with the fracture and fragmentation parameters, is then used in a wave propagation code to simulate the plate impact and springing experiments.

This paper reviews the application of SRI's fracture model to oil shale* and outlines a program designed to characterize and quantify failure of the eastern Devonian gas shales under dynamic loading. The application of the fracture model to oil shale involved four stages: (1) development of a constitu-

* Work supported by Los Alamos Scientific Laboratory, Los Alamos, New Mexico; Sandia Laboratories, Albuquerque, New Mexico; and Laramie Energy Research Center, Laramie, Wyoming.

tive model to describe stress wave propagation in the material, (2) a series of one-dimensional plate impact experiments to determine a set of preliminary fracture parameters, (3) a series of small-scale borehole (i.e., springing) experiments designed to characterize fracture in a two-dimensional cylindrical geometry, and (4) computations using the constitutive and fracture models to predict the stress and fracture distributions in oil shale. The initial work which was done on 20-gal/ton oil shale, is described in Sections II, III, and IV. At the time of this writing, data from the experiments on 40-gal/ton oil shale were still being analyzed, and are only briefly described in Sections IV and V. The program proposed for the Devonian shales is discussed in Section VI.

CONSTITUTIVE MODEL

Constitutive relations for 20-gal/ton oil shale were determined from low-stress-level gas gun data obtained by LASL (Olinger, 1976). Analysis of these data, using the Lagrange analysis technique (Cowperthwaite and Williams, 1971), yielded stress-volume curves for both loading and unloading. Additional data on compressive yield strengths were obtained from work by Johnson (1975); data on elastic moduli came from ultrasonic measurements by Olinger (1976) and data on very-high-pressure shock loading derived from work by Carter (1976). Data obtained by Schuler et al. (1976) on shock loading and unloading of a more clay-rich oil shale from Rock Springs, Wyoming, were compared with data from Rifle, Colorado. Stress-volume curves calculated separately from these various data are shown in Figure 1. Carter's curves are based on a linearized U_s-u_p (shock velocity versus particle velocity) fit to his modeling of high-pressure Hugoniot data (Carter, 1976). We used the average oil shale denisty of 2.27 g/cm^3 (corresponding to an average kerogen content of 25 gal/ton) measured by SRI from core samples in determining constitutive relation parameters.

Elastic loading and unloading moduli (both are defined by $K + 4G/3$; where K is the bulk modulus and G is the shear modulus) and yield strength were estimated from the Lagrange analysis results (Figure 1). We found the loading moduli to be accurately represented by Olinger's curve fit to longitudinal ultrasonic data (for propagation across the bedding planes). We derived a shear modulus from Olinger's curve fit to transverse ultrasonic velocity data, giving G = 11.8 GPa (118 kbar), corresponding to a low-pressure Poisson's ratio of 0.233. The assumption of a constant yield strength of 0.21 GPa estimated from the Lagrange analysis agrees best with Johnson's data on Rock Springs oil shale (ρ = 2.25 g/cm^3). With this yield strength, the initial bulk modulus (derived from the above loading and shear moduli) was used with Carter's high-pressure data to define the hydrostat. For initial solid density, ρ_{SO} = 2.27 g/cm^3, we found it to be

$$P = C\mu + D\mu^2 + S\mu^3, \qquad (1)$$

where, $\mu = (\rho/\rho_{SO}) - 1$, C = 18.2 GPa, D = 164.8 GPa, and S = -202.1 GPa. We found the density dependence under compressive stress of the unloading moduli ($K + 4G/3$) measured from the Lagrange analysis to agree approximately with that obtained by allowing K to be the slope of the hydrostat and holding G constant and its low-pressure value of 11.8 GPa.

The viscoelastic type of rate dependence observed in loading and unloading curves (from Lagrange analysis) was modeled by using larger that usual coefficients for the linear artifical viscosity employed in finite-difference calculations under relative compression (C_L = 0.15, C_Q = 4.0) and tension (C_L = 0.05).

The predictive quality of the constitutive relations is illustrated by the loading-unloading curve shown in Figure 1. We calculated this curve for an initial specific volume of 0.465 cm/g (ρ = 2.15 g/cm^3) to avoid overlap with other data in Figure 1.

PLATE IMPACT EXPERIMENTS

The material parameters in the NAG dynamic fracture model are usually determined by performing plate impact experiments, quantifying the resulting fracture damage, and correlating the damage with the causative stress history (Curran et al., 1977). A gas gun accelerates an impactor plate against a specimen plate to produce a uniaxial-strain tensile pulse in the specimen. Pulse amplitude and duration are controlled by the impact velocity and the plate thicknesses, respectively. The specimen's stress history can be calculated with a one-dimensional wave propagation code if the constitutive relations for the impacting materials are known or are measured with embedded gages or rear surface

interferometry.

The plate impact experiments produce a variety of stress histories and a range of fracture damage. The threshold conditions for fracture are inferred from experiments resulting in no damage and those resulting in incipient damage. The fracture damage in intact specimens is revealed on polished cross sections and quantified by counting and measuring individual fractures. Sieve analysis quantifies the damage in fragmented specimens. The dynamic fracture parameters are determined by iterative computational simulations of the plate impact experiments. Usually, two to four iterations give reasonable agreement between computed and measured crack and fragment size distributions.

A major objective in specimen design was to ensure that fracture damage occurs under one-dimensional-strain conditions (i.e., to minimize fracture damage produced by stress waves converging from the specimen's periphery). The problem of converging edge waves has been treated by Stevens and Jones (1972). The effect of these edge waves was minimized by press fitting the specimen into a guard ring.

Seven plate impact experiments using Lucite impactor plates were conducted on 20-gal/ton oil shale. The impact direction was normal to the bedding planes. The fracture parameters were estimated from the results of these experiments and from fracture toughness results of SLA (Schmidt, 1976).

The critical stress for flaw activation in the 20-gal/ton oil shale was determined to be 15 MPa (2.18 ksi) from the observed fracture threshold in the impact experiments. The inherent flaw size distribution, not directly observable on polsihed cross sections of oil shale, was inferred from the quasistatic fracture toughness results of SLA and the measured fragment size distribution from one of SRI's plate impact experiments. Assuming the dynamic fracture toughness to be approximately equal to the static toughness (i.e., neglecting rate dependence) and using Sneddon's expression for the stress intensity of a penny-shaped crack, we calculated the radius of the largest flaw R_{max} to be

$$R_{max} = \pi \left(\frac{K_{1c}}{2\sigma} \right)^2 = 0.08 \text{ in.} \approx 2 \text{ mm.} \qquad (2)$$

Because the volume of the plate impact specimens was about 5 cm^3, the concentration of largest flaws (those with radii of about 2 mm) in a specimen containing only one large crack would be about 0.2 crack cm^{-3}. Thus, our cumulative flaw size distribution curve N_g as a function of R (where N_g is the number of flaws per cubic centimeter of size equal to or greater than R) must contain or lie above the point $N_g = 0.2$ cm^{-3}, R = 0.2 cm. In the preliminary model discussed here, we allowed the size distribution curve to contain this point.

Fragmentation was produced in one of the impact experiments, and the fragment size distribution was determined. The smallest fragments had radii of about 0.002 cm, and the cumulative number of fragments per cubic centimeter was 176. The fragments averaged six sides; thus, the number of cracks was three times the number of fragments (each crack contributes to two fragments), producing a total number density of cracks equal to 528 cm^{-3}. We next assumed that these smallest cracks did not grow much from their original flaw sizes. Thus, our N_g (R) curve for flaws must also contain the point N_g = 528 cm^{-3}, R = 0.002 cm. Figure 2 shows the assumed inherent flaw size distribution drawn through the two points obtained and the crack size distribution assuming three cracks per fragment, upon coalescence.

From Figure 2 we infer that in this experiment the smallest cracks traveled shorter distances before coalescing than did the larger ones. The simplest explanation is that the larger cracks, on the average, traveled faster. Furthermore, the nearly parallel crack size distribution curves in Figure 2 indicate that the relative rate of growth is a constant,

$$\frac{\Delta R}{R_{avg}} \simeq 1.6, \qquad (3)$$

where, $R_{avg} = 0.5(R_{final} + R_{initial})$.

Previous work on rock fracture (Shockey et al., 1974, 1975) has shown the validity of a viscous growth law

$$\frac{\dot{R}}{R} = \frac{\sigma - \sigma_{go}}{4\eta} , \qquad (4)$$

where σ_{go} is the stress is required to maintain crack growth after a flaw is activated and η is the crack tip viscosity. In our preliminary model, we assume that σ_{go} is much less than the activation threshold stress and can be neglected.

Equation (3) would give

$$\frac{\dot{R}}{R} = \frac{\Delta R}{R\Delta t} \cong 0.8 \times 10^{6}\ s^{-1}. \tag{5}$$

Thus, we estimate η in Equation (4) by matching Equations (4) and (5):

$$\frac{\sigma}{4\eta} \cong 0.8 \times 10^{6}\ s^{-1},$$

where, σ in this experiment is taken to be 15 MPa, and $\sigma_{go} << 15$ MPa. This yields,

$$\eta \cong 47 \text{ poise}, \tag{6}$$

a value about half that obtained for microcrack growth in novaculite (85 poise). Later iterative calculations reduced this value to 12.5 poise.

The crack coalescence that leads to fragmentation of the shale is modeled as described by Shockey et al. (1974, 1975). Basically, after fulfilling a coalescence criterion, the cracks are used to form the fragments; the largest cracks make the largest fragments, the next largest cracks make the next largest fragments, and so on.

The discussion above presents the basis for selecting the parameters in a NAG model for dynamic fracture of oil shale. That is, we assume an initial flaw size distribution as shown in Figure 2, a threshold stress σ_{no} of 15 MPa (o.15 kbar), a growth law given by Equation (4), and the coalescence and fragmentation model documented by Shockey et al. (1974, 1975). Furthermore, the number of activated flaws may be obtained from our previously developed nucleation rate equation

$$\dot{N} = \dot{N}_o \exp\left[\frac{\sigma - \sigma_{no}}{\sigma_1}\right], \tag{7}$$

where, σ_{no} is the threshold activation stress, and $\dot{N}_o$ and σ_1 are material properties. The initial value of η was taken to be 47 poise. Interative wave propagation calculations were then performed, and these material parameters were adjusted to account for the improvements in computed stress histories as the effects of damage-induced stress relaxation were accounted for.

The fracture parameters were incorporated into the NAG fracture subroutine, and together with the constitutive relations, they were used in the PUFF wave propagation code to simulate the results of the experiment that produced fragmentation. Figure 3 compares computed and observed fragment size distributions after several iterations to obtain the best values for the fracture parameters. These final values for 20-gal/ton oil shale are listed below.

Nucleation threshold stress	σ_{no}	10 MPa
Nucleation stress sensitivity	σ_1	7.5 MPa
Threshold nucleation rate	$\dot{N}$	$1.6 \times 10^{10}\ cm^{-3}\ s^{-1}$
Growth threshold stress	σ_{go}	0.5 MPa
Growth viscosity	η	12.5 poise

SMALL-SCALE SPRINGING EXPERIMENTS

The oil shale used in these experiments was obtained from Dr. Karl Schuler of Sandia Laboratories and was from the Anvil Points mine in Colorado. The average initial density was 2.27 g/cm^3 for the 20-gal/ton shale and 1.99 g/cm^3 for the 40-gal/ton shale.

In the first experiment on 20-gal/ton oil shale, a 6.35-mm-diameter (0.25-in.-diameter) hole was drilled to a depth of 279 mm (11 in.) along the cylinder axis and filled with a mild detonating fuse (MDF), as shown in Figure 3. Strain gages were mounted on the periphery of the cylinder near the plane passing through the center (Figure 3). The cylinder was placed in a pressure vessel and a confining pressure of 3.45 MPa (500 psi) was applied to simulate the overburden present in a field experiment.

Afterwards, the cylinder was sectioned through the center, and 1-in. slices were cut from the bottom half and polished (see Figures 3 and 4). To ascertain what effect a second stress wave would have on the crack pattern formed by the first detonation, we repeated the experiment with the top half of the original cylinder under 3.45 MPa (500 psi) confining pressure. The sample was then sectioned perpendicularly to the cylinder axis (section F in Figure 3), and the surface was polished and photographed. Figure 5 shows the crack pattern resulting from this double shock experiment.

We performed two experiments on the 40-gal/ton oil shale. The experimental arrangement and procedure were the same as those described above [a hydrostatic pressure of 3.45 MPa (500 psi) was used in both cases], except that (1) the explosive charge (PETN) was the same diameter as the borehole; (2) the borehole was stemmed at both ends; and (3) ytterbium stress gages were placed at known distances from the borehole.

After detonation of the explosive, the cylinder was removed from the pressure vessel and sectioned perpendicularly to the axis. The crack size distribution was determined for each section (1) splitting each section into three concentric zones of equal width centered on the borehole; (2) determining the length and orientation of each crack in each zone; and (3) counting the number of cracks within a specified length and orientation interval. Cracks with actual lengths of slightly less than 1 mm could be resolved and counted.

The distribution of radial cracks for Zones 1, 2, and 3 (Zone 1 is closest to the borehole, Zone 3 is the furthest) from the mid-sections of the 20-gal/ton and from the first 40-gal/ton experiment are compared in Figure 6. Preliminary calculations suggest that the stress pulses from the explosives were nearly identical in both cases, and hence the agreement between the crack size distributions is not surprising.

The permeability of oil shale was determined by removing a 5-cm (2-in.) diameter x 3.8-cm (1.5 in.) long core centered on the borehole. The ends of the core were sealed, except at the top of the borehole, and the fluid flow rate through the cylinder wall into the borehole was measured. The permeability was (1) 3×10^{-8} darcies in the intact 40-gal/ton shale and (2) 8×10^{-3} darcies in the 40-gal/ton shale, shot once. The permeability of the 20-gal/ton oil shale, shot twice, was greater than 10 darcies. These results suggest that near the borehole the permeability may be increased by about 4 to 5 orders of magnitude by each shot.

It is also instructive to consider the microstructure of the oil shale. The regions shown in Figures 7a and 7b were about 1 cm apart in the original sample. Figure 7a shows a very porous, loosely cemented mixture of clay particles abutting the kerogen, whereas the region in Figure 7b is quite dense. Such differences in porosity and degree of cementing suggest that cracks may nucleate between grains or regions of differing physical properties. Figures 8a and 8b reveal cracks that have nucleated and propagated along grain boundaries. Examination of the oil shale microstructure therefore yields insight into the physical mechanism responsible for the formation and growth of these cracks and the consequent increase in permeability.

COMPUTATIONS

The maximum stresses produced by the borehole charge of MDF in the 20-gal/ton oil shale (Figure3) were estimated by performing a "no damage" calculation (Figure 9). The hoop tensile stress, radial tensile stress, and axial tensile stress are shown as a function of R/R_o; where, R is the distance from the center of the cylinder and R_o is the initial borehole radius (3.175 mm in our experiment). In this

calculation, we used the constitutive model previously developed for 20-gal/ton oil shale, and the oil shale was assumed to have infinite tensile strength (i.e., fracture was not allowed).

The calculation indicates that radial cracks (caused by the hoop tensile stress) should extend to about 16 borehole diameters (10 cm or 4 in.), with the largest concentration of cracks expected within about 4 borehole diameters (2.5 cm or 1 in.). We observed radial cracks extending to 12 borehole diameters, with the most cracks occurring at much smaller diameters. The calculation also predicts that circumferential cracks (caused by the radial tensile stress) should occur at approximately 8 borehole diameters (5 cm or 2 in.). We observed such cracks at about 6 borehole diameters (3.8 cm or 1.5 in.) on section B of Figure 3.

Of course, as fracture occurs the stresses are modified. Consequently, the maximum stresses predicted by the "no damage" calculation are likely to be an upper bound only. We are currently performing "damage" calculations using the constitutive and fracture models discussed previously. These "damage" calculations are iterated by (1) comparing the predicted to observed stress histories and fracture distributions and (2) varying the fracture parameters until observations and predictions are similar.

Many questions remain to be answered. The sensitivity of the fracture distributions to specific material (and fracture) parameters must be determined, as must the input pressure-time history. The next section outlines SRI's program on Devonian shales, in which we will attempt to answer some of these questions.

FRACTURE OF DEVONIAN SHALE BY TAILORED-PULSE LOADING

A. Introduction

Because of the inherently low permeability of Devonian shale, any stimulation technique applied to it must entail some type of formation fracturing. A principal objective of explosive techniques has been to load the rock dynamically to form multiple fractures and/or to propagate preferred fractures. Without a detailed knowledge of the relationships between the processes controlling rock fracture and the stress-time history of dynamic loading, efforts to optimize explosive stimulation are at best trial and error.

The SRI research program has three objectives:

(1) The determination of the relative and absolute importance of various rock properties in controlling rock fracture by the dynamic pressure of loading well bores.

(2) The determination of the ranges of the important properties that will permit successful well fracturing by tailored-pulse loading, and the correlation of these ranges with actual values found in rocks of interest.

(3) An evaluation of the prospects for successfully implementing a well stimulation technique, based on pressure-pulse tailoring.

The results of the research will have other applications beyond these specific objectives; the fracture models resulting from the research will directly apply to current or future programs for developing and field demonstrating a propellant-based well stimulation technique. The improved understanding of rock fracture and related processes will prove useful in the study and evaluation of other dynamic stimulation techniques such as the in-formation detonation of high explosives and well bore penetration with shaped charges.

B. Research Program on Devonian Shales

Because available cores of Devonian shale are limited in size, we propose a series of small-scale springing experiments in which cores 4 to 6 in. in diameter and about 12 in. long are cast in an impedance-matching epoxy. The total diameter will thus be 10 to 12 in., and the epoxy will minimize the reflection of the stress wave from the shale boundary. A central borehole 0.125 to 0.25 in. in diameter will be filled with a charge of PETN.

The experimental configuration of these tests will be similar to the oil shale experiments discussed above. By changing the density of PETN and the borehole diameter by venting or stemming the borehole,

the amplitude and duration of the input pressure pulse can be controlled. Some of the samples will be instrumented (stress, strain, and particle velocity gages are available), and the measured quantities will provide valuable constraints on later computations. The remaining springing experiments will not be instrumented (but will be otherwise identical to the instrumental shots) to enable observation of the fracture distribution.

After detonation of the charge, the noninstrumented sample will be sectioned, polished and photographed. The length and orientation of the cracks produced in the sample will be measured, and the fracture distributions will be correlated with the stress histories (known from the instrumented shots) to derive a preliminary set of fracture parameters.

The initial set of fracture parameters will be determined by using a single, one-dimensional finite difference code with a single test cell. The code includes the fracture subroutine and computes the stresses in the material. A strain rate equivalent to the measured strain rate will be imposed on the test cell and the stress will be computed at each time increment. When the stress in the cell exceeds the threshold activation stress (which initially can be assumed to be equivalent to the spall strength determined by Olinger, 1977), the fracture subroutine will be called, and the amount of damage (or cracking) will be computed. The crack volume will be computed from the nucleation and growth laws discussed previously, and the total volume change can thus be computed from the change in crack volume and solid volume. The overall volume change (estimated from the stresses) will be the constraint used on the calculations, and the computations will be iterated until comparisons between the overall volume change and the volume change produced by the damage are satisfactory. This procedure will be repeated by adjusting the fracture parameters until the observed and predicted fracture distributions agree.

This preliminary set of fracture parameters will then be used in a one-or two-dimensional finite difference code (i.e., PUFF or TROTT). We shall use as many cells as required by the experimental configuration to predict the stress-time histories and fracture distributions throughout this material. We shall vary the parameters again until suitable agreement is obtained between the observed and predicted quantities. The final result will be a set of parameters that allow the observed quantities (e.g., stress and fracture distributions) from the springing experiments to be reproduced.

Once the shale has been characterized in this fashion, a subset of the material (and fracture) parameters can be chosen for a parameter sensitivity study. Each parameter will be varied incrementally over some range of values (with the well bore load the same in each case), and the fracture distribution will be calculated for each increment in the parameter by using the one-dimensional finite difference code. This procedure will indicate those aspects of the failure process that are sensitive to changes in specific material parameters.

Then, using the original fracture parameters, we shall perform a similar set of calculations for variations in the well bore load (i.e., changing the pressure-time history). The sensitivity of the fracture distribution to changes in the well bore load will be determined and compared to the effect of variations in the material parameters. If the predicted effect of the well bore load differs substantially from the predicted effect of variations in the material parameters, we shall conduct springing experiments to verify these results.

In these experiments a well bore load will be chosen from those used in the calculations. This load will be (1) different from the input used in the first set of springing experiments, and (2) it will be expected from the calculations to yield a fracture distribution uniquely different from any distribution that might be the result of material property variations.

If the springing experiments (using this new well bore load) result in a fracture distribution unlike any distribution that could be produced by variations in the material properties, they will suggest that specific fracture patterns may be produced by tailoring the pressure-time history at the well bore boundary. The results of this study may then be used to evaluate the prospects for developing a well stimulation technique that uses high explosive and/or propellant induced fracturing.

REFERENCES

Carter, W. J. (1976) Hugoniots of Green River Oil Shale, Los Alamos Scientific Laboratory, March 31.

Cowperthwaite, M., and Williams, R. F. (1971) Determination of Constitutive Relations With Multiple Gages in Nondivergent Waves. J. Appl. Phys. 42, 456.

Curran, D. R., Seaman, L., and Shockey, D. A. (1977) Dynamic Failure in Solids. Physics Today pp. 46-55.

Johnson, J. N. (1975) Dynamic Anisotropic Constitutive Relations for Oil Shale. Final Report to Sandia Laboratories, TR75-25, Terra Tek.

Olinger, B. W., (1977) Eastern Gas Shales Under Dynamic Stress, Report LA-UR-77-1937, Los Alamos Scientific Laboratory, Los Alamos, New Mexico.

_____ (1976) Elastic Constants of Oil Shales. Los Alamos Scientific Laboratory, March 31.

_____ (1976) Los Alamos Scientific Laboratory, private communication.

Schmidt, R. A. (1976) Sandia Laboratories, Albuquerque, New Mexico, private communication.

Schuler, K. W., Lysne, P. C., and Stevens, A. L. (1976) Dynamic Mechanical Properties of Two Grades of Oil Shale. Int. J. Rock Mech. Min. Sci. 13, 91-95.

Shockey, D. A., Curran, D. R., Austin, M., and Seaman, L. (1975) Development of a Capability for Predicting Cratering and Fragmentation Behavior in Rock. Final Report DNA 3730F for Defense Nuclear Agency, Stanford Research Institute, Menlo Park, California, May.

Shockey, D. A. Curran, D. R., Seaman, L., Rosenberg, J. T., and Petersen, C. F. (1974) Fragmentation of Rock under Dynamic Loads. Int. J. Rock Mech. Sci. 11, 303-317.

Stevens, A. L., and Jones, O. E. (1972) Radial Stress Release Phenomena in Plate Impact Experiments: Compression-Release. J. Appl. Mech. 39, 359.

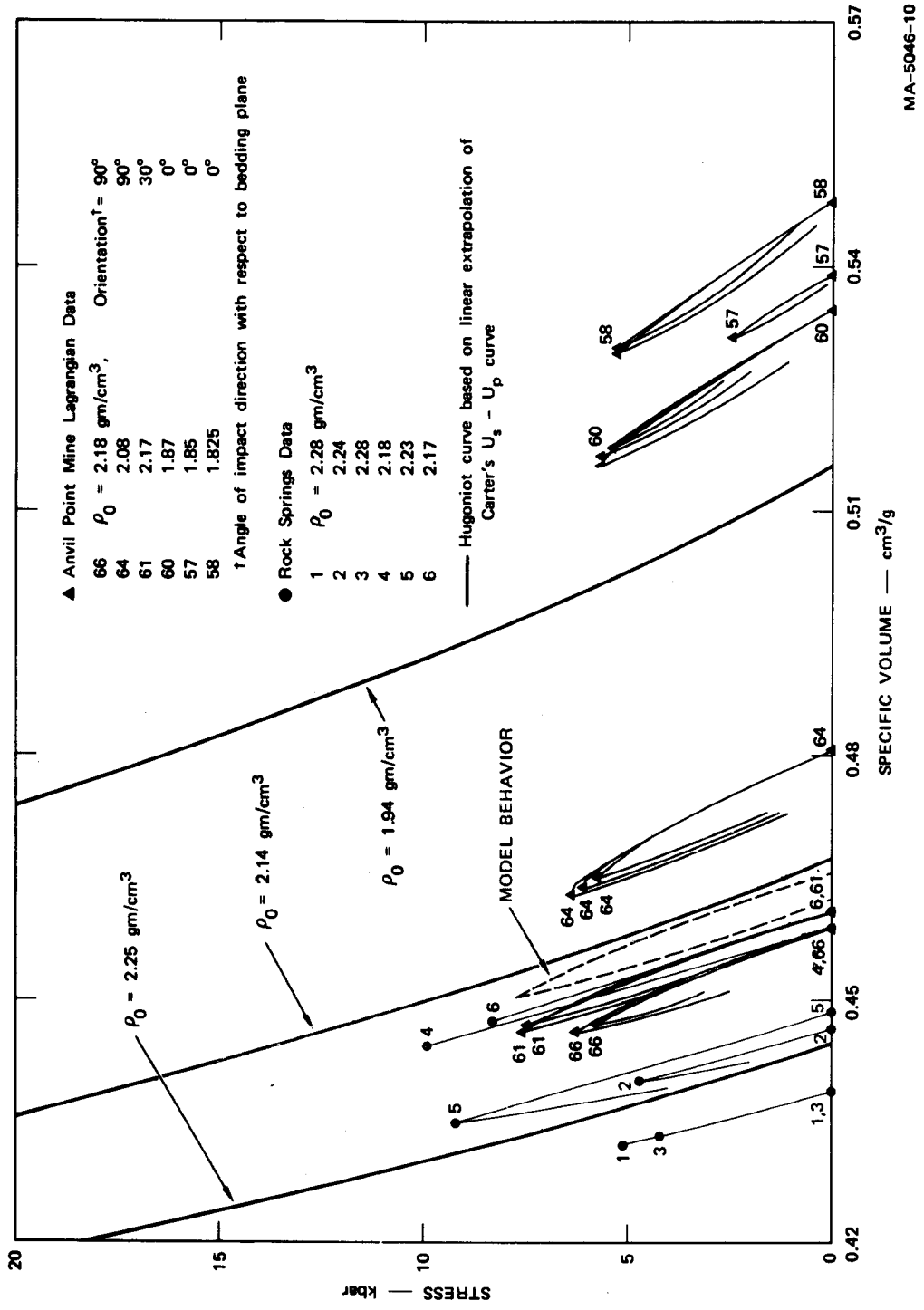

FIGURE 1 HUGONIOT DATA FOR GREEN RIVER OIL SHALE

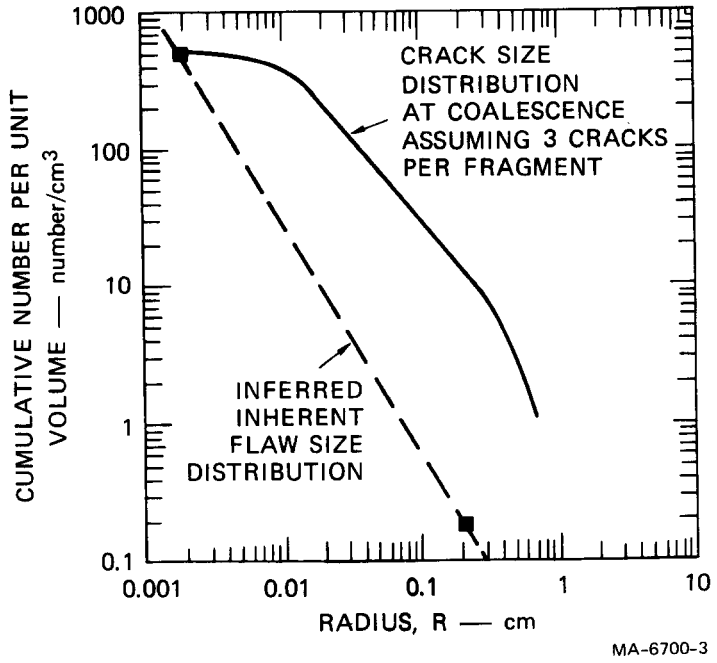

FIGURE 2 INFERRED INHERENT FLAW AND COALESCED CRACK SIZE DISTRIBUTION

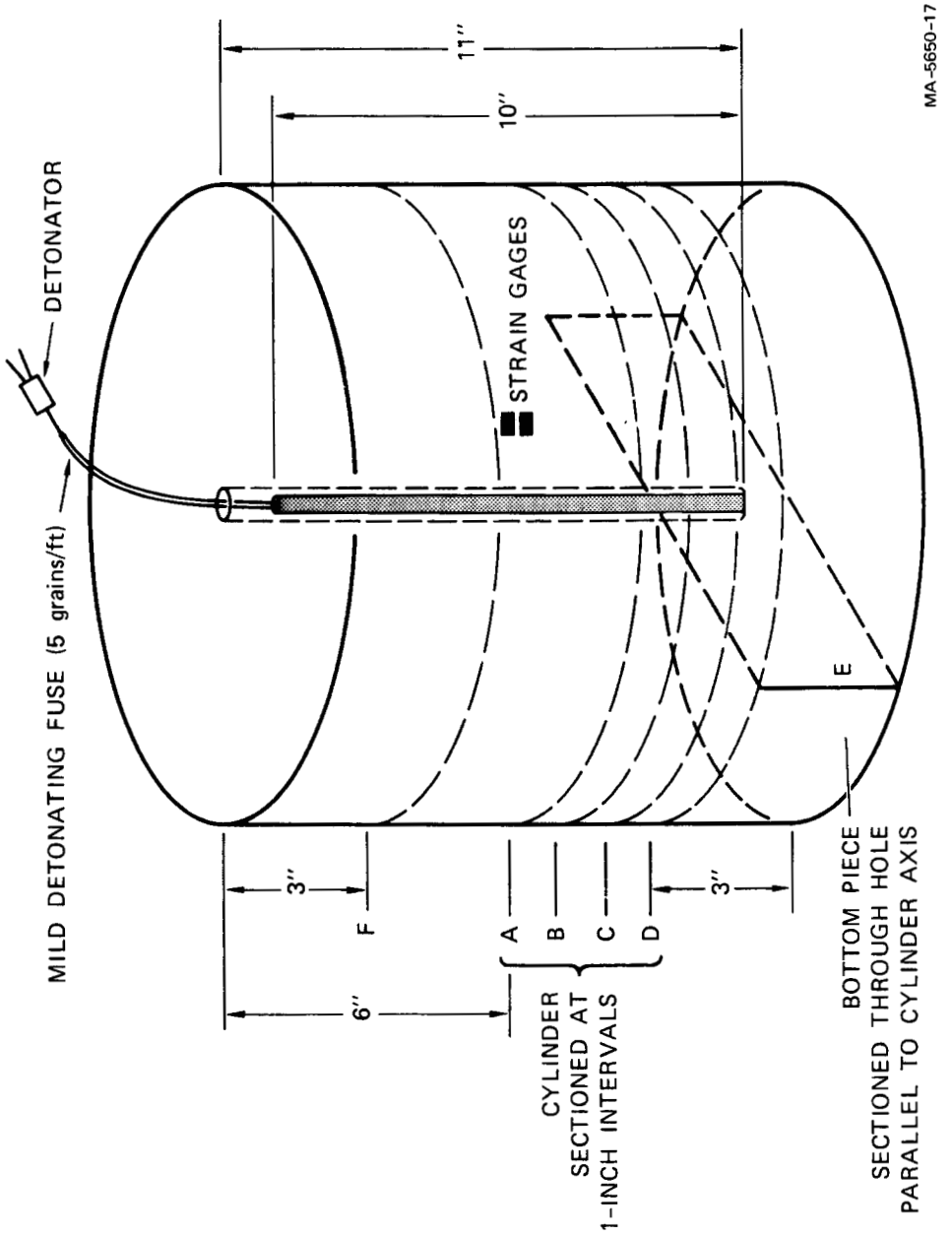

FIGURE 3 SCHEMATIC OF LABORATORY SCALE BOREHOLE EXPERIMENT
Oil shale cylinder is 12 inches in diameter by 12 inches high.

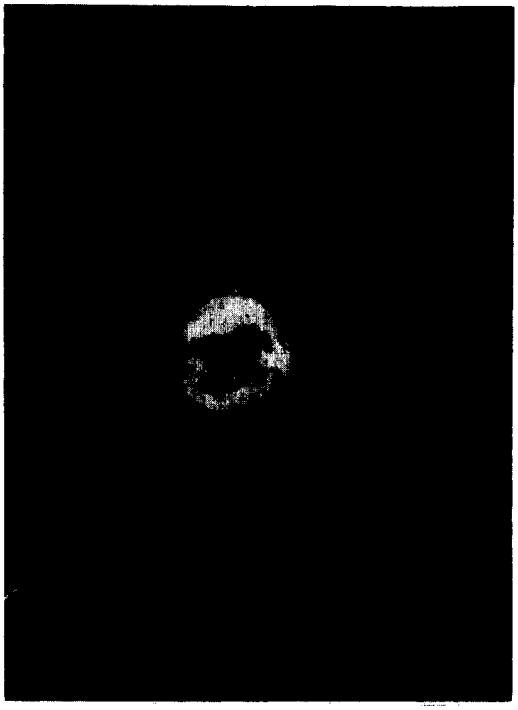

MP-5650-18a

2 x MAGNIFICATION

FIGURE 4 CRACK PATTERN ON SECTION A

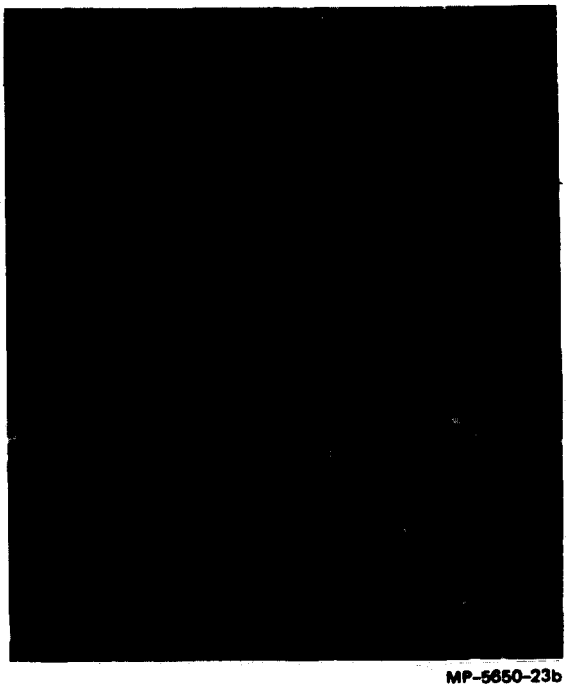

MP-5650-23b

2.5 x MAGNIFICATION

FIGURE 5 CRACK PATTERN ON SECTION F
(AFTER SECOND DETONATION)

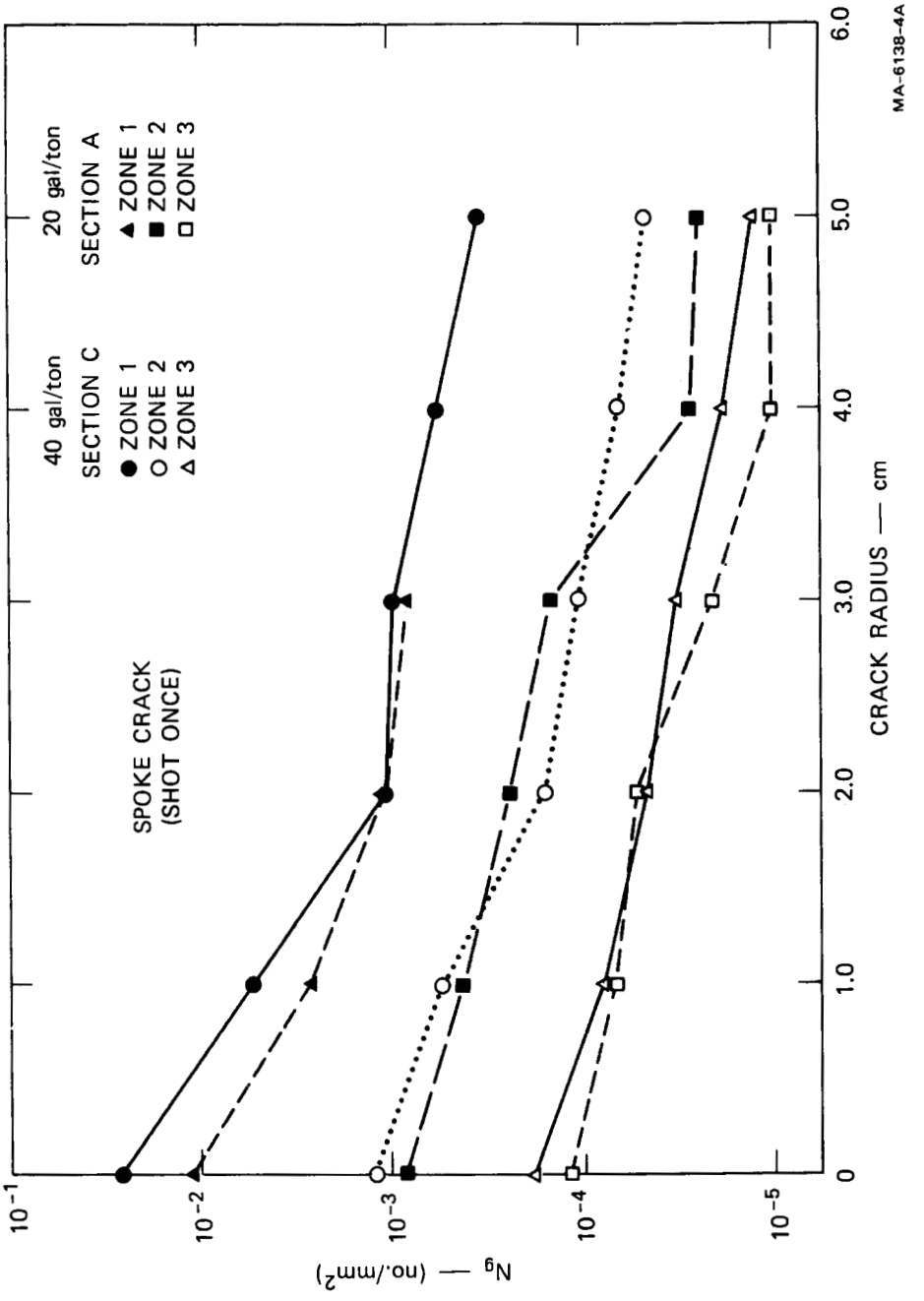

FIGURE 6 COMPARISON OF SPOKE CRACK SIZE DISTRIBUTIONS OF 20-GAL/TON AND 40-GAL/TON OIL SHALE

N_g is the cumulative crack density; R is the crack radius.

(a) THE BOUNDARY BETWEEN KEROGEN (BOTTOM) AND GRAINS OF CLAY AND CARBONATE (TOP)

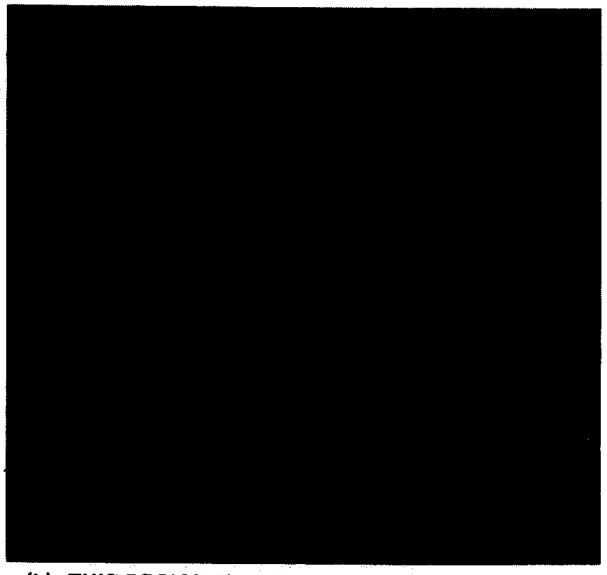

(b) THIS REGION IS ABOUT 1 cm FROM THE REGION SHOWN ABOVE

MP-6700-1

FIGURE 7 2000x MAGNIFICATION — SCANNING ELECTRON MICROPHOTOGRAPH OF 20-GAL/TON OIL SHALE

(a) 1900x MAGNIFICATION OF 20-GAL/TON OIL SHALE. THIS REGION IS ABOUT 1 cm FROM THE BOREHOLE AND IS FROM SECTION F IN FIGURE 3.

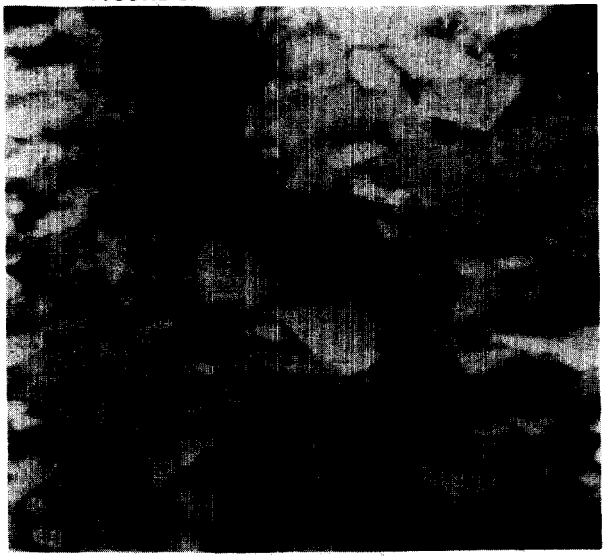

(b) 1300x MAGNIFICATION OF 40-GAL/TON OIL SHALE. THE FRACTURE IS AN INHERENT FLAW (i.e. WAS NOT PRODUCED BY DYNAMIC LOADING)

FIGURE 8 SCANNING OF ELECTRON MICROPHOTOGRAPHS OF OIL SHALE

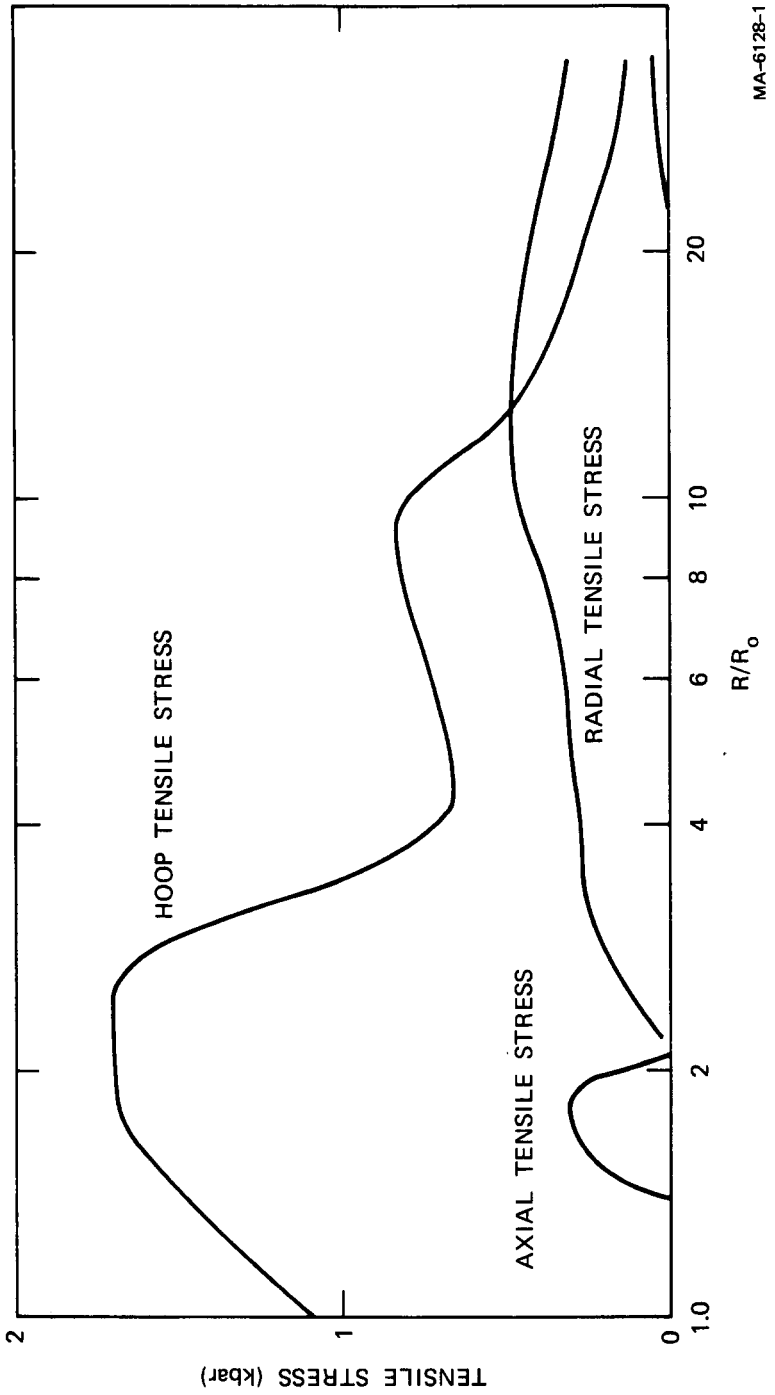

FIGURE 9 PEAK TENSILE STRESS PROFILES FOR NO DAMAGE CALCULATION OF SMALL-SCALE BOREHOLE EXPERIMENTS

GAS CHROMATOGRAPHIC ANALYSIS OF FISCHER RETORT PRODUCTS OF THE NEW ALBANY SHALE

by

Gianfranco Rinaldi
Paolo Ciccioli*
W. Bradley Wimberg
W. G. Meinschein, Department of Geology, Indiana University, Bloomington, IN 47401

SAMPLES OF THE NEW ALBANY SHALE WERE HEATED TO VARIOUS TEMPERATURES IN THE RANGE FROM 50° TO 500°C. THE MAIN ORGANIC CONSTITUENTS OF THE OIL AS WELL AS OF THE GAS PHASES THAT WERE OBTAINED FROM THE HEATED SAMPLES WERE COLLECTED AND THEN CHARACTERIZED AND QUANTIFIED BY MEANS OF GAS CHROMATOGRAPHY. n-ALKANES WERE THE MOST ABUNDANT COMPOUNDS IN THESE PHASES. ALL POSSIBLE ISOMERS OF ALKANES AND MONO-OLEFINIC ALKENES ARE PRESENT IN C_1 THROUGH C_4 PRODUCTS. BRANCHED CHAIN ALKANES AND STERANES WERE DEGRADED MORE RAPIDLY THAN n-ALKANES AT TEMPERATURES BETWEEN 150° AND 300°C. THE CONCENTRATIONS OF LOW MOLECULAR WEIGHT (C_1 TO C_4) HYDROCARBONS INCREASED WITH SAMPLE TEMPERATURE, BUT THE CONCENTRATIONS OF THE $> C_{17}$ ALKANES WERE DEPLETED IN THE HEATED SHALE SAMPLES RELATIVE TO THE UNHEATED SAMPLE.

*Laboratorio sull'Inquinamento Atmosferico del C. N. R., Via Montorio Romano 36, 00131 Roma, Italy

INTRODUCTION

Organic materials in sedimentary series undergo secular changes. Intensive studies have been conducted of the origin and evolution of hydrocarbons in selected sedimentary strata and basins. Special attention in these studies has been paid the effects of organic source materials [Breger and Brown, 1962] and depth of burial or temperature and pressure [Albrecht and Ourisson, 1969; Tissot et al., 1971; Vassoevich, 1974; Tissot and Espitalie, 1975] on the diagenesis of hydrocarbons and other organic substances which may be found in petroleum. An excellent review of the history and scope of investigations of the alterations of hydrocarbons in sedimentary environments is included in an article by Young et al. [1977] which discusses in detail a quantitative method for determining the ages of oils by calculations that utilize the concentrations of certain hydrocarbons in the oils.

Investigations are now being carried out on the New Albany Shale by various scientific groups. One phase of these investigations has as its major objective the evaluation of the potential of the New Albany Shale as a source of gases and liquid organic fractions that may be utilized to augment presently dwindling natural gas and petroleum resources. This evaluation involves the analyses of gases and liquids formed by heating or pyrolyzing the shale. Such an evaluation may furnish data that will clarify some of the ambiguities associated with the interpretations of the analyses of naturally occurring organic materials.

For example, Albrecht and Ourisson [1969] selected a thick sedimentary series of uniform lithological and geochemical compositions in the Douala basin for their investigation of the diagenesis of hydrocarbons. Similarly, Tissot et al. [1971] chose a continuous shale deposit of early Toarcian ($\simeq 180 \times 10^6$ yrs) age in the Paris basin for their study of the origin and evolution of hydrocarbons. Although these ingenious selections of sampling sites probably served to minimize the effects of variations in source materials and organic-inorganic interactions on the quantities, distributions, and structures of the hydrocarbons, the compositional controls exerted on hydrocarbons by biological, chemical, and physical processes specifically may not be completely resolved for natural systems without a precise knowledge of the reactions of sedimentary organic materials. For this reason, the investigation of the thermal production and alteration of hydrocarbons within the New Albany Shale under carefully controlled conditions may complement previous studies of the genesis of hydrocarbons. It should be emphasized, however, that the results obtained on heated samples of the New Albany Shale may not be generally representative. As Breger and Brown [1962] have reported, the compositions of kerogens and the yields of oil from shales vary with the depositional environments of the shales.

EXPERIMENTAL

Samples. The retort charges employed in this investigation were obtained from a large reference sample prepared by Mr. R. K. Leininger. The reference sample was gathered from the exposed part of the Blocher Member of the New Albany Shale at the Harding Street Quarry of the American Aggregates Company in Indianapolis, Indiana, and this collected shale was crushed to pass an 8 mesh sieve.

Analyses. Fig. 1 is a schematic outline of the procedures used in the analyses of the New Albany Shale sample. Each retorting experiment utilized a 100g charge from the reference sample. The individual charges were separately heated in a Fischer retort to a specific temperature in the 50° to 500°C range. A stream of He passed continuously through the retort and an attached silica gel trap which was submerged in liquid N_2. After each charge had been maintained at a specific temperature for one hour, the retort system was closed, the liquid N_2 trap was warmed and liquid products (if formed) were measured volumetrically and weighed, respectively, then separately retained for subsequent chromatographic analyses. Gas samples were obtained from charges maintained at room temperature, 50°, 100°, and 150°, 200°, 250°, 300°, and 500°C, respectively. The charge heated to 500°C was the only one that produced a significant quantity of an isolated liquid phase. Liquid products were obtained, however, from all the retorted samples by separately extracting each shale charge for 72 hrs using a 3/1 v/v benzene/menthanol solvent in a Soxhlet extractor. The solvents was removed from the individual extracts under a stream

of N_2 gas at 40°C, and each extract was chromatographed on silica gel using carbon tetrachloride (CCl_4), benzene (C_6H_6), and methanol (CH_3OH) as successive eluants [Meinschein and Kenny, 1957]. The CCl_4 eluates of the different extracts were each separated into alkane and alkene fractions by thin-layer chromatography (TLC) on glass plates coated with silica gel impregnated with 15% by weight of silver nitrate. The alkane and alkene or olefin bands were separately scraped from each TLC plate onto a filter and each fraction of alkanes and olefins was washed from the scrapings into a 2 ml vial with anhydrous diethyl ether. The ether was permitted to evaporate and the alkane and alkene residues were separately sealed with caps over aluminum foil covers until analyzed. Each alkane and alkene fraction was qualitatively and quantitatively characterized by gas-liquid chromatography (glc) using a modified Varian 1400 Series Gas Chromatograph equpped with a FID detector. A 0.2 x 200 cm stainless steel column packed with 5% by weight of PPE-20 liquid phase on Carbopack B as solid support was used for the temperature-programmed (100°-300°C at 4° C/min) glc analyses.

The gas fractions collected from the Fischer retort were each analyzed by glc using a 0.2 x 200 cm stainless steel column packed with 1.5% by weight FFAP liquid phase on Carbopack B as stationary phase. The glc analysis of each 1 ml gas sample was carried out isothermally at room temperature.

RESULTS AND DISCUSSION

The volumes of gas, water, and oil produced by heating the New Albany Shale to temperatures in the 50° to 500°C range are recorded in Table 1. These data show that the volumes of gas and water released by the shale increase as the temperature of the shale increases. No separate oil phase was distilled from the shale at temperatures of less than 500°C which are recorded in Table 1.

Liquid-solid chromatographic analyses of the soluble organic fractions of the heated shale samples are presented in Table 2. The CCl_4 eluates from silica gel are composed primarily of alkanes plus olefins. Aromatic hydrocarbons and nitrogen, oxygen, and sulfur containing organic compounds are the principal constituents of the C_6H_6 and CH_3OH eluates. As indicated in Table 2 the weights and percentage yields of the CCl_4 fractions decrease as the retort temperatures increase, whereas the weights and percentage yeilds of the C_6H_6 and CH_3OH eluates increase with increasing retort temperatures.

Organic constituents of the New Albany Shale undergo extensive thermal alterations at temperature 500°C. Evidence of the extent of some of these alterations is provided by the gas chromatograms shown in Fig. 2(a) and (b). The chromatogram in Fig. 2a represents the CCl_4 eluate from silica gel of the room temperature extract of the New Albany Shale. The chromatogram in Fig. 2b represents the distilled oil phase of the shale sample that was heated to 500°C. The following interpretations may be made of these chromatograms:

1. The alicyclic isoprenoids, pristane and phytane, which are the largest individual peaks in Fig. 2(a), the CCl_4 eluates of the room temperature extract, are relatively small peaks in Fig. 2(b), the combined 500°C distillates and extract. Likewise, the iso-C_{17} alkane and certain cycloalkanes, such as steranes, are less concentrated in 500°C distillate and extract than in the CCl_4 eluate.

2. The C_{15}-C_{20} n-alkanes, which are the most abundant n-alkanes in the CCl_4 eluate, are significantly less abundant than the C_4 to C_{12} n-alkanes in the 500°C distillate plus extract.

3. A marked peak which is probably formed by pyrolysis products, appears in Fig. 2(b).

Figs. 3(a) and (b) are gas chromatograms of the pure alkanes isolated from the fractions that provided the samples used to obtain the chromatograms in Figs. 2(a) and (b) respectively.

These alkanes were separated from the CCl_4 eluates of the room temperature extract and the combined 500° distillate and extract by thin layer chromatography (TLC)

on silica gel plus silver nitrate. Because peaks in the chromatograms shown in Fig. 3(a) and (b) are produced solely by alkanes, these chromatograms provide additional support for the interpretations of Fig. 2(a) and (b). As suggested above, pristane, phytane, steranes, and iso-C_{17} alkane are present in much higher concentrations in the unheated shale sample than in the sample heated to 500°C. Also noteworthy in Fig. 3(a) are the relative sizes of the peaks of the odd-carbon number and even-carbon number n-alkanes in the C_{15} to C_{20} range. The odd-carbon number n-alkane peaks are larger than the peaks of the even-carbon number homologs. Such a predominance of odd-carbon number n-alkanes is commonly attributed to the preferential production of odd-carbon number n-paraffins by organisms. As may be observed in Fig. 3(b) no "odd-carbon preference" exists in the alkanes that were thermally altered at 500°C. (The peaks of alkanes smaller than C_{12} which appear in Fig. 2(b) are absent in Fig. 3(b) because these relatively volatile alkanes were lost when the solvents were evaporated to recover the hydrocarbons from their liquid-solid and TLC chromatographic eluants.)

Fig. 4(a) presents plots of the weights of total alkanes, n-alkanes, total olefins, iso-C_{17} (2-methylhexodecane), and isoprenoids (pristane and phytane) in mg obtained from 100 g of shale at specific retort temperatures up to 500° C. The data plotted in Fig. 4(a) permit the following interpretations:

1. The degradation of total alkanes, n-alkanes, iso-C_{17}, and isoprenoids increases as the retort temperature increases.

2. The degradation rates of iso-C_{17} and isoprenoid alkanes are greater than the degradation rates of n-alkanes at temperatures above 150°C.

3. The maximum degradation rate of alkanes occurs initially in 150° to 200°C range.

4. The production rate of olefins increases to a maximum at 200°C at which temperature the degradation rate equals the production rate.

5. The olefinic degradation rate exceeds the olefinic production rate in the 200° to 250°C range.

6. At 250° C. the concentration of olefins reaches a minimum and then increases at 300° C.

Fig. 4(b) shows the plots of the odd carbon number C_{17} through C_{23} n-alkanes. It may be observed in Fig. 4(a) and 4(b) that the increase in olefin production in the 250° to 300° C range correlates with an increase in the concentrations of n-C_{19}, n-C_{21}, and n-C_{23} in the same temperature interval.

Degradation and production rates are plotted as the percentages of the differences of the concentrations of alkanes at room temperature (Q^{RT}) and at retort temperature (Q^{T}) divided by Q^{RT} versus the retort temperature (T°C) in Figs. 5(a) and (b). Because the concentration of olefins was a minimum at room temperature, the degradation and production curves for the olefins are plotted as the reverse difference $(Q^{T}-Q^{RT}/Q^{RT})$ function in Fig. 5(c).

As noted above, the maximum decay rates of various types of alkanes (see Fig. 5(a)) begins in the 150° to 200° C range, the temperature range in which the production rate of olefins increases to a maximum (see Fig. 5(c)). A rapid decrease in the concentration of olefins occurs between 200° and 250°C. This decrease is followed by an increase to a second maximum in the olefin plot at 300°C. The maximum in the n-C_{19} curve in Fig. 5(b) correlates with the second maximum in the olefin plot. These maxima and the inflections in these n-alkane plots suggest that degradations of organic non-hydrocarbons, i.e. kerogens, which occur at 250°-300°C, have preferentially produced C_{19}, C_{21}, and C_{23} n-paraffins.

Fig. 6 presents the ratios of odd-carbon number to even-carbon number C_{15}-C_{20} n-alkanes (carbon preference index or CPI), pristane to phytane, n-C_{17} to iso-C_{17}, and n-C_{17} to iso-C_{17} and the n-C_{17} to phytane plots at 250°C. These maxima may either be consequences of the concomitant increases in the degradation rates of the branched

chain alkanes relative to n-alkanes and in the production rate of n-C_{17} in the 150° to 250° C temperature interval. A smaller maximum occurs at 200° C in the pristane to phytane plot, but neither the cause nor the reality of this maximum is established. The variations in the pristane to phytane ratio in Fig. 6 do not greatly exceed the precision of measurement. The CPI plot decreases from 1.3 to 1 in the 100° to 250° C temperature interval and remains constant at 1 from 250° to 500° C. A rapid increase in the n-C_{17} to phytane ratio in the 300° to 500° C range is probably the result of phytane having a greater degradation rate than n-C_{17} at these temperatures. Because the n-C_{17} to iso-C_{17} increases only slightly in the 300° to 500° C interval, iso-C_{17} is apparently more stable than phytane in this temperature range.

Fig. 7(a) and (b) presents plots of the hydrocarbon gases isolated from the New Albany Shale at temperatures up to 500° C. The concentrations of the alkanes, see Fig. 7(a), and the yields of gases as reported in Table 1 increase with increasing temperature. Similar increases may be observed in the concentrations of ethylene (C_2H_4) and propylene (C_3H_6) in Fig. 7(b), but the concentrations of the three butenes reach maxima in the 150° and 200° C temperature interval.

CONCLUSIONS

Thermal alterations of the organic constituents of the New Albany Shale lead to increased yields of gaseous hydrocarbons and of liquid organic compounds containing oxygen, nitrogen, and/or sulfur atoms. Heating, however, substantially degrades and diminishes the concentration of the $\geq C_{17}$ alkanes in the New Albany Shale. The production of gaseous hydrocarbons reaches a maximum rate in the 100° - 200° C range that overlaps the 150° to 200° C interval in which the degradation rates of butenes and $\geq C_{17}$ alkanes reach a maximum. Correspondence between the temperatures at which the gaseous hydrocarbons other than the butenes are formed most rapidly, see Fig. 7(a) and (b), and the higher molecular weight olefins and alkanes are degraded most rapidly, see Fig. 5, indicates that these gases may be partially derived from their larger homologs. In that the butenes production rates apparently peak at lower temperatures than do the production rates of the other gaseous hydrocarbons, the butenes may be preferentially formed from organic non-hydrocarbons which are thermal more labile than hydrocarbons. The temperature dependencies of the relative abundances of certain hydrocarbons such as n-C_{17} to iso-C_{17} or phytane in the New Albany Shale suggests that these compounds can be used as thermal indicators.

REFERENCES

Albrecht P. and Ourisson G. (1969) Diagénèse des hydrocarbures saturés dans une série sédimentaire épaisse (Douala, Cameroun). Geochim. Cosmochim. Acta 33, 138-142.

Breger I. A. and Brown A. (1962) Kerogen in the Chattanooga Shale. Science 137, 221-224.

Meinschein W. G. and Kenny G. S. (1957) Analyses of a chromatographic fraction of organic extracts of soils. Anal. Chem. 29, 1153-1161.

Tissot B., Celifet-Debyer V, Derro G and Oudin J. L. (1971) Origin and evolution of hydrocarbons in Early Torcian Shales, Paris Basin, France. Bull. Am. Assoc. Petrol. Geologists 55, 2177-2193.

Tissot B. and Espitalie J. (1975) L'Evolution thermique de la matiére organique des sediments: applications d'une simulation matematique. Inst. Francais Petrole Rev. 30, 743-777.

Vassoevich N. B. (1974) More exact definition of oil age conception. Akad. Nauk SSSR Doklady 219, 1465-1467.

Young A., Monaghan P.H. and Schweisberger R.T. (1977) Calculation of ages of hydrocarbons in oils - Physical Chemistry applied to petroleum geochemistry I. Bull. Am. Assoc. Petrol. Geologists 61, 573-600.

TABLE 1. Total Volume of Gas, Water, and Oil Products Produced at Different Retort Temperatures

Retort Temperatures (°C)	Gas (cu. ft. ton)	Water (gal./ton)	Oil (gal./ton)
50	243	.239	--
100	333	1.91	--
150	378	3.53	--
200	422	3.59	--
250	445	4.3	--
300*	445	4.7	--
500	1,717	5.97	10

*Because a leak developed in the retort the value obtained for the gas volume at 300° C is low.

TABLE 2. Liquid-solid silica gel chromatographic analysis of the benzene-methanol extracts of New Albany Shale samples

Retort Temperature	Amounts in mg. of Extracts obtained from 100g of shale	Carbon Tetrachloride (CCl_4) fraction		Benzene (C_6H_6) fraction		Methanol (CH_3OH) fraction	
(°C)	(mg)	(mg)	(%)	(mg)	(%)	(mg)	(%)
R.T.	500.0	136.0	27.0	42.0	8.0	73.0	15.0
50	502.0	137.5	27.0	43.0	9.0	75.0	15.0
100	497.0	127.5	26.0	48.0	10.0	81.0	16.0
150	500.0	100.0	25.0	61.0	15.0	82.0	20.0
200	500.0	80.0	16.0	95.0	19.0	110.0	22.0
250	661.0	60.0	9.8	130.0	20.0	150.0	23.0
300	847.0	50.0	6.0	180.0	21.0	200.0	24.0

Figure 1

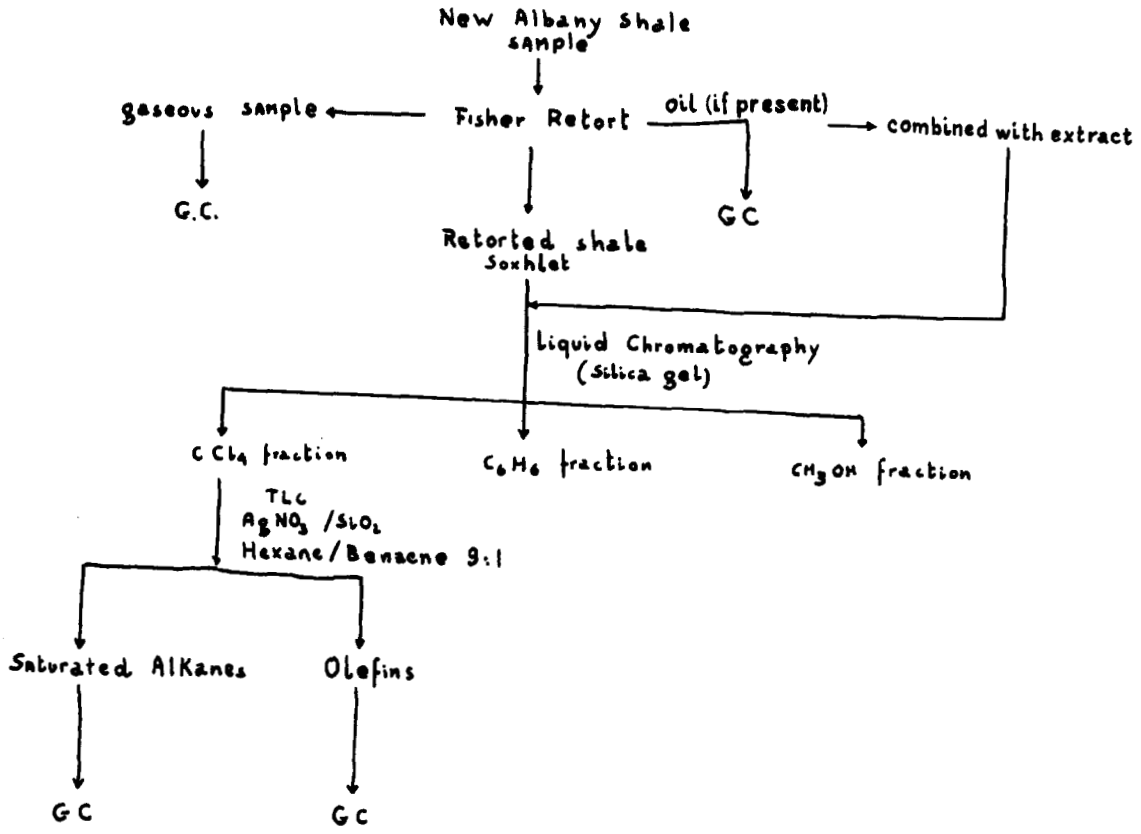

Fig. 1. Flow sheet of the extraction and separation of the New Albany shale pyrolysis products.

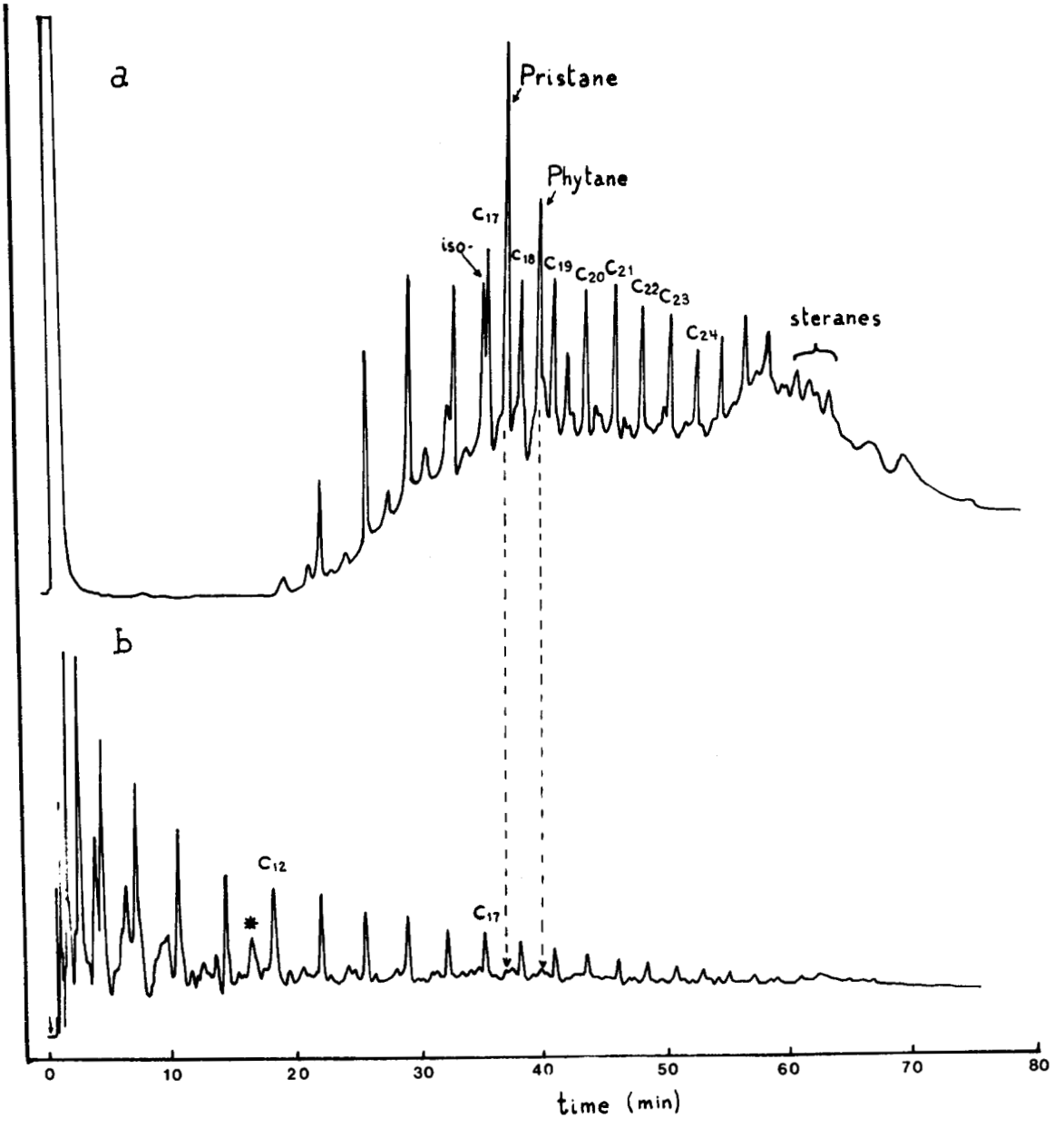

Figure 2

Fig. 2. Gas chromatograms of the New Albany Shale (a) CCl_4 fraction at room temperature and (b) of the oil phase obtained from the same shale after retorting at 500°C.

Figure 3

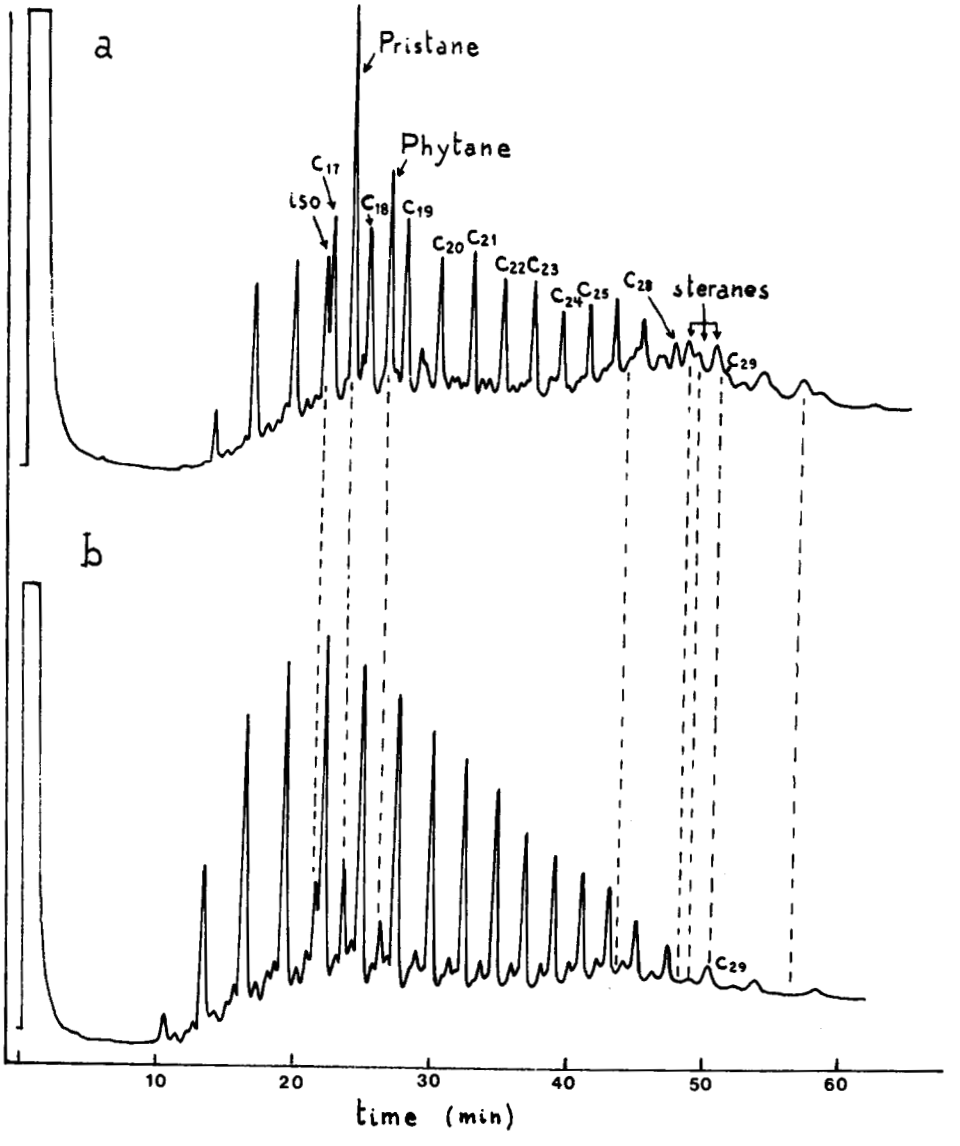

Fig. 3. Gas chromatograms of the CCl_4 fractions of the (a) room temperature extract of the New Albany Shale and (b) oil phase from a sample of the same shale which had been heated to 500°C.

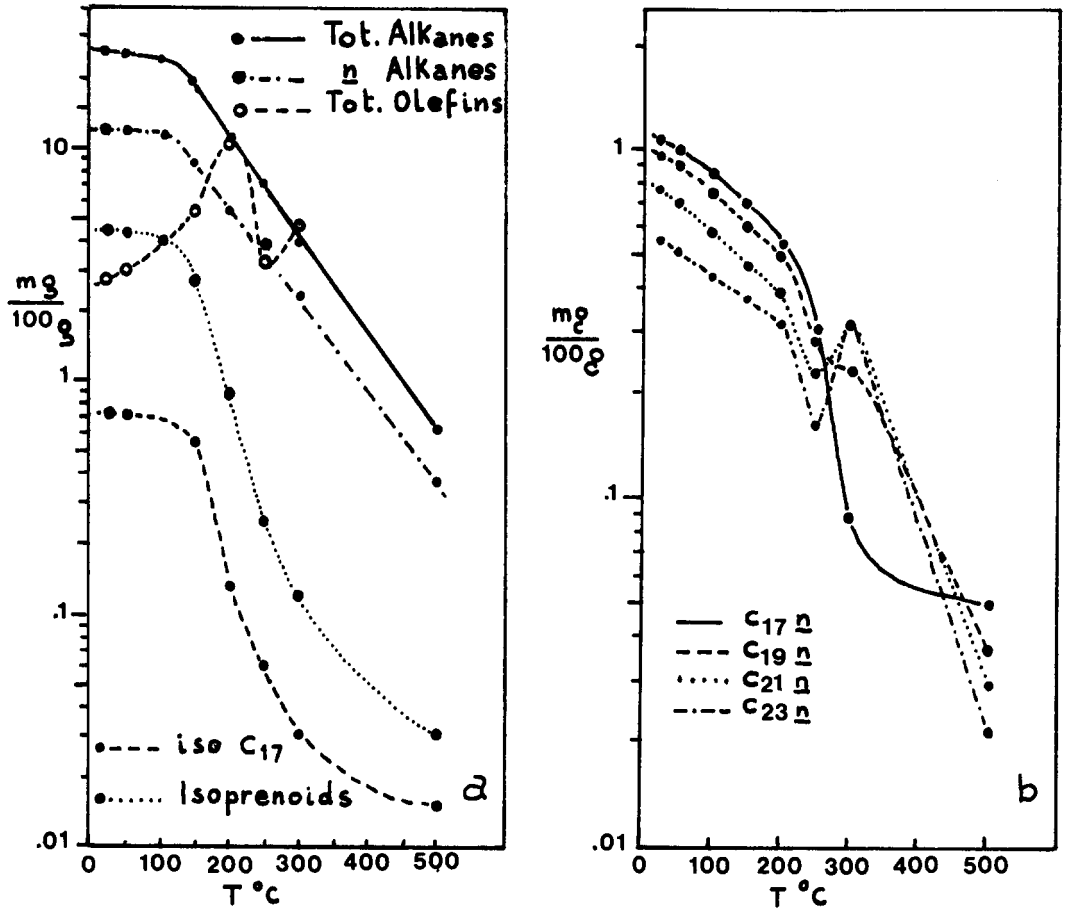

Figure 4

Fig. 4. Plots of the concentrations (a) of alkenes (olefins) and classes of alkanes (b) of individual n-alkanes vs. pyrolysis temperatures for samples of the New Albany Shale.

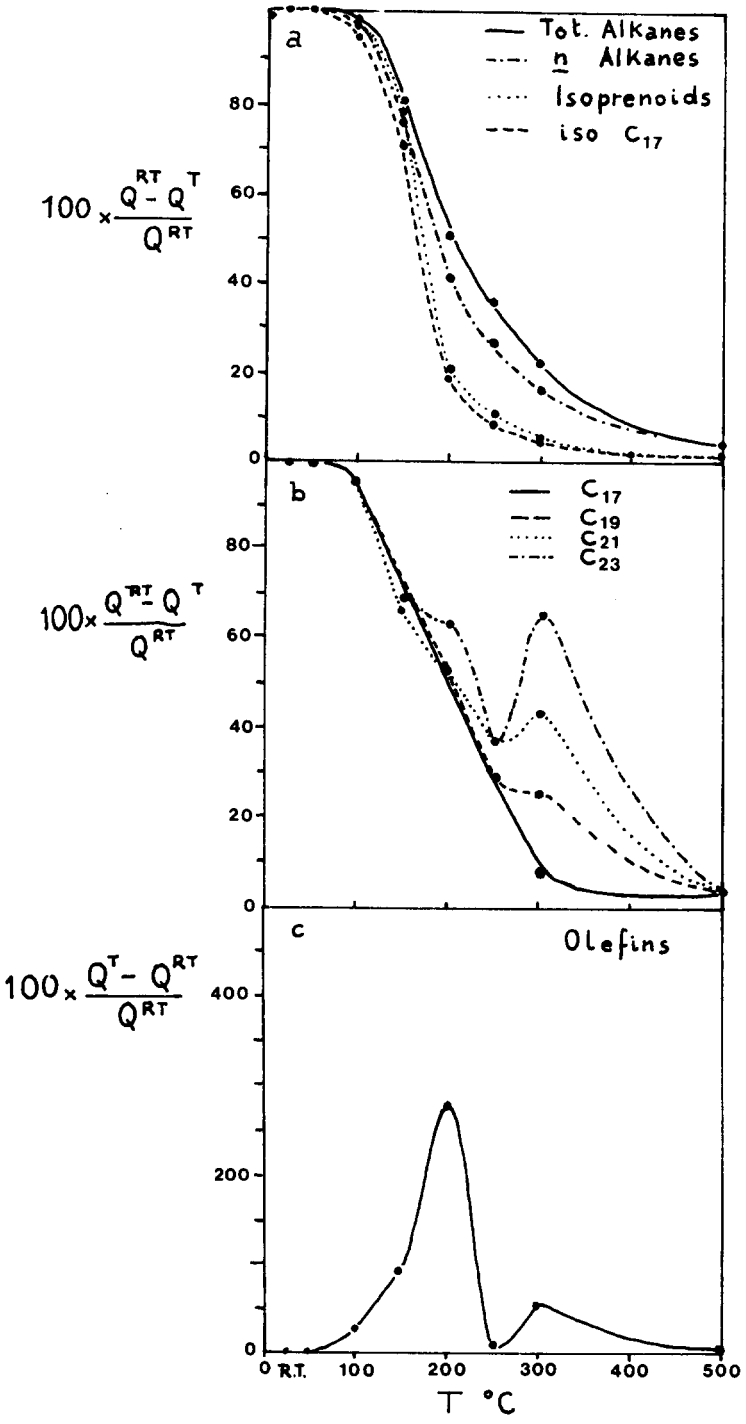

Figure 5

Fig. 5. Normalizeddecay rate curves, expressed as percent of the initial concentration vs. pyrolysis temperature for (a) classes of alkanes and (b) C_{17}, C_{19}, C_{21}, and C_{23} n-alkanes. Plot (c) is the production rate of olefins expressed as 100 x the difference in concentrations at the specified temperature (Q^T) and at room temperature Q^{RT}.

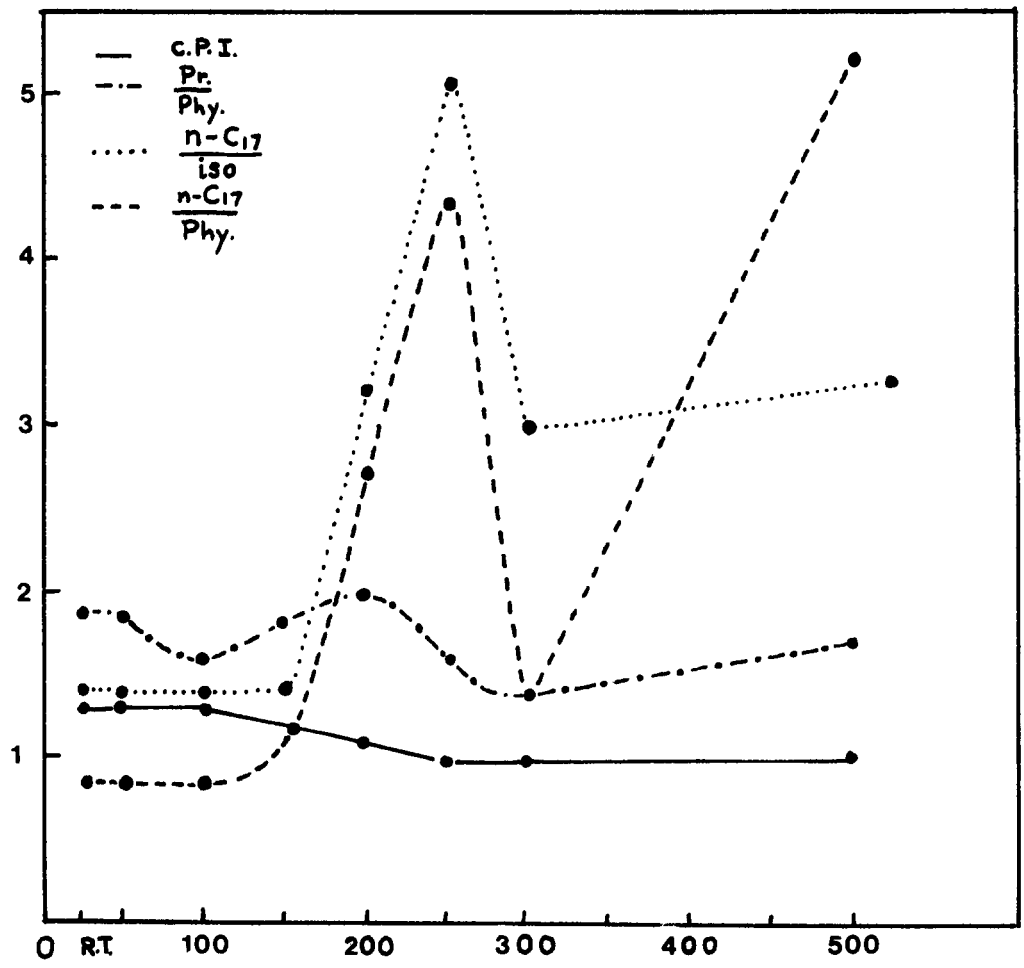

Figure 6

Fig. 6. Plots of the ratios of the concentrations odd-carbon number/seven-carbon number C_{15} to C_{20} n-alkanes (C.P.I.), $\frac{Pr}{Phy}$, $\frac{n\text{-}C_{17}}{iso}$ and $\frac{n\text{-}C_{17}}{Phy}$ vs. pyrolysis temperature for samples of the New Albany Shale.

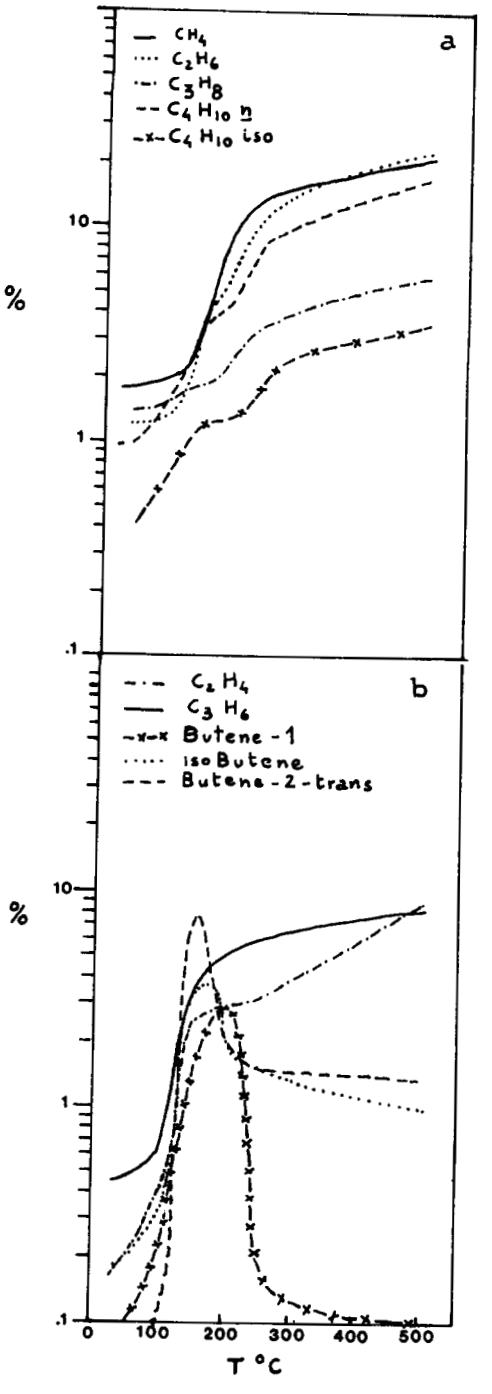

Figure 7

Fig. 7. Plots of the relative concentrations in percent vs. pyrolysis temperature for (a) C_1 to C_4 alkanes and (b) C_2 to C_4 alkenes obtained from the pyrolysis of the New Albany Shale.

AN INTERACTIVE DATA MANAGEMENT AND ANALYSIS SYSTEM FOR THE EASTERN GAS SHALE PROGRAM

Pyrtle W. Seabaugh and Ronald E. Zielinski

Monsanto Research Corporation*
Mound Facility
Miamisburg, Ohio 45342

ABSTRACT

A versatile, easy-to-use data base system is described. The system provides flexibility in display formats as well as input and output options such as format compatibility adaptive to field data. Both on- and off-line capability exists. Versatility is attained through logical, boolean, and arithmetic expressions. Consequently, computational capability is available so that data input can be minimized. Browsing and recursive searches are available through a search criteria command that allows the user to modify and narrow the request without restart. The system provides plotting options; data can be plotted in a well profile format. Through GEOLOG, a soft-wired synergistic log system, well log data can be integrated with geochemical and geophysical experimental data. This integration will provide a more accurate assessment of the resource potential of the well.

Utilization of these features provides not only a fully interactive data management system but also an enhanced statistical capability for data analysis.

*Mound Facility is operated for the U. S. Department of Energy by Monsanto Research Corporation (Contract No. EY-76-C-04-0053).

Current awareness of shortages in traditional energy sources for oil and natural gas has placed great emphasis on the characterization and development of new sources for these fuels. The Devonian Shales have produced gas for over 150 years, and similarly the brown shales have produced commercially along the western edge of the Appalachian Basin for approximately one hundred years.[1] The estimated amount of gas reserves contained in the shales of the Appalachian Basin vary between 460 quadrillion cubic feet[2] and 285 trillion cubic feet.[3] Using conservative figures based on the Appalachian Basin, at least a 10-year supply of natural gas is available from the Devonian Shales.

The U. S. Energy Research and Development Administration formally initiated the Eastern Gas Shale Program in 1976, and it is being directed by the Morgantown Energy Research Center. Currently, the program includes the systematic accumulation of a data bank for accurately assessing and characterizing the resource and providing for an economical and efficient production of the gas. Mound Laboratory is assisting in the determination of the resource inventory and is cooperating in studies designed to determine the geological, geophysical, and geochemical properties of the shale.

To collate the voluminous data that will be generated by this program, and to effectively use and efficiently distribute the data, an interactive data management and analysis system is required. This report describes some attributes of such a system.

In conjunction with MERC, a prototype data management system (DMS) which includes the capabilities of data storage, retrieval, and processing was established for demonstration purposes. This interactive system contains some of Mound's Eastern Gas Shale data in a technical data base and is currently available for on-line demonstrations. Both on-line and in the batch mode, the system provides browsing and recursive search capabilities needed to scan large volumes of data and to conveniently present data for analysis and interpretability. In part, these features are provided through logical, boolean, and arithmetic expressions which allow the user to modify, rephrase, or narrow his search criterion without restart, so that a redirected search need not include a retrace of previous paths. There is no practical restrictions on the size of the data base. The system allows users to manipulate their data with the basic system and then to interface user selected portions of the data with specialized routines linked with DMS to perform special calculations or manipulations. The system is easy to use because the entire two-way "conversation" between the user and the DMS is in English. (Mastery of a complex protocol language is not needed.) For the infrequent user, the system offers a practical convenience through an on-call instructional tutorial which is stylized to the user's preferences and background.

Often, at the inception of a major program, detailed specifications on format requirements and input media may not exist. Using the flexibility of the data system, input routines can be easily generated to convert data collected prior to completed specifications into selected DMS input formats. Although the system can interact with an array of input formats, all are processed through a common utility program. The system can be used to generate a variety of reporting formats, each tailored to specific report needs for various contractors or users. Consequently, the user is not required to adhere to a rigid format. In a similar manner, accommodations can be made for unplanned or unforeseen requirements with minimal economic impact. By use of the computational features of the system, many important sums, differences, and ratios can be provided for interpretative purposes. For example, the prototype system calculates total C_1-C_4, total C_2-C_4, % gas wetness (C_1-C_4/C_2-C_4), and the iC_4/nC_4 ratios. Furthermore, these computations also minimize data entry effort, both in a time and dollar sense. Other ratios and percents provided by the prototype are:

- 2-methylpentane/3-methylpentane
- isopentane/n-pentane
- cyclohexane/methylcyclopentane
- methylcyclopentane/methylcyclohexane
- % paraffin-naphthene (PN)
- % aromatic (A)
- % hydrocarbon
- PN/A

The latter four items are associated with the C_{15}+ Bitumen Extract. Collectively, the first four items provide insight into the maturity of the hydrocarbons.

Many of the data elements in the prototype Eastern Gas Shale data base require arithmetic manipulations. By use of arithmetic operators (greater than, less than, equal to, etc.), the DMS allows searching over ranges of data magnitudes. This arithmetic manipulation facilitates the interface of DMS with specialized output subroutines in higher level languages such as FORTRAN. Use of the FORTRAN Encode/Decode features is supported through use of the necessary FORTRAN compiler.

The statistical and modelling implications of the Eastern Gas Shale Program suggest the use of statistical packages such as SAS[4] and BMD. These can be provided through the host language (e.g., FORTRAN) extension facility. Other mathematical packages that provide simple optimization, data filters, cluster analysis, trend analysis, and plotting capabilities can be provided without severe economic impact. Examples of the plotting capability are shown in Figures 1 and 2, and some cluster results are shown in Figure 3. All the mathematical resources can be shared with all the various contractors involved in the program, at least to the degree that they may choose. These statistical and mathematical software packages can be used to tie the characterization data with logging data.

As an example, an extension to the interpretative capabilities of the data base is a system called GEOLOG. GEOLOG is a synergistic log system that will accurately integrate the log data on file from the A to D conversion and the geochemical data for that same well. This system ties together the well log and experimental data to provide a more accurate representation of the well.

These inputs will serve to produce an accurate synergistic log system that can be used in future applications with well log data.

The system equally supports project management and text files.

For project management files, a variety of searches are available. Some key examples are:

- Contractor
- Contractor's Address
- Principal Investigator
- Associate Investigator
- Technique/Technology Used
- Technical Objectives
- Approach
- Status
- Budget Code
- Project Title
- Start Date
- Funding Agency
- Procurement Method
- Completed Milestones
- Contractor Performance

Through the arithmetic features, annualized budgets can be divided into a monthly allocation; spending rates can be computed, projected and monitored for under or overrun; monthly expenditure values can be inserted; weekly, monthly, or yearly updates can be made; year-to-date information can be provided; milestones can be monitored; and variance flags can be set. Other provisions also are available for assessment of contractor performances in an objective manner.

The DMS provides security keys at multiple levels. Through these keys, both selective input, retrieval, and display can be imposed on the system. Files can be reserved solely for the project manager, so that no one else can breach them. Technical data files can be protected likewise, with the security level going down to the field level (e.g., single word). Transaction activities for all stations can be monitored and identified as to origin.

A highly useful feature for a text or report file is the capability to search on a word without knowing the complete spelling. The user can specify the first three or four letters or characters and then fill out the word with a default character such as an asterisk. A predetermined dictionary is not necessary, because each word entered into the text file becomes part of the dictionary. Another convenience provided by the system is a display function that allows the key word to be read in context with words highlighted on both sides of the key word. As a result key-word searches are more rapidly and accurately executed.

Remote data entry through cassettes, and/or cartridges, and remote terminals also is provided by the system. The data on a cassette or cartridge can be transmitted over a telephone line or mailed to an entry station. Entry also can be made via magnetic typewriter cards. This mode would be particularly useful for a report or text file.

In summary, a prototype data base system has been designed, tested, and implemented. The system provides the flexibility to meet changing and future needs that inevitably evolve with new programs. The system has already accommodated a request for format change that came after an initial format was fixed. It provides enhanced statistical capability for interpretation of characterization data through logical, boolean, and arithmetic searches that can be complemented by extensions to higher programming languages such as FORTRAN. These capabilities can be readily extended to text and project management files, including budgeting functions. Security keys are provided down to the word level. This interactive system contains some of Mound's Eastern Gas Shale data in a technical data base and is currently available for on-line demonstrations.

REFERENCES

1. Provo, Linda J., "Upper Devonian Black Shale -- Worldwide Distribution and What It Means," Published in the "Proceedings of the Seventh Annual Appalachian Petroleum Geology Symposium," Morgantown, West Virginia, March 1-4, 1976.

2. Shumaker, R. C., "Introduction," Published in the "Proceedings of the Seventh Annual Appalachian Petroleum Geology Symposium," Morgantown, West Virginia, March 1-4, 1976.

3. Symposium on Devonian Shale Development, Columbus, Ohio, May 21-22, 1973.

4. Barr, A.J., Goodnight, J. H., Sall, J.P., and Helwig, J.T., "A User's Guide to SAS," Sparks Press, Raleigh, North Carolina.

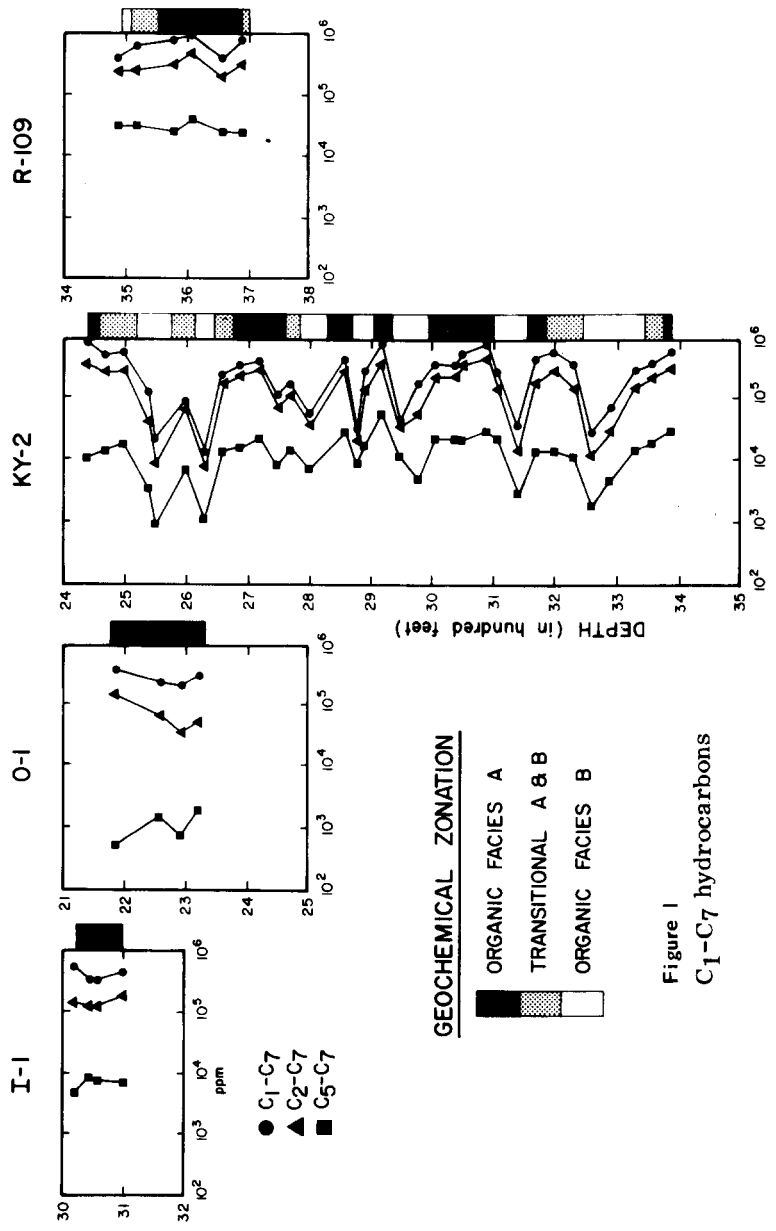

Figure 1
C_1-C_7 hydrocarbons

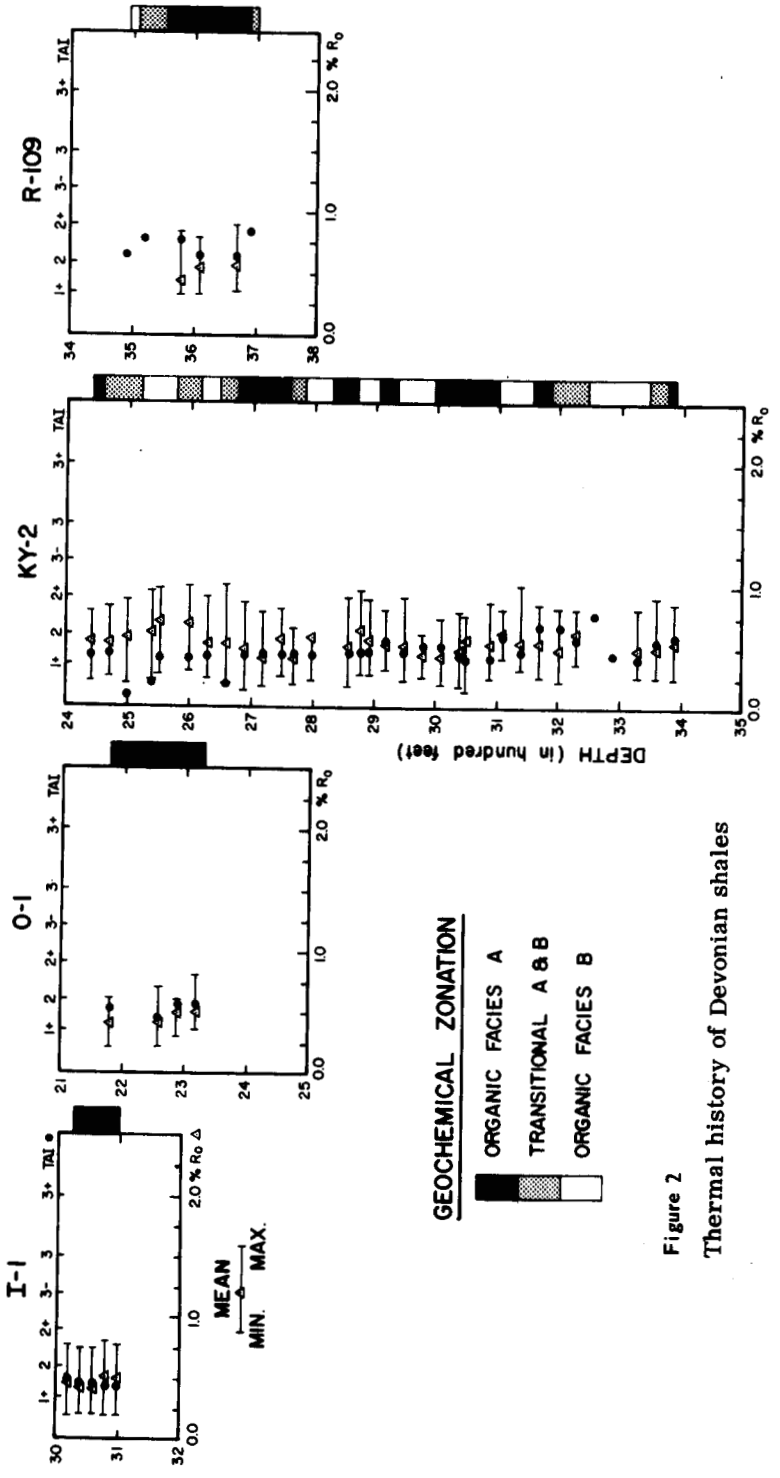

Figure 2
Thermal history of Devonian shales

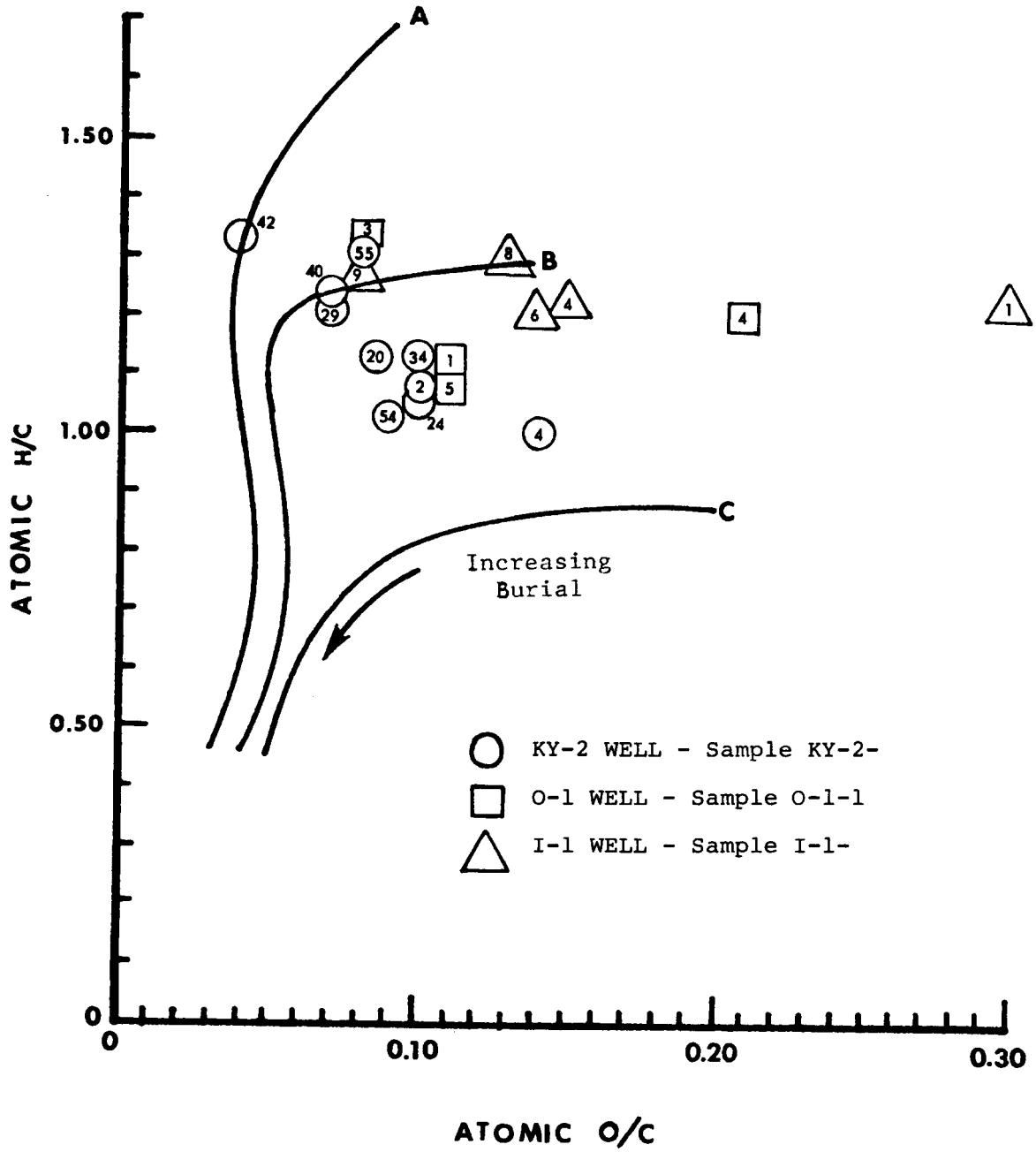

Figure 3
Kerogen composition

SUBMITTED BIOGRAPHICAL SKETCHES

STEPHEN P. CREMEAN, COLUMBIA GAS SYSTEM SERVICE CORPORATION

Mr. Creamean was born in Lima, Ohio and grew up in Columbus, Ohio. He attended the Ohio State University and graduated in 1968 with a Bachelor of Mechanical Engineering degree. After work one year with North American Rockwell, he joined the Research Department of the Columbia Gas System Service Corporation, where he is currently a Research Engineer. For the past five years with Columbia, he has been involved in several natural gas exploration and well stimulation research projects, and has authored several internal publications in these areas.

JOHN M. DENNISON, UNIVERSITY OF NORTH CAROLINA

Mr. Dennison was born in Keyser, West Virginia. Received his B.S. and M.S. degrees from West Virginia University and Ph.D. from University of Wisconsin. Taught at University of Illinois 1960-65, at University of Tennessee 1965-67, and at University of North Carolina since 1967. Broad research interests throughout the Appalachian basin have been dominated by work on the Catskill delta complex. Was American Association of Petroleum Geologists Distinguished Lecturer in 1974, on the subject of Appalachian basin hydrocarbons related to Paleozoic eustatic sealevel changes.

FRANK R. ETTENSOHN, UNIVERSITY OF KENTUCKY

Mr. Ettensohn was born in Cincinnati, Ohio. In 1969 he earned a B.S. degree in geology from the University of Cincinnati, and in 1970 received a M.S. degree in geology at the University of Cincinnati. During 1970-71 he served as an officer in the Army Corps of Engineers and as a high school math teacher at Greenhills, Ohio. In 1975 he received the Ph.D. degree from the University of Illinois at Urbana-Champaign, where he studied stratigraphy and paleoenvironments in the Newman Limestone of east-central Kentucky. Dr. Ettensohn is currently employed as an assistant professor of geology at the University of Kentucky where he is studying the stratigraphy, paleoenvironments, and paleontology of the Devonian-Mississippian black shales in eastern Kentucky under ERDA sponsorship. His principal fields of interest include paleontology, paleoenvironments, stratigraphy and sedimentation. He is a member of the Geological Society of America, the Paleontological Society, The Paleontological Association, Paleontological Research Institution, Ohio Academy of Science, Kentucky Geological Society, Sigma Xi and Sigma Gamma Epsilon.

LINDA P. FULTON, EXXON COMPANY

Dr. Fulton was born in Lyons, New York and earned her B.S. degree from Hope College, Holland, Michigan in 1971, and her M.S. degree in geology at the University of Illinois at Urbana-Champaign in 1973. In 1977, she received the Ph.D. degree from the University of Cincinnati where she studied Devonian and Mississippian shales of the central Appalachian Basin. Dr. Fulton is presently employed with Exxon Company, U.S.A. in New Orleans, Louisiana. Her principal fields of interest are sedimentation, stratigraphy, and micropalentology, and her professional affiliations include membership in The Geological Society of America, Society of Economic Paleontologists and Mineralogists, and The New Orleans Geological Society.

ANITA G. EPSTEIN HARRIS, U.S. GEOLOGICAL SURVEY

Dr. Epstein received her B.S. at Brooklyn College; M.S. Indiana University; Ph.D. Ohio State University. Paleontologic and stratigraphic studies in Paleozoic rocks in eastern Pennsylvania, New Jersey, and New York, 1960-1969. Geologic map editor, USGS, 1966-1974. Geologist-paleontologist, Paleontology and Stratigraphy Branch, USGS, specializing in conodont biostratigraphy of chiefly lower and middle Paleozoic rocks of the United States. Developed technique for assessing organic maturation using conodont color changes.

SUBMITTED BIOGRAPHICAL SKETCHES

RICHARD HARVEY, ILLINOIS STATE GEOLOGICAL SURVEY

Dr. Harvey studied geology at Indiana University at Bloomington, Indiana, where he specialized in mineralogy and petrography and received a Ph.D. degree in 1960. He has been with the Illinois State Geological Survey since 1960. He had conducted research on carbonate rocks in the Industrial Minerals Section, with emphasis on the use of carbonates in SO_2 sorption from flue gases. He transferred to the Coal Section in 1976 where he now directs research on the petrography of Illinois Coals. He is in charge of the petrographic studies of the New Albany Shales at the Illinois Survey.

ROY C. KEPFERLE, U.S. GEOLOGICAL SURVEY

Dr. Kepferle was born in Greeley, Colorado, December 28, 1926. He received his B.A., at the University of Colorado, 1950; M.S., at South Dakota School of Mines & Technology, 1954; Ph.D. at the University of Cincinnati, 1972. He is presently working for the U.S. Geological Survey from 1950 to present; strippable lignite and uraniferous lignite, Williston Basin; uraniferous shale, trace elements, South Dakota and Nebraska; Far East geology; areal geology in Kentucky; stratigraphy and sedimentology of Lower Mississippian and Devonian rocks, Illinois and Appalachian basins. Instructor, South Dakota School of Mines, 1953-1954 Elizabethtown Community College (University of Kentucky), 1964-1967; University, 1968-1970. Society membership: A.A.P.G., S.E.P.M., G.S.A., A.A.A.S., Geological Society of Kentucky. Home address: 915 Egan Hills Drive Cincinnati, Ohio 45229

ROBERT G. PIOTROWSKI, PENNSYLVANIA GEOLOGICAL SURVEY

Mr. Piotrowski received his B.S. degree in Geology at the University of Dayton in 1970. After two years service in the U.S. Army, he attended Duke University and received his M.S. degree in Geology in 1974. He immediately joined Amoco Production Company and worked in the New Orleans Division as an exploration geologist in the Smackover and Hosston trends of Mississippi and Alabama. In 1975, he joined the Pennsylvania Geological Survey and is a staff geologist in the Oil and Gas Geology Division in Pittsburgh. Mr. Piotrowski is a member of the Pittsburgh Geological Society and the American Association of Petroleum Geologists.

PAUL SCHETTLER, JUNIATA COLLEGE

Dr. Schettler is full professor and chairman of the Chemistry Department at Juniata College. He obtained his Ph.D. in Physical Chemistry at Yale University after receiving his Bachelor of Science degree in Chemistry at the University of Utah. His Ph.D. thesis is entitled "Liquid-Liquid Phase Separation in Metal Ammonia Solutions." Two postdoctoral fellowships subsequently extended his research interests outside of thermodynamics. At the University of Utah he concentrated on theoretical aspects of flow and diffusion as applied to chromatography. During a second postdoctoral at Yale, he concentrated on electrical properties of metal ammonia solutions. He has concentrated on physical chemical problems associated with natural gas in shale since 1974.

JAMES W. SCHMOKER, U.S. GEOLOGICAL SURVEY

Dr. Schmoker is a geophysicist in the Branch of Oil and Gas Resources of the U.S. Geological Survey. He holds B.S. and M.S. degrees in physics from the University of Minnesota and a Ph.D. degree in geophysics from Virginia Polytechnic Institute. He worked for Atlantic Richfield for nearly six years in various exploration-research assignments prior to joining the Survey, where he is presently working with the borehole gravity project.

SUBMITTED BIOGRAPHICAL SKETCHES

JOSEPH F. SCHWIETERING, WEST VIRGINIA GEOLOGICAL AND ECONOMIC SURVEY

Dr. Schwietering received B.Sc. (1956) and Ph.D. (1970) degrees from Ohio State University. Worked as an Exploration Geologist for Pure Oil Company in Mt. Pleasant, Michigan and Casper, Wyoming; as a Field Geologist for Harding Associates in California and the Ohio Department of Highways in Ohio; and as teacher at Hanover College, Hanover, Indiana and Cleveland State University, Cleveland, Ohio. Now employed by the West Virginia Geological and Economic Survey doing stratigraphic studies of Devonian rocks in West Virginia.

EDWARD R. TEGLAND, GEOPHYSICAL SERVICE

Mr. Tegland was born August 14, 1937 in Pierre, South Dakota. Attended the South Dakota School of Mines and Technology from 1955 through 1959. Received B.S. in Geological Engineering. Attended the University of Missouri at Rolla (formerly Missouri Mines) from 1959 through 1961 receiving M.S. in Petroleum Engineering. Employed for a brief period by the USGS prior to military service. Military service included a tour of duty as an officer in the Corps of Engineers in France and Germany. Employed by Geophysical Service in August 1963, as a Geophysical Engineer, and has held various positions involving data collection and processing of Gulf Coast seismic data. Currently residing in Dallas and assigned as Area Geophysicist in GSI's Eastern Division. Member of SEG, EAEG, and Society of Petroleum Engineers of AIME.

DANIEL A. TEXTORIS, UNIVERSITY OF NORTH CAROLINA

Dr. Textoris was born in Cleveland, Ohio. Received the B.A. degree from Western Reserve University, the M.S. degree from Ohio State University, and the Ph.D. degree from the University of Illinois. Served on the faculty at the University of Illinois for two years, and moved to the University of North Carolina in 1965. He is currently Professor of Geology and Associate Dean for Research Administration. His specialities in the field of geology are sedimentary petrology, with specific interests in carbonates and volcanic tuffs. One of his specialities as Associate Dean is coordination of research on energy at the University.

JOSEPHUS (JOE)THOMAS, JR., ILLINOIS STATE GEOLOGICAL SURVEY

Dr. Thomas, received his Ph.D. in analytical chemistry (emphasis on X-ray and electron diffraction) from the University of Illinois in 1957. After working 5 years at the Du Pont Experimental Station in Wilmington, Delaware, he returned to the Illinois campus in 1962, assuming duties as head of the Physical Chemistry Section of the Illinois State Geological Survey. His primary research interests have dealt with structure-property relationships in materials that, on the gross-structure scale, also involve porosity and internal surface area.

EDWARD N. WILSON, KENTUCKY GEOLOGICAL SURVEY

Mr. Wilson received his A.B. (Geology) Washington University, St. Louis, Missouri. Military experience: Major (ARTY) USAR (Ret) in 1943-1945, Algeria, Tunisia, Corsica, Italy. He then attended the Washington University, St. Louis, Missouri and received his M.S. In 1946-1948 he taught General Geology, University of Tennessee, Knoxville. In 1948-1957 he joined the O&G Division of Great Lakes Carbon Corporation, Evansville, Indiana as a District Geologist. In 1957-1959, Priviate Office in Evansville, Indiana. In 1959-to present outside state of Kentucky. Independent Consultant in O&G, Coal, Water Resources, Natural Gas Storage. 1959-1962 Coal & Pennsylvania Geologist, Henderson Field Office, 1963-1964 O&G Geologist, Editor, 1964-1976 Head, Oil and Gas Section: O&G, Underground Waste Disposal, 1977-present, Principal Investigator, Characterization and Data Processing of Black Shale (Ky. Research Group). A.B. degree, Washington University.

APPENDIX A-1

SUBMITTED BIOGRAPHICAL SKETCHES

JAFFERY S. ZAFAR, UNIVERSITY OF KENTUCKY

Mr. Zafar, is presently working fulltime as Petroleum Geologist at University of Kentucky on the Eastern Gas Shale Project of ERDA, from February 1977 to present. July 1970 to February 1977, geologist with Geological Sample Log Company. September 1968 to April 1970, Research Fellow at the University of Pittsburgh in Petroleum Engineering. January 1967 to September 1968, Geophysical Service Inc., work with Amerada in Canada. In 1964 received B.S. degree in Geology from University of Karachi and M.S. and D.I.C. degrees in 1967 from Imperial College of Science and Technology, London.

ATTENDEES--FIRST EASTERN GAS SHALES SYMPOSIUM

Sunder H. Advani
Professor of Mechanical
Engineering and Mechanics
525 E.S.
West Virginia University
Morgantown, WV 26506
Phone: 304/293-4031

Roberto Aguilera
Reservoir Engineer
SOQUIP
3340, de la Perade, Ste-foy
Quebec G1X217 CANADA
Phone: 418/651-9543

Javiad Alam
Staff Scientist
Science Applications Inc. (SAI)
Suite 8, Chestnut Ridge Professional Bldg.
Morgantown, WV 26505
Phone: 304/599-9696

Steven H. Alkire
Petroleum Engineer
National Petroleum Corporation
6161 Busch Blvd., P.O. Box 29228
Columbus, OH 43229
Phone: 614/888-4641

Arthur T. Anderson
Staff Scientist
NASA
Greenbelt Road
Greenbelt, MD 20771
Phone: 301/982-5240

Gordon D. Anderson
Lawrence Livermore Laboratory
P.O. Box 808
Livermore, CA 94550
Phone: 415/447-1100 x4446

Randall L. Anselment
Assistant District Manager
District 1320
Christensen Diamond Products, USA
P.O. Box 41136
Indianapolis, IN 46241
Phone: 317/243-9379

James Aronson
Associate Professor, Earth Sciences
Case Western Reserve University
Cleveland, OH 44106
Phone: 216/368-3763

David M. Ashbrook
District Geologist
Mitchell Energy Corporation
6230 Busch Blvd., Suite 226
Columbus, OH 43229
Phone: 614/888-7882

Roland C. Baer, Jr.
Vice President-Administration
Flex-O-Lite Div., General Steel Ind., Inc.
P.O. Box 4366
St. Louis, MO 63123
Phone: 314/351-4450

W. D. Bagnall
Columbia Gas Transmission Corp.
1700 MacCorkle Avenue, S.E.
Charleston, WV 25325
Phone: 304/346-0951

Philip O. Banks
Associate Professor
Case Western Reserve University
Cleveland, OH 44106
Phone: 216/368-3679 or 3690

John Bassett
Geologist
Indiana Geological Survey
611 N. Walnut Grove
Bloomington, IN 47401
Phone: 812/337-5412

Lamont S. Beers
District Geologist
National Fuel Gas Supply Corporation
10 Lafayette Square
Buffalo, NY 14203
Phone: 716/855-6982

Mary C. Behling
Data Processing
West Virginia Geological Survey
P.O. Box 879
Morgantown, WV 26505
Phone: 304/292-6331

O. R. Bergmann
Potomac River Development Laboratory
P.O. Box 761
Martinsburg, WV 25401
Phone: 304/267-2941

David Berstein
Science Applications Inc.
8201 Capwell
Oakland, CA 94621
Phone: 415/562-9163

APPENDIX A-2

Attendees (Cont.)

Phyllis A. Bialobok
Secretary
West Virginia Geological Survey
Devonian Shale Project
P.O. Box 879
Morgantown, WV 26505
Phone: 304/292-6331

Stephanie J. Bialobok
Chemist
MERC
Box 880 Collins Ferry Rd.
Morgantown, WV 26505
Phone: 304/599-7275

Gary S. Biesiadeck
Research Associate Geological Data
West Virginia Geological Survey
P.O. Box 879
Morgantown, WV 26505
Phone: 304/292-6331

William H. Blackburn
University of Kentucky/Black Shale Project
University of Kentucky
Lexington, KY 40506
Phone: 606/258-2702

Richard G. Blank
General Manager
Stratigraphic Services Company
1305 N.E. 43rd, Suite 406
Seattle, WA 98105
Phone: 206/634-1343

William F. Blank
General Manager
Stratigraphic Services Company
1305 N.E. 43rd, Suite 406
Seattle, WA 98105
Phone: 206/634-1343

Tom Blanton
Senior Engineer
Halliburton Services
Drawer 1431
Duncan, OK 73533
Phone: 405/251-3172

Thomas C. Boberg
Senior Engineering Assoc.
EXXON
P.O. Box 2189
Houston, TX 77002
Phone: 713/965-4396

L. C. Bonham
Senior Research Associate
Chevron Oil Field Research Company
P.O. Box 446
LaHabra, CA 90631
Phone: 213/691-2241

Ellis R. Boyd
Chief--Planning & Special Project
Branch
Federal Energy Regulatory Commission
825 N. Capitol Street
Washington, DC 20426
Phone: 202/566-9464

Michael C. Brannock
Senior Geologist
Quaker State Oil Refining Corporation
P.O. Box 1327
Parkersburg, WV 26101
Phone: 614/423-9543

Larry P. Brown
Technical Manager
Cities Service
Box 50408
Tulsa, OK 74150
Phone: 918/586-4246

William M. Brown
Director, Technological Studies
Hudson Institute, Inc.
Quaker Ridge Road
Croton-on-Hudson, NY 10520
Phone: 914/762-0700 x35

George Brunton
Union Carbide Nuclear Division
Box 4
Oak Ridge, TN 27820
Phone: 615/483-8611

Curtis W. Burgess, Jr.
Geological Manager-Enhanced Recovery
Cities Service Company
P.O. Box 300, 7th & Boulder
Cities Service Building
Tulsa, OK 74102
Phone: 918/586-3531

Charles W. Byrer
Geologist
MERC
P.O. Box 880
Morgantown, WV 26505
Phone: 304/599-7547

Joseph E. Campbell
Senior Production Engineer
Columbia Gas
P.O. Box 2946
Huntington, WV 25728
Phone: 304/529-4173

Attendees (Cont.)

Richard W. Carlton
Geologist
Ohio Geological Survey
Fountain Square, Bldg. 'B'
Columbus, OH 43224
Phone: 614/466-5344

William J. Carter
Project Manager
Los Alamos Scientific Laboratory
Group M-6, MS 970
Los Alamos, NM 87545
Phone: 505/667-6881

Sandra C. Chalton
Petroleum Economist
Lewin and Associates
470 L'Enfant Plz. SW.
Washington, DC 20024
Phone: 202/488-4300

Robert Chase
West Virginia University
College of Mineral Economic Resources
Morgantown, WV 26505
Phone: 304/293-5695

Martin E. Chenevert
President
Chenevert & Associates Inc.
2727 Kirby
Houston, TX 77098
Phone: 713/522-2122

George R. Clarkson
Geologist
West Virginia Geological Survey
P.O. Box 879
Morgantown, WV 26505
Phone: 304/292-6331

Robert C. Claus
Exploration Manager
Texas International Petroleum Corp.
1020 - One Valley Square
Charleston, WV 25301
Phone: 304/343-4609

George E. Claypool
Research Chemist
U.S. Geological Survey
Branch of Oil and Gas Resources
MS 977, Box 25046, Federal Center
Denver, CO 80225
Phone: 303/234-3561

John A. Clendening
Amoco Production Company
Box 3092
Houston, TX 77001
Phone: 713/652-4379

Robert Cluff
Illinois State Geological Survey
Urbana, IL 61801
Phone: 217/344-1481

Stan Coates
Geologist
Carl E. Smith Inc.
Sandyville, WV 25275
Phone: 304/273-9313

C. E. Coffey
Director
Potomac River Development Laboratory
P.O. Box 761
Martinsburg, WV 25401
Phone: 304/267-2941

Lou Cook
Columbia Gas System Service Corp.
1600 Dublin Road
Columbus, OH 43215
Phone: 614/486-3681

Ken Covell
Logging Engineer
International Petroleum Service Co.
P.O. Box 547
Sheffield, PA 16347
Phone: 814/968-3295

J. G. Craig
Chief, Computer/Math Branch
MERC
P.O. Box 880 Collins Ferry Rd.
Morgantown, WV 26505
Phone: 304/599-7178

Steve Cremean
Columbia Gas System Service Corp.
1600 Dublin Road
Columbus, OH 43215
Phone: 614/486-3681

Chapman Cronquist
Manager, Houston Operations
Gulf Universities Research Consortium
5909 W. Loop So. #600
Houston, TX 77401
Phone: 713/668-0992

APPENDIX A-2

Attendees (Cont.)

John B. Curtis
Geologist
Science Applications, Inc.
Chestnut Ridge Professional Bldg. Suite 8
Morgantown, WV 26505
Phone: 304/599-9696

C. S. Dean
Geologist
MERC
P.O. Box 880 Collins Ferry Road
Morgantown, WV 26505
Phone: 304/599-7211

William H. Dennen
Principal Investigator
University of Kentucky/Black Shale Proj.
Lexington, KY 40506
Phone: 606/258-2702

John M. Dennison
Professor
University of North Carolina
Mitchell Hall, UNC
Chapel Hill, NC 27514
Phone: 919/933-1211

Wallace de Witt, Jr.
Geologist
United States Geological Survey
MS 955, National Center Building
Reston, VA 22092
Phone: 703/860-6635

Jane de Wys
Devonian Shale Project
West Virginia University
313 White Hall
Morgantown, WV 26506
Phone: 304/293-3477

Mark G. Doherty
Project Engineer
Booz-Allen & Hamilton
4330 East West Highway
Bethesda, MD 20014
Phone: 301/951-2586

Jessie G. Donahue
Senior Research Geologist
Gulf Research and Development Co.
P.O. Drawer 2038
Pittsburgh, PA 15230
Phone: 412/362-1600 x2124

Jack Douglas
Division Manager
Schlumberger
1050 Kingsmill Parkway
Columbus, OH 43229
Phone: 614/888-3632

J. E. Downey
Computer Programmer
MERC
P.O. Box 880 Collins Ferry Road
Morgantown, WV 26505
Phone: 304/599-7523

Susan L. Duffield
Research Assoc. Geologist Data
West Virginia Geological Survey
P.O. Box 879
Morgantown, WV 26505
Phone: 304/292-6331

Paul B. DuMontelle
Illinois State Geological Survey
Urbana, IL 61801
Phone: 217/344-1481

Ted Dyman
Geologist
U.S. Geological Survey
P.O. Box 25046
Denver, CO 80225
Phone: 303/234-3435

David Earle
Geologist
Appalachian Exploration &
Development, Inc.
P.O. Box 628
Charleston, WV 25322
Phone: 304/344-8355

Brian Easterday
Geologist
West Virginia Geological Survey
P.O. Box 879
Morgantown, WV 26505
Phone: 304/292-6331

Art Ehlenberger
Vice President
Talley Frac
3500 N. Greenfield Road
Mesa, AZ 85201
Phone: 602/832-3830

Attendees (Cont.)

J. L. Elbel
Development Specialist
Dowell - Div. Dow Chemical Co.
P.O. Box 21
Tulsa, OK 74102
Phone: 918/582-0101 x505

Bruce E. Engquist
Coord. Geol. Exploration
Northern Illinois Gas Company
P.O. Box 190
Aurora, IL 60507
Phone: 312/355-8000 x687

Robert B. Erwin
WVGS/State Geologist
P.O. Box 879
Morgantown, WV 26505
Phone: 304/292-6331

Frank R. Ettensohn
University of Kentucky/ Black Shale Project
University of Kentucky
Lexington, KY 40506
Phone: 606/258-2702

Wayne Fallgatter
Research Chemist
Cities Service Energy Resources Group
P.O. Box 50408
Tulsa, OK 74150
Phone: 918/586-2526

Fred Ferris
Manager, Public Relations
Columbia Gas Transmission Corporation
P.O. Box 1273
Charleston, WV 25325
Phone: 304/346-0951 x2252

Robert F. Flagg
Senior Physicist
Physics International
2700 Merced Street
San Leandro, CA 94577
Phone: 415/357-4610

Gene Foglietta
Div. Exploration Manager
Tenneco Oil Co.
3000 United Founders Blvd.
Ciudad Bldg. Suite 139
Oklahoma City, OK 73112
Phone: 405/848-8551 x114

John M. Foster
Manager, Special Projects
Columbia Gas Transmission Corp.
P.O. Box 1273
Charleston, WV 25325
Phone: 304/346-0951

Harry E. Fritz
Geoscience Manager
Gulf Oil Company
P.O. Box 2619
Casper, WY 82601
Phone: 307/235-1311

K-H Frohne
Petroleum Engineer
MERC
P.O. Box 880
Morgantown, WV 26505
Phone: 304/599-7412

James Funk
Manager, 3-D Support
Geophysical Service, Inc.
P.O. Box 5621 MS 966
Dallas, TX 75222
Phone: 214/238-3057

Hota V. S. Gangarao
Associate Professor Civil Engineer
West Virginia University
507 E.S.
Morgantown, WV 26506
Phone: 304/293-3780

Stephen W. Gerrard
Geologist
West Virginia Geological Survey
P.O. Box 879
Morgantown, WV 26505
Phone: 304/292-6331

D. W. Gillmore
Section Leader
MERC
P.O. Box 880
Morgantown, WV 26505
Phone: 304/599-7526

James H. Griffith
Staff Geologist
Mobil Oil Corporation
Box 5444
Denver, CO 80217
Phone: 303/572-2464

APPENDIX A-2

Attendees (Cont.)

Jim Groves
Area Manager
Aircowell
P.O. Box 68
Cortland, OH 44410
Phone: 216/637-2085

Hugh D. Guthrie
Director, Oil, Gas & Shale Technology
DOE
20 Massachusetts Avenue, N.W.
Washington, DC 20545
Phone: 202/376-4693

James E. Gwinn
Production Engineer
Consolidated Gas Supply Corp.
445 West Main Street
Clarksburg, WV 26301
Phone: 304/623-3611 x239

Keith O. Halloran
Geologist
West Virginia Geological Survey
P.O. Box 879
Morgantown, WV 26505
Phone: 304/292-6331

Merle E. Hanson
Program Leader
Lawrence Livermore Laboratory
P.O. Box 808
Livermore, CA 94550
Phone: 415/447-1100 x3376

Bob Hardman
Regional Sales Engineer
Dowell
110 Westwood
Bridgeport, WV 26330
Phone: 304/842-2000

Anita G. Harris
Geologist
U.S. Geological Survey
6007 Windham Road
Laurel, MD 20810
Phone: 202/343-3495

Leonard D. Harris
Geologist
U.S. Geological Survey
6007 Windham Road
Laurel, MD 20810
Phone: 202/343-3495

James H. Hartsock
Senior Engineer
Gruy Federal, Inc.
Southwest Tower
Houston, TX 77002
Phone: 713/652-5753

Richard Harvey
Illinois State Geological Survey
403 W. Indiana
Urbana, Il 61801
Phone: 217/344-1481

Nancy Hassenmueller
Geologist
Indiana Geological Survey
611 North Walnut Grove
Bloomington, IN 47401
Phone: 812/337-5412

Ken C. Hays
Dome Petroleum Ltd.
P.O. Box 200
Calgary, Canada T2P 2H8
Phone: 403/232-5100

E. T. Heck
Executive Vice President
Minard Run Oil Company
P.O. Box 18
Bradford, PA 16701
Phone: 814/362-3531

William Henderson
Petroleum Geologist
Michigan Public Service Commission
6545 Merchantile Way
Box 30221
Lansing, MI 48909
Phone: 517/373-8636

W. M. Hennington, Manager
Exploration Eastern Division
Mitchell Energy Corporation
3900 One Shell Plaza
Houston, TX 77002
Phone: 713/224-4522

David Hight
Texas International Petroleum Corp.
1020 - One Valley Square
Charleston, WV 25301
Phone: 304/343-4609

Jon Hilton
District Manager
Schlumberger
1658 Smith Drive
Wooster, OH 44691
Phone: 216/264-6518

Attendees (Cont.)

Henry H. Hinch
Research Scientist
Amoco Production Co.
P.O. Box 591
Tulsa, OK 74102
Phone: 918/664-3540

W. A. (Bill) Hockings
Research Fellow
Institute of Mineral Research
Michigan Technological University
Houghton, MI 49931
Phone: 906/487-2600

Steven S. Holsclaw
Geologist
Pennzoil Company
P.O. Box 1588
Parkersburg, WV 26101
Phone: 304/422-6565

John W. Hosterman
Geologist
U.S. Geological Survey
Reston, VA 22092
Phone: 703/860-6913

Yvon Houde
Geologist - Special Proj.
Weaver Oil & Gas Corporation
5251 Westhimer
Houston, TX 77057
Phone: 713/626-1550

Pierre Houle
Production Engineer
SOQUIP
3340, de la Perade, Ste-Foy
Quebec G1X 217 - CANADA
Phone: 418/651-9543

Dr. James F. Howard
President
Howard and Associates, Inc.
2247 Twenty Grand Avenue
Owensboro, KY 42301
Phone: 502/926-3775

John P. Humphrey
Research Manager
Dow Chemical Company
734 Building
Midland, MI 48640
Phone: 517/636-2296

Arlen E. Hunt
Assistant Project Manager
Eastern Gas Shales Project
Morgantown Energy Research Center
P.O. Box 880
Collins Ferry Road
Morgantown, WV 26505
Phone: 304/599-7265

Thomas E. Huzzy
Commissioner
Oil and Gas Conservation Commission
1613 Washington Street, East
Charleston, WV 25311
Phone: 304/348-3092

John Janka
Manager, Process Analysis
Institute of Gas Technology
3424 S. State Street
Chicago, IL 60615
Phone: 312/567-3721

Dr. W. Gibson Jaworek
Consultant
7500 Old Chester Road
Bethesda, MD 20034
Phone: 301/320-5579

Ernest E. Jenkins
Chief Geologist
Kentucky West Virginia Gas Co.
Box 431
Prestonsburg, KY 41653
Phone: 606/886-2311

Arfon H. Jones
Vice President
Terra Tek, Inc.
420 Wakara Way
Salt Lake City, UT 84108
Phone: 801/582-2220

Victor T. Jones
Senior Research Geochemist
Gulf Science & Tech.
P.O. Drawer 2038
Pittsburgh, PA 15230
Phone: 412/362-1600

Rustu S. Kalyoncu
Principal Research Scientist
Battelle Columbus Labs
505 King Avenue
Columbus, OH 43201
Phone: 614/424-5821

APPENDIX A-2

Attendees (Cont.)

David Kamakaris
New York State Geological Survey
P.O. Box 1218
Alfred, NY 14802
Phone: 607/871-2407

Kris Kamath
Section Leader
Morgantown Energy Research Center
P.O. Box 880
Morgantown, WV 26505
Phone: 304/599-7555

William W. Kelly, Jr.
State Oil and Gas Inspector
Virginia Division of Mines
Drawer V
Big Stone Gap, VA 24219
Phone: 703/523-0335

Roy Kepferle
USGS
Old Technical Building
University of Cincinnati
Cincinnati, OH 45221
Phone: 513/475-3541

Norman F. Knapp
Chemist
Ohio G. S.
Fountain Square Bldg. 'B'
Columbus, OH 43224
Phone: 614/466-5344

Laura J. Knoff
Laboratory Technician
WVGS
P.O. Box 879
Morgantown, WV 26505
Phone: 304/292-6331

C. A. Komar
Asst. Project Manager, EGSP
MERC
Morgantown, WV 26505
Phone: 304/599-7107

Harev G. Kozik
Mngr. Special Engineering Studies
Mitchell Energy Corp.
3900 One Shell Plaza
Houston, TX 77002
Phone: 713/224-4522

Kit Krickenberger
The MITRE Corporation
1820 Dolley Madison Boulevard
Mail Stop W251
McLean, VA 22101
Phone: 703/790-6234

Patrick Kujawa
Program Manager
SAI
1651 Old Meadow Rd., Suite 620
McLean, VA 22101
Phone: 703/821-4890

Byron Kulander
Assoc. Prof. of Geology
Alfred University
Dept. of Geology, Box 851
Alfred, NY 14802
Phone: 607/871-2203

Steven C. Lamey
Research Chemist
MERC
Box 880 Collins Ferry Rd.
Morgantown, WV 26505
Phone: 304/599-7275

Richard N. Lane
President
Gruy Federal Incorporated
1911 Jefferson Davis Highway
Arlington, VA 22202
Phone: 703/979-2955

Bruce Langhus
Geologist
Gulf Energy and Minerals Co. - US
324 N. Robinson
Oklahoma City, OK 73102
Phone: 405/236-3071

Paul Lechler
Analyst
Indiana Geological Survey
611 N. Walnut Grove
Bloomington, IN 47401
Phone: 812/337-2504

R. K. Leininger
Geochemist
Indiana Geological Survey
611 N. Walnut Grove
Bloomington, IN 47401
Phone: 812/337-2504

APPENDIX A-2

Attendees (Cont.)

Joel S. Leventhal
Research Chemist
U.S. Geological Survey
Uranium and Thorium Branch
Denver, CO 80225
Phone: 303/234-3285

Reeves Lewenthal
Managing Partner
Reel Energy Program
2100 South Ocean Lane
Ft. Lauderdale, FL 33316
Phone: 305/522-6139 or 563-5066

Forrest W. Lewis
Director, Gas Storage
Texas Gas
3800 Frederish
Owensboro, KY 42301
Phone: 502/683-2431

Jerry Lineback
Illinois State Geological Survey
Urbana, IL 61801
Phone: 217/344-1481

F. A. Loving
Potomac River Development Laboratory
P.O. Box 761
Martinsburg, WV 25401
Phone: 304/267-2941

Chuck Lowe, Geologist
Quaker State Oil Refining Corp.
P.O. Box 1327
Parkersburg, WV 26101
Phone: 614/423-9543

Roger G. Ludwig
Geologist
Carnegie Natural Gas Company
3904 Main Street
Munhall, PA 15120
Phone: 412/462-7121

Gordon J. F. MacDonald
Chairman, Commission on Natural Resources
National Academy of Science
Mitre Corporation
1820 Dolly Madison Blvd.
McLean, VA 22101
Phone: 703/790-6000

Frank L. Majchszak
Geologist
Ohio Geological Survey
Fountian Square Building 'B'
Columbus, OH 43224
Phone: 614/466-5344

Philip L. Martin
Chief Geologist-Deep Fms.
Consolidated Gas Supply Corp.
445 W. Main Street
Clarksburg, WV 26301
Phone: 304/623-3611

J. C. Massey
Sales Engineer
Aircowell
3392 So. Union Avenue
Alliance, OH 44601
Phone: 216/821-0289

R. D. Matthews
District Geologist
Minerals Department
The Dow Chemical Company
1707 Building
Midland, MI 48640
Phone: 517/636-1187

F. F. McClish
Oil and Gas Energy Specialist
Ohio ERDA
30 E. Broad Street
Columbus, OH 43229
Phone: 614/466-8277

William T. McCormick, Jr.
Vice President
American Gas Association
1515 Wilson Boulevard
Arlington, VA 22209
Phone: 202/524-2000

William G. McGlade
Project Manager, EGSP
Science Applications, Inc.
Suite 8, Chestnut Ridge Professional Bldg.
Morgantown, WV 26505
Phone: 304/599-9696

Stuart McHugh
Geophysicist
SRI International
333 Ravenswood Avenue
Menlo Park, CA 94025
Phone: 415/326-6200 x4614

APPENDIX A-2

Attendees (Cont.)

Michael W. McKay
Senior Scientist
Science Applications Inc.
P.O. Box 2351
La Jolla, CA 92038
Phone: 714/459-0211 x438

George R. McManus
Production Engineer
Consolidated Gas Supply Corp.
445 W. Main Street
Clarksburg, WV 26301
Phone: 304/623-3611

Jim C. Mercer
Morgantown Energy Research Center
P.O. Box 880
Collins Ferry Road
Morgantown, WV 26505
Phone: 304/599-7523

Phil M. Miles
Geological Engineer
Self employed consultant
229 Barrow Road
Lexington, KY 40502
Phone: 606/266-1379

Robert C. Milici
Chief Geologist
Tennessee Department of Conservation
Division of Geology
G-5 State Office Building
Nashville, TN 37219
Phone: 615/588-6575

A. J. Miller
Senior Research Chemist
Mobil Oil R & D
3600 Duncanville Road
Dallas, TX 75211
Phone: 214/331-6531

Norman Mines
The Mitre Corporation
1820 Dolley Madison Blvd.
McLean, VA 22101
Phone: 703/790-6000

Paul D. Moffitt
Research Engineer
Phillips Petroleum Company
264 R.B.1 PRC
Bartlesville, OK 74004
Phone: 918/661-3310

Pedro A. Montano
Assistant Professor
West Virginia University
Department of Physics
Morgantown, WV 26506
Phone: 304/293-3422

E. T. Moore, Jr.
Vice President
Physics International Company
2700 Merced Street
San Leandro, CA 94577
Phone: 415/357-4610

David C. Morrill
Petroleum Exploration Specialist
Donohue, Anstey & Morrill
8 Arlington Street
Boston, MA 02116
Phone: 617/267-7600

Donald R. Morris-Jones
Research Analyst
Wisconsin State Planning and Energy Office
P.O. Box 511
Madison, WN 53701
Phone: 608/266-7707

William F. Morse
Director of Research
Columbia Gas System Service Corporation
1600 Dublin Road
Columbus, OH 43215
Phone: 614/486-3681

Don E. Napp
Staff Geologist
Tenneco Oil Company
3000 United Founders Bldg., Cuidad Bldg.
Suite 139
Oklahoma City, OK 73112
Phone: 405/848-8511 x222

Donald W. Neal
Research Association - Stratigraphy
West Virginia Geological Survey
P.O. Box 879
Morgantown, WV 26505
Phone: 304/292-6331

W. S. (Bill) Northern
Senior Sales Engineer
Schlumberger
2-0-3 Schroath Building
227 Washington Avenue
Clarksburg, WV 26301
Phone: 304/624-4635

Attendees (Cont.)

David A. Northrop
Division Supervisor
Sandia Laboratories - Division 5732
Albuquerque, NM 87115
Phone: 505/264-2302

Jerry L. Norton
Regional Engineer
Dowell
1021 Quarrier
Charleston, WV 25302
Phone: 304/343-7504

E. B. Nuckols
Devonian Shale Project
West Virginia University
313 White Hall
Morgantown, WV 26506
Phone: 304/293-3477

Edward B. Nuhfer
Petrologist
West Virginia Geological Survey
P.O. Box 879
Morgantown, WV 26505
Phone: 304/292-6331

William O'Brien
Geologist
Morgantown Energy Research Center
P.O. Box 880
Morgantown, WV 26505
Phone: 304/599-7249

William O'Conner
Vice President of Marketing
Talley Frac
3500 N. Greenfield Road
Mesa, AZ 85201
Phone: 602/832-3830

Robert S. Ottinger
Manager, Energy Resources Office
TRW Inc.
7600 Colshire Drive
McLean, VA 22101
Phone: 703/893-2000 x2421

W. K. Overbey, Jr.
Project Manager, EGSP
Morgantown Energy Research Center
P.O. Box 880
Morgantown, WV 26505
Phone: 304/599-7109

Fritz M. Overs
Director, School Plant Planning
Shaker Heights City Schools
Shaker Heights, OH 44120
Phone: 216/921-1400 x318

G. L. Owens
Research Engineer
Columbia Gas System Service Corporation
1600 Dublin Road
Columbus, OH 43215
Phone: 614/486-3681

Pat N. Parker
Product Development
The Western Company
P.O. Box 186
Fort Worth, TX 76101
Phone: 817/731-5419

J. Pasini, III
Senior Staff Specialist
Morgantown Energy Research Center
P.O. Box 880
Morgantown, WV 26505
Phone: 304/599-7103

Douglas G. Patchen
Oil and Gas Section
West Virginia Geological Survey
P.O. Box 879
Morgantown, WV 26505
Phone: 304/292-6331

Robert J. Pauken
Senior Research Geologist
Mobil Research and Development Corp.
P.O. Box 900
Dallas, TX 75221
Phone: 214/331-6531 x352

William J. Perry, Jr.
Geologist
U.S. Geological Survey
Mailstop 955 - National Center
Reston, VA 22092
Phone: FTS 928-6637

John C. Peterson
NYS Geological Survey
P.O. Box 1218
Alfred, NY 14802
Phone: 607/871-2407

APPENDIX A-2

Attendees (Cont.)

C. I. Pierce
Physicist
Morgantown Energy Research Center
U.S. Department of Energy
P.O. Box 880
Morgantown, WV 26505
Phone: 304/599-7752

Ken Pinkston
Sales Representative
McJunkin Corporation
1400 Hansford Street
Charleston, WV 25322
Phone: 304/348-5211

Robert Piotrowski
Staff Geologist
Pennsylvania Geological Survey
1201 Kossman Building
Pittsburgh, PA 15222
Phone: 412/565-5030

Harvey Price
Intercomp
1201 Dairy Ashford, Suite 200
Houston, TX 77079
Phone: 713/497-8400

Mike Price
Senior Geologist
Appalachian Exploration and
Development, Inc.
P.O. Box 628
Charleston, WV 25322
Phone: 304/344-8355

Wayne Proell
Manager
Cloud Hill Scientific Developments
Route 3
Seymour, IN 47274
Phone: 812/522-2570

Constance Putnam
Editor
Science Applications, Inc.
Suite 8, Chestnut Ridge Professional Building
Morgantown, WV 26505
Phone: 304/599-9696

E. O. Ray
Vice President
Kentucky West Virginia Gas Company
Box 431
Prestonsburg, KY 41653
Phone: 606/886-2311

Mark L. Reinhold
Research Assistant
Illinois State Geological
Survey
Natural Resources Building
Urbana, IL 61801
Phone: 217/344-1481 x201

John Reynolds
Staff Geologist
International Petroleum
Service Co.
P.O. Box 547
Sheffield, PA 16347
Phone: 814/968-3295

Stewart Rhoades
Geologist
WVGS
P.O. Box 879
Morgantown, WV 26505
Phone: 304/292-6331

Dudley D. Rice
Geologist
U.S. Geological Survey
Box 25046, MS 951, Federal Center
Denver, CO 80225
Phone: 303/234-4167

Herman Rieke
Technical Staff
TRW
Suite 12
Chestnut Ridge Prof. Bldg.
Morgantown, WV 26505
Phone: 304/599-8622

Debra Riester
Geologist
Don Richner & Associates, Inc.
Box 768
Painesville, OH 44077
Phone: 216/352-4090

Wayland Roberts
Amoco Production Company
Box 3092
Houston, TX 77001
Phone: 713/652-4379

J. L. Robertson
Chief Geologist
International Petroleum Service Co.
P.O. Box 547
Sheffield, PA 16347
Phone: 814/968-3295

Attendees (Cont.)

John B. Roen
Geologist
U.S. Geological Survey
Reston, VA 22092
Phone: 703/860-6635

Roberto Rosales
Supervisor
G. S. I.
2509 Glencliff
Plano, TX 75074

Roger L. Rowland
Regional Geologist
Gulf Energy & Minerals Co. U.S.
324 N. Robinson
Oklahoma City, OK 73102
Phone: 405/236-3071

Albert P. Ruotsala
Professor
Michigan Technological University
Geology, Geological Engineer
Houghton, MI 49931
Phone: 906/487-2535 or 2531

Phillip Russell
Research Scientist
Modges Hall
Department of Physics-WVU
Morgantown, WV 26506
Phone: 304/293-5769

F. Daniel Ryan
President, Vescorp Inc.
6660 N. High Street
Worthington, OH 43085
Phone: 614/436-5522

William M. Ryan
Geologist
Spartan Gas Co.
P.O. Box 766
Charleston, WV 25323
Phone: 304/925-0317

Erich Sarapuu
President
Electrofrac Corp.
308 W-99 Terrace
Kansas City, MO 64114
Phone: 816/942-5965

Walter K. Sawyer
Section Leader
Morgantown Energy Research Center
U.S. Department of Energy
P.O. Box 880
Morgantown, WV 26505
Phone: 304/599-7221

M. F. Scharff
Vice President
JAYCOR
P.O. Box 370
Del Mar, CA 92014
Phone: 714/453-6580

Barry F. Sheetz
Research Associate
Penn State University
223 Materials Research Lab
University Park, PA 16802
Phone: 814/865-3539

Paul D. Schettler
Professor of Chemistry
Juniata College
Huntingdon, PA 16652
Phone: 814/643-6288

C. F. Schlemmer, Jr.
Deputy Director of Research and
Development
Ohio Department of Energy
30 East Broad Street
Columbus, OH 43229
Phone: 614/466-8277

Dr. Hans-Hermann Schmitz
Mineralogist
Federal Insititute Geosciences and
Natural Resources
3000 Hanover 51
Germany

James W. Schmoker
Geophysicist
U.S. Geological Survey
MS 964, Denver Federal Center
Denver, CO 80225
Phone: 303/234-5601

Garry L. Schott
Los Alamos Scientific Lab
120 Monte Vista
Los Alamos, NM 87544
Phone: 505/672-1023

APPENDIX A-2

Attendees (Cont.)

Grover J. Schrayer
Senior Research Chemist
Gulf Research and Development Co.
P.O. Box 2038
Pittsburgh, PA 15230
Phone: 412/828-5000 x2355

Leo A. Schrider
Assistant Director
Morgantown Energy Research
P.O. Box 880
Morgantown, WV 26505
Phone: 304/599-7492

Carl L. Schuster
Division Supervisor
Sandia Laboratories
P.O. Box 5800, Div. 5733
Albuquerque, NM 87115
Phone: 505/264-9142

Louis Schwasnick
Sales Engineer
Schlumberger
1650 Smith Drive
Wooster, OH 44691
Phone: 216/345-5143

Joseph F. Schwietering
Stratigrapher
West Virginia Geological Survey
P.O. Box 879
Morgantown, WV 26505
Phone: 304/292-6331

P. W. Seabaugh
Senior Analytical Specialist
Monsanto Research Corporation
Mound Laboratory
Miamisburg, OH 45342
Phone: 512/866-7444 x7471

Mohindar Seehra
Professor of Physics
West Virginia University
Hodges Hall - WVU
Morgantown, WV 26506
Phone: 304/293-5769

Zane Shuck
Assoc. Dir., Engineering Exp. Sta.
125 ES
West Virginia University
Morgantown, WV 26506
Phone: 304/293-4821

Robert C. Shumaker
Principal Investigator
Devonian Shale Project, WVU
313 White Hall
Morgantown, WV 26506
Phone: 304/293-3477

A. Richard Sinclair
President
Fracturing Technology, Div. of
Maurer Engineering Inc.
10301 NW Freeway #202
Houston, TX 77018
Phone: 713/683-8227

Madan M. Singh
President
Engineers International, Inc.
2514 Wisconsin Avenue
Downers Grove, IL 60515
Phone: 312/968-6883

Charles R. Skillern
Senior Staff Engineer
TRW Inc.
7600 Colshire Drive
McLean, VA 22101
Phone: 703/893-2000 x2421

Marianna Slocum
Senior Engr. Specialist
Dept. of Energy
20 Massachusetts Avenue
Washington, DC 20545
Phone: 202/376-4840

M. L. Slusser
Engineering Associate
Mobil Research & Development Co.
P.O. Box 900
Dallas, TX 75221
Phone: 214/331-6531

Eric Smith
Columbia Gas System Service Corp.
1600 Dublin Road
Columbus, OH 43215
Phone: 614/486-3681

Harold B. Smith
Geologist
Louden Properties Company
2521 Evergreen Drive
Indiana, PA 15701
Phone: 412/349-2586

Attendees (Cont.)

Jeffrey B. Smith
Staff Geologist
U.S. DOE
20 Massachusetts Avenue
Washington, DC 20545
Phone: 202/376-4690

John Ward Smith
Division Manager - Resource Characterists
LERC-DOE
P.O. Box 3395
University Station
Larmie, WY 82071
Phone: 307/742-4236

Paul L. Smith
Engineer
Halliburton Services
Drawer 1431
Duncan, OK 73533
Phone: 405/251-3172

R. D. Smith
Geologist
MERC
P.O. Box 880 Collins Ferry Road
Morgantown, WV 26505
Phone: 304/599-7439

Walter L. Smith
Senior Geologist
Petroleum Information Corp.
1375 South Delaware
Denver, CO 80201
Phone: 303/825-2181

Jim Smitherman
Geologist
Weaver Oil and Gas Corporation
5251 Westheimer Road, Suite 800
Houston, TX 77056
Phone: 713/626-1550

Richard A. Smosna
Petrologist
West Virginia Geological Survey
P.O. Box 879
Morgantown, WV 26505
Phone: 304/292-6331

M. Jack Snyder
Manager, Materials Development
Battelle Columbus Labs
505 King Avenue
Columbus, OH 43201
Phone: 614/424-5821

Warren S. Spaulding
Senior Staff Research Specialist
AMOCO Production Company
P.O. Box 591
Tulsa, OK 74102
Phone: 918/664-3012

Wesley F. Spence
Technical Specialist
DuPont Company
Explosive Products Division
Wilmington, DE 19898
Phone: 302/744-5326

Art M. Spencer
Chief Chemist
Petroleum Technology Corporation
P.O. Box 537
Redmond, WA 98052
Phone: 206/885-5200 x475

Thomas E. Springer
Physicist
LASL - MS 580
P.O. Box 1663
Los Alamos, NM 87544
Phone: 705/667-6832

J. G. Stanley
Contract Specialist
The Dow Chemical Company
Building 566
Midland, MI 48640
Phone: 517/636-1348

Anthony T. Statler
Chief Geologist
Tennessee Dept. of Conservation
Division of Geology
G-5 State Office Building
Nashville, TN 37219
Phone: 615/741-2726

Frank M. Stead
U.S. Geological Survey
MS 954
Denver, CO 80225
Phone: 303/234-2261

Ronald T. Stearns
Project Engineer (Scientific)
U.S. Department of Energy
2753 S. Highland Drive
Las Vegas, NE 89114
Phone: 702/734-3251

APPENDIX A-2

Attendees (Cont.)

Dale Stein
District Manager
Christensen Diamond Inc.
510 W. Monroe
Jackson, MI 49202
Phone: 517/783-6425

Dave Stevenson
Assoc. Geologist
ISGS
Urbana, IL 61801
Phone: 217/344-1481

Roy Strait
Supervisor - Petroleum Engr. Section
Michigan Public Service Commission
6545 Merchantile Way, Box 30221
Lansing, MI 48909
Phone: 517/373-9636

James G. Strother
Division Petroleum Engineer
Tenneco Oil Company
3000 United Founders Blvd
Ciudad Building - Suite 139
Oklahoma City, OK 73112
Phone: 405/848-8551 x161

Richard A. Struble
Assistant Chief
Ohio Geological Survey
Building 'B', Fountain Square
Columbus, OH 43224
Phone: 614/466-5344

Jojok Sumartoio
Geology Department, Vanderbilt University
Nashville, TN 37235
Phone: 615/322-2420

Peter E. Susev
Manager, Energy Resources
Anchor - Hocking
109 Broad Street
Lancaster, OH 43130
Phone: 614/687-2441

Bruce E. Taylor
Sales Representative
Core Laboratories
1951 Commercial Drive
Mt. Pleasant, MI 48858
Phone: 517/773-9904

E. P. Tegland
Senior Area Geophysicist
Geophysical Service, Inc.
P.O. Box 5621, MS 966
Dallas, TX 75222
Phone: 214/238-3057

Daniel A. Textoris
Professor
University of North Carolina
Mitchell Hall
Chapel Hill, NC 27514
Phone: 919/933-1211

Josephus Thomas
Illinois State Geological Survey
Urbana, IL 61801
Phone: 217/344-1481

Charles M. Threlkeld
U.S. Geological Survey
Branch of Oil & Gas Resources
MS 977, Box 25046, Federal Center
Denver, CO 80225
Phone: 303/234-3561

Howard W. Thune
Research Geologist
Gulf Science Technology Co.
P.O. Drawer 2038
Pittsburgh, PA 15230
Phone: 412/362-1600 x319

Raymond Trempe
Regional Geologist
SOQUIP
3340, de la Perade
Ste-Foy, Quebec G1Y 2I7 CANADA
Phone: 418/651-9543

Mick Trentacoste
Science Applications, Inc.
1651 Old Meadow Road, Suite 620
McLean, VA 22101
Phone: 703/821-4590

George Troutman
Geologist
Consolidated Gas Supply Corp.
445 W. Main Street
Clarksburg, WV 26301
Phone: 304/623-3611

Attendees (Cont.)

Robert P. Trump
Senior Research Engineer
Gulf Research
P.O. Drawer 2038
Pittsburgh, PA 15230
Phone: 412/362-1600

Lynn D. Tyler
Staff Member
Sandia Lab
Kirtland AFB
Albuquerque, NM 87115
Phone: 505/264-8174

Robert N. M. Trash
General Manager
Serv.-Kor, Inc.
P.O. Box 389
Carmi, IL 62821
Phone: 618/382-4184

N. E. Vanderborgh
Staff Member
Los Alamos Scientific Laboratory
P.O. Box 1663
Los Alamos, NM 87545
Phone: 505/667-4896

Arthur Van Tyne
Senior Geologist
New York State Geological Survey
P.O. Box 1218
Alfred, NY 14802
Phone: 607/871-2407

Michael Vickers
Geologist
West Virginia Geological Survey
P.O. Box 879
Morgantown, WV 26505
Phone: 304/292-6331

Robert J. Vinopal
Res. Assoc. Petrology
WVGS
P.O. Box 879
Morgantown, WV 26505
Phone: 304/292-6331

Frank E. Walker
Member Prof. Staff
TRW
7600 Colshire Dr.
McLean, VA 22101
Phone: 703/893-2000

Laure C. Wallace
Geologist
U.S. Geological Survey
Nat'l Center, Sunrise Valley Dr.
Reston, VA 22092
Phone: 703/860-6635

Dale Wambler
Juniata College
Huntingdon, PA 16652
Phone: 814/643-6288

W. A. Watson, Jr.
Supt. Production Operations
The Inland Gas Company, Inc.
P.O. Box 1189
Ashland, KY 41101
Phone: 606/324-3171

Doyal J. Watts
Section Leader
MERC
P.O. Box 880
Morgantown, WV 26505
Phone: 304/599-7218

Thurlow Weed
Managing Partner
Ohio Shale Gas Limited
1765 Edgemont Road
Columbus, OH 43212
Phone: 614/488-4471

Edward D. Weinberger
Vice President
Peel Energy Program
2100 South Ocean Lane
Ft. Lauderdale, FL 33316
Phone: 305/522-6139 or 563-5066

Marcia West
Geologist
U.S. Geological Survey
928 National Center
Reston, VA 22092
Phone: 703/860-6743

Russell Wheeler
Devonian Shale Project
West Virginia University
313 White Hall
Morgantown, WV 26506
Phone: 304/293-3477

Attendees (cont.)

William T. White
Geologist
West Virginia Geological Survey
P.O. Box 879
Morgantown, WV 26505
Phone: 304/292-6331

Jeffrey Whitehair
Sand Survey, Inc.
RD #2
Cambridge, OH 43725
Phone: 614/432-3336

C. Ray Williams
Petroleum Engineer
Bartlesville Energy Research Center
P.O. Box 1398
Bartlesville, OK 74003
Phone: 918/336-2400 x369

Partick O. Williams
Geologist, Appalachian Basin
Cities Service Oil Company
3545 NW 58th
Oklahoma City, OK 73112
Phone: 405/943-9511

Robert F. Williams
Haddad and Brooks, Inc.
37 McMurray Road
Pittsburgh, PA 15241
Phone: 412/835-7400

Edward Norman Wilson
Principal Investigator
Kentucky Geological Survey
Mineral Industries Building
Lexington, KY 40506
Phone: 606/257-2696

Jack L. Wilson
Supervisory Geologist
Columbia Gas Transmission Corporation
1700 MacCorkle Avenue, SE
Charleston, WV 25325
Phone: 304/346-0951

Robert Wise
Chemical Engineer
Morgantown Energy Research Center
P.O. Box 880
Morgantown, WV 26505
Phone: 304/599-7715

Larry D. Woodfork
Assistant State Geologist
West Virginia Geological Survey-DS Project
P.O. Box 879
Morgantown, WV 26505
Phone: 304/292-6331

Michael F. Yarussi
Haddad and Brooks, Inc.
37 McMurray Road
Pittsburgh, PA 15241
Phone: 412/835-7400

T. F. Yen, PhD
Associate Professor
University of Southern California
PCE 201, USC
Los Angeles, CA 90007
Phone: 213/741-2066

Paul P. Yewisiak
Appalachian Exploration &
Development Inc.
1400 Charleston National Plaza
P.O. Box 628
Charleston, WV 25322
Phone: 304/344-8355

A. B. Yost
Petroleum Engineer
Morgantown Energy Research Center
P.O. Box 880
Morgantown, WV 26505
Phone: 304/599-7325

Channan Young
Science Applications Inc.
1608 Independence Court
Ft. Collins, CO 80521
Phone: 303/491-8419

Jeffrey S. Zafar
Petroleum Geologist
UKRF
307 Mineral Industrial Building
University of Kentucky
Lexington, KY 40506
Phone: 606/257-2696

R. E. Zielinski
Manager, Energy Systems Technology
Monsanto Research Corporation
Mound Laboratory
Miamisburg, OH 45342
Phone: 513/866-7444 x3607

Jim Zuber
District Engineer
Dowell Division of Dow Chemical
Box 1910
Newark, OH 43055
Phone: 614/344-1191

Symposium Keynote address is presented by Hugh Guthrie, Acting Director of the Oil, Gas and Shale Technology Division of the U. S. Department of Energy.

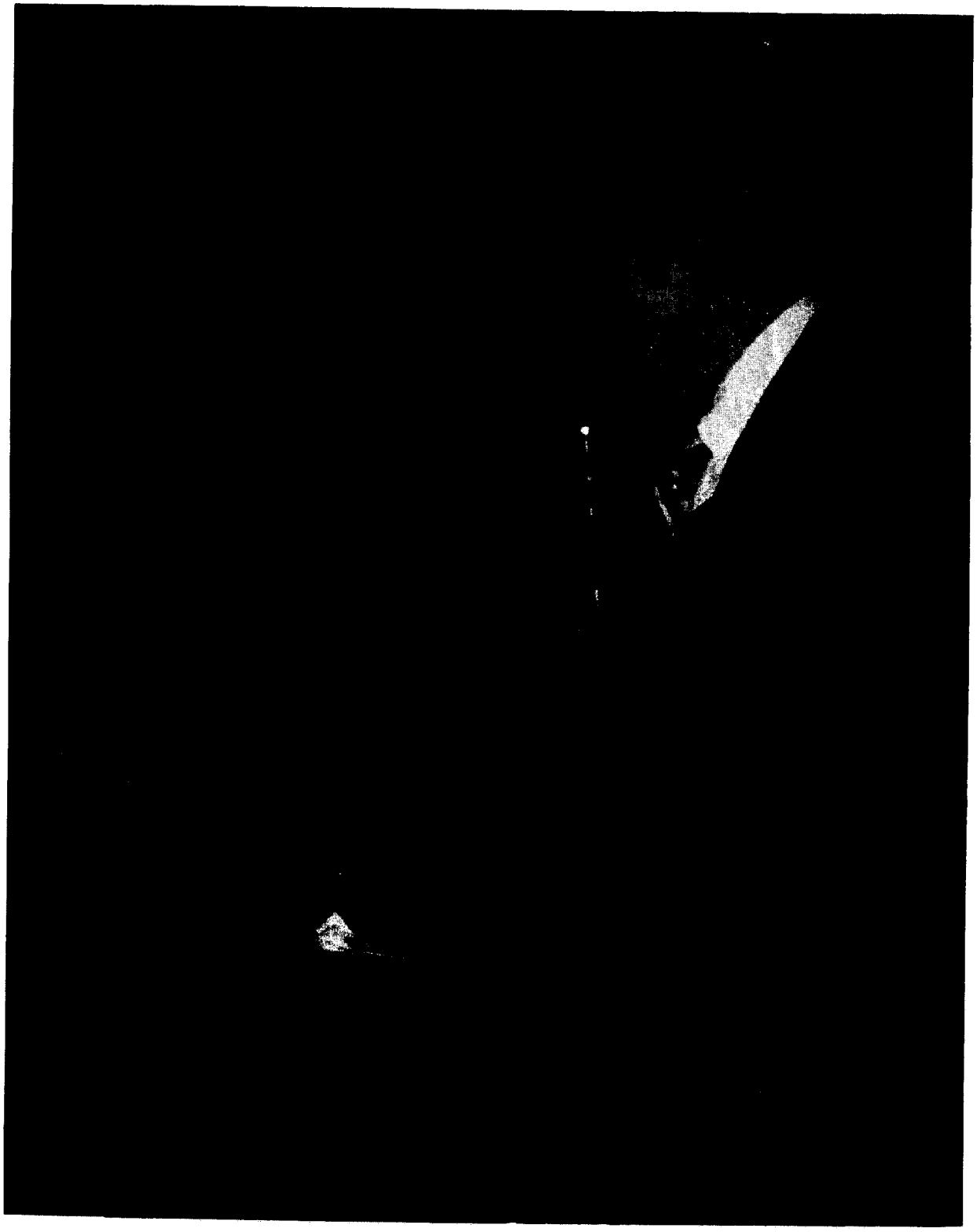

Mr. William T. McCormick, Vice-President of the American Gas Association, Arlington, VA, delivers the Banquet Address to an enthusiastic and interested audience.

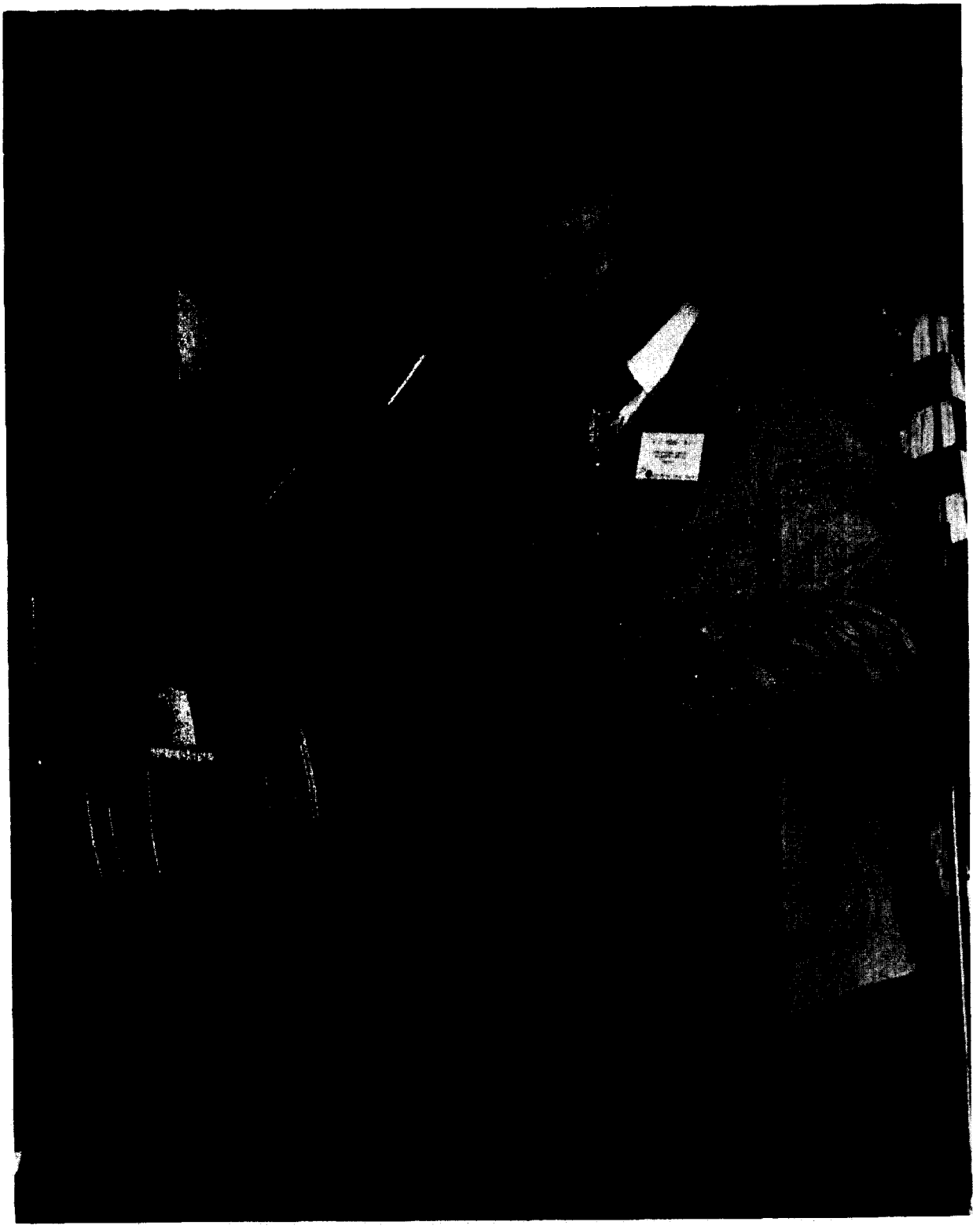

Bill Overbey, Symposium Chairman and Eastern Gas Shales Project Manager, presents opening address at First Eastern Gas Shales Project Symposium on October 18, 1977, Lakeview Inn, Morgantown, WV.

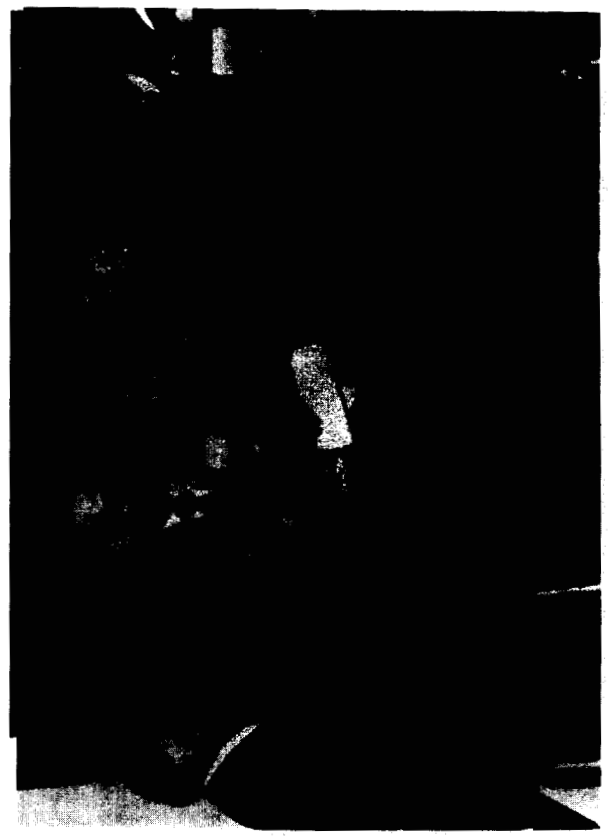

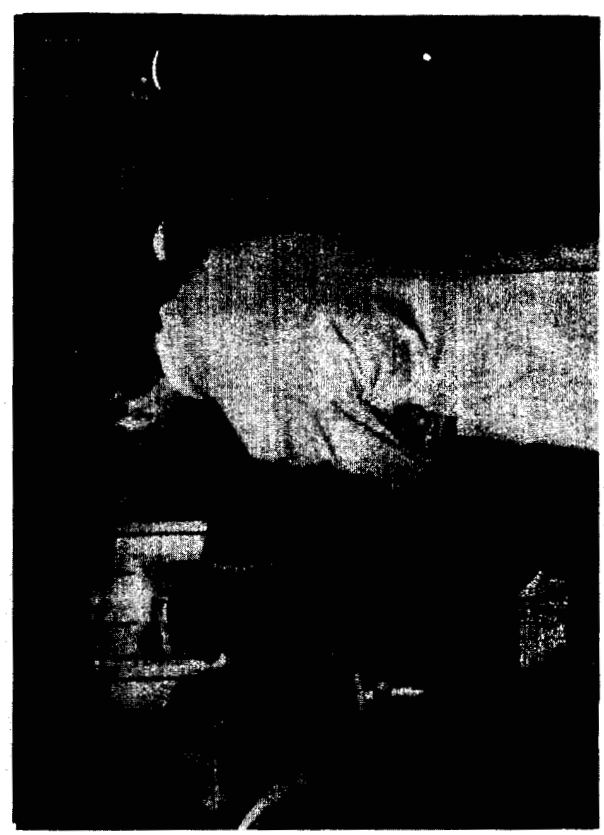

Many attendees enjoyed exhibits and discussions at the OPEN FORUM.

Symposium participants examine the first published cross sections for the Appalachian basin studies, USGS OC-80 "Preliminary Stratigraphic cross section showing Radioactive zones in the Devonian Black shales in the Western part of the Appalachian Basin" by Wallace, Roen & deWitt.

Symposium coordinator Ms. Hilma Barlow and assistants Diane Manilla
[illegible] participants.

U. S. GOVERNMENT PRINTING OFFICE 1978 747-795